

757

SANDIA REPORT SAND82-1647 • Unlimited Release
Printed December 1982

Effects of Ground Motion on Repository Depth The Yucca Flat Data

Luke J. Vortman, Jerald W. Long

Prepared by
Sandia National Laboratories
Albuquerque, New Mexico 87185 and Livermore, California 94550
for the United States Department of Energy
under Contract DE-AC04-76DP00789

Issued by Sandia National Laboratories, operated for the United States Department of Energy by Sandia Corporation.

NOTICE: This report was prepared as an account of work sponsored by an agency of the United States Government. Neither the United States Government nor any agency thereof, nor any of their employees, nor any of their contractors, subcontractors, or their employees, makes any warranty, express or implied, or assumes any legal liability or responsibility for the accuracy, completeness, or usefulness of any information, apparatus, product, or process disclosed, or represents that its use would not infringe privately owned rights. Reference herein to any specific commercial product, process, or service by trade name, trademark, manufacturer, or otherwise, does not necessarily constitute or imply its endorsement, recommendation, or favoring by the United States Government, any agency thereof or any of their contractors or subcontractors. The views and opinions expressed herein do not necessarily state or reflect those of the United States Government, any agency thereof or any of their contractors or subcontractors.

Printed in the United States of America
Available from
National Technical Information Service
U.S. Department of Commerce
5235 Port Royal Road
Springfield, VA 22161

NTIS price codes
Printed copy: A11
Microfiche copy: A01

TABLE OF CONTENTS

	<u>Page</u>
Abstract	iii
Preface	v
Acknowledgments	v
Chapter 1 Introduction	1
Chapter 2 Effects of Depth on Ground Motion - Single Peaks	3
Chapter 3 Effects of Depth on Ground Motion - Multiple Peaks	17
Chapter 4 Effects of Depth on Ground Motion - PSRV Ratios	25
Chapter 5 Ground Motion Waveforms	35
Chapter 6 Comparison of Results from Yucca Flat and Pahute Mesa	65
Chapter 7 Conclusions	69
References	75
Appendix A Tables of Ratios (Top/Bottom) for Peak Vector Motion - Multiple Peak Data	77
Appendix B Comparison of Ratios (Top/Bottom) of "Vector" PSRV's	91
Appendix C Comparison of Top and Bottom Waveforms at Station W-10	137
Appendix D Comparison of Top and Bottom Waveforms at Station W-4	223
Appendix E Comparison of Top and Bottom Waveforms at Station W-11	273
Appendix F Comparison of Top and Bottom Waveforms at Station W-3	359
Appendix G Comparison of Top and Bottom Waveforms at Station W-9	481

Appendix H	Comparison of Top and Bottom Waveforms at Station W-8	567
Appendix I	Comparison of Top and Bottom Waveforms at Stations W-15/W-16	581
Appendix J	Comparison of Top and Bottom Waveforms at Station W-13	619
Distribution List		669

ABSTRACT

Measurements of ground motion were made at some of seven locations on 28 different underground nuclear weapons tests in Yucca Flat. Each location had measurements at the surface and at a depth ranging from 61 m to 762m, permitting an assessment of the effect of depth on ground motion.

Measurements of vertical, radial, and tangential acceleration were made at each location and depth, and the three components were used to determine peak vector magnitudes of acceleration, velocity, and displacement. Top-to-bottom ratios of the peak vector values were plotted against depth and an exponential least squares fit made to the data. Ratios of the largest single peaks, averages of the 5, 10, 15, 20, and 25 largest peaks, and ratios of Pseudo Relative Response Velocity (PSRV) were examined. Fits for the multiple peaks were better than for single peaks, as evidenced by improvements in coefficients of determination. Except for acceleration, fits for PSRV's were better than for multiple peaks. While scatter from one event to the next contributes to small coefficients of determination, an even greater effect is produced by differences in geology at the seven locations. Fits to the data can be used as prediction equations. Examination of waveforms of individual components of motion showed influences of topography at two locations.

In some cases events detonated in proximity to one another had similar waveforms, and in other cases the waveforms were quite different. Surface displacement on Rainier Mesa showed three distinct relationships between vertical, radial, and tangential amplitudes. There was no correlation with event location within Yucca Flat.

ABSTRACT

(cont'd)

Similar measurements were made on Pahute Mesa and reported earlier. The better fit of prediction equations for the Pahute Mesa data could be attributed to the smaller number of events in that data set and to the smaller range of yields of those events.

PREFACE

The work reported here is essentially that performed under the Weapons Test Seismic Investigations (WBS 1.3.3.8) of the Nevada Nuclear Waste Storage Investigation (NNWSI) during FY 1982.

ACKNOWLEDGMENTS

We are grateful to L. S. Converse, Sandia National Laboratories, Livermore, California, for digitizing the analog data used in this report. L. N. Castle and J. D. Pearcey, EG&G, Inc., provided digital signal processing of data after it had been digitized. J. G. Lee directed data acquisition for Event 45 and subsequent events, and J. R. Dickinson and H. A. Stuckert for prior events.

EFFECTS OF REPOSITORY DEPTH ON GROUND MOTION

THE YUCCA FLAT DATA

CHAPTER 1

INTRODUCTION

This report is an extension of Reference 1, and as such its contents are similar, but the data analyzed are those from underground weapons tests in Yucca Flat rather than on Pahute Mesa. Chapter 1 of the reference describes the instrumentation, signal processing, canister orientation, station locations, event participation, and effects of geometry and geology. That information applies for all the analysis included in this report.

In the following chapters we will present the Yucca Flat data and also make comparisons between those data and data from Pahute Mesa events.

CHAPTER 2

EFFECTS OF DEPTH ON GROUND MOTION

SINGLE PEAKS

The reader is referred to applicable discussion in Chapter 2, Reference 1, which is not repeated here. The ratios (top/bottom) for peak vector acceleration, velocity, and displacement for shots fired in Yucca Flat are shown in Tables 2-1, 2-2, and 2-3, respectively. The stations are listed across the table in order of increasing depth, and the event numbers are listed in order of decreasing yield. As with the corresponding ratios from the Pahute Mesa data, there is no distinct trend with yield for any of the stations.

The ratios from the tables are plotted in Figures 2-1, 2-2, and 2-3 as a function of the depth below the surface to the downhole measurement. Separate symbols have been used to identify ratios from the numbered events. The flags note the average of ratios from all Yucca Flat for which measurements were made at each surface and downhole pair. An exponential least squares (ELS) fit to the averages was determined and is indicated by the dashed line. The ELS fit was weighted according to the number of events for which there were data at that depth. (See Tables 2-1, 2-2, and 2-3 for the number of events.)

Acceleration, velocity, and displacement all decrease with depth relative to those parameters at the surface. The change with depth is greatest for acceleration, and least for displacement. Station variations in geology and topography tend to obscure the effect of depth. Note (Figure 2-1) that the acceleration ratio for the shallowest station

TABLE 2-1
Ratios (Top/Bottom) for Peak Vector
Acceleration - Single Highest Peak

Event Number	Plot Symbol	STATION NUMBER								
		TOP (61m)	4 (130.5m)	10 (342.6m)	11 (345.6m)	3 (416.7m)	9 (431.6m)	8 (570m)	15/16 (580m)	13 (762m)
8	c	b	1.65	b	b	1.71	b	b	b	b
11	Δ	b	2.08	b	b	2.32	a	a	b	b
40	o	1.23	b	1.52	2.19	1.58	2.44	b	a	4.83
24	e	a	b	a	2.77	1.20	a	b	b	b
3	v	b	1.51	b	b	b	b	b	b	b
1	j	b	2.02	b	b	b	b	b	b	b
13	Δ	b	1.84	b	b	1.59	a	b	b	b
16	d	1.33	2.01	b	a	1.59	2.26	4.86	b	b
53	b	1.21	b	1.02	a	1.57	3.24	b	a	4.82
30	a	1.36	b	1.31	2.78	1.98	2.50	b	0.91	b
36	s	1.14	b	1.56	2.89	a	1.70	b	0.91	3.38
5	m	b	2.10	b	b	b	b	b	b	b
21	m	a	b	a	a	1.11	a	a	b	b
2	v	b	1.91	b	b	b	b	b	b	b
31	u	1.35	b	1.20	3.14	2.69	2.51	b	1.45	b
45	q	a	b	a	2.83	1.30	3.71	b	0.96	5.02
26	v	1.00	b	a	a	1.67	2.23	b	b	b
23	◆	a	b	a	a	1.90	a	b	b	b
55	q	a	b	a	a	2.01	a	b	a	a
39	n	1.20	b	1.84	3.06	a	4.06	b	2.25	5.07
43	r	1.20	b	3.24	3.33	1.02	a	b	2.38	3.61
37	p	1.21	b	1.50	2.73	1.42	2.95	b	a	4.20
50	o	d	b	d	3.09	a	a	b	d	d
38	e	d	b	d	3.34	a	3.36	b	d	d
9	k	d	a	d	d	1.79	b	2.87	d	d
42	x	d	b	d	1.90	1.59	3.77	b	d	d
49	f	d	b	d	2.78	1.38	3.23	b	d	d
46	t	d	b	d	3.25	2.48	4.57	b	d	5.82
No. of Events		10	8	8	14	20	14	2	6	8
Average		1.22	1.89	1.65	2.86	1.69	3.04	3.87	1.48	4.59

a - data inadequate

b - station not installed at time of event

d - station not operated for this event

$$R = 1.29e^{0.00135d} \quad \sigma_R = \pm 1.36$$

$$r^2 = 0.402 \quad CL_{R90} = \pm 1.87 \text{ to } 1.89$$

TABLE 2-2
 Ratios (Top/Bottom) for Peak Vector
 Velocity - Single Highest Peak

Event Number	Plot Symbol	STATION NUMBER								
		10P (61m)	4 (130.5m)	10 (342.6m)	11 (345.6m)	3 (416.7m)	9 (431.6m)	8 (570m)	15/16 (580m)	13 (762m)
8	c	b	1.39	b	b	2.08	b	b	b	b
11	Δ	b	1.52	b	b	1.77	a	a	b	b
40	o	1.09	b	1.75	2.96	1.16	3.47	b	a	1.77
24	o	a	b	a	3.61	1.56	a	b	b	b
3	v	b	1.47	b	b	b	b	b	b	b
1	j	b	2.07	b	b	b	b	b	b	b
13	Δ	b	1.36	b	b	1.29	a	b	b	b
16	d	1.02	1.53	b	a	1.27	3.75	3.16	b	b
53	b	1.02	b	1.56	a	1.16	4.23	b	a	2.03
30	a	1.05	b	2.90	2.62	1.07	2.93	b	1.98	b
36	a	1.11	b	1.93	5.14	a	2.89	b	2.12	2.00
5	m	b	1.68	b	b	b	b	b	b	b
21	m	a	b	a	a	1.12	a	a	b	b
2	v	b	1.26	b	b	b	b	b	b	b
31	u	1.11	b	1.99	4.67	1.01	3.54	b	2.10	b
45	u	a	b	a	3.54	1.11	3.67	b	1.67	2.08
26	v	1.04	b	a	a	1.14	3.67	b	b	b
23	q	a	b	a	a	1.14	a	b	b	b
55	q	a	b	a	a	1.54	a	b	a	a
39	n	1.08	b	1.61	3.06	a	4.79	b	2.53	2.60
43	r	1.23	b	2.62	3.53	1.07	a	b	3.05	2.32
37	p	1.06	b	1.80	2.80	1.48	4.27	b	a	2.15
50	o	d	b	d	2.95	a	a	b	d	d
38	k	d	b	d	2.87	a	4.22	b	d	d
9	k	d	a	d	d	1.42	b	2.40	d	d
42	x	d	b	d	2.03	1.35	a	b	d	d
49	f	d	b	d	2.58	2.12	4.05	b	d	d
46	t	d	b	d	3.13	1.50	6.04	b	d	3.16
No. of Events		10	8	9	14	20	13	2	6	8
Average		1.08	1.54	2.02	3.25	1.37	3.96	2.78	2.24	2.26

a - data inadequate
 b - station not installed at time of event
 d - station not operated for this event

$$R = 1.41e^{0.000992d} \quad \sigma_R = \pm 1.49$$

$$r^2 = 0.210 \quad CL_{R90} = \pm 2.25 \text{ to } 2.29$$

TABLE 2-3

Ratios (Top/Bottom) for Peak Vector
Displacement - Single Highest Peak

Event Number	Plot Symbol	STATION NUMBER								
		TOP (61m)	4 (130.5m)	10 (342.6m)	11 (345.6m)	3 (416.7m)	9 (431.6m)	8 (570m)	15/16 (580m)	13 (762m)
8	c	b	1.47	b	b	1.04	b	b	b	b
11	Δ	b	1.24	b	b	1.36	a	a	b	b
40	o	1.05	b	1.62	3.01	0.09	2.79	b	a	1.25
24	e	a	b	a	3.20	1.05	a	b	b	b
3	v	b	1.12	b	b	b	b	b	b	b
1	i	b	1.23	b	b	b	b	b	b	b
13	Δ	b	1.14	b	b	1.27	a	b	b	b
16	d	0.10	1.39	b	a	1.15	3.23	1.60	b	b
53	b	1.00	b	1.45	a	1.14	3.85	b	a	1.44
30	a	1.04	b	2.31	2.19	1.03	2.61	b	1.61	b
36	a	1.06	b	1.61	2.77	a	2.34	b	1.95	1.02
5	a	b	1.58	b	b	b	b	b	b	b
21	m	a	b	a	a	1.05	a	a	b	b
2	v	b	1.20	b	b	b	b	b	b	b
31	u	1.08	b	1.67	3.53	1.02	3.99	b	2.14	b
45	q	a	b	a	2.85	0.87	3.10	b	1.64	1.56
26	v	1.05	b	a	a	0.96	3.14	b	b	b
23	q	a	b	a	a	0.96	a	b	b	b
55	q	a	b	a	a	1.32	a	b	a	a
39	n	1.04	b	1.45	2.95	a	2.97	b	1.85	2.06
43	r	1.08	b	1.78	4.18	0.92	a	b	3.29	2.23
37	p	1.07	b	1.73	3.43	1.19	3.45	b	a	1.24
50	o	d	b	d	3.43	a	a	b	d	d
38	e	d	b	d	2.86	a	2.92	b	d	d
9	k	d	a	d	d	1.09	b	1.79	d	d
42	x	d	b	d	2.64	1.09	a	b	d	d
49	f	d	b	d	2.78	1.35	5.03	b	d	d
46	t	d	b	d	2.58	1.45	4.98	b	d	
No. of Events		10	8	8	14	20	13	2	6	8
Average		1.05	1.30	1.70	3.03	1.11	3.42	1.69	2.08	1.69

a - data inadequate

b - station not installed at time of event

d - station not operated for this event

$$R = 1.34e^{0.000708d} \quad \sigma_R = \pm 1.54$$

$$r^2 = 0.087 \quad CL_{R90} = \pm 2.39 \text{ to } 2.44$$

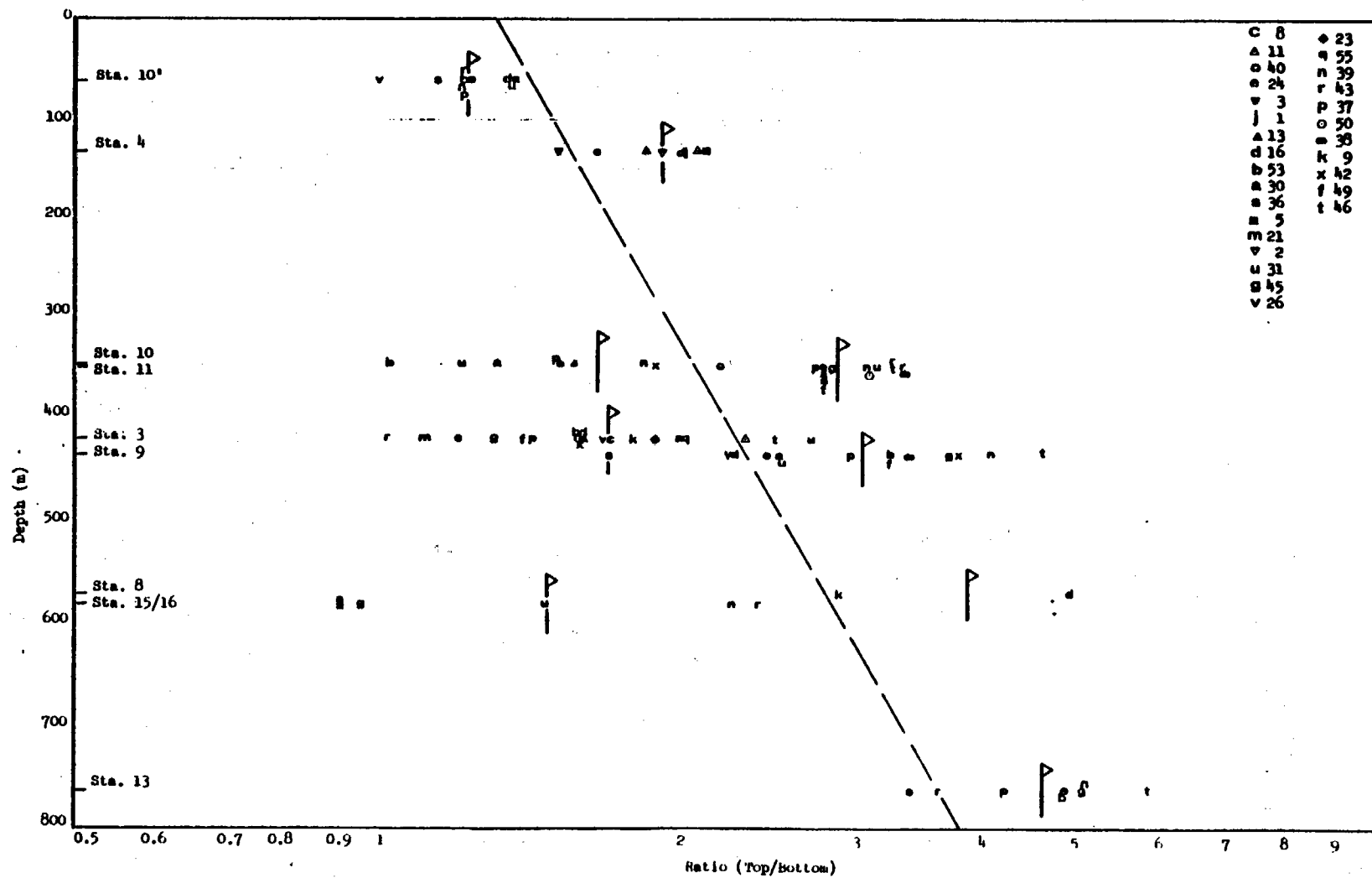
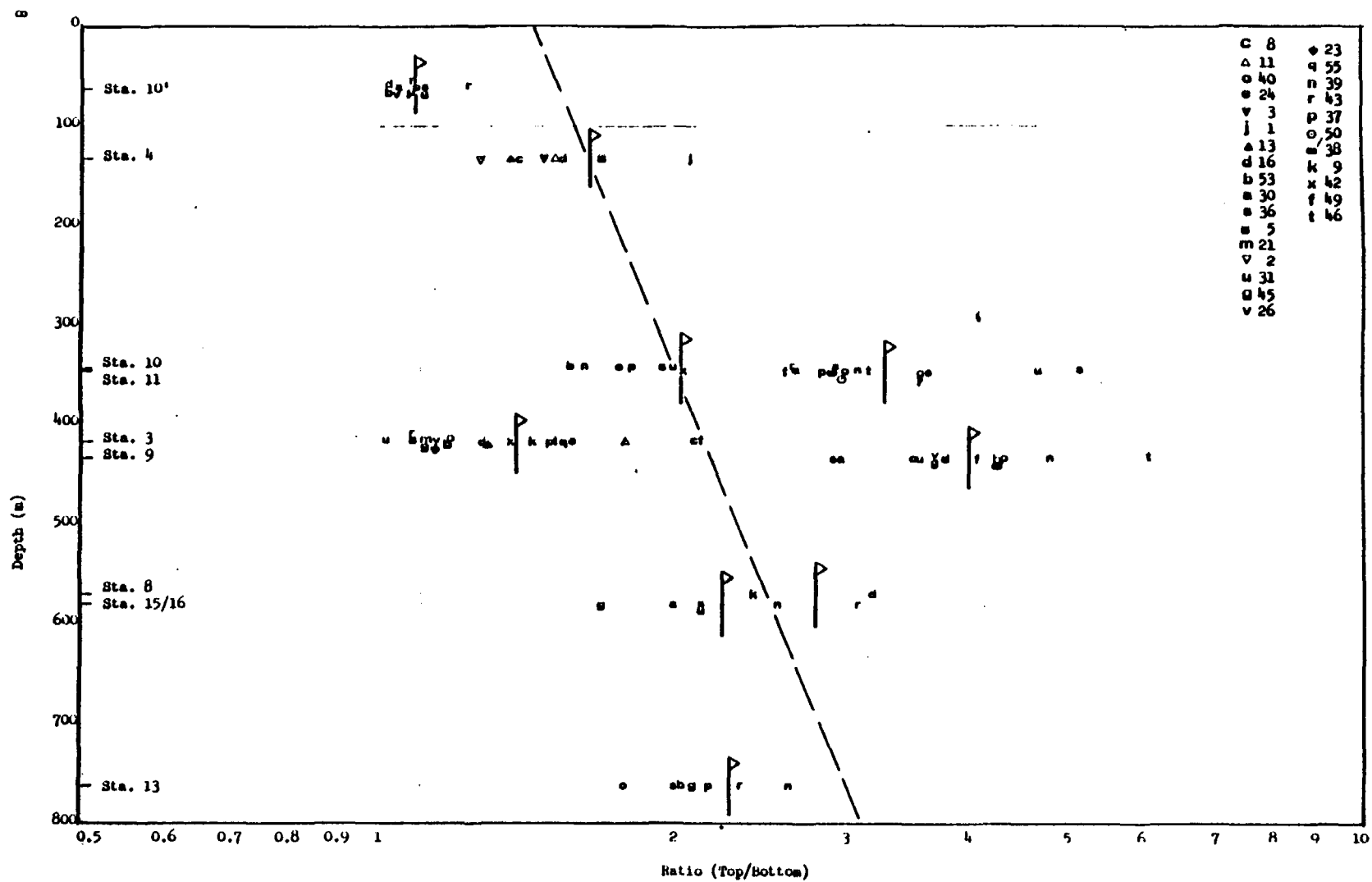


Figure 2-1 Ratios (Top/Bottom) for
Peak Vector Acceleration Plotted
Versus Station Depth



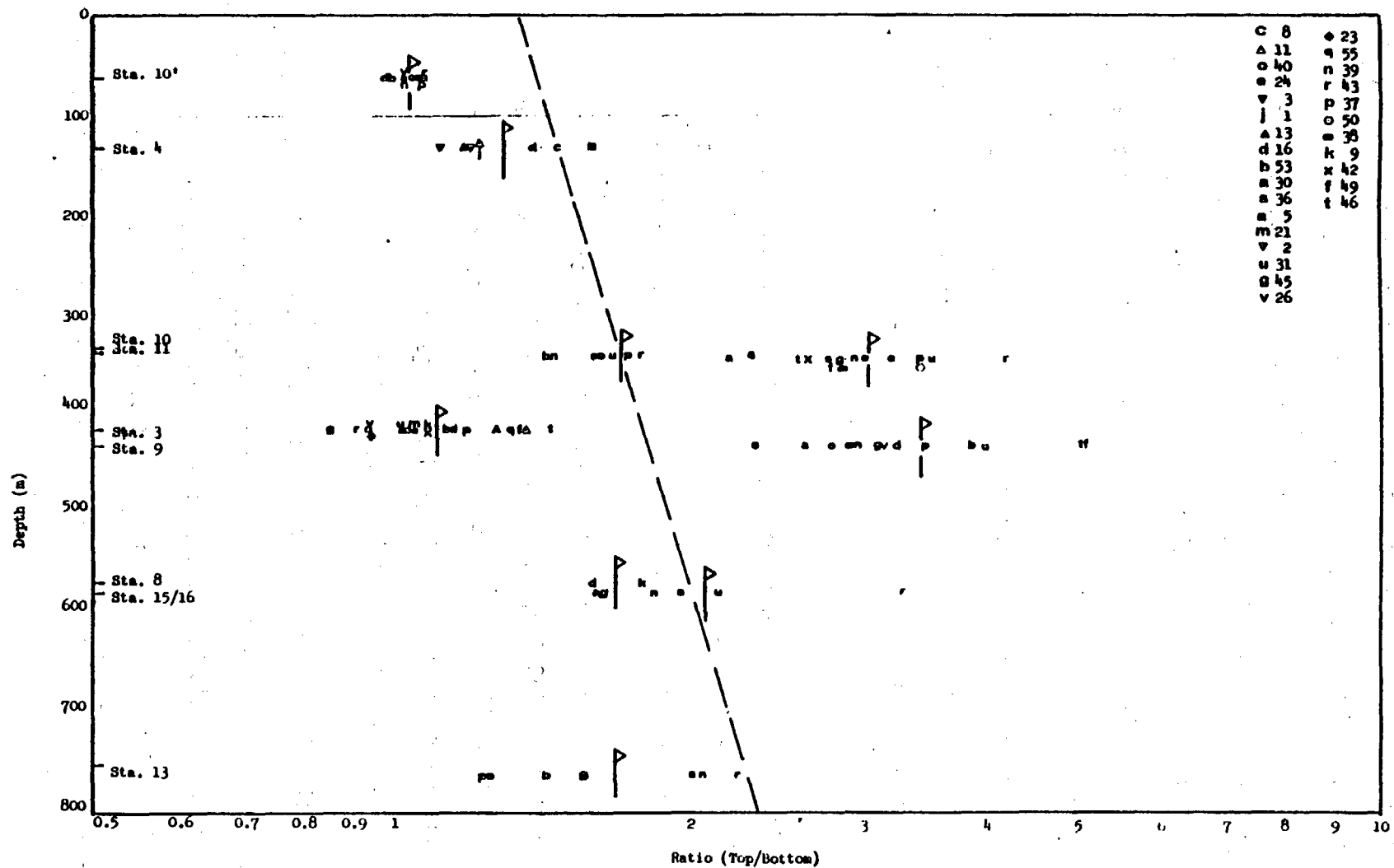


Figure 2-3 Ratios (Top/Bottom) for
Peak Vector Displacement Plotted
Versus Station Depth

is enough larger than that at the surface that a relatively rapid change in acceleration ratio appears to be taking place in the first 60 metres of depth. Velocity and displacement ratios (Figures 2-2 and 2-3) are only slightly larger than those at the surface. Acceleration peaks are usually those in the p-wave, whereas those for displacement are in the surface wave. Peaks for velocity can be in either. Scatter in the ratios from shot to shot for any station is greatest for acceleration and least for displacement.

The surface intercept of the ELS fit to all three parameters is larger than 1 because of the rapid change at shallow depth, as noted above. It is in order to review station characteristics which account for these differences.

Station 10 Prime has both the surface and bottom stations in alluvium. The bottom station, at 61m, is well above the alluvium/basalt interface at 312 m and the water table at 316 m.

Station 4 is in alluvium throughout the length of the hole. The bottom, at 130.5 m, is 333 m above the alluvium/tuff interface, and about 338 m above the water table. Thus, it is not clear why there should be such a large difference in top/bottom ratios between Stations 4 and 10 Prime.

Station 10 has the bottom canister at 342.6 m. This is 30.6 m below the alluvium/basalt interface and 26.6 m below the water table. Thus, it would be expected that the basalt around the bottom canister would offer restraint which would cause the top/bottom ratio to be large. This does not appear to be so, especially when compared

with Station 11. Station 11 has the bottom canister at 346.6 m. This is above the water table and 10.4 m above the alluvium/paleozoic interface. Top/bottom ratios are relatively large. Topography is not a factor. Thus, the bottom is moving less than expected relative to the top. The difference can be seen in the spectra of Stations 10 and 11. Because Station 11 is in Yucca Flat, as are the nuclear events being considered here, there is more energy in the spectra (both top and bottom) for Station 11 than for Station 10 which is in Jackass Flats, 35 to 40 km farther away. Station 11 shows the greatest spectral difference between top and bottom at 1 Hz where the difference is more than a factor of 8. Station 11 is so close to events in Yucca Flat that almost all the energy is in the direct wave at both the top and bottom.

Station 3 is perhaps the easiest to understand. Both top and bottom are in granite, the latter at a depth of 416.7 m. Since the granite is a large intrusive mass (pluton), water table and interfaces are of little or no consequence. Top/bottom ratios are small because the mass moves very much as a unit.

Station 9 is in Rainier Mesa. Top and bottom are separated by a series of tuff strata, and the bottom is about 230 (± 30) m above the tuff/paleozoic interface. In an east-west direction at the location of the station, Rainier Mesa is about 1.07 km wide at the top. The surface station is located about 0.5 km from the south edge of the mesa. Northward there is no appreciable relief for over 4 km. Table 2-4 shows the difference in vertical, north-south,

TABLE 2-4

Peak-to-Peak Ground Motion at Station 9 for Event 49

<u>Motion and Component</u>		<u>Top Motion</u>	<u>Ratio to Vertical</u>	<u>Bottom Motion</u>	<u>Ratio to Vertical</u>	<u>Top/Bottom Ratio</u>	<u>Top/Bottom Ratio (Vector)</u>
Accel. (g's)	Vert	0.00812		0.00327		2.48	
	270°	0.00975	1.20	0.00381	1.17	2.56	
	0°	<u>0.01401</u>	1.73	<u>0.00457</u>	1.40	<u>3.07</u>	
	Ave	0.01063		0.00388		2.70	3.08
Velocity (cm/s)	Vert	0.337		0.183		1.84	
	270°	0.817	2.42	0.192	1.05	4.26	
	0°	<u>1.033</u>	3.07	<u>0.244</u>	1.33	<u>4.23</u>	
	Ave	0.729		0.206		3.44	3.96
Disp. (cm)	Vert	0.0416		0.0309		1.35	
	270°	0.1337	3.21	0.0281	0.909	4.76	
	0°	<u>0.1535</u>	3.69	<u>0.0250</u>	0.809	<u>6.14</u>	
	Ave	0.1096		0.0280		4.08	3.43

and east-west motion at both the top and bottom, together with ratios of top to bottom for individual components and ratios of each of the horizontal components to the vertical. Acceleration, velocity, and displacement values shown are peak-to-peak values. The station was on an azimuth of 311.76° clockwise from north about event 49. Thus the north-south gage (0° , positive north) and the east-west gage (270° , positive west) are within $\pm 5^{\circ}$ of 45° from the event. At these distances, in the absence of topographic effects, motions, especially displacements, are within $\pm 50\%$ of the average of the three components, and horizontal motion is closer to the vertical than is observed here. At the top, horizontal motion for both components is significantly greater than vertical, and that for 0° greater than for 270° . At the bottom, acceleration and velocity follow the same trends, but with much smaller differences -- differences more like those commonly observed. For displacement the trend is reversed, producing large top/bottom ratios for horizontal displacement. Curiously, the largest motion at the top is in the direction of the long axis of the mesa.

Station 8 provided data from only 2 events. It was located in Ue-1L. The top canister was in alluvium. The alluvium-paleozoic interface was at 61 m. The paleozoic medium was argillite of the eleana formation, which extended to the total depth of the hole at 1627 m. The station was at 570 m because the hole was closed just below that depth. Water table is at 520 m or less. There are no topographic effects at this location, although some of the effects of proximity to the explosions noted above for Station 11 would apply to Station

8, but to a lesser extent since distances are slightly greater.

Stations 15/16 are not a true surface/downhole pair, the former on Dome Mountain and the latter in Fortymile Canyon. They are separated by 2300 m horizontally and 580 vertically. Topographic effects were observed for the Pahute Mesa events, and are seen for the Yucca Flat events as well.

Station 13 is in Hole Ue-18r which had been used as a water well. The total depth is 1525 m, and the hole is cased to 496 m. The canister is at 762 m, 344 m below the water table at 418 m. The medium from the surface to the canister consists of 9 units of ash-flow and bedded tuffs and one each rhyolite lava and gravel and tuffaceous sediments. The medium in the lower half of the hole is similar.

The results of the effects of depth for Yucca Flat are:

For single peak vector ratios:

Acceleration	$R = 1.29e^{0.00135d}$	$\sigma_R = \pm 1.36$
	$r^2 = 0.399$	$CL_{R90} = \pm 1.87 \text{ to } 1.89$
Velocity	$R = 1.41e^{0.000992d}$	$\sigma_R = \pm 1.49$
	$r^2 = 0.210$	$CL_{R90} = \pm 2.25 \text{ to } 2.29$
Displacement	$R = 1.34e^{0.000708d}$	$\sigma_R = \pm 1.54$
	$r^2 = 0.087$	$CL_{R90} = \pm 2.39 \text{ to } 2.44$

where R is the ratio of the peak vector value at the surface to that at the bottom, and r^2 is the coefficient of determination which indicates the quality of fit achieved by the regression. Values of r^2 close to 1 indicate a better fit than values close to zero. Standard errors of the estimate, σ_R , and 90 percent

confidence limits, CL_{R90} , are also shown above and in the tables. The CL_{R90} values are multipliers (+) or divisors (-) of the value given by the equations.

CHAPTER 3
EFFECTS OF DEPTH ON GROUND MOTION
MULTIPLE PEAKS

It was noted in Reference 1 that using single peaks can distort the top/bottom ratios when either record contains a single large peak due to simultaneous arrivals via different paths which is not present in the other. As for the Pahute Mesa data, averages of the highest 5, 10, 15, 20, and 25 peaks were determined separately for top and bottom, and the ratio of the corresponding averages obtained. Ratios for the 15 highest peaks are shown in Tables 3-1, 3-2, and 3-3, for acceleration, velocity, and displacement, respectively. (Corresponding ratios for the 5, 10, 20, and 25 highest peaks are included as Appendix A.) Changes in the ratios going from 15 to 25 peaks are usually small relative to those going from 1 to 15.

Figures 3-1, 3-2, and 3-3 show the ratios for the average of the 15 highest peaks plotted against depth. Changes in average values (indicated by the flags) going from 1 to 15 peaks can be seen by comparing Figures 2-1, 2-2, and 2-3 with 3-1, 3-2, and 3-3. There are significant changes for Station 8 for acceleration, velocity, and displacement; for Station 11 for velocity; and for Stations 9 and 13 for displacement. Only for displacement is the slope of the fit to the data changed appreciably in going from 1 to 15 peaks. For each motion parameter the coefficient of determination was improved by going from 1 to 15 peaks.

The effect of geology at the station locations exerts a greater influence on fit than does the effect of depth. The results are:

TABLE 3-1
 Ratios (Top/Bottom) for Peak Vector
 Acceleration - 15 Highest Peaks

Event Number	Plot Symbol	STATION NUMBER								
		TOP (61m)	4 (130.5m)	10 (342.6m)	11 (345.6m)	3 (416.7m)	9 (431.6m)	8 (570m)	15/16 (580m)	13 (762m)
8	c	b	1.98	b	b	1.71	b	b	b	b
11	Δ	b	1.74	b	b	2.38	a	a	b	b
40	o	1.32	b	1.50	2.76	1.70	2.42	b	a	4.85
24	e	a	b	a	2.88	1.56	a	b	b	b
3	v	b	1.59	b	b	b	b	b	b	b
1	j	b	1.90	b	b	b	b	b	b	b
13	Δ	b	1.75	b	b	1.72	a	b	b	b
16	d	1.29	1.60	b	a	1.73	2.51	3.79	b	b
53	b	1.23	b	1.01	a	1.97	3.29	b	a	4.68
30	a	1.37	b	1.49	3.04	2.00	2.70	b	1.15	b
36	e	1.24	b	1.70	3.34	a	2.14	b	1.41	3.64
5	m	b	2.06	b	b	b	b	b	b	b
21	m	a	b	a	a	1.64	a	a	b	b
2	v	b	1.74	b	b	b	b	b	b	b
31	u	1.25	b	1.03	2.75	2.05	3.00	b	1.73	b
45	g	a	b	a	2.48	1.45	3.67	b	1.55	5.33
26	v	1.14	b	a	a	1.66	2.40	b	b	b
23	e	a	b	a	a	1.47	a	b	b	b
55	q	a	b	a	a	2.23	a	b	a	a
39	n	1.16	b	1.73	3.79	a	3.92	b	1.89	4.47
43	r	1.21	b	2.82	3.25	1.21	a	b	2.02	3.79
37	p	1.27	b	1.53	3.00	1.67	3.15	b	a	4.09
50	o	d	b	d	2.56	a	a	b	d	d
38	u	d	b	d	3.20	a	3.51	b	d	d
9	k	d	a	d	d	1.90	b	2.60	d	d
42	x	d	b	d	2.31	1.46	4.00	b	d	d
49	f	d	b	d	2.68	1.92	2.74	b	d	d
46	t	d	b	d	3.23	2.36	4.03	b	d	5.05
No. of Events		10	8	8	14	20	14	2	6	8
Average		1.25	1.79	1.60	2.95	1.79	3.11	3.20	1.63	4.49

a - data inadequate

b - station not installed at time of event

d - station not operated for this event

$$R = 1.30e^{0.00137d} \quad \sigma_R = \pm 1.33$$

$$r^2 = 0.446 \quad CL_{R90} = \pm 1.78 \text{ to } 1.81$$

TABLE 3-2

Ratios (Top/Bottom) for Peak Vector
Velocity - 15 Highest Peaks

Event Number	Plot Symbol	STATION NUMBER								
		TOP (61m)	4 (130.5m)	10 (342.6m)	11 (345.6m)	3 (416.7m)	9 (431.6m)	8 (570m)	15/16 (580m)	13 (762m)
8	c	b	1.53	b	b	1.22	b	b	b	b
11	A	b	1.60	b	b	1.49	a	a	b	b
40	o	1.07	b	2.13	2.59	1.19	2.94	b	a	2.56
24	o	a	b	a	2.79	1.24	a	b	b	b
3	v	b	1.28	b	b	b	b	b	b	b
1	j	b	1.67	b	b	b	b	b	b	b
13	A	b	1.47	b	b	1.23	a	b	b	b
16	d	1.02	1.49	b	a	1.25	3.38	3.22	b	b
53	b	1.06	b	1.54	a	1.31	4.74	b	a	2.69
30	a	1.07	b	2.45	2.50	1.19	3.07	b	1.65	b
36	a	1.08	b	1.71	3.32	a	3.55	b	2.18	2.57
5	m	b	1.55	b	b	b	b	b	b	b
21	m	a	b	a	a	1.18	a	a	b	b
2	v	b	1.42	b	b	b	b	b	b	b
31	u	1.09	b	1.67	3.57	1.28	4.06	b	2.14	b
45	u	a	b	a	3.46	1.08	4.09	b	1.66	2.59
26	v	1.04	b	a	a	1.19	3.20	b	b	b
23	v	a	b	a	a	1.14	a	b	b	b
55	q	a	b	a	a	1.32	a	b	a	a
39	q	1.06	b	1.75	4.34	a	5.34	b	2.08	2.57
43	r	1.12	b	2.30	3.69	1.07	a	b	2.49	2.83
37	p	1.09	b	1.79	3.26	1.34	4.59	b	a	2.58
50	o	d	b	d	2.89	a	a	b	d	d
38	a	d	b	d	3.28	a	4.48	b	d	d
9	k	d	a	d	d	1.46	b	2.59	d	d
42	x	d	b	d	2.16	1.25	a	b	d	d
49	t	d	b	d	2.96	1.82	3.95	b	d	d
46	t	d	b	d	3.07	1.60	5.03	b	d	2.93
No. of Events		10	8	8	14	20	13	2	6	8
Average		1.07	1.50	1.92	3.13	1.29	4.03	2.91	2.03	2.66

a - data inadequate

b - station not installed at time of event

d - station not operated for this event

$$R = 1.30e^{0.00115d} \quad \sigma_R = \pm 1.50$$

$$r^2 = 0.221 \quad CL_{R90} = \pm 2.28 \text{ to } 2.33$$

TABLE 3-3
 Ratios (Top/Bottom) for Peak Vector
 Displacement - 15 Highest Peaks

Event Number	Plot Symbol	STATION NUMBER								
		TOP (61m)	4 (130.5m)	10 (342.6m)	11 (345.6m)	3 (416.7m)	9 (431.6m)	8 (570m)	15/16 (580m)	13 (762m)
8	c	b	1.32	b	b	1.06	b	b	b	b
11	▲	b	1.25	b	b	1.17	a	a	b	b
40	o	1.05	b	2.06	3.51	1.08	3.15	b	a	1.66
24	e	a	b	a	2.56	1.08	a	b	b	b
3	v	b	1.09	b	b	b	b	b	b	b
1	j	b	1.32	b	b	b	b	b	b	b
13	▲	b	1.16	b	b	1.04	a	b	b	b
16	d	0.99	1.23	b	a	1.06	2.94	2.38	b	b
53	b	1.02	b	1.39	a	1.16	4.09	b	a	1.84
30	a	1.03	b	2.19	2.82	0.97	3.19	b	1.73	b
36	a	1.05	b	1.51	2.84	a	3.36	b	2.05	2.15
5	a	b	1.46	b	b	b	b	b	b	b
21	m	a	b	a	a	1.10	a	a	b	b
2	v	b	1.26	b	b	b	b	b	b	b
31	u	1.04	b	1.53	2.97	1.10	4.01	b	2.16	b
45	u	a	b	a	2.47	0.94	3.42	b	1.55	1.78
26	v	1.02	b	a	a	1.05	2.96	b	b	b
23	◆	a	b	a	a	1.01	a	b	b	b
55	q	a	b	a	a	1.25	a	b	a	a
39	n	1.02	b	1.42	3.98	a	3.74	b	2.09	2.09
43	r	1.07	b	1.71	2.96	0.97	a	b	2.57	2.22
37	p	1.10	b	1.67	3.72	1.04	4.21	b	a	1.73
50	o	d	b	d	2.76	a	a	b	d	d
38	e	d	b	d	2.99	a	3.70	b	d	d
9	k	d	a	d	d	1.28	b	1.69	d	d
42	x	d	b	d	2.32	1.11	a	b	d	d
49	f	d	b	d	3.20	1.37	5.07	b	d	d
46	t	d	b	d	2.54	1.46	3.98	b	d	2.01
No. of Events		10	8	8	14	20	13	2	6	8
Average		1.04	1.32	1.68	2.97	1.12	3.68	2.04	2.02	1.93

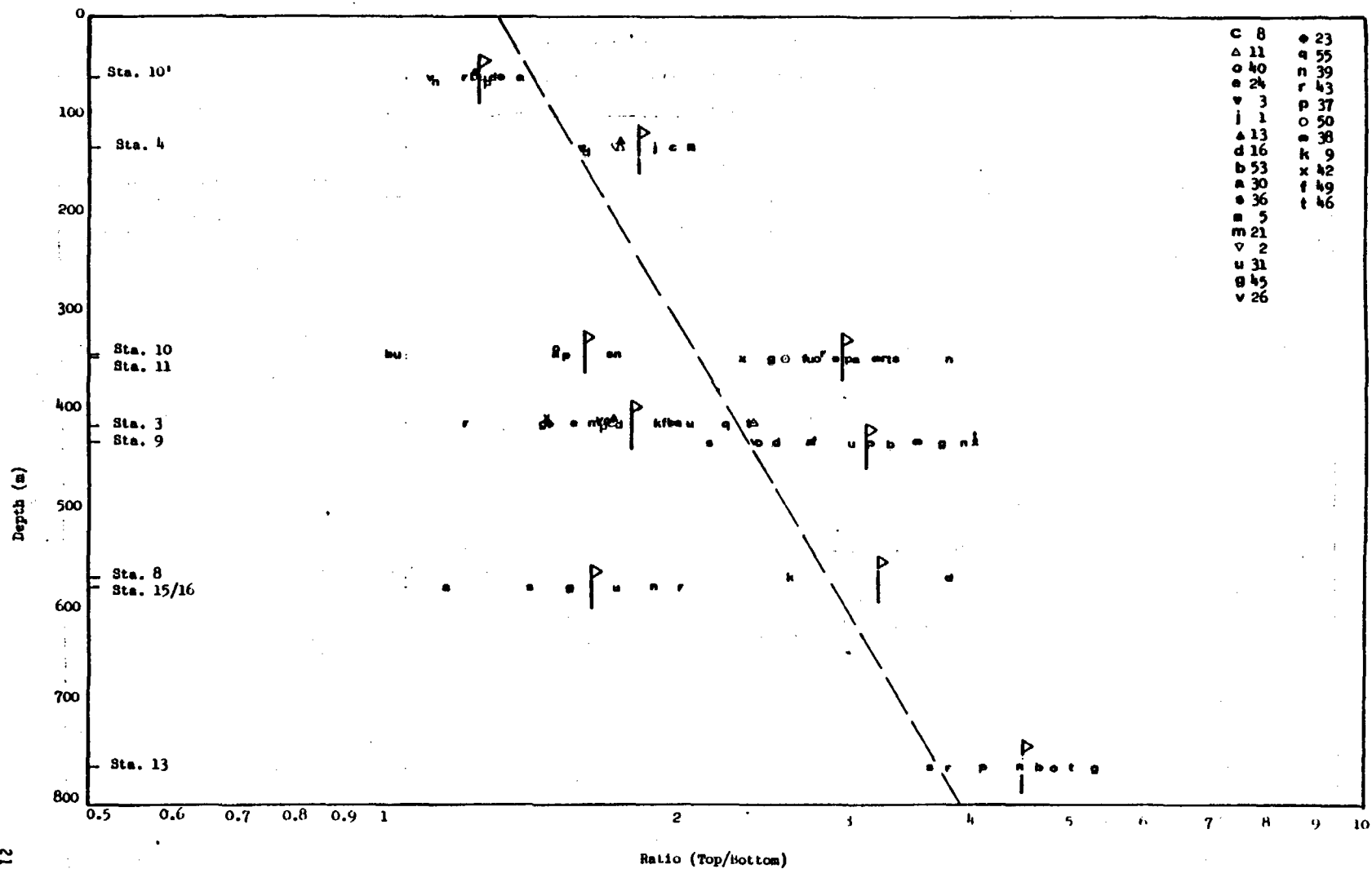
a - data inadequate

b - station not installed at time of event

d - station not operated for this event

$$R = 1.27e^{0.000898d} \quad \sigma_R = \pm 1.55$$

$$r^2 = 0.131 \quad CL_{R90} = \pm 2.41 \text{ to } 2.46$$



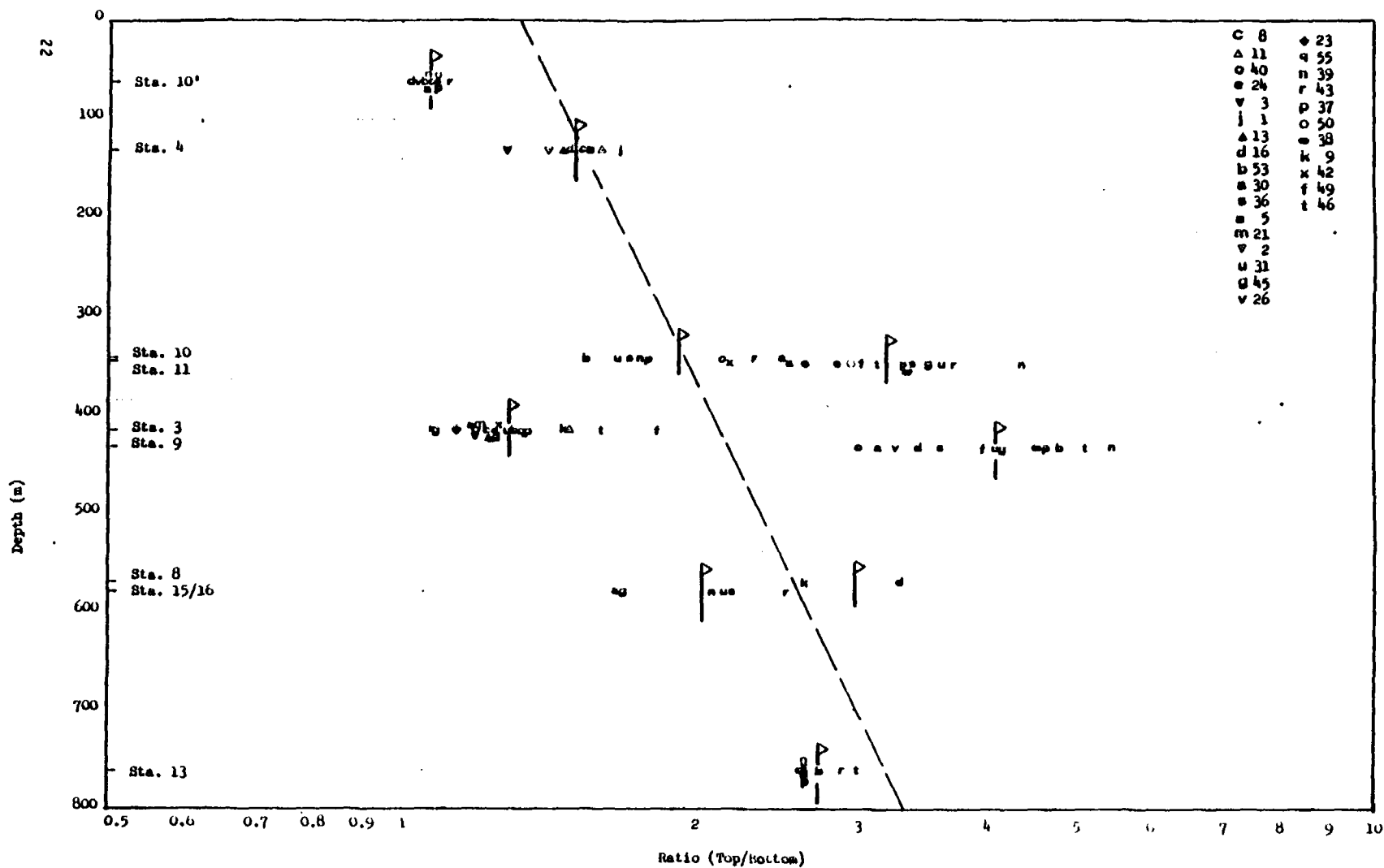


Figure 3-2 Ratios (Top/Bottom) for
Peak Vector Velocity (15 Highest
Peaks) Plotted Versus Station Depth

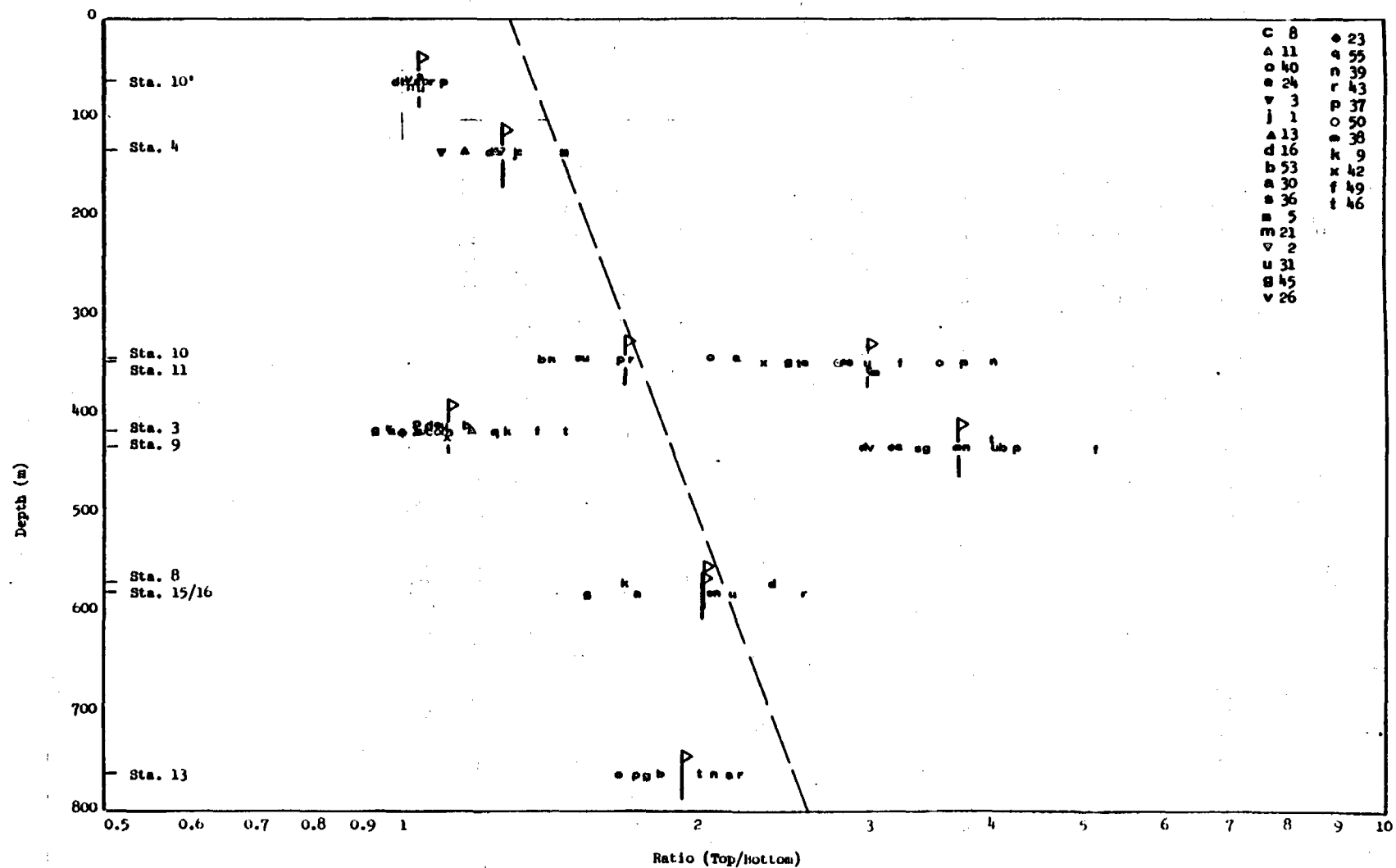


Figure 3-3 Ratios (Top/Bottom) for
Peak Vector Displacement (15 Highest
Peaks) Plotted Versus Station Depth

For the 15 highest peaks:

Acceleration	$R = 1.30e^{0.00137d}$	$\sigma_R = \pm 1.33$
	$r^2 = 0.446$	$CL_{R90} = \pm 1.78 \text{ to } 1.81$
Velocity	$R = 1.30e^{0.00115d}$	$\sigma_R = \pm 1.50$
	$r^2 = 0.221$	$CL_{R90} = \pm 2.28 \text{ to } 2.33$
Displacement	$R = 1.27e^{0.000898d}$	$\sigma_R = \pm 1.55$
	$r^2 = 0.131$	$CL_{R90} = \pm 2.41 \text{ to } 2.46$

The exponents indicate that acceleration changes most with depth and displacement least. The coefficients of determination reflect the differences due to station geology. Since average values for all events were used in computing the equations, the scatter from one event to the other is not included except indirectly.

Comparison of the error estimates with those in Chapter 2 for single peaks shows that for there is a very slight improvement for acceleration and essentially no change for velocity and displacement. For the coefficient of determination, r^2 , there was considerable improvement for all three. For the 90 percent confidence limits there was a slight degradation of the error estimate in going from 1 to 15 peaks.

CHAPTER 4
EFFECTS OF DEPTH ON GROUND MOTION
PSRV RATIOS

A portion of the text of Reference 1 is repeated here for reader convenience.

The Psuedo-Relative Response Spectra (PSRV) plots used in this work result from a calculation at about 75 frequencies with equal log frequency intervals over three decades. Ordinarily the plots are made separately for each of the three components. By taking the square root of the sum of the squares of the velocity value at each of the frequencies, a composite PSRV has been constructed which will be referred to as a "vector" PSRV.

Just as for single-component PSRV's, the "vector" PSRV can be constructed for a specified damping. Here, 5, 10, 20, 35, and 50 percent of critical damping were chosen arbitrarily to illustrate the effect of changing the damping coefficient. To examine the effect of depth, the velocity value of the top "vector" PSRV was divided by the corresponding value of the bottom at each of the 75 frequencies permitting a plot of the ratio as a function of frequency. Also, the average value of the ratio over the 75 points was calculated and printed at the lower left corner of the plot. An example is shown in Figure 4-1. In what follows, only the 5 percent damping is treated, although the data exist in file for exploring corresponding results with the other damping values.

The "vector" PSRV ratio between top and bottom is especially useful in showing how different frequencies are decreased at depth relative to those at the surface. In the following discussion of the ratios the plots in

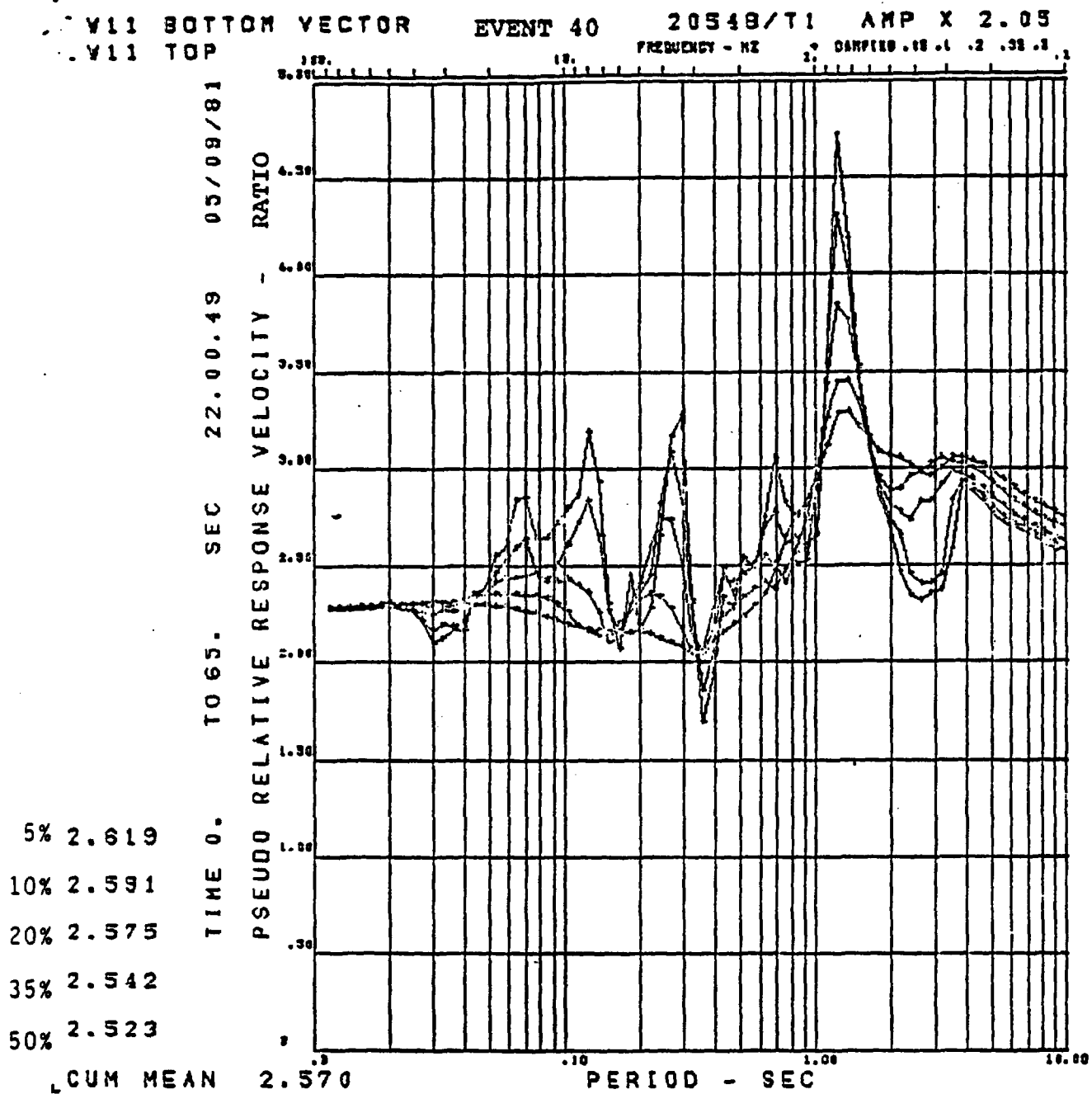


Figure 4-1 PSRV "Vector" Ratios for Five Damping Percentages

Appendix B* have been arranged in the order of the shallowest to the deepest hole, and for a given hole in the order of decreasing yield. The left portion of the plotted ratio should become asymptotic (barring the first two or three data points) at about the ratio of the peak vector accelerations. Actually, most fall between that value (listed in Table 2-1) and the ratio of the average of 15 highest peaks (Table 3-1). The right portion becomes asymptotic between the ratio of the peak displacement for single peaks (Table 2-3) and the ratio of the average of the 15 highest displacement peaks (Table 3-3). The following discussion will point out similarities and differences.

Station W-10 Prime

This was the shallowest station. The ratios (Figures B-1 through B-5) are small for all events, as would be expected from the small vertical separation. The most common feature is a peak in the ratio at between 35 and 45 Hz. Only Event 26 (Figure B-4a) has a higher peak at 80 Hz. Event 36 (Figure B-3a) has two equal peaks at 45 and 70 Hz., and Event 43 (Figure B-5a) has no single well-defined peak. Events 16 and 26 (Figures B-1b and B-4a) both show dips at 18 and 15 Hz., respectively. These are an artifact resulting from use of the times 1 output because of failure to get a useable record on the amplified channel. One horizontal component was involved for Event 16 and all three components for Event 26. Times 1 output signals have electrical noise at these frequencies.

*The plots of Appendix B were produced at different times and with different plotting instructions. As a result, scales of the vertical axis are not the same for all plots. This difference in scales should be kept in mind when comparing the figures in Appendix B.

Station W-4

The PSRV ratios for this station are shown in Figures B-6 through B-9. All signatures show peaks at 1.6 to 2.1 Hz. For Event 13 (Figure B-8a), the large peak at 16 Hz was occasioned by an excess of that frequency in the top AR signal and a deficiency in the bottom AR signal. The peak at about 6 Hz. for Event 8 (Figure B-6a) is a result of an excess of that frequency in the vertical signal at the top. For Event 2 (Figure B-9b) the peak at 16 Hz. results from a frequency component which occurs at the top in all three components, but not at the bottom. The most pertinent observation on the "vector" PSRV ratios is that they are so different considering that both are in alluvium and the vertical separation is only 130 m.

Station W-10

Figures B-10 through B-13 show the ratios for this station. It was noted² that the bottom canister was installed in a cased hole, and that at the location of the canister lack of grout or other cause allowed the casing to ring when excited by ground motion. The ringing affects both horizontal components and not the vertical. Ringing was observed in the 3 to 5 Hz range. In Figures B-10 through B-13 this shows up as a low value when the top signal is divided by the bottom which has the ringing. Each of the figures shows a low peak at 3 to 3.5 Hz. Four have an additional low at 6 Hz. The most consistent feature for all stations is the pronounced peak between 1 and 2 Hz. This is caused by the surface wave introducing strong pulses in this frequency range at the top, whereas these same pulses are significantly reduced at the bottom.

Station W-11

PSRV ratios for Station W-11 are shown in Figures B-14 through B-20. The most striking feature of the ratio profiles is the large high which peaks between 0.8 and 1.25 Hz. Again, these are frequencies characteristic of the surface wave. In the case of Event 36 (Figure B-15b) where the station was only 5.35 km almost due south of the event, the radial component at the surface had a large peak at these frequencies. At the bottom the radial component was depleted in this frequency range relative to both higher and lower frequencies. The result is the large peak shown in Figure B-15b. If the reader will refer to Figures E-19 through E-24 the manifestation of this effect on the wave train will be more apparent. Event 46 (Figure B-20b) has a smaller peak at 0.8 to 1.25 Hz. than the other events, and another of comparable amplitude at about 2.5 Hz. This is evident on PSRV's for all three components at both top and bottom, but it is much more pronounced at the surface. The peak in the ratio for Event 30 (Figure B-15a) in the 5 to 20 Hz. region results from high frequency content of the surface signal, particularly for the vertical component. (See Figure E-13.)

Station W-3

Figures B-21 through B-30 show the PSRV ratios for Station W-3. The ratio profile for Event 9 (Figure B-29a) has two peaks, one at 7 Hz., and one at about 3.1 Hz. Profiles for all the other events fall into three categories. The first has a single dominant peak at about 3 Hz. Events 8 (Figure B-21a) and 21 (Figure B-25a) are examples. The second has a dominant peak around 3 Hz. and a second lower peak between 10 and 25 Hz. Examples are Events 40, 24, 23, 43, 42, 49, and 46 (Figures B-22a, B-22b, B-27a, B-28a,

B-29b, B-30a, and B-30b). The third has the dominant peak in the 10 to 40 Hz. range and a lesser peak in the 2.5 to 4.0 Hz. range (Figures B-21b, B-23a, B-23b, B-24a, B-24b, B-25b, B-26a, B-26b, B-27b, B-28b and B-29a). All of the above have ratios which are small compared with peak values at the other stations, attesting to the fact that the top and bottom in the granite pluton move more or less as a unit. The profiles indicate the frequencies at which there are differences.

Station W-9

PSRV ratios for Station 9 are shown in Figures B-31 through B-37. All events have the dominant peak in the frequency range between 0.9 and 1.6 Hz. This is indicative of the frequency with which the top of Rainier Mesa resonates. Several of the events show a lesser peak at between 6 and 10 Hz. Reference to the PSRV's for the individual components of motion show that this was a contribution of the vertical component in the case of Events 16, 53, 30, 45, and 27; of the vertical and tangential in the case of Event 31; and of all three components in the case of Event 26. One outstanding feature of this set of ratio plots is the relatively large values of the left and right asymptotes, signifying the relatively large differences between top and bottom for acceleration (left) and displacement (right). This is in contrast to Station 3 where the displacement (right) asymptote was small. Event 42 is an exception because of a poor quality displacement record from the bottom gages.

Station W-8

The PSRV ratios for this station are shown in Figure B-38. Relatively few measurements were made at this station before it was discontinued when the Eleana Formation was dropped from consideration for a repository. Both of

the two ratios obtained show peaks in the 1 to 1.5 Hz. range. Left and right asymptotes are similar, and the dip at 25 Hz. in the case of Event 9 is the contribution of high frequencies observed by all three components at the bottom.

Stations W-15 and W-16

It is repeated that these two stations do not constitute a true pair, since they have a 2300 m horizontal separation as well as 580 m vertically. The plots of PSRV ratios are shown in Figures B-39 through B-41. All six events show peaks between 0.5 and 1 Hz. For Events 30, 31, 39, 43, and 45 the peaks of the vertical component PSRV's are about the same for W-15 and W-16, while the radial and tangential component peaks are larger at W-15. This is interpreted as a surface effect. Events 39, 43, and 45 have inverted V-shaped peaks at station W-15 and M-shaped peaks at W-16 which accounts for the sharp peaks in the ratios. Events 30, 31, 36, and 45 have ratios at or below 1 in the 10 to 20 Hz. region. This is because the PSRV's for W-16 are rich in those frequencies. This richness is in all three components.

Station W-13

PSRV ratios for Station W-13 are shown in Figures B-42 through B-45. They are characterized by single or multiple peaks in the 2.5 to 8 Hz. region, and in all but three cases by a dip in the 12 to 50 Hz. range. The latter is caused by these frequencies being greater in all three components at the top than at the bottom.

The mean value for the 5 percent damping PSRV ratios are printed at the lower left in the figures in Appendix B. These values can be used as an

index of the effects of depth. The ratios are listed in Table 4-1, and they are plotted as a function of depth in Figure 4-2. The trend with depth is similar to that observed in Chapters 2 and 3 for single and multiple peaks. The strong effect of medium at the station location is preserved and the scatter of the data at each depth is not appreciably different from that observed in Figures 3-1, 3-2, and 3-3.

The ELS fit to the data gives for the PSRV ratio:

$$R = 1.34e^{0.00120d} \quad \sigma_R = \pm 1.36 \quad r^2 = 0.350 \quad CL_{R90} = \pm 1.86 \text{ to } 1.89$$

TABLE 4-1
 Ratios (Top/Bottom) for
 "Vector" PSRV Mean Values

Event Number	Plot Symbol	STATION NUMBER								
		TOP (61m)	4 (130.5m)	10 (342.6m)	11 (345.6m)	3 (416.7m)	9 (431.6m)	8 (570m)	15/16 (580m)	13 (762m)
8	c	b	1.67	b	b	1.51	b	b	b	b
11	Δ	b	1.75	b	b	1.80	a	a	b	b
40	o	1.36	b	1.53	2.62	1.48	2.69	b	a	4.22
24	e	a	b	a	2.99	1.44	a	b	b	b
3	v	b	1.40	b	b	b	b	b	b	b
1	j	b	1.76	b	b	b	b	b	b	b
13	Δ	b	1.67	b	b	1.58	a	b	b	b
16	d	1.29	1.59	b	a	1.50	3.00	3.29	b	b
53	b	1.28	b	1.46	a	1.74	3.75	b	a	4.04
30	a	1.41	b	2.13	2.86	1.56	2.89	b	1.39	b
36	s	1.23	b	1.83	3.40	a	2.49	b	1.30	3.53
5	m	b	1.90	b	b	b	b	b	b	b
21	Δ	a	b	a	a	1.29	a	a	b	b
2	v	b	1.63	b	b	b	b	b	b	b
31	u	1.25	b	1.61	3.10	1.66	3.21	b	1.70	b
45	g	a	b	a	2.86	1.34	3.18	b	1.58	3.98
26	v	1.15	b	a	a	1.50	2.55	b	b	b
23	♦	a	b	a	a	1.63	a	b	b	b
55	q	a	b	a	a	1.97	a	b	a	a
39	n	1.26	b	1.71	3.20	a	3.67	b	1.77	4.17
43	r	1.18	b	2.40	3.13	1.12	a	b	2.16	3.39
37	p	1.21	b	1.79	3.34	1.42	3.62	b	a	3.15
50	o	d	b	d	3.33	a	a	b	d	d
38	•	d	b	d	3.08	a	3.36	b	d	d
9	k	d	a	d	d	1.71	b	2.18	d	d
42	x	d	b	d	2.43	1.38	a	b	d	d
49	f	d	b	d	3.00	1.71	3.68	b	d	d
46	t	d	b	d	3.09	2.59	3.91	b	d	4.18
No. of Events		10	8	8	14	20	13	7	6	8
Average		1.26	1.68	1.81	3.03	1.57	3.23	2.74	1.65	3.83

a - data inadequate

b - station not installed at time of event

d - station not operated for this event

$$R = 1.36e^{0.00117d} \quad \sigma_R = \pm 1.36$$

$$r^2 = 0.350 \quad CL_{R90} = \pm 1.86 \text{ to } 1.89$$

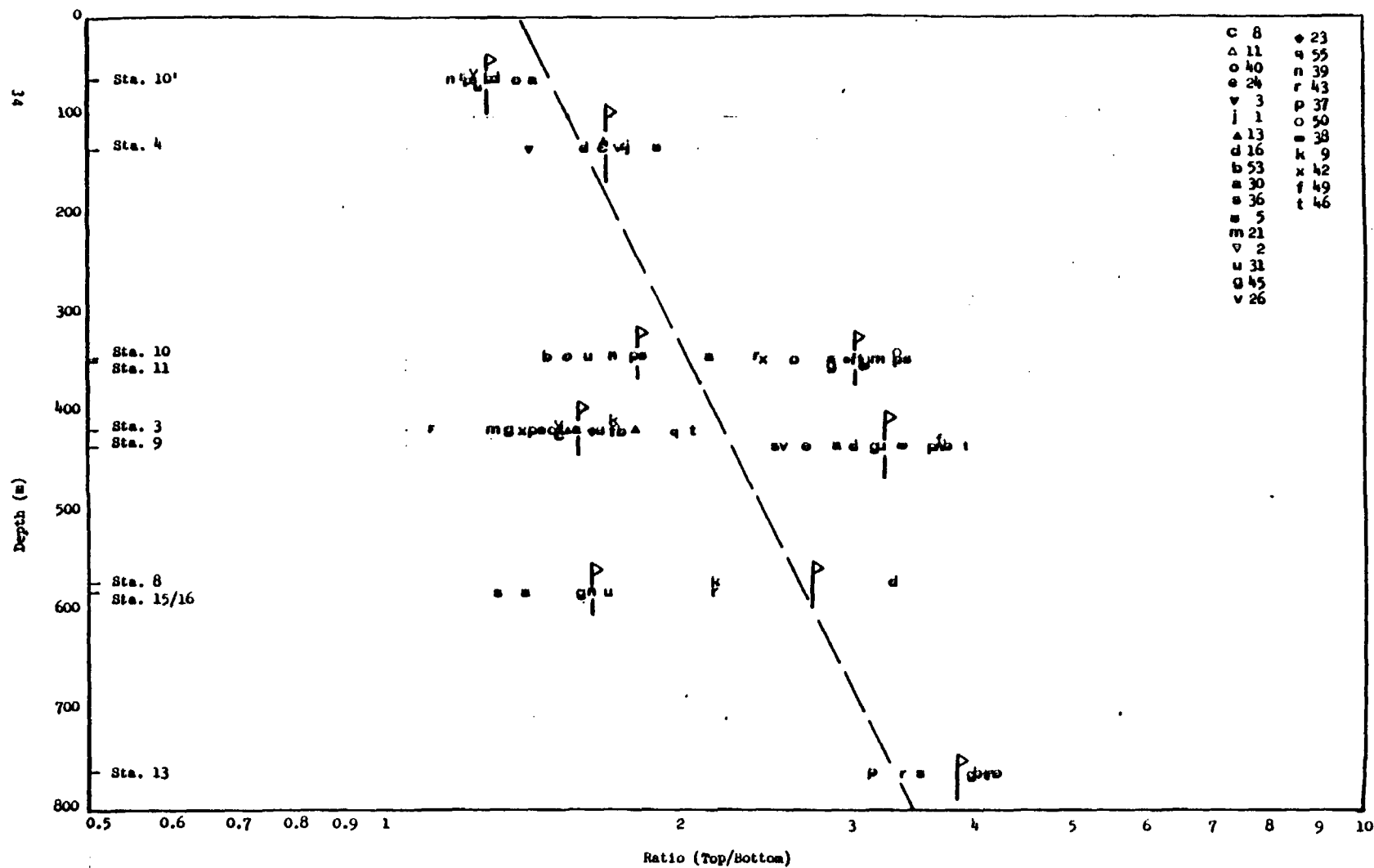


Figure 4-2 Ratios (Top/Bottom) for
"Vector" PSRV Mean Values Plotted
Versus Station Depth

CHAPTER 5

GROUND MOTION WAVEFORMS

The attempts in the preceding chapters to provide a quantitative measure of the effects of depth do not reveal some of the qualitative aspects of ground motion. These can best be observed by comparing acceleration, velocity, and displacement at the surface and at each depth. In Appendices C through J these waveforms for vertical, radial, and tangential motion are presented for comparison. The appendices are arranged in order of depth, Appendix C treating the shallowest depth and Appendix J the deepest. An exception is Station W-10 which is included in Appendix C because of its proximity to the shallowest hole. Within each appendix the data are presented in order of decreasing yield. For each event the amplitude scales are the same for top and bottom to facilitate comparisons.

There are some common features to be pointed out before going into more detailed discussion. First motion of the vertical component is upward and first motion of the radial component is outward from the source. Direction of first tangential motion can be either clockwise or counterclockwise and is unpredictable with no prior experience for a shot in a given location. It can become predictable for an event sufficiently near an earlier event for which direction of first motion is known. First motion at the bottom is usually a few milliseconds earlier than that at the top. And, first motion of the radial and tangential motion is generally a few milliseconds behind that of the vertical component. Except for Station W-11, which is in Yucca Flat and relatively close to most of the events, the maximum acceleration is found in the body wave

and the maximum displacement in the surface wave. The maximum amplitude of the vertical component of the surface wave is attenuated relatively little with depth over the range of depths and wave lengths of concern here. At the ground surface the maximum amplitude of the radial component is about $2/3$ that of the vertical component. It becomes smaller relative to the vertical component as depth increases. These observations are based on a theoretical treatment by Pilant,³ and it can be seen in these data that there are some apparent exceptions.

In the following discussion the stations will be treated in order of increasing depth of the bottom canister (except for W-10 bottom), and the events in order of decreasing yield. To facilitate visualizing the relative locations of the numbered events with respect to the stations, it is suggested that the reader have available Appendix A of Reference 1 while reading this chapter.

● Station W-10 (Appendix C)

It was noted earlier that casing ringing was involved at W-10 bottom in Well J-11. It occurs for both horizontal components, and is significant during the early portion of the acceleration records. The ringing is discernible on the velocity records, and is hardly noticeable on the displacement records. The frequency at which the ringing is maximum is between 3 and 3.5 Hz as noted in Chapter 4. Another feature common to all events is the relatively small difference between W-10 top and W-10' (the plots without the top or bottom notation). This small difference is seen in all three components of acceleration, velocity, and displacement.

Event 40 (Figures C-1 through C-9) Comparison of Figures C-1 and C-3 show that the vertical component of displacement has changed relatively little from top to bottom. A similar comparison of Figures C-4 with C-6 and C-7 with C-9 illustrates the significant reduction in the horizontal component displacements.

Event 16 (Figures C-10 through C-15) This was the first event on which measurements were made at W-10 top and W-10'. The bottom canister had not been installed. For W-10' no data was obtained from the high sensitivity channels, and the use of the direct output channels (no amplification) results in more than the usual amount of system noise.

Event 53 (Figures C-16 through C-24) A close examination of the vertical, radial, and tangential displacements shows that the signals are in phase at all three levels. The ringing of the pipe is especially large on the tangential record (Figure C-24).

Event 30 (Figures C-25 through C-33) The similarity of the records at the three levels is an obvious feature of this set of records. An interesting aspect is seen in Figures C-28 and C-29, where there is a small high frequency in the former at 22 to 26 seconds which is not in the latter.

Event 36 (Figures C-34 through C-42) A comparison of the displacements in these nine figures shows that at all levels the tangential motion is greater than either the vertical or radial. The stations are at an azimuth of 203.6° from the event, compared with 209.9° for Event 30, where displacement amplitudes of the three components were similar.

Event 31 (Figures C-43 through C-51) While it is expected that the radial displacement amplitudes would be attenuated with depth more than the vertical, no trend can be predicted for the tangential component. Here, there is less attenuation for the tangential component. In addition, the tangential displacements are larger than those of the vertical or radial components, as was the case for Event 36. In this case the stations were at an azimuth of 204.7° from the event.

Event 26 (Figures C-52 through C-57) Data from the bottom canister was obscured after three seconds following signal arrival by a burst of RF noise. In this case the tangential displacement at the surface is only slightly larger than the radial, and at the 61-m level the tangential displacement is considerably larger. The vertical displacement is smaller than either radial or tangential at both levels. For this event, the stations were at an azimuth of 205° from the event.

Event 39 (Figures C-58 through C-66) Again the tangential displacements are much larger than vertical and radial, the latter two being essentially equal. The stations were at an azimuth of 207.22° from the event.

Event 37 (Figures C-76 through C-84) Vertical, radial, and tangential displacements are about the same at each level. The vertical displacement at the top (Figure C-76) has a low frequency background resulting from a VCO malfunction. By comparing these figures for motion generated by the smallest yield in this data set with the corresponding figures in Figures 1 through 9 for the largest yield, it can be seen that peak displacements are roughly a factor of 10 smaller for the smaller yield.

In five of the ten events described above, Events 26, 31, 36, 39,

and 43, the tangential displacement was markedly larger than the radial and vertical displacements. These five events were all located in Area 2 at azimuths between 203.6° and 207.2° , and at distances between 38.30 and 40.85 km. The other five events without enhanced tangential displacements were located in Areas 4 and 7, at azimuths between 209.7 and 212.7 and distances between 42.07 and 44.92 km. This is one manifestation of how small differences in source locations can affect the direction of largest motion. Of the five events in Areas 4 and 7, four were in tuff and one (Event 37) in alluvium 2 m above the alluvium/tuff interface. Four were below the water table and Event 37 was 18 m above. Of the five events in Area 2, two (Events 26 and 31) were in tuff and the others in alluvium; only Event 26 was below the water table. Thus there is no indication that the medium in the immediate vicinity of the detonation causes differences in energy coupling which contributes to the strong tangential displacements. Since the larger amplitudes in the displacements are from the surface wave, we can only speculate that there are differences in geology in the region of surface wave formation which contribute the large tangential displacements from events in Area 2 and which do not exist in the region of Areas 4 and 7.

● Station W-4 (Appendix D)

Since the bottom canister at this station is only 130.5 m deep, the differences in motion between top and bottom are relatively small.

Event 8 (Figures D-1 through D-6) The unamplified ($\times 1$) data are used here because the amplified data was limited by band edge. Accelerations are reduced by depth more than displacements.

Event 11 (Figures D-7 through D-12) There are no special or unusual features in these records.

Event 3 (Figures D-13 through D-18) Radial velocity in the body wave portion at the beginning of the record is considerably reduced by depth.

Event 1 (Figures D-19 through D-24) These records were from the first surface and downhole canisters installed as a part of this program, and are particularly good records.

Event 13 (Figures D-25 through D-30) This event was separated from Event 1 by 409 m radially and 32 m vertically. Both were in tuff and below the water table. A comparison with the six foregoing figures shows that the waveforms, especially for displacement, are very similar, except that the bottom tangential is smaller than that of Event 1. Comparison of Figure D-23 with D-29, the top tangential component, shows enough similarity to conclude that the tangential motion is determined by geology, even though it is not predictable for the first event in a particular location.

Event 16 (Figures D-31 through D-36) There was a 964 m radial and 61 m vertical separation between this event and Event 3. Both were in tuff and below the water table. Comparing these figures with Figures D-13 through D-18 shows that the waveforms are similar, but not as alike as for Events 1 and 13. The signals are in phase. Amplitudes for Event 16 are larger than for Event 3 even though the yield of the latter was larger. Again, similarity of the tangential components indicates the displacements are determined by geology.

Event 5 (Figures D-37 through D-42) Although this event was in Area 2 along with Events 1, 11, and 13, the radial distance separating it from the others was between 2.4 and 3.1 km. Comparison with the figures for those events shows that the waveforms from Event 5 have little in common with waveforms from the others. A most notable difference is the large tangential displacement in the interval of 40 to 50 seconds, when in the records of the other events the motion was almost damped out. This was not one of the events which provided large tangential displacements at Station 10, but it was near Event 31 which did.

Event 2 (Figures D-43 and D-48) This event and Event 8 were detonated in Area 7, but about 3.19 km apart. Comparison of these figures with Figures D-1 through D-6 shows little similarity.

● Station W-11 (Appendix E)

This station is 342.6 m deep, and is the closest to weapons tests in Yucca Flat. As a result, p waves dominate the signals and surface waves are poorly developed. Also, signals are of shorter duration than at the more distant stations.

Event 40 (Figures E-1 through E-6) The top canister was 3872 m from the detonation and the bottom canister was at 3828 m. The bottom canister was about 320 m above the detonation point. As a result, vertical motion at both top and bottom is quite strong. It shows much less decrease with depth than does either the radial or tangential.

Event 24 (Figures E-7 through E-12) The top canister was 4278 m from

the detonation point and the bottom one at 4238 m. The bottom canister was 324 m above the detonation. There was an 11° azimuthal difference from this event to the station relative to the preceding event. Thus a similarity in signals would be expected, since both were fired in tuff below the water table, and yields were about the same. In fact, the signals are very much alike, the principal difference being that amplitudes of the tangential component of Event 24 were slightly larger than those of Event 40.

Event 30 (Figures E-13 through E-18) For this event, the top canister was 3793 m and the bottom one 3710 m from the detonation point. The latter was about 250 m above the explosion. The azimuthal separation from the other events was greater. There were 24.7° separating this event from Event 40 and 36.7° separating it from Event 24. This event was also in tuff below the water table. Yield was smaller than for the two preceding events. Vertical and radial motion at top and bottom were similar in waveform, but the amplitudes were smaller. Tangential motion at both top and bottom had amplitudes comparable to those of Events 24 and 40, but phasing was different, especially at the top where Event 30 appeared to have higher frequencies in the displacement.

Event 36 (Figures E-19 through E-24) This event was 5367 m (average for top and bottom) away from the station, and on quite a different azimuth. All signals "ring down" over a longer period of time than for the closer events. Only the vertical component at the bottom shows a similarity of waveform compared with the preceding events, and the amplitude is considerably less.

Event 31 (Figures E-25 through E-30) This event was even farther away than the foregoing ones, and its azimuth was 11° from that of Event 36. Waveforms are different from those discussed above. The vertical component at the bottom shows a decrease relative to the top, greater than the decrease noted for the preceding events.

Event 45 (Figures E-31 through E-36) This event was 394 m farther away than Event 30, and there is an azimuthal separation of only 6.3° . Even so, the waveforms of the vertical and radial signals are quite different from those of Event 30. Tangential displacements at the top from the two events have a similar dominant frequency, and in both cases tangential motion at the bottom is much less than that at the top. This decrease with depth was greater for both events than for the vertical and radial components.

Event 39 (Figures E-37 through E-42) Event 39 was 26 m closer than Event 40, and there was a 61° azimuthal separation. There is some similarity in the first cycle of the vertical records of the two events and in the first two cycles of the radial records. Tangential motion at the top is in reasonable agreement for the two events. Amplitudes for Event 39 are much smaller than those for Event 40. Event 39 was 115 m above the bottom canister compared with 324 m below for Event 40. This difference as well as the relatively large azimuthal separation may have contributed to some difference in waveforms.

Event 43 (Figures E-43 through E-48) The top tangential record (Figure E-47) came from the unamplified channel. This event was 465 m closer

than Event 31, and the azimuthal separation was 7.5° . Comparison with the waveforms for Event 31 shows a similarity in the p-wave portion of the record except for the top tangential.

Event 37 (Figures E-49 through E-54) This event is the closest to the station of all events in the data set. The top canister is 2586 m from the detonation point and the bottom canister 2546 m. The elevation of the detonation point is 126 m above the bottom canister. The tangential motion at the bottom is very small compared with that at the top. Event 37 is 1.64 km closer to the station than Event 24 and the two are separated azimuthally by 5.9° . Records from all components, top and bottom, are dissimilar for the two events.

Event 50 (Figures E-55 through E-60) Event 50 was 248 m farther than Event 36, and the azimuthal separation was only 3.1° . Waveforms for the two events are unlike. Those from Event 50 contain quite high frequencies in the p-wave portion of the signal. The bottom vertical displacement is not valid because of a malfunction of the VCO for that channel.

Event 38 (Figures E-61 through E-66) Event 38 was 11.8 km from the station on an azimuth quite different from the foregoing events. As a result, the surface wave is more thoroughly developed and there is a longer time before the motion "rings down."

Event 42 (Figures E-67 through E-72) This event is separated azimuthally from Event 50 by 4.1° and it is 2.09 km closer than that event. There is no similarity in the records of the two events. The singularly large displacement pulse that occurs between 12 and 14 seconds on the records

of Event 50 is completely missing on the records of Event 42.

Event 49 (Figures E-73 through E-78) This event and Events 38 and 46 are the only ones in the Station W-11 data set which were fired in Area 3. Thus they would not be expected to have waveforms similar to events fired in other areas. Event 49 is at about half the distance from the station as are Events 38 and 46, and the waveforms of Event 49 are not like those of the other two events.

Event 46 (Figures E-79 through E-84) Event 46 is 685 m farther than Event 38, and the two events have an azimuthal separation of only 3.8° . In spite of these small differences in the locations, there is essentially no similarity in the waveforms produced. Both events were in tuff and above the water table. Although the yields were not appreciably different, the peak displacements for Event 46 were about half those of Event 38.

● Station W-3 (Appendix F)

The bottom canister at this station is 416.7 m deep. Both top and bottom are in granite of the Climax Stock. Experience with the Pahute Mesa data indicates the granite moves pretty much monolithically. The information in Chapters 2, 3, and 4 substantiates that the difference in top and bottom vector motion is much less than would be expected for the depth.

Event 8 (Figures F-1 through F-6) The waveforms from this event have dominant p-wave accelerations and dominant surface wave displacements. Vertical and tangential displacement at top and bottom are virtually the same. Radial displacement at the bottom is slightly smaller than at the top, but not as much reduced as for the waveforms shown in Appendix E for Station W-11 where the shots were closer.

Event 11 (Figures F-7 through F-12) The comments made for Event 8 apply, except that the tangential displacement at the bottom is smaller than at the top.

Event 40 (Figures F-13 through F-18) For this event the top and bottom vertical and radial displacements are about equal. Peak displacement amplitudes of the radial at the bottom are about equal to those at the top, but maxima occur at 4 to 6 seconds at the bottom and at 14 to 16 seconds at the top.

Event 24 (Figures F-19 through F-24) The comments for Event 8 above apply to Event 24. This event was about 900 m farther away from the station than Event 40, and on essentially the same azimuth. They were at the same depth, were in tuff below the water table, and had comparable yields. Making allowance for the longer travel time for Event 24 in comparing the records, one finds that the top and bottom vertical displacements are virtually the same for both events. There is less similarity in the case of the radial and tangential displacements.

Event 13 (Figures F-25 through F-30) For this event the maximum radial and tangential displacements are in the p-wave portion of the wave train.

Event 16 (Figures F-31 through F-36) Event 16 was on essentially the same azimuth as Events 8, 40, and 24, but it was from 1.5 to 3.3 km closer. Comparison with Figures F-13 through F-18 for Event 40, which was closest to Event 13, shows some similarity in the vertical displacements but very little in the radial and tangential. There is as much agreement with Event 24, but less for Event 8.

Event 53 (Figures F-37 through F-42) This event was also on about the same azimuth as Events 8, 40, 24, and 16, and 150 m farther away than Event 40. Vertical displacements are in good agreement with those of Event 40, especially at the bottom. Radial and tangential displacements for the two events are in phase, but the amplitudes are considerably greater for Event 40.

Event 30 (Figures F-43 through F-48) Event 30 is another on about the same azimuth as the four referred to above. It was 57 m closer than Event 16, and the azimuthal separation was 1.4° . Vertical displacements for the two events are very much in agreement. Vertical accelerations at the beginning of the surface signal from Event 30 are much greater than those of Event 16. Agreement is not quite as good for the radial tangential components. The top tangential signal from Event 30 is quite different in the p-wave portion from that of Event 16.

Event 21 (Figures F-49 through F-54) This event was on exactly the same azimuth as Event 53 and 915 m farther away. It was 167 m farther than Event 24, and separated azimuthally from that event by 2.4° . Agreement between Events 21 and 53 is good for the vertical displacements and the top tangential displacements and only fair for the radial. Agreement between Events 21 and 24 is especially good for vertical and radial displacements, and moderately good for the tangential. Thus we conclude that at least for these three events a separation in distance leads to more dissimilarity than a small azimuthal difference.

Event 31 (Figures F-55 through F-60) This was the closest event to Station W-3. It has a very strong vertical acceleration at the beginning

of the record from the top canister. Vertical displacements at top and bottom are large relative to radial and tangential displacements.

Event 45 (Figures F-61 through F-66) This event has a distance separation of 275 m from Event 16, and an azimuthal separation of 7.6° . There is only moderate agreement between the vertical displacements of the two events, even less agreement between the radial displacements, and little agreement for the tangential displacements.

Event 26 (Figures F-67 through F-72) For this event, the radial displacements at both top and bottom were small relative to the vertical and tangential. The event was 147 m closer than Event 13, but there was an azimuthal separation of about 9.4° . The vertical displacements of the two events were in phase during the first few seconds, and out of phase thereafter. There was little similarity between the radial and tangential motions of the two events. Whereas an azimuthal separation of 2.4° between Events 21 and 24 led to similar waveforms, the separation here was too great for there to be agreement.

Event 23 (Figures F-73 through F-78) The system noise on the acceleration records for this event resulted from only a small portion of the band width being used. This was done intentionally to permit recording larger signals from another event when the time interval between the events did not permit changing gain settings at the station. The location of the event made it comparable only to the event below.

Event 55 (Figures F-79 through F-84) Events 23 and 55 were separated radially by 603 m and azimuthally by 4° . There is little similarity in the waveforms of the two events. One exception is the two positive and

one negative tangential displacement peaks in the vicinity of 10 seconds for both events.

Event 43 (Figures F-85 through F-90) Events 11 and 43 were separated by only 0.3° but by 1.6 km radially. The distance separation was so great that there is no similarity in the waveforms. The yield of Event 43 was smaller than that of Event 11, and that may have contributed to the difference in waveforms.

Event 37 (Figures F-91 through F-96) This event was separated from Event 40 by 5.7° and 473 m, and from Event 24 by 6° and 425 m. Both had yields larger than that of Event 37. There is no similarity in the records from Event 37 with those of either Event 40 or 24. One notable characteristic is the higher frequency of the displacement from Event 37, compared with Events 40 and 24. This is probably a result of the smaller yield.

Event 9 (Figures F-97 through F-102) Event 9 is one of three events detonated in Area 3, and would not be expected to produce motion comparable to that of any of the above events.

Event 42 (Figures F-103 through F-108) Event 42 and Event 26 had a radial separation of 116 m and an azimuthal separation of 2° . The vertical and radial displacements of the two events are in good agreement to about 7 seconds, after which they are out of phase because of the higher-frequency motion of the lower-yield Event 42. There is no agreement between the tangential displacements.

Event 49 (Figures F-109 through F-114) This is the second of the three events detonated in Area 3. Because it is relatively remote from the

other two, the motions would not be expected to be similar—and they are not.

Event 46 (Figures F-115 through F-120) This event is separated from Event 9 by 2.6° and 1.868 km. Although the azimuthal difference is small, the distance separation is sufficiently large that the signals from the two events are quite dissimilar.

● Station W-9 (Appendix G)

The depth to the bottom canister at this station is 431.6 m. Both the surface and bottom canisters are in tuff. It was noted in the previous chapters that because of topography the top of the Rainier Mesa experiences large horizontal motions relative to those at the bottom.

Event 40 (Figures G-1 through G-6) Peak-to-peak radial displacements at the surface are 2.7 times those at the bottom, and peak-to-peak tangential displacements are 5.0 times the bottom values. Figure 5-1 shows the ratio of top and bottom peak-to-peak displacements as a function of azimuth. Whereas the maximum difference is only a few degrees from the tangential, the minimum occurs at about the $170-350^\circ$ axis, almost midway between the radial and tangential motion. This latter is approximately along the long, or stiff, axis of Rainier Mesa. Corresponding ratios for the vertical displacements are between 1.25 and 1.30.

It is in order to compare these displacements with those measured at Station W-3 where there were no topographic effects. There maximum difference between top and bottom was about 1.5 and the minimum 0.5. Averaged over 360 degrees the displacement at top and bottom was equal. Orientation of maximum displacement is within 10 degrees for the two

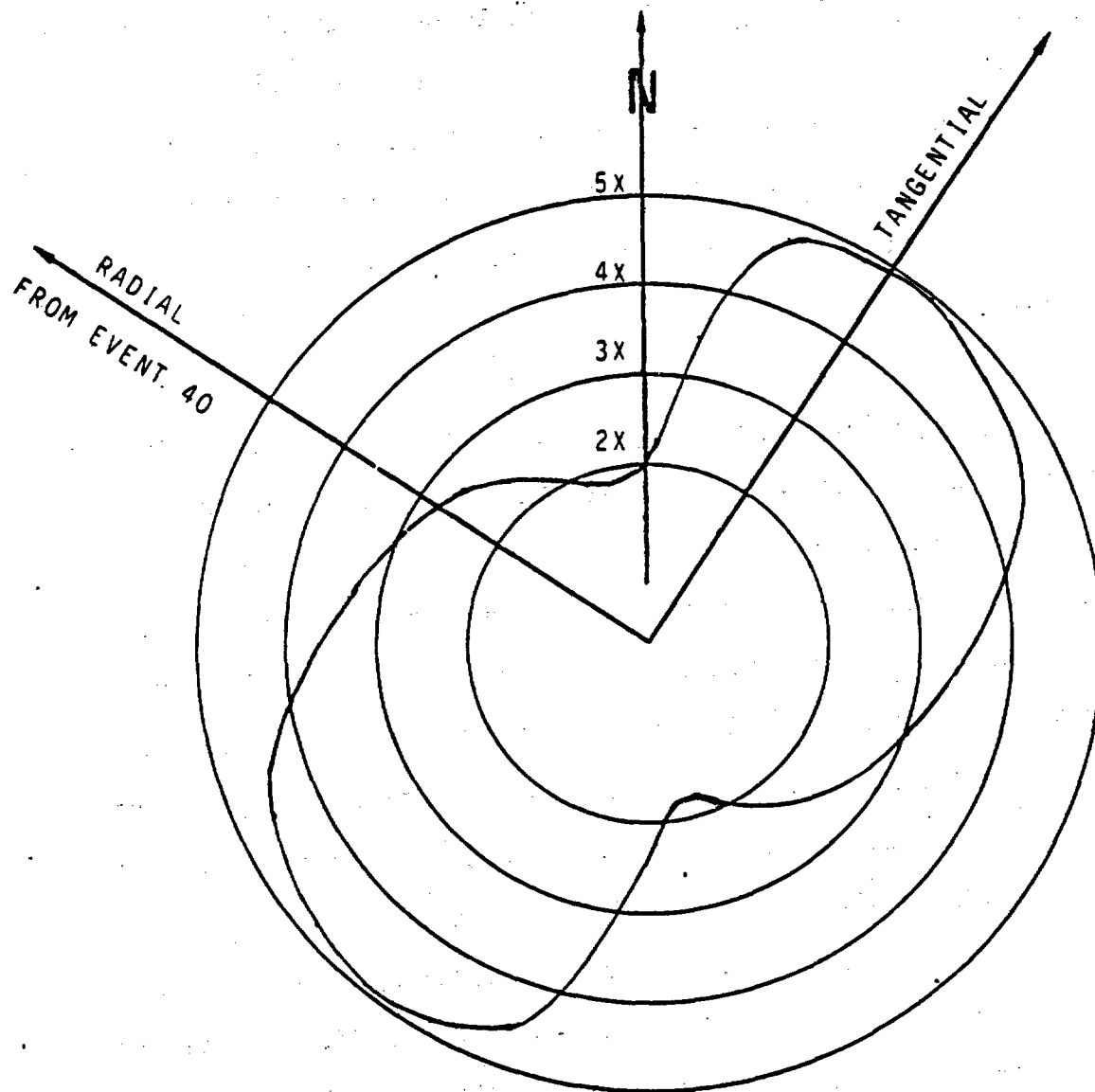


Figure 5-1. . Ratio of peak-to-peak displacement at top and bottom as a function of azimuth at Rainier Mesa

events and that of the minimum within 30 degrees.

Event 16 (Figures G-7 through G-12) Event 16 was about 671 m closer than Event 40, and there was an azimuthal separation of 4.8° . In spite of the latter, there is a surprising similarity in the signals which can be seen best in the top radial and tangential components of the two events. This can be observed by comparing Figures G-3 with G-9, and G-5 with G-11.

Event 53 (Figures G-13 through G-18) This event was about 650 m farther away than Event 40 and 1.32 km farther than Event 16. There was an azimuthal separation of 1° from Event 40 and of 3.8° from Event 16. There is considerable similarity in the radial motion of the surface station, and in the tangential motion as well, until about 15 seconds. After that time differences in both phase and amplitude are observed. Figure 5-2 shows the ratio of top and bottom peak-to-peak displacements as a function of azimuth for Event 53. Event 53 was chosen because it was close to Event 40. (See Figure 5-3.) There is a similarity between Figures 5-1 and 5-2, but the length to width ratio of the pattern in Figure 5-2 is less than that of Figure 5-1. Maximum difference between top and bottom is about 4.7 times and occurs along the $70-250^\circ$ axis, rotated clockwise from the tangential by about 37° . At the minimum the top displacement is about 2.7 times the bottom along the $150-330^\circ$ axis.

Event 30 (Figures G-19 through G-24) Event 30 is separated from Event 40 by a radial distance of 940 m, from Event 16 by 270 m, and from Event 53 by 1590 m. Azimuthal separations are 4.4° , 0.34° , and 3.4° ,

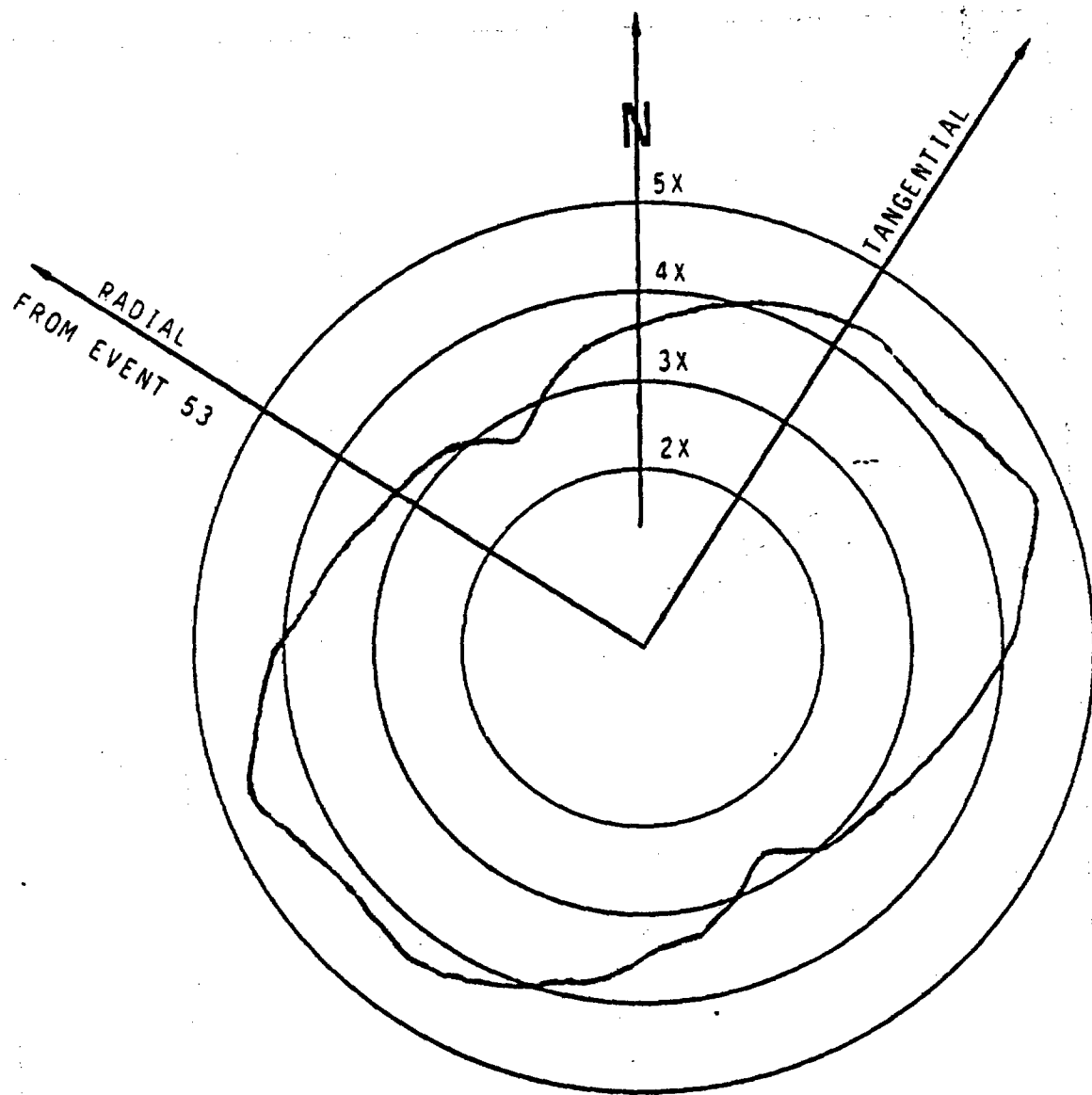


Figure 5-2. Ratio of top and bottom peak-to-peak displacements as a function of azimuth at Rainier Mesa

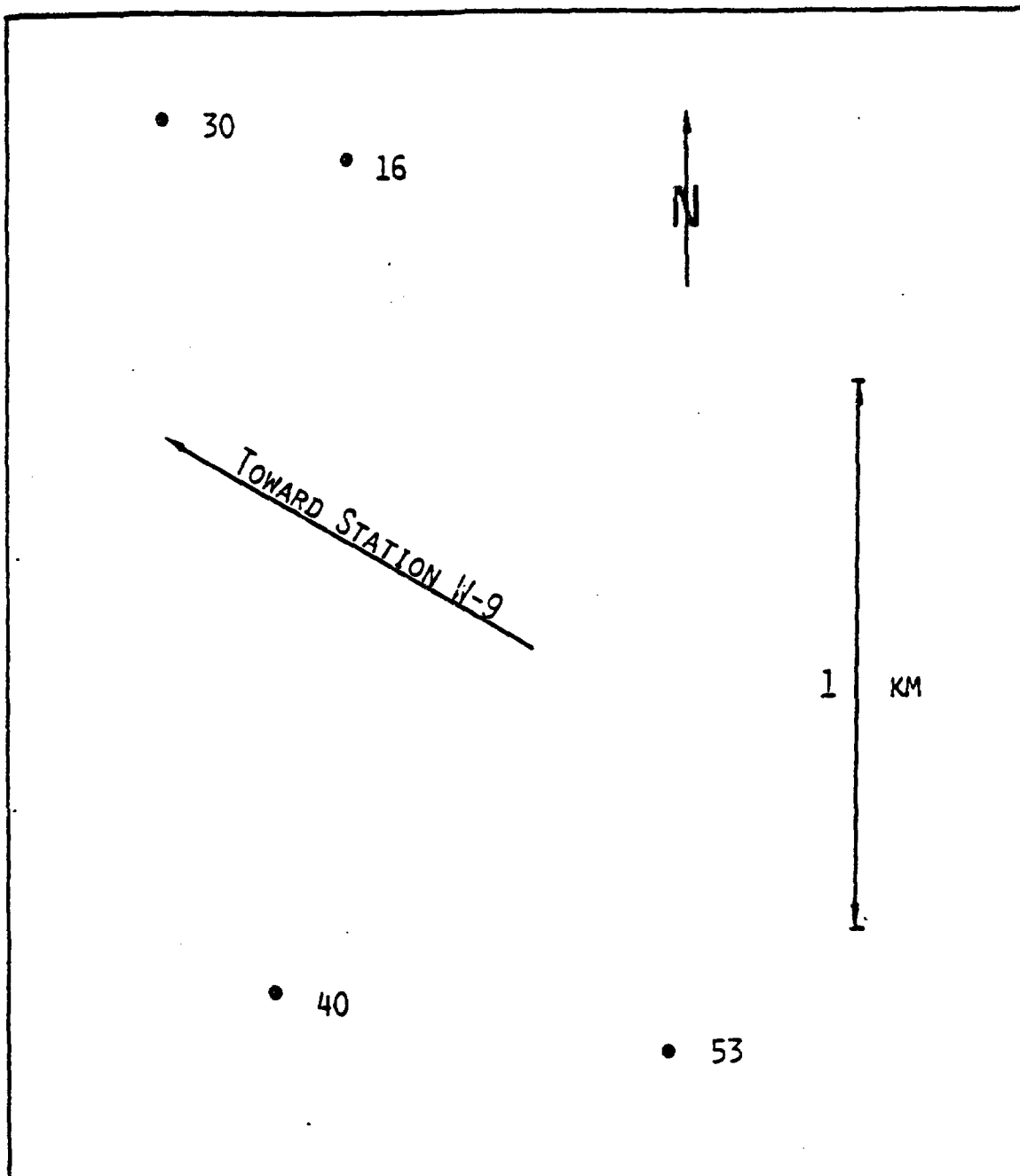


Figure 5-3. Relative locations of Events 16, 30, 40, and 53.

respectively. A comparison of top radial motion for the four events indicates the greatest similarity between Events 30 and 16 and the least between Events 30 and 53. This is as would be expected from the distance and azimuthal separations. The same similarity exists for the top tangential motion. The scales on the figures have been set to accommodate the maximum positive and negative excursion occurring in top vertical, radial, and tangential motion. Thus where there is a large difference between top and bottom, the scales for the bottom records result in small amplitudes in the figures. Figures G-1 and G-19 for Events 40 and 30 show that the vertical motion was comparable to the radial (Figures G-3 and G-21) and tangential (Figures G-5 and G-23). Figures G-7 and G-13 show that for Events 16 and 53 the vertical motion was small relative to the radial and tangential (Figures G-9, G-11, G-15, and G-17). This is unexpected, since Events 16 and 30 were close to each other as were Events 40 and 53, but the two pairs were separated by a greater distance. Figure 5-3 shows the relative locations of the four events. Event 30 was in alluvium above the water table; the others were in tuff and below the water table.

Event 36 (Figures G-25 through G-30) This event was the closest to Station W-9. It is separated too far in both azimuth and distance to be comparable with any other event.

Event 31 (Figures G-31 through G-36) Like the preceding event, this one is separated in distance or azimuth from the other events, and comparisons cannot be made.

Event 45 (Figures G-37 through G-42) Event 45 was separated from Event 53 by about 315 m and 6.5° . Comparison of the top radial and tangential

displacements for the two events shows moderately good agreement to about 12 seconds for the radial and to about 16 seconds for the tangential. Thereafter there are differences in both phase and amplitude.

Event 26 (Figures G-43 through G-48) The most obvious characteristic of the records from this event is the large amplitude of the top tangential displacements. Those amplitudes are over three times the vertical and radial displacements. Vertical and radial displacements show very little difference between top and bottom.

Event 39 (Figures G-49 through G-54) This event was separated from the previous one by only 0.3° , but by 1.64 km in radial distance. Even though the alignment is the same the distance separation is so large that the waveforms are quite different. The one common characteristic is the large amplitude of the top tangential signal.

Event 37 (Figures G-55 through G-60) This event is only about 25 m closer to W-9 than Event 30, but the azimuthal separation is 8.9° . There is no similarity in the ground motion because of the azimuthal separation and because of the difference in yield. Difference in burial depth may have been a factor, since Event 37 was in alluvium above the water table and Event 30 was in tuff and below the water table.

Event 38 (Figures G-61 through G-66) This is the first of the three events detonated in Area 3. It, too, has unusually large tangential displacement at the top relative to the other five measurements.

Event 42 (Figures G-67 through G-72) The vertical velocity and displacement at the bottom (Figure G-68) are not valid because of a malfunction of

the VCO for this channel. Only the acceleration was used in the treatment in Chapters 2 and 3. Event 42 was separated from Event 26 by about 370 m and 1°. In spite of the small separation, there is no similarity in the waveforms of the two events. There was a difference in yield and burial depth. Event 26 was in tuff and Event 42 was in alluvium. Both were above the water table.

Event 49 (Figures G-73 through G-78) This event in Area 3 is separated too far from the other two for the motions to be comparable.

Event 46 (Figures G-79 through G-84) Events 38 and 46 had a radial separation of about 600 m and an azimuthal separation of 2°. There is no similarity between the waveforms of the two events. It is interesting to categorize the waveforms in Appendix G according to the amplitudes of the displacements from the top canister. They fall into three categories.

1. Amplitudes of vertical, radial, and tangential components are comparable.
2. Amplitudes of the vertical component are small relative to those of the radial and tangential components which are larger.
3. Amplitudes of the vertical and radial components are small relative to those of the tangential component which are larger.

Events in Category 1 are 30, 36, and 40, in Areas 4, 2, and 4, respectively. Those in Category 2 are 16, 31, 37, 42, 45, 46, 49, and 53, in Areas 4, 2, 4, 2, 2, 3, 3, and 7, respectively. In Category 3 are 26, 38, and 39, in Areas 2, 3, and 2, respectively. Figure 5-4 shows the relative

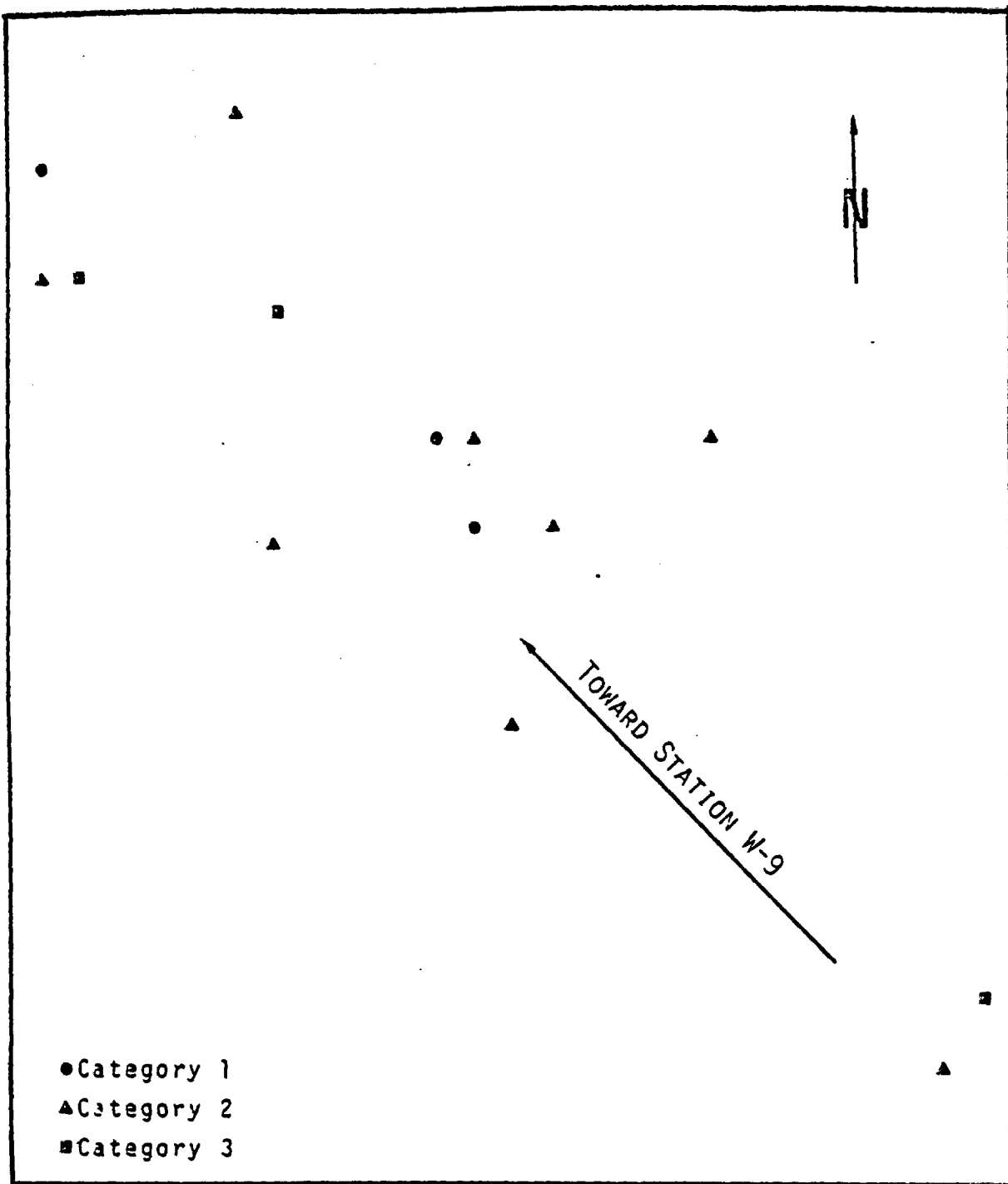


Figure 5-4. Relative locations of events falling into three ground motion categories

locations of the events in each category. There is no pattern in the horizontal locations of the events in the three categories which would explain the observed motion. In Category 1, Events 30 and 40 were in tuff below the water table, and Event 36 was in alluvium below. In Category 2, Events 16, 45, and 53 were in tuff below the water table and Events 31, 46, and 49 were in tuff above. Events 37 and 42 were in alluvium above the water table and Event 39 was in alluvium above. Thus the environment surrounding the burst does not appear to contribute to the observed motion in any consistent way.

● Station W-8 (Appendix H)

Data were recorded at this station on only two Yucca Flat events. One of these was in Area 4 and the other in Area 3. The data are of interest primarily because of the depth of the hole and the fact that it was on the western edge of Area 1.

Event 16 (Figures H-1 through H-6) Because of the depth of the hole there was a significant decrease in radial and tangential motion seen by the bottom canister. The event in Area 4 was 8.7 km away from the station and produced nearly sinusoidal vertical displacements, but quite irregular radial and tangential displacements. This suggests some higher-frequency content in the horizontal motion that was not present in the vertical.

Event 9 (Figures H-7 through H-12) This event in Area 3 was 10.6 km from the station. Vertical motions contain high frequencies which were not seen in the vertical motion records for the previous event. There are greater differences in vertical displacements between top and bottom

than would be expected from the data examined to this point.

● Stations W-15 and W-16 (Appendix I)

Station W-15 on Dome Mountain and W-16 in Fortymile Canyon did not constitute a true surface/downhole pair, since there was a 2300 m horizontal separation as well as the 580 m vertically.

Event 30 (Figures I-1 through I-6) Vertical displacement at the two stations is quite similar after allowance is made for difference in arrival time. There is less similarity for the radial and tangential displacement. In Figure 5-5 the ratio of top to bottom peak-to-peak horizontal displacements is plotted as a function of azimuth. The dashed line parallels the edge of Fortymile Canyon. The direction of maximum displacement is 20° counterclockwise from a perpendicular to the canyon edge. Thus there is a demonstrated edge effect of the canyon.

Event 36 (Figures I-7 through I-12) Both the radial and tangential displacements in Fortymile Canyon are smaller relative to those on Dome Mountain than was the case for Event 30.

Event 31 (Figures I-13 through I-18) Event 31 was 1.7 km farther from both stations than Event 36, and both were on the same azimuth. There are portions of the surface wave during which the displacements at both stations for the two events are in phase if the difference in arrival time is taken into account. The most obvious difference is that the maximum displacement in the vertical and radial components occurs later for Event 31 than for Event 36, even though Event 36 was the closer of the two.

Event 45 (Figures I-19 through I-24) Event 45 was 1.9 km farther than

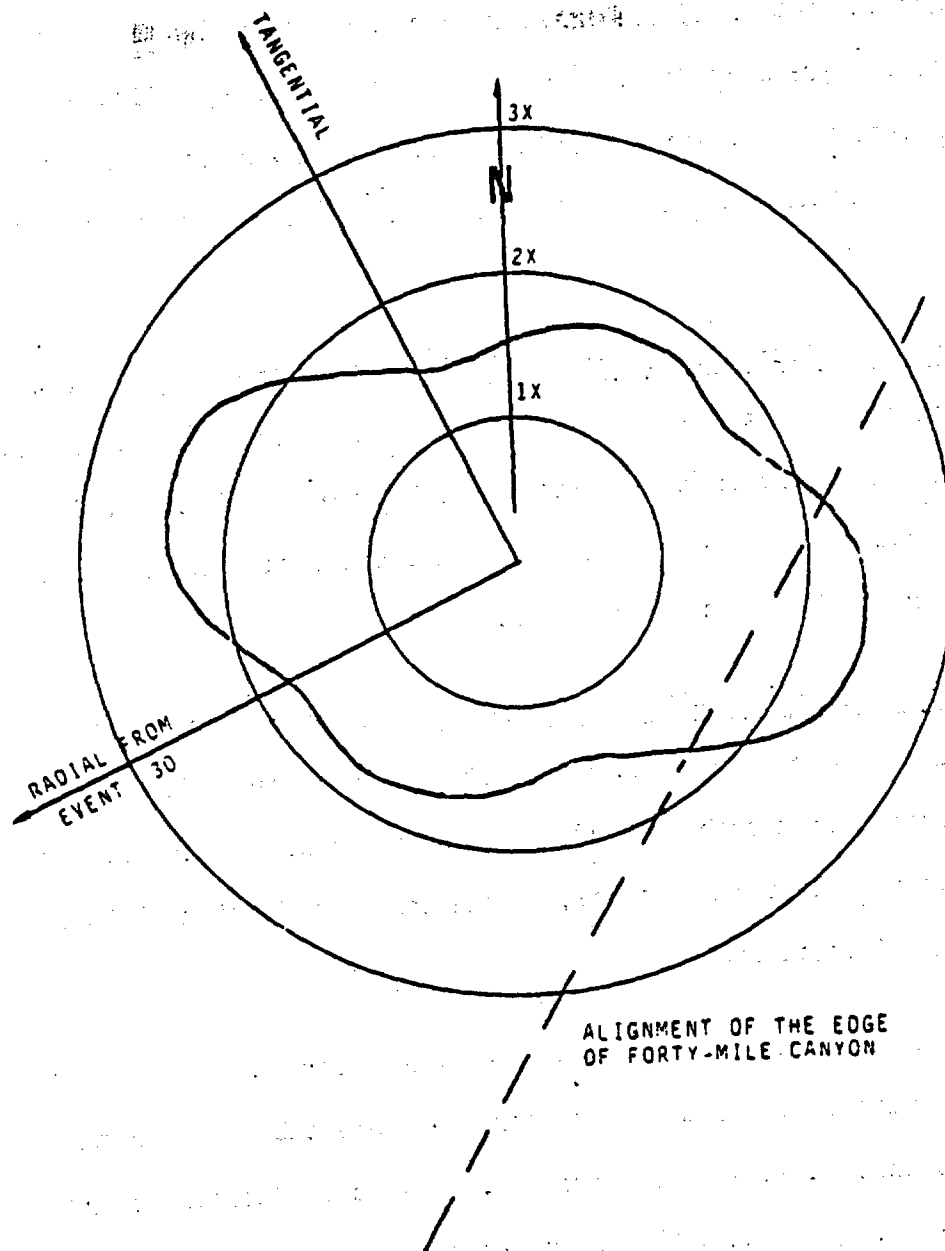


Figure 5.5. Ratio of peak-to-peak displacement at Dome Mountain and Fortymile Canyon as a function of azimuth

Event 30, and there was a 1.9° azimuthal separation. Vertical displacements at Station 15 are smaller than the radial and tangential displacements, whereas at Station 16 all have comparable amplitudes. This suggests topographic effects permitting greater horizontal motion for Dome Mountain. There are few similarities in the waveforms of Events 30 and 45.

Event 39 (Figures I-25 through I-30) Again, the larger horizontal displacements at Station 15 suggest topographic effects. Event 45 is about 120 m closer than Event 30, and there is an azimuthal separation of about 4.2° . There are no obvious similarities in the motion at either station from the two events.

Event 43 (Figures I-31 through I-36) This event has a radial separation of about 280 m from Event 36 and 1610 m from Event 31. The azimuthal separation from both is 0.6° . The only common feature for the three events is that the horizontal displacement at Station 15 is larger than that at Station 16.

Since Dome Mountain is susceptible to topographic effects on the motion, the displacements from the top canister were subjected to the same categorization as was done for W-9. Events in Category 2 were 30, 31, 36, 39 and 45. Event 43 was in Category 3. None were in Category 1. Of the five events for which there were also data at Station W-9, only Events 31 and 45 were in the same categories at both stations. This difference in the two cases would tend to confirm the observation made with respect to Station W-9, that the mechanism affecting the relative amplitudes of the three components is not related to source environment.

● Station W-13 (Appendix J)

Station W-13 is of interest because at 762 m the bottom canister is the deepest in the program. It is also of interest because of the complex geology of the Timber Mountain Cauldera in which it is located.

Event 40 (Figures J-1 through J-6) Vertical displacement is virtually identical at top and bottom. Radial and tangential displacement at the bottom is much reduced.

Event 53 (Figures J-7 through J-12) Events 40 and 53 are on the same azimuth and have a radial separation of about 720 m. Displacements of all three components of Event 40 are in phase with those of Event 53. Peak-to-peak displacements of Event 53 are about half those of Event 40, except for the top tangential which was less than half. Top/bottom ratios of the events were about 1.1 for vertical, 2.6 (Event 40) and 3.1 (Event 53) for radial, and 1.9 (Event 40) and 1.7 (Event 53) for tangential displacements.

Event 36 (Figures J-13 through J-18) Event 36 was located away from the preceding two, and the waveforms are dissimilar. Waveforms of Event 36 show higher frequencies in the displacement.

Event 45 (Figures J-19 through J-24) Because of location the motion of Event 45 is not comparable to that of any other events in this set. The top vertical displacement is small relative to that for the radial and tangential components.

Event 39 (Figures J-25 through J-30) Event 39 is closest to Event 36. There is a radial separation of 1880 m and an azimuthal separation of

4.2°. There is no similarity in the waveforms.

Event 43 (Figures J-31 through J-36) This event has a 490-m radial separation from Event 36 and a 1.3° azimuthal separation. Only in the tangential displacement at the top is there any appreciable similarity in the waveforms. Differences in waveforms may be due to differences in yield. Vertical displacement at the top for Event 42 is small relative to the radial and tangential displacements. For Event 36 all three components have comparable components.

Event 37 (Figures J-37 through J-42) This event is 2.04 km farther away from the station than Event 53, and separated from it azimuthally by 1.2° . The yield of Event 37 was considerably smaller than that of Event 53. As a result of differences in location and yield, there is no similarity in waveforms from the two events.

Event 46 (Figures J-43 through J-48) This event is the only one in this set which was detonated in Area 3; hence it is comparable with no other.

CHAPTER 6

COMPARISON OF RESULTS FROM YUCCA FLAT AND PAHUTE MESA

In Chapters 2, 3, and 4 and the same chapters in Reference 1, the top/bottom ratios were fit to depth with an exponential curve fit of the form

$$R = ce^{\beta d}.$$

In Table 6-1 the values of c and β and those for the coefficients of determination (r^2) are tabulated the highest peak, the average of the 5, 10, 15, 20, and 25 highest peaks, and the PSRV's for both the Yucca Flat and Pahute Mesa Data.

For the Yucca Flat data the coefficients of determination for acceleration increase to 0.449 for the average of the 10 highest peaks, then decrease. Those for velocity drop from 1 to 5 peaks, then increase. Those for displacement increase from 1 to 25 peaks. The coefficient for PSRV ratios is larger than those for velocity and displacement, but smaller than that for acceleration. This would be expected, since the PSRV contains elements of all three parameters.

For the Pahute Mesa set the coefficients for all three parameters increase from 1 to 25 peaks. However, the coefficient for PSRV ratios is larger than all three. The better fit to the Pahute Mesa data could also be to differences in the geologic structure between Pahute Mesa and Yucca Flat which cause a wider range of top/bottom ratio for the latter.

TABLE 6-1

Comparison of Results from Yucca Flat and Pahute Mesa

	<u>Yucca Flat Data</u>			<u>Pahute Mesa Data</u>		
	c	B	r ²	c	B	r ²
Highest Single Peak (Chapter 2)						
a	1.29	0.00134	0.399	1.48	0.000867	0.282
u	1.37	0.000991	0.210	1.06	0.00163	0.494
d	1.35	0.000692	0.084	1.08	0.00113	0.322
Ave 5 Highest Peaks						
a	1.30	0.00135	0.436	1.38	0.00108	0.359
u	1.38	0.00101	0.178	1.07	0.00159	0.502
d	1.31	0.000760	0.103	1.06	0.00123	0.324
Ave 10 Highest Peaks						
a	1.30	0.00137	0.449	1.32	0.00121	0.398
u	1.33	0.00108	0.202	1.07	0.00156	0.505
d	1.30	0.000823	0.117	1.03	0.00122	0.359
Ave 15 Highest Peaks (Chapter 3)						
a	1.31	0.00136	0.441	1.29	0.00127	0.416
u	1.32	0.00113	0.215	1.07	0.00157	0.514
d	1.29	0.000869	0.124	1.01	0.00132	0.404
Ave 20 Highest Peaks						
a	1.31	0.00135	0.432	1.27	0.00131	0.429
u	1.30	0.00118	0.227	1.07	0.00158	0.516
d	1.29	0.000909	0.131	0.99	0.00140	0.430
Ave 25 Highest Peaks						
a	1.31	0.00134	0.424	1.27	0.00133	0.435
u	1.30	0.00121	0.237	1.06	0.00160	0.518
d	1.28	0.000944	0.138	1.00	0.00143	0.437
PSRV (Chapter 4)						
	1.36	0.00117	0.335	1.29	0.00125	0.569

For velocity and displacement the coefficients are in all cases larger in the case of the Pahute Mesa data, indicating a better fit. For acceleration the coefficients are smaller for 15 peaks or less, about the same for 20, and slightly larger for 25 peaks. For PSRV ratios the coefficient is considerably better for the Pahute Mesa data.

A larger value of the exponential constant, β , means a greater change in the top/bottom ratio with depth, i.e., a greater decrease in downhole motion with depth relative to that at the top. For the Yucca Flat data set the values of β for acceleration show no change from 1 to 25 peaks. Those for velocity increase after a low for 5 peaks, while the values for displacement increase continuously. For PSRV ratio β is as expected from the fact that all three parameters are involved in a PSRV.

For the Pahute Mesa data set β for acceleration and displacement increases as the number of peaks increases, and is relatively unchanged for velocity. The value for PSRV ratio is smaller than those for the three parameters for 25 peaks.

Values of β for acceleration are smaller in the case of events on Pahute Mesa. For velocity, displacement, and PSRV ratio they are smaller for Yucca Flat shots. Thus downhole acceleration decreases with depth more slowly for Pahute Mesa shots than for shots in Yucca Flat. Similarly, downhole velocity, displacement, and PSRV decrease more slowly for Yucca Flat shots than for Pahute Mesa events.

It would be useful to seek understanding of the differences in motion generated in Yucca Flat and on Pahute Mesa. The only station with measurements made at nearly comparable distances from events in the two

locations was W-10. The two events were 31 in Yucca Flat and 41 on Pahute Mesa, and there was a considerable difference in yield between the two. There was also an azimuthal separation of 33° . When PSRVs for the vertical component at the surface of W-10 are adjusted for yield differences, it appears that the smaller yield of Event 31 produced relatively more motion in the 0.3 to 0.7 Hz region. At the bottom of W-10 it appeared that the event on Pahute Mesa produced more motion in the 3.5 to 10 Hz region than the event in Yucca Flat. Without more data, it is not possible to tell whether these differences are attributable to the two location or to the yield differences. Such differences may or may not be consistent from one event to another.

A similar comparison between the two areas using the standard error of the estimate or the 90 percent confidence limits has not been presented because those error functions were not determined for the Pahute Mesa data.

CHAPTER 7

CONCLUSIONS

There were seven locations at which measurements were made on the surface and at an available depth as a part of the Weapons Test Seismic Investigation project. The depths at which measurements were made ranged from 61 m to 762 m. Measurements were made at some of the seven locations on 28 different underground nuclear weapons tests in Yucca Flat. This data set became the basis for assessing the effects of depth of measurement on ground motion. The assessment made use of ratios (top/bottom) of single peak vector accelerations, velocities, and displacements; averages of multiple peaks of the same parameters; and top/bottom ratios of PSRVs. Also, waveforms of the individual vertical, radial, and tangential components of the same three parameters were compared at top and bottom.

The results confirmed what was observed with the Pahute Mesa data, namely, that change in motion with depth is strongly dependent on the geology at the location where surface and downhole measurements are made. The difference between top and bottom was small for the granite of the Climax stock (Station W-3), and large for Rainier Mesa (Station 9) where the added effect of topography increased the difference.

A relative trend with depth was determined for each of the ratios noted above. The trends for Yucca Flat and Pahute Mesa data were compared in Chapter 6. Better fits to the data were obtained from the Pahute Mesa than from the Yucca Flat data. The better fit for Pahute Mesa data could be attributed to a smaller number of events in the data set and to the smaller range of yields the events represented. There were changes

in quality of fit as the number of peaks was increased. For PSRV ratios the better fit was for the Pahute Mesa data.

The equations show that downhole acceleration decreased with depth more slowly for Pahute Mesa shots than for shots in Yucca Flat. Also, downhole velocity, displacement, and PSRV decrease more slowly for Yucca Flat shots than for Pahute Mesa events.

Only one event on Pahute Mesa and one in Yucca Flat were at about the same distance from one station (Station 10). There was considerable azimuthal separation between shots in the two locations as well as differences in yield. Differences in PSRVs for the vertical component were noted from a comparison, but with data from only two events it is not possible to tell whether the observed differences are attributable to yield or location.

A number of observations can be made concerning the ground motion waveforms. First motion of the vertical component is upward and first motion of the radial component is outward from the source. First motion of the tangential component is unpredictable and can be either clockwise or counterclockwise about the source. There was evidence in the Yucca Flat data that where shots were fired sufficiently close together the first tangential motion would be in the same direction. Relatively small differences in radial distance from the source and in azimuth to the source can change the direction of first tangential motion. First motion at the bottom is usually a few milliseconds earlier than at the top. And first motion of the radial and tangential motion is generally a few milliseconds behind that of the vertical component. Except for Station W-11 in the case of the Yucca Flat data only, the maximum

acceleration is usually found in the body wave and the maximum displacement in the surface wave. Usually, the maximum amplitude of the vertical displacement of the surface wave is reduced with depth much less than radial and tangential displacements. However, there were exceptions.

At Station W-10 there were five of ten events where the surface tangential displacement was notably larger than that for the radial and vertical component. All five were in Area 2 and relatively close together, and the other five were in Areas 4 and 7. The five in Area 2 differed in their location with respect to both the water table and the alluvium/tuff interface. Thus there is no indication that the medium in the immediate vicinity of the detonation causes differences in energy coupling which contributes to the strong tangential displacements. It is speculated that there are characteristics in geology in the region of surface wave formation which contribute the large tangential displacements from events in Area 2 which do not exist in the corresponding region with respect to Areas 4 and 7.

Station W-11 in Yucca Flat was so close to events detonated there that a fully developed surface wave was usually not seen.

By comparison with other stations, Station W-3 in the Climax granite stock showed relatively small differences between top and bottom motion, because the granite pluton moved monolithically.

Station W-9 had motion which indicated strong effects of topography on top displacement relative to that at the bottom. Comparison of top and bottom horizontal displacement as a function of azimuth about the station

showed that, for the two cases examined, the maximum motion was nearly tangential, and the minimum displacement was close to the long axis of Rainier Mesa.

Three categories of surface displacement were observed on Rainier Mesa:

(1) Amplitudes of vertical, radial, and tangential components are comparable; (2) amplitudes of the vertical component are small relative to those of the radial and tangential; and (3) amplitudes of the vertical and radial components are small relative to those of the tangential component. There was no pattern in the horizontal locations of the events in the three categories which would explain the observed motion. Also, the environment surrounding the burst does not appear to contribute to the observed motion in any consistent way.

Stations 15 and 16 on Dome Mountain and in Fortymile Canyon, respectively, were treated as a surface/downhole pair. Analysis for one event comparing ratios of displacement as a function of azimuth about the stations showed that the maximum displacement of Dome Mountain was aligned 20° from a perpendicular to the edge of Fortymile Canyon. This demonstrates a topographic effect of the free surface of the canyon wall. This led to categorizing the motion as was done for Station W-9. Of the five events for which there were data at both Stations 9 and 15, only two were in the same categories at both stations, tending to confirm that the mechanism affecting the relative amplitudes of the three components is not related to the source environment.

A Note Concerning Yucca Mountain

Of the surface/downhole pairs in the ground motion net, the one at Rainier Mesa (Station W-9) is in a geology most nearly comparable to the

geology of Yucca Mountain. Rainier Mesa exhibited topographic effects, and similar effects would be expected at Yucca Mountain. There the effects would be greater for surface stations on or near the top of the mountain than for surface stations in valleys or near the base of the mountain.

Azimuthal differences would be expected, also. Station W-9 has an azimuthal window from 99° to 128° for shots in Yucca Flat and from 282° to 317° for Pahute Mesa events. By contrast, Yucca Mountain has a window from 59° to 77° for Yucca Flat events and from 357° to 23° for shots on Pahute Mesa. We have only recently begun to collect data downhole at Yucca Mountain, and it will be some time before comparisons can be made with Rainier Mesa motion.

REFERENCES

1. Vortman, L. J., and Long, J. W., Effects of Repository Depth on Ground Motion—The Pahute Mesa Data, SAND82-0174, Sandia National Laboratories, Albuquerque, NM, May 1982.
2. Long, J. W., An Investigation of Resonant Signals Recorded at Well J-11, Nevada Test Site, SAND81-1323, Sandia National Laboratories, Albuquerque, NM, July 1981.
3. Pilant, W. L., Elastic Waves in the Earth. Elsevier Scientific Publishing Company, 1979.

APPENDIX A

TABLES OF RATIOS (TOP/BOTTOM) FOR PEAK VECTOR MOTION -- MULTIPLE PEAK DATA

TABLE A-1
 Ratios (Top/Bottom) for Peak Vector
 Acceleration - 5 Highest Peaks

Event Number	Plot Symbol	STATION NUMBER								
		10P (61m)	4 (130.5m)	10 (342.6m)	11 (345.6m)	3 (416.7m)	9 (431.6m)	8 (570m)	15/16 (580m)	13 (762m)
8	c	b	1.81	b	b	1.67	b	b	b	b
11	Δ	b	1.80	b	b	2.38	a	a	b	b
40	o	1.31	b	1.43	2.63	1.69	2.17	b	a	4.75
24	e	a	b	a	2.76	1.54	a	b	b	b
3	v	b	1.56	b	b	b	b	b	b	b
1	j	b	1.88	b	b	b	b	b	b	b
13	Δ	b	1.77	b	b	1.65	a	b	b	b
16	d	1.32	1.70	b	a	1.76	2.39	3.72	b	b
53	b	1.21	b	1.01	a	1.77	3.14	b	a	4.74
30	a	1.39	b	1.48	3.24	1.85	2.54	b	0.94	b
36	a	1.25	b	1.72	3.33	a	2.05	b	1.21	3.62
5	m	b	2.12	b	b	b	b	b	b	b
21	m	a	b	a	a	1.40	a	a	b	b
2	v	b	1.74	b	b	b	b	b	b	b
31	u	1.22	b	1.07	2.78	2.32	2.87	b	1.56	b
45	g	a	b	a	2.60	1.32	3.47	b	1.34	5.31
26	v	1.10	b	a	a	1.63	2.41	b	b	b
23	e	a	b	a	a	1.67	a	b	b	b
55	q	a	b	a	a	2.36	a	b	a	a
39	n	1.16	b	1.75	3.38	a	3.75	b	2.08	4.75
43	r	1.22	b	3.17	3.14	1.13	a	b	2.24	3.64
37	p	1.25	b	1.54	3.02	1.65	3.17	b	a	4.13
50	o	d	b	d	2.70	a	a	b	d	d
38	e	d	b	d	3.37	a	3.51	b	d	d
9	k	d	a	d	d	1.84	b	2.87	d	d
42	x	d	b	d	1.95	1.57	3.85	b	d	d
49	f	d	b	d	2.76	1.70	2.62	b	d	d
46	t	d	b	d	3.33	2.51	4.37	b	d	5.32
No. of Events		10	8	8	14	20	14	2	6	8
Average		1.24	1.80	1.64	2.93	1.77	3.02	3.30	1.56	4.53

a - data inadequate

b - station not installed at time of event

d - station not operated for this event

$$R = 1.32e^{0.00128d} \quad \sigma_R = \pm 1.34$$

$$r^2 = 0.409 \quad CL_{R90} = \pm 1.79 \text{ to } 1.82$$

TABLE A-2.

Ratios (Top/Bottom) for Peak Vector
Velocity - 5 Highest Peaks

Event Number	Plot Symbol	STATION NUMBER								
		10P (61m)	4 (130.5m)	10 (342.6m)	11 (345.6m)	3 (416.7m)	9 (431.6m)	8 (570m)	15/16 (580m)	13 (762m)
8	c	b	1.43	b	b	1.42	b	b	b	b
11	Δ	b	1.67	b	b	1.59	a	a	b	b
40	o	1.08	b	2.04	2.78	1.20	3.11	b	a	1.91
24	o	a	b	a	3.09	1.35	a	b	b	b
3	v	b	1.33	b	b	b	b	b	b	b
1	j	b	1.84	b	b	b	b	b	b	b
13	Δ	b	1.52	b	b	1.21	a	b	b	b
16	d	1.03	1.56	b	a	1.19	3.74	2.90	b	b
53	b	1.05	b	1.53	a	1.30	4.43	b	a	2.27
30	a	1.05	b	2.69	2.38	1.12	3.23	b	1.75	b
36	a	1.08	b	1.69	3.96	a	3.43	b	2.10	2.15
5	a	b	1.65	b	b	b	b	b	b	b
21	v	a	b	a	a	1.14	a	a	b	b
2	v	b	1.38	b	b	b	b	b	b	b
31	u	1.11	b	1.71	4.14	1.16	4.09	b	2.10	b
45	g	a	b	a	3.47	1.11	4.12	b	1.70	2.54
26	v	1.03	b	a	a	1.14	3.21	b	b	b
23	♦	a	b	a	a	1.14	a	b	b	b
55	q	a	b	a	a	1.36	a	b	a	a
39	n	1.04	b	1.66	3.43	a	4.98	b	2.24	2.60
43	r	1.13	b	2.48	3.82	1.00	a	b	3.00	2.46
37	p	1.06	b	1.73	3.00	1.41	4.33	b	a	2.24
50	o	d	b	d	2.84	a	a	b	d	d
38	o	d	b	d	3.23	a	4.32	b	d	d
9	k	d	a	d	d	1.50	b	2.47	d	d
42	x	d	b	d	1.88	1.20	a	b	d	d
49	f	d	b	d	2.77	1.95	3.84	b	d	d
46	t	d	b	d	2.93	1.61	5.53	b	d	2.80
No. of Events		10	8	8	14	20	13	2	6	8
Average		1.07	1.55	1.93	3.12	1.30	4.03	2.69	2.14	2.37

a - data inadequate

b - station not installed at time of event

d - station not operated for this event

$$R = 1.36e^{0.00103d} \quad \sigma_R = \pm 1.50$$

$$r^2 = 0.186 \quad CL_{R90} = \pm 2.28 \text{ to } 2.33$$

TABLE A-3
 Ratios (Top/Bottom) for Peak Vector
 Displacement - 5 Highest Peaks

Event Number	Plot Symbol	STATION NUMBER								
		10P (61m)	4 (130.5m)	10 (342.6m)	11 (345.6m)	3 (416.7m)	9 (431.6m)	8 (570m)	15/16 (580m)	13 (762m)
8	c	b	1.37	b	b	1.03	b	b	b	b
11	Δ	b	1.22	b	b	1.26	a	a	b	b
40	o	1.04	b	1.91	2.74	1.04	2.89	b	a	1.55
24	e	a	b	a	2.81	1.04	a	b	b	b
3	v	b	1.12	b	b	b	b	b	b	b
1	j	b	1.27	b	b	b	b	b	b	b
13	Δ	b	1.12	b	b	1.05	a	b	b	b
16	d	0.99	1.30	b	a	1.08	3.40	1.99	b	b
53	b	1.01	b	1.40	a	1.13	3.69	b	a	1.66
30	a	1.03	b	2.24	2.10	1.00	2.76	b	1.54	b
36	a	1.05	b	1.55	2.73	a	2.85	b	1.92	2.01
5	m	b	1.53	b	b	b	b	b	b	b
21	m	a	b	a	a	1.03	a	a	b	b
2	v	b	1.24	b	b	b	b	b	b	b
31	u	1.06	b	1.53	3.24	1.04	3.37	b	2.12	b
45	u	a	b	a	2.40	0.93	3.03	b	1.58	1.72
26	v	1.03	b	a	a	1.05	2.92	b	b	b
23	♦	a	b	a	a	0.99	a	b	b	b
55	q	a	b	a	a	1.30	a	b	a	a
39	n	1.04	b	1.46	3.28	a	3.17	b	2.01	2.00
43	r	1.07	b	1.76	3.48	0.97	a	b	3.22	2.02
37	p	1.07	b	1.68	3.42	1.08	4.10	b	a	1.43
50	o	d	b	d	2.79	a	a	b	d	d
38	o	d	b	d	3.02	a	3.67	b	d	d
9	k	d	a	d	d	1.19	b	1.52	d	d
42	x	d	b	d	2.18	1.13	a	b	d	d
49	f	d	b	d	3.44	1.35	4.71	b	d	d
46	t	d	b	d	2.46	1.48	4.51	b	d	1.75
No. of Events		10	8	8	14	20	13	2	6	8
Average		1.04	1.27	1.69	2.87	1.11	3.47	1.75	2.07	1.77

a - data inadequate

b - station not installed at time of event

d - station not operated for this event

$$R = 1.29e^{0.000786d} \quad \sigma_R = \pm 1.52$$

$$r^2 = 0.110 \quad CL_{R90} = \pm 2.35 \text{ to } 2.40$$

TABLE A-4

Ratios (Top/Bottom) for Peak Vector
Acceleration - 10 Highest Peaks

Event Number	Plot Symbol	STATION NUMBER								
		TOP (61m)	4 (130.5m)	10 (342.6m)	11 (345.6m)	3 (416.7m)	9 (431.6m)	8 (570m)	15/16 (580m)	13 (762m)
8	c	b	1.93	b	b	1.68	b	b	b	b
11	Δ	b	1.76	b	b	2.43	a	a	b	b
40	o	1.32	b	1.46	2.76	1.72	2.33	b	a	4.82
24	o	a	b	a	2.83	1.56	a	b	b	b
3	v	b	1.60	b	b	b	b	b	b	b
1	j	b	1.89	b	b	b	b	b	b	b
13	Δ	b	1.74	b	b	1.73	a	b	b	b
16	d	1.31	1.65	b	a	1.76	2.41	3.79	b	b
53	b	1.22	b	1.00	a	1.91	3.22	b	a	4.73
30	a	1.37	b	1.50	3.14	1.96	2.61	b	1.07	b
36	a	1.26	b	1.73	3.35	a	2.14	b	1.35	3.67
5	m	b	2.07	b	b	b	b	b	b	b
21	m	a	b	a	a	1.61	a	a	b	b
2	v	b	1.73	b	b	b	b	b	b	b
31	u	1.23	b	1.04	2.76	2.16	2.99	b	1.68	b
45	B	a	b	a	2.55	1.41	3.61	b	1.50	5.35
26	v	1.11	b	a	a	1.67	2.42	b	b	b
23	◆	a	b	a	a	1.66	a	b	b	b
55	q	a	b	a	a	2.29	a	b	a	a
39	n	1.17	b	1.73	3.71	a	3.81	b	2.00	4.58
43	r	1.23	b	2.95	3.03	1.19	a	b	2.10	3.73
37	p	1.26	b	1.53	3.01	1.66	3.23	b	a	4.09
50	o	d	b	d	2.54	a	a	b	d	d
38	e	d	b	d	3.27	a	3.55	b	d	d
9	k	d	a	d	d	1.90	b	2.77	d	d
42	x	d	b	d	2.08	1.49	4.00	b	d	d
49	f	d	b	d	2.75	1.87	2.65	b	d	d
46	t	d	b	d	3.26	2.40	4.13	b	d	5.12
No. of Events		10	8	8	14	20	14	2	6	8
Average		1.25	1.80	1.62	2.93	1.80	3.07	3.28	1.62	4.51

a - data inadequate

b - station not installed at time of event

d - station not operated for this event

$$R = 1.30e^{0.00137d} \quad \sigma_R = \pm 1.33$$

$$r^2 = 0.453 \quad Cl_{R90} = \pm 1.77 \text{ to } 1.80$$

TABLE A-5
 Ratios (Top/Bottom) for Peak Vector
 Velocity - 10 Highest Peaks

Event Number	Plot Symbol	STATION NUMBER								
		10P (61m)	4 (130.5m)	10 (342.6m)	11 (345.6m)	3 (416.7m)	9 (431.6m)	8 (570m)	15/16 (580m)	13 (762m)
8	c	b	1.50	b	b	1.27	b	b	b	b
11	Δ	b	1.62	b	b	1.49	a	a	b	b
40	o	1.07	b	2.08	2.58	1.18	2.90	b	a	2.23
24	e	a	b	a	2.84	1.26	a	b	b	b
3	v	b	1.31	b	b	b	b	b	b	b
1	j	b	1.74	b	b	b	b	b	b	b
13	Δ	b	1.52	b	b	1.23	a	b	b	b
16	d	1.03	1.53	b	a	1.20	3.46	3.14	b	b
53	b	1.05	b	1.53	a	1.30	4.55	b	a	2.55
30	a	1.06	b	2.52	2.34	1.17	3.12	b	1.67	b
36	a	1.09	b	1.71	3.47	a	3.47	b	2.18	2.36
5	e	b	1.56	b	b	b	b	b	b	b
21	m	a	b	a	a	1.18	a	a	b	b
2	v	b	1.40	b	b	b	b	b	b	b
31	u	1.09	b	1.69	3.78	1.25	3.95	b	2.13	b
45	u	a	b	a	3.57	1.09	4.06	b	1.65	2.62
26	v	1.04	b	a	a	1.20	3.24	b	b	b
23	♦	a	b	a	a	1.15	a	b	b	b
55	q	a	b	a	a	1.33	a	b	a	a
39	n	1.05	b	1.67	3.93	a	5.20	b	2.16	2.55
43	r	1.12	b	2.32	3.67	1.02	a	b	2.63	2.69
37	p	1.08	b	1.77	3.10	1.36	4.51	b	a	2.45
50	o	d	b	d	2.82	a	a	b	d	d
38	e	d	b	d	3.25	a	4.53	b	d	d
9	k	d	a	d	d	1.49	b	2.49	d	d
42	x	d	b	d	1.90	1.23	a	b	d	d
49	f	d	b	d	2.86	1.87	3.96	b	d	d
46	t	d	b	d	2.91	1.60	5.21	b	d	2.84
No. of Events		10	8	8	14	20	13	2	6	8
Average		1.07	1.52	1.91	3.07	1.29	4.01	2.82	2.07	2.53

a - data inadequate

b - station not installed at time of event

d - station not operated for this event

$$R = 1.32e^{0.00110d} \quad \sigma_R = \pm 1.50$$

$$r^2 = 0.208 \quad CL_{R90} = \pm 2.27 \text{ to } 2.31$$

TABLE A-6

Ratios (Top/Bottom) for Peak Vector
Displacement - 10 Highest Peaks

Event Number	Plot Symbol	STATION NUMBER								
		TOP (61m)	4 (130.5m)	10 (342.6m)	11 (345.6m)	3 (416.7m)	9 (431.6m)	8 (570m)	15/16 (580m)	13 (762m)
8	c	b	1.34	b	b	1.06	b	b	b	b
11	Δ	b	1.23	b	b	1.21	a	a	b	b
40	o	1.04	b	2.01	3.26	1.06	3.01	b	a	1.64
24	o	a	b	a	2.57	1.06	a	b	b	b
3	v	b	1.11	b	b	b	b	b	b	b
1	j	b	1.31	b	b	b	b	b	b	b
13	Δ	b	1.15	b	b	1.04	a	b	b	b
16	d	0.99	1.24	b	a	1.07	2.96	2.26	b	b
53	b	1.01	b	1.39	a	1.14	3.93	b	a	1.79
30	a	1.04	b	2.21	2.58	1.01	3.00	b	1.60	b
36	s	1.05	b	1.52	2.86	a	3.08	b	2.00	2.04
5	m	b	1.47	b	b	b	b	b	b	b
21	m	a	b	a	a	1.06	a	a	b	b
2	v	b	1.26	b	b	b	b	b	b	b
31	u	1.04	b	1.53	3.04	1.09	3.75	b	2.13	b
45	g	a	b	a	2.32	0.90	3.10	b	1.54	1.78
26	v	1.04	b	a	a	1.07	2.86	b	b	b
23	e	a	b	a	a	1.01	a	b	b	b
55	q	a	b	a	a	1.27	a	b	a	a
39	n	1.04	b	1.41	3.77	a	3.55	b	2.03	2.07
43	r	1.07	b	1.71	3.04	0.96	a	b	2.77	2.12
37	p	1.08	b	1.66	3.76	1.04	4.23	b	a	1.58
50	o	d	b	d	2.77	a	a	b	d	d
38	e	d	b	d	3.02	a	3.72	b	d	d
9	k	d	a	d	d	1.24	b	1.60	d	d
42	x	d	b	d	2.19	1.11	a	b	d	d
49	f	d	b	d	3.32	1.39	5.02	b	d	d
46	t	d	b	d	2.48	1.48	4.08	b	d	1.92
No. of Events		10	8	8	14	20	13	2	6	8
Average		1.05	1.26	1.68	2.03	1.11	3.56	1.93	2.01	1.87

a - data inadequate

b - station not installed at time of event

d - station not operated for this event

$$R = 1.28e^{0.000850d} \quad \sigma_R = \pm 1.53$$

$$r^2 = 0.123 \quad CL_{R90} = \pm 2.37 \text{ to } 2.42$$

TABLE A-7
 Ratios (Top/Bottom) for Peak Vector
 Acceleration - 20 Highest Peaks

Event Number	Plot Symbol	STATION NUMBER								
		TOP (61m)	4 (130.5m)	10 (342.6m)	11 (345.6m)	3 (416.7m)	9 (431.6m)	8 (570m)	15/16 (580m)	13 (762m)
8	c	b	2.00	b	b	1.72	b	b	b	b
11	Δ	b	1.74	b	b	2.39	a	a	b	b
40	o	1.33	b	1.51	2.85	1.65	2.46	b	a	4.88
24	e	a	b	a	2.92	1.57	a	b	b	b
3	v	b	1.59	b	b	b	b	b	b	b
1	j	b	1.89	b	b	b	b	b	b	b
13	Δ	b	1.74	b	b	1.71	a	b	b	b
16	d	1.28	1.58	b	a	1.74	2.58	3.75	b	b
53	b	1.24	b	1.02	a	1.97	3.34	b	a	4.66
30	a	1.38	b	1.50	2.91	1.98	2.74	b	1.21	b
36	e	1.23	b	1.68	3.40	a	2.18	b	1.40	3.62
5	m	b	2.05	b	b	b	b	b	b	b
21	m	a	b	a	a	1.67	a	a	b	b
2	v	b	1.73	b	b	b	b	b	b	b
31	u	1.25	b	1.03	2.76	2.00	2.95	b	1.76	b
45	g	a	b	a	2.45	1.49	3.68	b	1.57	5.31
26	v	1.17	b	a	a	1.65	2.37	b	b	b
23	e	a	b	a	a	1.42	a	b	b	b
55	q	a	b	a	a	2.19	a	b	a	a
39	n	1.15	b	1.71	3.78	a	3.95	b	1.81	4.34
43	r	1.21	b	2.72	3.38	1.20	a	b	1.99	3.89
37	p	1.28	b	1.53	3.11	1.69	3.18	b	a	4.05
50	o	d	b	d	2.59	a	a	b	d	d
38	e	d	b	d	3.19	a	3.49	b	d	d
9	k	d	a	d	d	1.90	b	2.46	d	d
42	x	d	b	d	2.50	1.47	3.96	b	d	d
49	f	d	b	d	2.63	1.98	2.82	b	d	d
46	t	d	b	d	3.22	2.29	4.01	b	d	5.01
No. of Events		10	8	8	14	20	14	2	6	8
Average		1.25	1.79	1.59	2.98	1.78	3.12	3.11	1.62	4.47

a - data inadequate

b - station not installed at time of event

d - station not operated for this event

$$R = 1.30e^{0.00136d} \quad \sigma_R = \pm 1.34$$

$$r^2 = 0.437 \quad CL_{R90} = \pm 1.80 \text{ to } 1.82$$

TABLE A-8
Ratios (Top/Bottom) for Peak Vector
Velocity - 20 Highest Peaks

Event Number	Plot Symbol	STATION NUMBER								
		10P (61m)	4 (130.5m)	10 (342.6m)	11 (345.6m)	3 (416.7m)	9 (431.6m)	8 (570m)	15/16 (580m)	13 (762m)
8	c	b	1.58	b	b	1.20	b	b	b	b
11	Δ	b	1.59	b	b	1.48	a	a	b	b
40	o	1.07	b	2.16	2.61	1.22	2.95	b	a	2.83
24	o	a	b	a	2.81	1.25	a	b	b	b
3	v	b	1.26	b	b	b	b	b	b	b
1	j	b	1.65	b	b	b	b	b	b	b
13	Δ	b	1.44	b	b	1.20	b	b	b	b
16	d	1.02	1.46	b	a	1.26	3.32	3.29	b	b
53	b	1.05	b	1.56	a	1.36	4.78	b	a	2.86
30	a	1.07	b	2.40	2.65	1.19	3.07	b	1.70	b
36	a	1.08	b	1.73	3.32	a	3.65	b	2.19	2.70
5	u	b	1.55	b	b	b	b	b	b	b
21	m	a	b	a	a	1.19	a	a	b	b
2	v	b	1.42	b	b	b	b	b	b	b
31	u	1.09	b	1.64	3.57	1.33	4.18	b	2.17	b
45	u	a	b	a	3.37	1.08	4.11	b	1.69	2.59
26	v	1.05	b	a	a	1.19	3.20	b	b	b
23	v	a	b	a	a	1.16	a	b	b	b
55	q	a	b	a	a	1.33	a	b	a	a
39	n	1.06	b	1.78	4.59	a	5.24	b	2.05	2.62
43	r	1.12	b	2.28	3.65	1.04	a	b	2.40	2.97
37	p	1.09	b	1.84	3.44	1.32	4.55	b	a	2.67
50	o	d	b	d	2.98	a	a	b	d	d
38	e	d	b	d	3.36	a	4.41	b	d	d
9	k	d	a	d	d	1.45	b	2.62	d	d
42	x	d	b	d	2.35	1.28	a	b	d	d
49	f	d	b	d	3.01	1.79	3.98	b	d	d
46	t	d	b	d	3.17	1.60	4.94	b	d	2.99
No. of Events		10	8	8	14	20	13	2	6	8
Average		1.07	1.49	1.92	3.20	1.30	4.03	2.95	2.03	2.78

a - data inadequate
b - station not installed at time of event
d - station not operated for this event

$$R = 1.29e^{0.00120d} \quad \sigma_R = \pm 1.51$$

$$r^2 = 0.232 \quad CL_{R90} = \pm 2.29 \text{ to } 2.32$$

TABLE A-9
 Ratios (Top/Bottom) for Peak Vector
 Displacement - 20 Highest Peaks

Event Number	Plot Symbol	STATION NUMBER								
		TOP (61m)	4 (130.5m)	10 (342.6m)	11 (345.6m)	3 (416.7m)	9 (431.6m)	8 (570m)	15/16 (580m)	13 (762m)
8	c	b	1.32	b	b	1.09	b	b	b	b
11	Δ	b	1.24	b	b	1.17	a	a	b	b
40	o	1.06	b	2.09	3.62	1.09	3.27	b	a	1.64
24	e	a	b	a	2.54	1.09	a	b	b	b
3	v	b	1.10	b	b	b	b	b	b	b
1	j	b	1.33	b	b	b	b	b	b	b
13	Δ	b	1.17	b	b	1.04	a	b	b	b
16	d	0.99	1.22	b	a	1.07	3.03	2.40	b	b
53	b	1.01	b	1.41	a	1.17	4.17	b	a	1.93
30	a	1.02	b	2.13	2.91	0.97	3.35	b	1.81	b
36	s	1.06	b	1.51	2.86	a	3.56	b	2.04	2.23
5	m	b	1.44	b	b	b	b	b	b	b
21	m	a	b	a	a	1.12	a	a	b	b
2	v	b	1.26	b	b	b	b	b	b	b
31	u	1.05	b	1.50	3.05	1.11	4.15	b	2.56	b
45	g	a	b	a	2.63	0.95	3.58	b	1.64	1.81
26	v	1.04	b	a	a	1.05	3.00	b	b	b
23	♦	a	b	a	a	0.99	a	b	b	b
55	q	a	b	a	a	1.24	a	b	a	a
39	n	1.02	b	1.44	4.04	a	3.83	b	2.15	2.14
43	r	1.07	b	1.73	3.02	0.98	a	b	2.53	2.31
37	p	1.11	b	1.66	3.73	1.04	4.29	b	a	1.84
50	o	d	b	d	2.82	a	a	b	d	d
38	e	d	b	d	3.04	a	3.73	b	d	d
9	k	d	a	d	d	1.29	b	1.70	d	d
42	x	d	b	d	2.39	1.13	a	b	d	d
49	f	d	b	d	3.10	1.37	5.06	b	d	d
46	t	d	b	d	2.70	1.46	3.98	b	d	2.04
No. of Events		10	8	8	14	20	13	2	6	8
Average		1.04	1.26	1.68	3.03	1.12	3.77	2.05	2.06	1.99

a - data inadequate

b - station not installed at time of event

d - station not operated for this event

$$R = 1.27e^{0.000936d} \quad \sigma_R = \pm 1.56$$

$$r^2 = 0.138 \quad CL_{R90} = \pm 2.44 \text{ to } 2.55$$

TABLE A-10
 Ratios (Top/Bottom) for Peak Vector
 Acceleration - 25 Highest Peaks

Event Number	Plot Symbol	STATION NUMBER								
		TOP (61m)	4 (130.5m)	10 (342.6m)	11 (345.6m)	3 (416.7m)	9 (431.6m)	8 (570m)	15/16 (580m)	13 (762m)
8	c	b	2.03	b	b	1.72	b	b	b	b
11	Δ	b	1.75	b	b	2.39	a	a	b	b
40	o	1.33	b	1.53	2.88	1.63	2.51	b	a	4.83
24	e	a	b	a	2.82	1.56	a	b	b	b
3	v	b	1.59	b	b	b	b	b	b	b
1	j	b	1.89	b	b	b	b	b	b	b
13	Δ	b	1.73	b	b	1.73	a	b	b	b
16	d	1.27	1.59	b	a	1.73	2.63	3.64	b	b
53	b	1.24	b	1.02	a	1.96	3.41	b	a	4.64
30	a	1.38	b	1.50	2.89	1.96	2.79	b	1.26	b
36	a	1.23	b	1.66	3.44	a	2.24	b	1.38	3.63
5	m	b	2.03	b	b	b	b	b	b	b
21	m	a	b	a	a	1.68	a	a	b	b
2	v	b	1.73	b	b	b	b	b	b	b
31	u	1.24	b	1.02	2.77	1.97	2.92	b	1.76	b
45	g	a	b	a	2.47	1.52	3.65	b	1.57	5.26
26	v	1.18	b	a	a	1.66	2.36	b	b	b
23	♦	a	b	a	a	1.39	a	b	b	b
55	q	a	b	a	a	2.15	a	b	a	a
39	n	1.15	b	1.70	3.79	a	3.96	b	1.76	4.26
43	r	1.21	b	2.65	3.42	1.22	a	b	1.98	3.99
37	p	1.27	b	1.53	3.19	1.70	3.20	b	a	4.03
50	o	d	b	d	2.67	a	a	b	d	d
38	k	d	b	d	3.17	a	3.45	b	d	d
9	k	d	a	d	d	1.89	b	2.37	d	d
42	x	d	b	d	2.64	1.47	3.96	b	d	d
49	f	d	b	d	2.59	2.06	2.91	b	d	d
46	t	d	b	d	3.17	2.25	3.99	b	d	5.02
No. of Events		10	8	8	14	20	14	2	6	8
Average		1.25	1.79	1.58	2.99	1.78	3.14	3.01	1.62	4.46

a - data inadequate
 b - station not installed at time of event
 d - station not operated for this event

$$R = 1.31e^{0.00135d} \quad \sigma_R = \pm 1.34$$

$$r^2 = 0.429 \quad CL_{R90} = \pm 1.81 \text{ to } 1.83$$

TABLE A-11

Ratios (Top/Bottom) for Peak Vector
Velocity - 25 Highest Peaks

Event Number	Plot Symbol	STATION NUMBER								
		TOP (61m)	4 (130.5m)	10 (342.6m)	11 (345.6m)	3 (416.7m)	9 (431.6m)	8 (570m)	15/16 (580m)	13 (762m)
8	c	b	1.64	b	b	1.19	b	b	b	b
11	Δ	b	1.59	b	b	1.49	a	a	b	b
40	o	1.09	b	2.18	2.57	1.25	2.97	b	a	3.01
24	e	a	b	a	2.81	1.27	a	b	b	b
3	v	b	1.26	b	b	b	b	b	b	b
1	j	b	1.65	b	b	b	b	b	b	b
13	Δ	b	1.43	b	b	1.17	a	b	b	b
16	d	1.02	1.44	b	a	1.25	3.30	3.29	b	b
53	b	1.05	b	1.56	a	1.41	4.69	b	a	2.99
30	a	1.07	b	2.35	2.71	1.20	3.09	b	1.76	b
36	e	1.08	b	1.77	3.27	a	3.75	b	2.21	2.81
5	m	b	1.55	b	b	b	b	b	b	b
21	m	a	b	a	a	1.20	a	a	b	b
2	v	b	1.42	b	b	b	b	b	b	b
31	u	1.09	b	1.63	3.67	1.38	4.27	b	2.19	b
45	u	a	b	a	3.30	1.10	4.18	b	1.72	2.70
26	v	1.05	b	a	a	1.18	3.18	b	b	b
23	q	a	b	a	a	1.19	a	b	b	b
55	q	a	b	a	a	1.33	a	b	a	a
39	n	1.06	b	1.80	4.81	a	5.14	b	2.05	2.69
43	r	1.12	b	2.27	3.74	1.09	a	b	2.34	3.09
37	p	1.09	b	1.89	3.47	1.31	4.48	b	a	2.75
50	o	d	b	d	3.09	a	a	b	d	d
38	e	d	b	d	3.43	a	4.36	b	d	d
9	k	d	a	d	d	1.45	b	2.58	d	d
42	x	d	b	d	2.49	1.31	a	b	d	d
49	f	d	b	d	3.02	1.77	4.03	b	d	d
46	t	d	b	d	3.23	1.59	4.91	b	d	3.05
No. of Events		10	8	8	14	20	13	2	6	8
Average		1.07	1.50	1.93	3.26	1.31	4.03	2.93	2.04	2.89

a - data inadequate

b - station not installed at time of event

d - station not operated for this event

$$R = 1.29e^{0.00123d} \quad \sigma_R = \pm 1.51$$

$$r^2 = 0.242 \quad CL_{R90} = \pm 2.29 \text{ to } 2.33$$

TABLE A-12

Ratios (Top/Bottom) for Peak Vector
Displacement - 25 Highest Peaks

Event Number	Plot Symbol	STATION NUMBER								
		10P (61m)	4 (130.5m)	10 (342.6m)	11 (345.6m)	3 (416.7m)	9 (431.6m)	8 (570m)	15/16 (580m)	13 (762m)
8	c	b	1.35	b	b	1.10	b	b	b	b
11	Δ	b	1.24	b	b	1.16	a	a	b	b
40	o	1.06	b	2.13	3.63	1.10	3.32	b	a	1.64
24	e	a	b	a	2.53	1.09	a	b	b	b
3	v	b	1.11	b	b	b	b	b	b	b
1	j	b	1.33	b	b	b	b	b	b	b
13	Δ	b	1.18	b	b	1.04	a	b	b	b
16	d	0.99	1.23	b	a	1.07	3.12	2.38	b	b
53	b	1.01	b	1.41	a	1.16	4.21	b	a	2.02
30	a	1.02	b	2.08	2.96	0.97	3.47	b	1.84	b
36	a	1.06	b	1.51	2.91	a	3.69	b	2.02	2.30
5	m	b	1.43	b	b	b	b	b	b	b
21	m	a	b	a	a	1.18	a	a	b	b
2	v	b	1.27	b	b	b	b	b	b	b
31	u	1.05	b	1.50	3.05	1.12	4.33	b	2.12	b
45	g	a	b	a	2.12	0.97	3.70	b	1.70	1.94
26	v	1.05	b	a	a	1.05	3.01	b	b	b
23	◆	a	b	a	a	0.98	a	b	b	b
55	q	a	b	a	a	1.24	a	b	a	a
39	n	1.02	b	1.46	4.12	a	3.92	b	2.21	2.19
43	r	1.07	b	1.73	3.06	0.99	a	b	2.54	2.38
37	p	1.11	b	1.70	3.71	1.04	4.35	b	a	1.91
50	o	d	b	d	2.90	a	a	b	d	d
38	k	d	b	d	3.11	a	3.77	b	d	d
9	k	d	a	d	d	1.29	b	1.69	d	d
42	x	d	b	d	2.43	1.14	a	b	d	d
49	f	d	b	d	3.08	1.37	5.04	b	d	d
46	t	d	b	d	2.90	1.46	3.98	b	d	2.10
No. of Events		10	8	8	14	20	13	2	6	8
Average		1.04	1.27	1.69	3.08	1.13	3.84	2.03	2.07	2.06

a - data inadequate

b - station not installed at time of event

d - station not operated for this event

$$R = 1.26e^{0.000970d} \quad \sigma_R = \pm 1.56$$

$$r^2 = 0.144 \quad CL_{R90} = \pm 2.46 \text{ to } 2.51$$

APPENDIX B

COMPARISON OF RATIOS (TOP/BOTTOM)

OF "VECTOR" PSRV'S

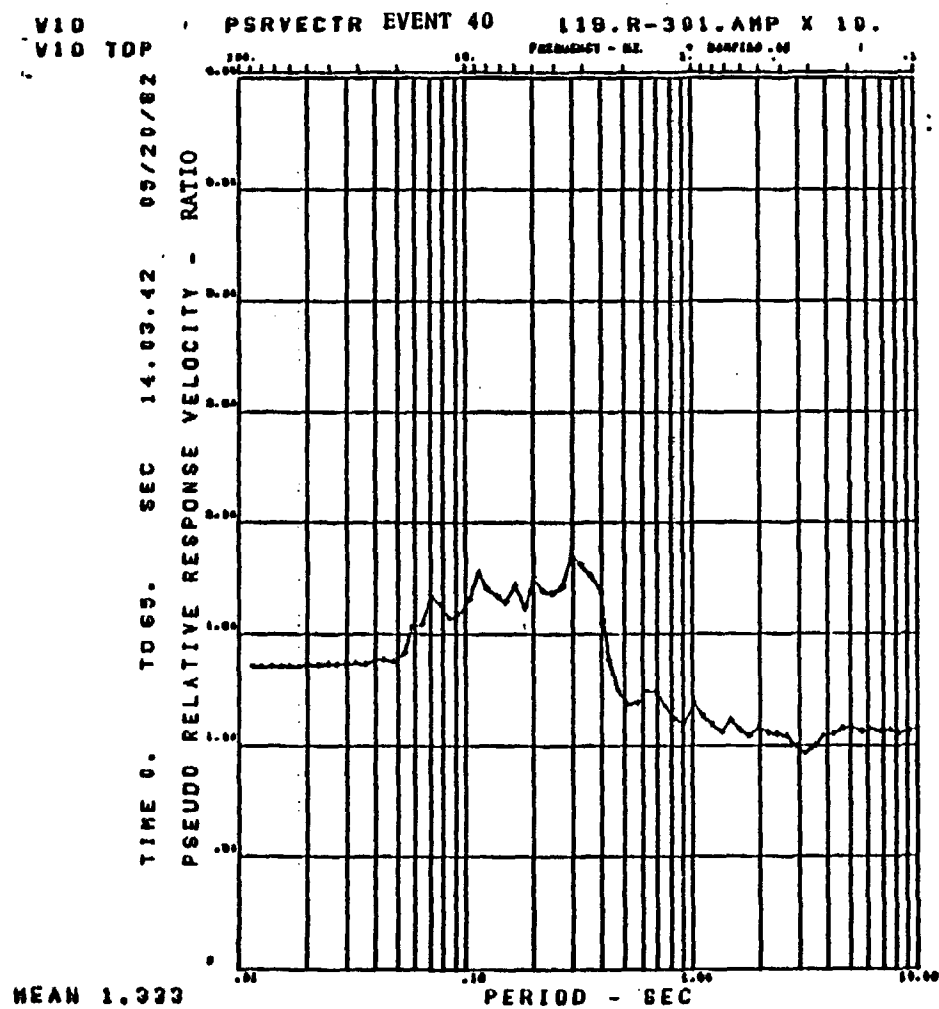


Figure B-1a

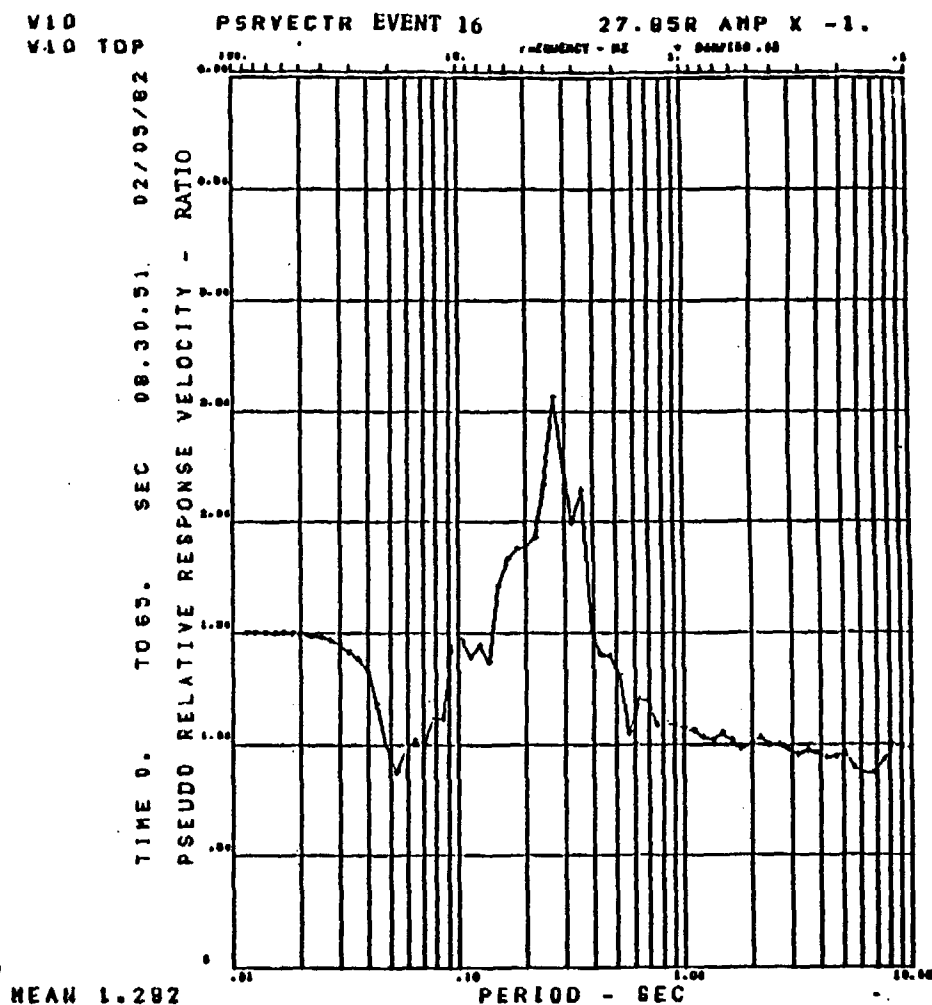


Figure B-1b

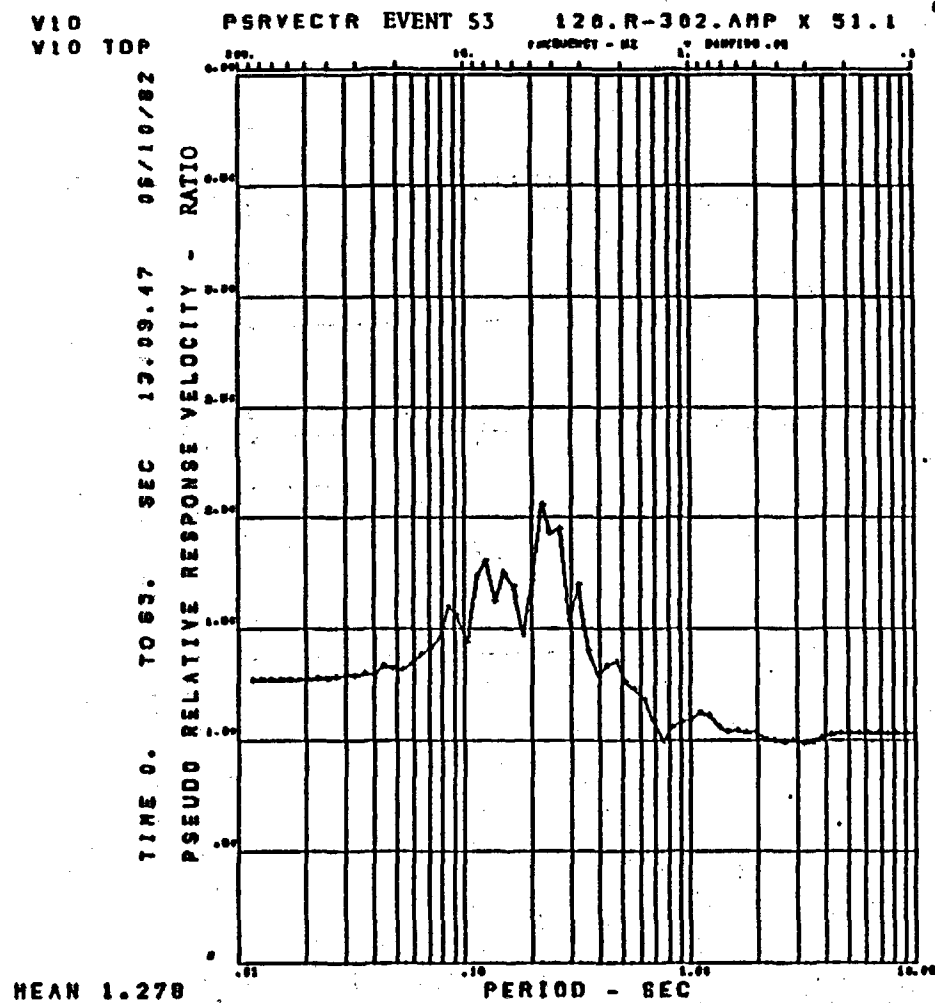


Figure B-2a

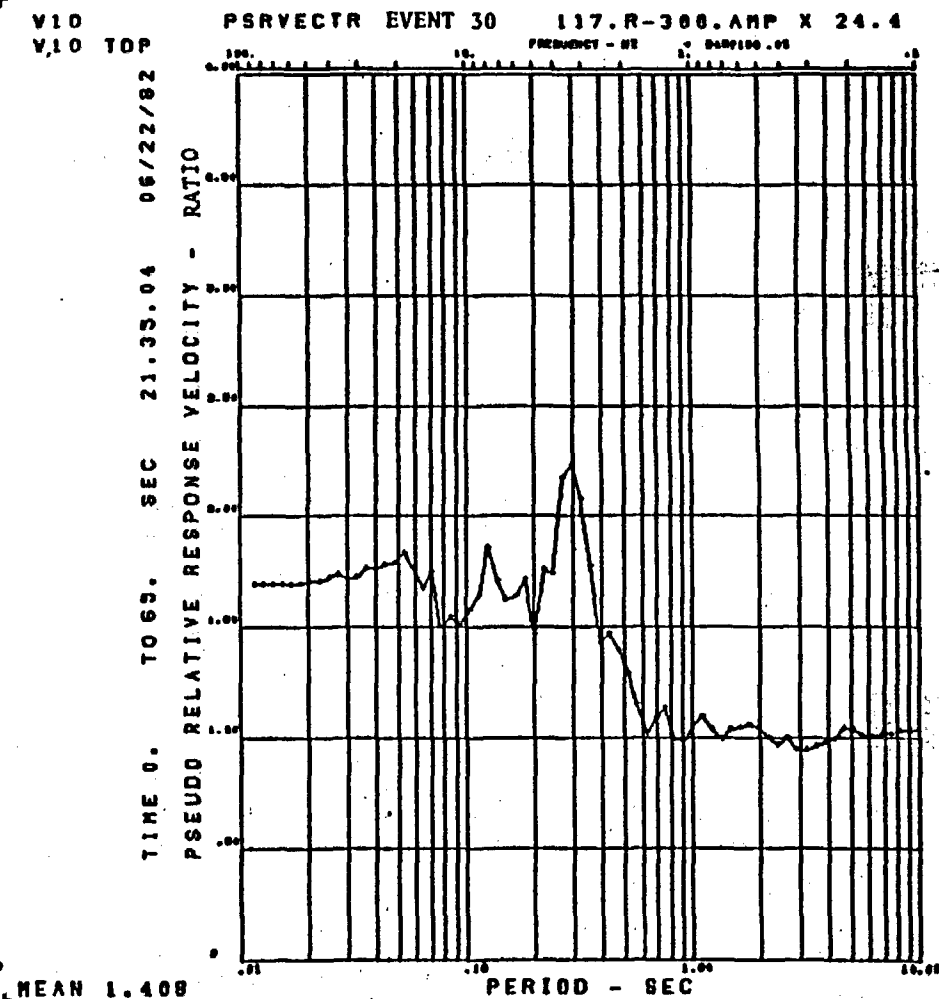


Figure B-2b

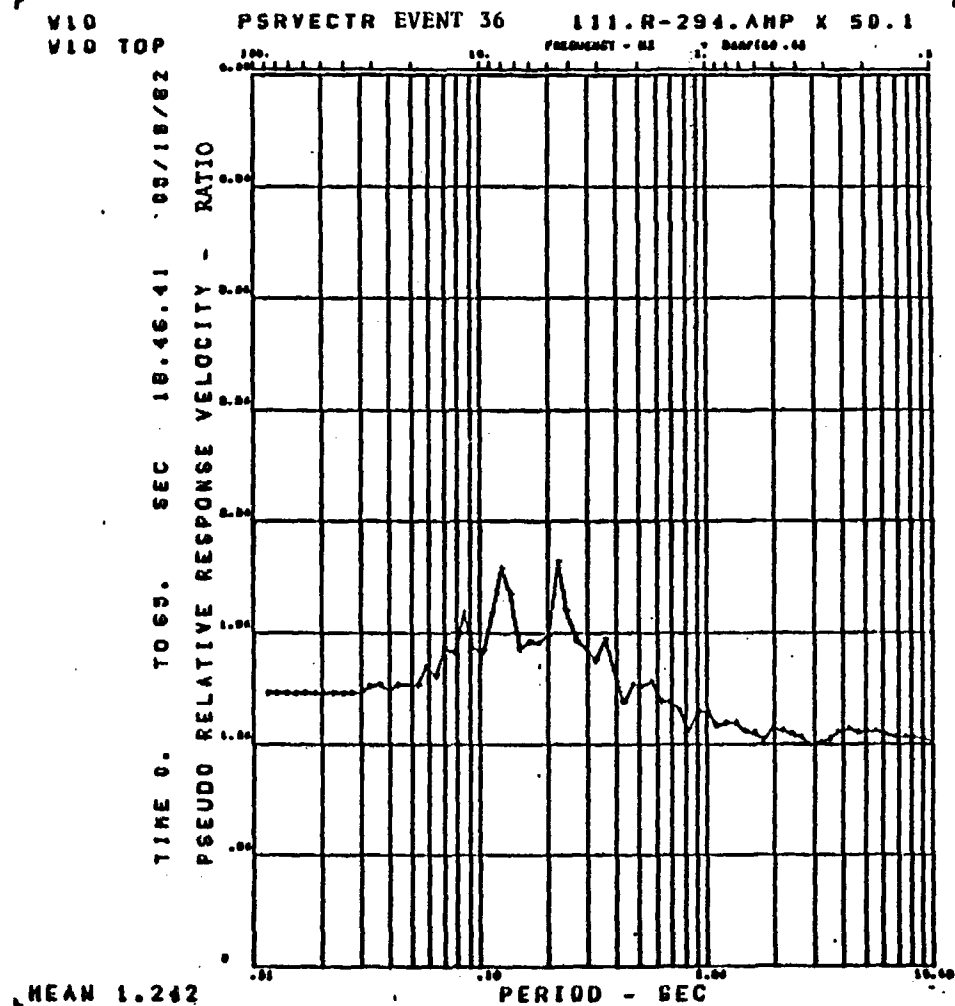


Figure B-3a

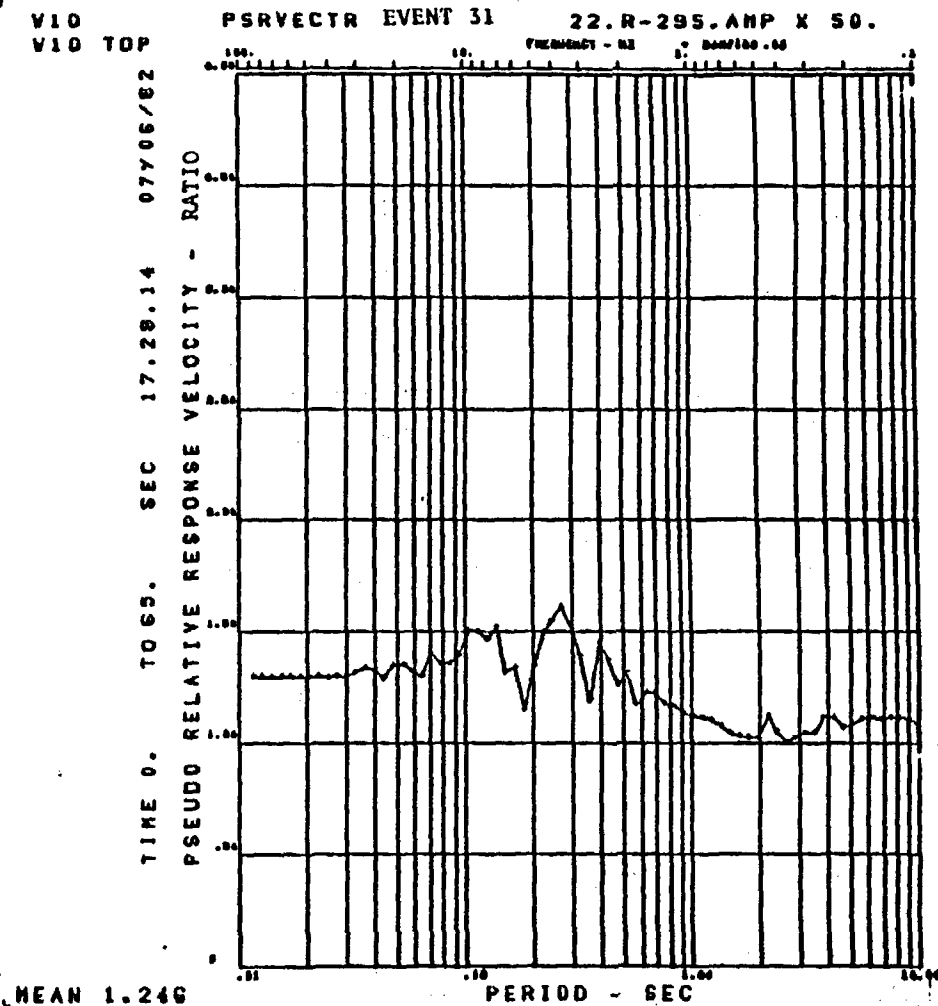


Figure B-3b

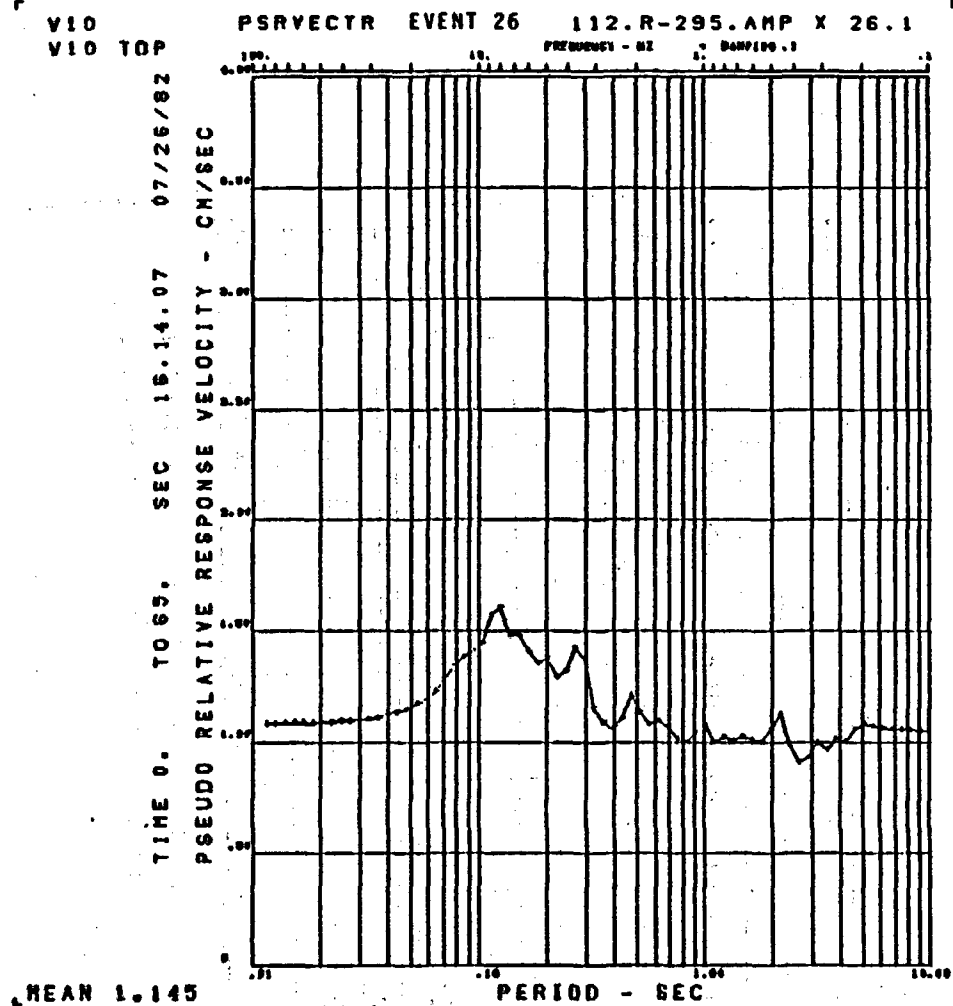


Figure B-4a

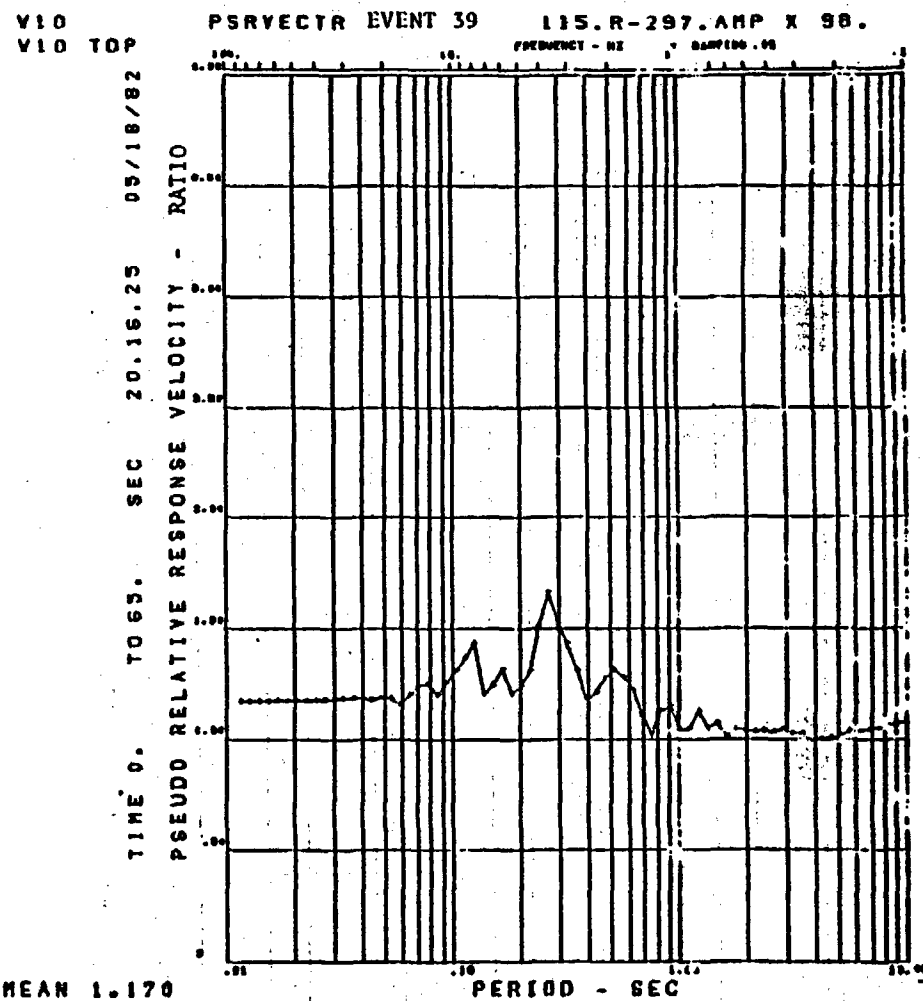


Figure B-4b

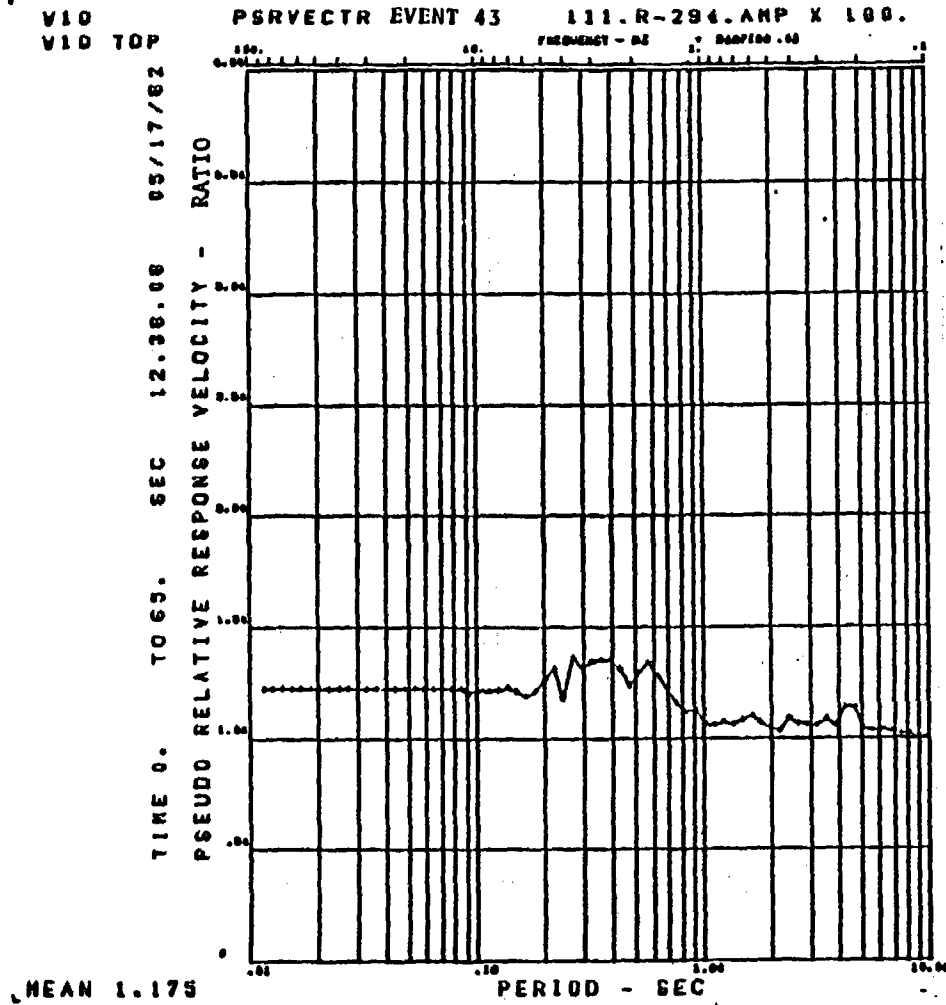


Figure B-5a

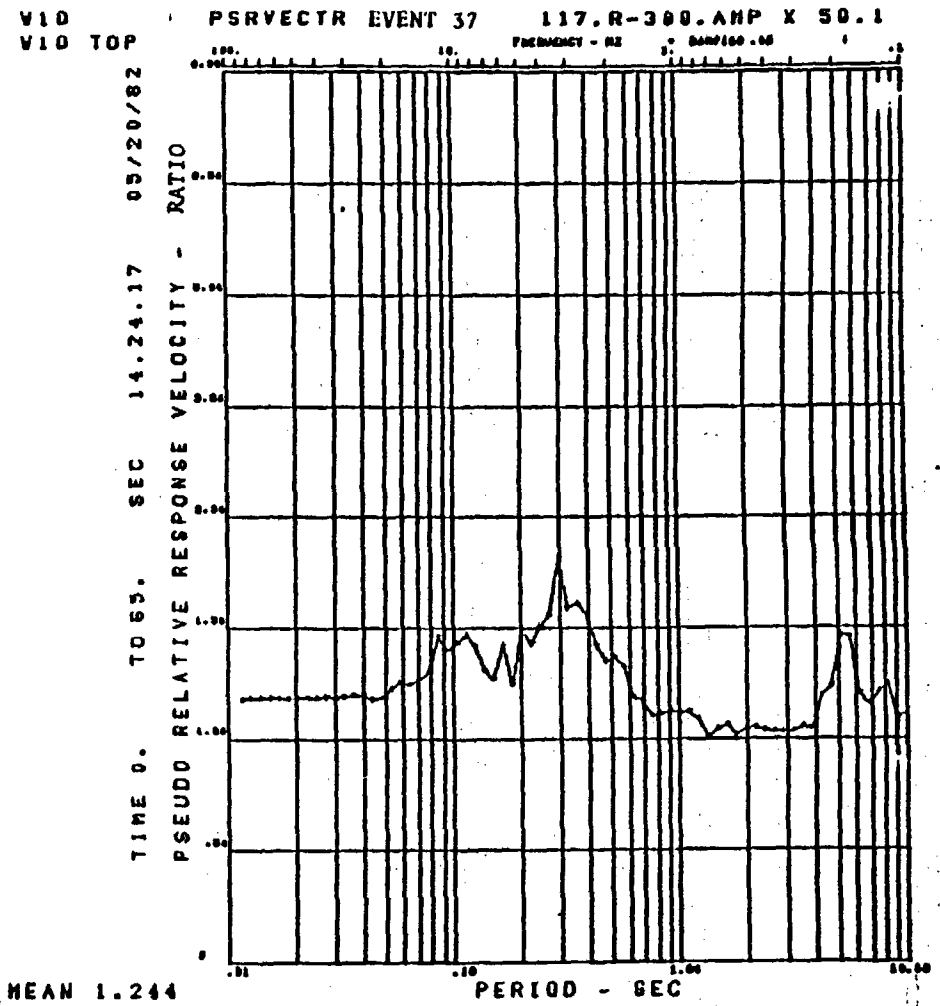


Figure B-5b

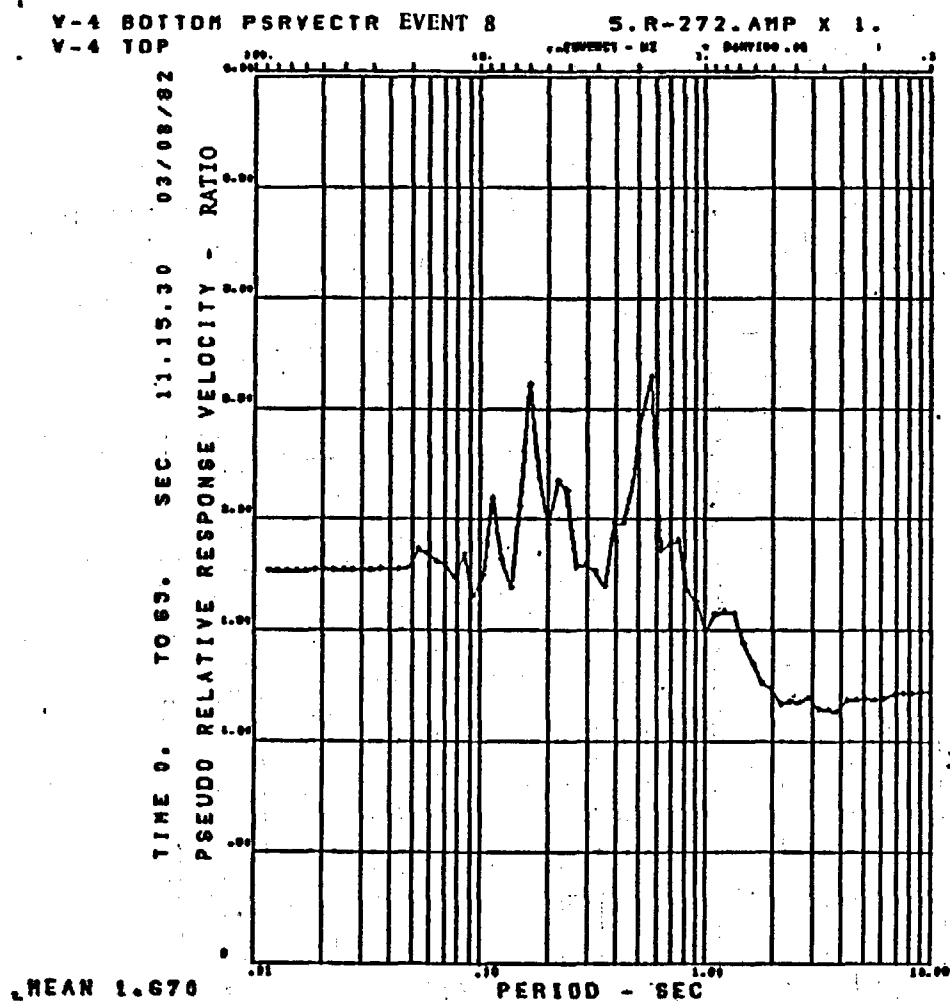


Figure B-6a

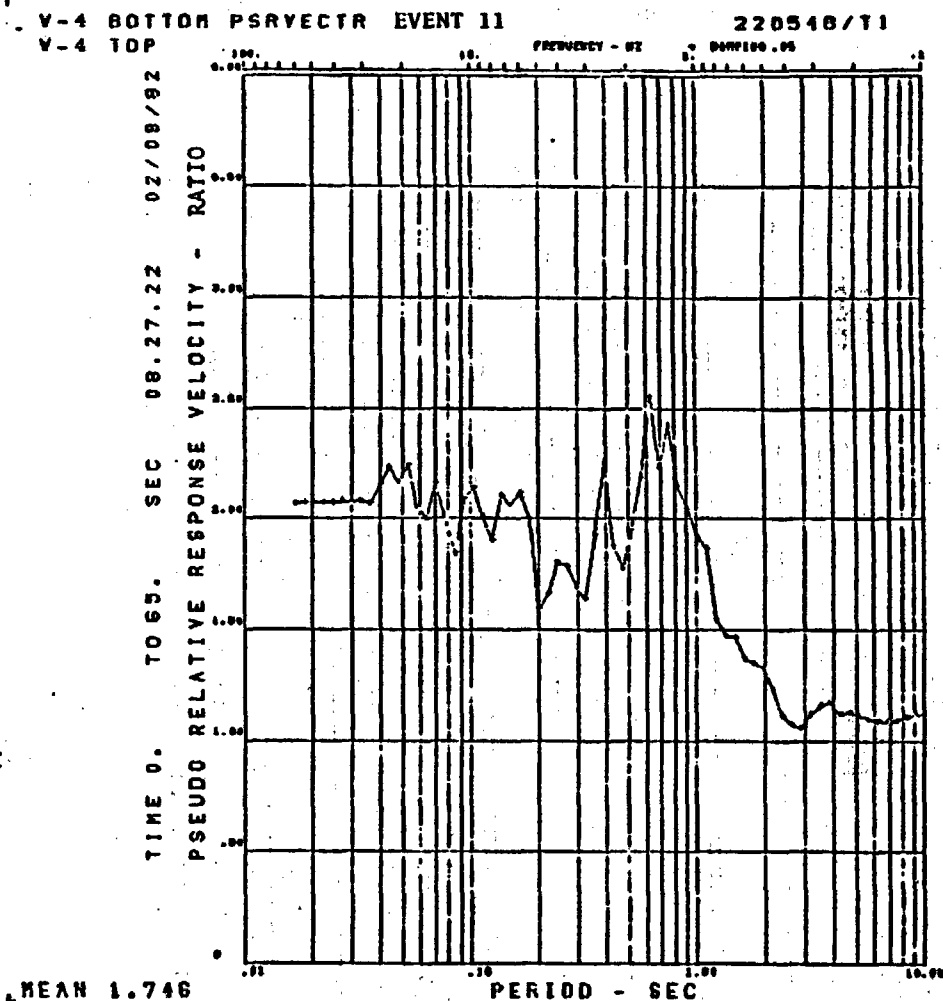


Figure 3-6b

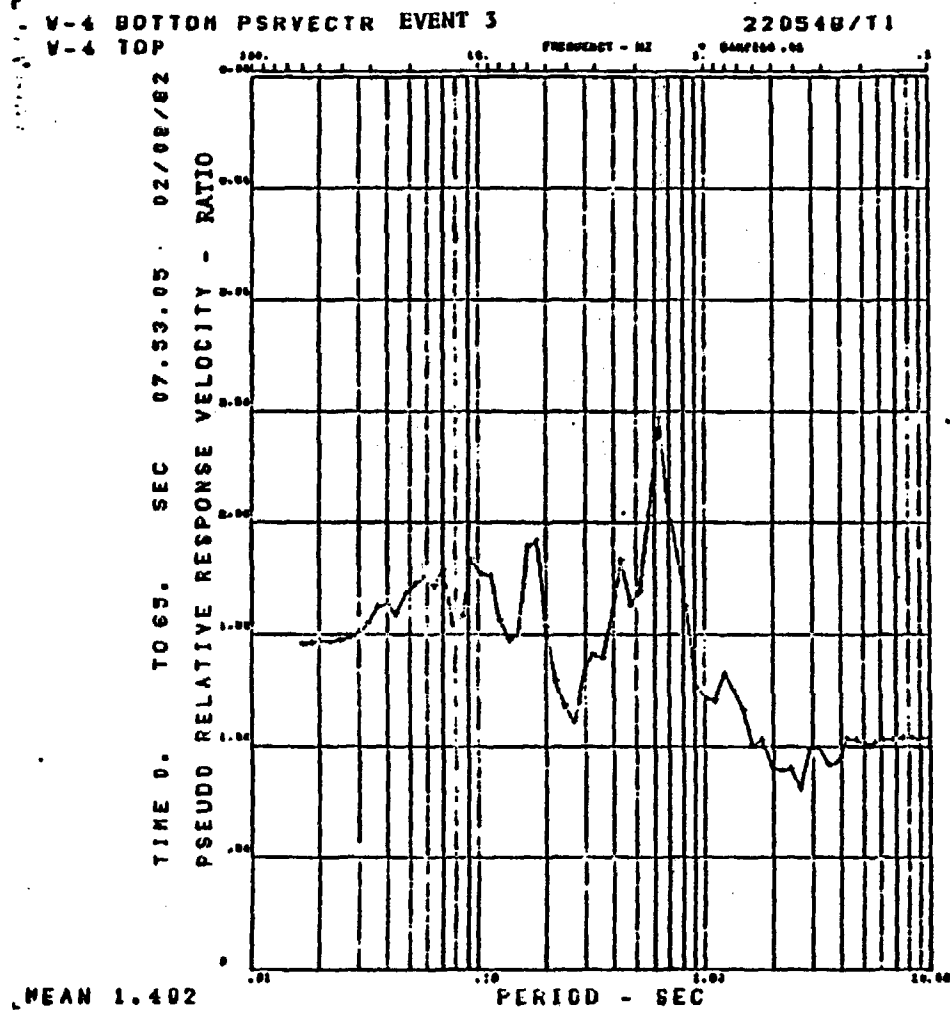


Figure B-7a

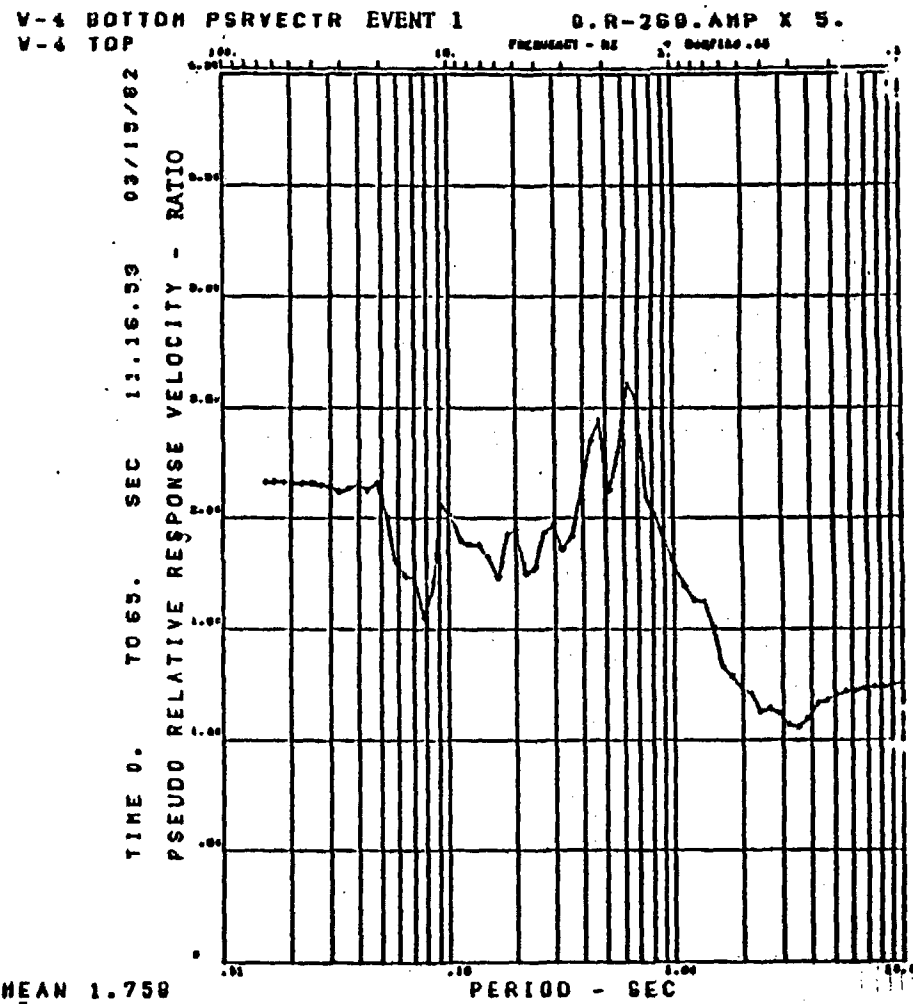


Figure B-7b

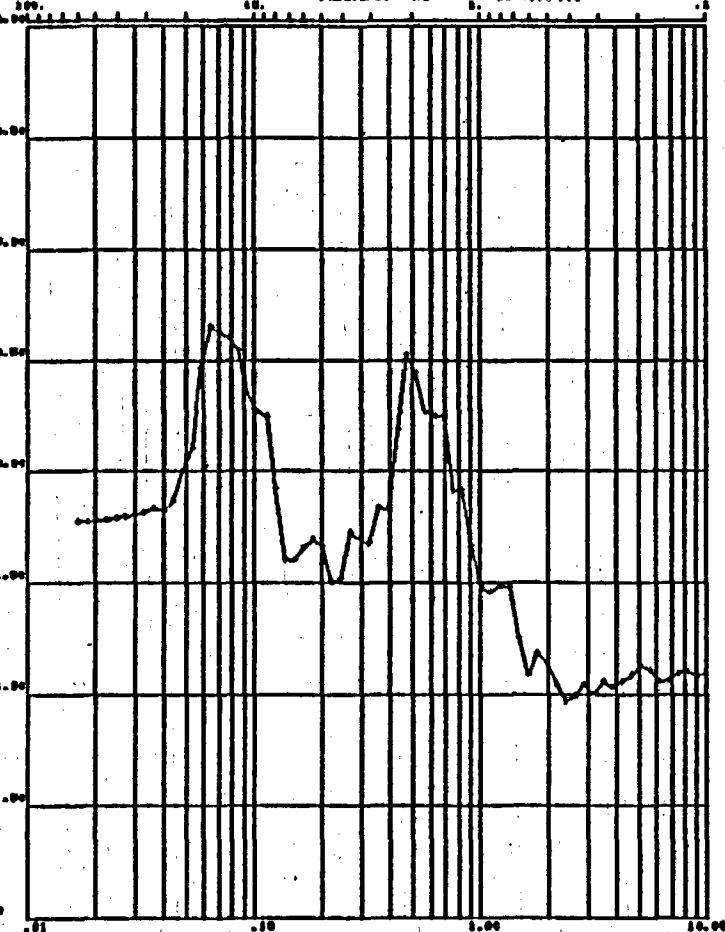
V-4 BOTTOM PSRVECTR EVENT 13

220548/1

V-4 TOP

TIME 0. TO 65. SEC 13.12.16 08/09/82

PSEUDO RELATIVE RESPONSE VELOCITY - CM/SEC



MEAN 1.669

PERIOD - SEC

Figure B-8a

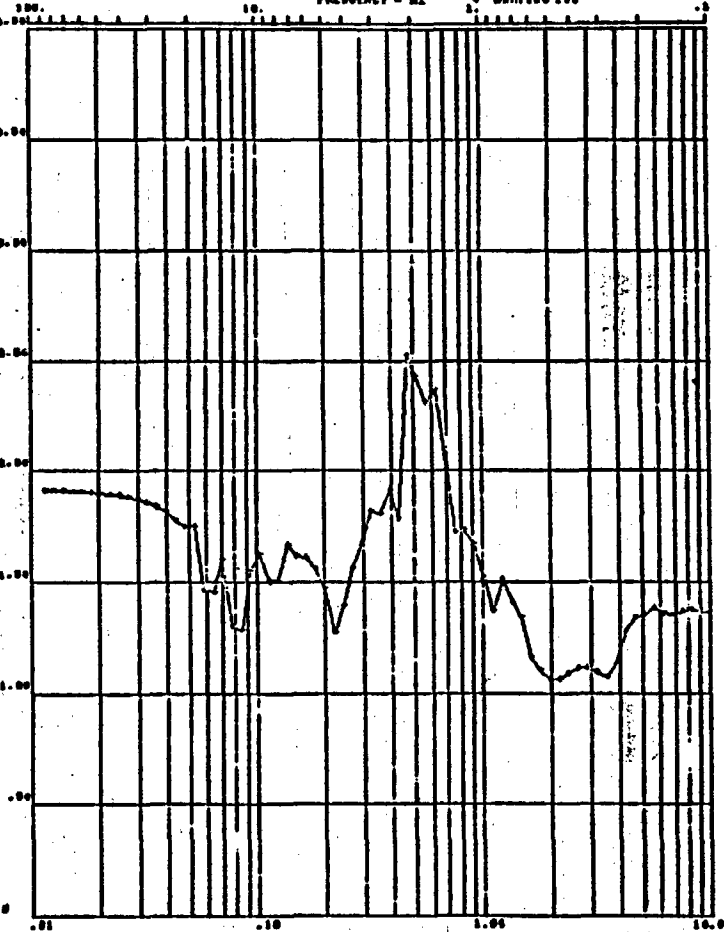
V-4 BOTTOM PSRVECTR EVENT 16

3.79R AMP X 5.

V-4 TOP

TIME 0. TO 65. SEC 08.19.34 02/08/82

PSEUDO RELATIVE RESPONSE VELOCITY - RATIO



MEAN 1.591

PERIOD - SEC

Figure B-8b

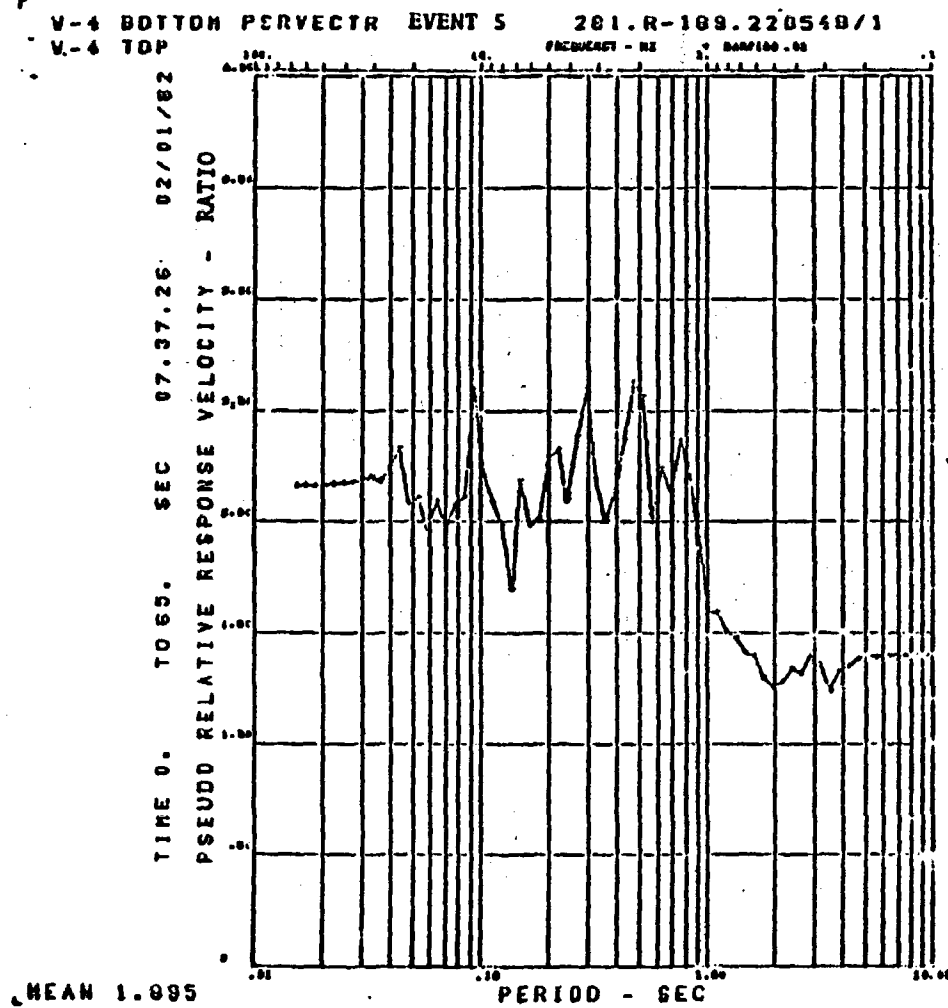


Figure B-9a

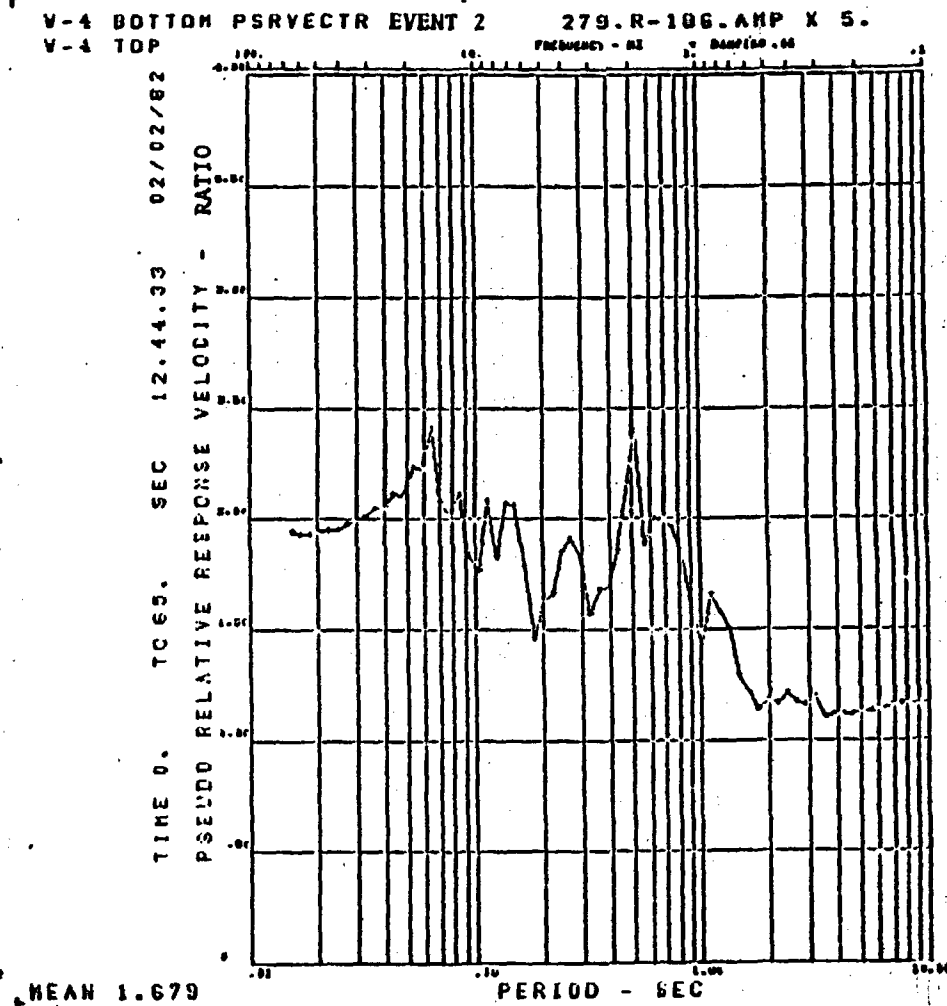


Figure B-9b

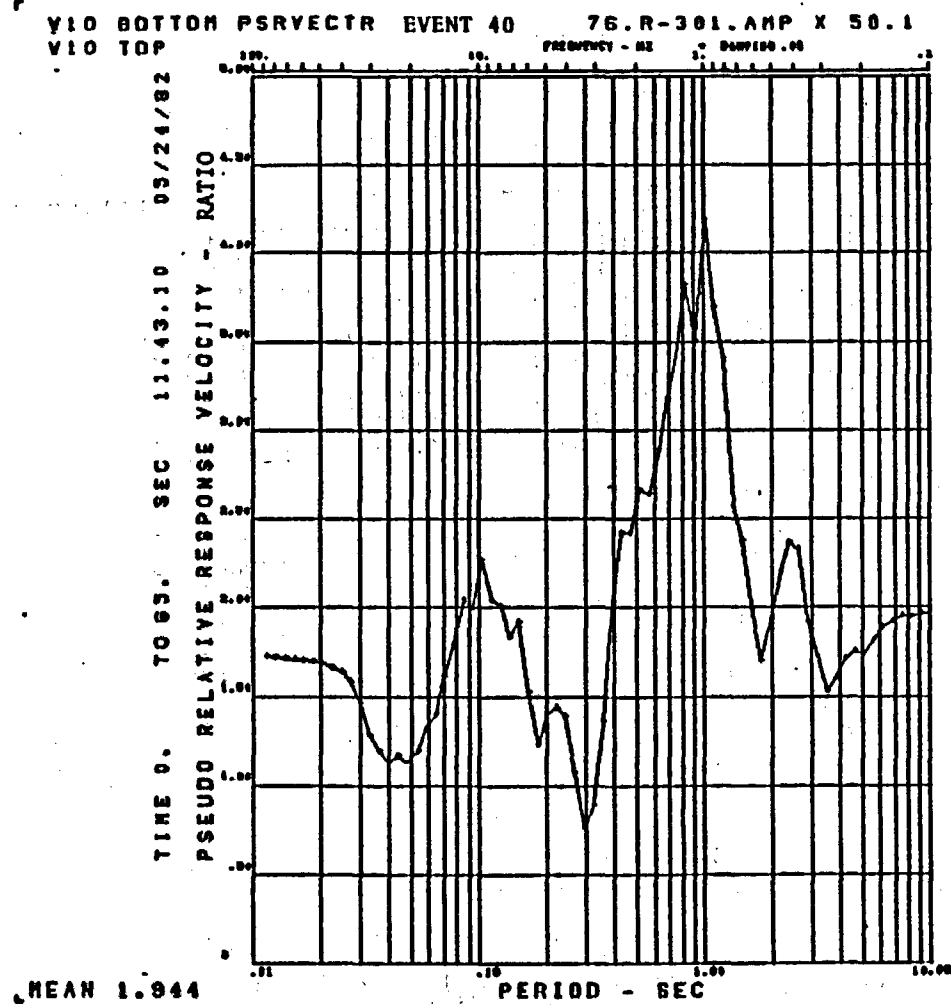


Figure B-10a

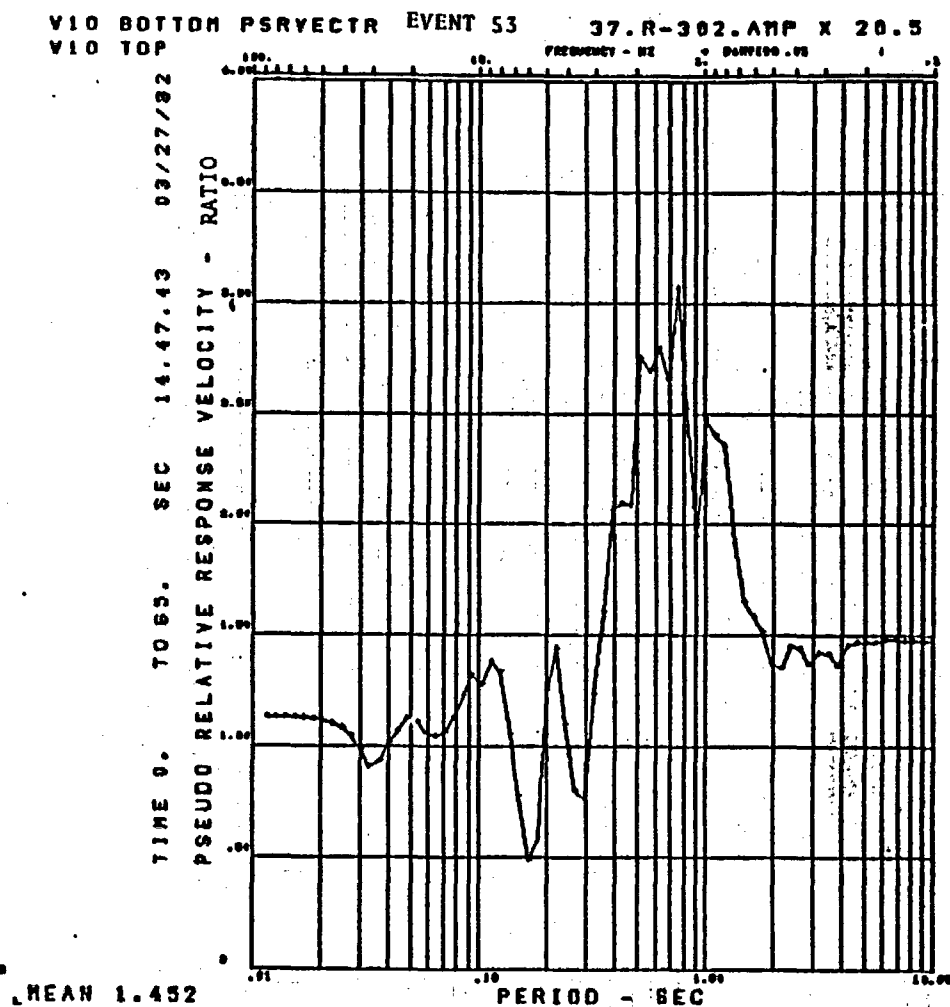


Figure B-10b

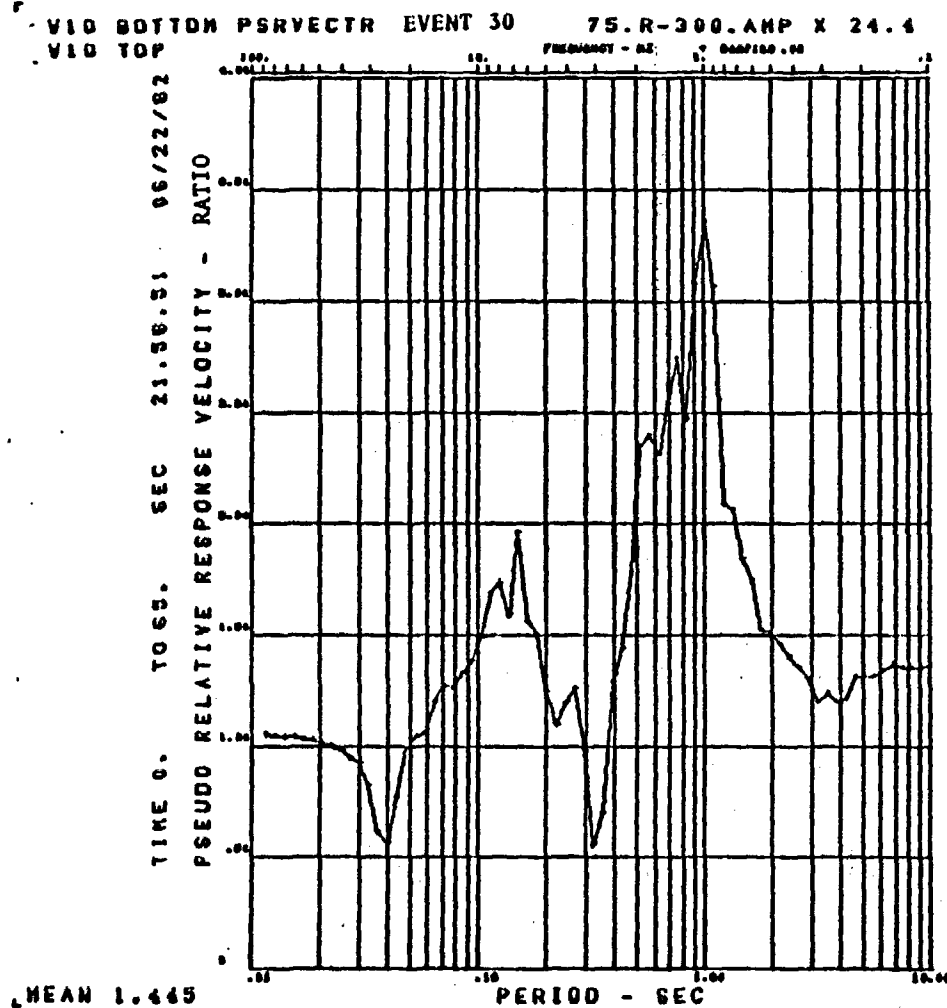


Figure 8-11a

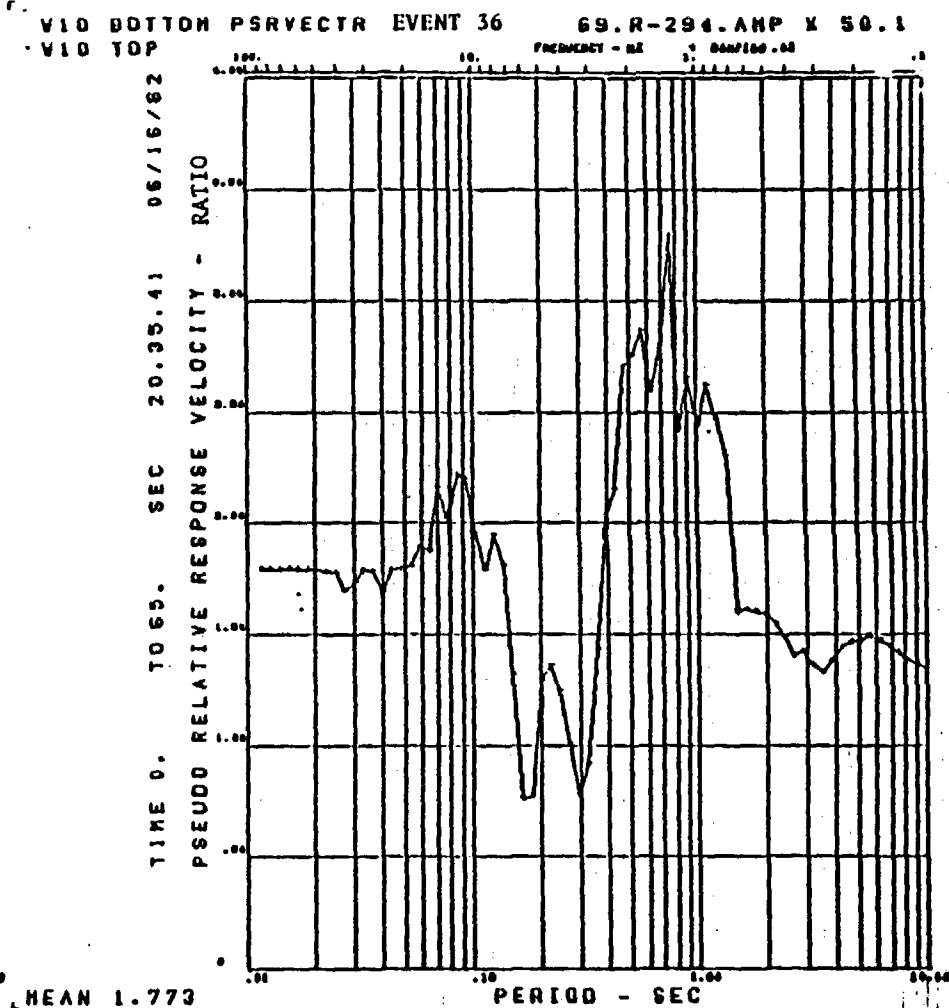


Figure 8-11b

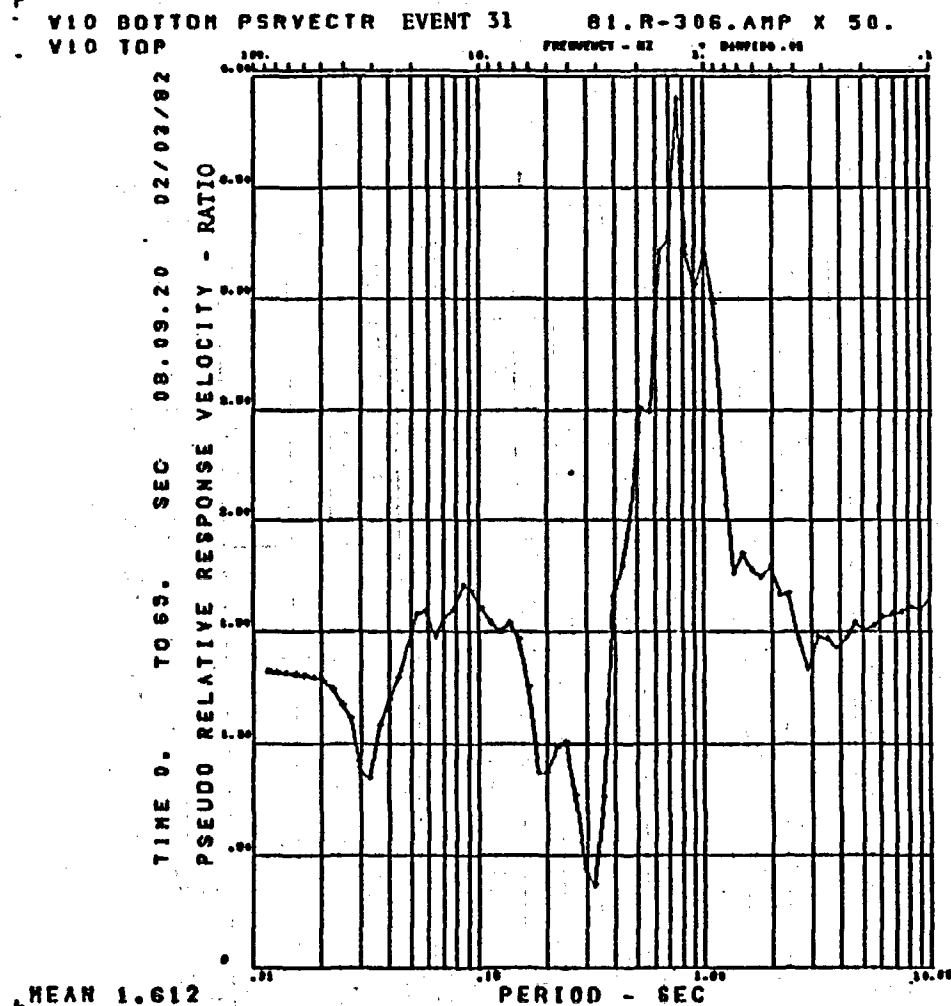


Figure B-12a

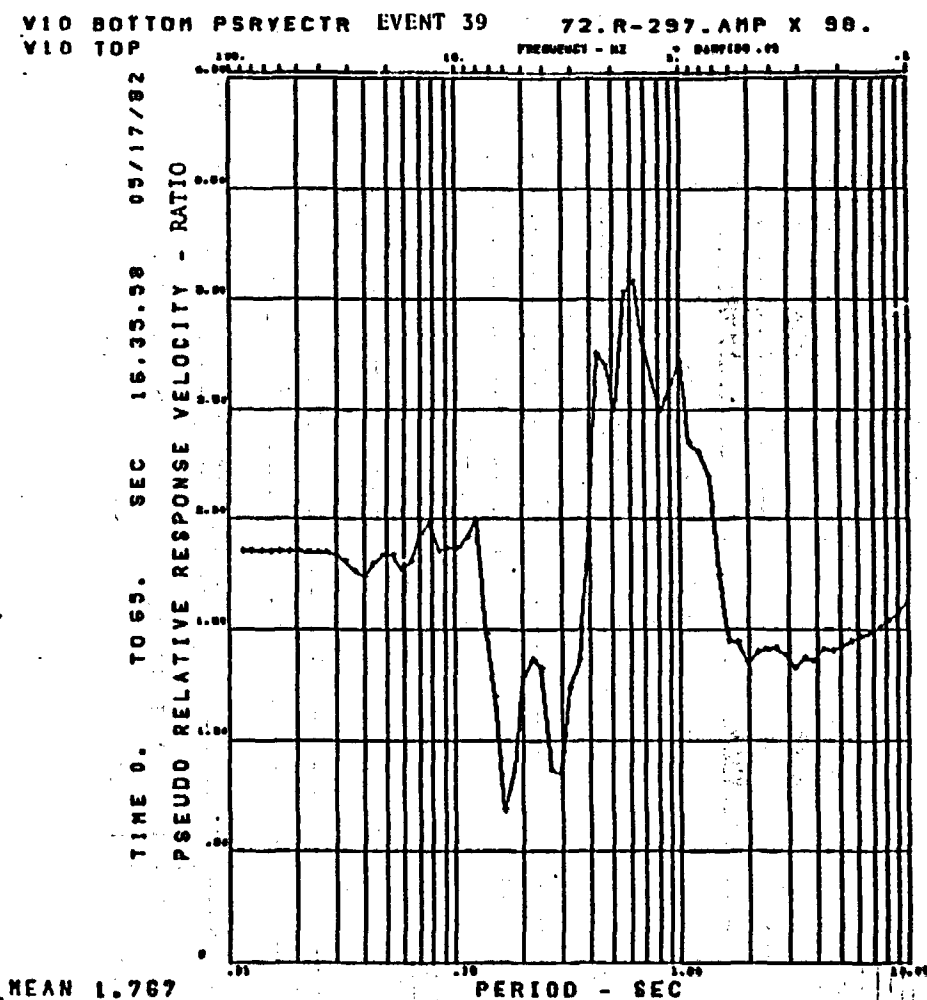


Figure B-12b

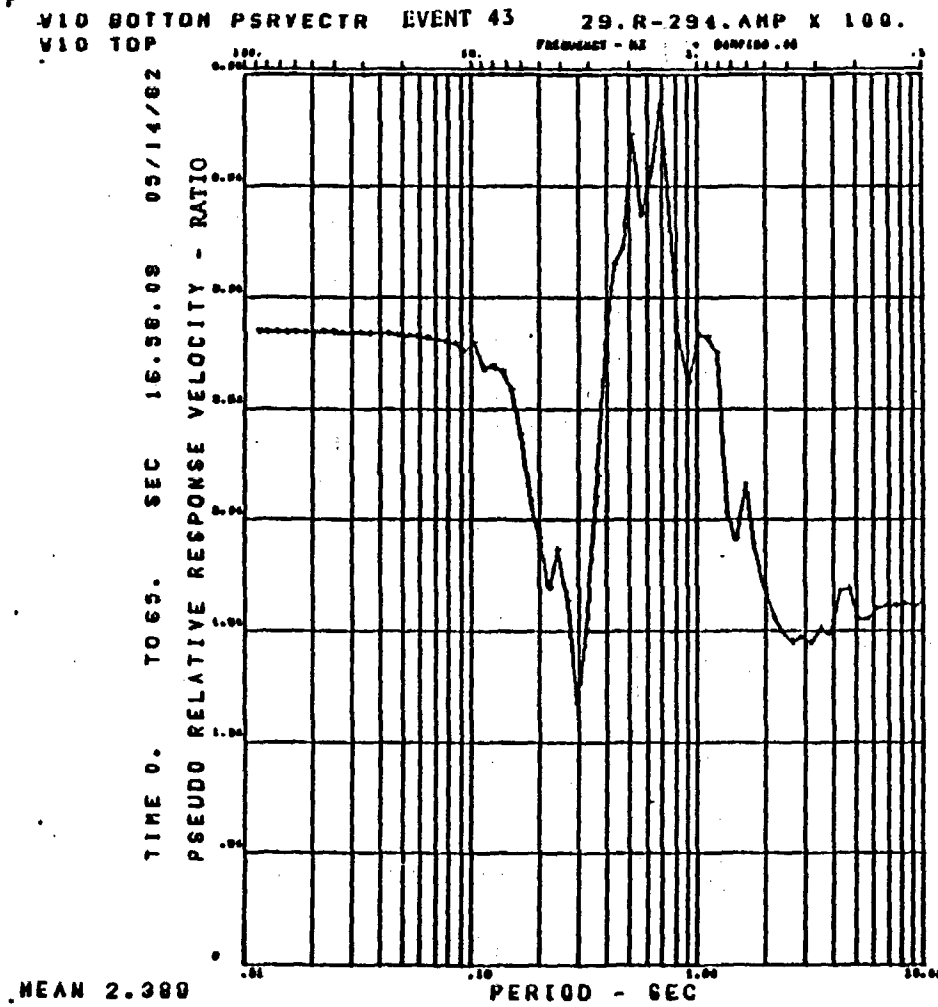


Figure B-13a

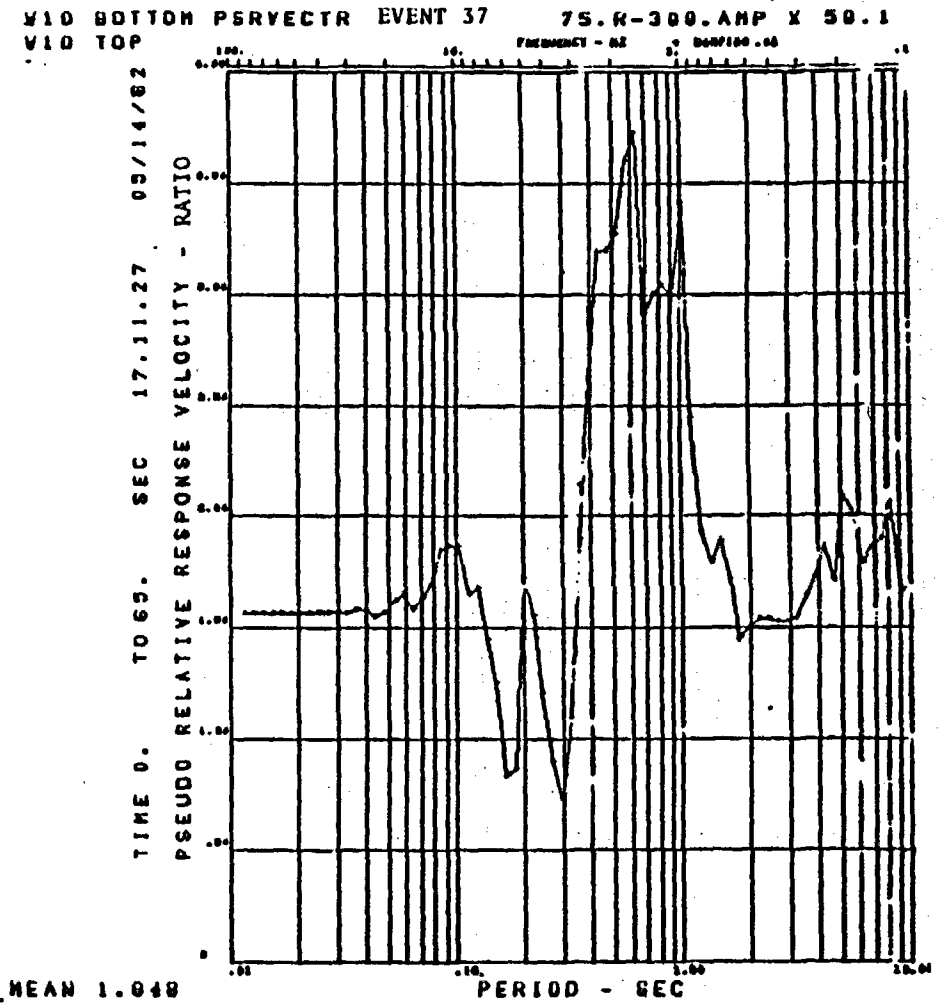


Figure B-13b

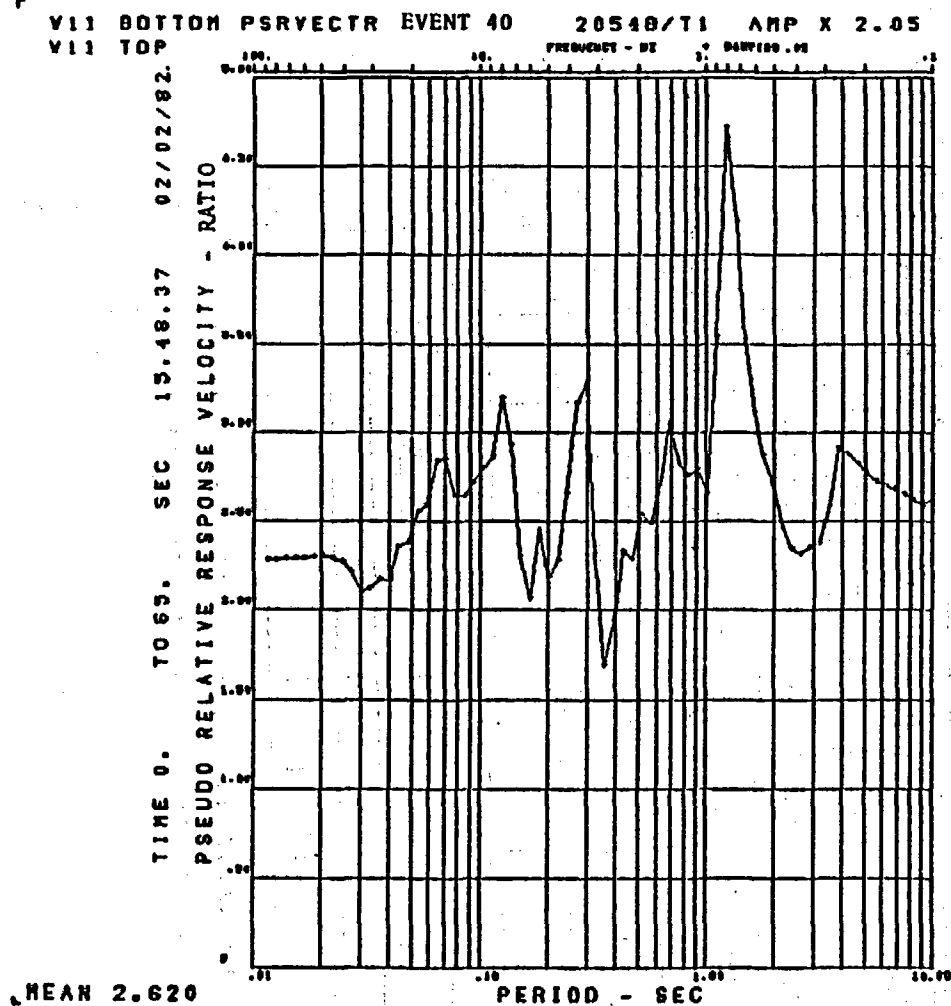


Figure B-14a

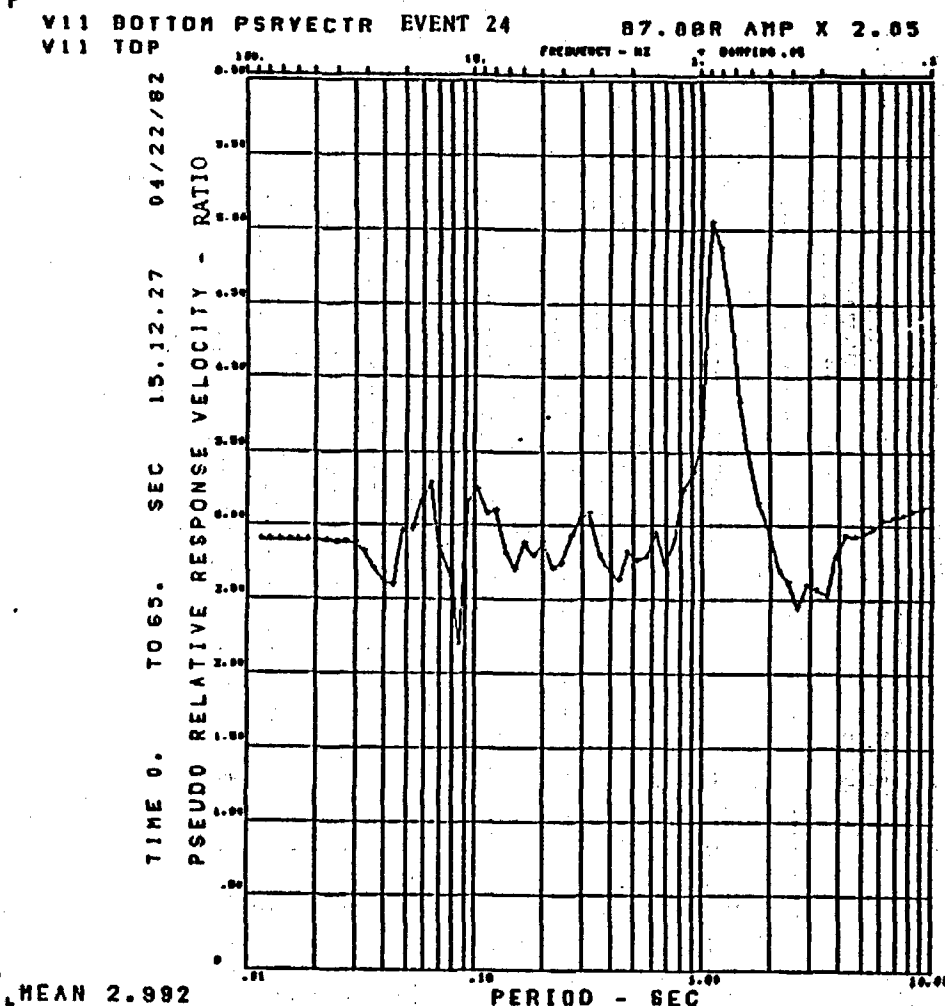


Figure B-14b

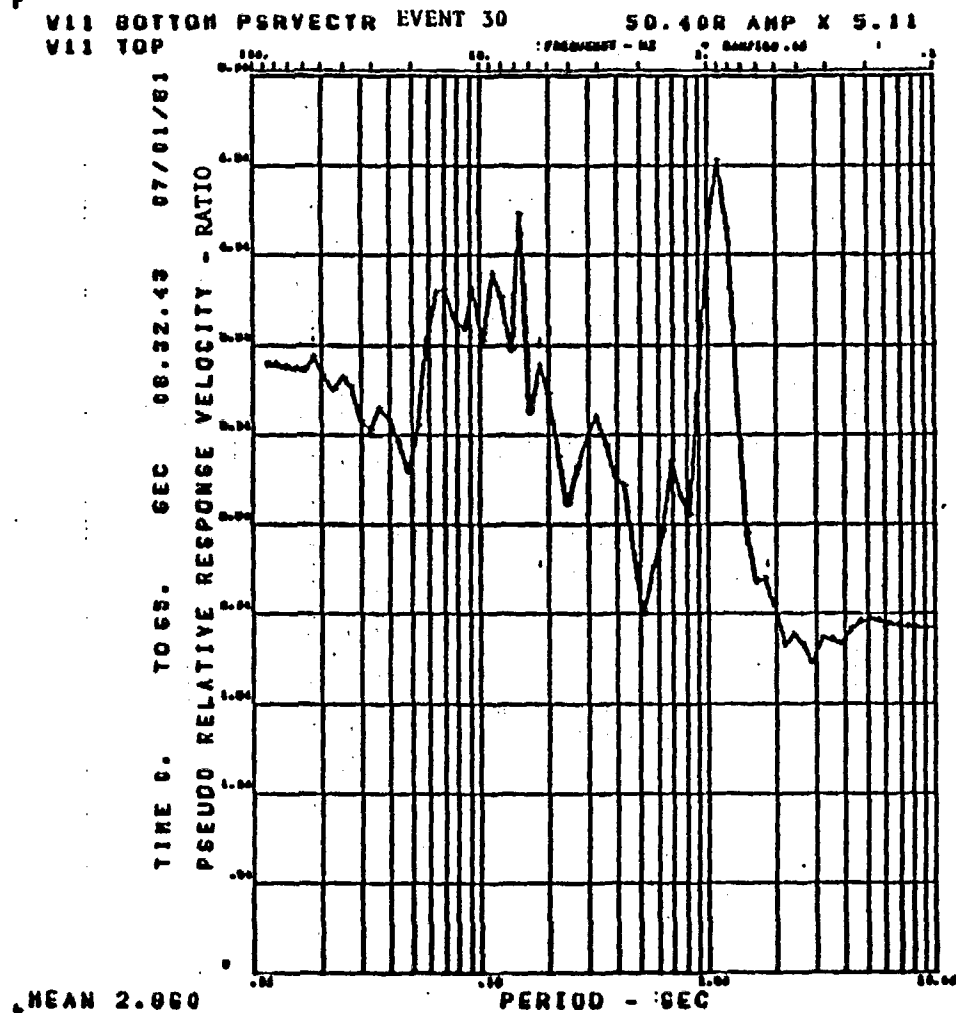


Figure B-15a

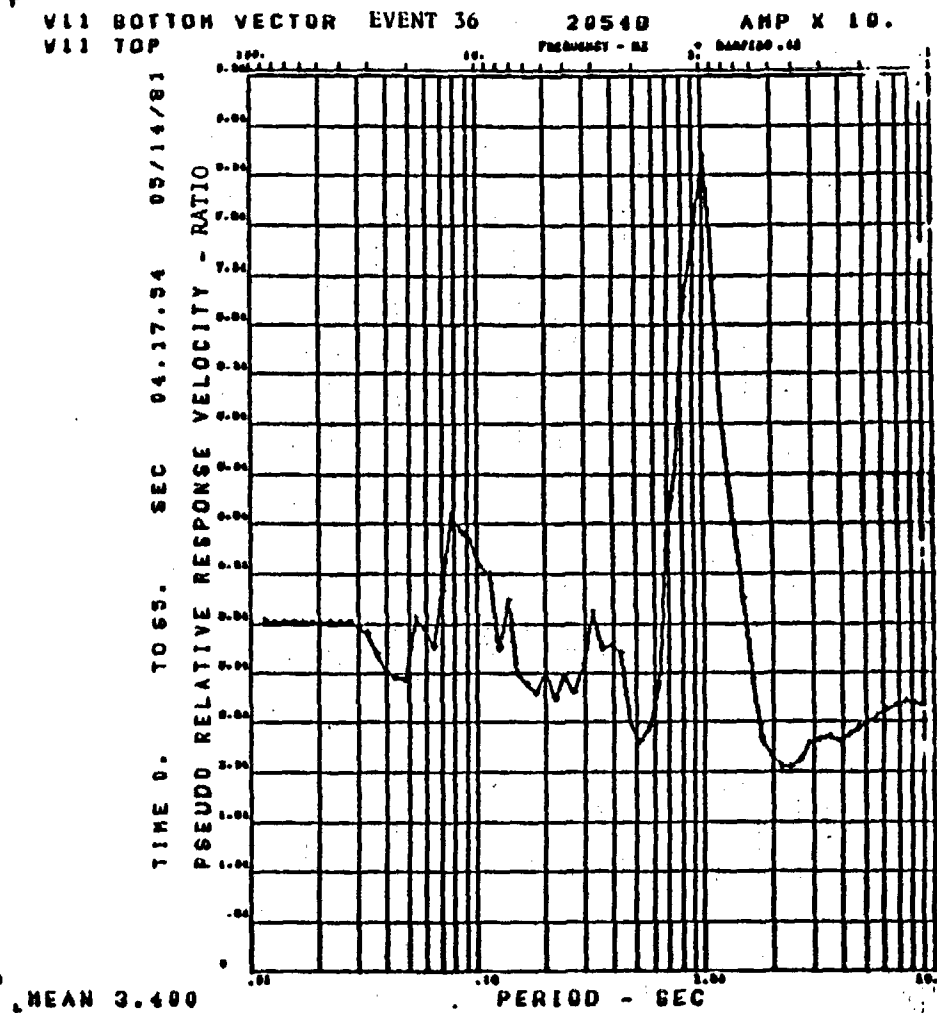


Figure B-15b

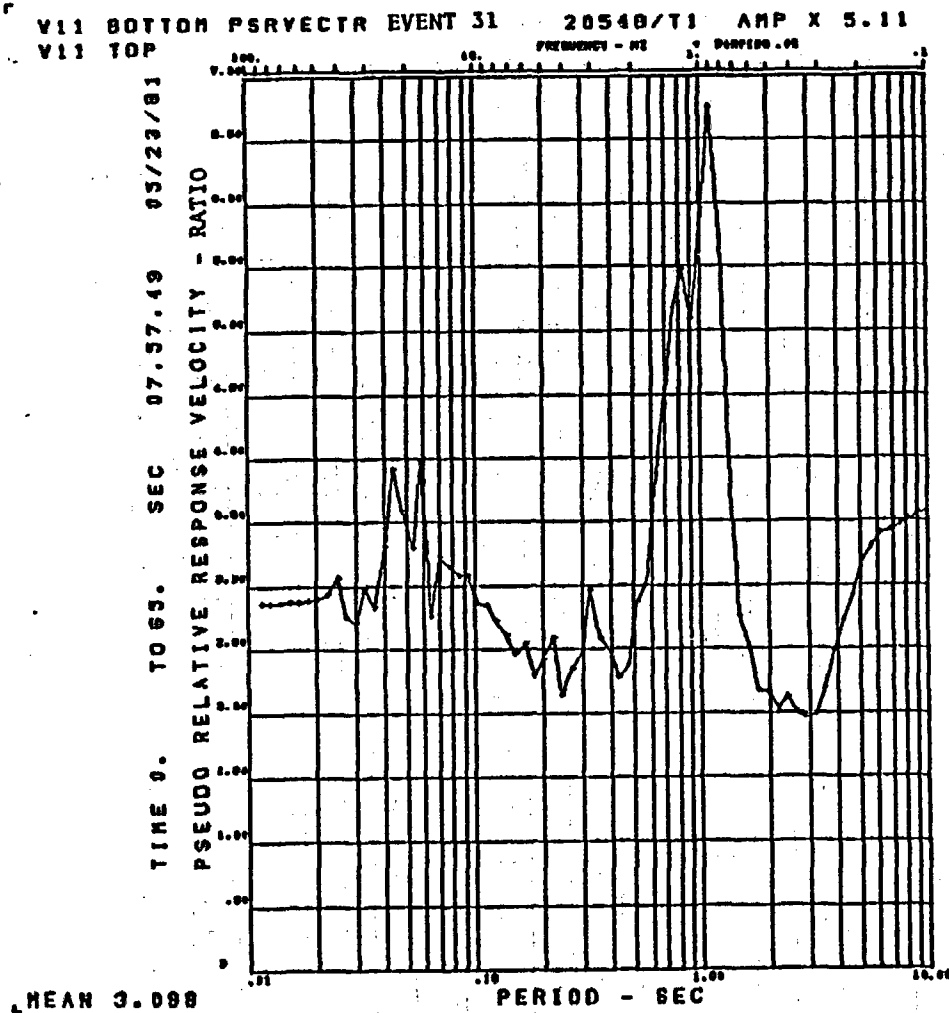


Figure 8-16a

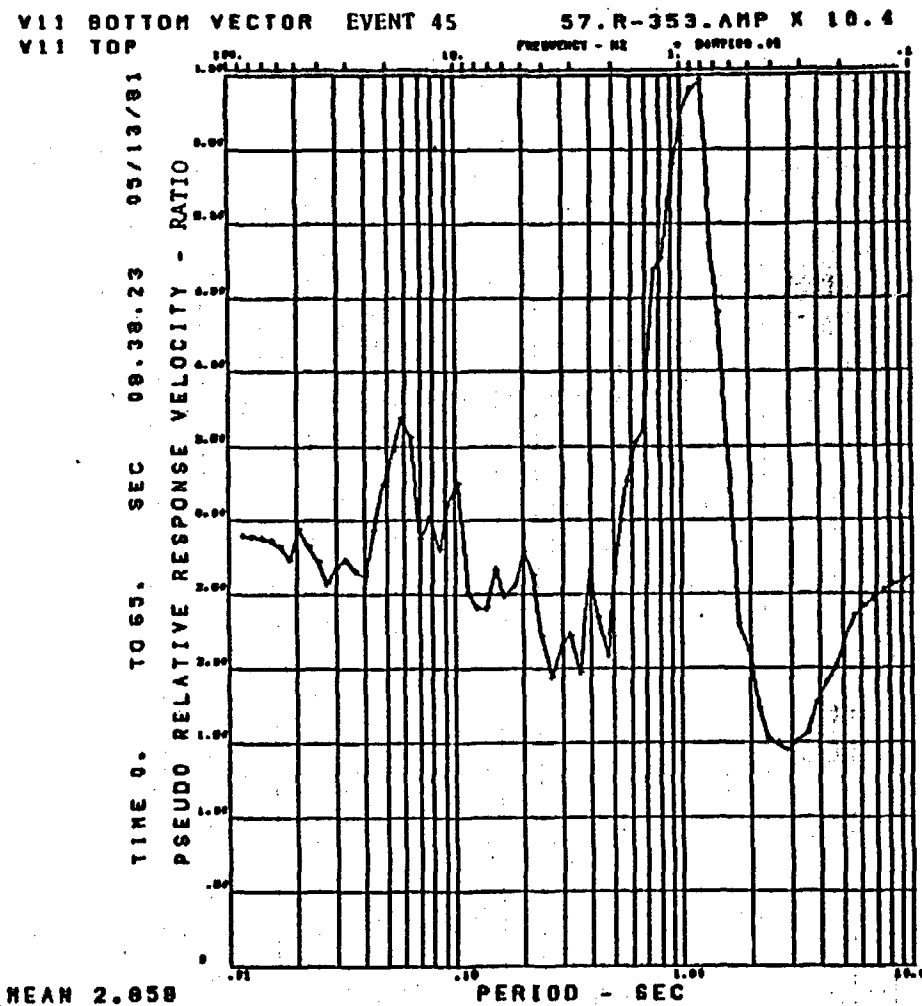


Figure 8-16b

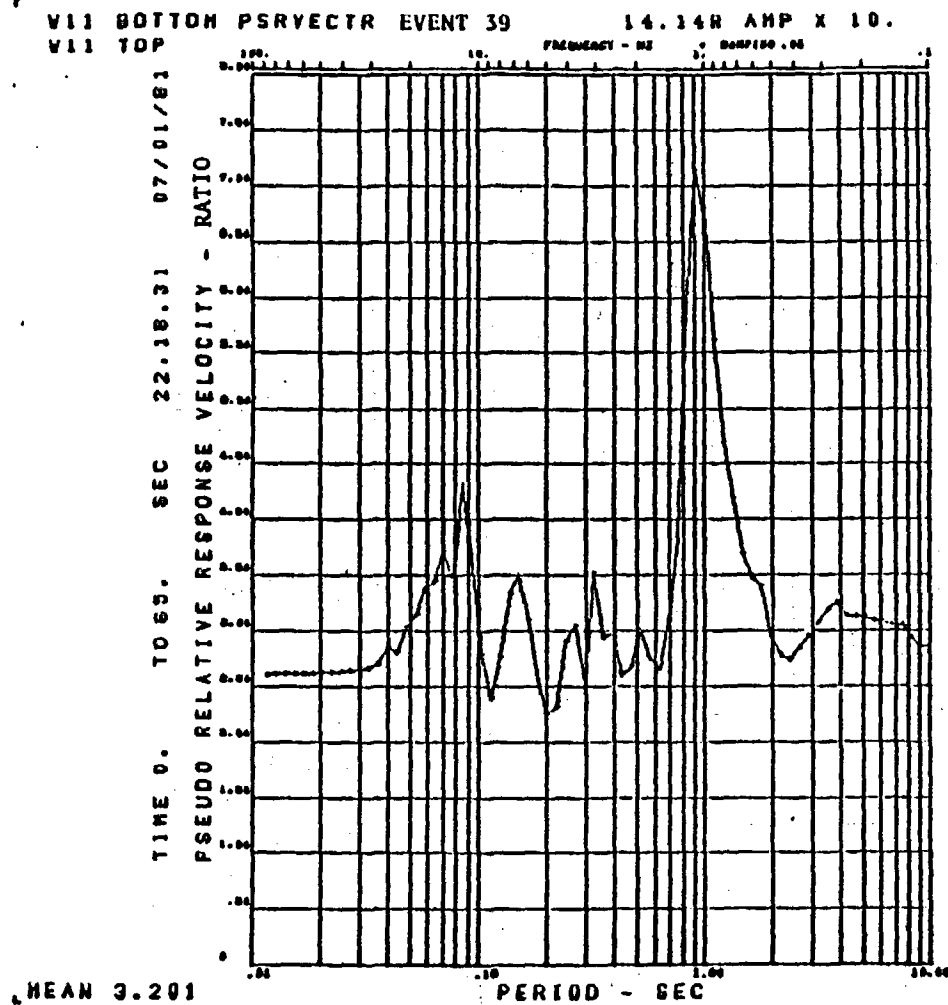


Figure B-17a

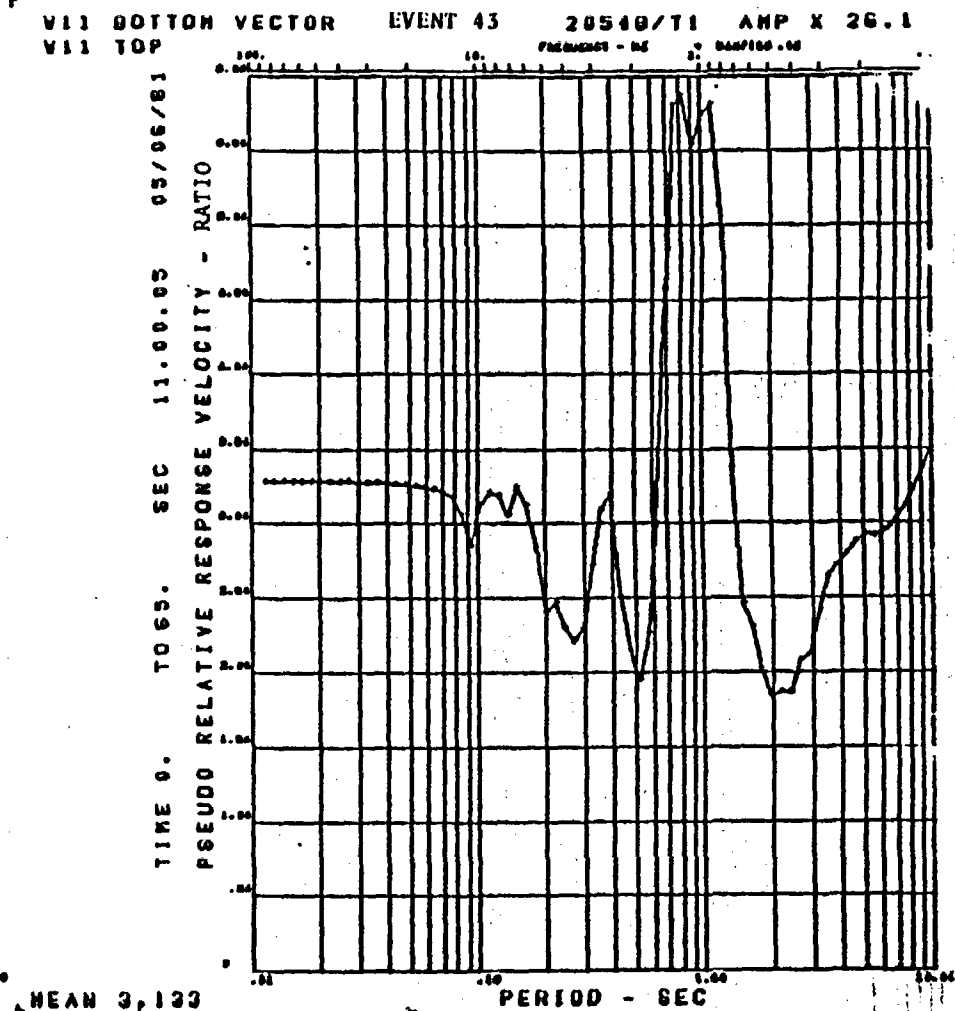


Figure B-17b

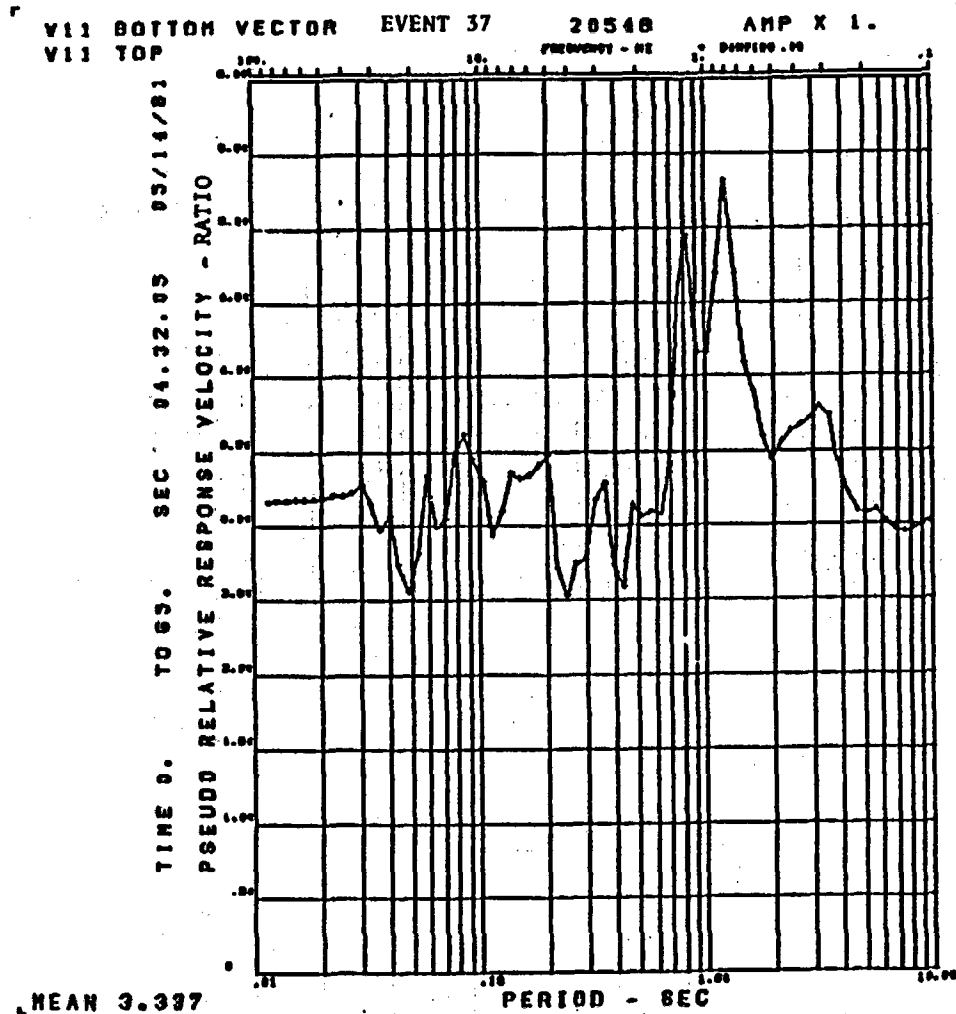


Figure B-18a

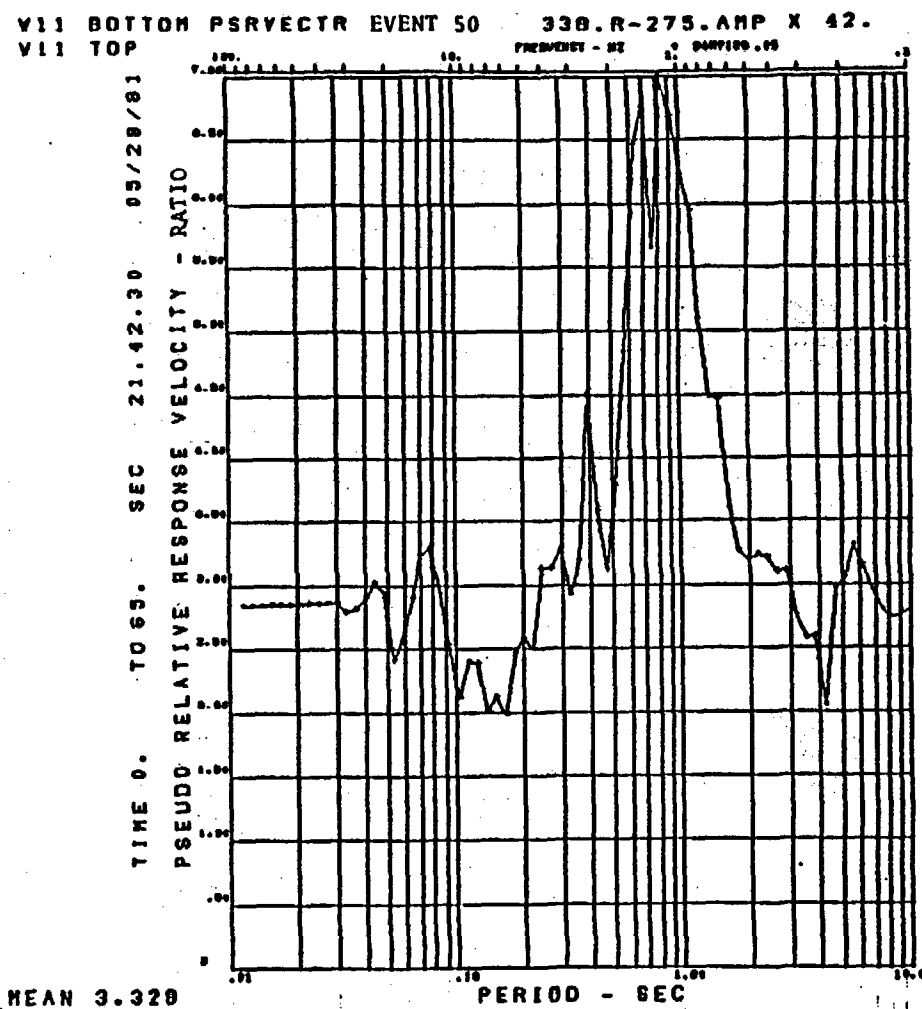


Figure B-18b

V11 BOTTOM VECTOR EVENT 38 20548 AMP X 100.
V11 TOP

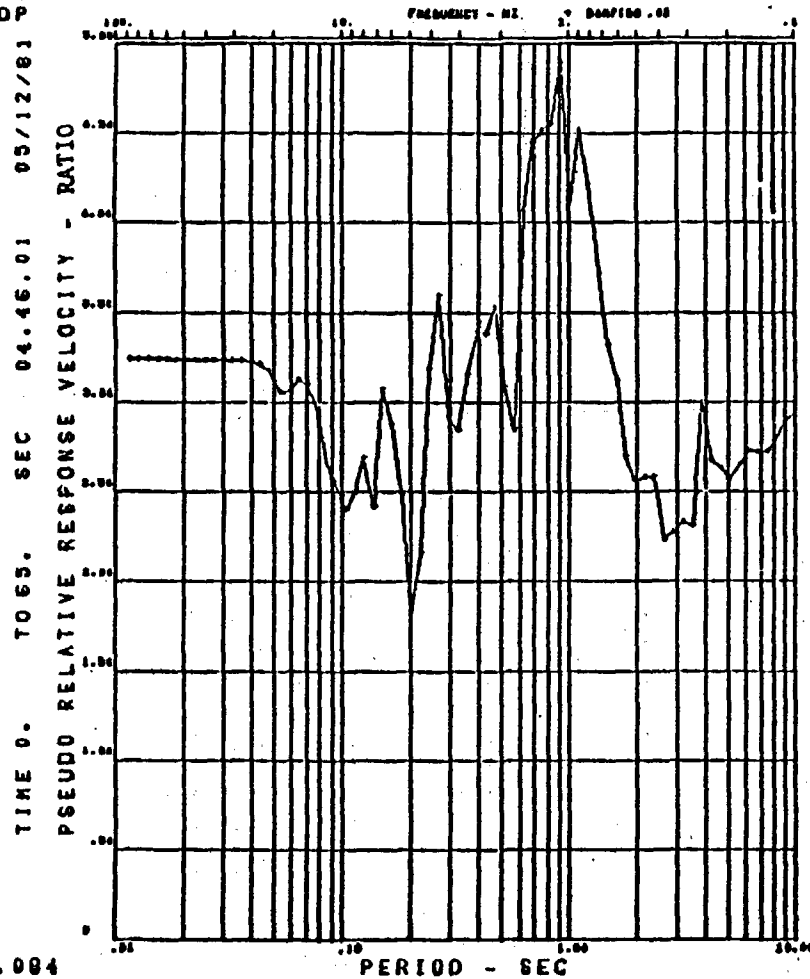


Figure B-19a

V11 BOTTOM VECTOR EVENT 42 342.R-279, AMP X 10.
V11 TOP

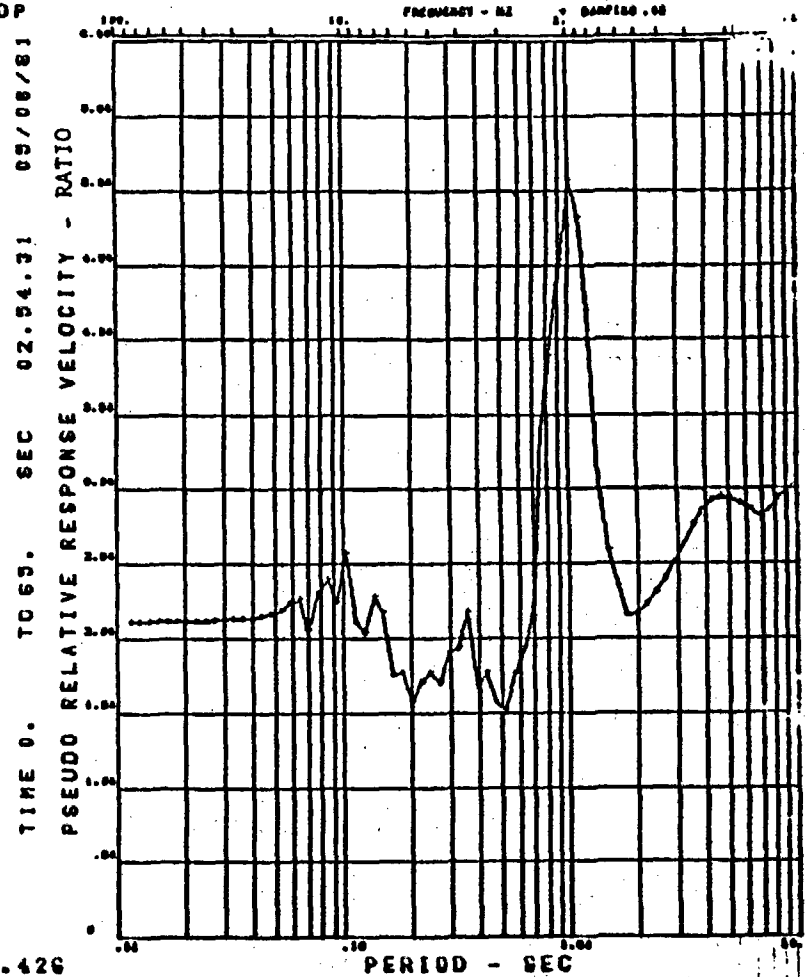


Figure B-19b

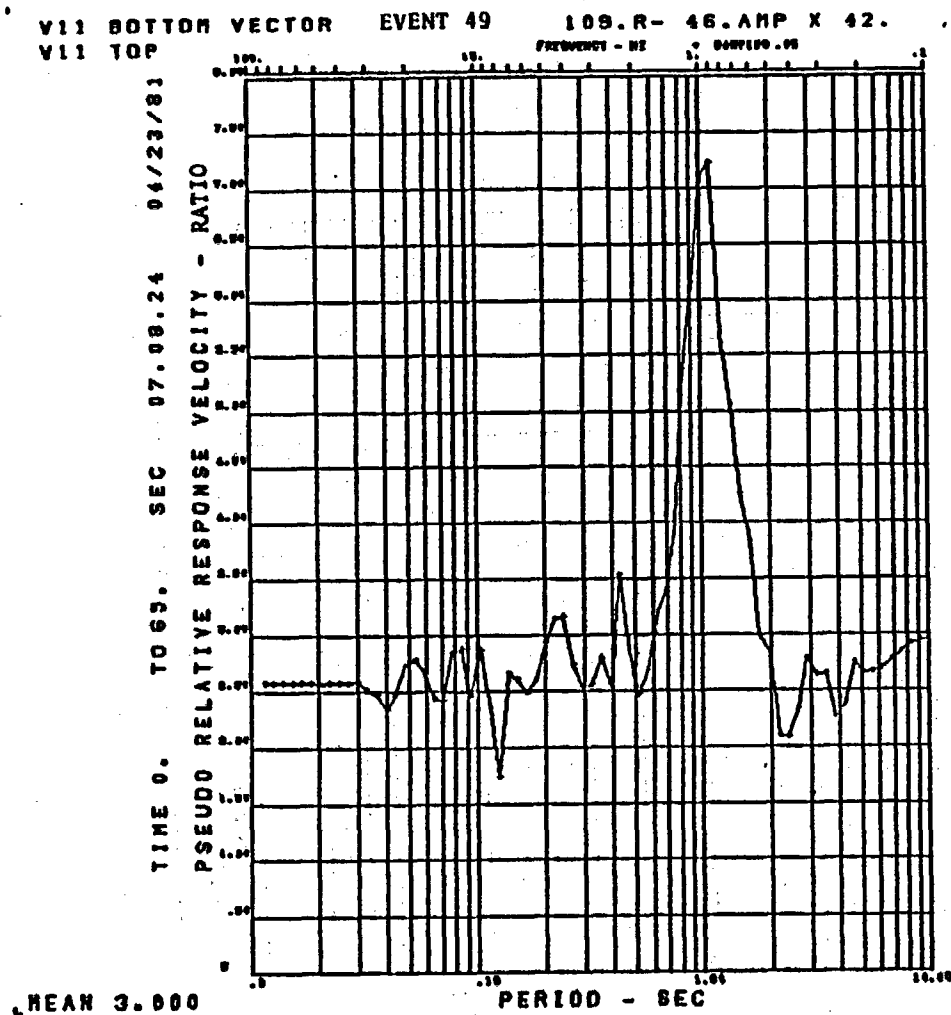


Figure B-20a

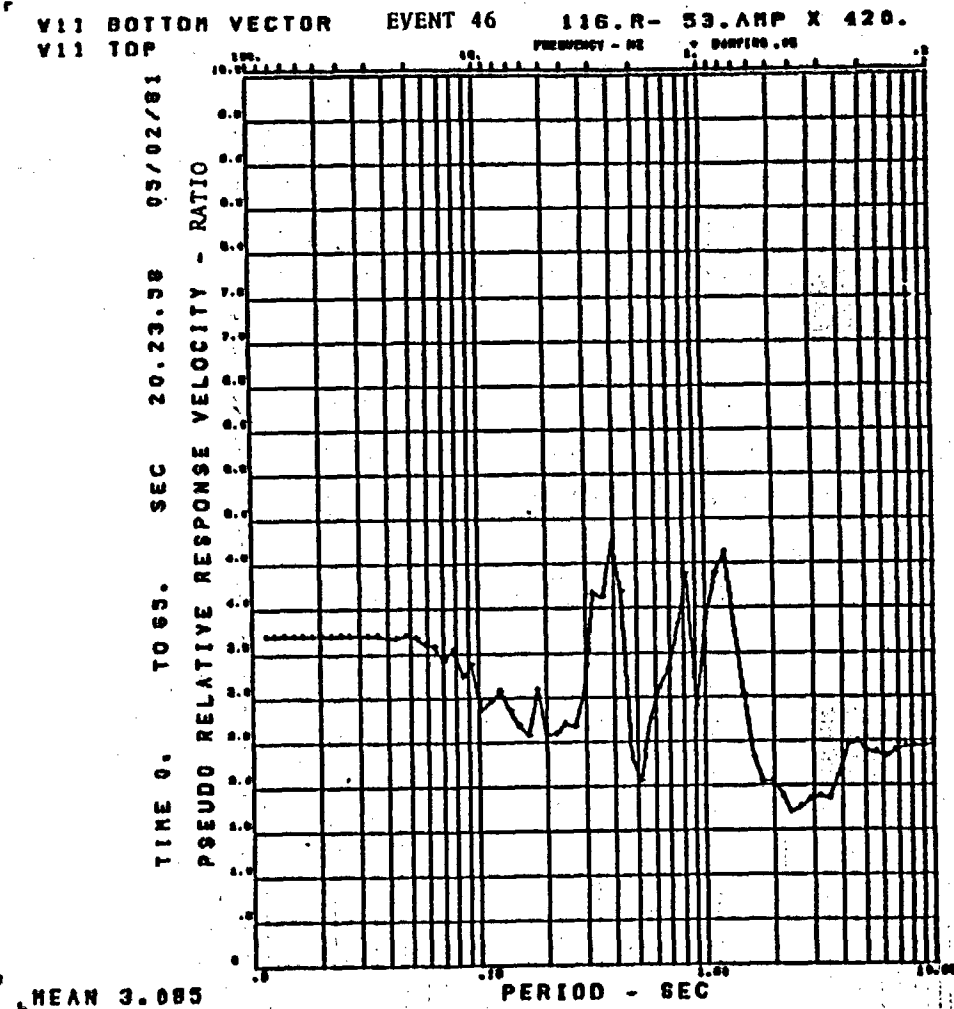


Figure B-20b

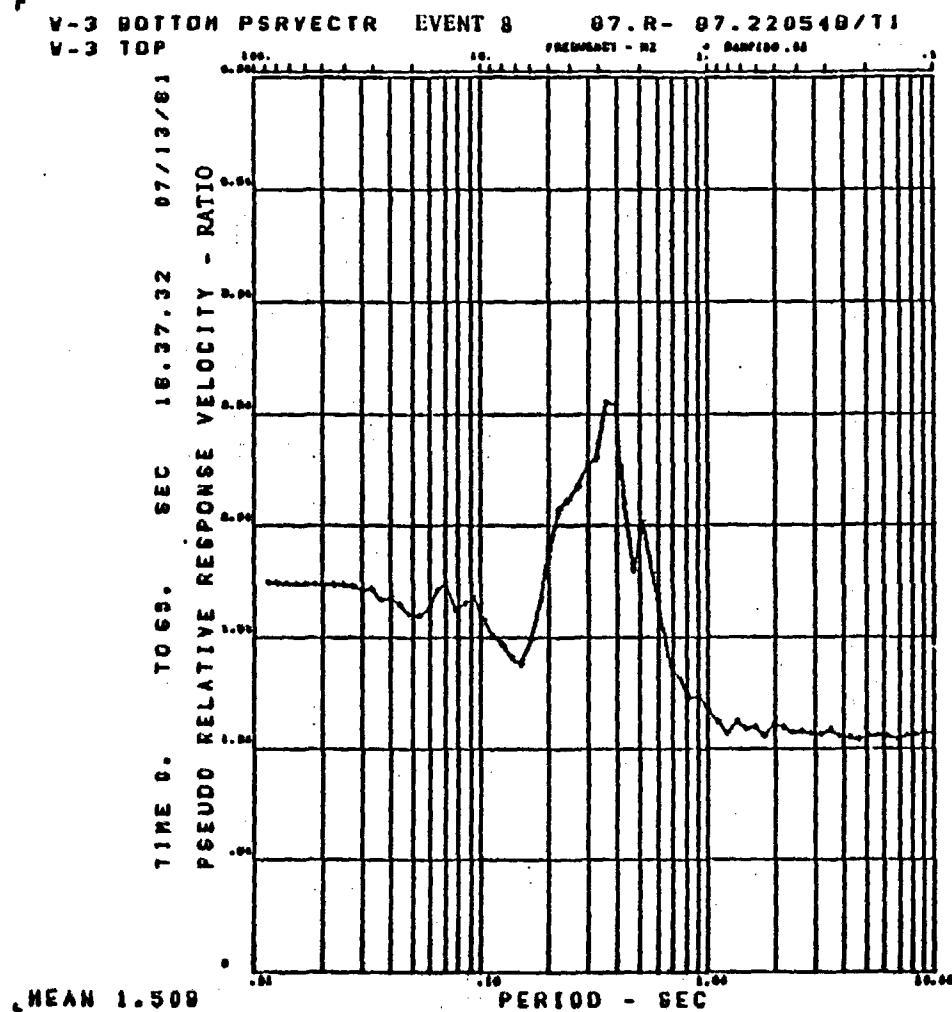


Figure B-21a

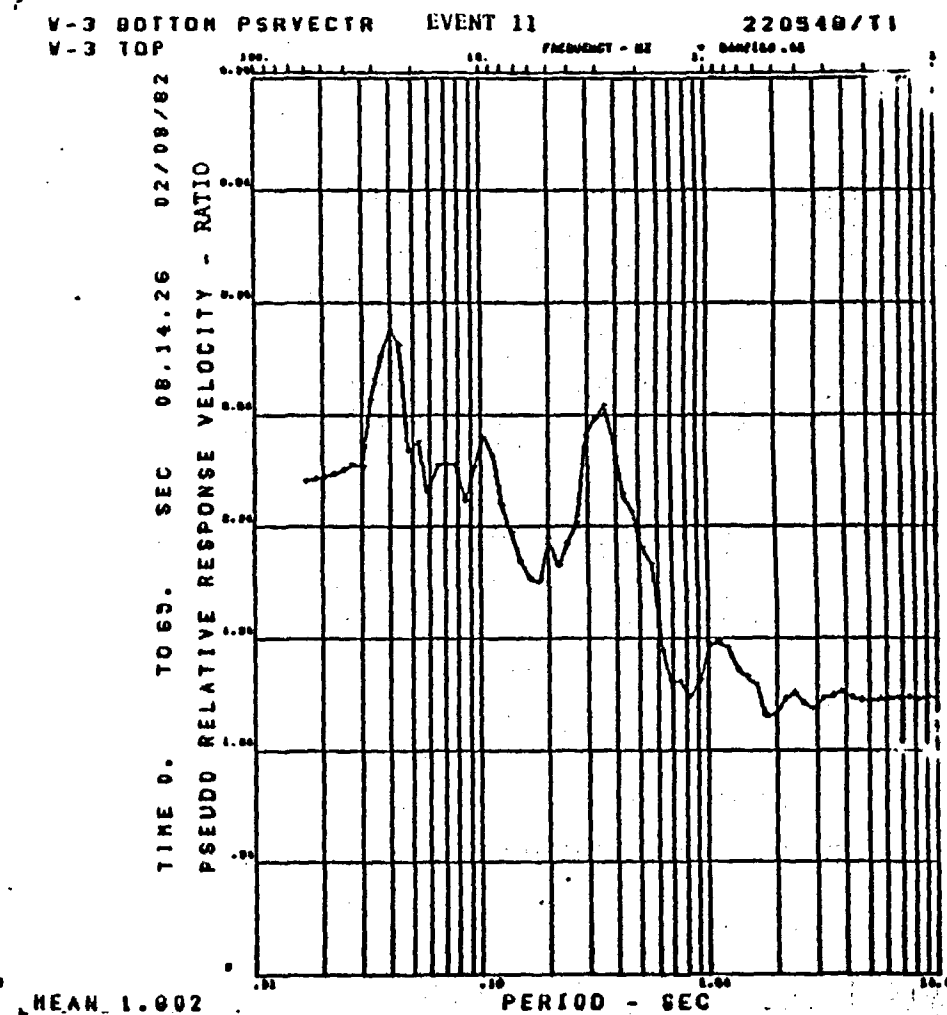


Figure B-21b

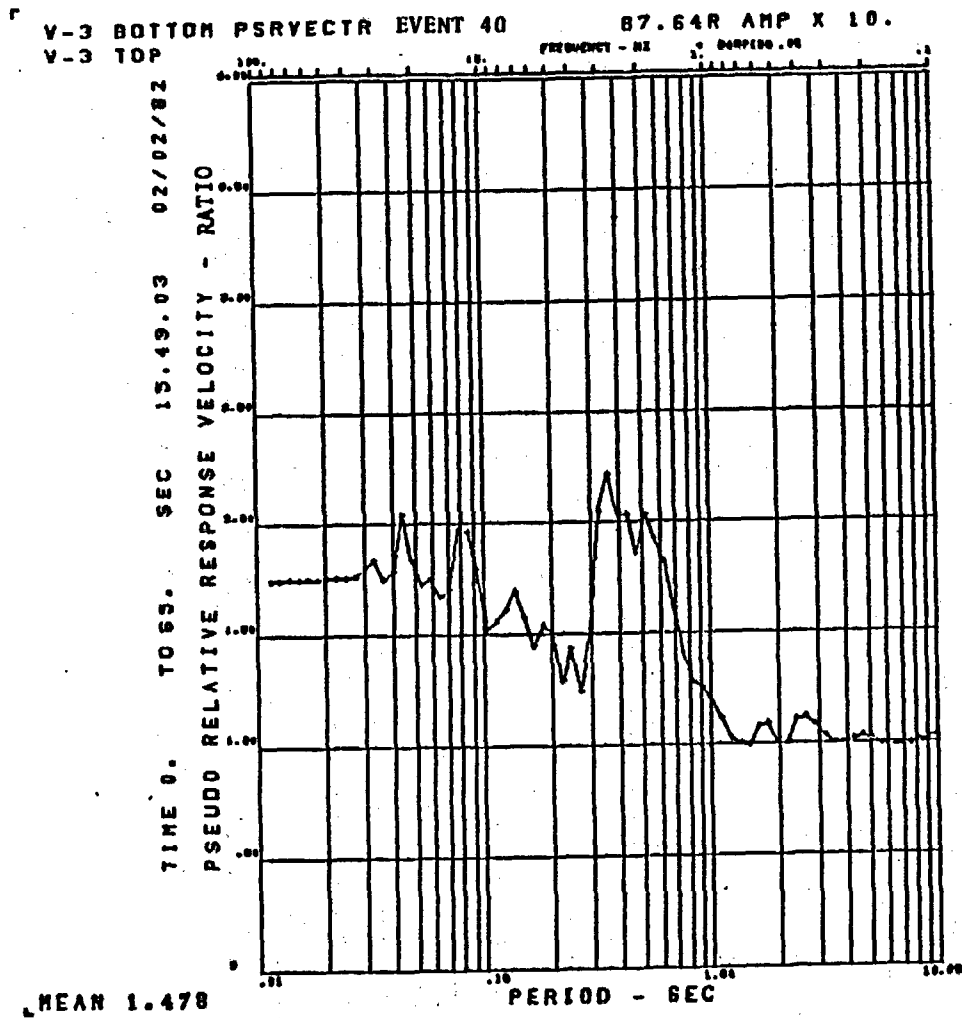


Figure B-22a

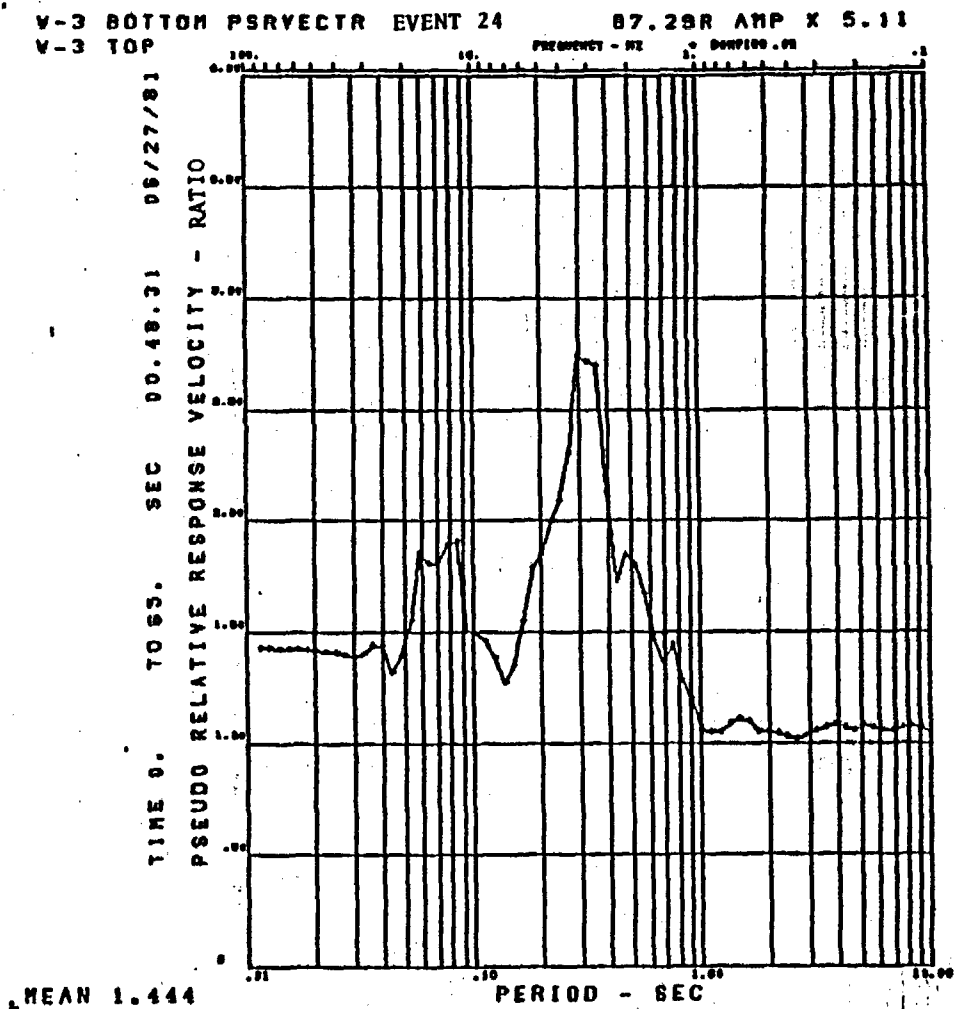


Figure B-22b

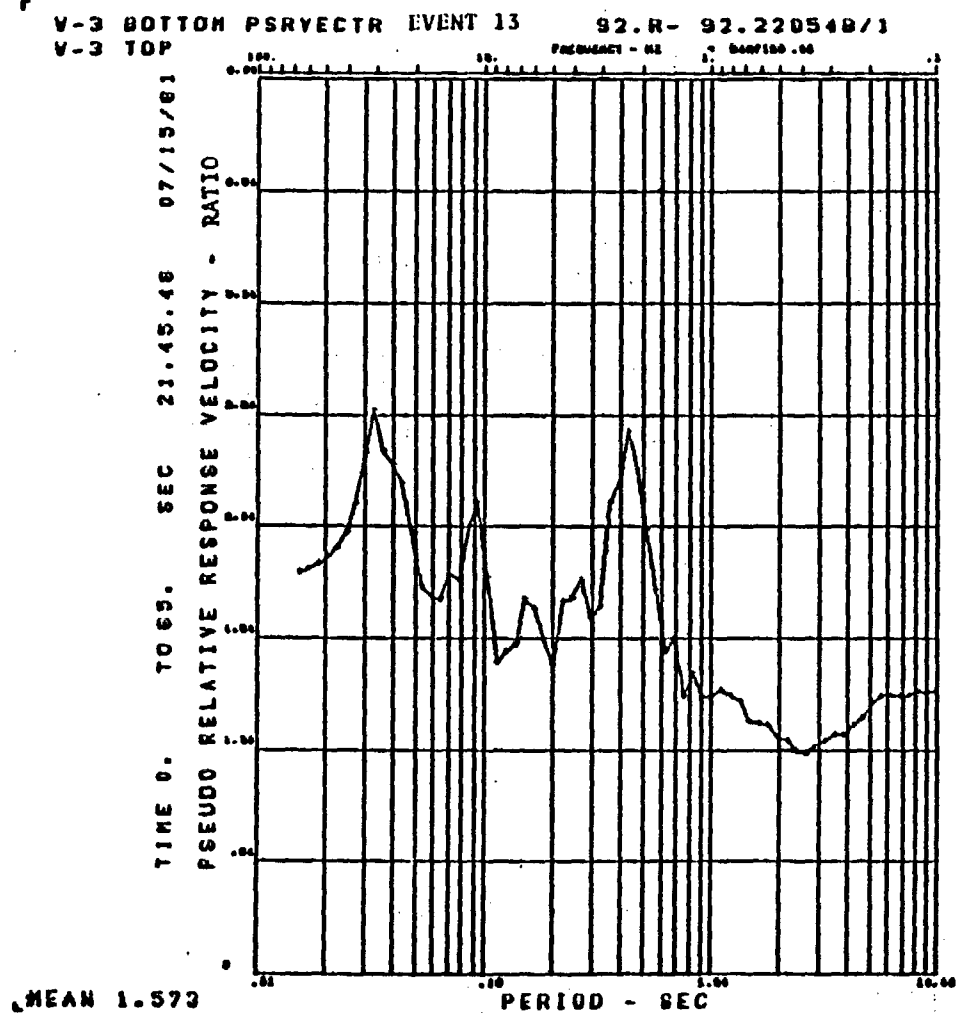


Figure B-23a

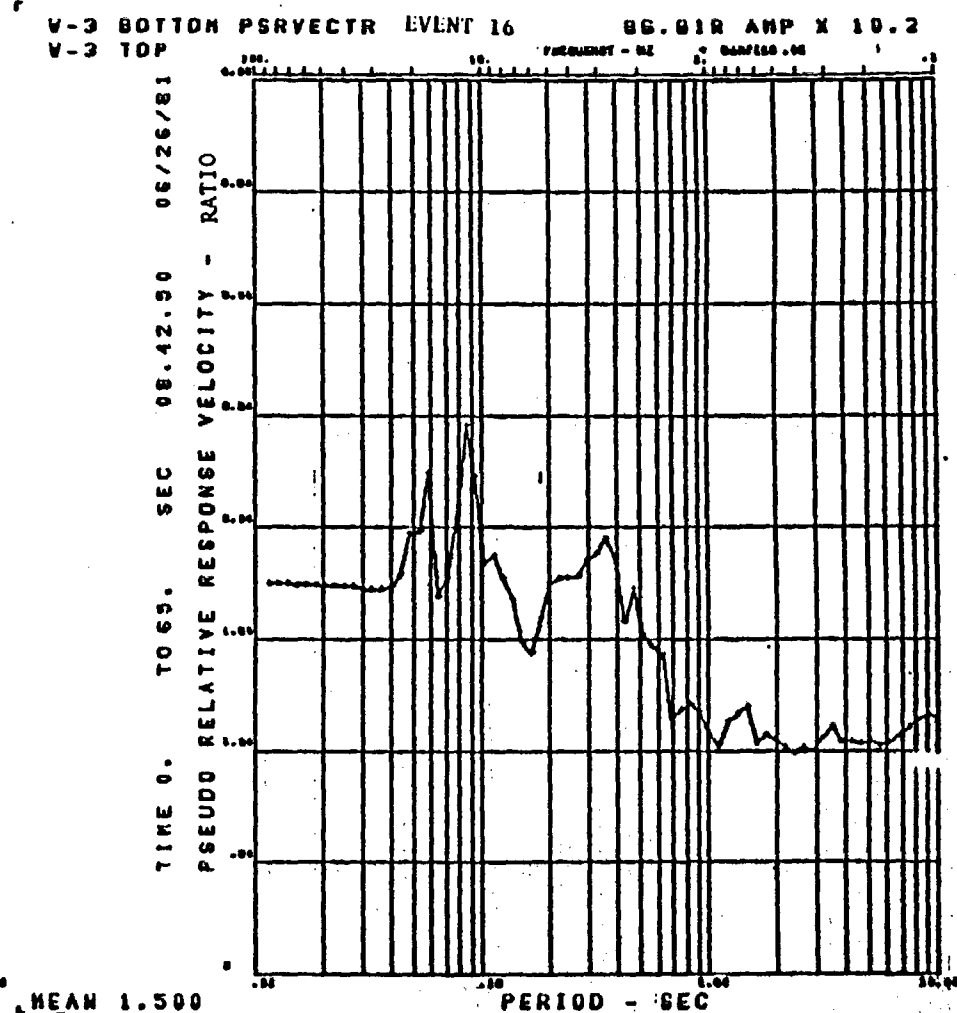


Figure B-23b

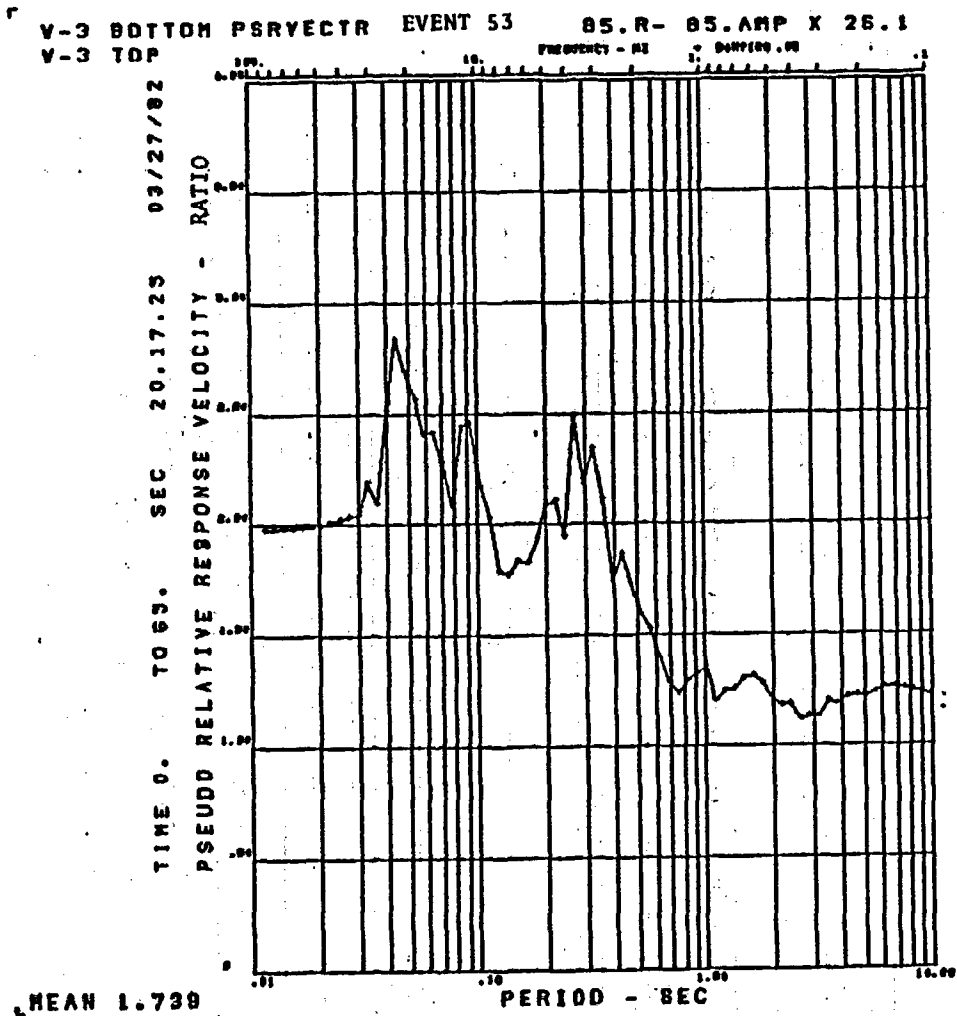


Figure B-24a

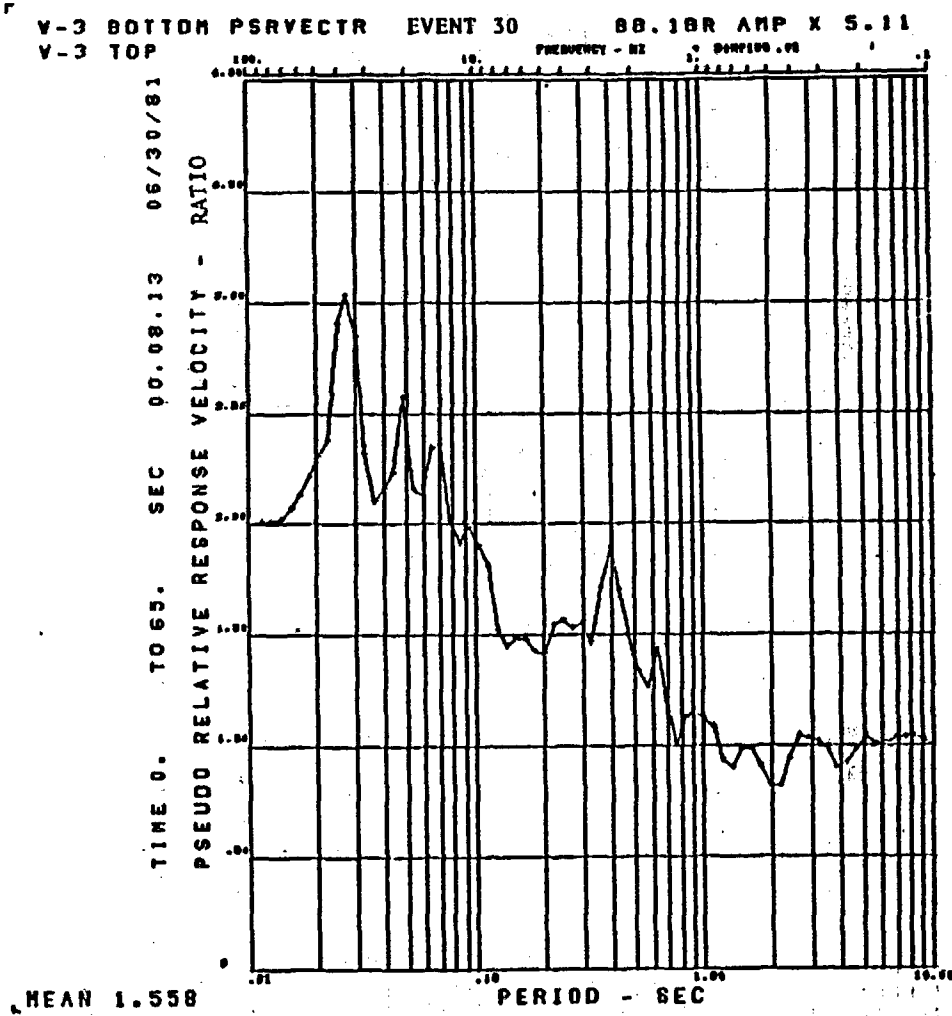


Figure B-24b

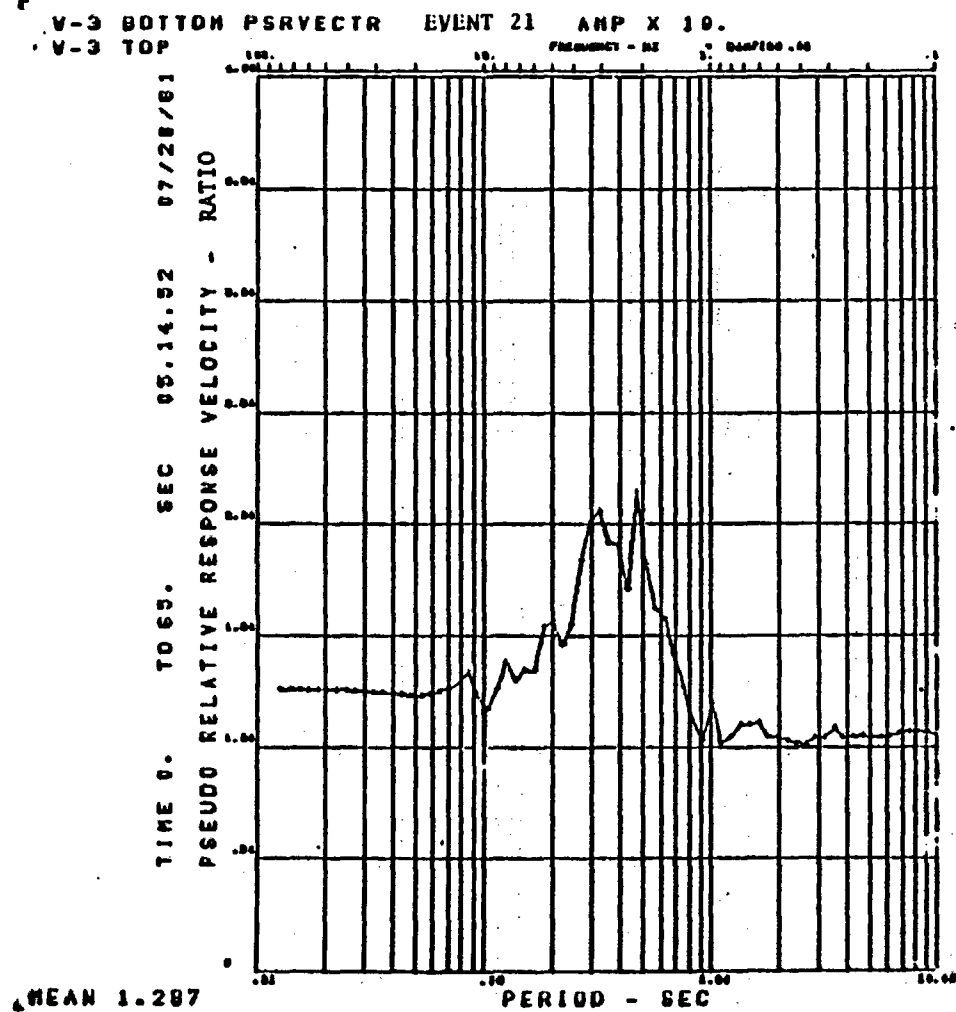


Figure B-25a

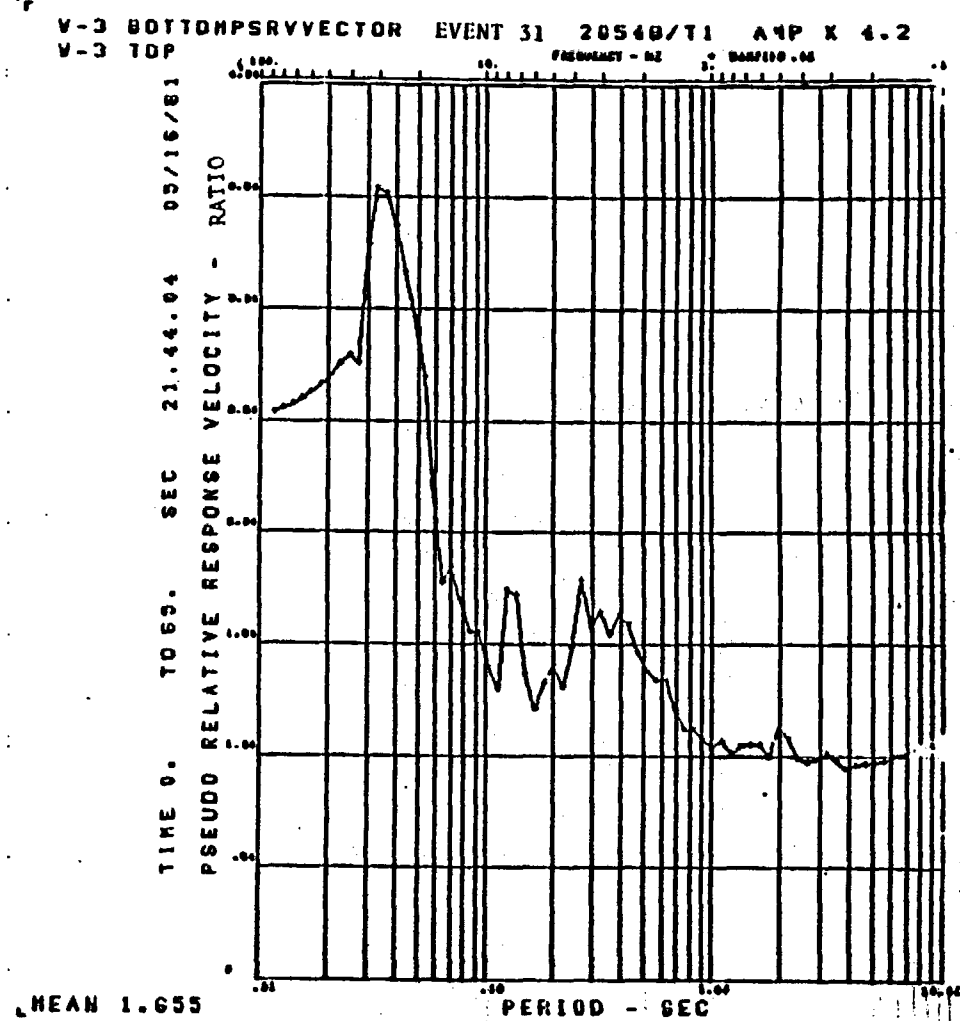


Figure B-25b

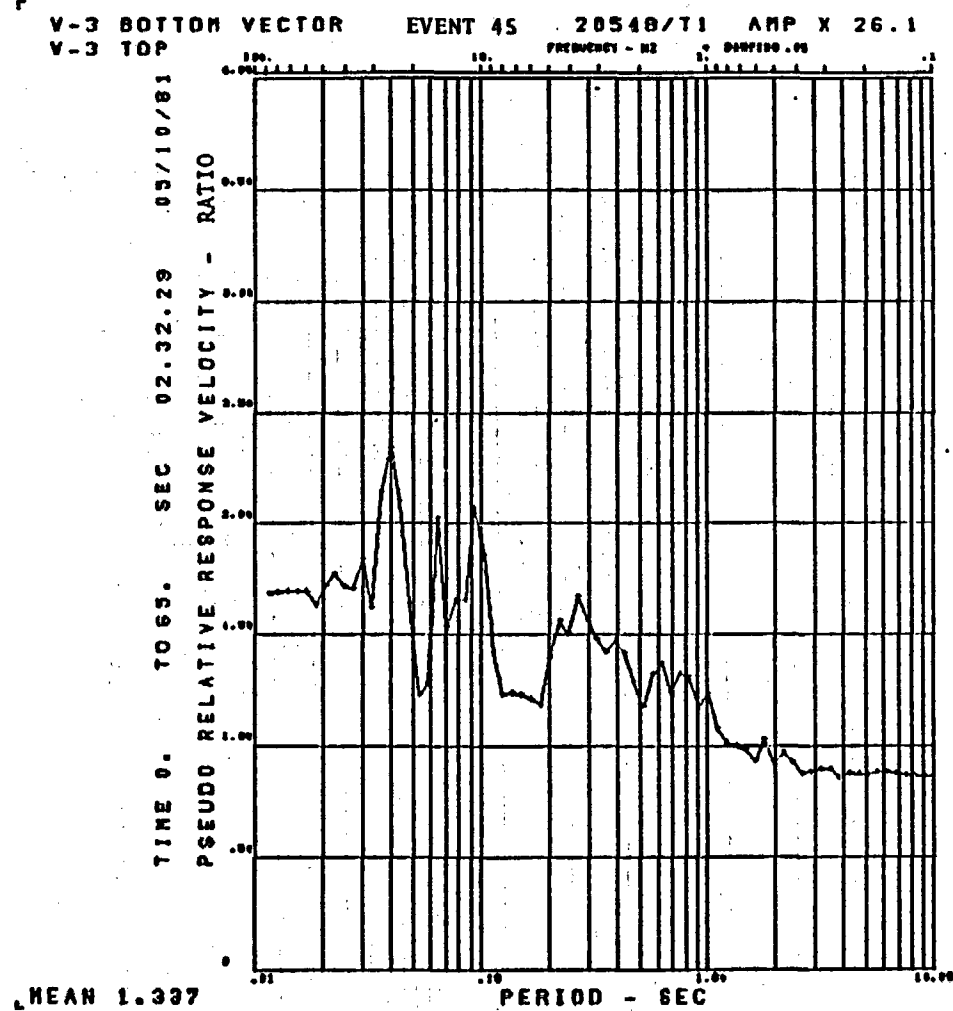


Figure B-26a

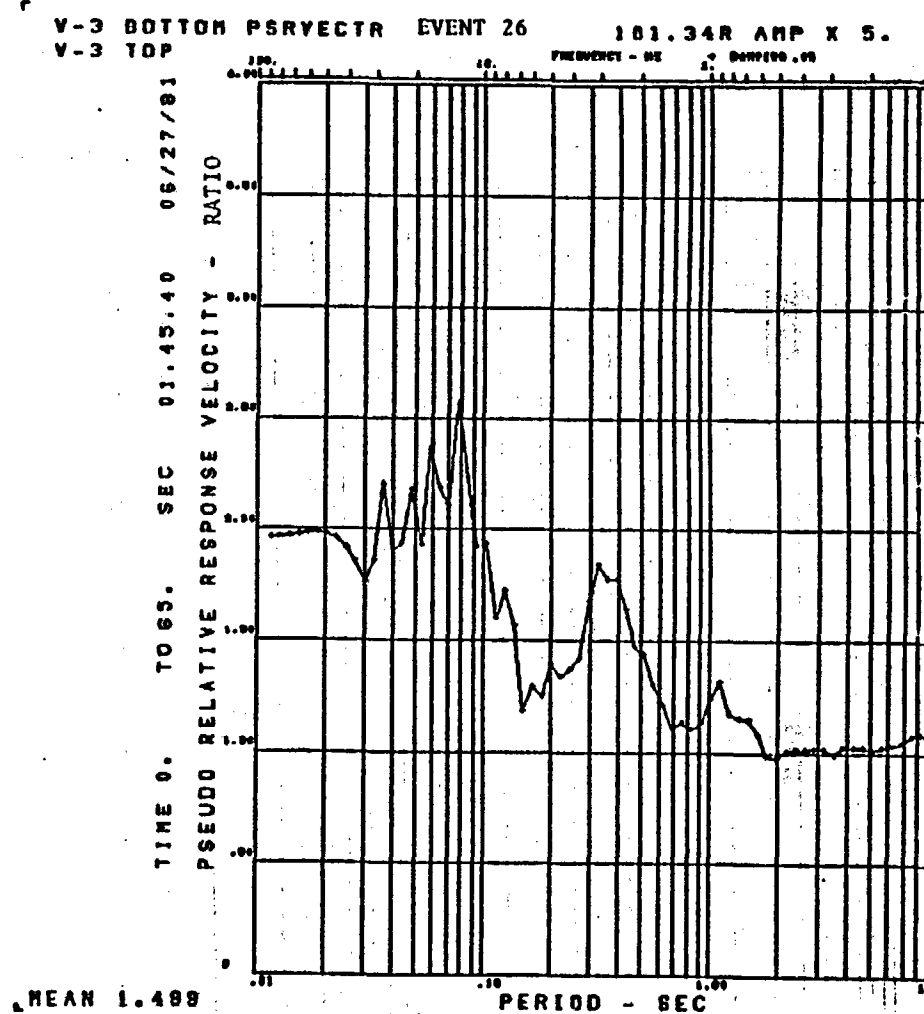


Figure B-26b

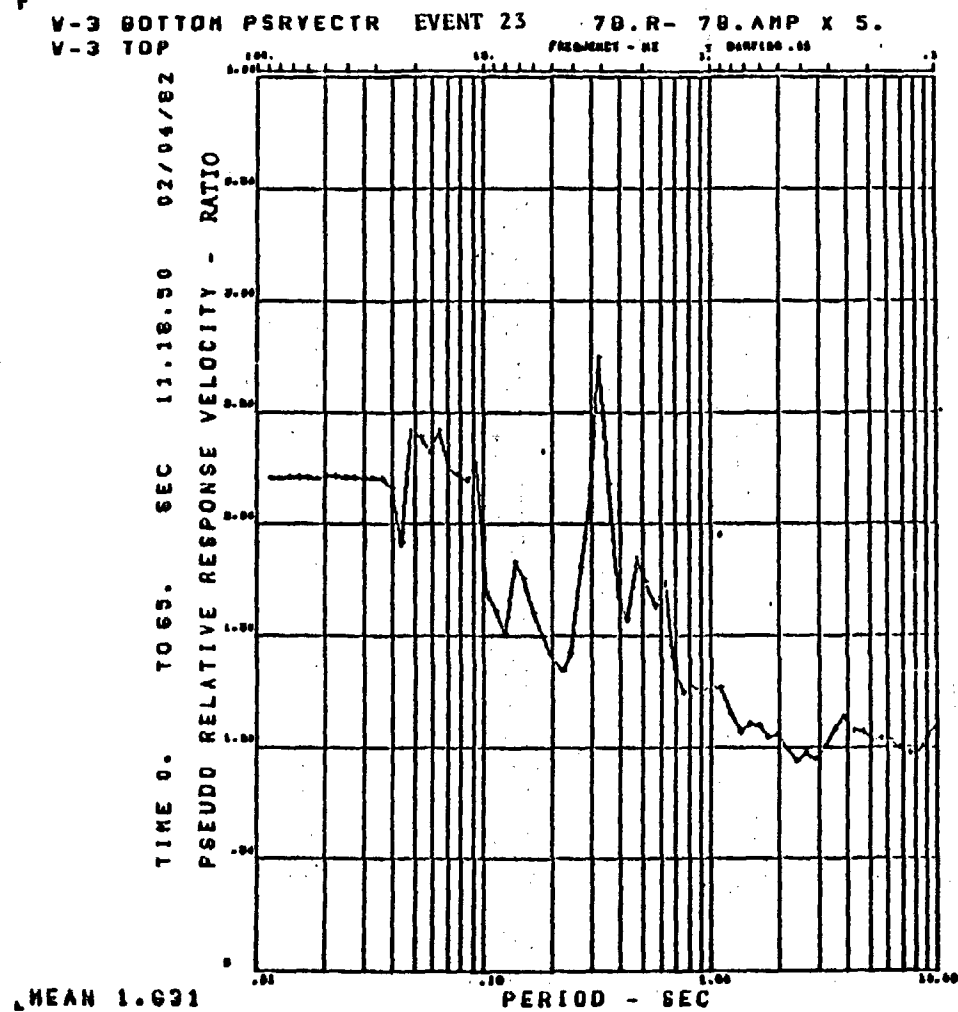


Figure B-27a

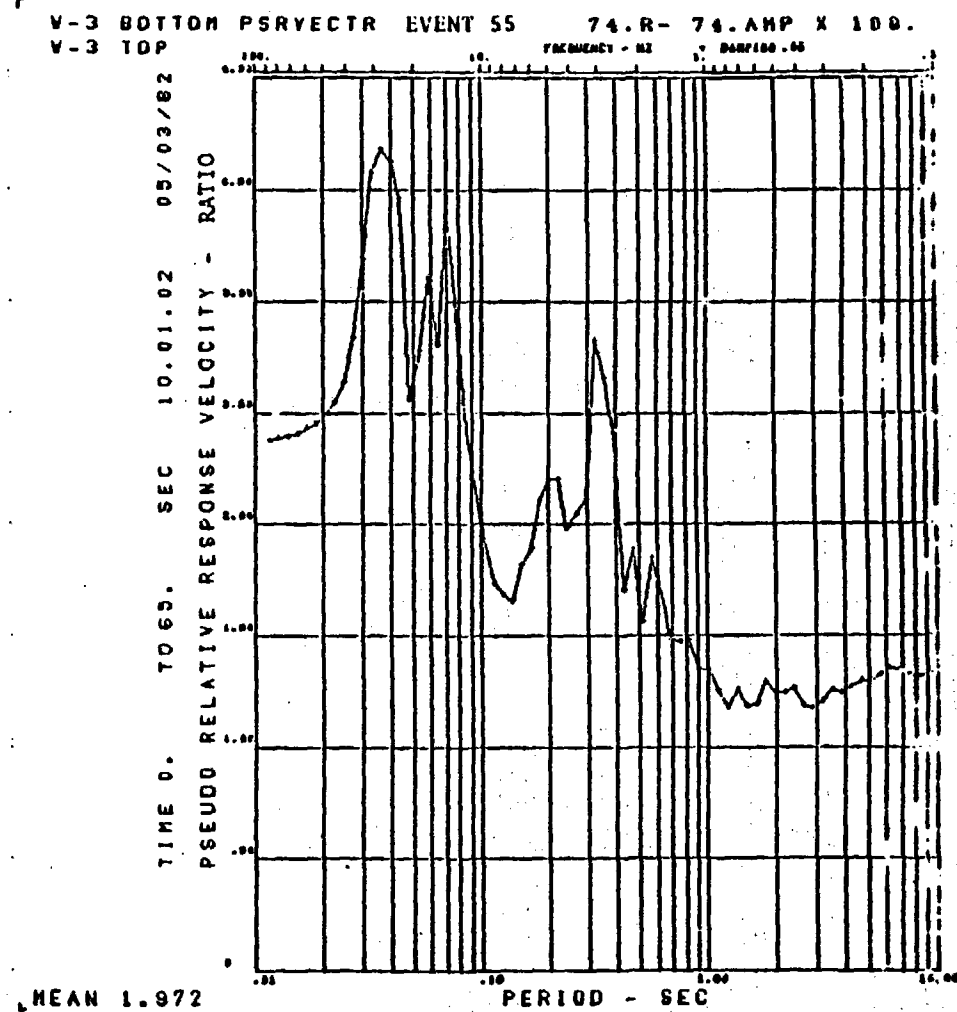


Figure B-27b

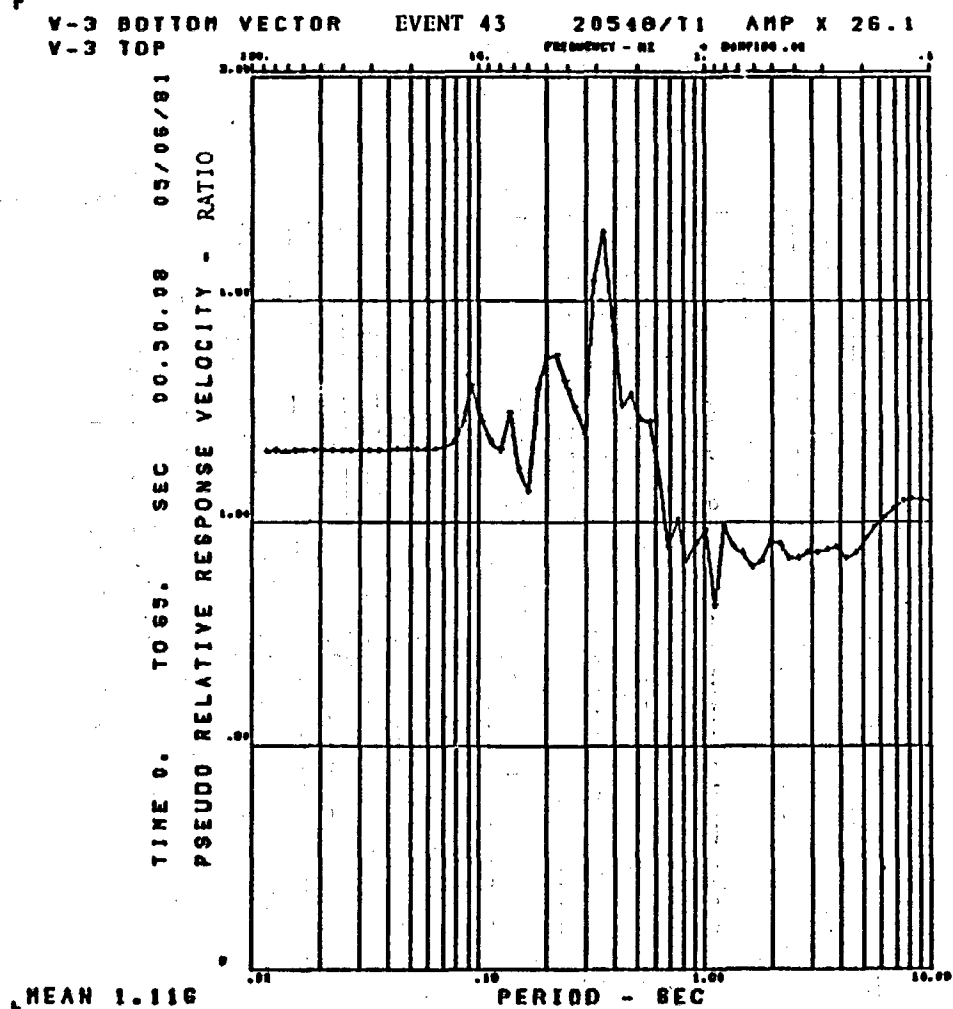


Figure B-28a

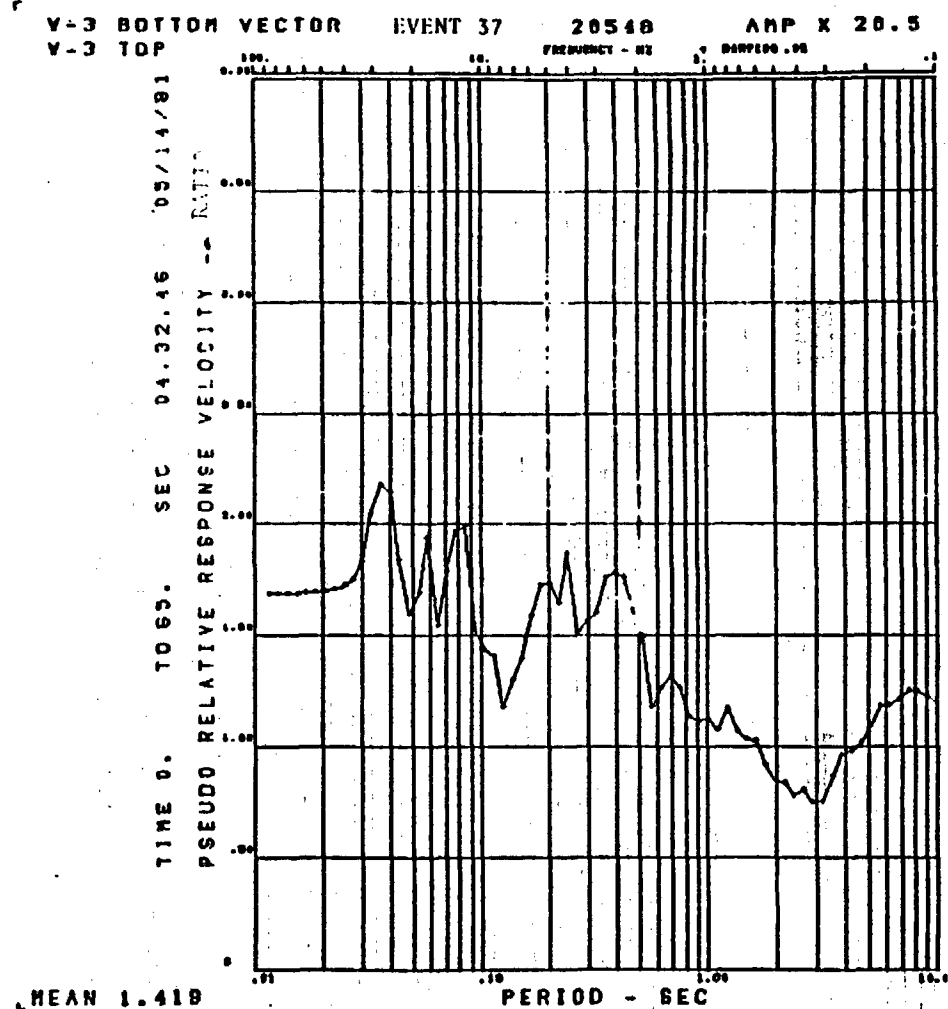


Figure B-28b

V-3 BOTTOM PSRYECTR EVENT 9

02.R- 02.

V-3 TOP

FREQUENCY - HZ

DAMPING - DB

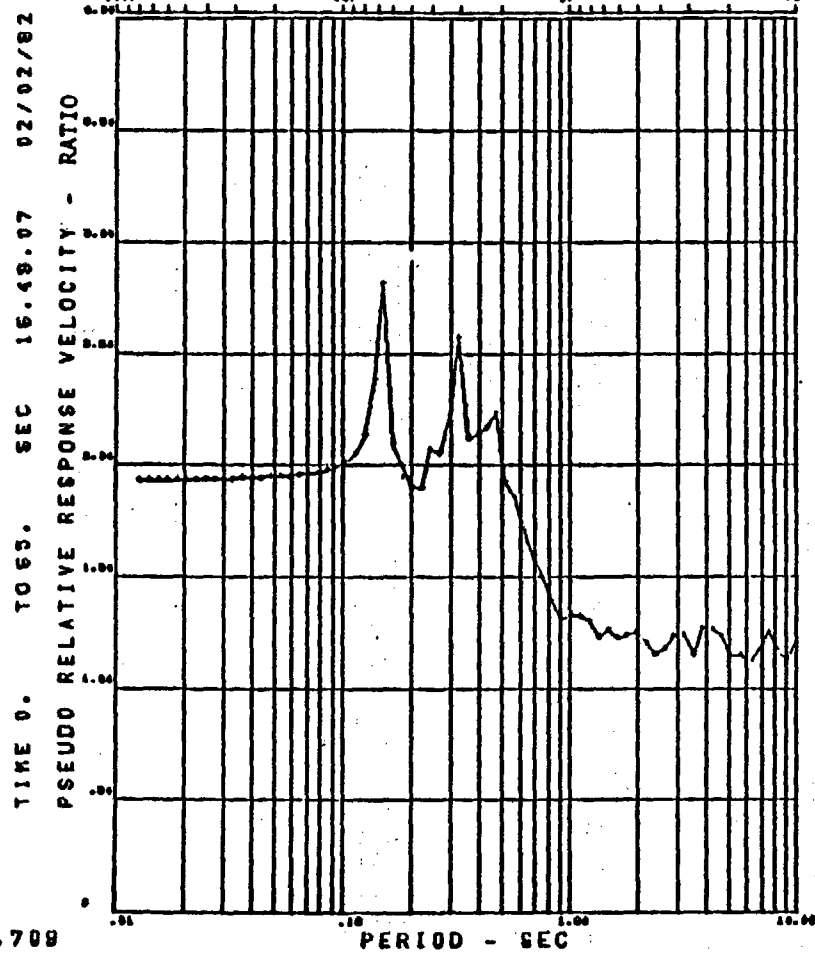


Figure B-29a

V-3 BOTTOM PSRYECTR EVENT 42

103.R-103.AMP X 104.

V-3 TOP

FREQUENCY - HZ

DAMPING - DB

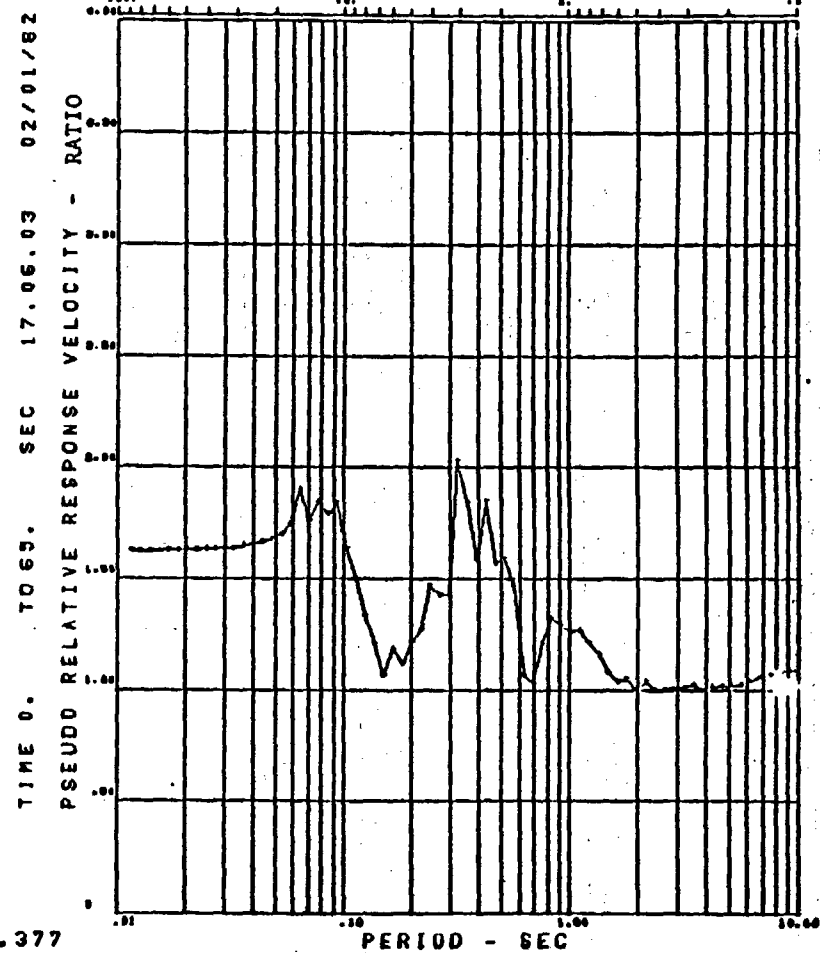


Figure B-29b

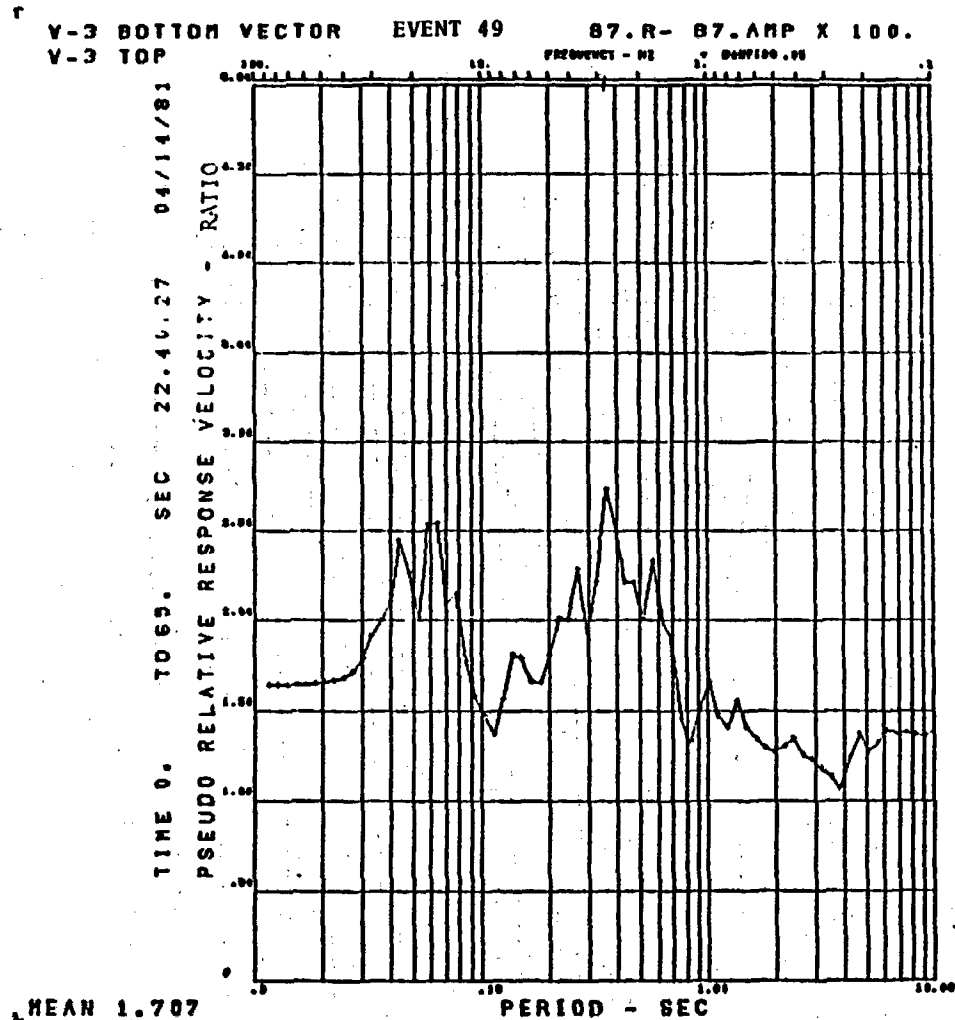


Figure B-30a

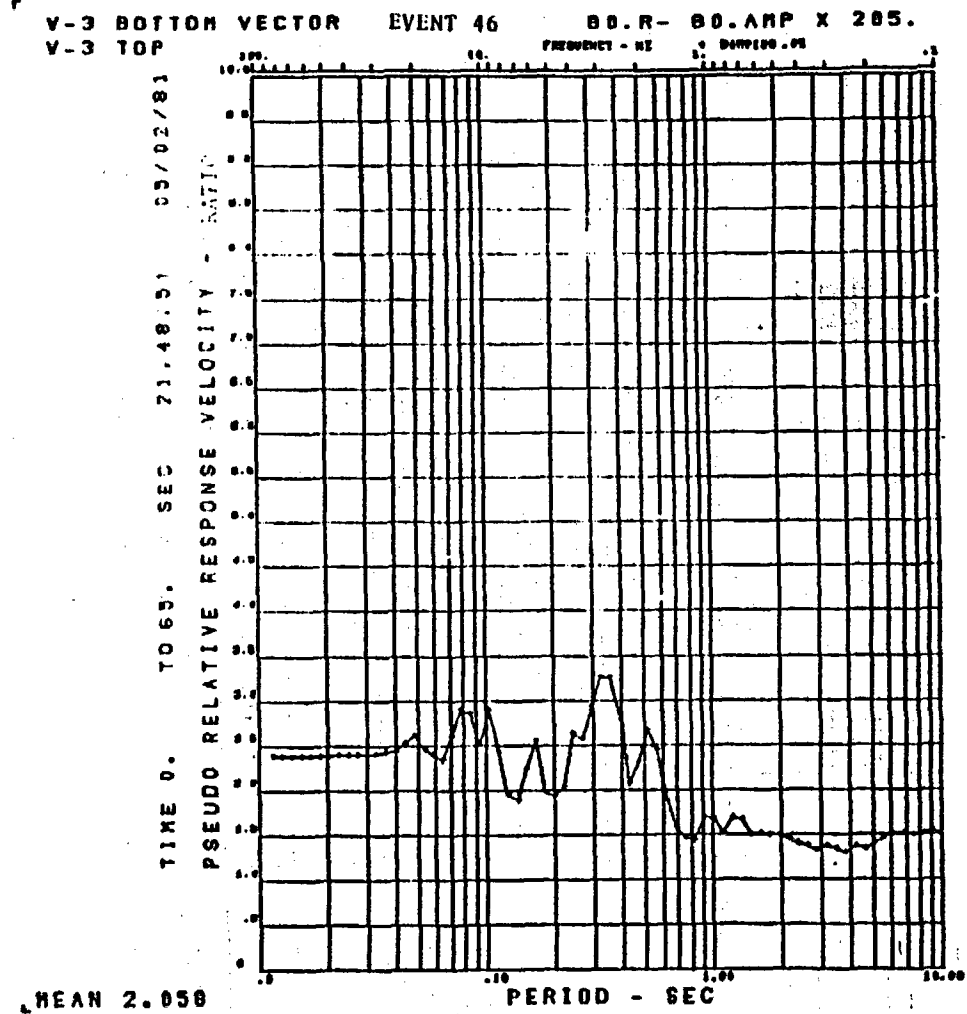


Figure B-30b

V-9 BOTTOM VECTOR EVENT 40
V-9 TOP

33.71R AMP X 10.

FREQUENCY - HZ DAMPING - 10

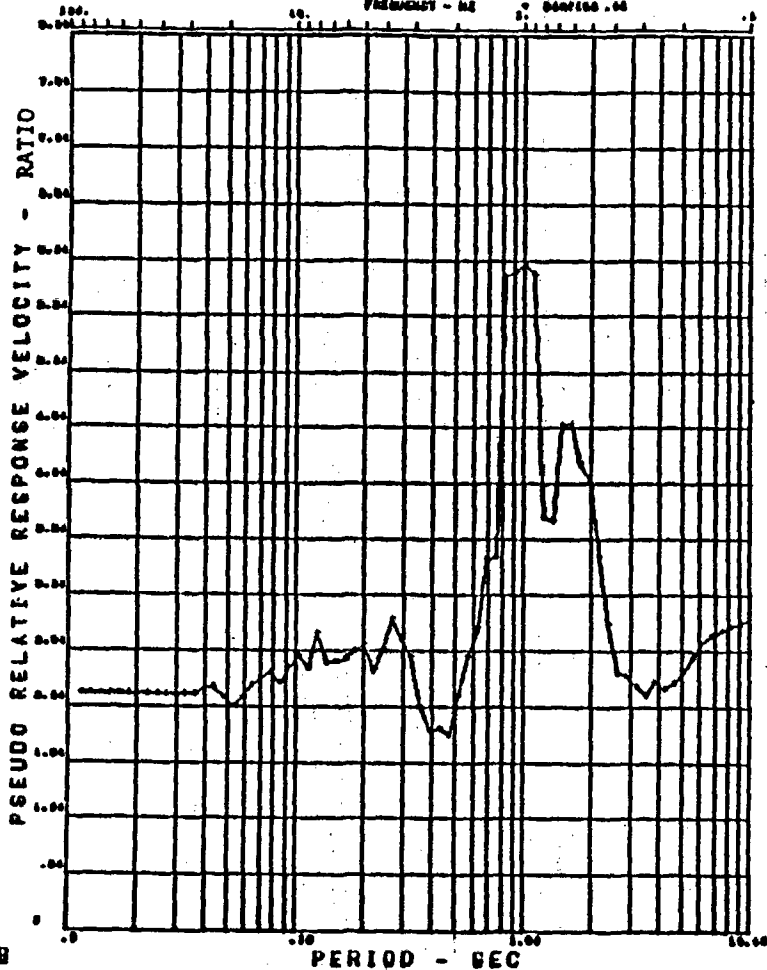


Figure B-31a

V-9 BOTTOM PSRVECTR EVENT 16
V-9 TOP

29.95R AMP X 5.11

FREQUENCY - HZ DAMPING - 10

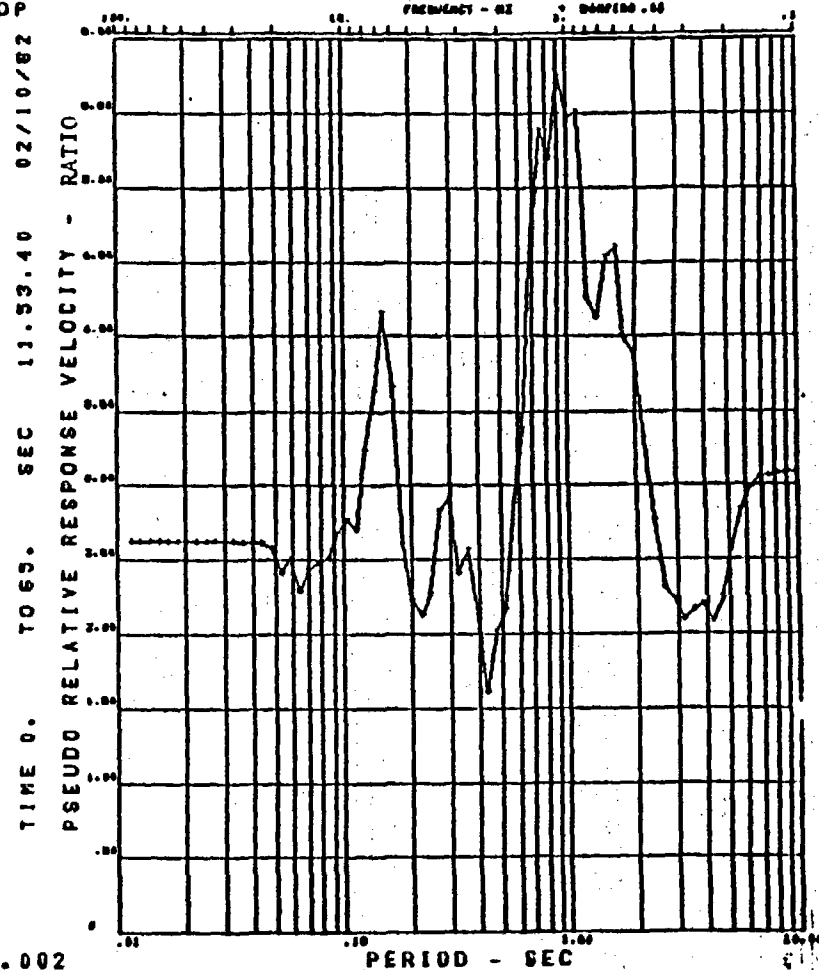


Figure B-31b

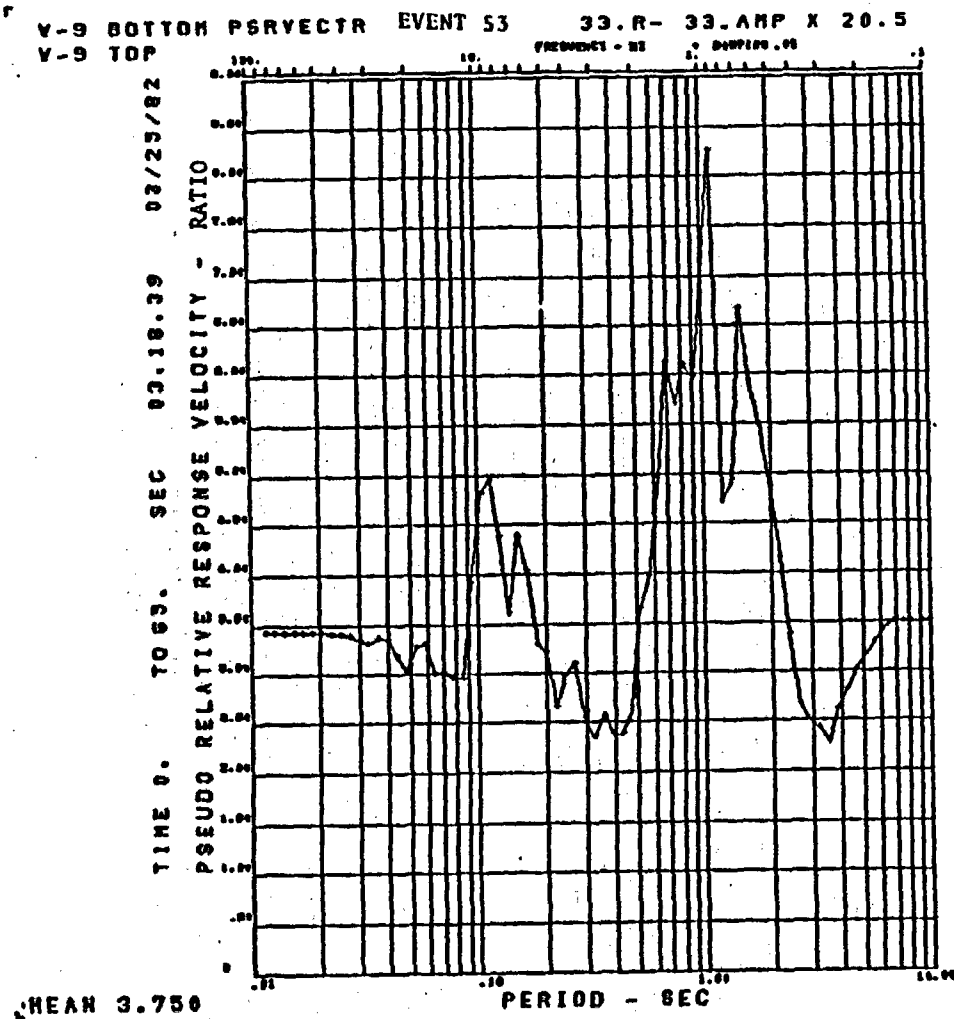


Figure B-32a

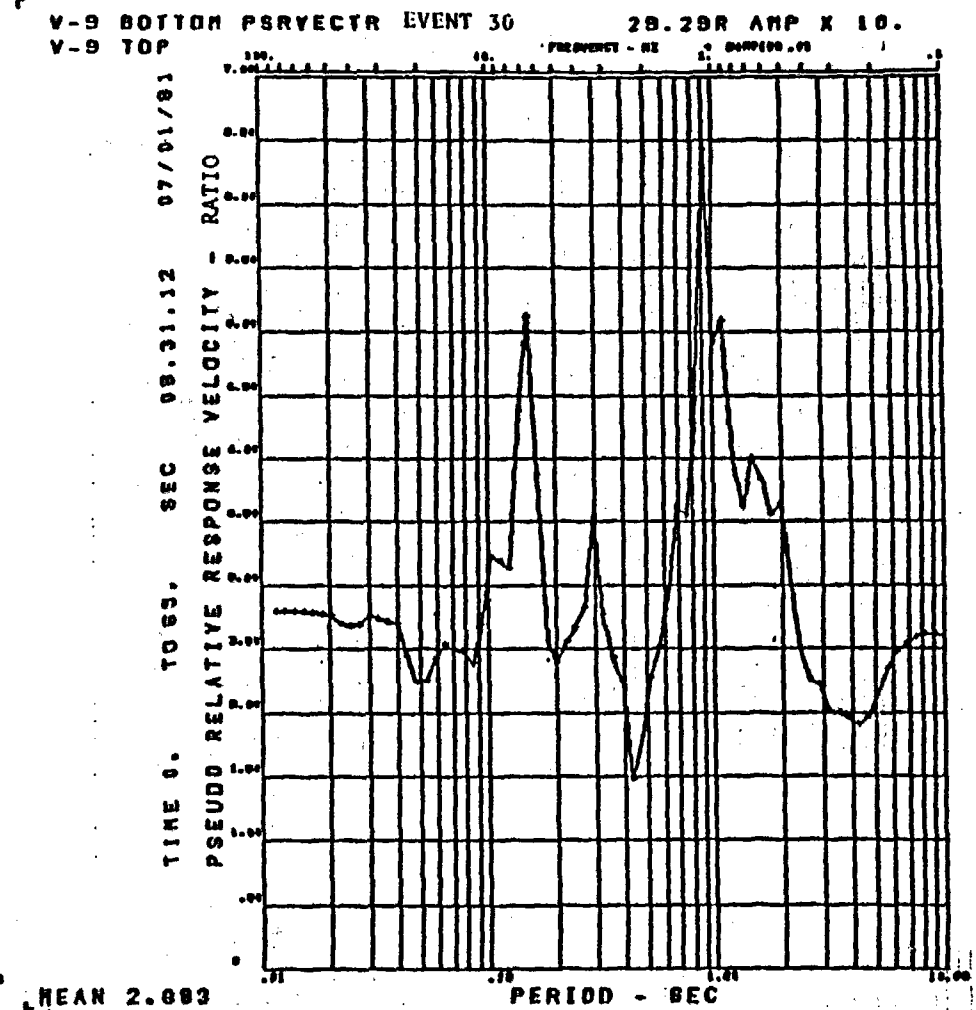


Figure B-32b

V-B BOTTOM VECTOR EVENT 36 20549 AMP X 5.1
V-B TOP FREQUENCY - HZ DAM/100.00

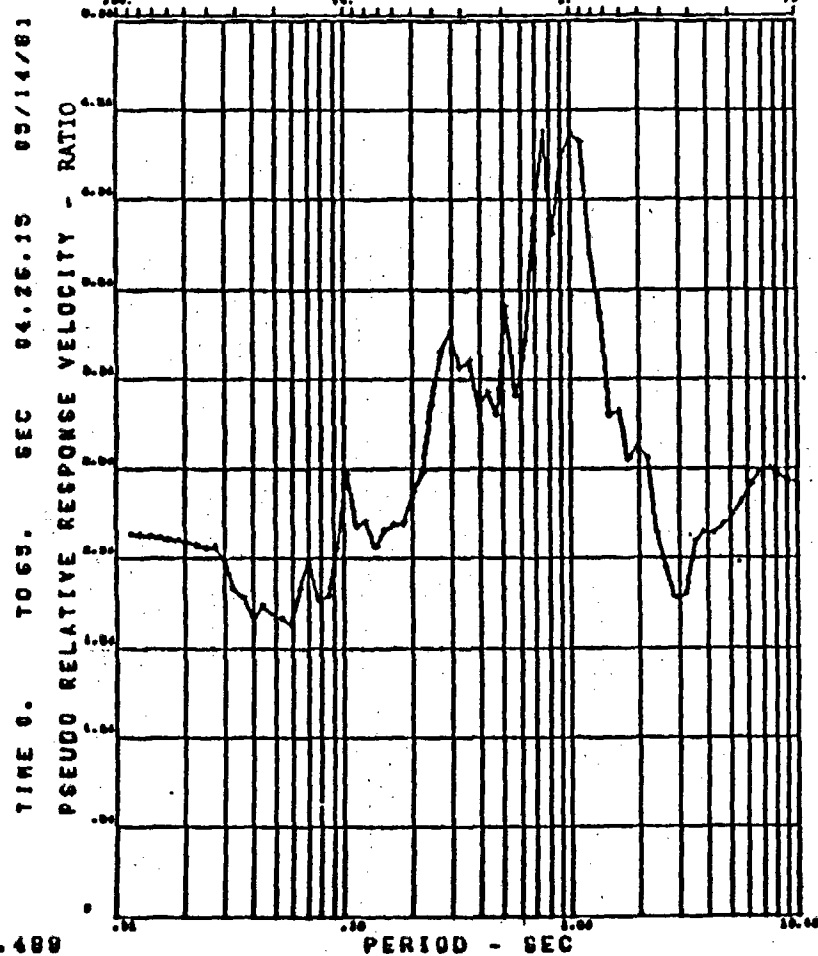


Figure B-33a

V-B BOTTOMPSRVVECTOR EVENT 31 20549/T1 AMP X 10.
V-B TOP FREQUENCY - HZ DAM/100.00

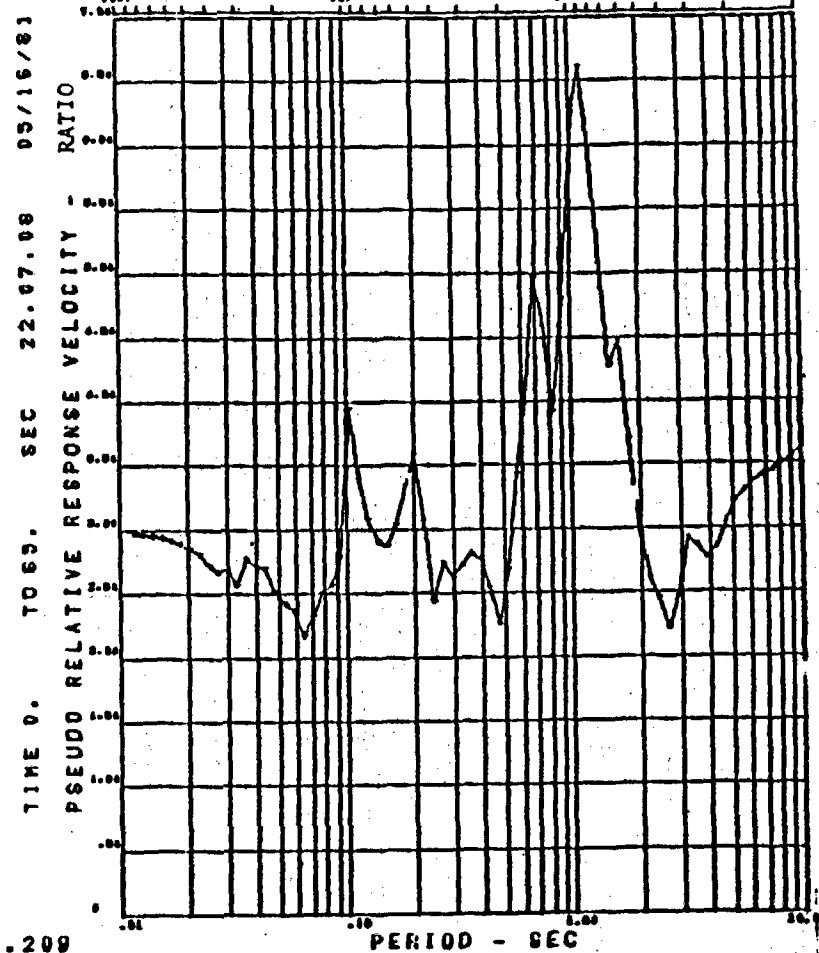


Figure B-33b

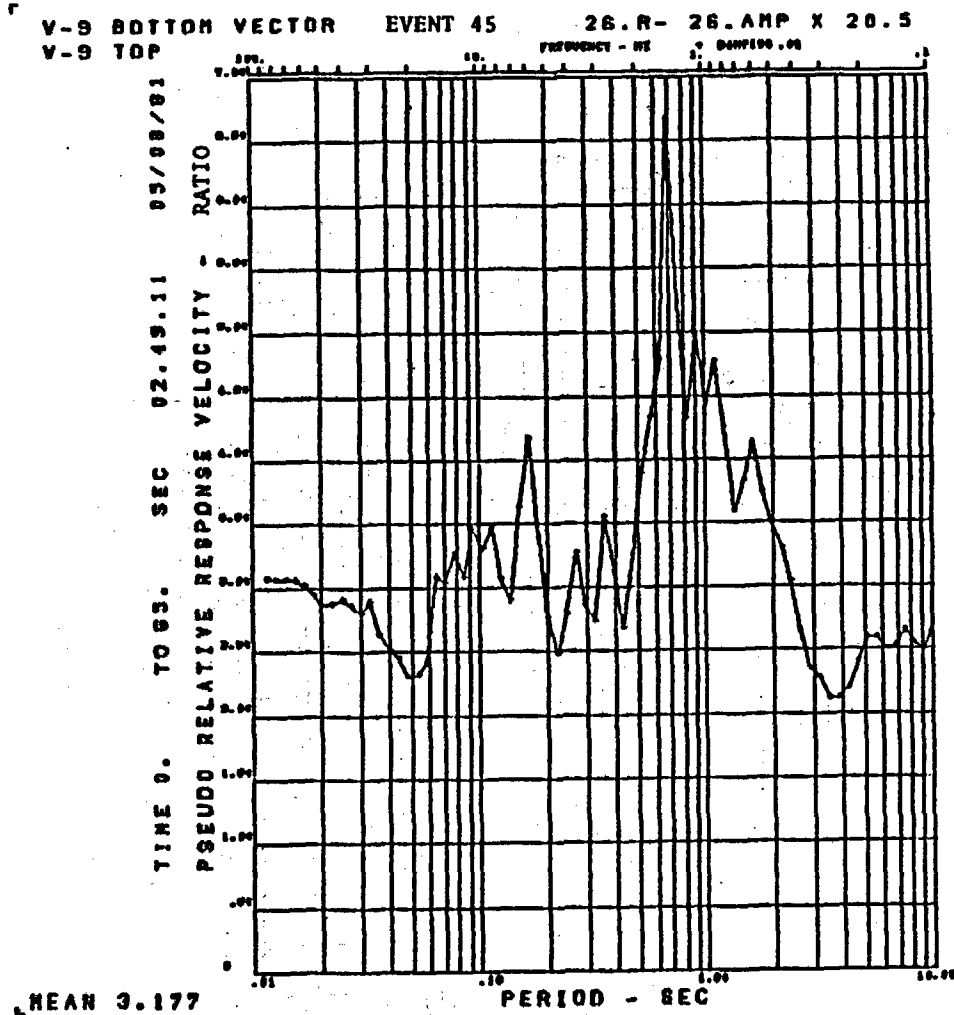


Figure B-34a

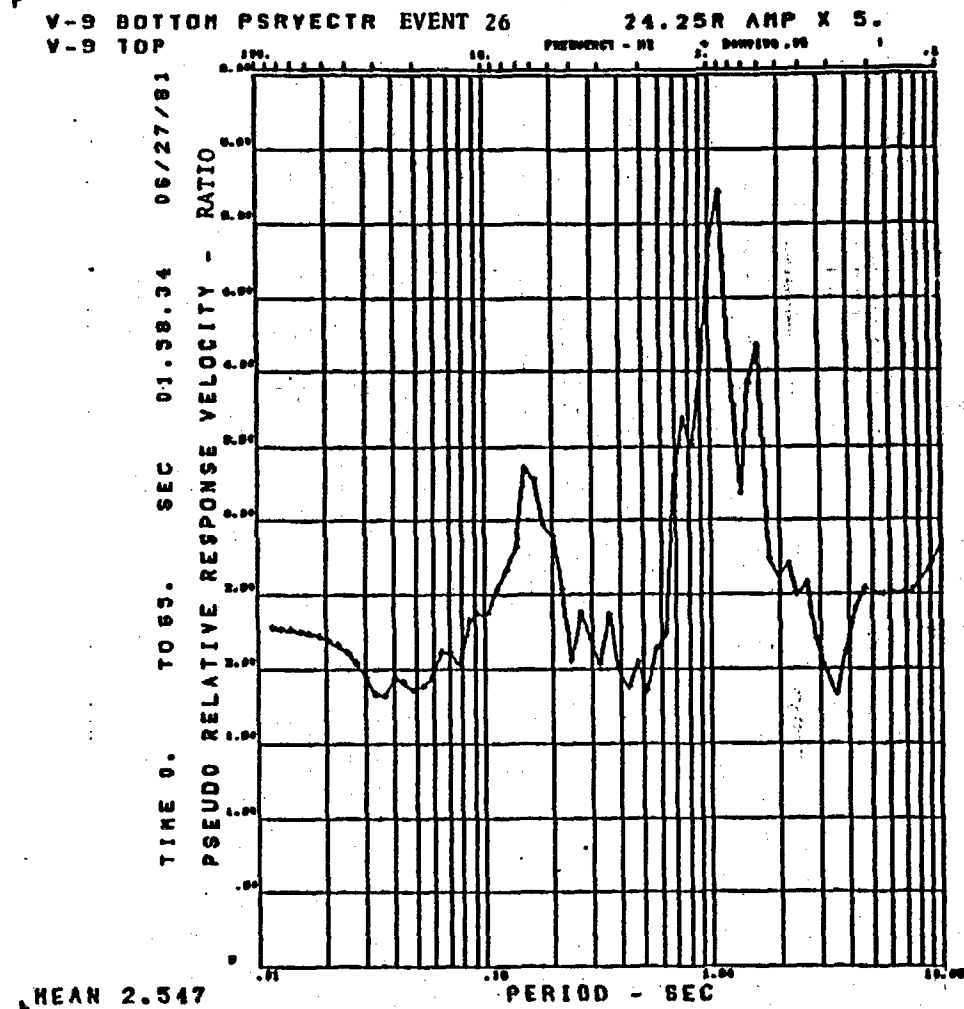


Figure B-34b

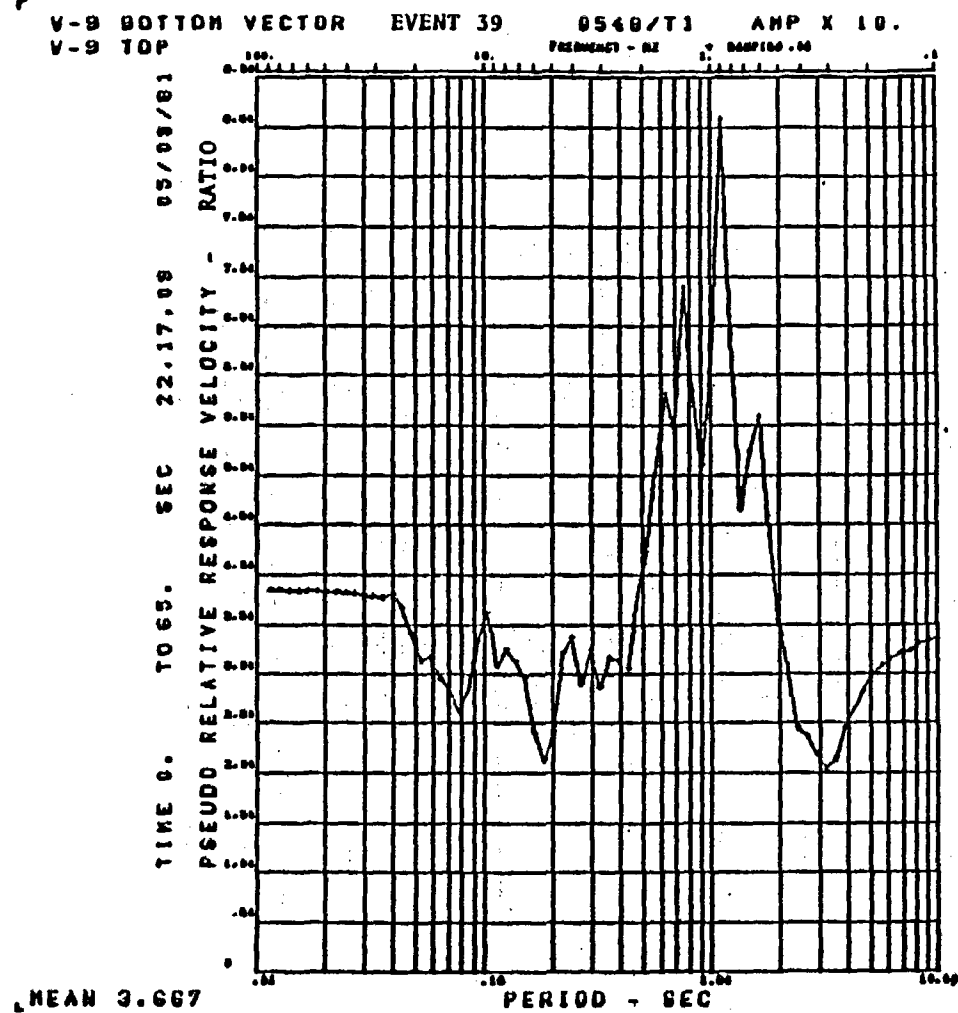


Figure B-35a

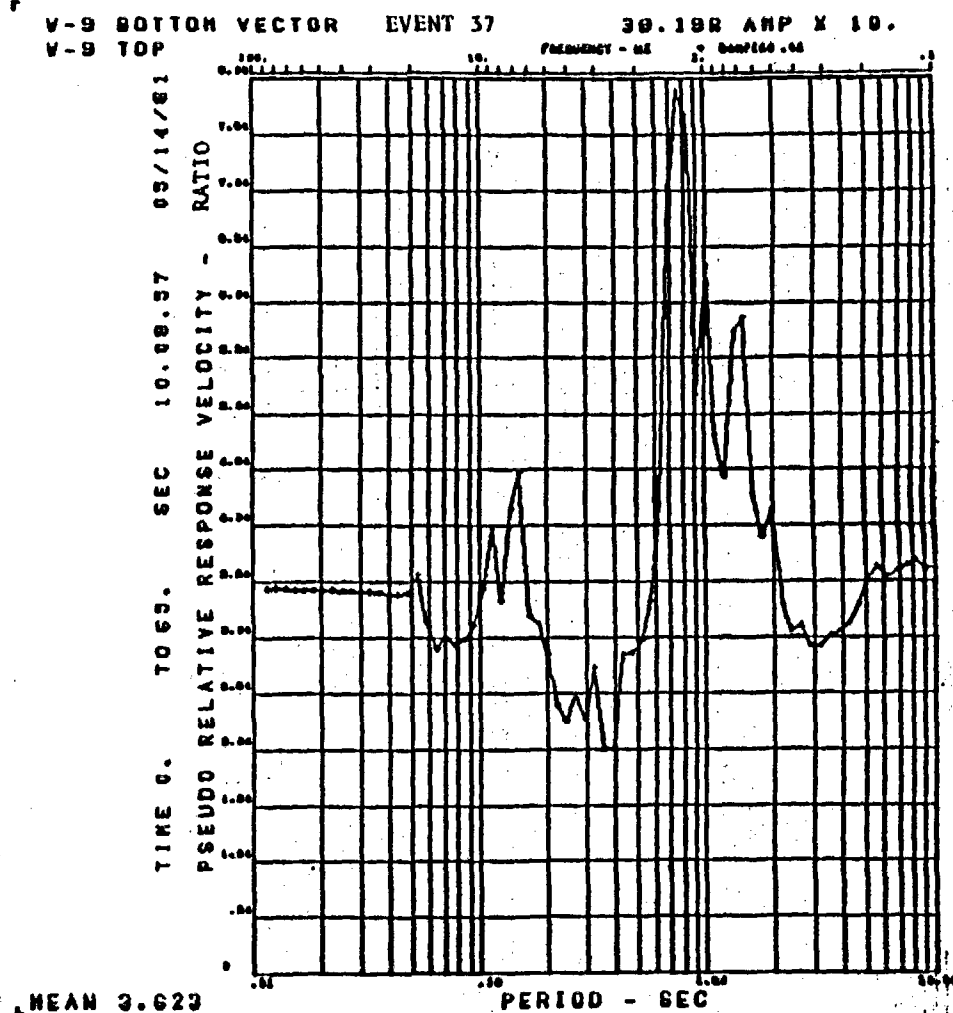


Figure B-35b

MEAN 3.355

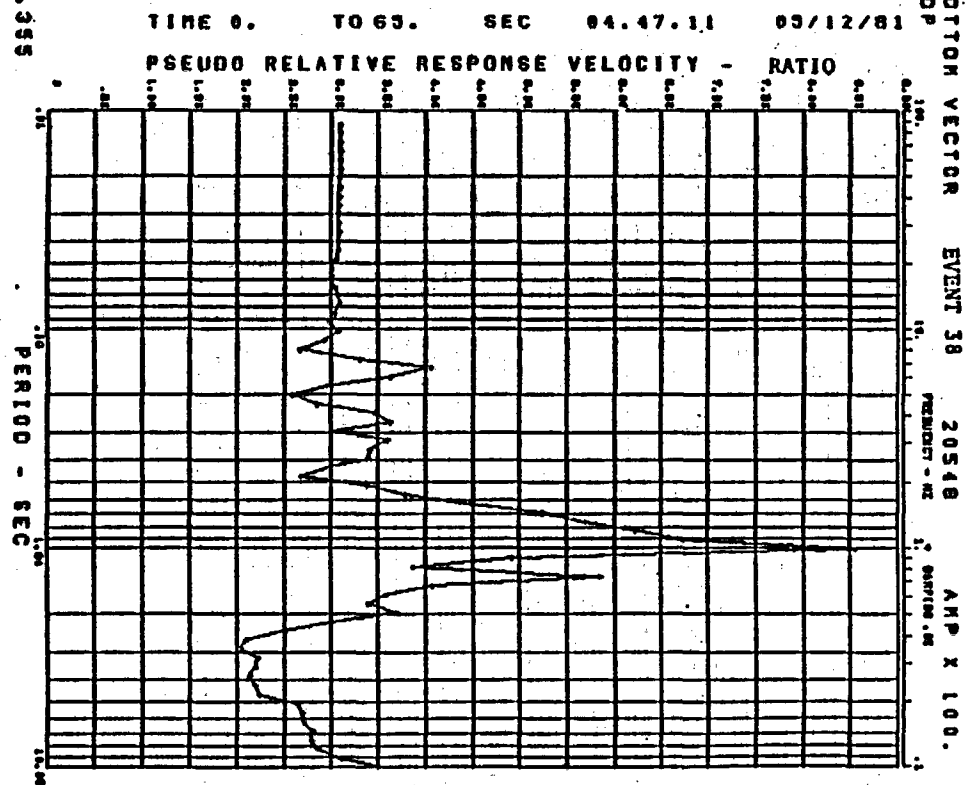


Figure B-36a

V-S BOTTOM VECTOR EVENT 42 25.R- 25.AMP X 10.
V-S TOP

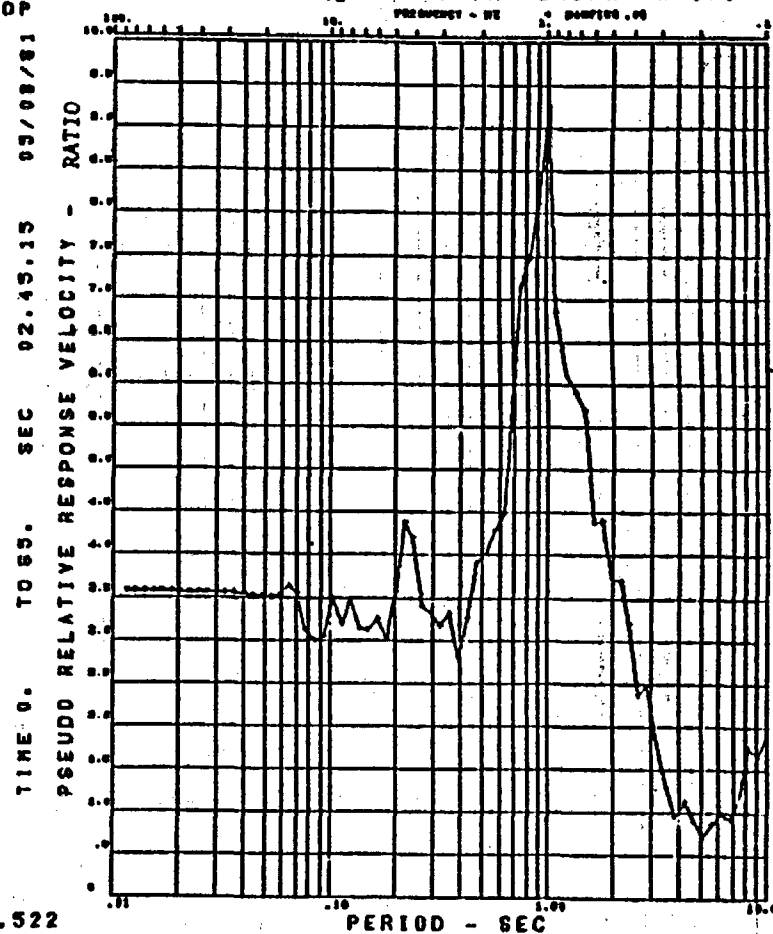


Figure B-36b

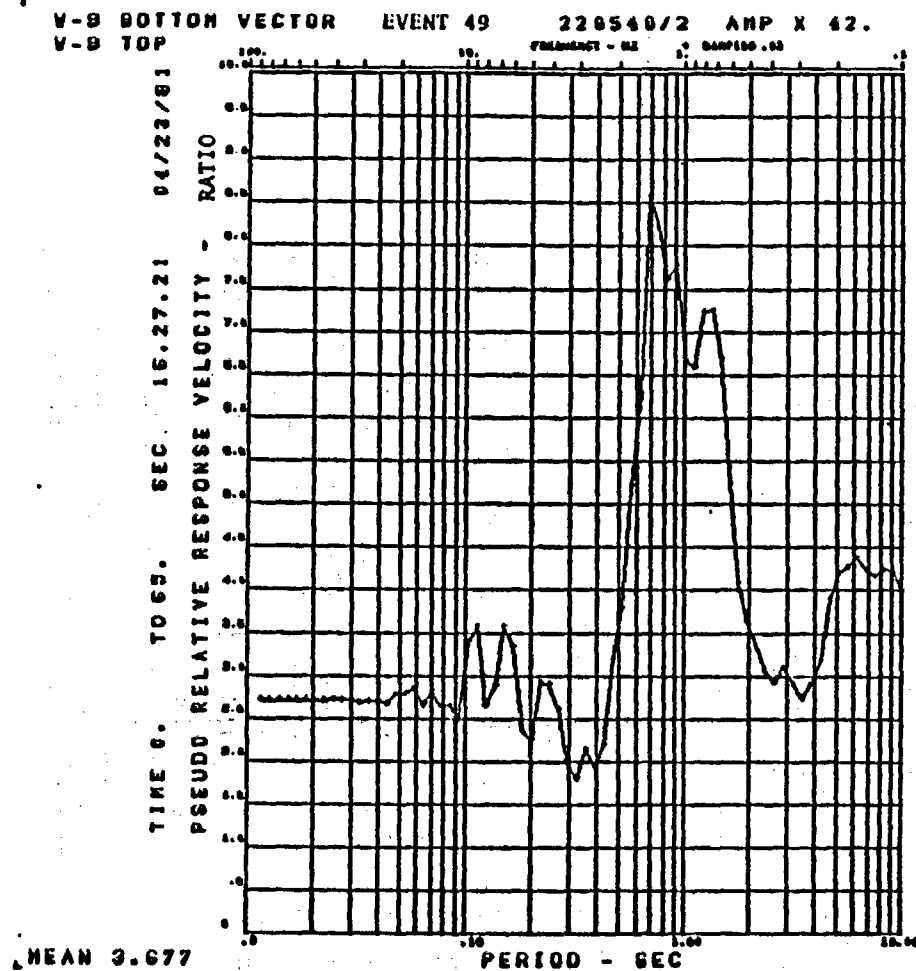


Figure B-37a

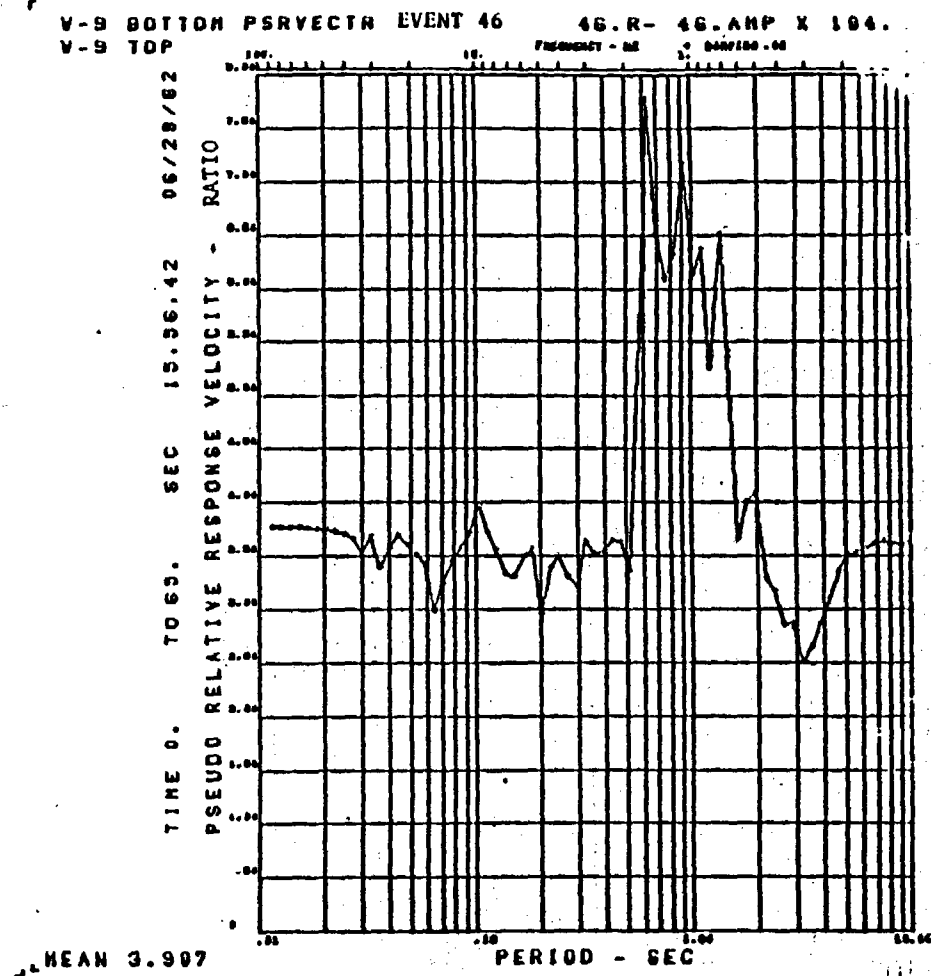


Figure B-37b

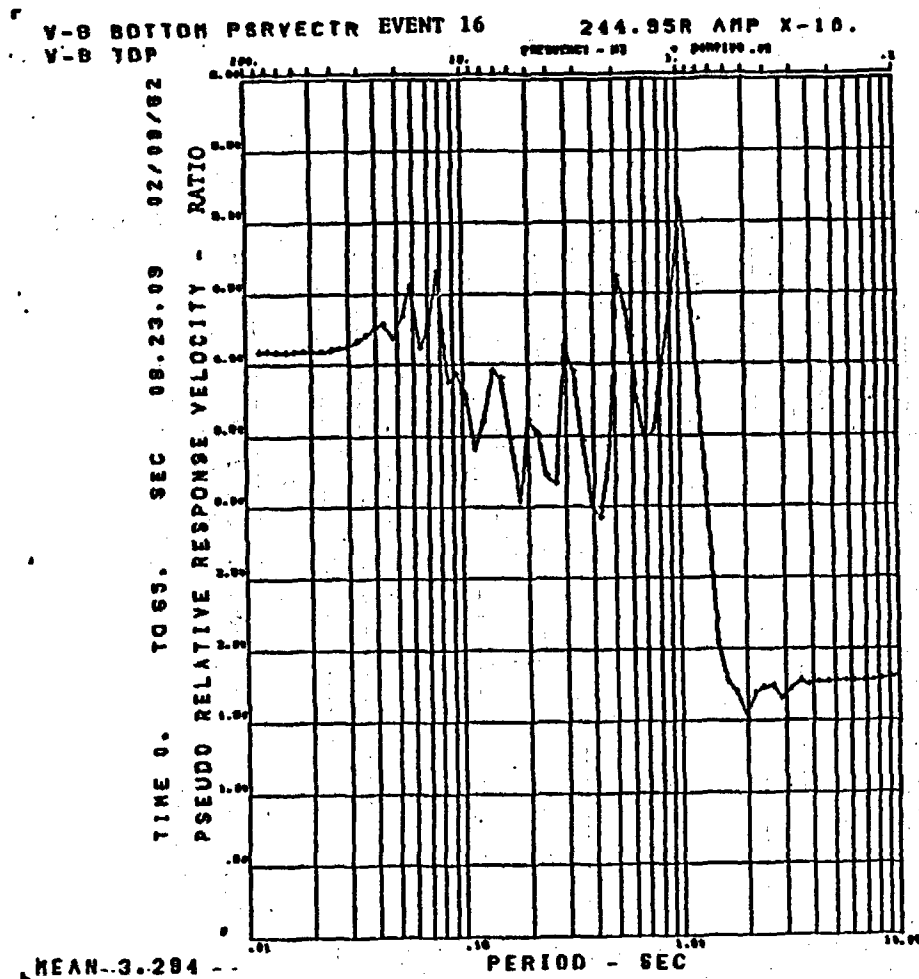


Figure B-38a

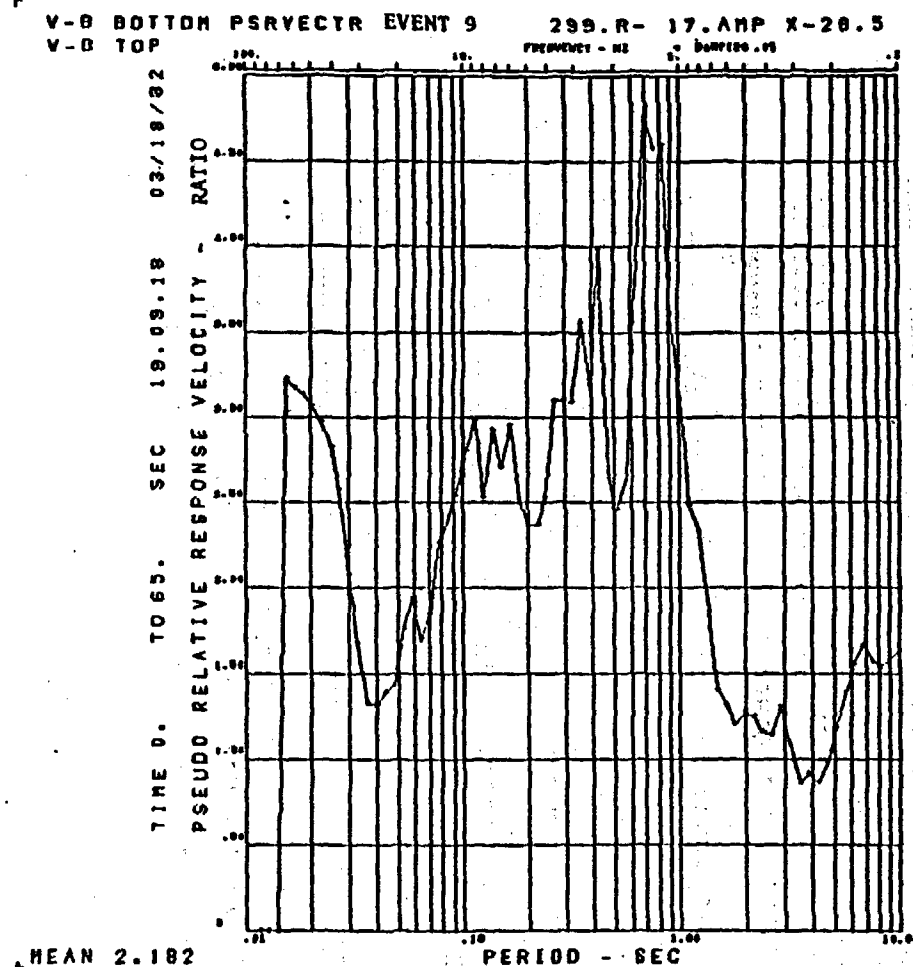


Figure B-38b

130
V16
V15

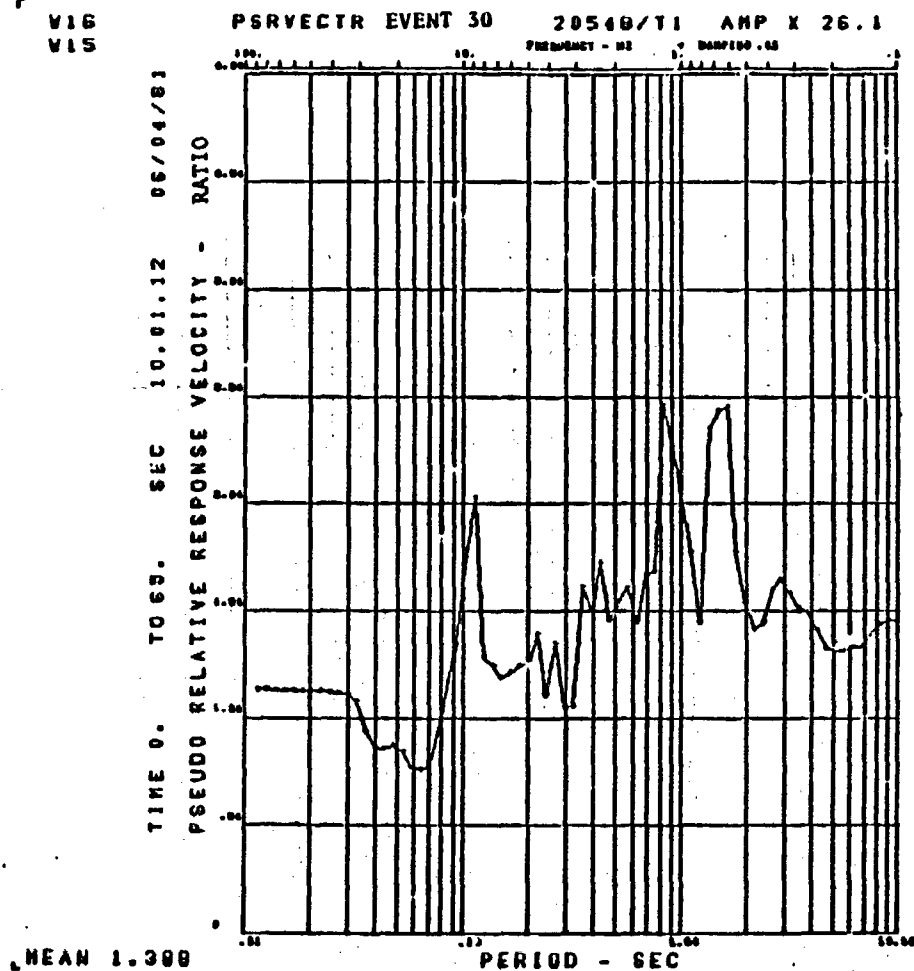


Figure B-39a

V16
V15

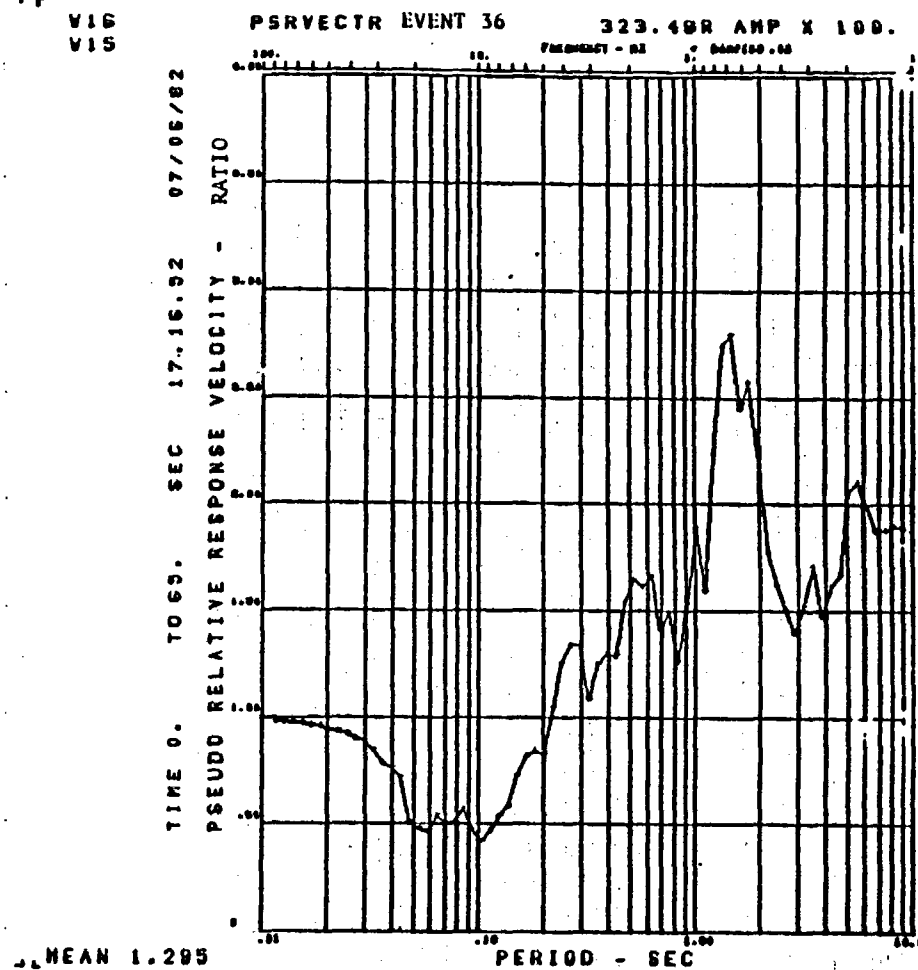


Figure B-39b

V18
V15

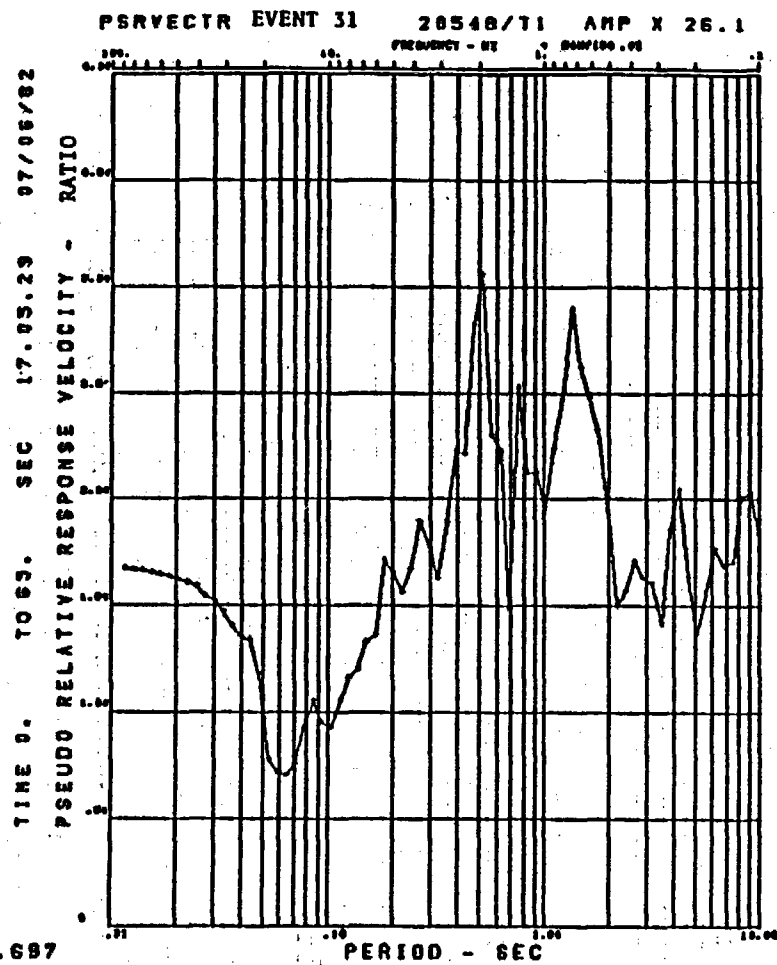


Figure B-40a

V16
V15

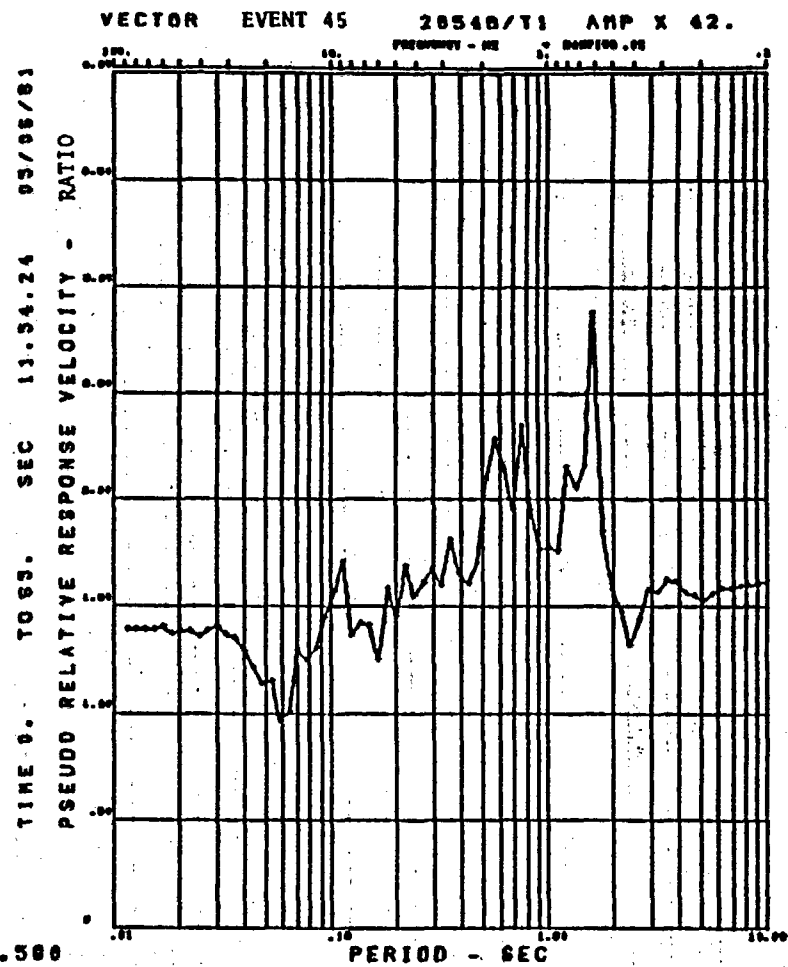


Figure B-40b

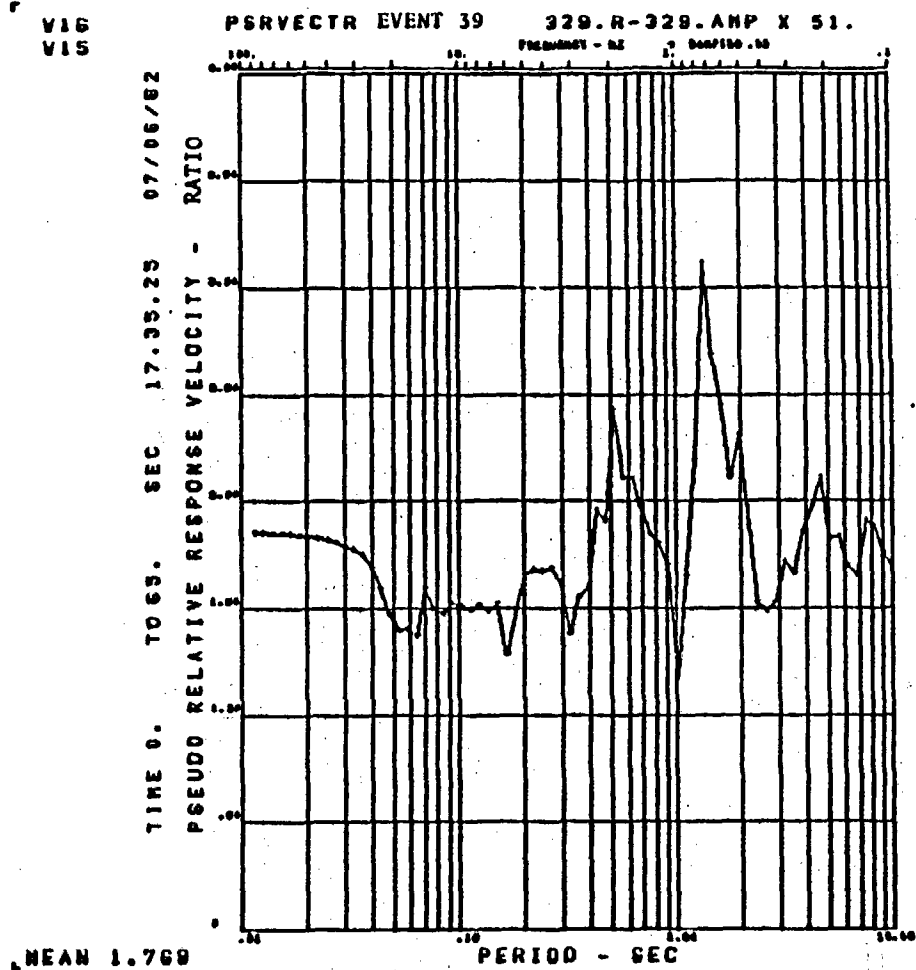
V16
V15

Figure B-41a

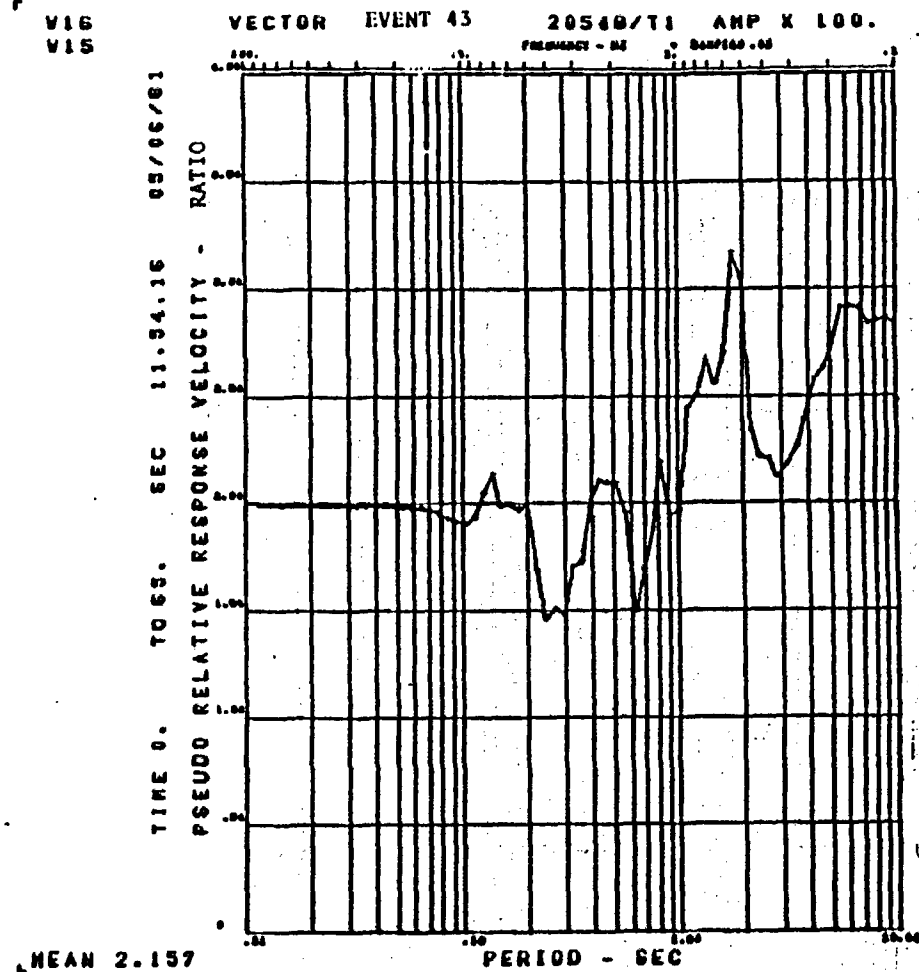
V16
V15

Figure B-41b

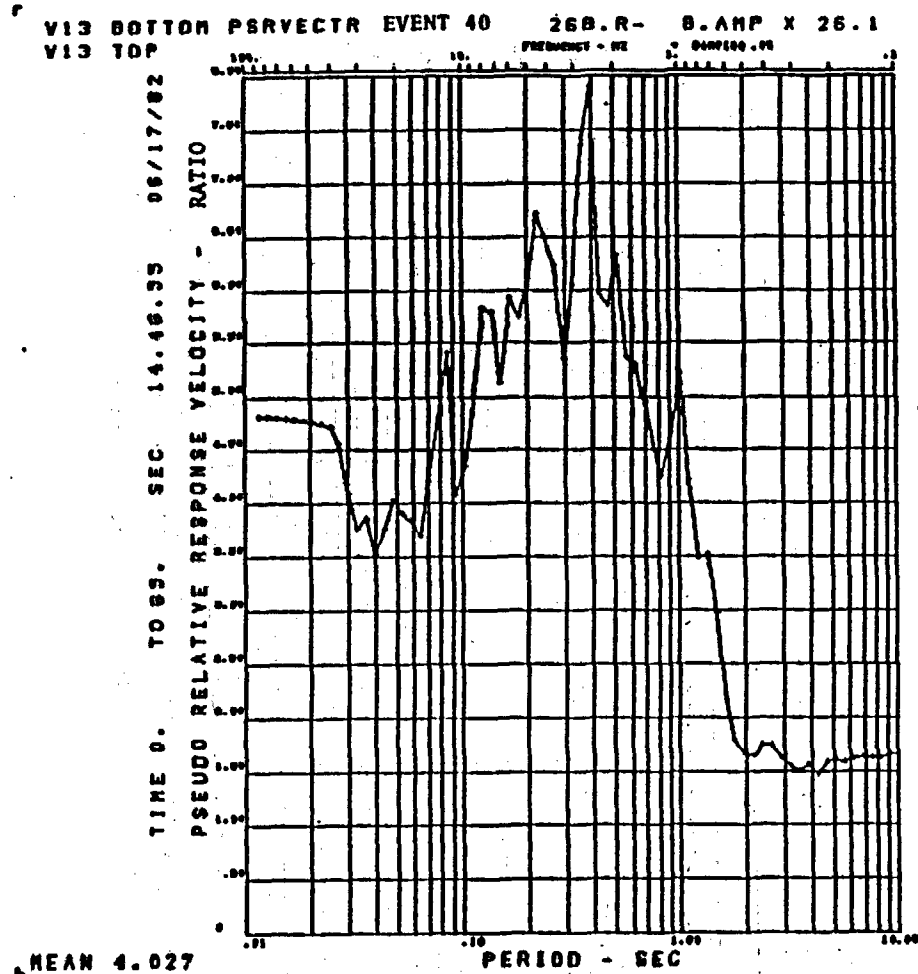


Figure B-42a

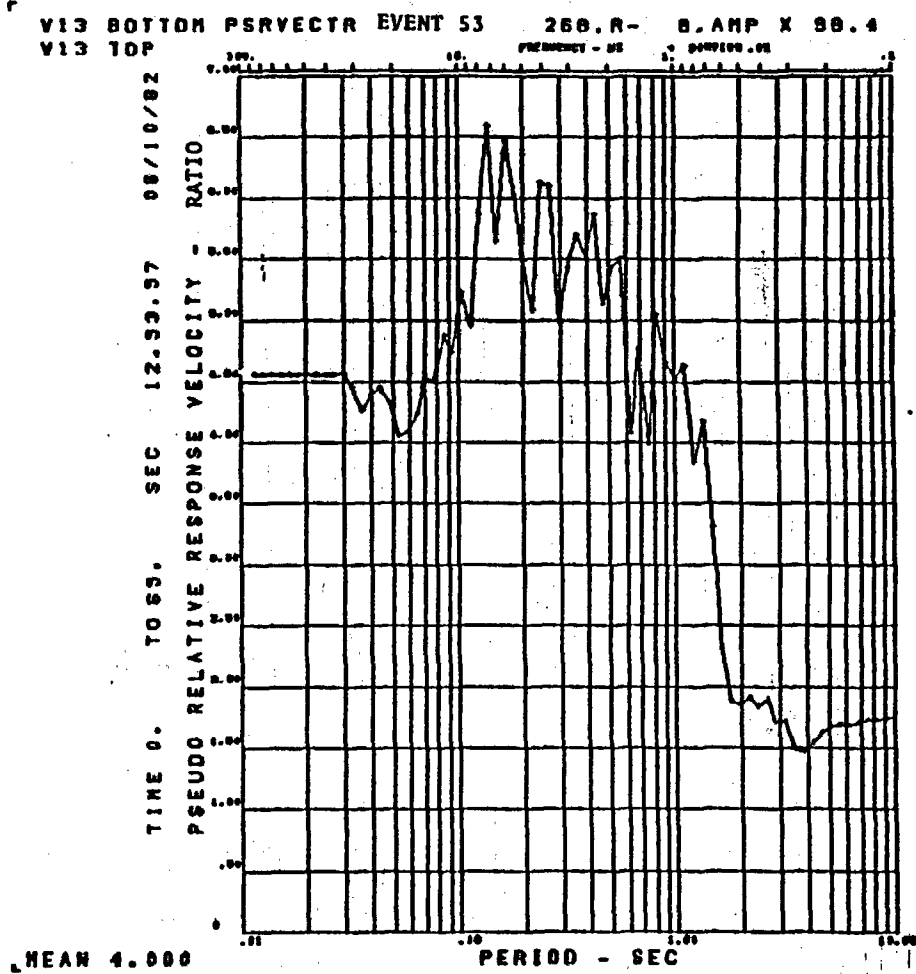


Figure B-42b

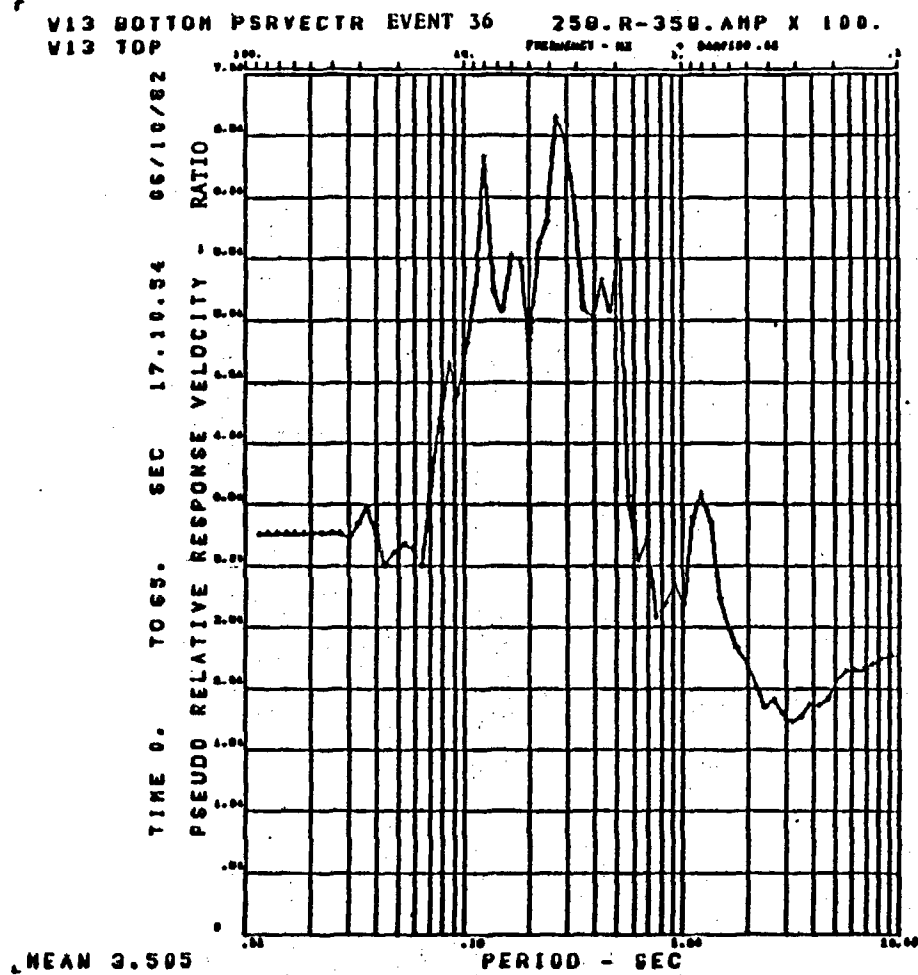


Figure B-43a

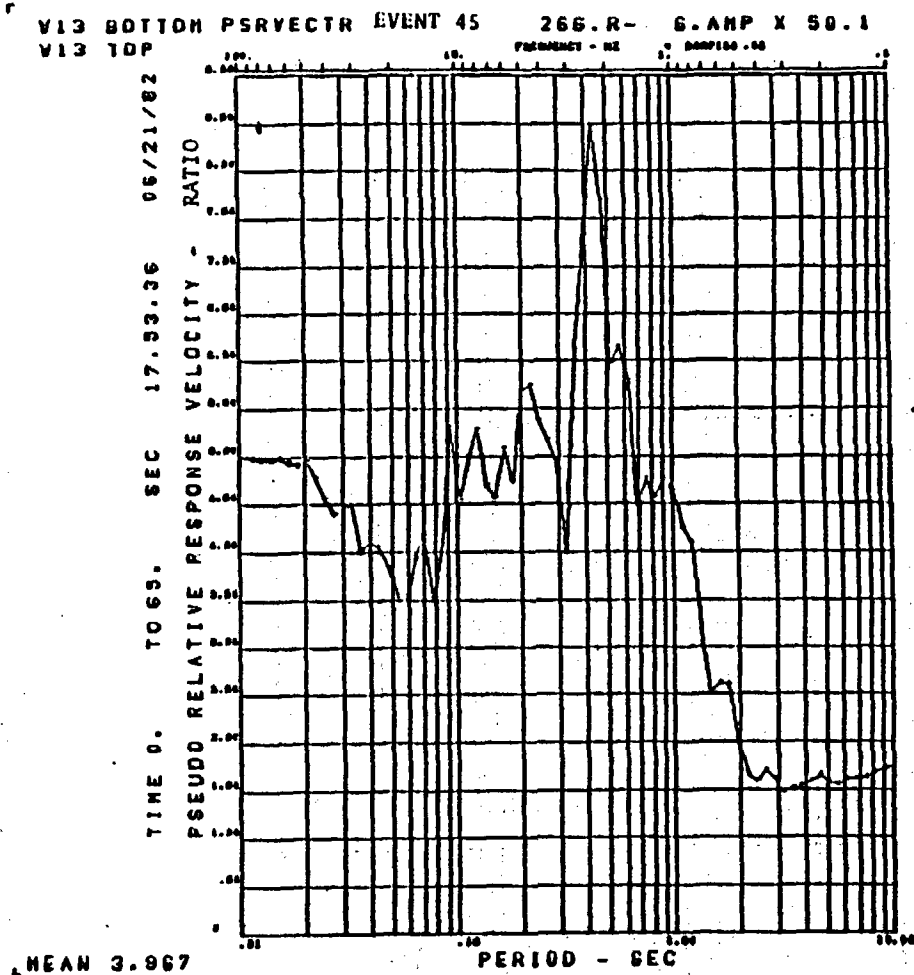


Figure B-43b

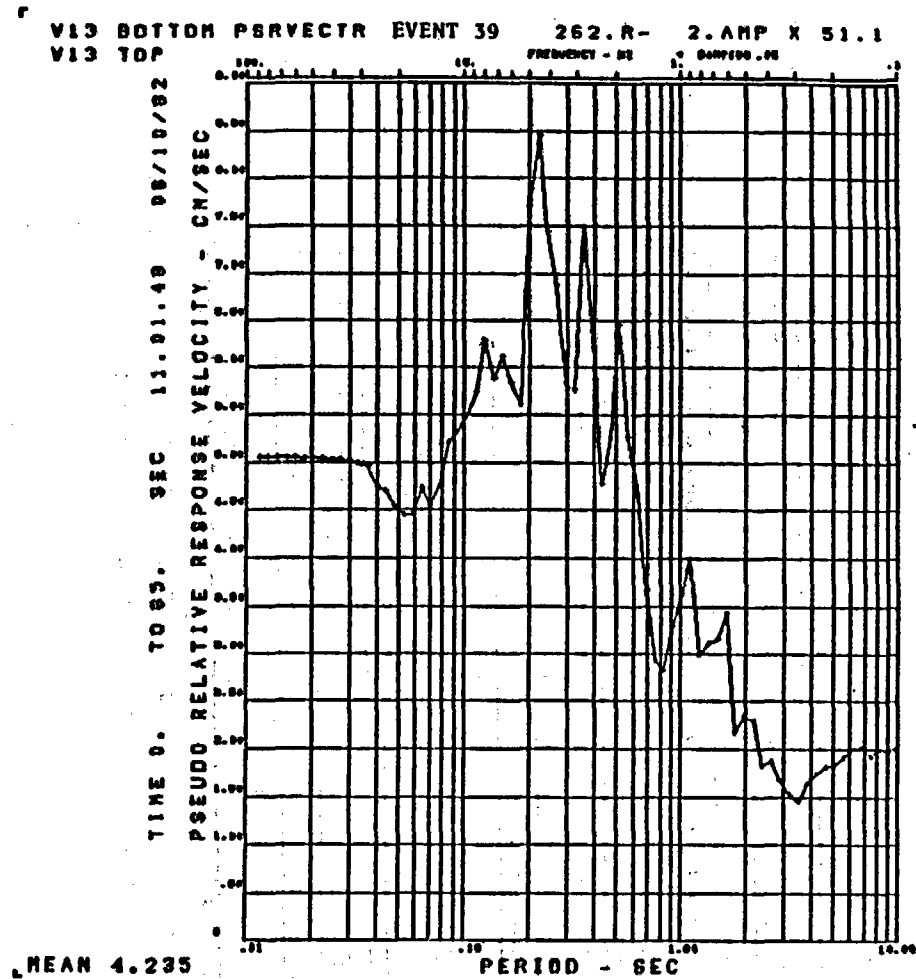


Figure B-44a

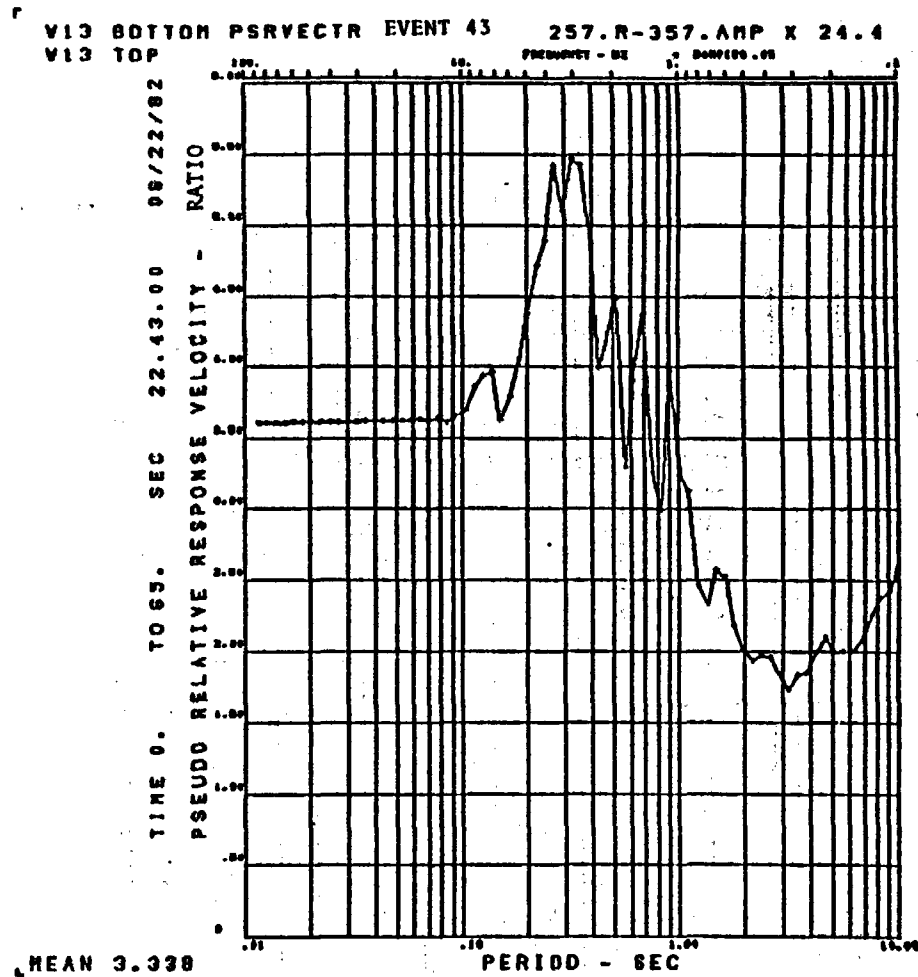


Figure B-44b

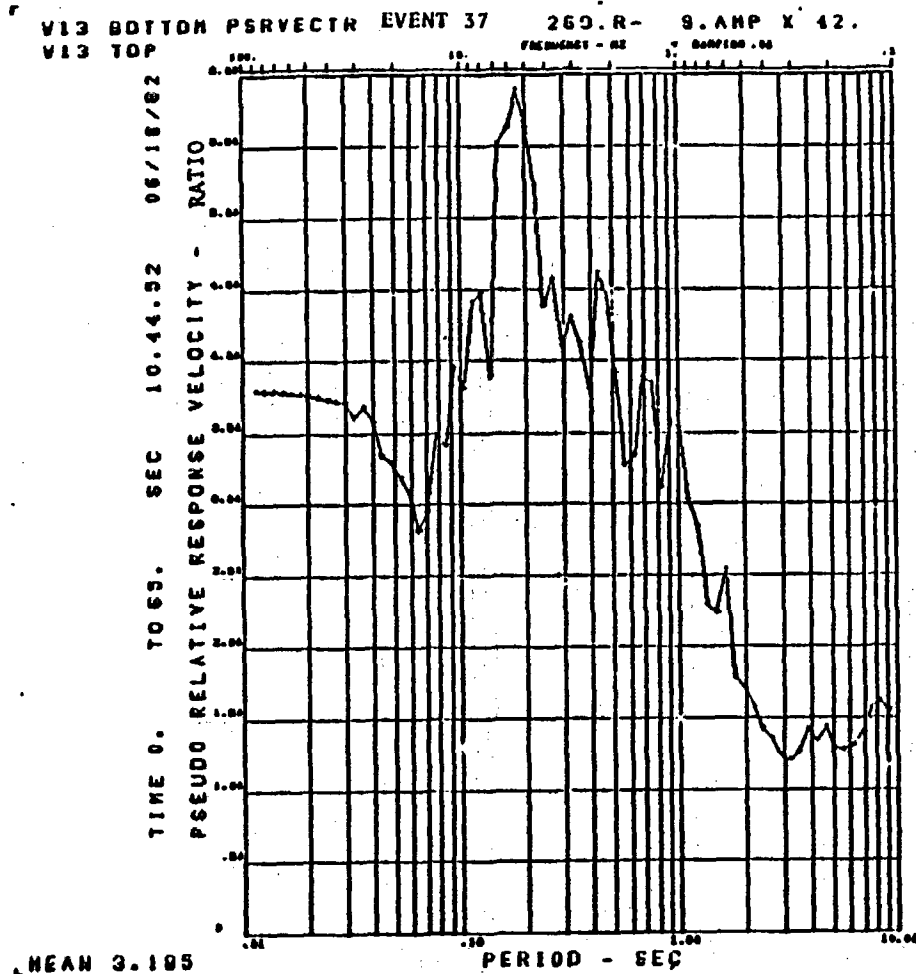


Figure B-45a

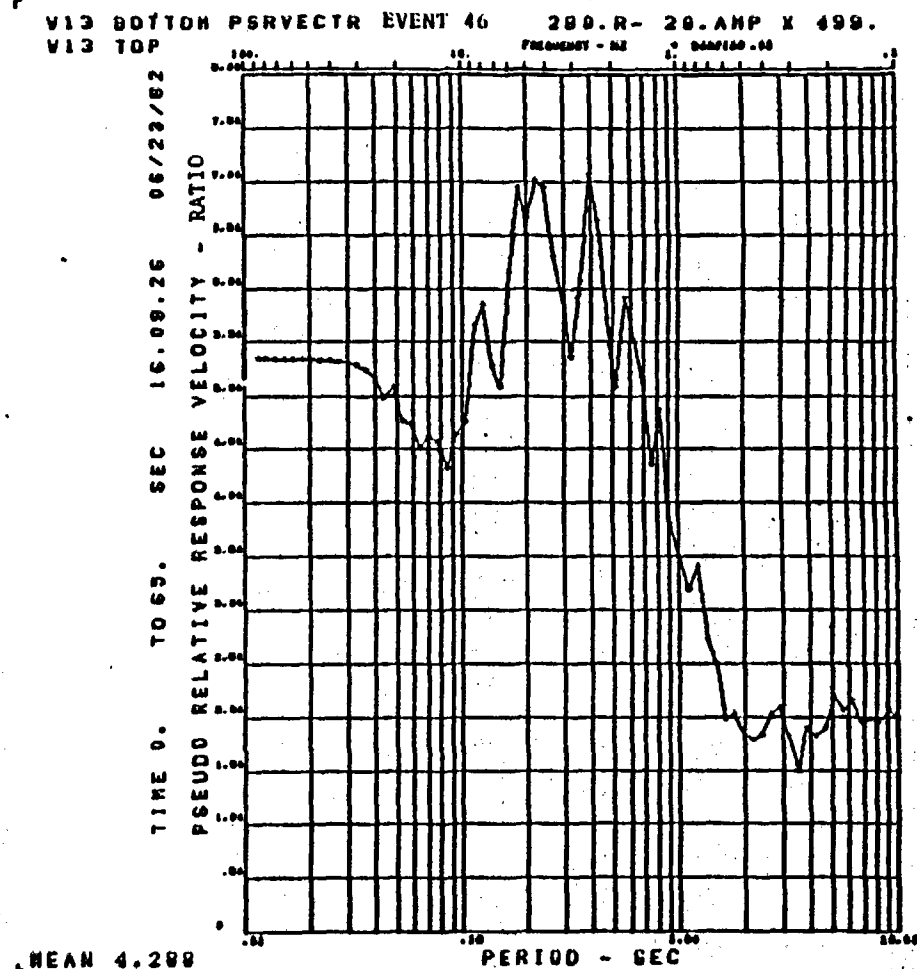
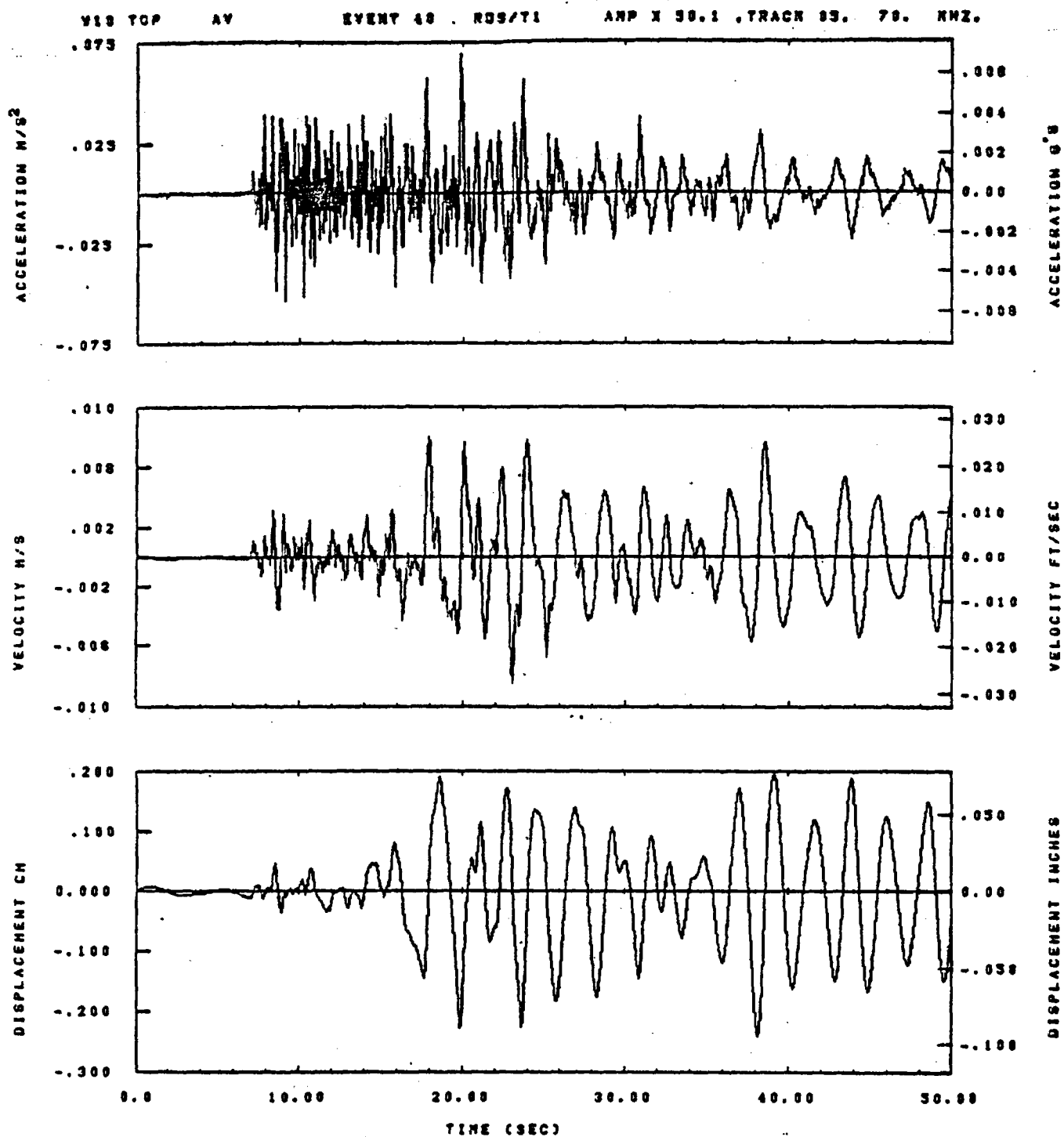


Figure B-45b

APPENDIX C

COMPARISON OF TOP AND BOTTOM

WAVEFORMS AT STATION W-10

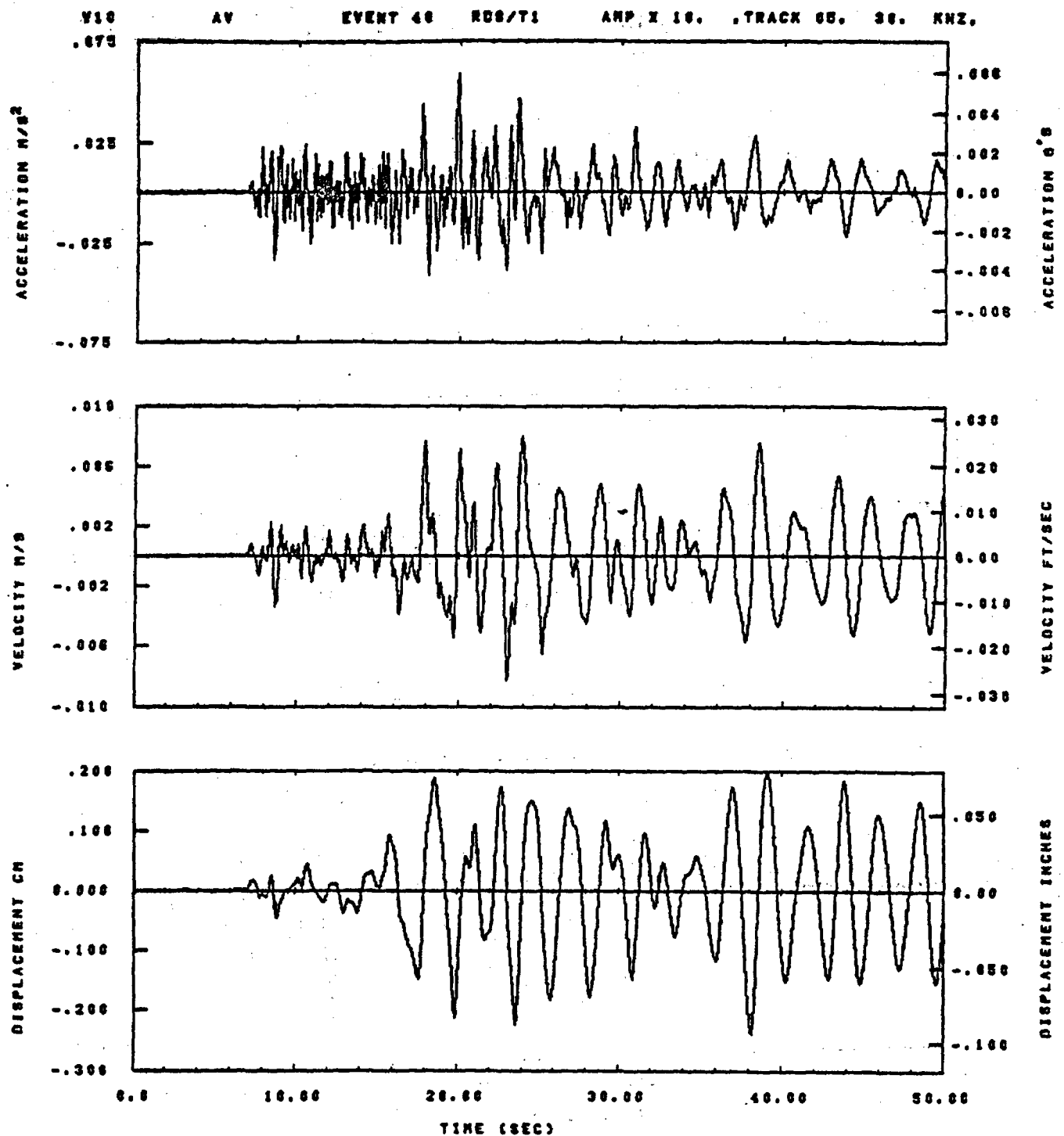


IOT= .0029	ODT= .003	FIX=	AAS= 0.
HPF= .25	BYH= .18	HLH= 187	ASB=
LPF= 27.	BYL= 6.	HLL= 2339	ASE=
VTS= .230	VTE= .188	FLL= -20.	VSE= 0.
DPS= 0.	DPE= 83.	FLN= 0	DSE= 0.

10.04.40.

08/22/82

Figure C-1

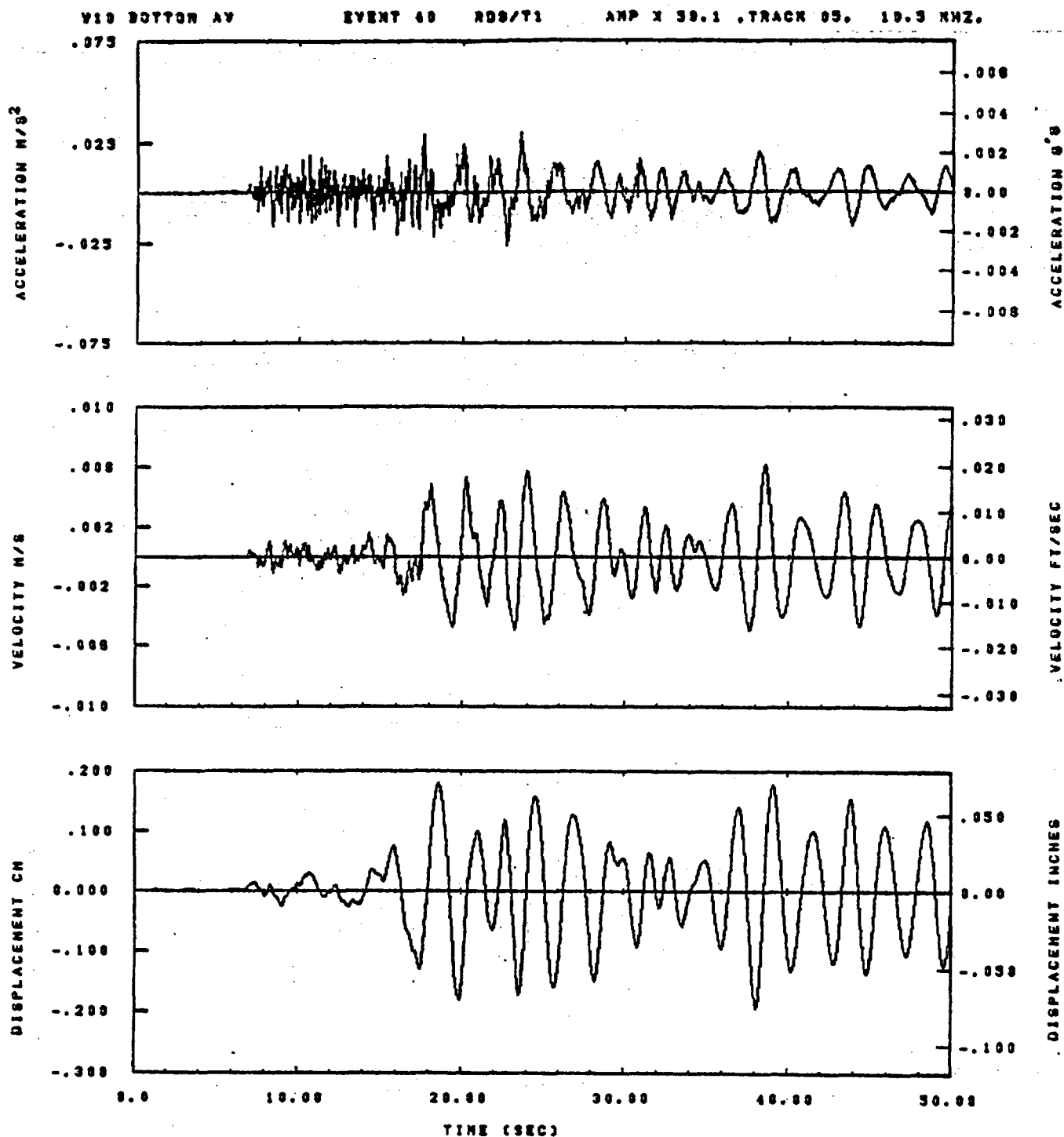


IDT= .0020	ODT= .000	FIX=	AAS= 0.
HPF= .25	BVN= .10	HLN= 107	ASB=
LPF= 27.	BVL= 0.	HLL= 2300	ASE=
VTS= .250	VTE= .100	FLL= -20.	VSE= 0.
DPS= 0.	DPE= 00.	FLH= 0	DSE= 0.

10.13.31.

06/22/02

Figure C-2

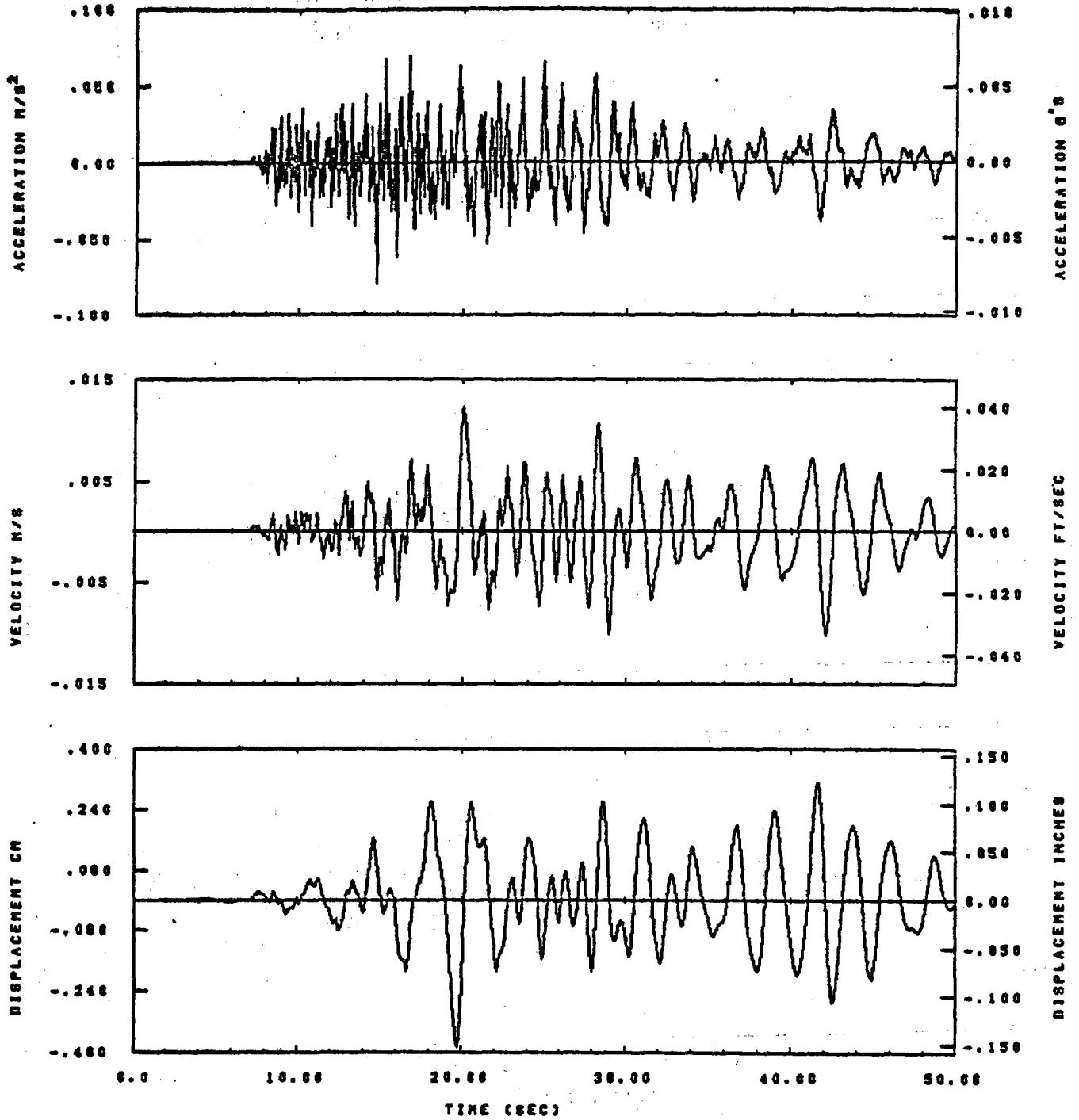


IDT= .0028	ODT= .003	FIX=	AAS= 0.
HPP= .25	BYH= .18	HLH= 187	ASB=
LPP= 27.	BYL= 8.	HLL= 2399	ASE=
VTB= .259	VTE= .188	FLL= -20.	VSE= 0.
DPS= 0.	DPE= 95.	FLH= 0	DSE= 0.

09.38.58.

08/22/92

V10 TOP AR EVENT 40 301.R-211. ANP X 88.1 .TRACK 03. 82.5 KHZ.

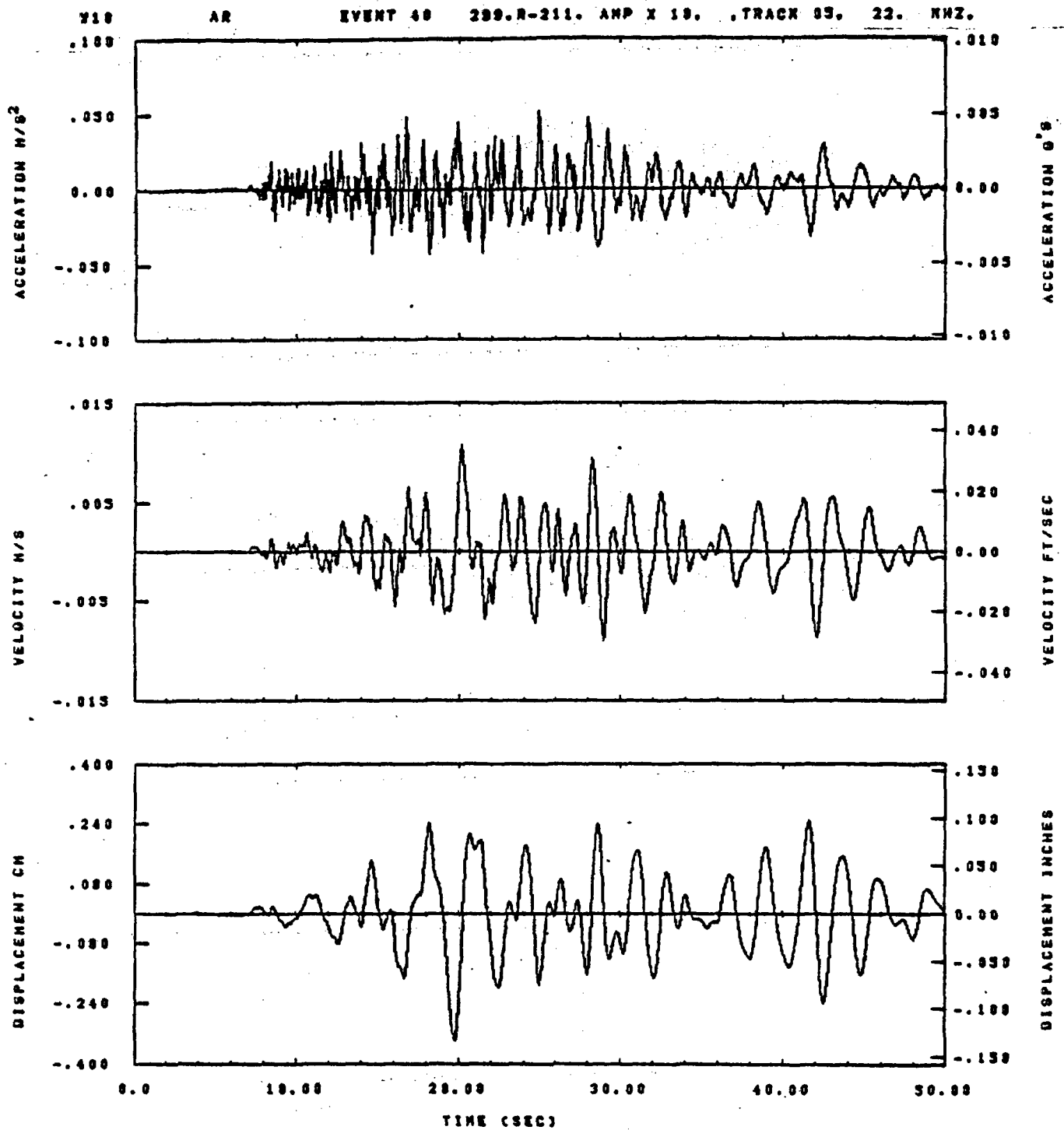


IDT= .0020	ODT= .005	FIX=	AAS= 0.
HPP= .25	BYH= .18	HLN= 187	ASB=
LPP= 27.	BYL= 6.	HLL= 2380	ASE=
VTB= .250	VTE= .160	FLL= -20.	VSE= 0.
DPS= 0.	DPE= 100.	FLH= 0	DSE= 0.

10.04.58.

06/22/82

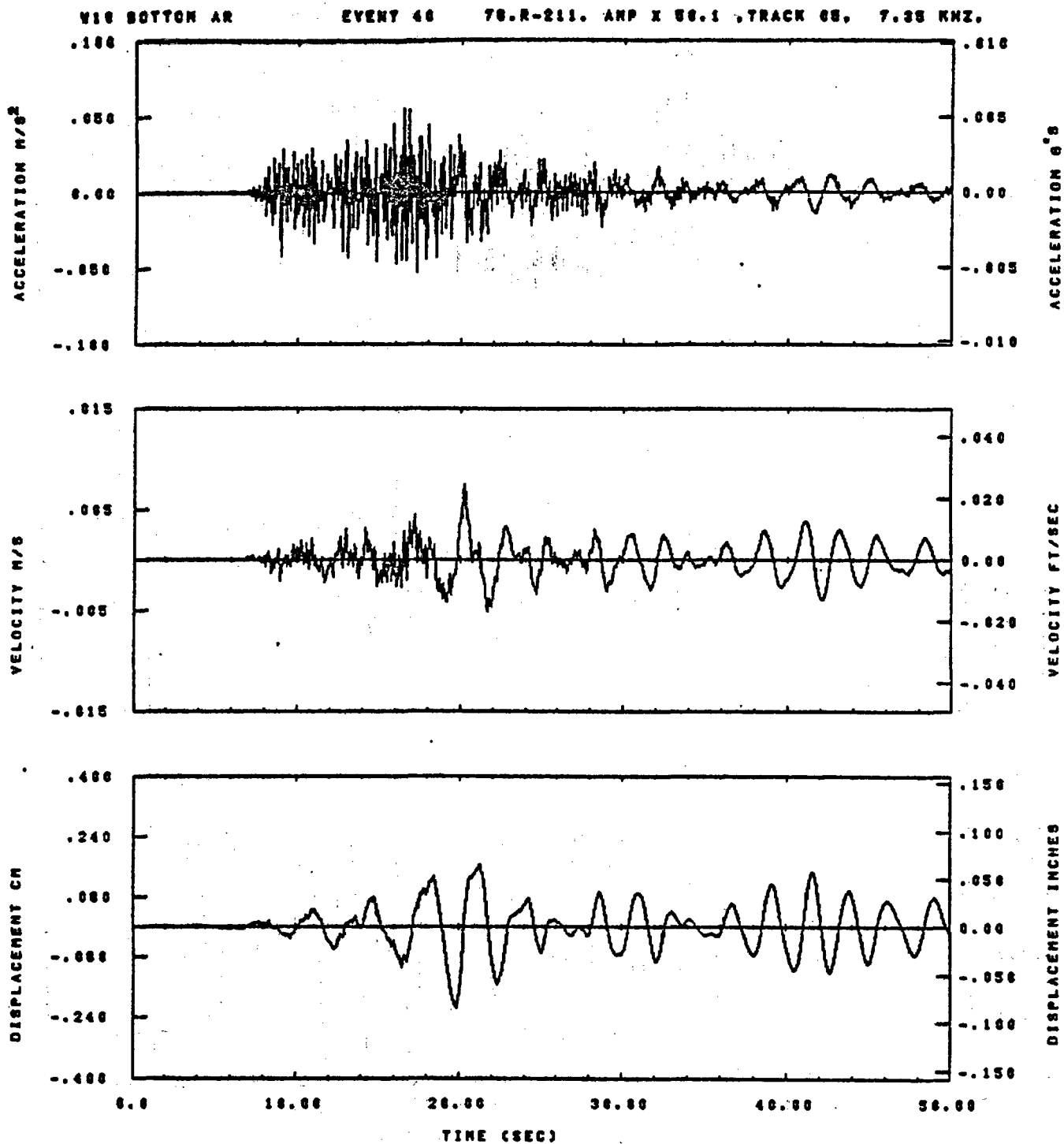
Figure C-4



IDT= .0020	DDT= .003	FIX=	AAS= 0.
HPP= .23	BYH= .18	HLH= 187	ASB=
LPP= 27.	BYL= 8.	HLL= 2399	ASE=
VTE= .250	VTE= .168	FLL= -20.	VSE= 0.
DPS= 0.	DPE= 99.	FLH= 0	DSE= 0.

10.13.42.

08/22/92

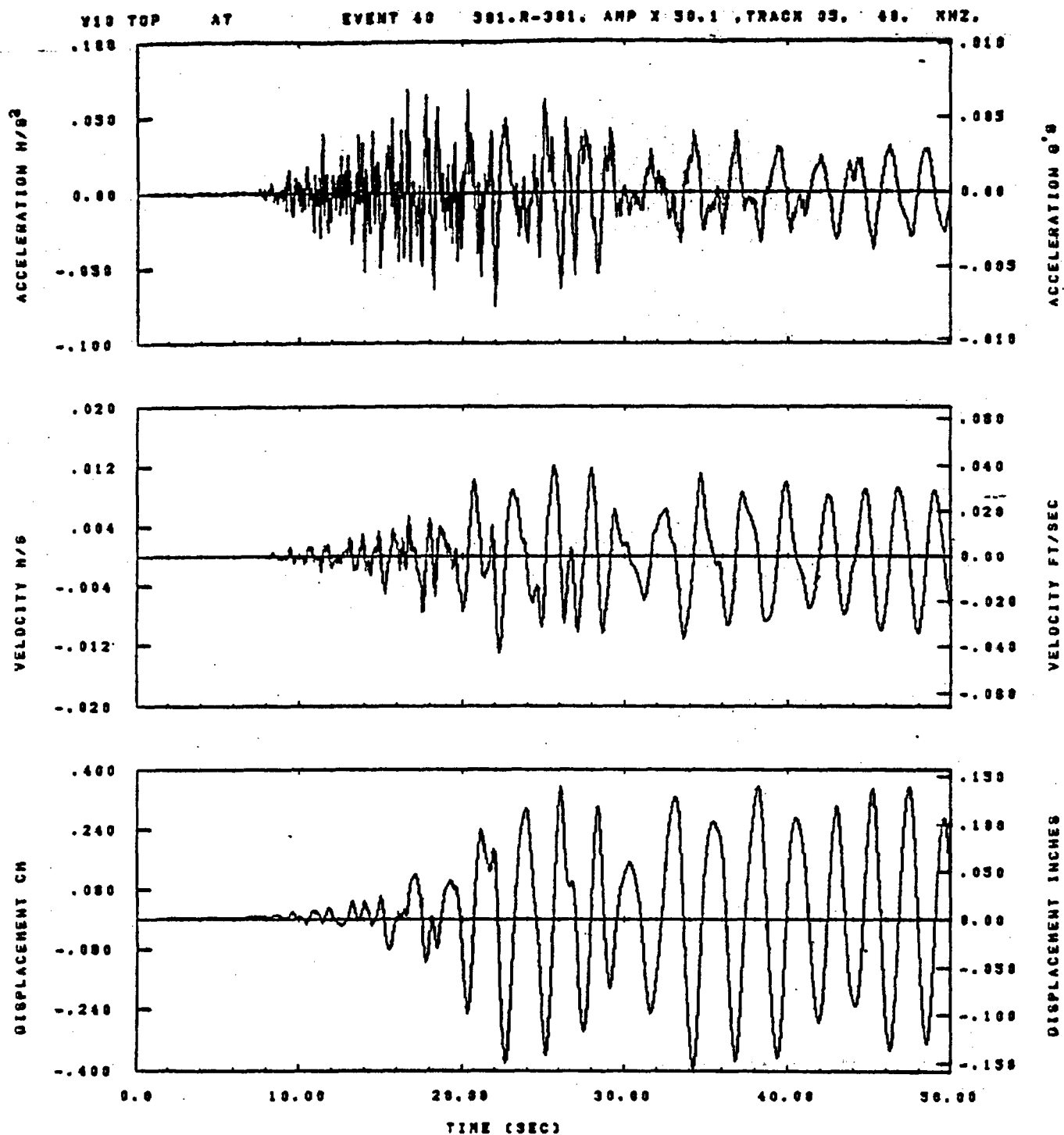


IDT= .0020	QDT= .005	FIX=	AAS= 0.
HFF= .25	BYH= .10	HLH= 107	ASH=
LFF= 27.	BYL= 0.	HLL= 2380	ASE=
VTS= .250	VTE= .100	FLL= -20.	VSE= 0.
DPS= 0.	DPE= 05.	FLH= 0	DSE= 0.

00.57.00.

06/22/02

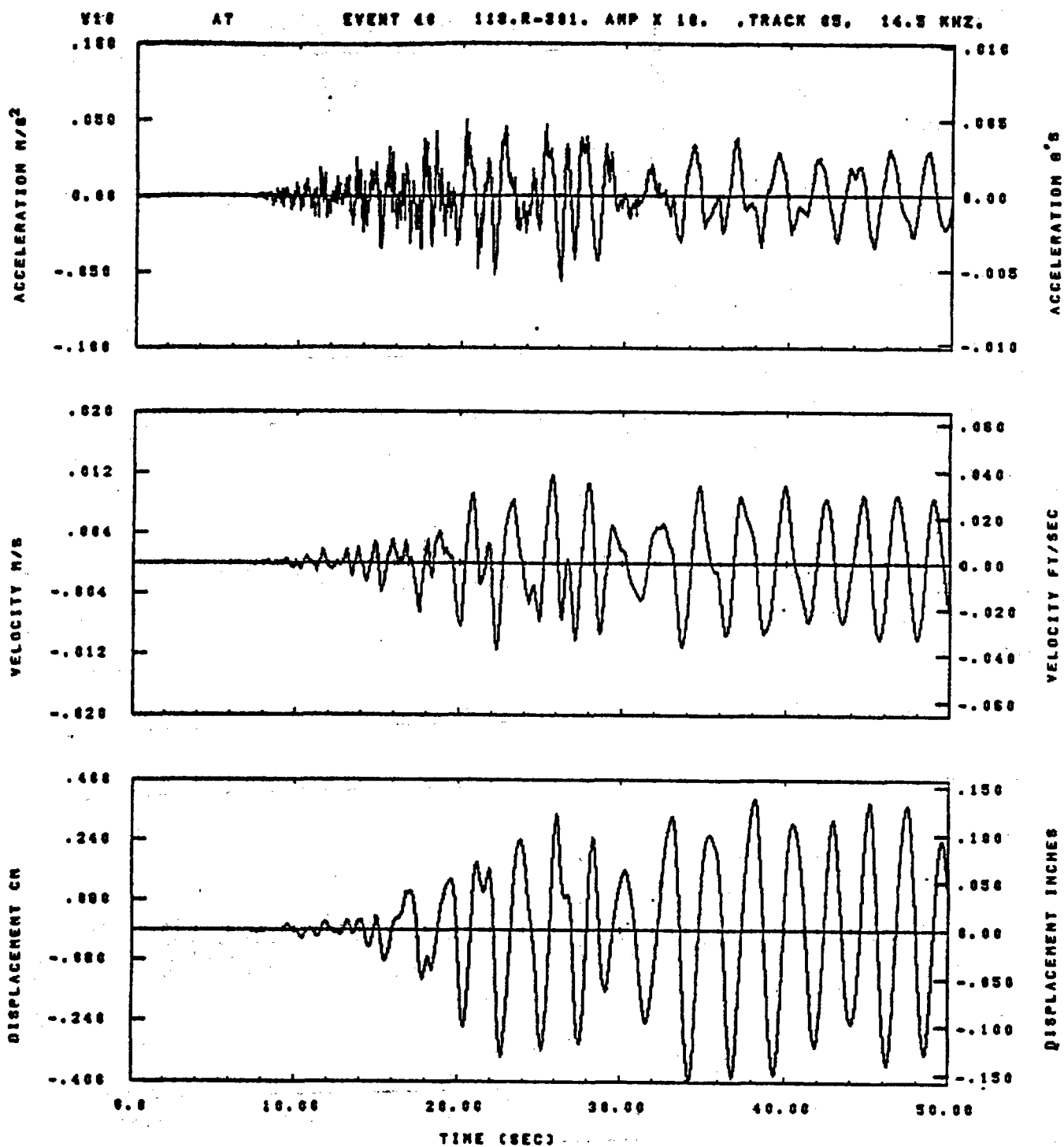
Figure C-6



IDT= .0020	ODT= .003	FIX=	AAS= 0.
MPF= .25	BYM= .10	HLH= 107	ASB=
LPF= 27.	BYL= 0.	HLL= 2333	ASE=
VTS= .250	VTE= .100	FLL= -20.	VSE= 0.
DPS= 0.	DPE= 100.	FLH= 0	DSE= 0.

10.05.03.

08/22/02



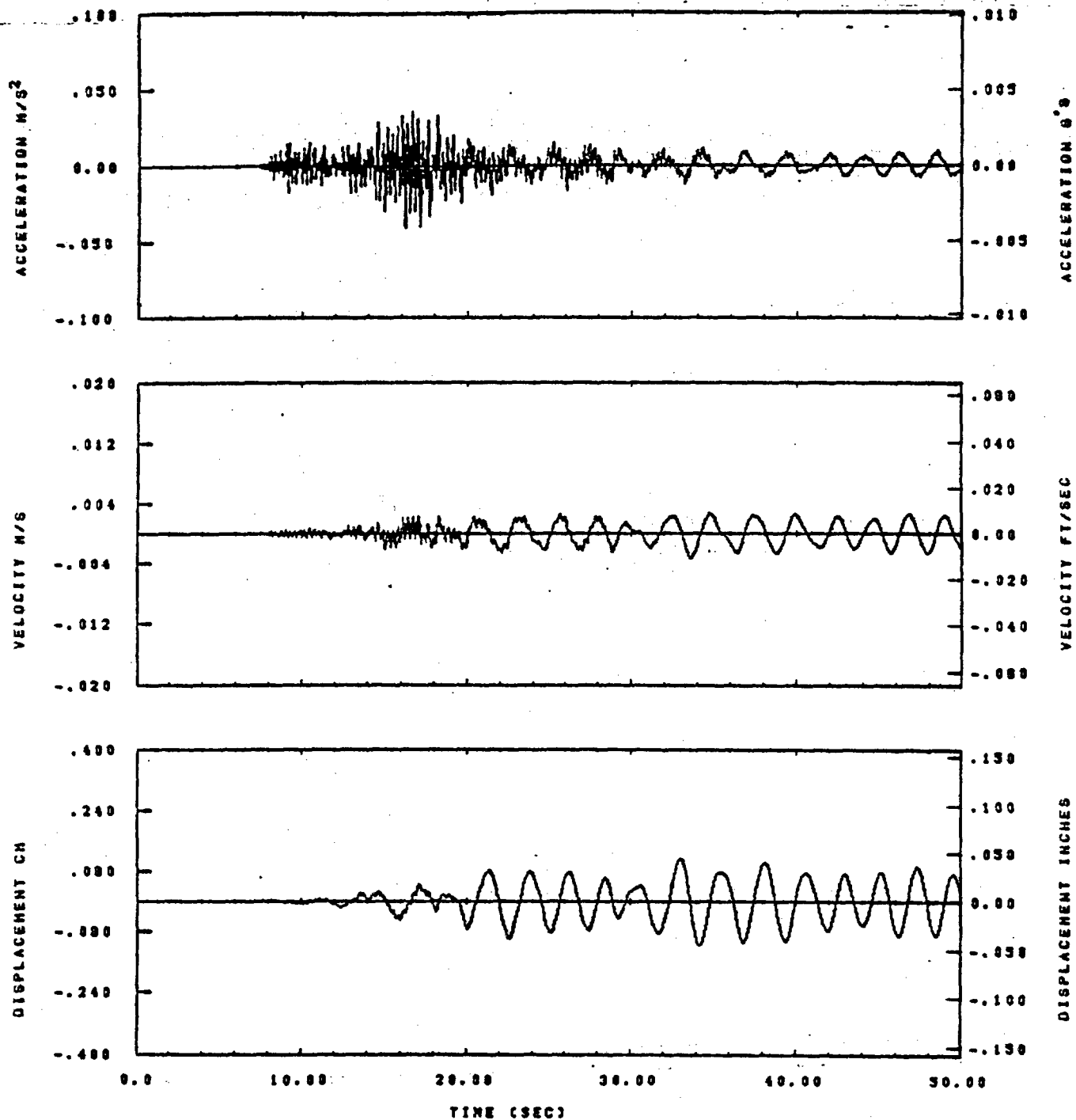
IDT= .0020	OST= .005	FIX=	AAS= 0.
HPP= .25	SVN= .10	HLH= 167	ASB=
LPP= 27.	SVL= 6.	HLL= 2390	ASE=
VTS= .250	VTE= .100	FLL= -20.	VSE= 0.
DPS= 0.	DPE= 05.	FLH= 0	DSE= 0.

10.13.55.

06/22/82

Figure C-8

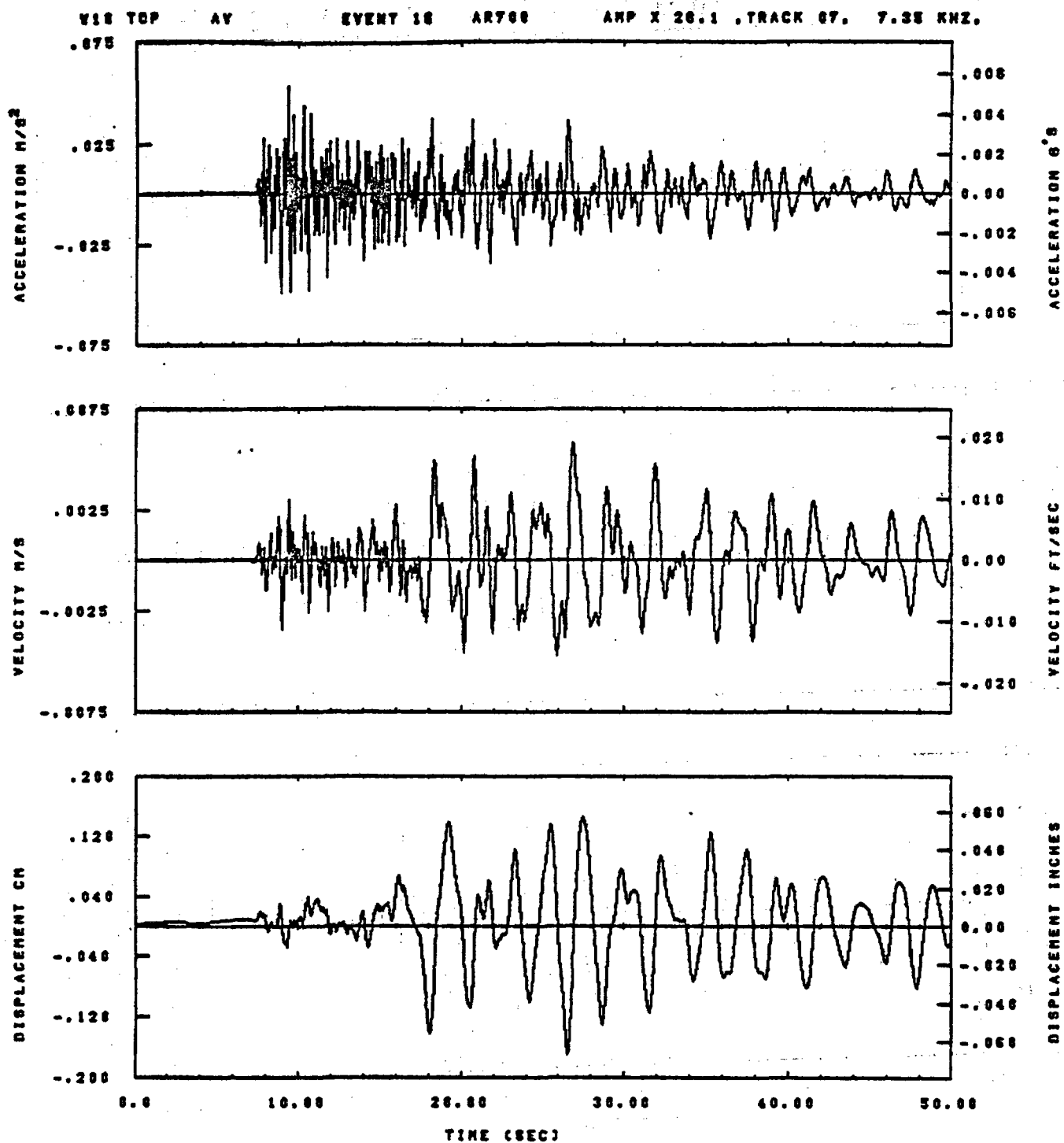
Y10 BOTTOM AT EVENT 48 78.R-301. AMP X 50.1 .TRACK 03. 3.4 KHZ.



IDT= .0020	ODT= .003	FIX=	AAS= 0.
HPP= .25	BYH= .18	HLH= 187	ASH=
LPP= 27.	BYL= 8.	HLL= 2399	ASE=
VTB= .250	VTE= .180	FLL= -20.	VSE= 0.
DPS= 0.	DPE= 93.	FLH= 0	DSE= 0.

09.37.19.

08/22/92

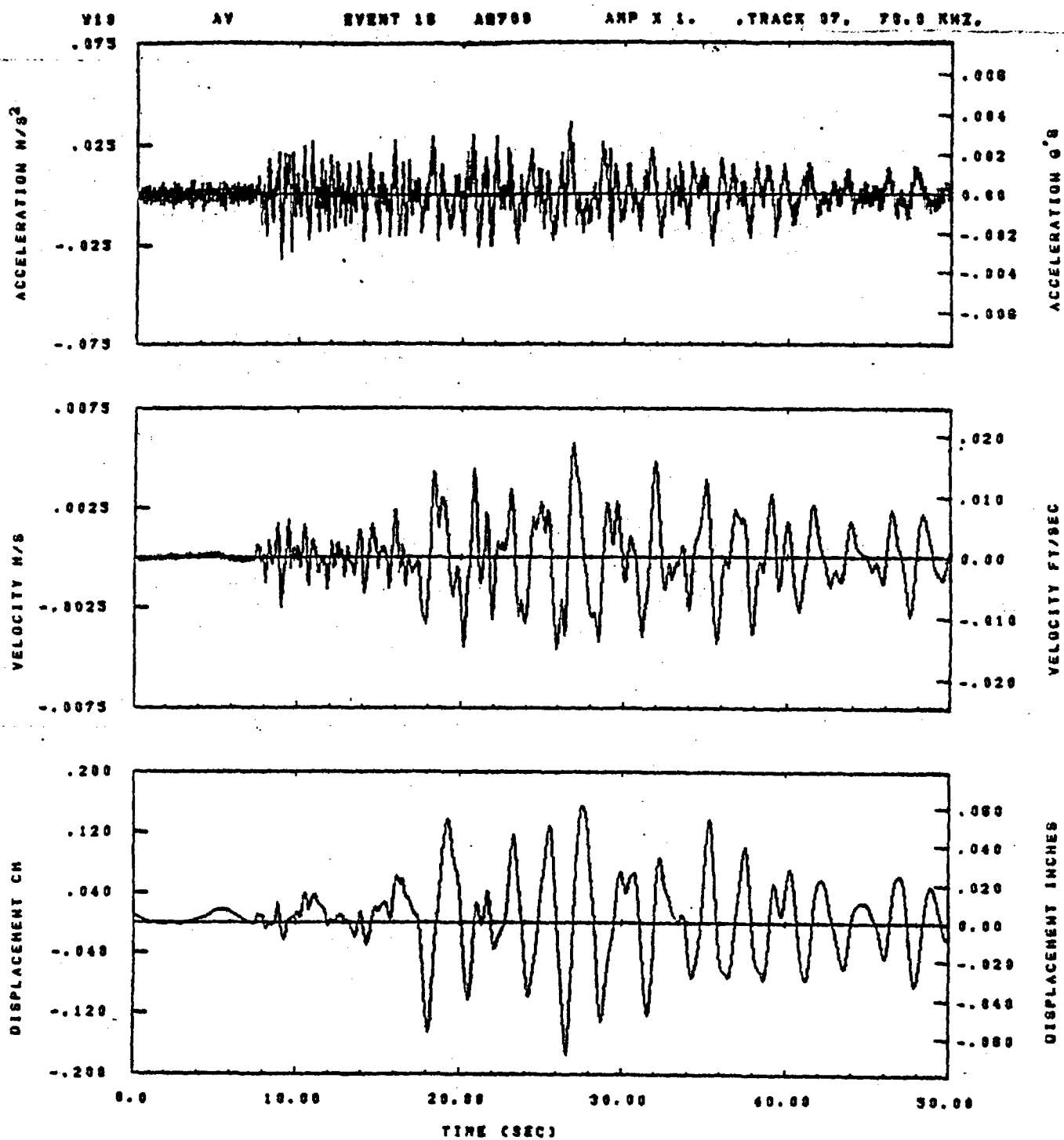


IDT= .0020	QDT= .005	FIX=	AAS= 0.
HPF= .20	BYH= .13	HLH= 251	ASB=
LPF= 18.	BYL= 4.	HLL= 2888	ASE=
VTS= .200	VTE= .133	FLL= -20.	VSE= 0.
DPS= 0.	DPE= 100.	FLH= A-.1	DSE= A+.1

00.48.00.

07/02/02

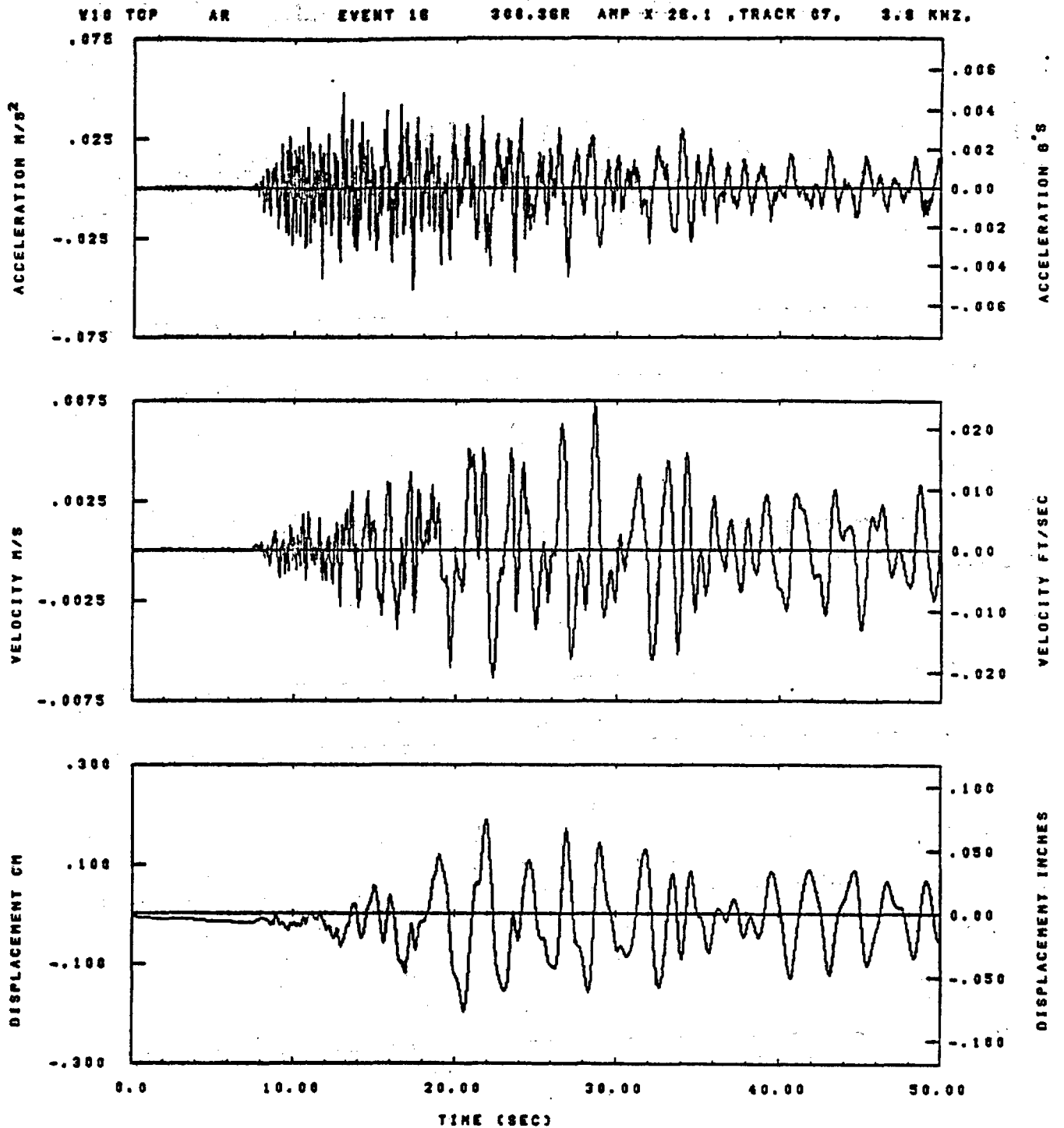
Figure C-10



IDT= .0020	QDT= .005	FIX=	AAS= 0.
HPP= .20	BYN= .13	HLH= 251	ASB=
LPP= 18.	BVL= 4.	HLL= 2999	ASE=
YTS= .200	YTE= .133	PLL= -20.	VSE= 0.
OPS= 0.	OPE= 100.	PLH= A+.1	DSE= A+.1

09.48.24.

07/02/82

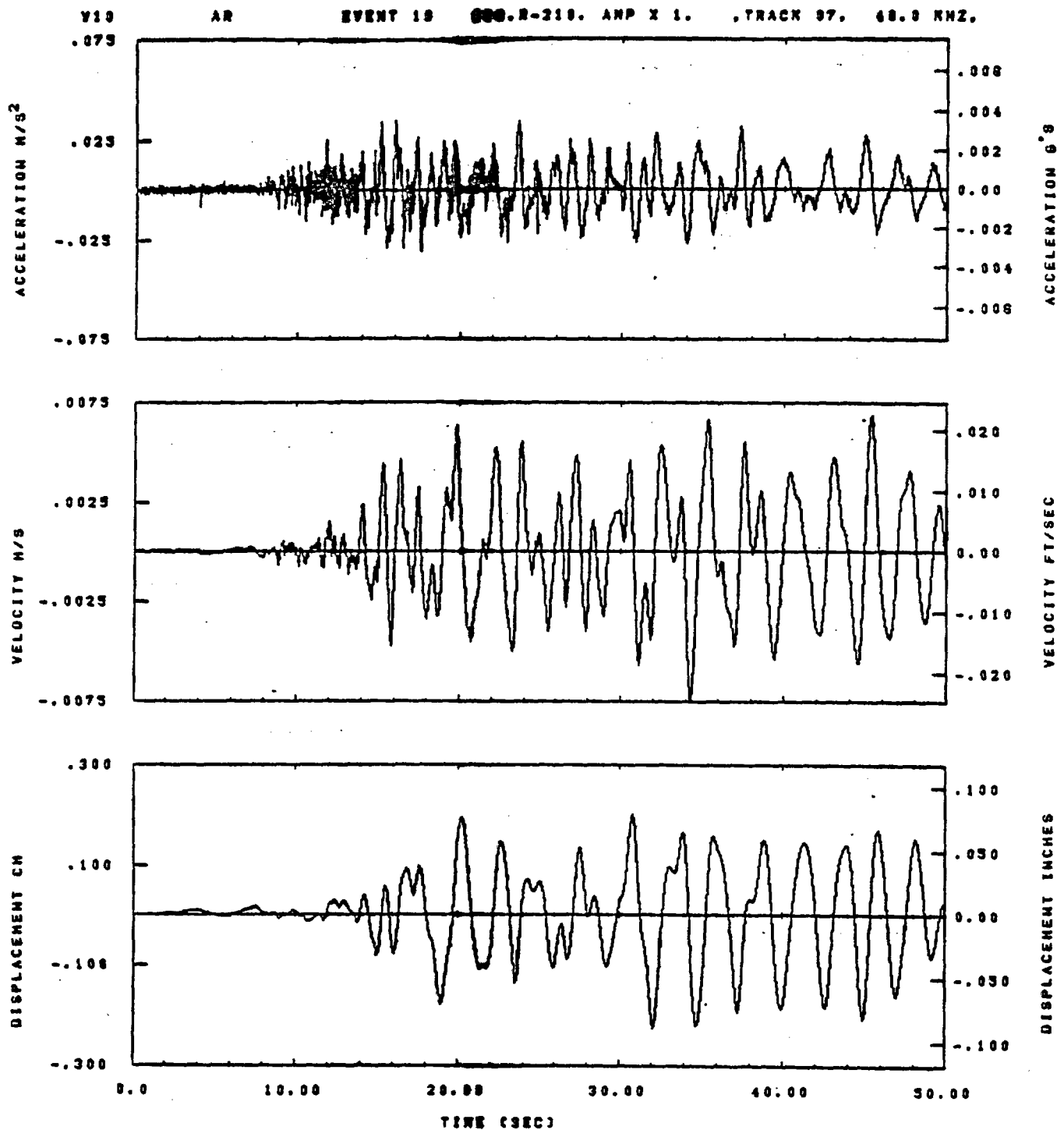


IDT= .0020	ODT= .005	FIX=	AAS= 0.
HPF= .20	BYH= .13	HLH= 251	ASB=
LPF= 18.	BYL= 4.	HLL= 2989	ASE=
VTE= .200	VTE= .133	FLL= -20.	VSE= 0.
DPS= 0.	DPE= 100.	FLH= A-.1	DSE= A+.1

11.21.27.

07/15/02

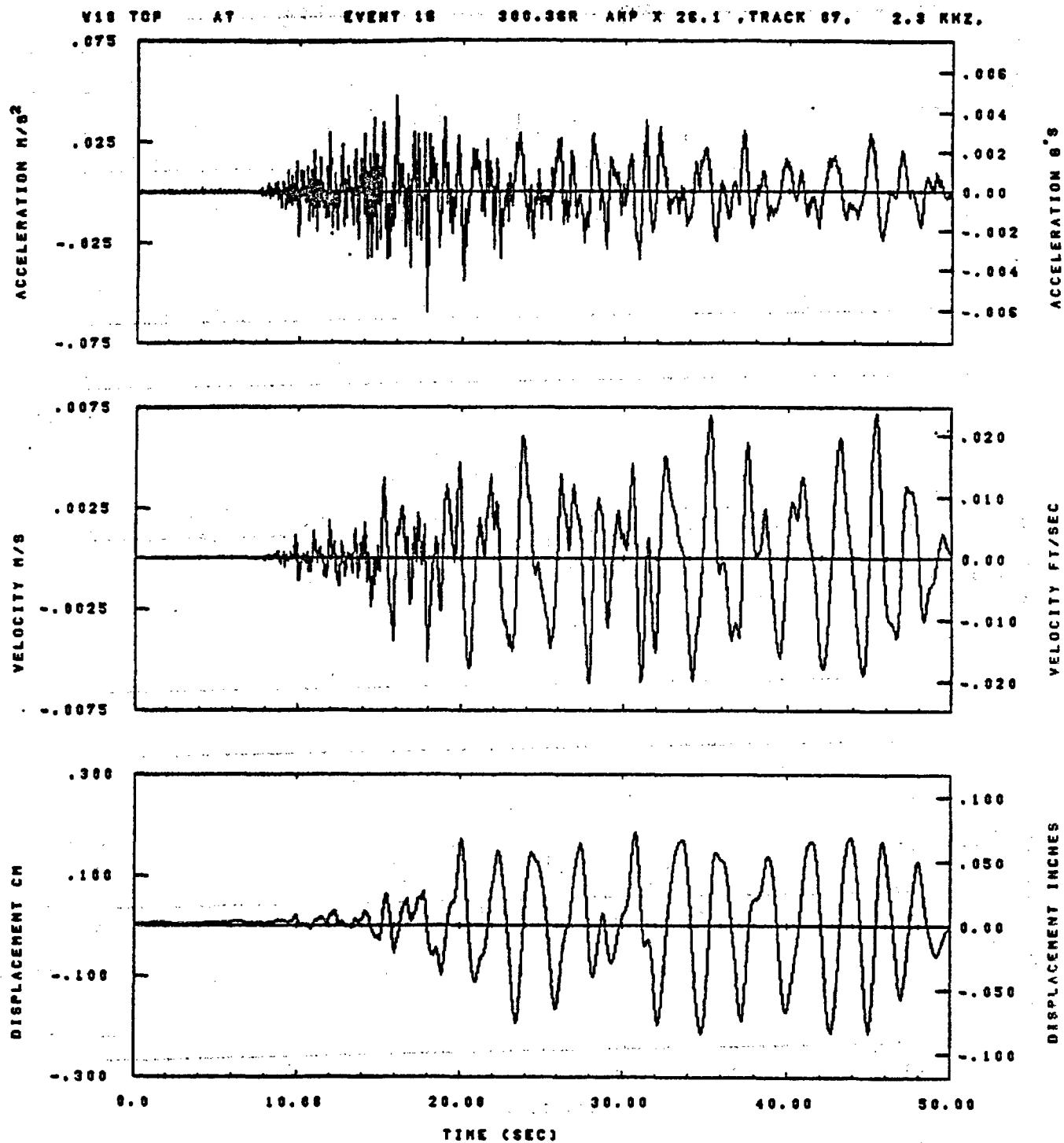
Figure C-12



IDT= .0020	QDT= .003	FIX=	AAS= 0.
HPP= .20	BYN= .13	NLN= 251	ASB=
LPP= 18.	BVL= 4.	NLL= 2399	ASE=
VTS= .200	VTE= .133	FLL= -20.	VSE= 0.
DPS= 0.	DPE= 100.	PLN= A-.1	DSE= A+.1

10.51.14.

07/15/92

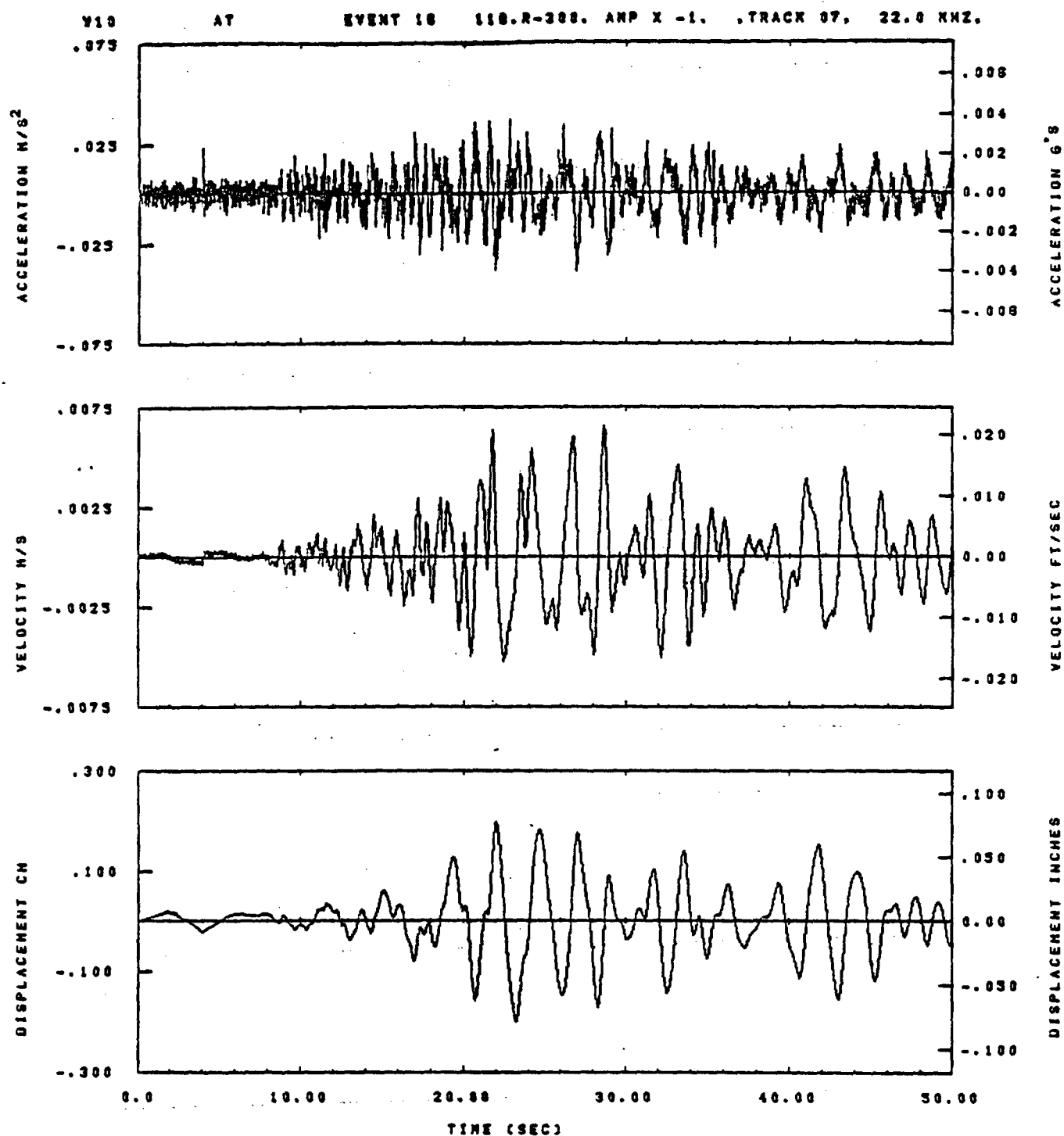


IDT= .0020	QDT= .005	FIX=	AAS= 0.
HPF= .20	SVN= .13	HLN= 251	ASS=
LPF= 18.	SVL= 4.	HLL= 2885	ASE=
VTB= .200	VTE= .133	FLL= -20.	VSE= 0.
DPS= 0.	DPE= 100.	FLH= A-.1	DSE= A+.1

11.21.36.

07/15/82

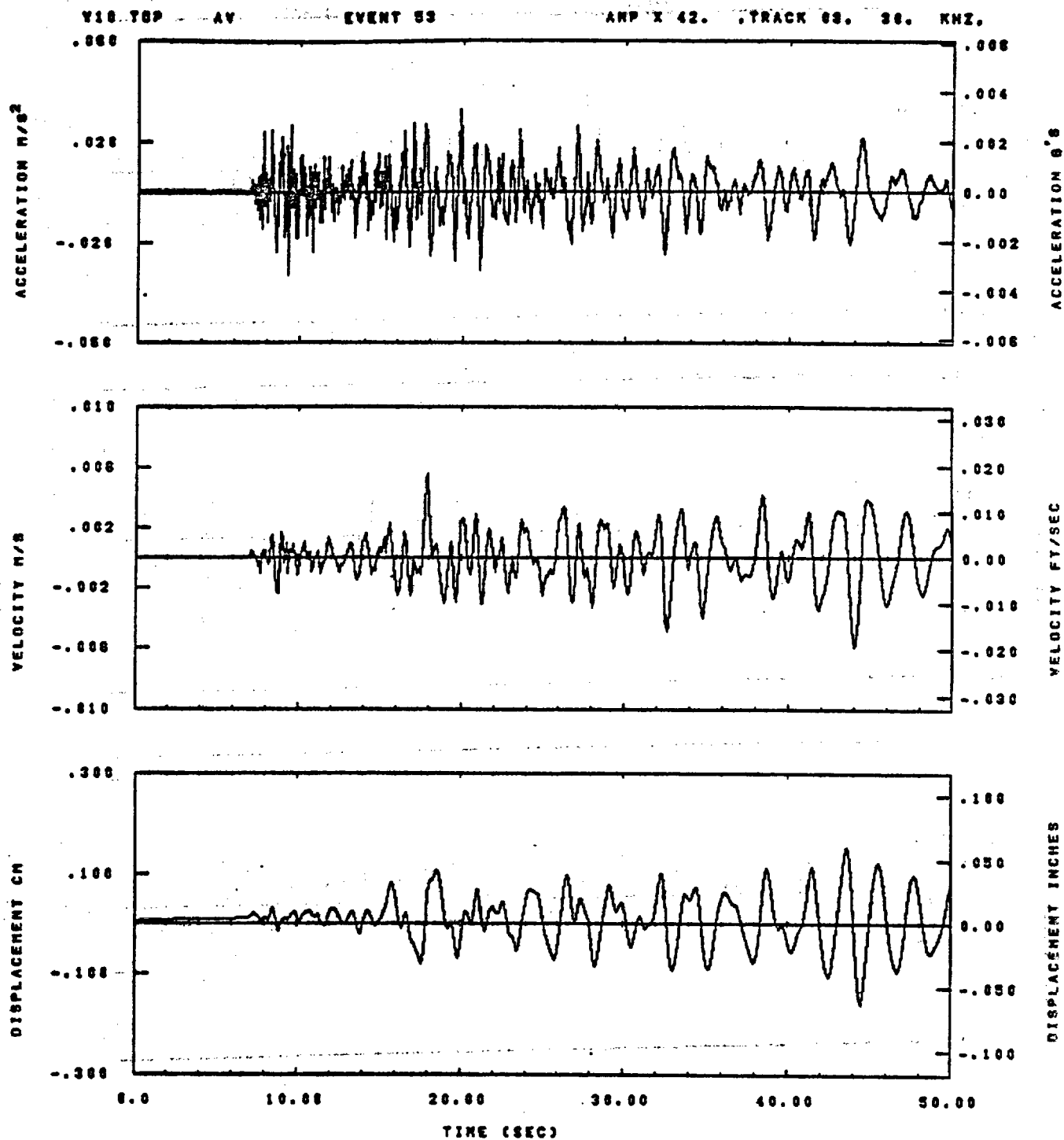
Figure C-14



IOT= .0020	QOT= .005	FIX=	AAS= 0.
HPP= .20	BYH= .13	HLH= 251	ASB=
LPP= 18.	BYL= 4.	HLL= 2999	ASE=
VTS= .200	VTE= .133	FLL= -20.	VSE= 0.
DPS= 0.	DPE= 100.	PLH= A-.1	DSE= A+.1

10.31.23.

07/15/82

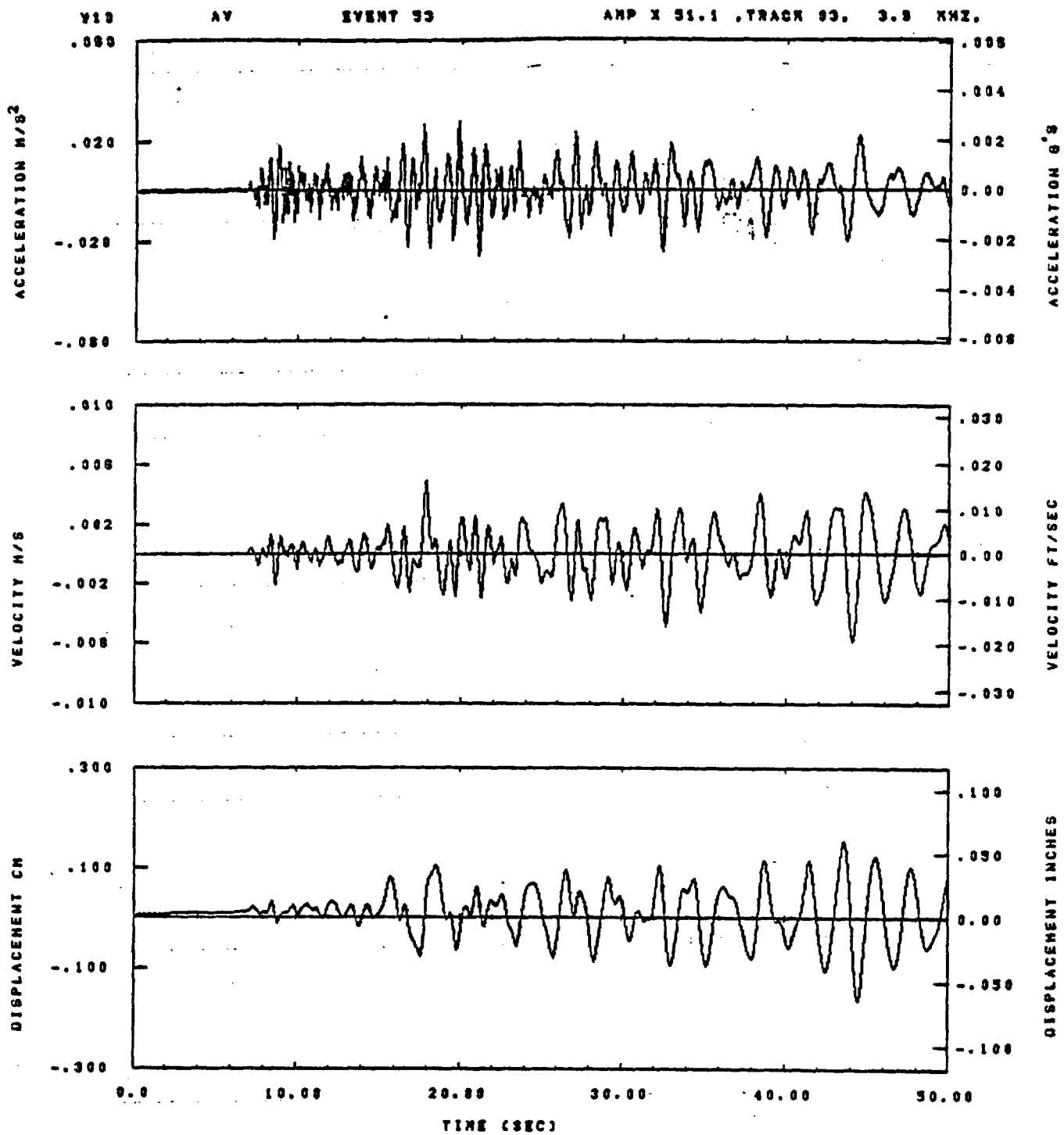


IDT= .0020	ODT= .0	FIX=	AAS=
HFF= .3	BYH= .20	HLH= 167	ASB=
LPF= 27.	BVL= 6.	HLL= 1888	ASE=
YTB= .30	YTE= .200	FLL=	VSE=
DPE=	DPE=	FLH= 0	DSE= 0.

08.34.18.

07/02/82

Figure C-16

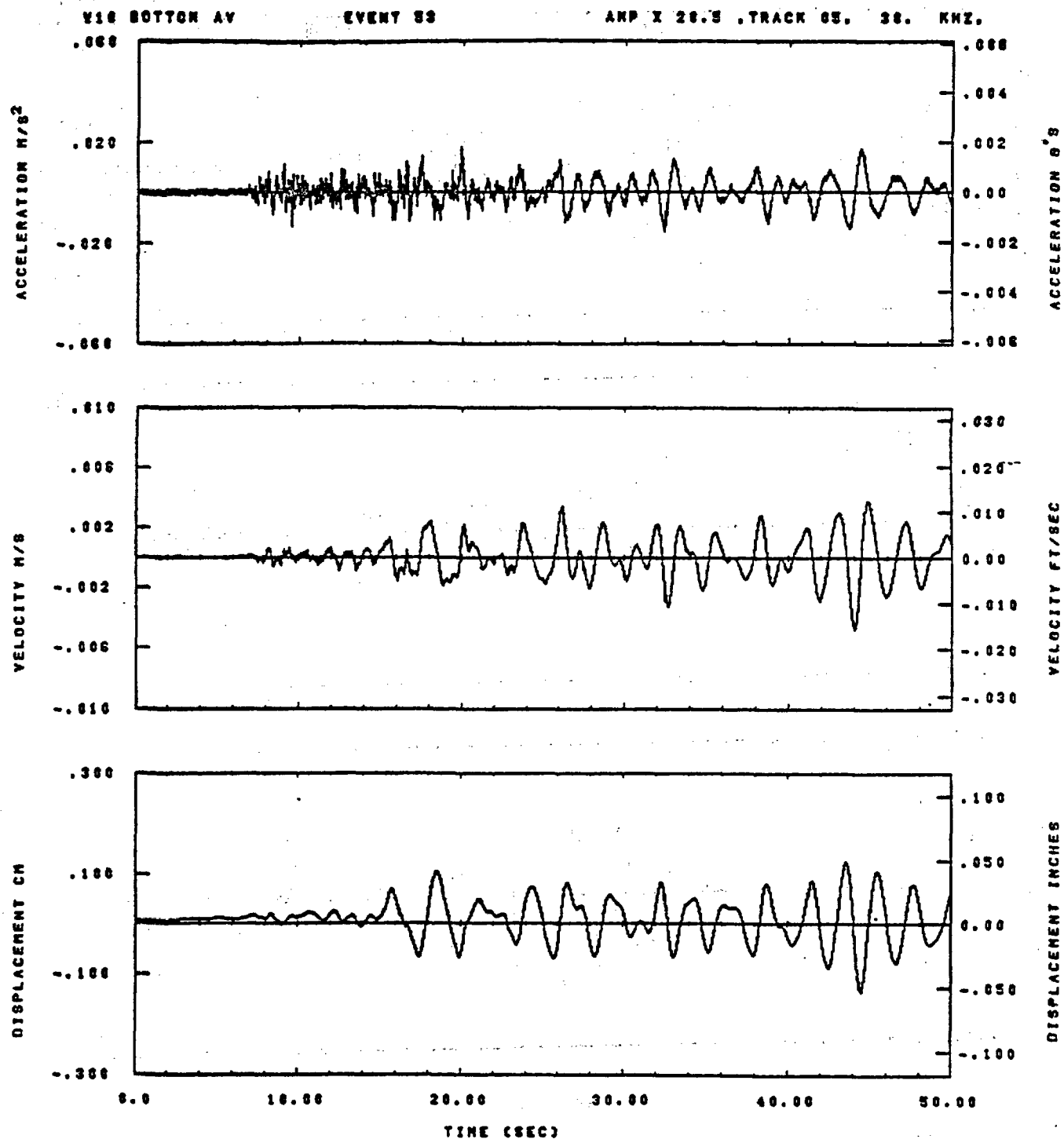


IDT= .0028	QDT= .0	FIX=	AAS=
HPP= .3	BYN= .20	HLH= 187	ASB=
LPP= 27.	BYL= 8.	HLL= 1999	ASZ=
VTS= .38	VTE= .200	FLL=	VSE=
DPS=	DPE=	FLH= 0	DSE= 0.

09.35.04.

07/82/82

Figure C-17

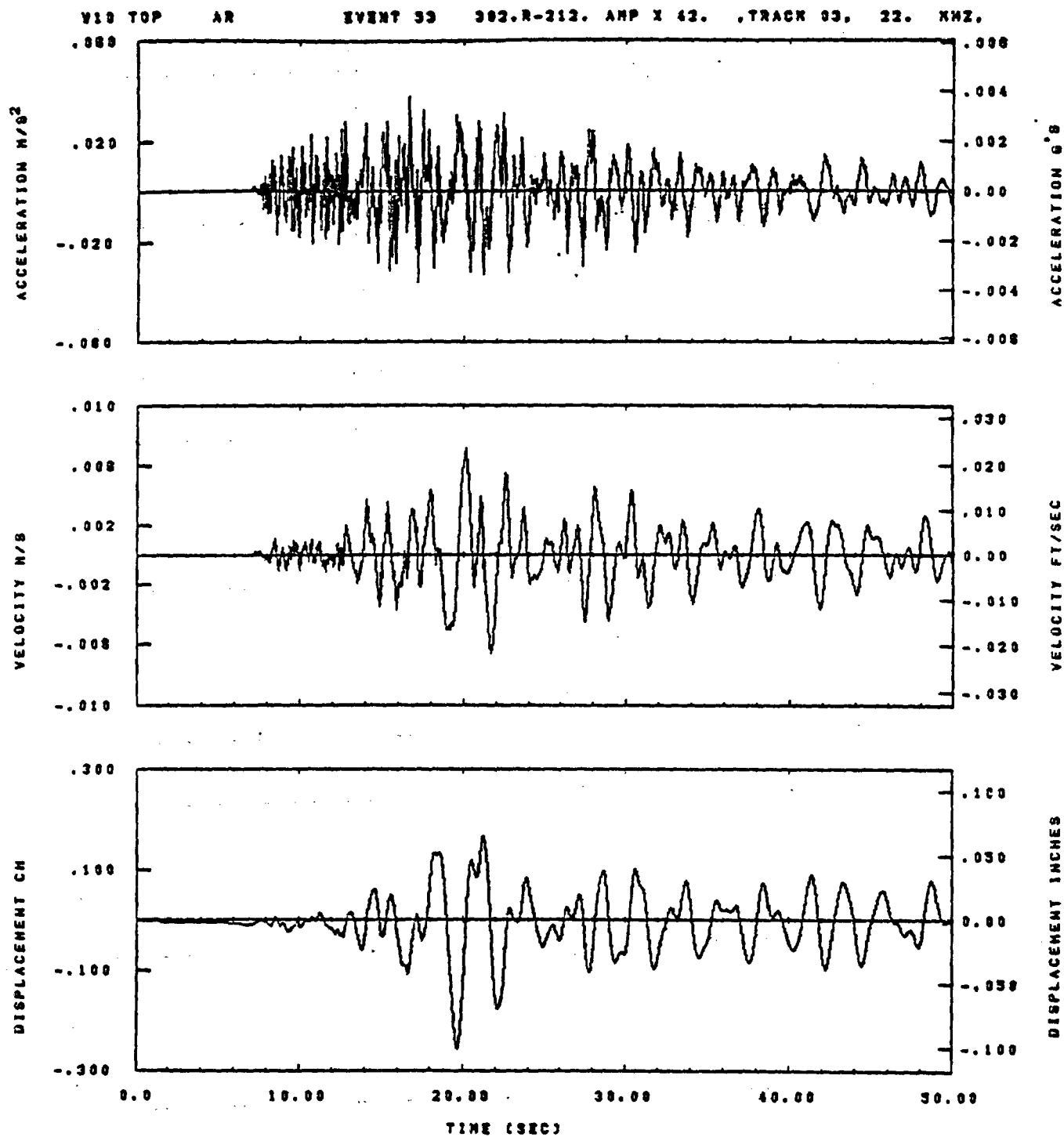


IDT= .0020	QDT= .0	FIX=	AAS=
HPF= .3	BYH= .20	HLH= 167	ASB=
LPF= 27.	BYL= 8.	HLL= 1888	ASE=
VTE= .38	VTE= .200	FLL=	VSE=
DPS=	OPE=	FLH= 0	DSE= 0.

08.35.07.

07/02/02

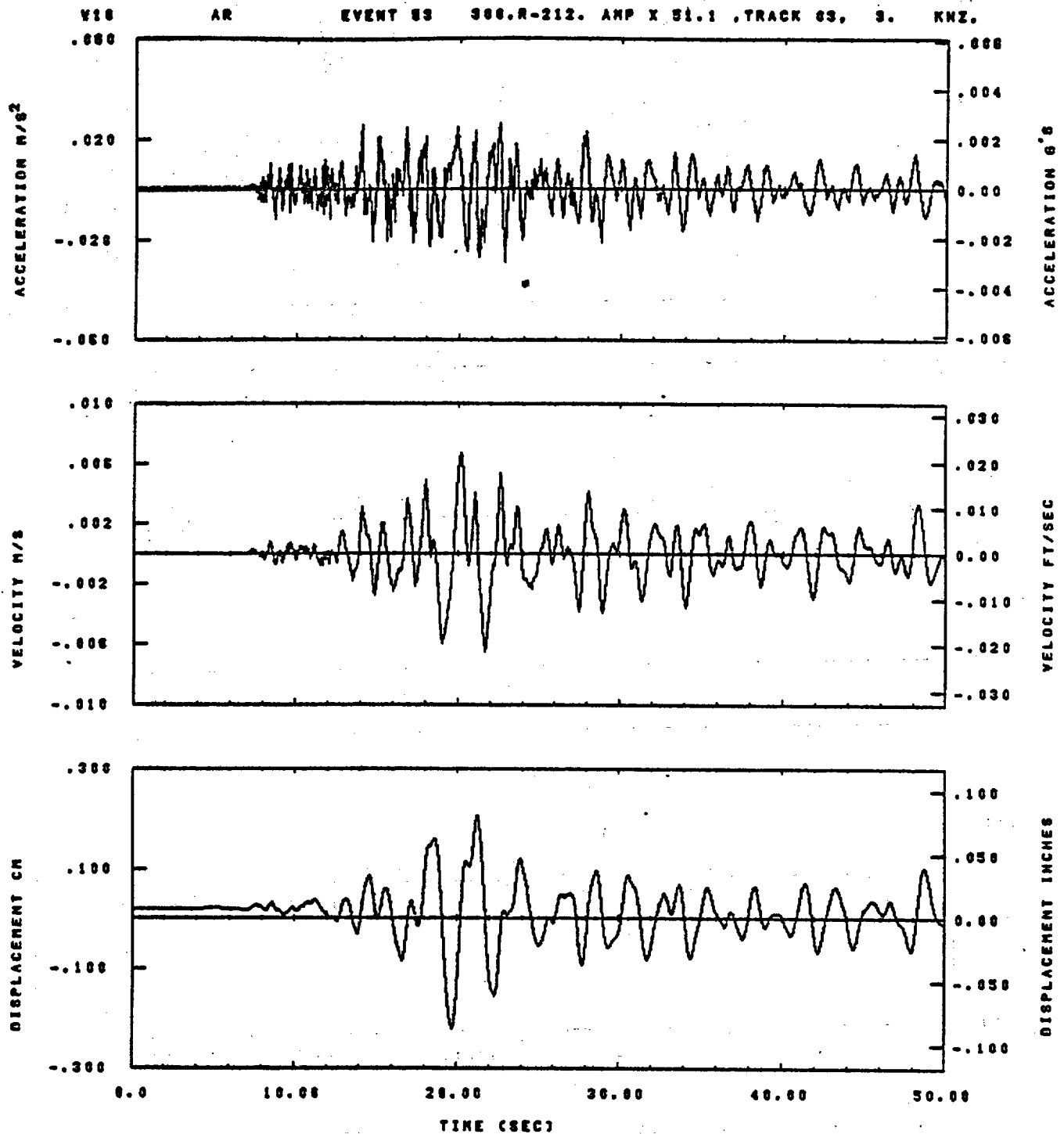
Figure C-18



IDT= .0020	ODT= .0	FIX=	AAS=
HPP= .3	BYN= .20	MLN= 167	ASB=
LPP= 27.	BYL= 0.	MLL= 1999	ASE=
VTS= .30	VTE= .200	FLL=	VSE=
OPS=	OPE=	PLN= 0	OSE= 0.

09.34.23.

07/02/82

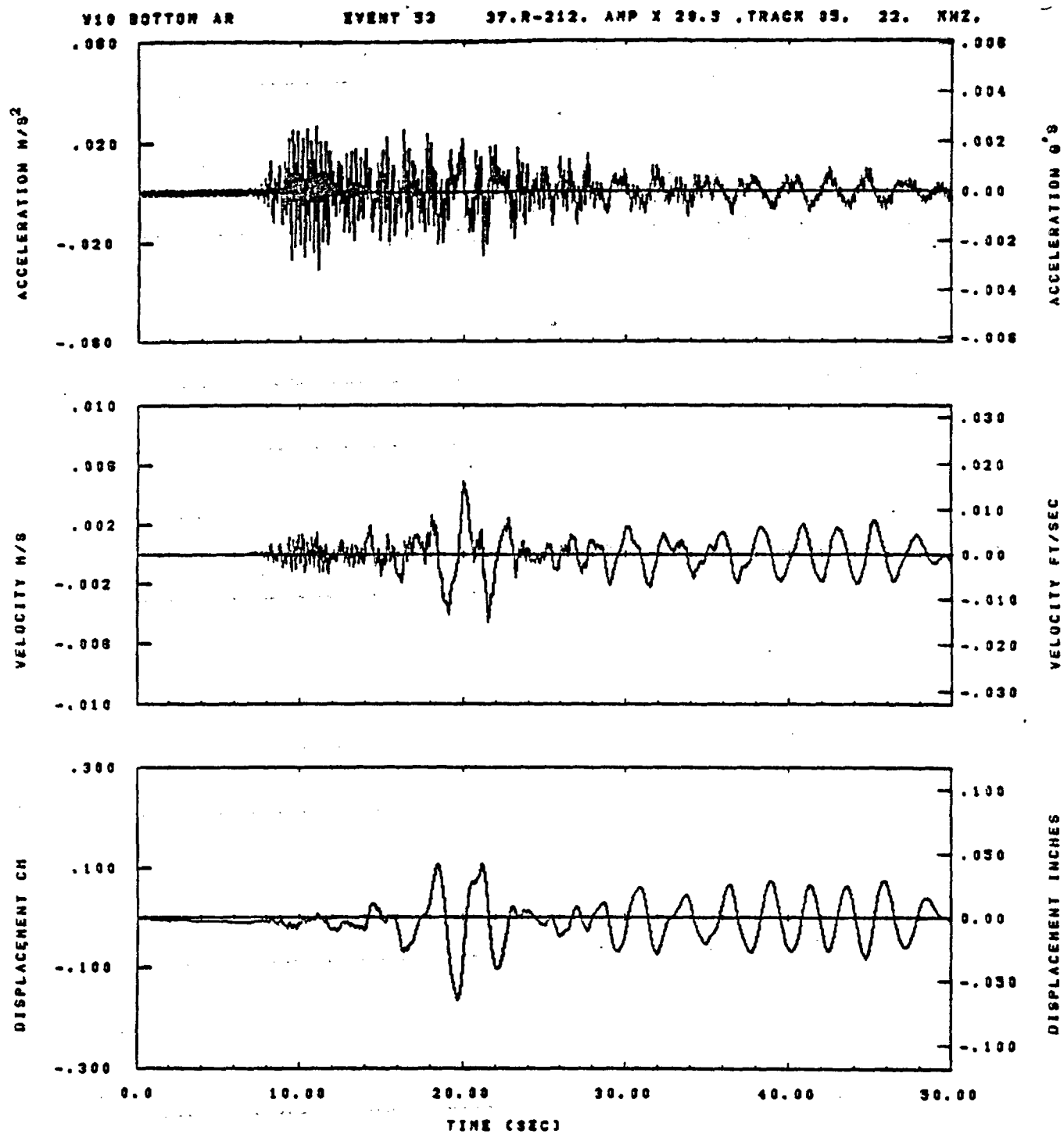


IDT= .0020	ODT= .0	FIX=	AAS=
HPF= .3	BYH= .20	HLH= 167	ASB=
LPF= 27.	BYL= 6.	HLL= 1999	ASE=
VTS= .30	VTE= .200	FLL=	VSE=
DPS=	DPE=	FLH= 0	DSE= 0.

09.35.20.

07/02/02

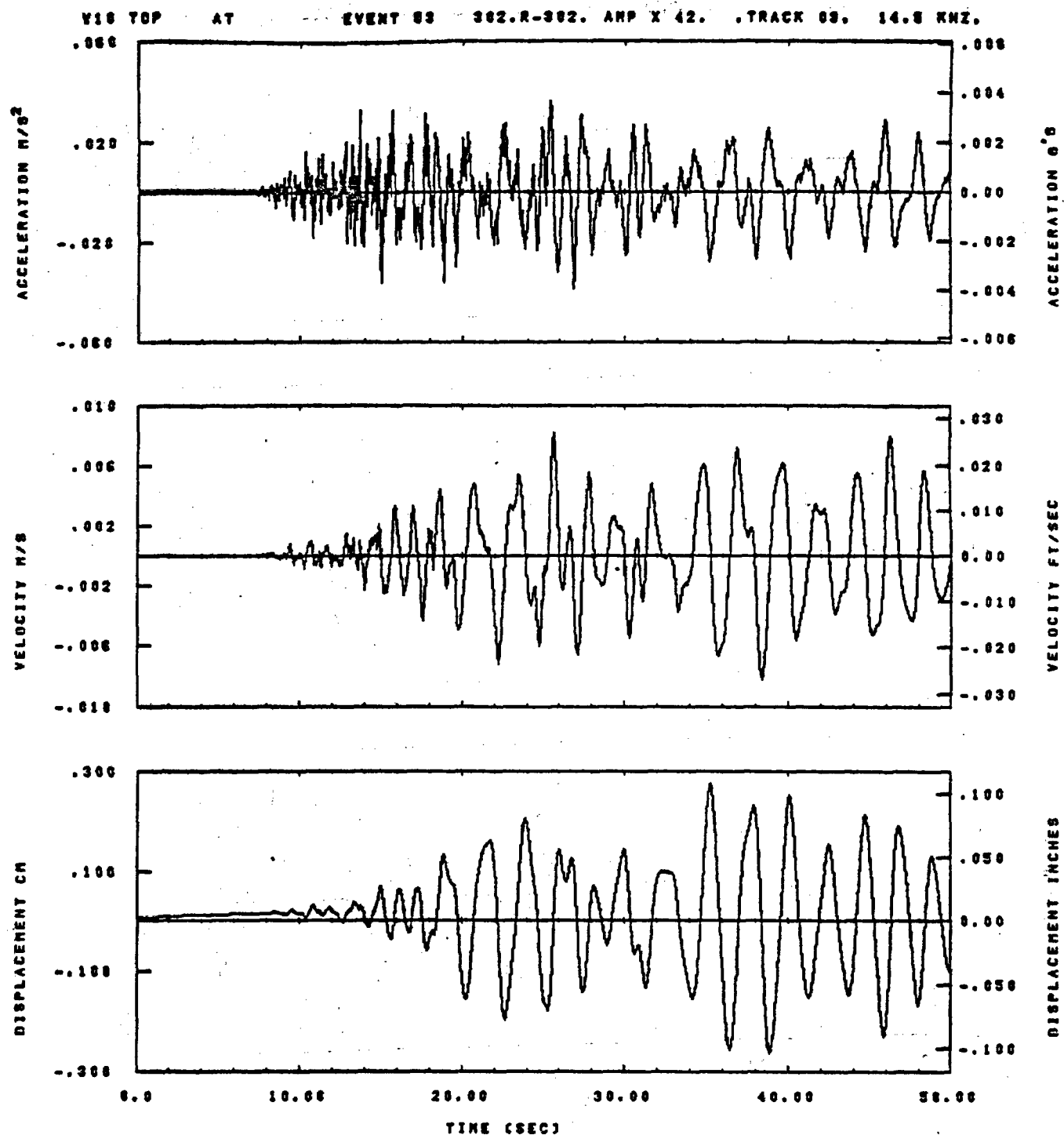
Figure C-20



IDT= .0020	ODT= .0	FIX=	AAS=
HPP= .3	BYH= .20	HLH= 187	ASB=
LPP= 27.	BYL= 8.	HLL= 1999	ASE=
VTS= .30	VTE= .200	FLL=	VSE=
OPS=	OPE=	FLH= 0	DSE= 0.

09.35.11.

07/02/82

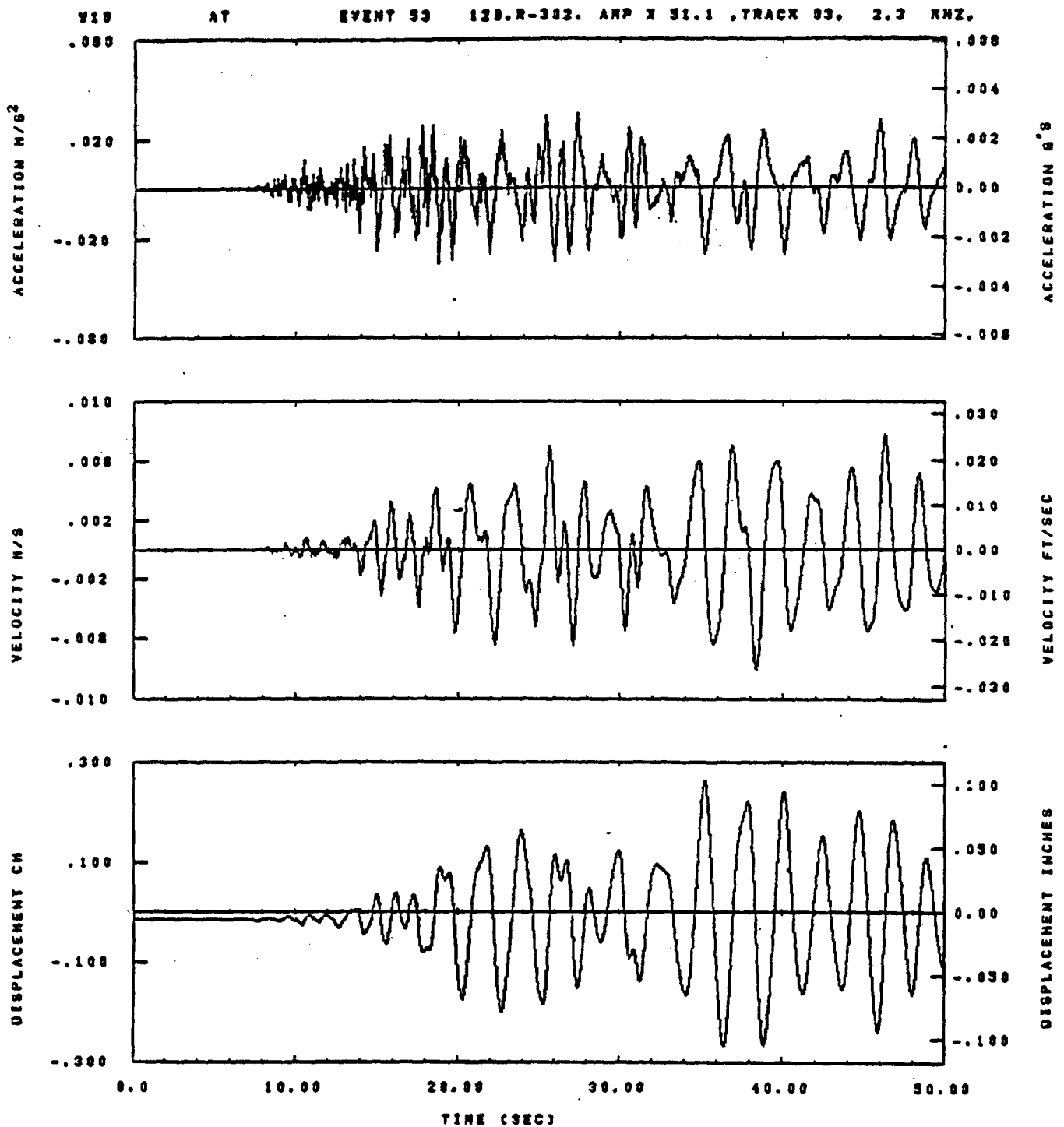


IDT= .0020	QDT= .0	FIX=	AAS=
HPF= .3	SVN= .20	MLH= 167	ASB=
LPF= 27.	BVL= 6.	MLL= 1000	ASE=
VTB= .30	VTE= .200	FLL=	VSE=
DPS=	DPE=	FLH= 0	DSE= 0.

08.34.58.

07/02/82

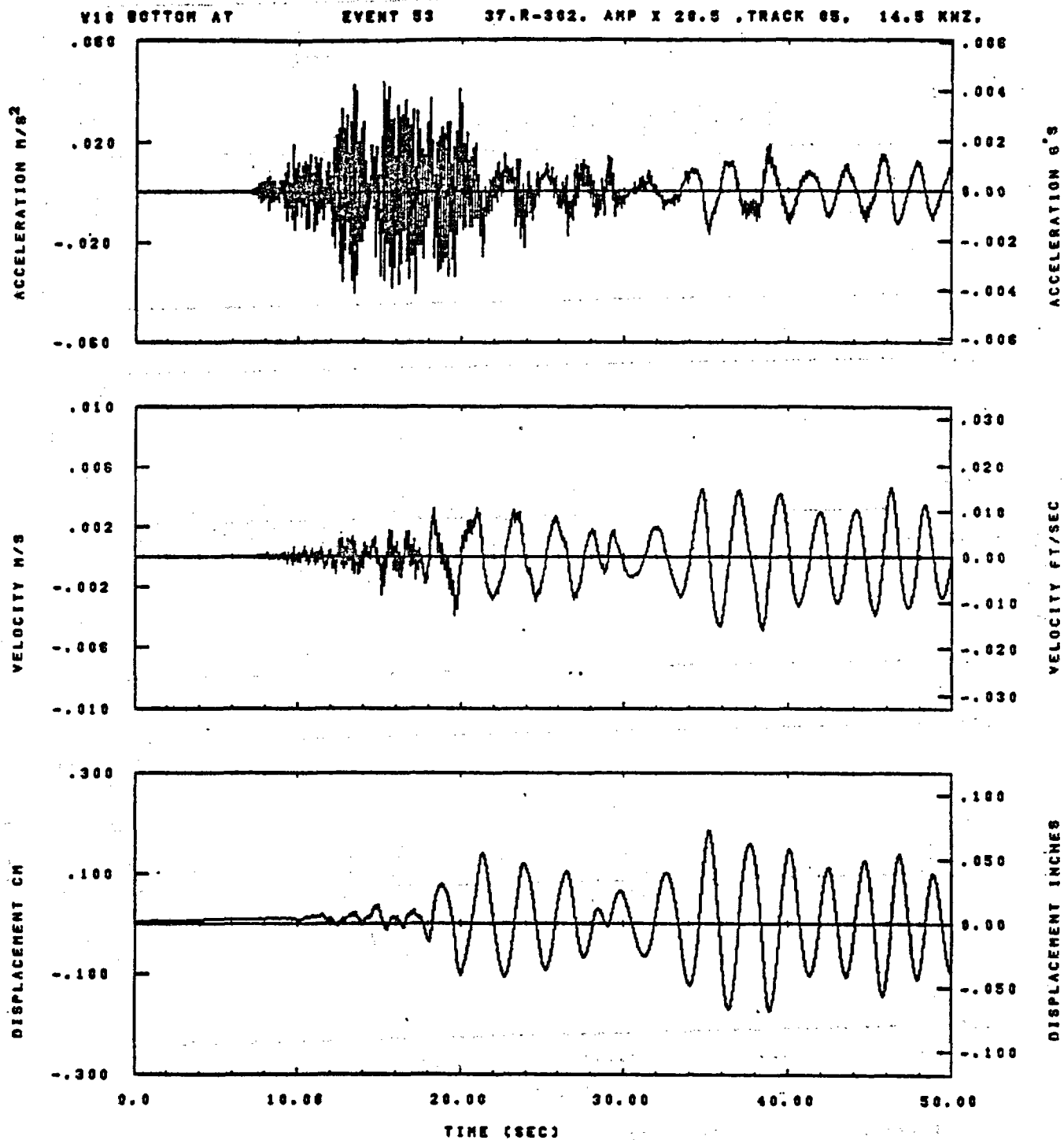
Figure C-22



IDT= .0020	ODT= .0	FIX=	AAS=
HPF= .3	BYH= .20	HLH= 187	ASB=
LPF= 27.	BYL= 8.	HLL= 1999	ASZ=
VTS= .30	VTE= .200	FLL=	VSE=
OPS=	OPE=	FLH= 0	OSZ= 0.

09.33.23.

07/02/82

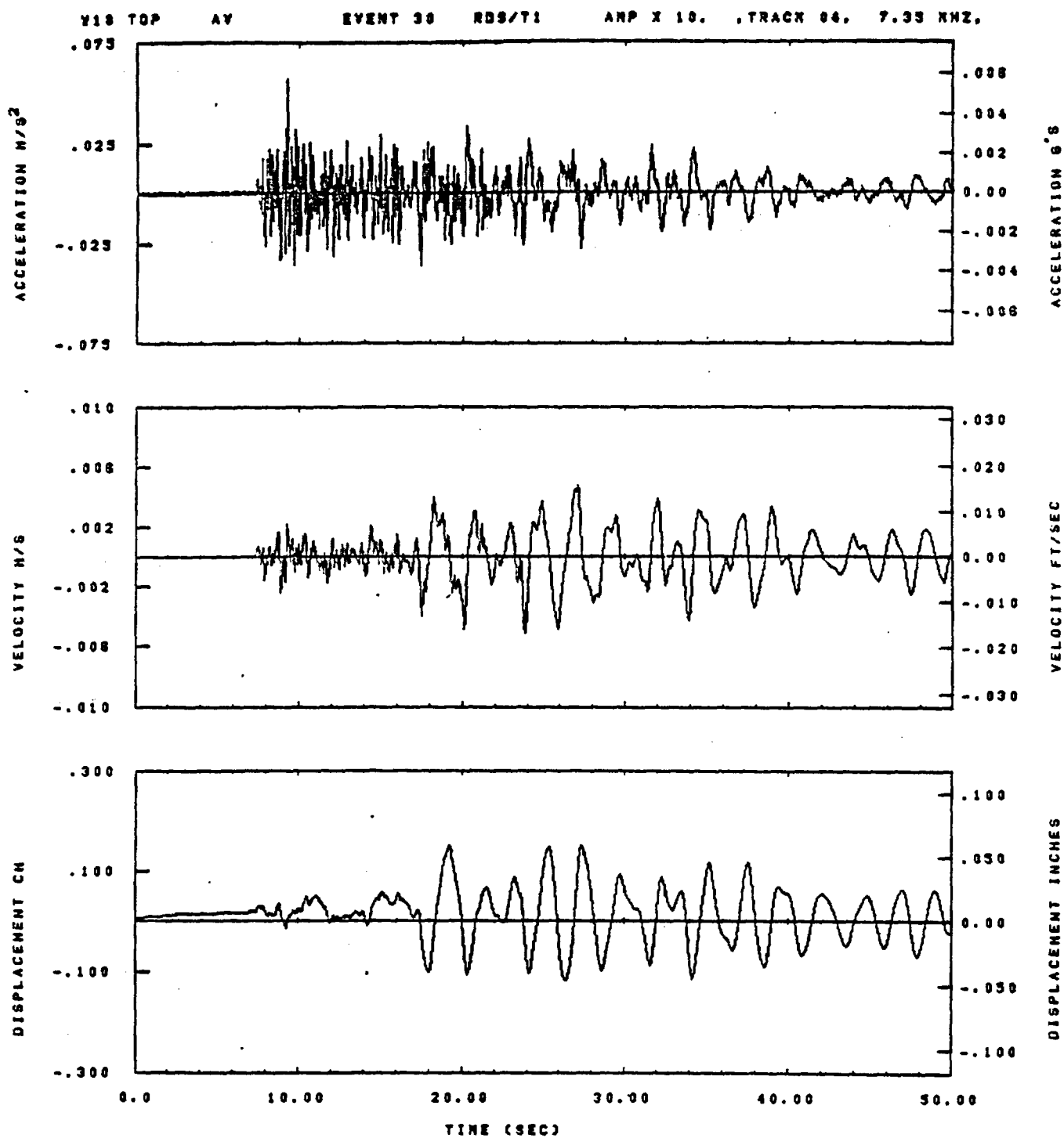


IDT= .0020	QDT= .0	FIX=	AAS=
NPF= .3	SVH= .20	HLH= 167	ASS=
LPF= 27.	SVL= 6.	HLL= 1888	ASE=
VTS= .30	VTE= .200	FLL=	VSE=
DPS=	DPE=	FLH= 0	DSE= 0.

08.35.14.

67/02/82

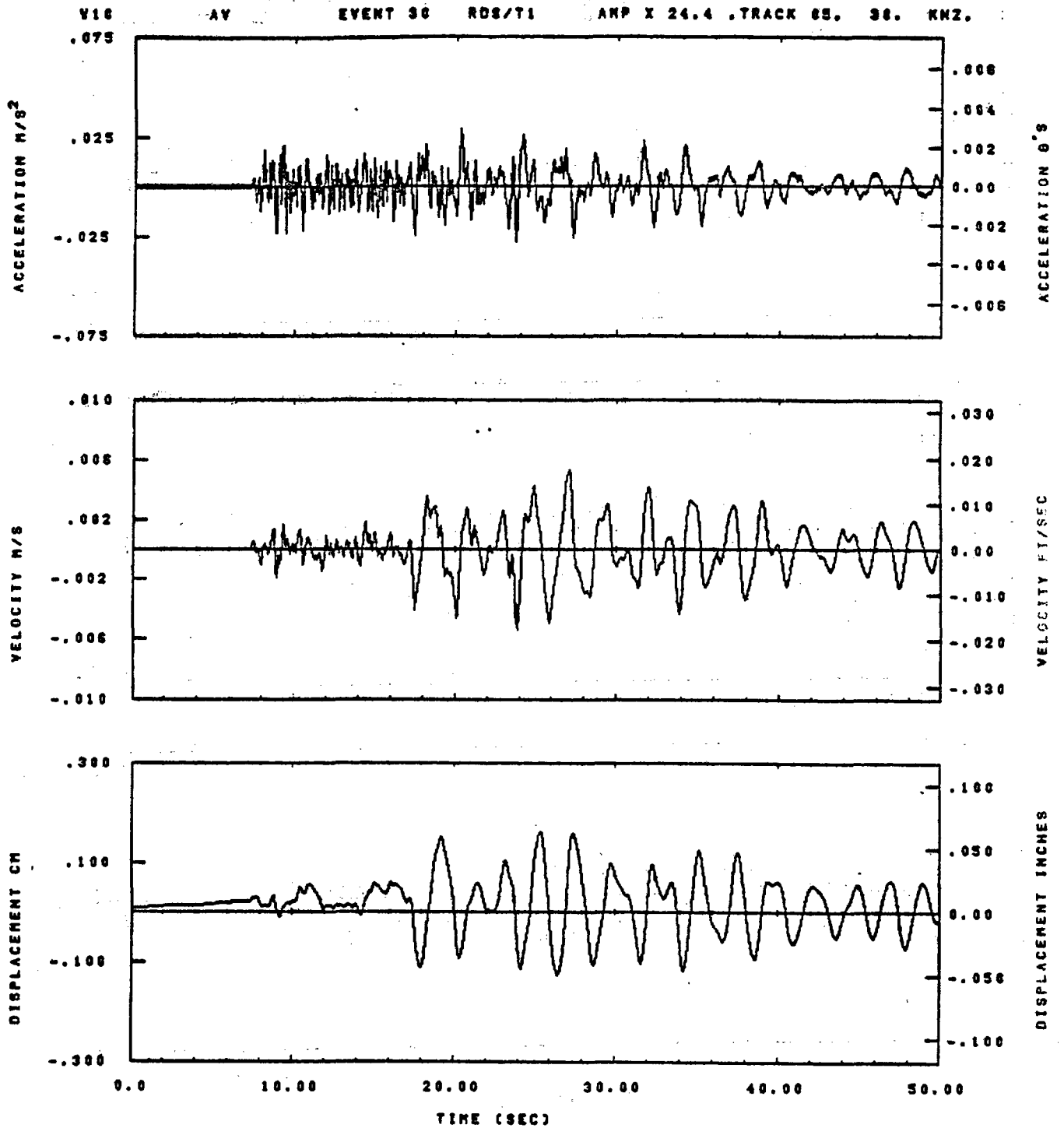
Figure C-24



IDT= .0020	ODT= .003	FIX=	AAS= 0.
HPP= .20	SVH= .13	HLN= 123	ASS=
LPP= 38.	SVL= 8.	HLL= 2999	ASE=
VTS= .200	VTE= .133	FLL= -20.	VSE= 0.
DPS= 0.	OPE= 100.	FLN= 0	OSE= 0.

14.57.32.

07/12/82

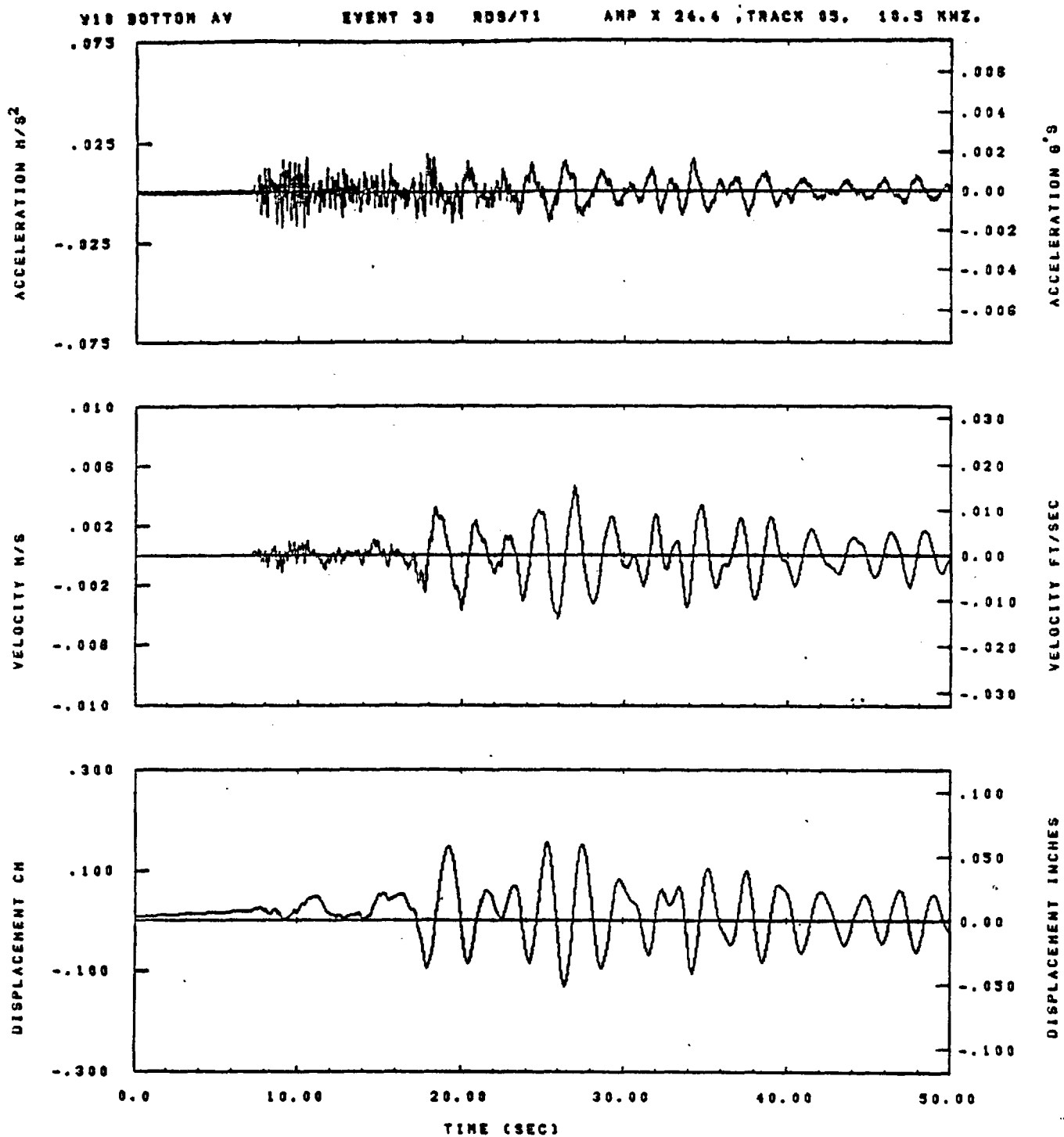


IDT= .0020	ODT= .005	FIX=	AAG= 0.
HPF= .20	SVH= .13	HLH= 125	ASB=
LPF= 36.	SVL= 8.	HLL= 2888	ASE=
VTS= .200	VTE= .133	FLL= -20.	VSE= 0.
DPS= 0.	DPE= 100.	FLH= 0	DSE= 0.

14.37.45.

07/12/82

Figure C-26

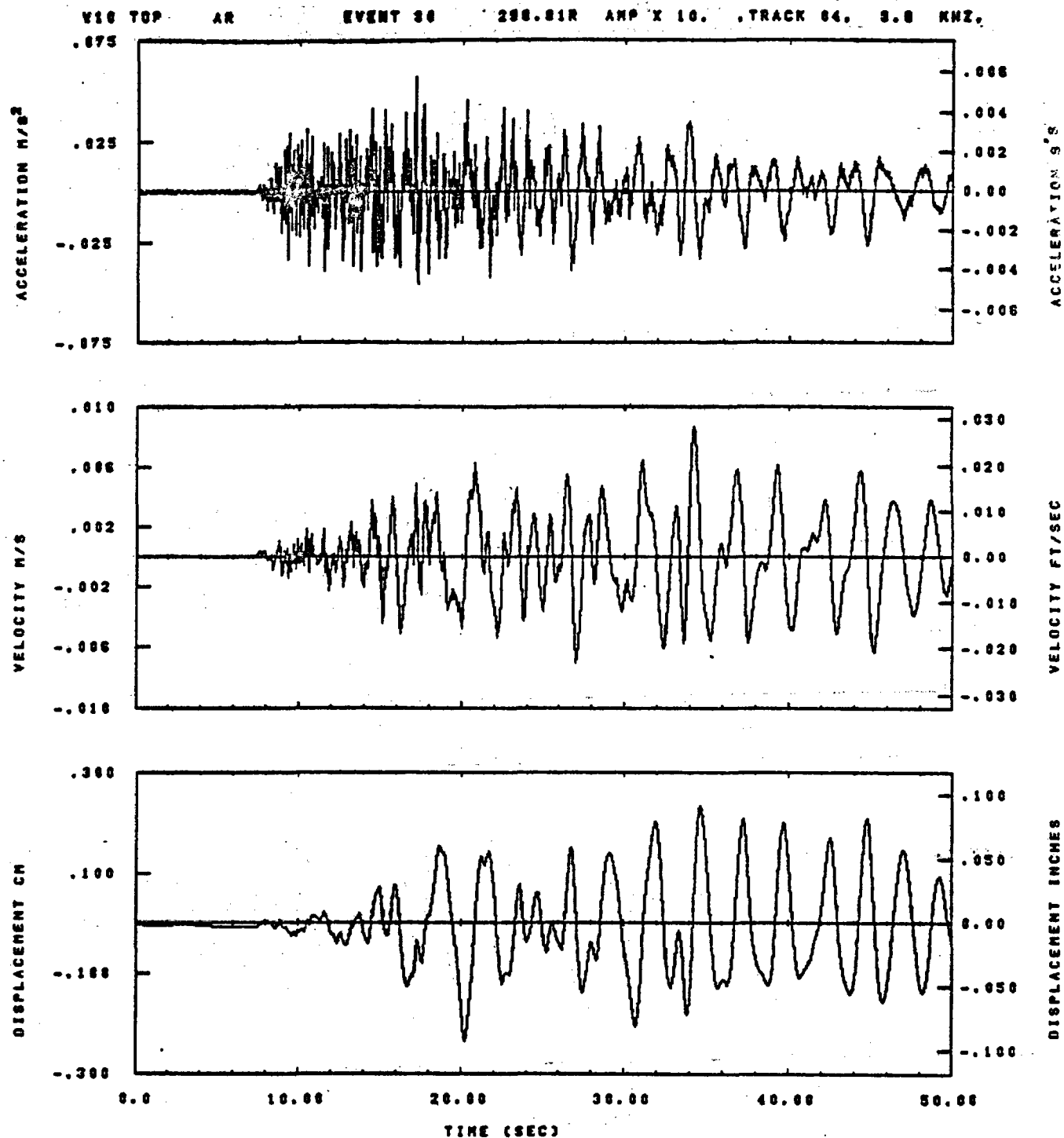


IDT= .0020	ODT= .003	FIX=	AAS= 0.
HPP= .20	BYH= .13	HLH= 123	ASB=
LPP= 38.	BYL= 8.	HLL= 2999	ASE=
VTB= .200	VTE= .133	PLL= -20.	VSE= 0.
OPB= 0.	OPE= 100.	FLH= 0	DSE= 0.

14.58.43.

07/12/82

Figure C-27

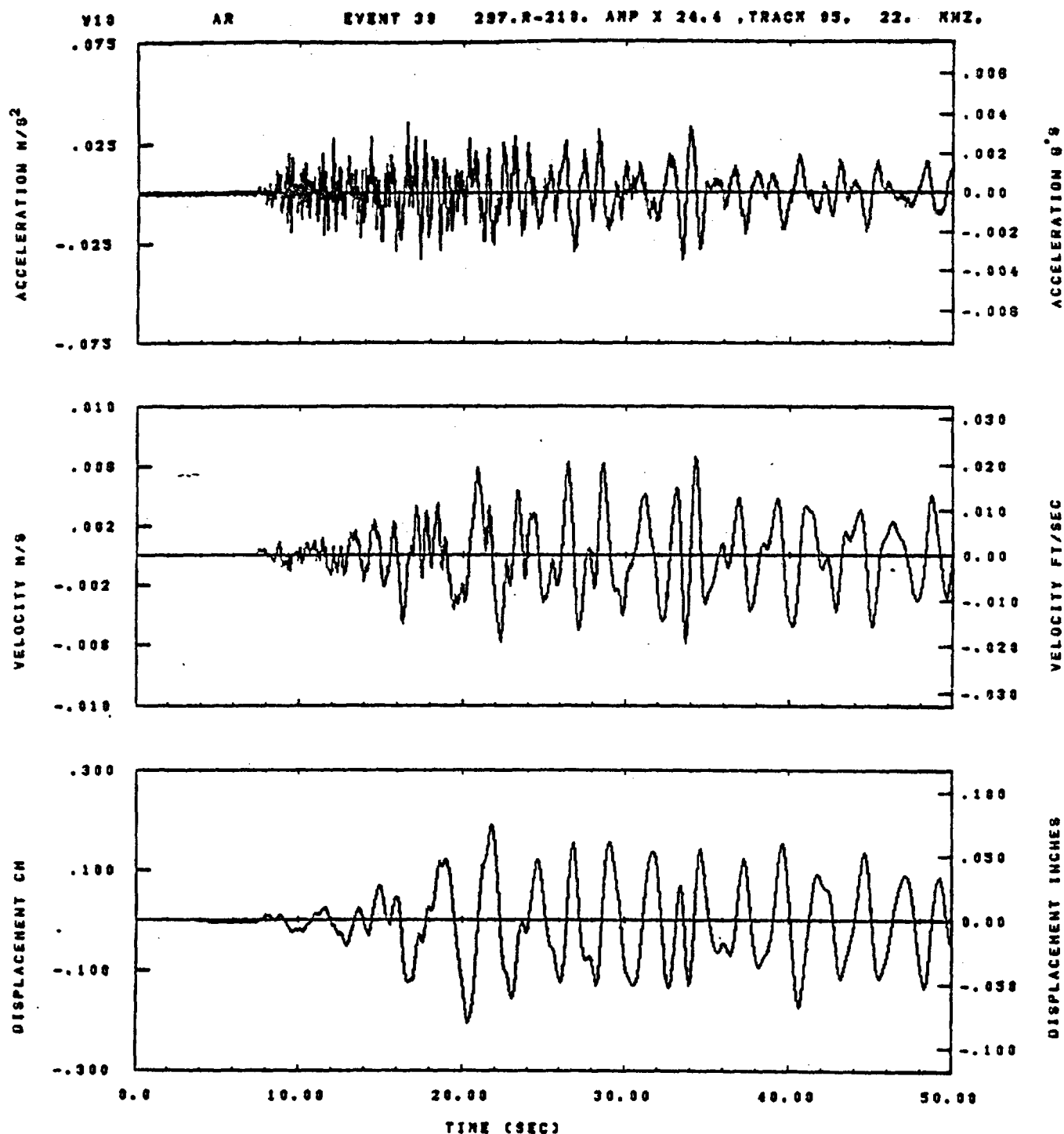


IDT= .0020	QDT= .005	FIX=	AAS= 0.
HPP= .20	BYN= .13	MLH= 125	ASS=
LPP= 36.	BYL= 0.	MLL= 2550	ASE=
VTS= .200	VTE= .133	FLL= -20.	VSE= 0.
DPS= 0.	DPE= 100.	FLH= 0	DSE= 0.

15.32.01.

06/22/82

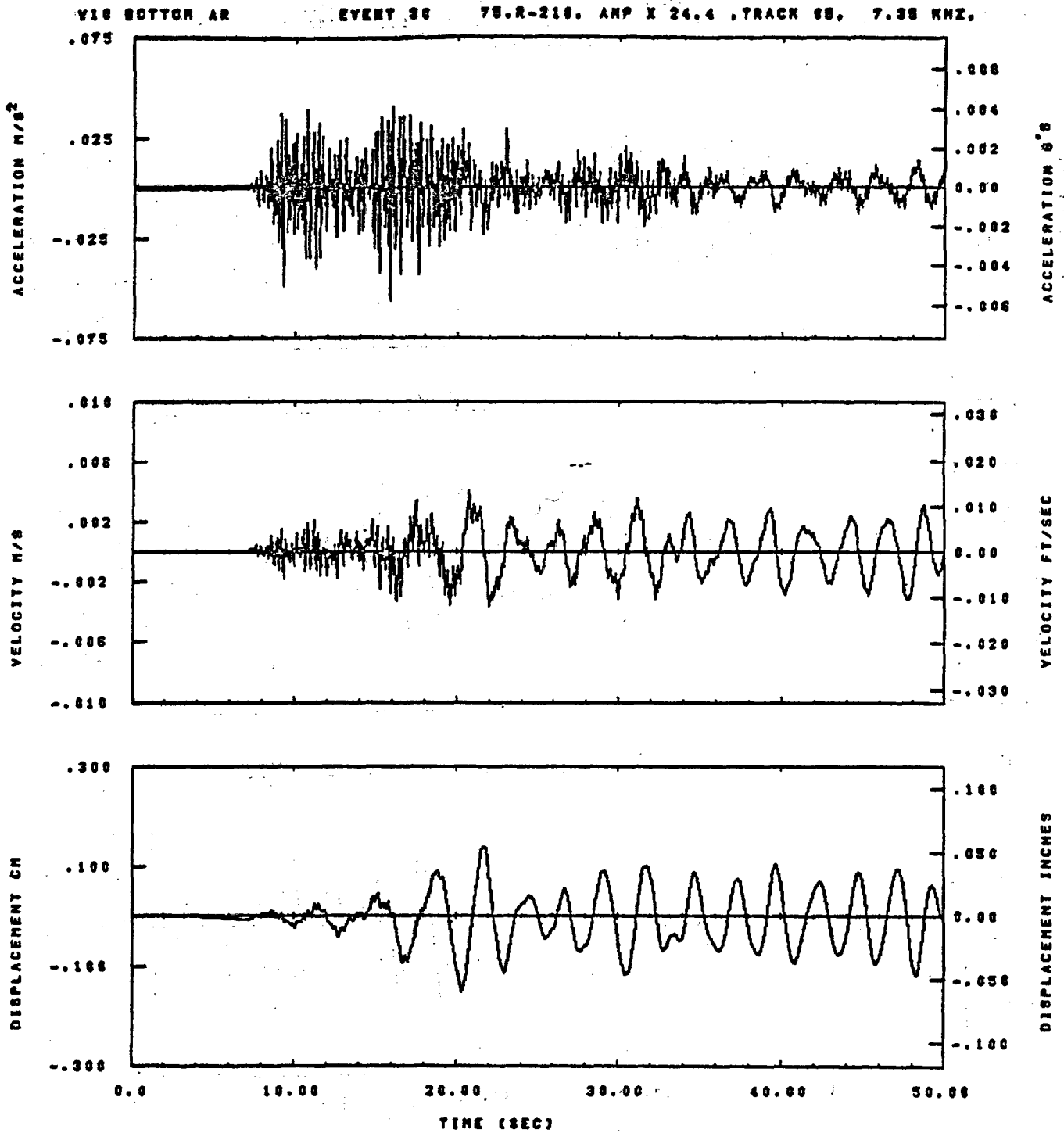
Figure C-28



IDT= .0020	ODT= .003	FIX=	AAS= 0.
HPF= .20	BYH= .13	HLH= 125	ASB=
LPF= 38.	BYL= 8.	HLL= 2999	ASE=
VTB= .200	VTE= .133	FLL= -20.	VSE= 0.
DPB= 8.	OPE= 100.	FLH= 0	DSE= 0.

15.34.33.

08/22/92



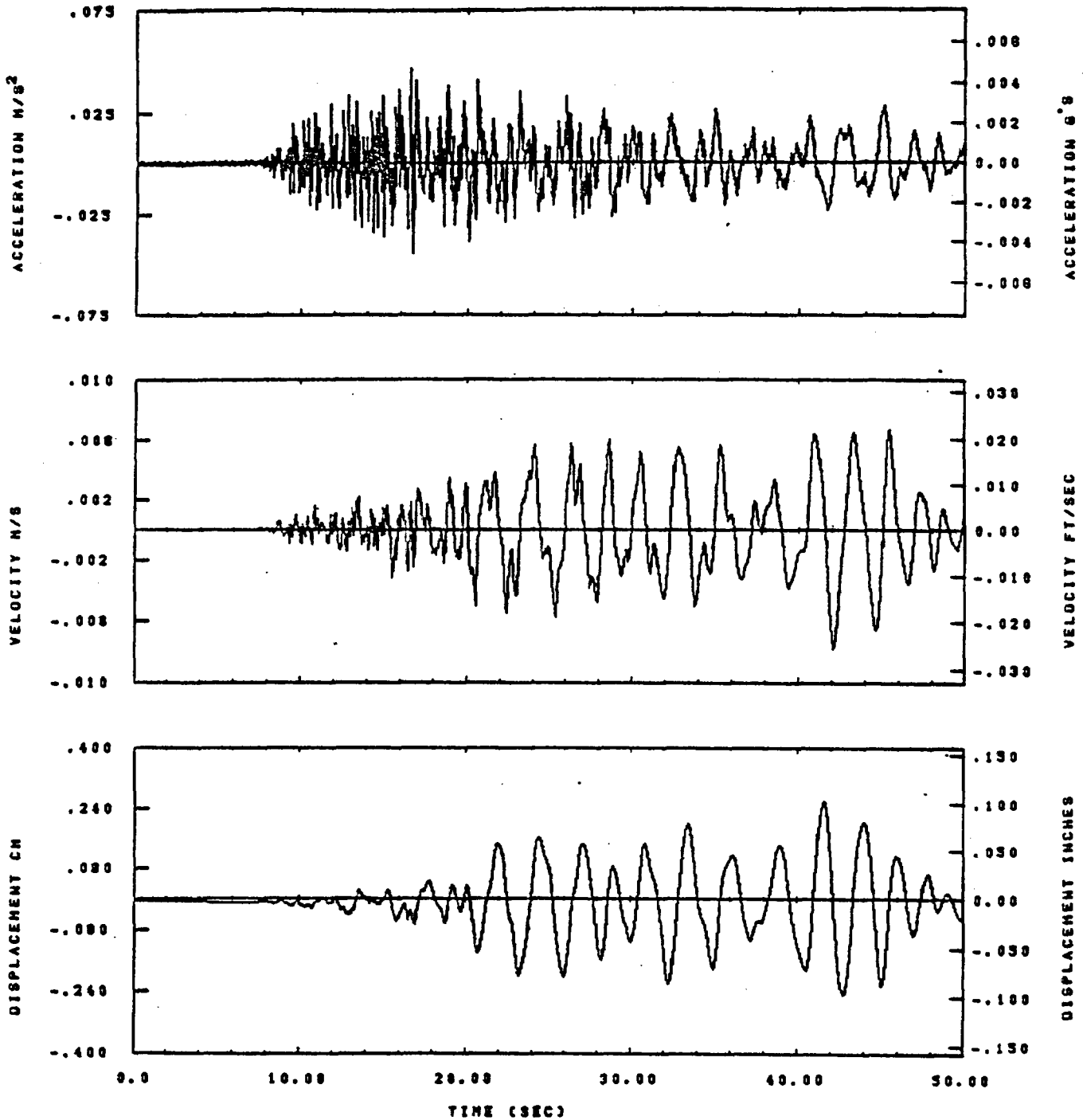
IDT= .0020	ODT= .005	FIX=	AAS= 0.
HPP= .28	BYH= .13	HLH= 125	ASH=
LPP= 36.	BYL= 6.	HLL= 2998	ASE=
VTB= .200	VTE= .133	FLL= -20.	VSE= 0.
DPS= 0.	DPE= 100.	FLH= 0	DSE= 0.

15.33.56.

06/22/82

Figure C-30

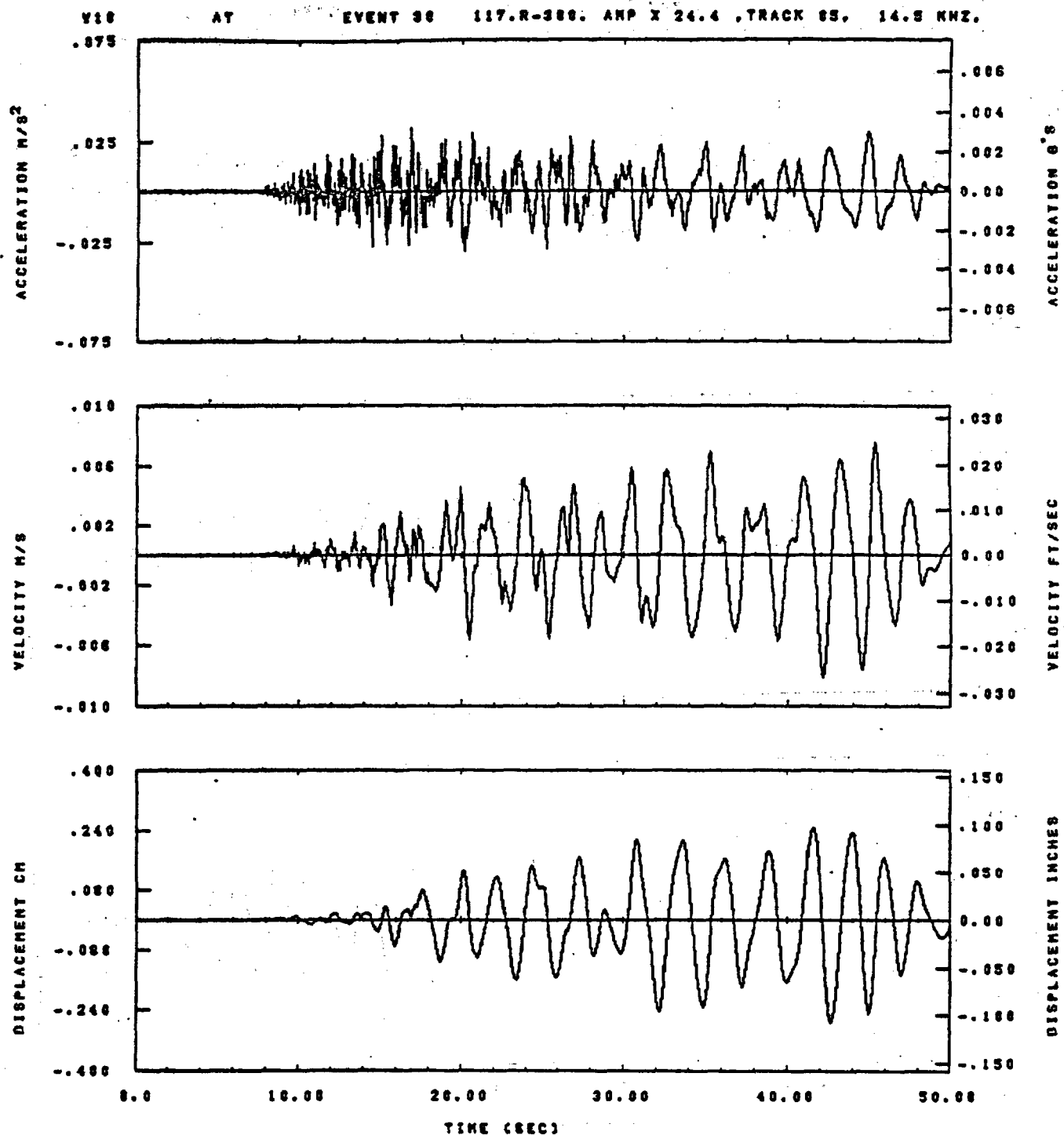
Y10 TOP AT EVENT 30 299.91R AMP X 10. TRACK 04. 2.3 KHZ,



IDT= .0020	ODT= .005	FIX=	AAS= 0.
HPF= .20	BYH= .13	HLH= 123	ASB=
LPF= 38.	BYL= 9.	HLL= 2999	ASE=
VTS= .200	VTE= .133	FLL= -20.	VSE= 0.
DPS= 0.	DPE= 100.	FLH= 0	DSE= 0.

15.32.89.

08/22/82



IDT= .0020	ODT= .005	FIX=	AAS= 0.
HFF= .20	SVH= .13	MLH= 125	ASB=
LFF= 36.	BVL= 6.	MLL= 2998	ASE=
VTS= .208	VTE= .133	FLL= -20.	VSE= 0.
DPS= 6.	DPE= 100.	FLH= 0	DSE= 0.

15.34.38.

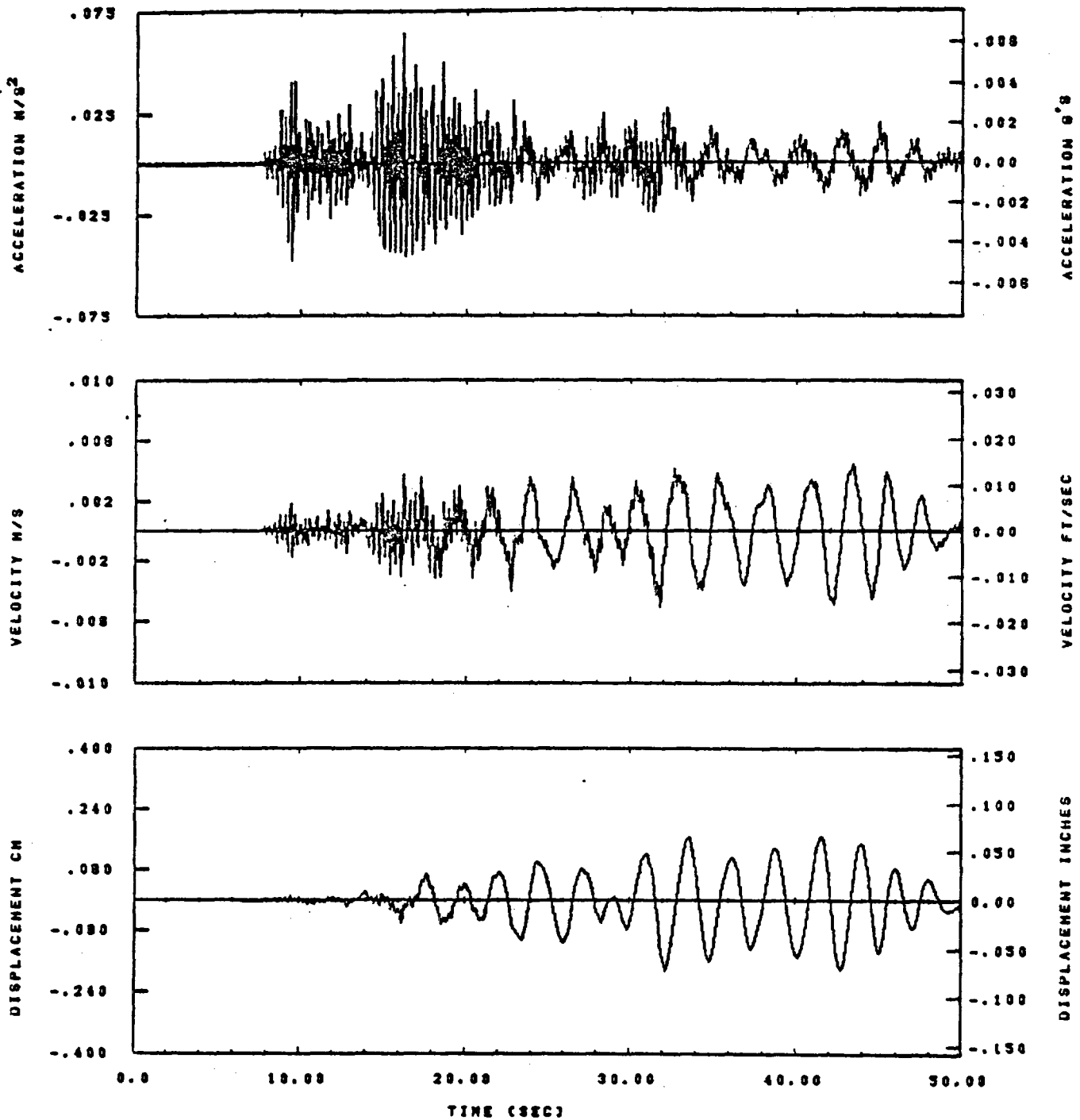
06/22/82

Figure C-32

V13 BOTTOM AT

EVENT 30

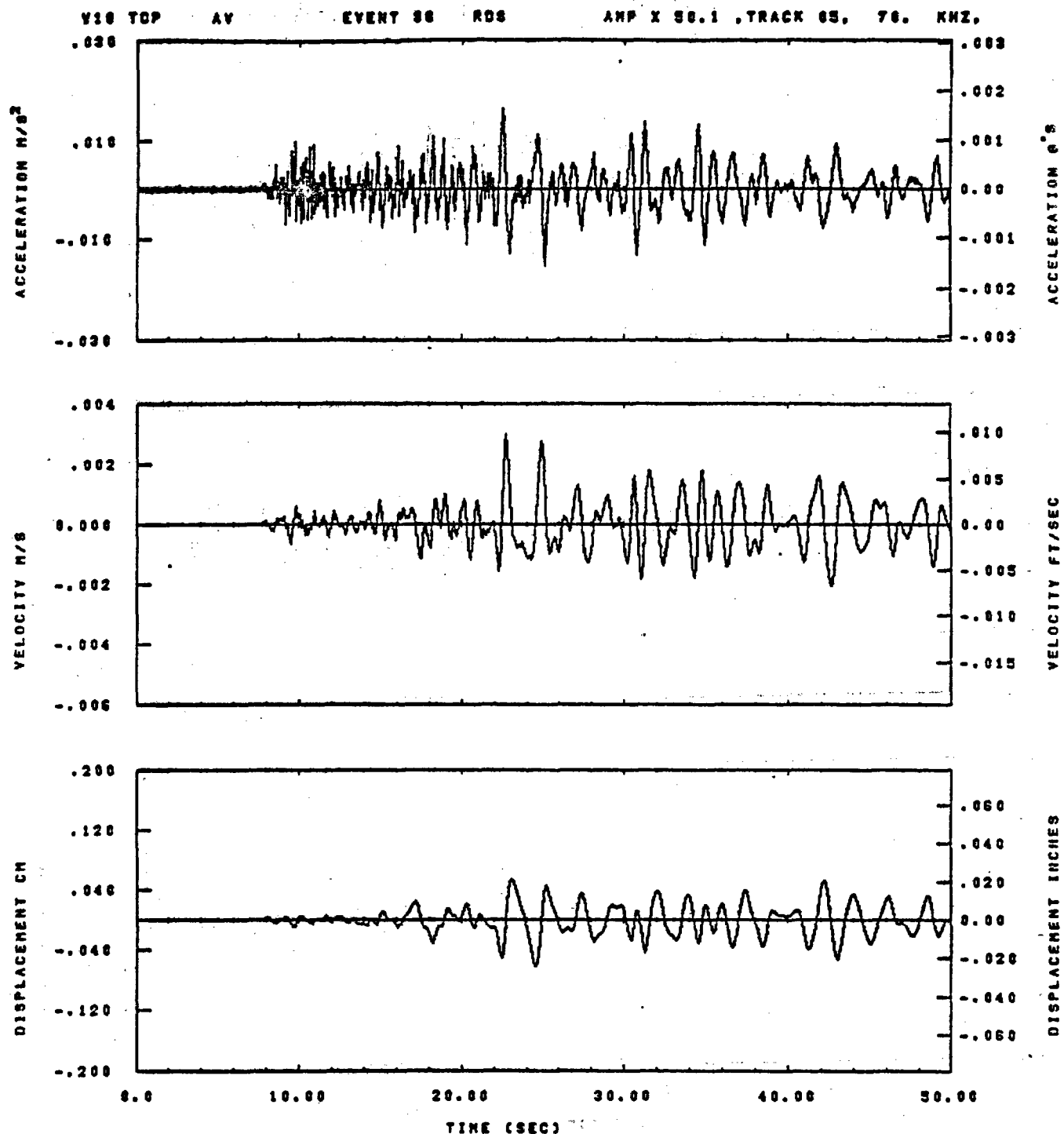
79.R-300. AMP X 24.4 .TRACK 03. 3.4 KHZ.



IDT= .8020	QDT= .003	FIX=	AAS= 0.
HPF= .20	BYM= .13	HLH= 125	ASS=
LPF= 38.	BYL= 9.	HLL= 2999	ASE=
VTB= .200	YTE= .133	FLL= -20.	VSE= 0.
DPS= 0.	DPE= 100.	FLH= 0	DSE= 0.

13.34.08.

08/22/02

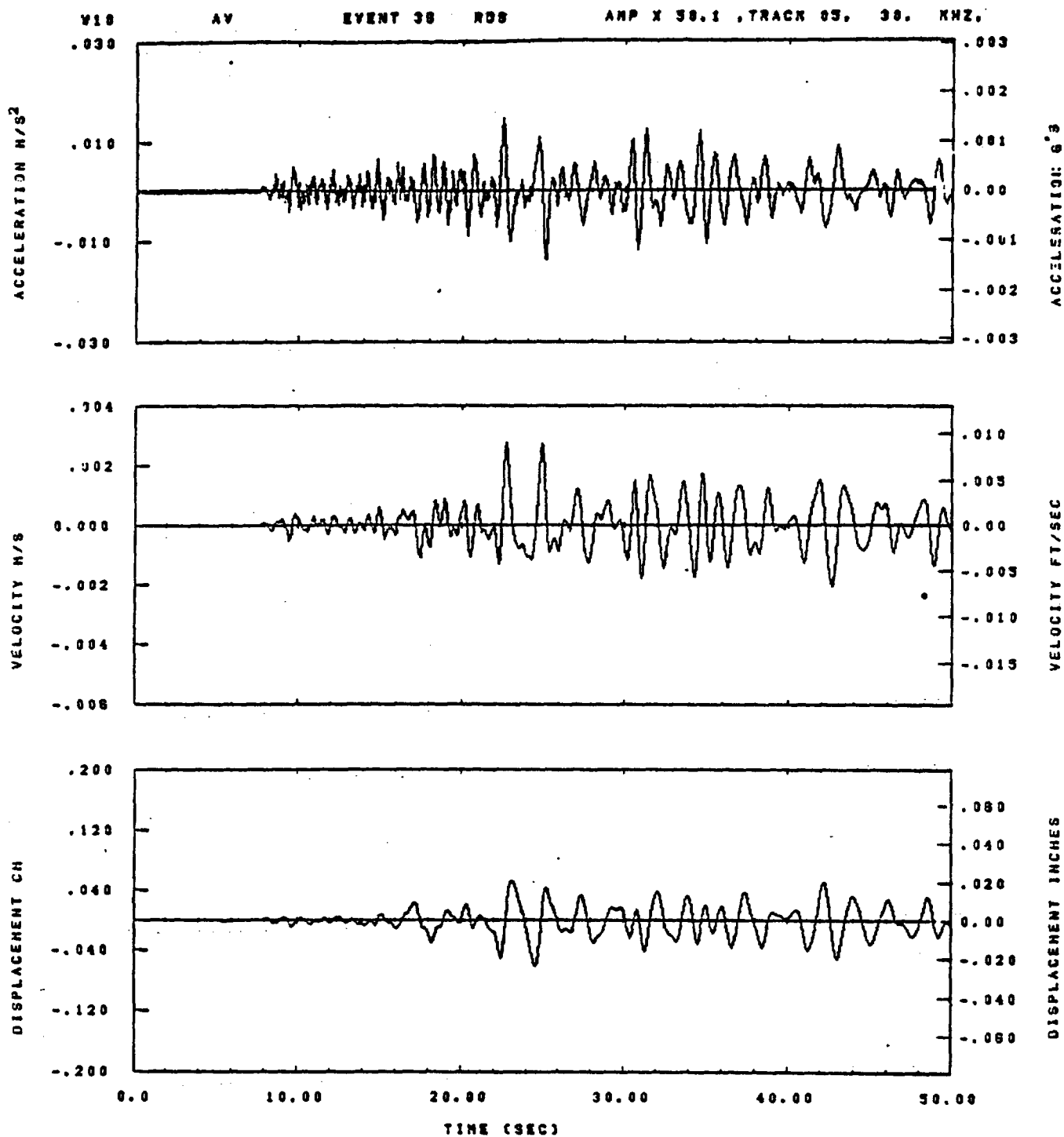


IDT= .0020	ODT= .005	FIX=	AAS= 0.
HPF= .25	BYH= .16	HLH= 143	ASB=
LPF= 31.	BVL= 7.	HLL= 2388	ASE=
VTB= .256	VTE= .160	FLL= -20.	VSE= 0.
DPS= 6.	DPE= 100.	FLH= 0	DSE= 0.

16.10.58.

07/12/02

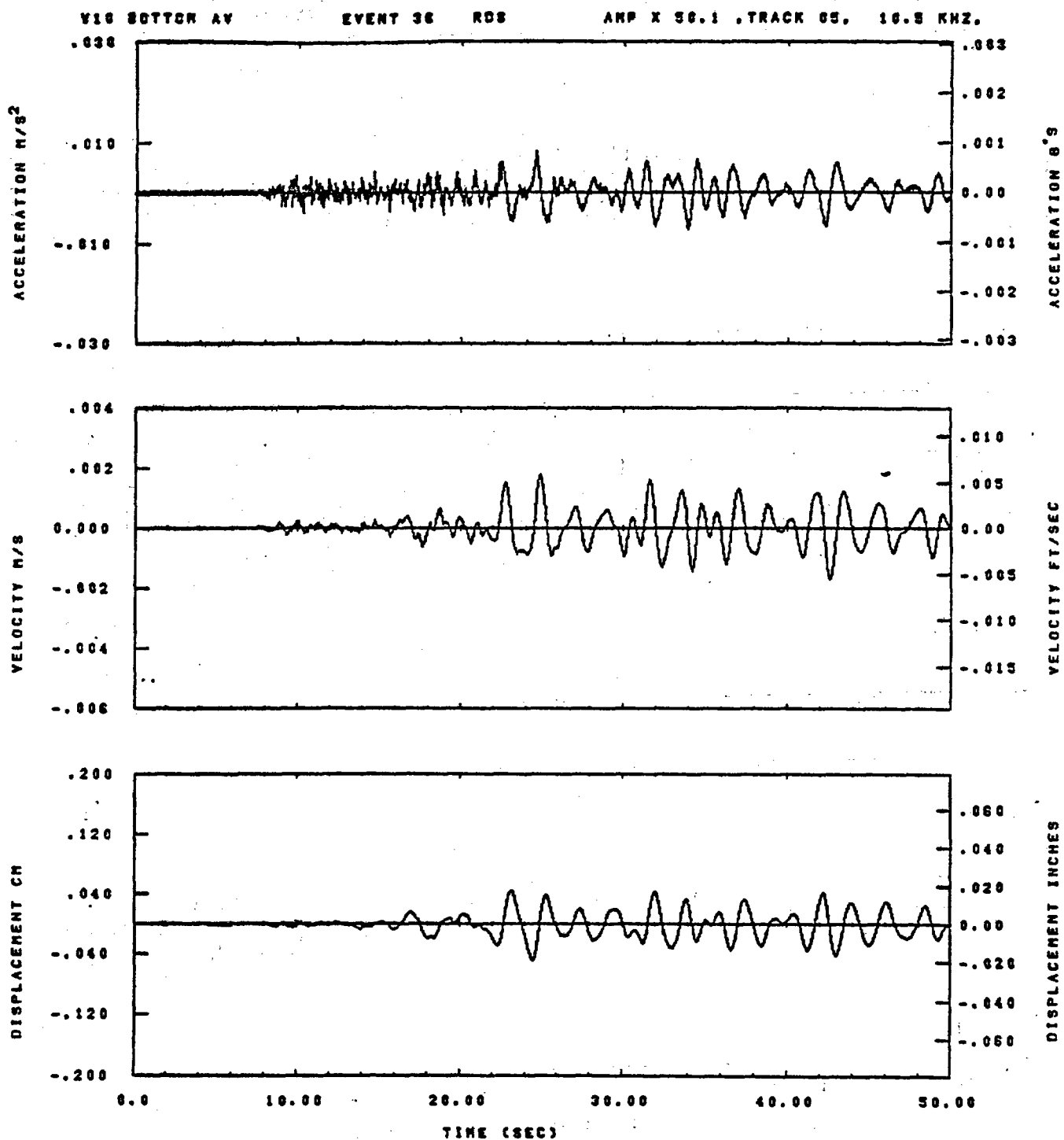
Figure C-34



IOT= .0020	OOT= .003	FIX=	AAS= 0.
HFF= .25	SVH= .18	HLH= 143	ASB=
LFF= 31.	SVL= 7.	HLL= 2339	ASE=
VTS= .250	VTE= .188	FLL= -20.	VSE= 0.
OPB= 6.	OPE= 100.	FLH= 0	OSE= 0.

11.53.13.

08/21/82

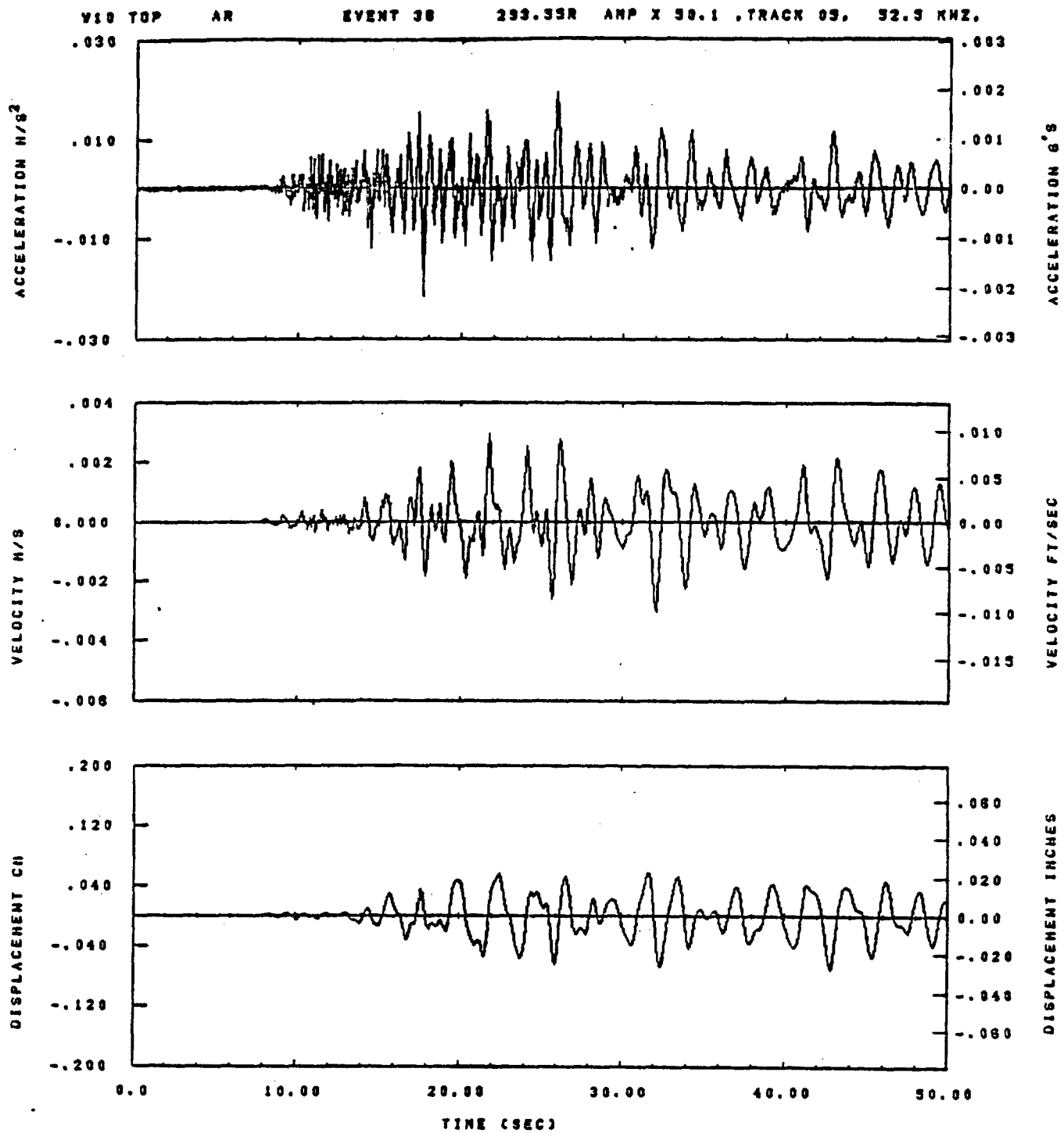


IDT= .0020	ODT= .005	FIX=	AAS= 0.
HPF= .25	SVN= .16	HLN= 143	ASS=
LPF= 31.	SVL= 7.	HLL= 2388	ASE=
VTS= .250	VTE= .168	FLL= -20.	VSE= 0.
DPS= 0.	DPE= 100.	FLH= 0	DSE= 0.

08.43.18.

06/23/82

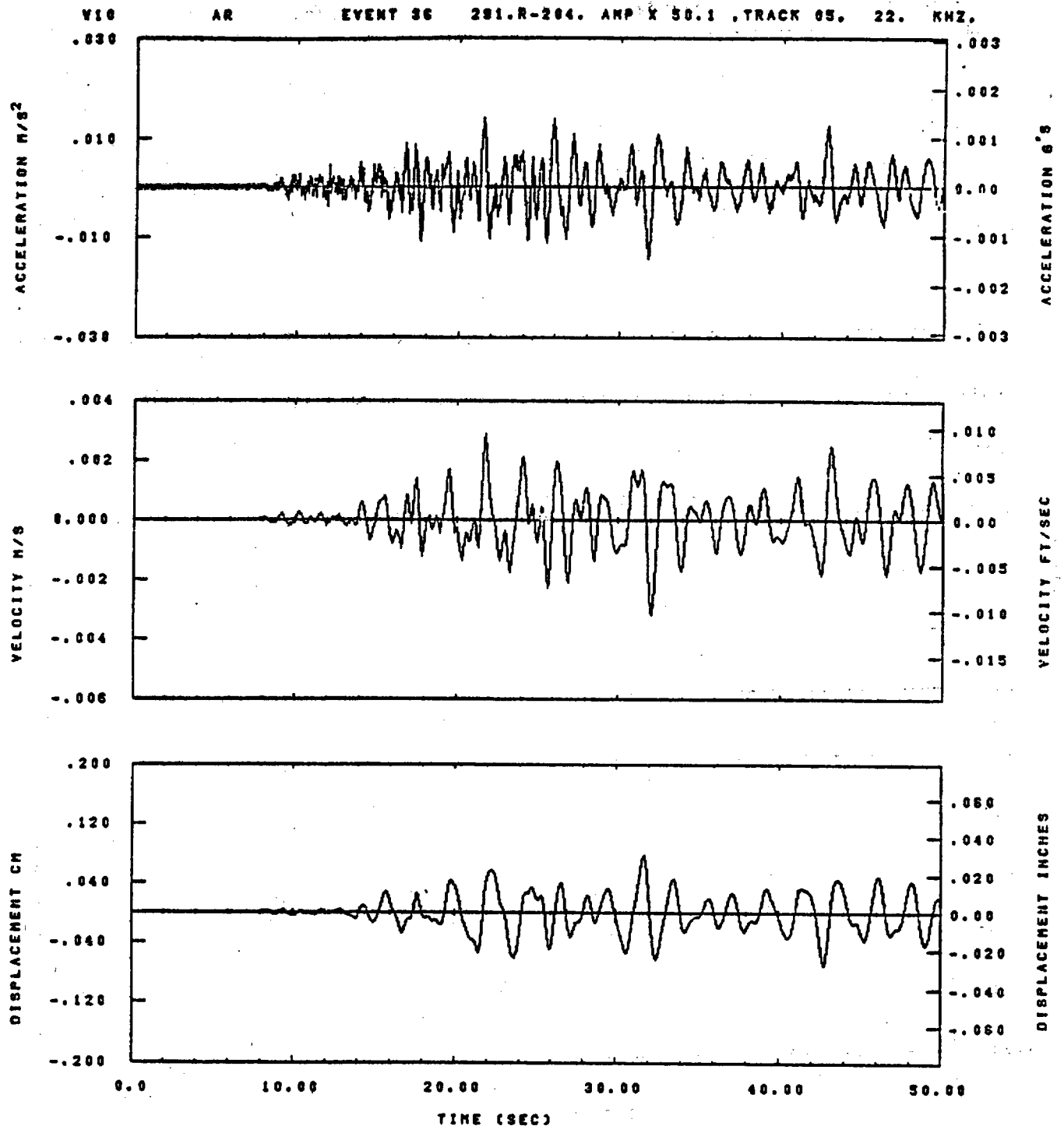
Figure C-36



IDT= .0020	DDT= .005	FIX=	AAS= 0.
HPP= .25	BYH= .18	HLH= 143	ASB=
LPP= 31.	BYL= 7.	HLL= 2399	ASZ=
VTS= .250	VTE= .188	FLL= -20.	VSE= 0.
OPS= 0.	OPE= 100.	FLH= 0	DSE= 0.

11.33.01.

08/21/82

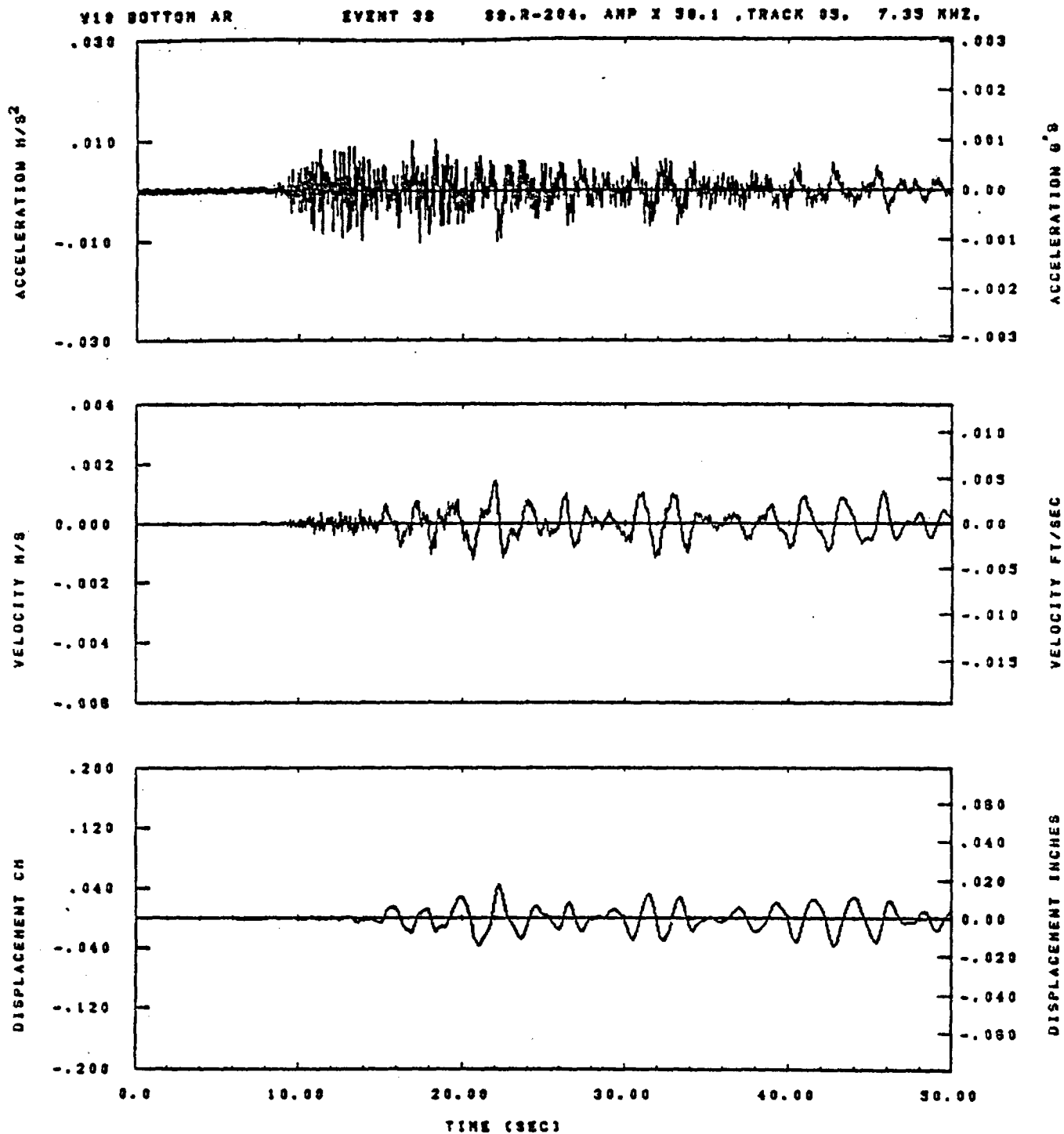


IDT= .0028	ODT= .005	FIX=	AAS= 0.
HPF= .25	BVH= .16	HLH= 143	ASB=
LPP= 31.	BVL= 7.	HLL= 2388	ASE=
VTB= .258	VTE= .166	FLL= -20.	VSE= 0.
DPS= 0.	DPE= 100.	FLH= 0	DSE= 0.

11.53.18.

06/21/82

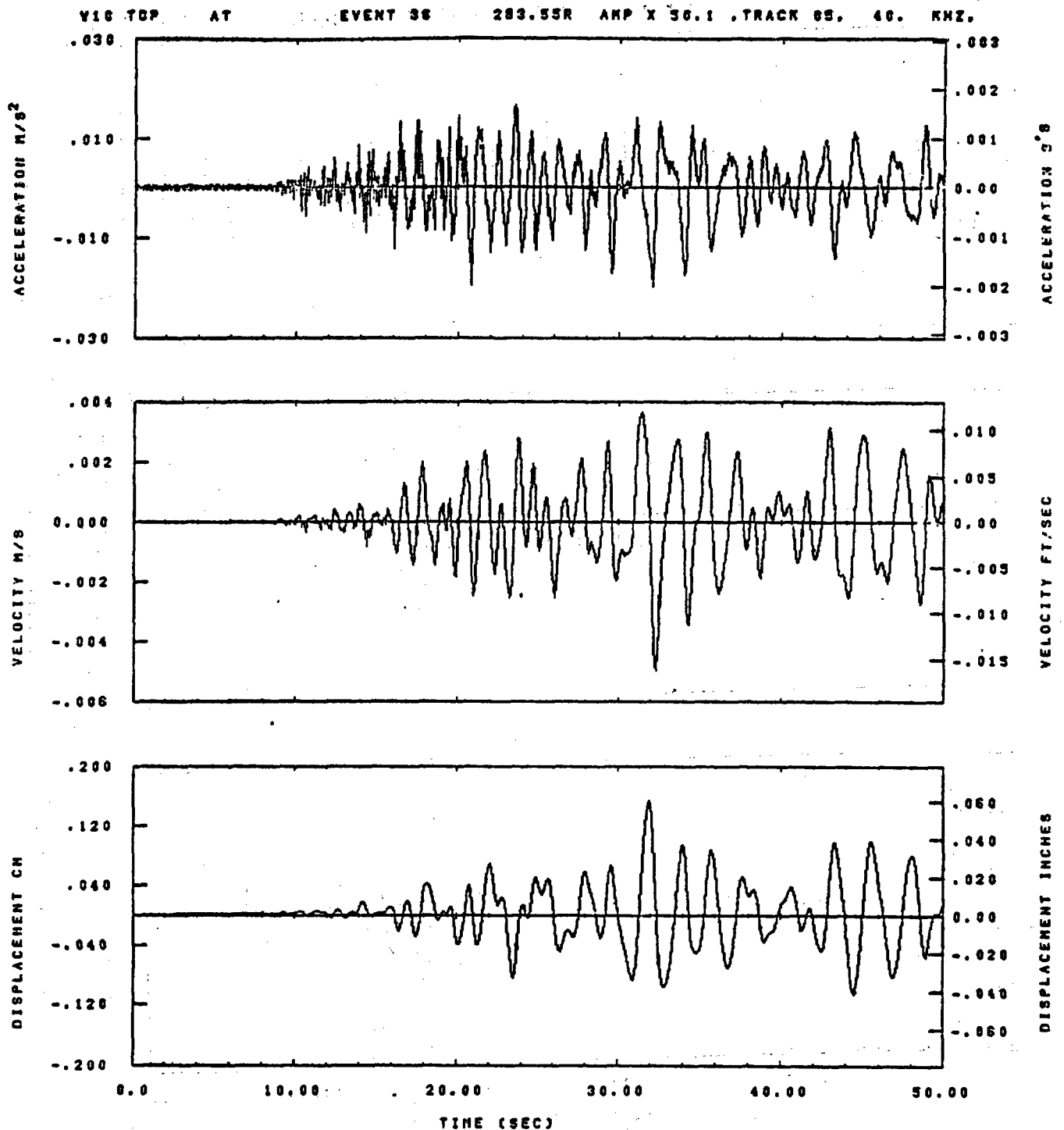
Figure C-38



IDT= .0020	OOT= .003	FIX=	AAS= 0.
HPF= .25	BYH= .16	HLH= 143	ASS=
LPF= 31.	BYL= 7.	HLL= 2333	ASE=
VTB= .250	VTZ= .188	FLL= -20.	VSE= 0.
DPS= 0.	DPE= 100.	FLH= 0	DSE= 0.

08.43.28.

08/23/82

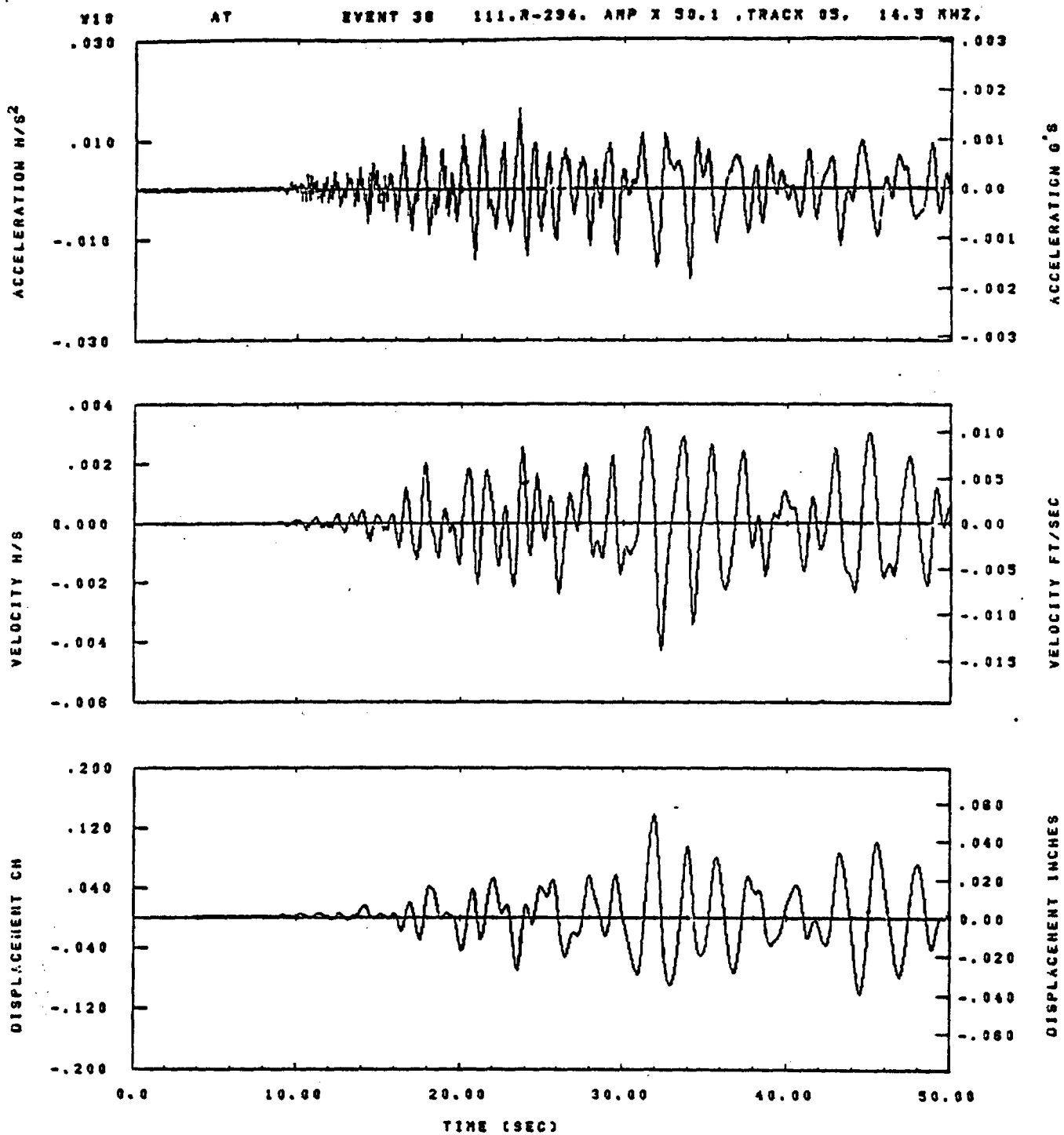


IDT= .0020	ODT= .005	FIX=	AAS= 0.
HPP= .25	BVH= .16	HLN= 143	ASS=
LPP= 31.	BVL= 7.	HLL= 2388	ASE=
VTB= .250	VTE= .166	FLL= -20.	VSE= 0.
DPB= 0.	DPE= 100.	FLN= 0	DSE= 0.

11.53.06.

06/21/82

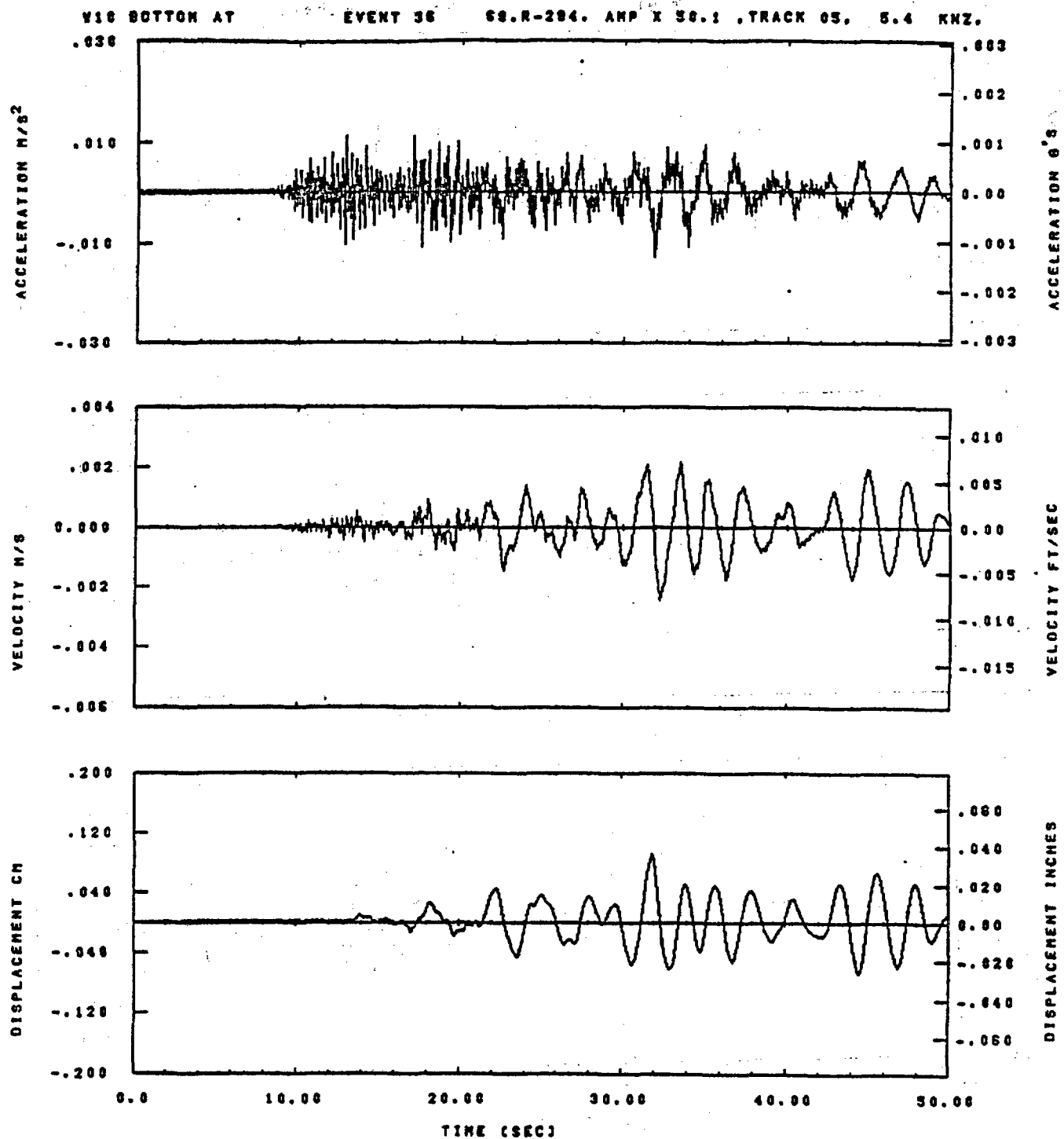
Figure C-40



IDT= .0020	ODT= .003	FIX=	AAS= 0.
HPP= .25	BYH= .18	HLH= 143	ASS=
LPP= 31.	BYL= 7.	HLL= 2399	ASE=
VTB= .250	VTE= .188	FLL= -20.	VSE= 0.
OPB= 0.	OPE= 100.	FLH= 0	DSE= 0.

11.53.23.

06/21/82

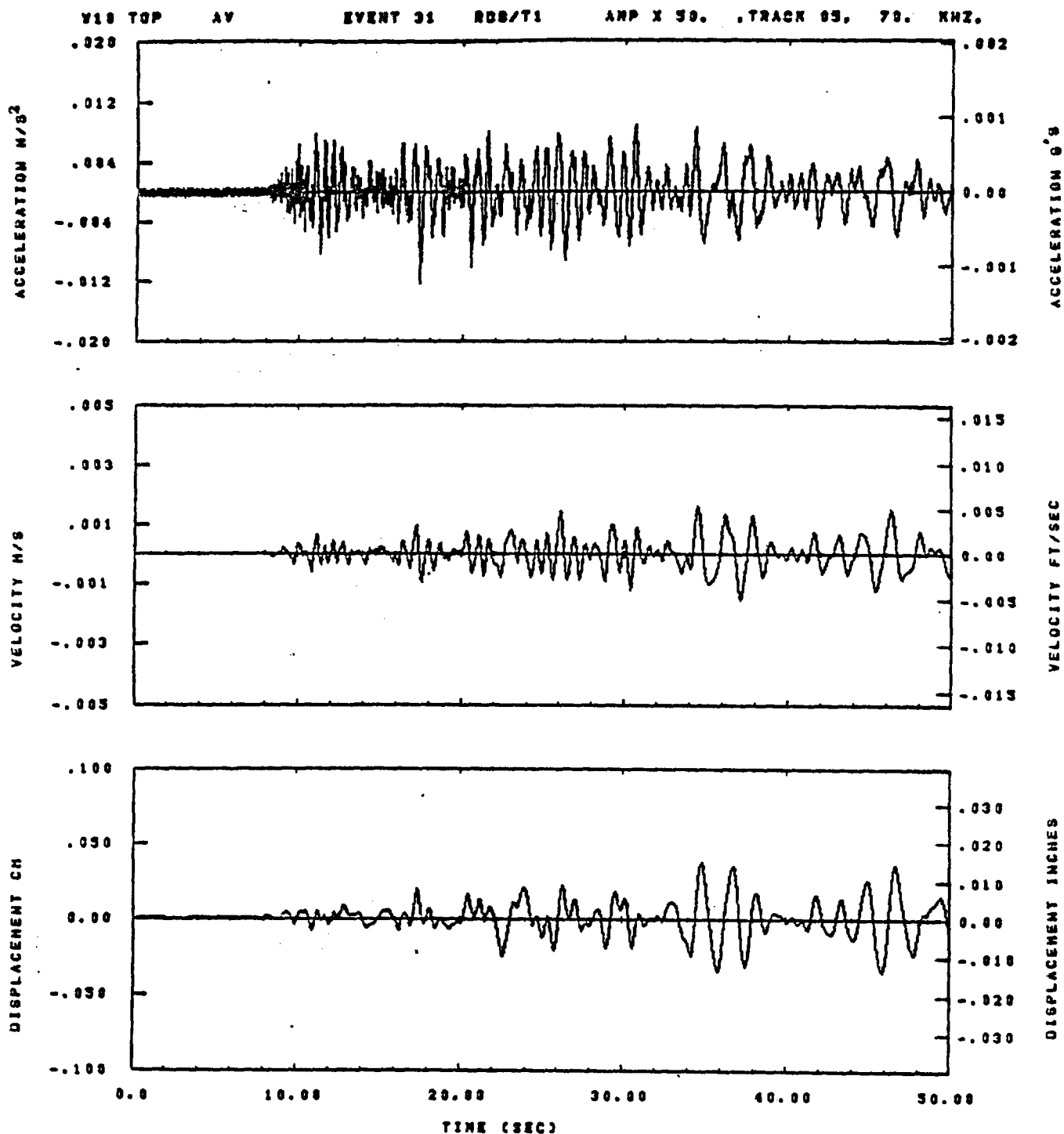


IDT= .0020	ODT= .005	FIX=	AAS= 0.
HPP= .25	SVH= .16	HLH= 143	ASB=
LPP= 31.	SVL= 7.	HLL= 2388	ASE=
VTS= .250	VTE= .166	PLL= -20.	VSE= 0.
DPS= 0.	DPE= 100.	FLH= 0	DSE= 0.

08.43.38.

06/23/82

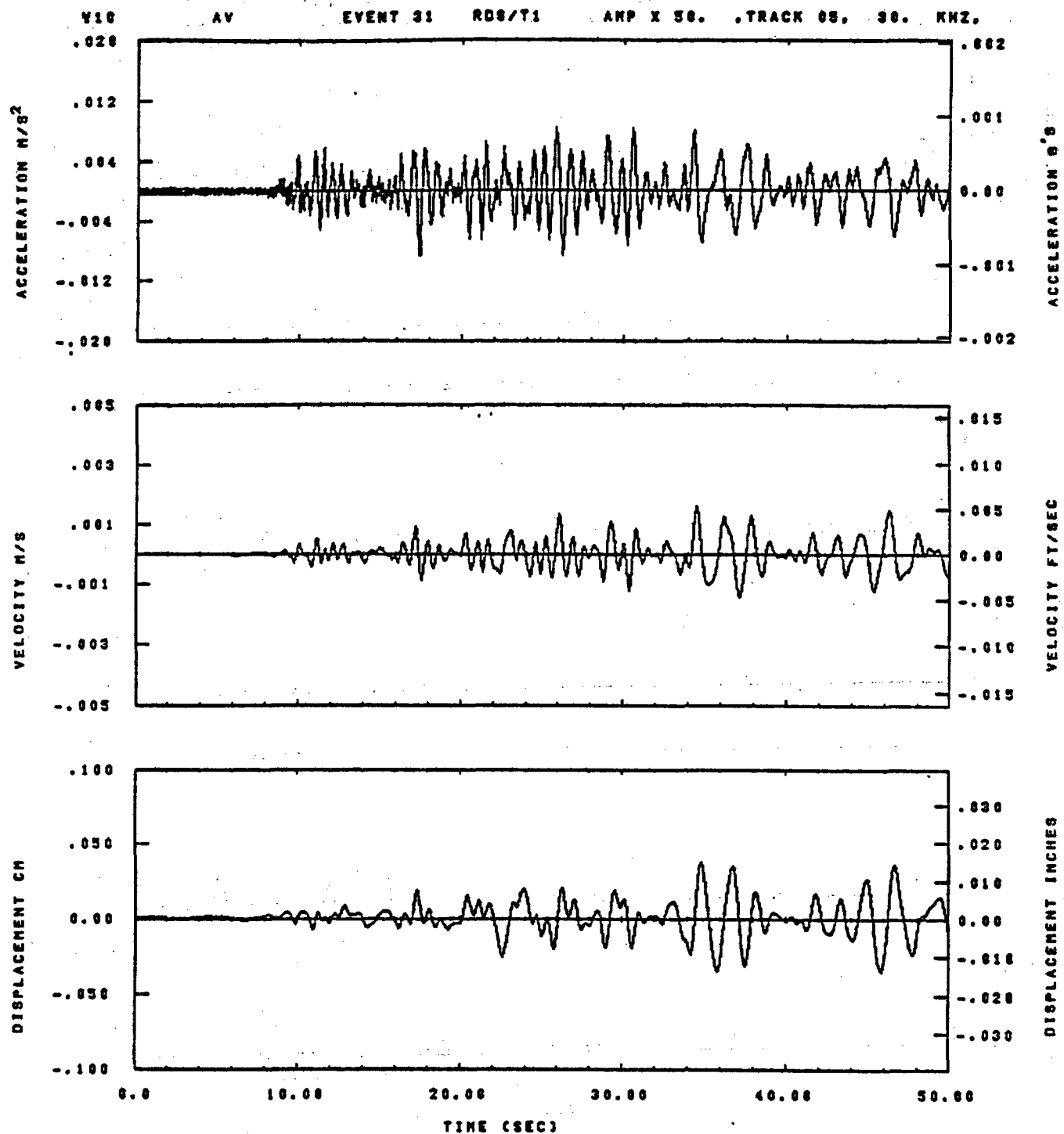
Figure C-42



IDT= .0020	ODT= .005	FIX=	AAS= 0.
HPP= .25	BYN= .18	HLH= 143	ASB=
LPP= 31.	BYL= 7.	HLL= 2399	ASE=
VTS= .250	VTE= .100	FLL= -20.	VSE= 0.
DPS= 0.	DPE= 100.	FLH= 0	DSE= 0.

14.53.48.

08/24/82

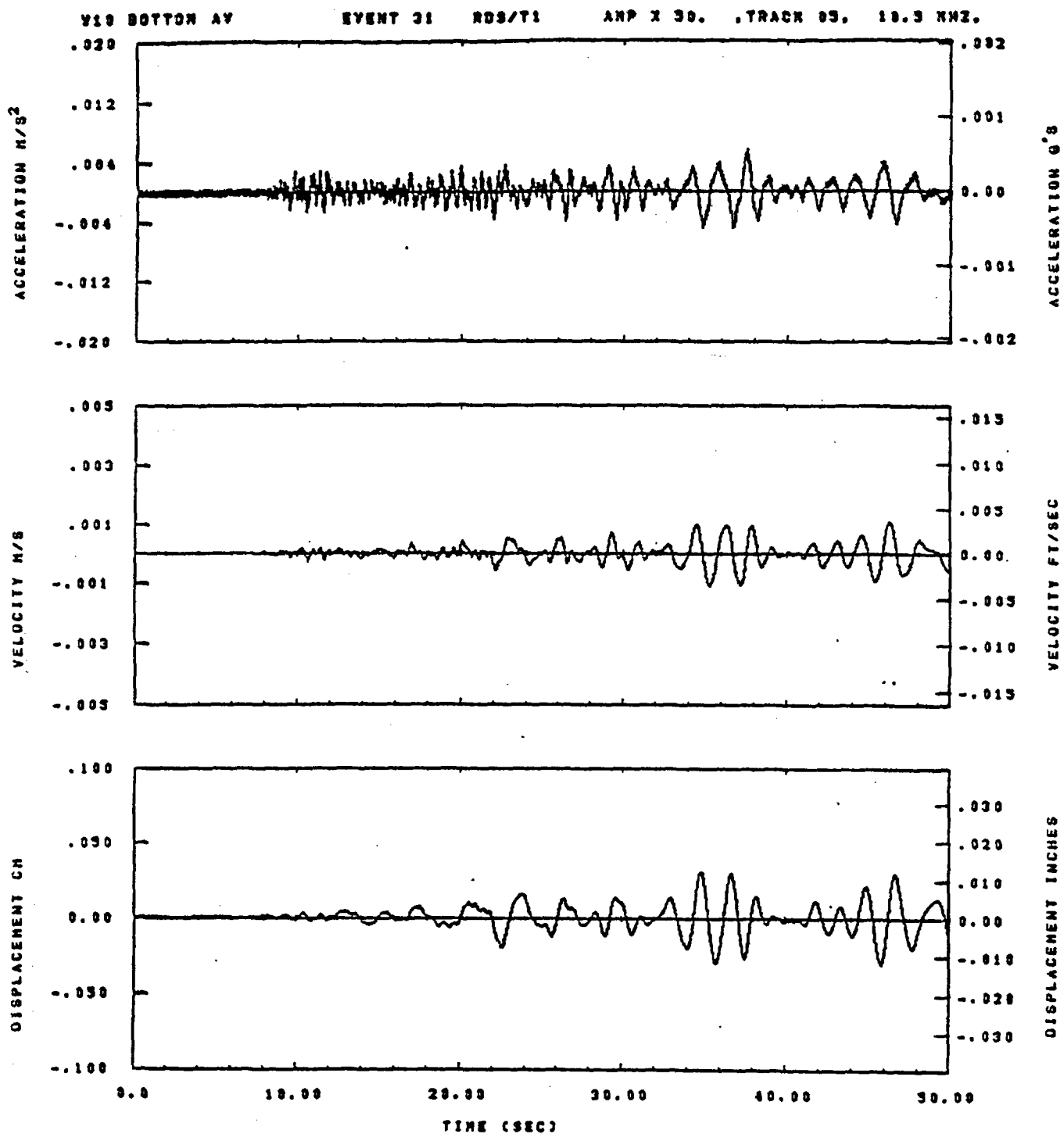


IDT= .0020	QDT= .005	FIX=	AAS= 0.
HFF= .25	BYH= .16	HLH= 143	ASS=
LFF= 31.	BYL= 7.	HLL= 2388	ASE=
VTS= .250	VTE= .160	FLL= -20.	VSE= 0.
DPS= 0.	DPE= 100.	FLH= 0	DSE= 0.

14.53.52.

06/24/82

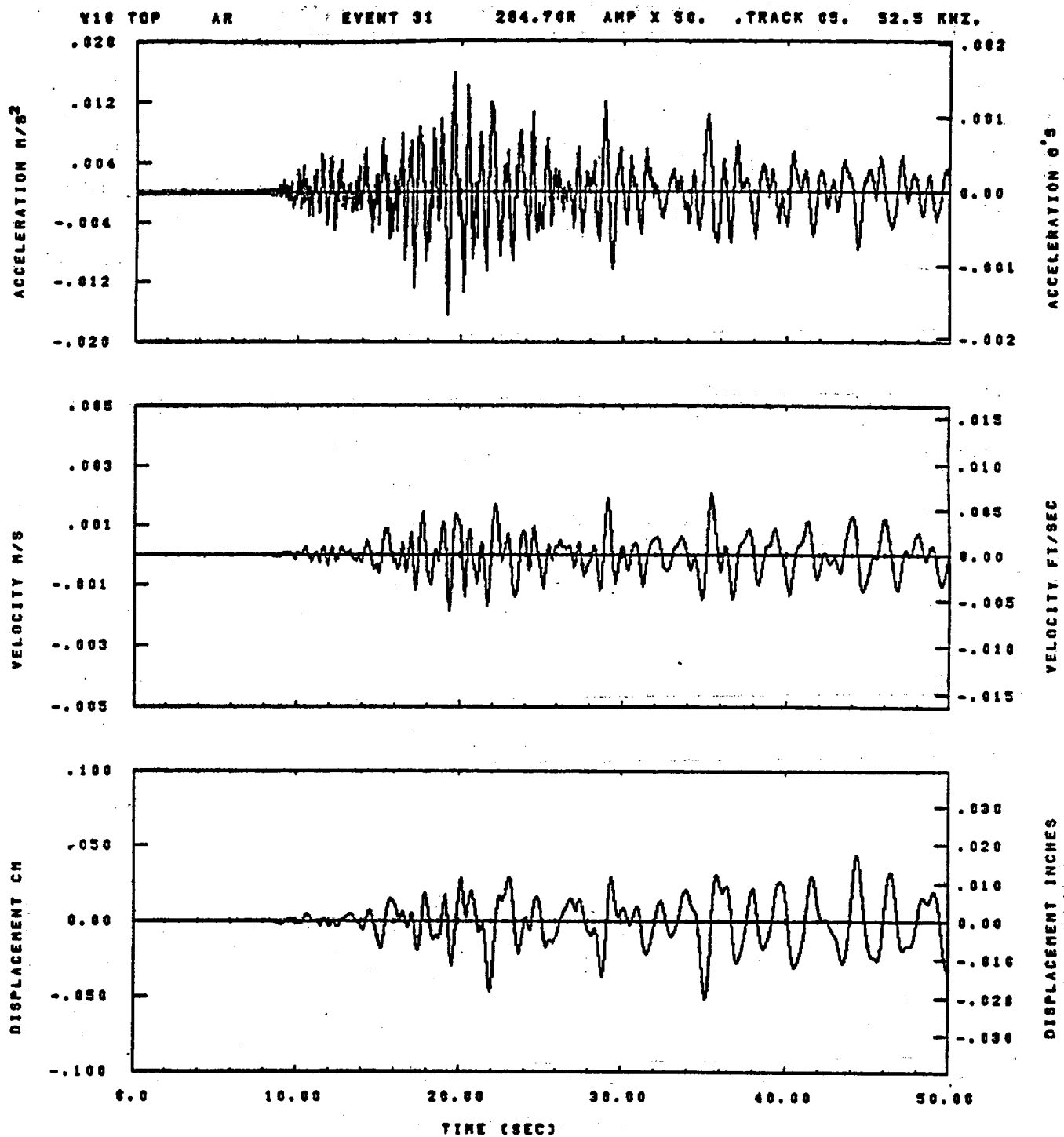
Figure C-44



IDT= .0020	ODT= .003	FIX=	AAS= 0.
HPP= .25	BYH= .18	HLH= 143	ASB=
LPP= 31.	BYL= 7.	HLL= 2399	ASE=
VTB= .250	VTE= .180	FLL= -20.	VSE= 0.
OPS= 0.	OPE= 100.	FLH= 0	DSE= 0.

14.33.38.

08/26/92

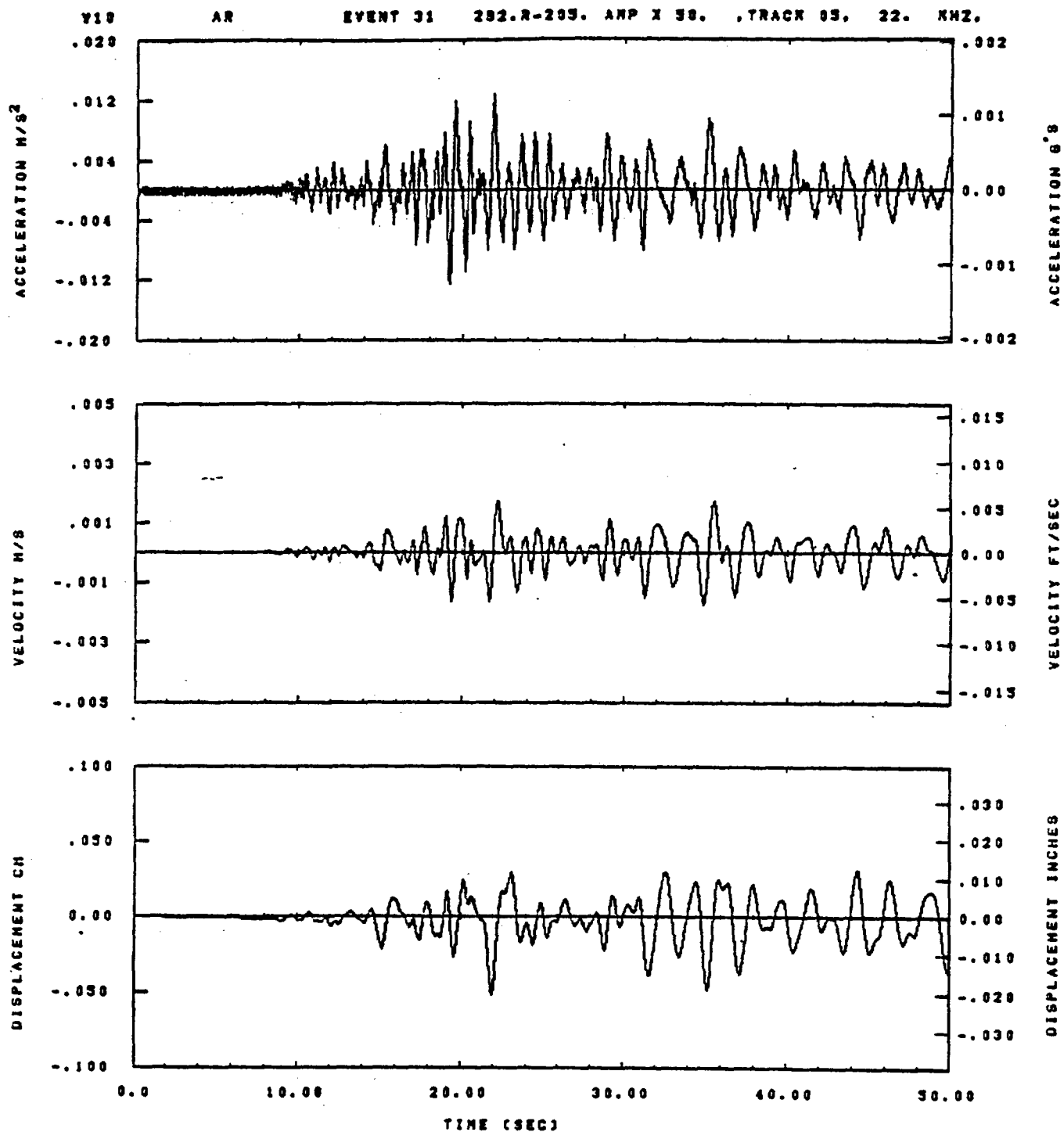


IDT= .0020	ODT= .005	FIX=	AAS= 0.
HFF= .25	SVH= .16	HLH= 143	ASB=
LFF= 31.	SVL= 7.	HLL= 2388	ASE=
VTB= .258	VTE= .166	FLL= -26.	VSE= 0.
DPE= 0.	DPE= 188.	FLH= 0	DSE= 0.

14.53.38.

06/24/82

Figure C-46

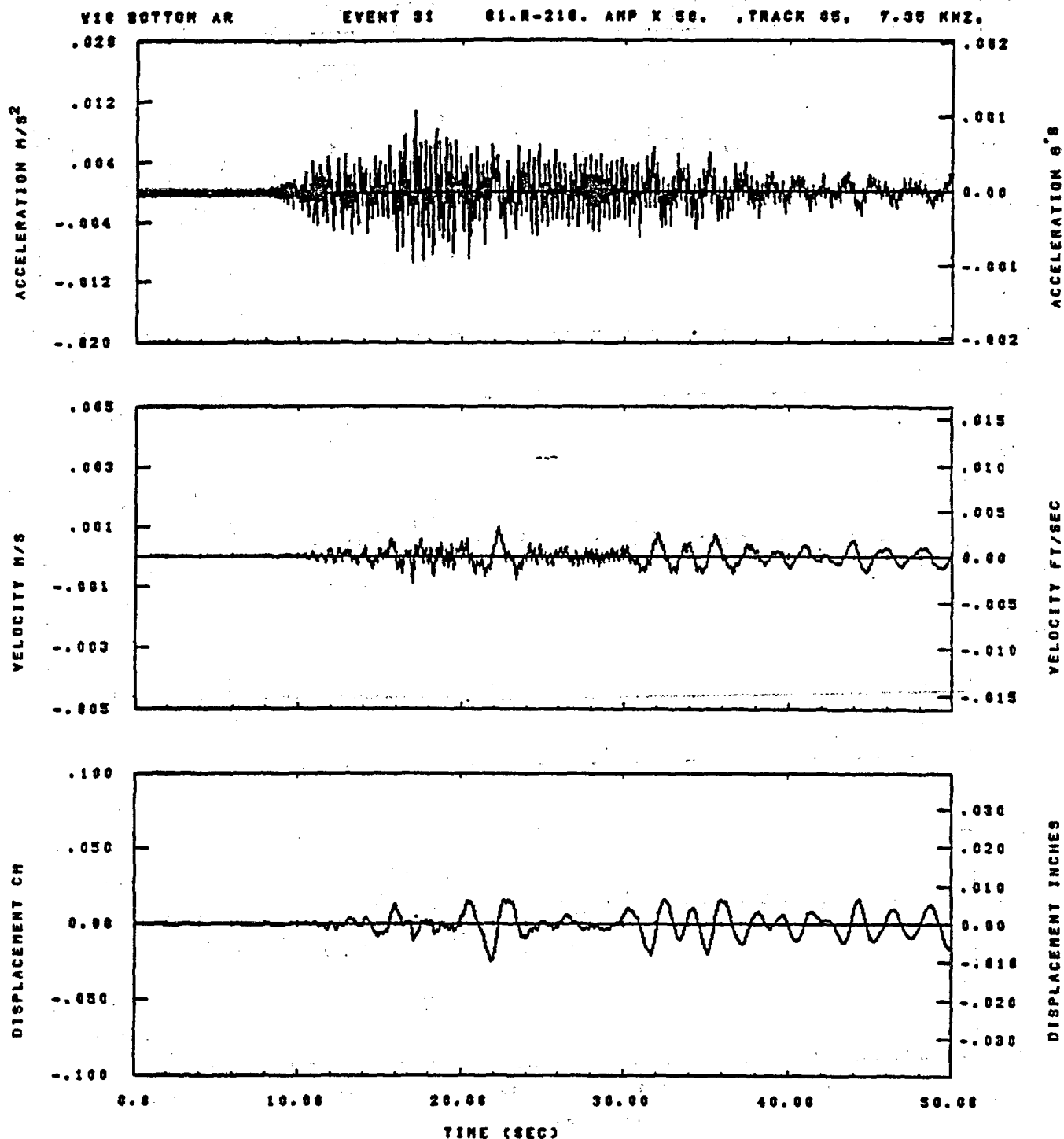


IDT= .0020	ODT= .005	FIX=	AAS= 0.
HPP= .25	BWH= .18	HLH= 143	ASS=
LPP= 31.	BVL= 7.	HLL= 2393	ASE=
VTS= .250	VTE= .188	FLL= -20.	VSE= 0.
DPS= 0.	DPE= 100.	FLH= 0	DSE= 0.

08.23.23.

07/02/82

Figure C-47

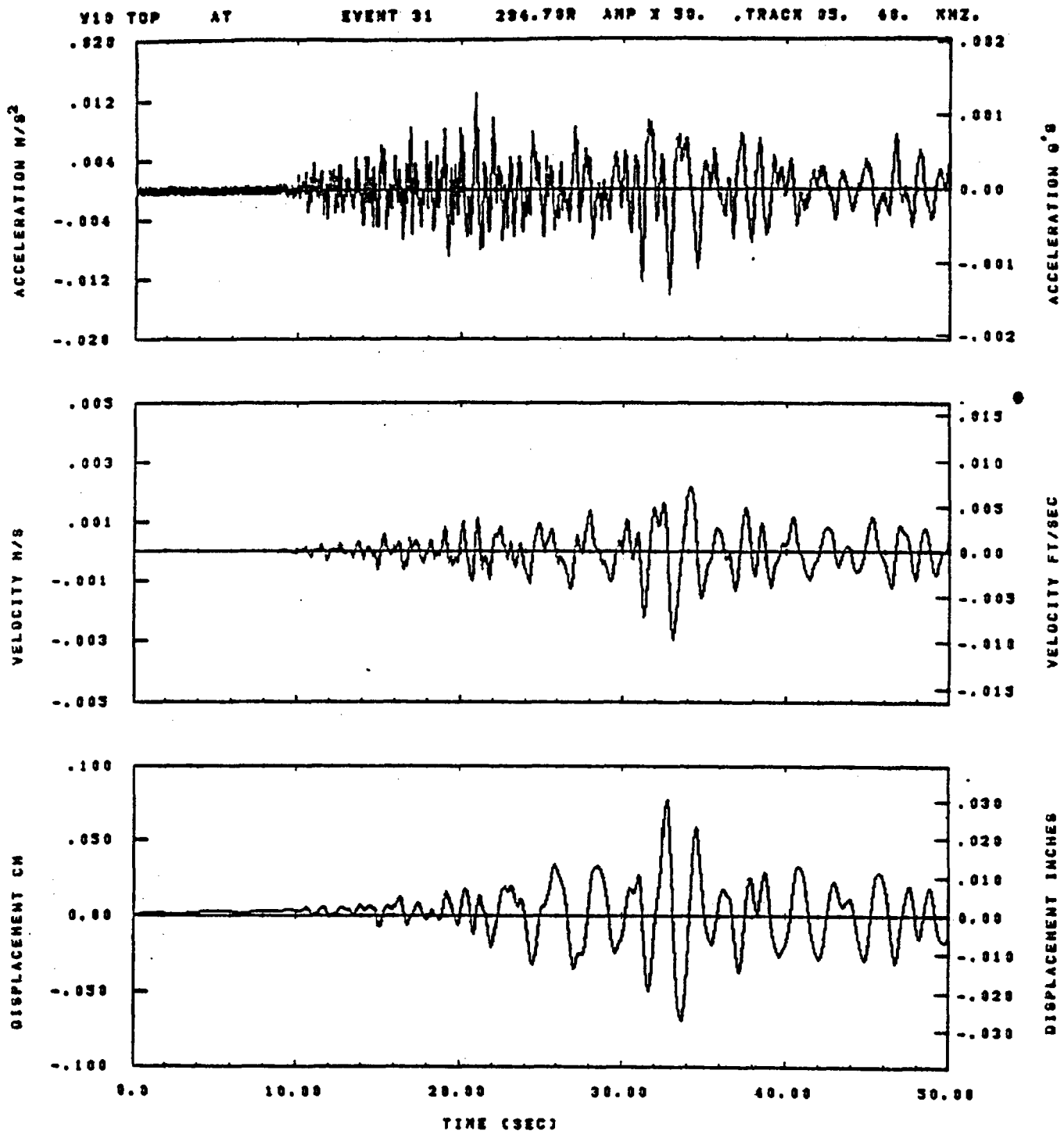


IDT= .0020	ODT= .005	FIX=	AAS= 0.
HPF= .25	BYH= .10	HLN= 143	ASB=
LPF= 31.	BYL= 7.	HLL= 2300	ASE=
VTD= .250	VTE= .100	FLL= -20.	VSE= 0.
DPS= 0.	DPE= 100.	FLH= 0	DSE= 0.

14.54.82.

08/24/82

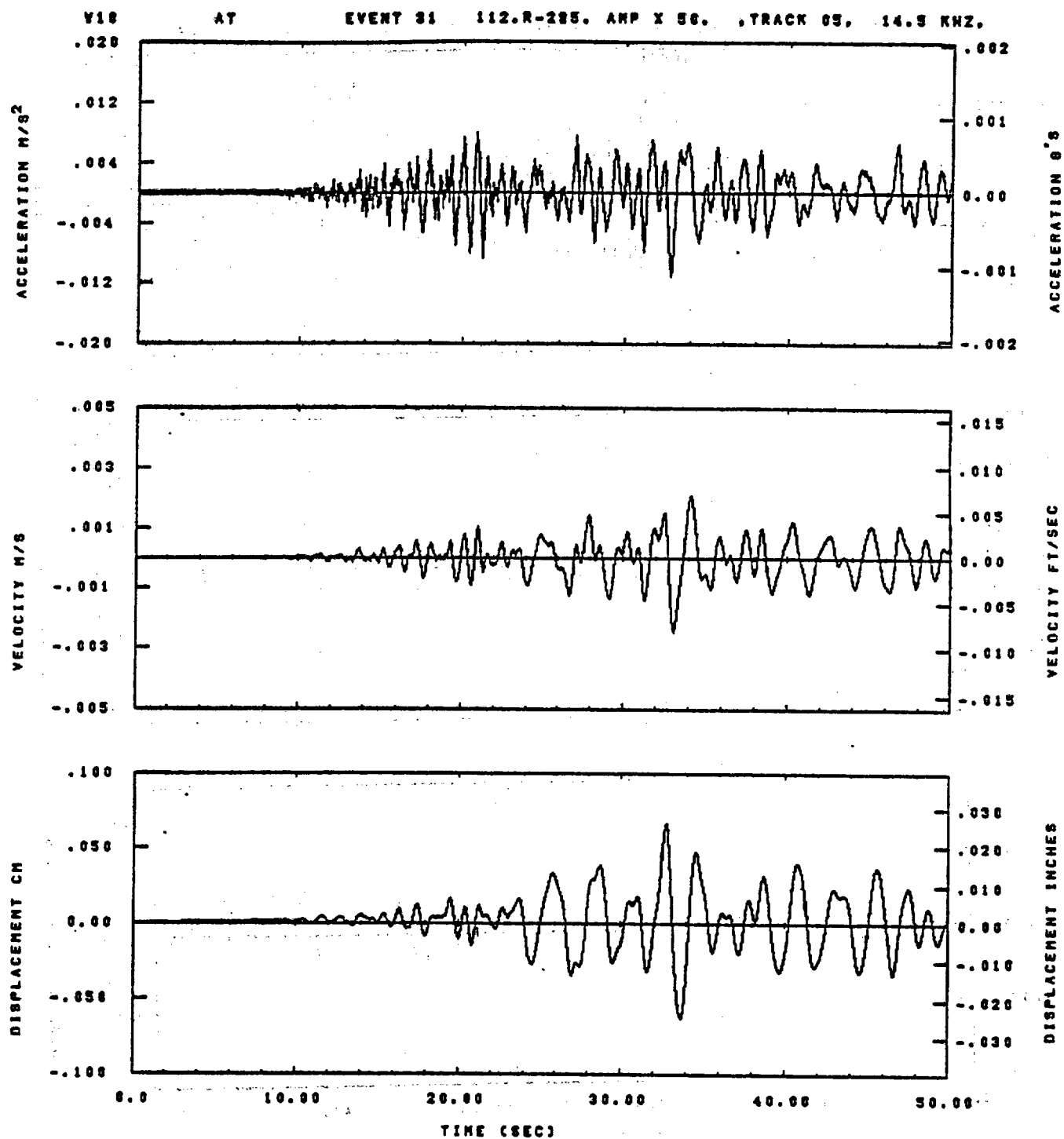
Figure C-48



IDT= .0020	OOT= .003	FIX=	AAS= 0.
HPP= .25	BYH= .10	HLH= 143	ASB=
LPP= 31.	BYL= 7.	HLL= 2399	ASE=
YTS= .250	YTE= .188	FLL= -20.	VSE= 0.
DPS= 0.	DPE= 100.	FLH= 0	DSE= 0.

14.53.42.

08/26/82

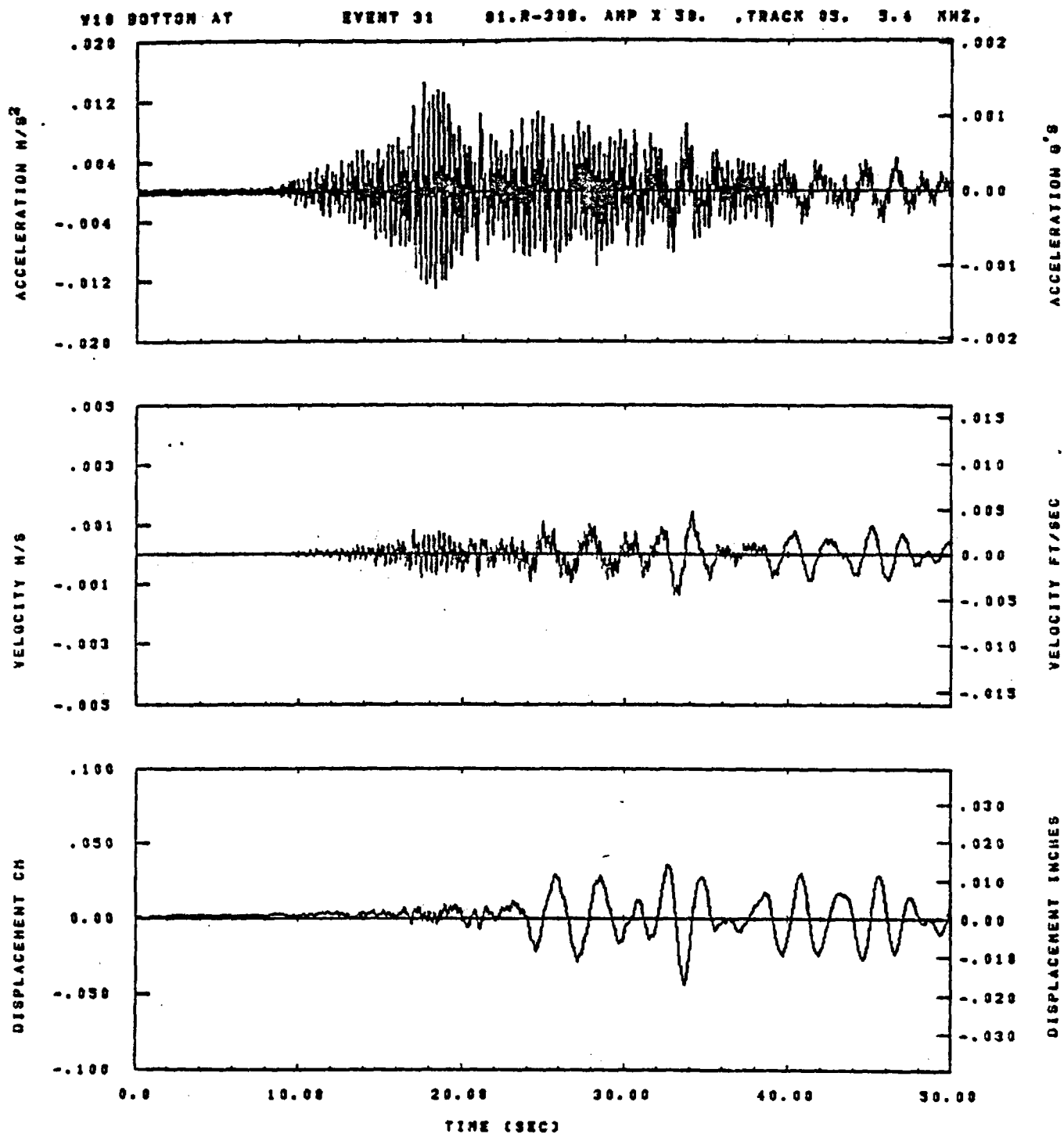


IDT= .0028	ODT= .005	FIX=	AAS= 0.
HPP= .25	BYH= .16	HLH= 143	ASE=
LPP= 31.	BYL= 7.	HLL= 2388	ASE=
VTS= .256	VTE= .166	FLL= -20.	VSE= 0.
DPS= 0.	DPE= 100.	FLH= 0	DSE= 0.

06.28.28.

07/02/82

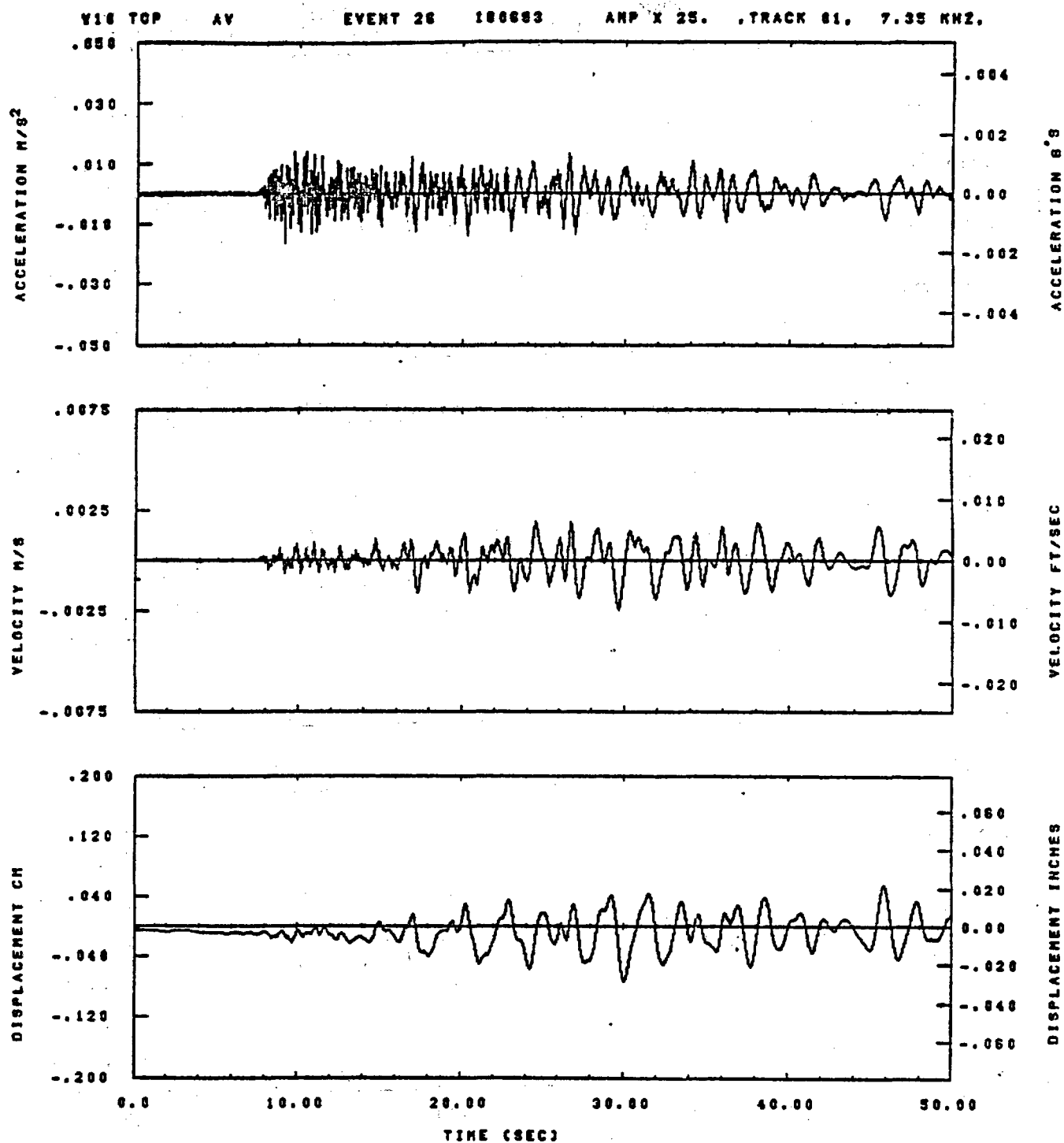
Figure C-50



IDT= .0020	QDT= .003	FIX=	AAS= 0.
HPP= .23	BYN= .18	HLH= 143	ASB=
LPP= 31.	BVL= 7.	HLL= 2399	ASE=
VTB= .238	VTE= .188	FLL= -20.	VSE= 0.
OPB= 0.	OPE= 188.	PLH= 8	OSE= 0.

14.36.87.

08/24/82

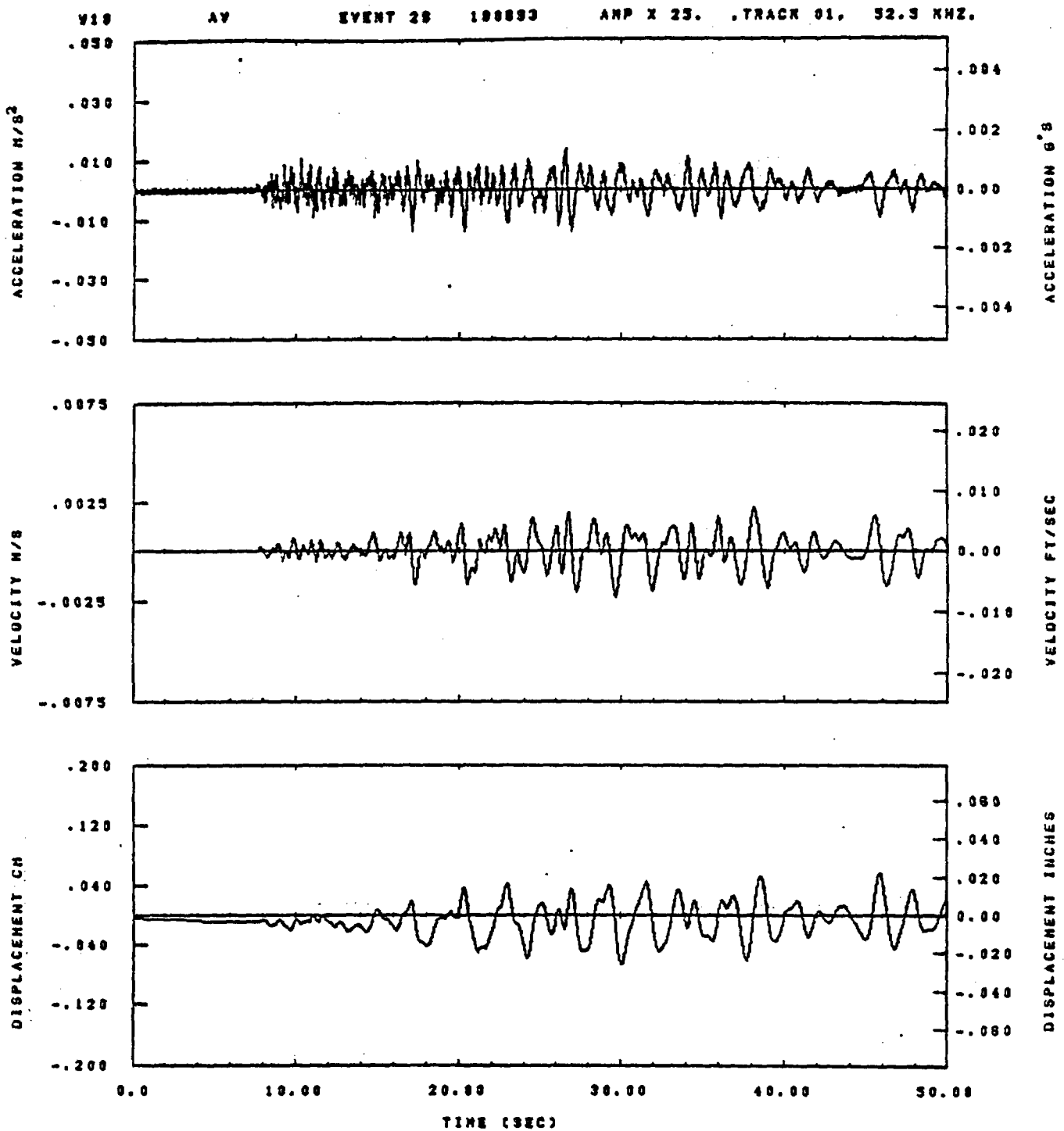


IDT= .0020	ODT= .005	FIX=	AAS= 0.
HPF= .20	SVH= .13	HLH= 251	ASB=
LPF= 18.	SVL= 4.	HLL= 2888	ASE=
YTE= .208	YTE= .133	FLL= -50.	VSE= 0.
DPS= 8.	DPE= 100.	FLH= A-.1	DSE= A+.1

08.05.51.

08/25/82

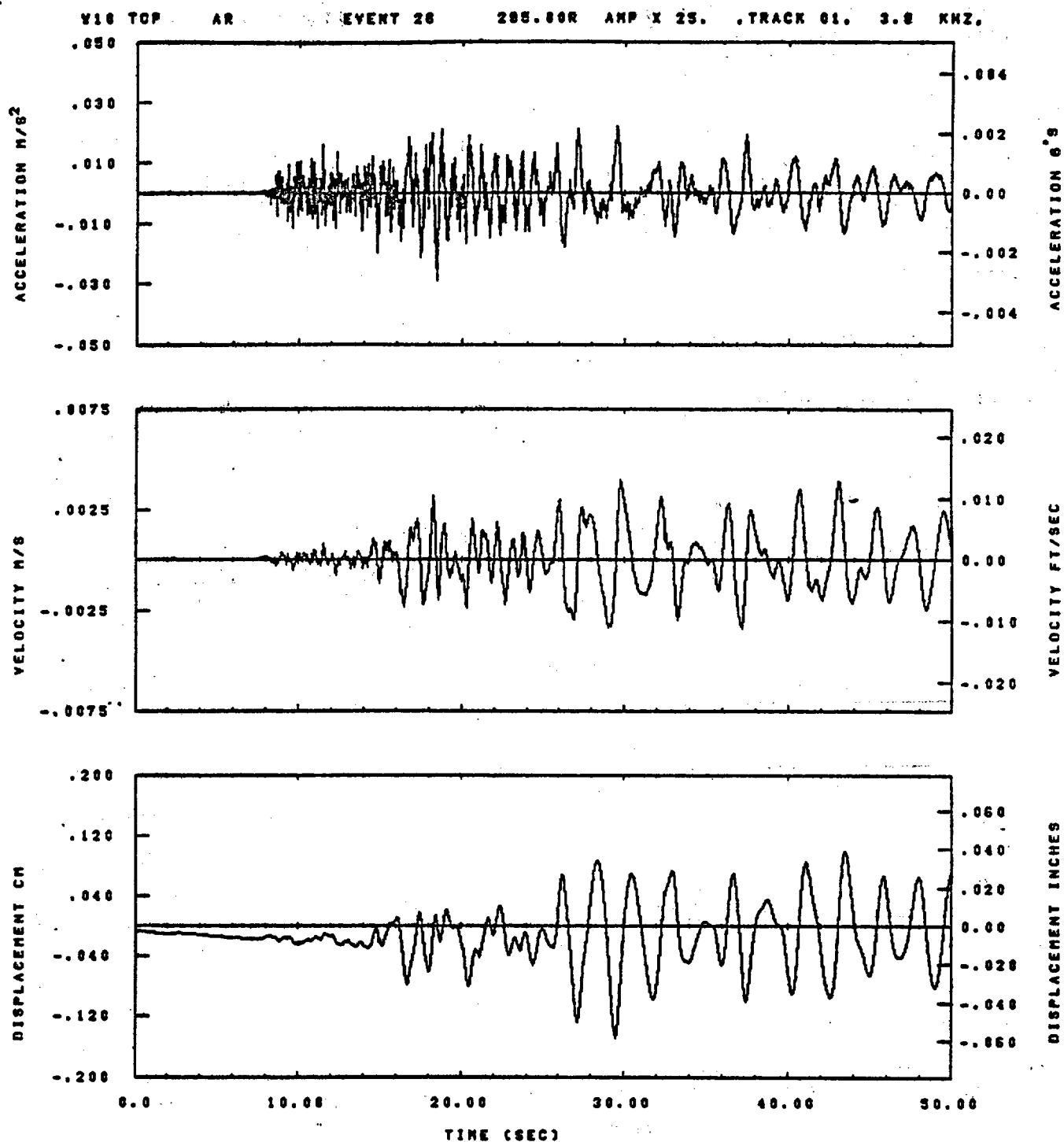
Figure C-52



IDT= .0020	ODT= .005	FIX=	AAS= 0.
HPP= .20	BYH= .13	HLH= 187	ASS=
LPP= 27.	BYL= 8.	HLL= 2333	ASE=
VTS= .200	VTE= .133	FLL= -20.	VSE= 0.
DPS= 8.	DPE= 100.	FLH= 0	DSE= 0.

08.08.20.

08/25/82

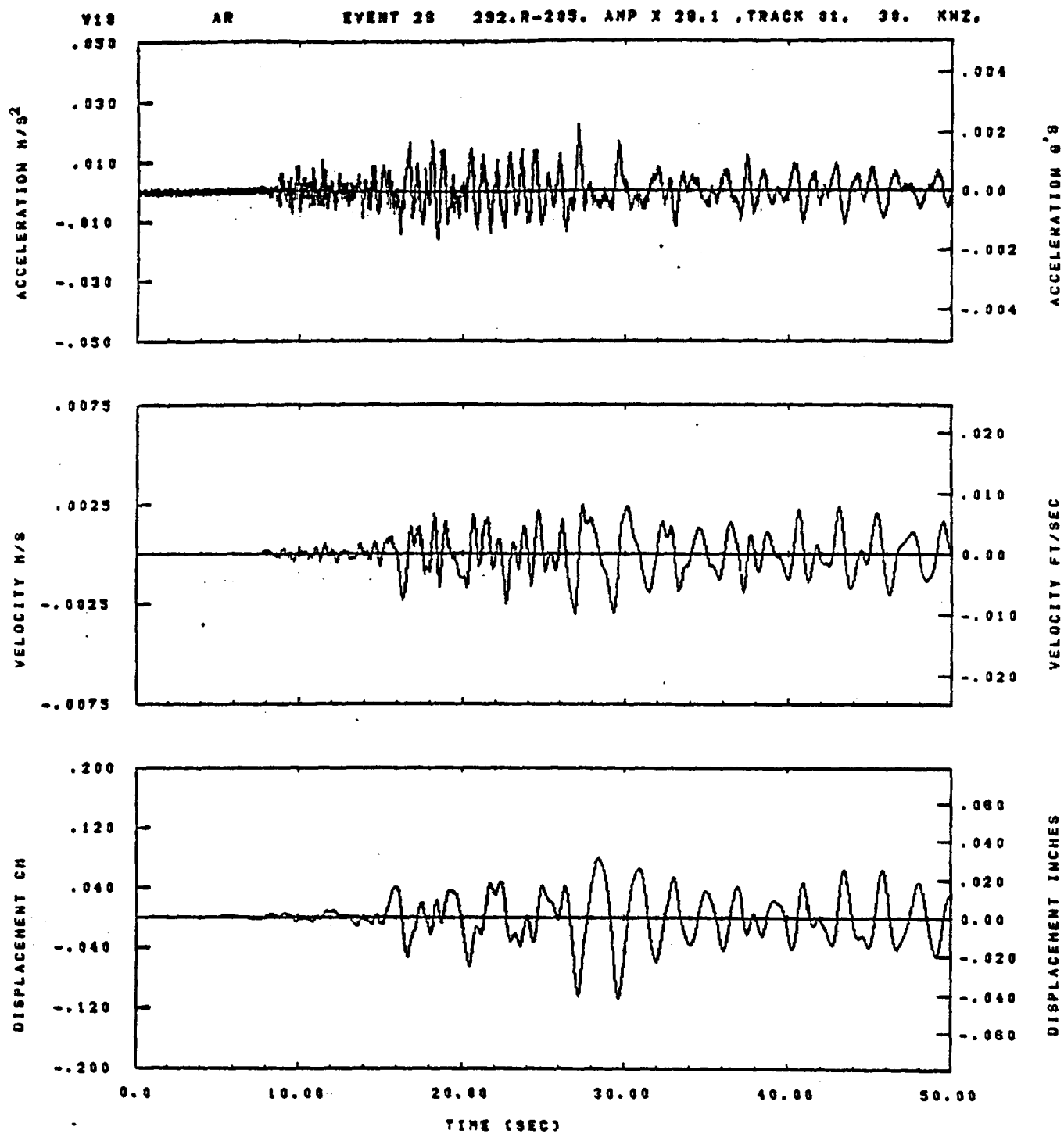


IDT= .0020	ODT= .005	FIX=	AAS= 0.
HPF= .20	BYH= .13	HLN= 251	ASS=
LPF= 18.	BYL= 4.	HLL= 2888	ASE=
VTS= .200	VTE= .133	PLL= -50.	VSE= 0.
DPS= 0.	DPE= 100.	FLH= A-.1	DSE= A+.1

08.05.26.

06/25/82

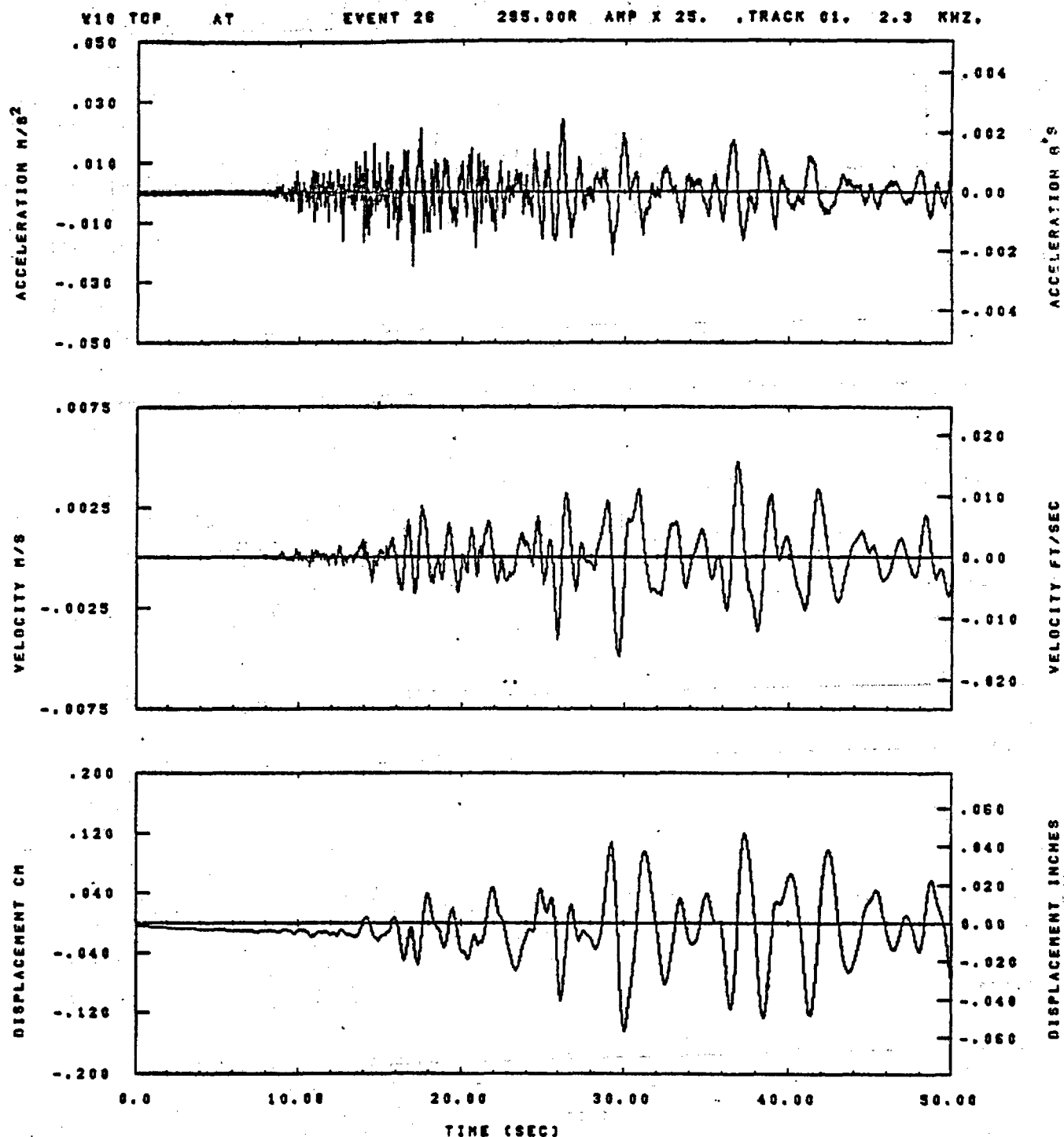
Figure C-54



IDT= .0020	ODT=	FIX=	AAS=
HPF= .3	BYH= .20	HLH= 167	RNG=
LPF= 27.	BYL= 6.	HLL= 1999	AZN=
VTB= .30	VTE= .200	FLL=	VSE=
DPS=	DPE=	FLH= 0	HLT=

13.33.28.

07/26/82

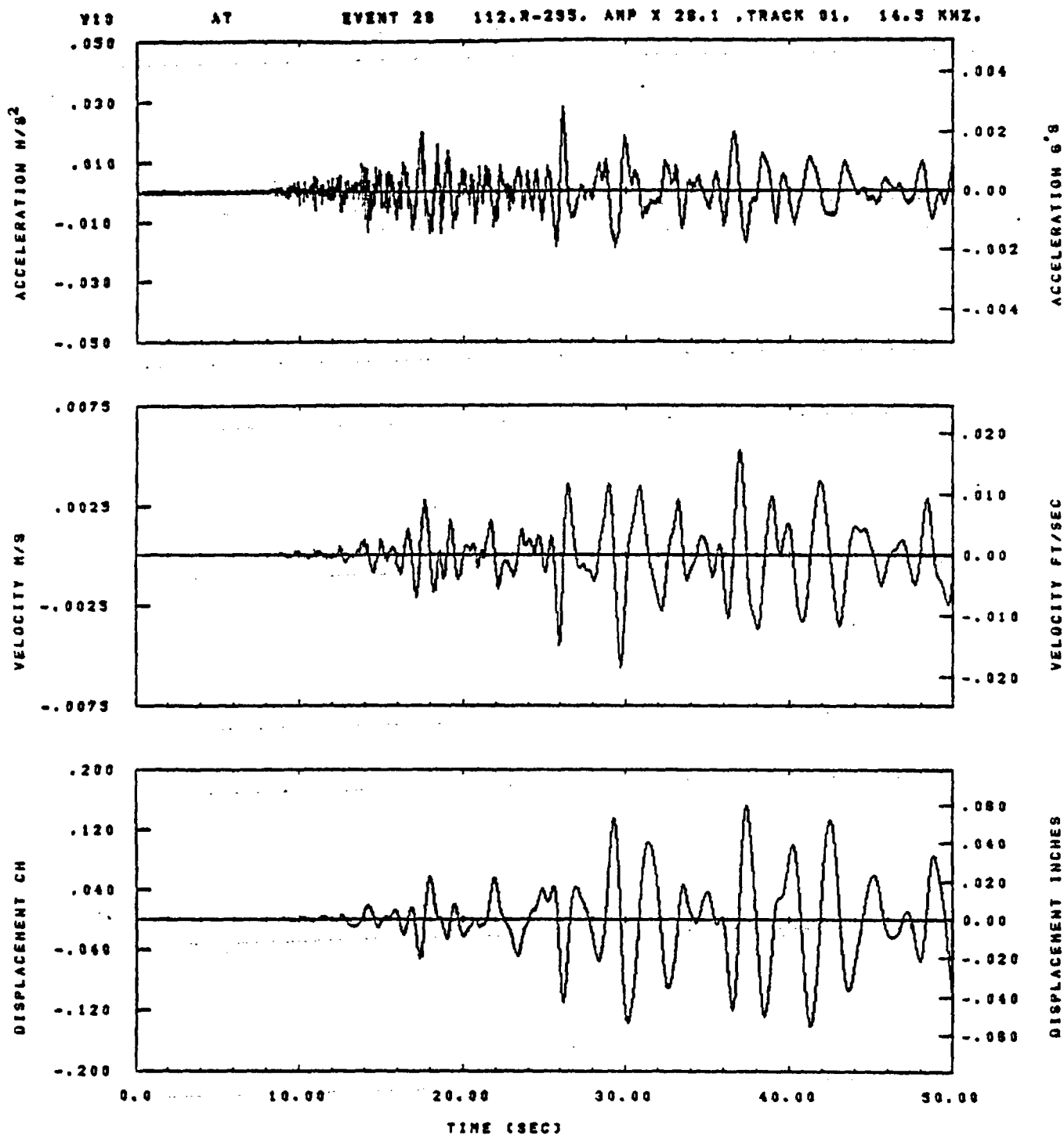


IDT= .0020	ODT= .005	FIX=	AAS= 0.
HPF= .20	BNH= .13	HLH= 251	ASB=
LPF= 18.	BVL= 4.	HLL= 2989	ASE=
VTS= .200	VTE= .133	FLL= -50.	VSE= 0.
DPE= 0.	DPE= 100.	FLH= A-.1	DSE= A+.1

08.05.44.

06/25/82

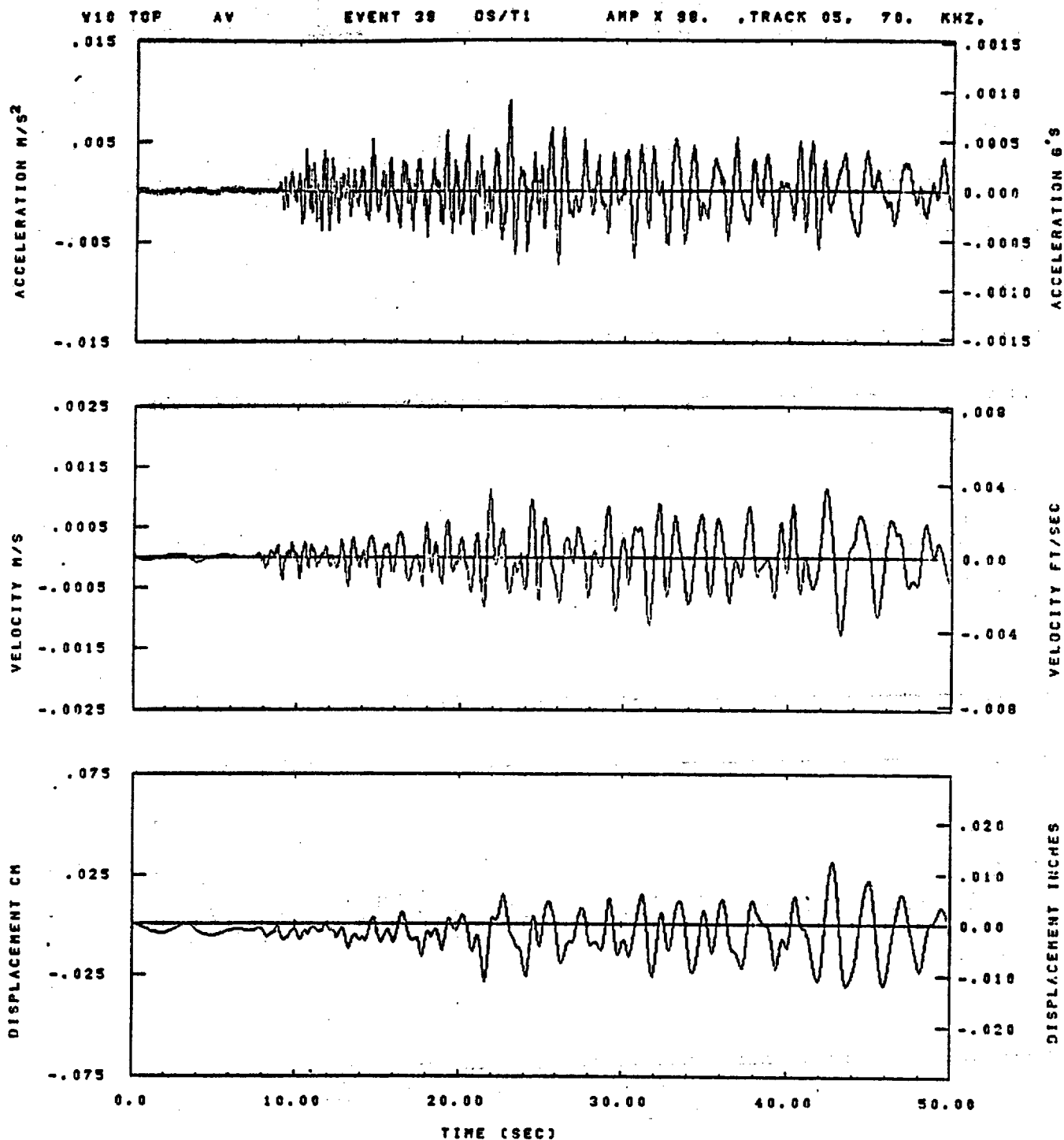
Figure C-56



IDT= .0020	ODT=	FIX=	AAS=
HPP= .3	BYH= .20	HLH= 167	RNG=
LPP= 27.	BYL= 6.	HLL= 1999	AZN=
VTB= .30	VTE= .200	PLL=	VSE=
DPS=	DPE=	FLH= 0	MLT=

13.54.11.

07/28/92

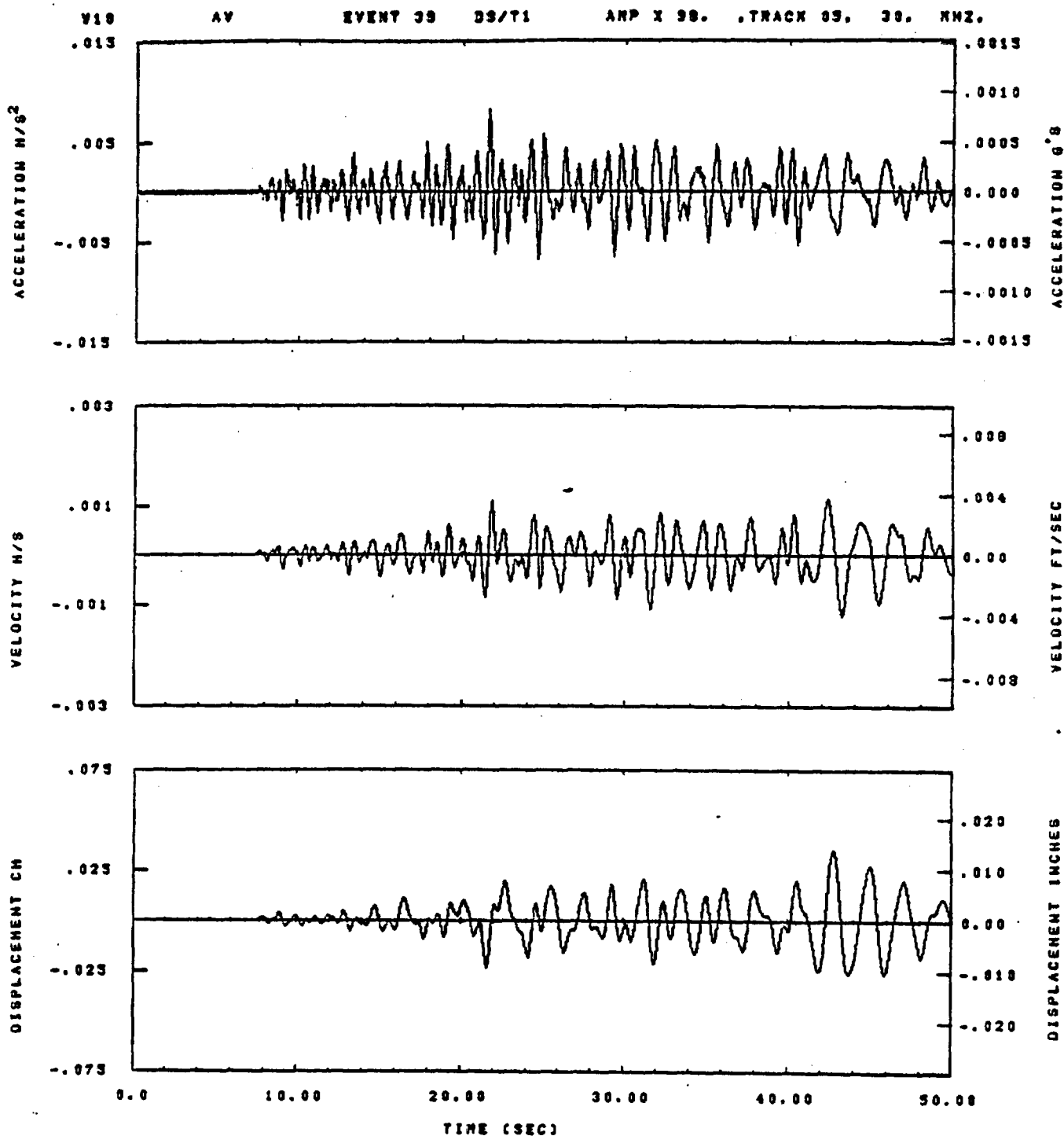


IDT= .0020	ODT= .005	FIX=	AAS= 0.
HPP= .30	SVH= .20	HLH= 199	ASD=
LPP= 22.	BVL= 5.	HLL= 1999	ASE=
YTS= .300	YTE= .200	FLL= -20.	VSE= 0.
OPB= 0.	OPE= 100.	FLH= 0	DSE= 0.

11.56.42

06/11/82

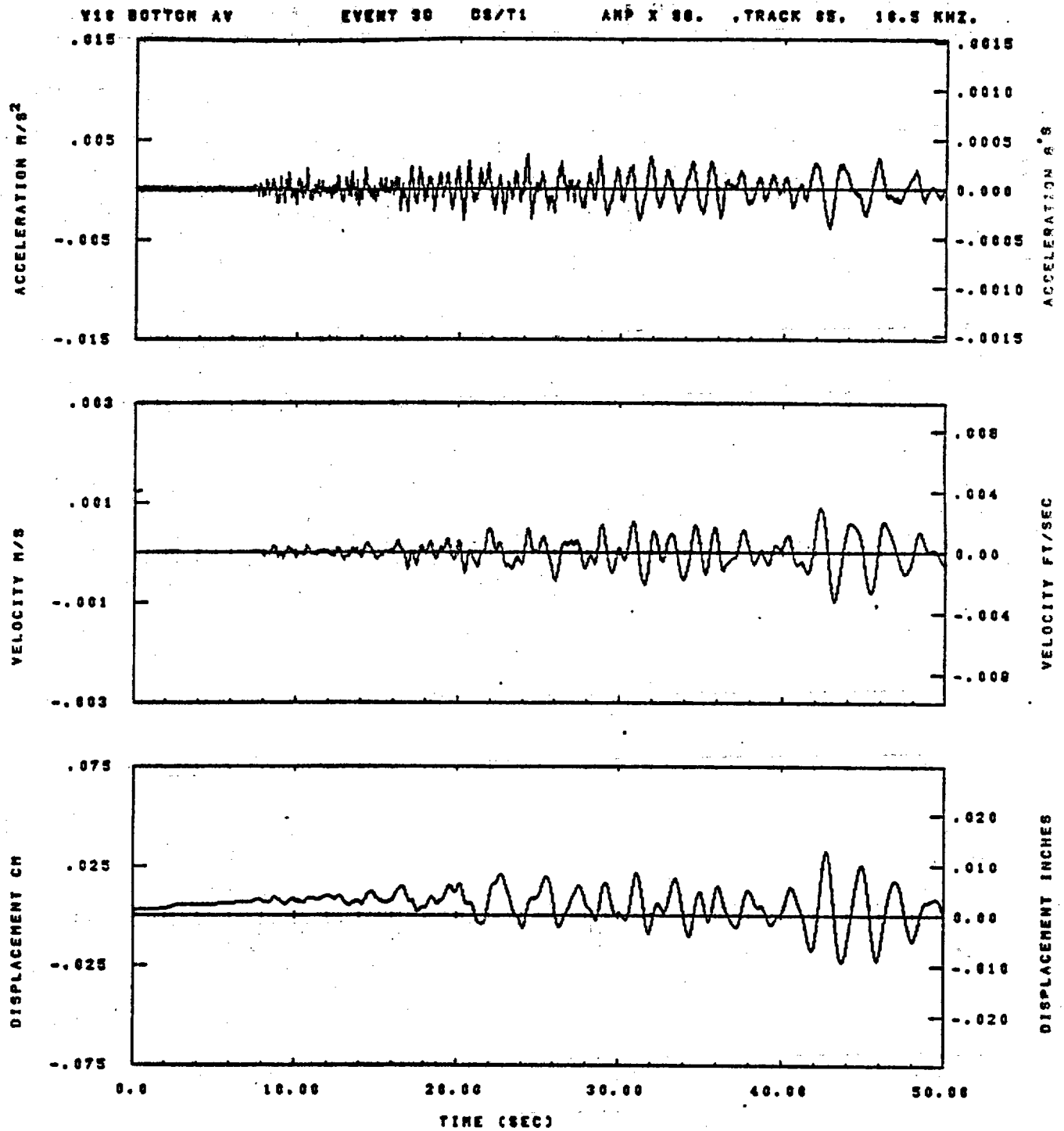
Figure C-58



IDT= .0020	QDT= .0	FIX=	AAS=
HPP= .3	SVH= .20	NLH= 187	ASB=
LPP= 27.	SVL= 8.	NLL= 1339	ASE=
YTS= .30	YTE= .200	PLL=	VSE=
OPS=	OPE=	PLH= 0	OSE= 0.

10.19.05.

07/01/92

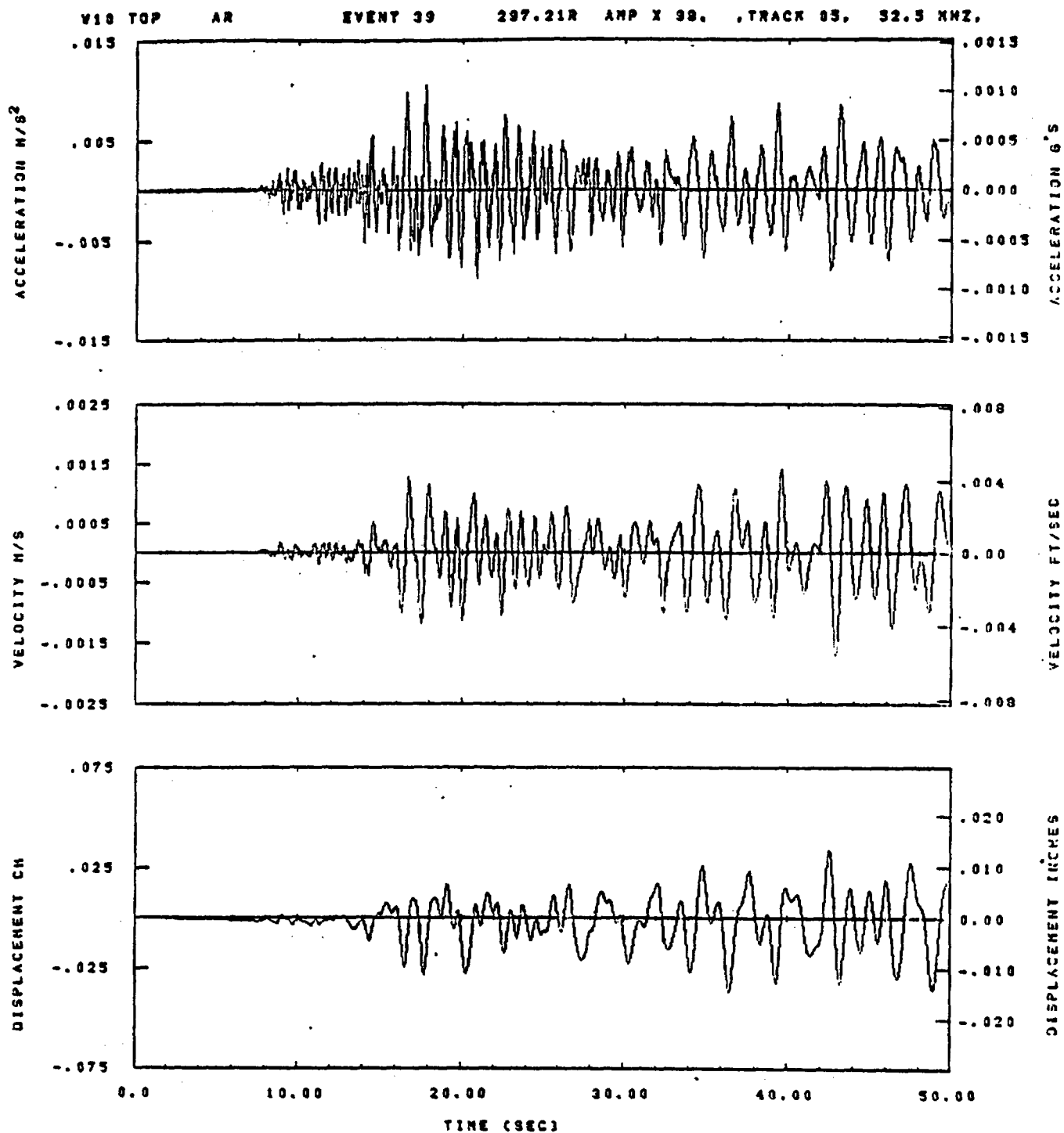


IDT= .0020	QDT= .005	FIX=	AAS= 0.
HFF= .30	BYH= .20	HLH= 100	ASB=
LFF= 22.	BYL= 5.	HLL= 1000	ASE=
VTS= .300	VTE= .200	FLL= -20.	VSE= 0.
DPS= 0.	DPE= 100.	FLH= 0	DSE= 0.

10.10.25.

07/01/82

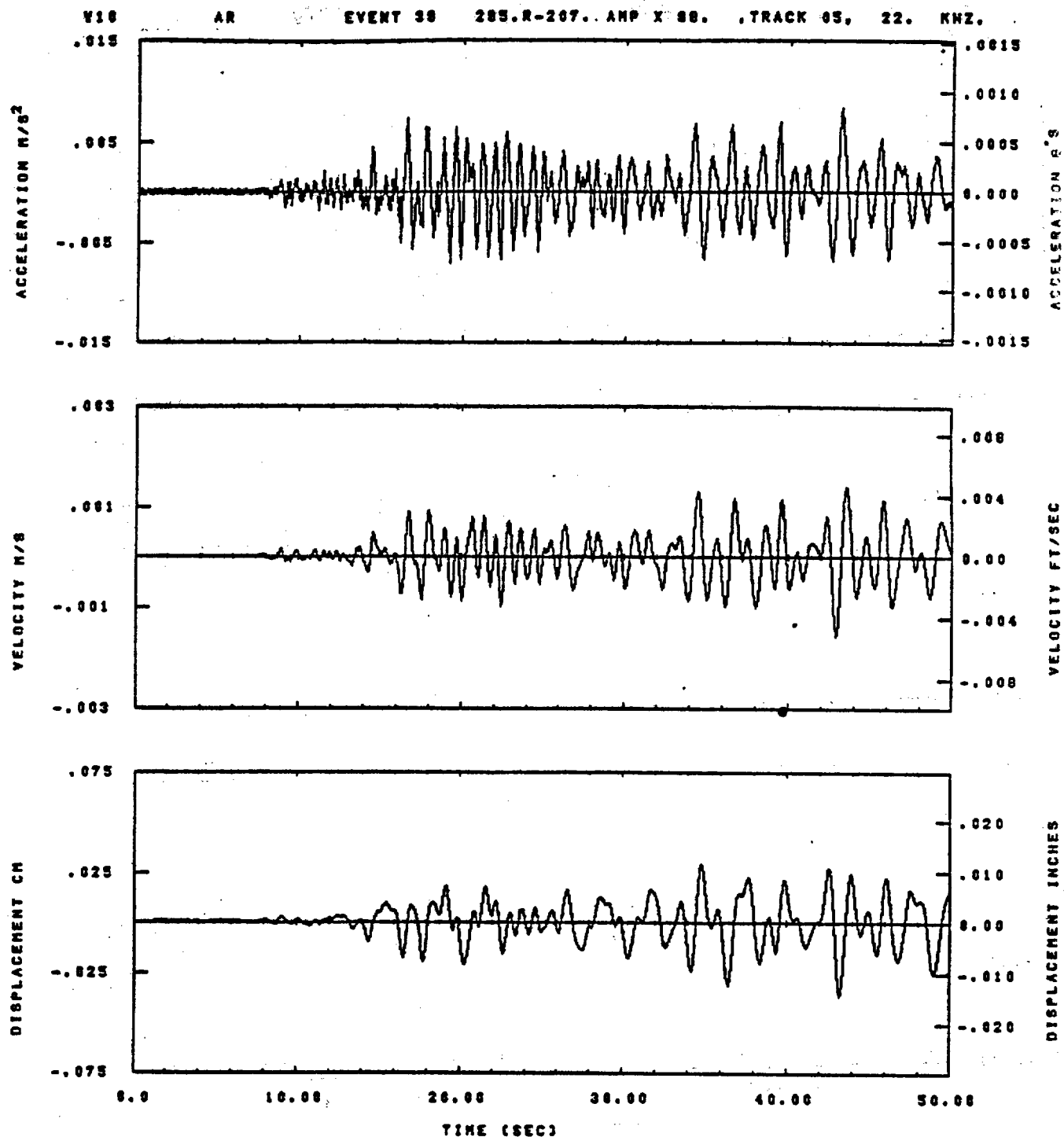
Figure C-60



IDT= .0020	ODT= .005	FIX=	AAS= 0.
HPP= .30	BYH= .20	HLH= 199	ASD=
LPP= 22.	BYL= 5.	HLL= 1999	ASE=
YTB= .300	YTE= .200	FLL= -20.	VSE= 0.
OPS= 0.	OPE= 100.	FLH= 0	QSE= 0.

11.58.32

08/11/92



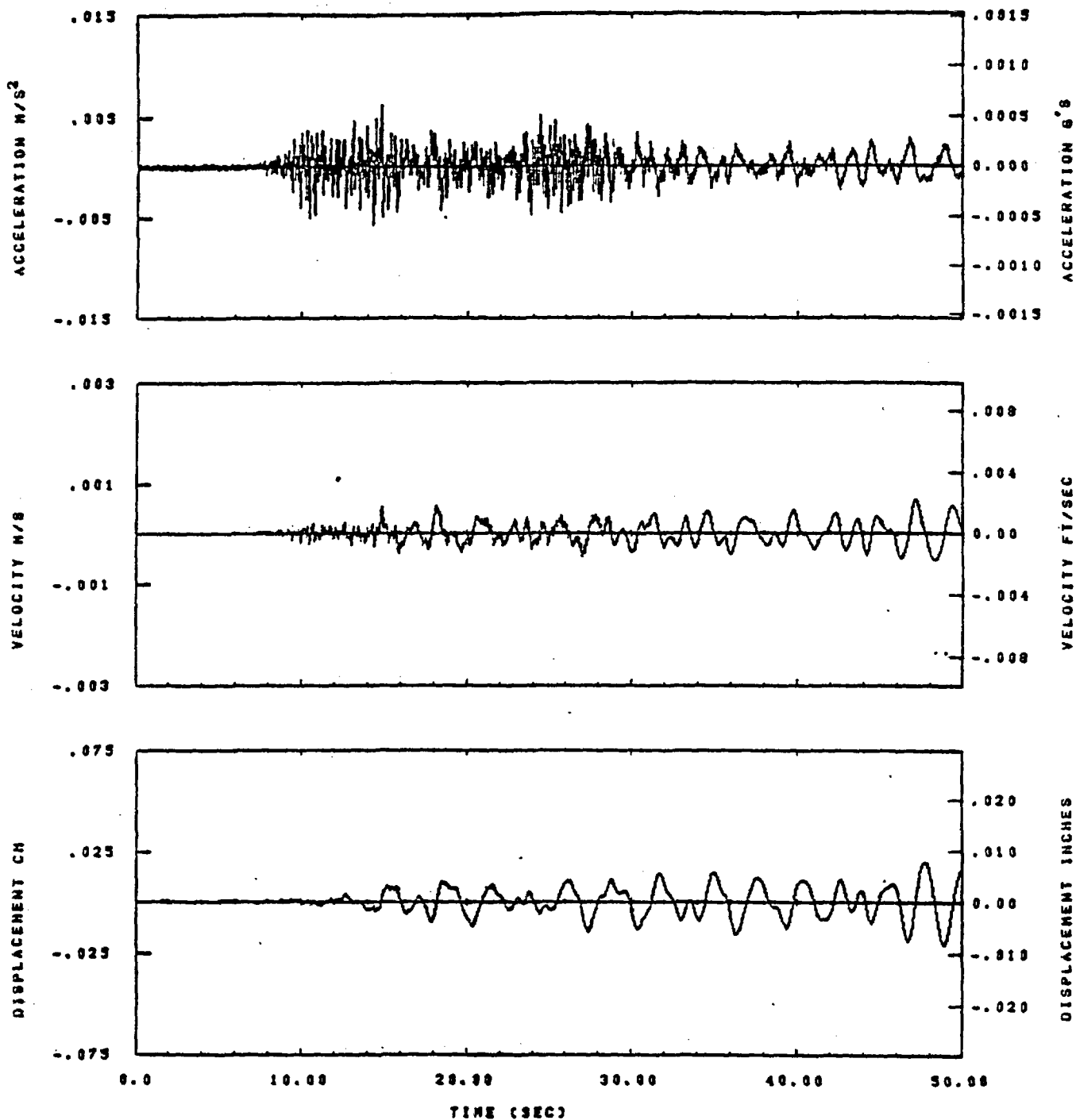
IDT=	.0020	QDT=	.0	FIX=		AAS=	
HPF=	.3	SVH=	.20	NLM=	187	ASB=	
LPF=	27.	SVL=	6.	NLL=	1888	ASE=	
VTS=	.38	VTE=	.208	FLL=		VSE=	
DPS=		DPE=		FLH=	0	DSE=	0.

10.18.00.

07/01/82

Figure C-62

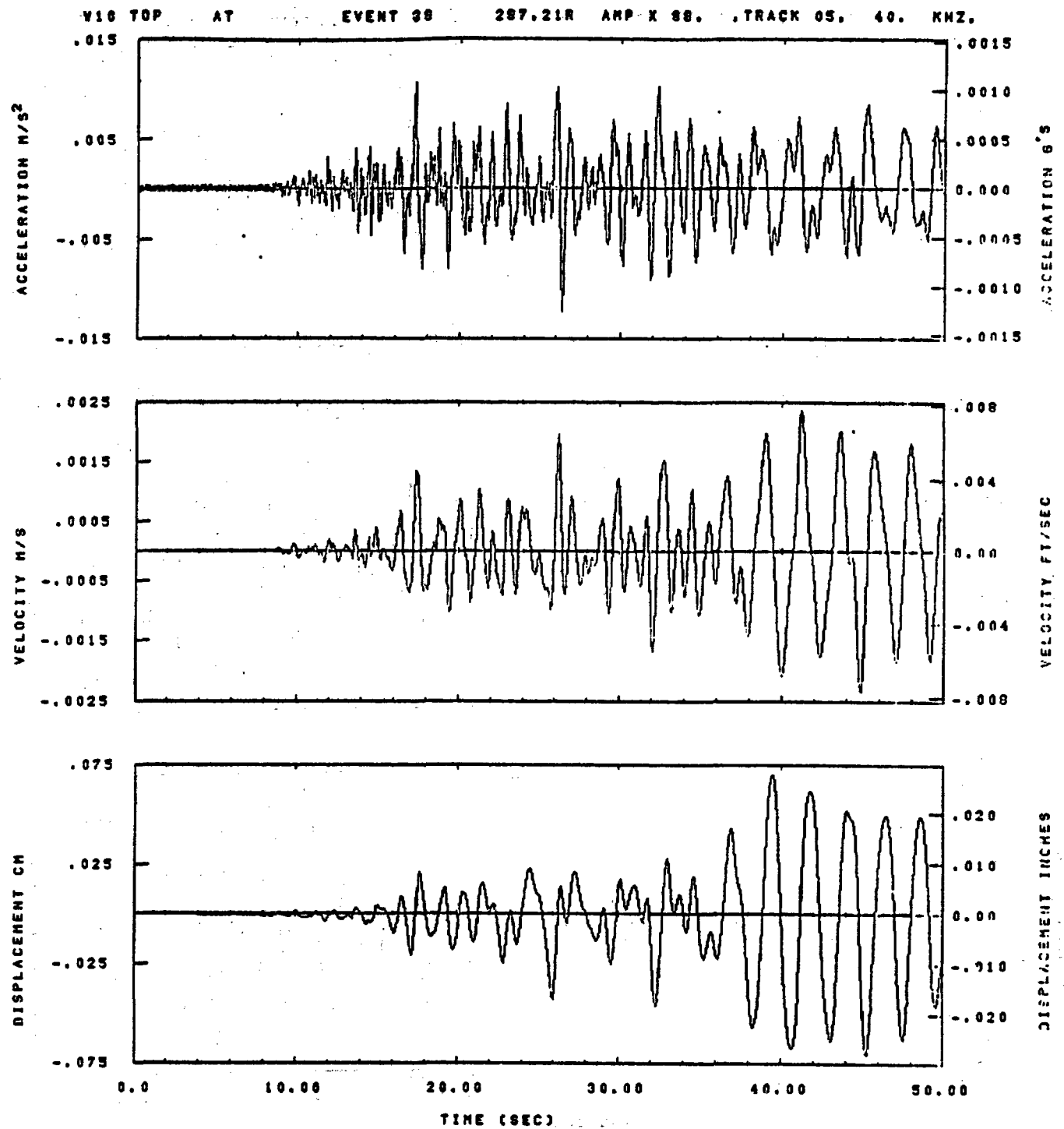
Y18 BOTTOM AR EVENT 38 72.R-287..AMP X 98. .TRACK 03. 7.35 KHZ.



IDT= .0020	OST= .0	FIX=	AAS=
HPF= .3	SVH= .20	HLH= 187	ASB=
LPF= 27.	BVL= 8.	HLL= 1999	ASE=
VTB= .38	VTE= .288	PLL=	VSE=
DPS=	DPE=	PLH= 0	DSE= 0.

18.19.17.

07/01/82

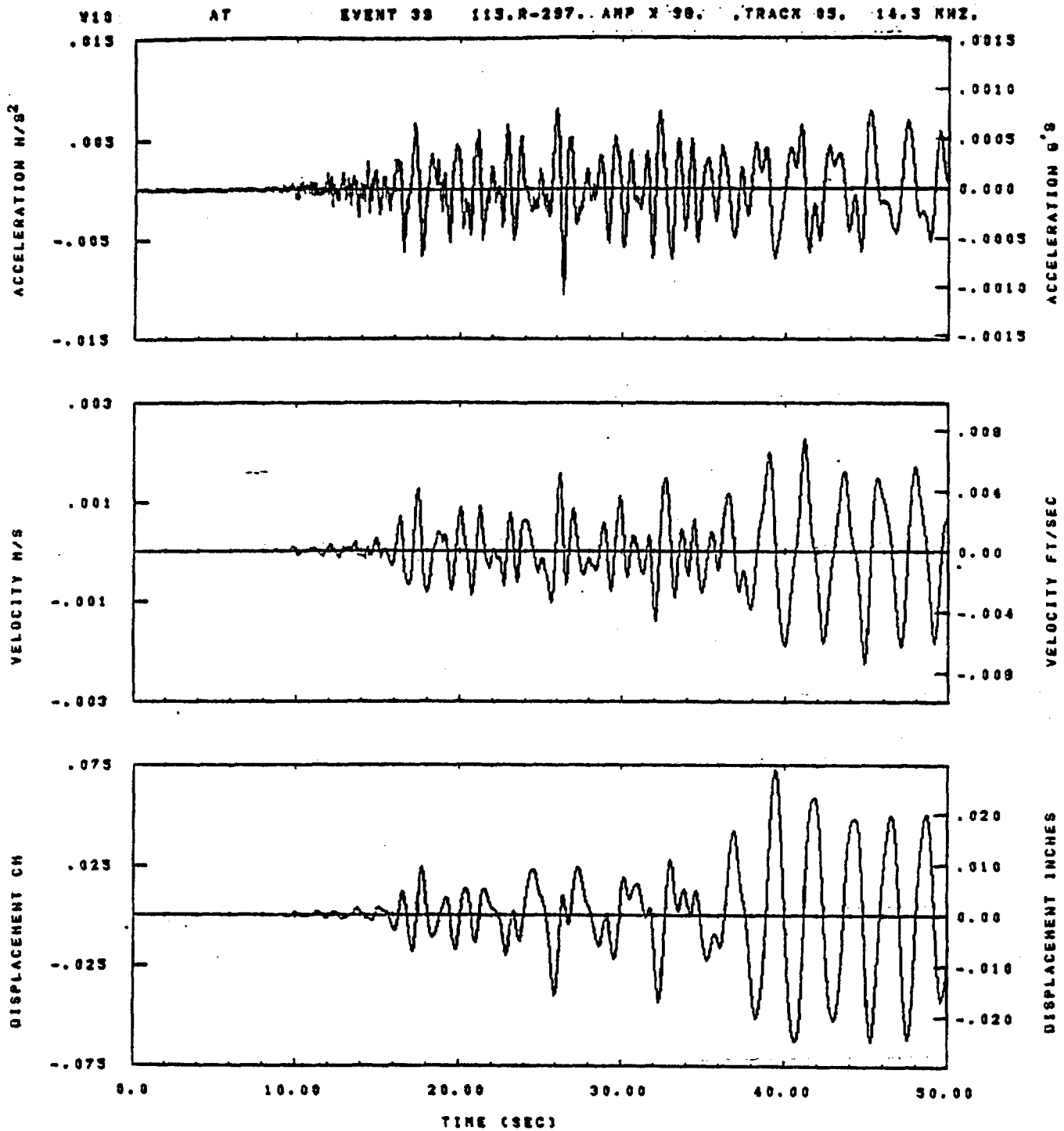


IDT= .0020	ODT= .005	FIX=	AAS= 0.
HPF= .30	BWH= .20	HLH= 199	ASD=
LPF= 22.	BYL= 5.	HLL= 1999	ASE=
VTS= .300	VTE= .200	FLL= -20.	VSE= 0.
DPS= 0.	DPE= 100.	FLH= 0	DSE= 0.

11.56.58

08/11/82

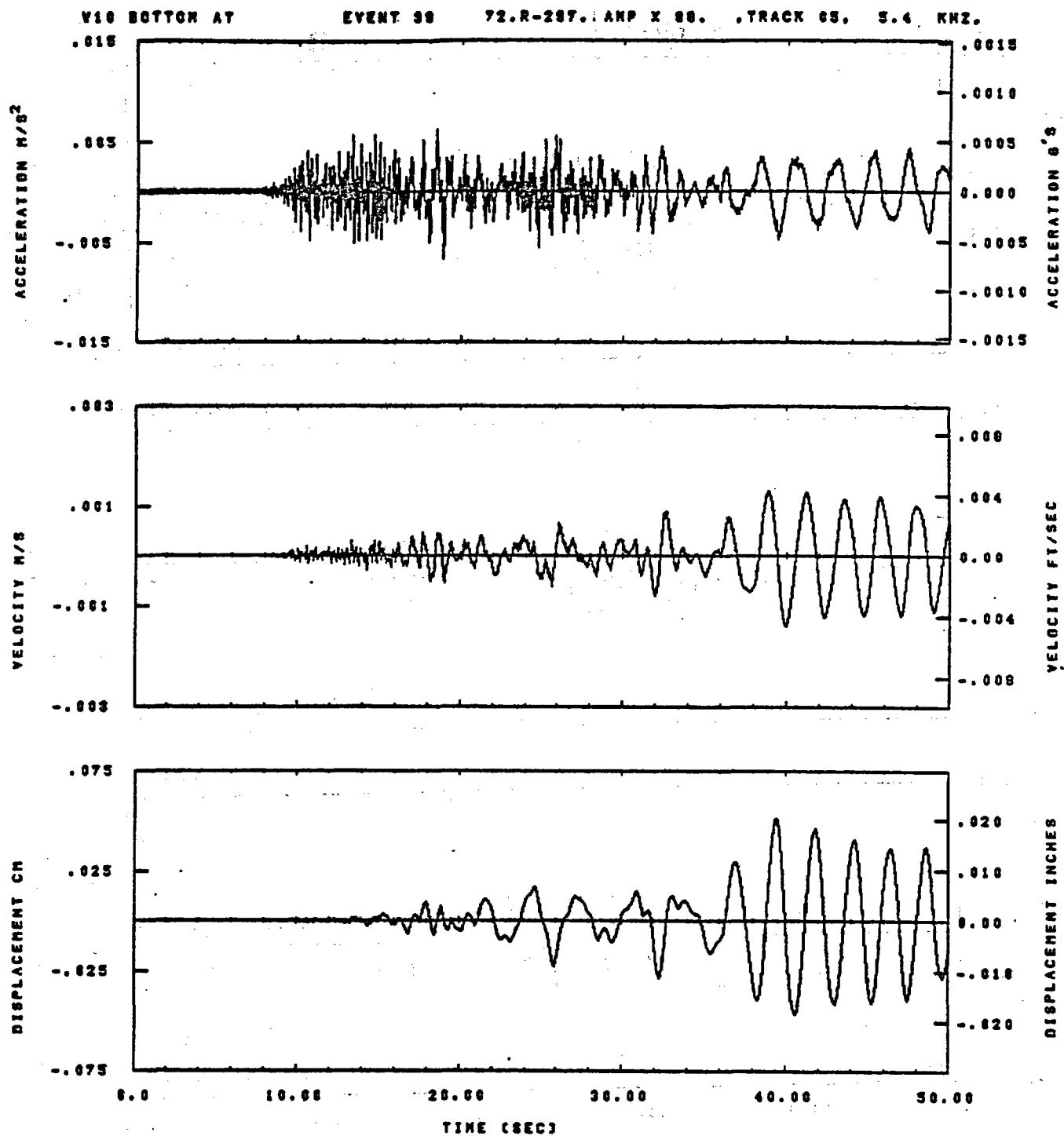
Figure C-64



IDT= .0020	ODT= .0	FIX=	AAS=
HPP= .3	BYN= .20	HLN= 187	ASB=
LPP= 27.	BVL= 8.	HLL= 1999	ASE=
VTS= .30	VTE= .200	FLL=	VSE=
OPS=	OPE=	FLH= 0	DSE= 0.

10.13.13.

07/01/82

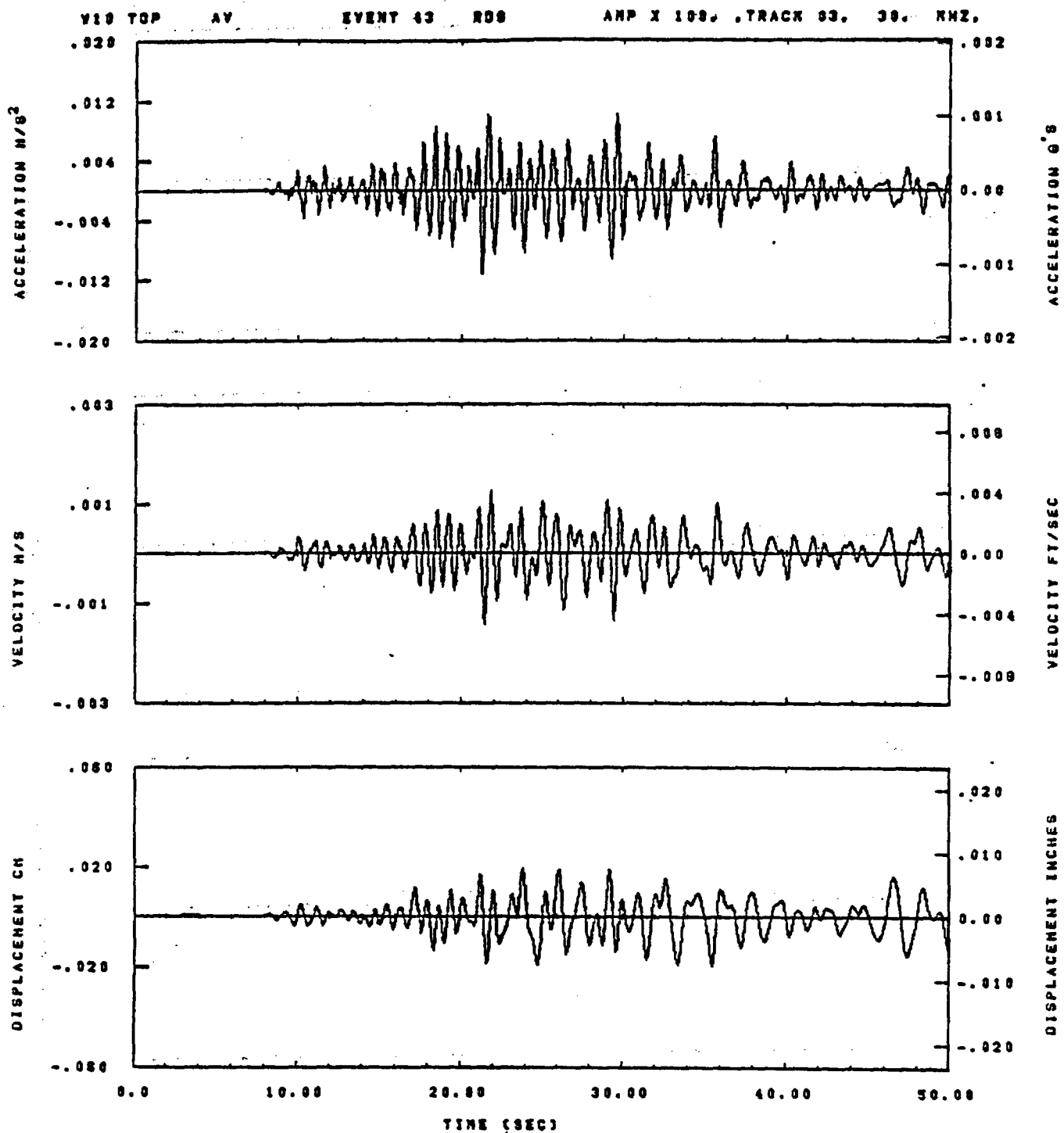


IDT= .0020	ODT= .0	FIX=	AAS=
HPF= .3	SVN= .20	MLN= 167	ASB=
LPF= 27.	SVL= 6.	MLL= 1988	ASE=
VTS= .36	VTE= .200	FLL=	VSE=
DPS=	DPE=	FLN= 0	DSE= 6.

10.18.26.

07/01/82

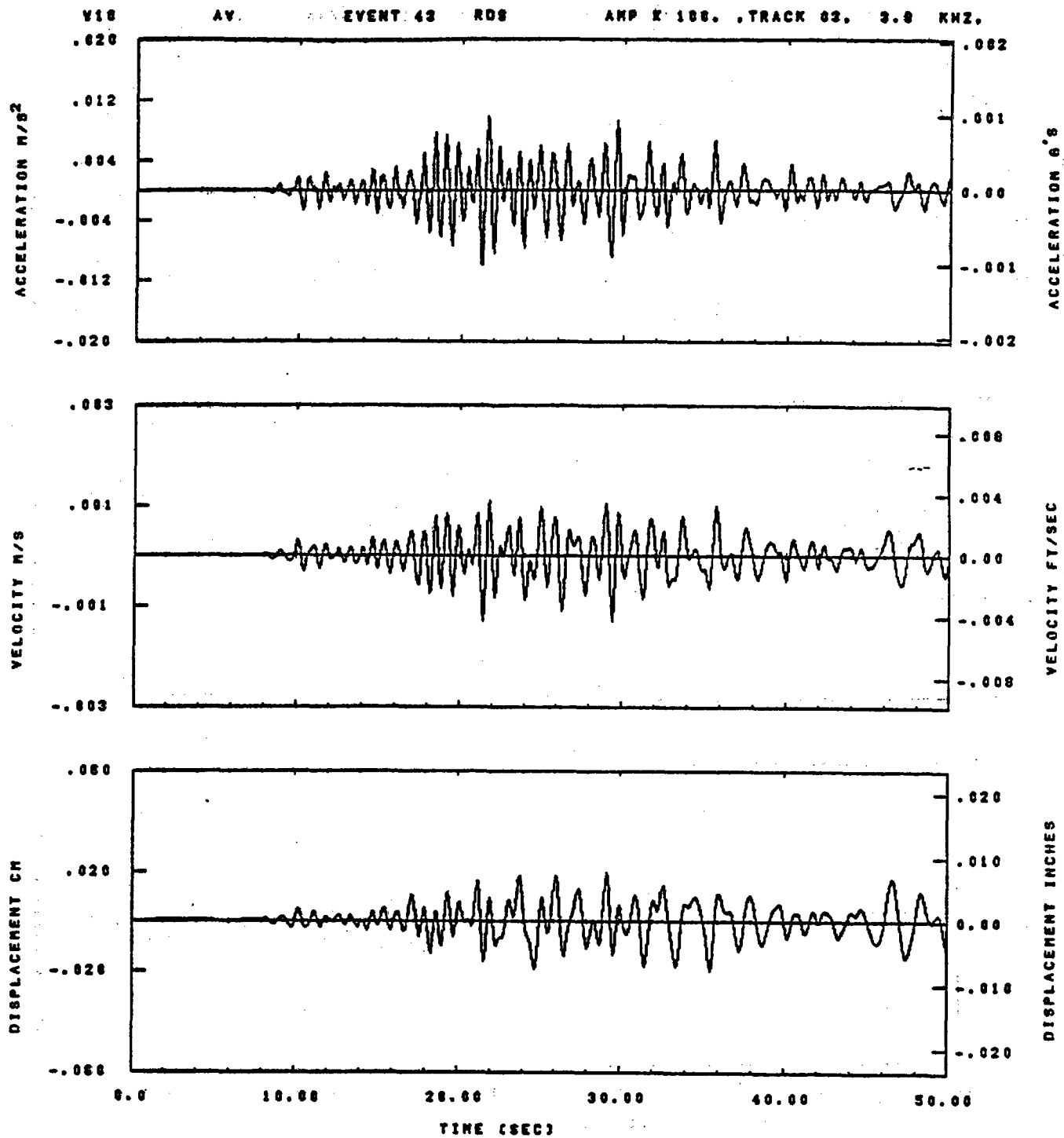
Figure C-66



IDT= .0020	ODT= .003	FIX=	AAS= 0.
HPF= .20	BYH= .13	HLH= 417	ASS=
LPF= 10.	BYL= 2.	HLL= 2999	ASE=
VTB= .200	VTE= .133	FLL= -20.	VSE= 0.
DPS= 0.	DPE= 100.	FLH= 0	DSE= 0.

14.11.24.

08/23/02

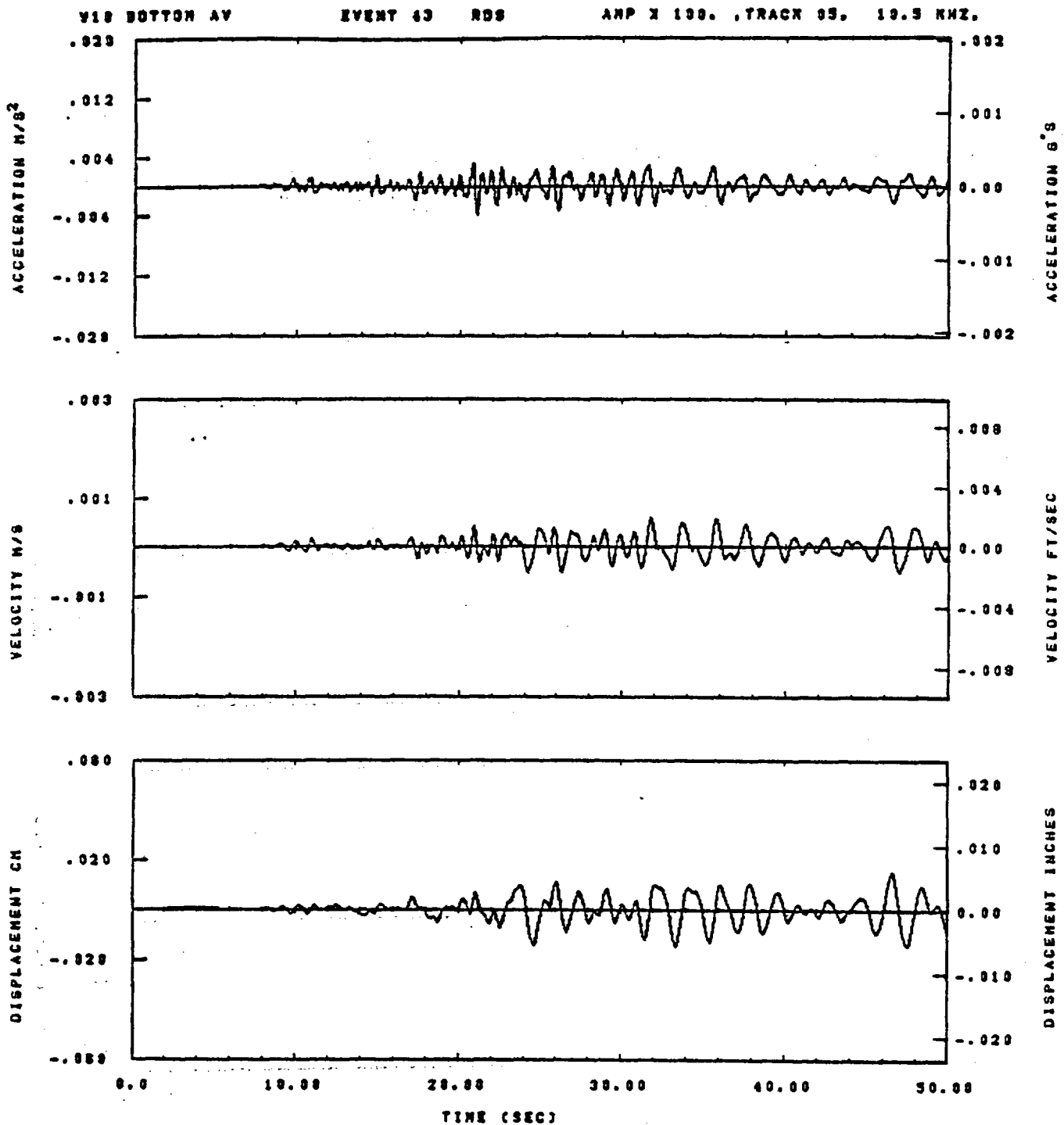


IDT= .0020	QDT= .005	FIX=	AAS= 0.
HFF= .20	SVN= .13	HLN= 417	ASB=
LFF= 10.	SVL= 2.	HLL= 2988	ASE=
VTS= .200	VTE= .133	FLL= -20.	VSE= 0.
DPS= 0.	DPE= 100.	FLH= 0	DSE= 0.

14.11.46.

06/23/82

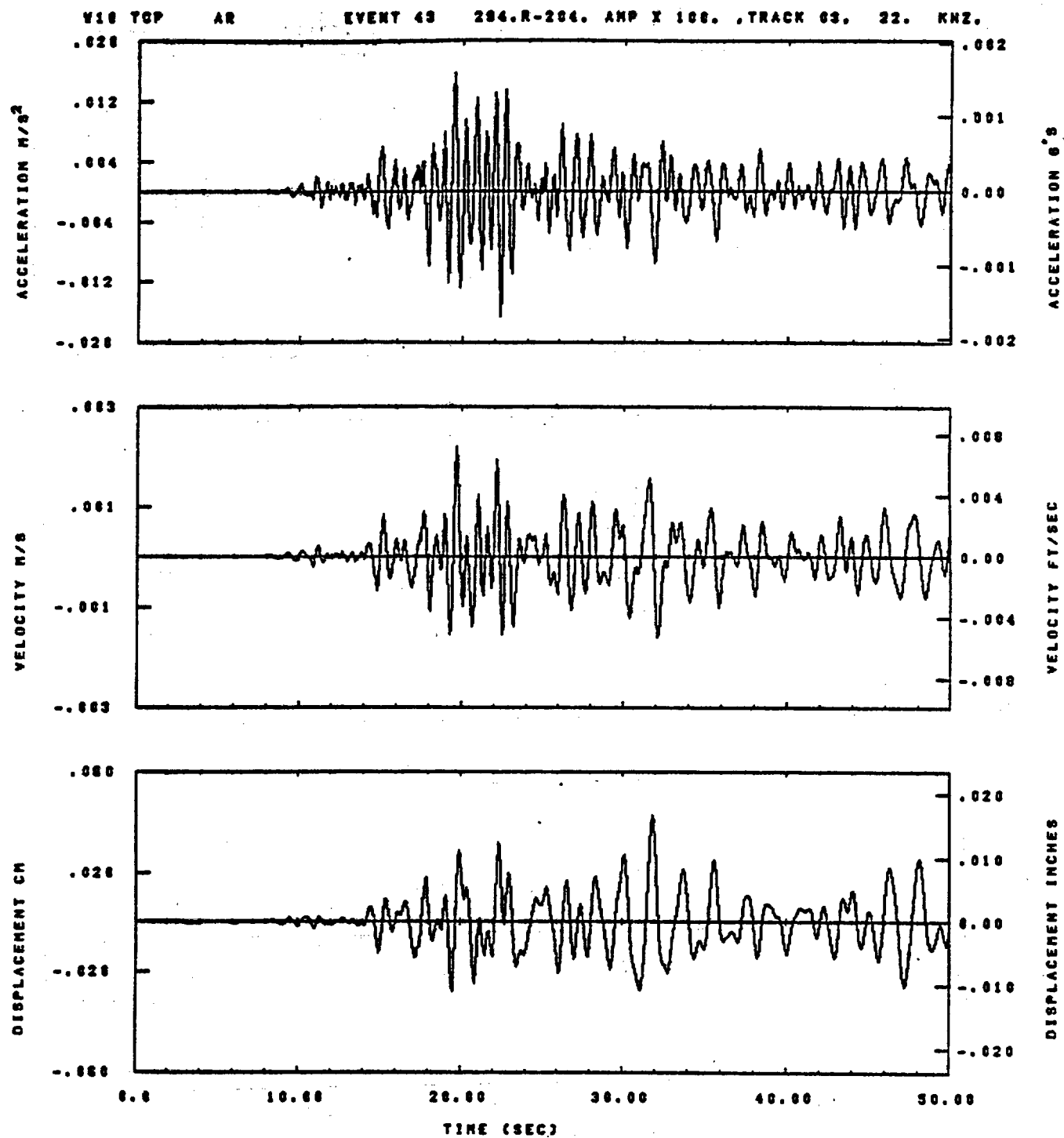
Figure C-68



IDT= .0020	ODT=	FIX=	AAS= 0.
HPP= .20	BYH= .13	HLN= 417	ASB=
LPP= 10.	BYL= 2.	HLL= 2999	ASE=
VTB= .200	VTE= .133	FLL= -20.	VSE= 0.
OPB= 0.	OPE= 100.	FLH= 0	DSE= 0.

14.13.12.

08/23/92

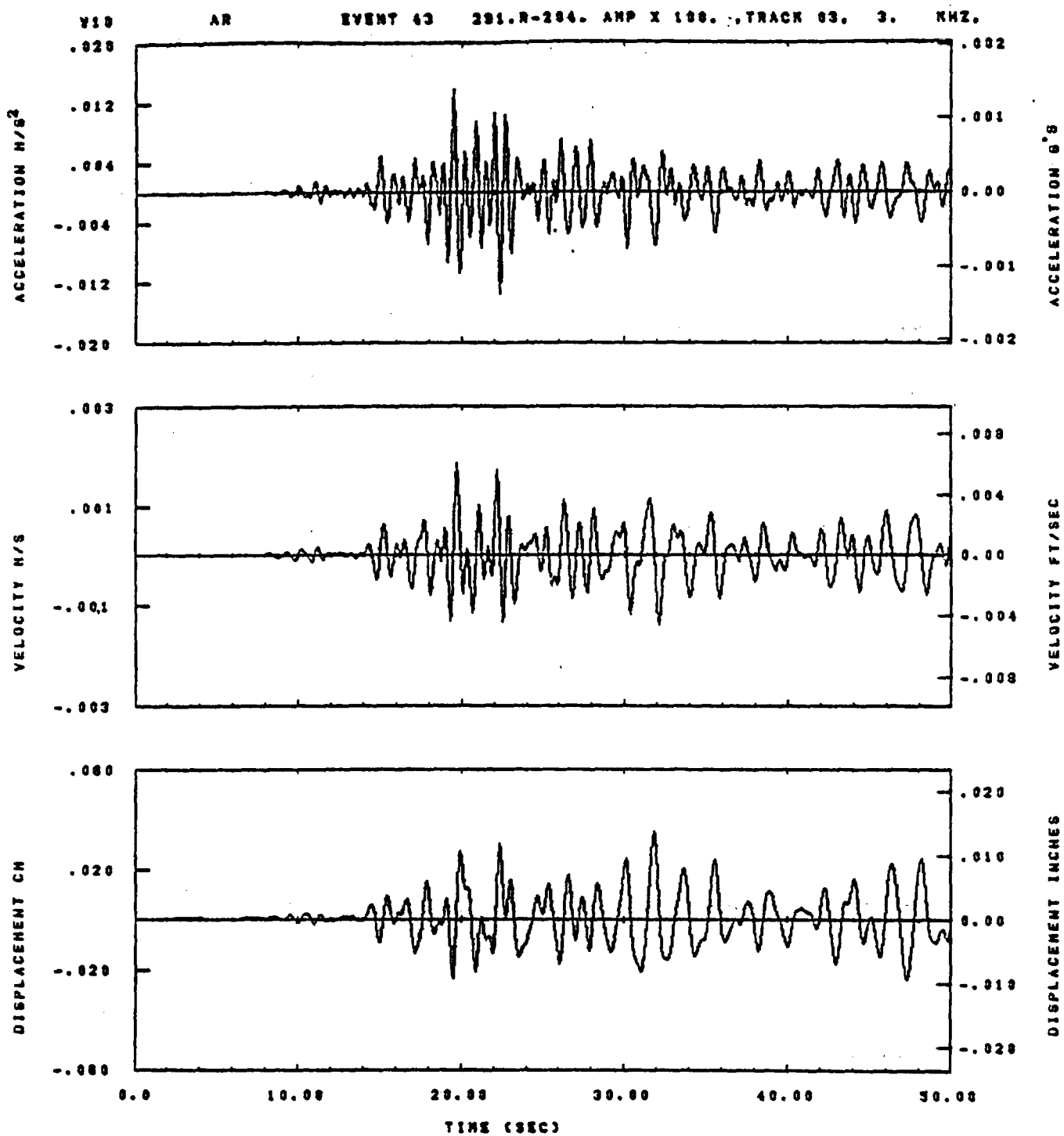


IDT= .0020	QDT= .005	FIX=	AAS= 0.
HPP= .20	BYH= .13	HLH= 417	ASB=
LPP= 10.	BVL= 2.	HLL= 2588	ASE=
VTD= .200	VTE= .133	FLL= -20.	VSE= 0.
DPB= 0.	DPE= 100.	FLH= 0	DSE= 0.

14.11.33.

06/23/82

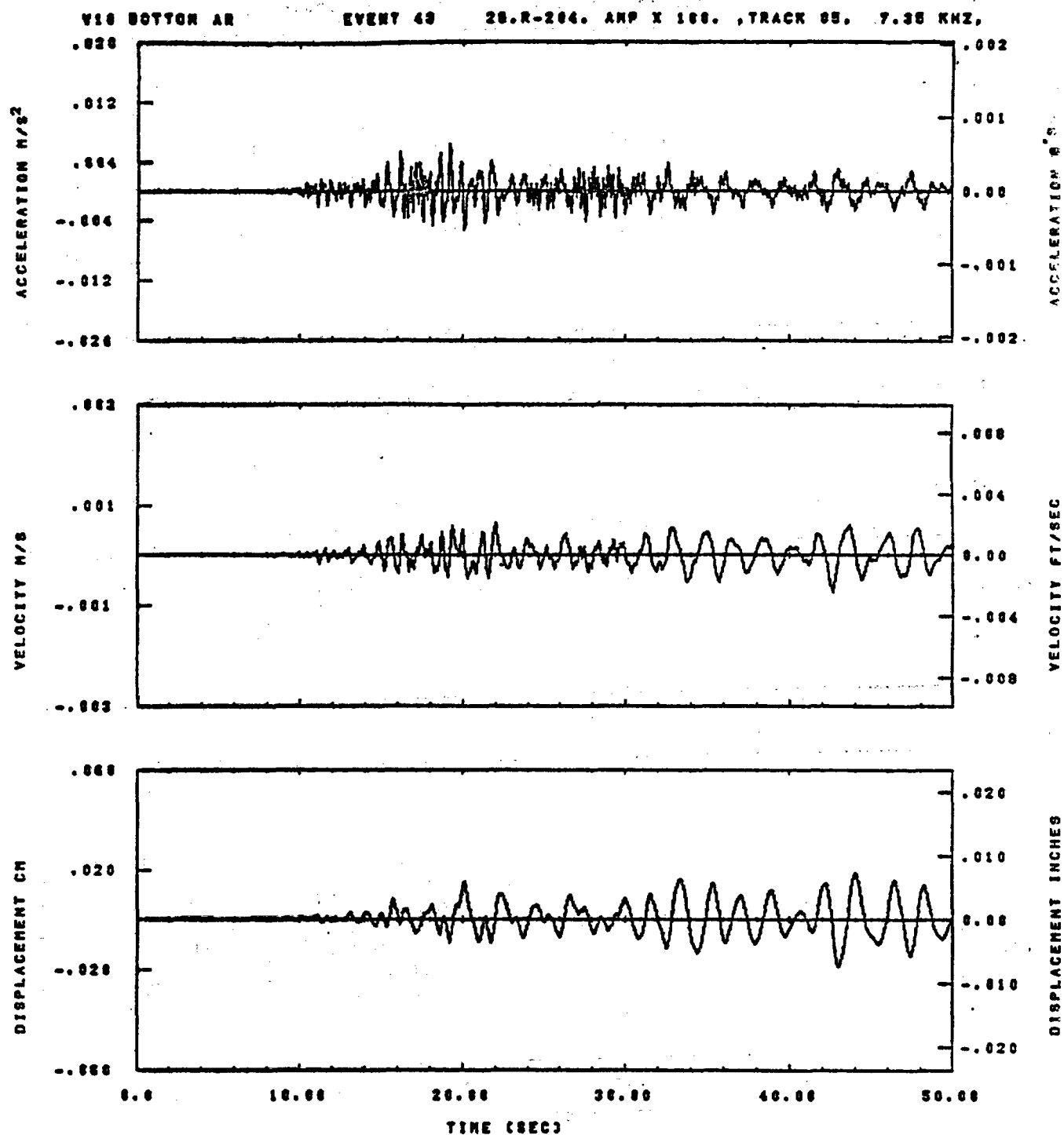
Figure C-70



IDT= .0020	ODT= .003	FIX=	AAS= 0.
HPP= .20	BYH= .13	HLH= 417	ASB=
LPP= 10.	BYL= 2.	HLL= 2999	ASE=
YTB= .200	YTE= .133	PLL= -20.	VSE= 0.
OPS= 0.	OPE= 100.	PLH= 0	OSE= 0.

14.12.68.

06/23/82

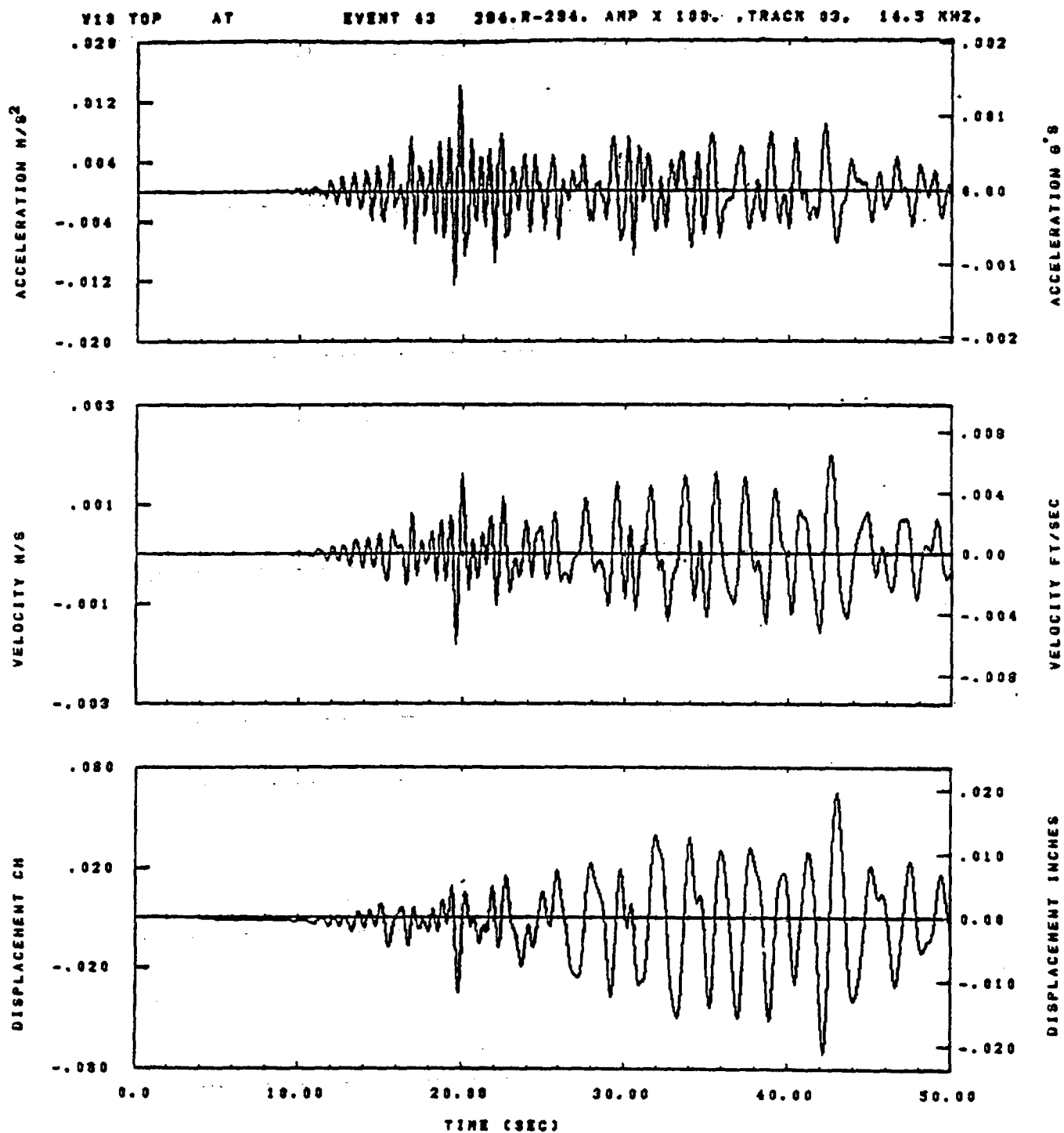


IDT= .0020	QDT=	FIX=	AAS= 0.
HPP= .20	BYH= .13	HLH= 417	ASB=
LPP= 10.	BYL= 2.	HLL= 2000	ASE=
VTS= .200	VTE= .133	FLL= -20.	VSE= 0.
OPS= 0.	BPE= 100.	FLH= 0	DSE= 0.

14.13.38.

06/23/82

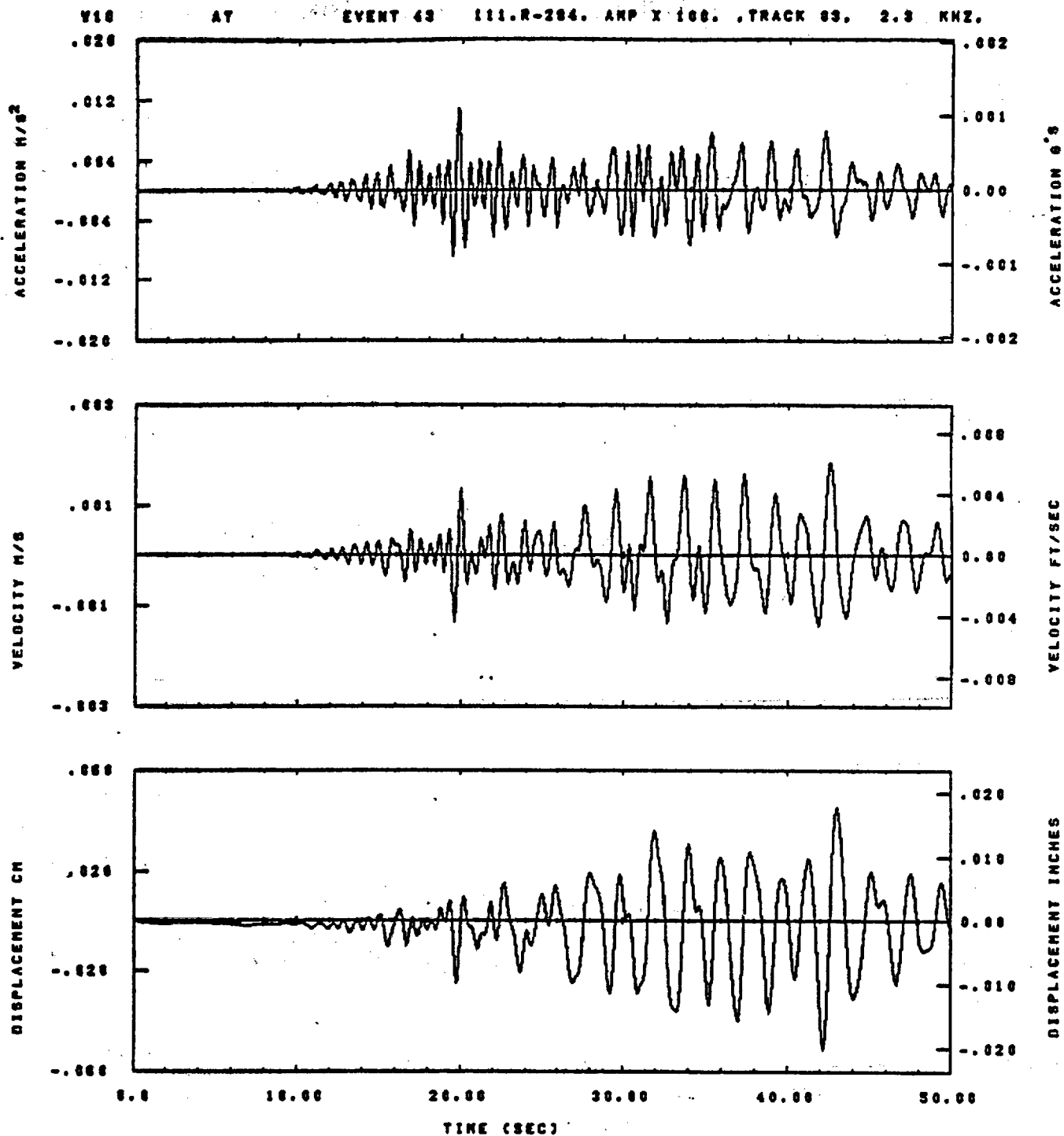
Figure C-72



IDT= .0020	ODT= .003	FIX=	AAS= 0.
HPP= .20	BYH= .13	HLH= 417	ASB=
LPP= 10.	SYL= 2.	HLL= 2999	ASE=
VTB= .200	VTE= .133	FLL= -20.	VSE= 0.
OPS= 0.	OPE= 100.	FLH= 0	DSE= 0.

14.11.39.

08/23/92

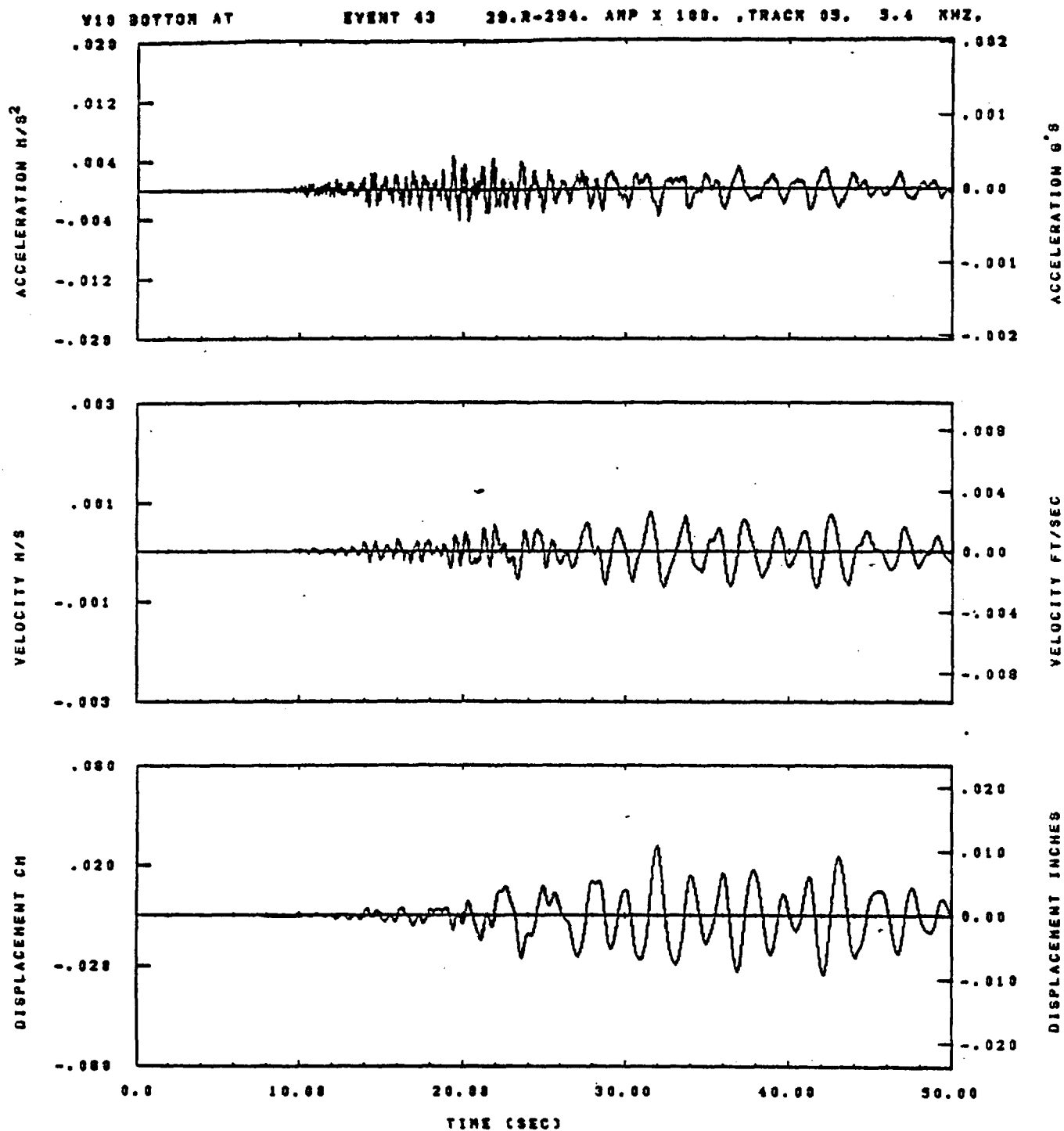


IDT= .0020	QDT= .005	FIX=	AAS= 0.
HPP= .20	BVM= .13	HLH= 417	ASB=
LPP= 10.	BVL= 2.	HLL= 2888	ASE=
YTB= .200	YTE= .193	FLL= -20.	VSE= 0.
DPS= 0.	DPE= 100.	FLH= 0	DSE= 0.

14.13.08.

06/23/82

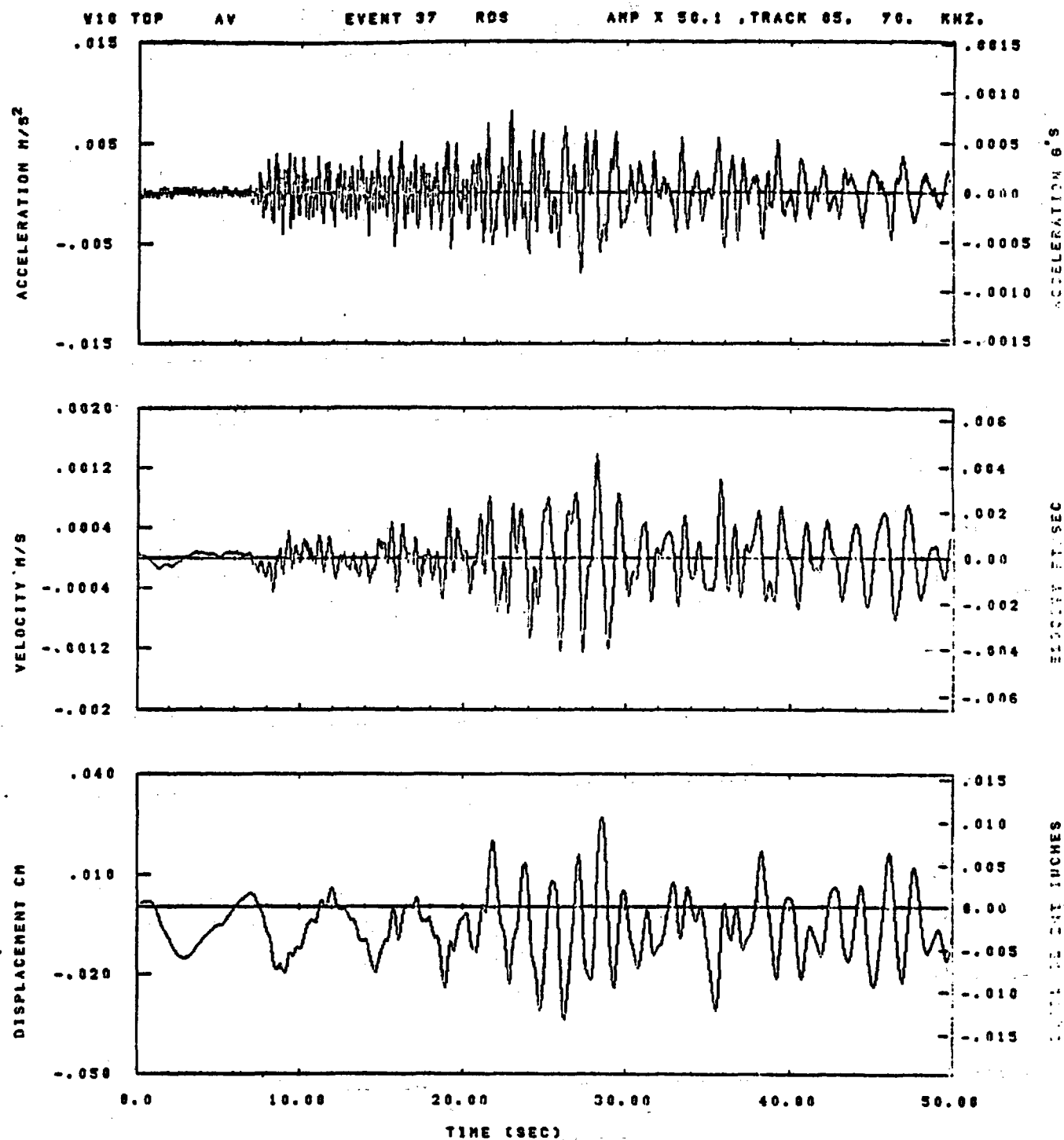
Figure C-74



IDT= .0020	ODT=	FIX=	AAS= 0.
HPP= .20	BYH= .13	HLH= 417	ASB=
LPP= 10.	BYL= 2.	HLL= 2999	ASE=
VTS= .200	VTE= .133	FLL= -20.	VSE= 0.
DPS= 0.	DPE= 100.	FLH= 0	DSE= 0.

14.13.33.

08/23/82

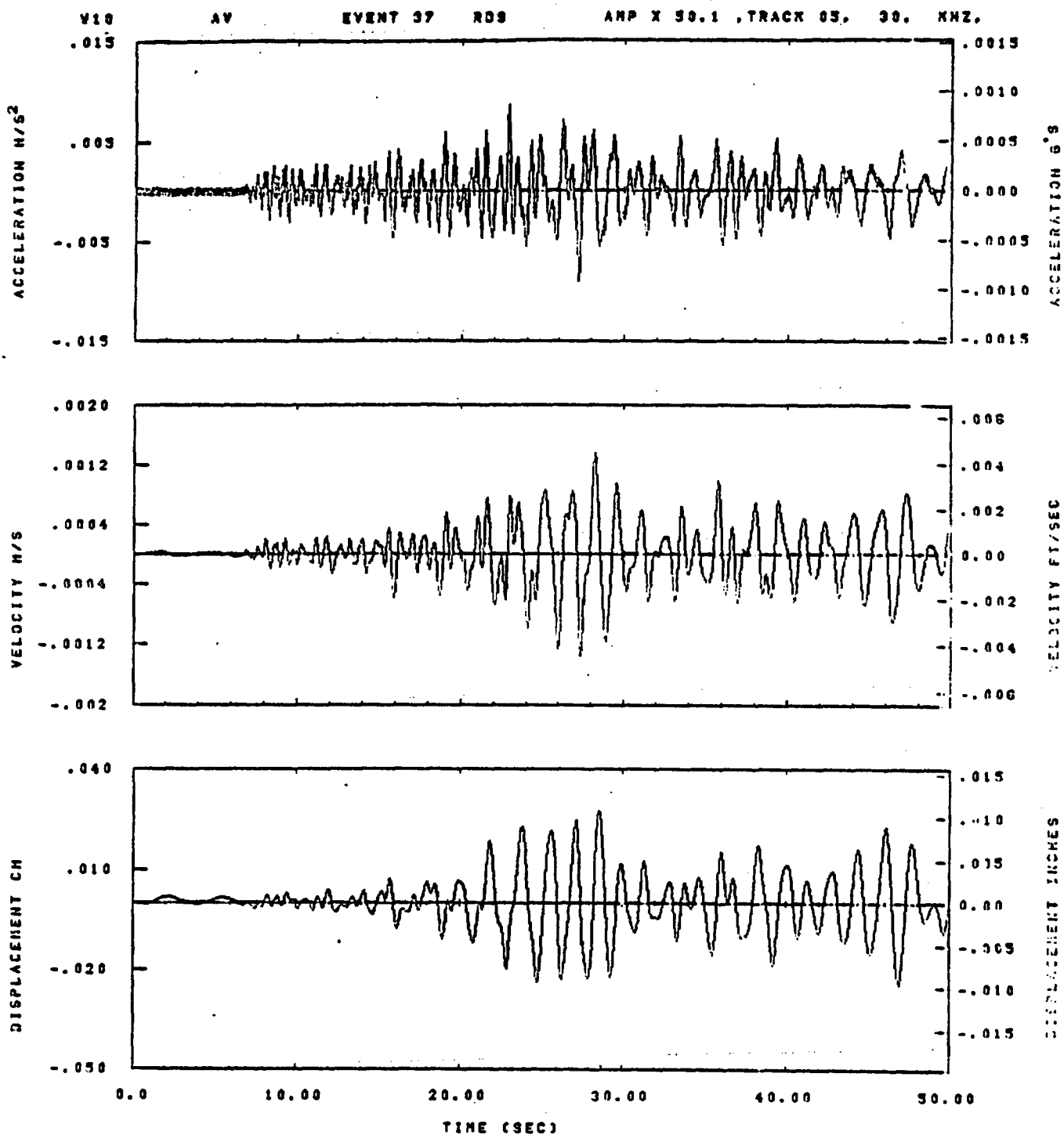


IDT= .0020	ODT= .005	FIX=	AAS= 0.
HPP= .20	BYH= .13	HLH= 249	ASD=
LPP= 18.	BYL= 4.	HLL= 2000	ASE=
VTB= .200	VTE= .133	FLL= -20.	VSE= 0.
DPS= 0.	DPE= 100.	FLH= 0	DSE= 0.

14.58.37

06/11/82

Figure C-76

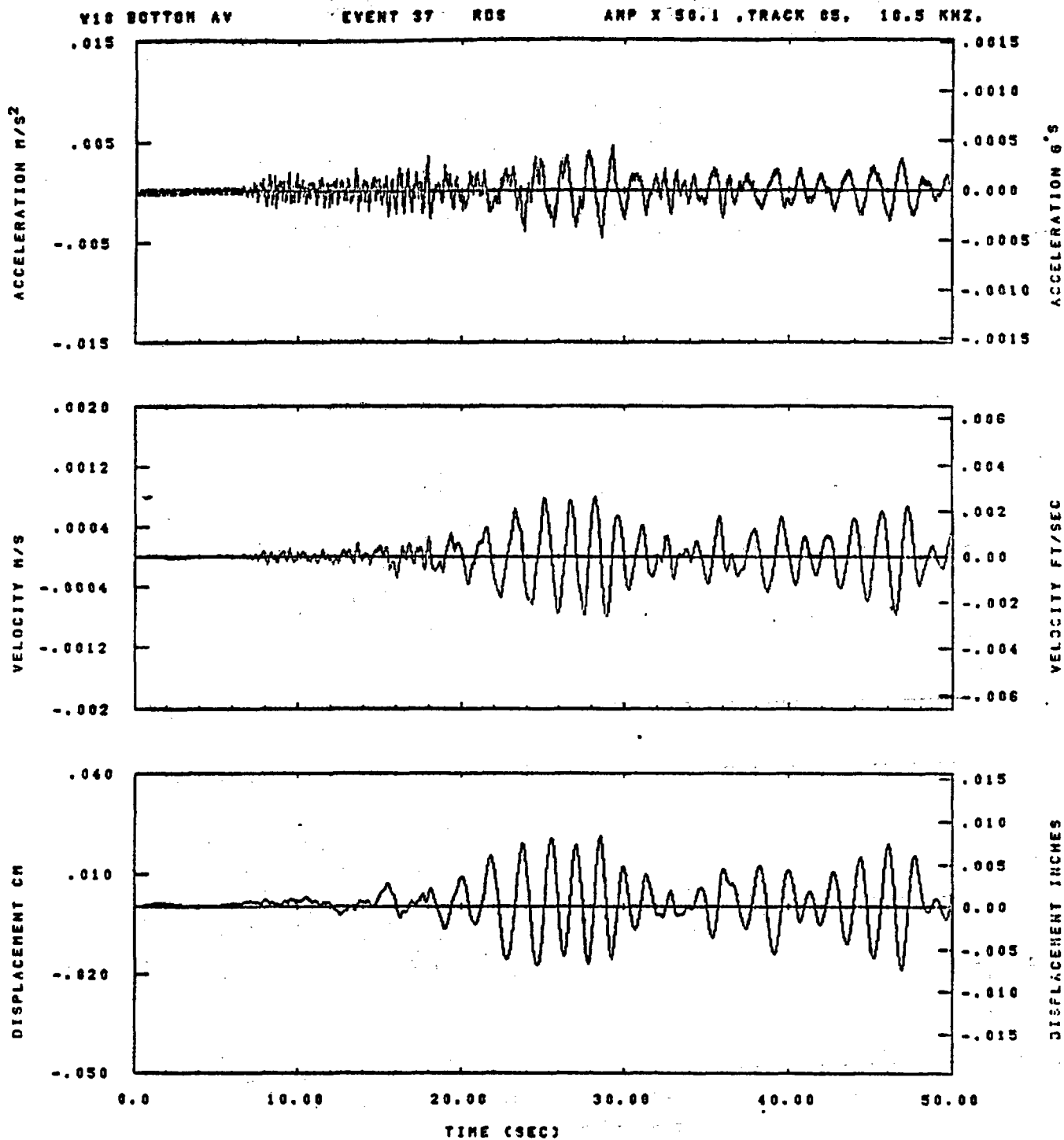


IDT= .0020	ODT=	FIX=	AAS= 0.
HPP= .30	BYN= .20	HLH= 167	ASD=
LPP= 27.	BYL= 6.	HLL= 1000	ASE=
YTB= .300	VTE= .200	FLL= -20.	VSE= 0.
GPB= 0.	DPE= 100.	FLH= 0	DSE= 0.

14.59.50

08/11/82

Figure C-77



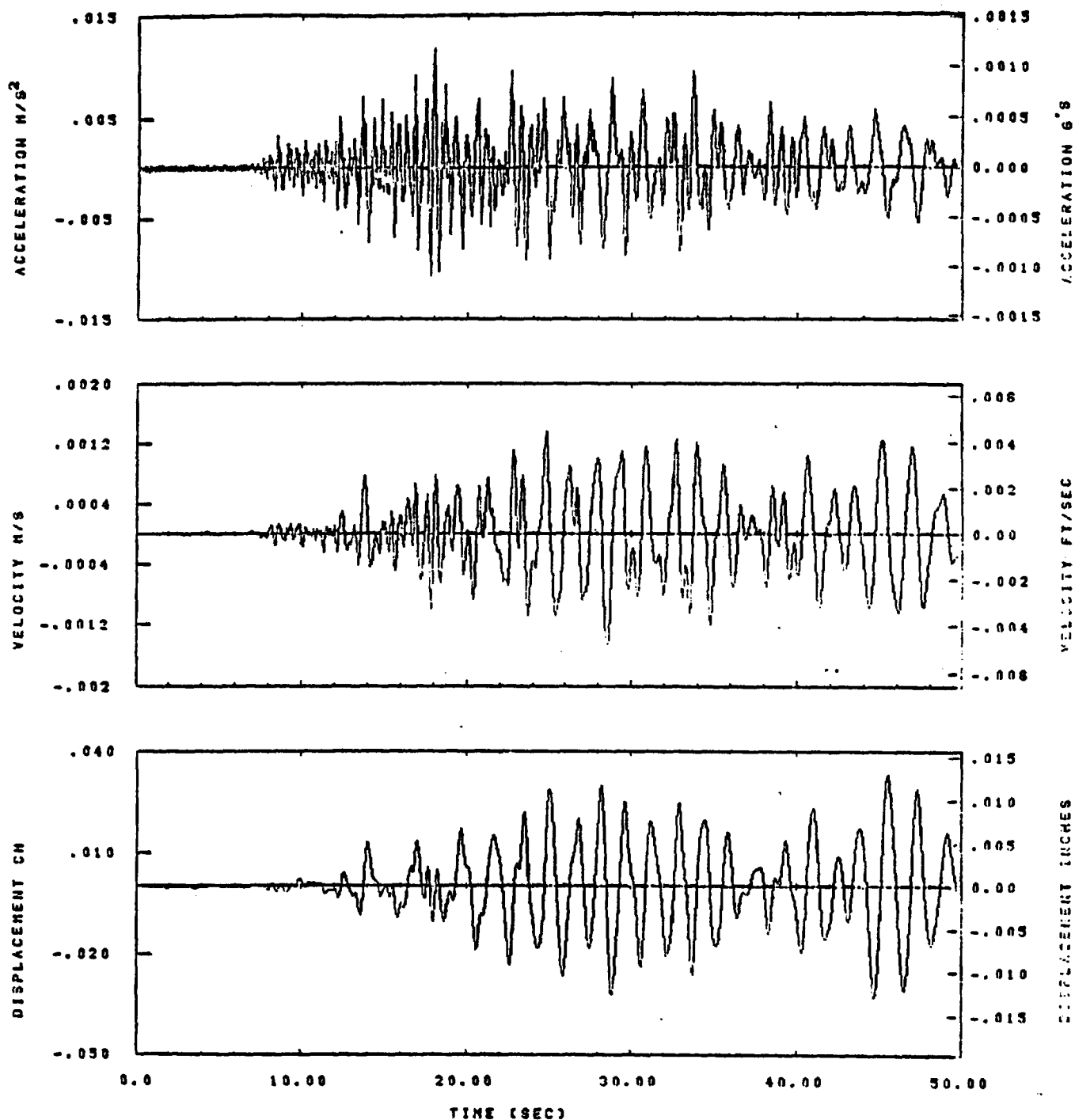
IDT= .0020	QDT= .0005	FIX=	AAS= 0.
HFF= .20	BYH= .13	HLH= 249	ASR=
LFF= 18.	SVL= 4.	HLL= 2999	ASE=
VTB= .200	VTE= .133	FLL= -20.	VSE= 0.
DPB= 0.	DPE= 100.	FLH= 8	DSE= 0.

14.58.24

06/11/82

Figure C-78

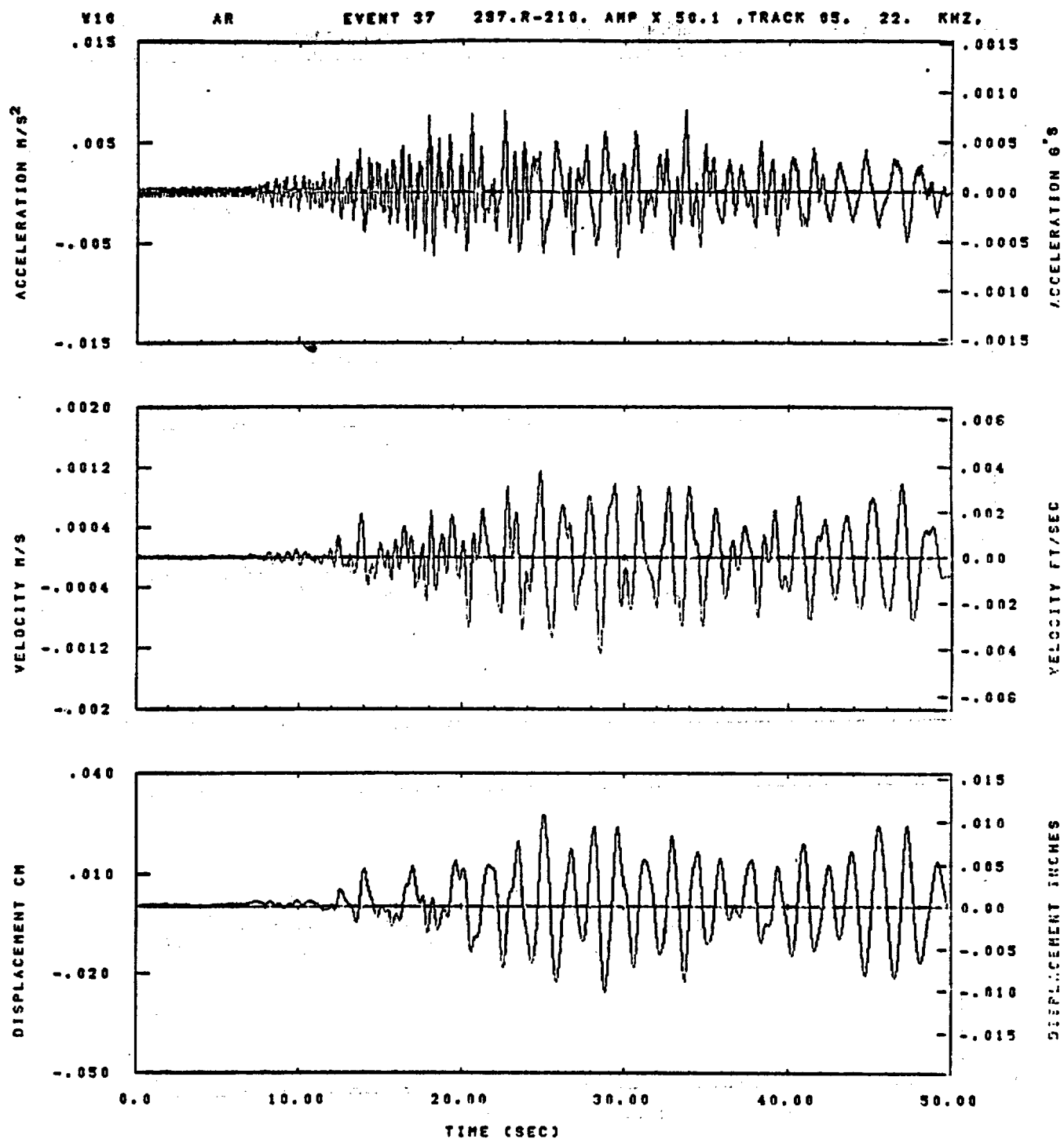
V18 TOP AR EVENT 37 388.R-218. AMP X 50.1 ,TRACK 03, 52.3 KHZ.



IDT= .0020	ODT=	FIX=	AAS= 0.
HPP= .30	OVN= .20	HLH= 107	ASB=
LPP= 27.	SVL= 6.	HLL= 1930	AGE=
VTB= .300	VTE= .200	FLL= -20.	VSE= 0.
DPB= 0.	DPE= 100.	FLH= 0	DSE= 0.

14.59.41

06/11/82



IDT= .0020	ODT= .005	FIX=	AAS= 0.
HPP= .20	OVH= .13	HLH= 249	ASD=
LPP= 18.	OVL= 4.	HLL= 2909	ASE=
VTS= .200	VTE= .133	FLL= -20.	VSE= 0.
DPS= 0.	DPE= 180.	FLH= 0	DSE= 0.

14.58.53

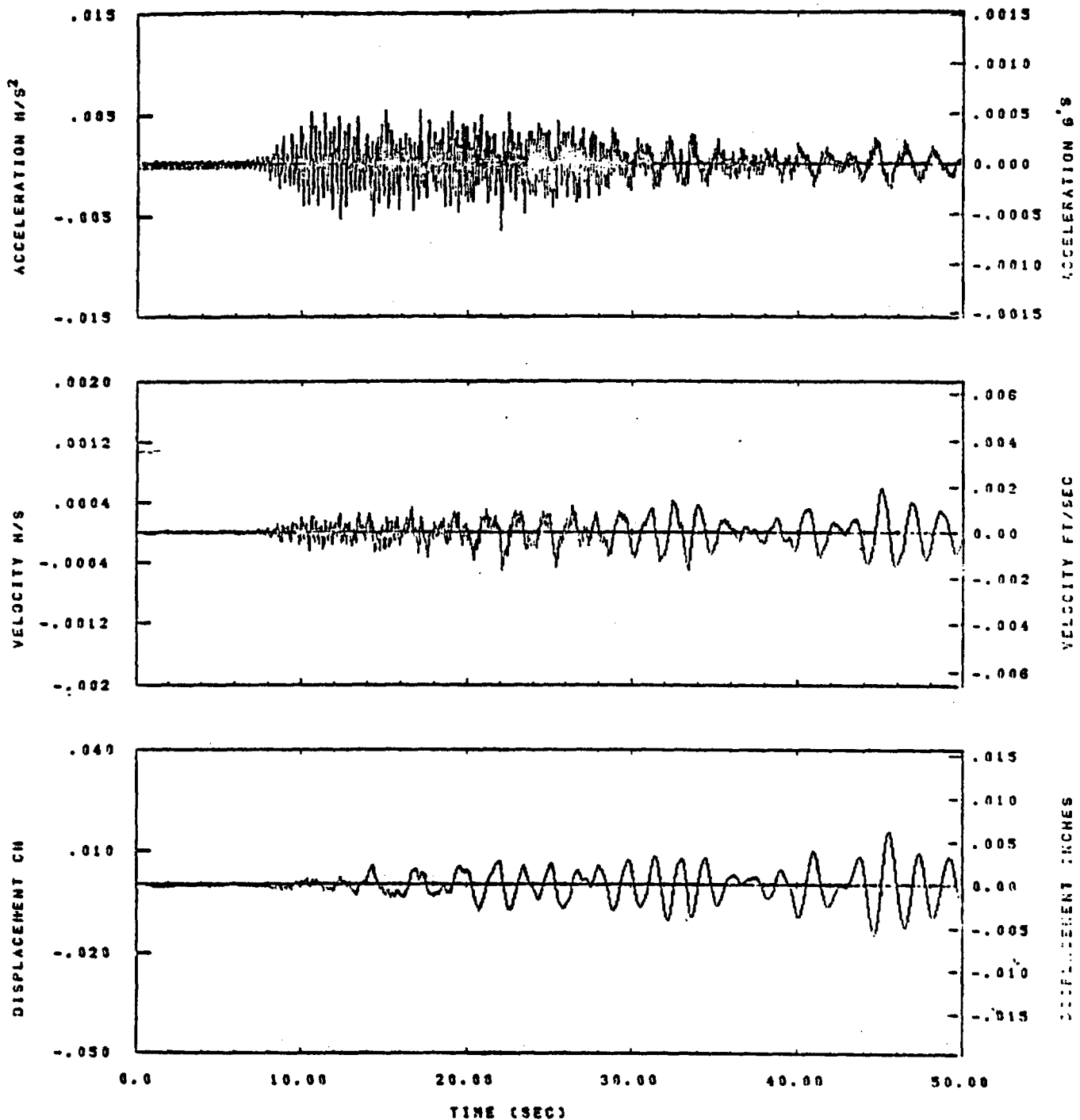
06/11/82

Figure C-80

V10 BOTTOM AN

EVENT 37

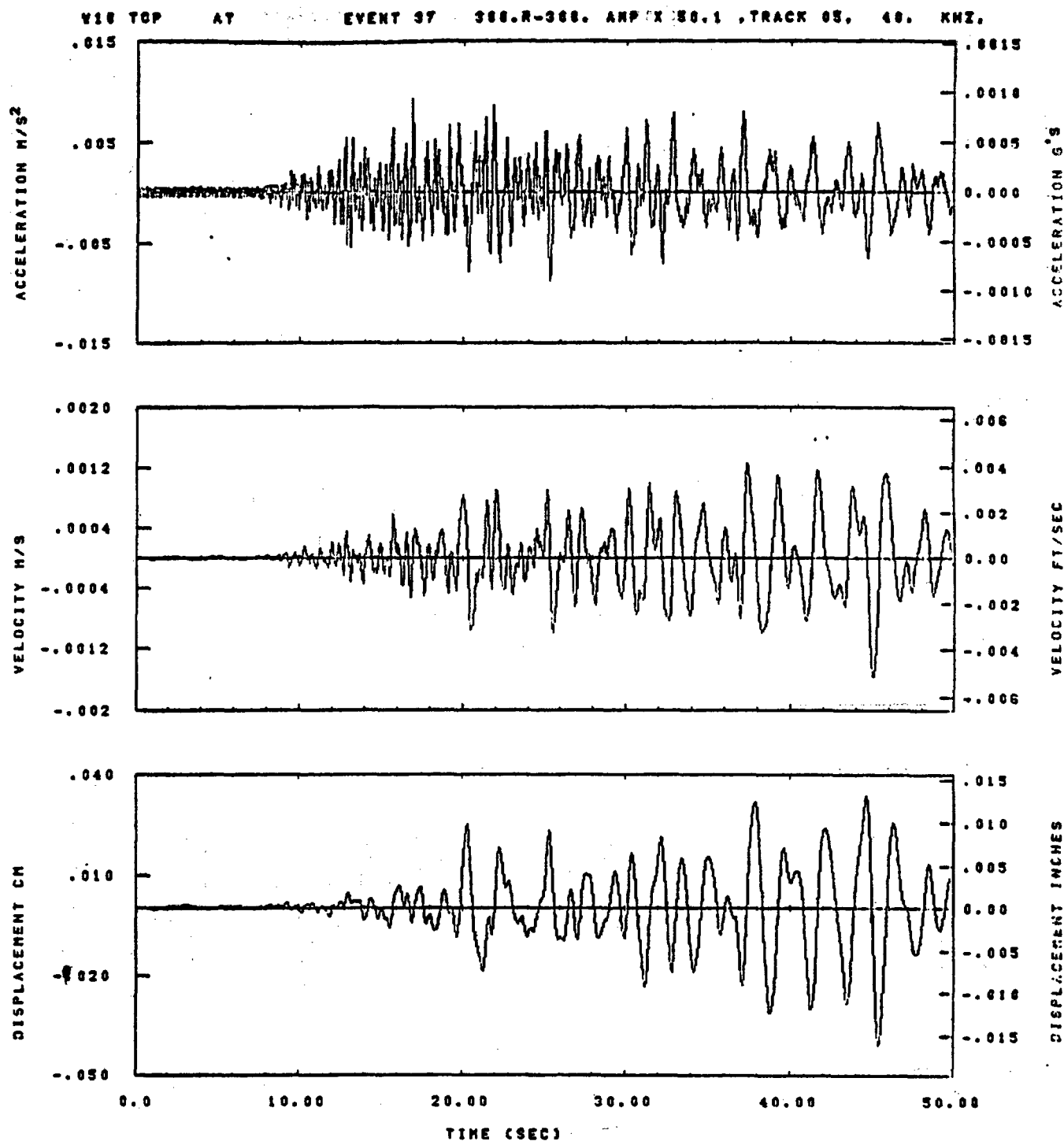
75.R-210. AMP X 50.1 TRACK 09. 7.33 NMZ.



IDT= .0020	ODT= .003	FIX=	AAS= 0.
HPF= .20	BYH= .13	HLH= 249	ASB=
LPF= 18.	BYL= 4.	HLL= 2999	ASE=
VTD= .200	VTE= .133	FLL= -20.	VSE= 0.
DPS= 0.	DPE= 100.	FLH= 0	DSE= 0.

14.59.29

06/11/82

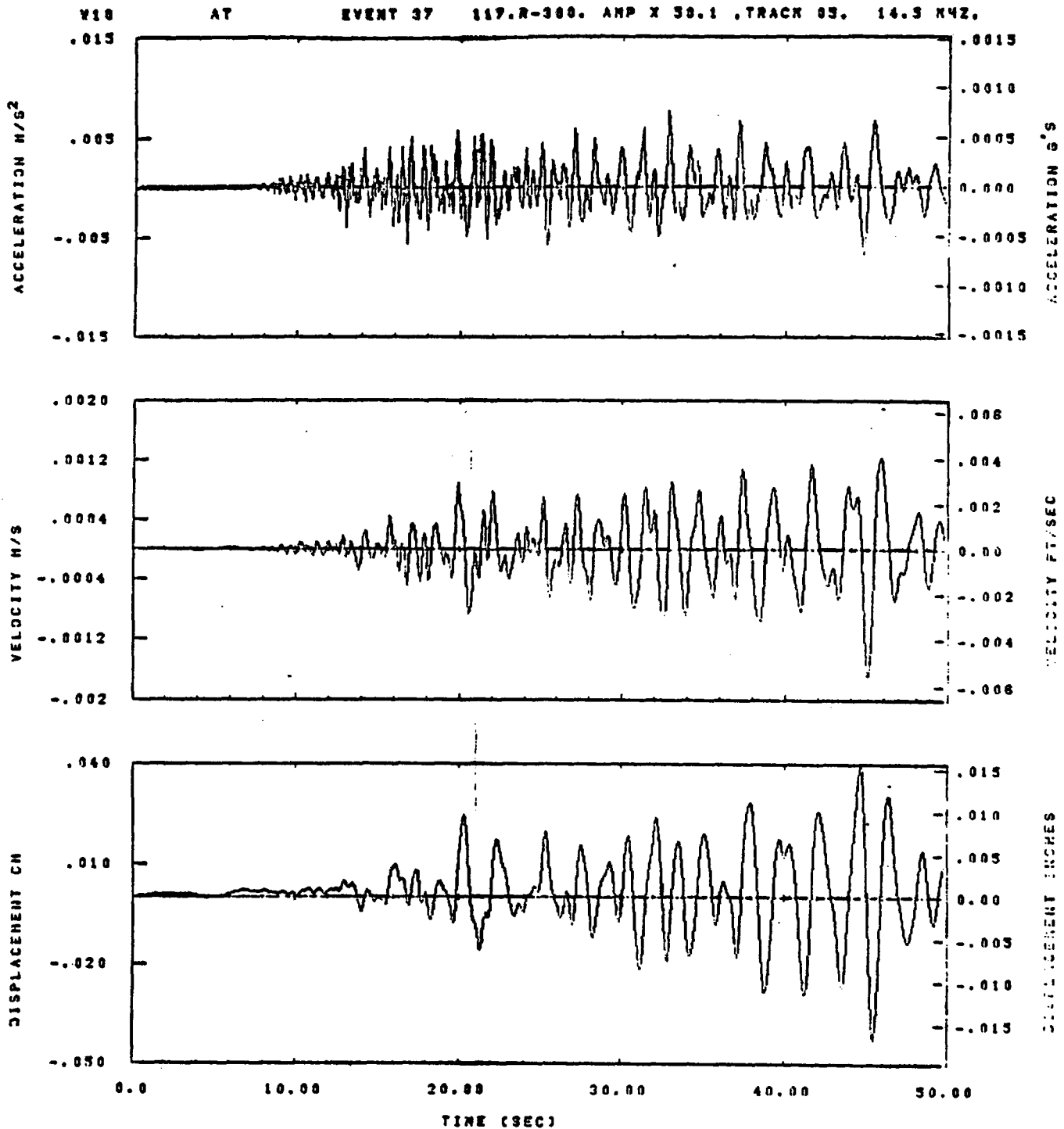


IDT= .0020	QDT=	FIX=	AAS= 0.
HPP= .30	SVH= .20	NLM= 167	ASB=
LPF= 27.	SVL= 6.	NLL= 1989	ASE=
YTS= .300	VTE= .200	PLL= -20.	VSE= 0.
OPB= 0.	OPE= 100.	FLH= 0	DSE= 0.

14.58.45

06/11/92

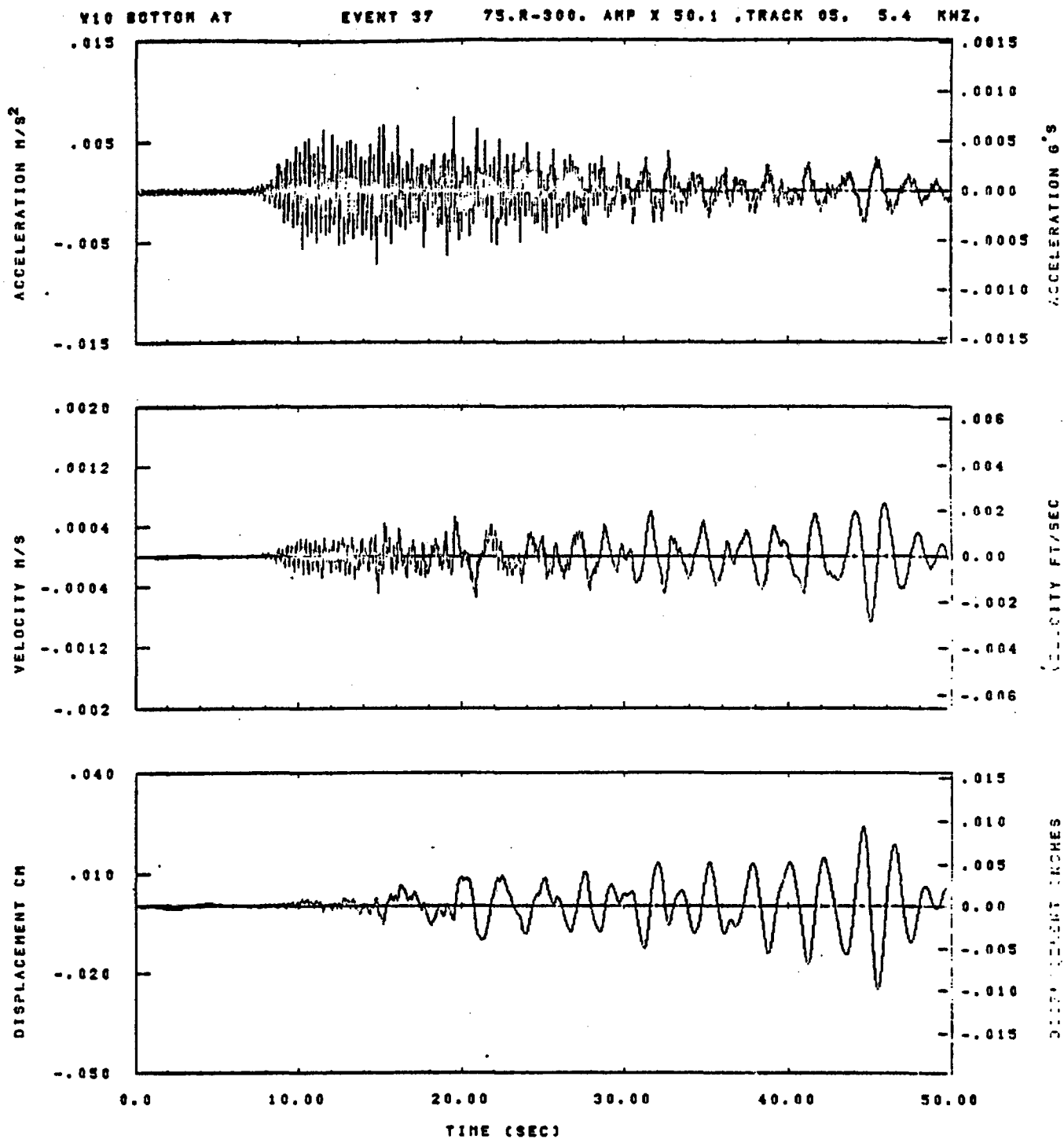
Figure C-82



IDT= .0020	ODT= .005	FIX=	AAS= 0.
HPF= .20	BYH= .13	HLH= 249	ASD=
LPF= 10.	BYL= 4.	HLL= 2990	AGE=
VTD= .200	VTE= .133	PLL= -20.	VSE= 0.
DPS= 0.	DPE= 100.	FLH= 0	DSE= 0.

14.39.98

08/11/82



IDT= .0020	ODT= .005	FIX=	AAS= 0.
HPF= .20	BYM= .13	MLH= 249	ASD=
LPF= 18.	BYL= 4.	MLL= 2999	ASE=
VTD= .200	VTE= .133	FLL= -20.	VSE= 0.
DPS= 0.	OPE= 100.	FLH= 0	DSE= 0.

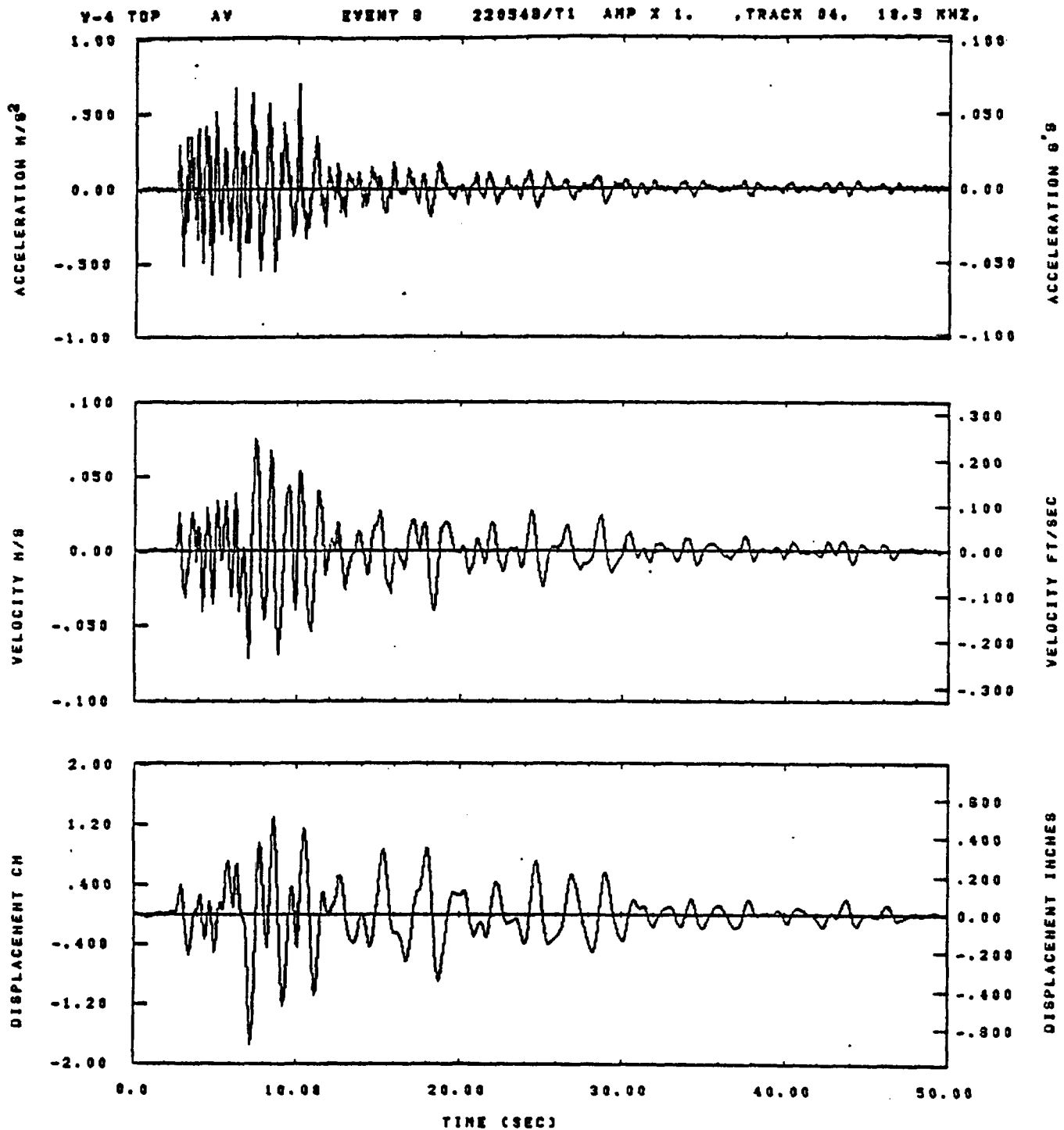
14.59.33

06/11/82

Figure C-84

APPENDIX D

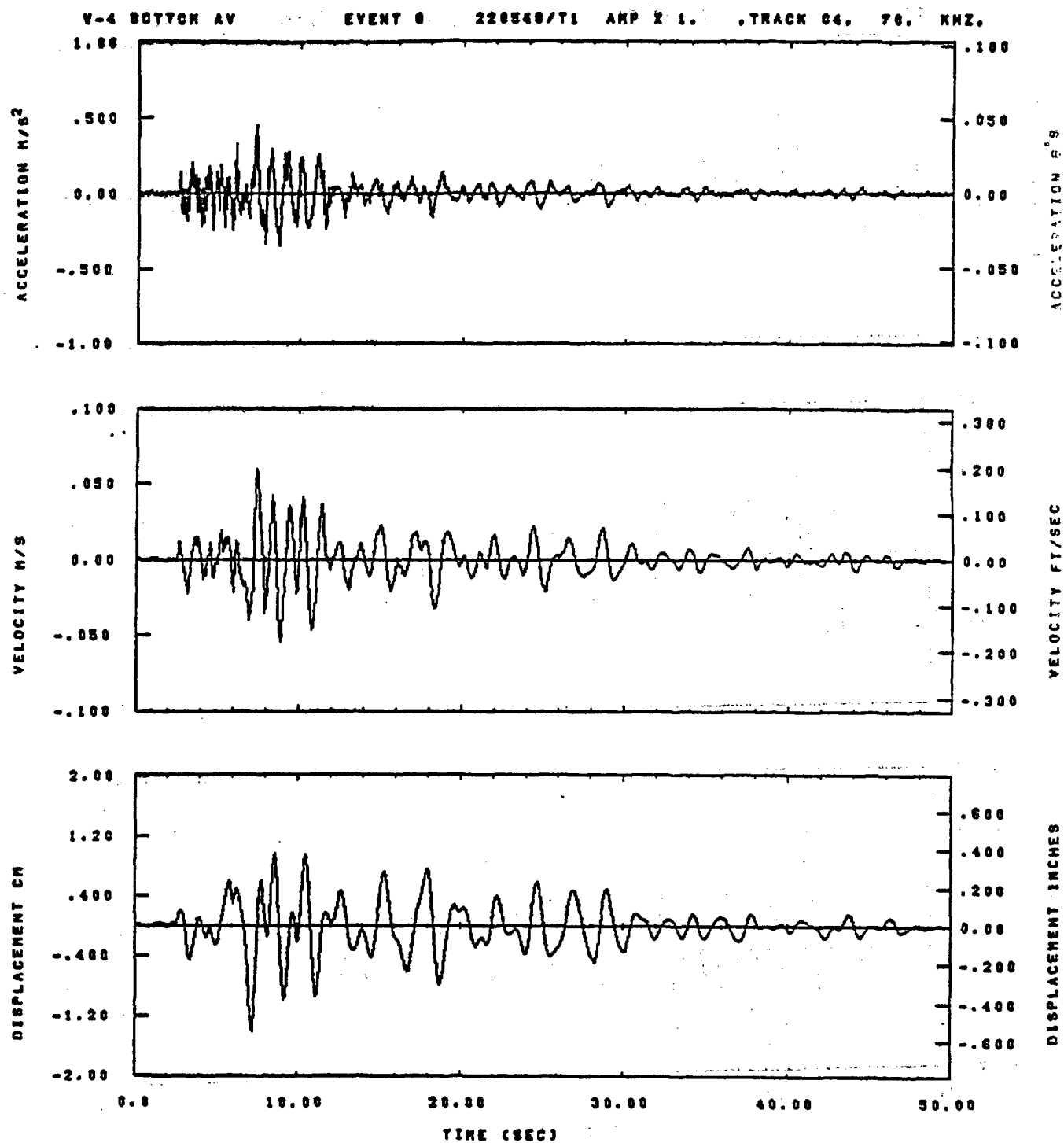
COMPARISON OF TOP AND BOTTOM WAVEFORMS AT STATION W-4



IDT= .0028	ODT= .003	FIX=	AAS= 0.
HPP= .20	BYN= .13	HLN= 249	ASB=
LPP= 18.	BYL= 4.	HLL= 2999	ASE=
VTS= .200	VTE= .133	FLL= -19.	VSE= 0.
DPS= 0.	DPE= 100.	FLH= A-.1	DSE= A+.1

14.34.38.

07/19/92

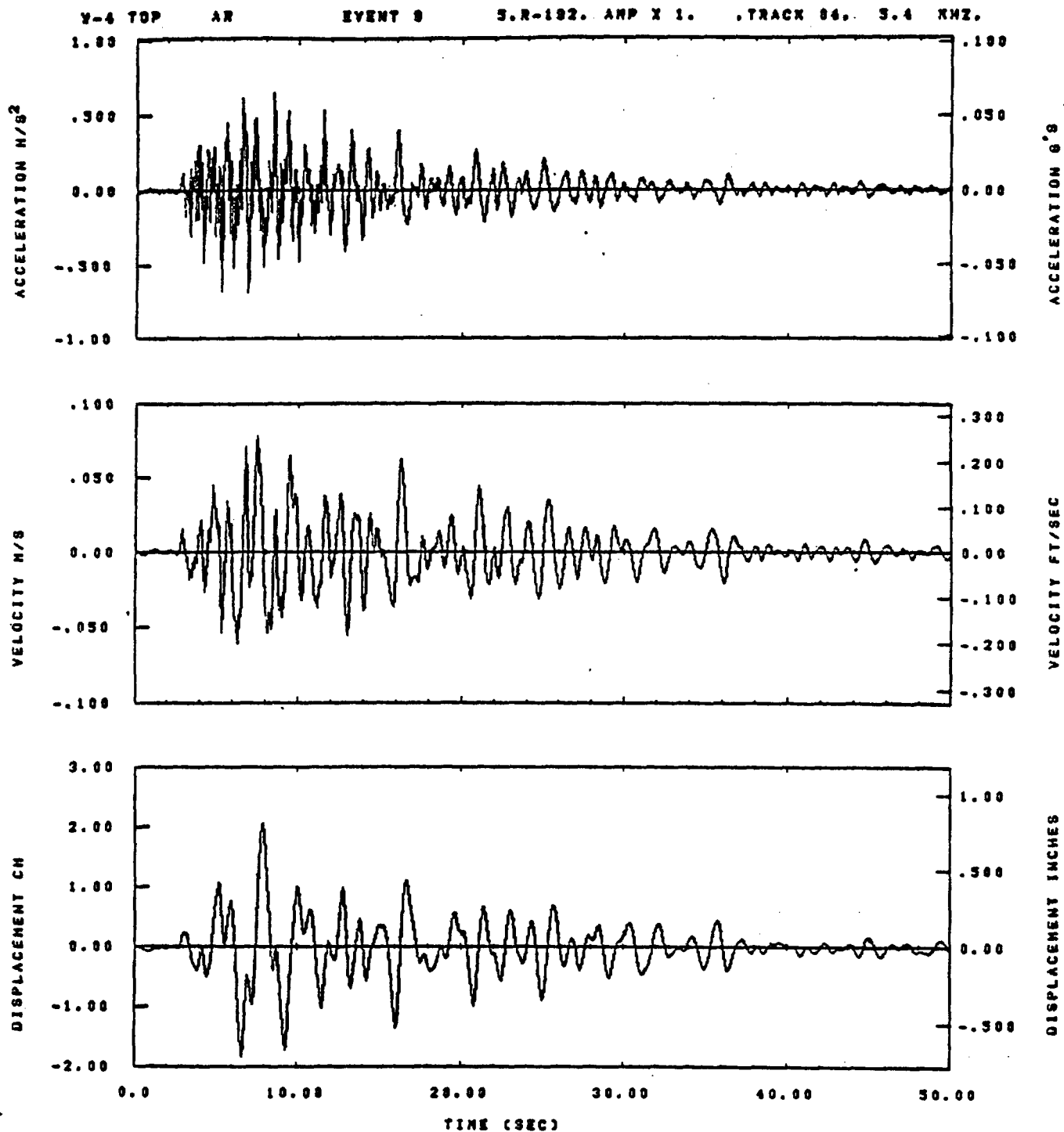


IDT= .0020	ODT= .005	FIX=	AAS= 0.
HPF= .20	BYH= .13	MLH= 245	ASB=
LPF= 10.	BYL= 4.	MLL= 2888	ASE=
VTS= .200	VTE= .133	FLL= -18.	VSE= 0.
DPS= 0.	DPE= 100.	FLH= A-.1	DSE= A+.1

14.08.28.

07/19/82

Figure D-2

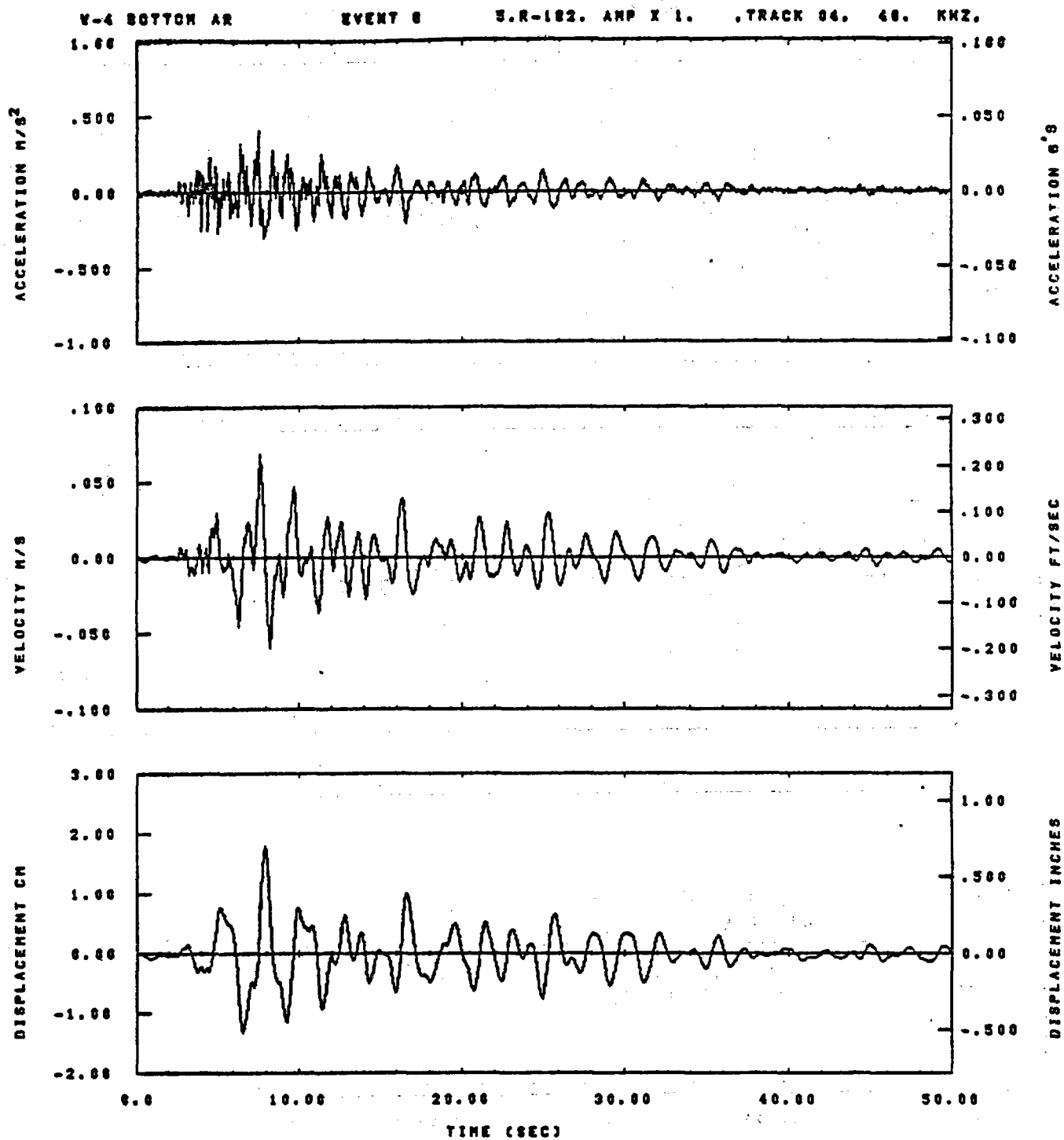


IDT= .0020	ODT= .003	FIX=	AAS= 0.
HPP= .20	BYH= .13	HLH= 249	ASB=
LPP= 10.	BYL= 4.	HLL= 2999	ASE=
VTB= .200	VTE= .133	FLL= -19.	VSZ= 0.
DPS= 0.	DPE= 100.	FLH= A-.1	DSE= A+.1

14.33.00.

07/19/82

Figure D-3

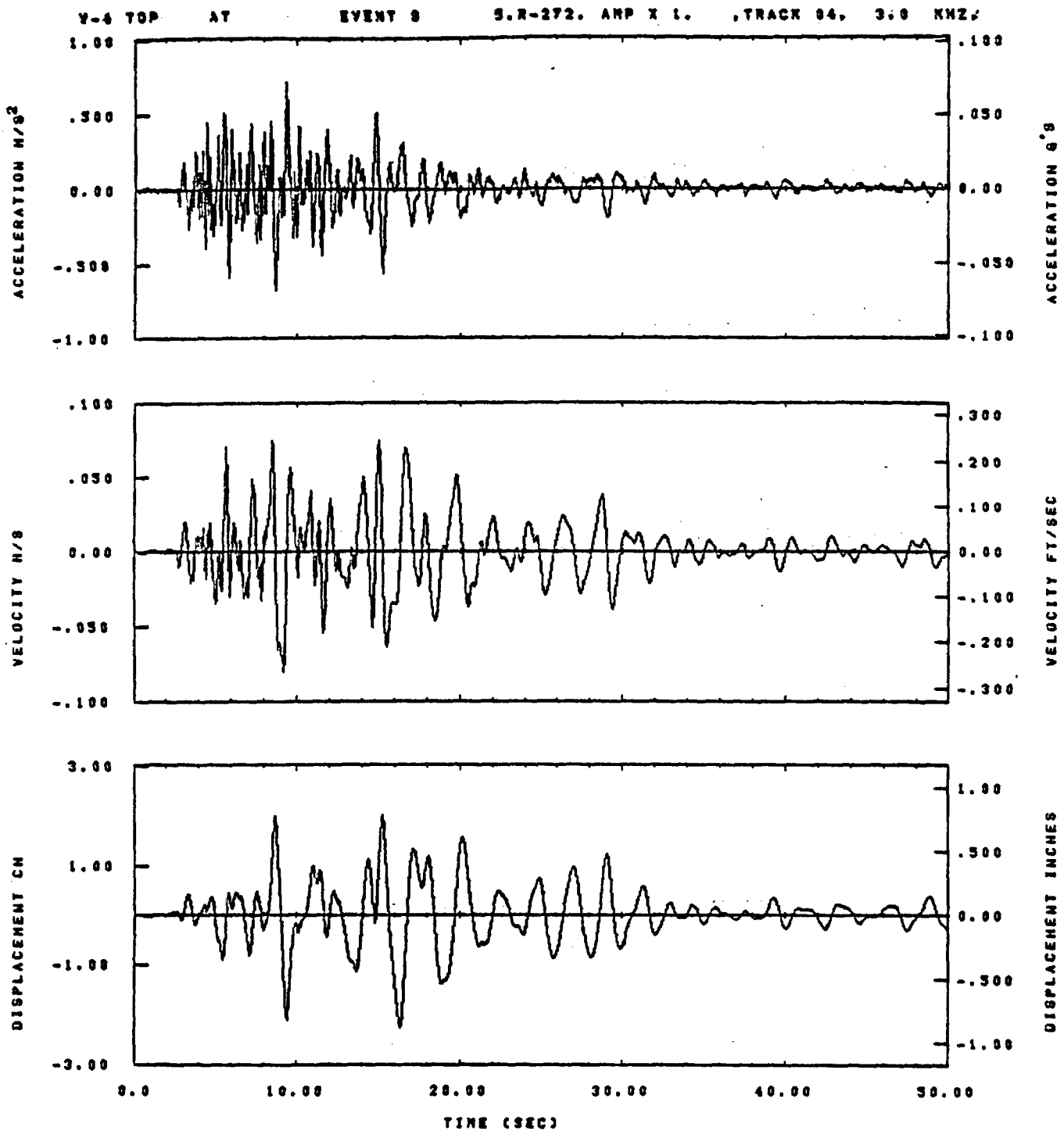


IDT= .0020	ODT= .005	FIX=	AAS= 0.
HPF= .20	BYH= .13	NLM= 249	ASB=
LPF= 10.	BYL= 4.	NLL= 2899	ASE=
VTS= .200	VTE= .133	FLL= -19.	VSE= 0.
OPE= 0.	OPE= 100.	FLH= A-.1	DSE= A+.1

14.08.40.

07/18/82

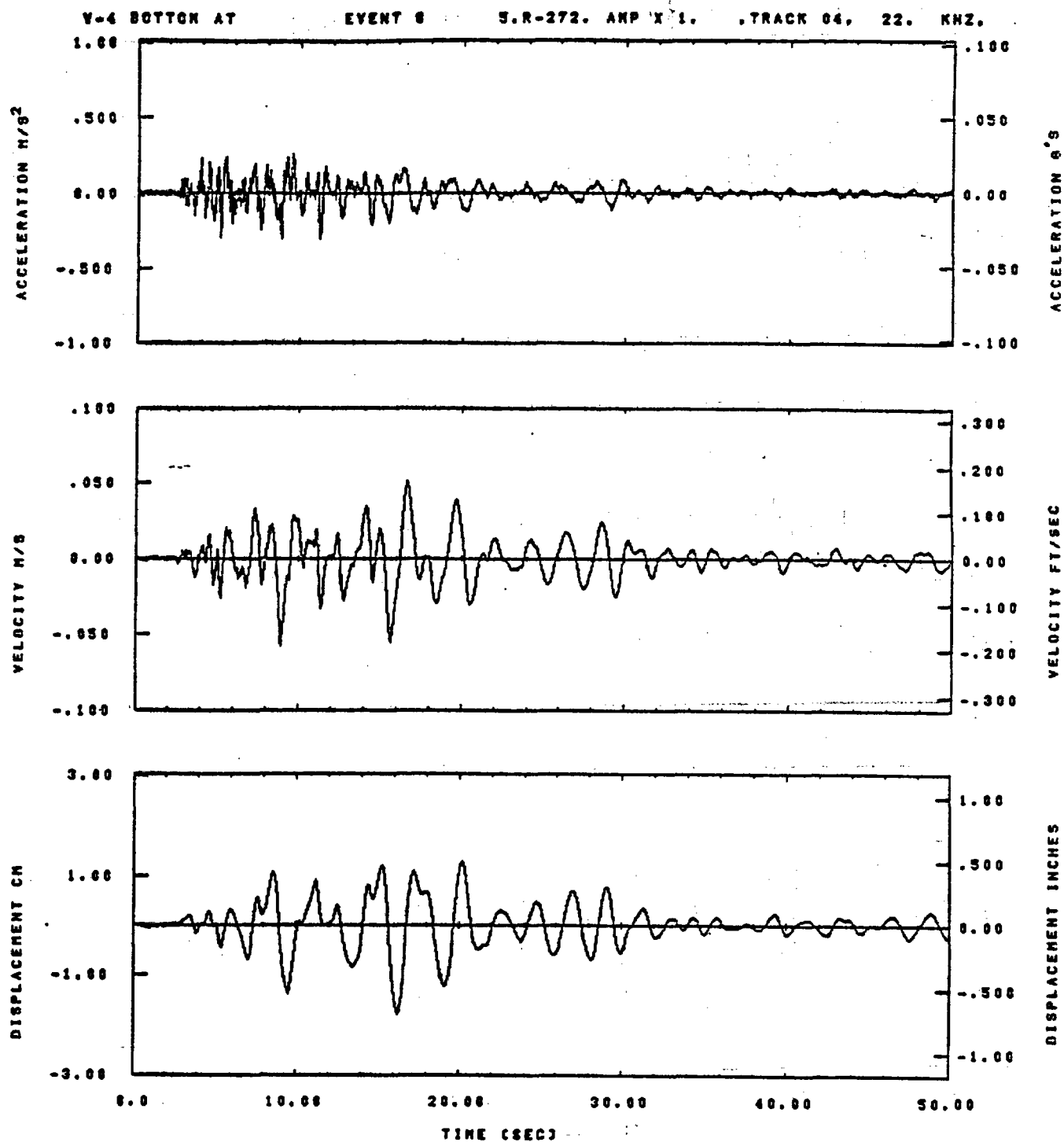
Figure D-4



IDT= .0028	ODT= .005	FIX=	AAS= 0.
HPF= .20	BYH= .13	HLH= 249	ASB=
LPF= 18.	BYL= 4.	HLL= 2999	ASE=
VTB= .200	VTE= .133	FLL= -19.	VSE= 0.
DPS= 0.	DPE= 100.	FLH= A+.1	DSE= A+.1

14.33.04.

07/19/82

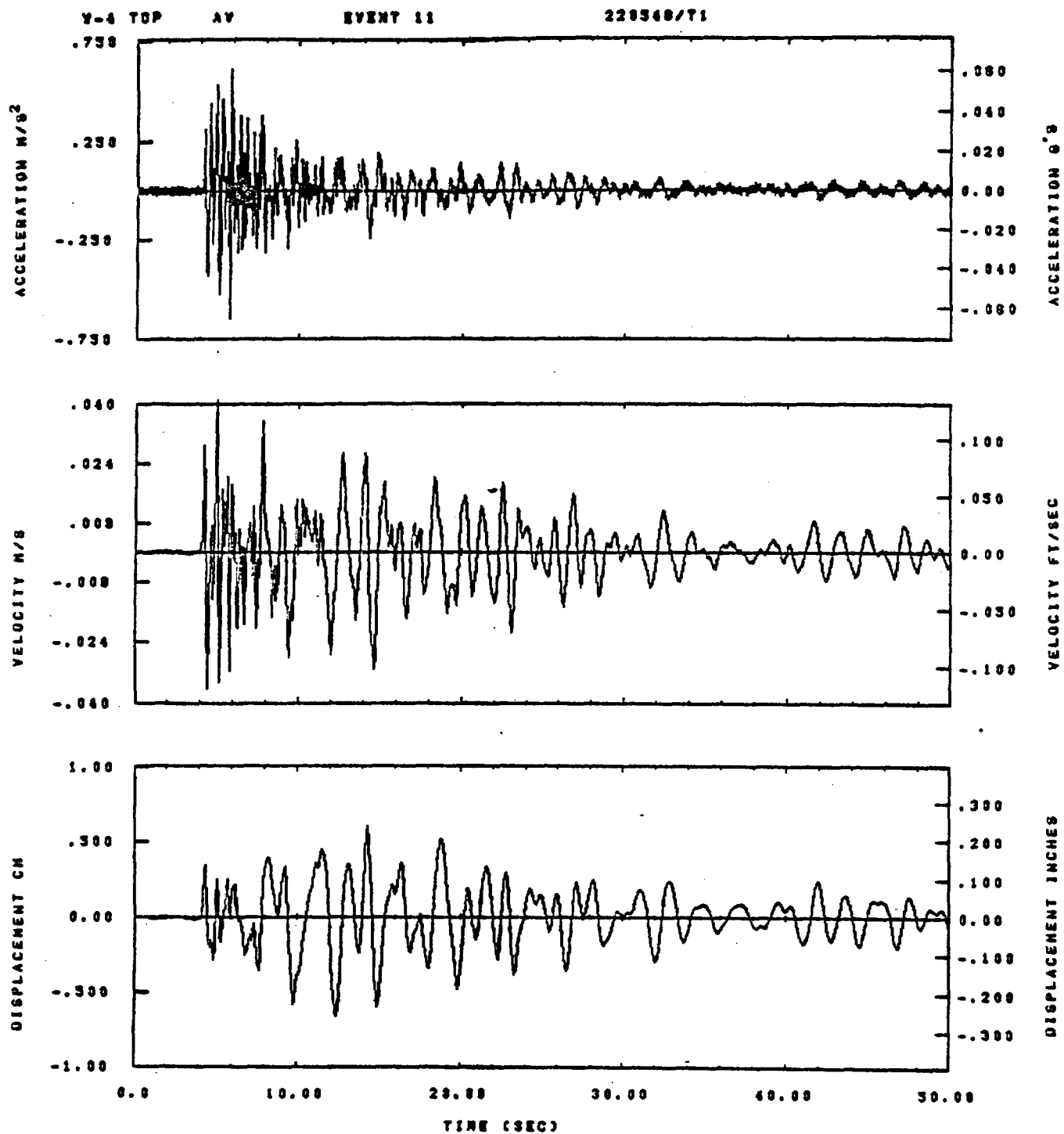


IDT= .0020	ODT= .005	FIX=	AAS= 0.
HPF= .20	BYH= .10	HLH= 240	ASB=
LPF= 18.	BYL= 4.	HLL= 2000	ASE=
VTB= .200	VTE= .133	FLL= -10.	VSE= 0.
OPS= 0.	OPE= 100.	FLH= A-.1	DSE= A+.1

14.10.03.

07/10/02

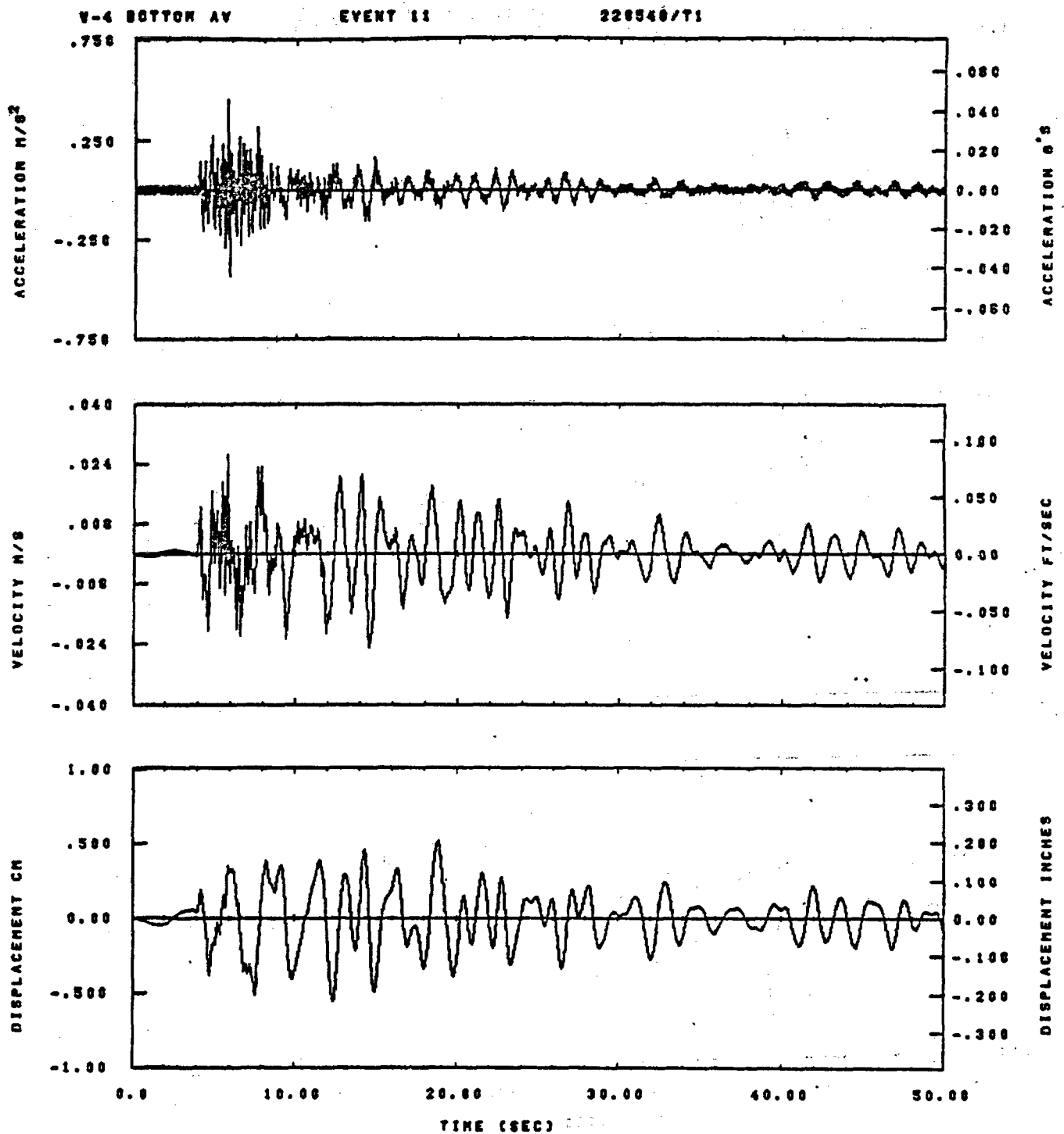
Figure D-6



IDT= .0020	QDT= .003	FIX=	AAS= 0.
HPP= .3	SVH= .20	MLH= 187	ASB=
LPP= 27.	SVL= 8.	HLL= 1999	ASE=
VTB= .30	VTE= .200	PLL= -20.	VSE= 0.
DPB= 0.	OPE= 100.	FLH= 0	DSE= 0.

18.58.53.

07/07/92

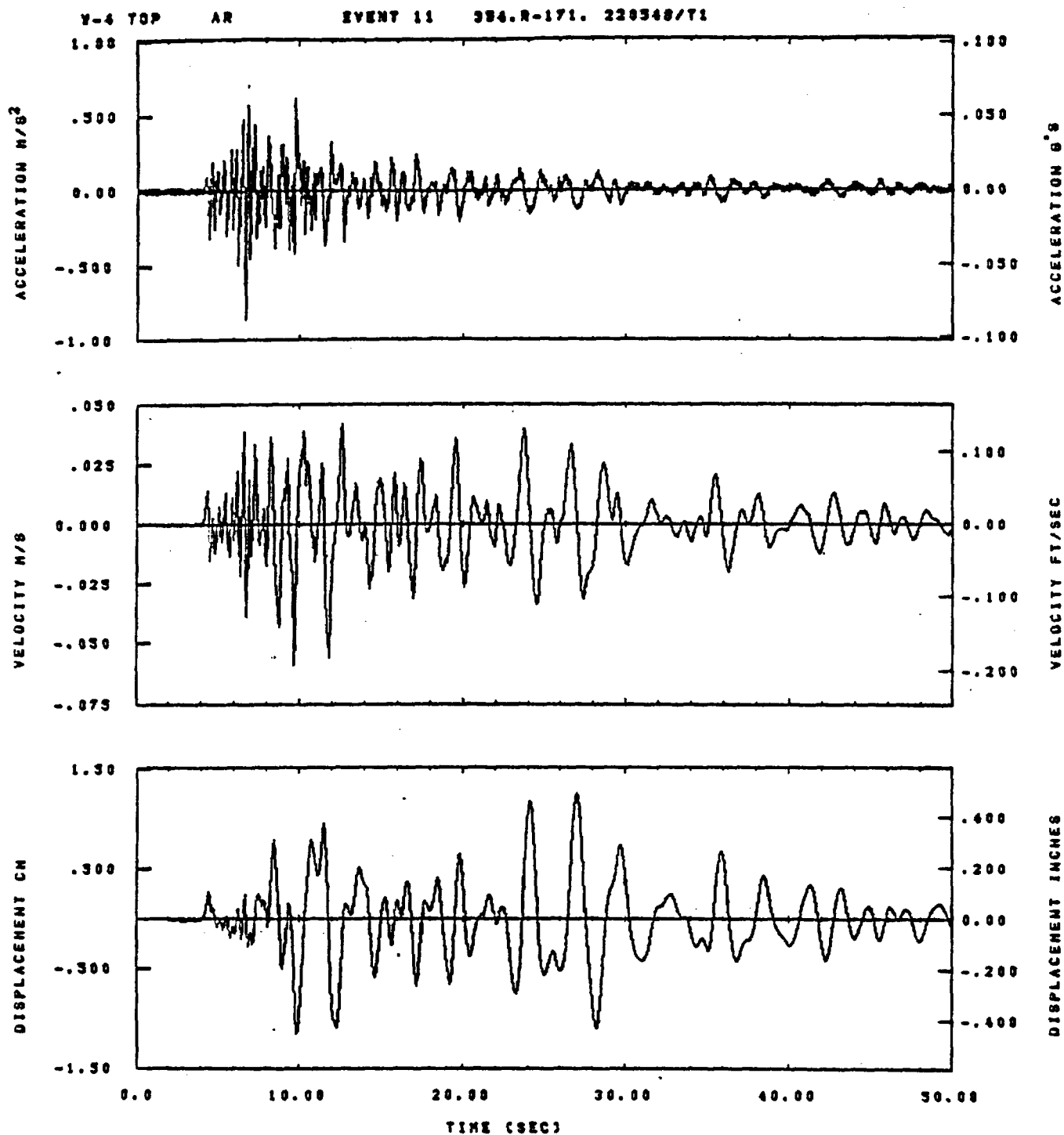


IDT= .0020	QDT= .0005	FIX=	AAS= 0.
HPF= .3	SVH= .20	HLH= 167	ASS= 0.
LPF= 27.	BVL= 8.	HLL= 1888	ASE=
VTB= .30	VTE= .208	FLL= -20.	VSE= 0.
DPS= 0.	DPE= 100.	FLH= 0	DSE= 0.

18.56.41.

07/07/82

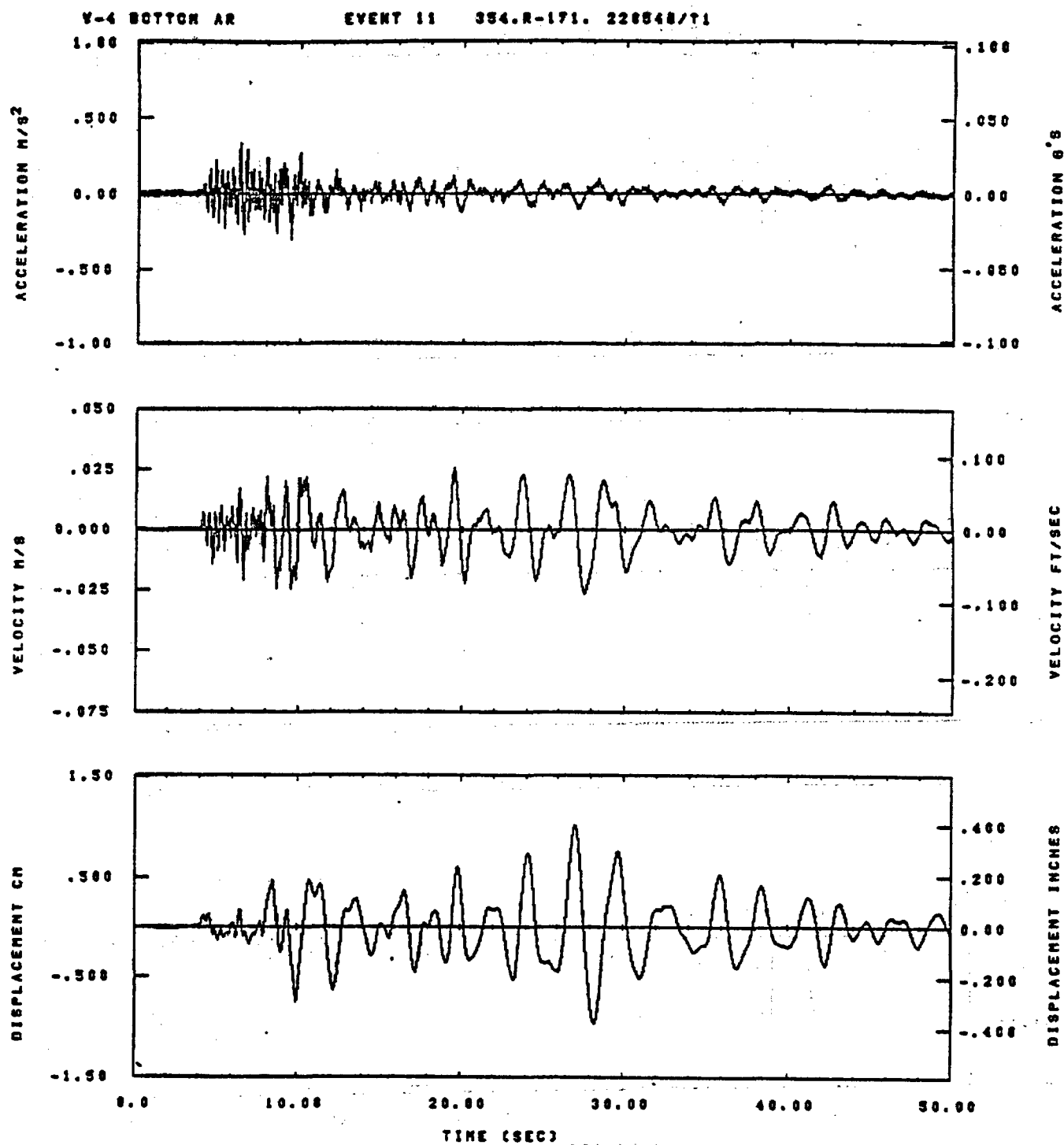
Figure D-8



IDT= .0020	ODT= .003	FIX=	AAS= 0.
HPP= .3	BYN= .20	HLH= 187	ASB=
LPP= 27.	BYL= 8.	HLL= 1999	ASE=
VTB= .30	VTE= .200	FLL= -20.	VSE= 0.
DPS= 0.	DPE= 100.	FLH= 0	DSE= 0.

10.37.04.

07/07/82

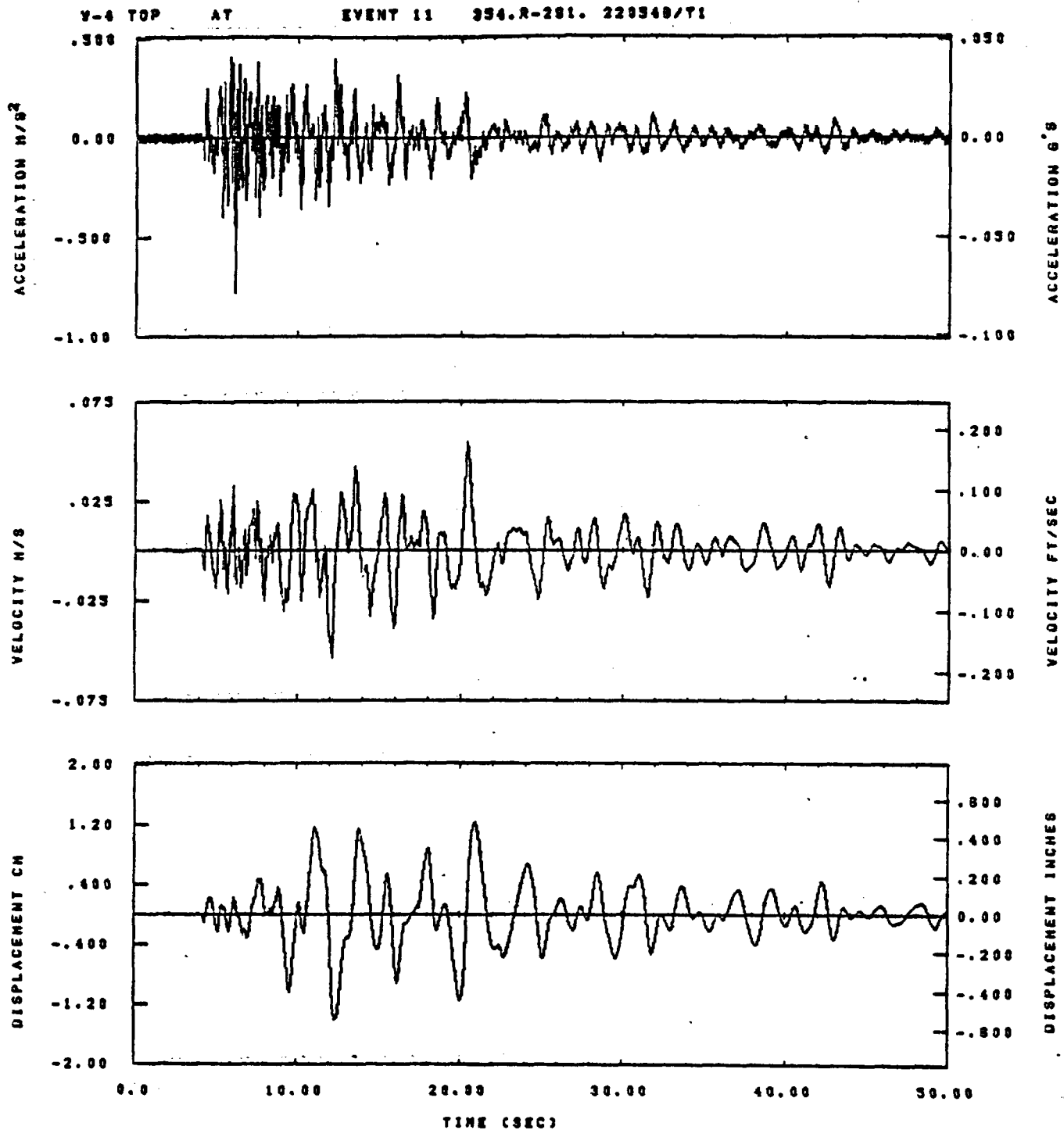


IDT= .0020	ODT= .005	FIX=	AAS= 0.
HPF= .3	BYH= .20	HLH= 167	ASB= "
LPF= 27.	BYL= 6.	HLL= 1988	ASE= "
VTE= .30	VTE= .200	PLL= -20.	VSE= 0.
DPS= 0.	DPE= 100.	PLH= 0	DSE= 0.

10.58.53.

07/07/82

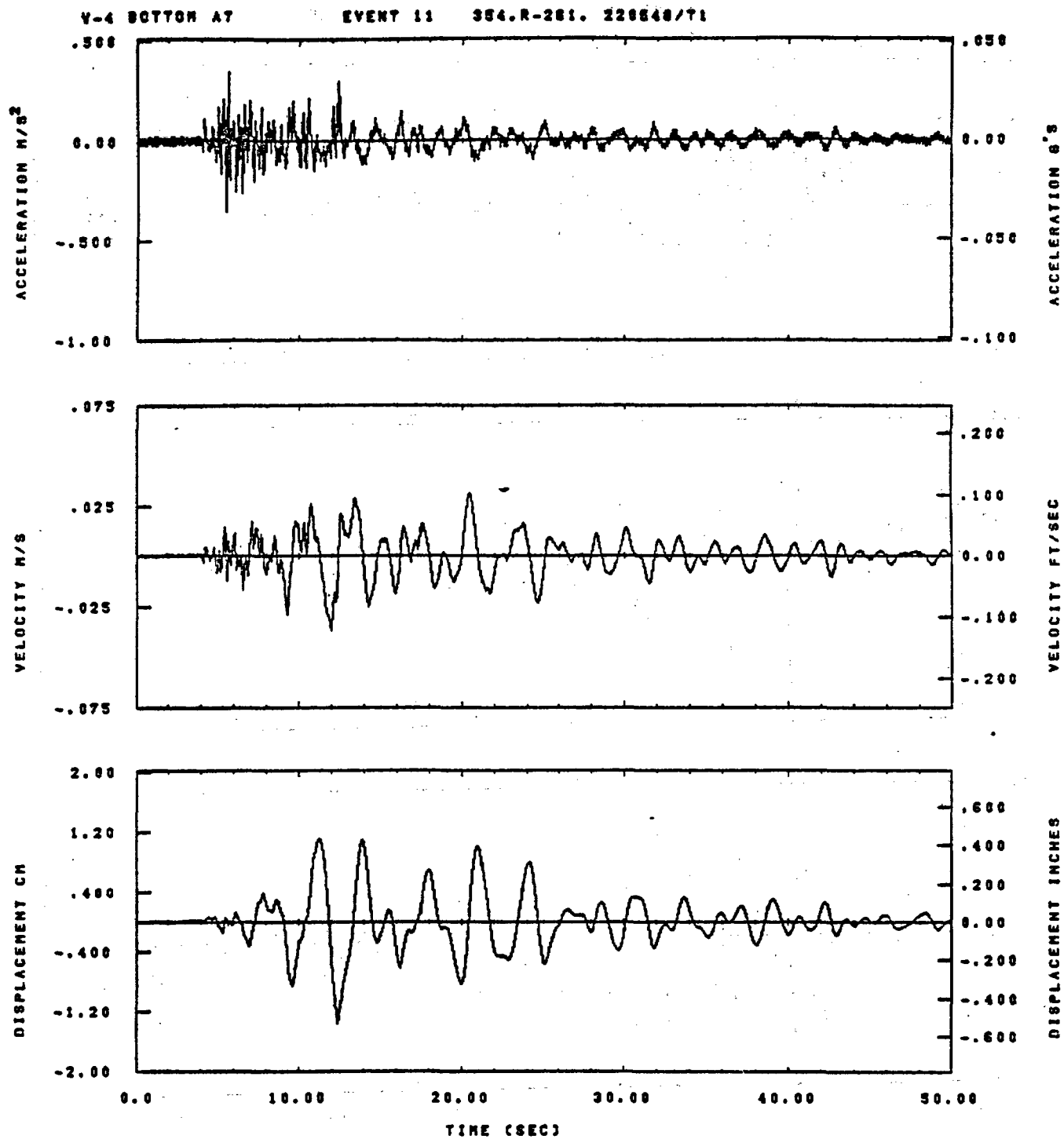
Figure D-10



IDT= .0020	ODT= .003	FIX=	AAS= 0.
HPF= .3	BYH= .20	HLH= 187	ASB=
LPF= 27.	BYL= 8.	HLL= 1999	ASE=
VTS= .30	VTE= .200	FLL= -20.	VSE= 0.
DPS= 0.	DPE= 100.	FLH= 0	DSE= 0.

10.37.21.

07/07/92

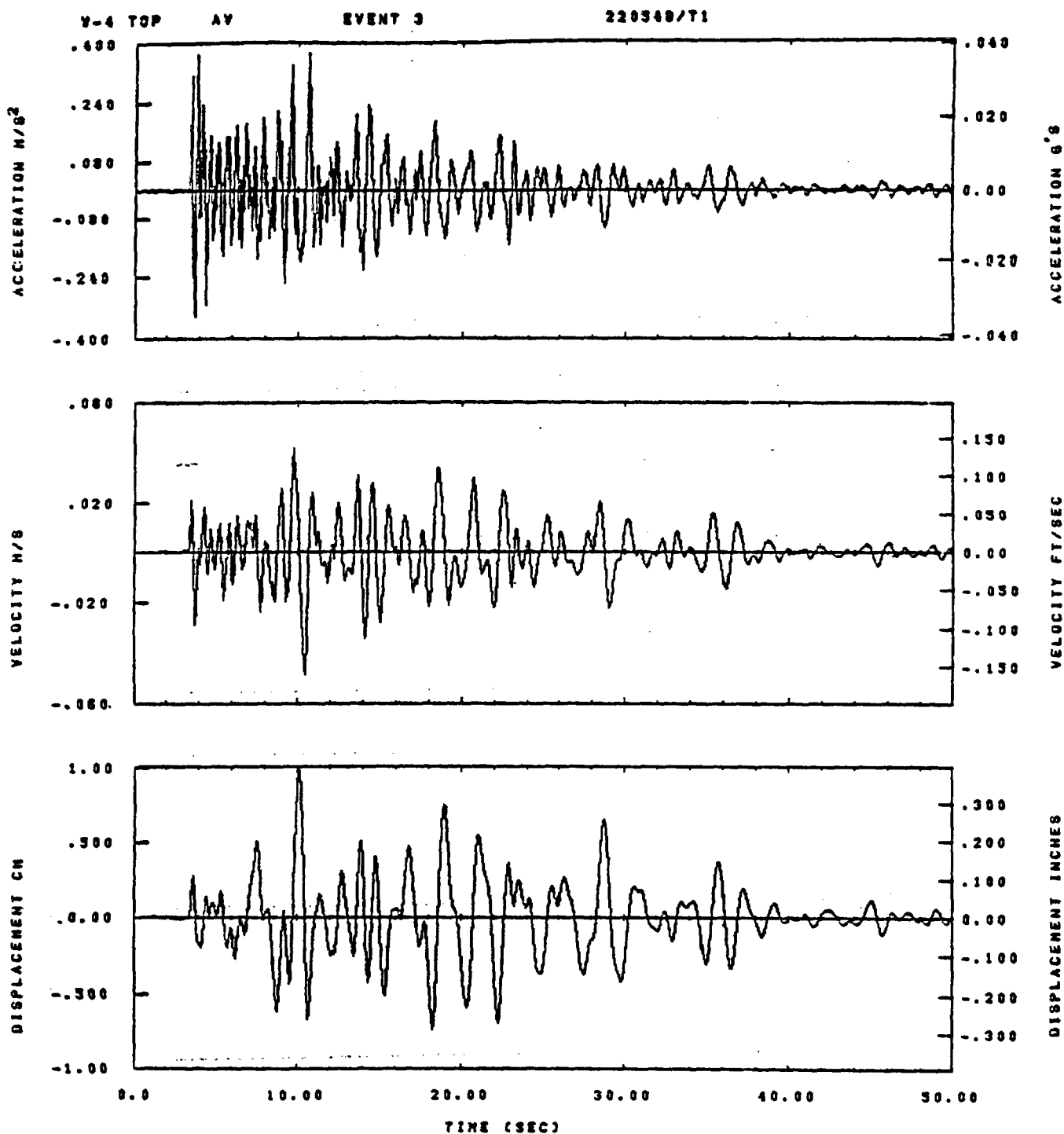


IDT= .0020	ODT= .005	FIX=	AAS= 0.
HPP= .3	BYH= .20	HLH= 167	ASS=
LPP= 27.	BYL= 6.	HLL= 1888	ASE=
VTE= .30	VTE= .200	FLL= -20.	VSE= 0.
DPS= 0.	DPE= 100.	FLH= 0	DSE= 0.

10.57.41.

07/87/82

Figure D-12



IDT= .0020	ODT= .003	FIX=	AAS= 0.
HPF= .3	SVH= .20	HLH= 187	ASB=
LPF= 27.	BVL= 8.	HLL= 1999	ASE=
VTB= .30	VTE= .200	FLL= -4.	VSE= 0.
DPS= 0.	DPE= 100.	FLH= 0	DSE= 0.

13.48.37.

07/09/82

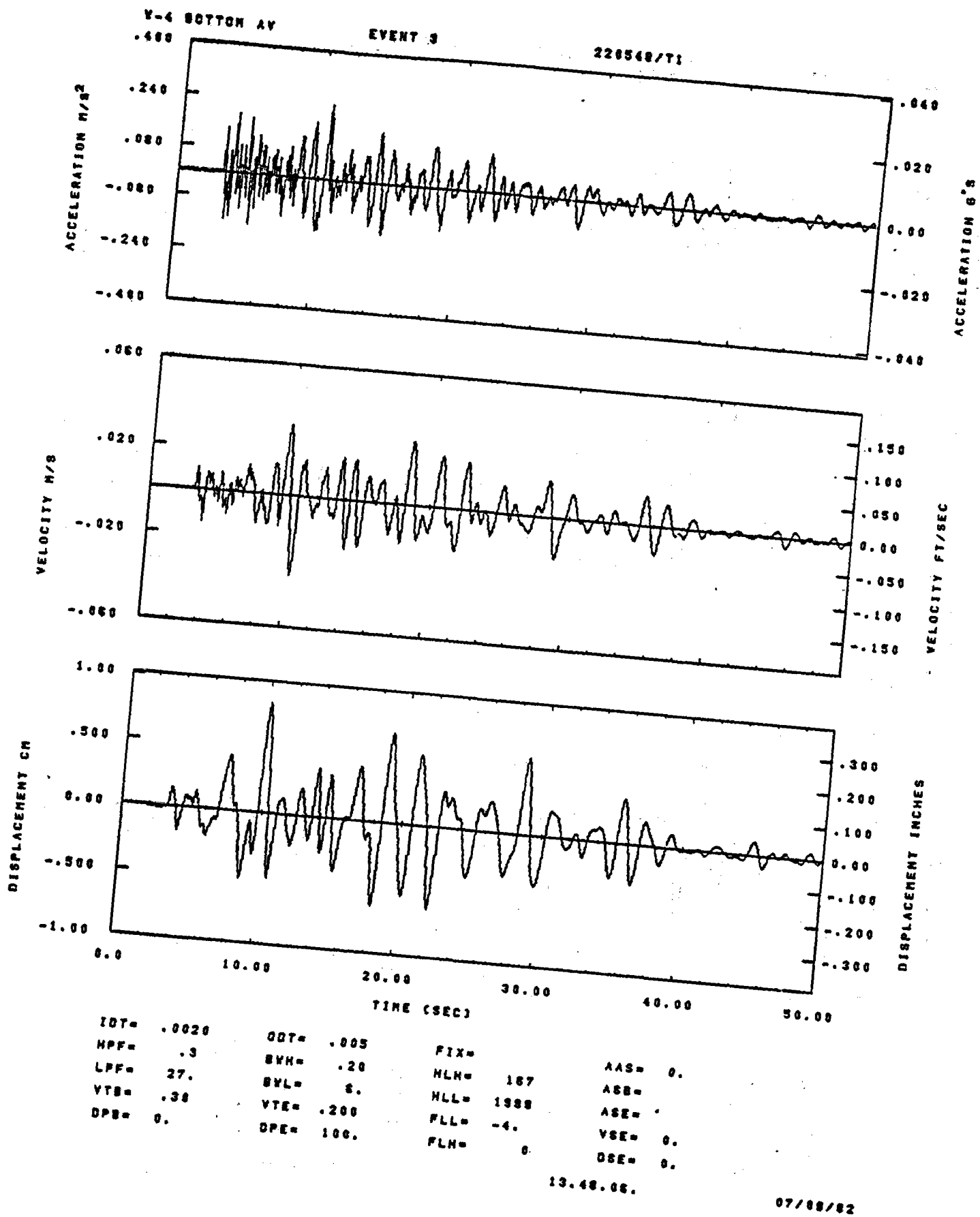
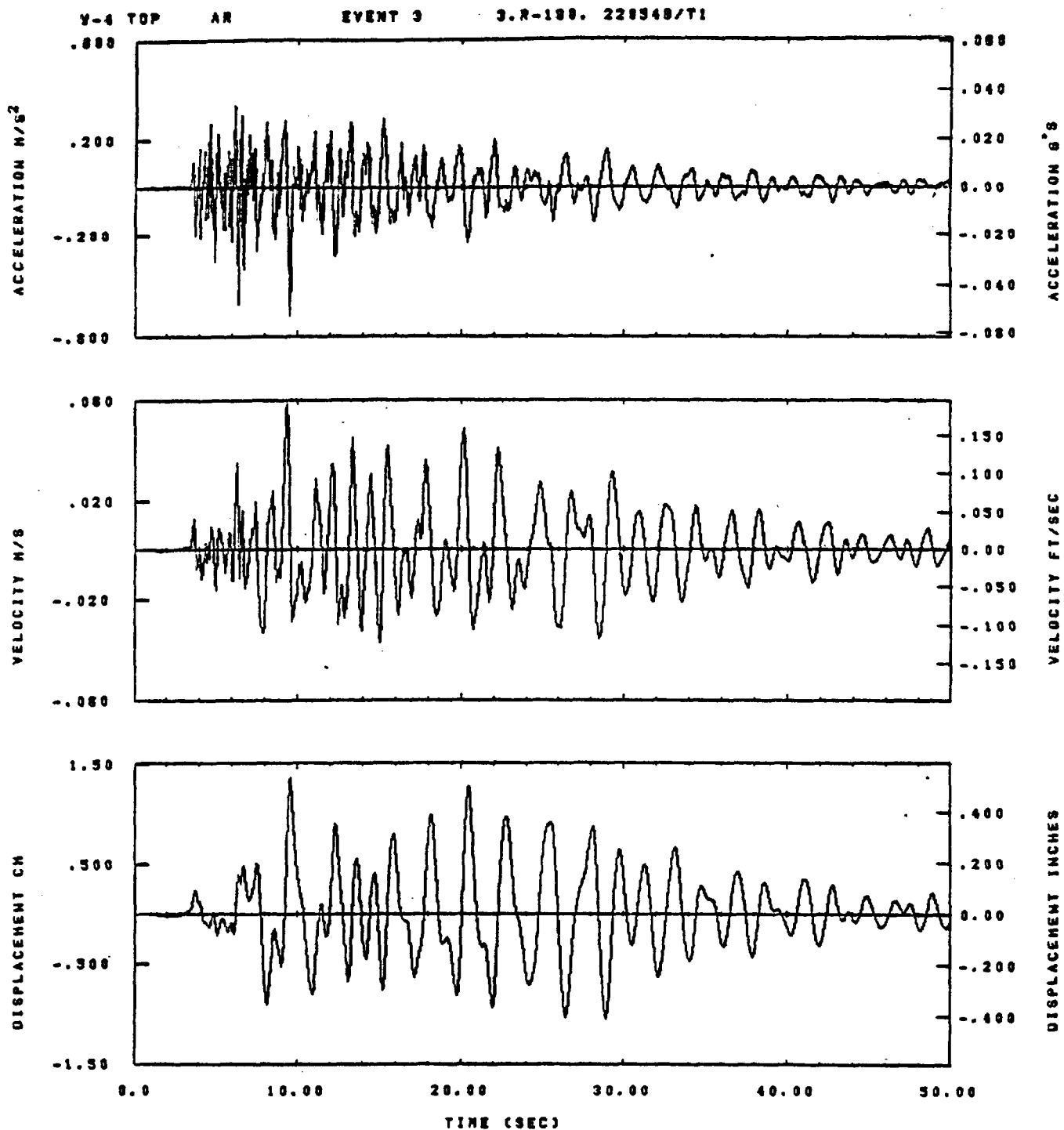


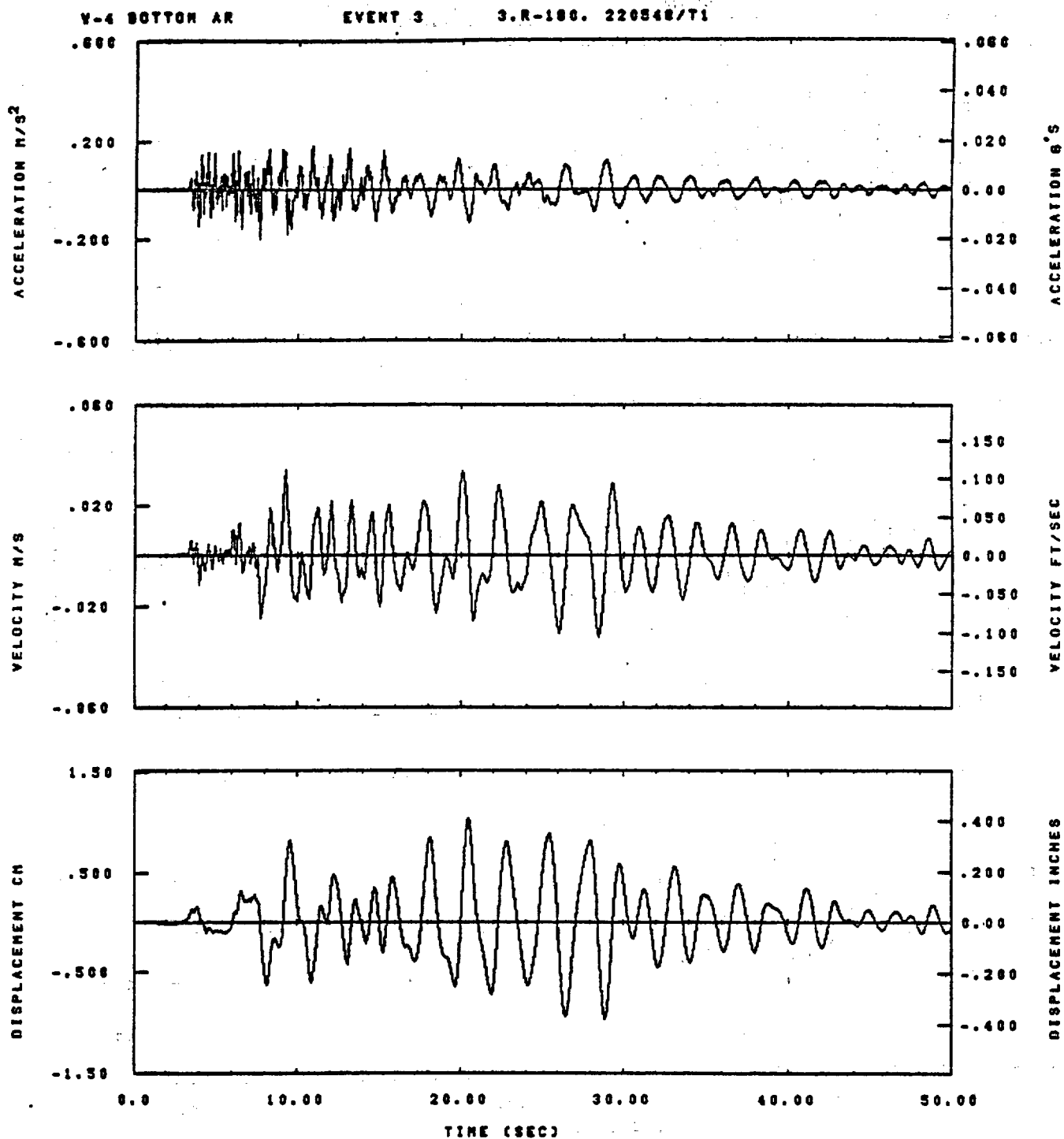
Figure D-14



IDT=	.0028	QDT=	.003	FIX=		AAS=	0.
HPP=	.3	SVH=	.20	HLH=	187	ASB=	
LPP=	27.	SVL=	6.	HLL=	1399	ASE=	
VTS=	.38	VTE=	.200	FLL=	-4.	VSE=	0.
DPS=	0.	DPE=	100.	FLH=	0	DSE=	0.

13.48.43.

07/09/82

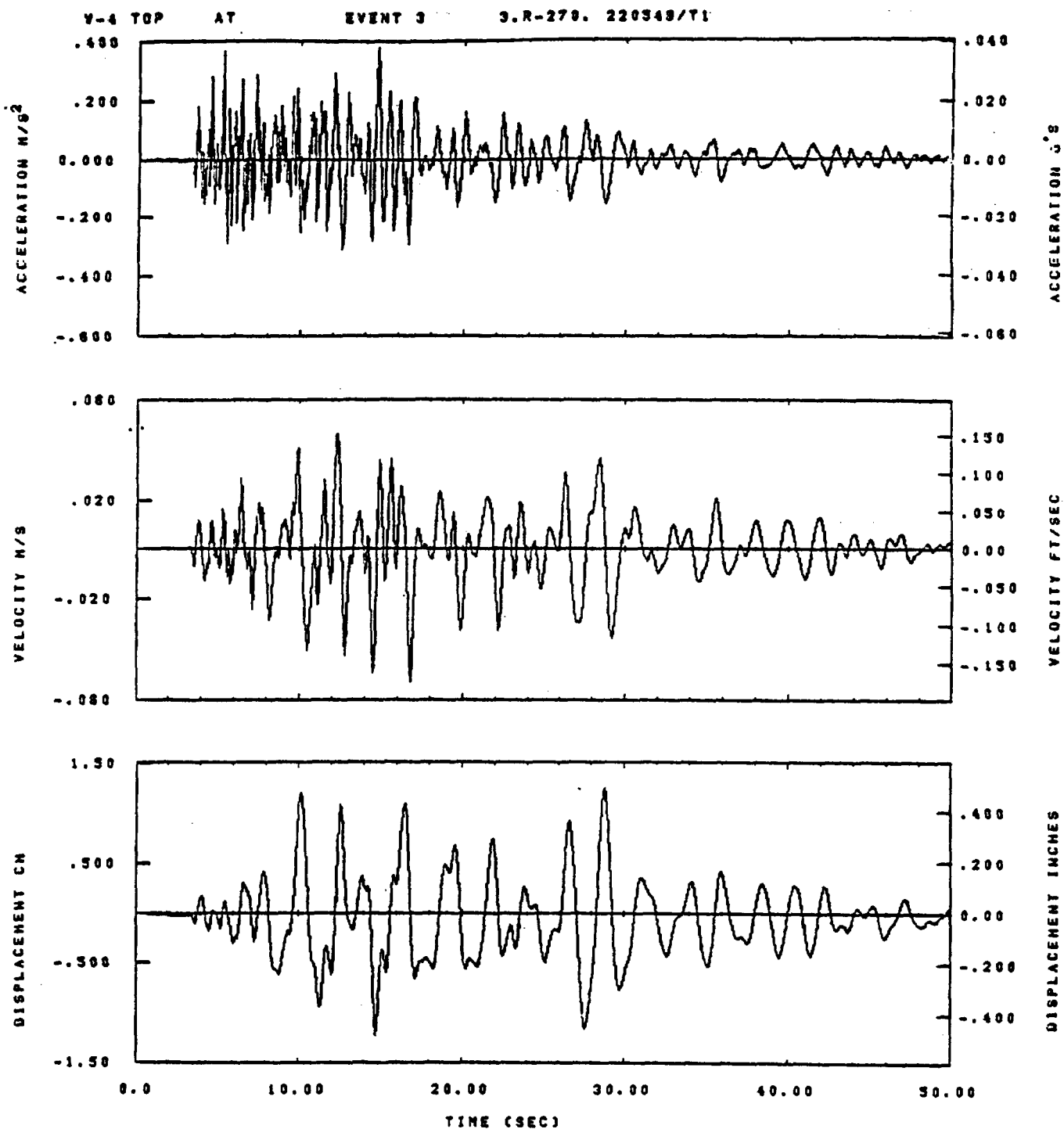


IDT= .0020	ODT= .005	FIX=	AAS= 0.
HPF= .3	BYH= .20	HLH= 167	ASB=
LPF= 27.	BYL= 6.	HLL= 1999	ASE=
VTS= .30	VTE= .200	FLL= -4.	VSE= 0.
DPS= 0.	DPE= 100.	FLH= 0	DSE= 0.

13.48.14.

07/08/82

Figure D-16

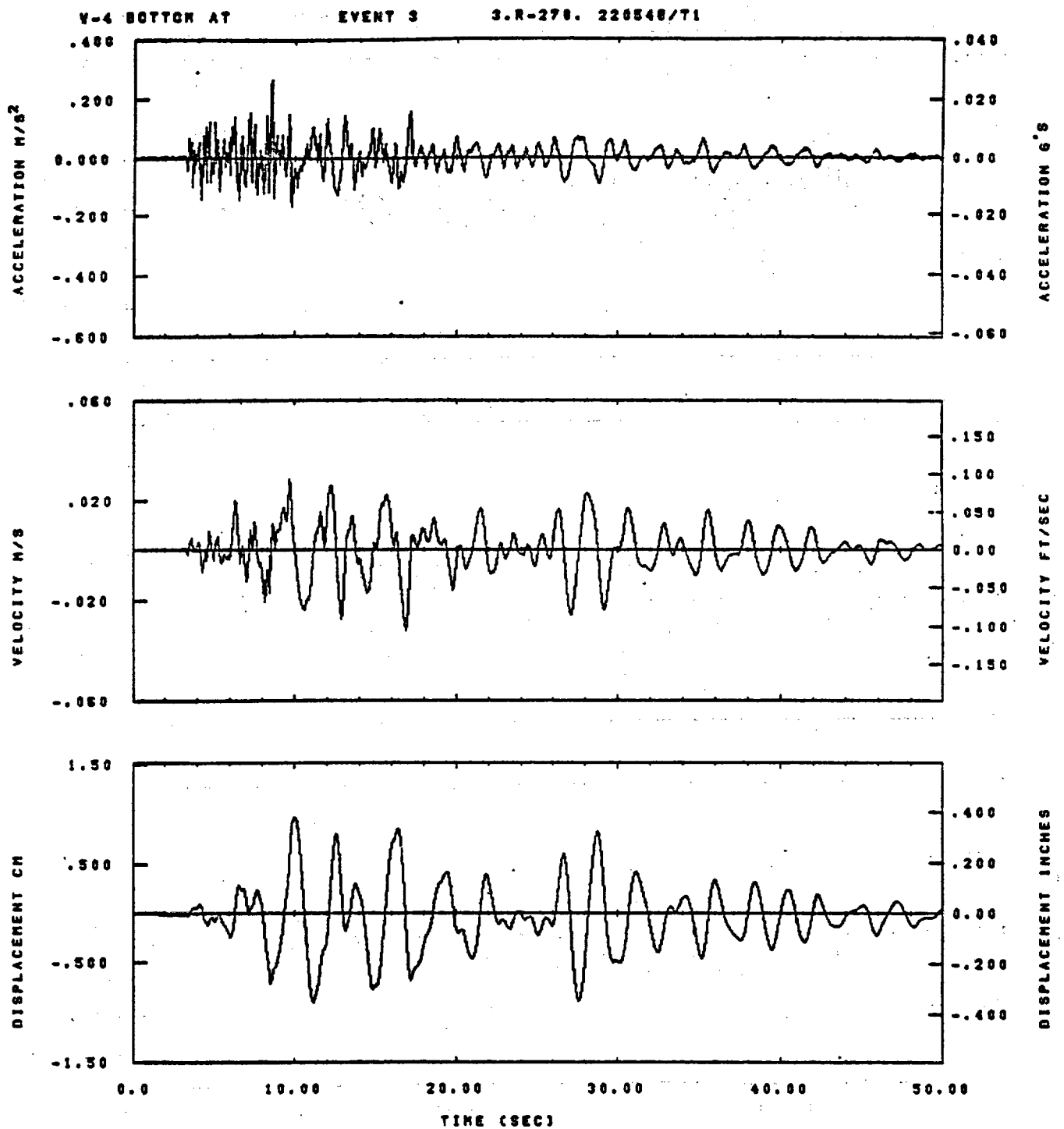


IDT= .0020	ODT= .005	FIX=	AAS= 0.
HPP= .3	SYH= .20	HLH= 187	ASB=
LPP= 27.	SYL= 6.	HLL= 1399	ASE=
VTB= .30	VTE= .200	FLL= -4.	VSE= 0.
DPS= 0.	DPE= 100.	FLH= 0	DSE= 0.

13.48.33.

07/09/82

Figure D-17

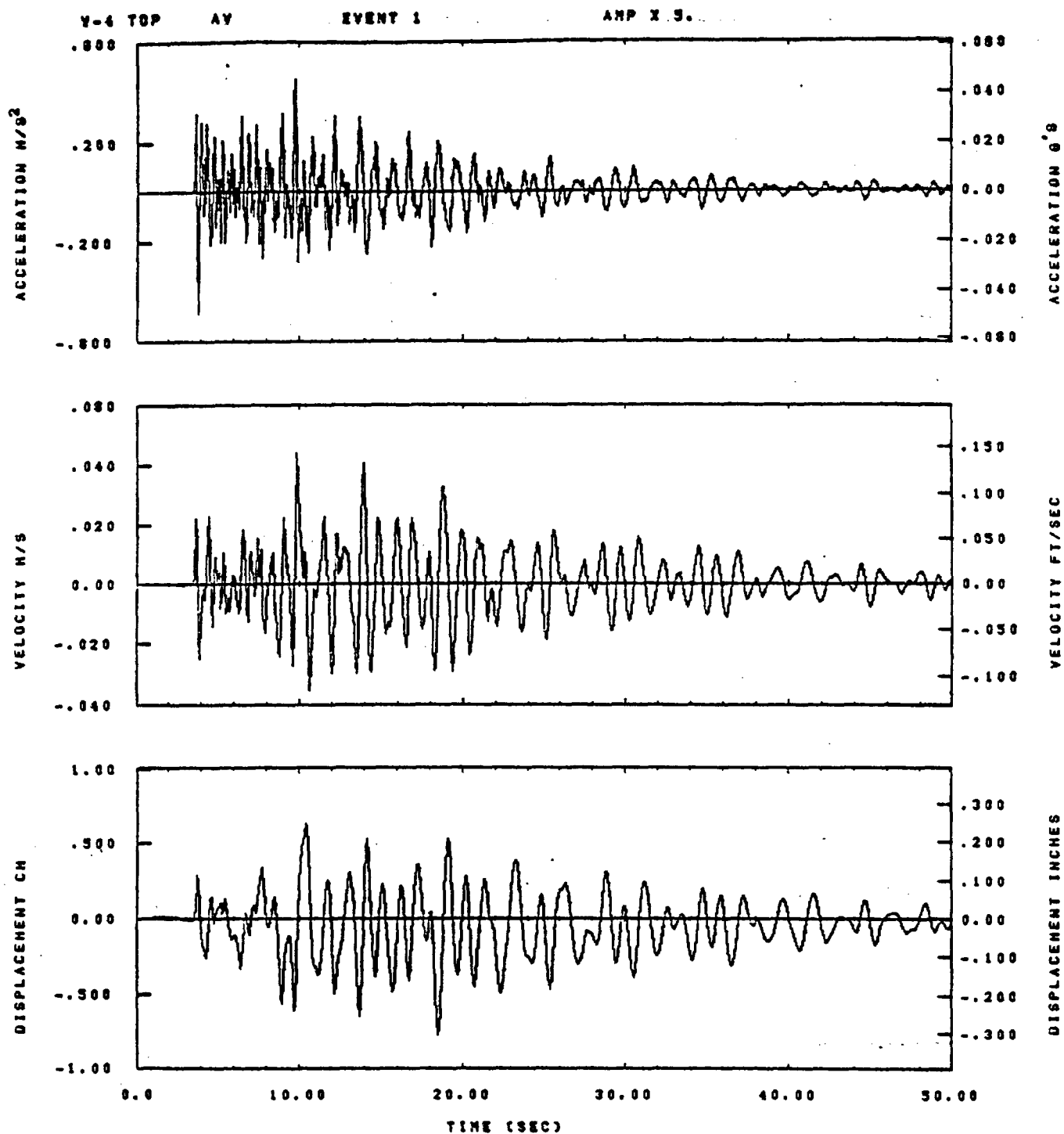


IDT= .0020	ODT= .005	FIX=	AAS= 0.
HPP= .3	SVH= .20	HLH= 167	ASB=
LPP= 27.	SVL= 6.	HLL= 1998	ASE=
VTS= .30	VTE= .200	FLL= -4.	VSE= 0.
DPS= 0.	DPE= 100.	FLH= 0	DSE= 0.

13.48.23.

07/68/82

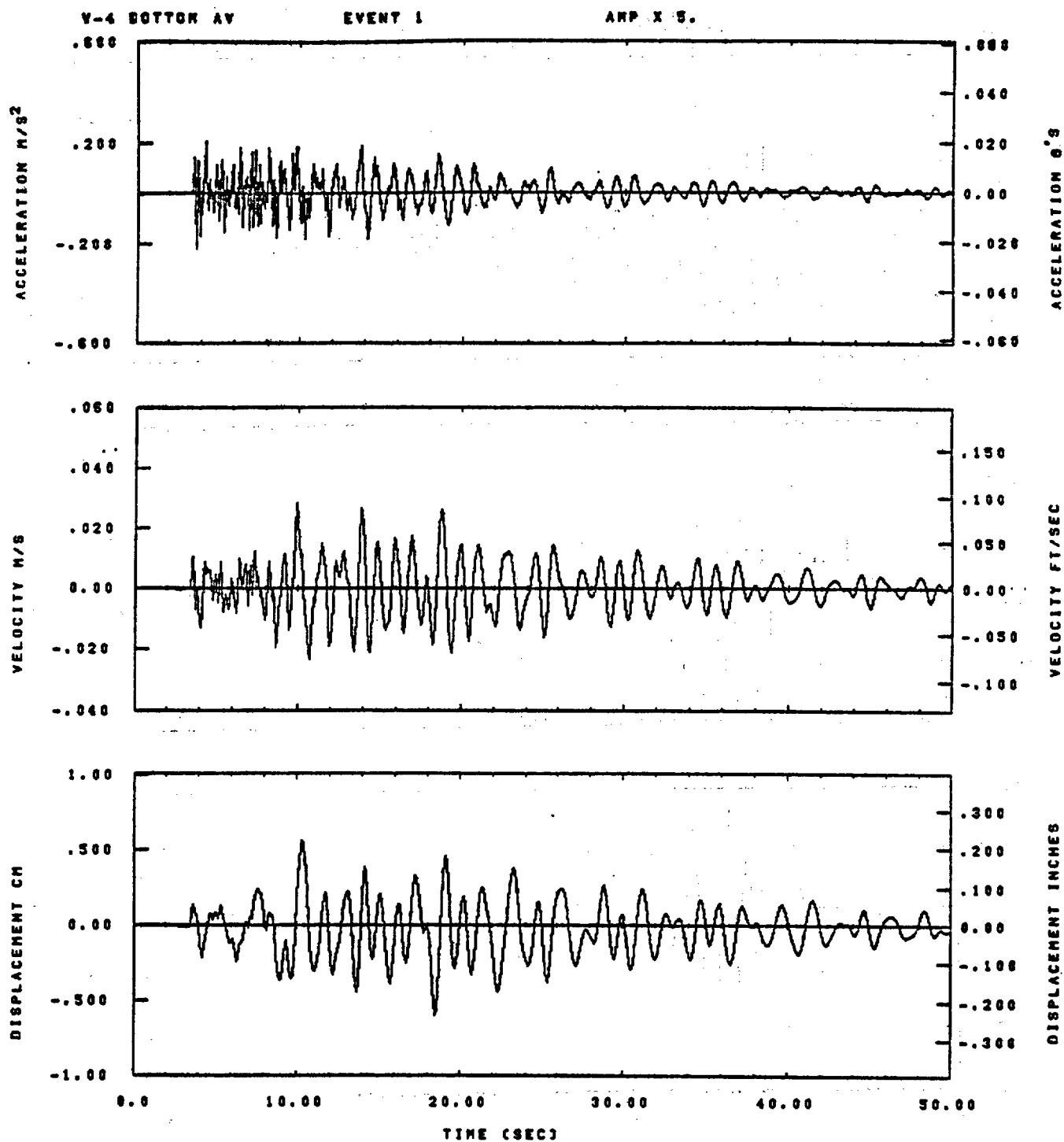
Figure D-18



IDT= .0005	ODT=	FIX=	AAS= 0.
HPP= .3	BYH= .20	HLH= 667	ASS=
LPP= 27.	BYL= 8.	HLL= 1999	ASE=
VTS= .30	VTE= .200	FLL= -20.	VSE= 0.
DPS= 0.	DPE= 100.	FLH= 0	DSE= 0.

09.50.44.

07/88/82

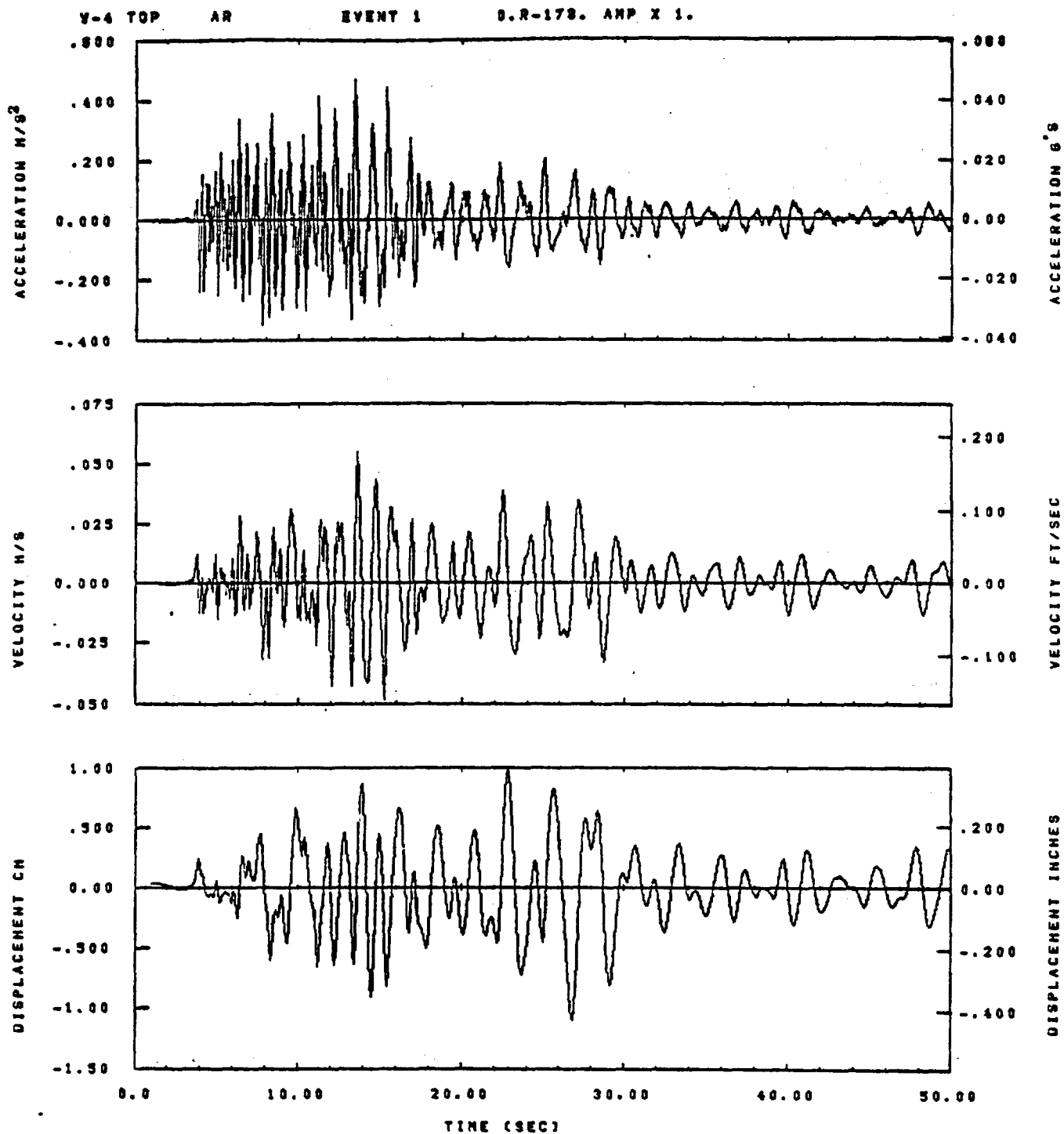


IDT= .0005	ODT=	FIX=	AAS= 0.
HPF= .3	BYH= .20	HLH= 667	ASB=
LPF= 27.	BYL= 6.	HLL= 1989	ASE=
VTS= .30	VTE= .200	FLL= -20.	VSE= 0.
OPB= 0.	DPE= 100.	PLH= 0	DSE= 0.

10.45.28.

07/06/02

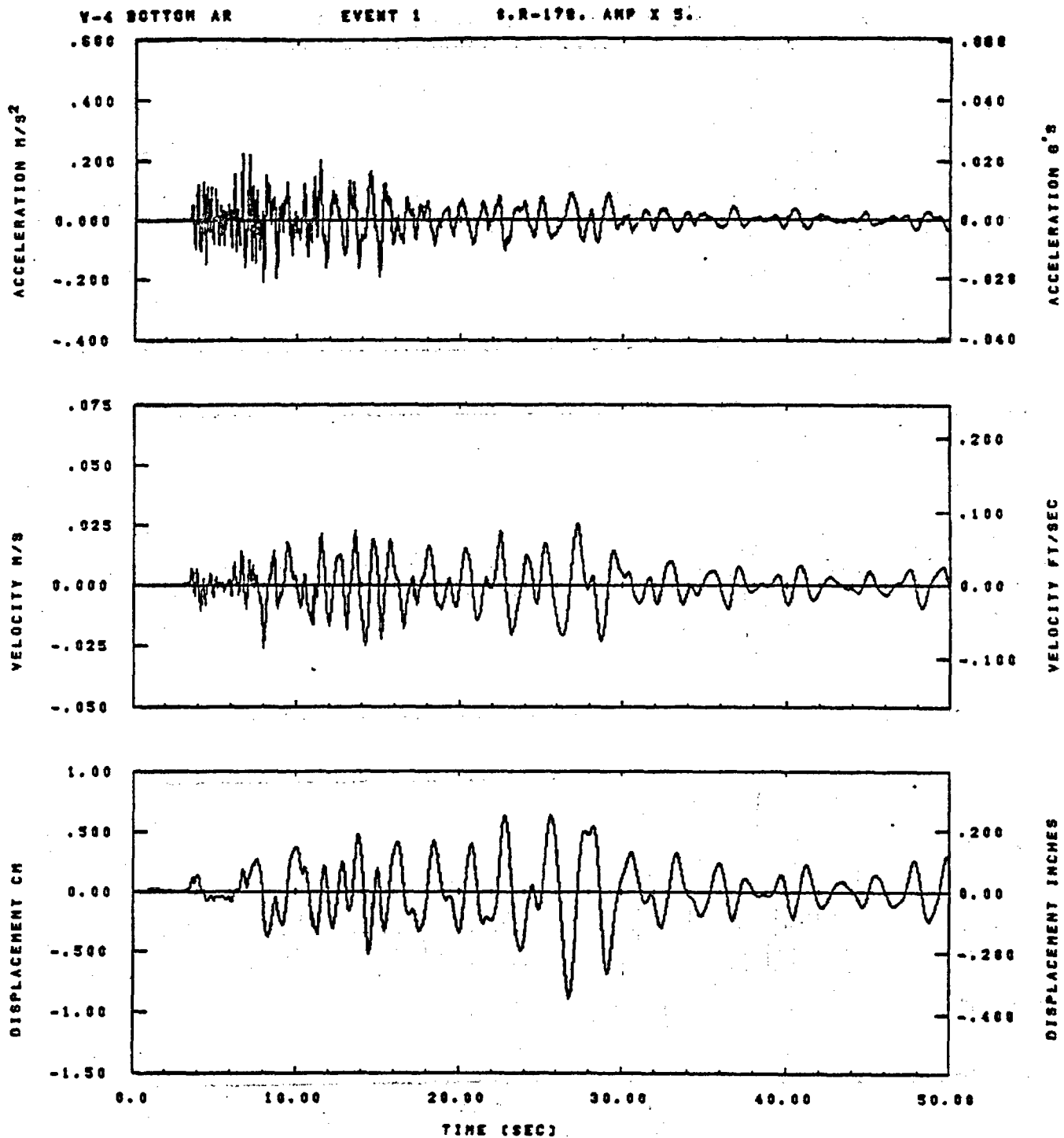
Figure D-20



IDT= .0085	ODT=	FIX=	AAS= 0.
HPP= .3	BYH= .20	HLH= 867	ASS=
LPP= 27.	BYL= 8.	HLL= 1999	ASE=
VTS= .30	VTE= .200	FLL= -20.	VSE= 0.
DPS= 0.	DPE= 100.	FLH= 0	DSE= 0.

09.30.48.

07/08/92

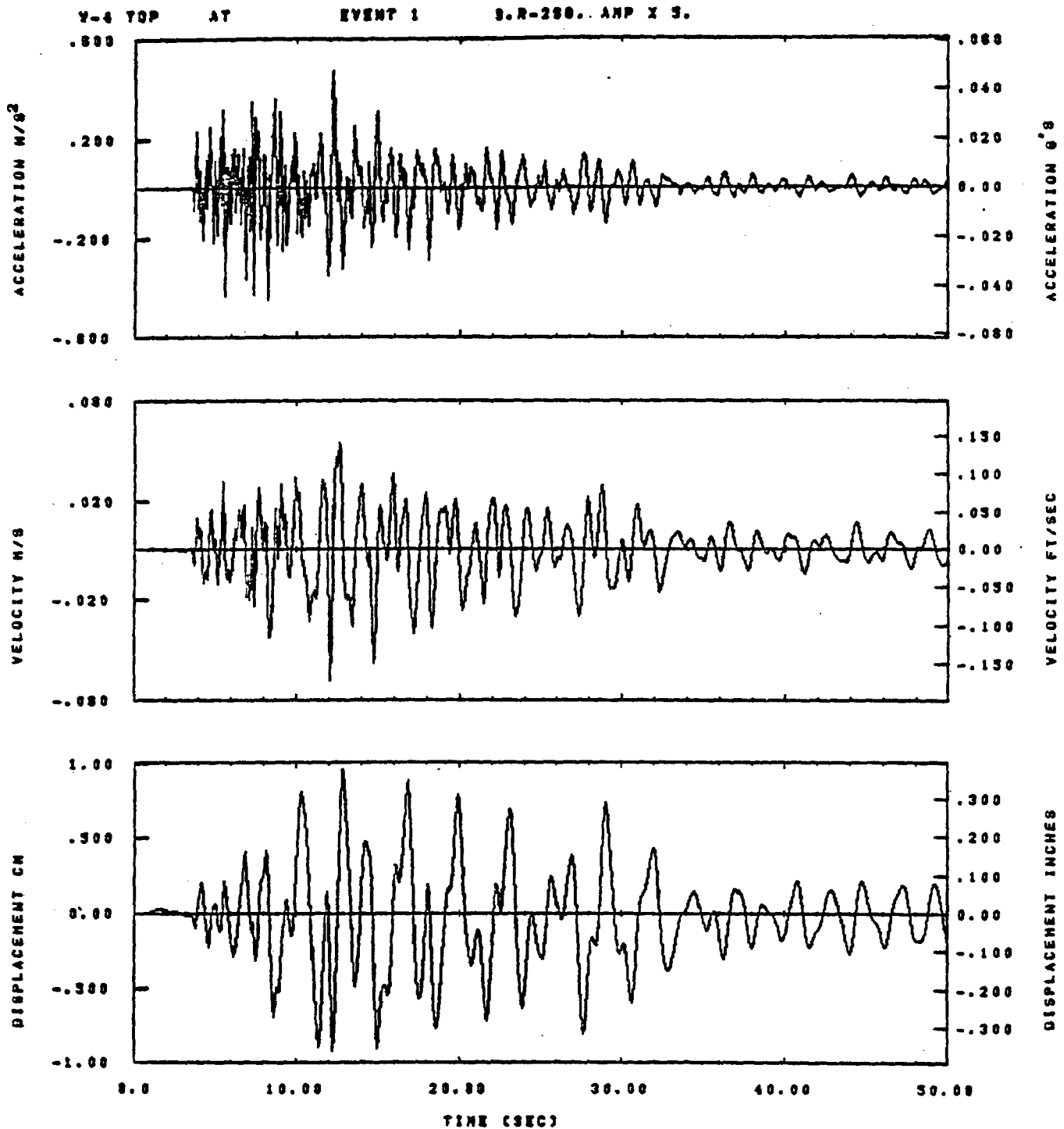


IDT= .0005	ODT=	FIX=	AAS= 0.
HPF= .3	EVH= .20	HLH= 667	ASS=
LFF= 27.	SVL= 6.	HLL= 1988	ASE= ②
VTS= .30	VTE= .200	FLL= -20.	VSE= 0.
DPS= 0.	DPE= 100.	FLH= 0	DSE= 0.

10.45.32.

07/05/82

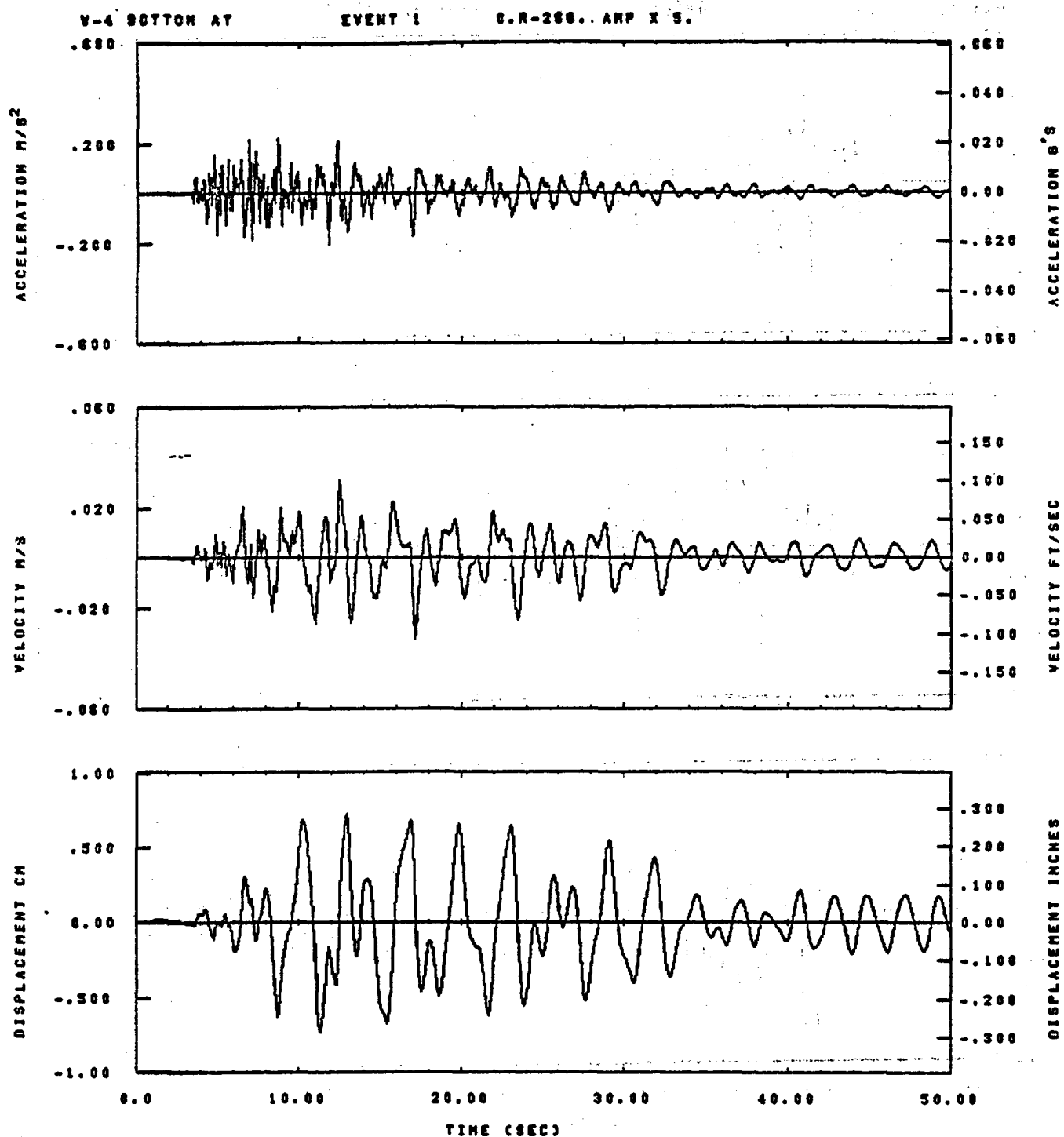
Figure D-22



IDT= .0003	ODT=	FIX=	AAS= 0.
HPP= .3	BYN= .20	HLH= 887	ASB=
LPP= 27.	BYL= 8.	HLL= 1339	ASE=
VTB= .38	VTE= .200	FLL= -20.	VSE= 0.
DPS= 0.	DPE= 100.	FLH= 0	DSE= 0.

09.30.33.

07/08/82

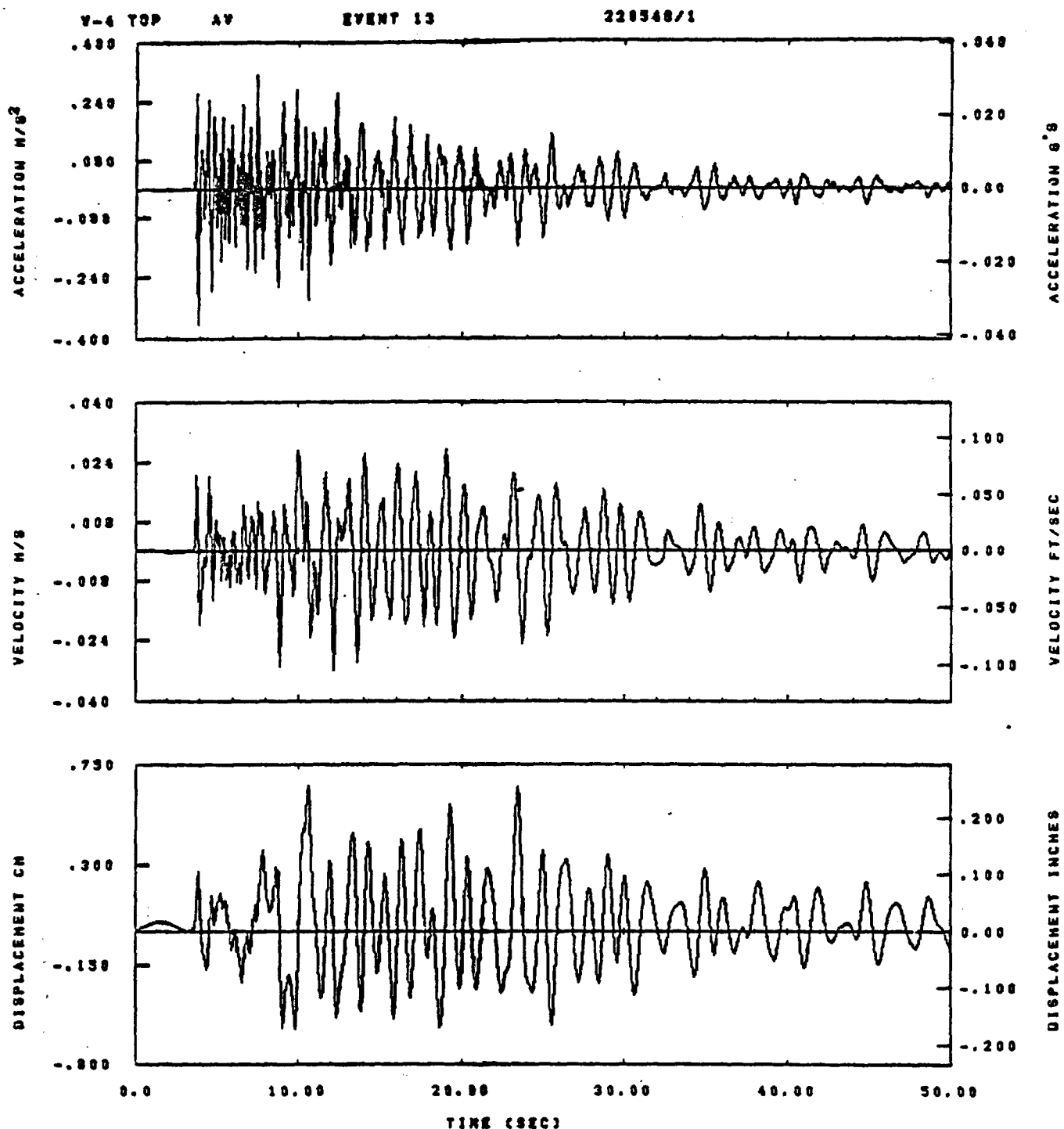


IDT=	.0005	ODT=		FIX=		AAS=	0.
HPP=	.3	BYH=	.20	HLH=	667	ASB=	.
LPP=	27.	BYL=	6.	HLL=	1888	ASE=	
VTB=	.30	YTE=	.200	FLL=	-20.	VSE=	0.
OPB=	0.	OPE=	100.	FLH=	0	DSE=	0.

10.45.38.

87/88/82

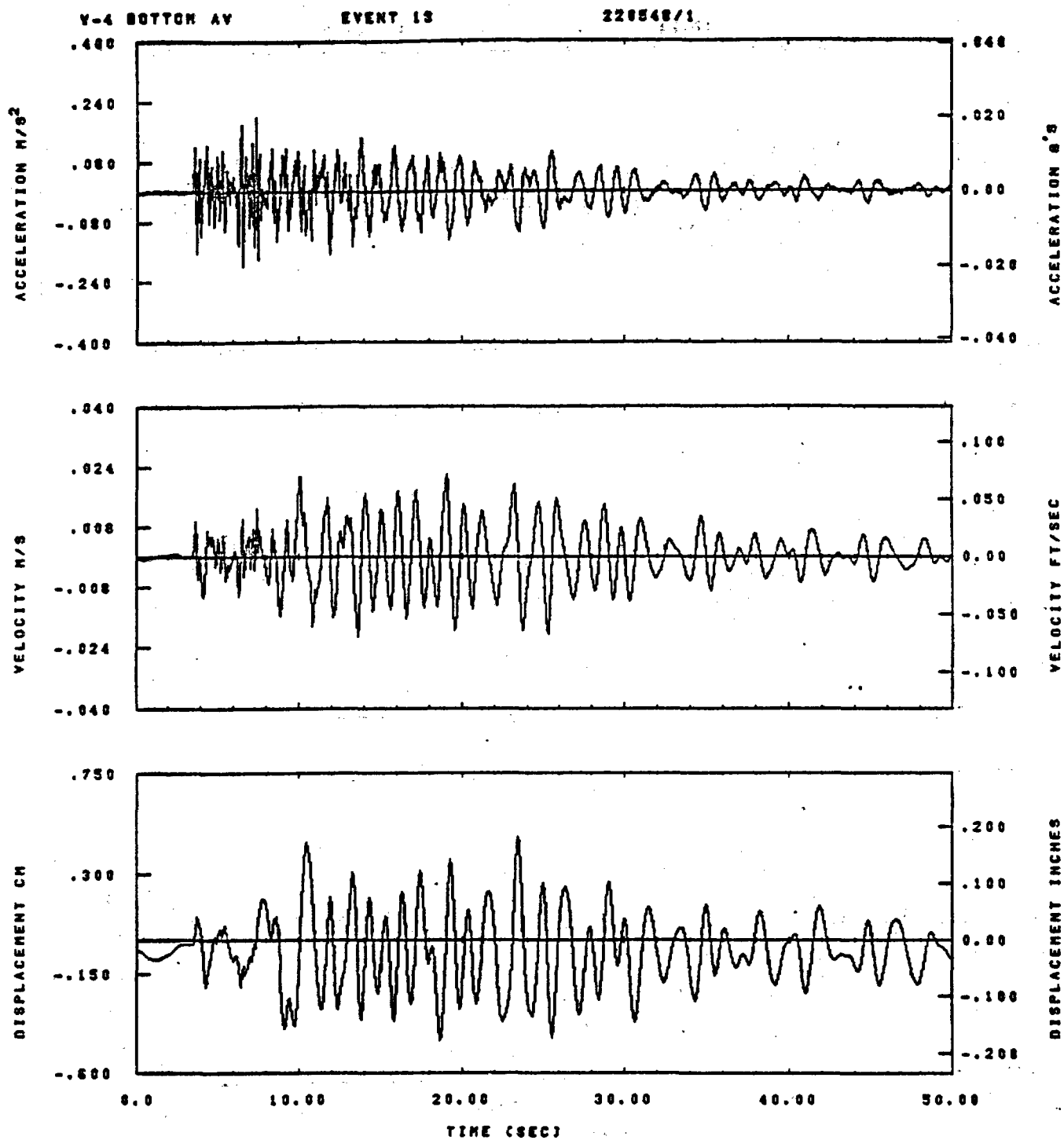
Figure D-24



IGT= .0020	ODT= .003	FIX=	AAS= 0.
HPF= .3	SVH= .20	HLH= 201	ASB=
LPF= 22.	SVL= 5.	HLL= 1999	ASE=
VTB= .38	VTE= .200	FLL= -20.	VSE= 0.
DPS= 0.	DPE= 100.	FLH= 0	DSE= 0.

13.48.27.

07/09/82

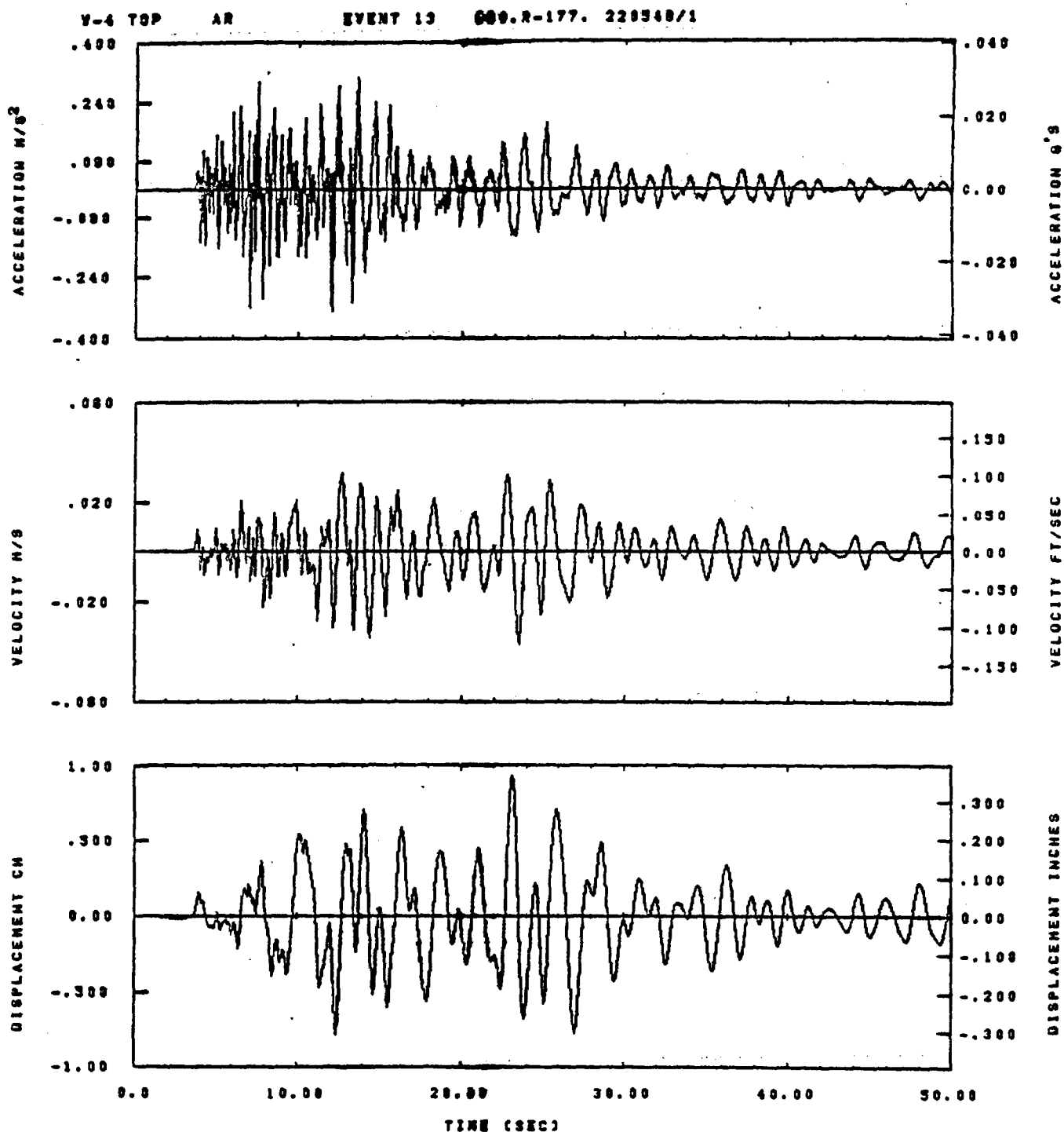


IOT= .0020	ODT= .005	FIX=	AAS= 4.
HPP= .3	BYH= .20	HLH= 201	ASB=
LPP= 22.	BYL= 5.	HLL= 1338	ASE=
VTB= .30	VTE= .200	FLL= 0.	VSE= 4.
DPS= 4.	DPE= 100.	FLH= 4	DSE= 0.

13.44.45.

07/08/82

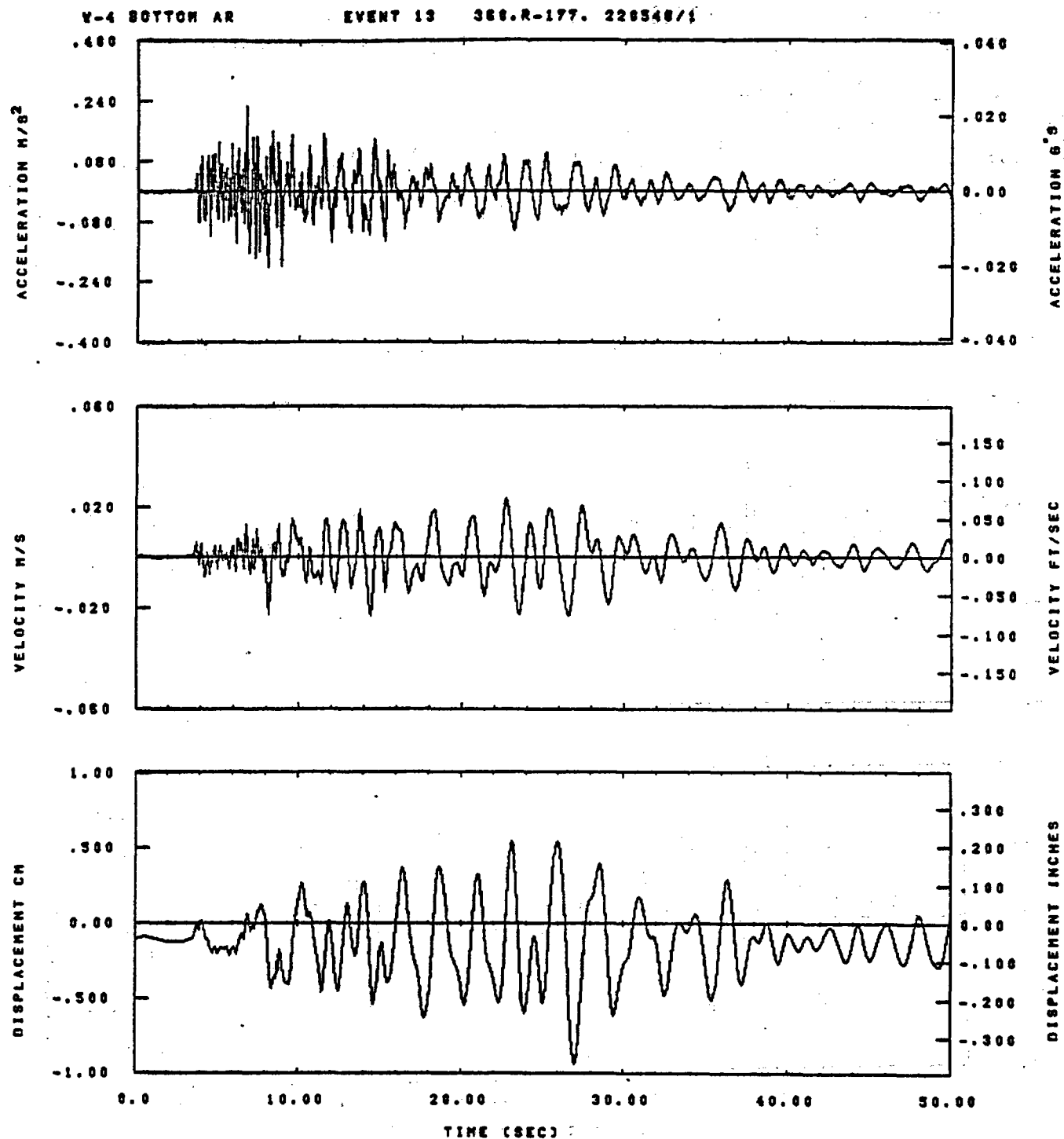
Figure D-26



IDT= .0020	ODT= .003	FIX=	AAS= 0.
HPP= .3	BYM= .20	HLH= 201	ASS=
LPP= 22.	BVL= 5.	HLL= 1999	ASE=
VTS= .30	VTE= .200	FLL= -20.	VSE= 0.
DPS= 0.	DPE= 100.	FLH= 0	DSE= 0.

13.48.34.

07/09/82

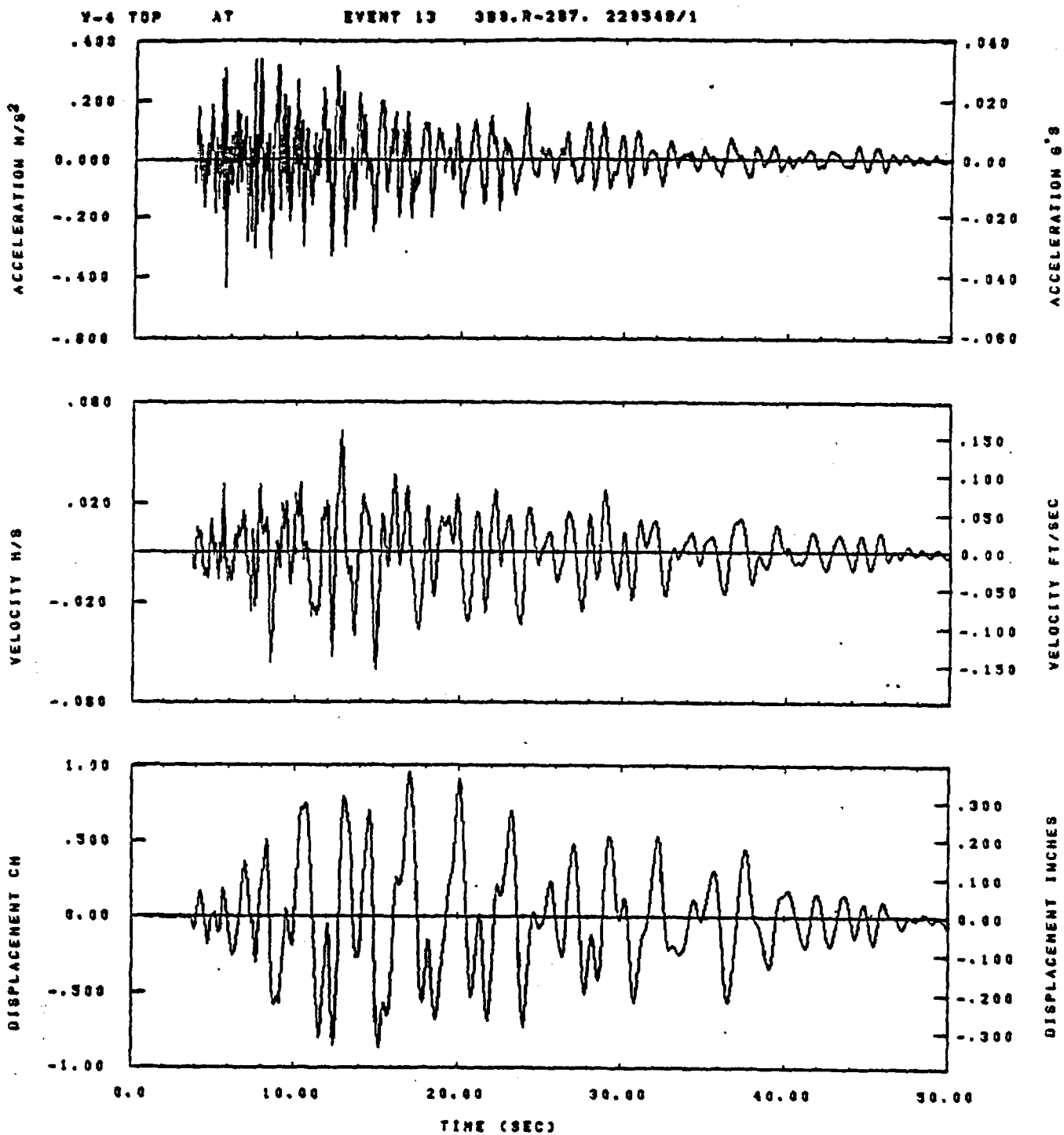


IDT= .0020	ODT= .005	FIX=	AAS= 4.
HPF= .3	BYH= .20	HLH= 201	ASS=
LPF= 22.	BYL= 3.	HLL= 1988	ASE=
VTS= .30	VTE= .200	FLL= 0.	VSE= 4.
DPS= 4.	DPE= 100.	FLH= 4	OSE= 0.

13.44.51.

07/08/82

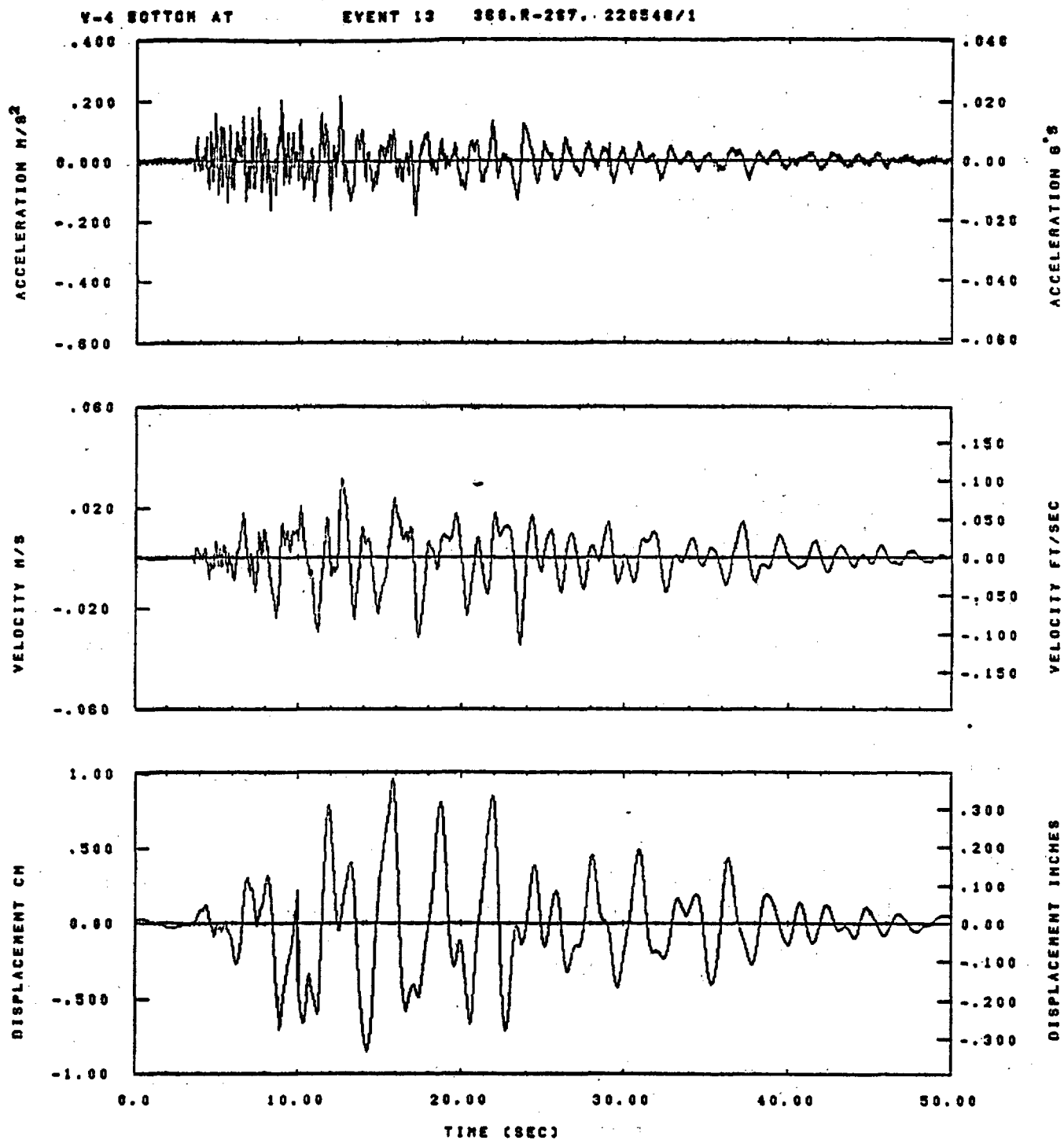
Figure D-28



IDT= .0028	ODT= .003	FIX=	AAS= 0.
HPP= .3	BYH= .20	HLH= 201	ASB=
LPP= 22.	BYL= 5.	HLL= 1399	ASE=
VTB= .38	VTE= .200	FLL= -20.	VSE= 0.
DPS= 0.	DPE= 100.	FLH= 0	DSE= 0.

13.48.41.

07/09/82

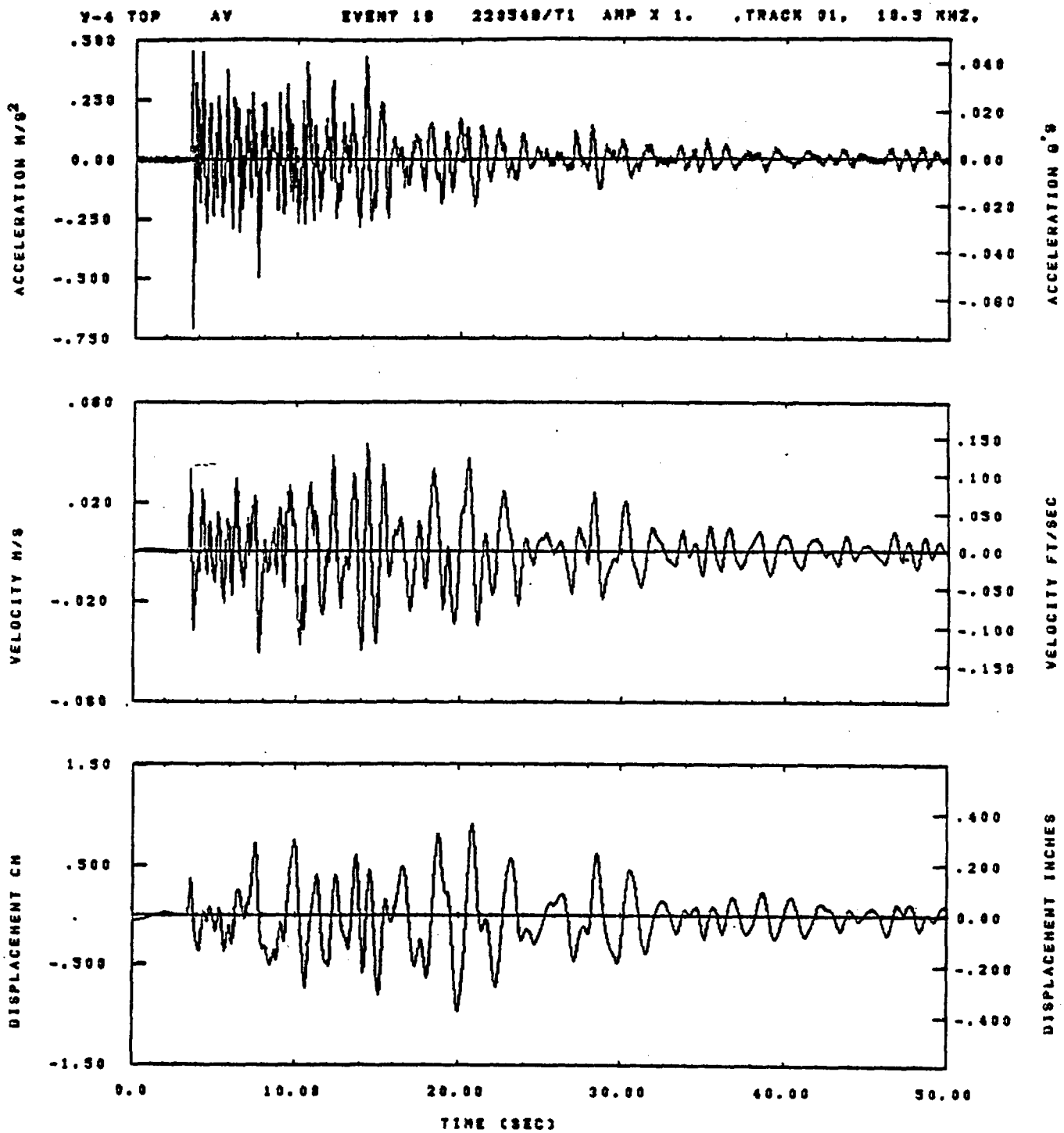


IDT= .0020	ODT= .005	FIX=	MIN=
HPF= .3	BVH= .20	HLH= 201	MAX=
LPF= 22.	BVL= 5.	HLL= 1999	AZH=
YTB= .30	YTE= .200	FLL= -10.	RNG=
OPB= 0.	OPE= 100.	FLH= 0	MLT=

15.24.02.

06/06/82

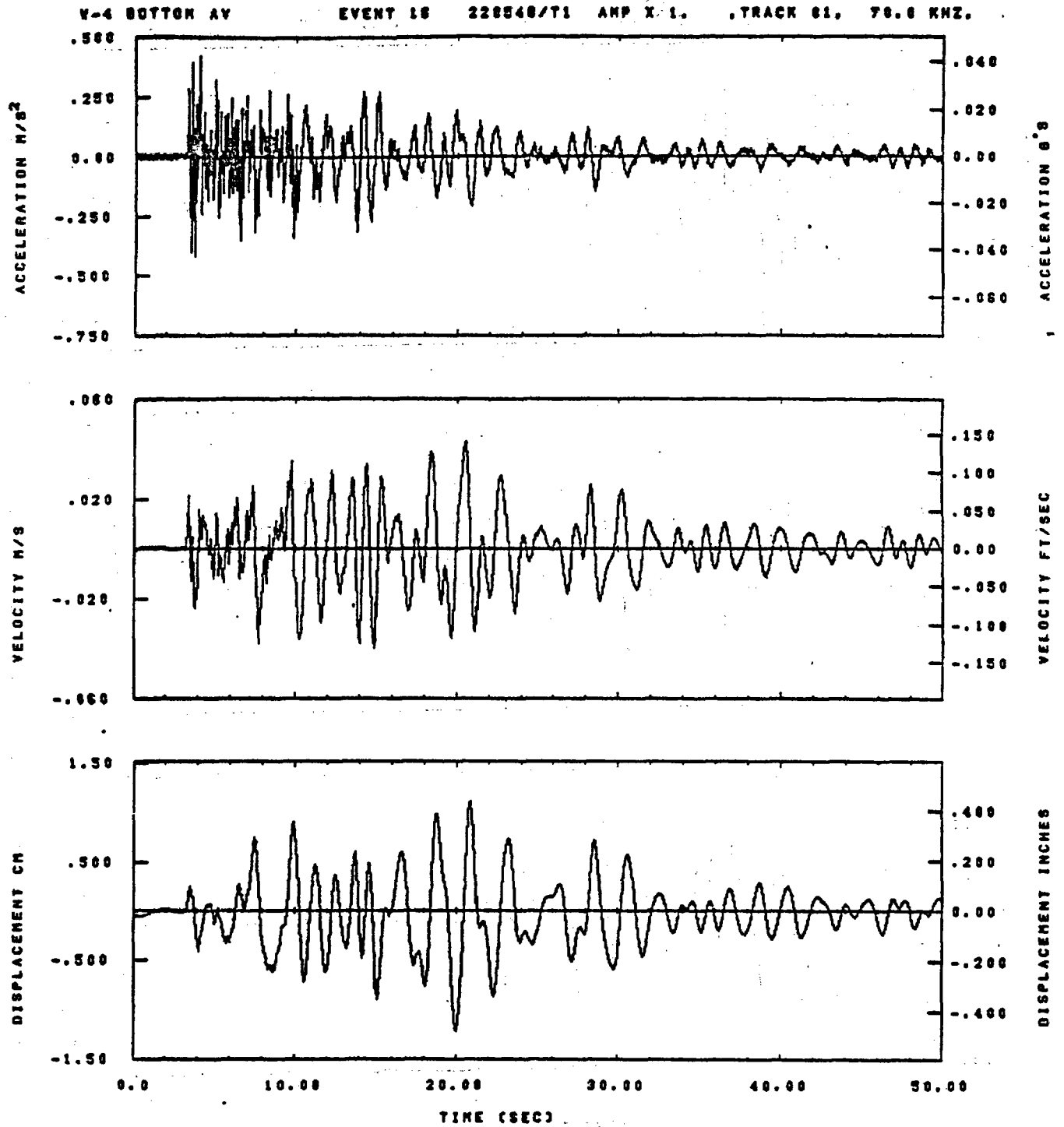
Figure D-30



IDT= .0020	ODT= .005	FIX=	AAS= 0.
HPP= .20	BYN= .13	MLN= 231	ASS=
LPP= 18.	BYL= 4.	MLL= 2399	ASE=
VTS= .200	VTE= .133	FLL= -20.	VSE= 0.
OPS= 0.	OPE= 100.	FLN= A-.1	DSE= A+.1

14.08.22.

07/02/92

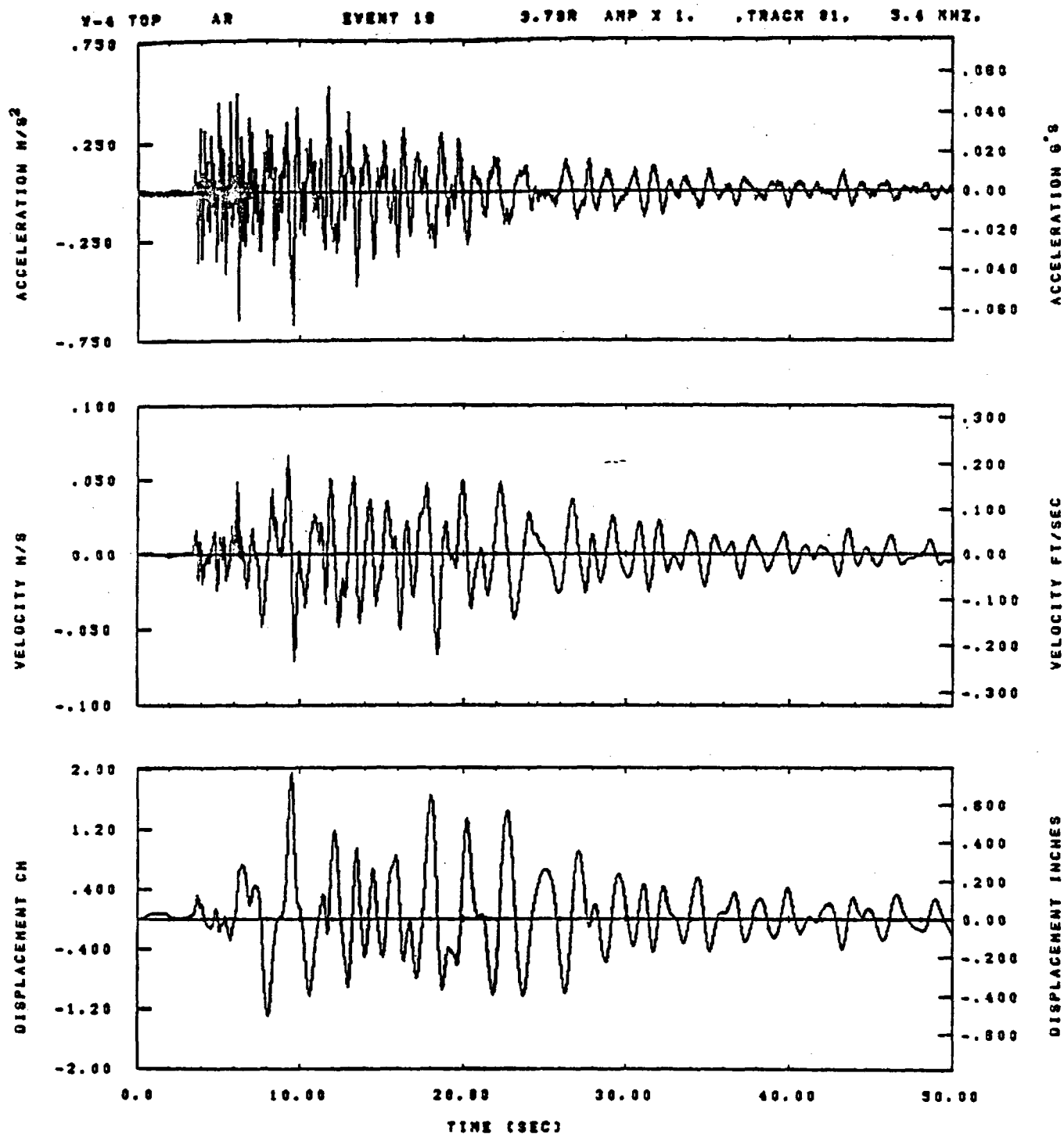


IDT= .0020	QDT= .005	FIX=	AAS= 0.
NPF= .20	BYH= .13	HLH= 251	ASB=
LPF= 18.	BYL= 4.	HLL= 2988	ASE=
VTS= .200	VTE= .133	FLL= -17.	VSE= 0.
DPS= 0.	DPE= 100.	FLH= A-.1	DSE= A+.1

14.08.41.

07/02/82

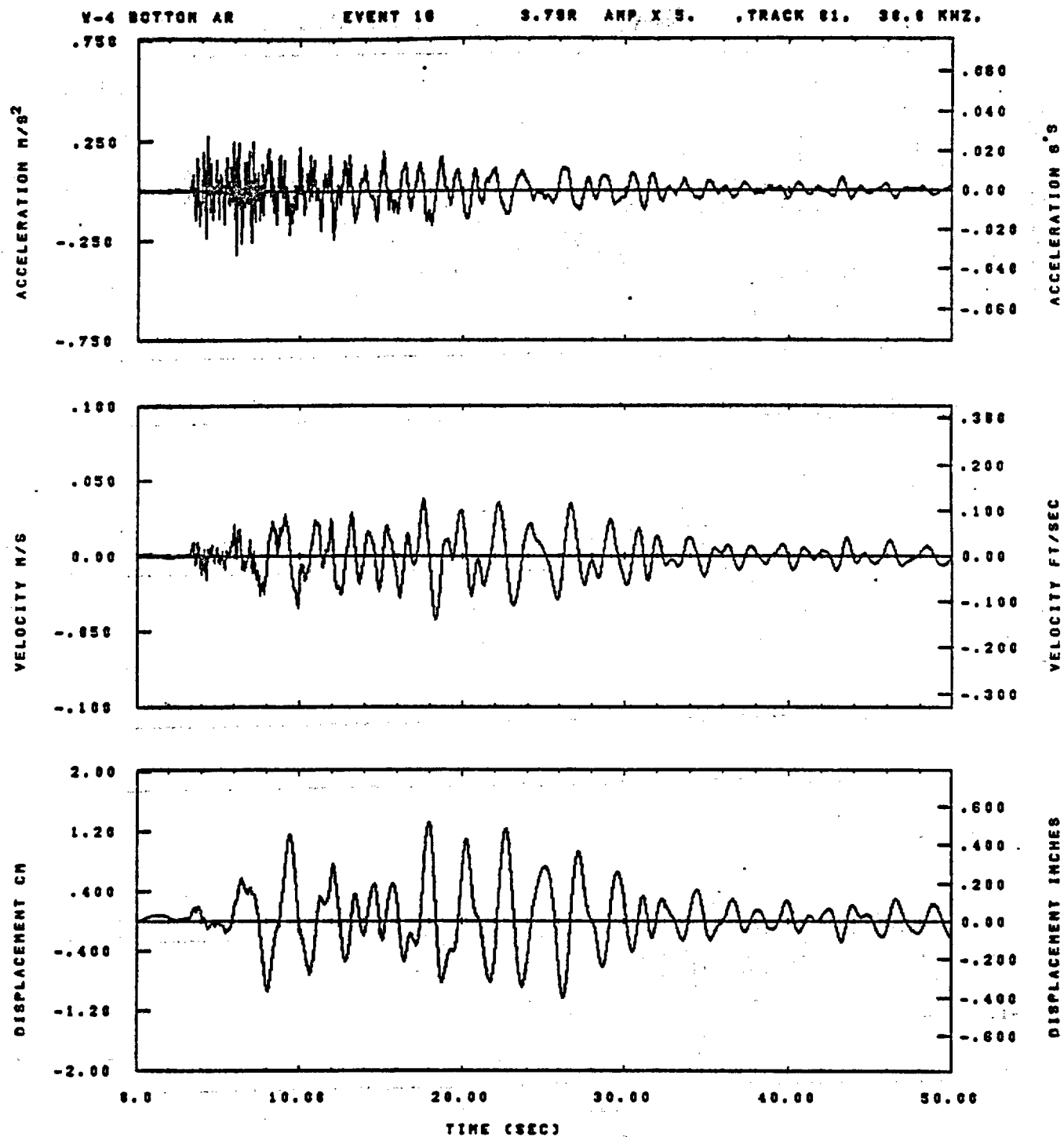
Figure D-32



IDT= .0020	ODT= .003	FIX=	AAS= 0.
HPP= .20	BYN= .13	HLN= 251	ASS=
LPP= 19.	BYL= 4.	HLL= 2999	ASE=
VTB= .200	VTE= .133	FLL= -20.	VSE= 0.
OPB= 0.	DPE= 100.	FLH= A-.1	DSE= A+.1

14.08.25.

07/02/82

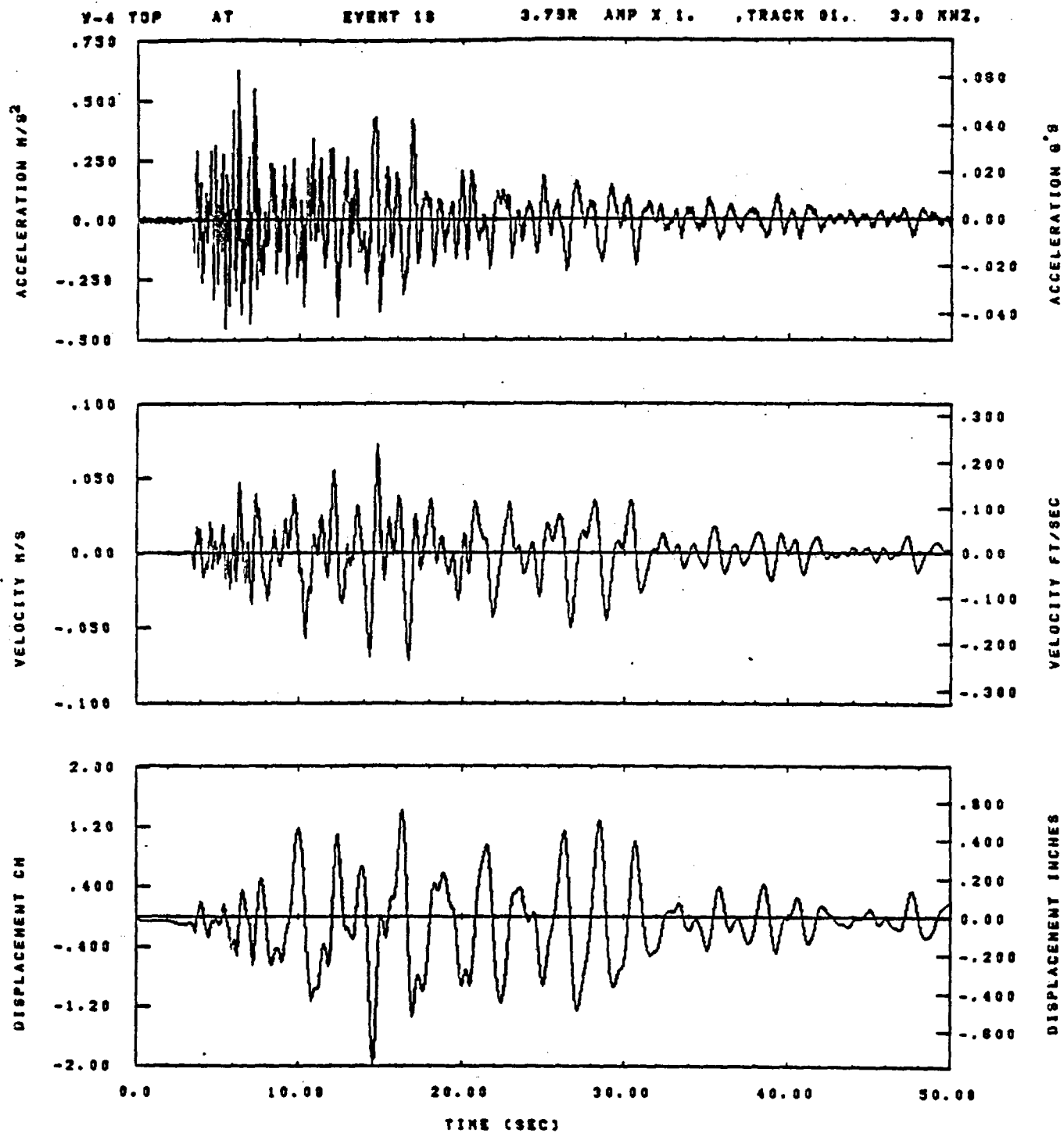


IDT= .0028	QDT= .005	FIX=	AAS= 0.
MPF= .20	BNH= .13	MLH= 251	ASB=
LPF= 10.	BVL= 4.	NLL= 2888	ASE=
VTB= .200	VTE= .133	FLL= -17.	VSE= 0.
DPS= 0.	DPE= 100.	FLH= A-.1	DSE= A+.1

14.08.45.

07/02/82

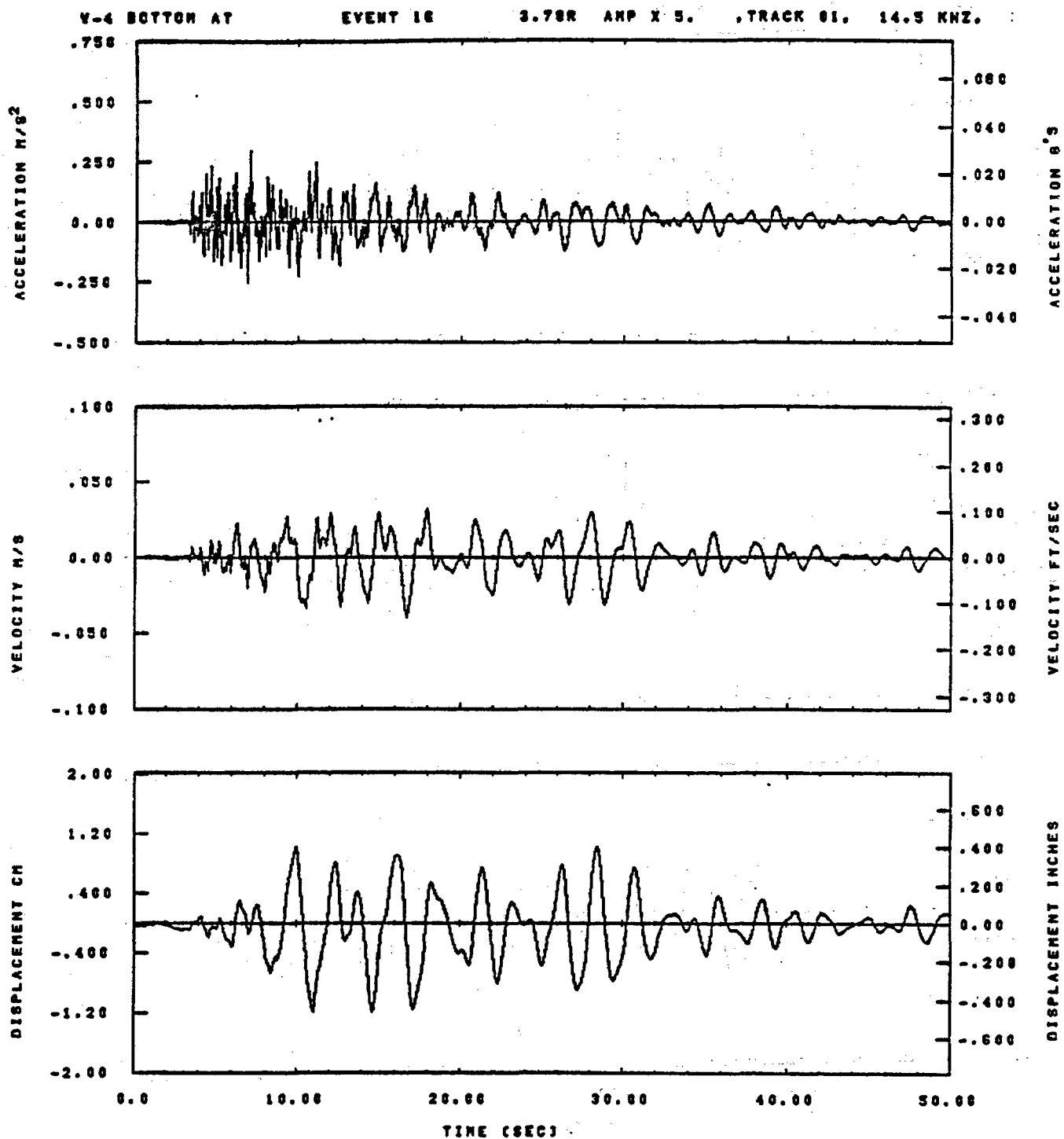
Figure D-34



IDT= .0020	ODT= .005	FIX=	AAS= 0.
HPP= .20	SVH= .13	HLH= 251	ASB=
LPP= 18.	SVL= 4.	HLL= 2889	ASE=
VTS= .208	VTE= .133	FLL= -20.	VSE= 0.
GPS= 0.	GPE= 100.	FLH= A-.1	DSE= A+.1

14.08.28.

07/02/92

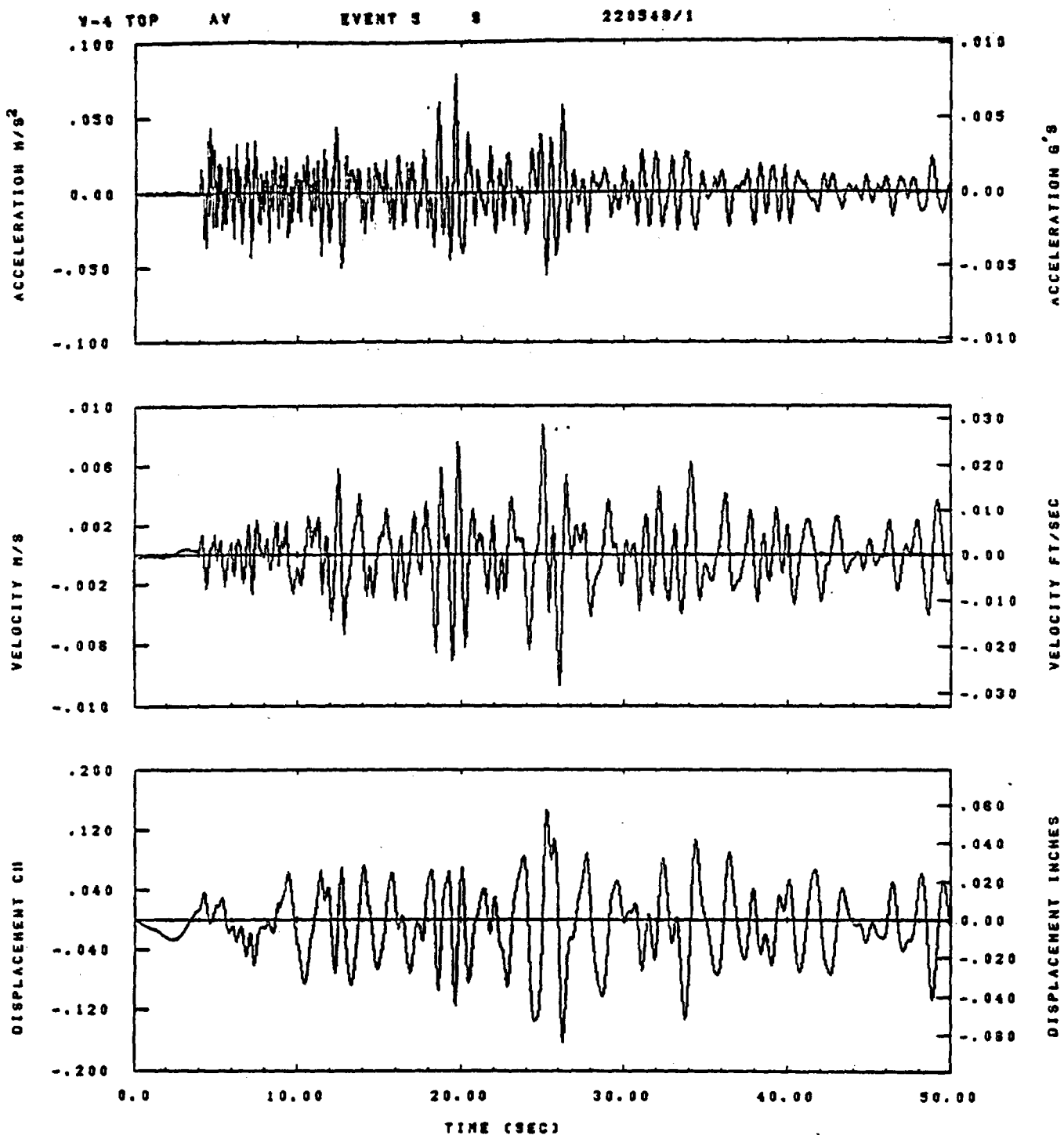


IDT= .0020	GDT= .005	FIX=	AAS= 0.
HPF= .20	BVM= .13	MLH= 251	ASB=
LPF= 18.	BYL= 4.	MLL= 2998	ASE=
VTS= .200	VTE= .133	FLL= -17.	VSE= 0.
DPS= 0.	DPE= 100.	FLH= A-.1	DSE= A+.1

14.08.48.

07/02/02

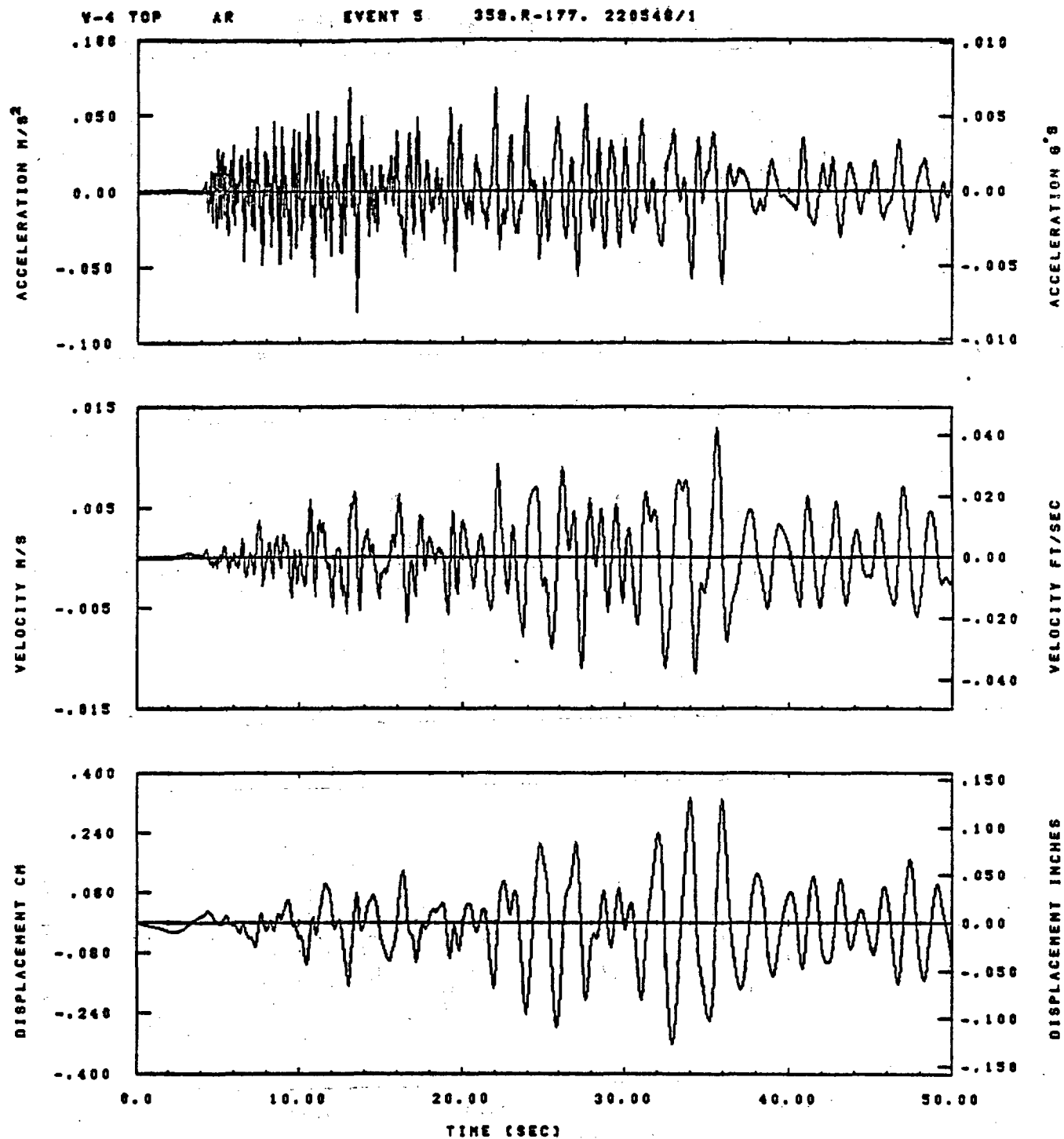
Figure D-36



IDT= .0020	ODT= .005	FIX=	AAS= 0.
HPF= .20	SVH= .13	HLH= 167	RNG=
LPF= 27.	SVL= 8.	HLL= 2999	AZN=
VTS= .200	VTE= .133	FLL= -20.	VSE= 0.
DPS= 0.	DPE= 100.	FLH= A-.1	HLT= 1A00

09.38.06.

07/20/82

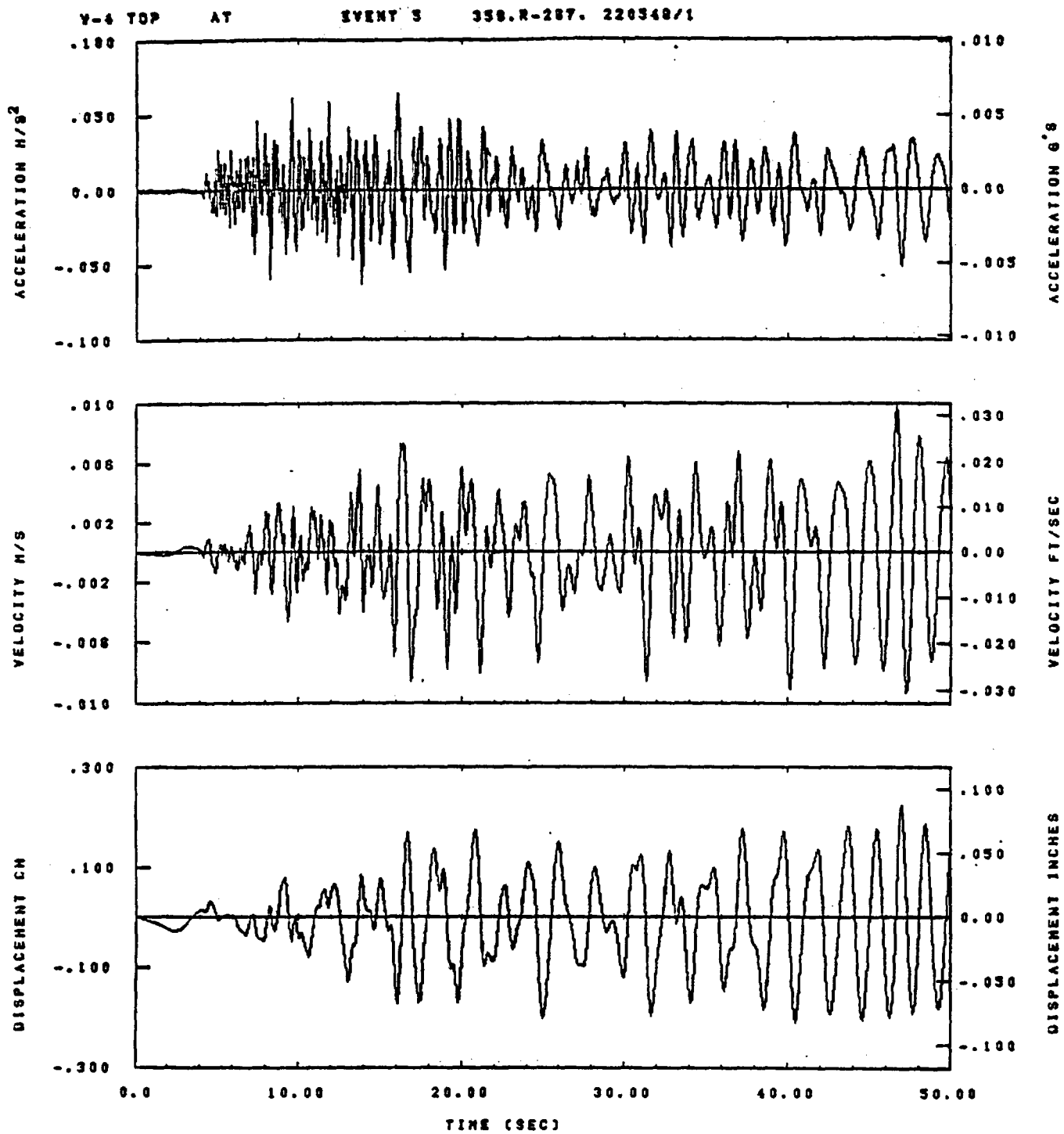


IDT= .0020	ODT= .005	FIX=	AAS= 0.
HPP= .20	SVH= .13	MLH= 167	RNS=
LPP= 27.	SVL= 6.	MLL= 2388	AZN=
YTB= .200	VTE= .133	FLL= -20.	VSE= 0.
DPS= 0.	DPE= 100.	FLH= A-.1	MLT= 1A00

09.38.12.

07/28/82

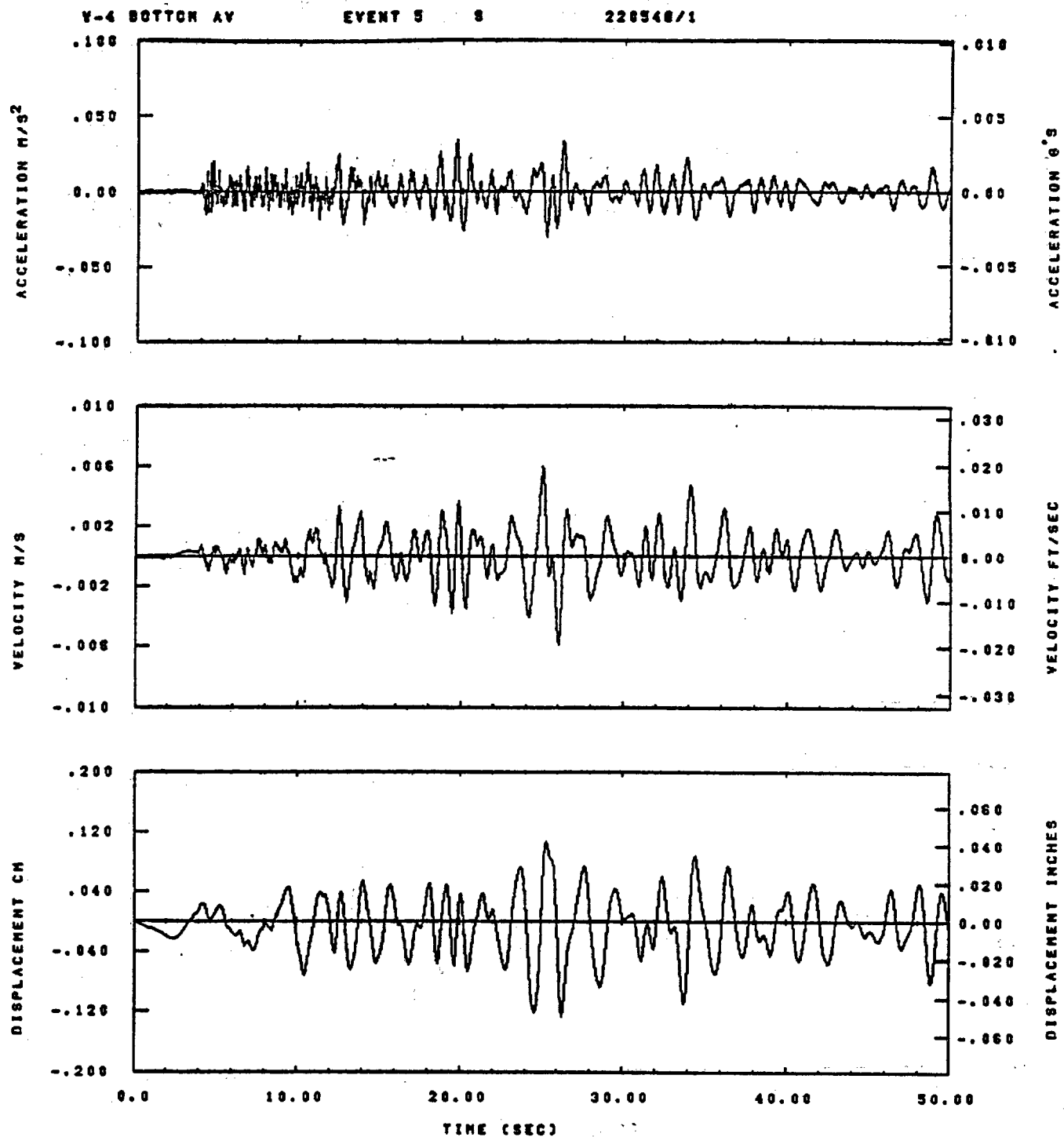
Figure D-38



IDT= .0020	ODT= .005	FIX=	AAS= 0.
HPP= .20	BYN= .13	HLH= 187	RNG=
LPP= 27.	BYL= 8.	HLL= 2999	AZN=
VTS= .208	YTE= .133	FLL= -20.	VSE= 0.
DPB= 0.	OPE= 100.	FLH= A-.1	MLT= 1A00

09.38.17.

07/20/82

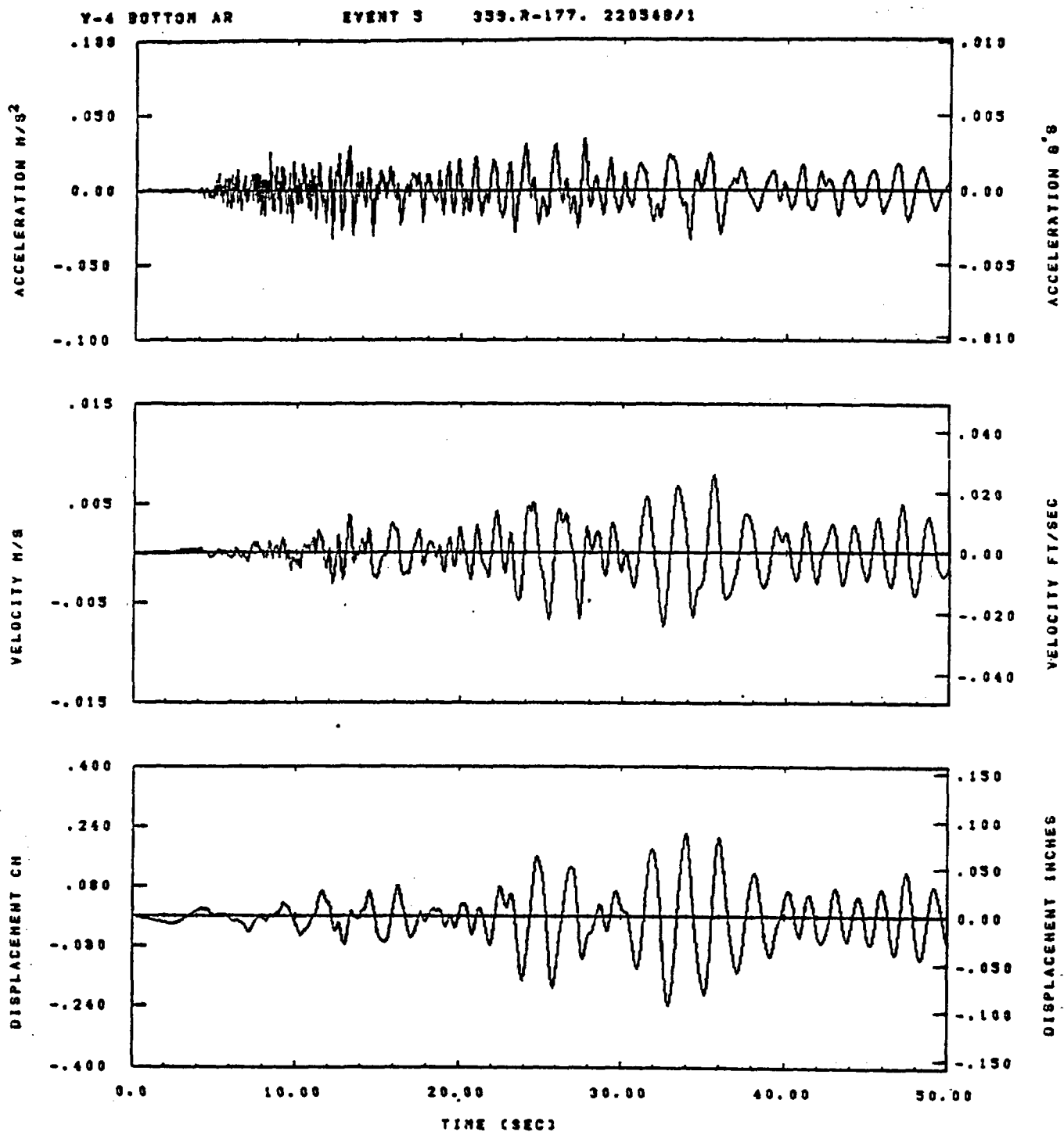


IDT= .0020	ODT= .005	FIX=	AAS= 0.
HPP= .20	BVH= .13	HLH= 167	RNS=
LPP= 27.	BVL= 6.	HLL= 2998	AZH=
VTS= .200	VTE= .133	PLL= -20.	VSE= 0.
DPS= 0.	DPE= 100.	FLH= A-.1	HLT= 1A00

08.38.35.

07/26/82

Figure D-40

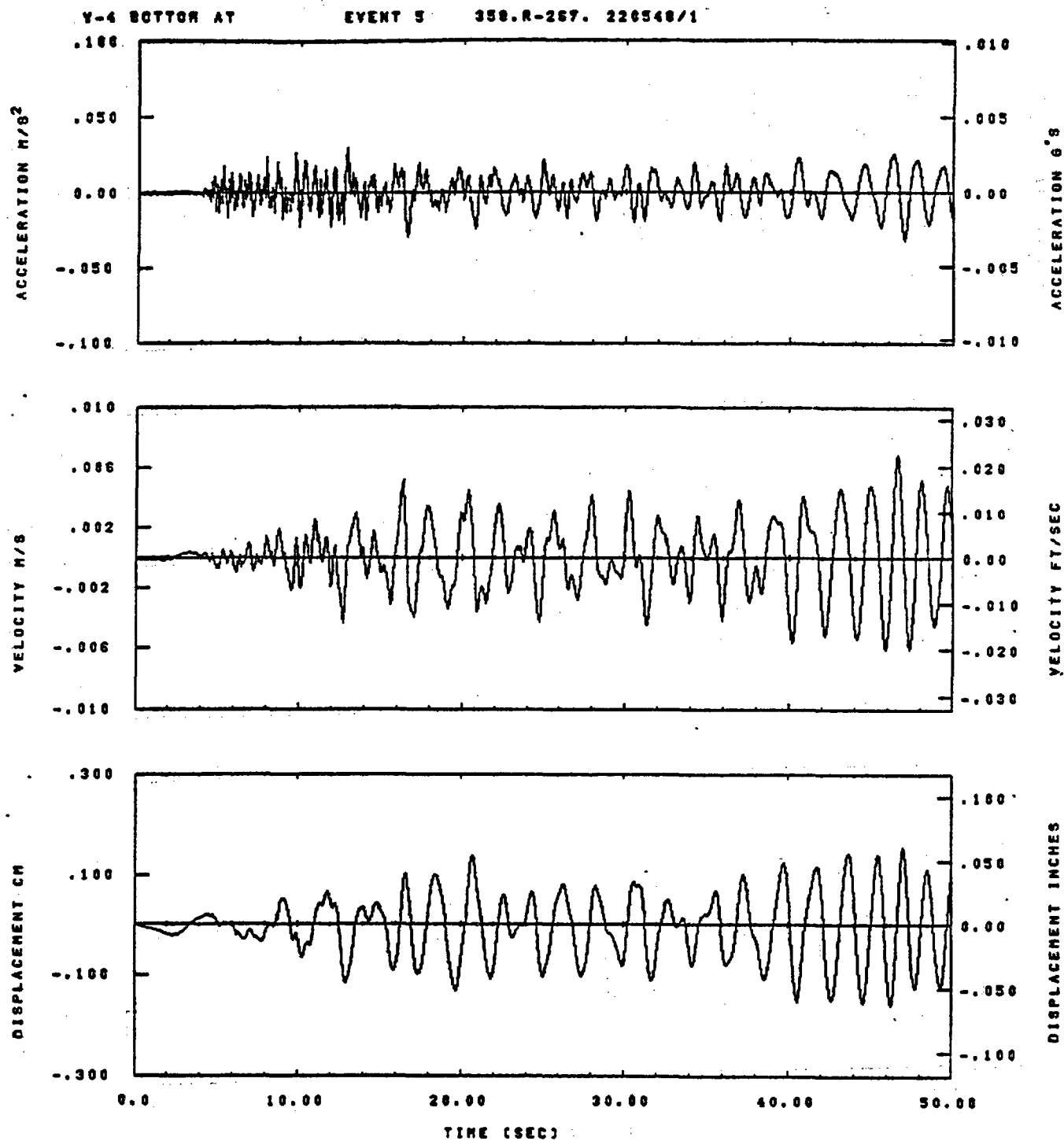


IDT= .0020	ODT= .003	FIX=	AAS= 0.
HPP= .20	SVN= .13	HLN= 187	RNS=
LPP= 27.	SVL= 8.	HLL= 2333	AZN=
VTS= .200	VTE= .133	FLI= -20.	VSE= 0.
OPS= 0.	OPE= 100.	FLH= A-1	MLT= 1A00

09.38.40.

07/20/82

Figure D-41

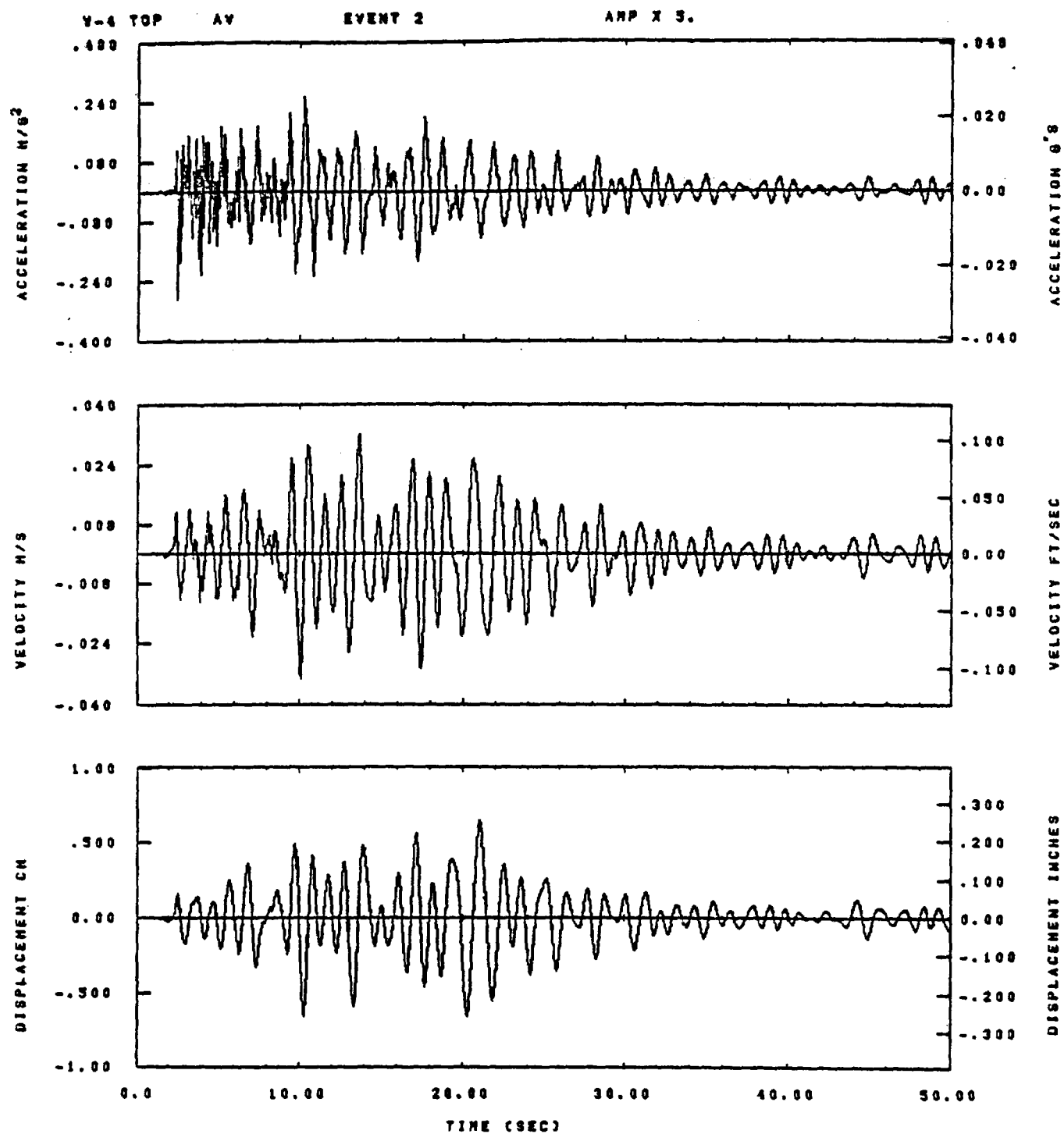


IDT= .0020	QDT= .005	FIX=	AAS= 0.
HPF= .20	BYH= .13	HLH= 167	RNG=
LPF= 27.	BYL= 6.	HLL= 2988	AZN=
YTB= .200	YTE= .133	FLL= -20.	VSE= 0.
DPE= 0.	DPE= 100.	FLH= A-.1	NLT= 1A00

09.38.45.

07/20/82

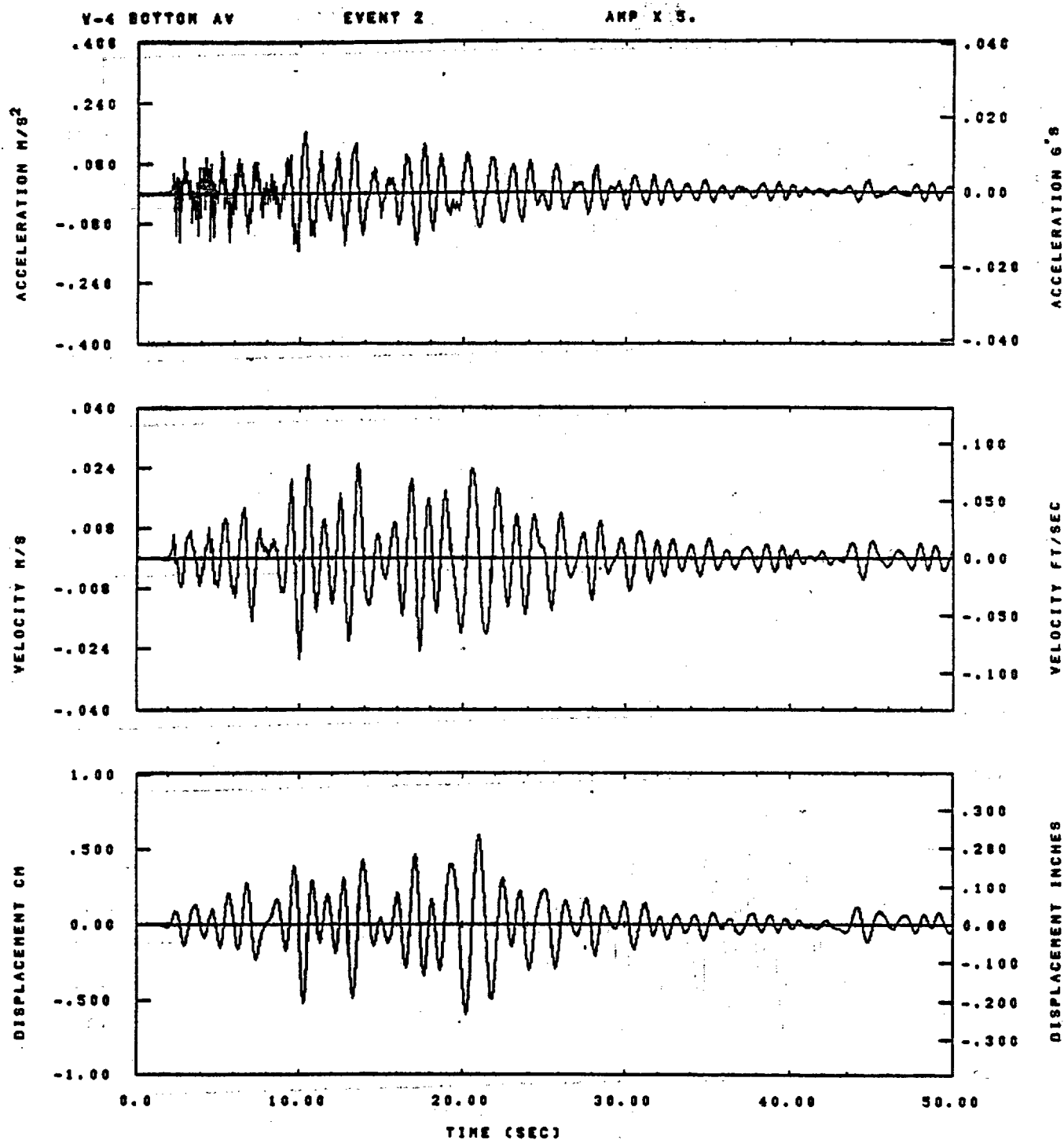
Figure D-42



IGT= 00050	QDT= .0025	FIX= 15	AAS= 0.
HPP= .4	SVH= .2	HLH= 2000	ASB=
LPP= 100.	SVL= 50.	HLL= 0300	ASE=
VTB= .4	VTE= .2	FLL=	VSE=
DPS= -5.	DPE= 80.	FLH= 0.	DSE= .1

00.28.19.

07/13/82

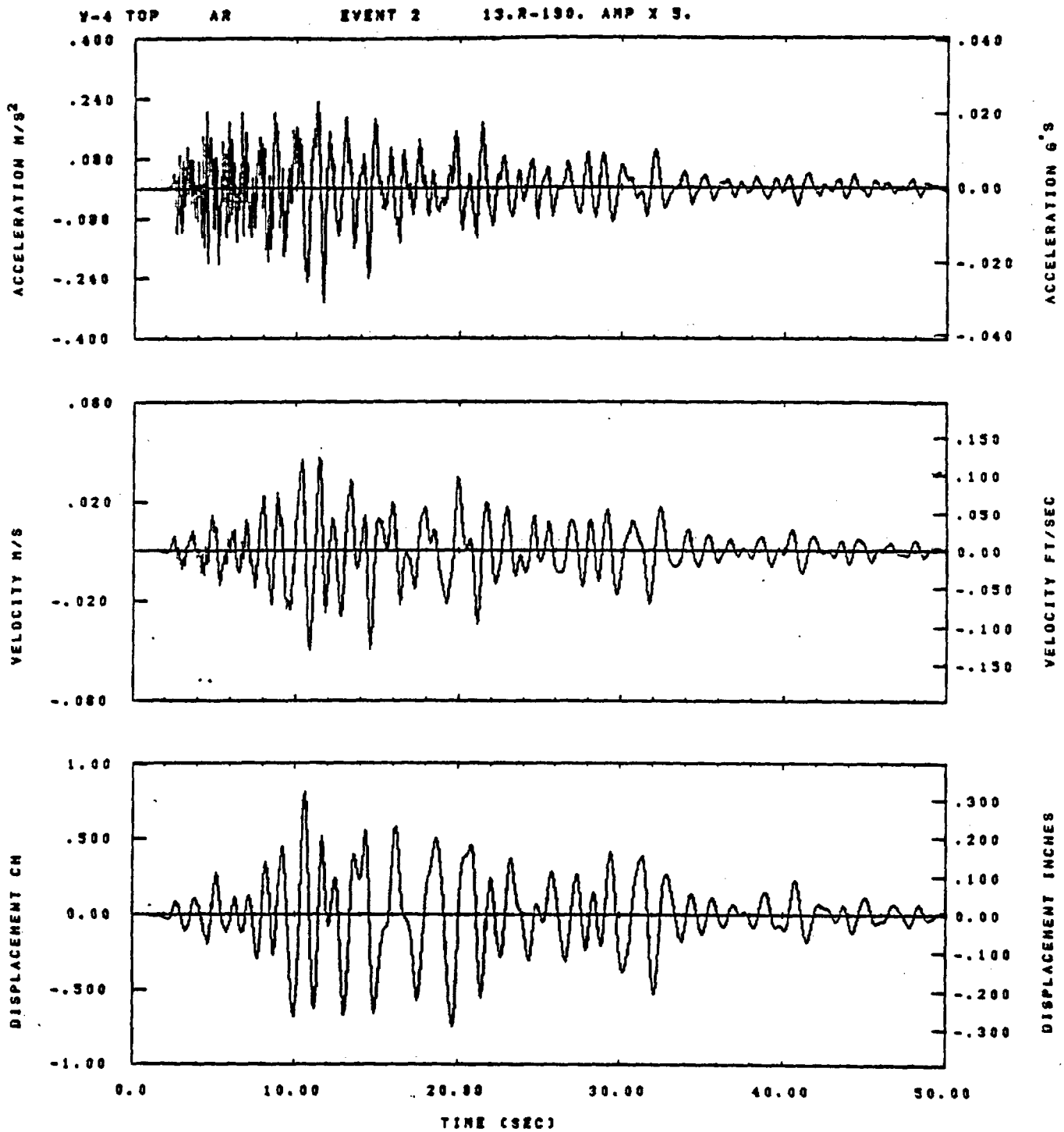


IDT= 00050	QDT= .0025	FIX= 15	AAS= 0.
HPF= .4	BYH= .2	HLH= 2000	ASB=
LPF= 100.	BYL= 50.	HLL= 0300	ASE=
VTB= .4	VTE= .2	FLL=	VSE=
DPS= -5.	DPE= 80.	FLH= 0.	DSE= .1

08.28.12.

07/13/82

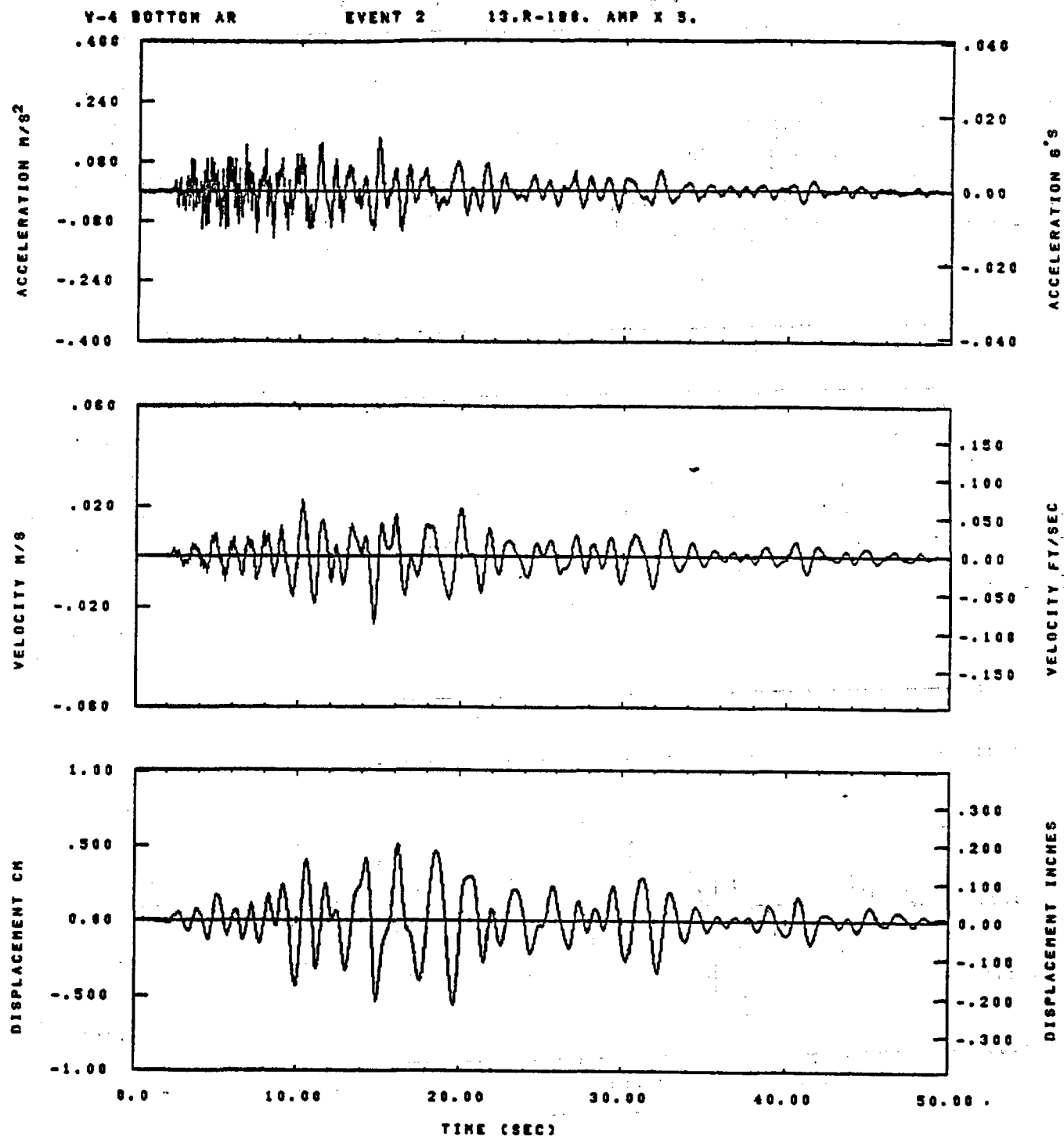
Figure D-44



IDT= 00030	ODT= .0023	FIX= 13	AAS= 0.
HPP= .4	BYM= .2	HLH= 2000	ASB=
LPP= 100.	BYL= 30.	HLL= 0300	ASE=
YTS= .4	YTE= .2	FLL=	VSE=
OPS= -3.	OPE= 80.	FLH= 0.	OSE= .1

08.28.25.

07/13/82

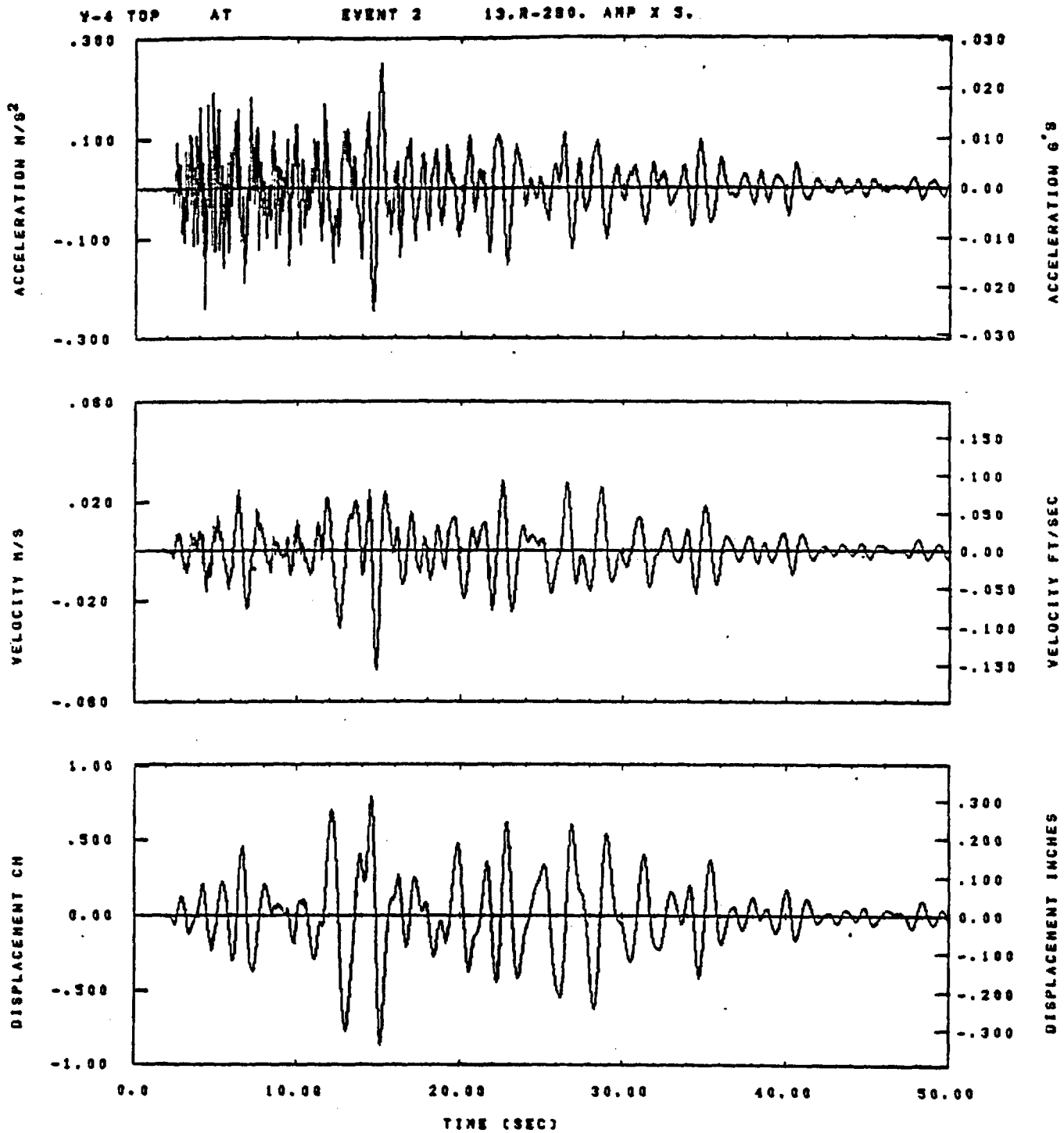


IDT= 00050	ODT= .0025	FIX= 15	AAS= 0.
HPP= .4	BYH= .2	HLH= 2000	ASB= .
LPP= 100.	BYL= 50.	HLL= 0300	ASE= .
VTE= .4	VTE= .2	FLL= .	VSE= .
DPE= -5.	DPE= 66.	FLH= 0.	DSE= .1

08.28.16.

07/13/82

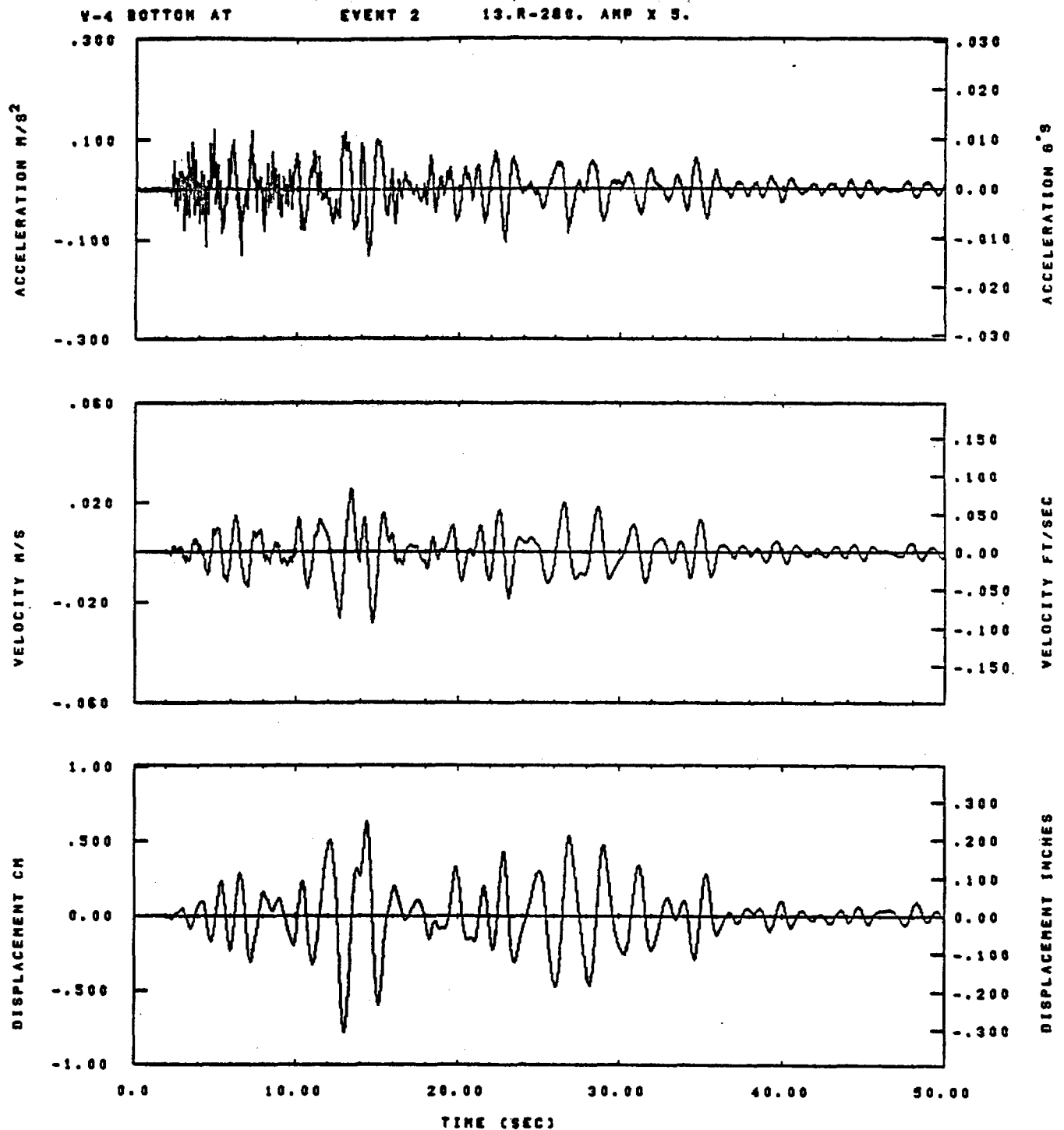
Figure D-46



IDT= 00050	QDT= .0025	FIX= 15	AAS= 0.
HPP= .4	BYH= .2	HLH= 2000	ASS=
LPF= 100.	BYL= 50.	HLL= 0300	ASE=
VTS= .4	VTE= .2	FLL=	VSE=
OPS= -3.	OPE= 80.	FLH= 0.	DSE= .1

08.28.98.

07/13/82



IDT= 08050	QDT= .0025	FIX= 15	AAS= 0.
HPP= .4	BYH= .2	HLH= 2000	ASH=
LPP= 100.	BVL= 50.	HLL= 0300	ASE=
VTS= .4	VTE= .2	FLL=	VSE=
DPE= -5.	DPE= 60.	FLH= 0.	DSE= .1

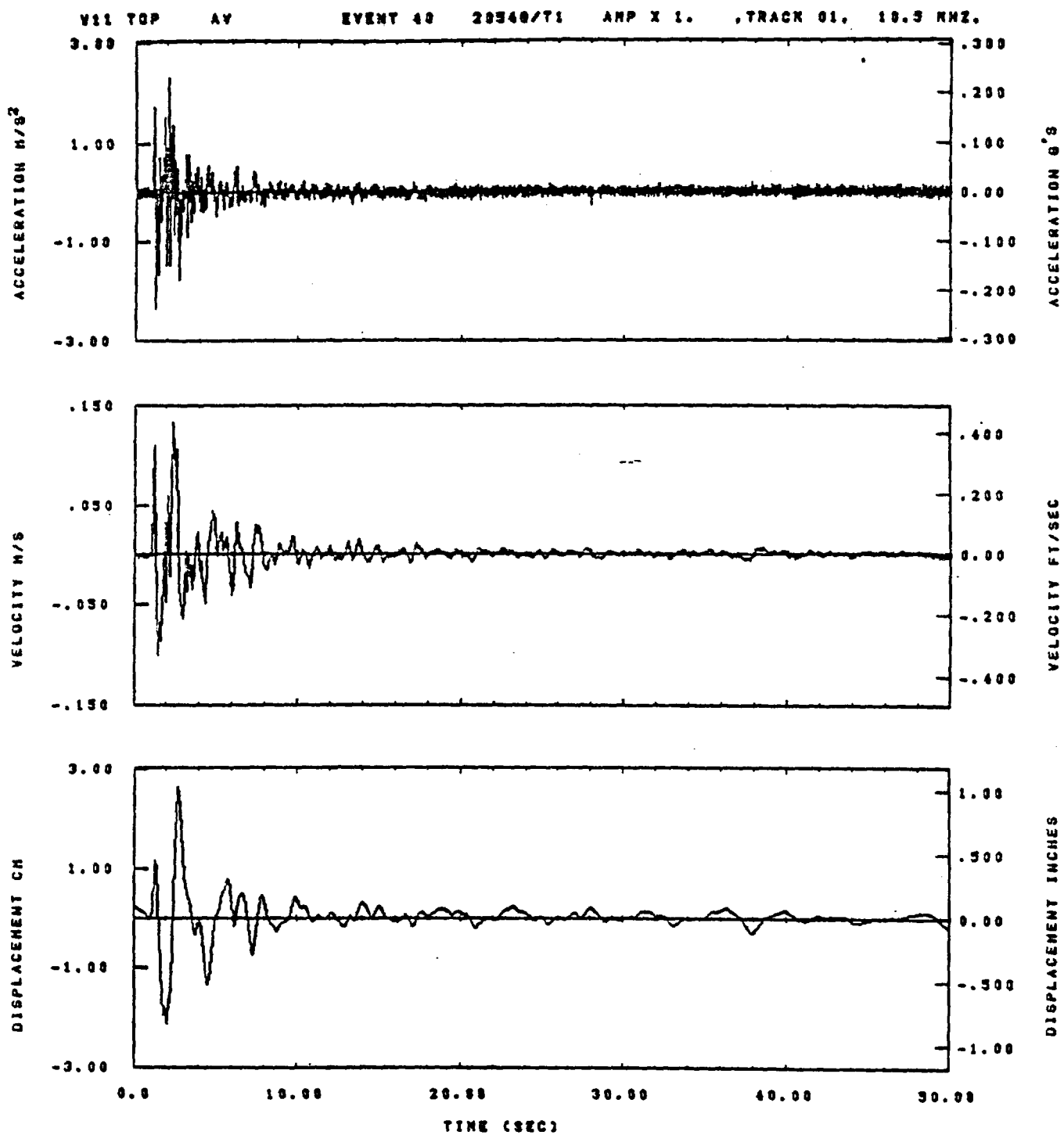
08.28.25.

07/13/82

Figure D-48

APPENDIX E

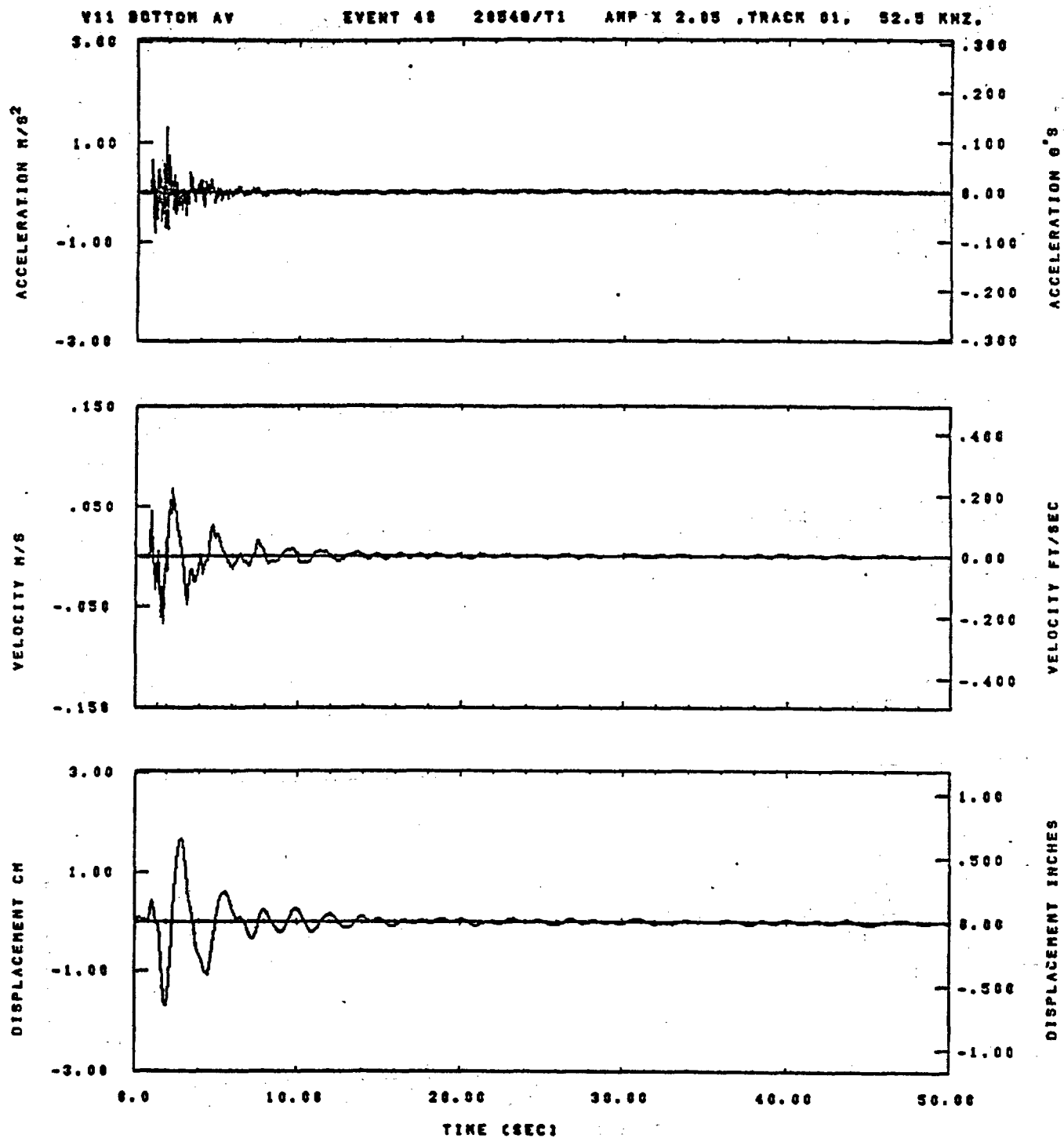
COMPARISON TO TOP AND BOTTOM WAVEFORMS AT STATION W-11



IDT= .0020	ODT= .003	FIX=	AAS= 0.
HPF= .25	BYH= .10	HLH= 107	ASB=
LPF= 27.	BYL= 0.	HLL= 2300	ASE=
VTS= .250	VTE= .100	FLL= -20.	VSE= 0.
OPS= 0.	OPE= 93.	FLH= 0	DSE= 0.

14.04.22.

00/24/02

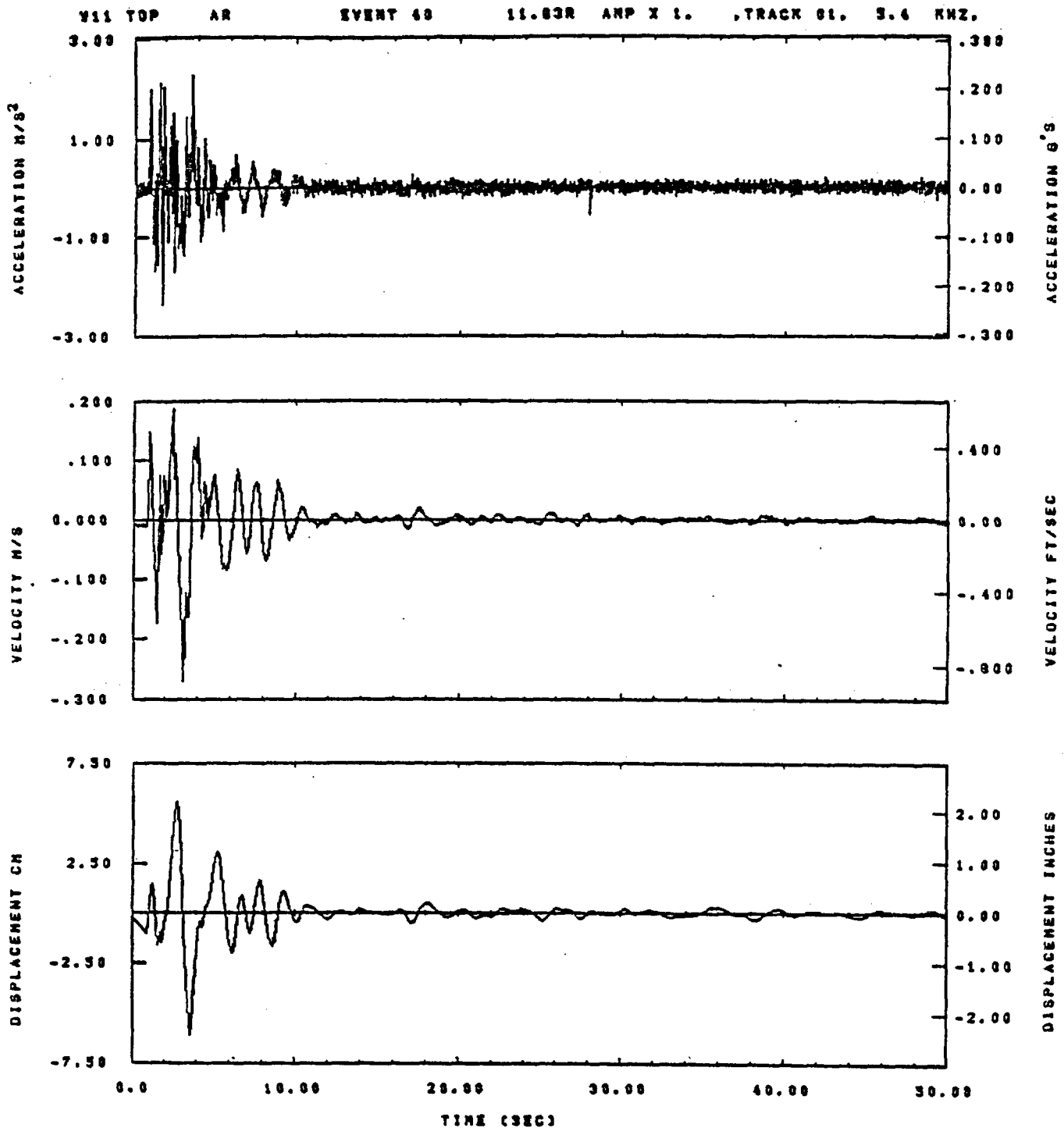


IDT= .0028	ODT= .005	FIX=	AAS= 0.
HFF= .25	BYH= .16	MLH= 167	ASB=
LFF= 27.	BYL= 6.	MLL= 2389	ASE=
VTH= .258	VTE= .168	FLL= -20.	VSE= 0.
OPB= 0.	DPE= .85.	FLH= 0	DSE= 0.

14.86.44.

06/26/82

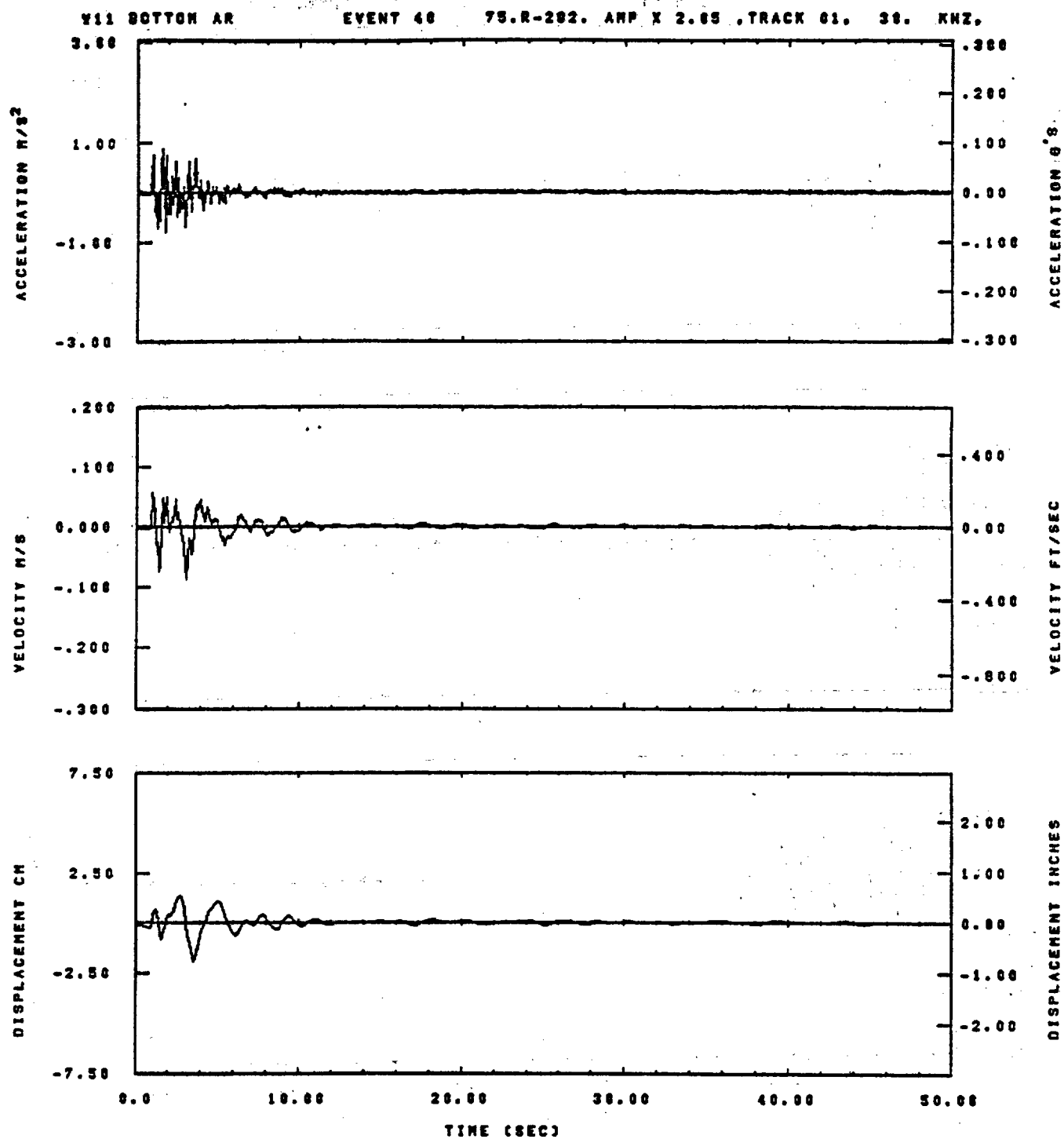
Figure E-2



IDT= .0029	ODT= .009	FIX=	AAS= 0.
HPP= .25	BYH= .10	HLH= 187	ASB=
LPP= 27.	BYL= 8.	HLL= 2393	ASE=
VTB= .250	VTH= .100	FLL= -20.	VSE= 0.
DPB= 0.	DPE= 93.	PLH= 0	DSE= 0.

14.04.12.

08/24/82

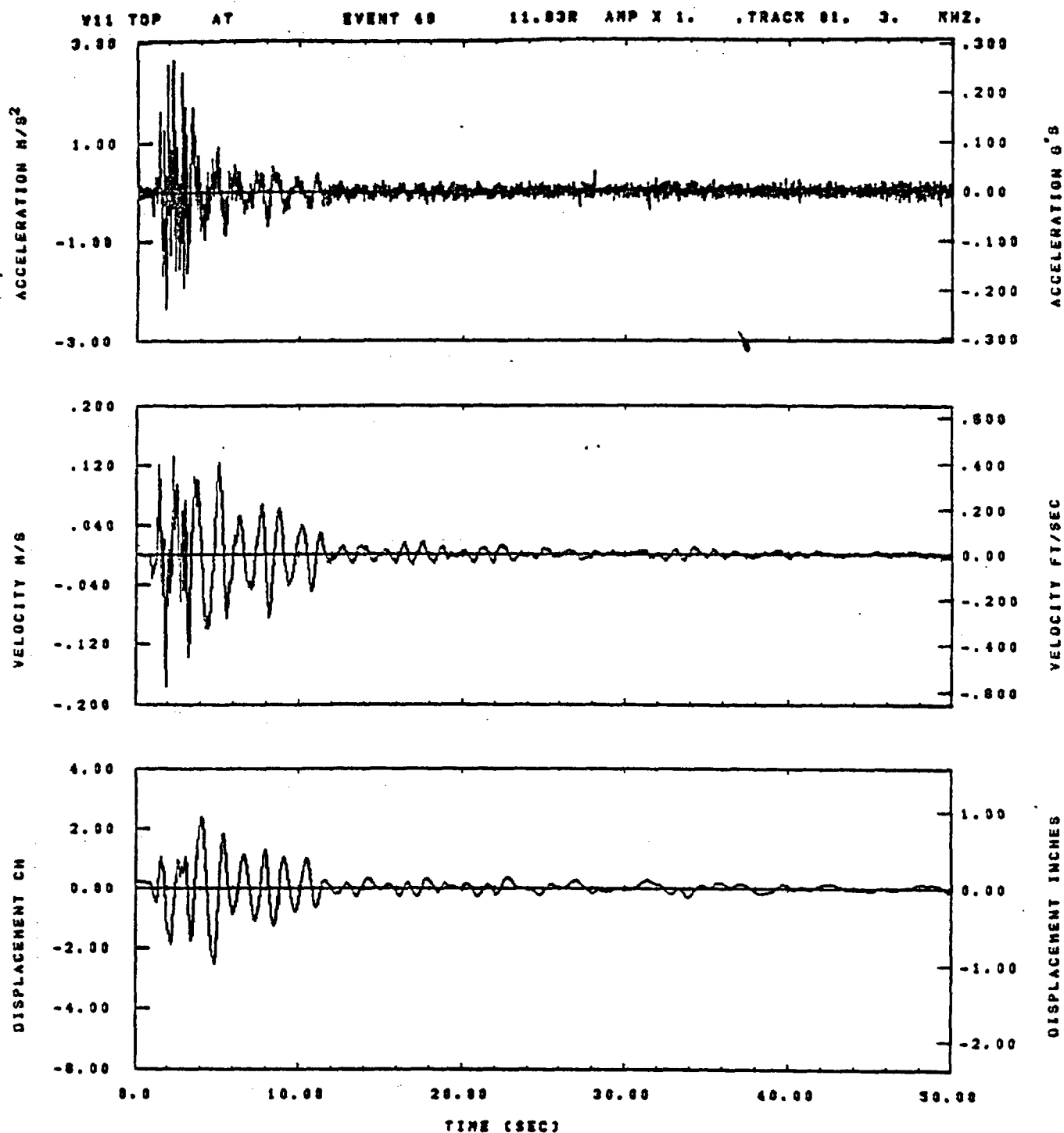


IDT= .0020	QDT= .005	FIX=	AAS= 0.
HPF= .25	BYH= .16	HLH= 167	ASS=
LPF= 27.	BYL= 6.	HLL= 2388	ASE=
VTS= .250	VTE= .168	FLL= -20.	VSE= 0.
OPS= 0.	OPE= 85.	FLH= 0	DSE= 0.

14.06.37.

06/24/82

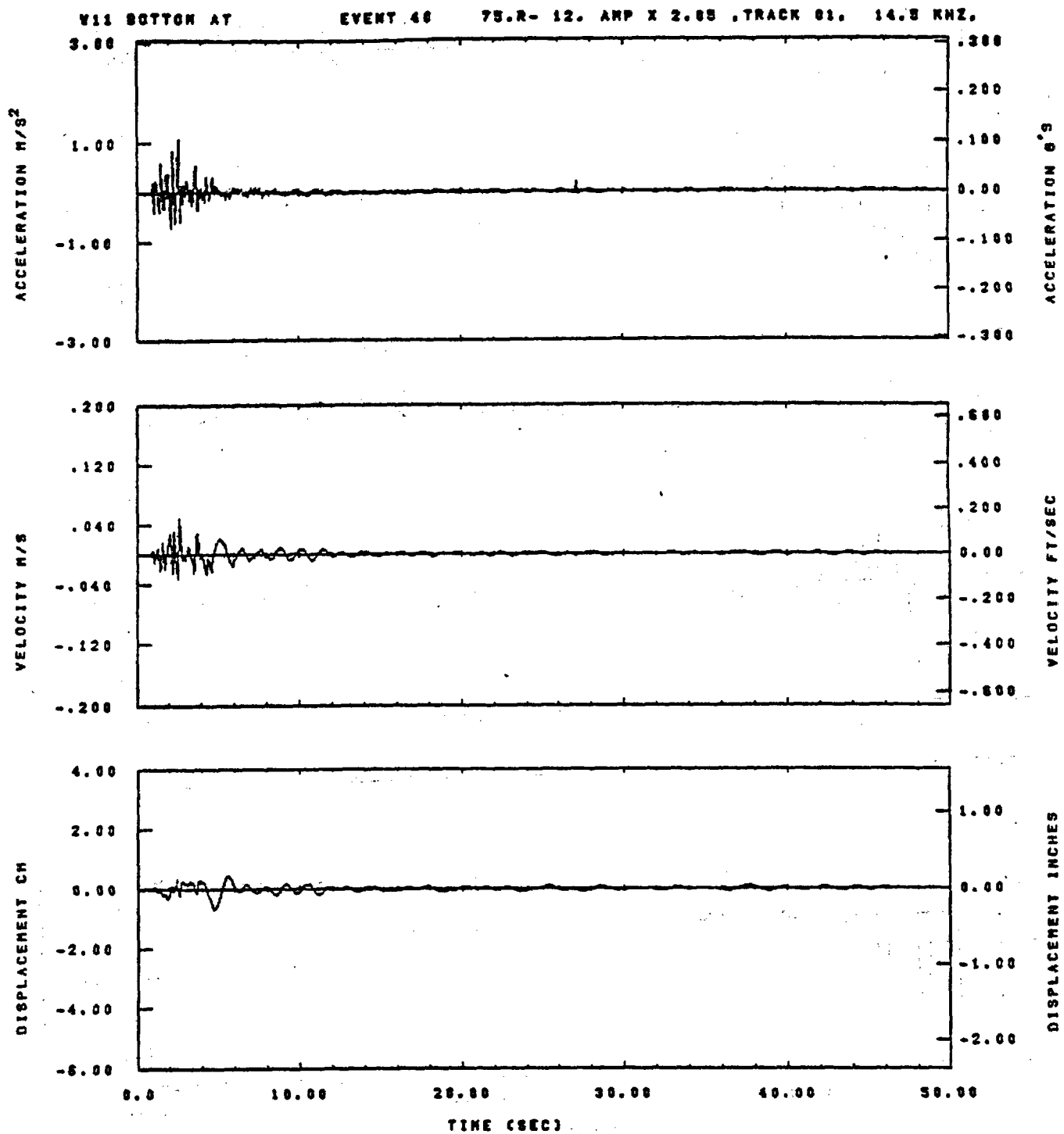
Figure E-4



IDT= .0020	ODT= .005	FIX=	AAS= 0.
HPP= .25	BYH= .18	HLH= 187	ASS=
LPP= 27.	BYL= 8.	HLL= 2399	ASE=
VTB= .250	VTZ= .188	FLL= -20.	VSE= 0.
OPB= 8.	OPE= 95.	FLH= 0	OSE= 0.

14.04.18.

08/24/92

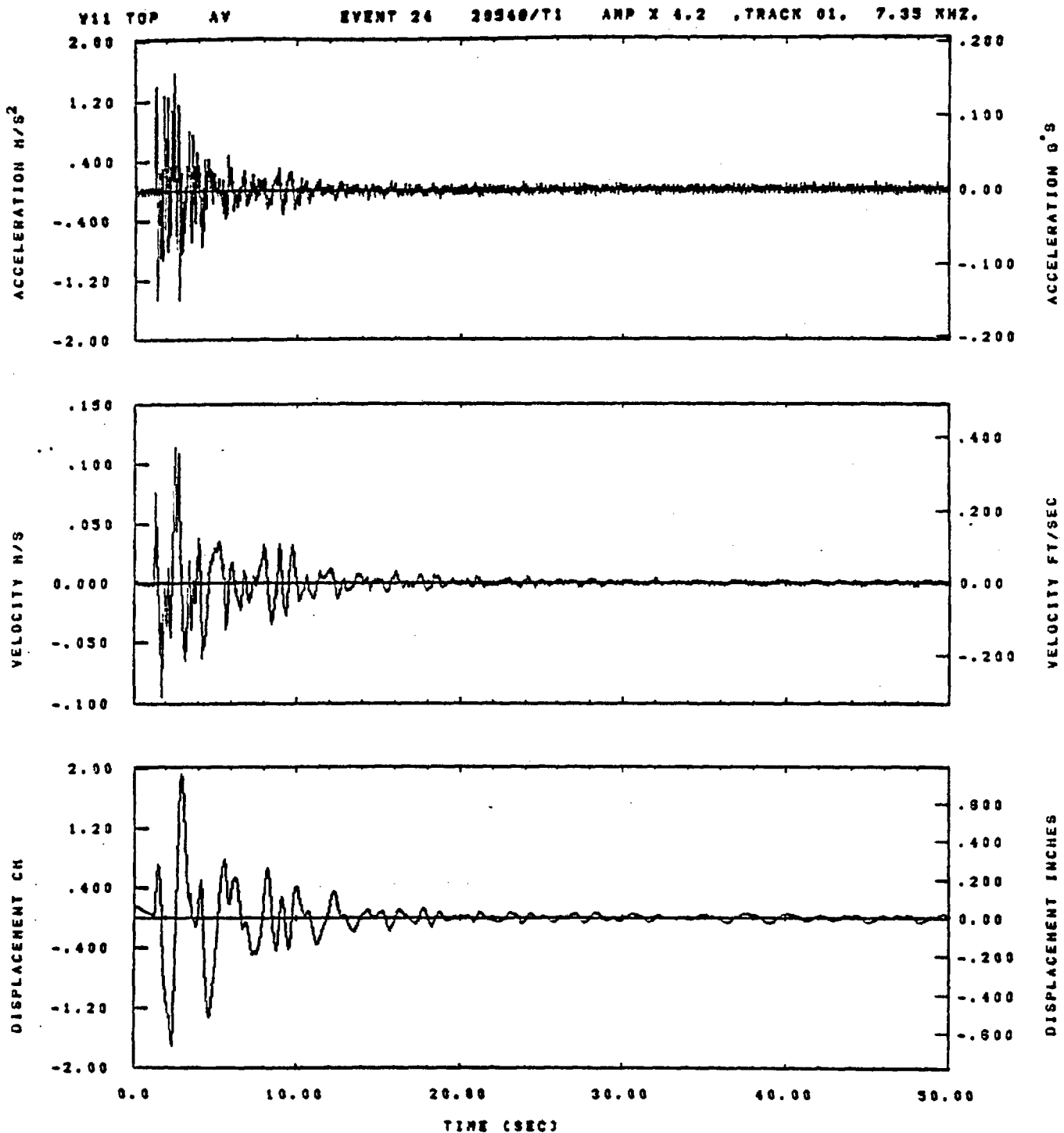


IDT= .0020	ODT= .005	FIX=	AAS= 0.
NPF= .25	SVH= .16	HLH= 167	ASB=
LPF= 27.	BYL= 6.	HLL= 2388	ASE=
VTS= .258	VTE= .166	FLL= -20.	VSE= 0.
OPS= 0.	OPE= 85.	FLH= 0	DSE= 0.

14.06.40.

06/24/82

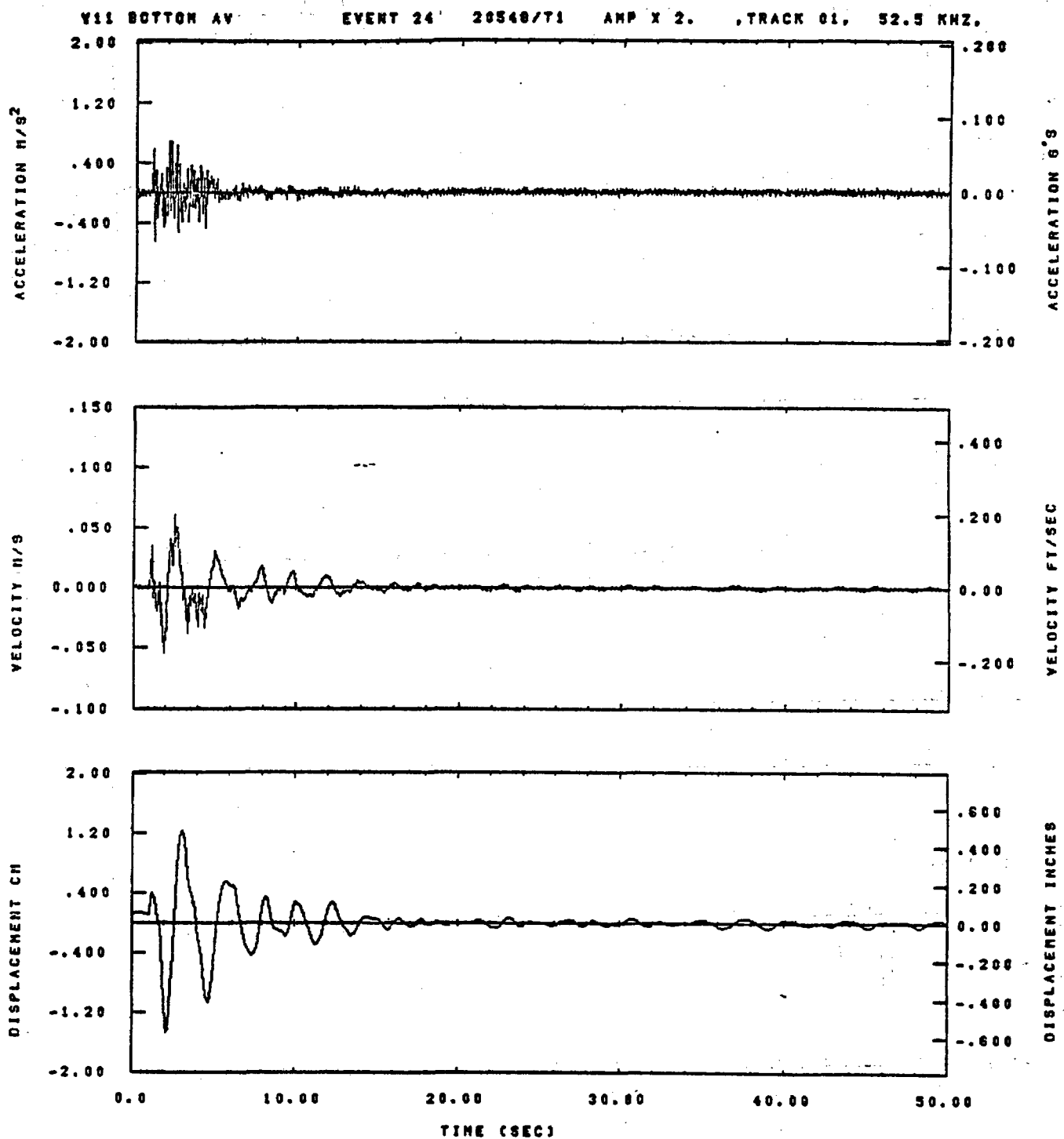
Figure E-6



IDT= .0020	ODT= .003	FIX=	AAS= 0.
HPP= .3	BYH= .20	MLH= 187	ASB=
LPP= 27.	BYL= 8.	MLL= 1393	ASE=
VTB= .38	VTE= .200	FLL= -3.	VSE= 0.
OPB= 0.	OPE= 100.	PLH= 0	DSE= 0.

15.35.09.

07/15/82

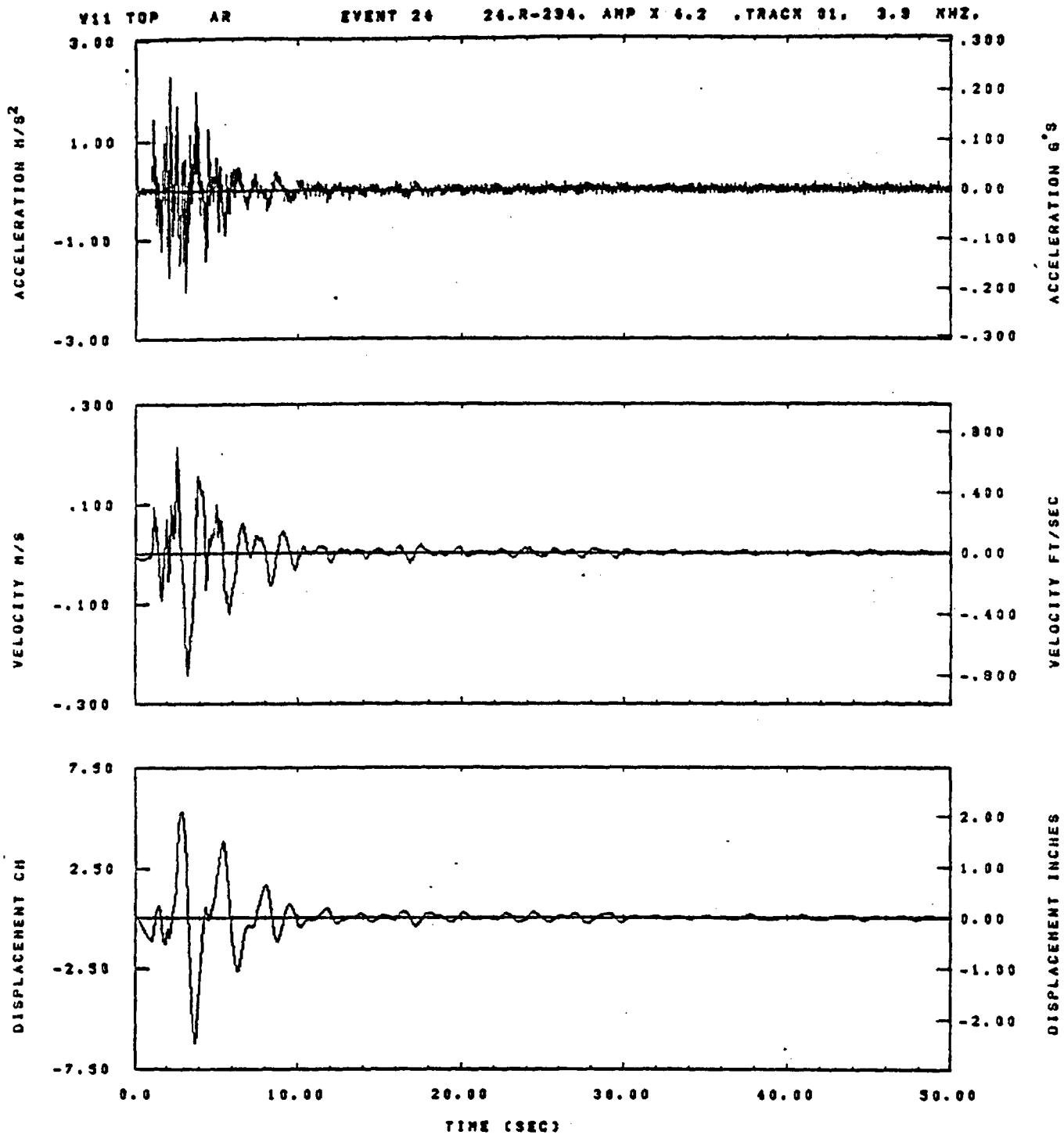


IDT= .0020	ODT= .005	FIX=	AAS= 0.
HPF= .3	BYH= .20	MLH= 167	ASS=
LPF= 27.	BYL= 6.	MLL= 1999	ASE=
VTB= .30	VTE= .200	FLL= -5.	VSE= 0.
DPB= 0.	DPE= 100.	FLH= 0	DSE= 0.

14.56.20.

07/18/82

Figure E-8

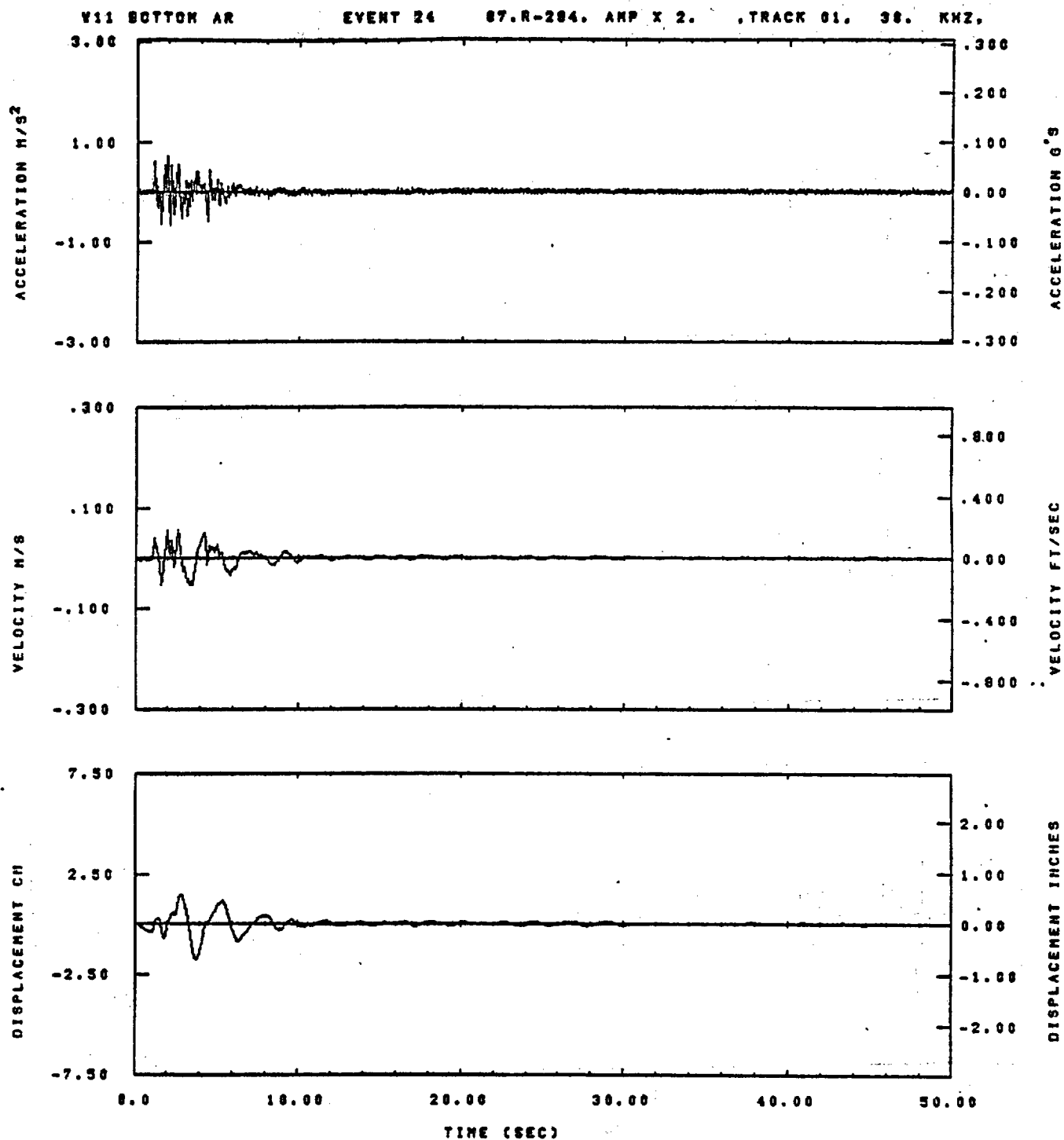


IDT= .0020	ODT= .003	FIX=	AAS= 0.
HPF= .3	BYH= .20	HLH= 167	ASB=
LPF= 27.	BYL= 6.	HLL= 1999	ASE=
VTS= .30	VTE= .200	FLL= -5.	VSE= 0.
DPS= 0.	DPE= 100.	FLH= 0	DSE= 0.

13.33.14.

07/13/82

Figure E-9

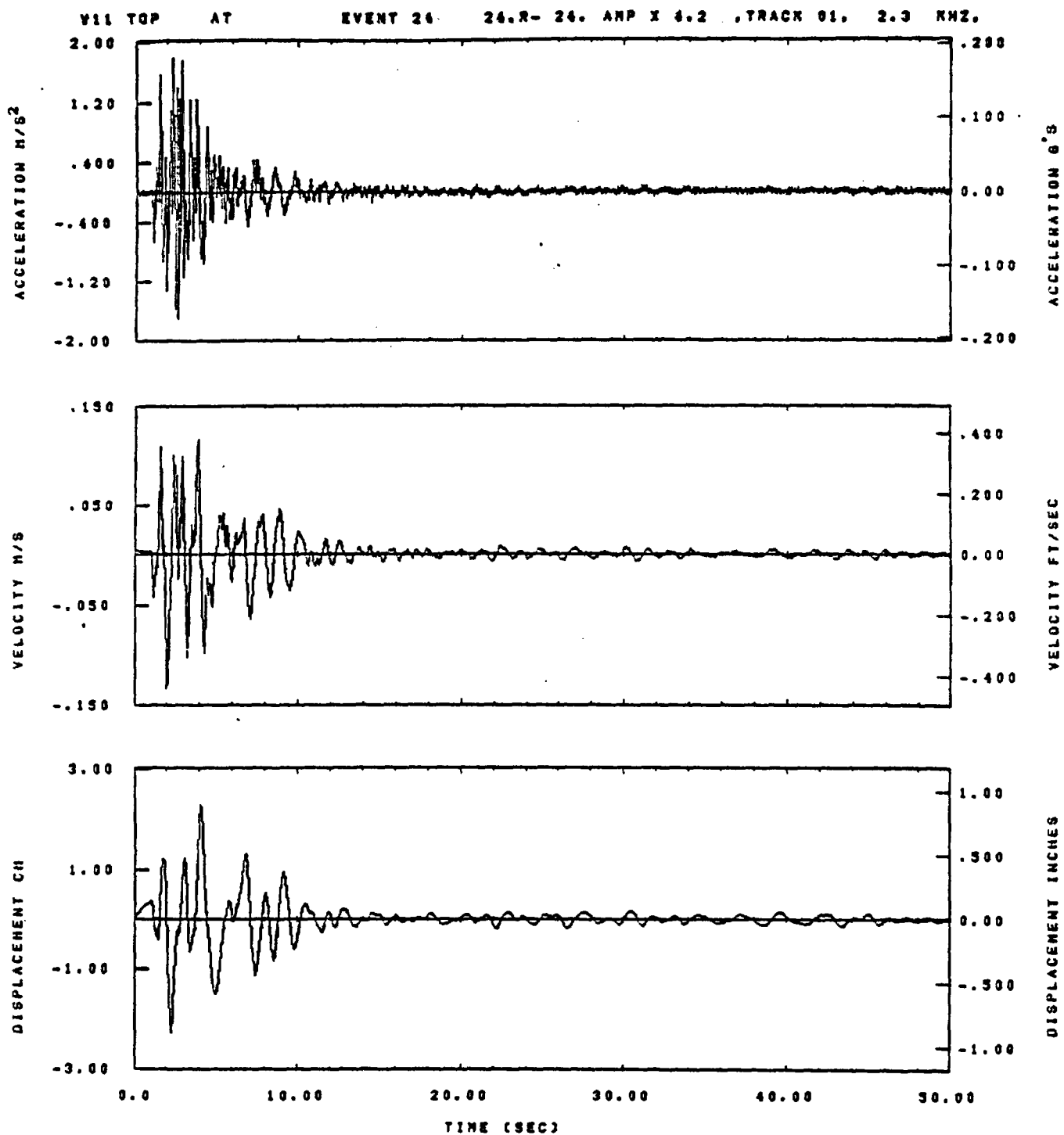


IDT= .0020	ODT= .005	FIX=	AAS= 0.
HPP= .3	BYH= .20	HLH= 167	ASB=
LPP= 27.	BYL= 6.	HLL= 1999	ASE=
VTS= .30	VTE= .208	FLL= -5.	VSE= 0.
DPS= 0.	DPE= 100.	FLH= 0	DSE= 0.

14.56.33.

07/18/82

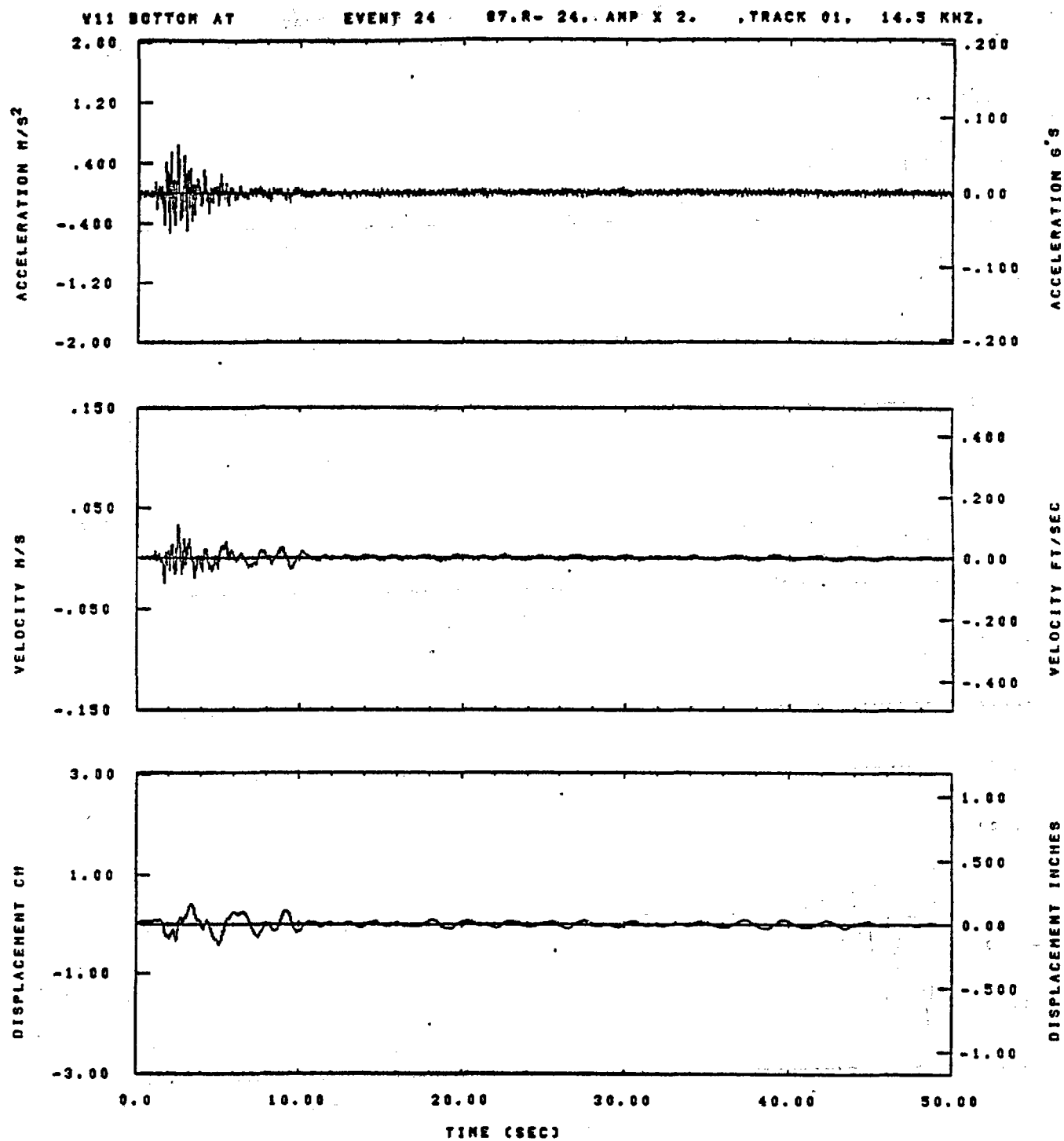
Figure E-10



IDT= .0020	ODT= .003	FIX=	AAS= 0.
HPF= .3	SVH= .20	HLH= 167	ASB=
LPF= 27.	SVL= 6.	HLL= 1999	ASE=
VTB= .30	VTE= .200	FLL= -5.	VSE= 0.
OPB= 0.	OPE= 100.	FLH= 0	DSE= 0.

19.35.20.

07/15/82

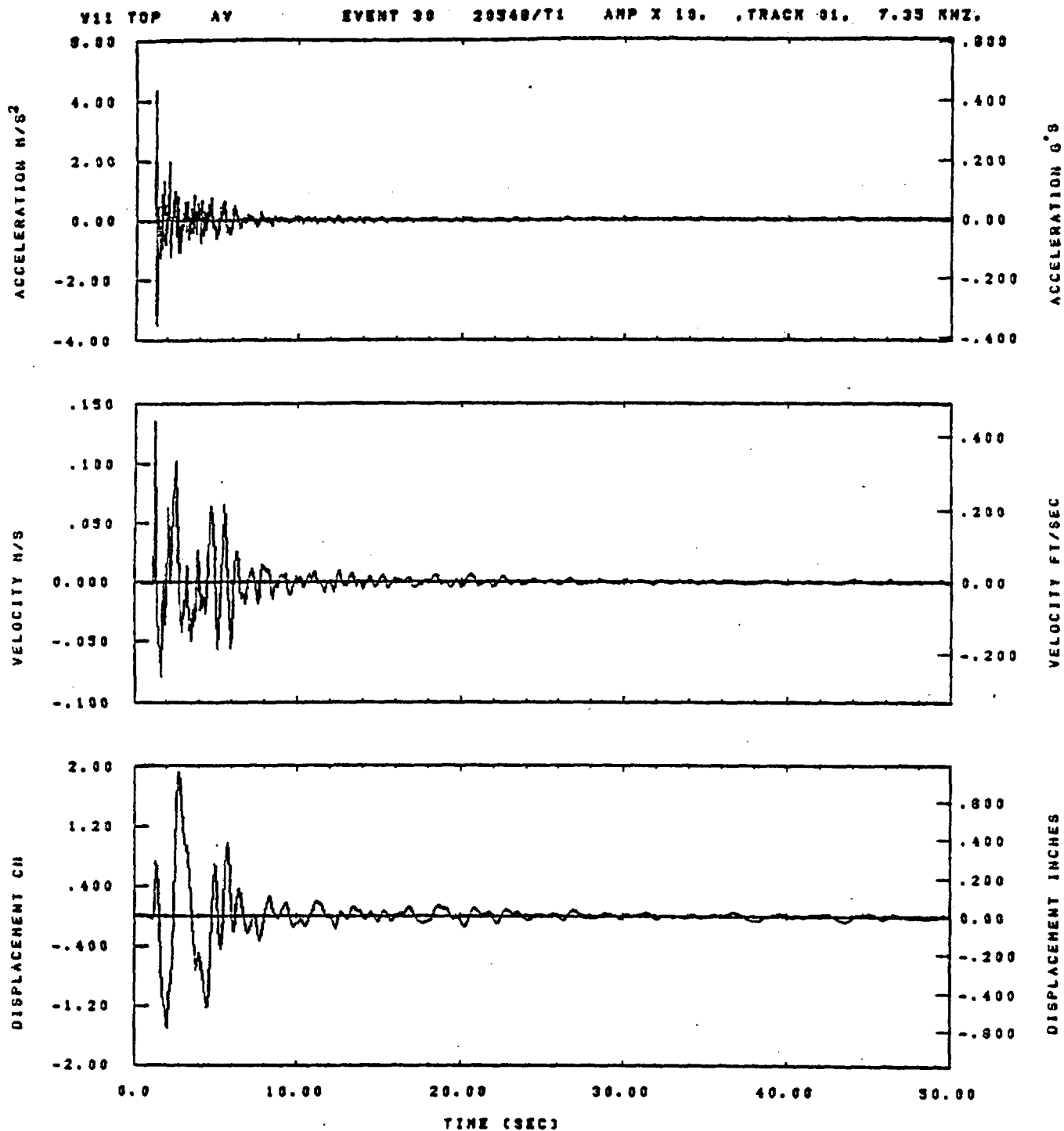


IDT= .0020	ODT= .005	FIX=	AAS= 0.
HPF= .3	BYN= .20	NLM= 167	ASS=
LPF= 27.	BYL= 6.	NLL= 1999	ASE=
VTB= .30	VTE= .200	FLL= -5.	VSE= 0.
OPB= 0.	OPE= 100.	FLH= 0	DSE= 0.

14.56.51.

07/18/82

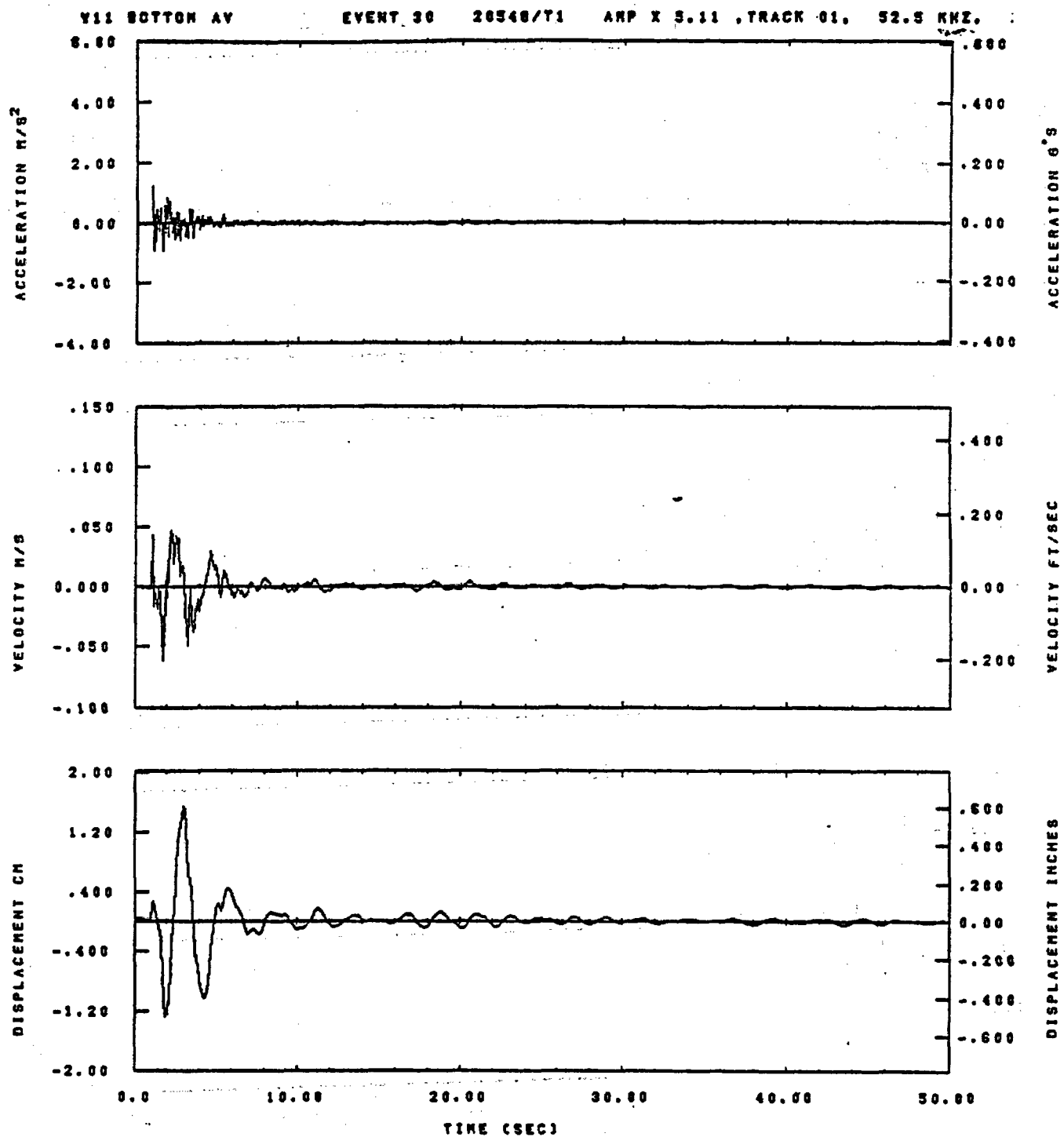
Figure E-12



IDT= .0020	ODT= .005	FIX=	AAS= 0.
HPP= .20	SYM= .13	MLH= 101	ASB=
LPP= 45.	SVL= 10.	HLL= 2933	ASE=
VTB= .200	VTE= .133	FLL= -20.	VSE= 0.
DPS= 0.	DPE= 100.	FLH= 0	DSE= 0.

09.13.48.

07/01/82

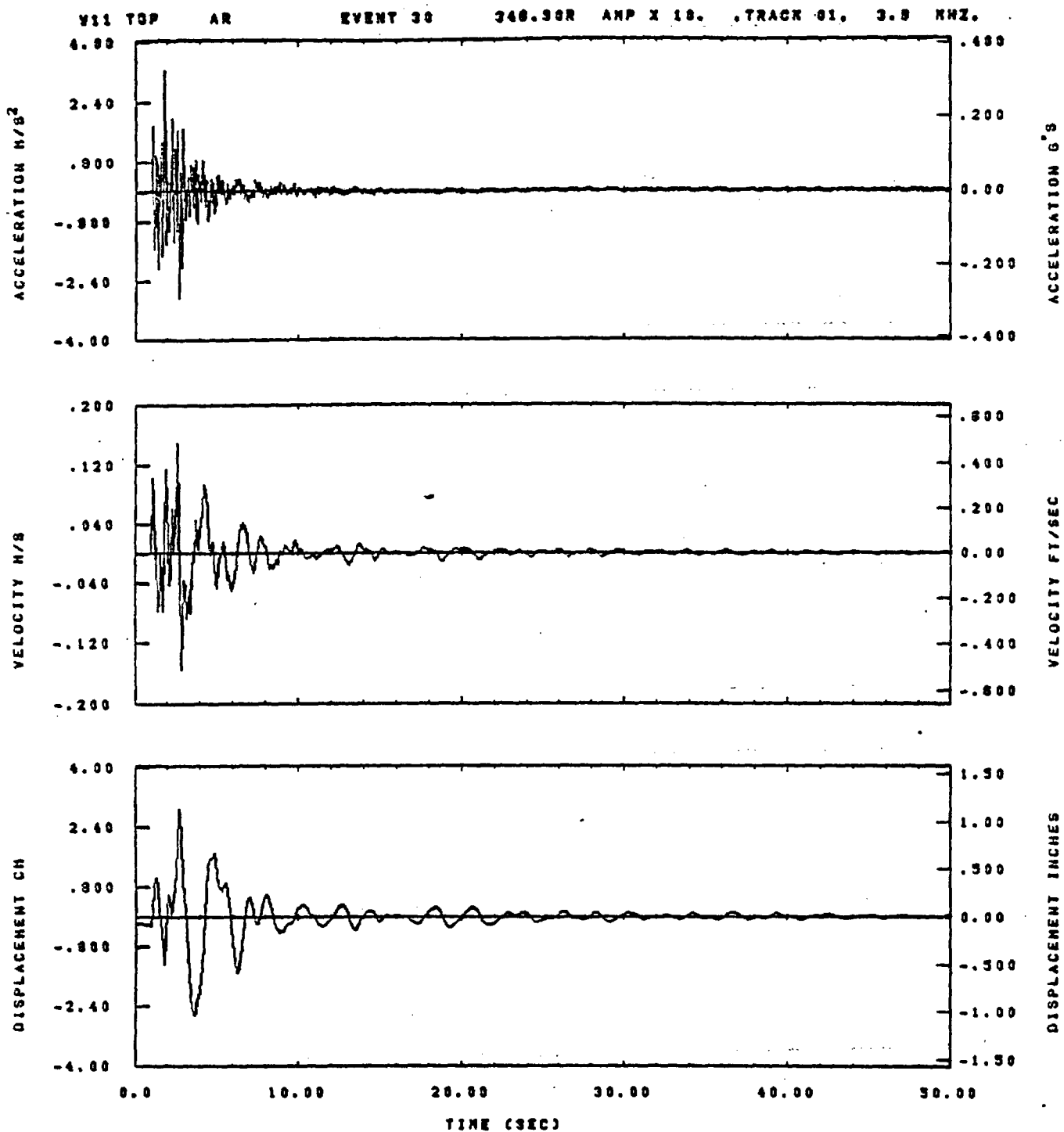


IDT= .0020	ODT= .005	FIX=	AAS= 0.
HPP= .20	BYH= .13	HLH= 101	ASB=
LPP= 45.	BVL= 10.	HLL= 2888	ASE=
VTS= .200	VTE= .133	FLL= -20.	VSE= 0.
DPS= 0.	DPE= 100.	FLH= 0	DSE= 0.

09.16.32.

07/01/02

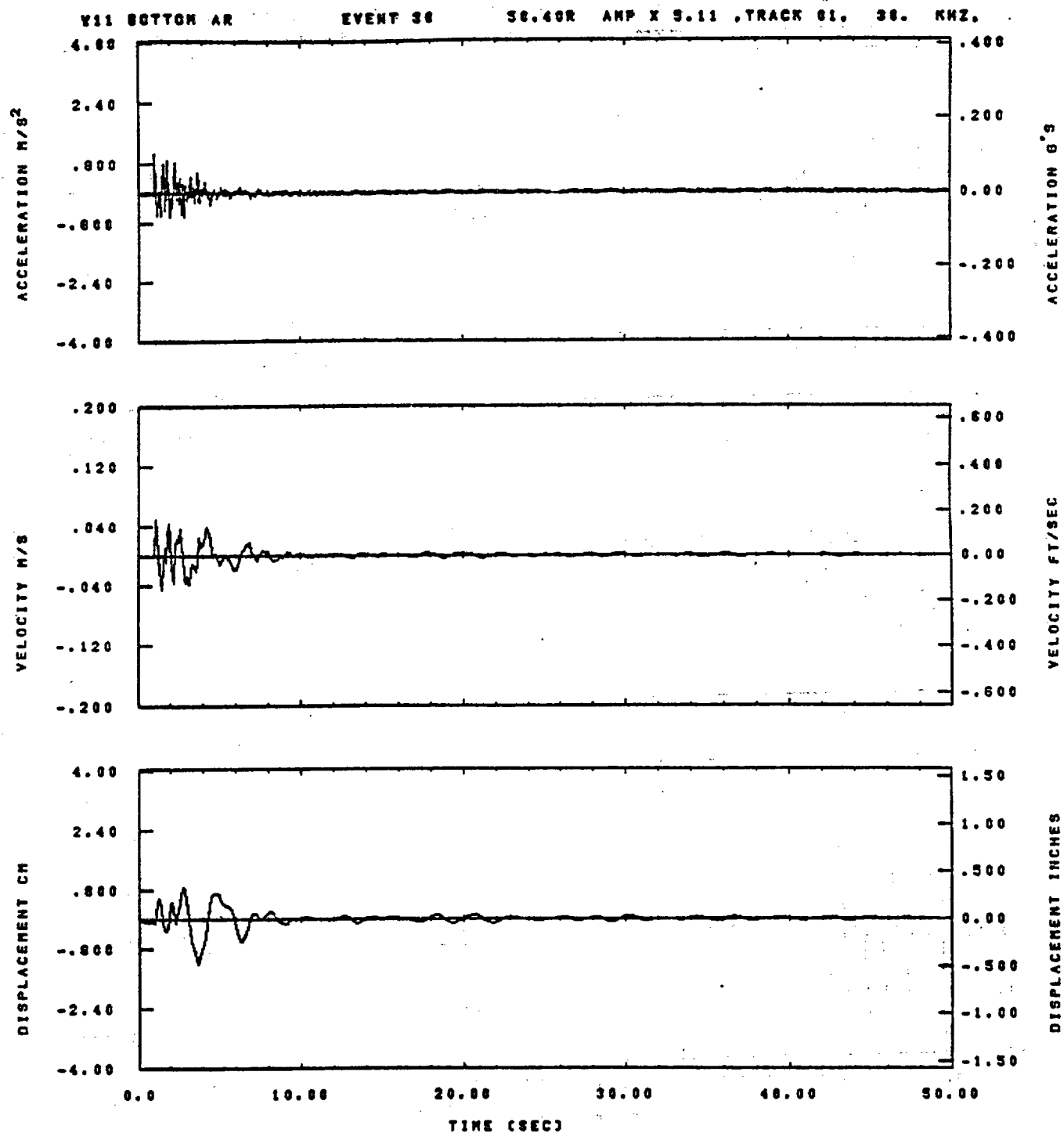
Figure E-14



IOT= .0020	ODT= .005	FIX=	AAS= 0.
HPP= .20	BYH= .13	HLH= 101	ASB=
LPP= 45.	BYL= 10.	HLL= 2999	ASE=
VTS= .200	VTE= .133	FLL= -20.	VSE= 0.
OPS= 0.	OPE= 100.	FLH= 0	DSE= 0.

03.13.38.

07/01/82

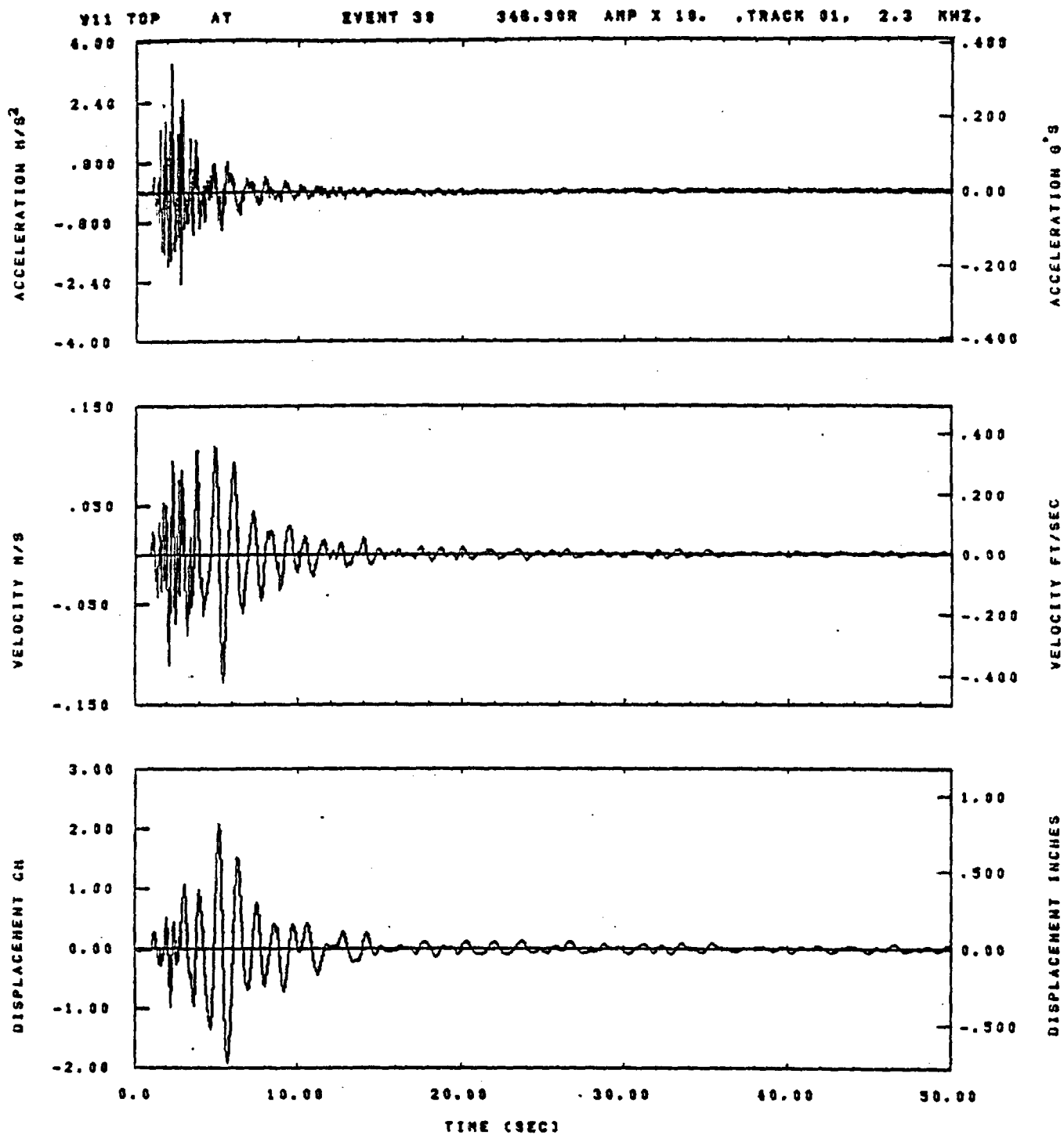


IDT= .0020	ODT= .005	FIX=	AAS= 0.
HPP= .20	BYH= .13	HLH= 101	ASB=
LPP= 45.	BYL= 10.	HLL= 2880	ASE=
VTE= .200	VTE= .133	FLL= -20.	VSE= 0.
DPE= 0.	DPE= 100.	FLH= 0	DSE= 0.

09.16.45.

07/01/82

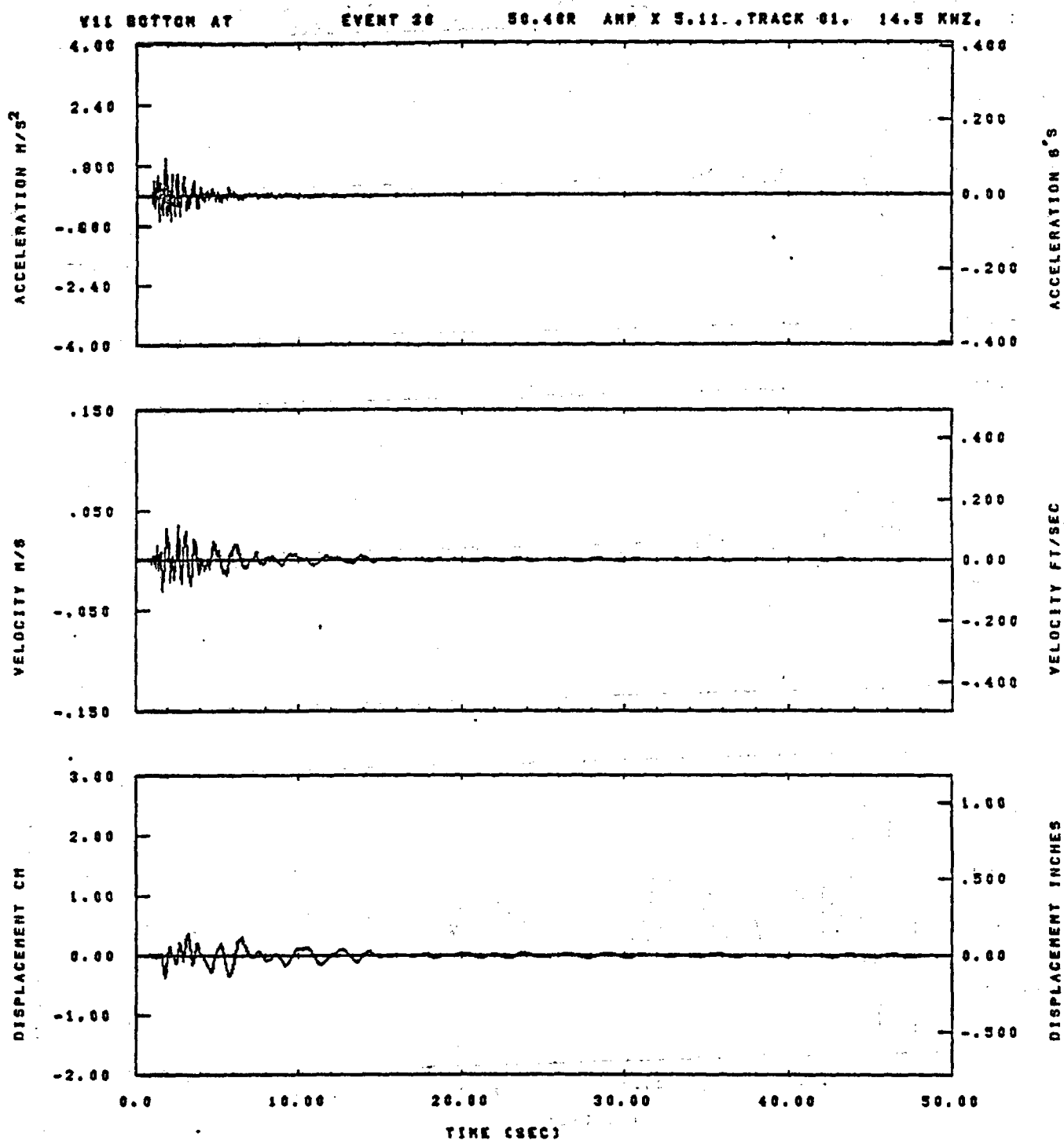
Figure E-16



IDT= .0020	ODT= .003	FIX=	AAS= 0.
HPF= .20	BYH= .13	HLH= 101	ASB=
LPF= 45.	BYL= 10.	HLL= 2939	ASE=
YTS= .200	YTE= .133	FLL= -20.	VSE= 0.
DPS= 0.	DPE= 100.	FLH= 0	DSE= 0.

09.18.08.

07/01/92

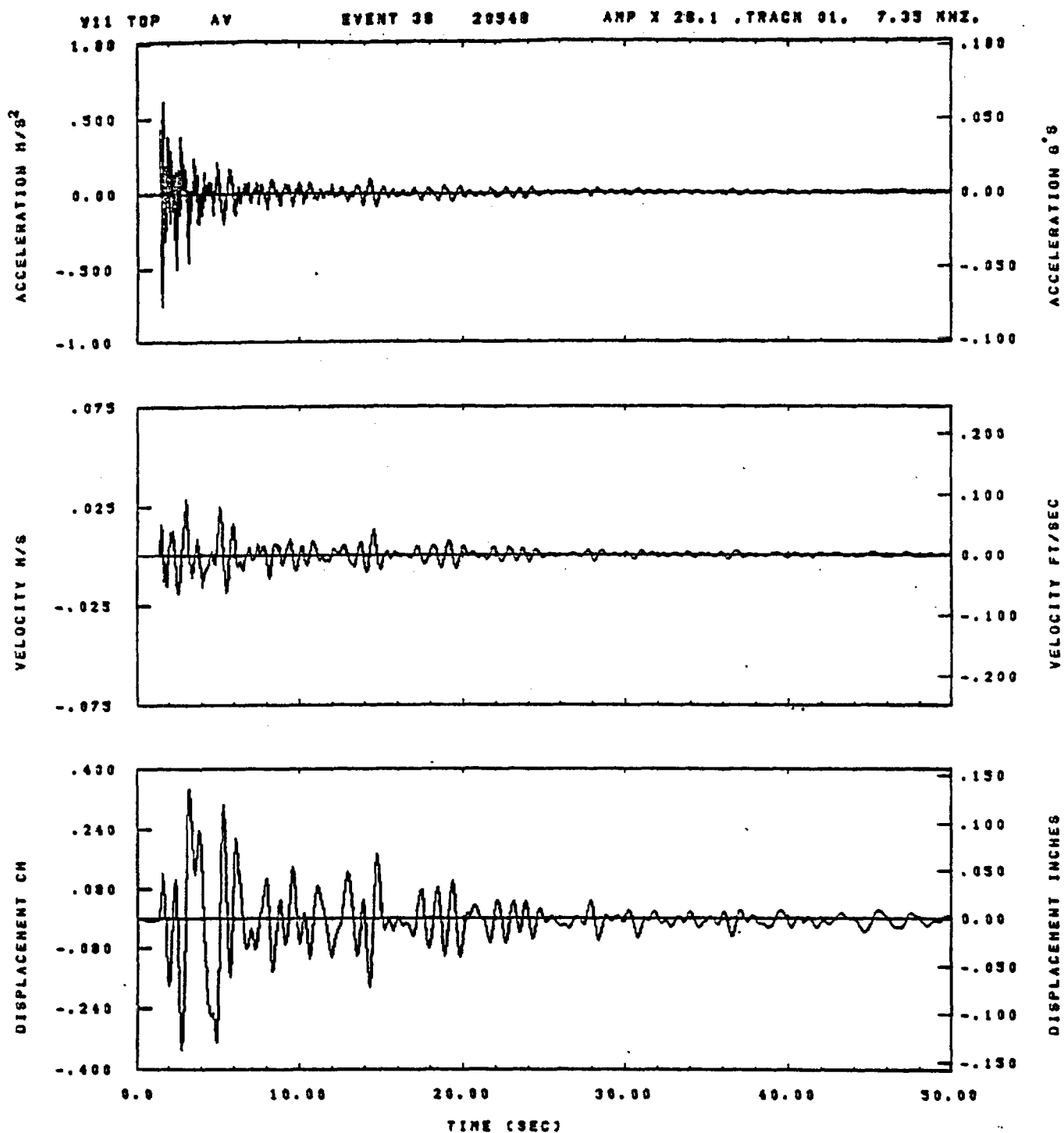


IDT= .0020	ODT= .005	FIX=	AAS= 0.
HPP= .20	BYH= .13	HLH= 101	ASS=
LPP= 45.	BYL= 10.	HLL= 2888	ASE=
VTS= .200	VTE= .133	FLL= -20.	VSE= 0.
DPS= 0.	DPE= 100.	FLH= 0	DSE= 0.

08.16.53.

07/01/82

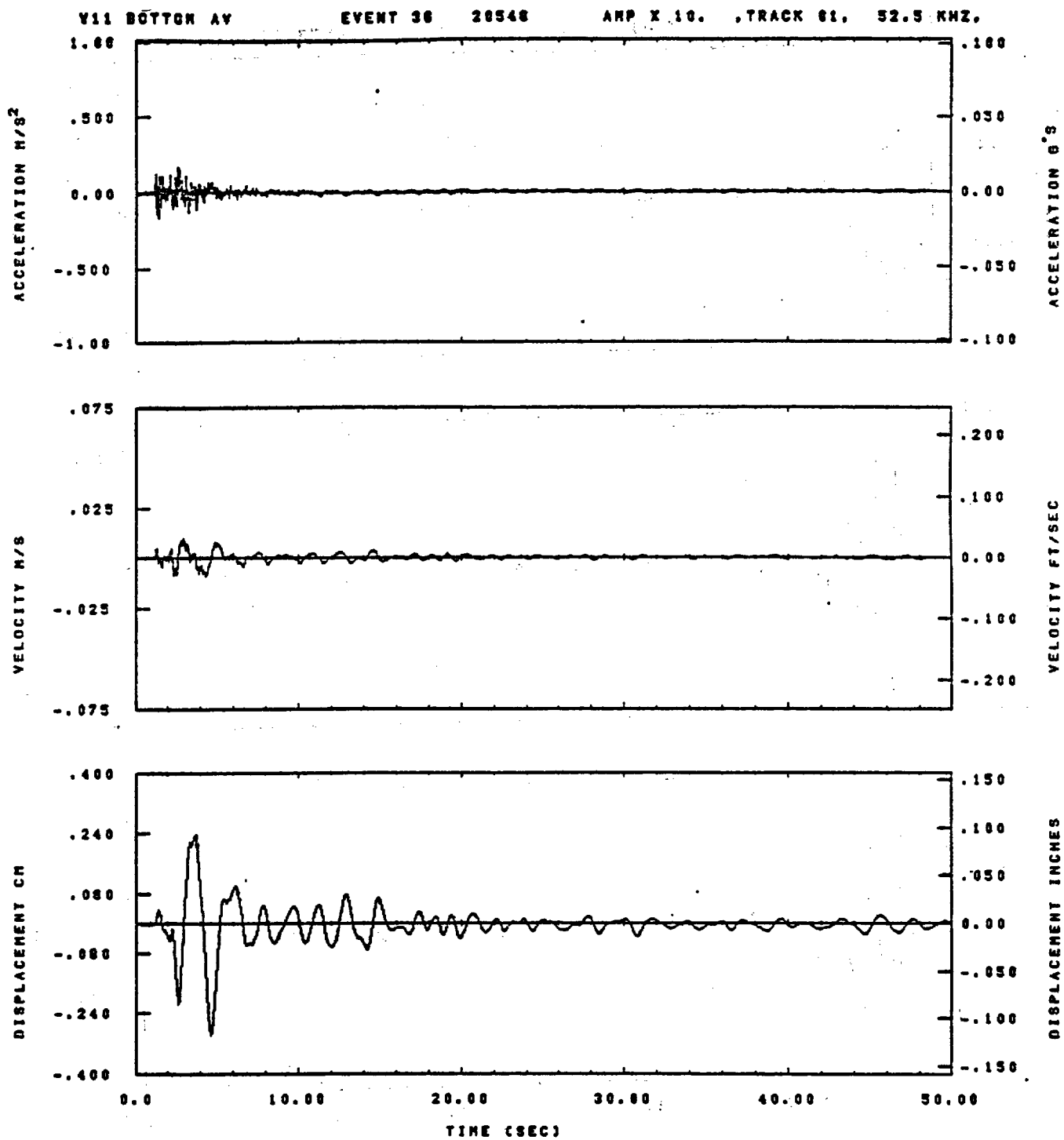
Figure E-18



IDT= .0020	ODT= .005	FIX=	AAS= 0.
HPP= .25	BYH= .18	HLH= 143	ASB=
LPP= 31.	BYL= 7.	HLL= 2399	ASE=
VTS= .250	VTE= .189	FLL= -20.	VSE= 0.
OPS= 0.	DPE= 100.	FLH= 0	DSE= 0.

08.10.22.

08/24/82

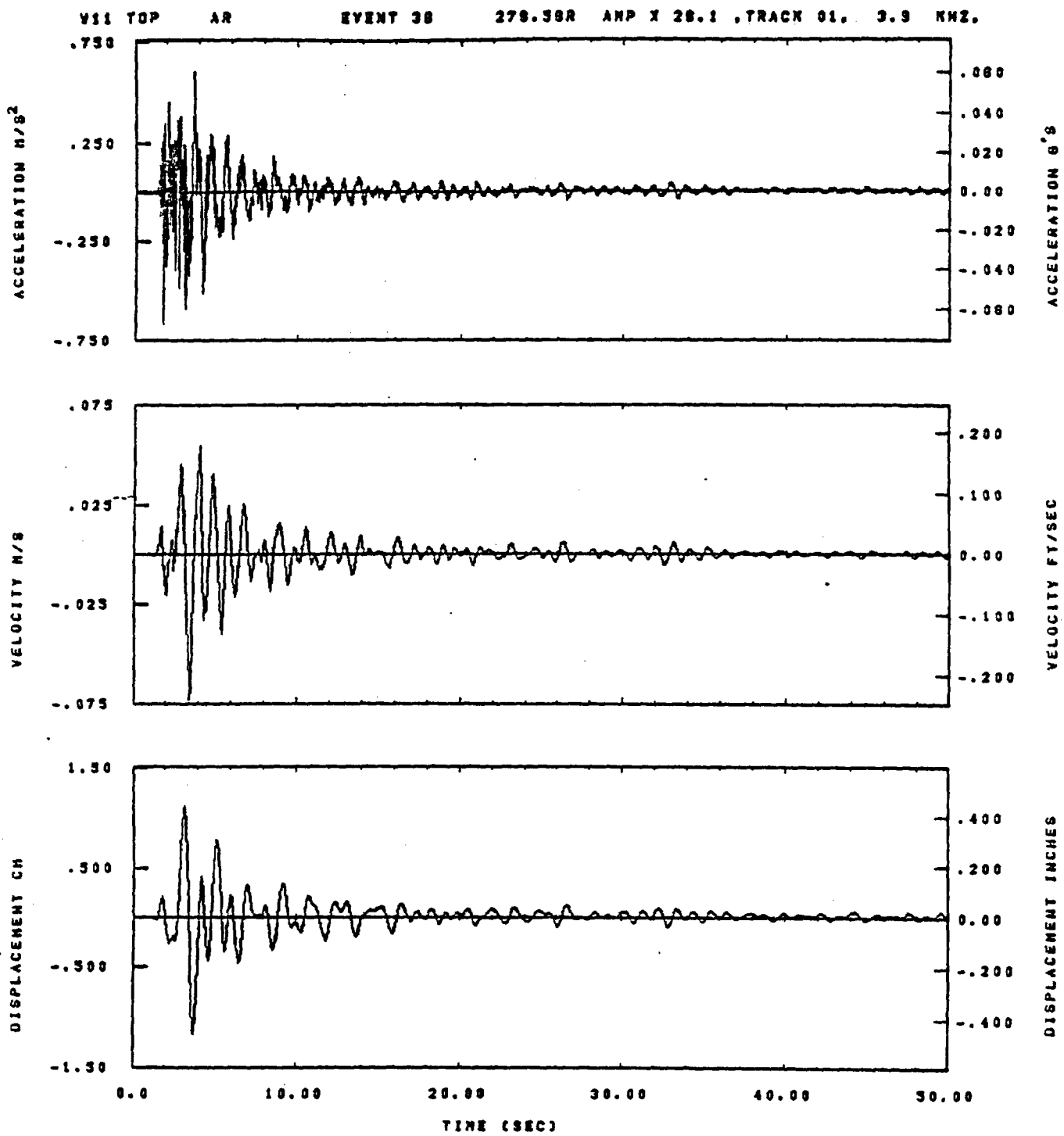


IDT= .0020	ODT= .005	FIX=	AAS= 0.
HPF= .25	BYH= .16	HLH= 143	ASB=
LPF= 31.	BYL= 7.	HLL= 2388	ASE=
VTS= .250	VTE= .166	FLL= -20.	VSE= 0.
DPS= 0.	DPE= 100.	FLH= 0	DSE= 0.

00.11.17.

06/24/82

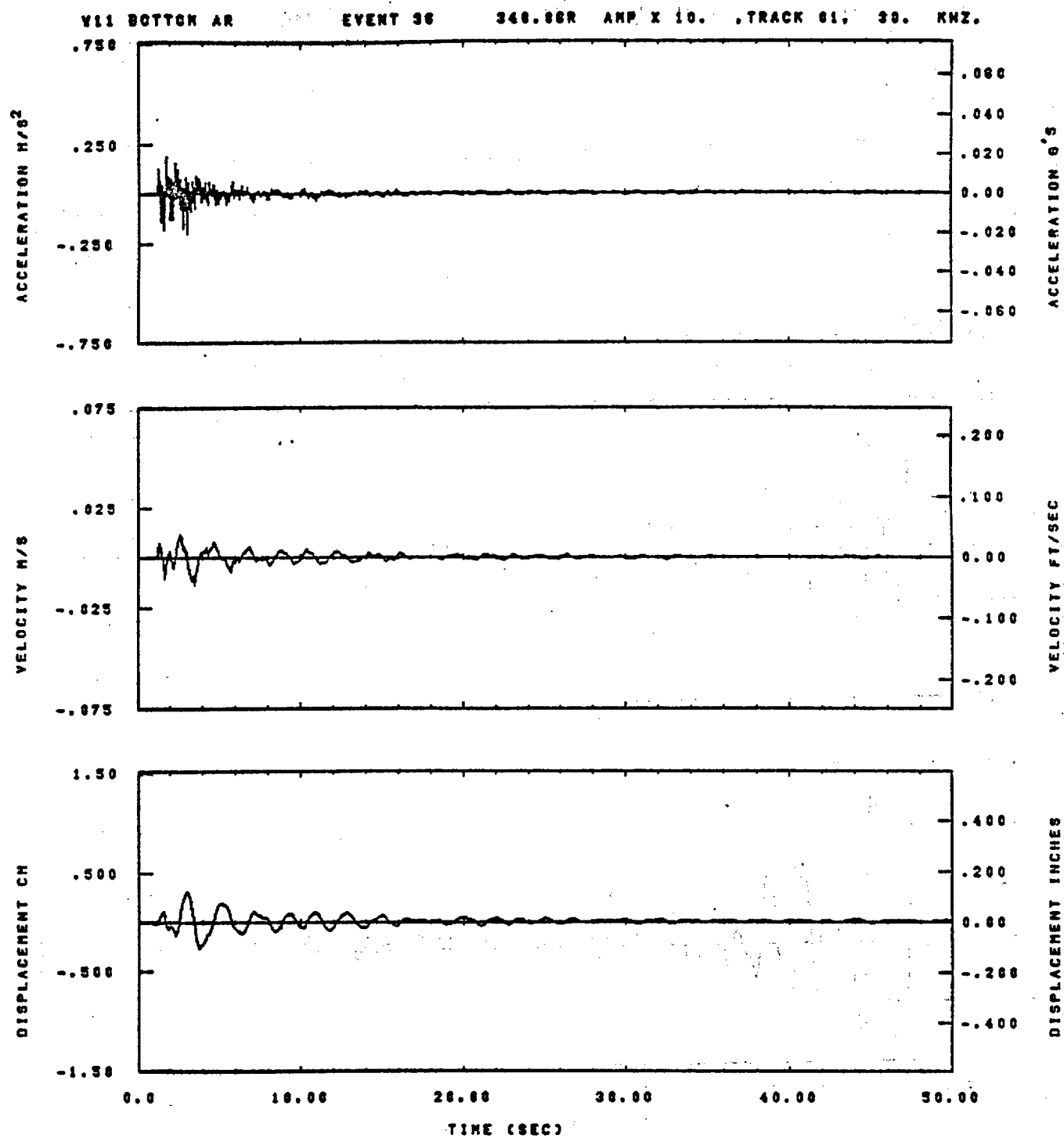
Figure E-20



LOT= .0028	ODT= .003	FIX=	AAS= 0.
HPP= .25	BYN= .18	HLN= 143	ASD=
LPP= 31.	BYL= 7.	HLL= 2399	ASE=
VTB= .230	VTE= .188	FLL= -20.	VSE= 0.
OPS= 0.	OPE= 100.	FLH= 0	DSE= 0.

00.10.34.

06/24/82

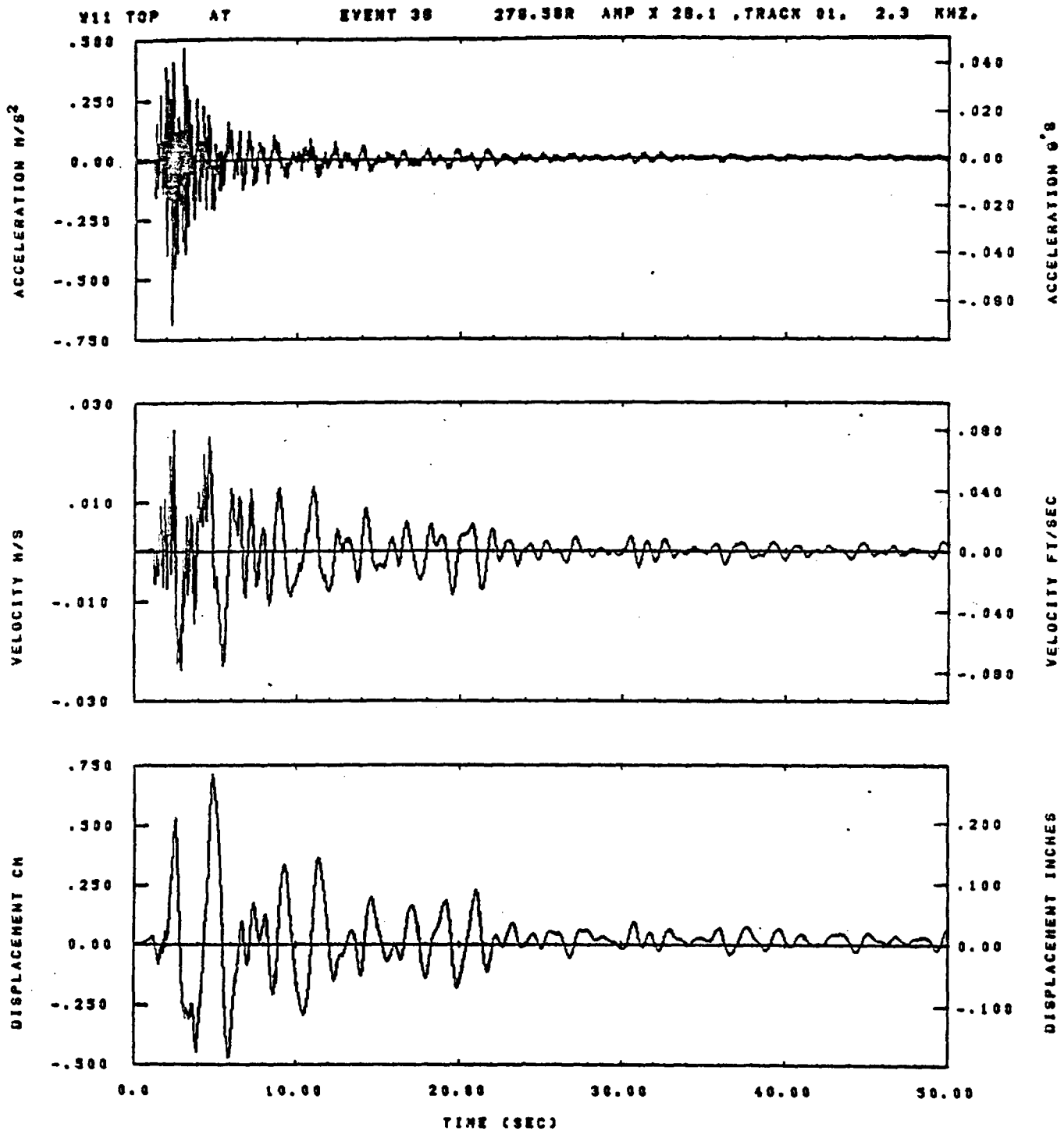


IDT= .0020	QDT= .005	FIX=	AAS= 0.
HPP= .25	BYH= .16	HLH= 143	ASS=
LPP= 31.	BYL= 7.	HLL= 2389	ASE=
VTB= .250	VTE= .166	FLL= -20.	VSE= 0.
DPS= 0.	DPE= 100.	FLH= 0	DSE= 0.

08.12.21.

06/24/82

Figure E-22



IDT= .0028	ODT= .005	FIX=	AAS= 0.
HPP= .25	BYN= .18	HLN= 143	ASB=
LPP= 31.	BVL= 7.	HLL= 2399	ASE=
VTB= .250	VTE= .188	FLL= -20.	VSE= 0.
DPS= 0.	DPE= 100.	FLN= 0	DSE= 0.

08.11.22.

08/24/82

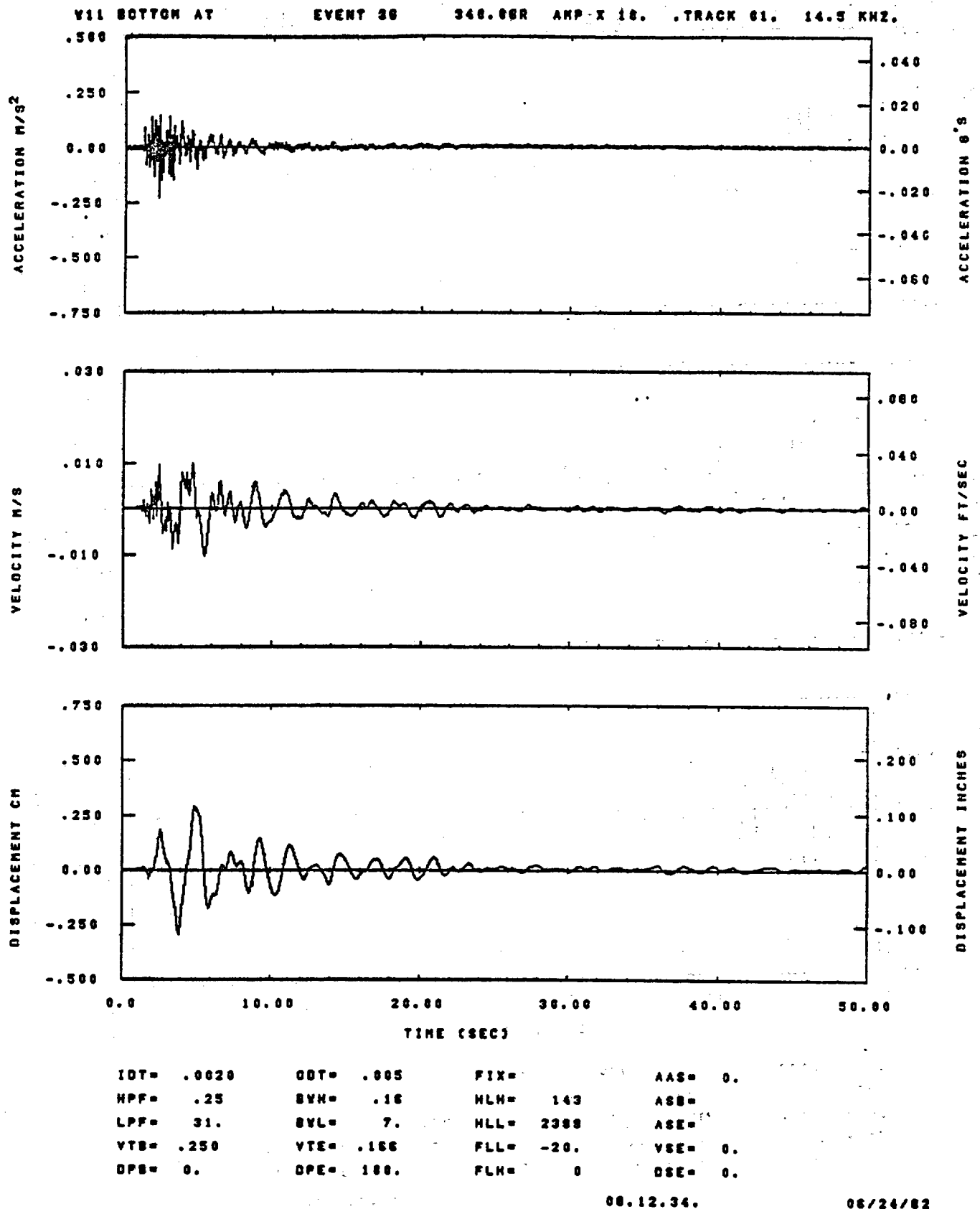
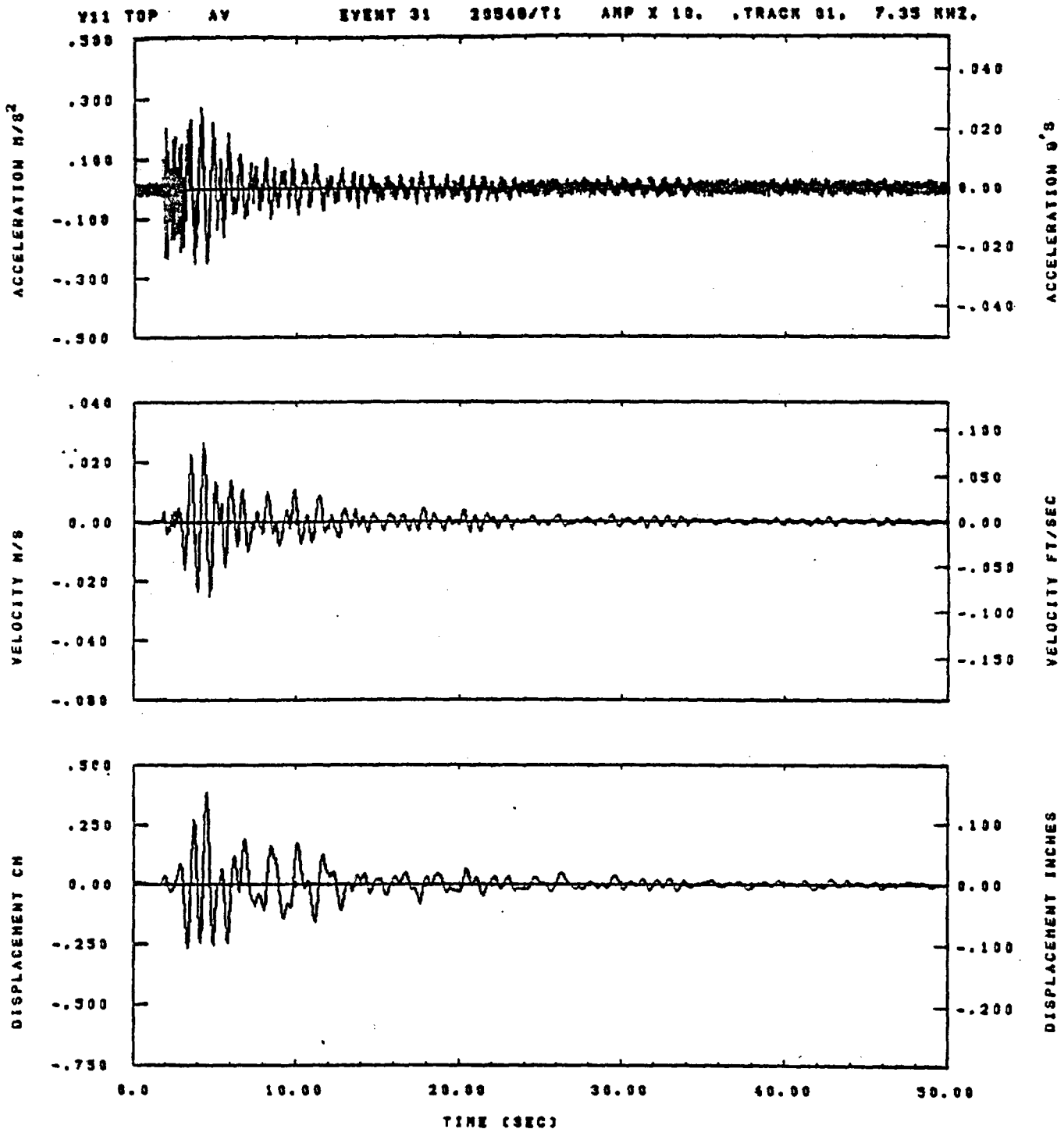


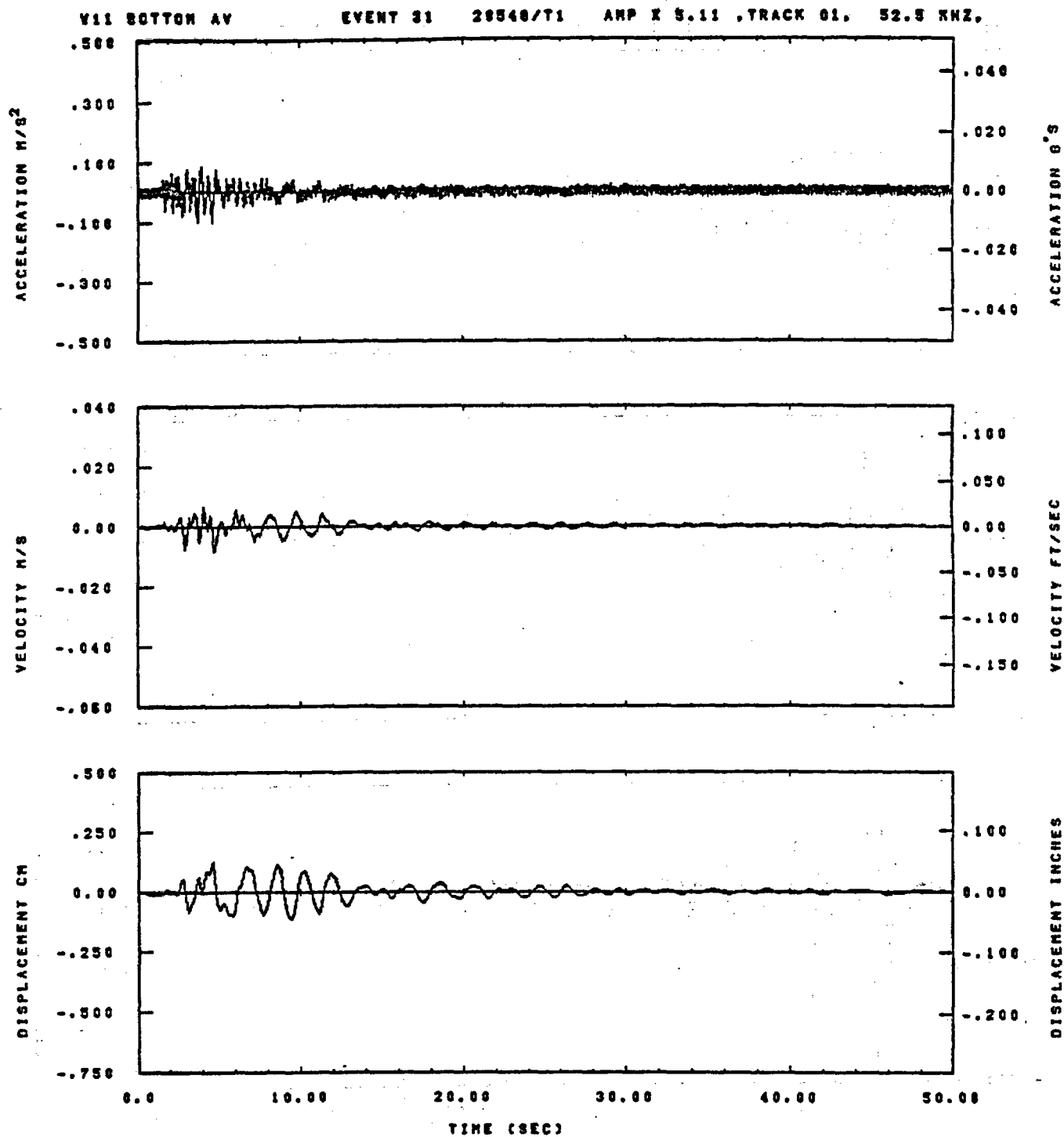
Figure E-24



IDT= .0020	QDT= .005	FIX=	AAS= 0.
HPP= .25	BYH= .10	HLH= 143	ASB=
LPP= 31.	BYL= .7.	HLL= 2399	ASE=
YTS= .250	YTS= .100	FLL= -20.	VSE= 0.
OPS= 0.	OPE= 100.	FLH= 8	DSE= 0.

14.40.29.

08/24/82

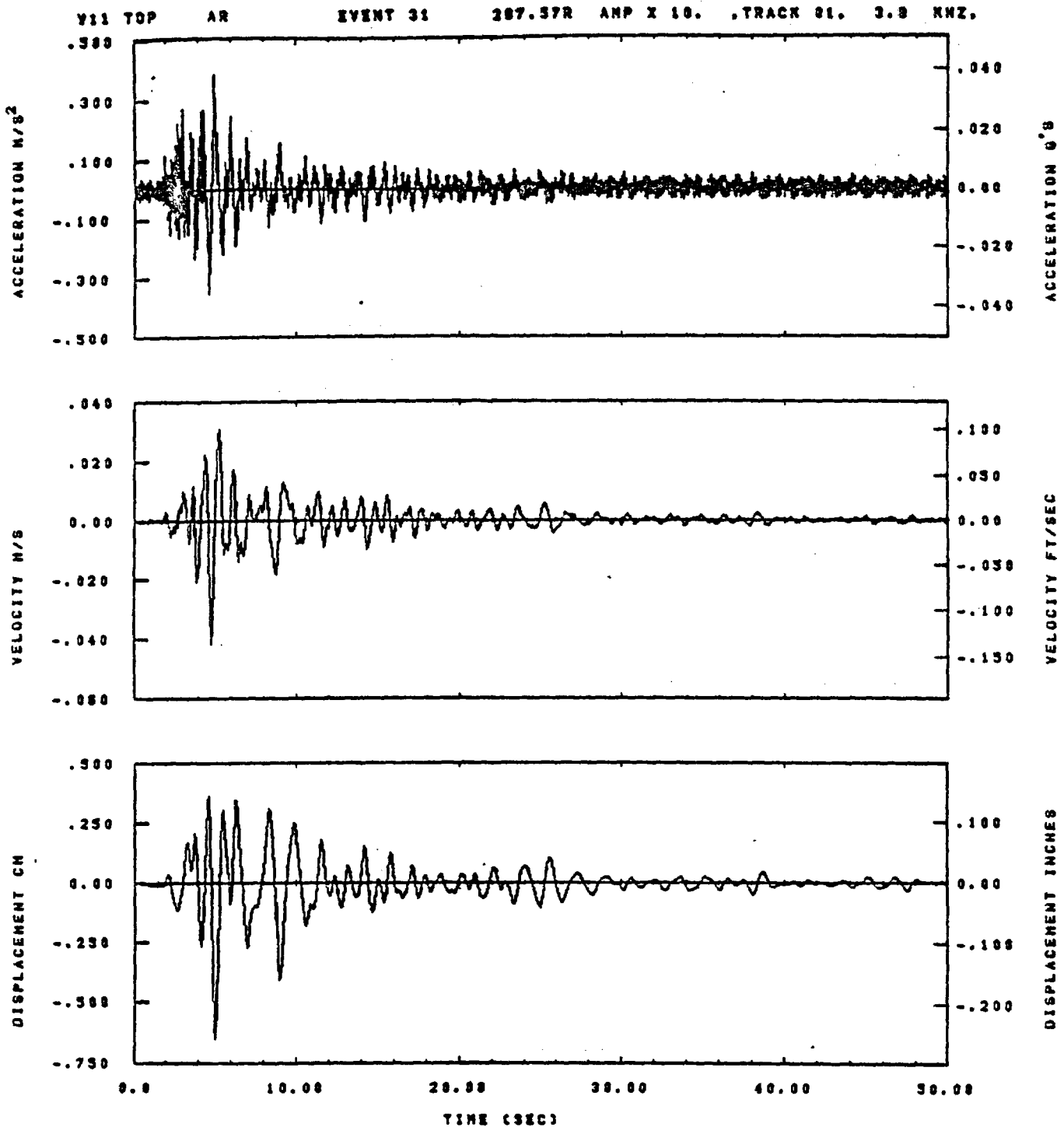


IDT= .0020	QDT= .005	FIX=	AAS= 0.
HPF= .25	SVN= .16	HLN= 143	ASB=
LPF= 31.	SVL= 7.	HLL= 2398	ASE=
VTB= .250	VTE= .166	FLL= -20.	VSE= 0.
DPS= 0.	DPE= 100.	FLN= 0	DSE= 0.

14.41.86.

08/24/82

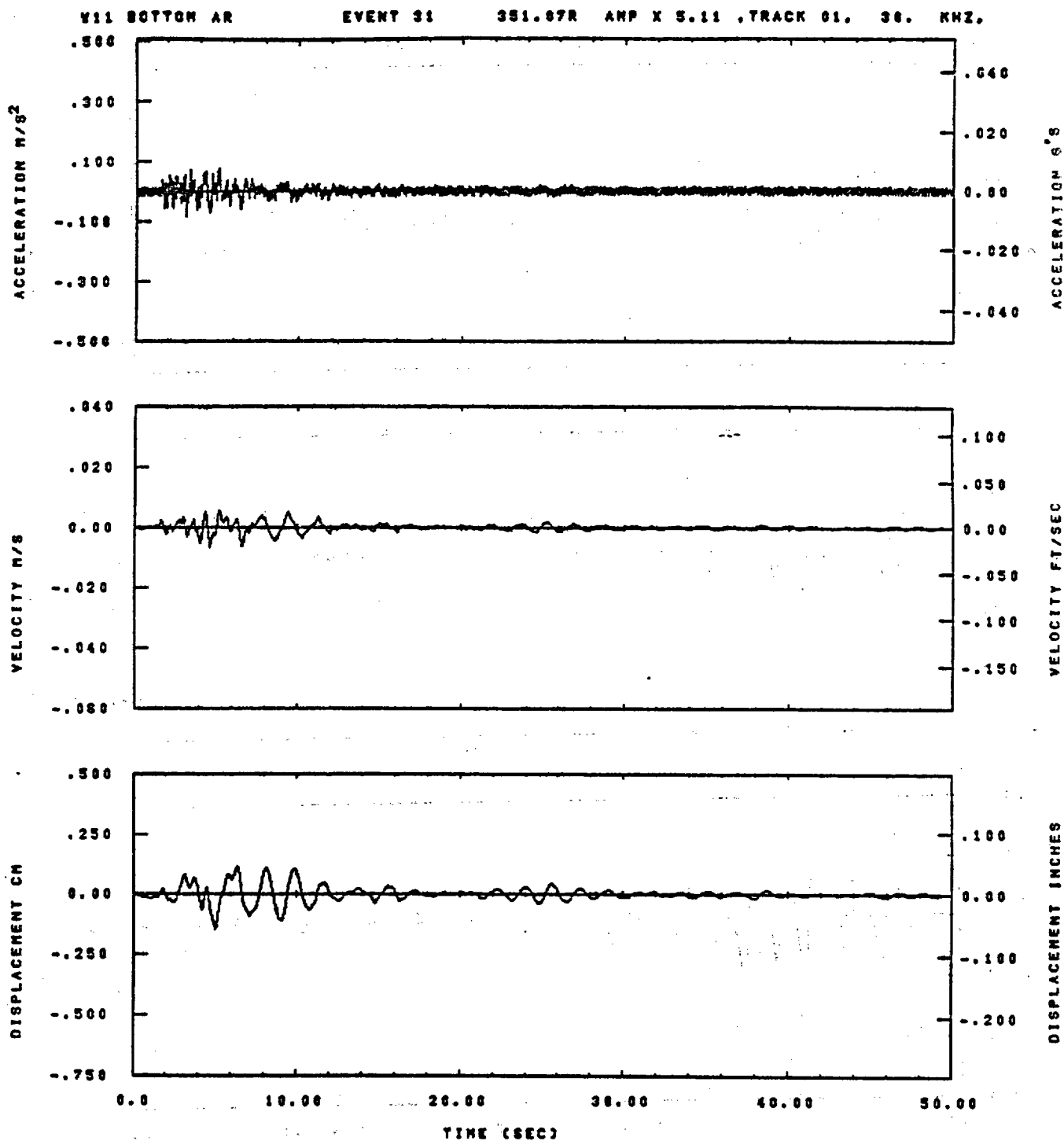
Figure E-26



IDT= .0028	ODT= .005	FIX=	AAS= 0.
HFF= .25	BYH= .18	HLH= 143	ASB=
LFF= 31.	BYL= 7.	HLL= 2399	ASE=
VTB= .250	VTE= .188	FLL= -20.	VSE= 0.
DPB= 0.	DPE= 180.	FLH= 0	DSE= 0.

14.48.33.

08/24/92

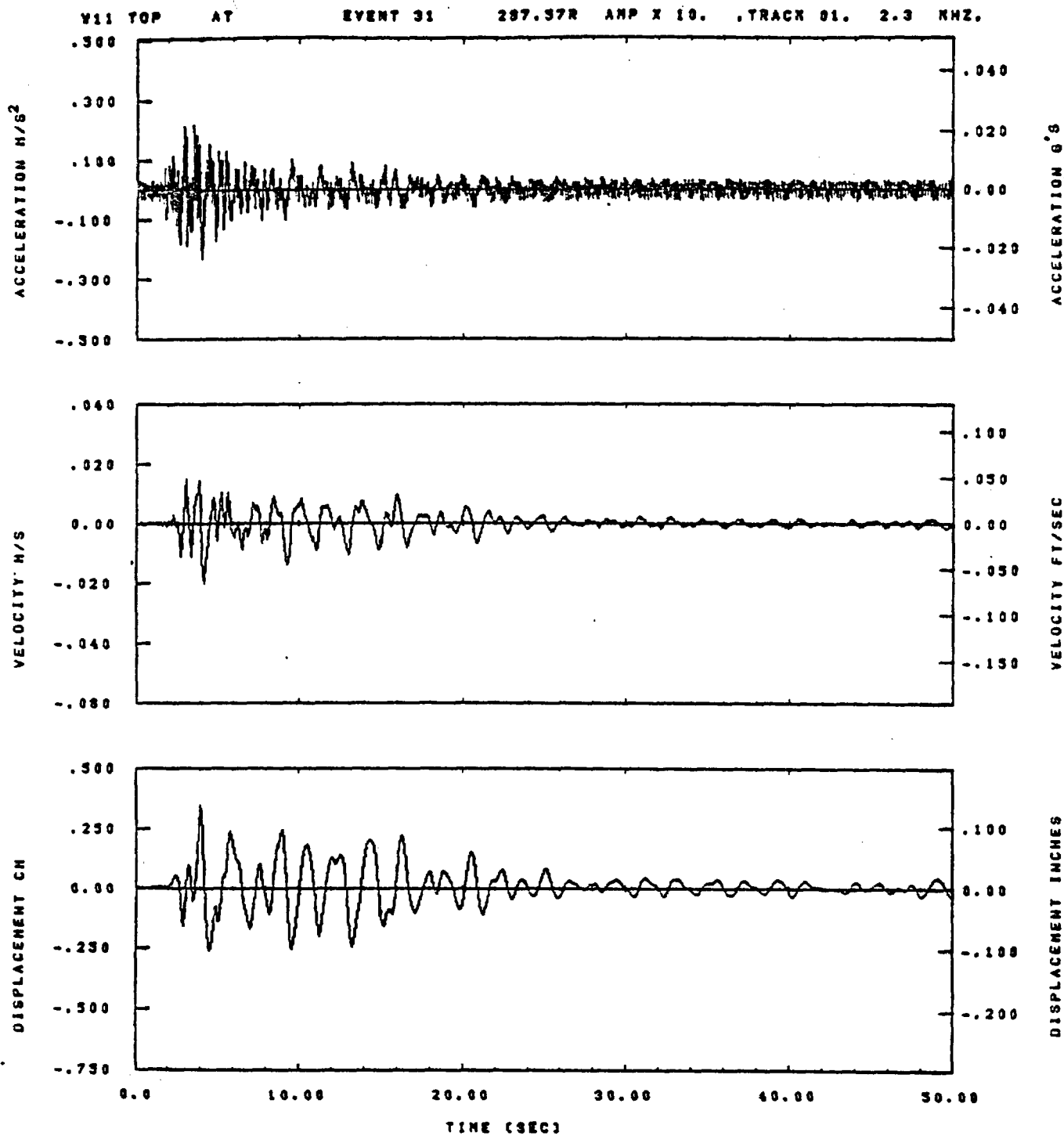


IDT= .0020	ODT= .005	FIX=	AAS= 0.
HPP= .25	BYH= .16	HLH= 143	ASS=
LPP= 31.	BYL= 7.	HLL= 2388	ASE=
VTE= .250	VTE= .160	FLL= -20.	VSE= 0.
OPB= 0.	OPE= 100.	FLH= 0	OSE= 0.

14.40.42.

08/24/82

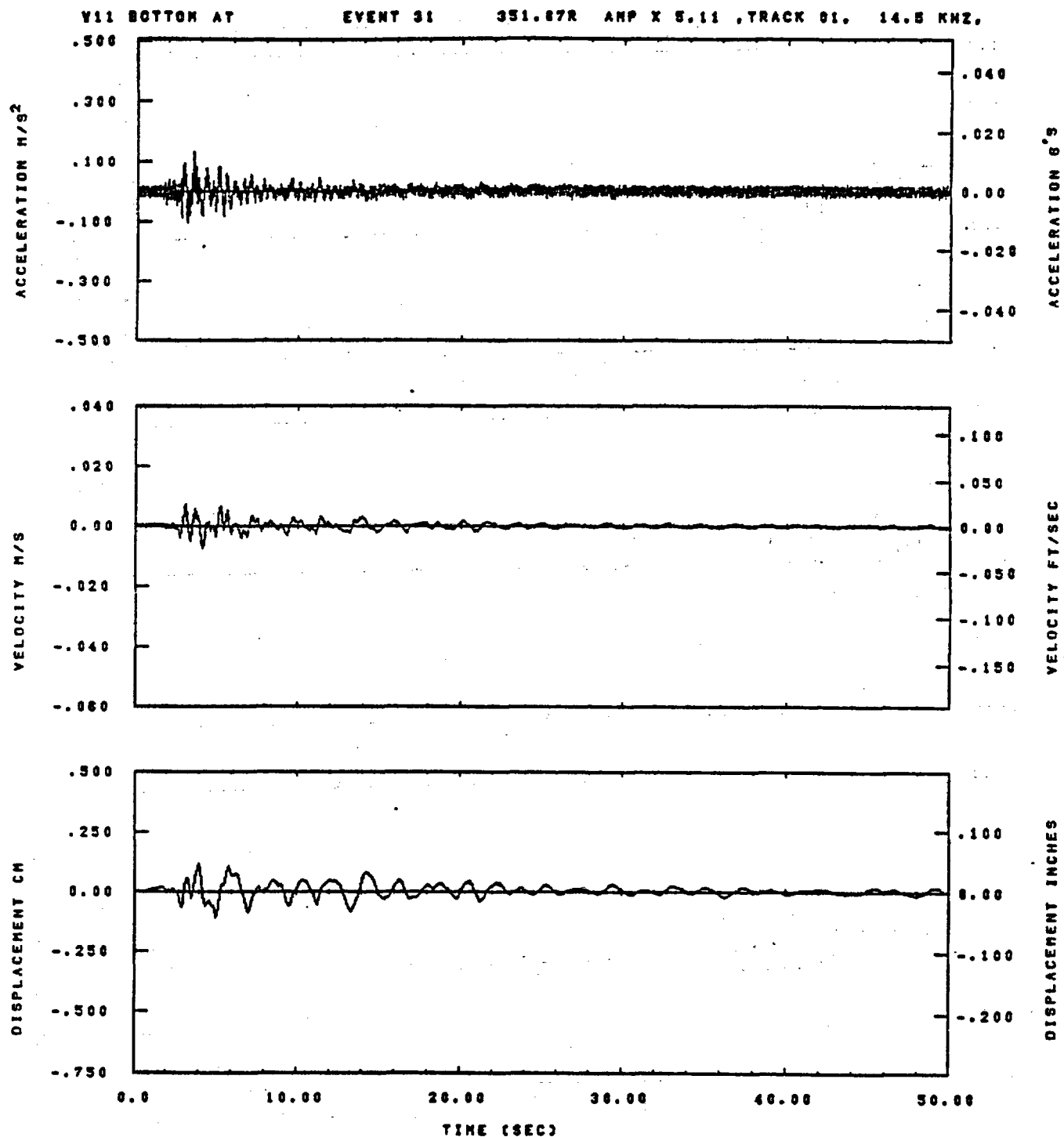
Figure E-28



IDT= .0020	ODT= .003	FIX=	AAS= 0.
HPP= .25	BYH= .16	HLH= 143	ASB=
LPP= 31.	BYL= 7.	HLL= 2339	ASE=
VTS= .250	VTE= .188	FLL= -20.	VSE= 0.
DPS= 0.	DPE= 100.	FLH= 0	DSE= 0.

14.40.38.

08/24/92

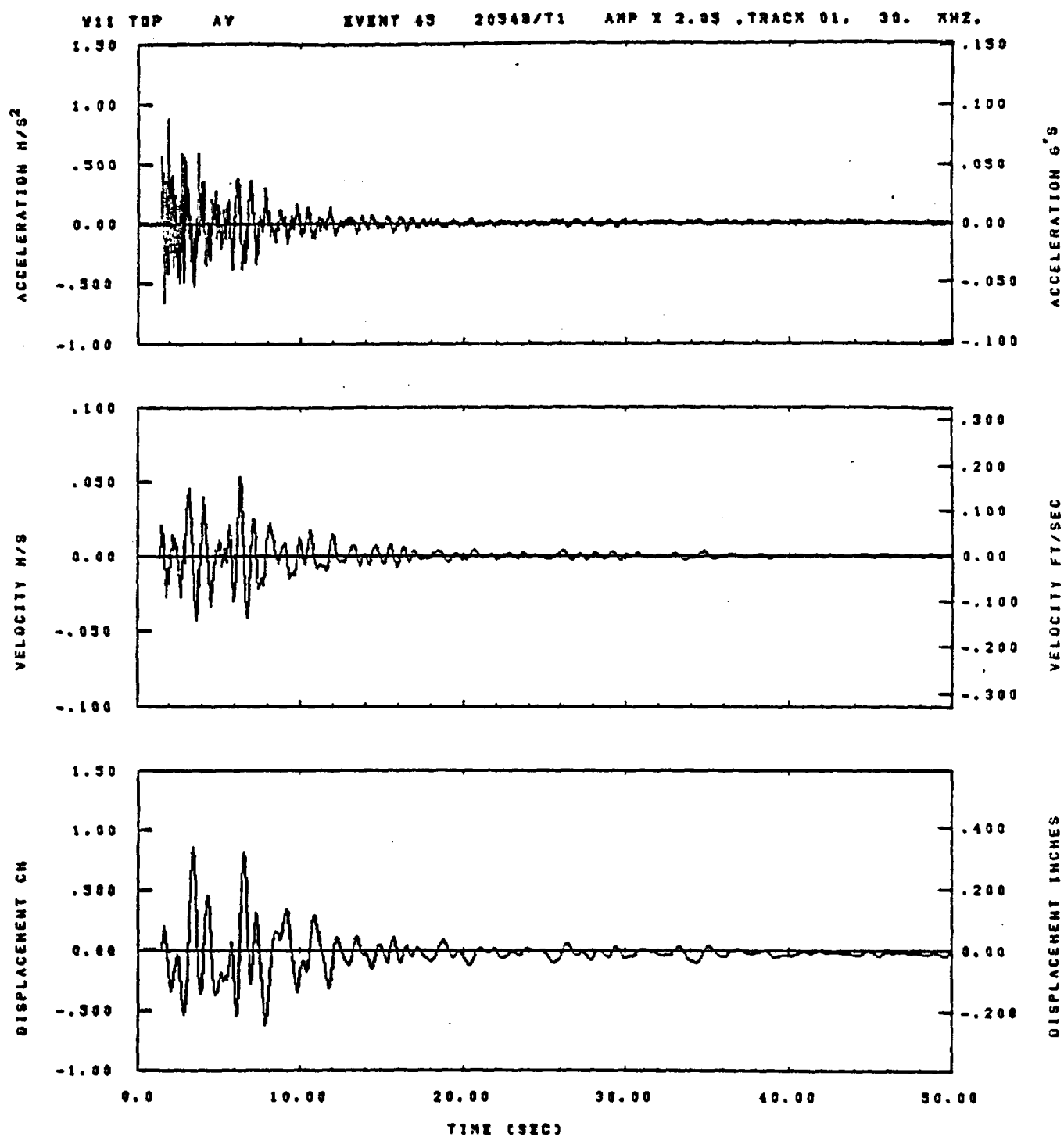


IDT= .0020	ODT= .005	FIX=	AAS= 0.
HPP= .25	BVH= .16	HLH= 143	ASB=
LPP= 31.	BVL= 7.	HLL= 2388	ASE=
VTS= .250	VTE= .188	FLL= -20.	VSE= 0.
DPS= 0.	DPE= 100.	FLH= 0	DSE= 0.

14.46.55.

06/24/82

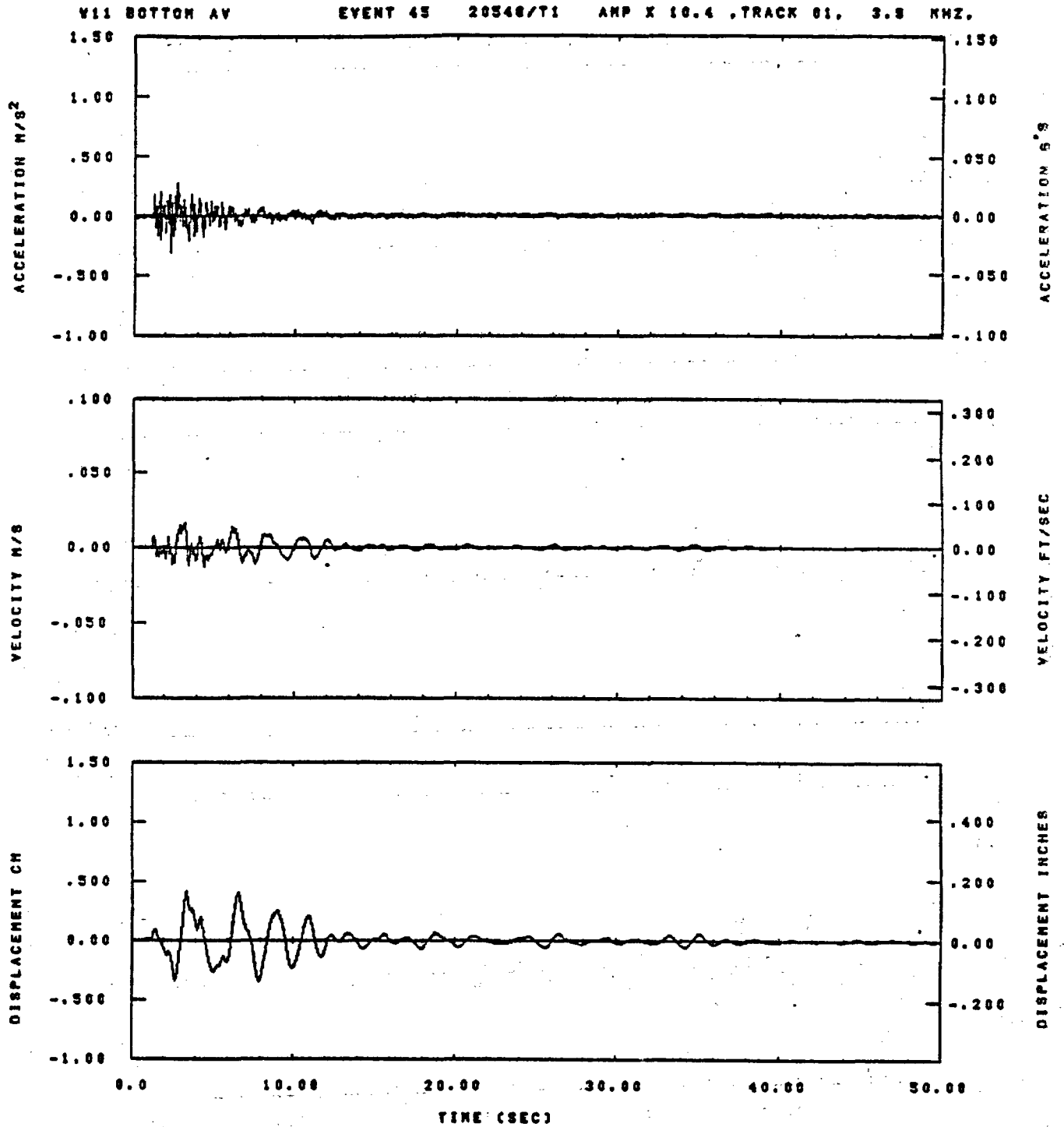
Figure E-30



IDT= .0020	ODT= .003	FIX=	AAS= 0.
MPF= .20	BYH= .13	HLX= 33	ASB=
LPF= 43.	BYL= 10.	HLL= 2999	ASE=
VTB= .200	VTE= .133	FLL= -20.	VSE= 0.
DPS= 0.	DPE= 100.	FLH= 0	DSE= 0.

13.34.43.

08/30/92

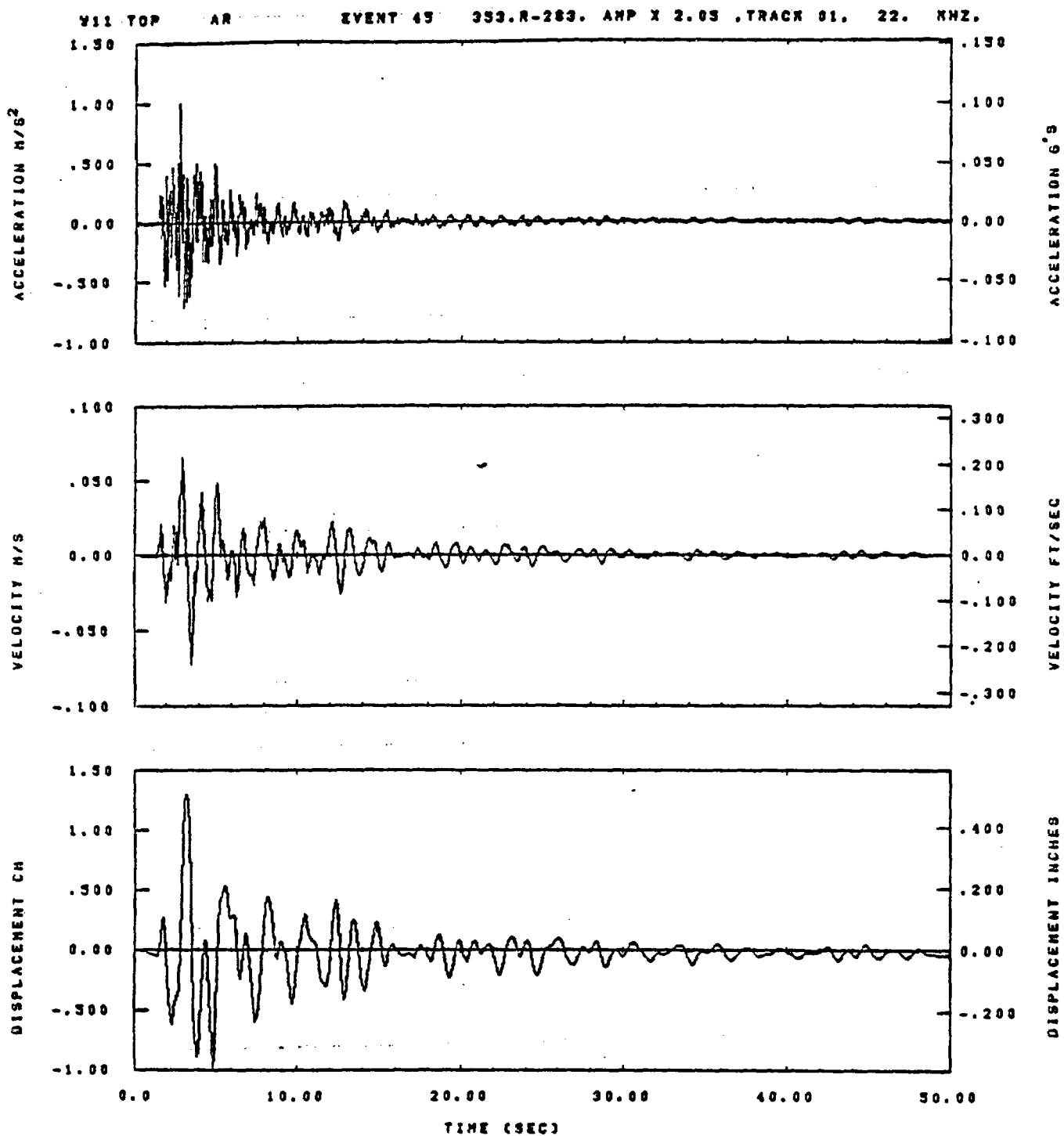


IDT= .0020	GDT= .005	FIX=	AAS= 0.
HFF= .20	SVH= .13	HLH= 99	ASB=
LFF= 45.	SVL= 10.	HLL= 2989	ASE=
VTB= .200	VTE= .133	FLL= -20.	VSE= 0.
DPE= 0.	DPE= 100.	FLH= 8	DSE= 0.

15.55.03.

06/30/02

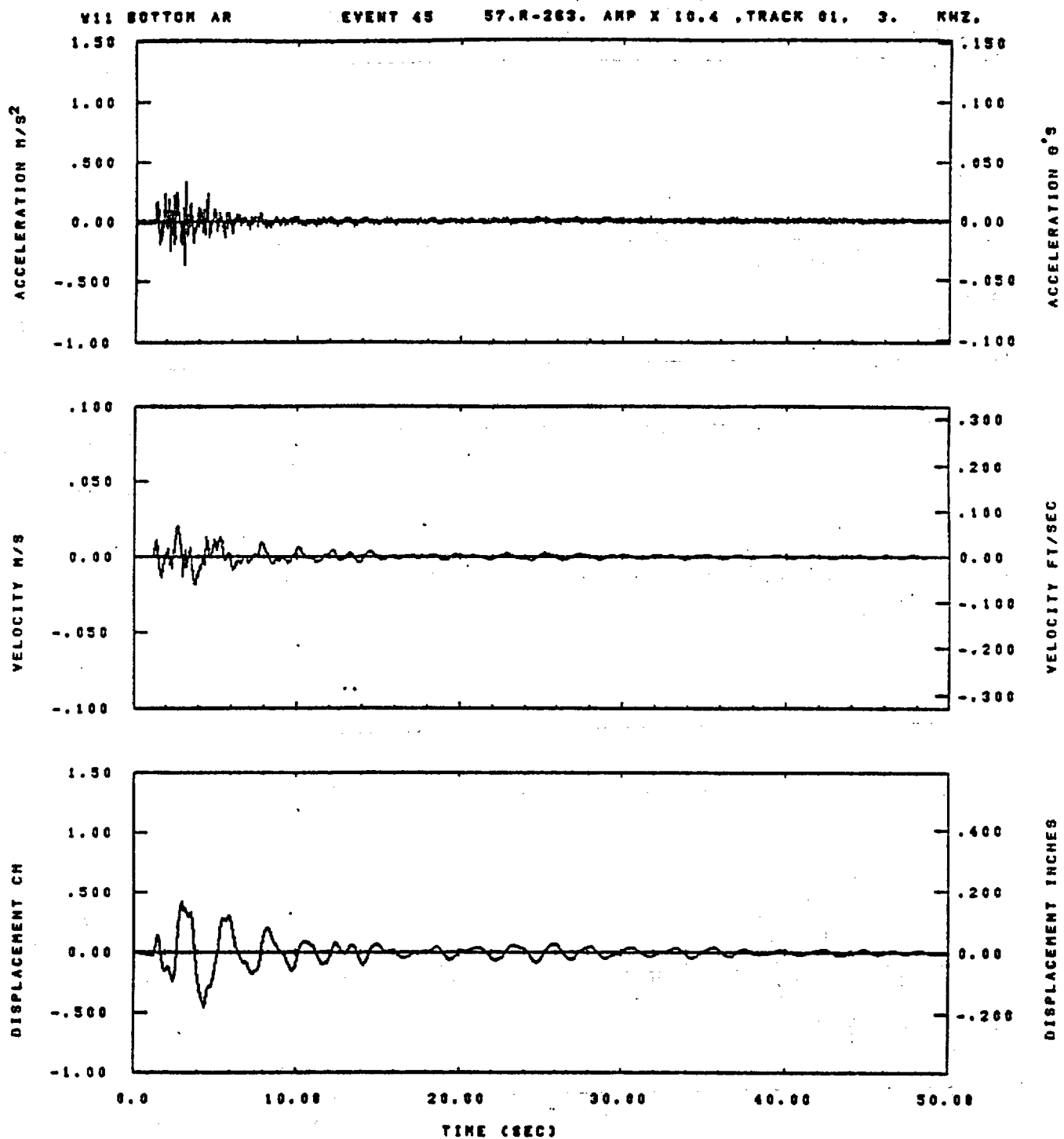
Figure E-32



IDT= .0020	ODT= .005	FIX=	AAS= 0.
HPP= .20	BYH= .13	HLH= 93	ASS=
LPP= 43.	BYL= 10.	HLL= 2999	ASE=
VTB= .200	VTE= .133	FLL= -20.	VSE= 0.
OPB= 0.	OPE= 100.	FLH= 0	OSE= 0.

13.54.34.

08/30/92

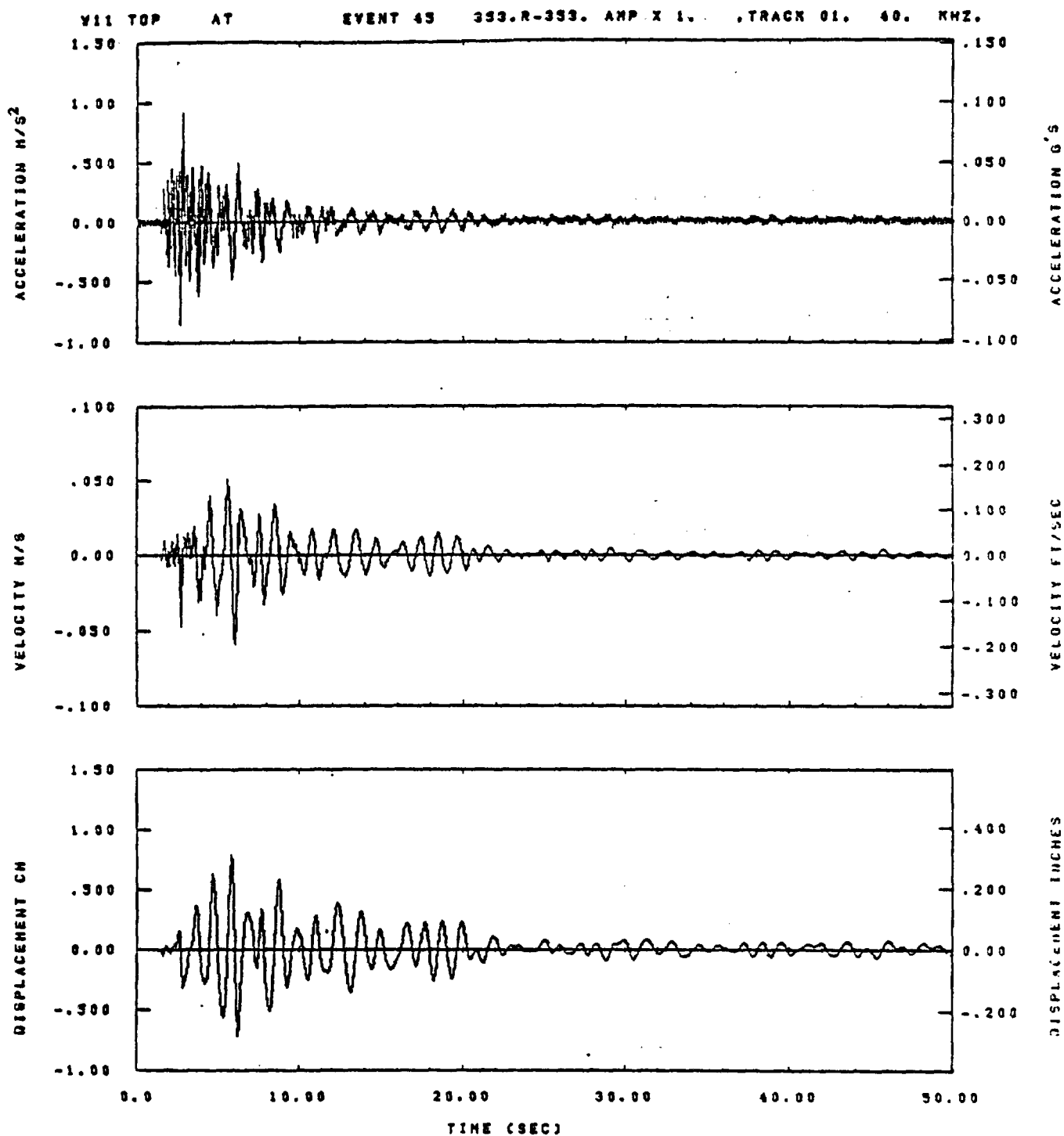


LOT= .0020	ODT= .005	FIX=	AAS= 0.
HFF= .20	SVH= .13	HLH= 99	ASS=
LFF= 45.	SVL= 10.	HLL= 2888	ASE=
VTB= .200	VTE= .133	PLL= -20.	VSE= 0.
OPB= 0.	OPE= 100.	PLH= 0	OSE= 0.

15.55.07.

06/30/82

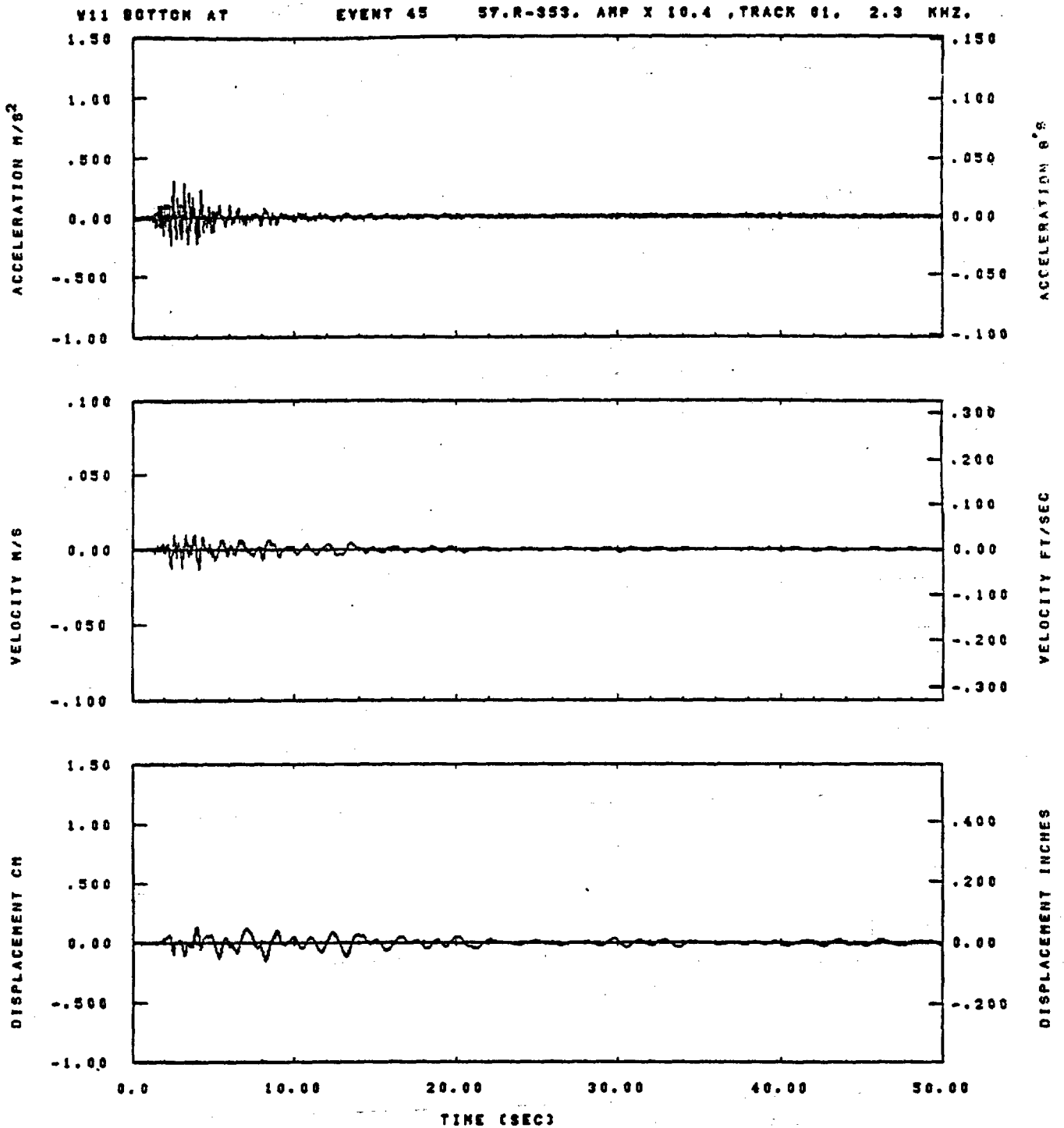
Figure E-34



IDT= .0020	QDT= .005	FIX=	AAS= 0.
HPP= .20	BYH= .13	HLH= 99	ASS=
LPP= 45.	BYL= 10.	HLL= 2999	ASE=
VTS= .200	VTE= .133	FLL= -20.	VSE= 0.
OPS= 0.	OPE= 100.	FLH= 0	OSE= 0.

13.34.58.

08/30/82

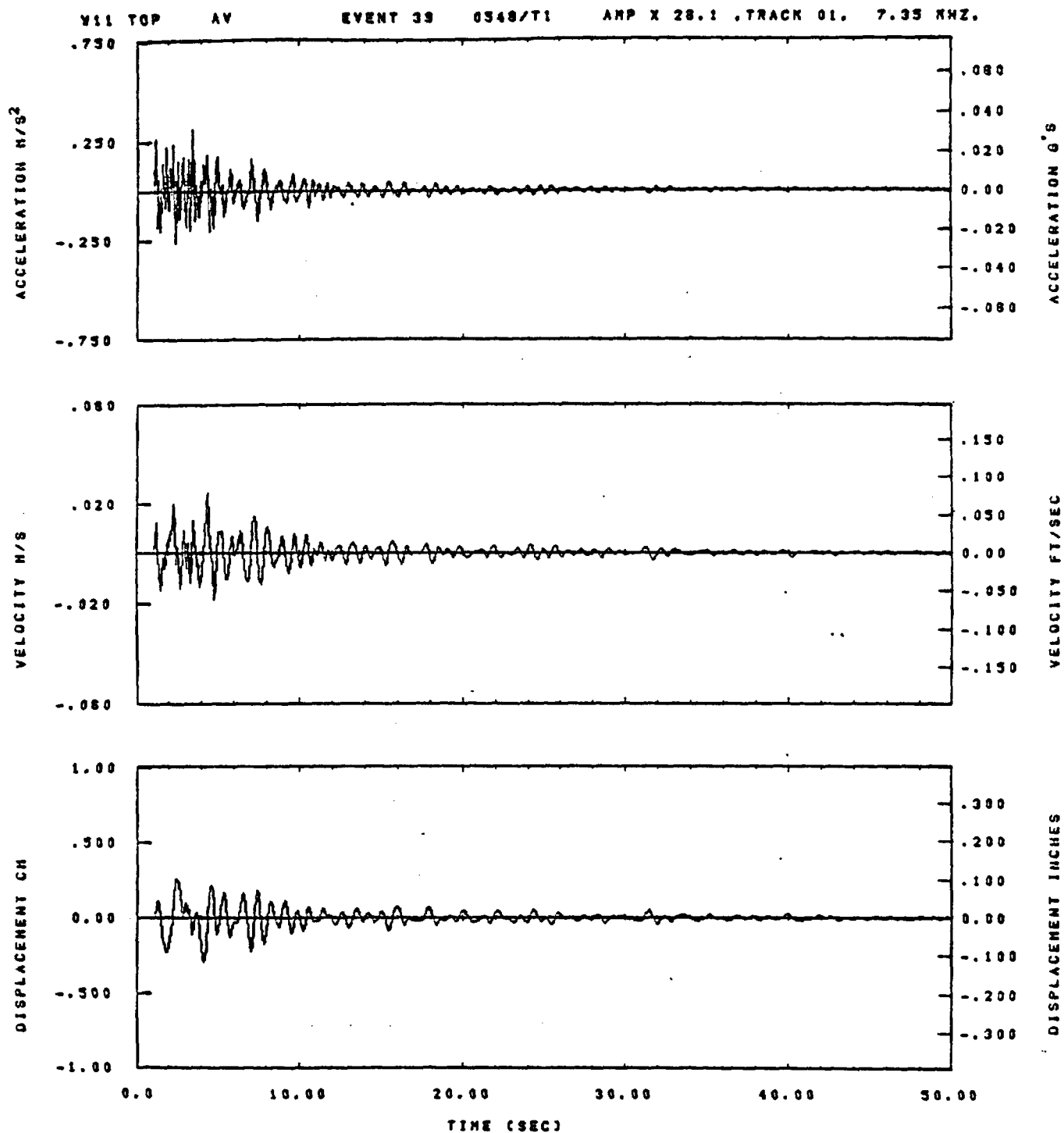


IDT= .0020	ODT= .005	FIX=	AAS= 0.
HPF= .20	BYH= .13	HLH= 88	ASB=
LPF= 45.	BYL= 10.	HLL= 2989	ASE=
VTB= .200	VTE= .133	FLL= -20.	VSE= 0.
DPS= 0.	DPE= 100.	FLH= 0	DSE= 0.

15.55.14.

06/30/82

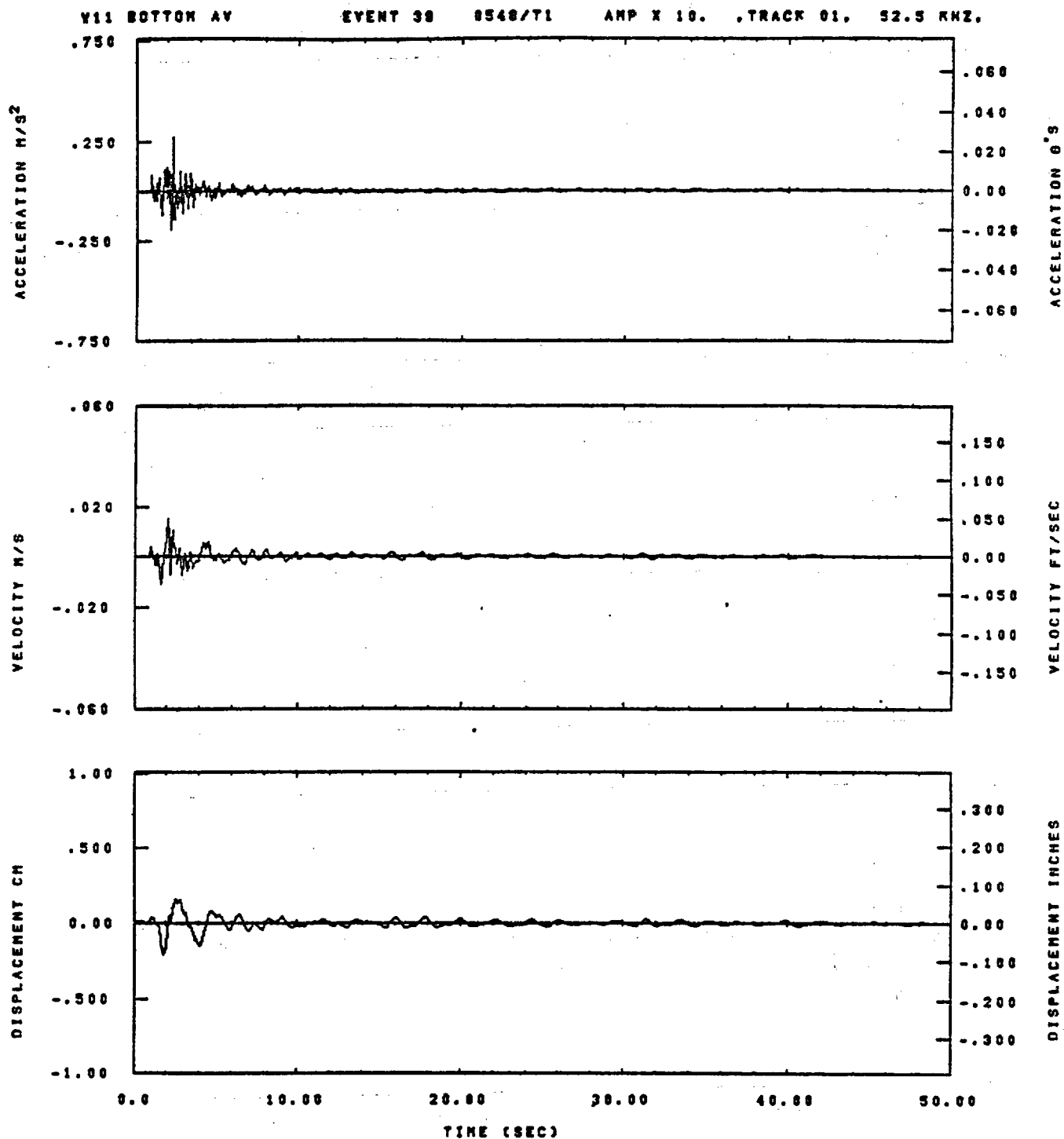
Figure E-36



IDT= .0020	ODT= .005	FIX=	AAS= 0.
HPF= .30	BYH= .20	HLH= 133	ASB=
LPF= 22.	BYL= 5.	HLL= 1333	ASE=
VTB= .300	VTZ= .200	FLL= -20.	VSE= 0.
DPS= 0.	DPE= 100.	FLH= 0	DSE= 0.

08.19.24.

08/24/92

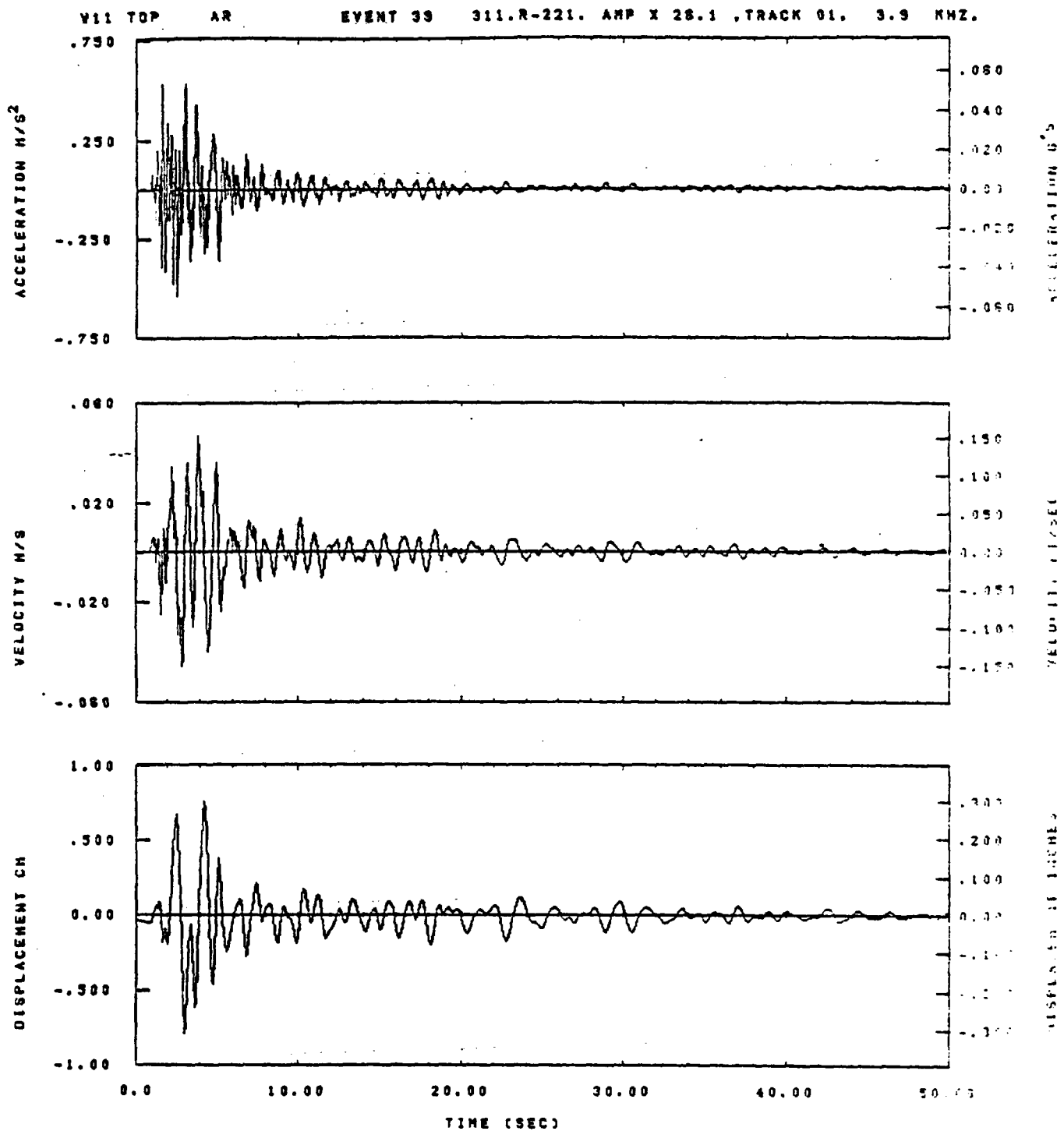


IDT= .0020	ODT= .005	FIX=	AAS= 0.
HPP= .38	BYH= .28	HLH= 198	ASH=
LPP= 22.	BYL= 5.	HLL= 1988	ASE=
VTB= .300	VTE= .200	FLL= -20.	VSE= 0.
OPB= 0.	OPE= 100.	FLH= 0	OSE= 0.

08.20.17.

08/24/82

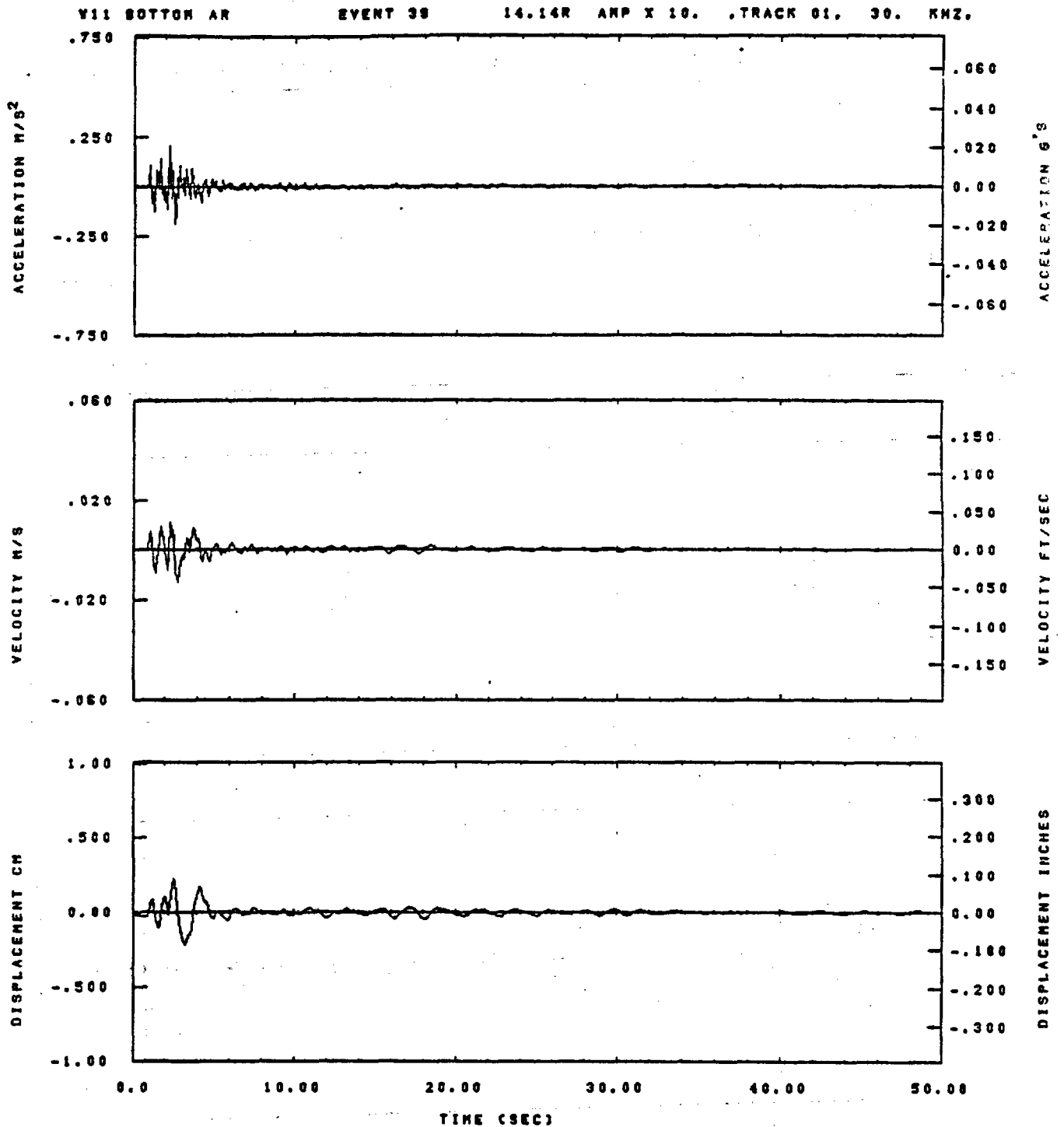
Figure E-38



IDT= .0020	ODT= .005	FIX=	AAS= 0.
HPF= .30	BYH= .20	HLH= 199	ASB=
LPF= 22.	BYL= 5.	HLL= 1999	ASE=
VTB= .300	VTE= .200	FLL= -20.	VSE= 0.
DPS= 0.	DPE= 100.	FLH= 0	DSE= 0.

08.19.32.

05/24/82

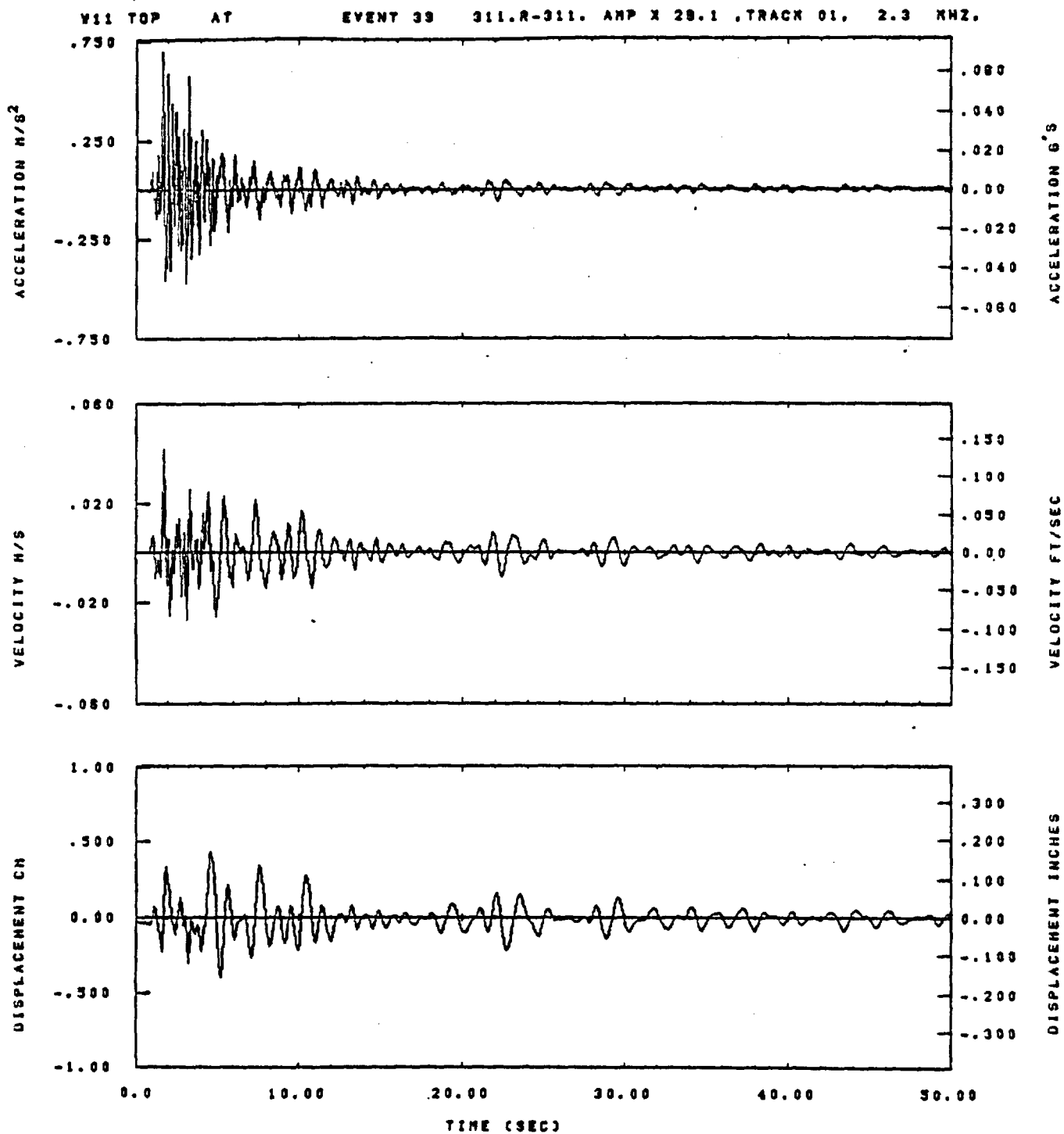


IDT= .0020	ODT= .005	FIX=	AAS= 0.
HPP= .30	SVH= .20	HLH= 189	ASB=
LPP= 22.	SVL= 5.	HLL= 1899	ASE=
VTB= .300	VTE= .200	FLL= -20.	VSE= 0.
DPS= 0.	DPE= 100.	FLH= 8	DSE= 0.

08.20.24.

06/24/82

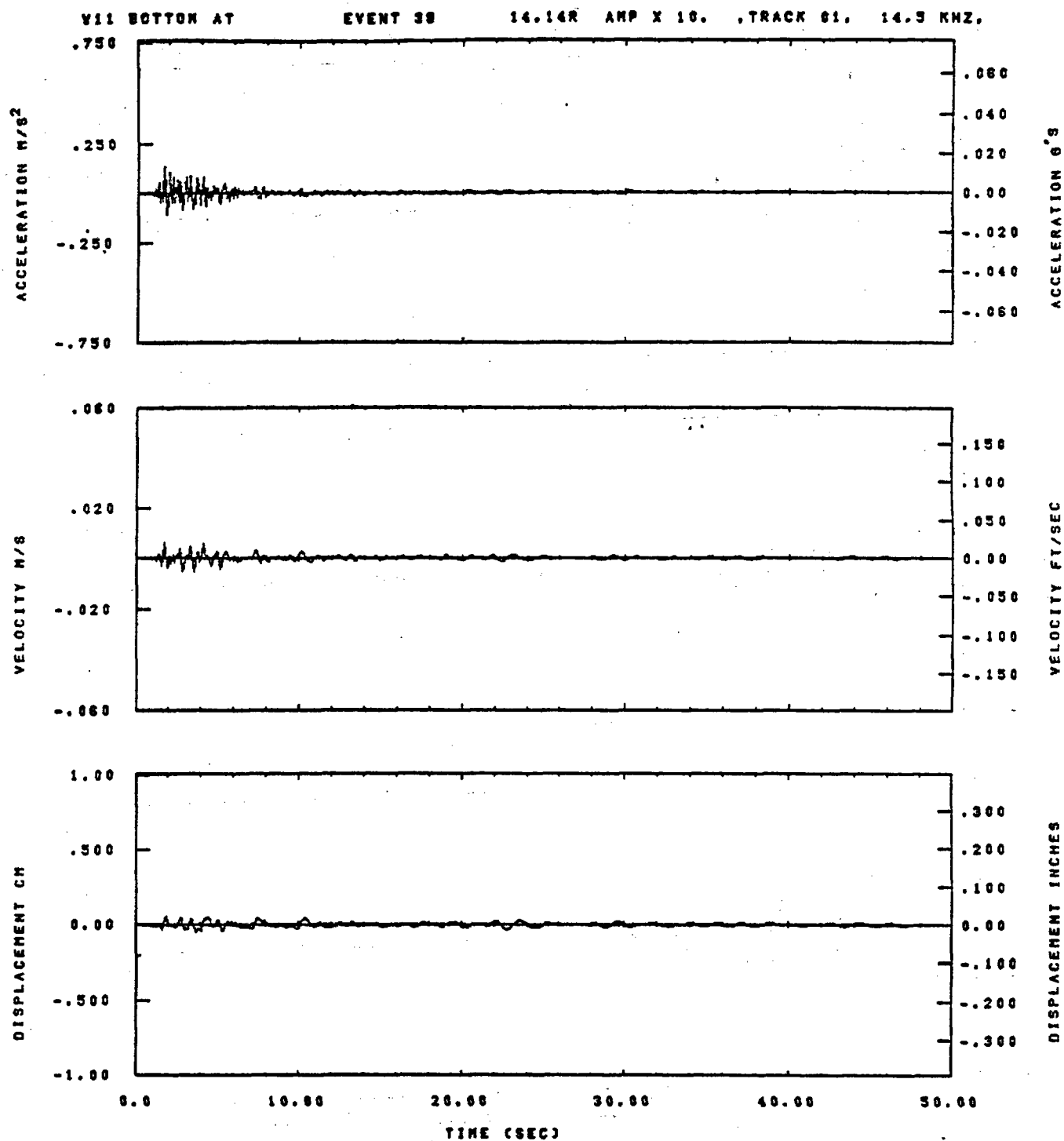
Figure E-40



IOT= .0020	ODT= .003	FIX=	AAS= 0.
HPP= .3	BVH= .20	HLH= 199	ASB=
LPP= 22.	SWL= 5.	HLL= 1999	ASZ=
VTB= .30	VTE= .200	FLL= -20.	VSE= 0.
OPB= 0.	DPE= 100.	FLH= 0	DSE= 0.

08.13.50.

08/24/82

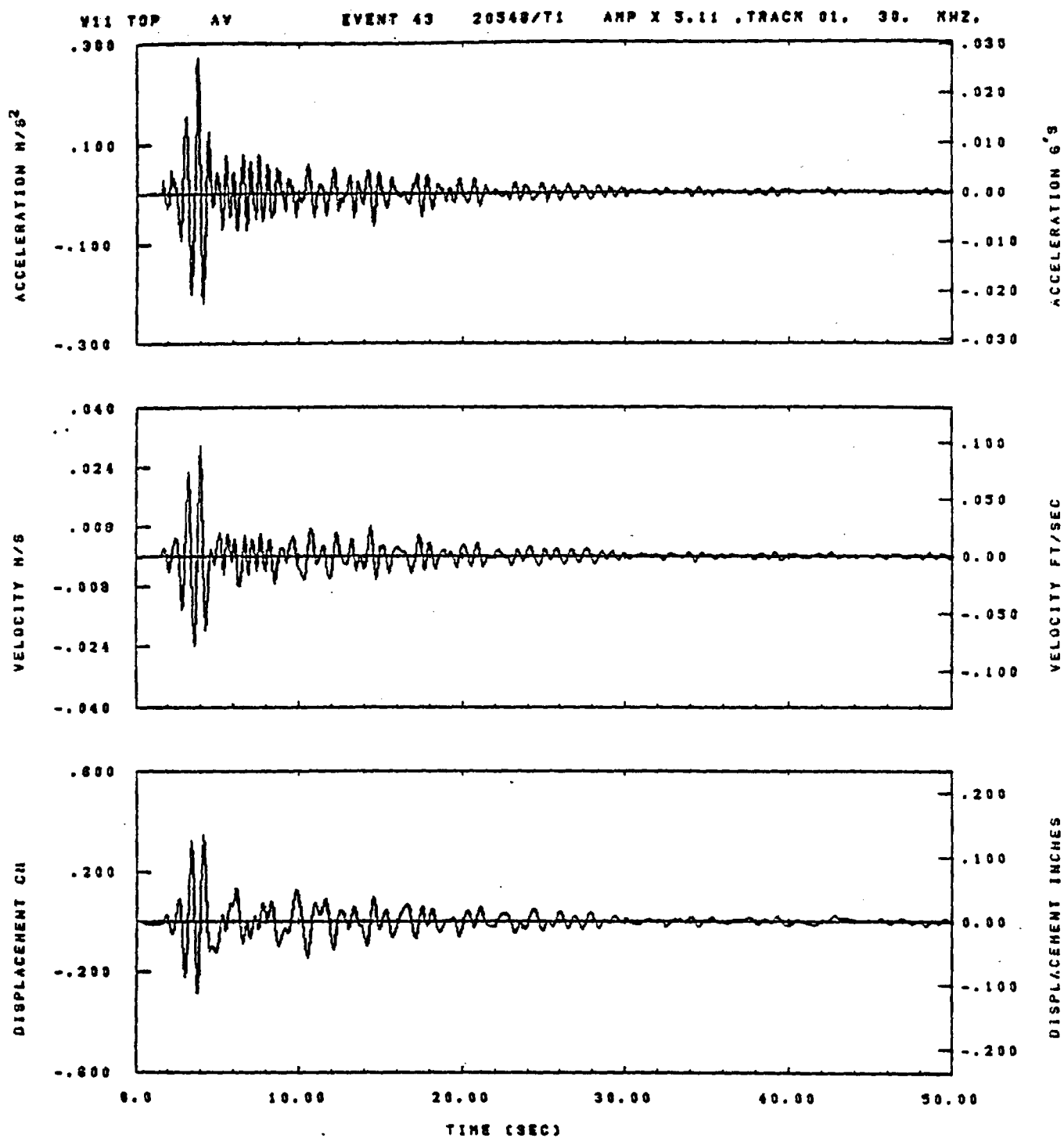


IDT= .0020	ODT= .005	FIX=	AAS= 0.
HPP= .30	BVH= .20	HLH= 189	ASB=
LPP= 22.	BVL= 5.	HLL= 1888	ASE=
VTB= .300	VTE= .208	FLL= -20.	VSE= 0.
DPS= 0.	DPE= 100.	FLH= 0	DSE= 0.

08.28.32.

06/24/82

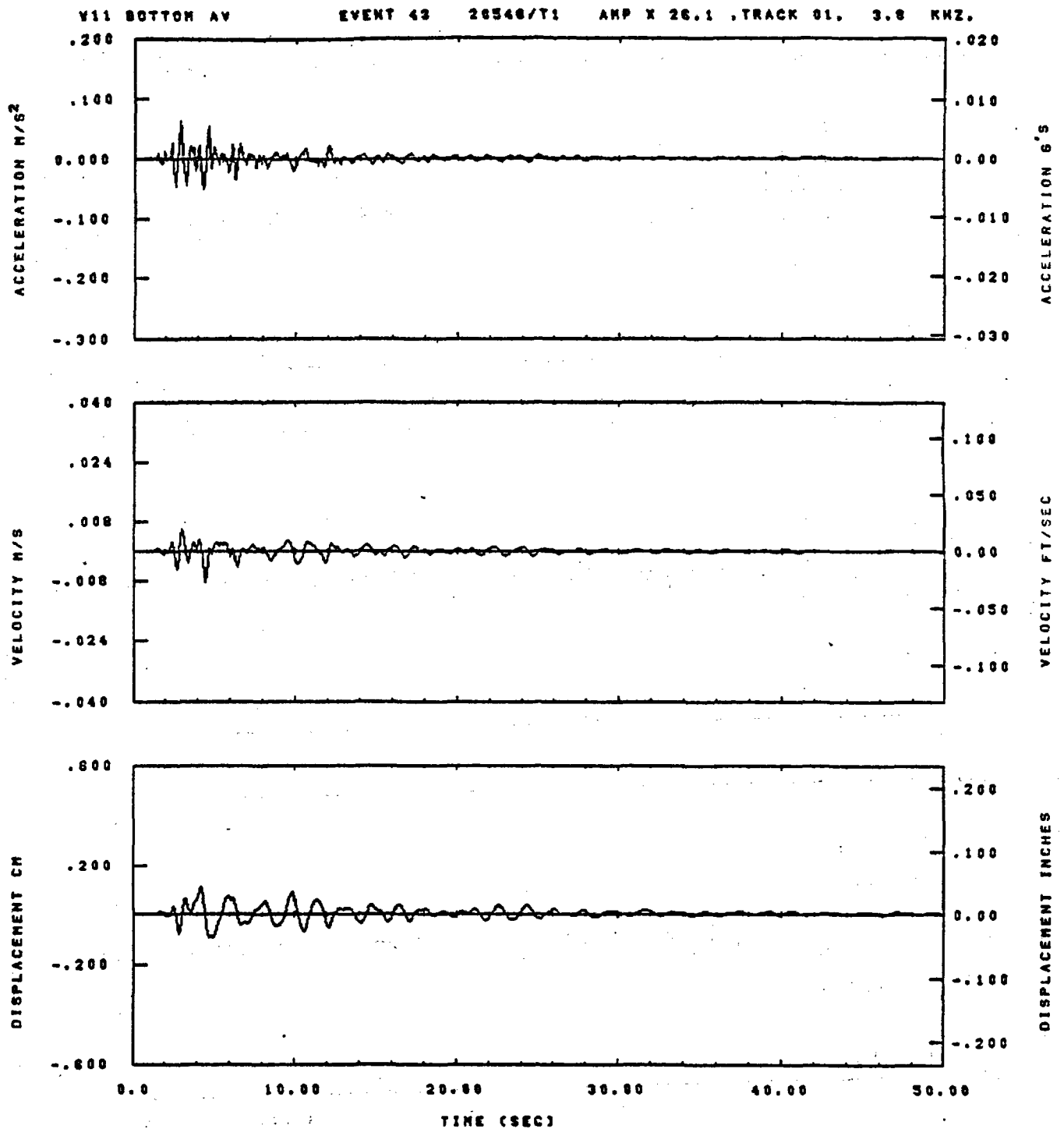
Figure E-42



IDT= .0020	ODT=	FIX=	AAS= 0.
HPP= .20	BYH= .13	HLH= 417	ASB=
LPP= 10.	BYL= 2.	HLL= 2993	ASE=
VTB= .200	VTE= .133	FLL= -20.	VSE= 0.
DPB= 0.	OPE= 100.	FLH= 0	DSE= 0.

10.48.28.

08/23/82

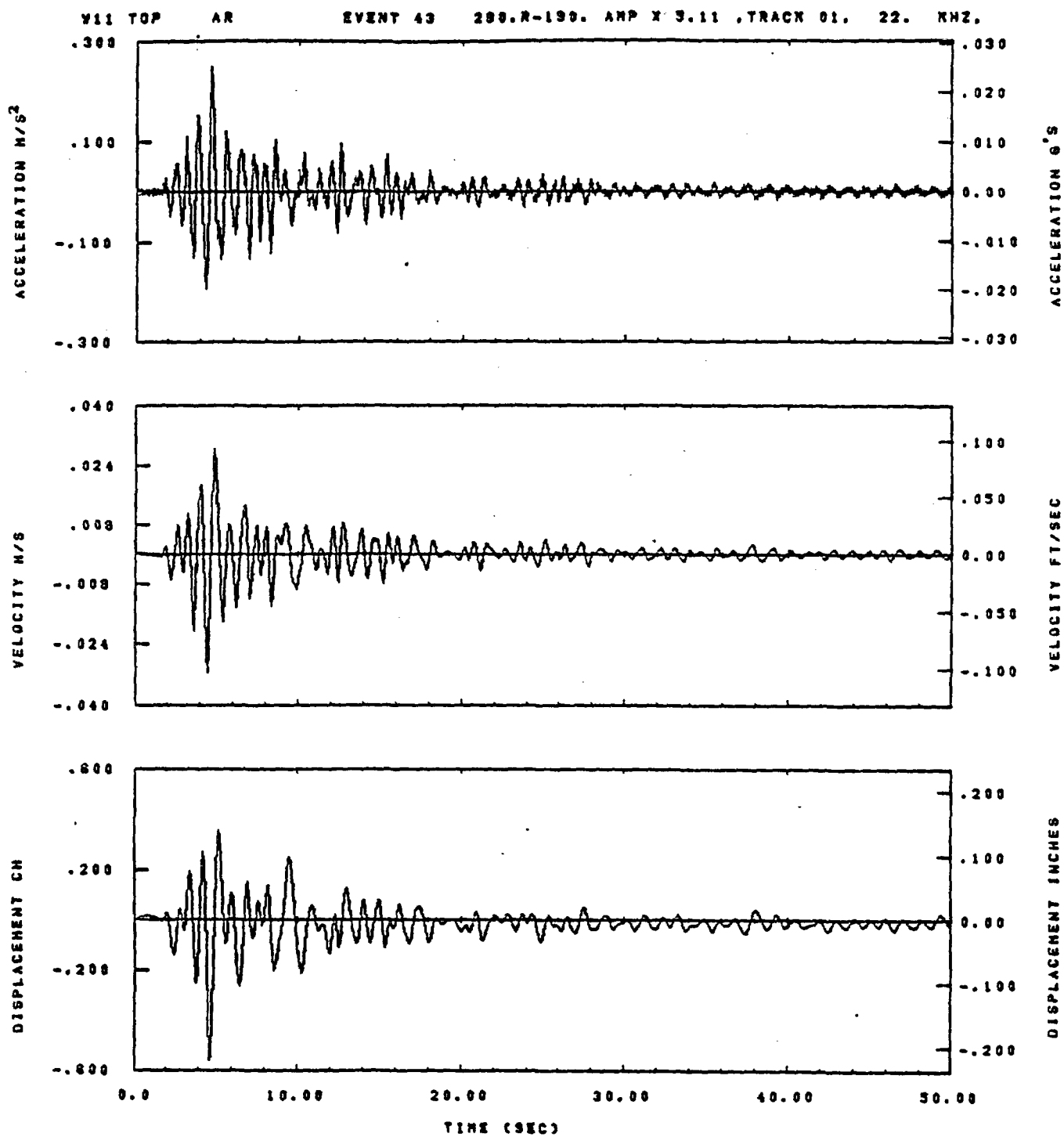


IDT= .0020	ODT= .005	FIX=	AAS= 0.
HPF= .20	BYN= .13	NLH= 417	AGB=
LPF= 10.	BYL= 2.	NLL= 2000	ASE=
YTB= .200	YTE= .133	FLL= -20.	VSE= 0.
DPS= 0.	DPE= 100.	FLW= 0	DSE= 0.

10.49.21.

06/23/82

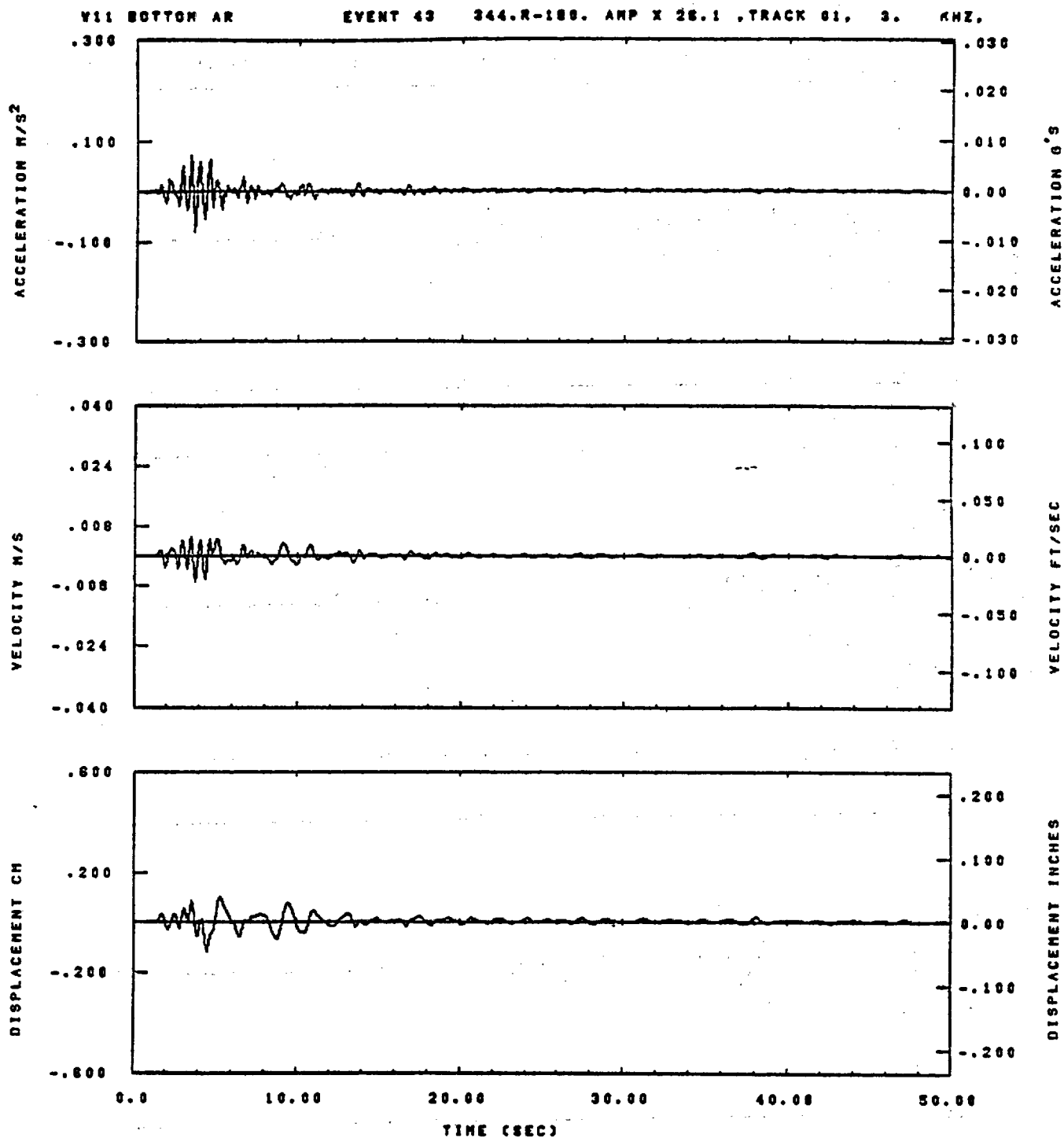
Figure E-44



IDT= .0020	ODT=	FIX=	AAS= 0.
HPP= .20	SVH= .13	HLH= 417	ASB=
LPP= 10.	SVL= 2.	HLL= 2999	ASE=
VTS= .200	VTE= .133	PLL= -20.	VSE= 0.
DPS= 0.	OPE= 100.	PLH= 0	DSE= 0.

10.48.44.

08/23/82

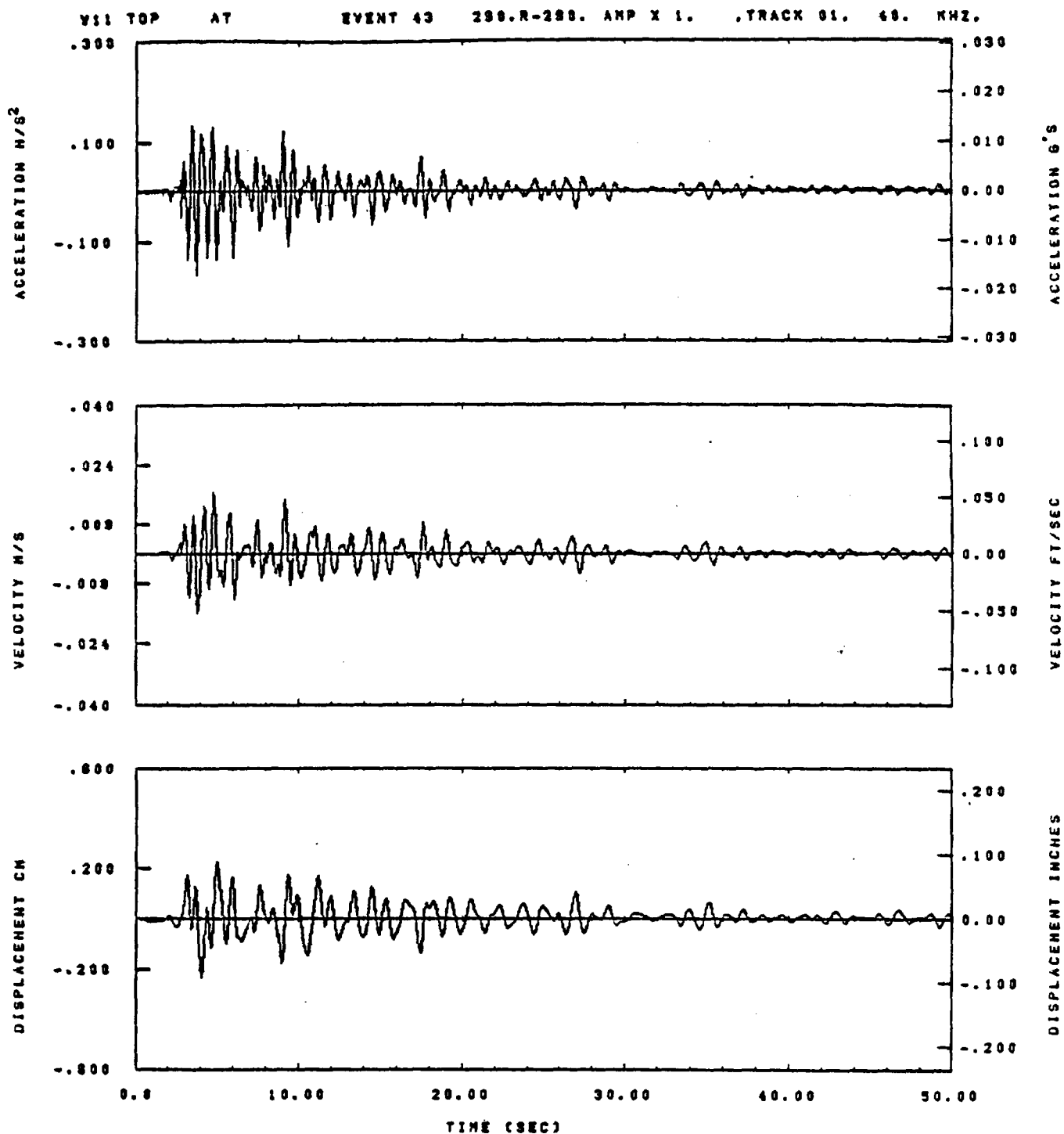


IDT= .0020	ODT= .005	FIX=	AAS= 0.
HPF= .20	BYH= .13	MLH= 417	ASS=
LPF= 10.	BYL= 2.	NLL= 2888	ASE=
VTS= .200	VTE= .133	FLL= -20.	VSE= 0.
DPS= 0.	DPE= 100.	FLH= 0	DSE= 0.

10.48.27.

06/23/82

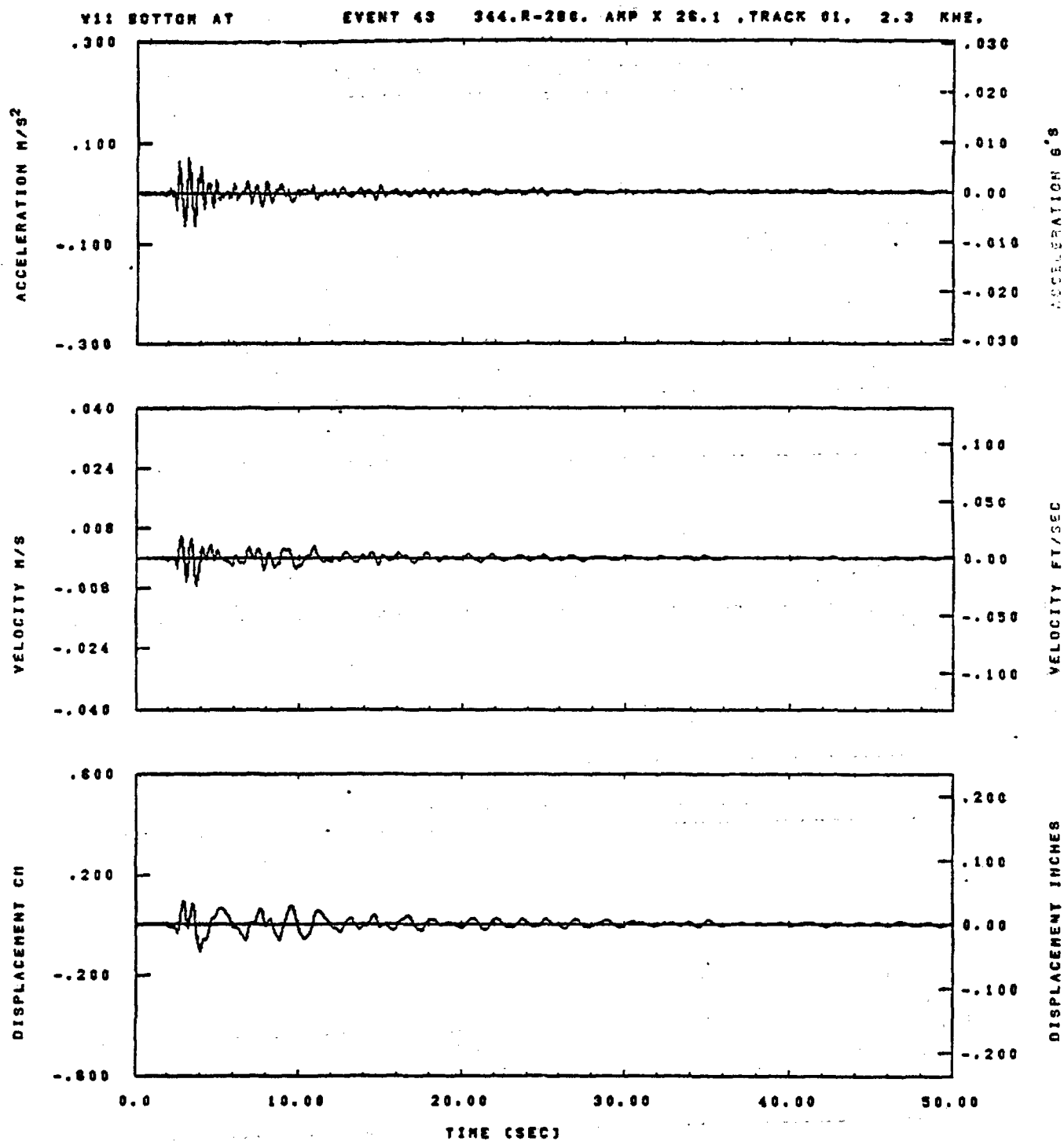
Figure E-46



IDT= .0020	QDT=	FIX=	AAS= 0.
HPP= .20	BYH= .13	HLH= 417	ASB=
LPP= 10.	BYL= 2.	HLL= 2999	ASE=
VTS= .200	VTE= .133	FLL= -20.	VSE= 0.
DPS= 0.	DPE= 100.	FLH= 0	DSE= 0.

10.49.01.

08/23/82

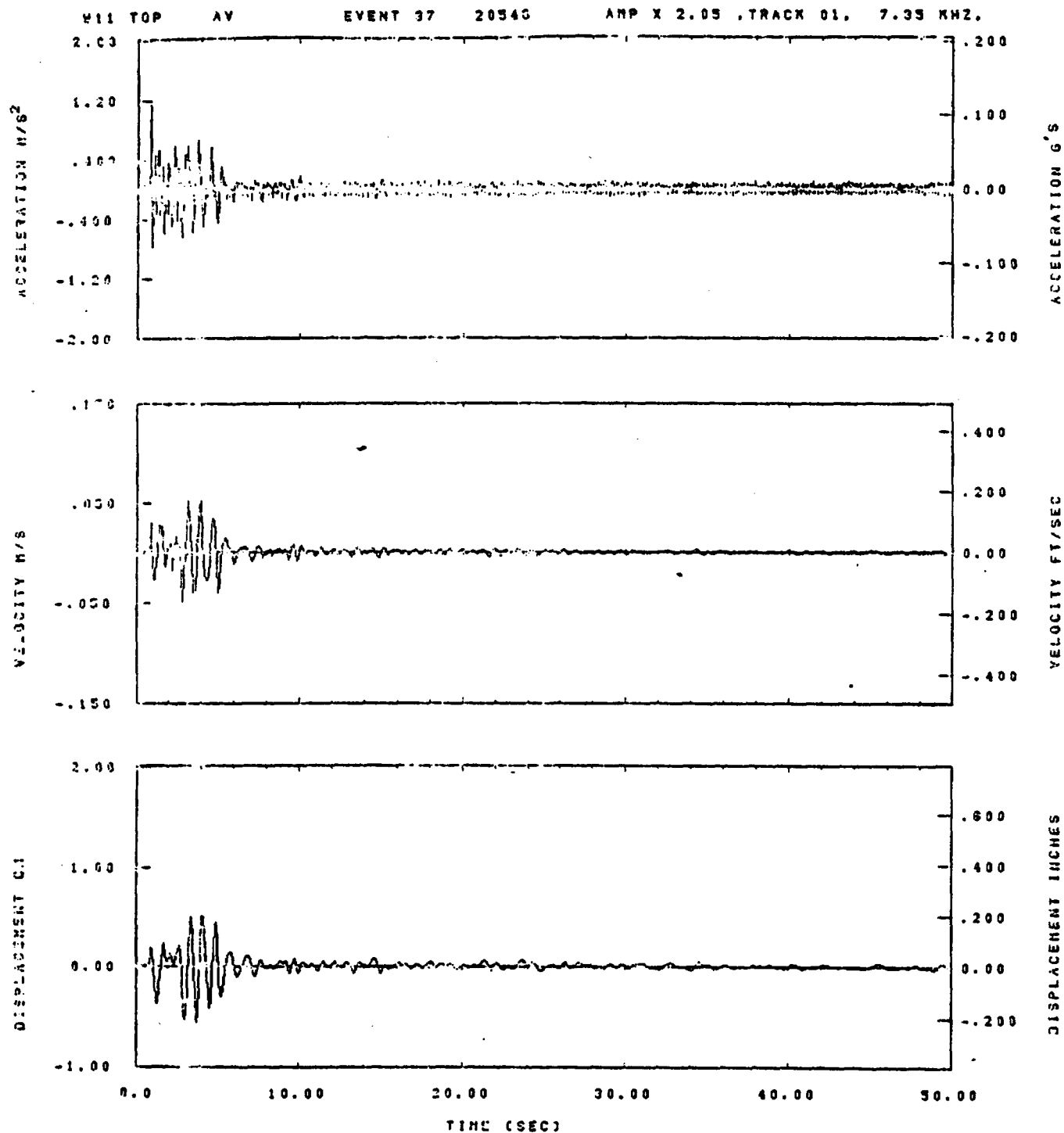


IDT= .0020	ODT= .005	FIX=	AAS= 0.
HPP= .20	BYH= .13	HLH= 417	ASB=
LPP= 10.	BYL= 2.	HLL= 2988	ASE=
VTB= .200	VTE= .133	FLL= -20.	VSE= 0.
DPS= 0.	DPE= 100.	FLH= 0	DSE= 0.

10.48.35.

06/23/82

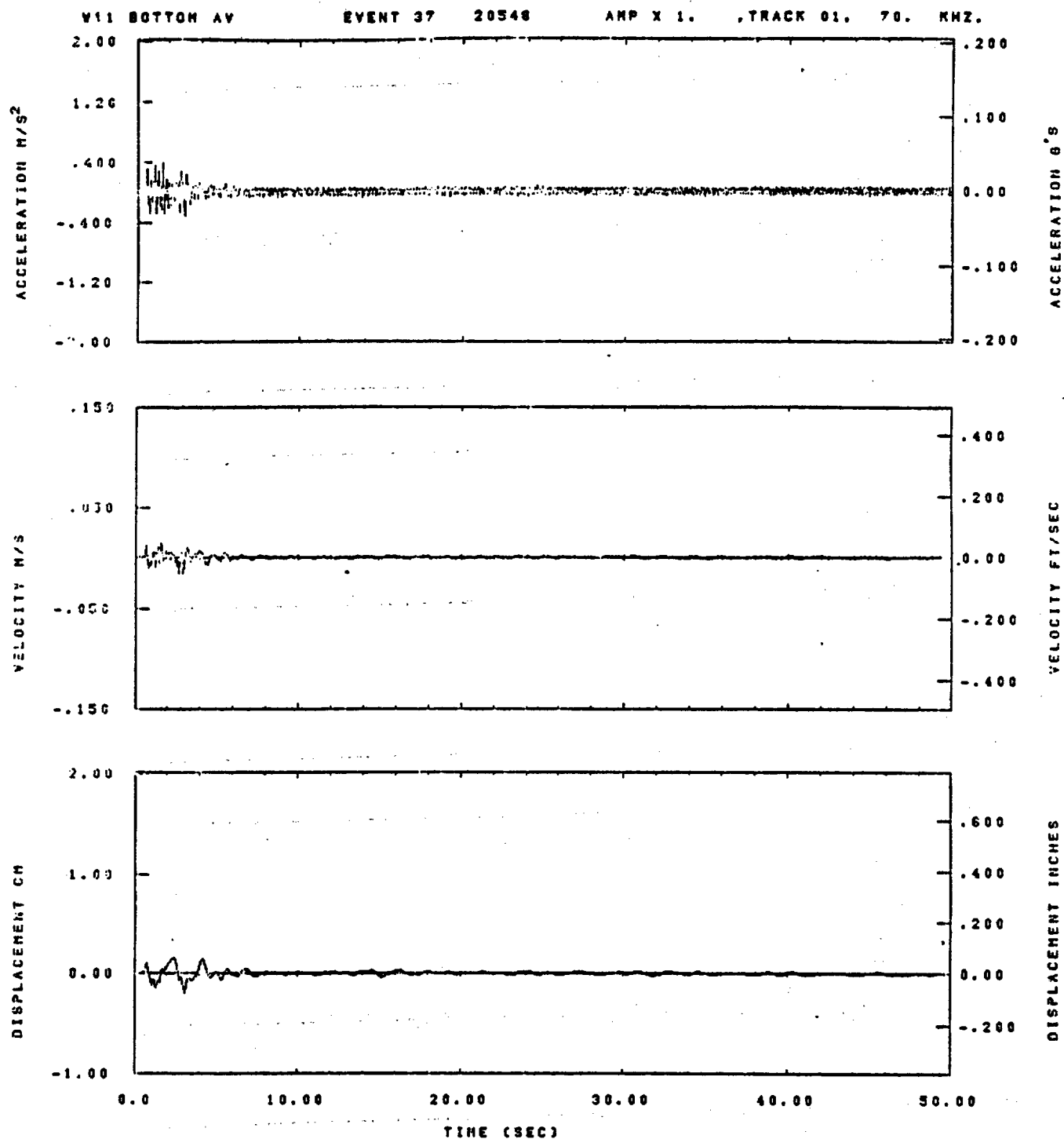
Figure E-48



IDT= .0020	ODT= .005	FIX=	AAS= 0.
HPFA= .40	SVH= .26	HLH= 167	ASB=
LPF= 27.	BVL= 6.	HLL= 1499	ASE=
VTB= .400	VTE= .267	FLL= -20.	VSE= 0.
DPC= 0.	DPE= 100.	FLH= 0	DSE= 0.

19.17.03.

08/16/82



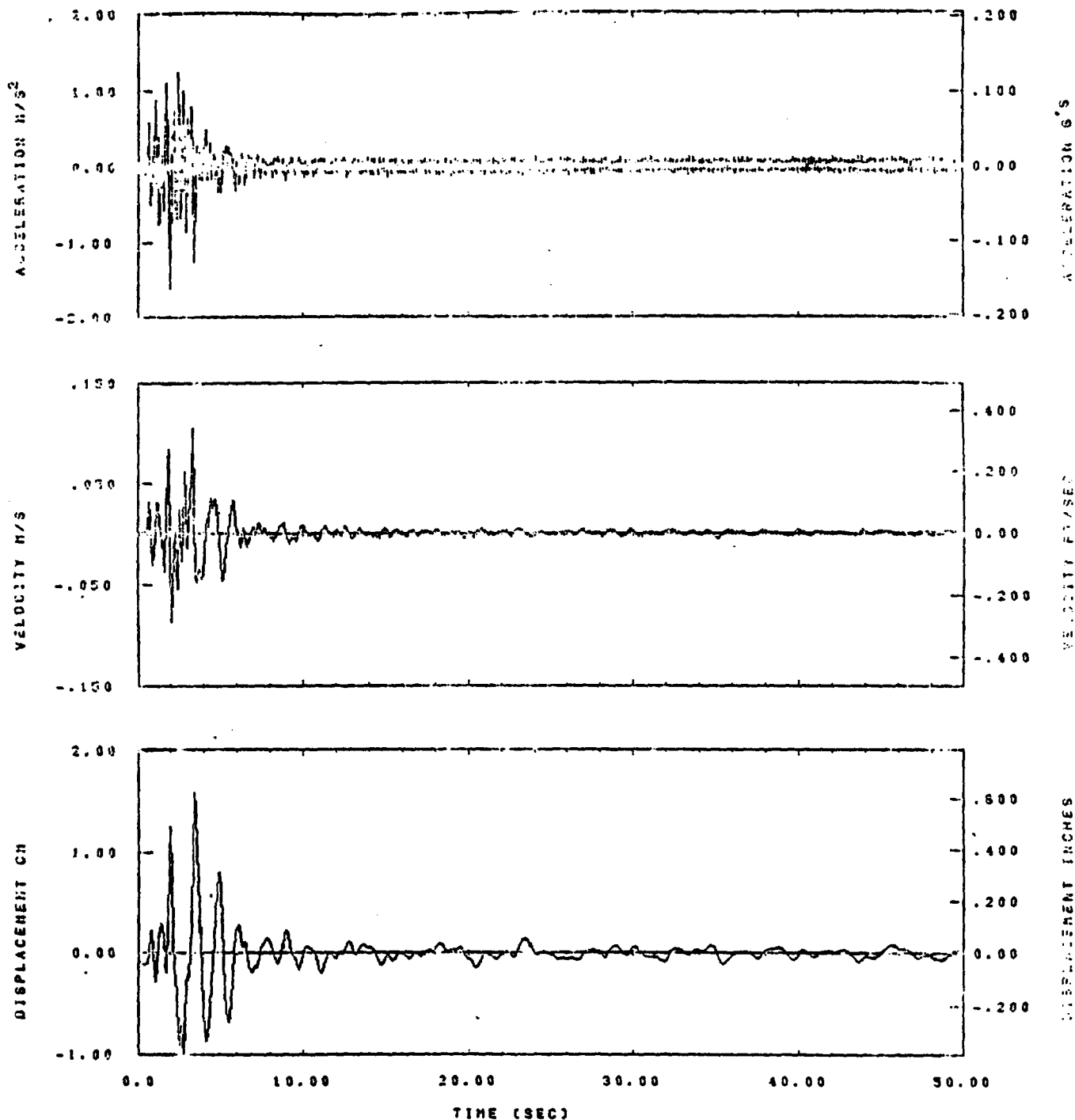
IDT= .0020	ODT= .005	FIX=	AAS= 0.
HPF= .40	SVH= .28	HLH= 167	ASB=
LPF= 27.	SVL= 8.	HLL= 1499	ASE=
VTS= .400	VTE= .267	FLL= -20.	VSE= 0.
CPS= 0.	OPE= 100.	FLH= 0	OSE= 0.

18.17.15.

06/16/82

Figure E-50

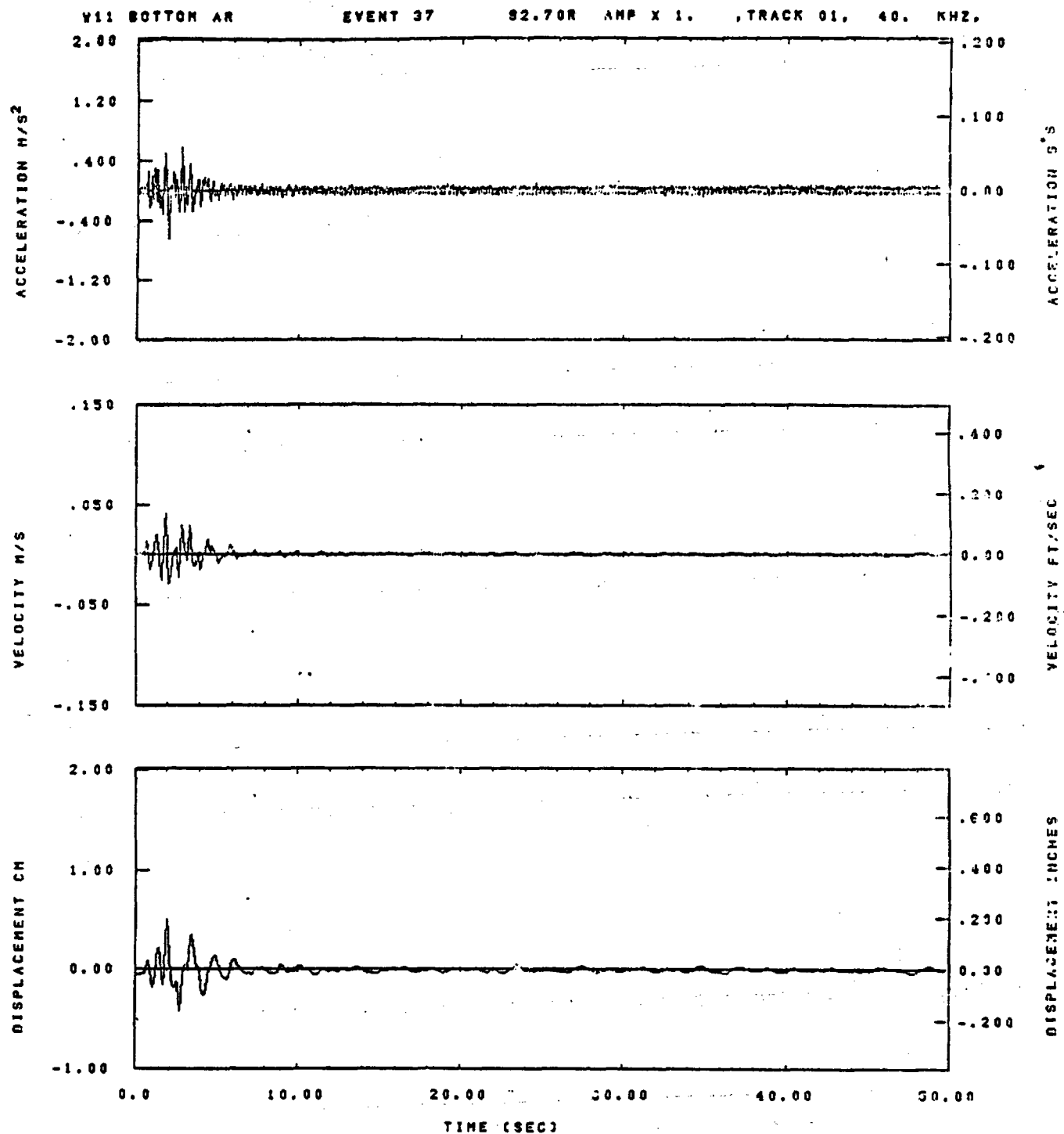
V11 TOP AR EVENT 37 29.20R AMP X 2.05 , TRACK 01. 3.9 KHZ.



IDT= .0020	ODT= .005	FIX=	AAS= 0.
HPP= .20	SVH= .13	HLH= 249	ACB=
LPP= 18.	SVL= 4.	HLL= 2999	ASE=
YTS= .200	YTE= .133	FLL= -20.	VSE= 0.
OPB= 0.	OPE= 100.	FLH= 0	OSE= 0.

19.16.58.

06/16/92

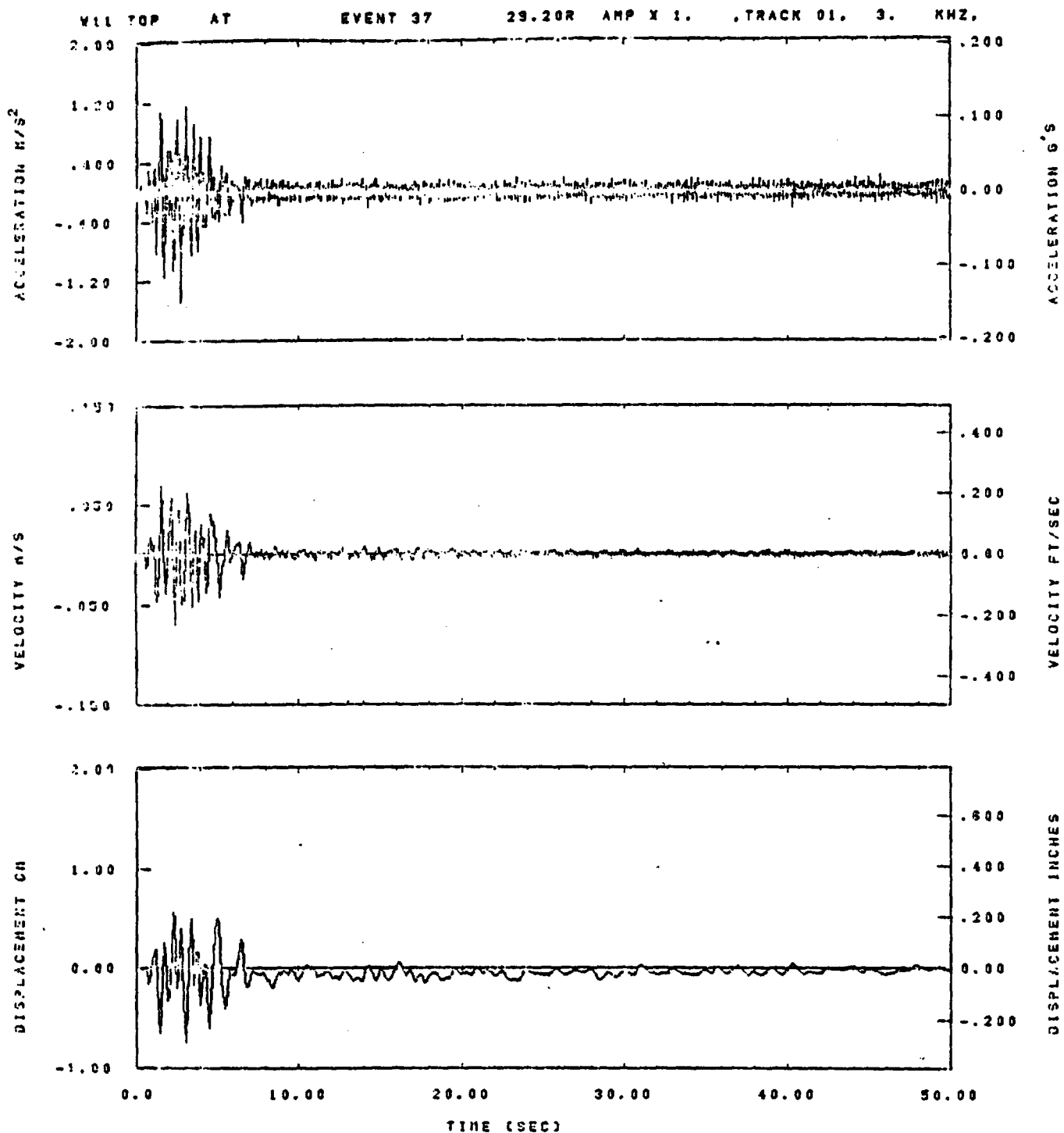


IOD= .0020	ODT= .005	FIX=	AA3= 0.
HPI= .40	BMH= .26	HLH= 167	AD0=
LPI= 27.	BYL= 6.	HLL= 1490	ARE=
VTB= .400	VTE= .267	PLL= -20.	VSE= 0.
DPS= 0.	DPE= 100.	PLH= 0	DSE=

15.45.57.

03/16/82

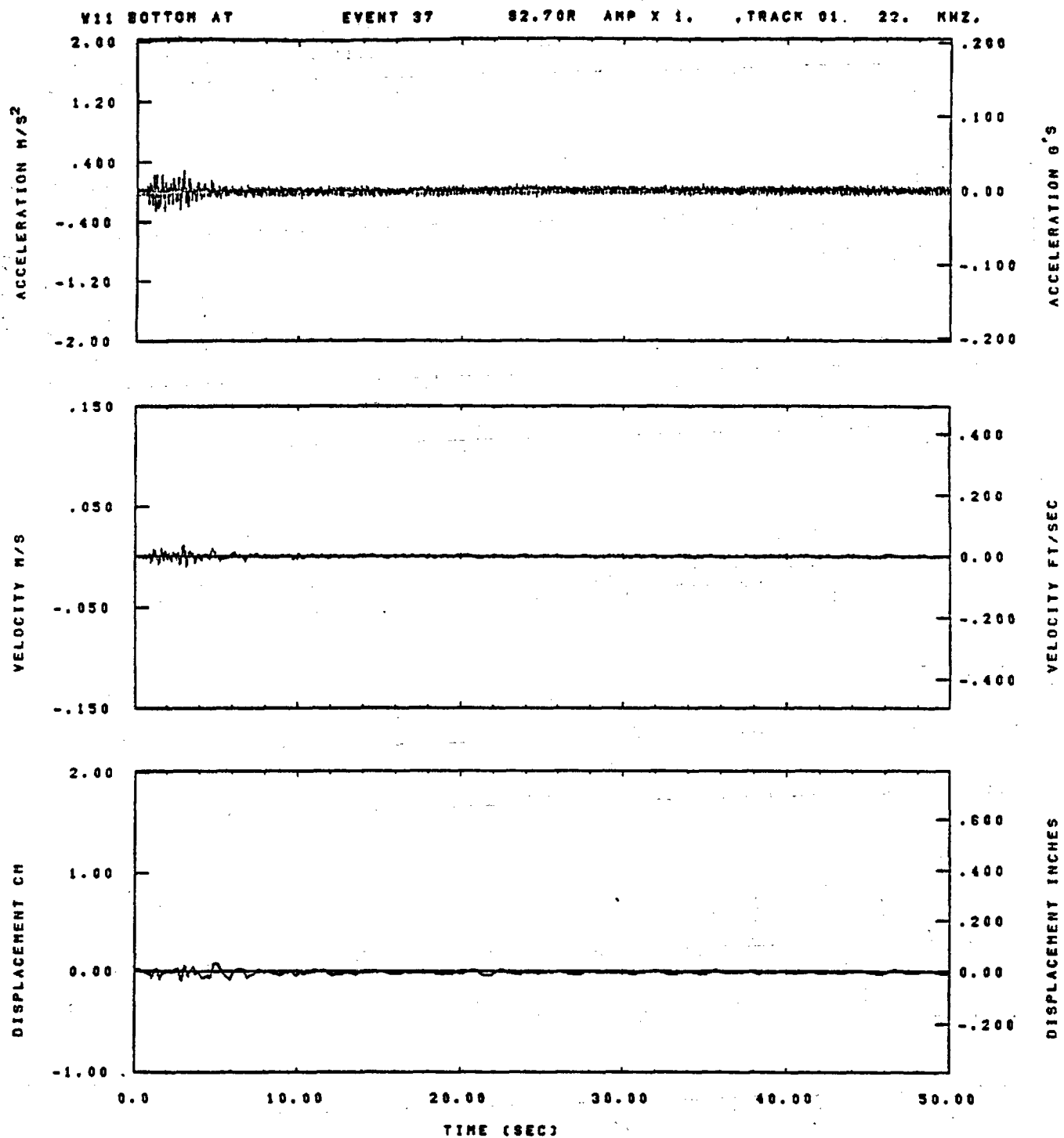
Figure E-52



IDT= .0020	OOT= .003	FIX=	AAS= 0.
HFF= .40	GVH= .26	HLH= 249	ASB=
LPF= 18.	SVL= 4.	HLL= 1439	ASE=
VTD= .400	VTE= .267	FLL= -20.	VSE= 0.
DPU= 0.	DPE= 100.	FLH= 0	DSE= 0.

19.17.02.

08/18/82

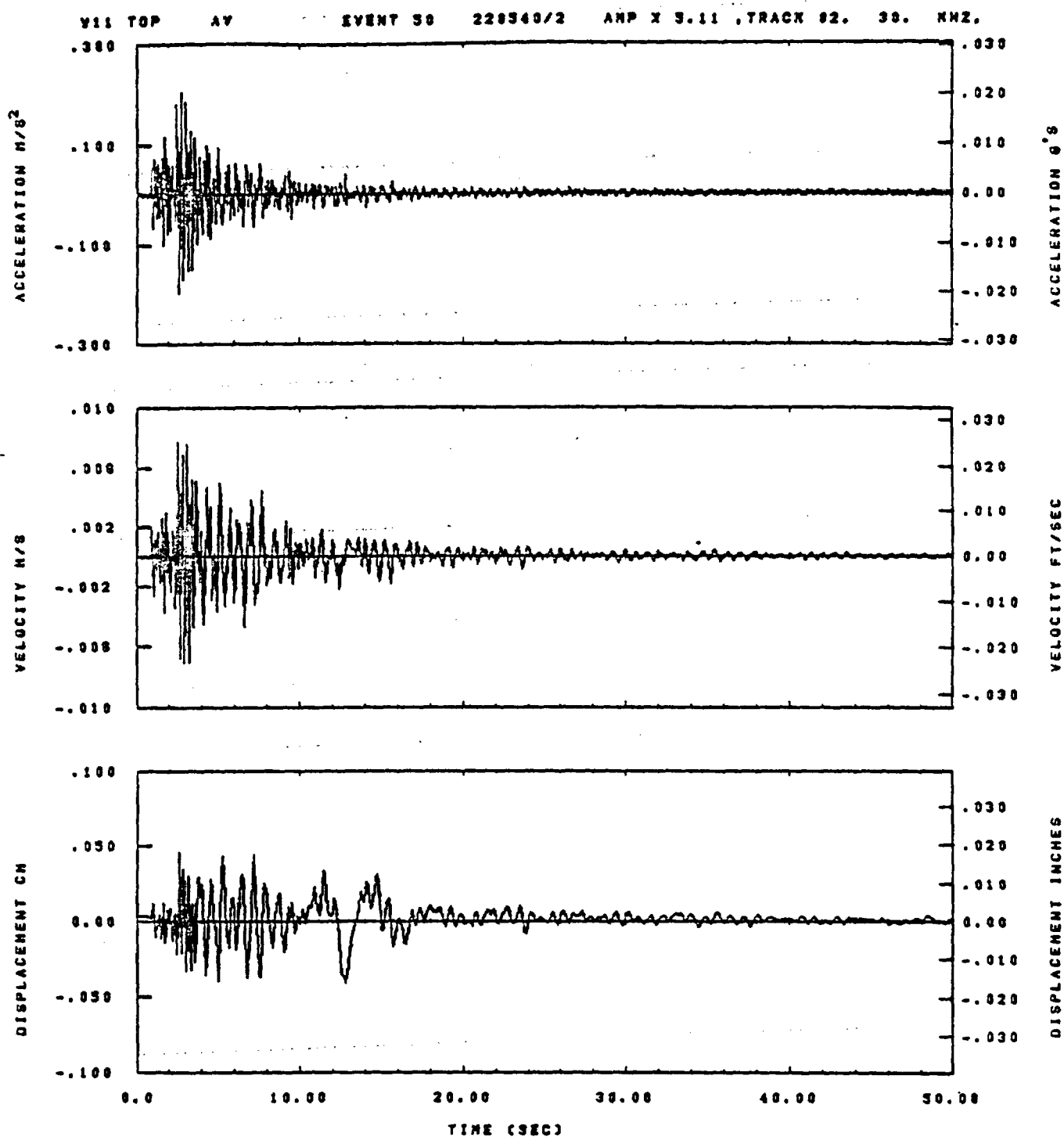


IDT= .0020	ODT= .005	FIX=	AAS= 0.
HPF= .40	BVN= .26	HLH= 167	ASB=
LPF= 27.	BVL= 6.	HLL= 1488	ASE=
VTS= .400	VTE= .267	FLL= -20.	VSE= 0.
DPS= 0.	DPE= 100.	FLH= 0	DSE= 0.

15.38.05.

06/17/82

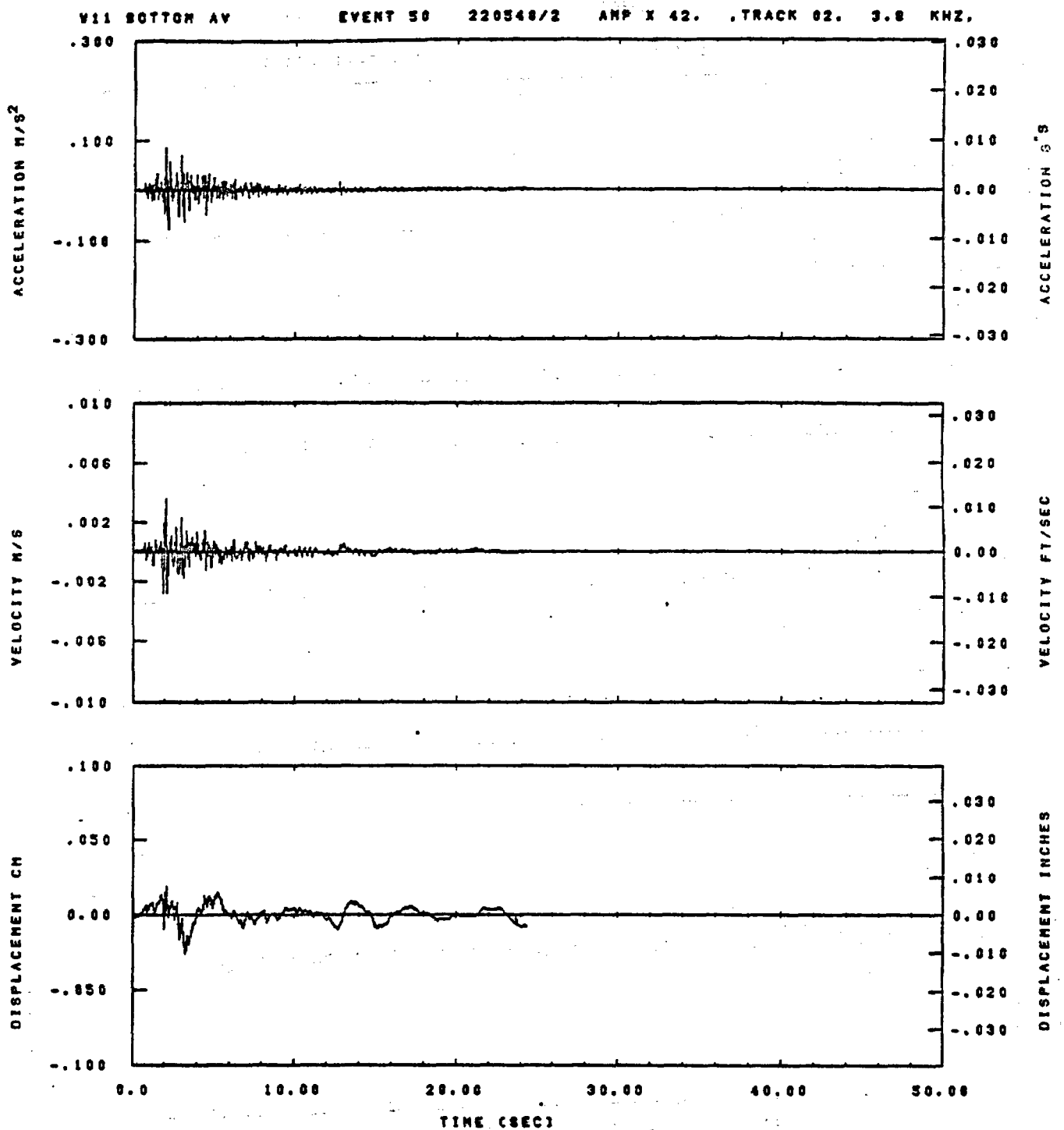
Figure E-54



IDT= .0020	ODT= .003	FIX=	AAS= 0.
HPP= .3	BYM= .20	MLH= 187	ASS=
LPP= 27.	BYL= 6.	MLL= 1999	ASE=
VTB= .39	VTE= .200	FLL= -20.	VSE= 0.
DPS= 0.	DPE= 100.	FLH= 0	DSE= 0.

13.42,15.

08/30/82

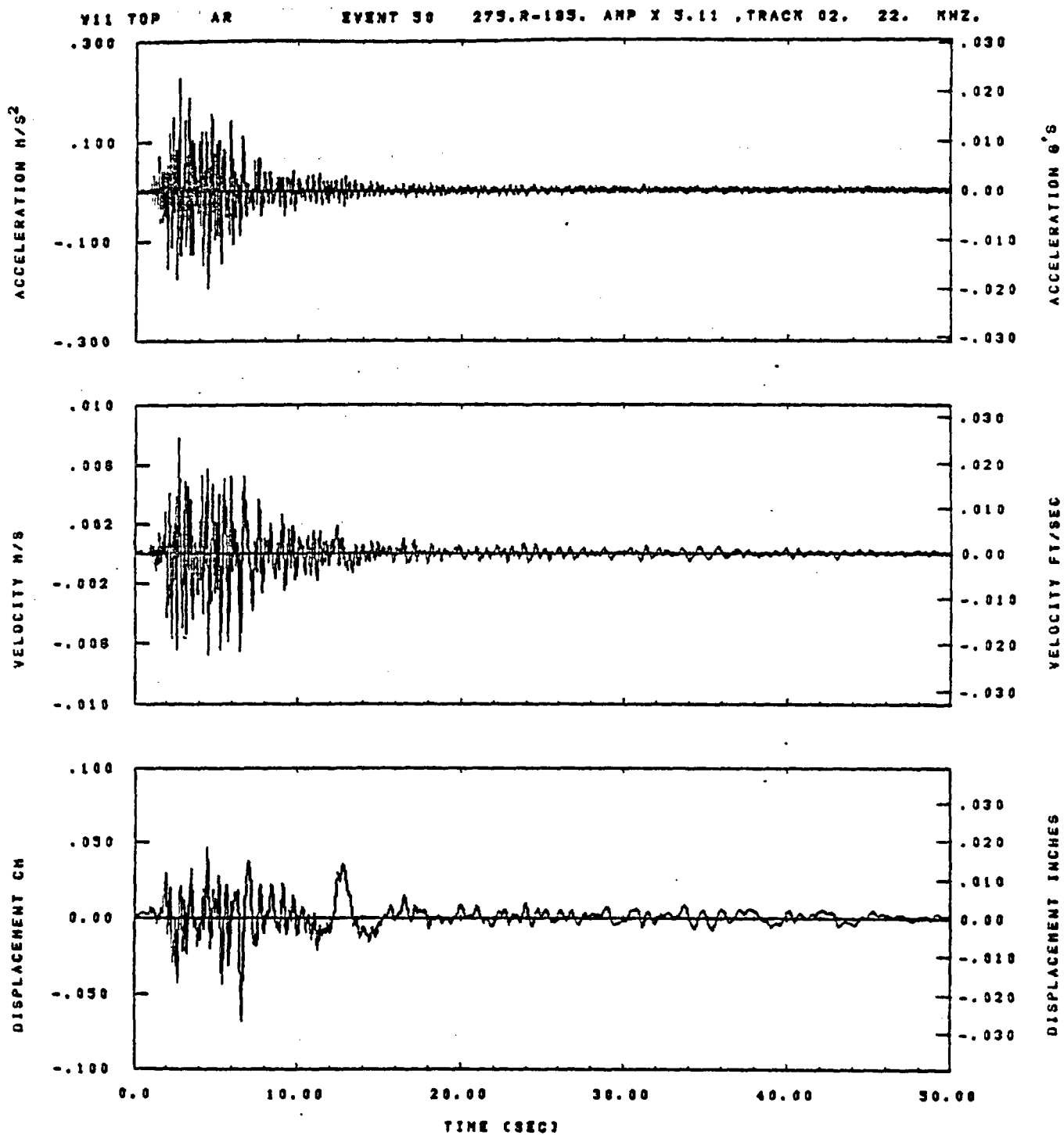


IOT= .0020	QDT= .005	FIX=	AAS= 0.
HPP= .3	BYH= .20	HLH= 167	ASS=
LPP= 27.	BYL= 6.	HLL= 1999	ASE=
VTB= .30	VTE= .200	FLL= -10.	VSE= 0.
OPS= 0.	OPE= 40.	FLH= 0	DSE= 0.

15.42.35.

06/30/82

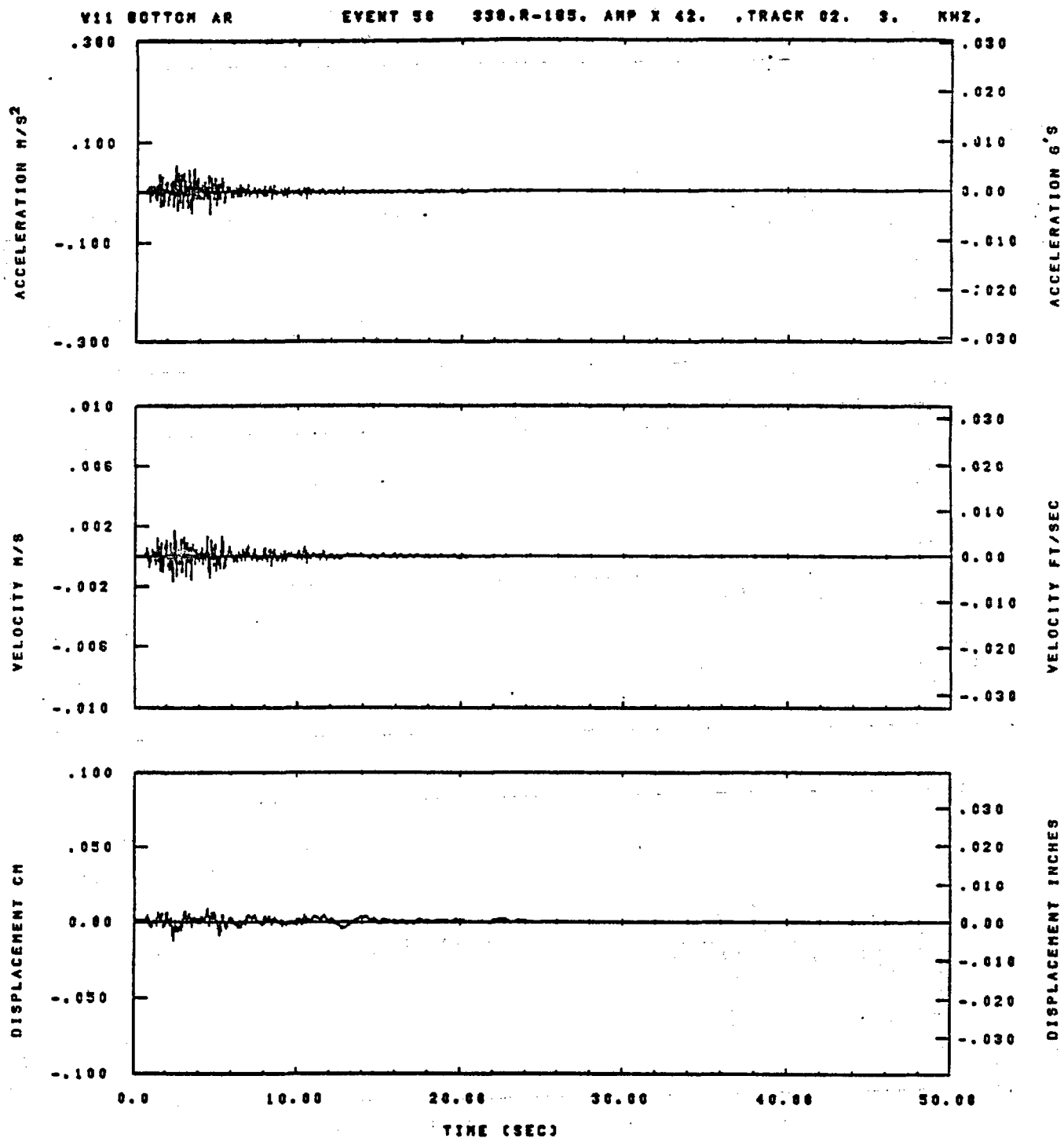
Figure E-56



IOT= .0020	ODT= .005	FIX=	AAS= 0.
HFF= .3	BYH= .20	HLH= 187	ASB=
LFF= 27.	BYL= 8.	HLL= 1999	ASE=
VTB= .30	VTE= .200	FLL= -20.	VSE= 0.
DPB= 0.	OPE= 100.	FLH= 0	DSE= 0.

13.42.21.

06/30/92

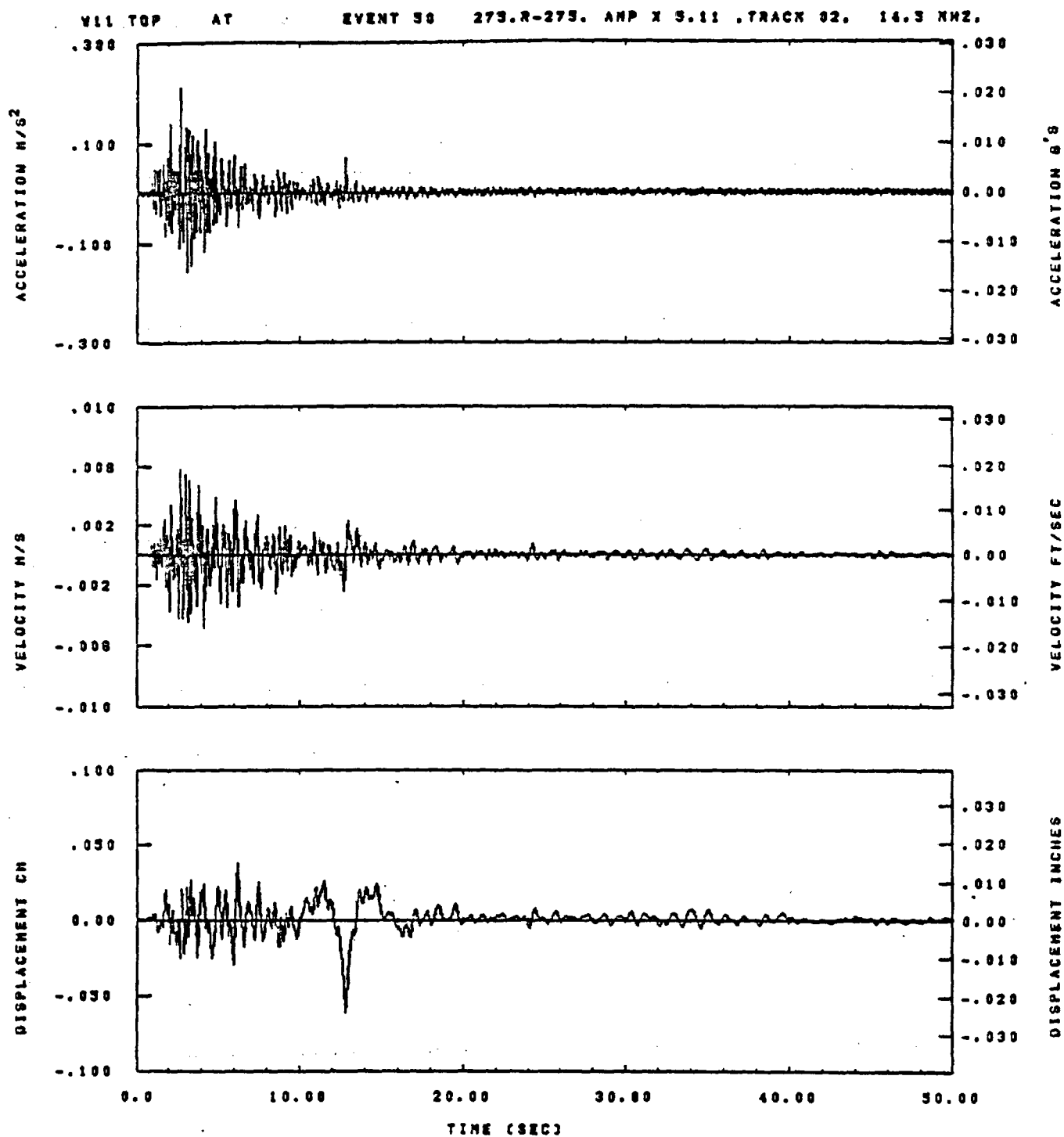


IDT= .0020	ODT= .005	FIX=	AAS= 0.
HPP= .3	BYH= .20	HLH= 167	ASS=
LPP= 27.	BYL= 6.	HLL= 1883	ASE=
VTB= .38	VTE= .288	FLL= -28.	VSE= 0.
DPE= 0.	DPE= 188.	FLH= 0	DSE= 0.

15.42.42.

06/30/82

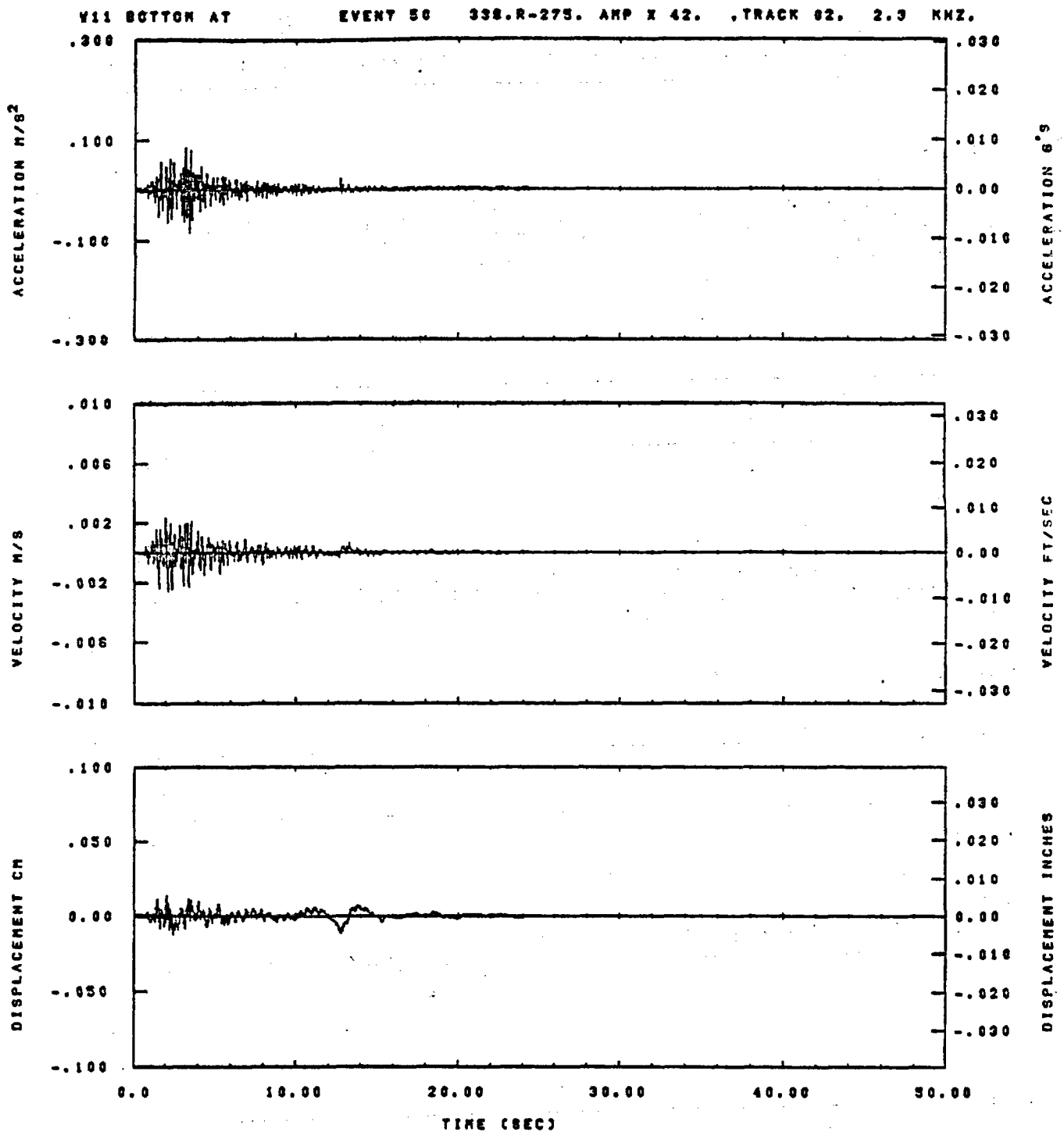
Figure E-58



IDT= .0020	ODT= .003	FIX=	AAS= 0.
HPP= .3	BYH= .20	HLH= 187	ASB=
LPP= 27.	BYL= 8.	HLL= 1999	ASE=
VTS= .38	VTE= .200	FLL= -20.	VSE= 0.
OPS= 0.	OPE= 100.	FLH= 0	DSE= 0.

15.42.28.

06/30/82



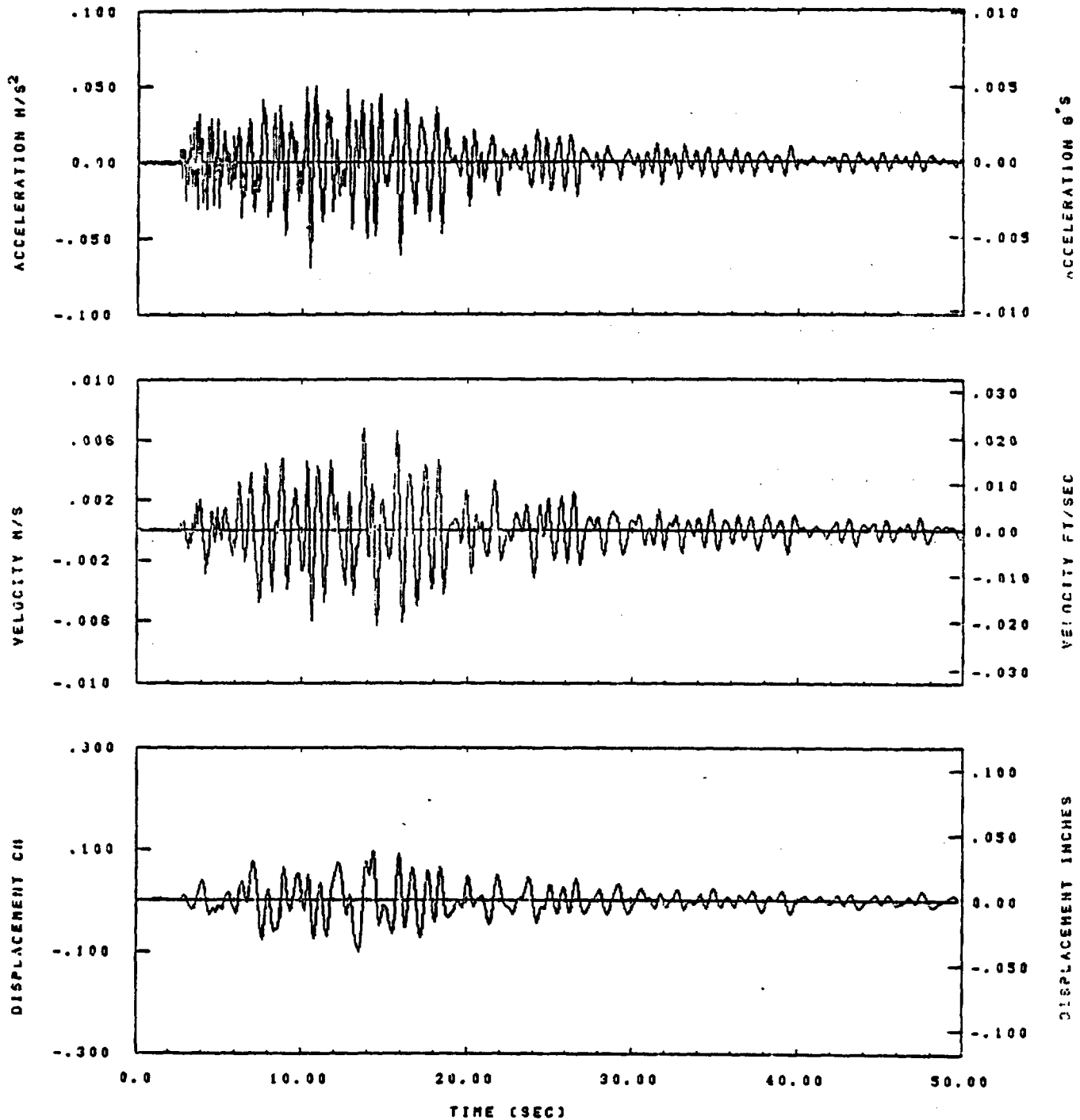
IDT= .0020	QDT= .005	FIX=	AAS= 0.
HPF= .3	BVH= .20	HLH= 167	ASS=
LPF= 27.	BVL= 6.	HLL= 1988	ASE=
VTS= .30	VTE= .200	FLL= -20.	VSE= 0.
DPS= 0.	DPE= 100.	FLH= 0	DSE= 0.

15.42.44.

06/30/82

Figure E-60

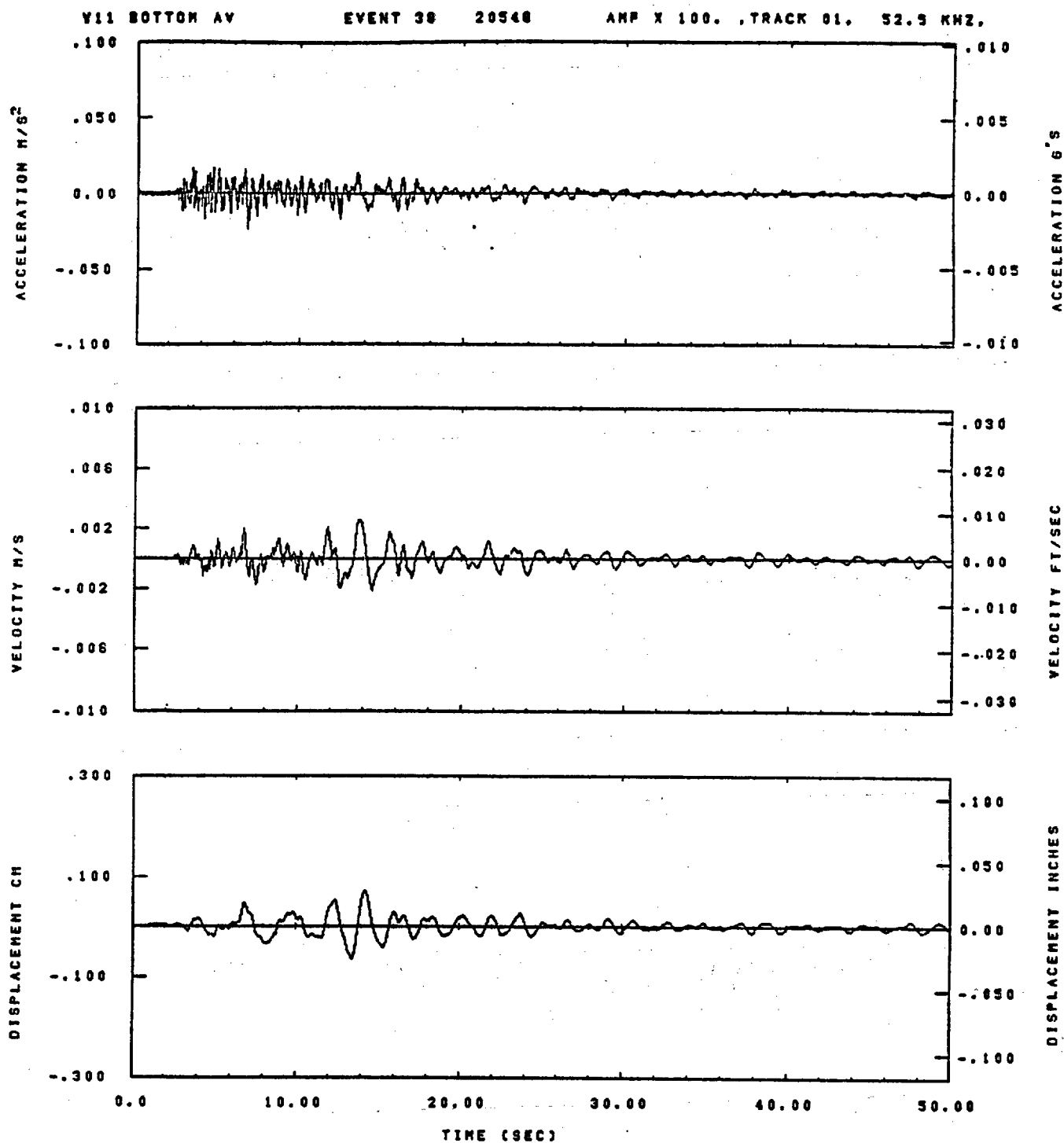
V11 TOP AV EVENT 38 20548 AMP X 205. TRACK 01. 7.35 MHZ.



IDT= .0020	ODT= .003	FIX=	AAS= 0.
HPF= .20	BYH= .13	HLH= 251	ASB=
LPF= 18.	BYL= 4.	HLL= 2999	ASE=
VTB= .200	VTE= .133	FLL= -20.	VSE= 0.
DPS= 0.	DPE= 100.	FLH= 0	DSE= 0.

10.09.54.

06/28/82

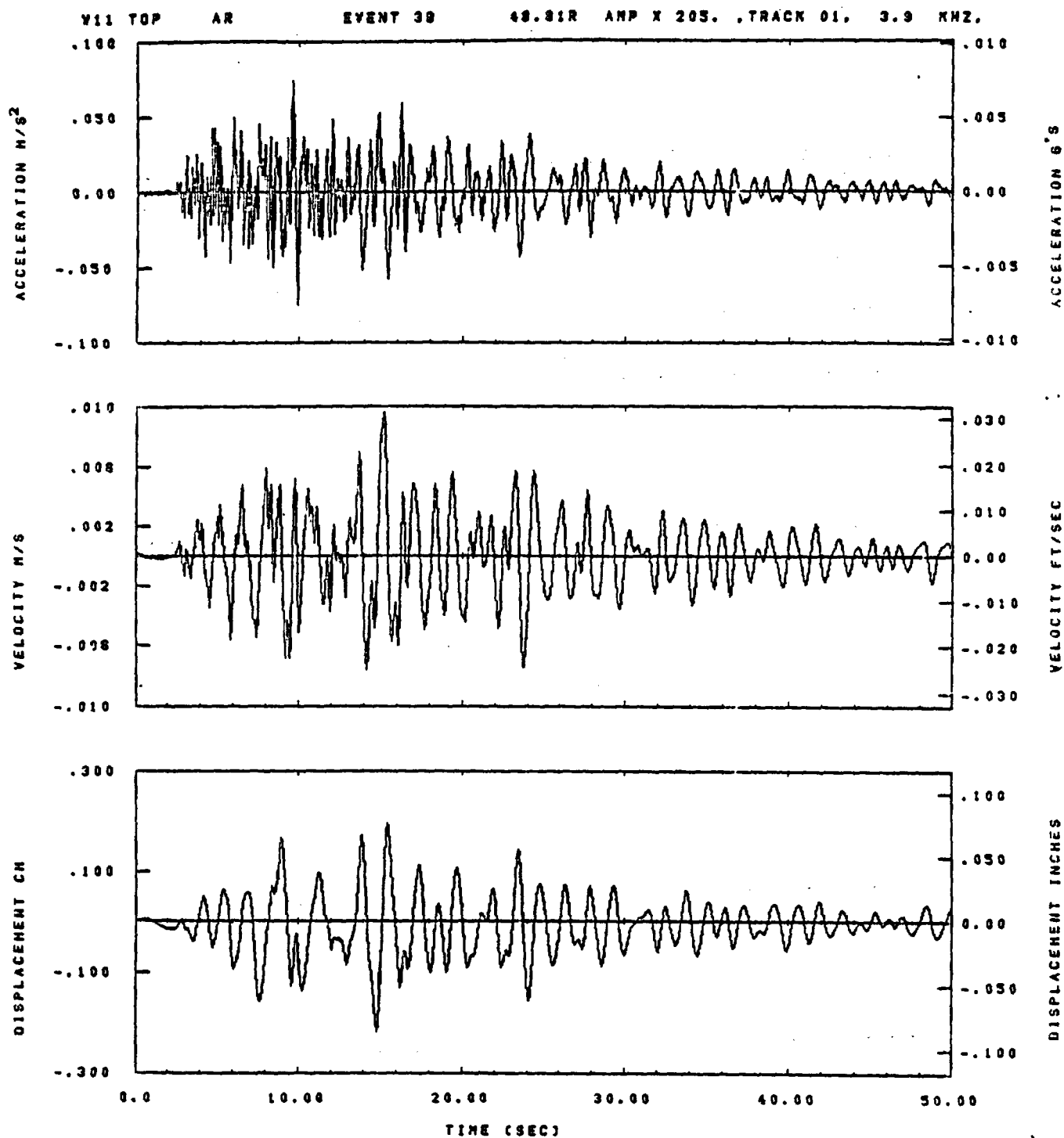


IDT= .0020	ODT= .005	FIX=	AAS= 0.
HPP= .20	BYN= .13	HLN= 251	ASB=
LPP= 10.	BVL= 4.	HLL= 2888	AGE=
VTB= .200	VTE= .133	FLL= -20.	VCE= 0.
DPE= 0.	DPE= 100.	FLW= 0	DCE= 0.

10.10.42.

06/28/82

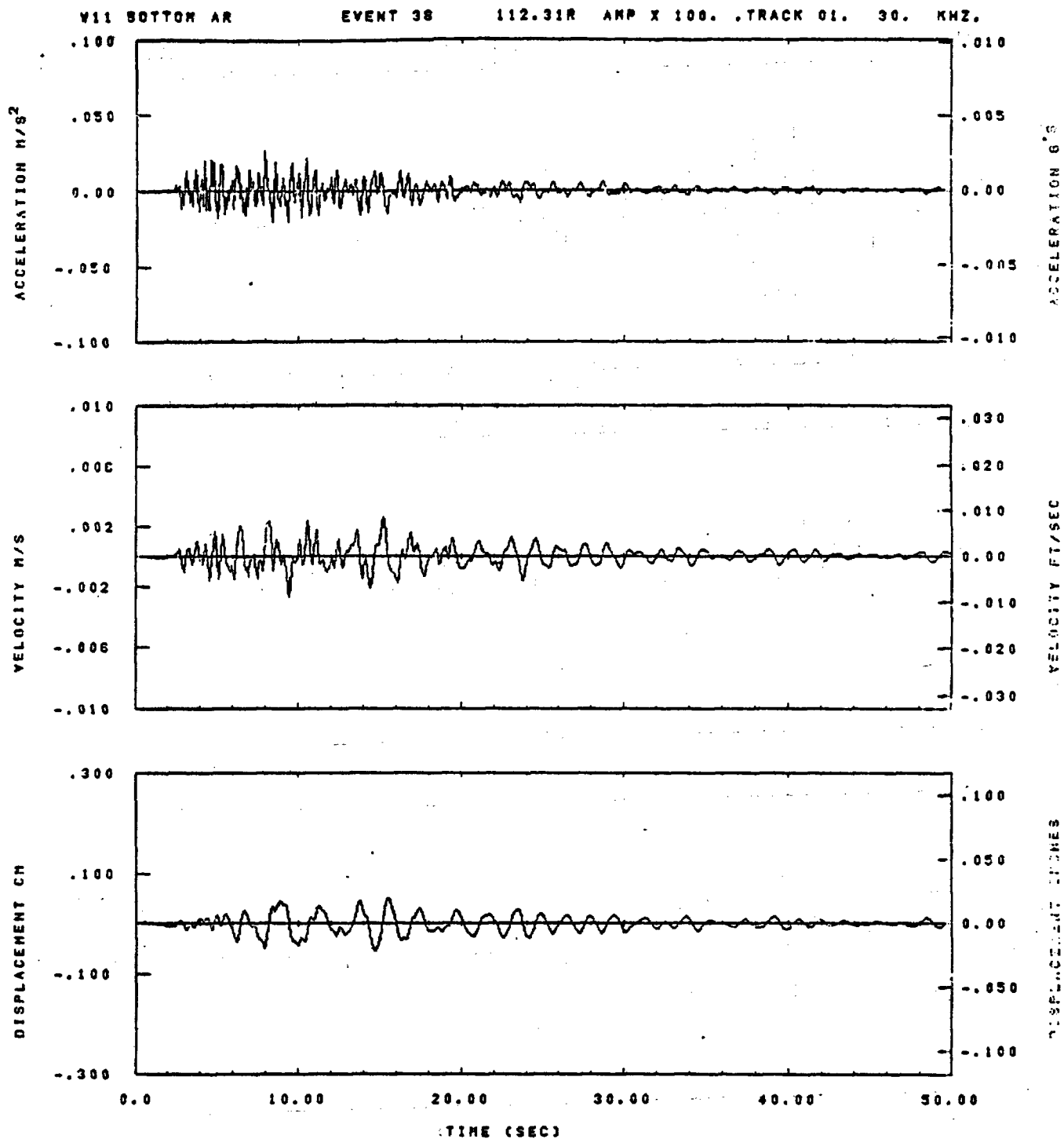
Figure E-62



IDT= .0020	OOT= .005	FIX=	AAS= 0.
HPP= .20	SVH= .13	HLH= 251	ASB=
LPP= 18.	SVL= 4.	HLL= 2983	ASE=
VTB= .200	VTE= .133	PLL= -20.	VSE= 0.
UPB= 0.	OPE= 100.	PLH= 0	USE= 0.

10.09.27.

08/28/82

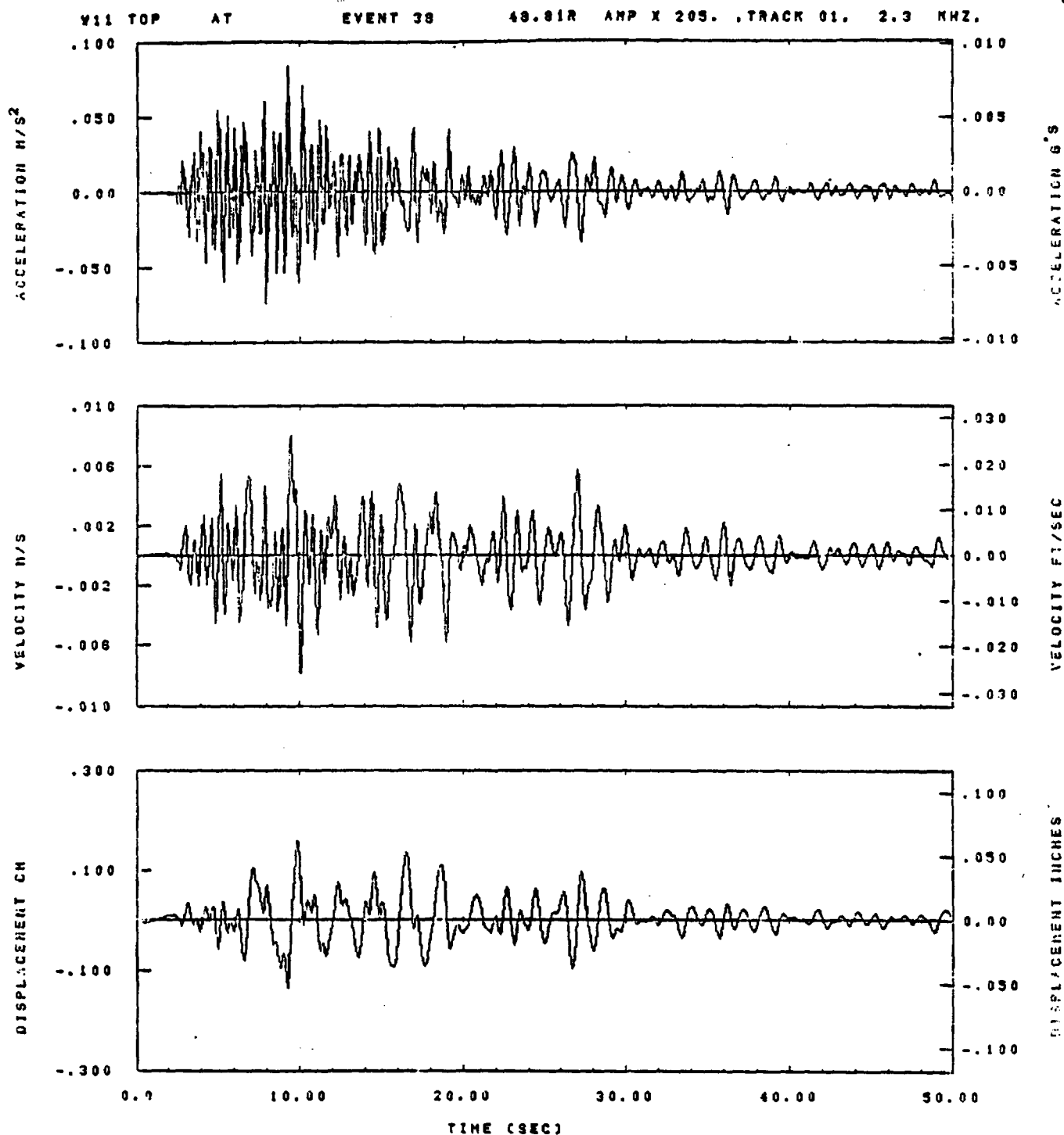


IDT= .0020	ODT= .005	FIX=	AAS= 0.
HPF= .20	SVH= .13	HLH= 251	ASB=
LPF= 18.	SVL= 4.	HLL= 2999	ASE=
VTS= .200	VTE= .133	FLL= -20.	VSE= 0.
DPS= 0.	DPE= 100.	FLH= 0	DSE= 0.

10.10.03.

06/28/82

Figure E-64



IOT= .0020	OOT= .005	FIX=	AAS= 0.
HPF= .20	BYH= .13	HLH= 251	ACB=
LPF= 18.	BYL= 4.	HLL= 2999	ASE=
YTB= .200	VTE= .133	FLL= -20.	VSE= 0.
CPB= 0.	OPE= 100.	FLW= 0	OPE= 0.

10.09.34.

08/28/92

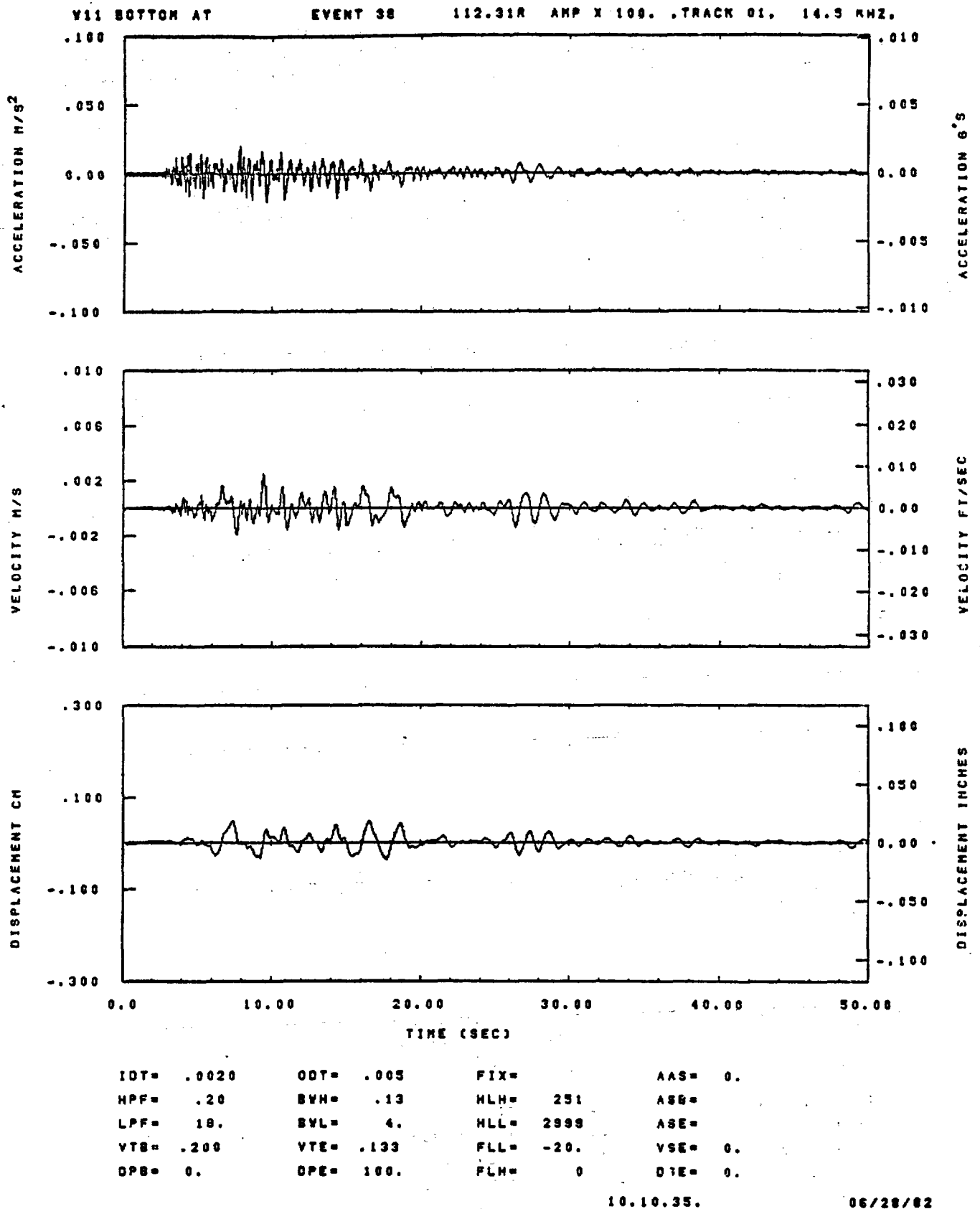
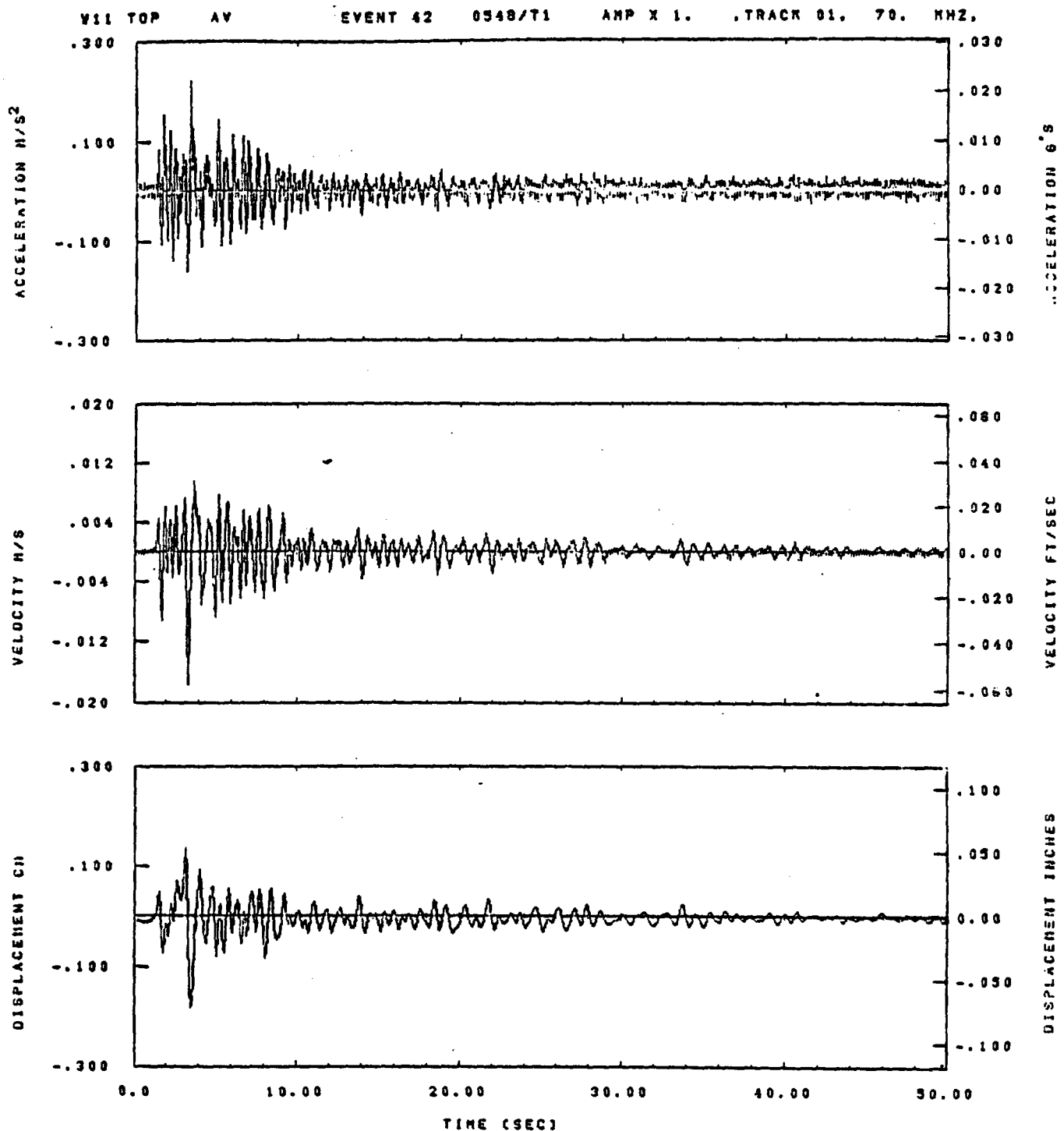


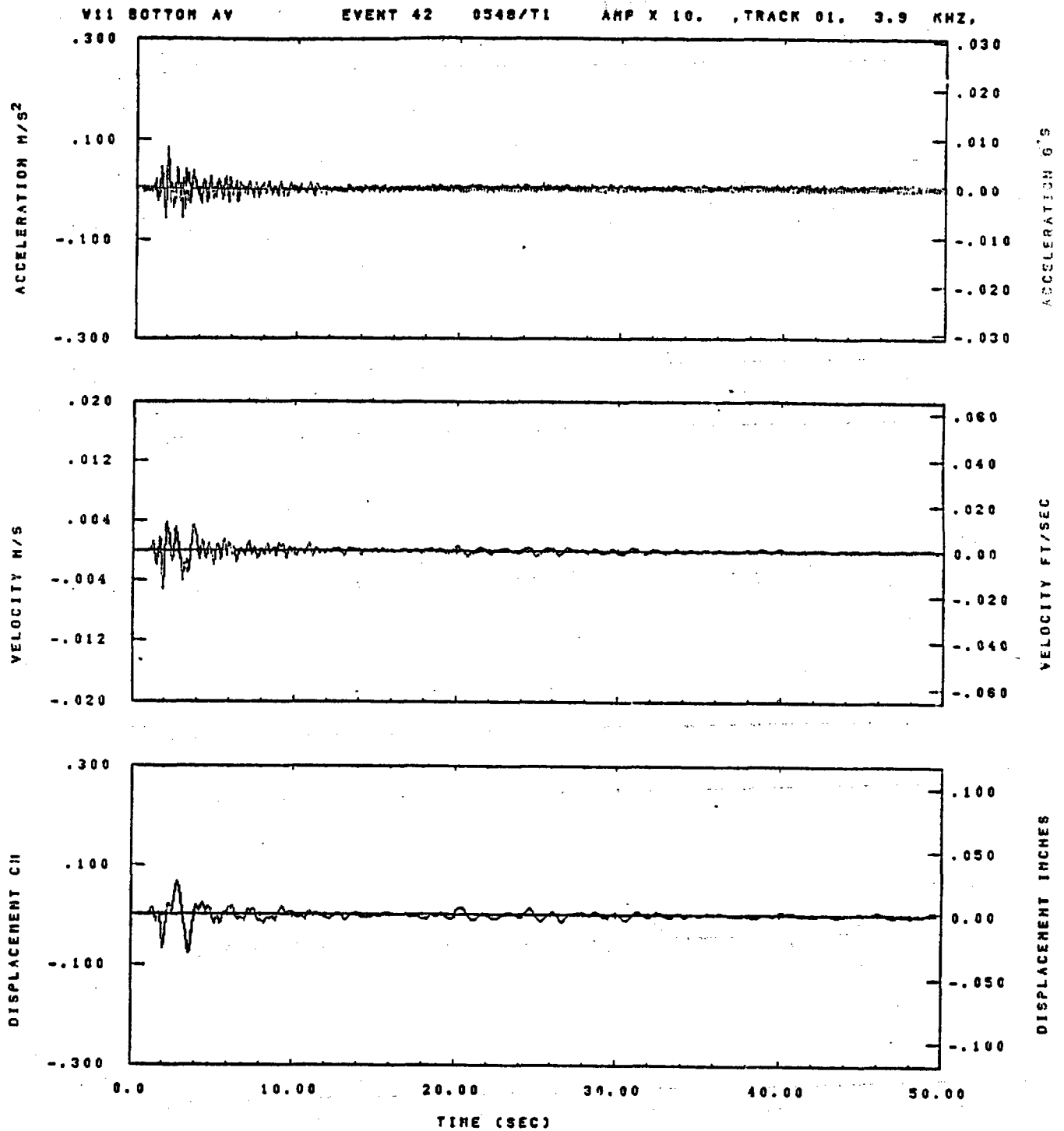
Figure E-66



IDT= .0020	ODT= .005	FIX=	AAS= 0.
HPF= .25	BVH= .16	HLH= 333	ASB=
LPF= 13.	BVL= 3.	HLL= 2399	ASE=
VTB= .250	VTE= .166	FLL= -20.	VSE= 0.
OPB= 0.	OPE= 100.	FLH= 0	OSE= 0.

13.21.16.

08/28/02



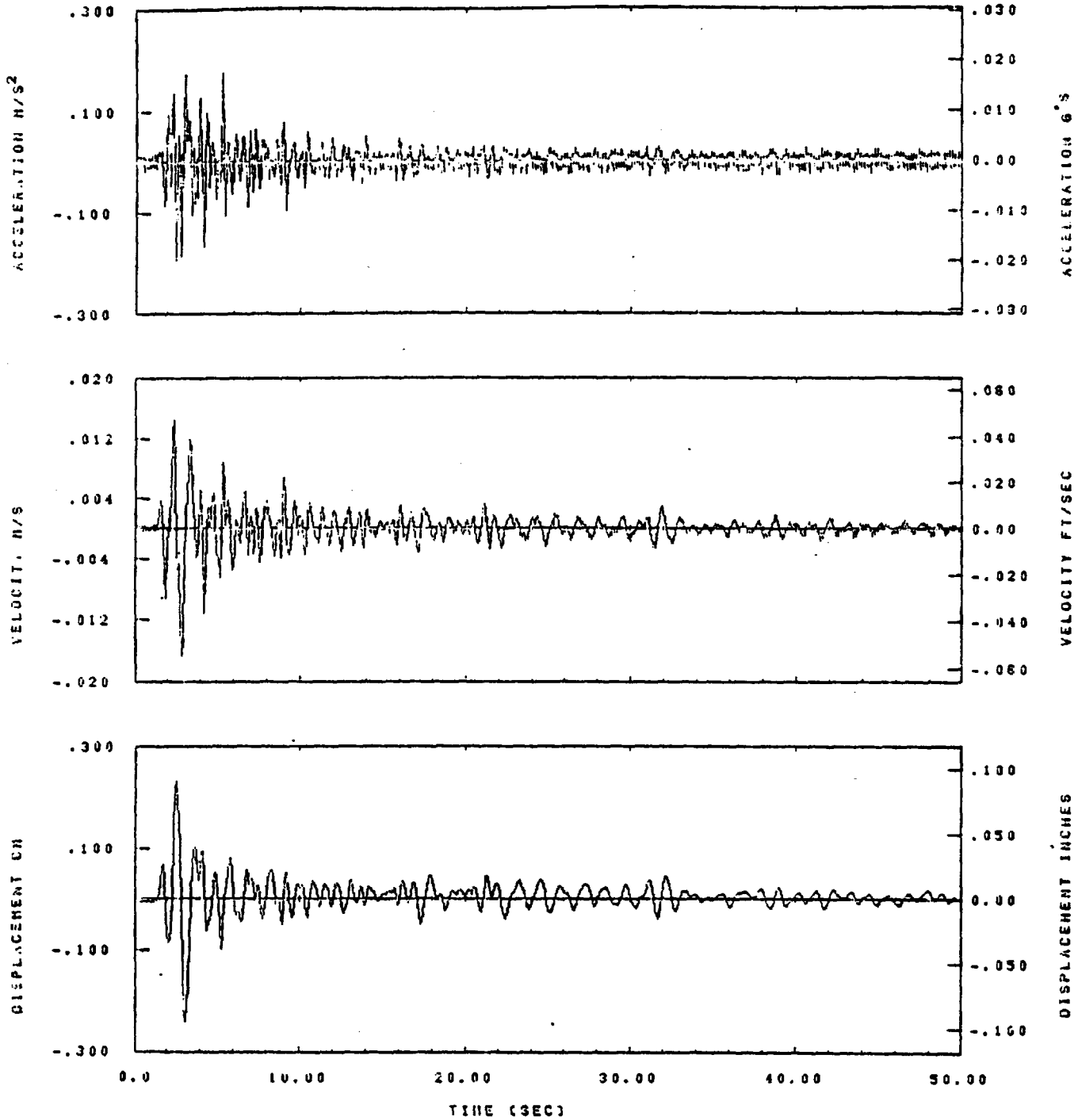
IDT= .0020	ODT= .005	FIX=	AAS= 0.
HPF= .25	BYH= .16	HLH= 333	ASB=
LPF= 13.	BYL= 3.	HLL= 2399	ASE=
YTB= .250	YTE= .166	FLL= -20.	VSE= 0.
DPB= 0.	OPE= 100.	FLH= 0	OGE= 0.

13.21.56.

06/29/82

Figure E-68

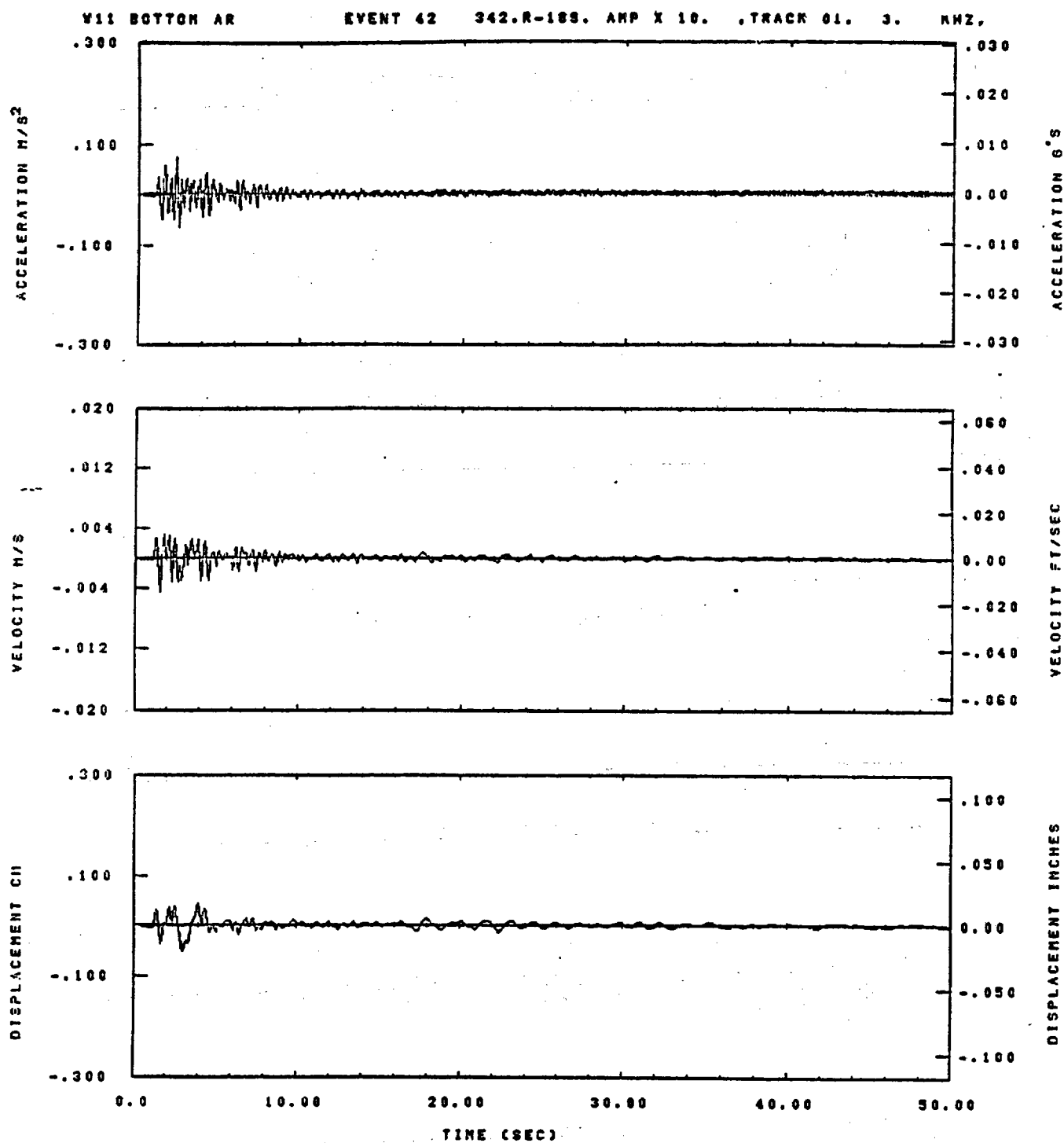
Y11 TOP AR EVENT 42 279.R-100. AMP X 1. , TRACK 01. 92.5 KHZ.



IDT= .0020	QDT= .005	FIX=	AAS= 0.
HPF= .25	GVH= .16	HLH= 333	ASD=
LPF= 10.	QVL= 3.	HLL= 2399	ASE=
YTD= .250	YTE= .166	FLL= -20.	YSE= 0.
UPB= 0.	UPE= 100.	FLH= 0	DSE= 0.

13.21.22.

06/28/82

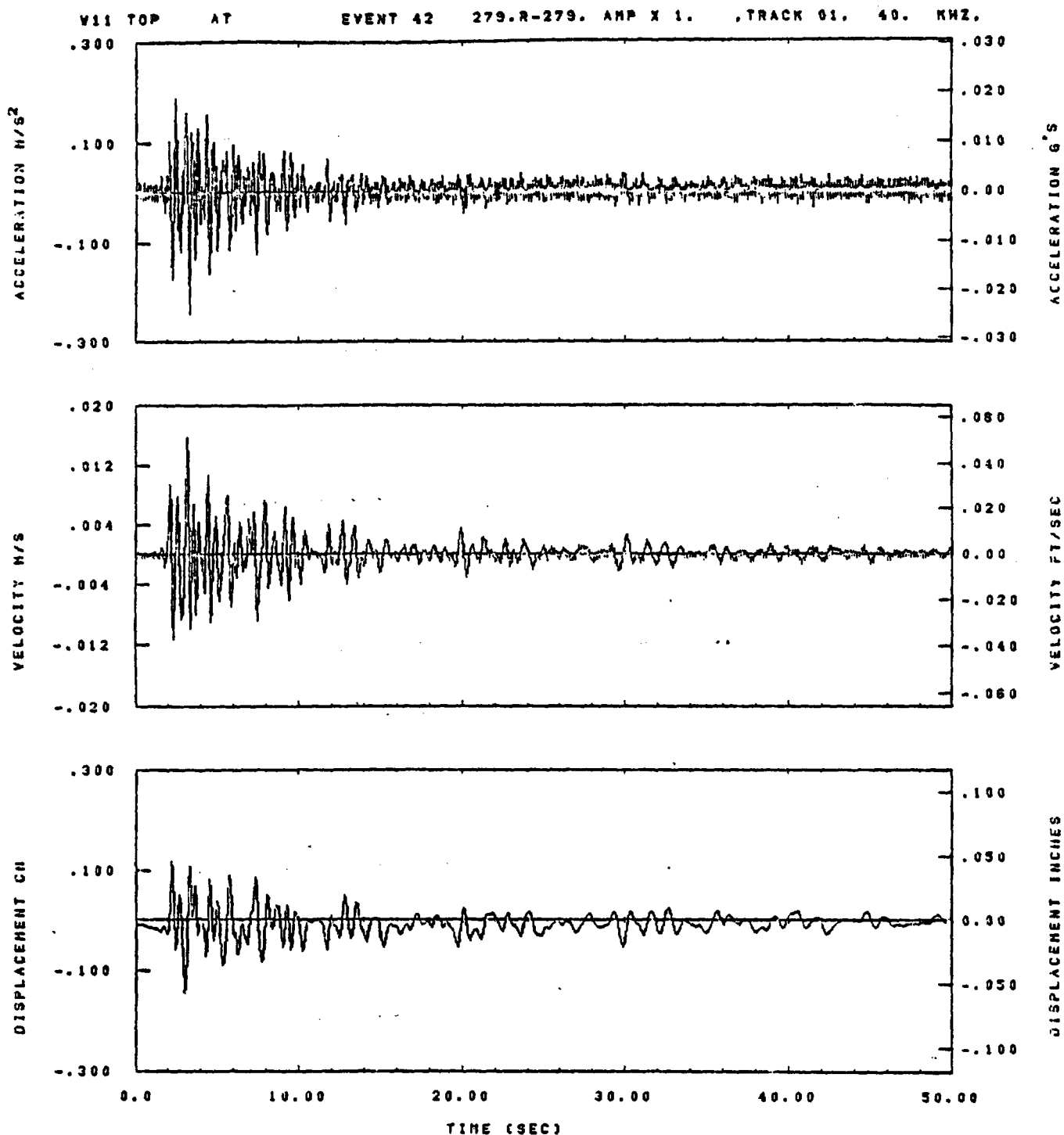


IDT= .0020	ODT= .005	FIX=	AAS= 0.
HPF= .25	BYH= .16	HLH= 333	ASB=
LPF= 13.	BYL= 3.	HLL= 2388	ASE=
YTD= .250	YTE= .166	FLL= -20.	VSE= 0.
DPS= 0.	DPE= 100.	FLH= 0	DSE= 0.

13.21.31.

06/28/82

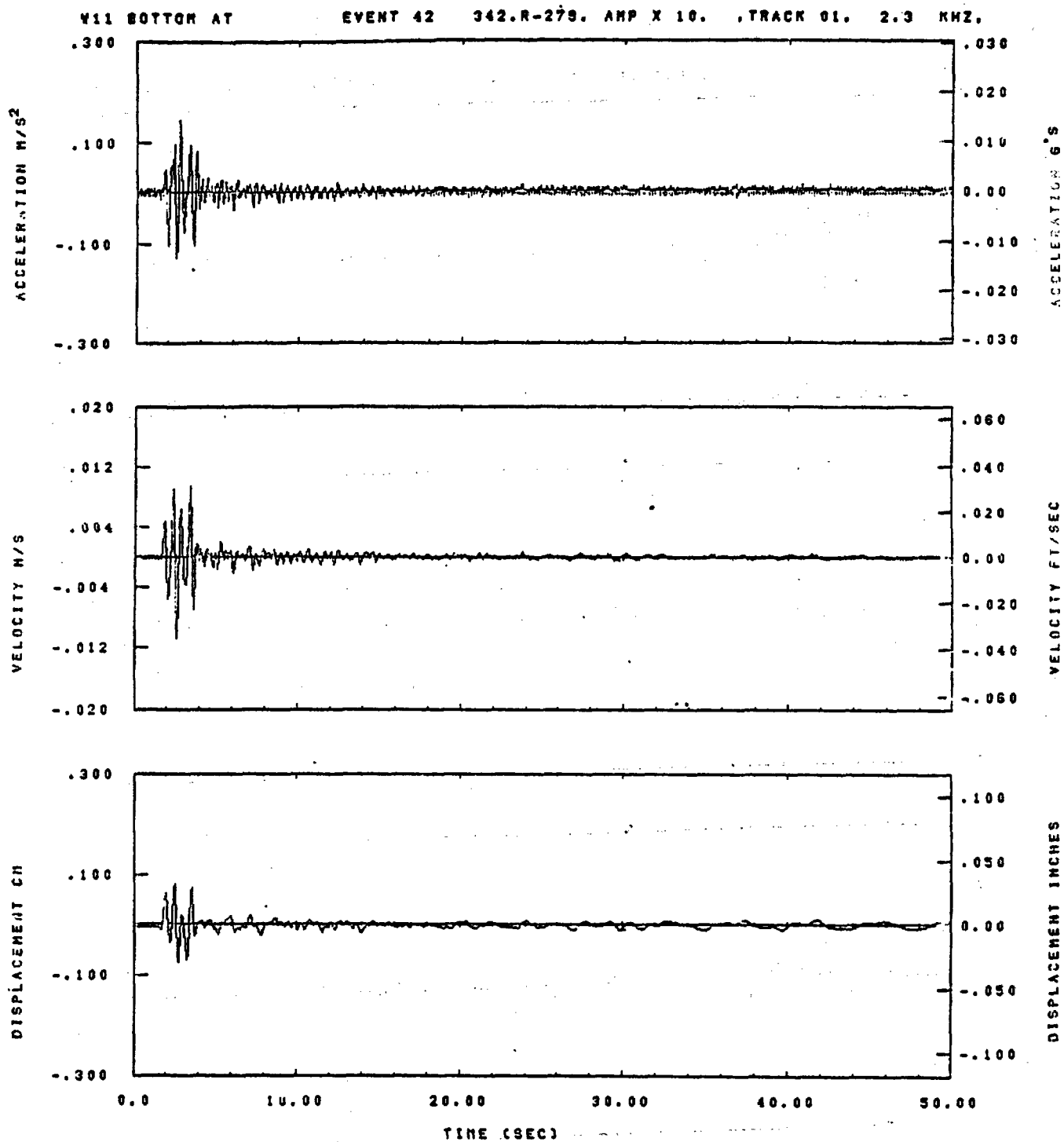
Figure E-70



IDT= .0020	QOT= .003	FIX=	AAC= 0.
HPF= .25	BYH= .16	HLH= 330	ASC=
LPF= 13.	QVL= 3.	HLL= 2399	ASE=
VTB= .250	VTE= .168	FLL= -20.	VSE= 0.
QPS= 0.	DPE= 100.	FLH= 0	DSE= 0.

13.21.26.

08/28/82

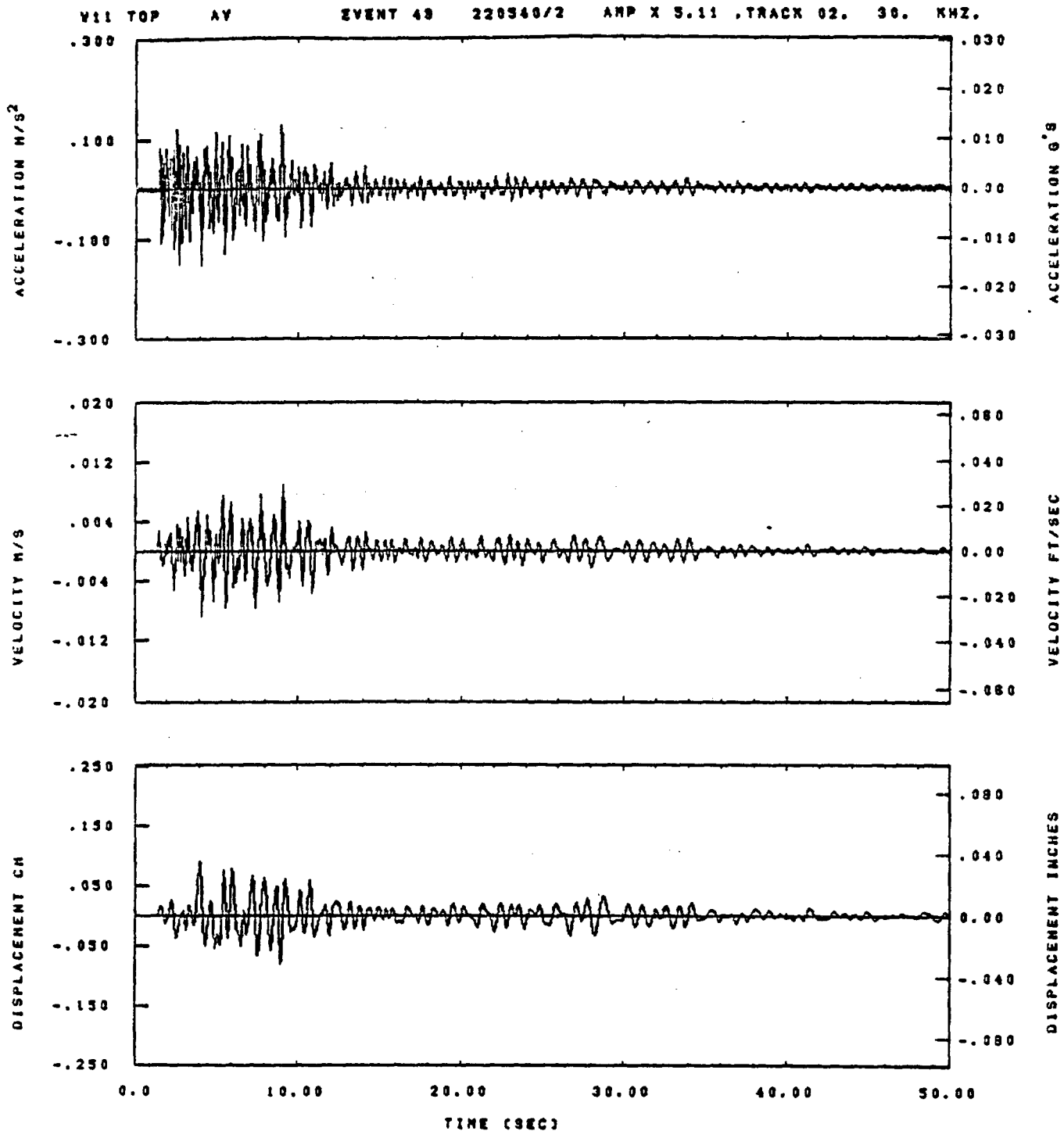


IDT= .0020	ODT= .005	FIX=	AAS= 0.
HPF= .25	BYH= .16	HLH= 333	ASB=
LPF= 13.	BYL= 3.	HLL= 2308	ASE=
VTB= .250	YTE= .166	FLL= -20.	VSE= 0.
OPB= 0.	OPE= 100.	FLH= 0	OSE= 0.

13.21.37.

06/28/82

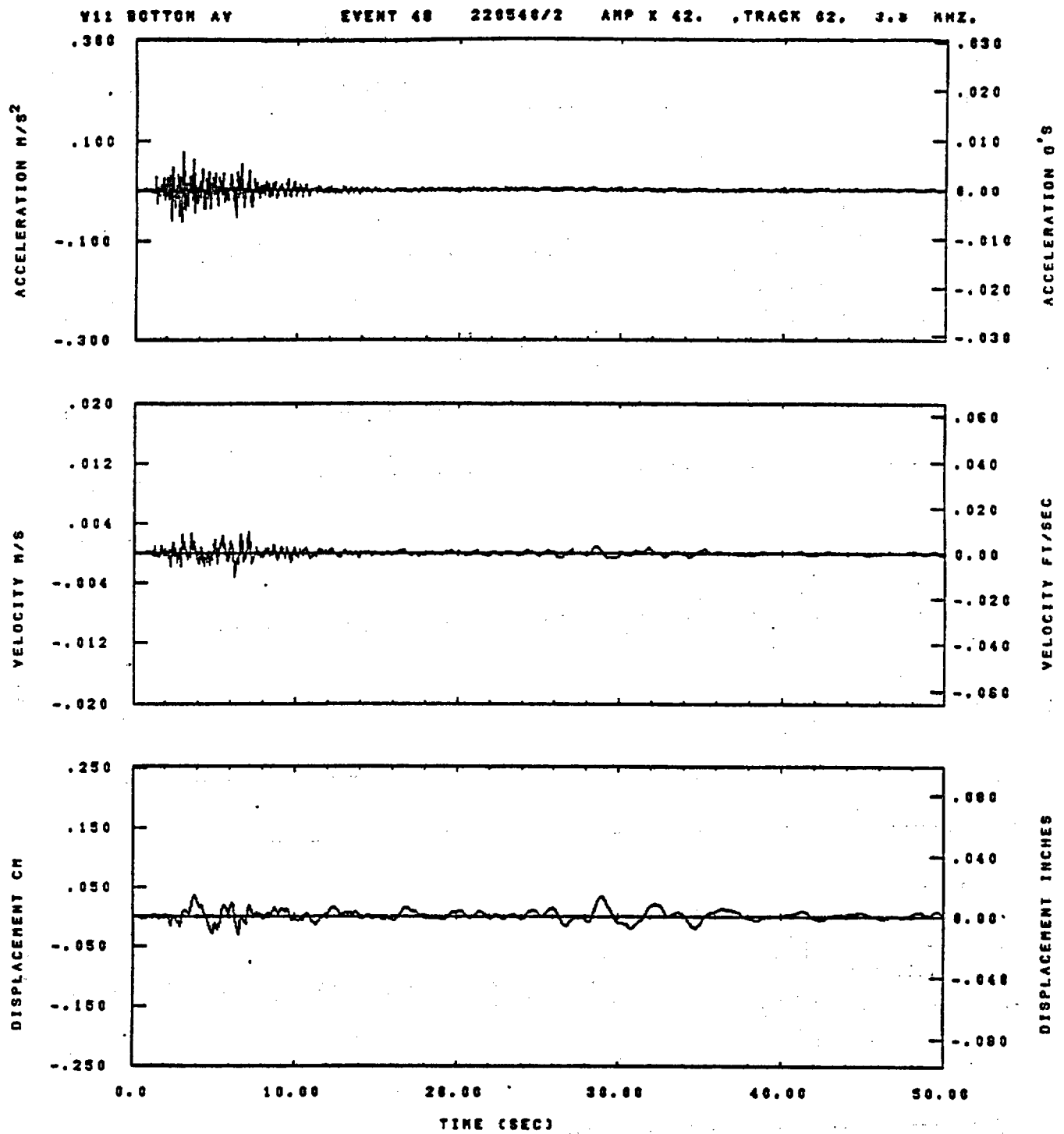
Figure E-72



IOT= .0020	ODT= .005	FIX=	AAS= 0.
HPP= .30	SVH= .20	HLH= 187	ASB=
LPP= 27.	SVL= 8.	HLL= 1939	ASE=
VTS= .300	VTE= .200	FLL= -20.	VSE= 0.
DPS= 0.	DPE= 100.	FLH= 0	DSE= 0.

15.48.28.

08/30/82

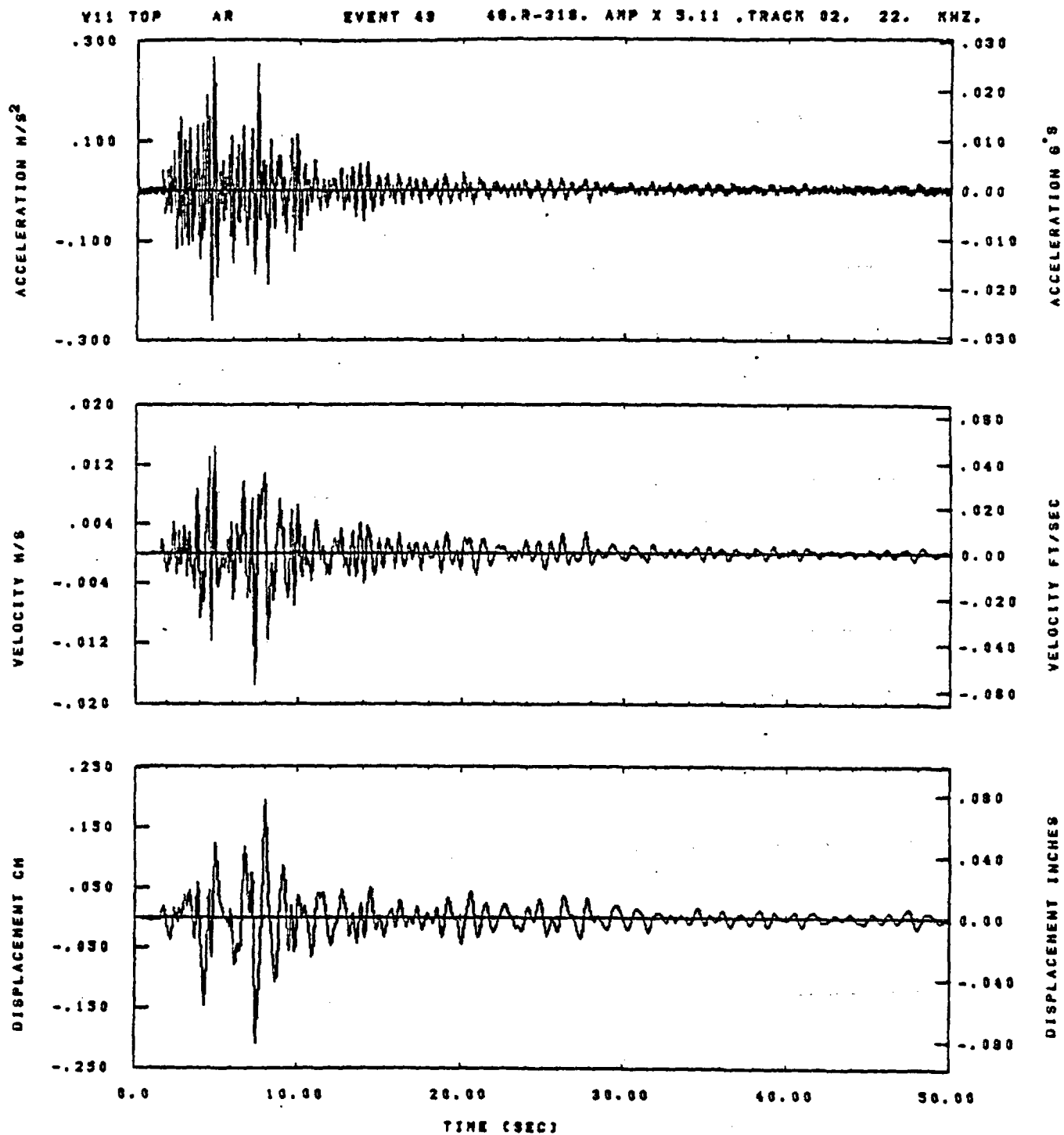


IDT= .0020	ODT= .005	FIX=	AAS= 0.
HPP= .30	BYH= .20	HLH= 167	ASB=
LPP= 27.	BYL= 6.	HLL= 1888	ASE=
VTS= .308	VTE= .288	FLL= -4.5	VSE= 0.
DPS= 0.	DPE= 100.	FLH= 0	DSE= 0.

15.48.57.

06/30/82

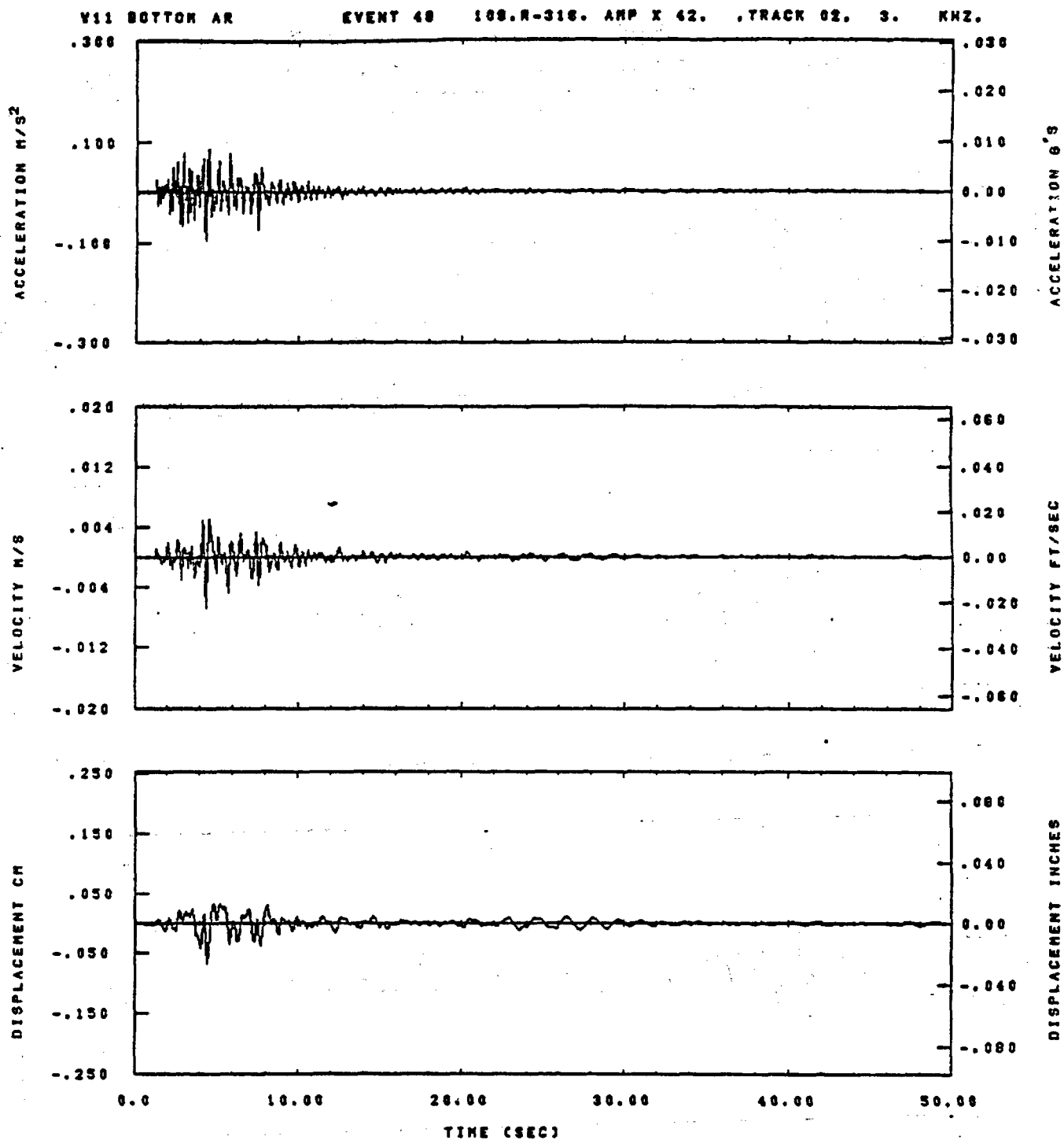
Figure E-74



IOT= .0020	QDT= .003	FIX=	AAS= 0.
HPP= .30	BYH= .20	HLH= 187	ASB=
LPP= 27.	BYL= 8.	HLL= 1999	ASE=
YTS= .300	YTE= .200	FLL= -20.	VSE= 0.
DPS= 0.	DPE= 100.	FLH= 0	DSE= 0.

13.48.32.

08/30/82

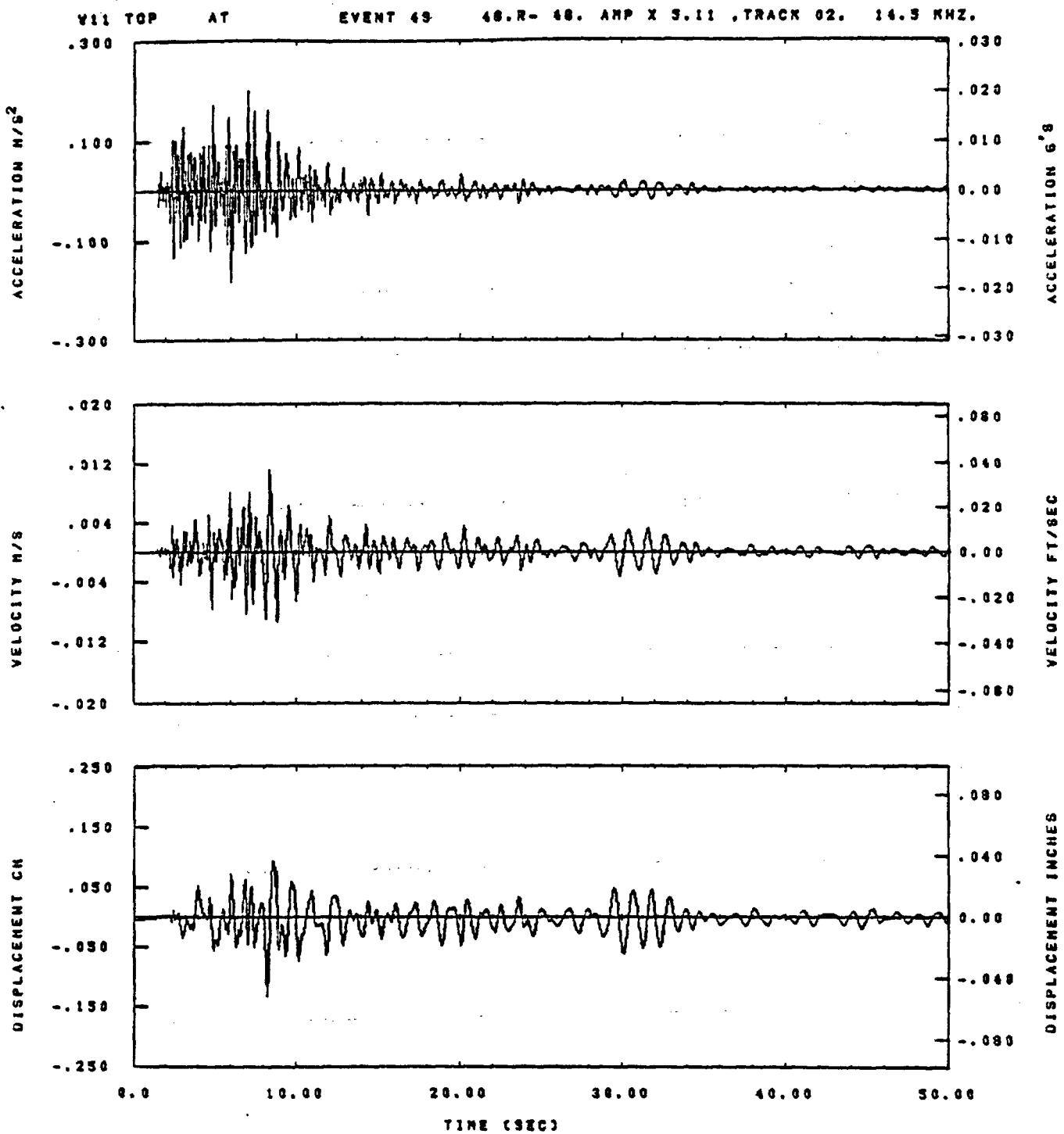


IDT= .0020	ODT= .005	FIX=	AAS= 0.
HPP= .30	SVH= .20	HLH= 167	ASS=
LPP= 27.	SVL= 8.	HLL= 1989	ASE=
VTS= .300	VTE= .200	FLL= -20.	VSE= 0.
OPE= 0.	OPE= 100.	FLH= 0	DSE= 0.

15.48.47.

06/30/82

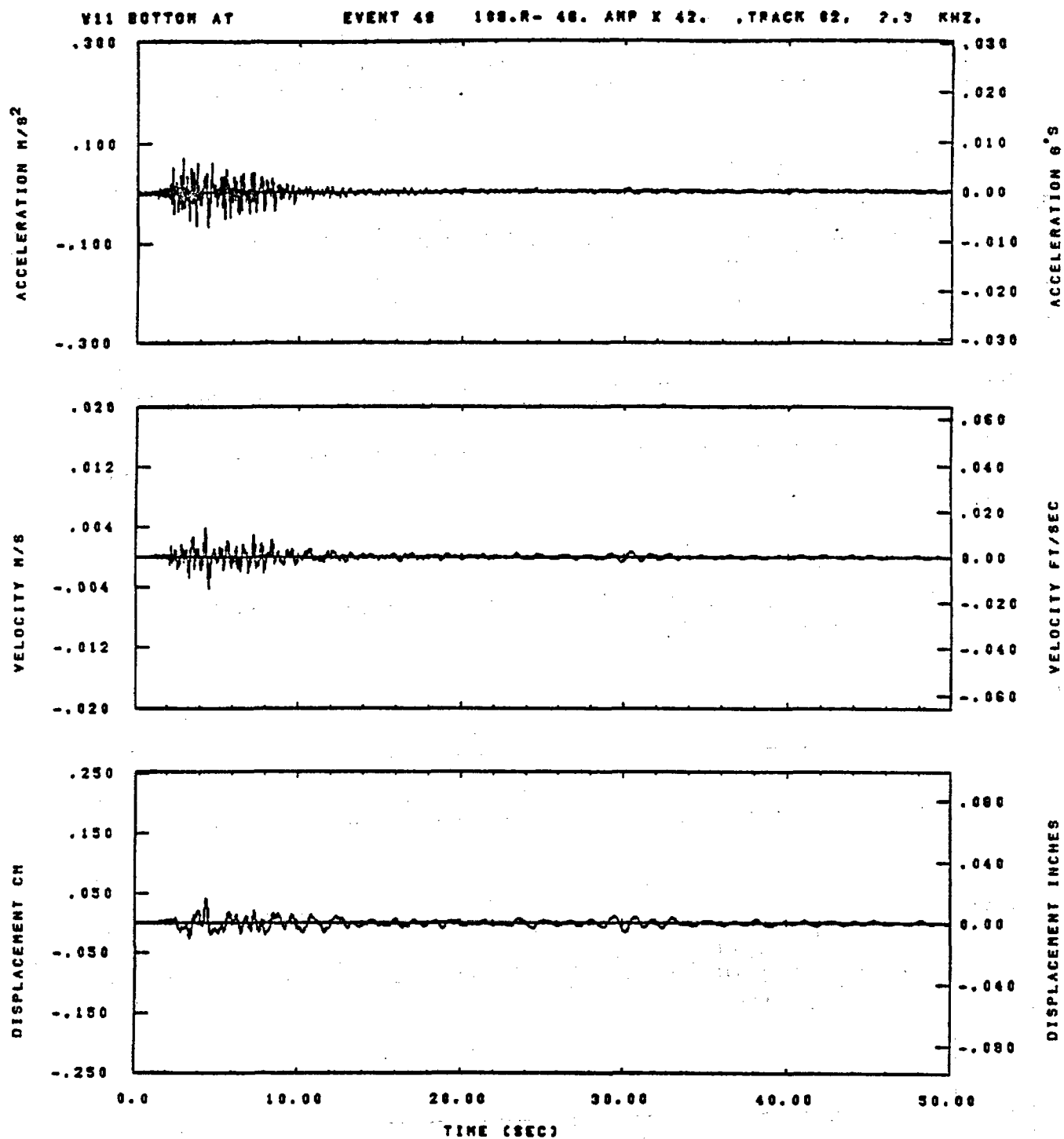
Figure E-76



IDT= .0020	OOT= .005	FIX=	AAS= 0.
HPP= .30	SVH= .20	HLH= 167	ASB=
LPP= 27.	SVL= 6.	HLL= 1333	ASE=
VTS= .300	VTE= .200	FLL= -20.	VSE= 0.
DPS= 0.	DPE= 100.	FLH= 0	DSE= 0.

15.48.38.

06/30/82



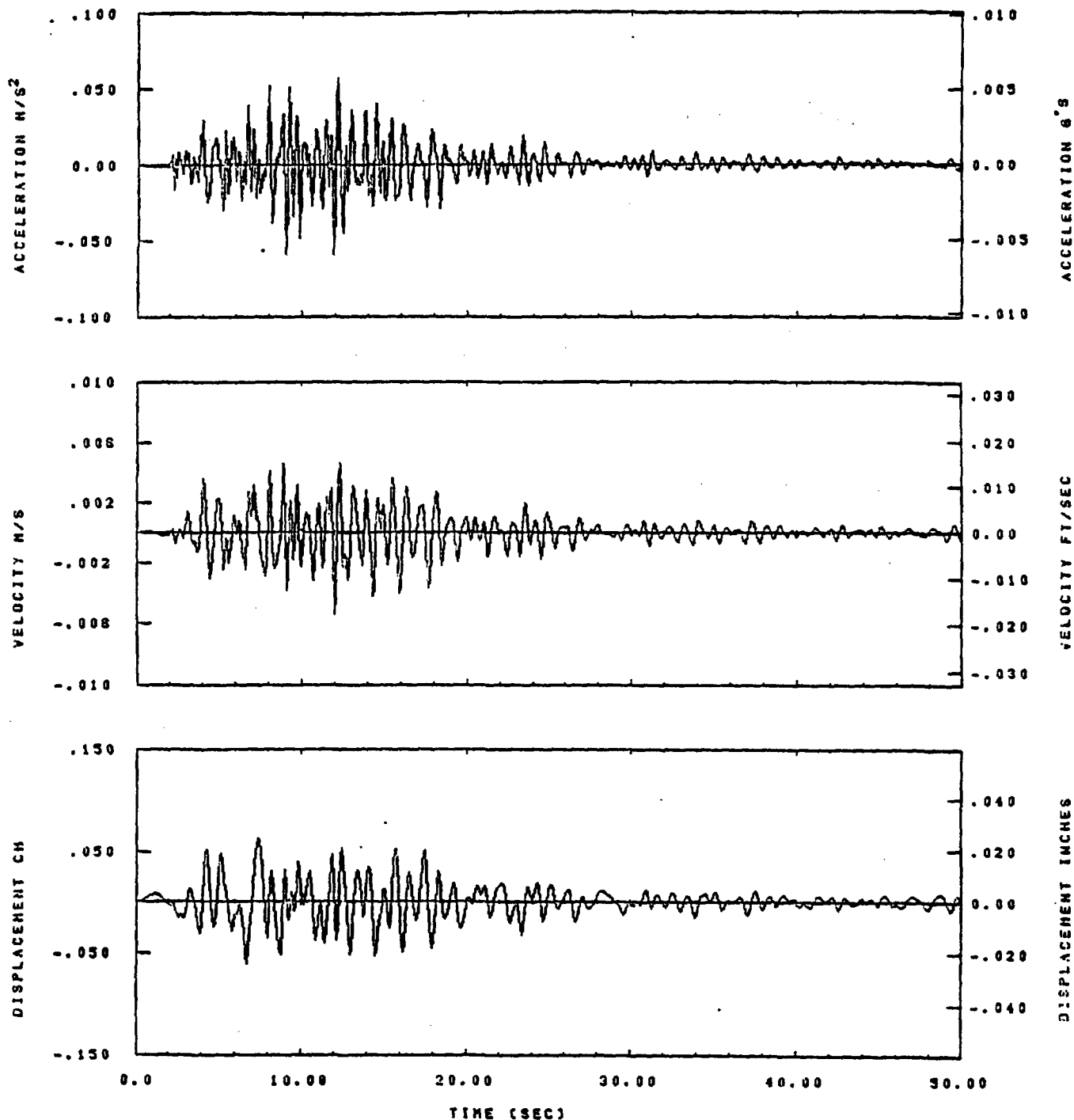
IDT= .0020	ODT= .005	FIX=	AAS= 0.
HPP= .30	BYH= .20	HLH= 167	ASH=
LPP= 27.	BYL= 6.	HLL= 1988	ASE=
VTB= .308	VTE= .200	FLL= -20.	VSE= 0.
OPB= 0.	OPE= 100.	FLH= 0	DSE= 0.

15.48.50.

06/30/82

Figure E-78

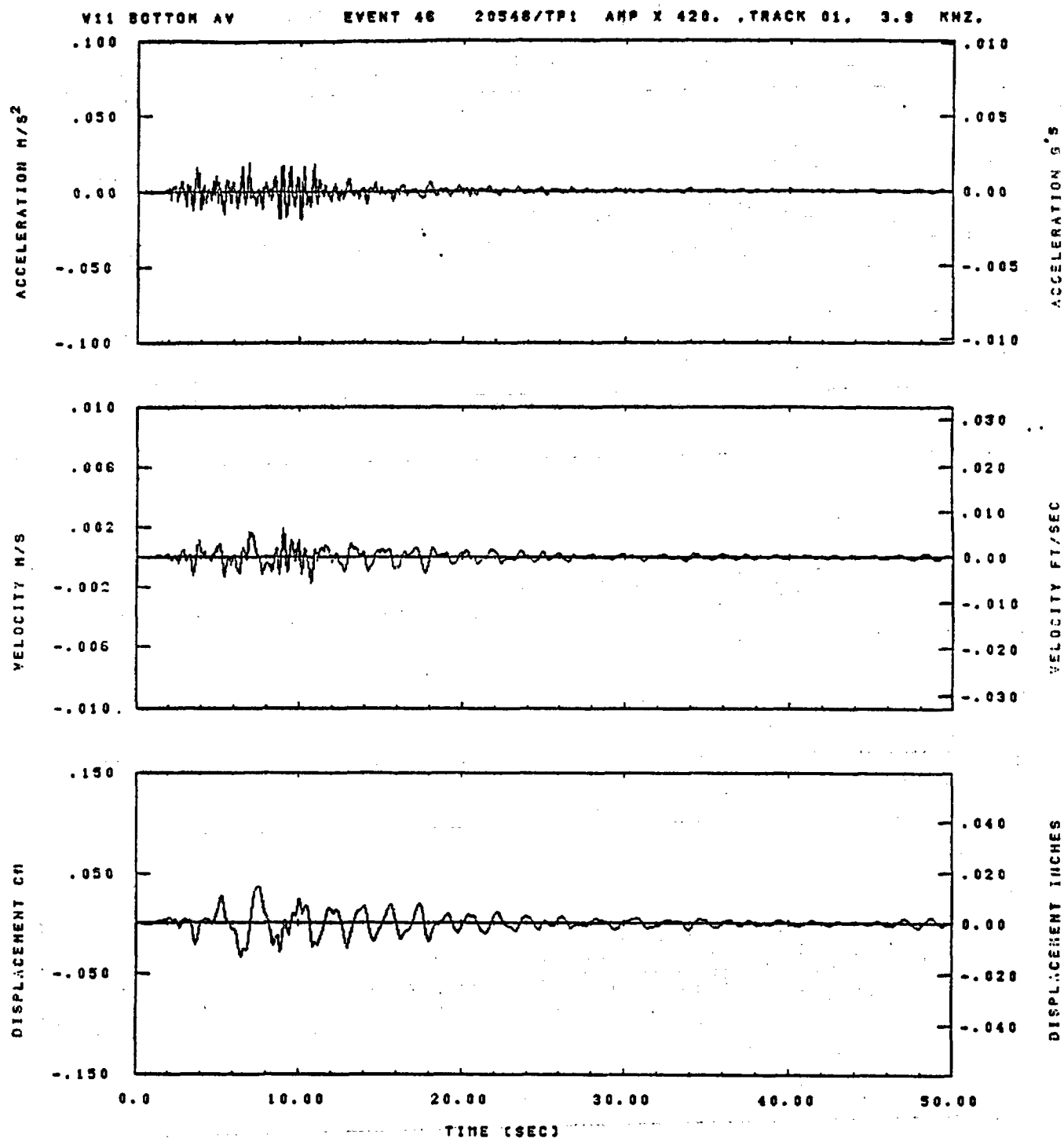
Y11 TOP AV EVENT 48 20548/TPI AMP X 28.1 TRACK 01. 30. KMZ.



IDT= .0020	ODT= .005	FIX=	AAS= 0.
HPP= .30	BYH= .20	HLH= 501	ASB=
LPP= 9.	BYL= 2.	HLL= 1999	ASE=
YTB= .300	VTE= .200	FLL= -20.	VSE= 0.
OPB= 0.	DPE= 100.	FLH= 0	DSE= 0.

13.47.22.

08/21/92

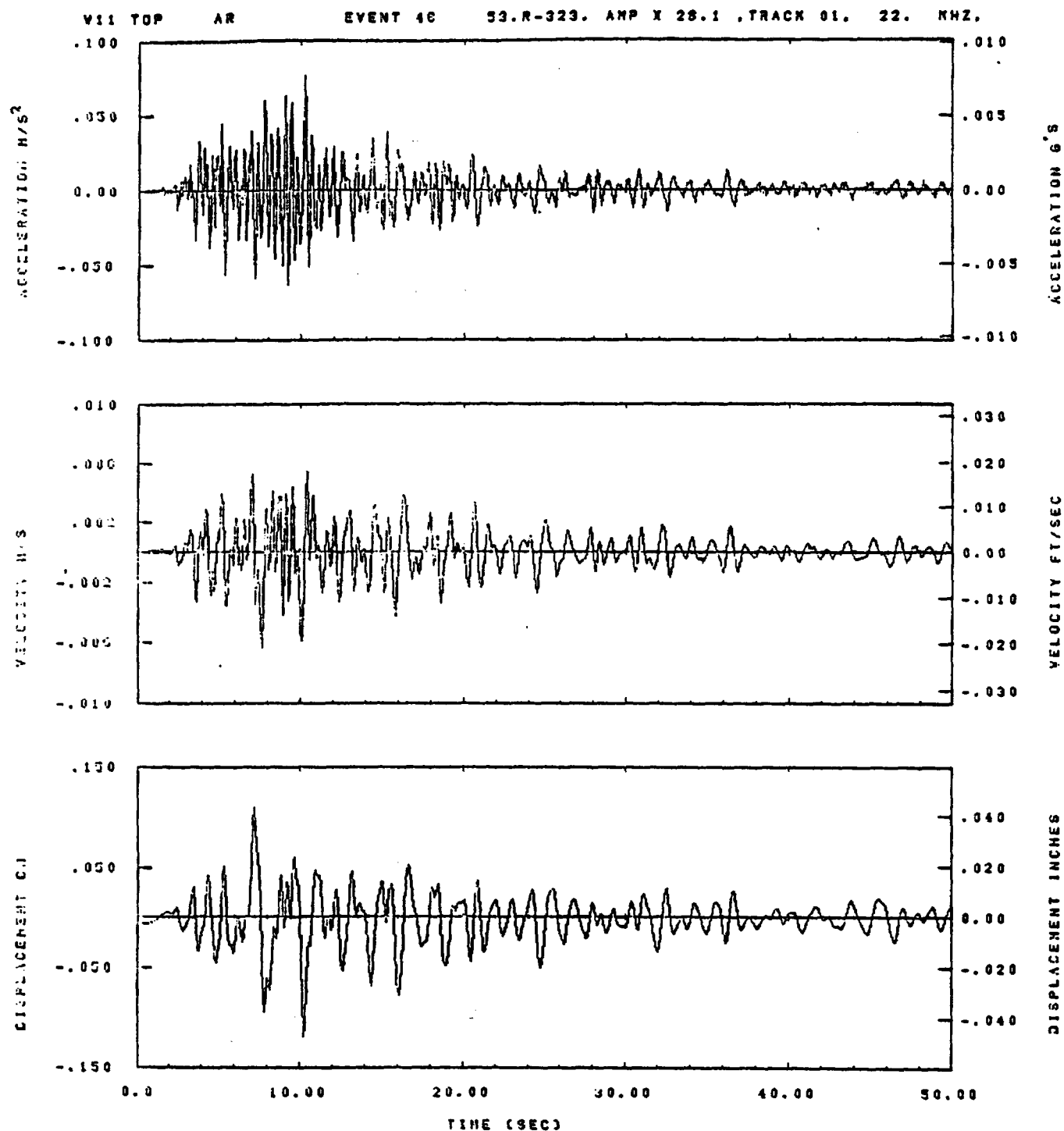


IDT= .0020	ODT= .005	FIX=	AAS= 0.
HPF= .30	BVH= .20	HLH= 201	ASS=
LPF= 22.	BYL= 5.	HLL= 1998	ASE=
VTB= .300	VTE= .200	FLL= -20.	VSE= 0.
DPS= 0.	DPE= 100.	FLH= 0	DSE= 0.

15.47.51.

06/21/82

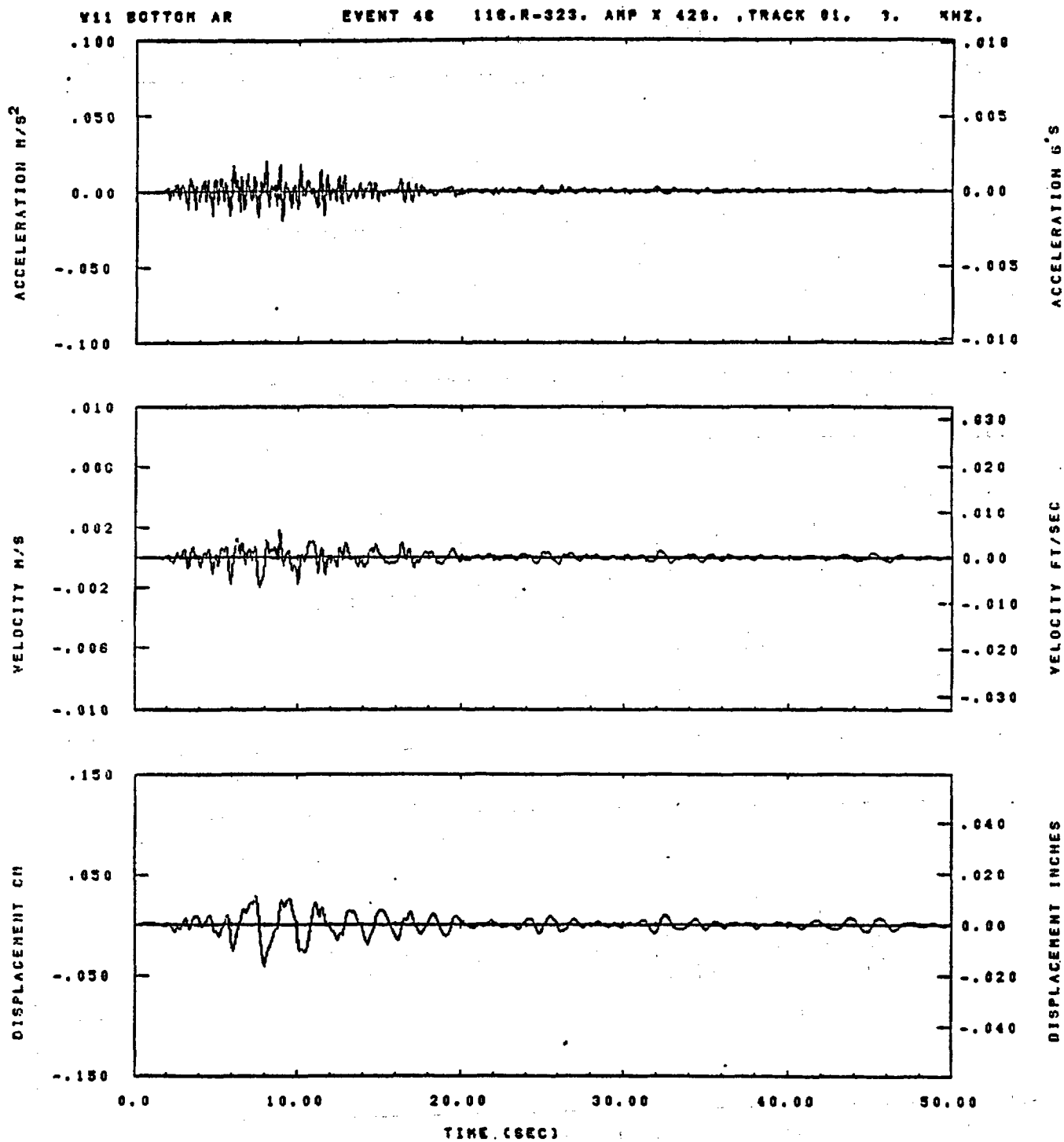
Figure E-80



IDT= .0020	OOT= .005	FIX=	AAS= 0.
HPF= .38	BNH= .20	HLH= 501	ASB=
LPF= 9.	BVL= 2.	HLL= 1989	ASE=
YTU= .300	VTE= .200	FLL= -20.	VSE= 0.
DPB= 0.	OPE= 100.	FLH= 0	DSE= 0.

15.47.27.

08/21/82

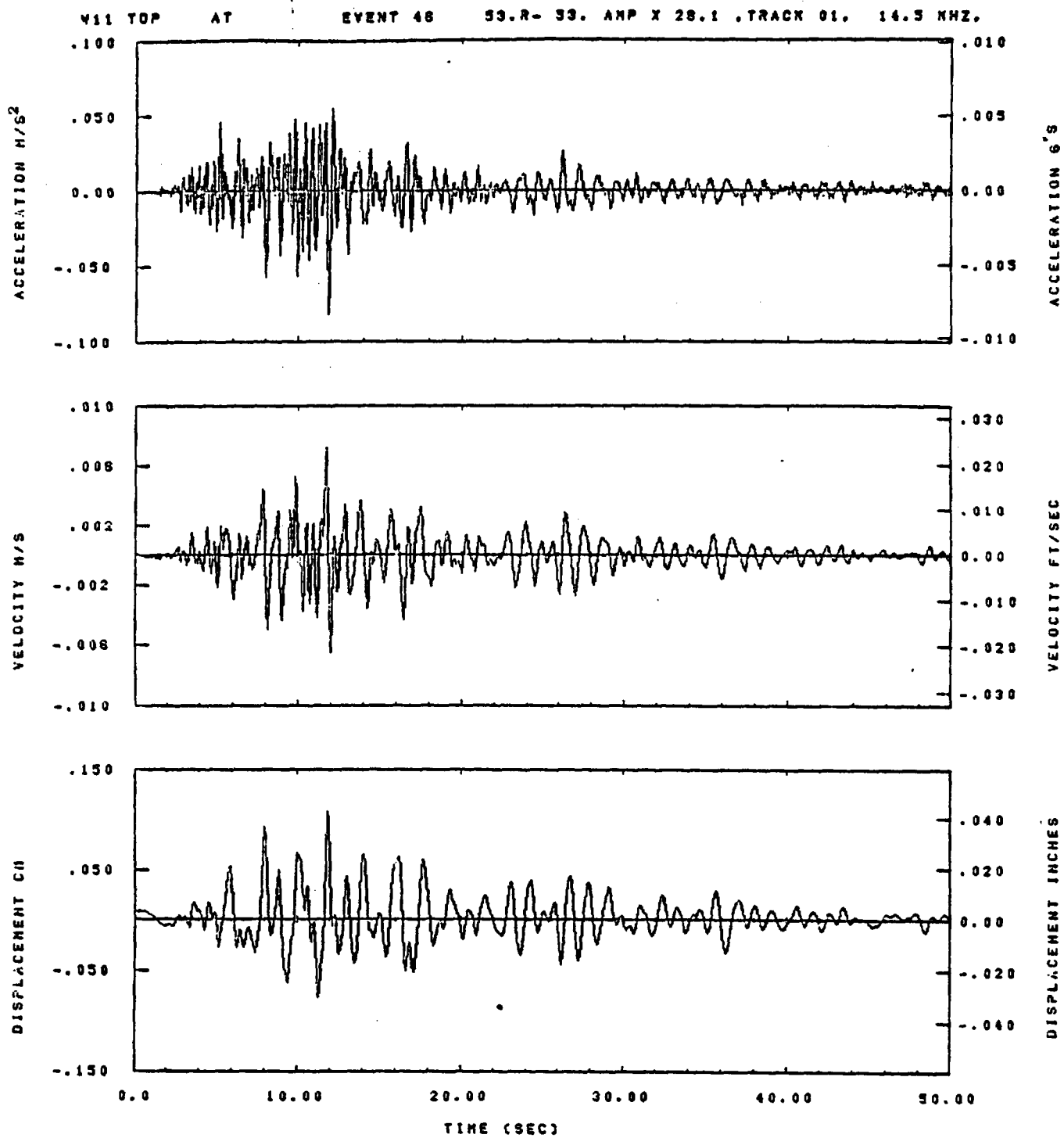


IDT= .0020	ODT= .005	FIX=	AAS= 0.
HPF= .30	BYN= .20	HLN= 201	ASB=
LPF= 22.	BVL= 5.	HLL= 1999	ASE=
VTB= .300	YTE= .200	FLL= -20.	VSE= 0.
DPS= 0.	DPE= 100.	FLH= 0	DSE= 0.

15.47.38.

06/21/82

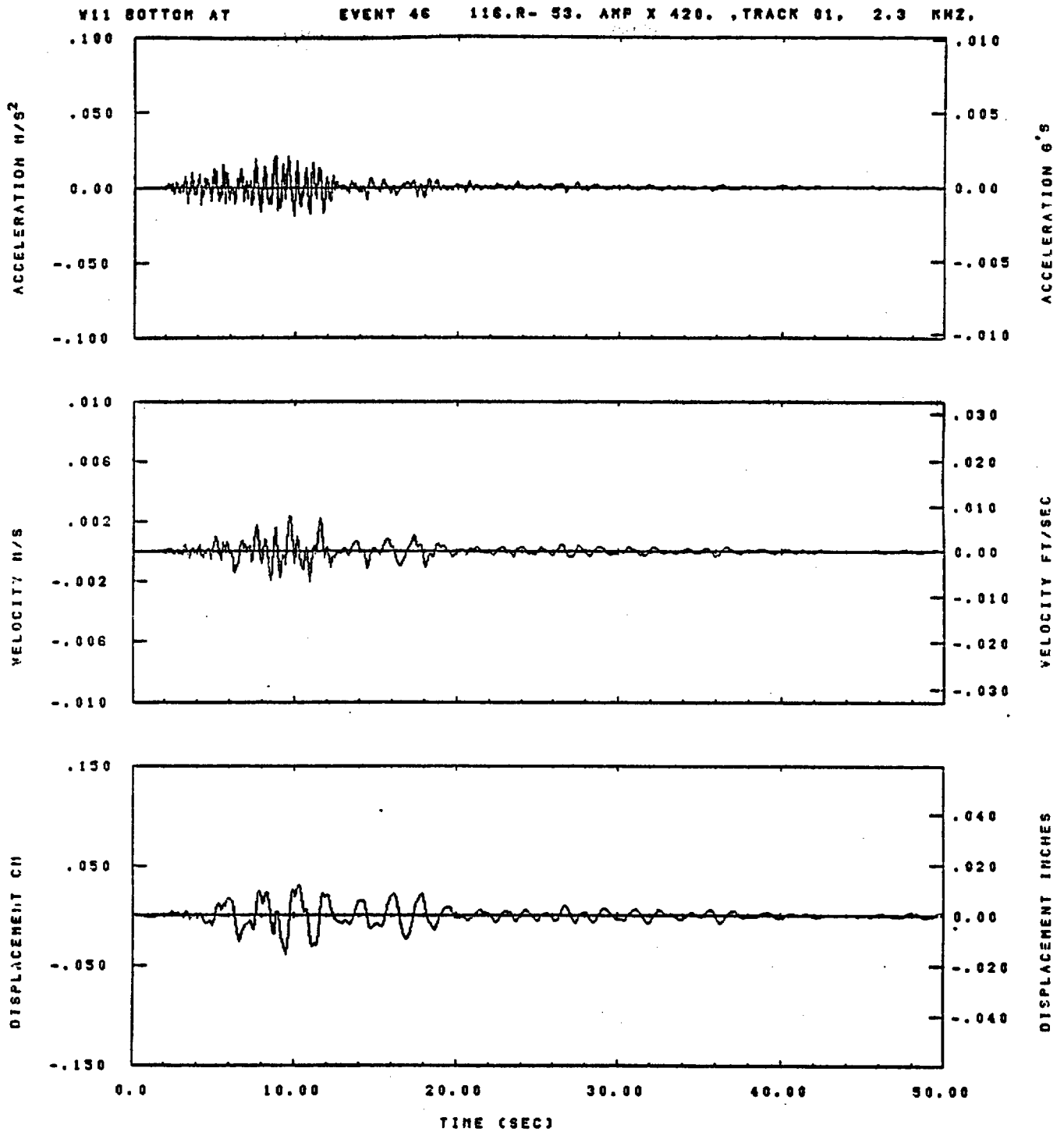
Figure E-82



IDT= .0020	ODT= .005	FIX=	AAS= 0.
HPF= .30	BYH= .20	HLH= 501	ASB=
LPF= 9.	BYL= 2.	HLL= 1399	ASE=
VTB= .300	VTE= .200	FLL= -20.	VSE= 0.
DPB= 0.	DPE= 100.	FLH= 0	DSE= 0.

13.47.31.

08/21/82



IDT= .0020	ODT= .005	FIX=	AAS= 0.
HPF= .30	SVH= .20	HLH= 201	ASS=
LPF= 22.	SVL= 5.	HLL= 1999	ASE=
VTB= .300	VTE= .200	FLL= -20.	YSE= 0.
OPB= 0.	DPE= 100.	FLH= 0	OSE= 0.

15.47.45.

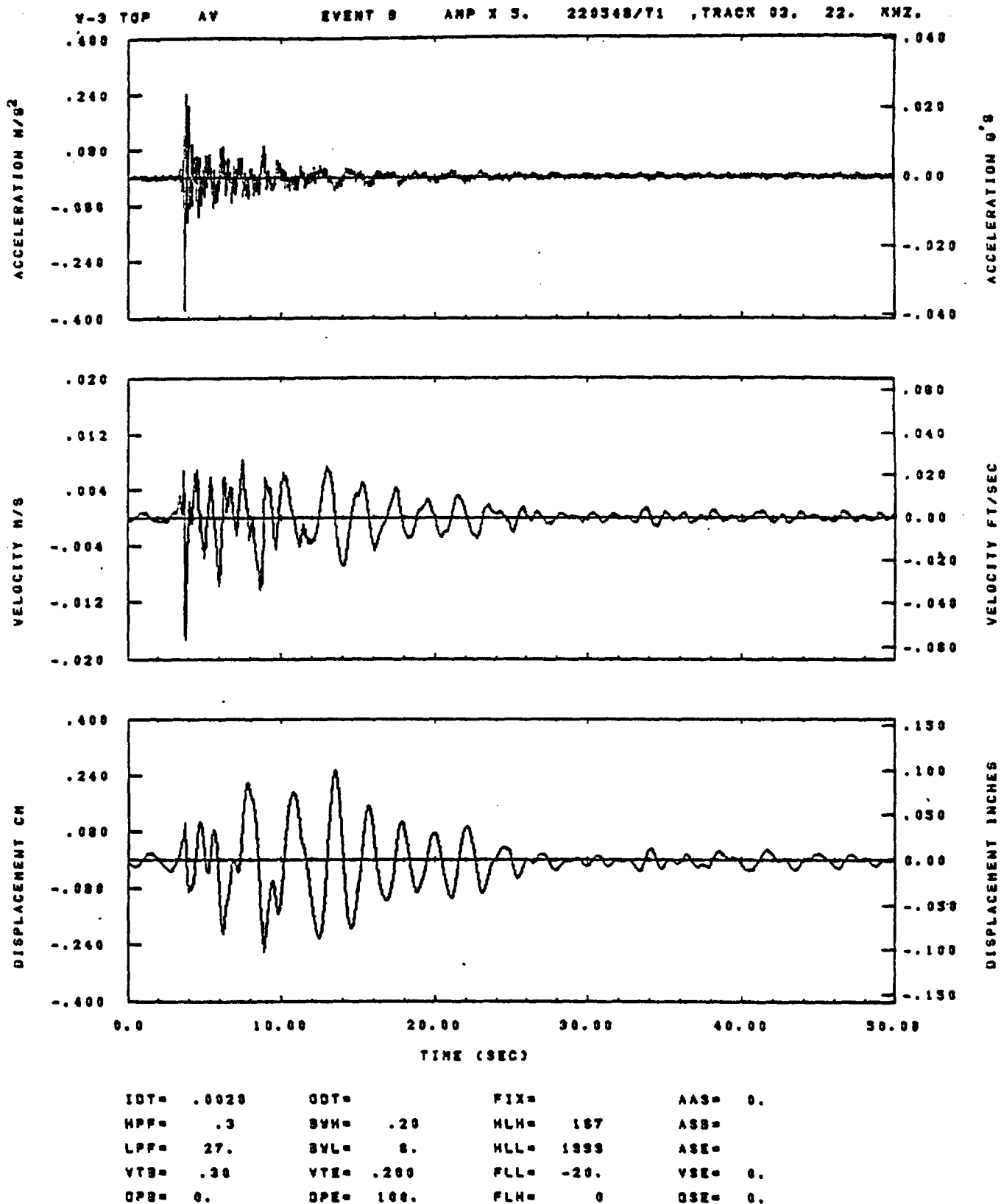
06/21/82

Figure E-84

APPENDIX F

COMPARISON OF TOP AND BOTTOM

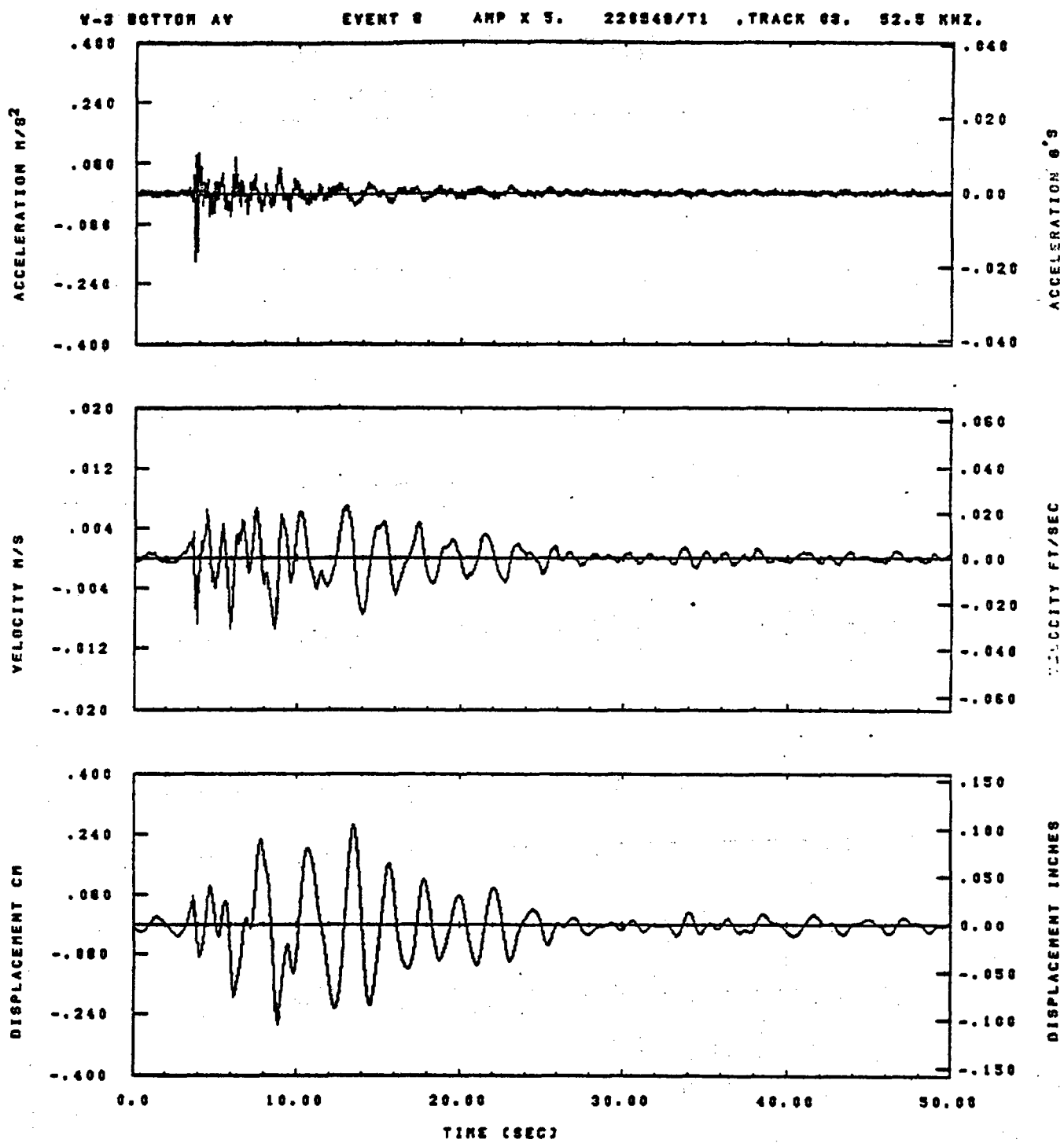
WAVEFORMS AT STATION W-3



14.48.09.

08/29/82

Figure F-1

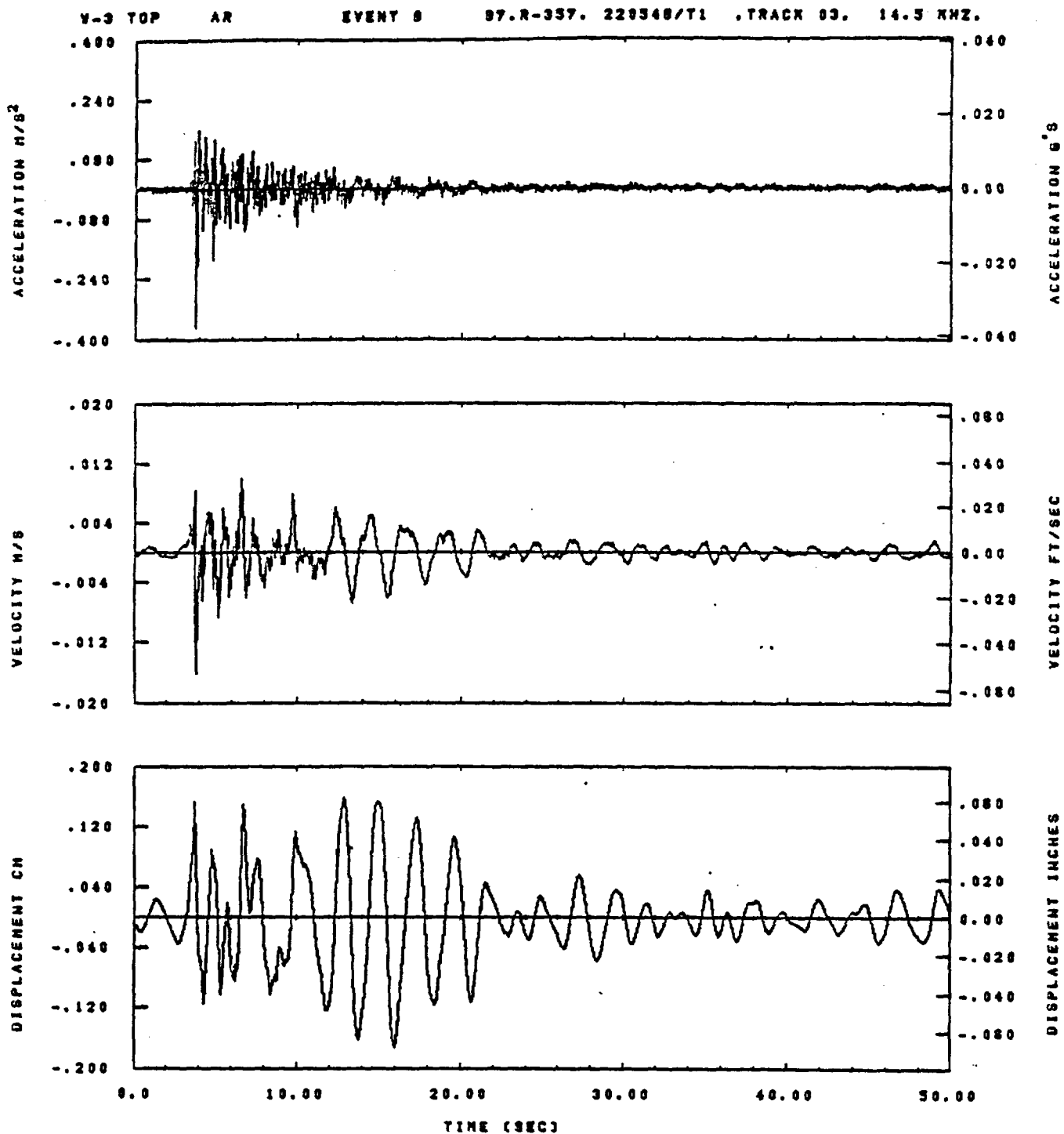


IDT= .0020	ODT=	FIX=	AAS= 0.
HPF= .3	BYH= .20	HLH= 167	ASS=
LPF= 27.	BYL= 6.	HLL= 1888	ASE=
VTB= .30	VTE= .200	FLL= -20.	VSE= 0.
DPS= 0.	DPE= 100.	FLH= 0	DSE= 0.

14.48.20.

06/30/82

Figure F-2

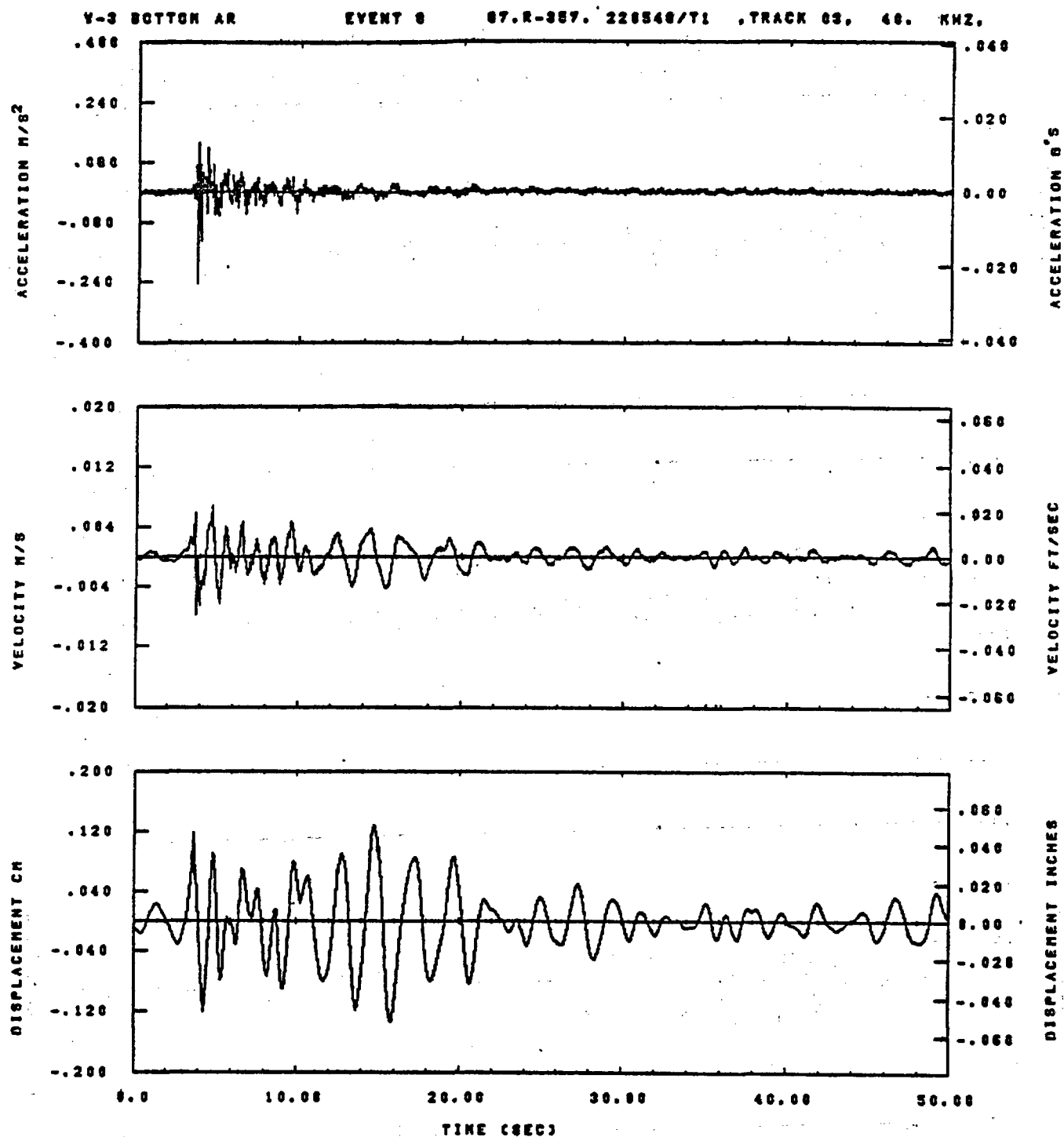


IDT= .0020	ODT=	FIX=	AAS= 0.
HPP= .3	BYH= .20	HLH= 187	ASB=
LPP= 27.	BYL= 8.	HLL= 1393	ASE=
VTB= .38	VTE= .200	FLL= -20.	VSE= 0.
DPS= 0.	DPE= 100.	FLH= 0	DSE= 0.

14.48.31.

08/30/82

Figure F-3

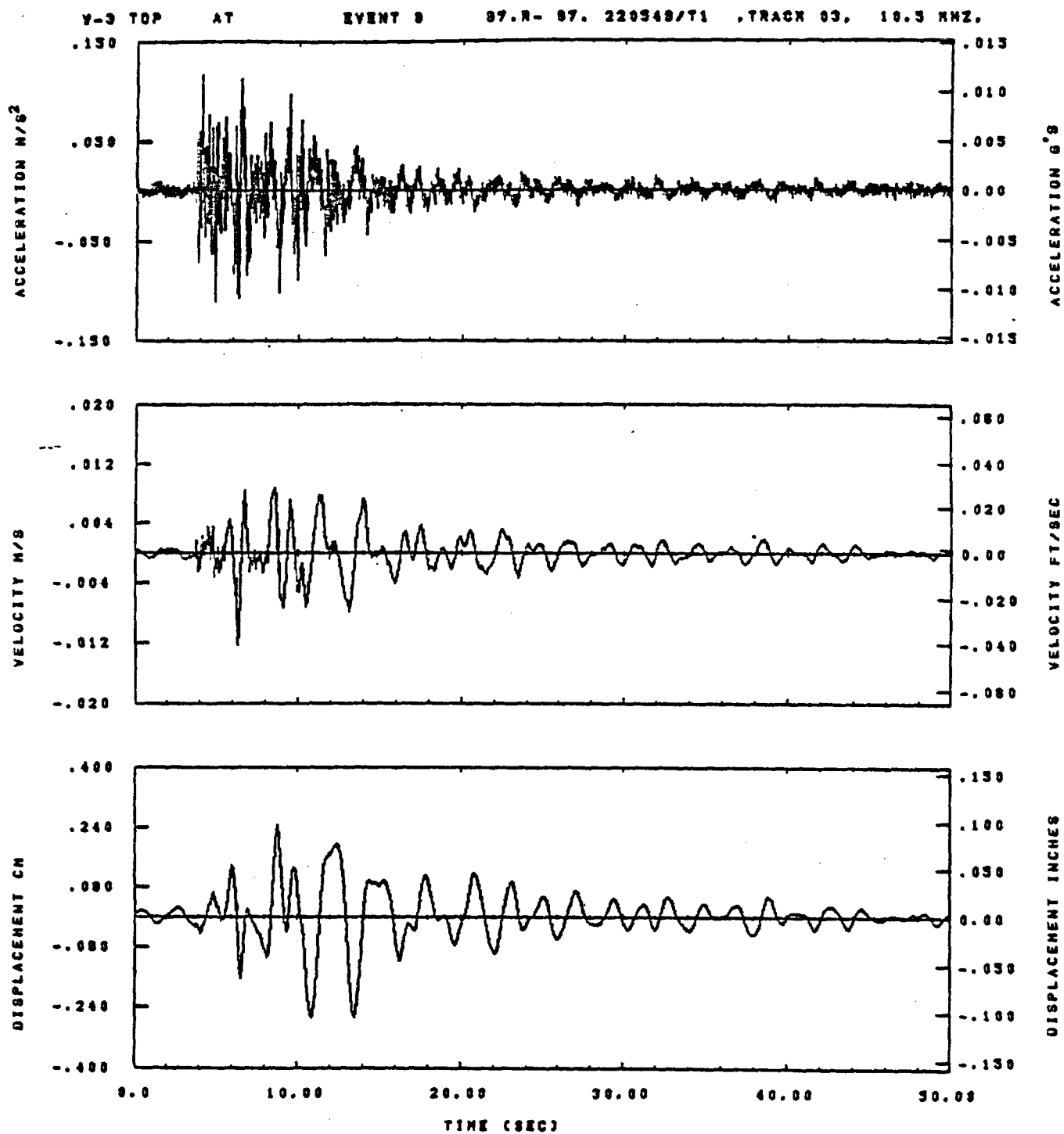


IDT= .0020	ODT=	FIX=	AAS= 0.
HPF= .3	BYN= .20	MLH= 167	ASB=
LPF= 27.	BYL= 6.	NLL= 1888	ASE=
VTS= .30	VTE= .200	FLL= -20.	VSE= 0.
DPS= 0.	DPE= 100.	FLH= 0	DSE= 0.

14.48.24.

06/30/82

Figure F-4

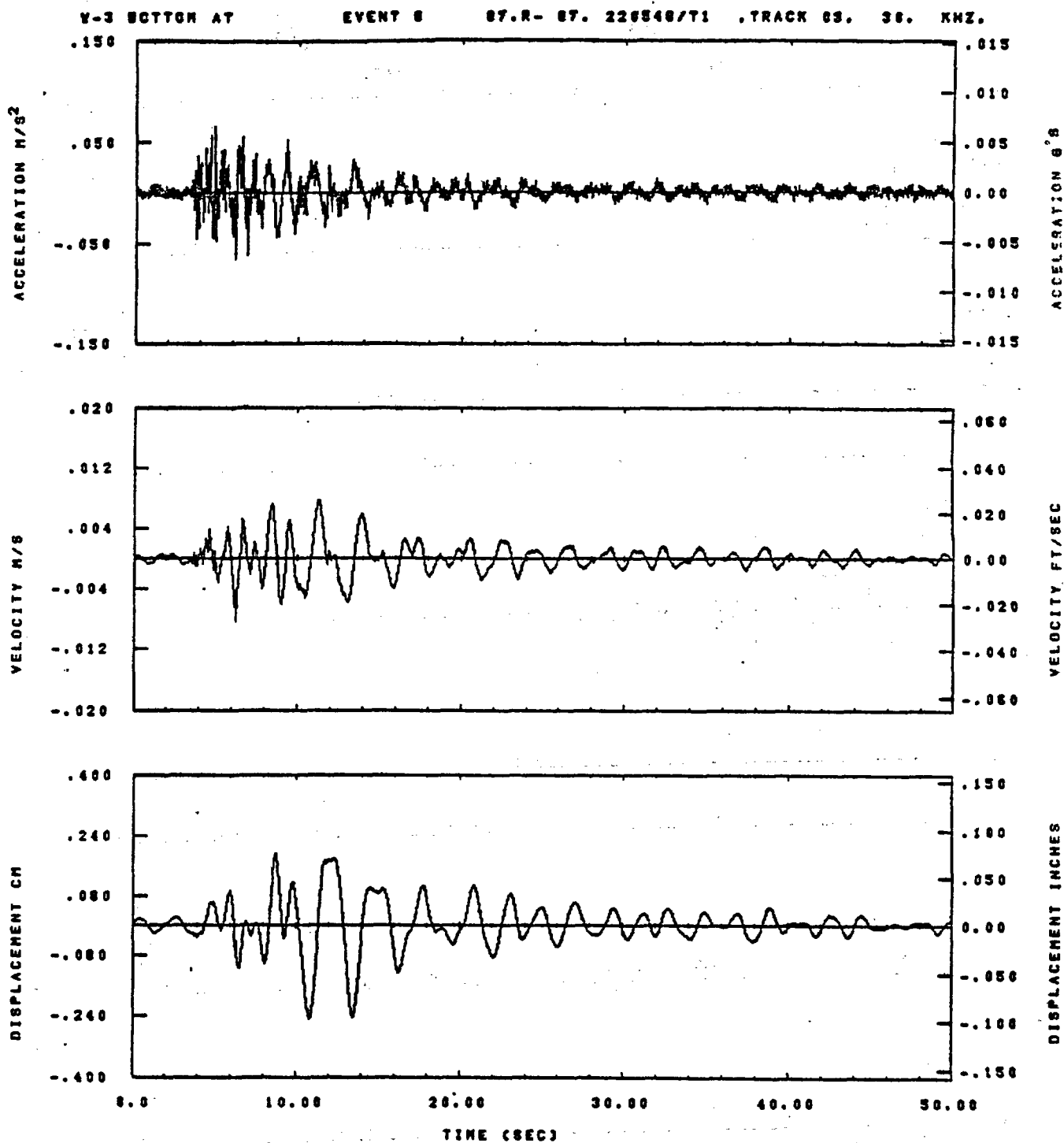


IDT= .0020	ODT=	FIX=	AAS= 0.
HPP= .3	BYN= .20	HLN= 187	ASS=
LPP= 27.	BYL= 0.	MLL= 1999	ASE=
YTS= .33	YTE= .200	FLL= -20.	VSE= 0.
DPS= 0.	DPE= 100.	FLH= 0	DSE= 0.

14.49.33.

08/30/82

Figure F-5

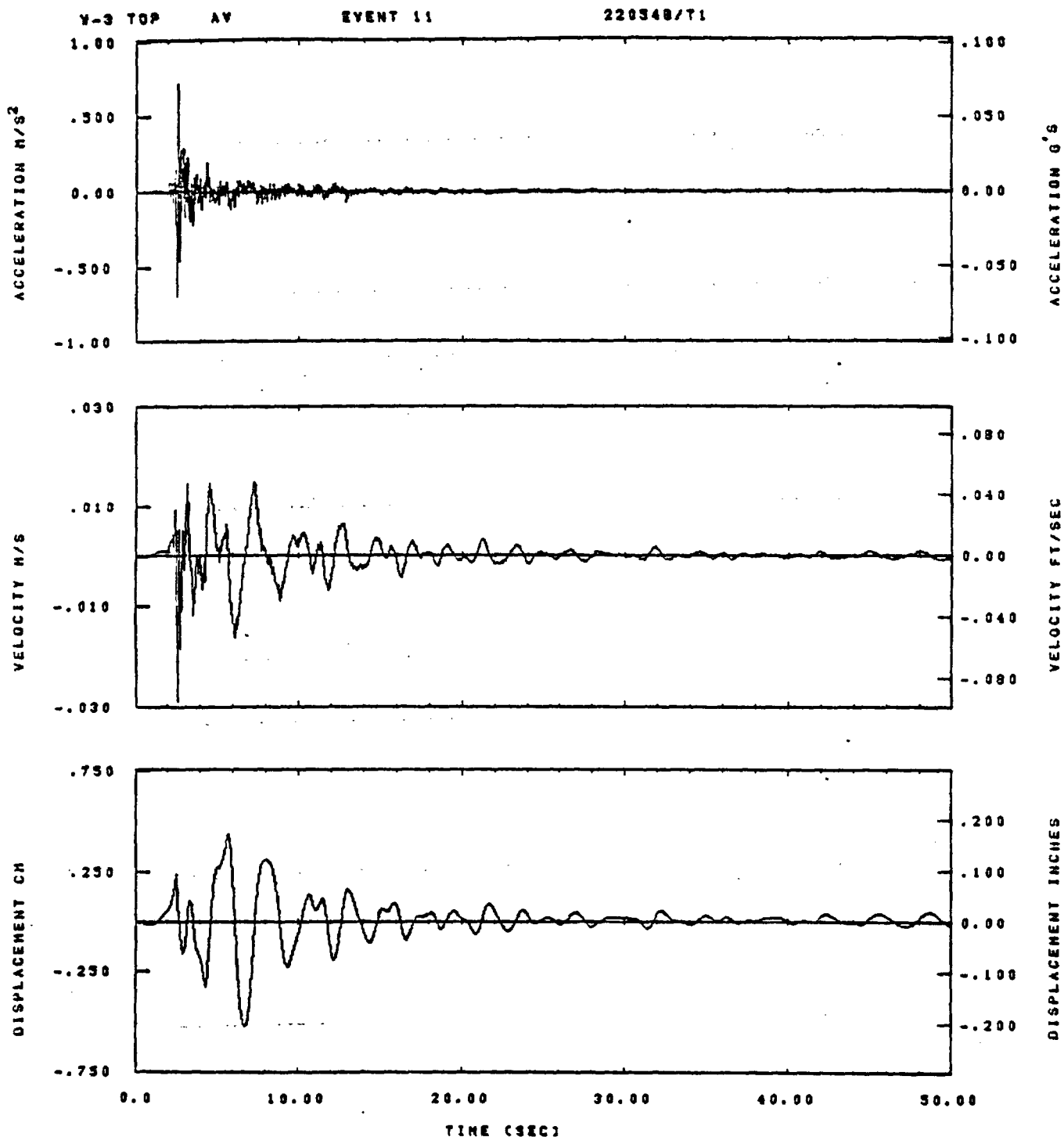


IDT= .0020	ODT=	FIX=	AAS= 0.
HPP= .3	BYH= .28	HLH= 167	ASS=
LPP= 27.	BYL= 6.	HLL= 1888	ASE=
VTS= .30	VTE= .200	FLL= -20.	VSE= 0.
OPE= 0.	OPE= 100.	FLH= 0	DSE= 0.

14.48.27.

06/30/82

Figure F-6

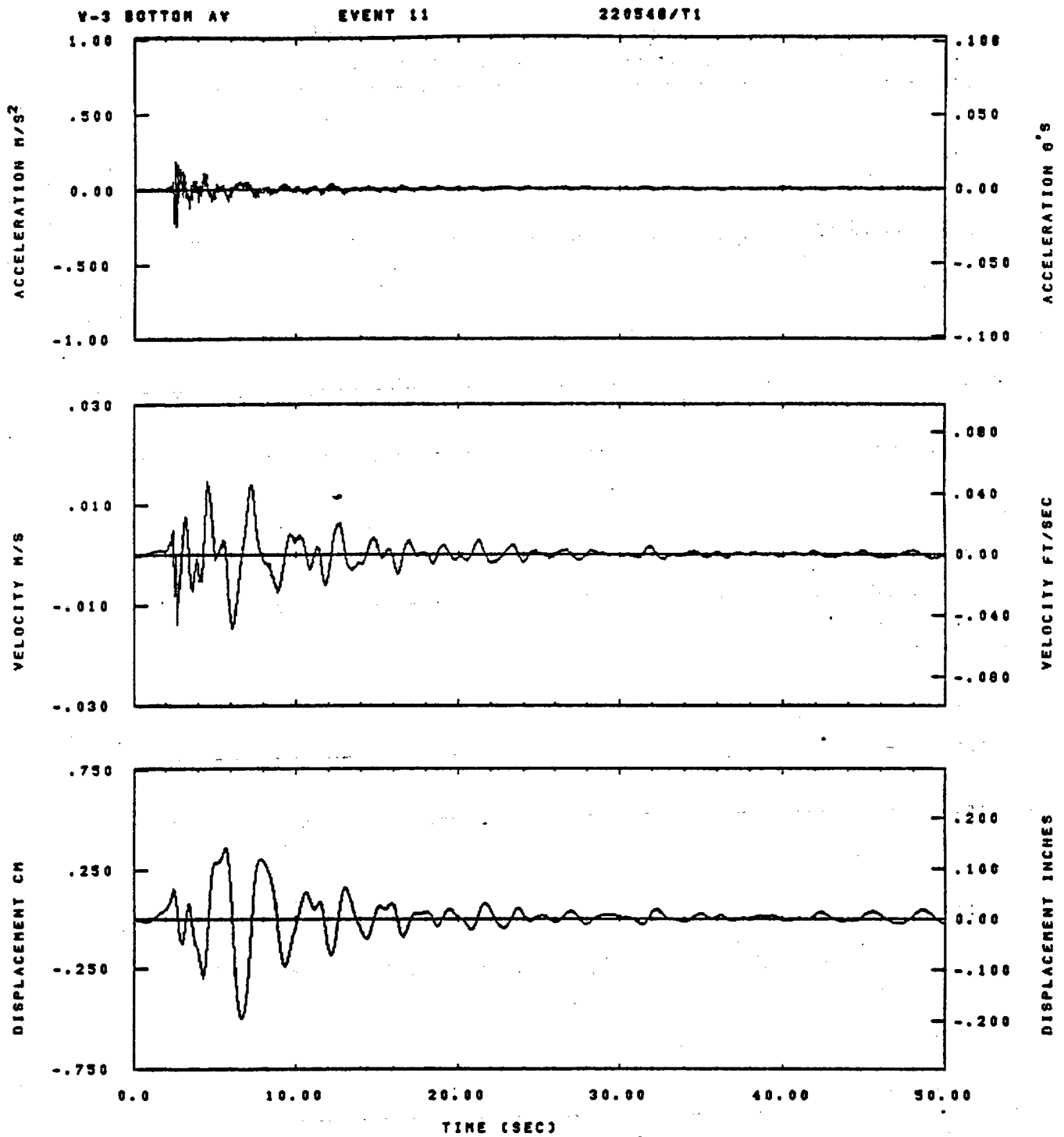


IDT= .0020	QDT= .005	FIX=	AAS= 0.
HPP= .3	BVM= .20	HLH= 187	ASB=
LPP= 27.	BVL= 8.	HLL= 1393	ASE=
VTB= .30	VTE= .200	FLL= -20.	VSE= 0.
DPS= 0.	DPE= 100.	FLH= 0	DSE= 0.

08.53.47.

07/09/82

Figure F-7

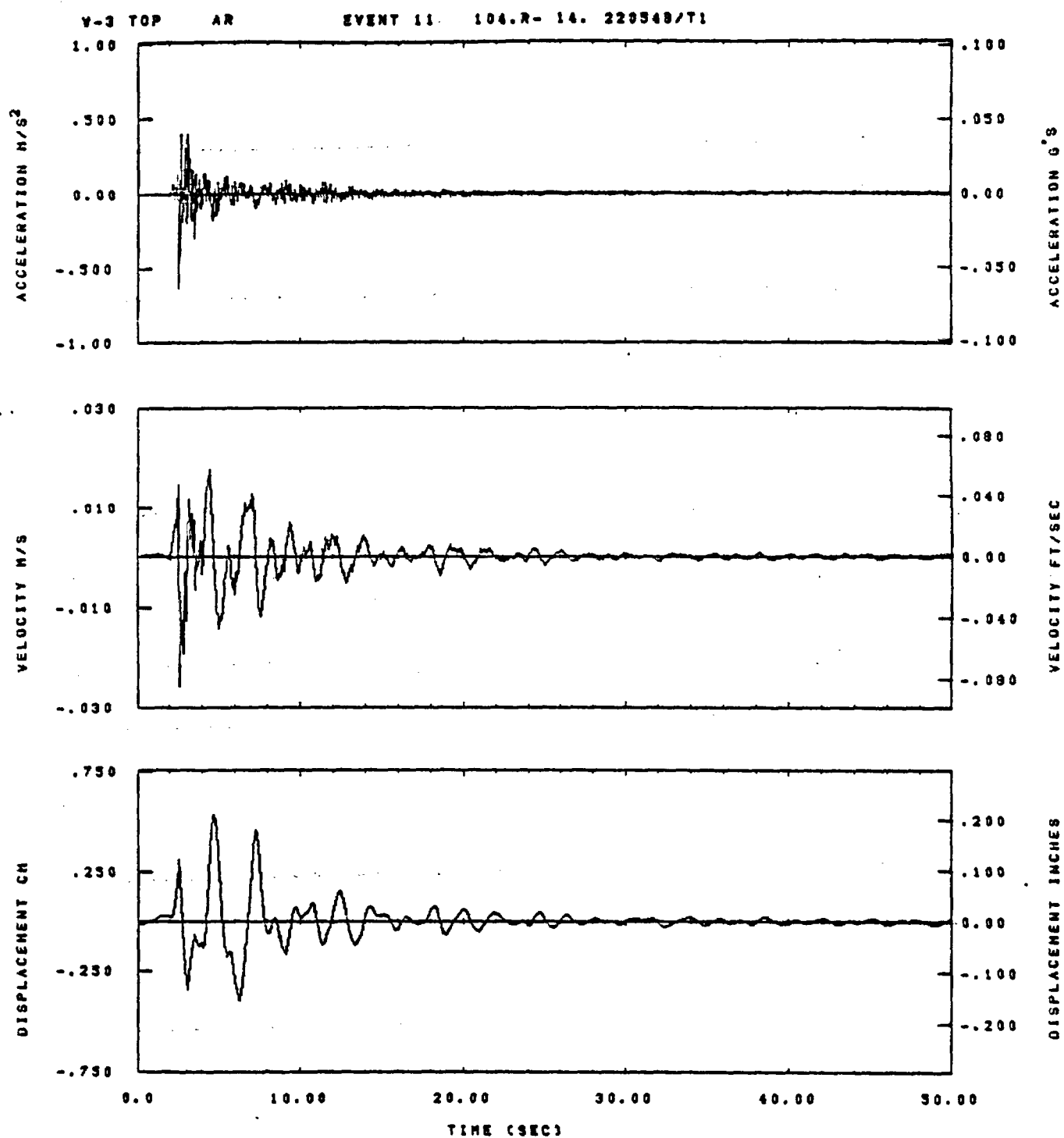


IDT= .0020	ODT= .005	FIX=	AAS= 0.
HPF= .3	BYH= .20	HLH= 187	ASB=
LPF= 27.	BYL= 6.	HLL= 1989	ASE=
VTB= .30	VTE= .200	FLL= -20.	VSE= 0.
DPS= 0.	DPE= 100.	FLH= 0	DSE= 0.

09.01.08.

07/08/82

Figure F-8

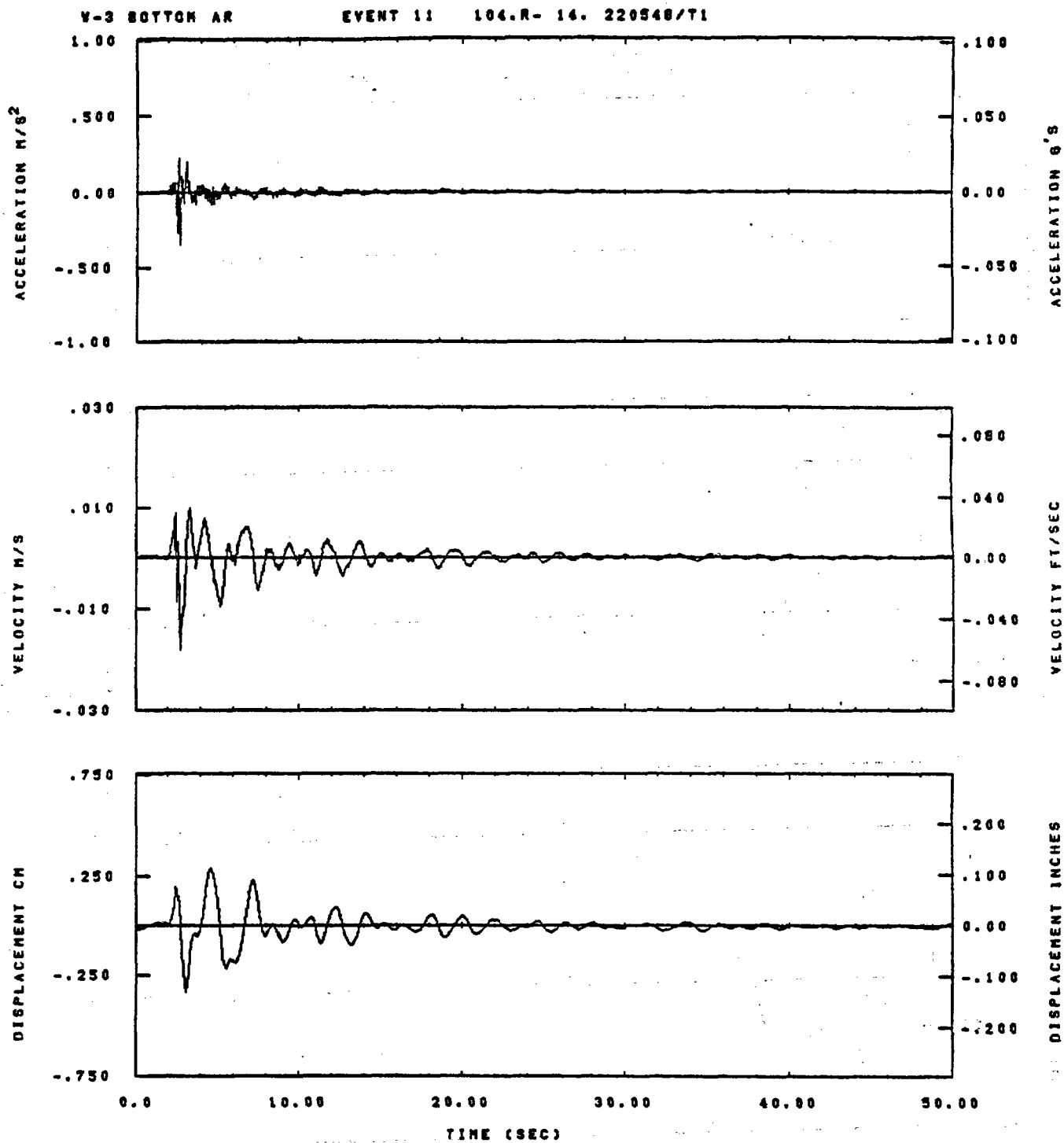


IDT= .0020	ODT= .003	FIX=	AAS= 0.
HPF= .3	BVH= .20	HLH= 187	ASB=
LPF= 27.	BVL= 6.	HLL= 1999	ASE=
VTB= .30	VTE= .200	FLL= -20.	VSE= 0.
DPB= 0.	DPE= 100.	FLH= 0	DSE= 0.

08.33.38.

07/03/82

Figure F-9

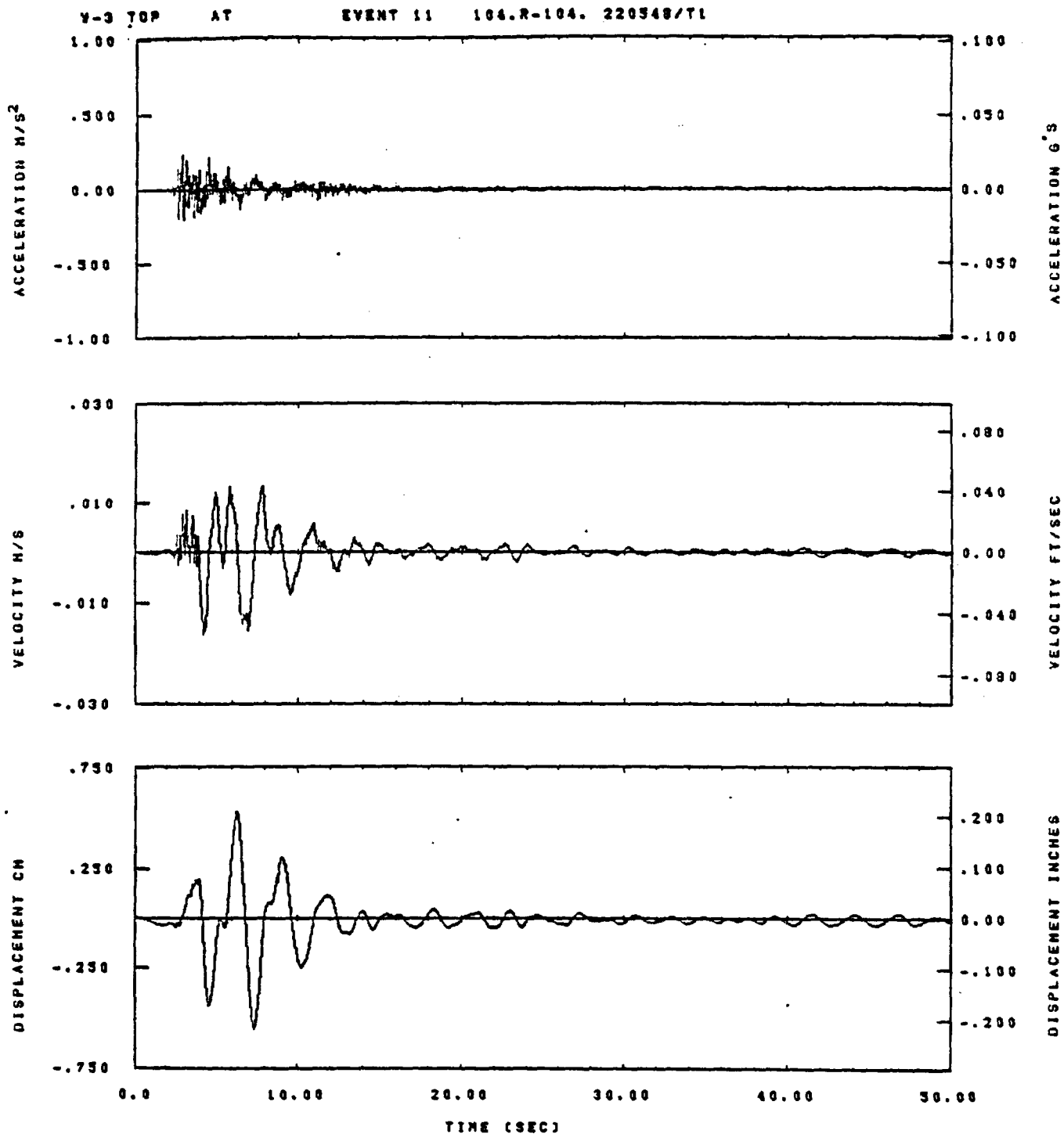


IDT= .0020	ODT= .005	FIX=	AAS= 0.
HPF= .3	SVH= .20	HLH= 167	ASB=
LPF= 27.	SVL= 6.	HLL= 1999	ASE=
VTS= .30	VTE= .200	FLL= -20.	VSE= 0.
DPS= 0.	DPE= 100.	FLH= 0	DSE= 0.

08.01.50.

07/08/82

Figure F-10

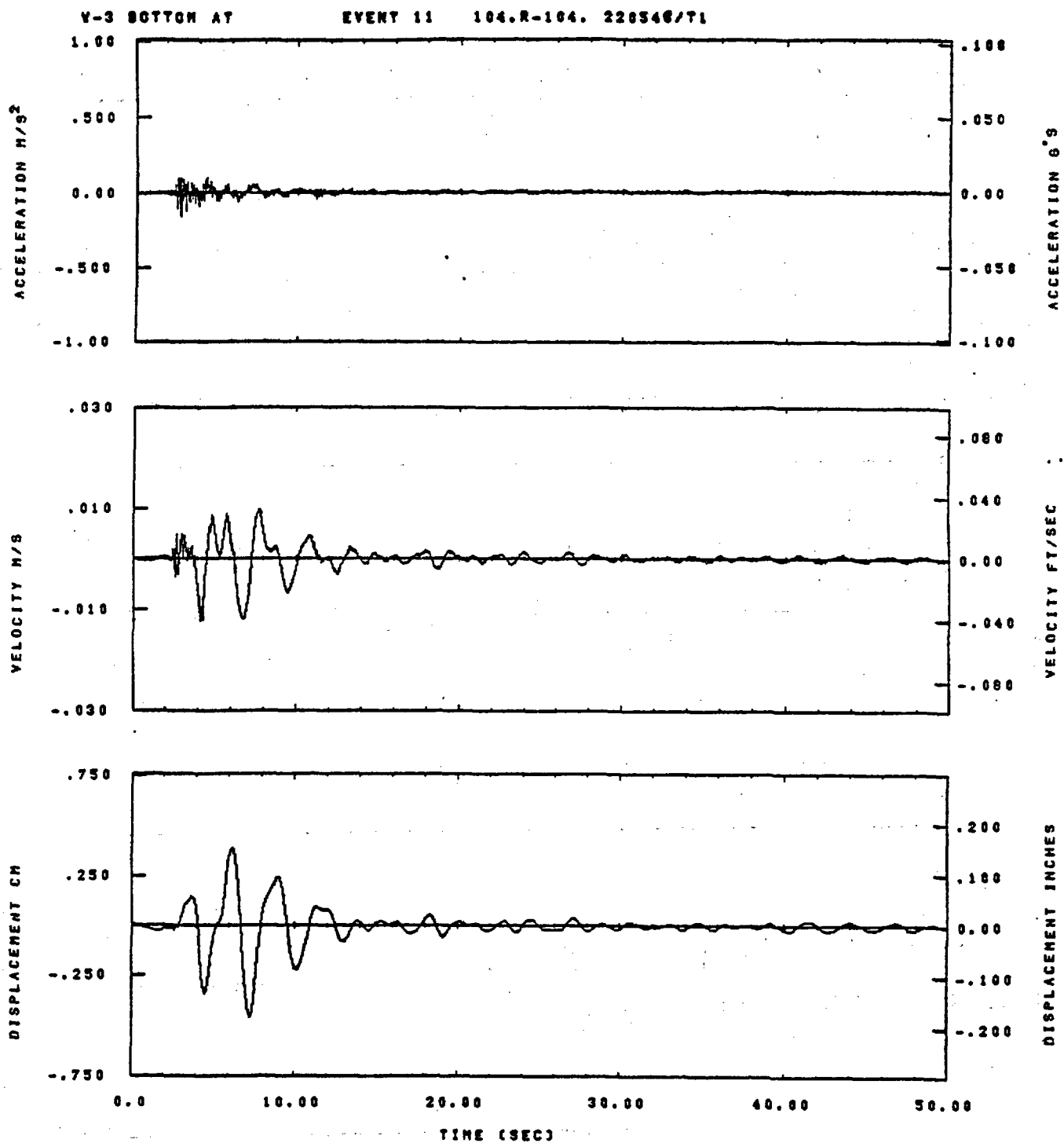


IDT= .0020	ODT= .005	FIX=	AAS= 0.
HPP= .3	SVH= .20	HLH= 187	ASB=
LPP= 27.	SVL= 8.	HLL= 1333	ASE=
VTB= .30	VTE= .200	FLL= -20.	VSE= 0.
DPS= 0.	DPE= 100.	FLH= 0	DSE= 0.

09.00.14.

07/09/82

Figure F-11

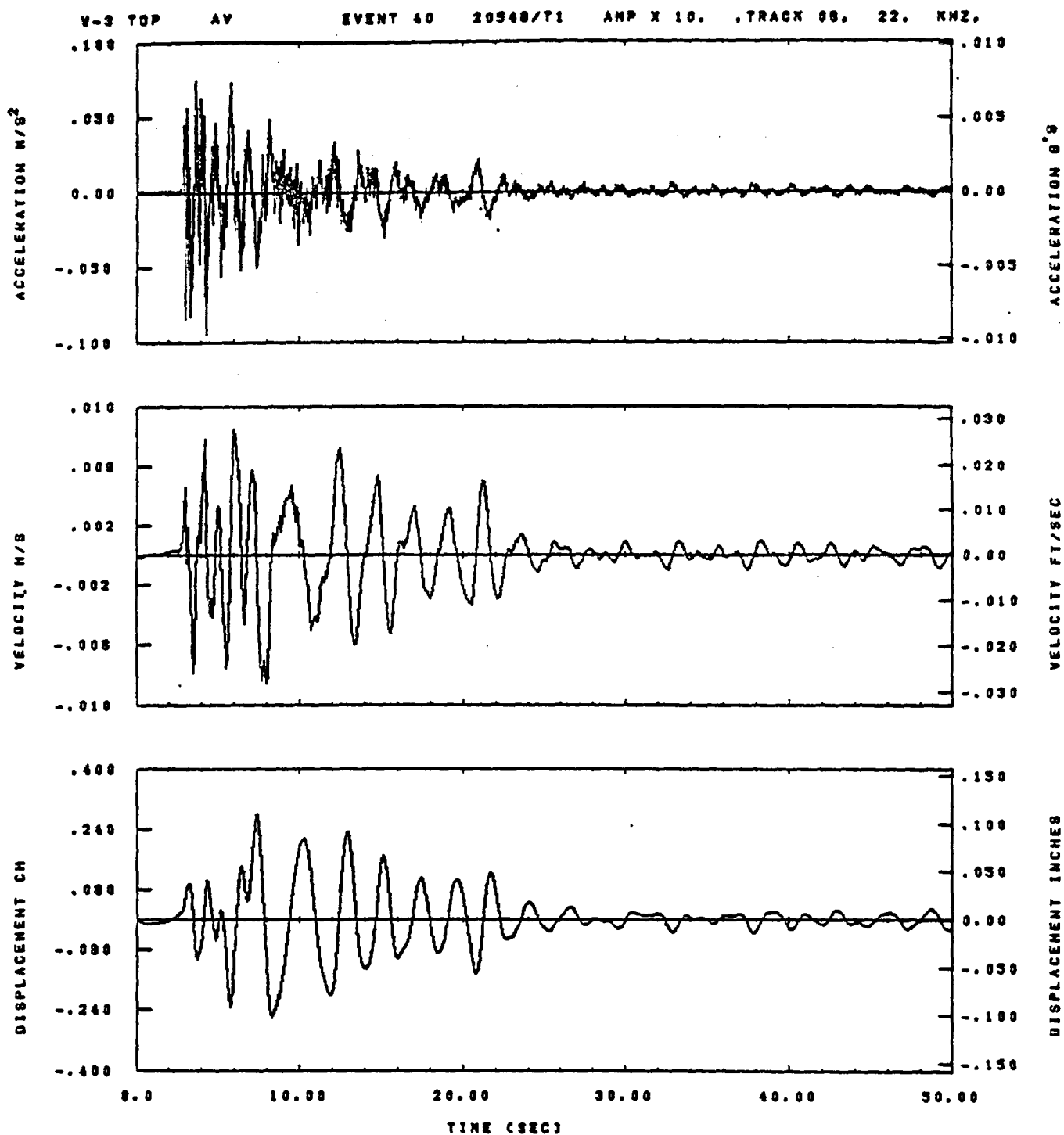


IOT= .0020	OCT= .005	FIX=	AAS= 0.
HPF= .3	BYH= .20	HLH= 167	ASB=
LPF= 27.	BYL= 6.	HLL= 1989	ASE=
VTS= .30	VTE= .208	FLL= -20.	VSE= 0.
DPB= 0.	DPE= 100.	FLH= 0	DSE= 0.

09.01.57.

07/08/82

Figure F-12

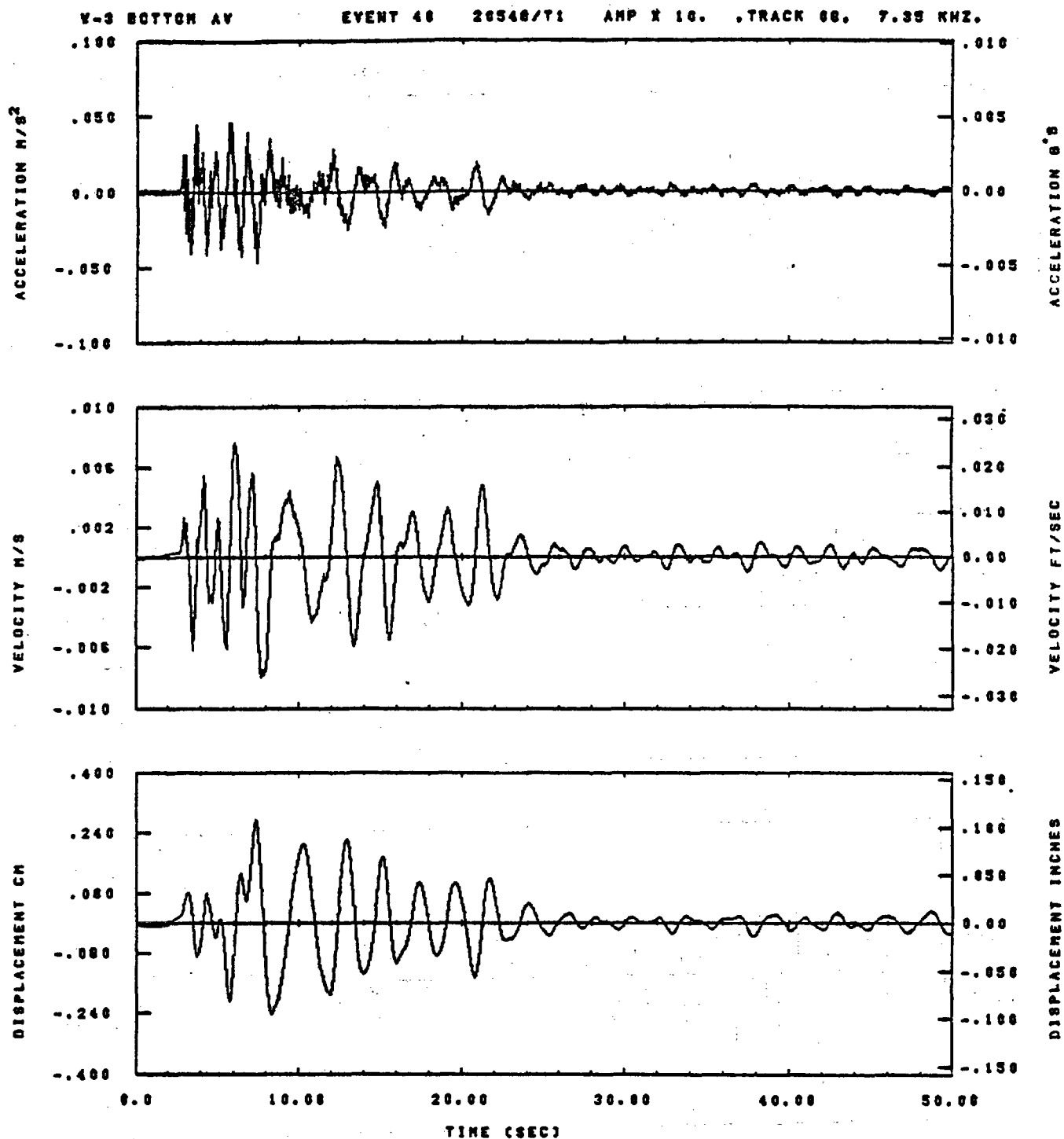


IDT= .0020	ODT= .003	FIX=	AAS= 0.
HPP= .23	BYH= .18	HLH= 187	ASB=
LPP= 27.	BYL= 8.	HLL= 2399	ASE=
VTB= .250	VTE= .180	FLL= -20.	VSE= 0.
DPS= 0.	DPE= 93.	FLH= 0	DSE= 0.

13.34.38.

08/30/82

Figure F-13

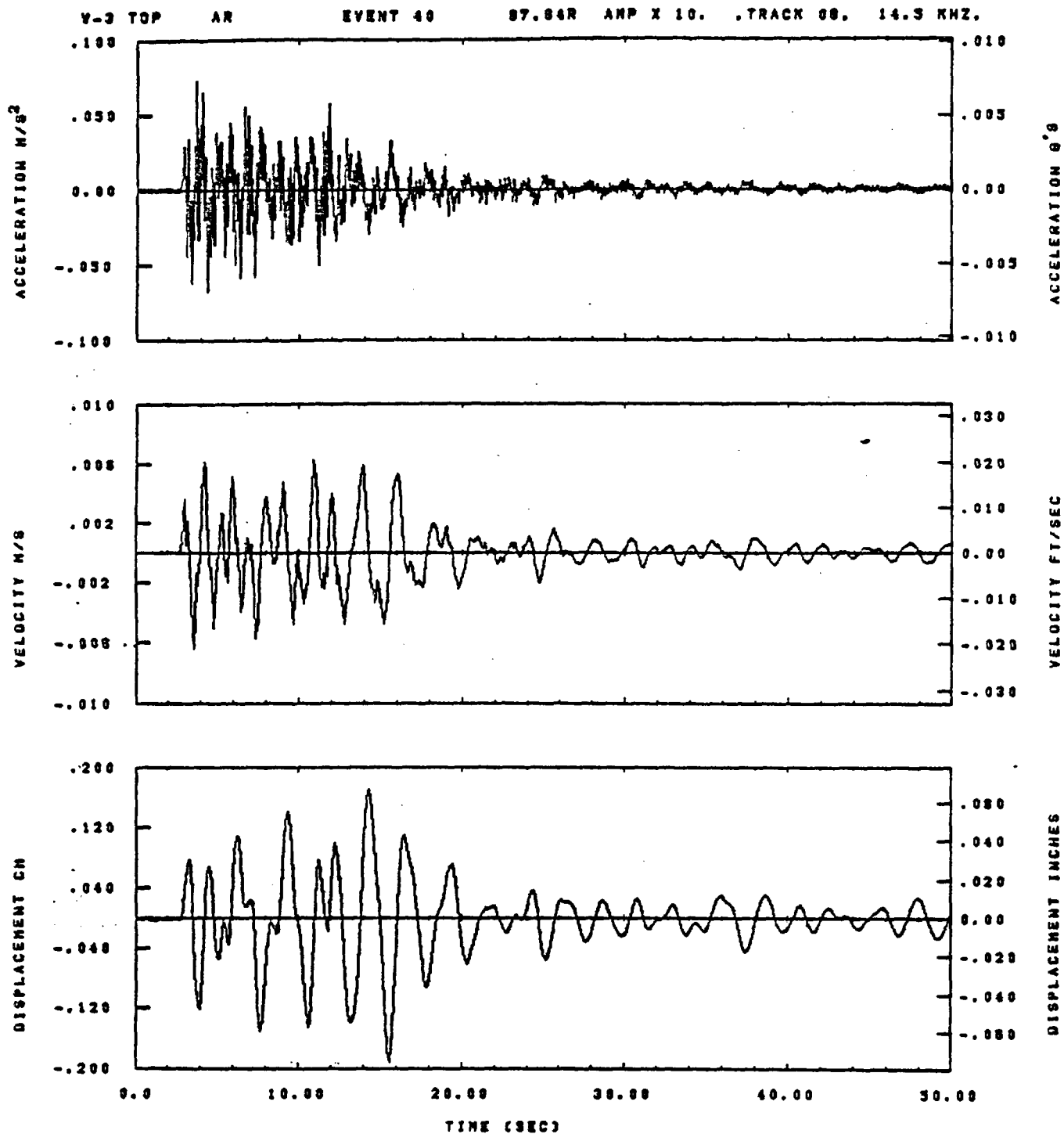


IGT= .0020	QDT= .0005	FIX=	AAS= 0.
HPP= .25	SVH= .16	HLH= 187	ASB=
LPP= 27.	SVL= 6.	HLL= 2388	ASE=
VTE= .250	VTE= .186	FLL= -20.	VSE= 0.
OPB= 0.	DPE= 85.	FLH= 0	DSE= 0.

13.54.58.

06/30/02

Figure F-14

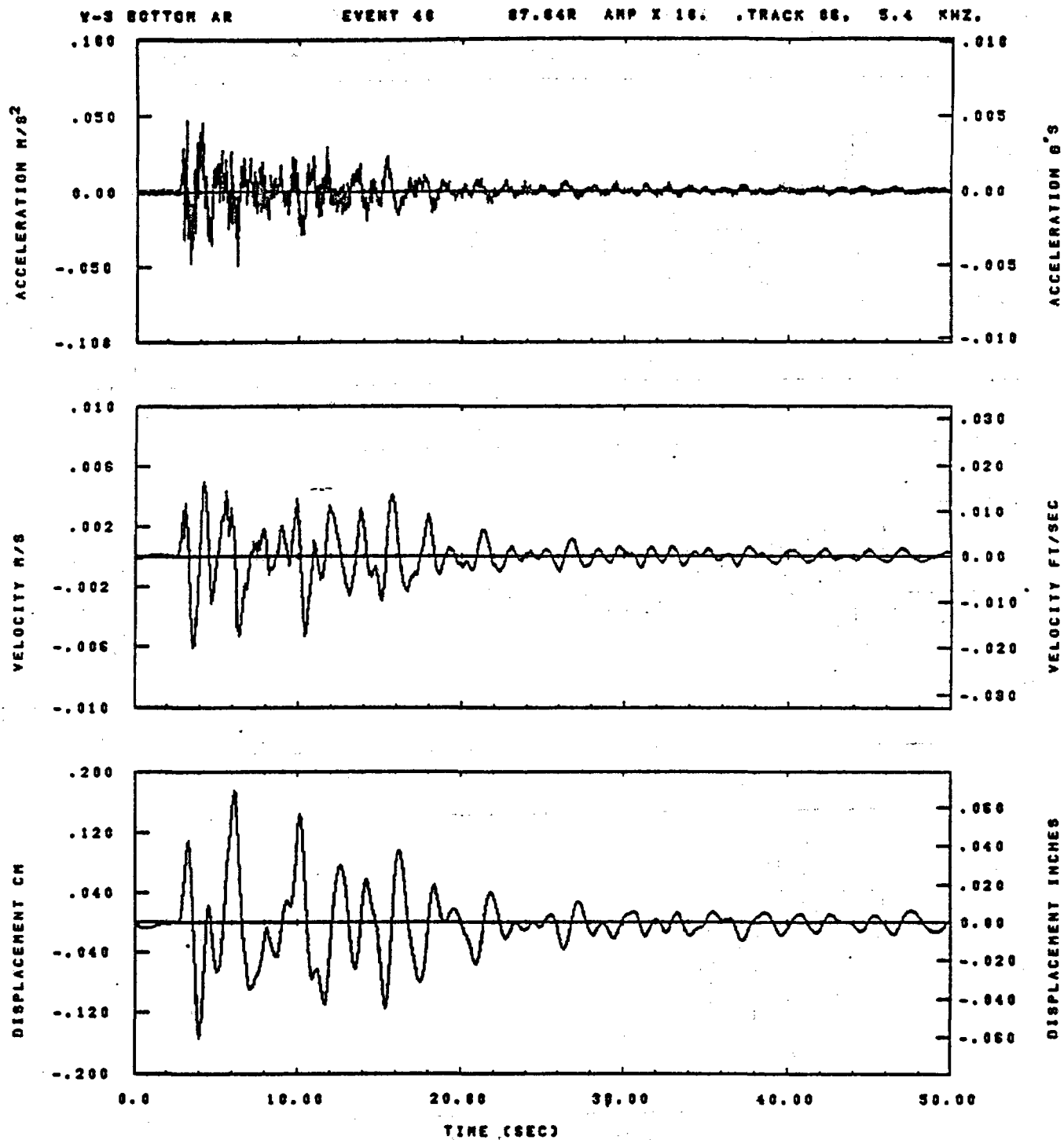


IOT= .0020	ODT= .003	FIX=	AAS= 0.
HPP= .23	BYH= .18	NLH= 187	ASB=
LPP= 27.	BYL= 8.	NLL= 2339	ASE=
VTS= .238	VTE= .188	FLL= -20.	VSE= 0.
OPS= 0.	OPE= 95.	FLH= 8	OSE= 0.

13.34.18.

06/30/92

Figure F-15

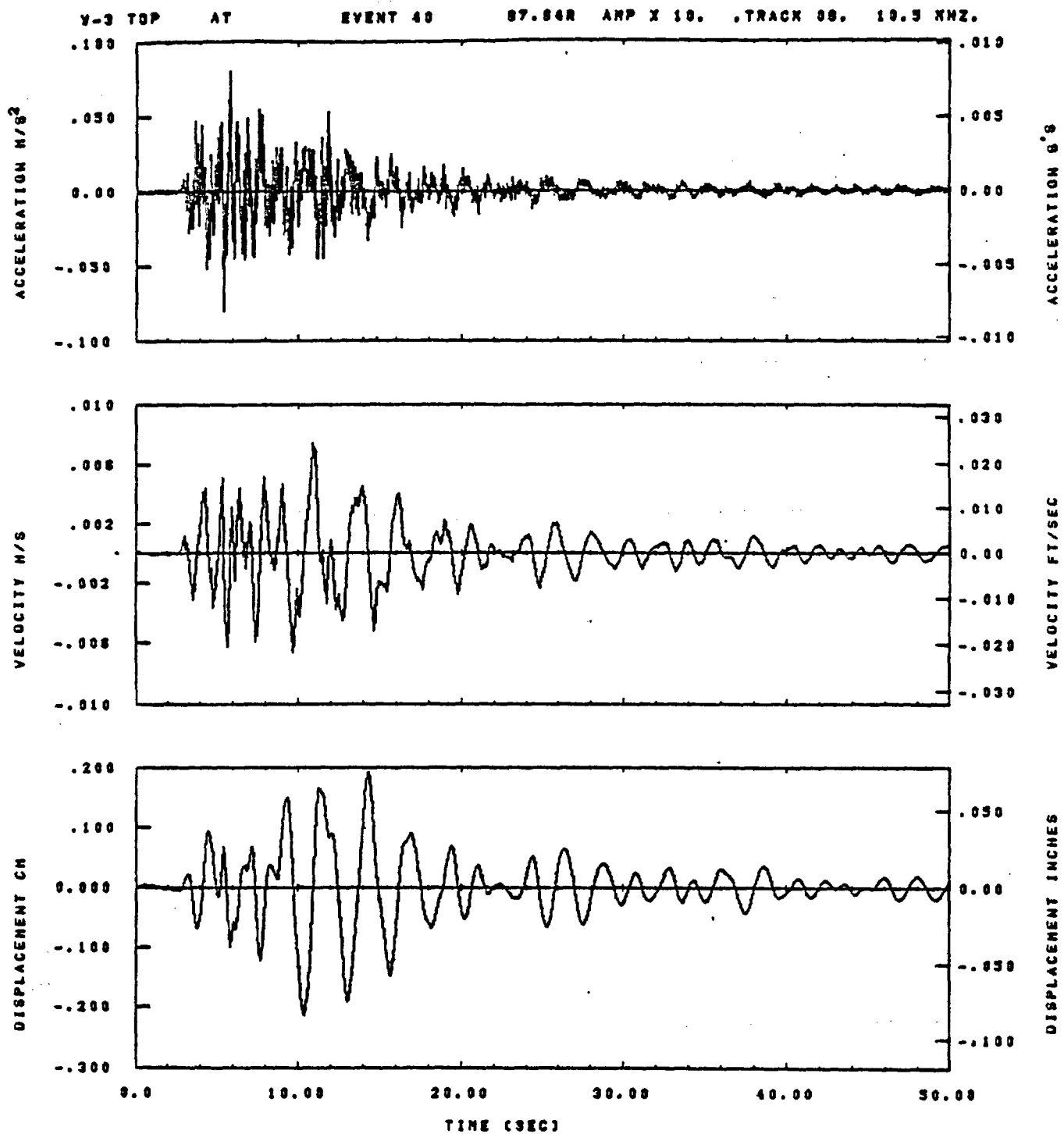


IDT= .0026	QDT= .005	FIX=	AAS= 0.
HPF= .25	SVH= .16	HLH= 167	ASB=
LPF= 27.	SVL= 6.	HLL= 2389	ASE=
VTS= .256	VTE= .166	FLL= -20.	VSE= 0.
OPS= 6.	OPE= 85.	FLH= 0	OSE= 0.

13.54.47.

06/30/82

Figure F-16

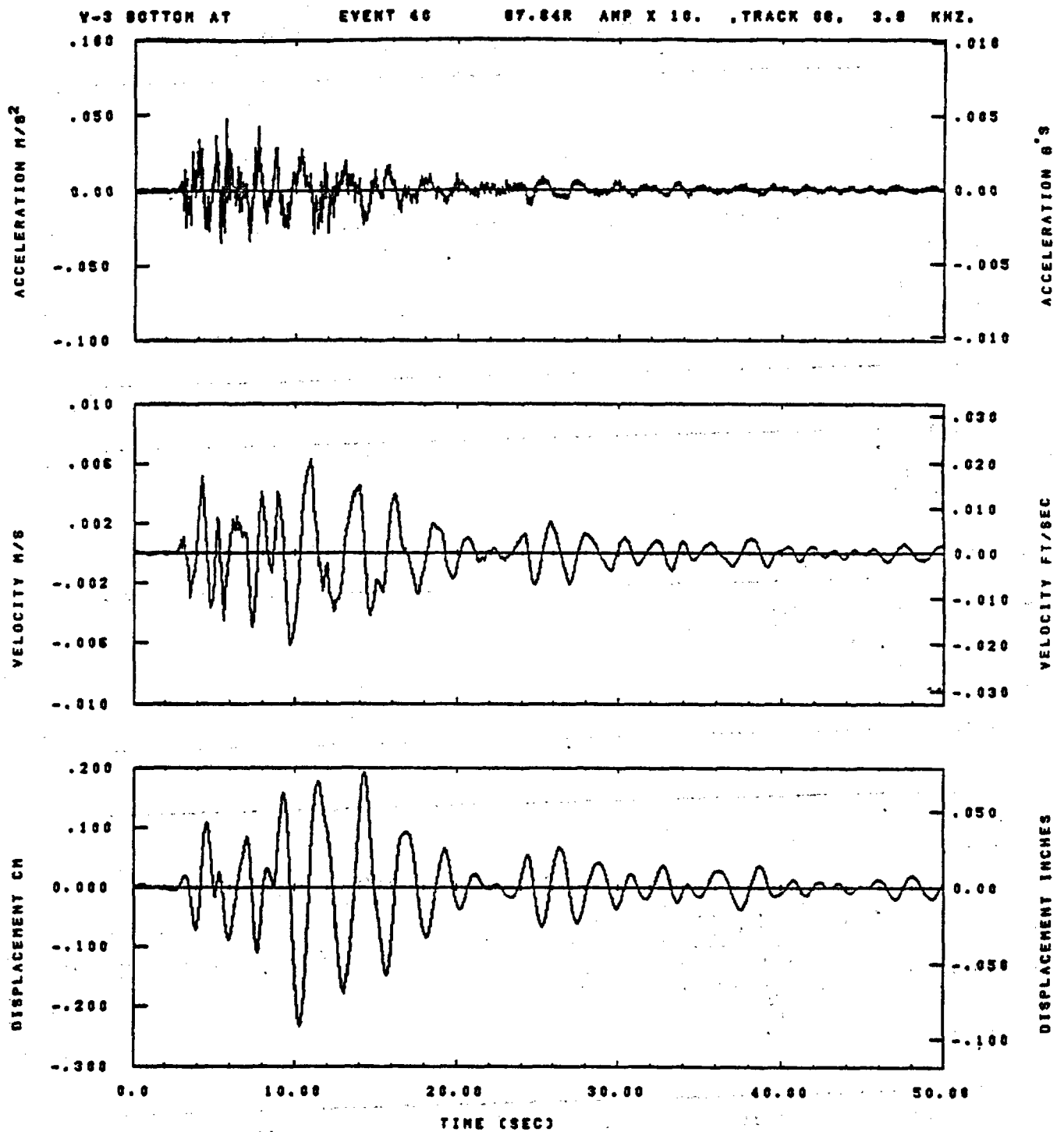


IDT= .0020	ODT= .003	FIX=	AAS= 0.
HPP= .25	BYH= .18	HLH= 187	ASB=
LPP= 27.	BVL= 8.	NLL= 2399	ASE=
VTS= .233	VTE= .188	PLL= -20.	VSE= 0.
DPS= 0.	DPE= 93.	PLH= 0	DSE= 0.

13.34.22.

08/30/82

Figure F-17

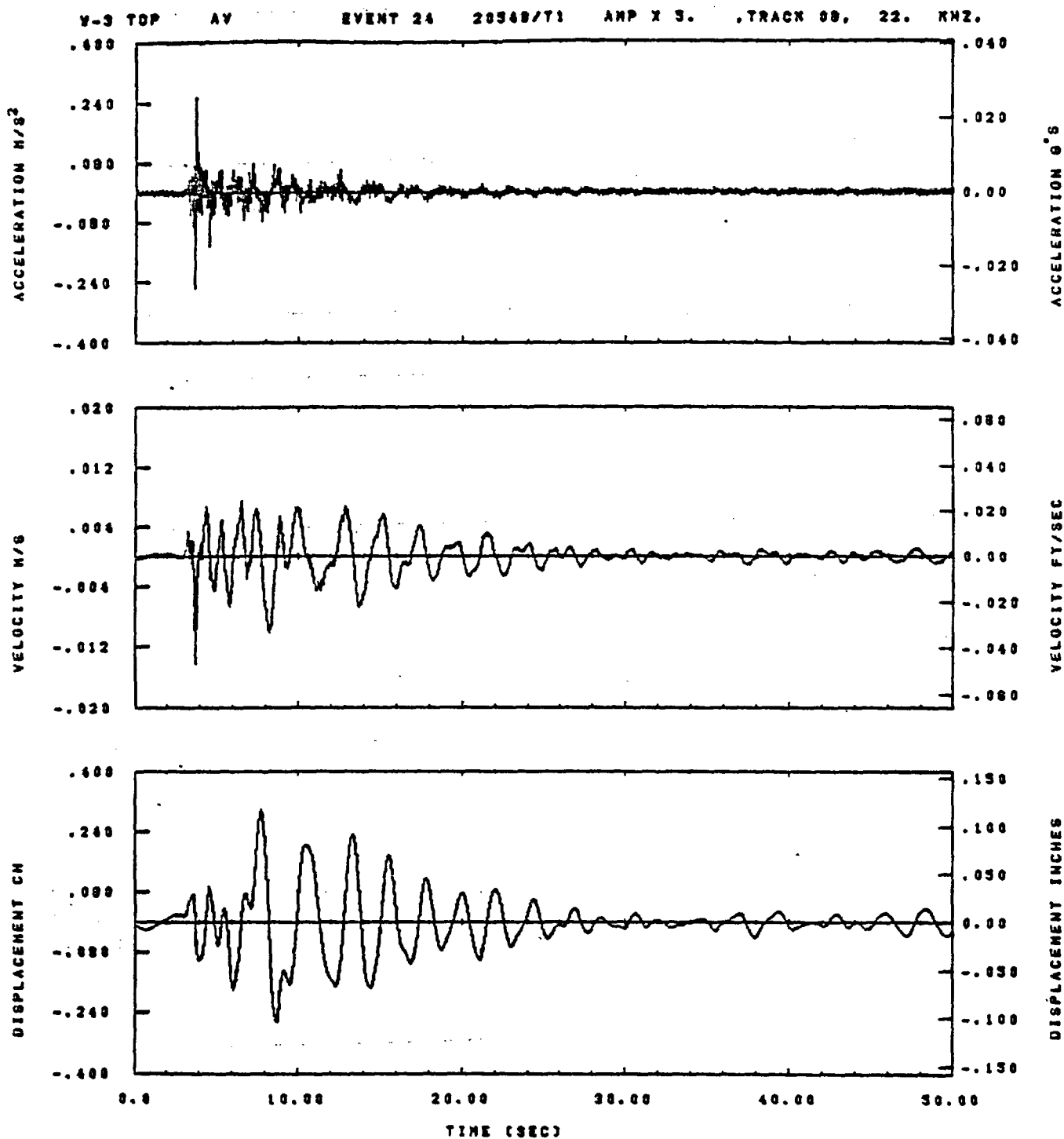


IDT= .0020	ODT= .085	FIX=	AAS= 0.
HFF= .25	SVH= .16	HLH= 167	ASB=
LPF= 27.	SVL= 6.	HLL= 2385	ASE=
VTB= .250	VTE= .166	FLL= -20.	VSE= 0.
DPS= 0.	DPE= 85.	FLH= 0	DSE= 0.

13.54.52.

06/30/82

Figure F-18

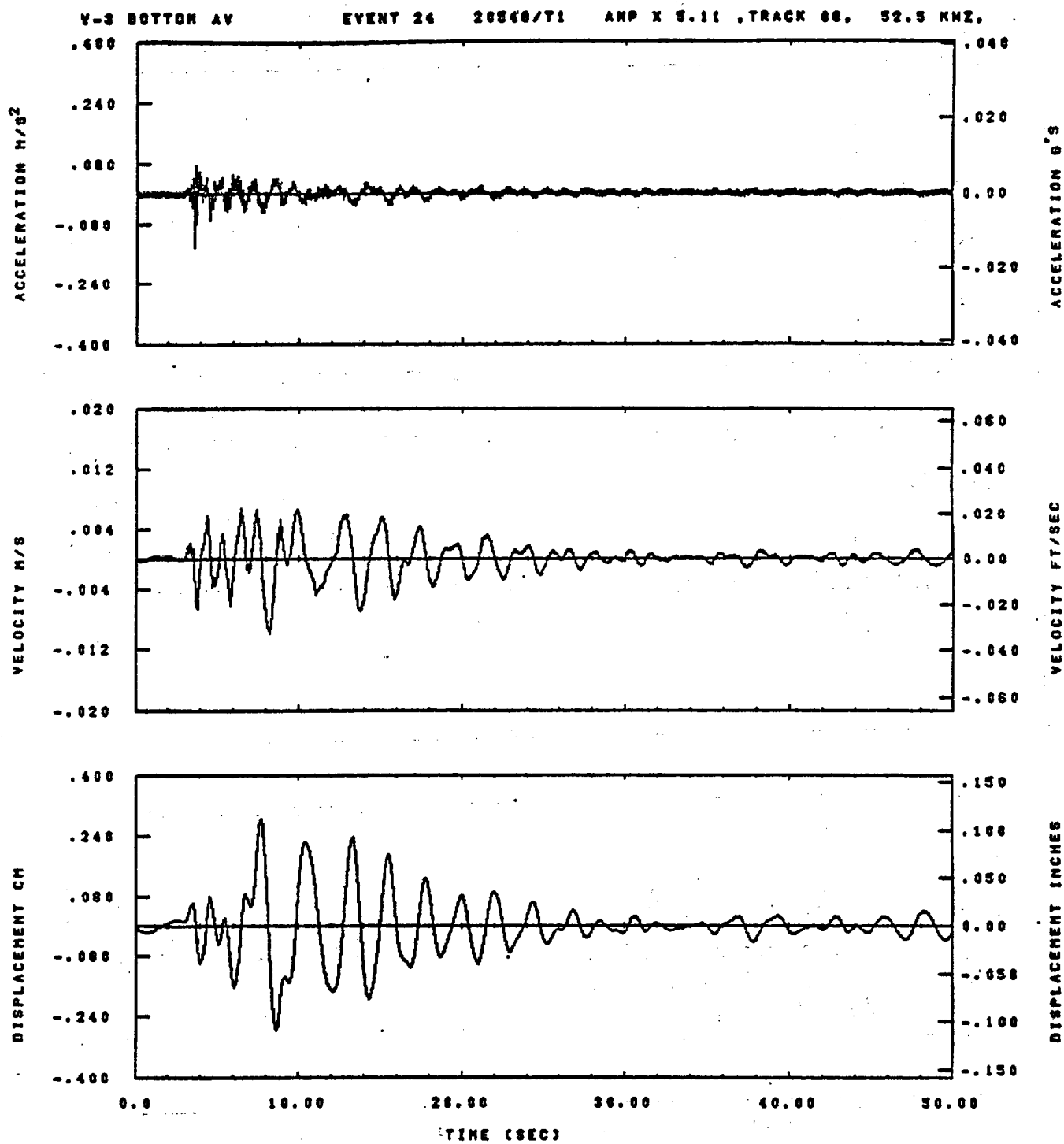


IGT= .0020	ODT= .005	FIX=	AAS= 0.
HPP= .20	BYH= .13	HLH= 187	ASB=
LPP= 27.	BYL= 8.	HLL= 2393	ASE=
VTB= .200	VTE= .133	PLL= -20.	VSE= 0.
DPS= 3.	DPE= 100.	PLH= A-.1	DSE= A+.1

14.34.20.

06/30/82

Figure F-19

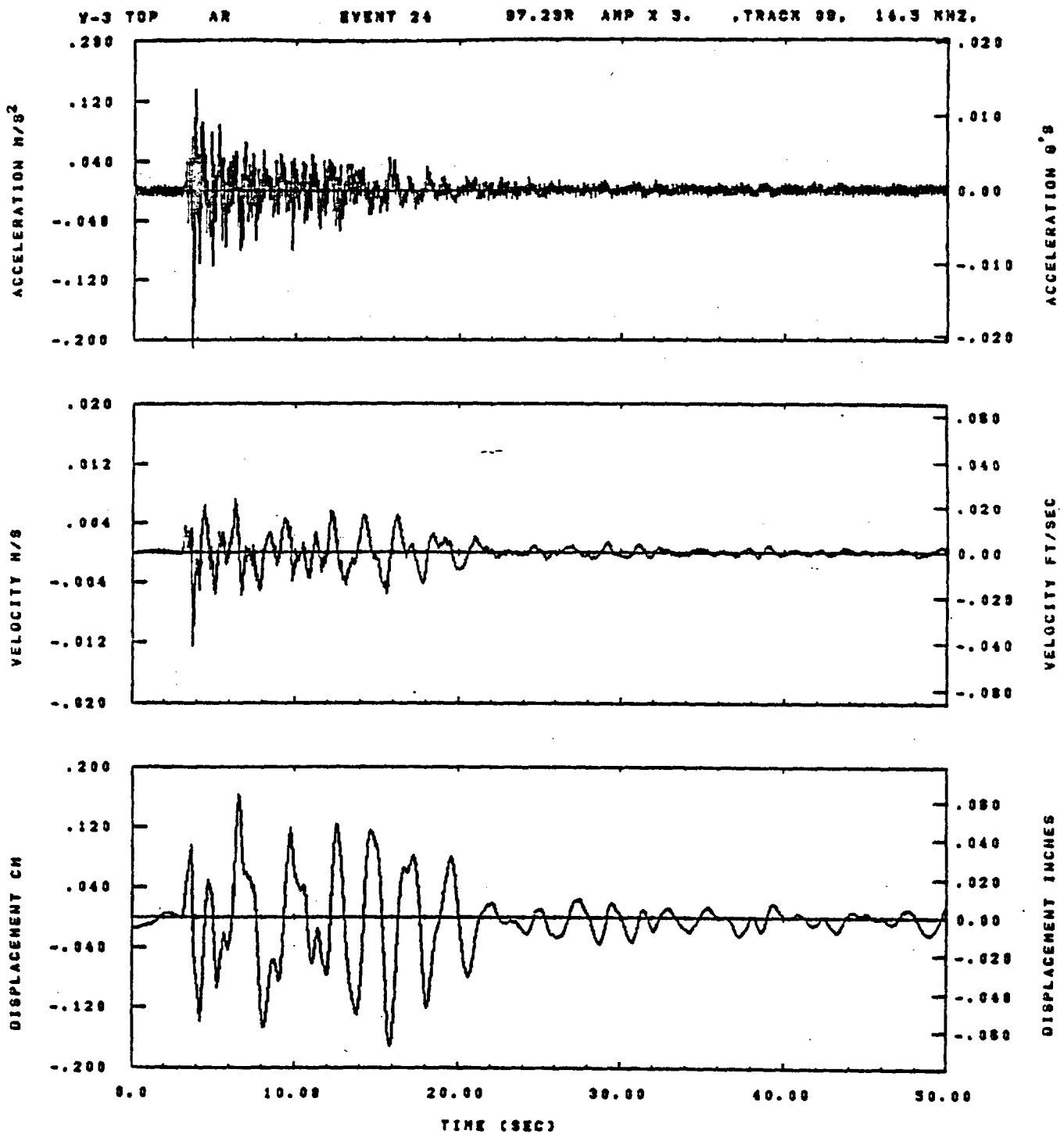


IDT= .0020	ODT= .005	FIX=	AAS= 0.
HPF= .20	BVH= .13	MLH= 167	ASB=
LPF= 27.	BVL= 6.	MLL= 2988	ASE=
VTS= .200	VTE= .133	FLL= -20.	VSE= 0.
OPS= 0.	OPE= 100.	FLH= A-.1	OSE= A+.1

14.55.05.

08/30/82

Figure F-20

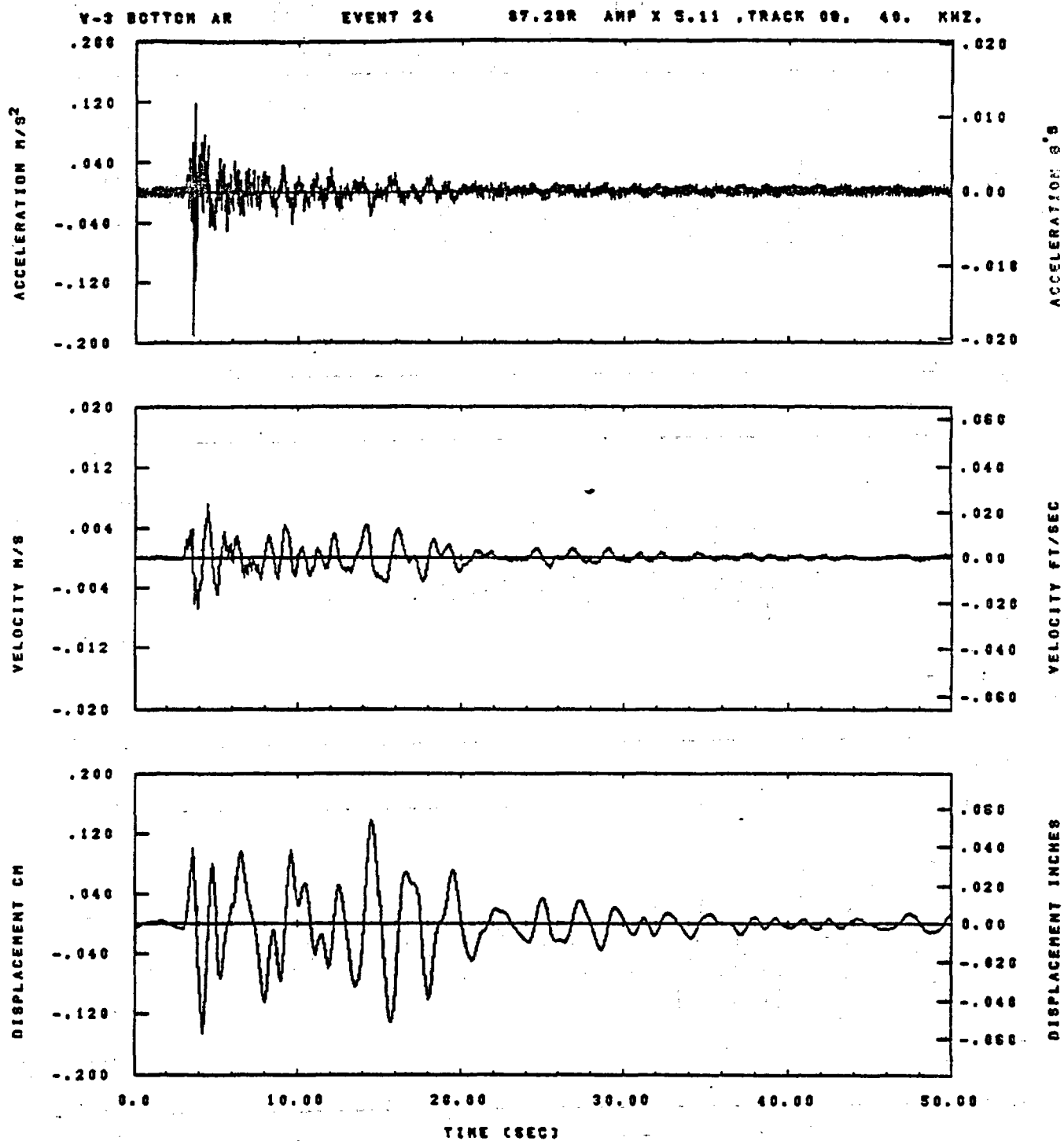


IDT= .0028	ODT= .003	FIX=	AAS= 0.
HPF= .28	BYH= .13	HLH= 187	ASB=
LPF= 27.	BVL= 8.	HLL= 2989	ASE=
VTS= .200	VTE= .133	PLL= -20.	VSE= 0.
DPS= 0.	DPE= 100.	PLH= A-.1	DSE= A+.1

14.34.25.

08/30/82

Figure F-21

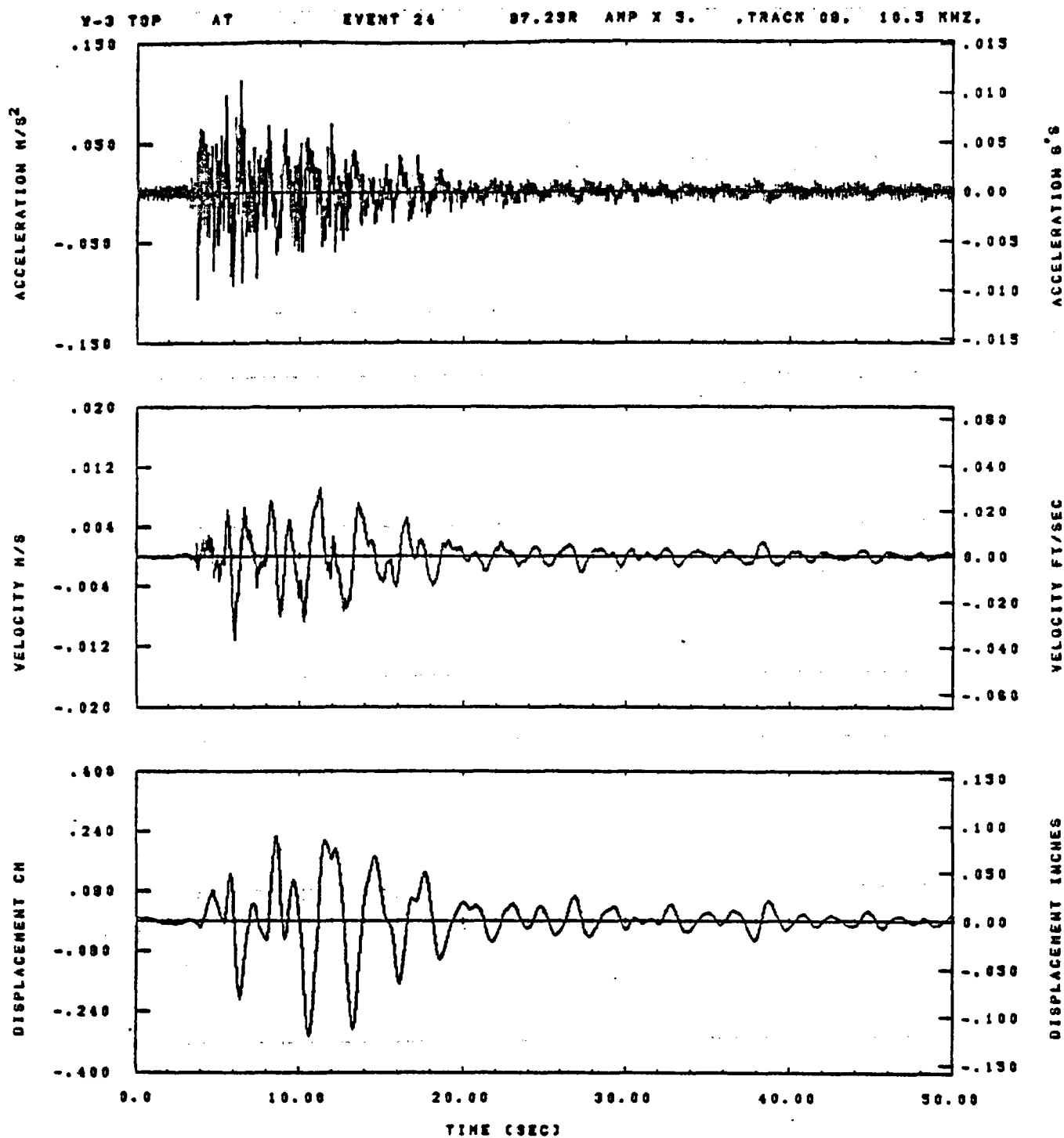


IDT= .0020	DDT= .085	FIX=	AAS= 0.
HPP= .20	BVH= .13	HLH= 167	ASS=
LPP= 27.	SVL= 6.	MLL= 2988	ASE=
VTS= .200	VTE= .133	PLL= -20.	VSE= 0.
OPE= 0.	OPE= 100.	FLH= A-.1	OSE= A+.1

14.55.17.

06/30/82

Figure F-22

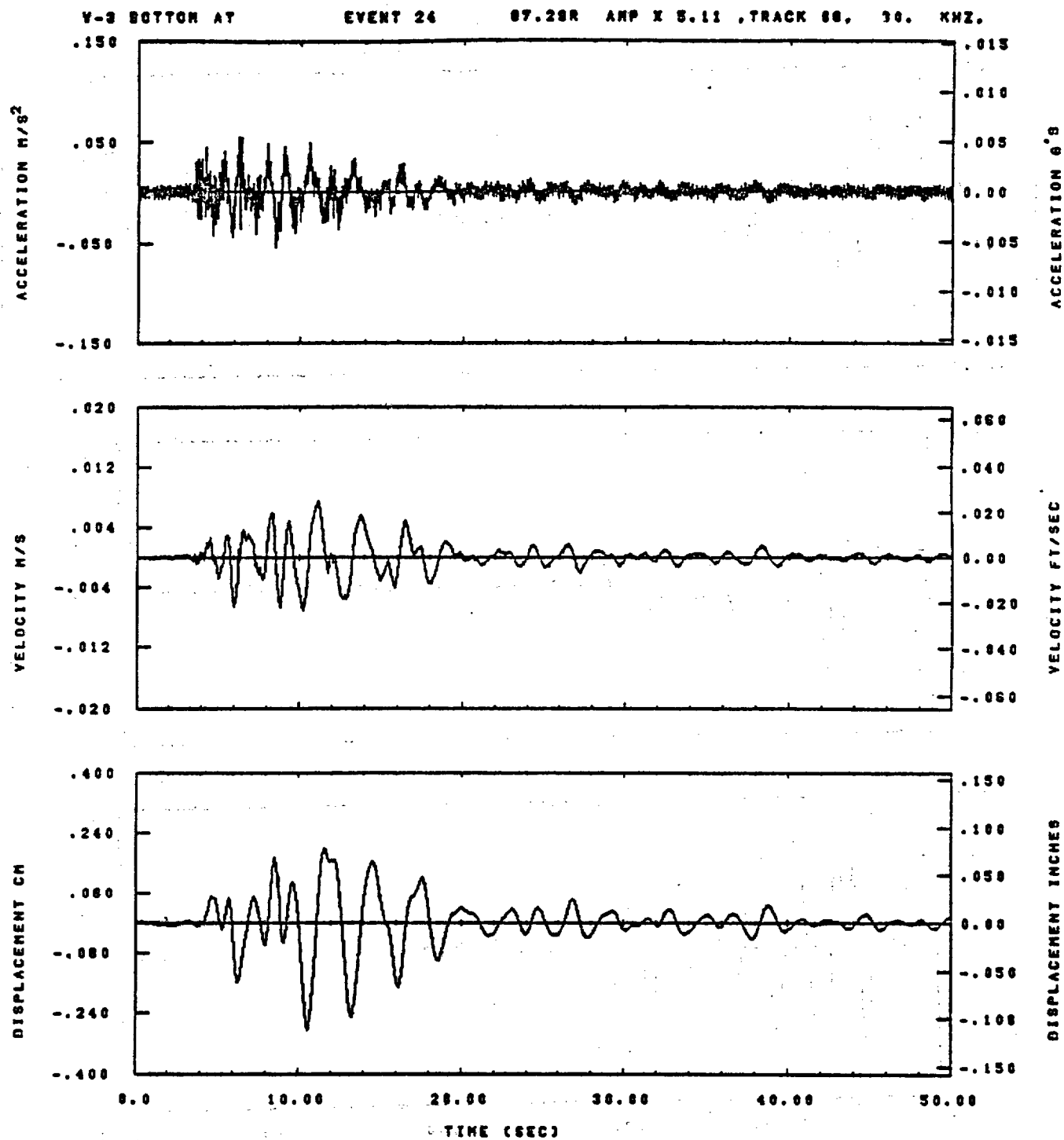


IDT= .0020	ODT= .005	FIX=	AAS= 0.
HPP= .20	BYN= .13	HLH= 187	ASB=
LPP= 27.	BYL= 8.	HLL= 2999	ASE=
VTS= .200	VTE= .133	FLL= -20.	VSE= 0.
QPS= 9.	QPE= 100.	FLH= A-.1	QSE= A+.1

14.56.34.

08/30/82

Figure F-23

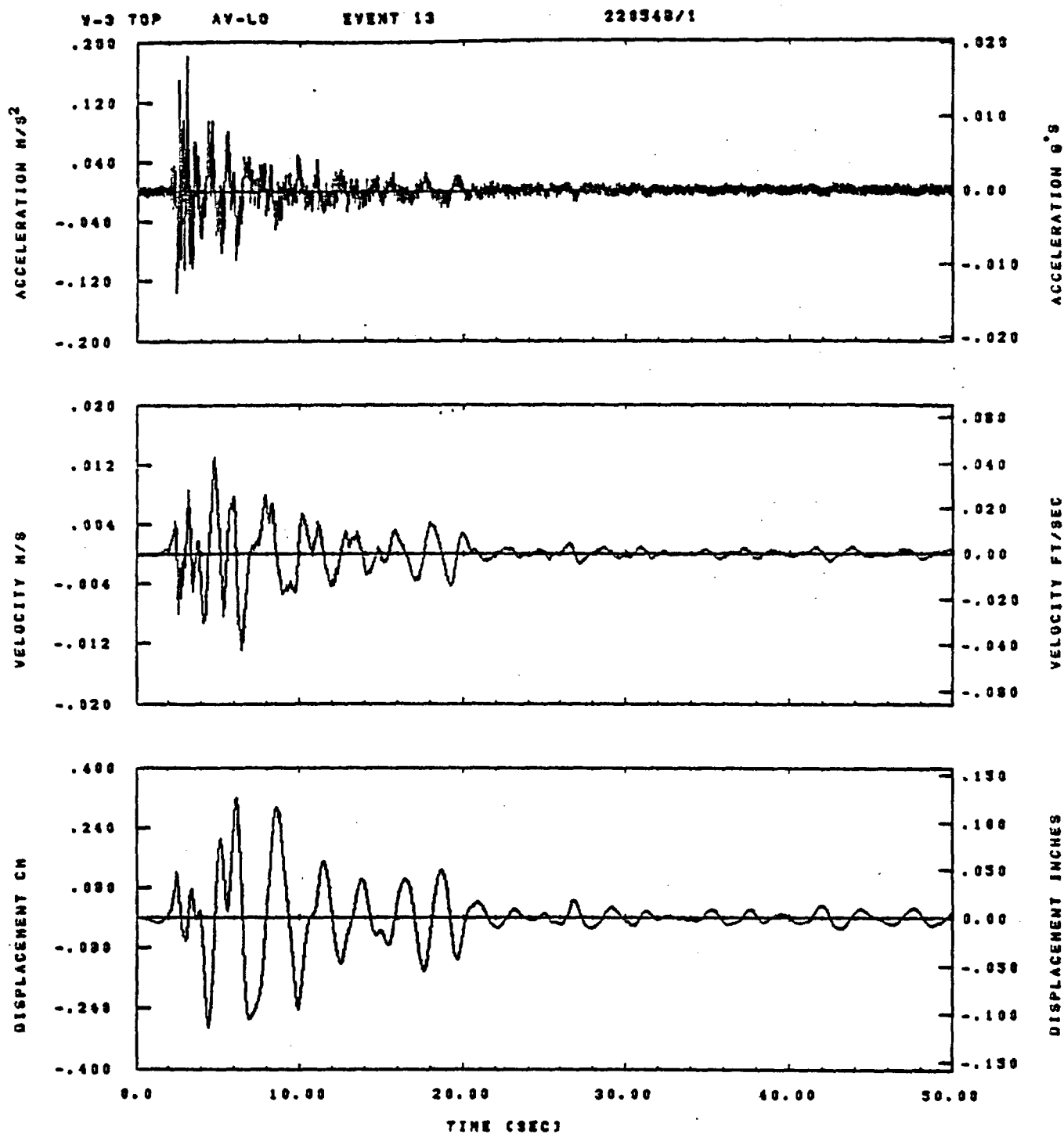


IDT= .0020	QDT= .005	FIX=	AAS= 0.
HPF= .20	BYN= .13	HLN= 167	ASB=
LPF= 27.	BYL= 6.	HLL= 2898	ASE=
VTS= .200	VTE= .133	FLL= -20.	VSE= 0.
OPS= 0.	OPE= 100.	FLN= A-.1	OSE= A+.1

14.55.21.

06/30/82

Figure F-24

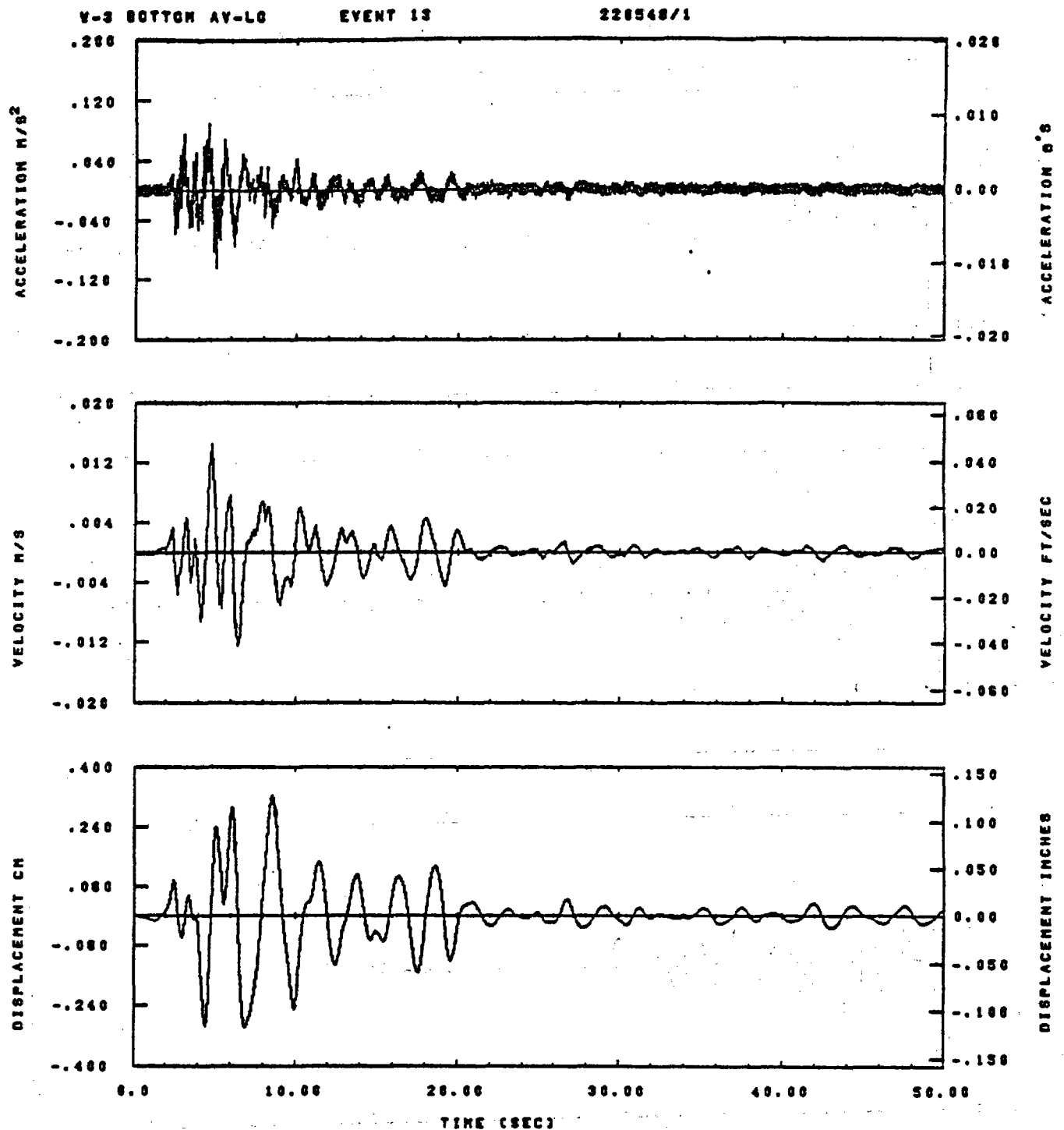


IDT= .0020	ODT= .003	FIX=	AAS= 0.
HPP= .30	BYH= .20	MLH= 187	ASB=
LPP= 27.	BYL= 0.	MLL= 1999	ASE=
YTB= .300	YTE= .200	FLL= -20.	VSE= 0.
DPS= 0.	DPE= 99.	PLH= 0	DSE= 0.

13.38.35.

08/30/82

Figure F-25

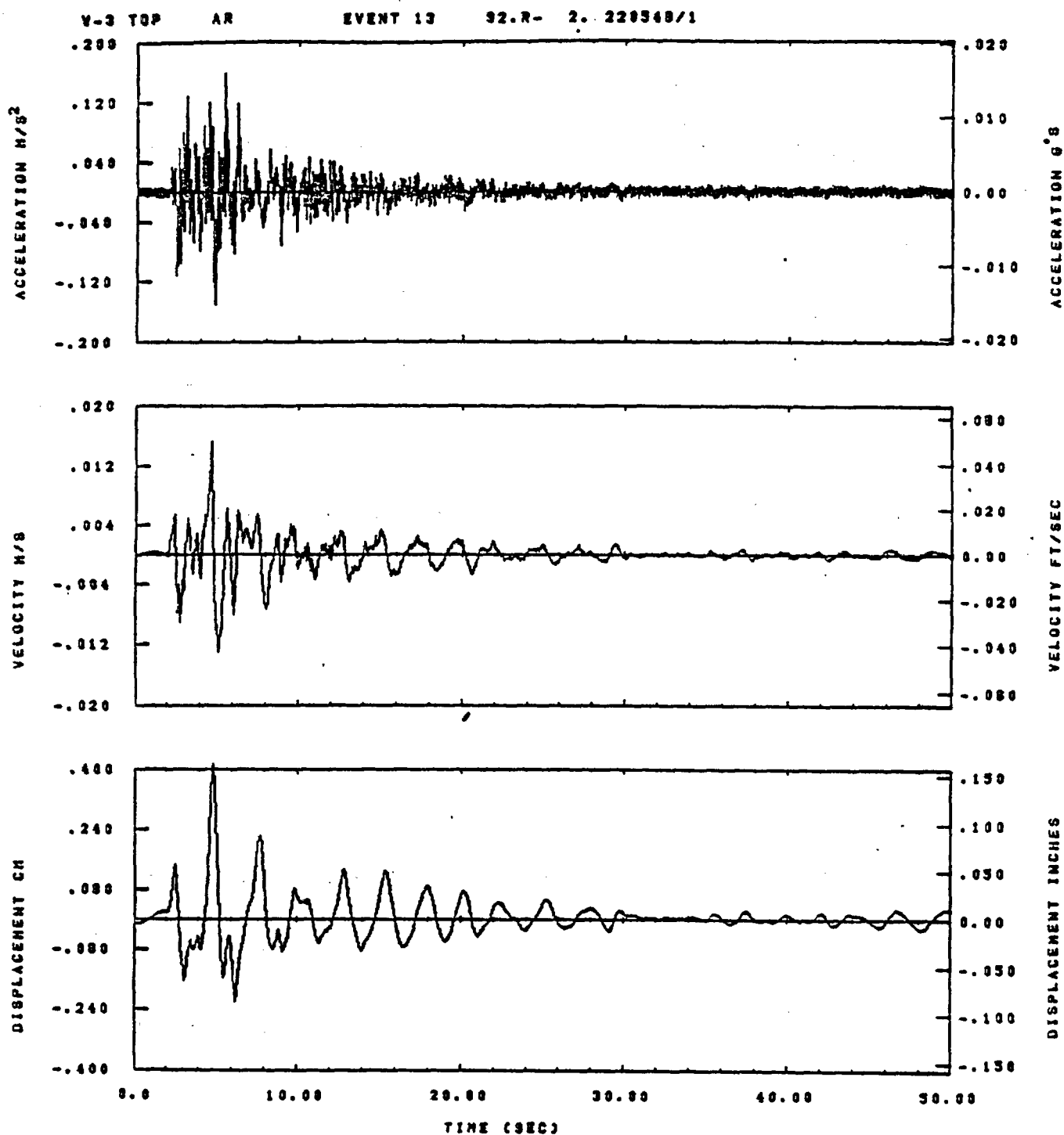


IDT= .0020	ODT= .005	FIX=	AAS= 0.
HPF= .30	BYN= .20	HLN= 167	ASB=
LPF= 27.	BYL= 8.	HLL= 1988	ASE=
VTS= .300	VTE= .200	PLL= -20.	VSE= 0.
OPS= 0.	DPE= 88.	PLH= 0	DSE= 0.

13.57.00.

06/30/82

Figure F-26

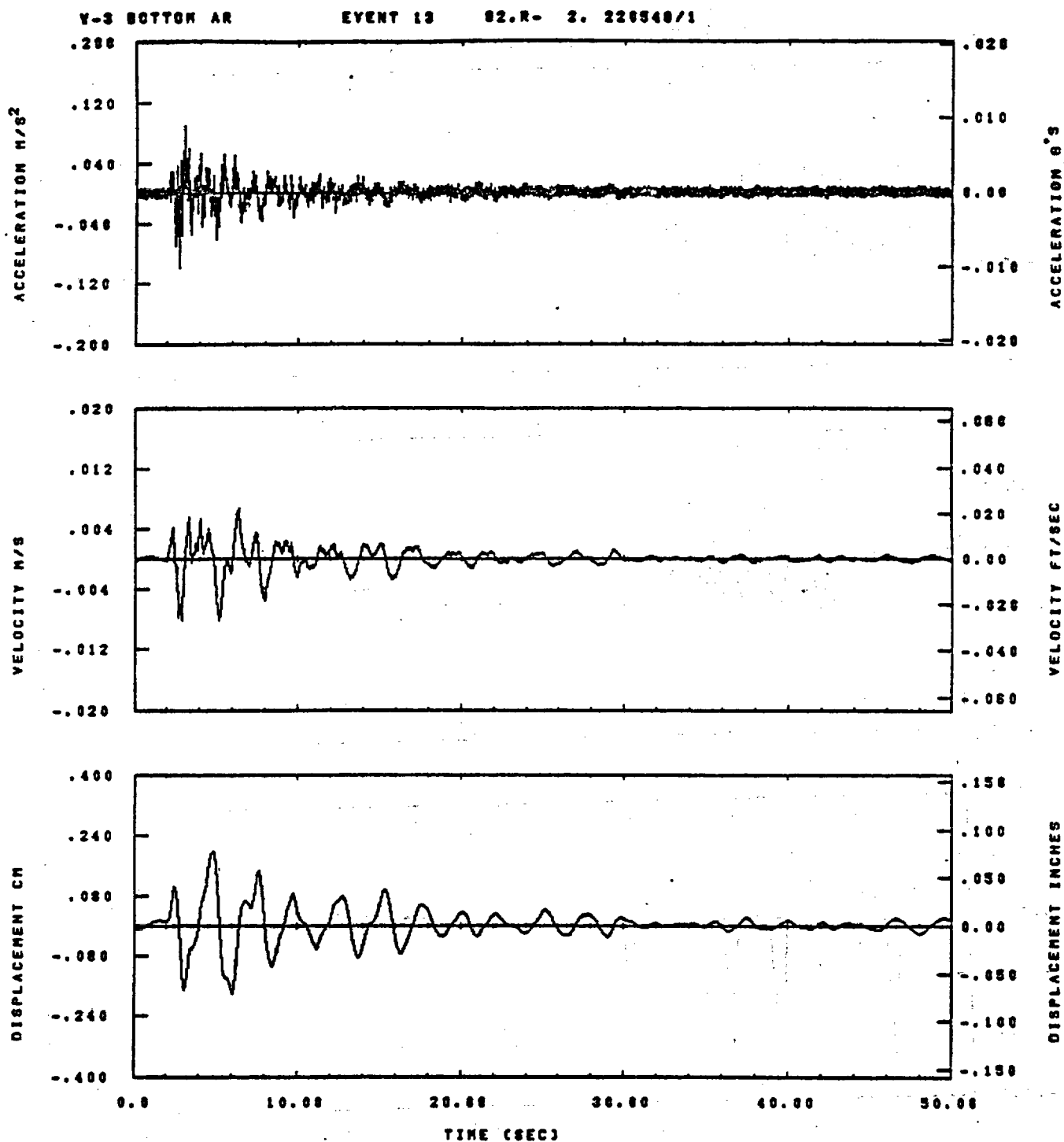


IOT= .0020	QOT= .003	FIX=	AAS= 0.
HPP= .30	BYH= .20	MLH= 107	ASB=
LPP= 27.	BYL= 8.	HLL= 1999	ASE=
VTS= .300	VTE= .200	FLL= -20.	VSE= 0.
DP9= 8.	DPE= 99.	FLH= 0	DSE= 0.

13.58.48.

06/30/82

Figure F-27

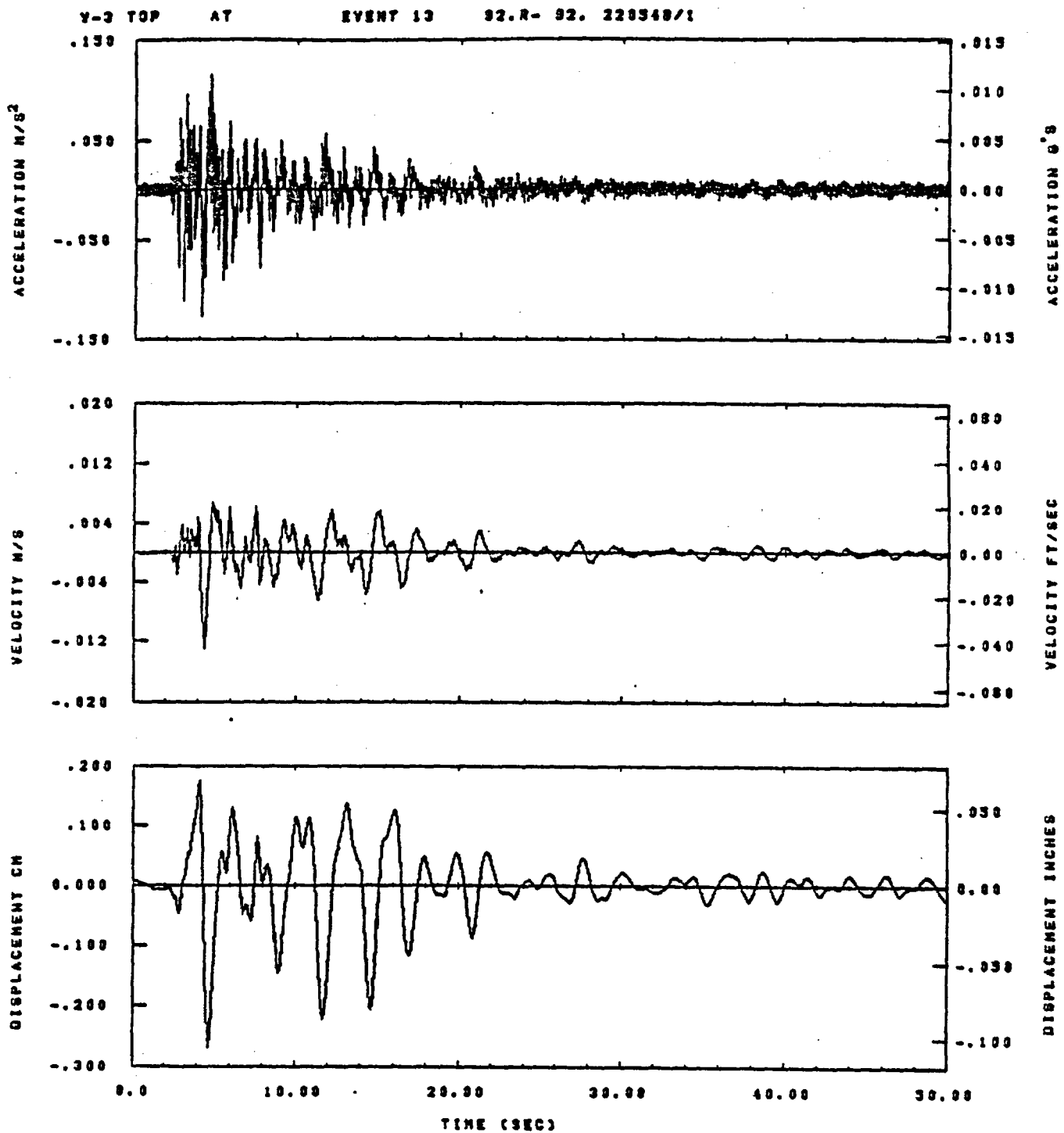


IDT= .0020	ODT= .005	FIX=	AAS= 0.
HPF= .30	BYH= .20	HLH= 167	ASB=
LPF= 27.	BYL= 6.	HLL= 1888	ASE=
VTS= .308	VTE= .200	FLL= -20.	VSE= 0.
DPS= 6.	DPE= 88.	FLH= 0	DSE= 0.

13.57.12.

06/30/82

Figure F-28

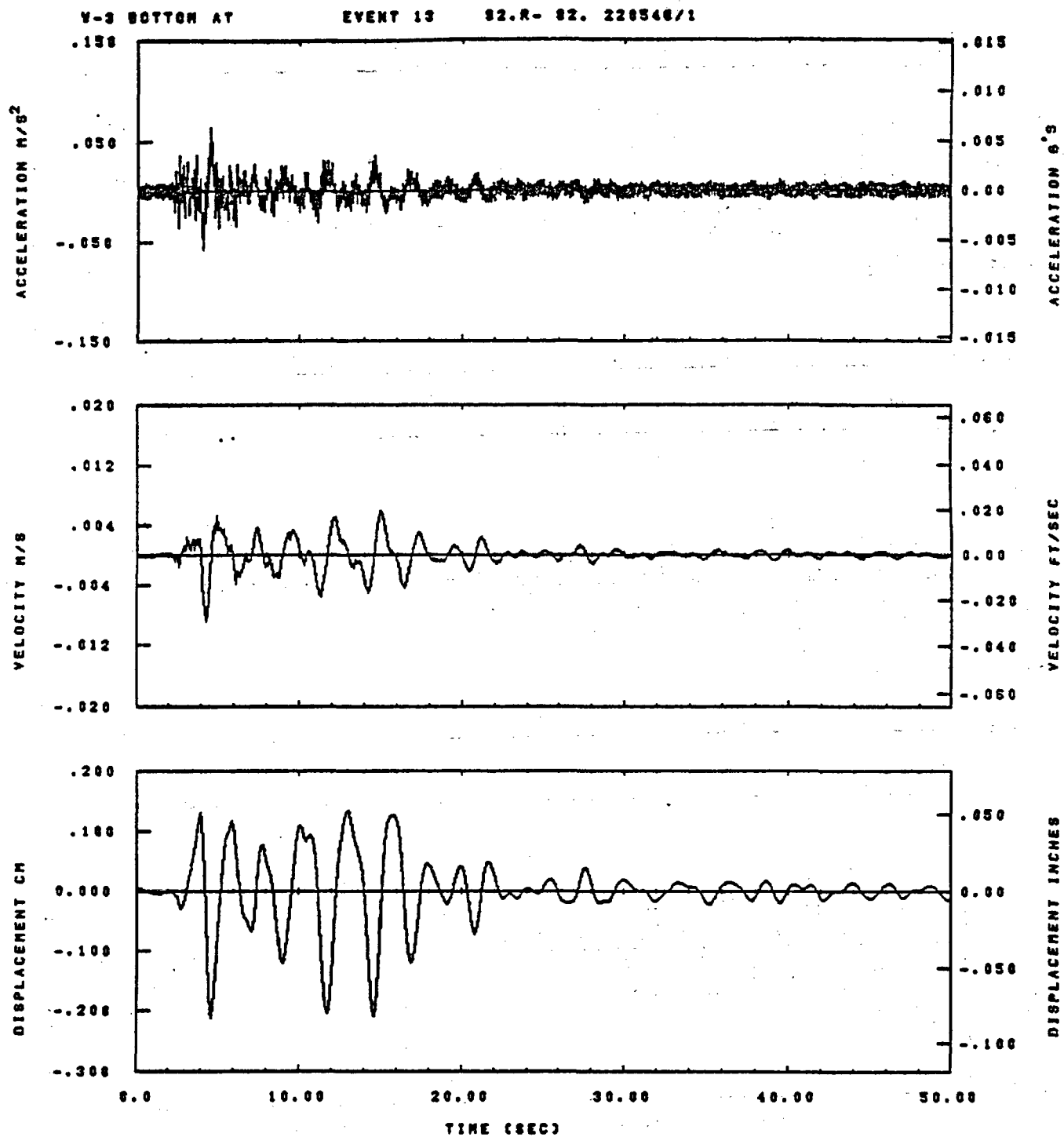


IDT= .0020	OOT= .005	FIX=	AAS= 0.
HPP= .30	SVN= .20	HLH= 187	ASB=
LPP= 27.	SVL= 8.	HLL= 1999	ASE=
VTS= .300	VTE= .200	FLL= -20.	VSE= 0.
DPS= 0.	DPE= 99.	FLH= 0	DSE= 0.

13.37.08.

08/30/82

Figure F-29

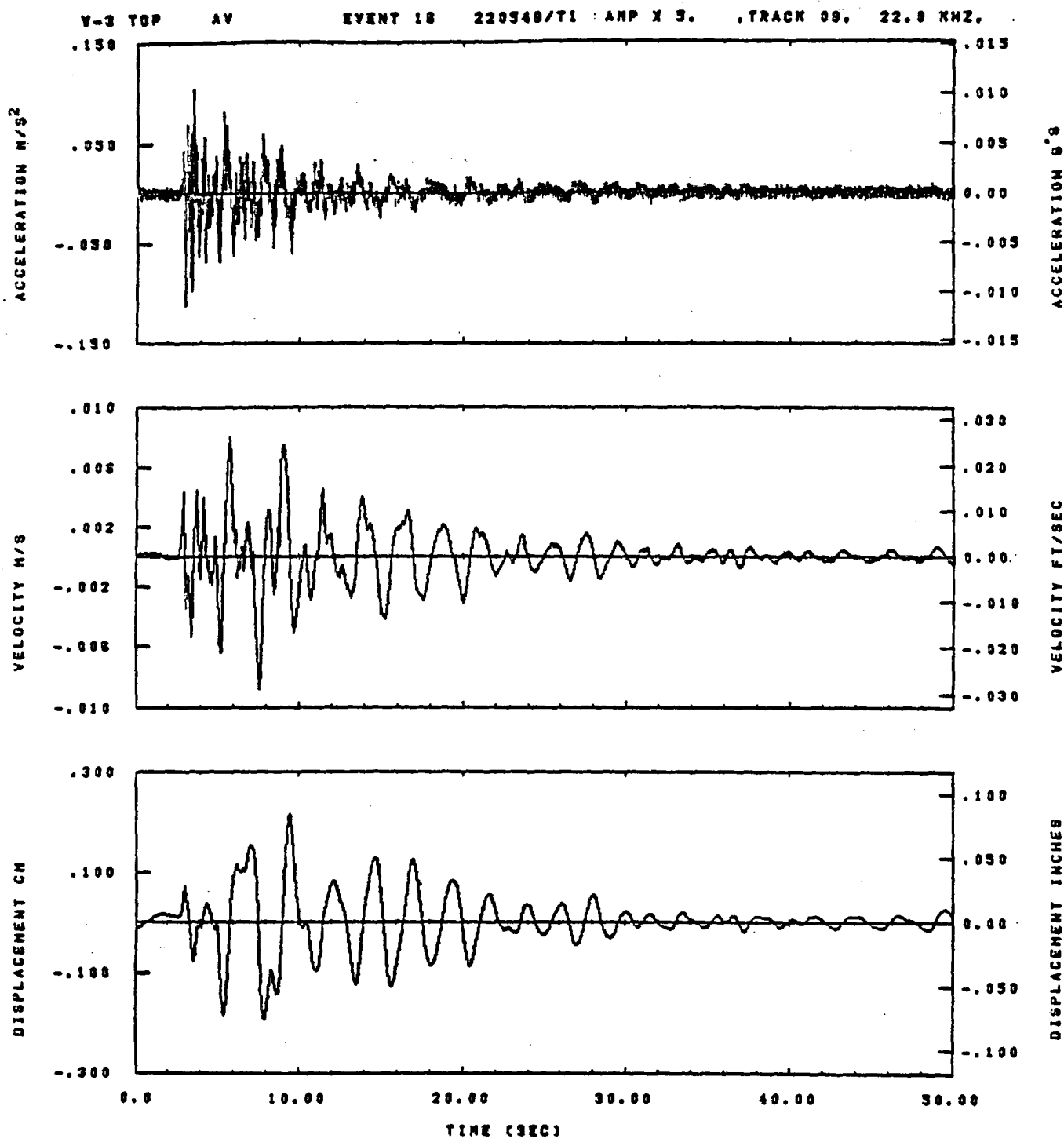


IDT= .0020	QDT= .005	FIX=	AAS= 0.
HPP= .30	BYN= .20	MLH= 167	ASB=
LPP= 27.	BYL= 6.	MLL= 1988	ASE=
VTS= .308	VTE= .200	PLL= -20.	VSE= 0.
DPS= 0.	DPE= 88.	FLH= 0	DSE= 0.

13.57.16.

08/30/82

Figure F-30

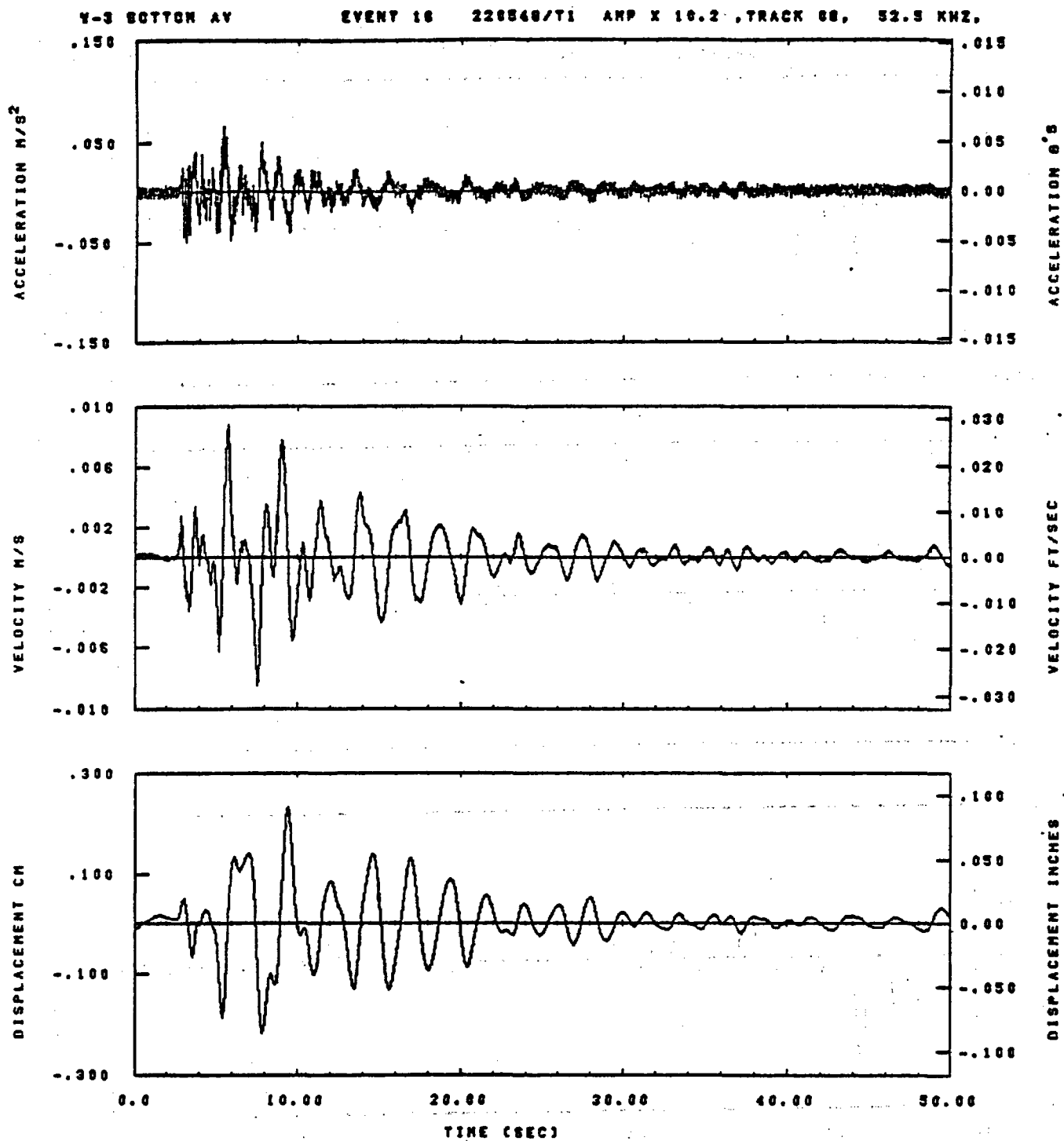


IDT= .0020	OOT= .003	FIX=	AAS= 0.
HPP= .20	BYH= .13	HLH= 251	ASB=
LPP= 10.	BYL= 4.	HLL= 2999	ASE=
VTB= .200	VTE= .133	PLL= -17.	VSE= 0.
OPS= 0.	OPE= 100.	PLH= A-.1	DSE= A+.1

15.02.57.

07/01/02

Figure F-31

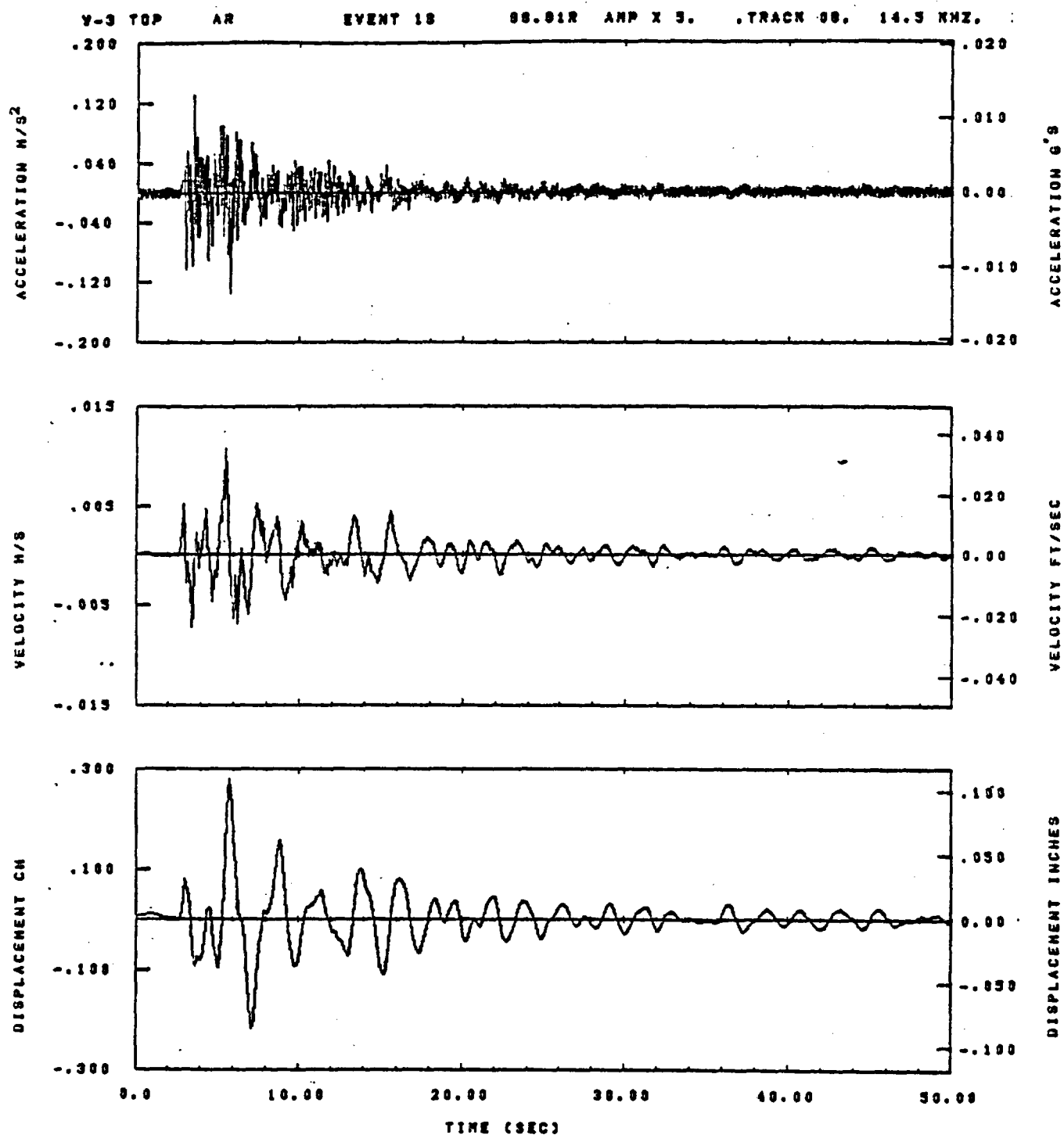


IDT= .0020	ODT= .005	FIX=	AAS= 0.
HPF= .20	BVM= .13	HLH= 251	ASS=
LPF= 18.	BVL= 4.	HLL= 2998	ASE=
VTS= .200	VTE= .133	FLL= -17.	VSE= 0.
DPS= 0.	DPE= 100.	FLH= A-.1	DSE= A+.1

08.44.23.

07/02/82

Figure F-32

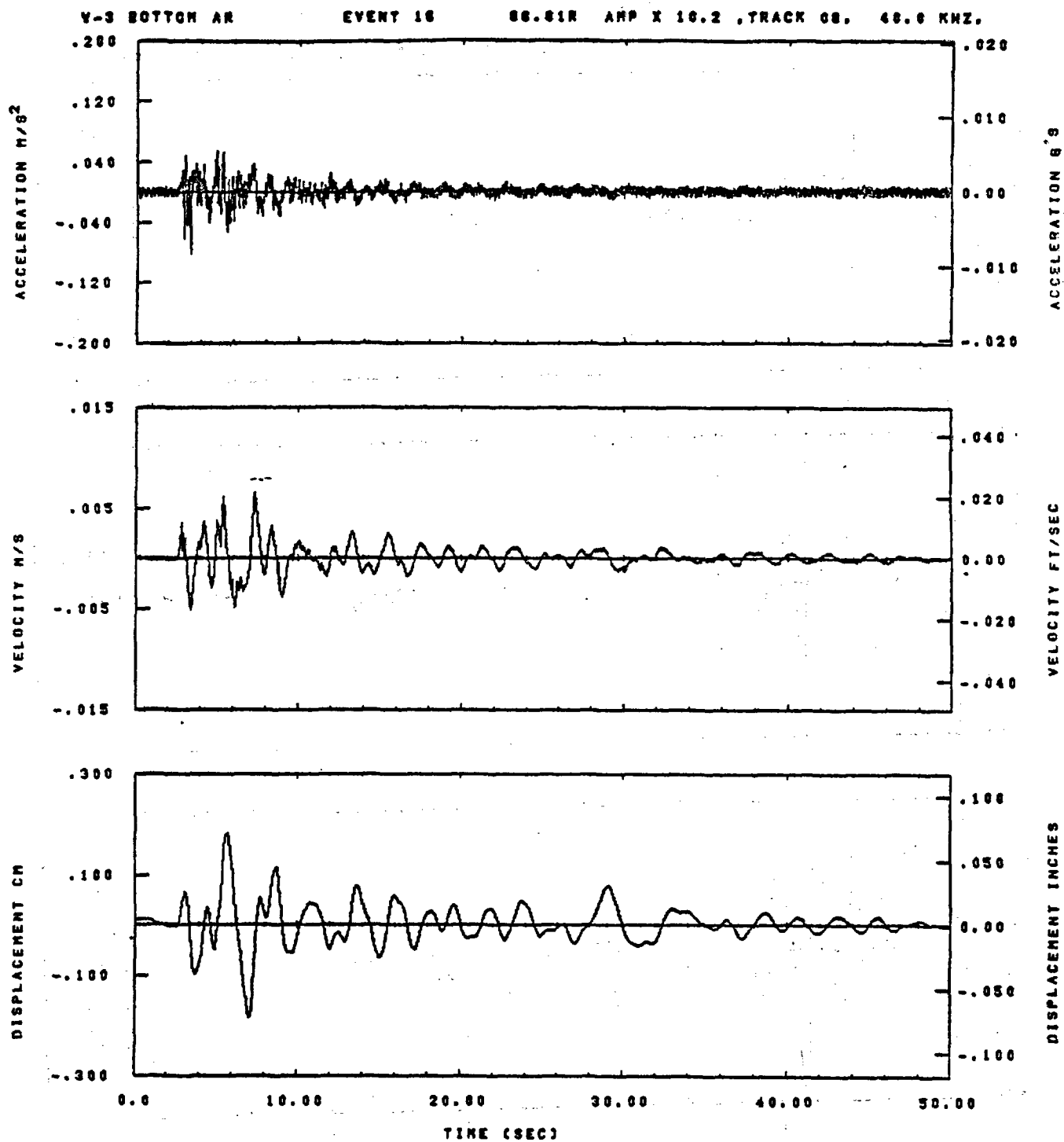


IDT= .0020	ODT= .005	FIX=	AAS= 0.
HPP= .20	SVH= .13	HLH= 251	ASB=
LPP= 18.	SVL= 4.	HLL= 2999	ASE=
VTS= .200	VTE= .133	FLL= -17.	VSE= 0.
OPS= 0.	OPE= 100.	FLH= A-.1	OSE= A+.1

15.03.01.

07/01/92

Figure F-33

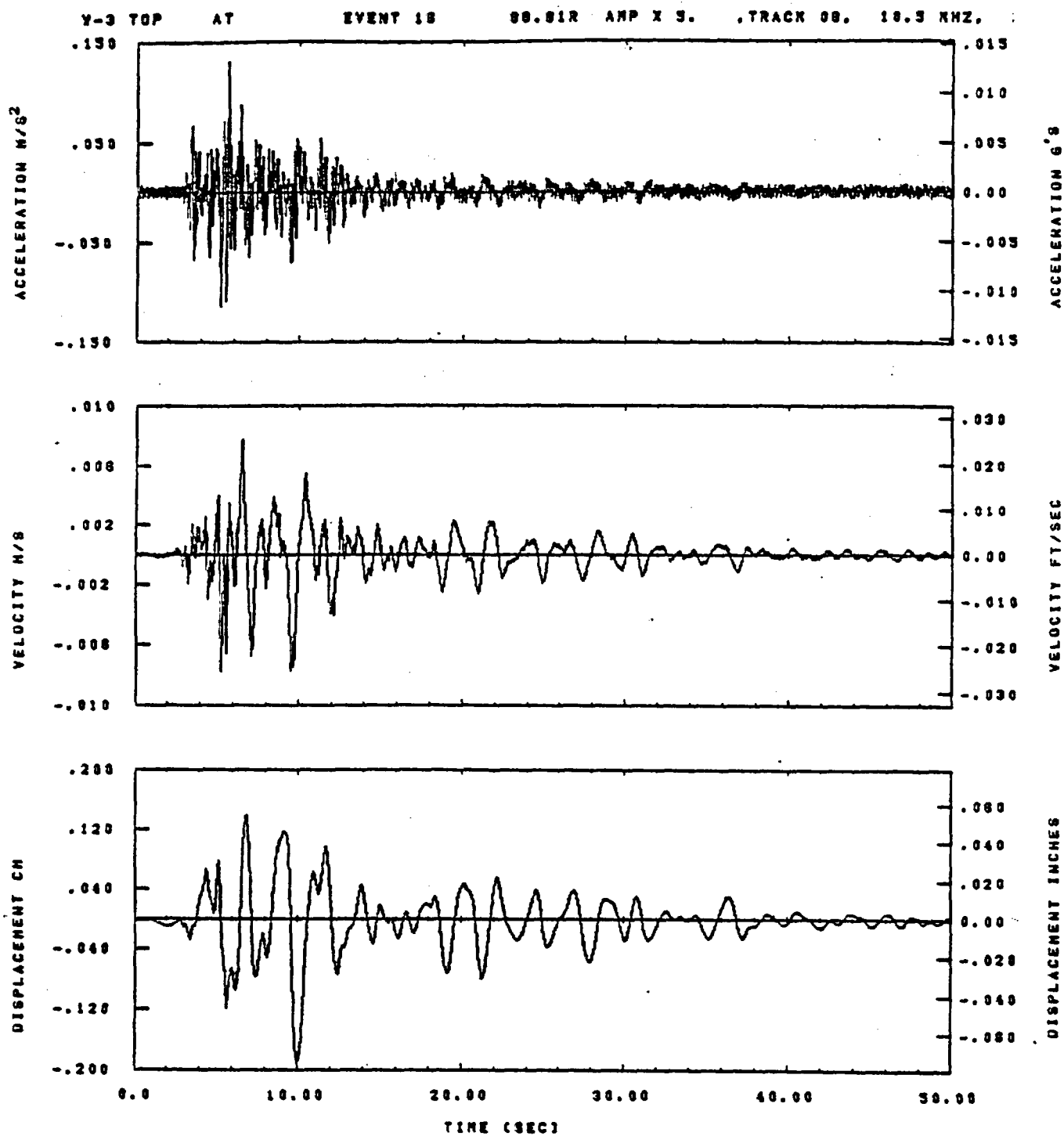


IDT= .0020	ODT= .005	FIX=	AAS= 0.
HPP= .20	BYH= .13	MLH= 251	ASB=
LPP= 18.	BYL= 4.	MLL= 2889	ASE=
VTB= .200	VTE= .133	PLL= -17.	VSE= 0.
DPS= 0.	DPE= 100.	PLH= A-.1	DSE= A+.1

08.44.26.

07/02/82

Figure F-34

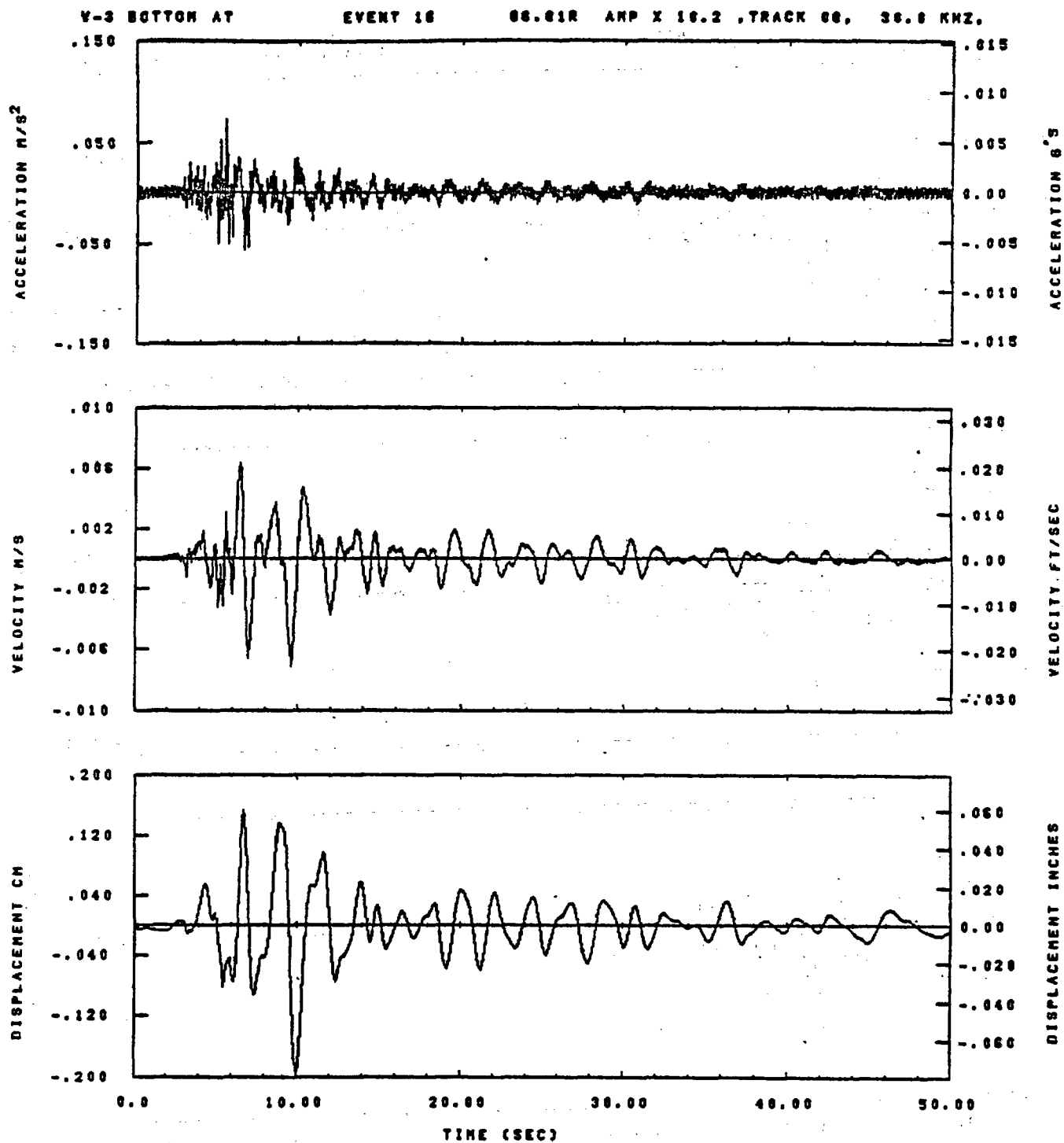


IDT= .0020	ODT= .003	FIX=	AAS= 0.
HPP= .20	BYH= .13	HLN= 231	ASB=
LPP= 18.	BYL= 4.	HLL= 2999	ASE=
VTS= .200	VTE= .133	FLL= -17.	VSE= 0.
DPS= 0.	DPE= 100.	FLH= A-.1	DSE= A+.1

13.03.03.

07/01/92

Figure F-35

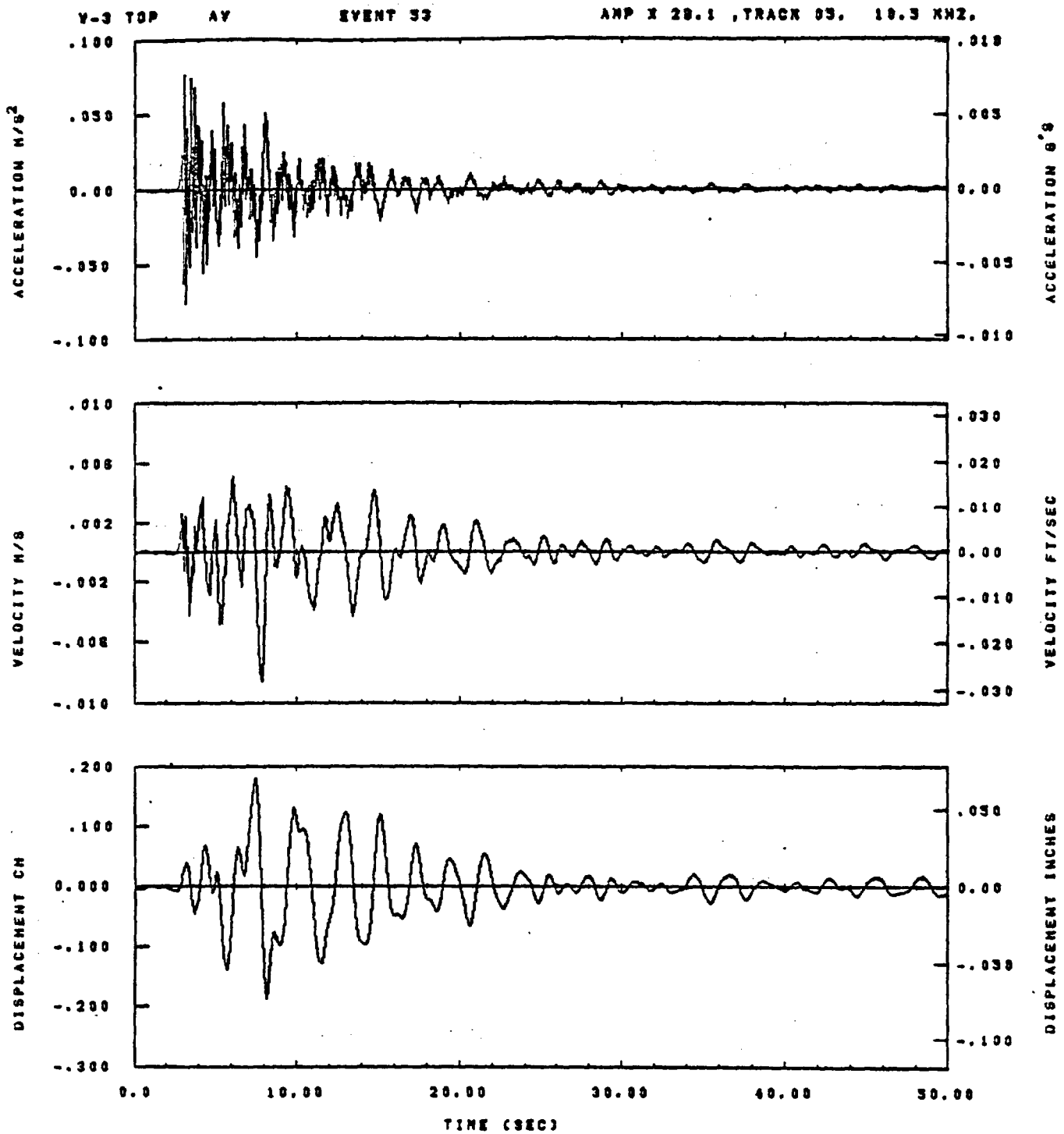


IDT= .0020	ODT= .005	FIX=	AAS= 0.
HPF= .20	SVH= .13	HLN= 251	ASB=
LPF= 10.	SVL= 4.	HLL= 2988	ASE=
VTS= .200	VTE= .133	FLL= -17.	VSE= 0.
OPS= 0.	DPE= 100.	FLN= A-.1	DSE= A+.1

08.44.30.

07/02/82

Figure F-36

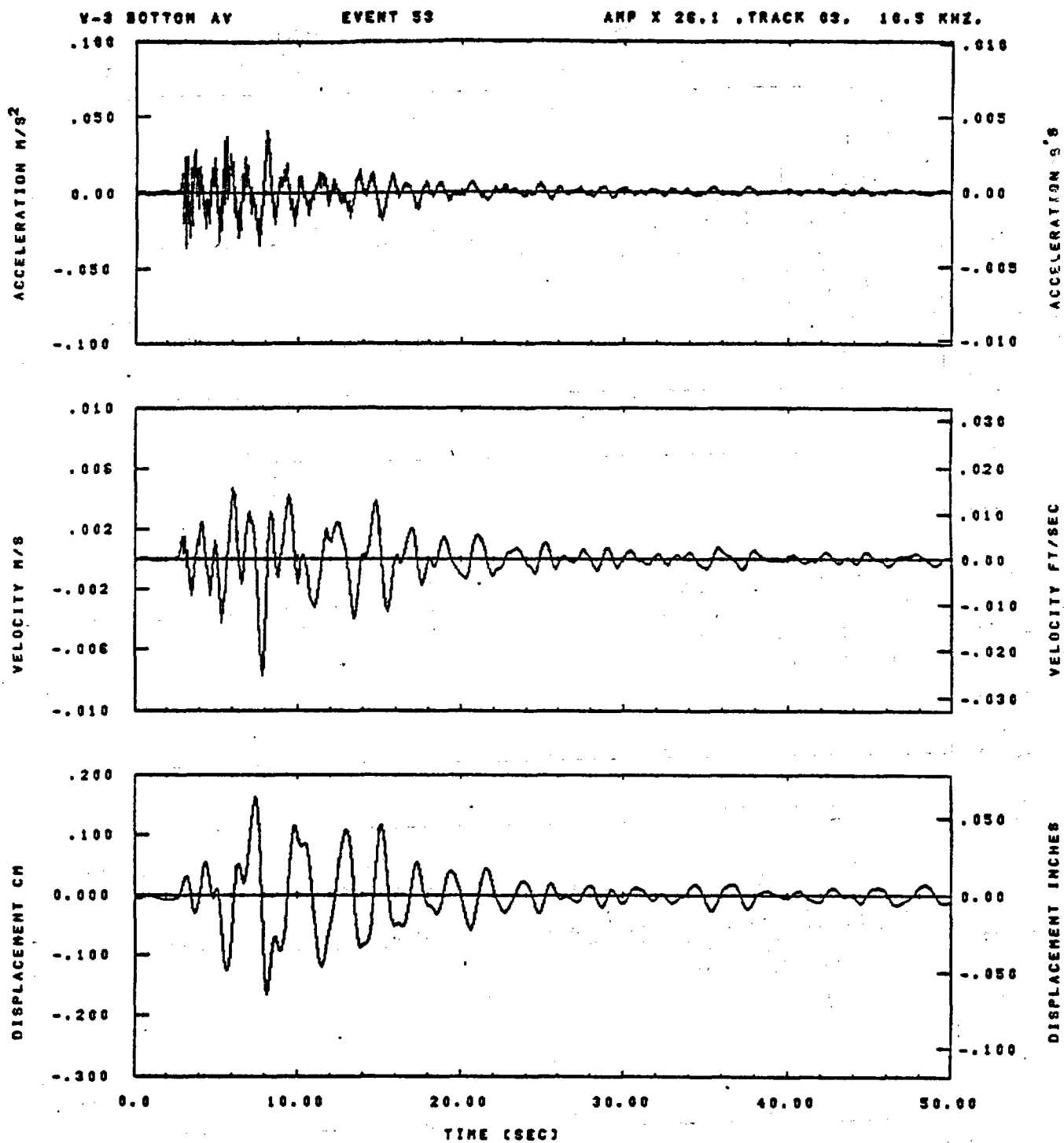


IDT= .0020	QDT= .0	FIX=	AAS=
HPP= .3	SVH= .20	HLH= 187	ASS=
LPP= 27.	SVL= 8.	HLL= 1999	ASE=
VTB= .30	VTE= .200	FLL=	VSE=
OPB=	OPE=	FLH= 0	OSE= 0.

09.38.32.

07/02/92

Figure F-37

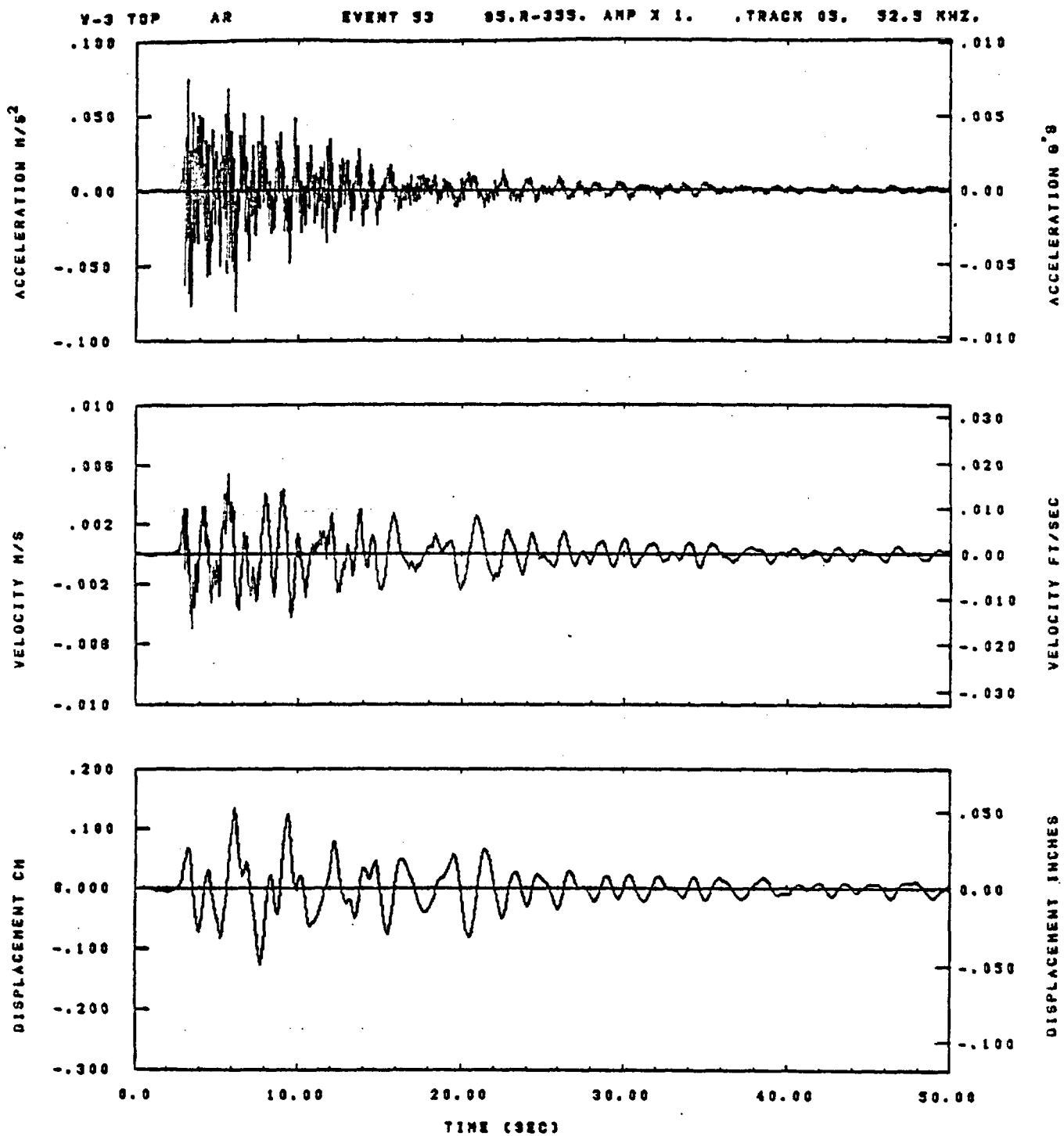


IDT= .0020	ODT= .0	FIX=	AAS=
HPP= .3	BYH= .20	HLH= 167	ASS=
LPP= 27.	BYL= 6.	HLL= 1999	ASE=
YTS= .30	YTE= .200	FLL=	VSE=
DPS=	DPE=	FLH= 0	DSE= 0.

09.31.04.

07/02/02

Figure F-38

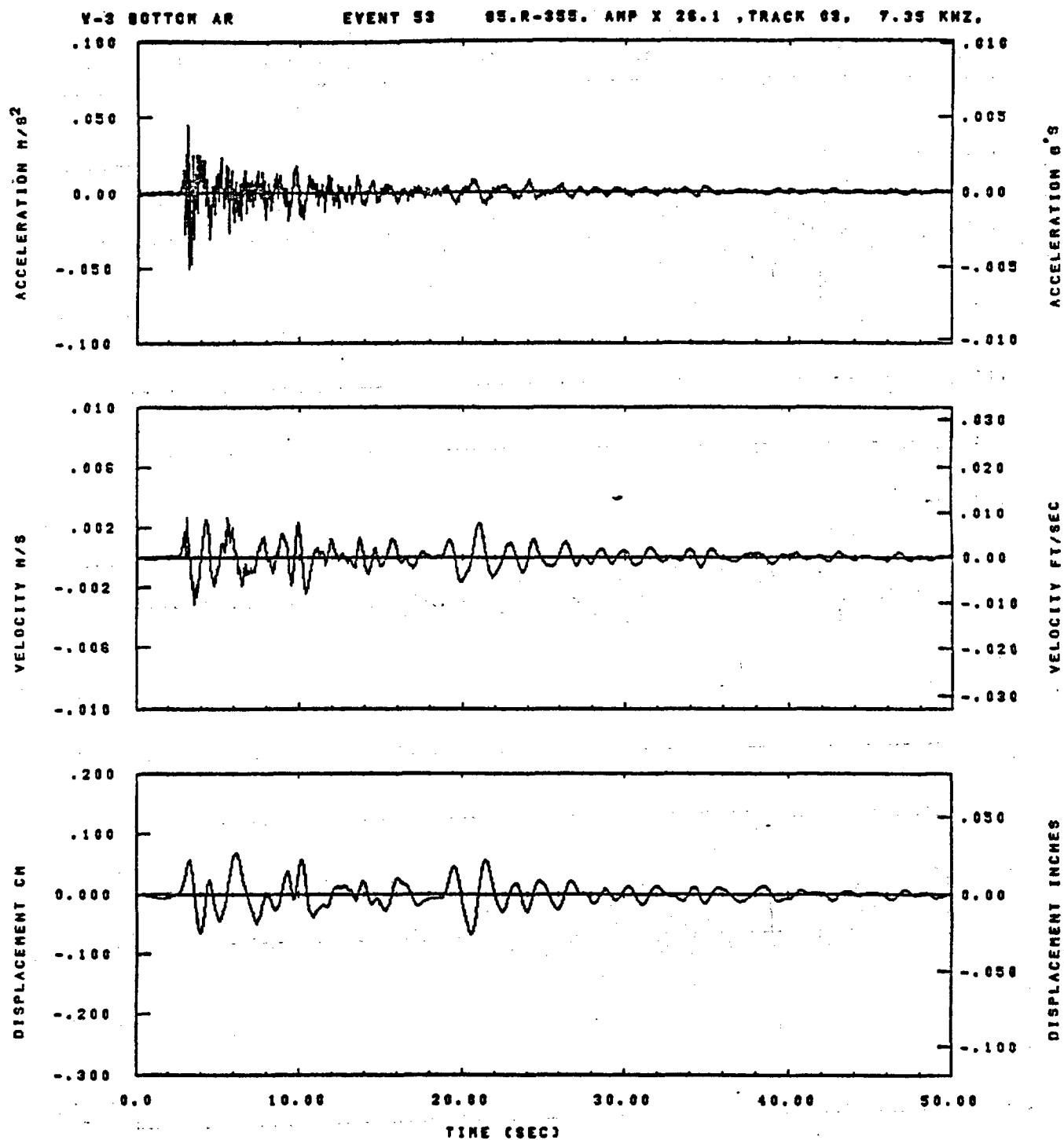


IDT= .0020	ODT= .0	FIX=	AAS=
HPP= .3	BYN= .20	HLH= 187	ASS=
LPP= 27.	SYL= 8.	HLL= 1999	ASE=
VTS= .30	VTE= .200	FLL=	VSE=
OPB=	OPE=	FLH= 0	DSE= 0.

03.30.58.

07/02/82

Figure F-39



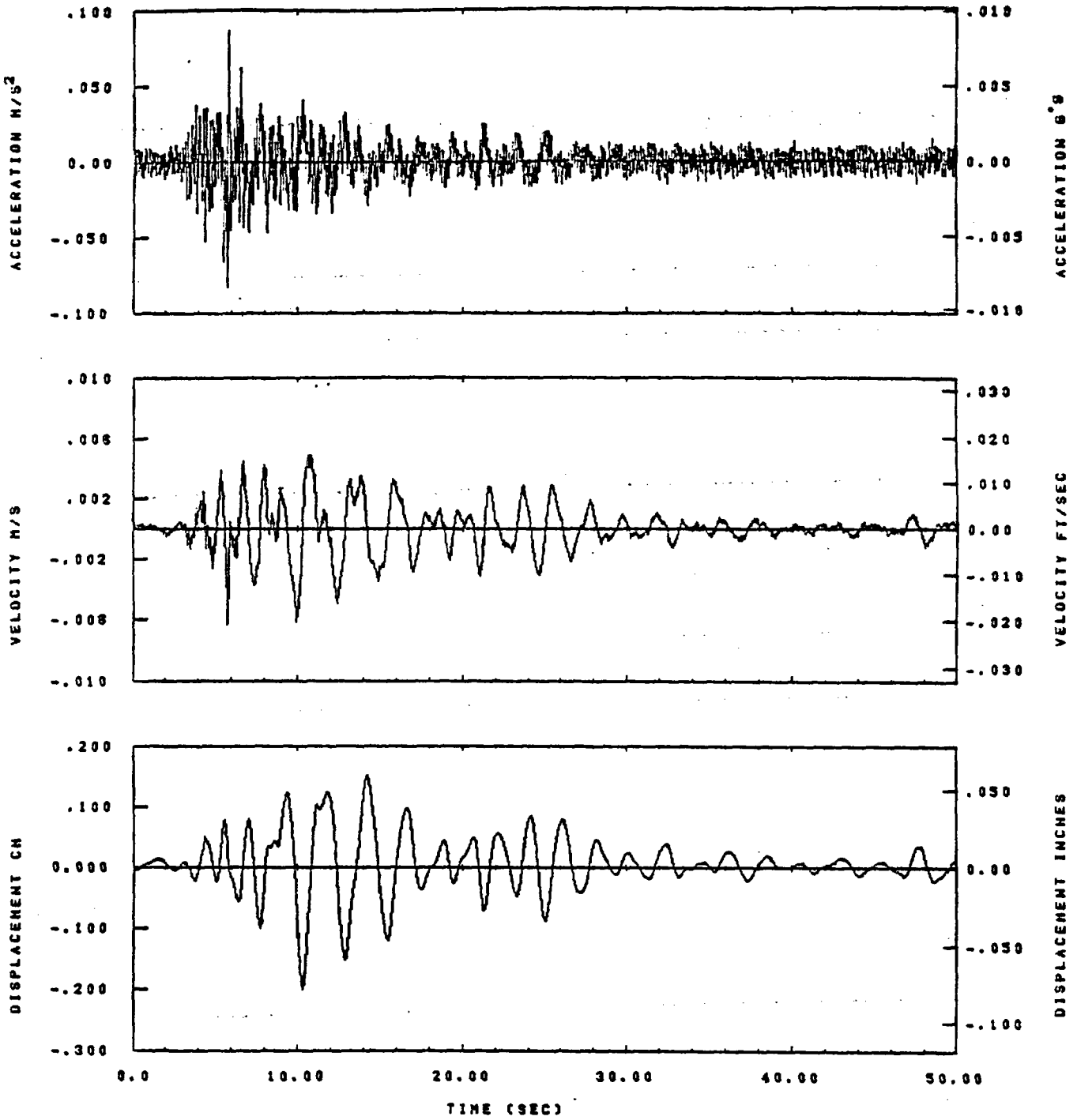
IDT= .0020	ODT= .0	FIX=	AAS=
HPP= .3	BYH= .20	HLH= 167	ASB=
LPP= 27.	BYL= 6.	HLL= 1898	ASE=
VTB= .38	VTE= .208	FLL=	VSE=
DPS=	DPE=	FLH= 0	DSE= 0.

08.31.08.

67/02/62

Figure F-40

V-3 TOP AT EVENT 99 95.R- 95. AMP X 28.1 .TRACK 03. 9.4 KHZ.

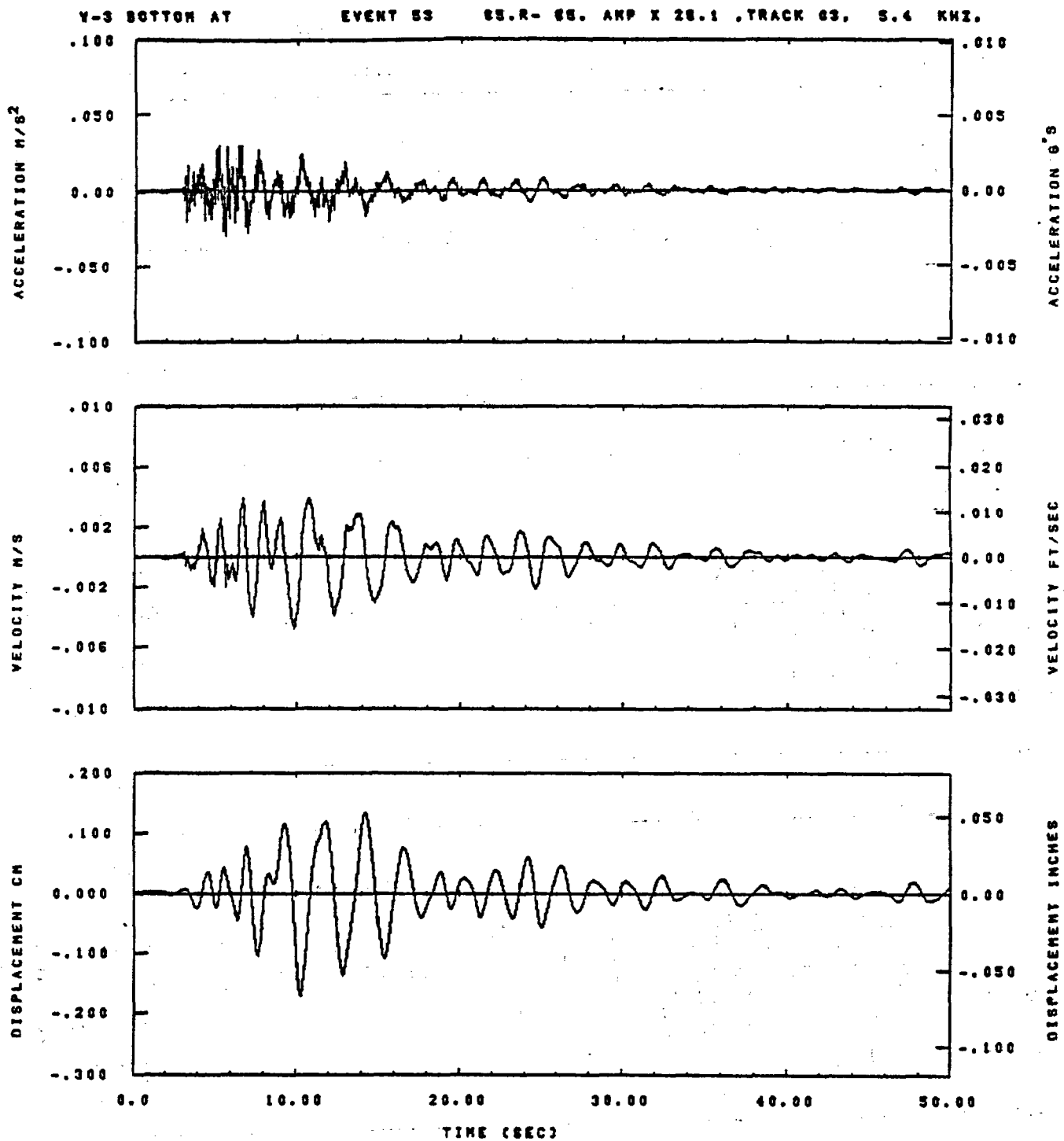


IDT= .0020	QDT= .0	FIX=	AAS=
HPF= .3	SVH= .20	HLH= 187	RNS=
LPP= 27.	SVL= 8.	HLL= 1999	AZN=
VTS= .30	VTE= .200	FLL=	VSE=
DPS=	DPE=	FLH= 0	HLT=

10.03.50.

07/28/82

Figure F-41

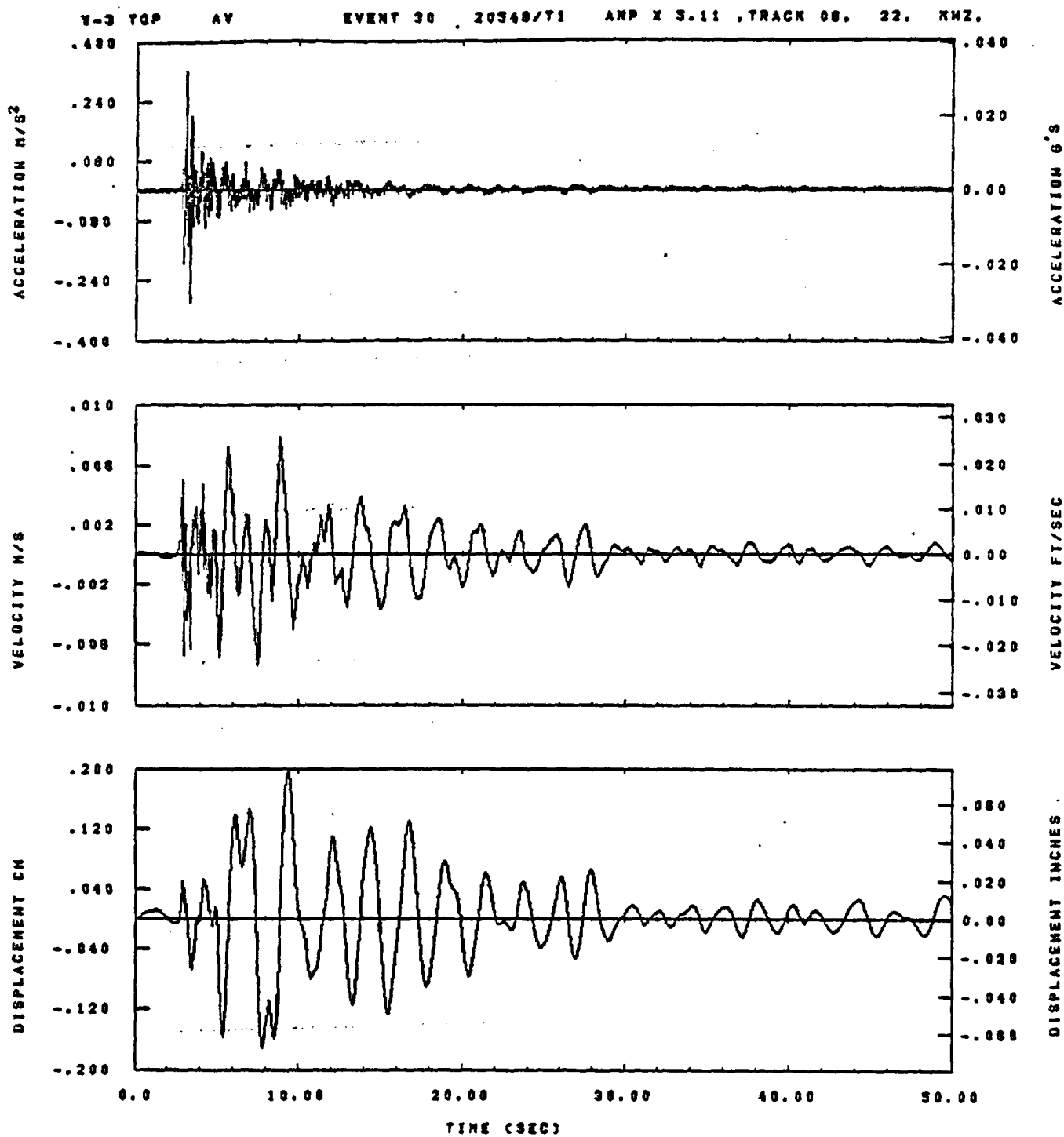


IDT= .0020	OOT= .0	FIX=	AAS=
HPF= .3	BYH= .20	HLH= 167	ASB=
LPF= 27.	BYL= 6.	HLL= 1999	ASE=
VTS= .30	VTE= .200	FLL=	VSE=
DPS=	DPE=	FLH= 0	DSE= 0.

08.31.13.

07/02/82

Figure F-42

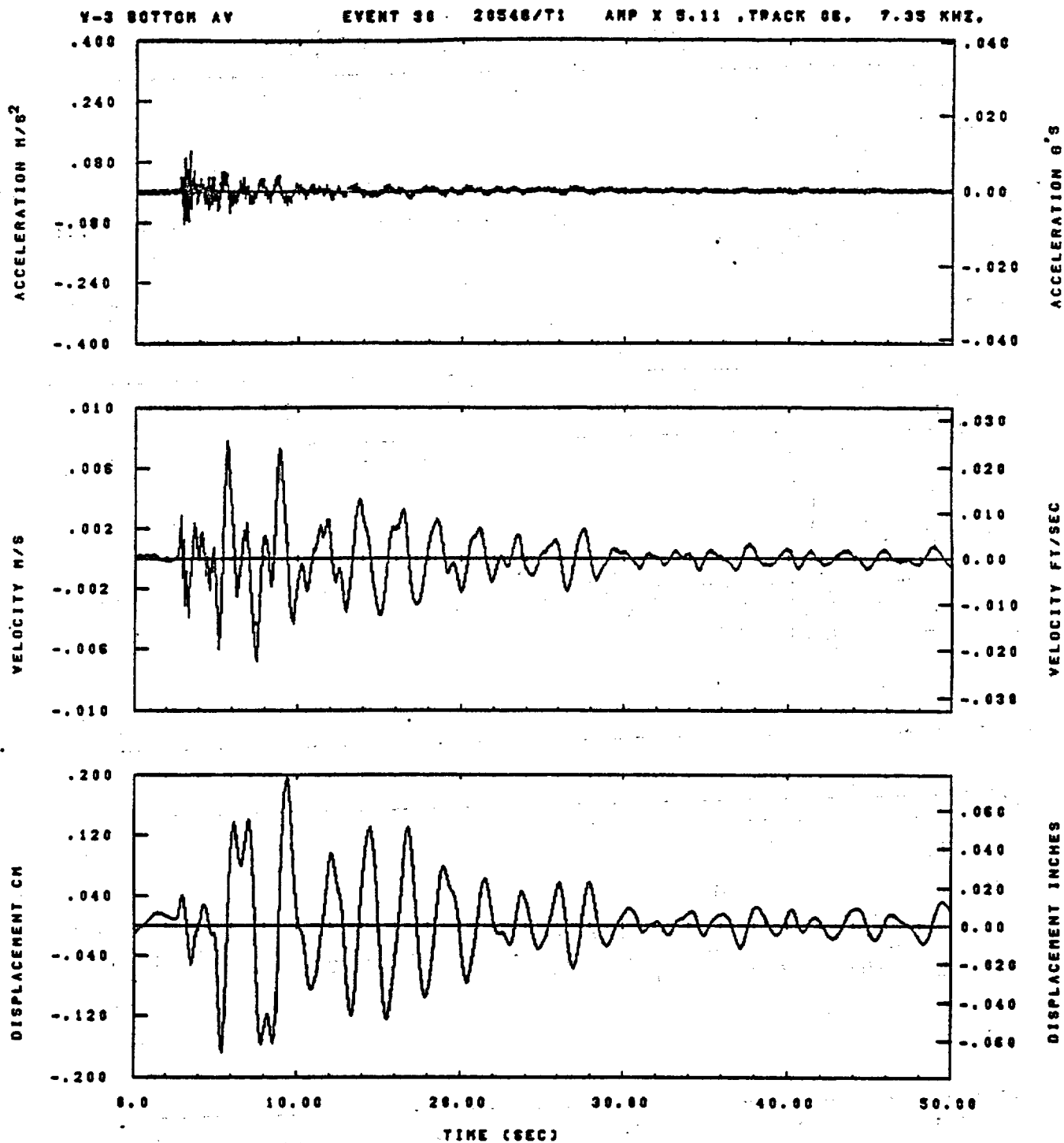


IDT= .0020	ODT= .005	FIX=	AAS= 0.
HPP= .20	SVH= .13	HLH= 123	ASB=
LPP= 38.	BVL= 8.	NLL= 2989	ASE=
VTB= .200	VTE= .133	PLL= -20.	VSE= 0.
DPB= 0.	DPE= 100.	PLH= 0	DSE= 0.

14.59.41.

08/30/82

Figure F-43

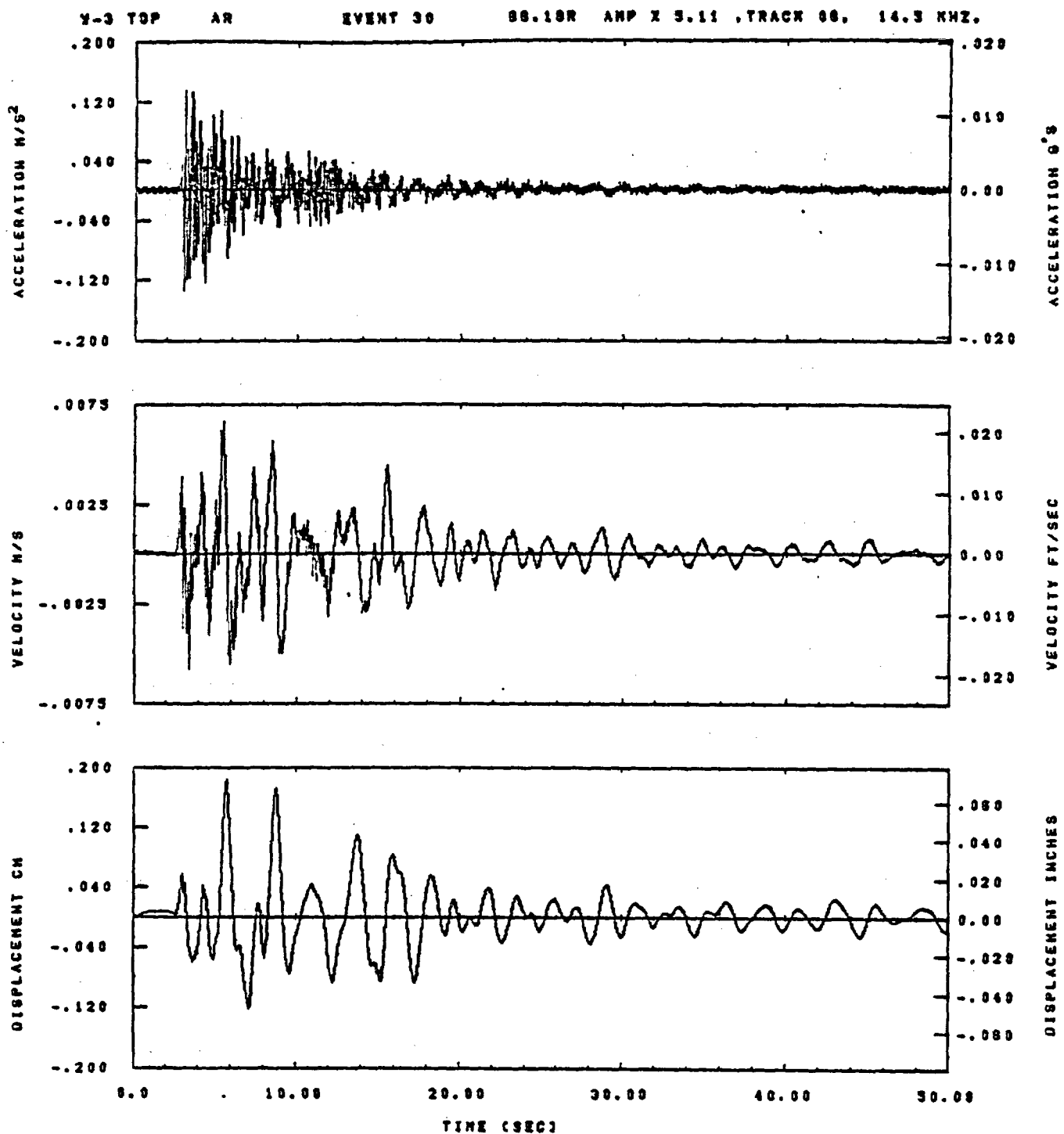


IDT= .0020	ODT= .005	FIX=	AAS= 0.
HPF= .20	SVH= .13	HLH= 125	ASH=
LPF= 36.	SVL= 8.	HLL= 2888	ASE=
YTS= .200	YTE= .133	FLL= -20.	VSE= 0.
DPS= 0.	DPE= 100.	FLH= 0	DSE= 0.

14.52.32.

06/30/82

Figure F-44

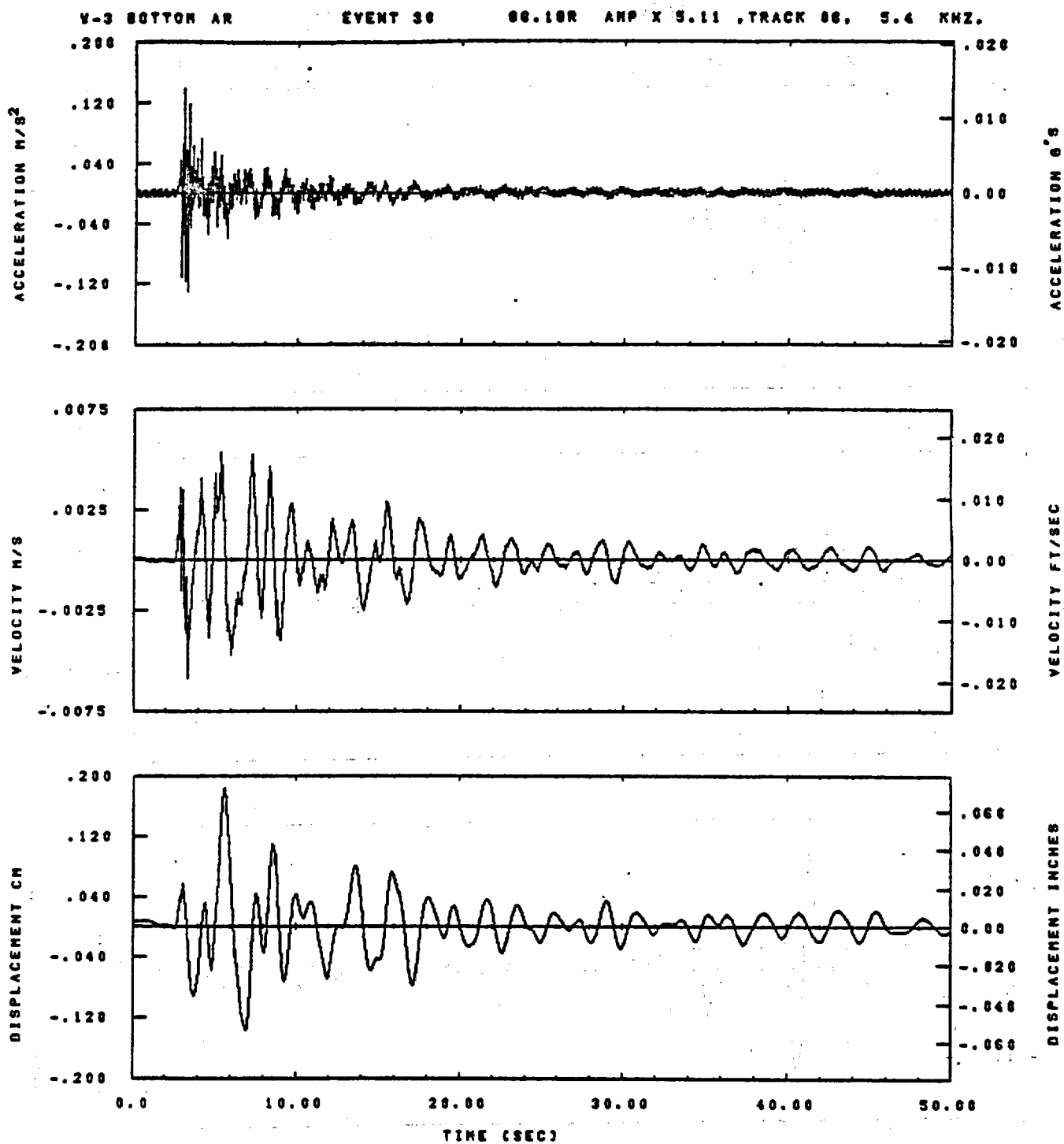


IDT= .0020	ODT= .003	FIX=	AAS= 0.
HPP= .20	BYH= .13	HLH= 123	ASS=
LPP= 38.	BYL= 8.	HLL= 2999	ASE=
VTS= .200	VTE= .133	FLL= -20.	VSE= 8.
DPB= 0.	OPE= 100.	FLH= 8	DSE= 0.

14.50.21.

08/30/92

Figure F-45

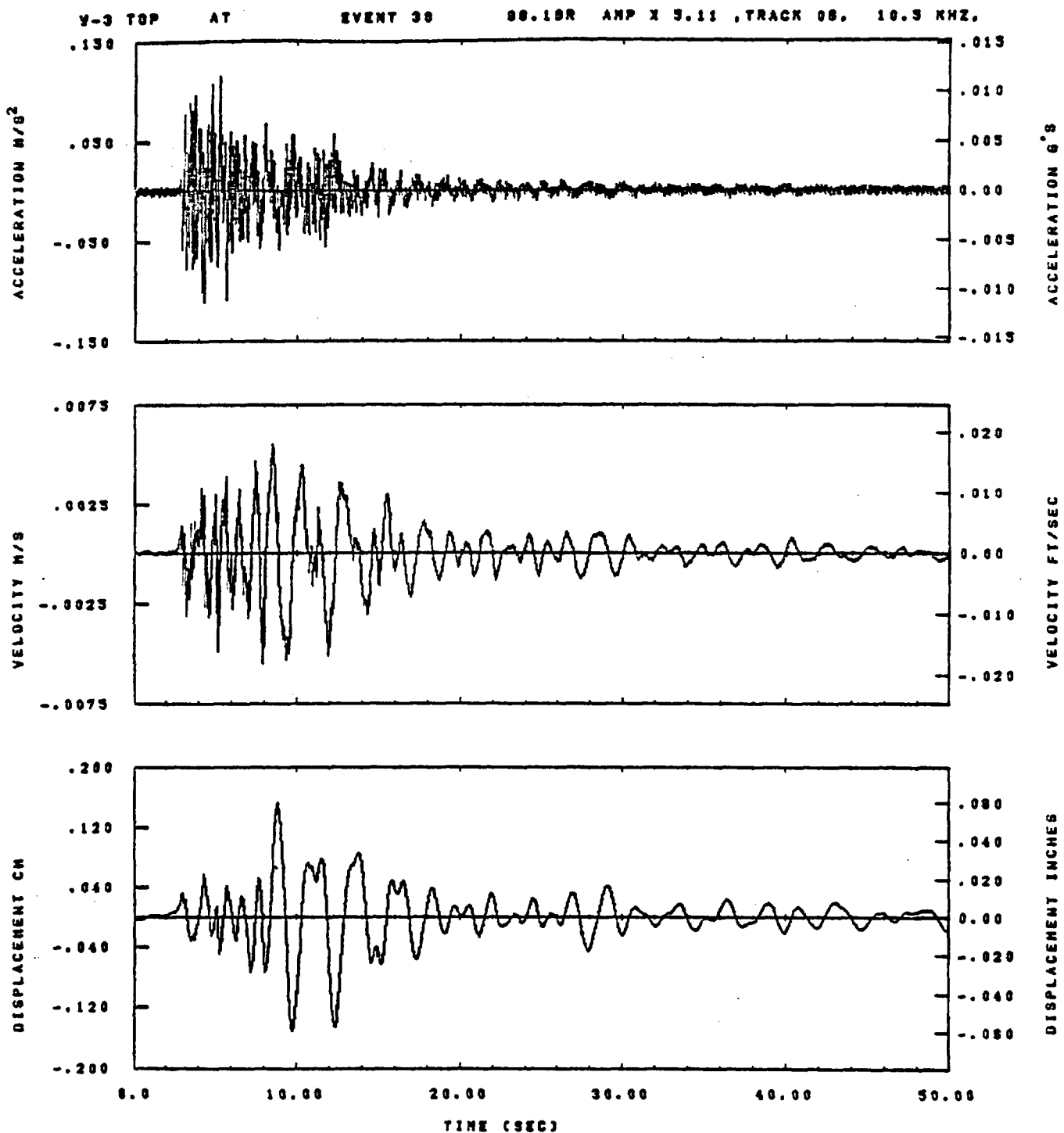


IDT= .0020	QDT= .005	FIX=	AAS= 0.
HPF= .20	BVH= .13	HLH= 125	ASS=
LPF= 36.	BYL= 8.	HLL= 2888	ASE=
VTB= .200	YTE= .133	FLL= -20.	VSE= 0.
OPB= 0.	OPE= 100.	FLH= 0	DSE= 0.

14.52.18.

06/30/82

Figure F-46

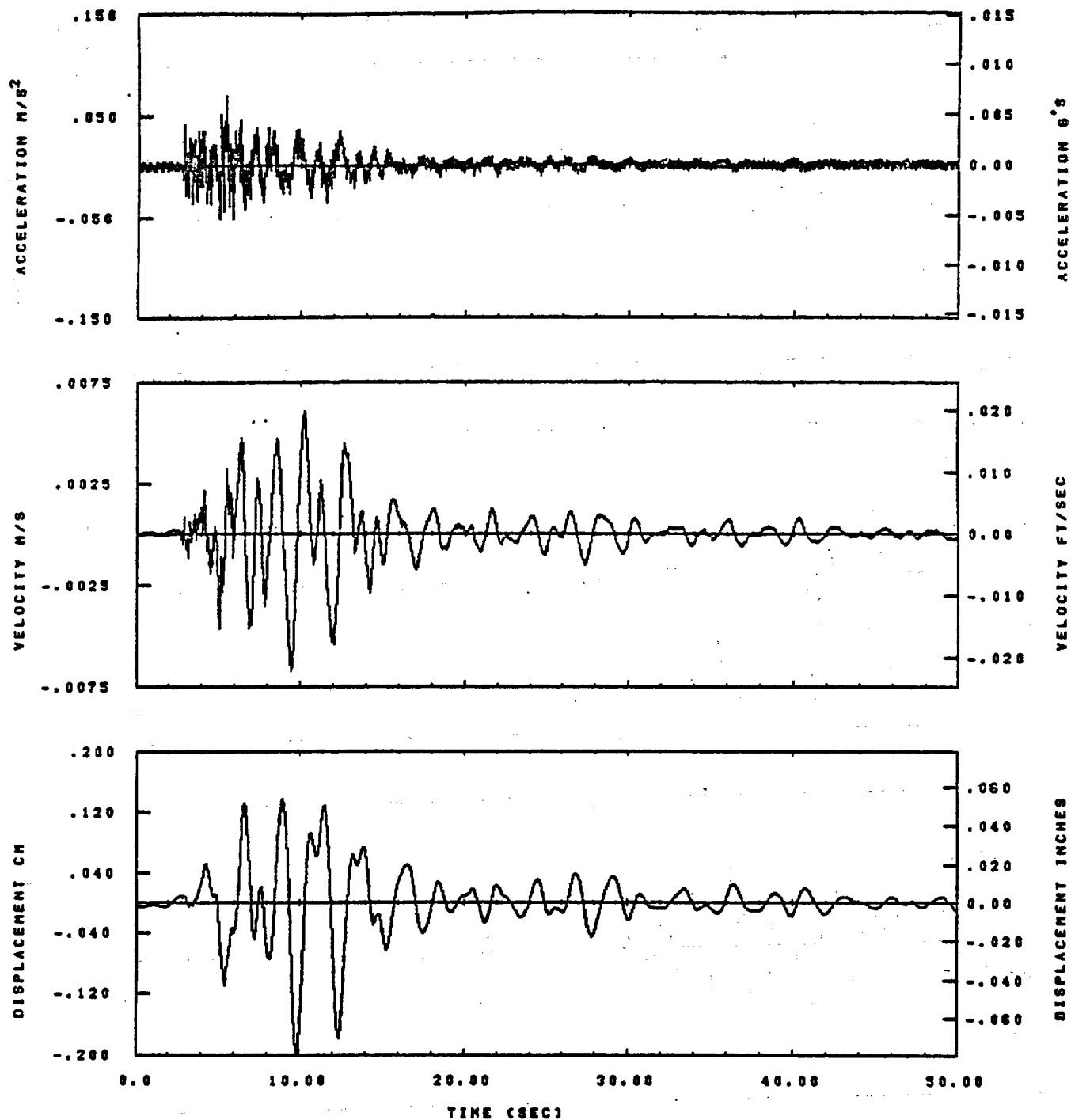


IDT= .0020	OOT= .003	FIX=	AAS= 0.
HPP= .28	BYH= .13	HLH= 125	ASB=
LPP= 38.	BYL= 8.	HLL= 2999	ASE=
VTB= .208	VTE= .133	FLL= -20.	VSE= 0.
DPB= 0.	DPE= 180.	PLH= 0	DSE= 0.

14.50.29.

08/30/82

V-3 BOTTOM AT EVENT 38 08.18R AMP X 5.11 ,TRACK 06. 3.8 KHZ.

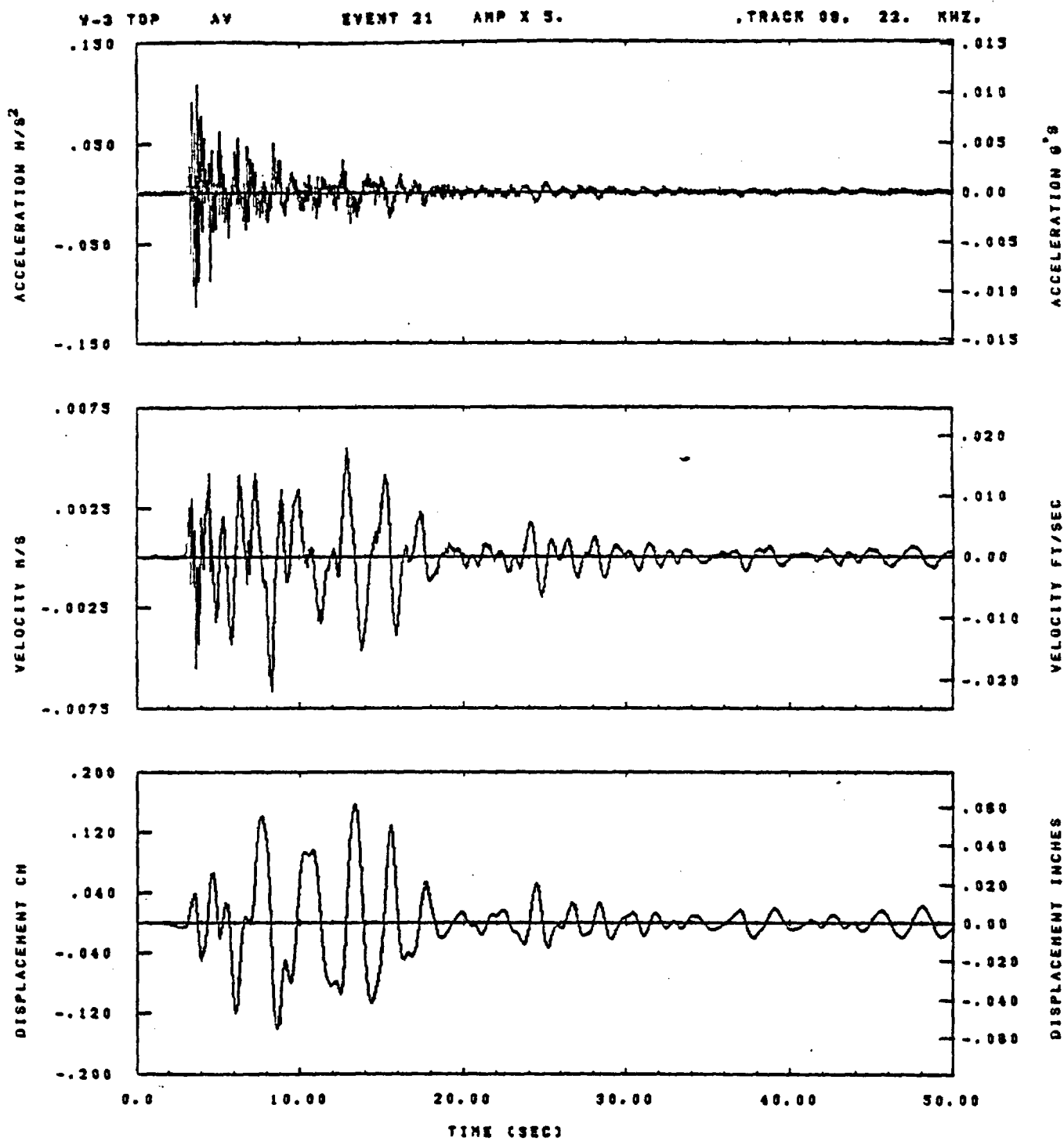


IDT= .0020	OOT= .005	FIX=	AAS= 0.
HPP= .20	BYH= .13	HLH= 125	ASB=
LPP= 36.	BYL= 0.	HLL= 2999	ASE=
VTB= .200	VTE= .133	FLL= -20.	VSE= 0.
OPB= 0.	OPE= 100.	FLH= 0	OSE= 0.

14.52.25.

06/30/82

Figure F-48

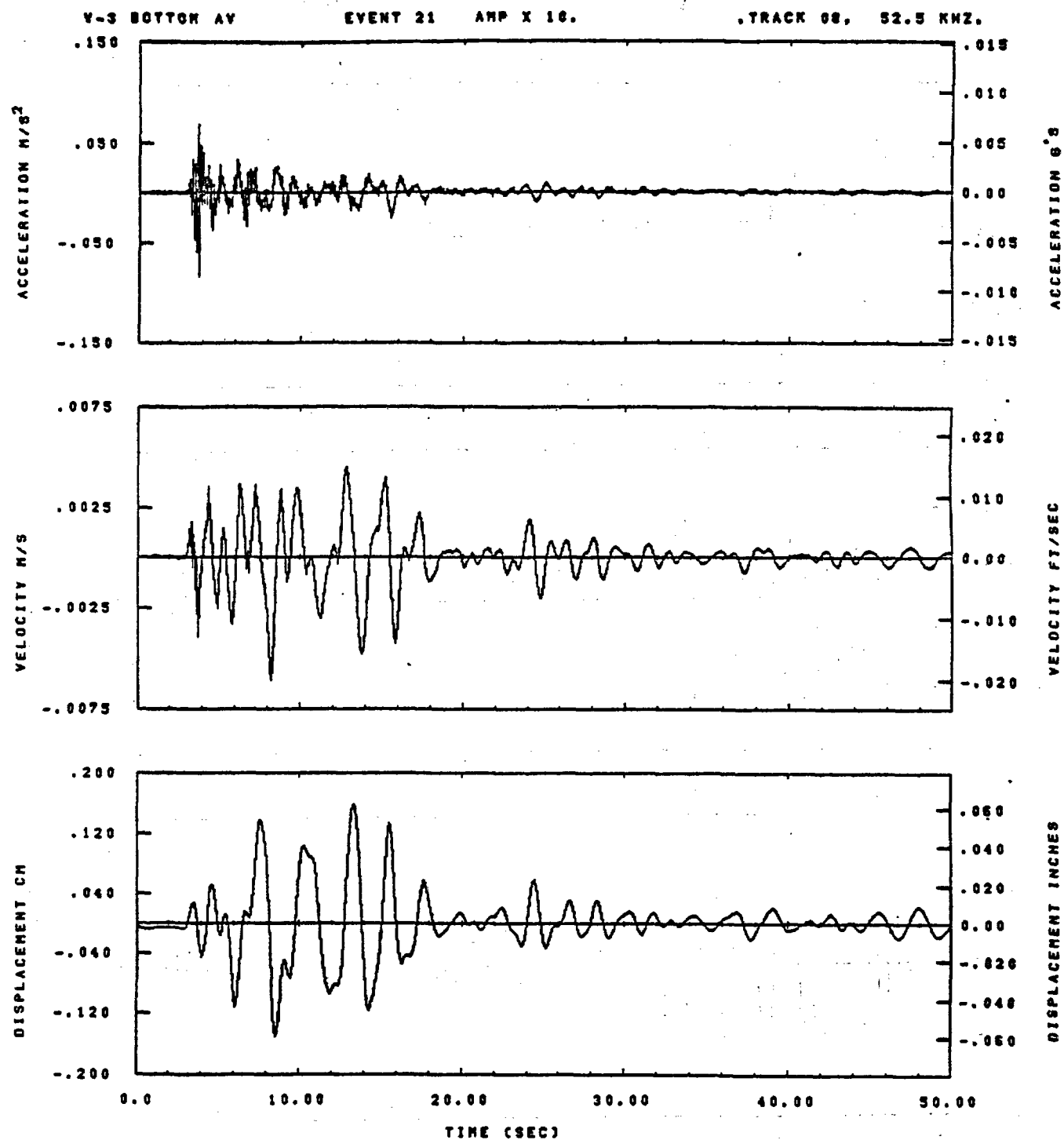


IDT= .0020	QDT=	FIX=	AAS= 0.
HPP= .3	BYH= .20	HLH= .417	ASB=
LPP= 10.	BYL= 2.	HLL= 1999	ASE=
VTS= .30	VTE= .200	FLL= -20.	VSE= 0.
DPS= 0.	DPE= 100.	FLH= 0	DSE= 0.

09.31.43.

07/82/82

Figure F-49

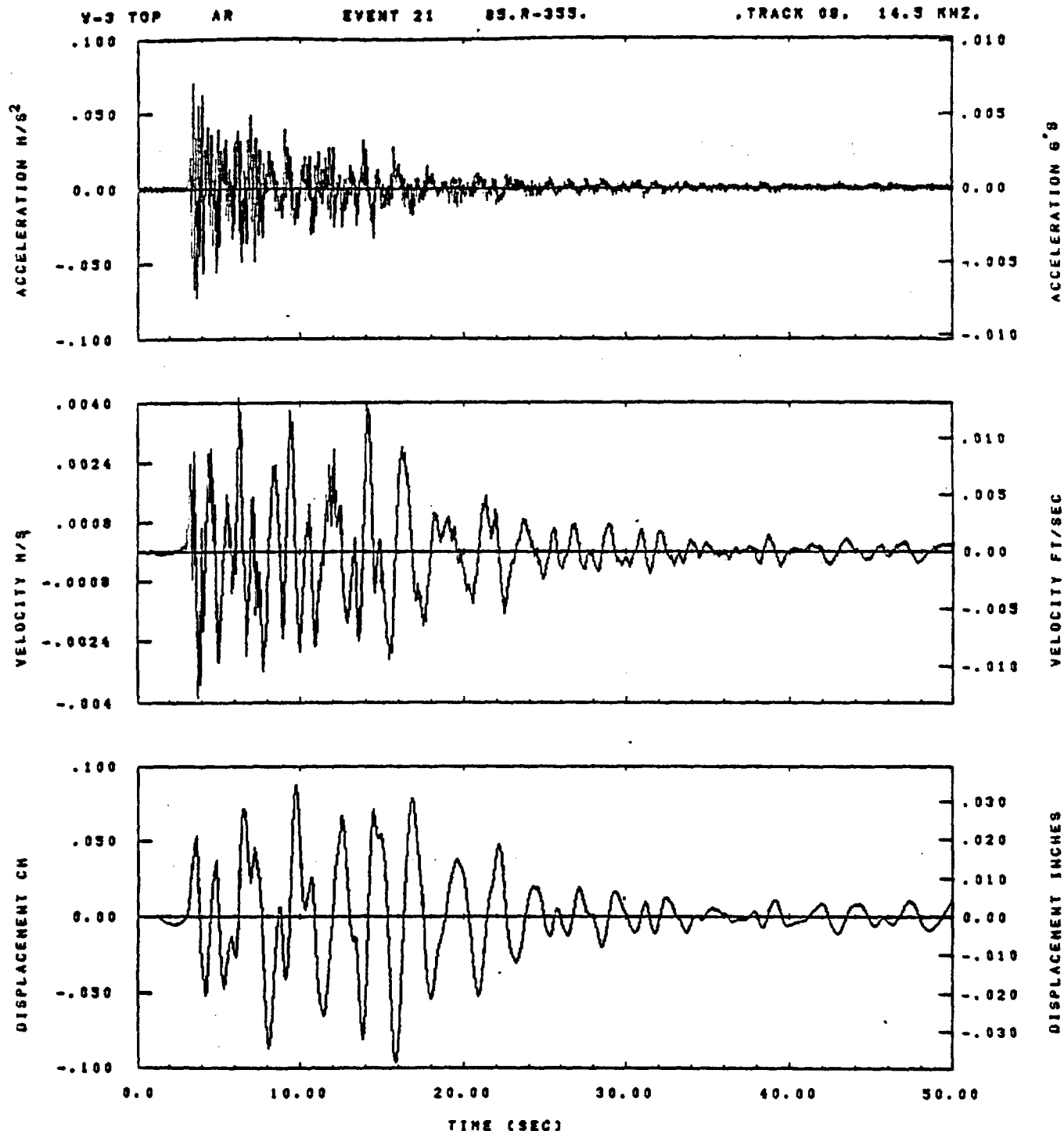


IDT= .0020	QDT=	FIX=	AAS= 0.
HPP= .3	BYH= .20	HLH= 417	ASB=
LPP= 10.	BVL= 2.	HLL= 1999	ASE=
VTB= .38	VTE= .200	FLL= -20.	VSE= 0.
DPS= 0.	DPE= 100.	FLH= 0	DSE= 0.

08.52.17.

07/02/82

Figure F-50

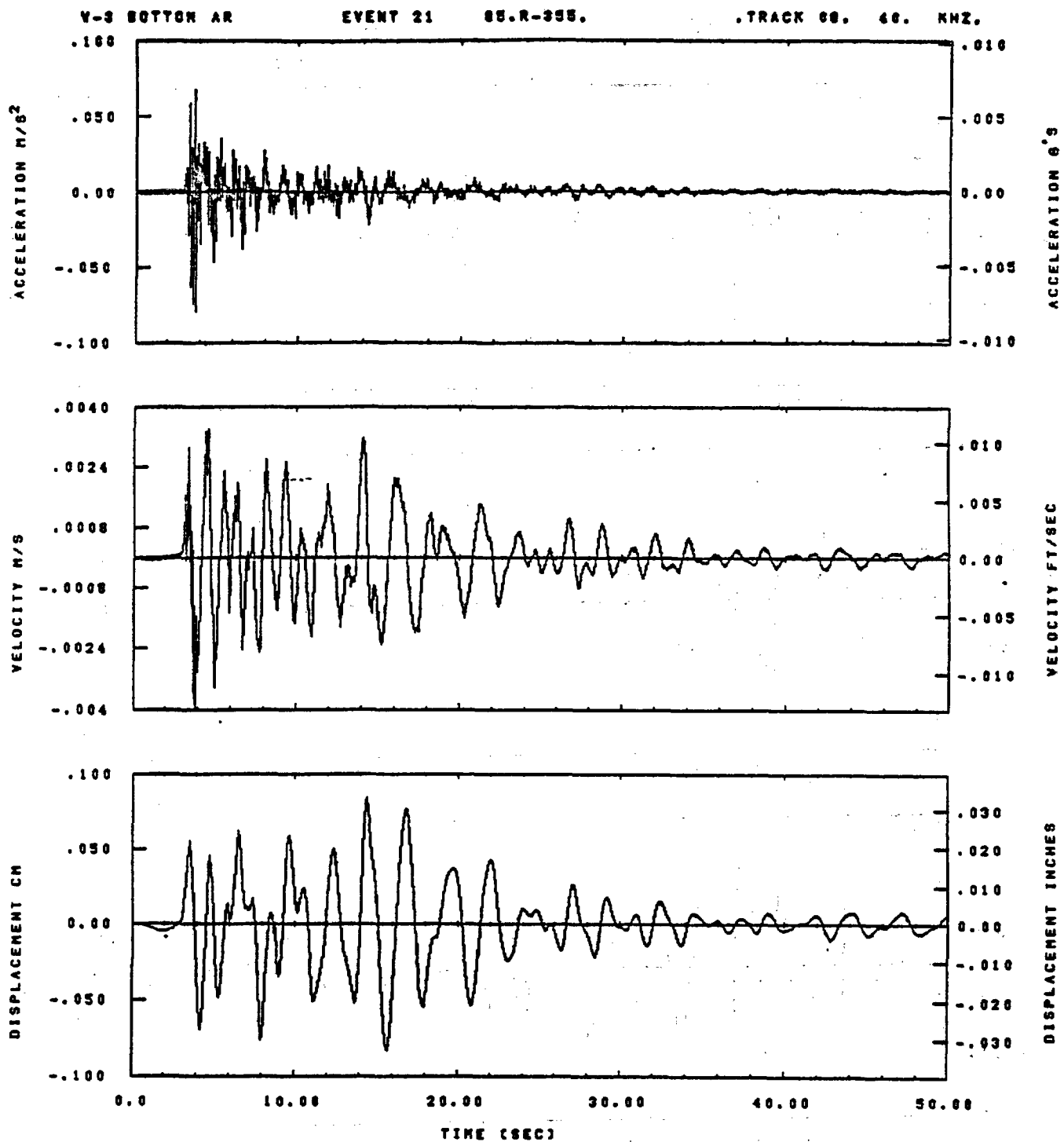


IDT= .0020	ODT=	FIX=	AAS= 0.
HPF= .3	BYM= .20	HLH= 417	ASS=
LFF= 10.	BYL= 2.	HLL= 1999	ASE=
VTS= .30	VTE= .200	FLL= -20.	VSE= 0.
DPS= 0.	DPE= 100.	FLH= 0	OSE= 0.

09.51.49.

07/02/82

Figure F-51



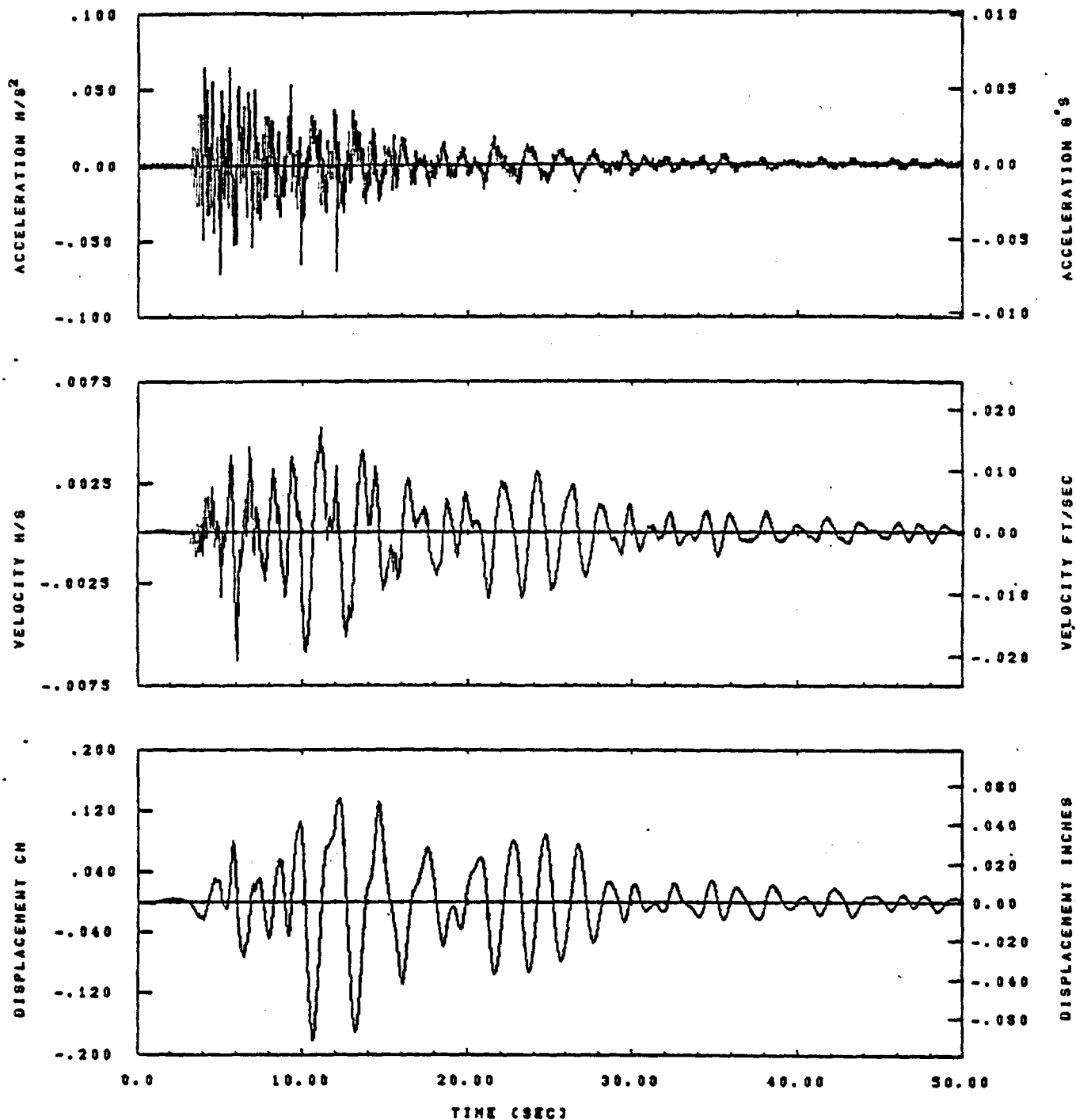
IDT= .0020	ODT=	FIX=	AAS= 0.
HPP= .3	SVN= .20	HLN= 417	ASB=
LPP= 10.	SVL= 2.	HLL= 1883	ASE=
VTS= .36	VTE= .200	FLI= -20.	VSE= 0.
DPS= 0.	DPE= 100.	FLH= 0	DSE= 0.

88.52.21.

07/02/02.

Figure F-52

Y-3 TOP AT EVENT 21 85.R- 85. TRACK 09. 10.3 KHZ.

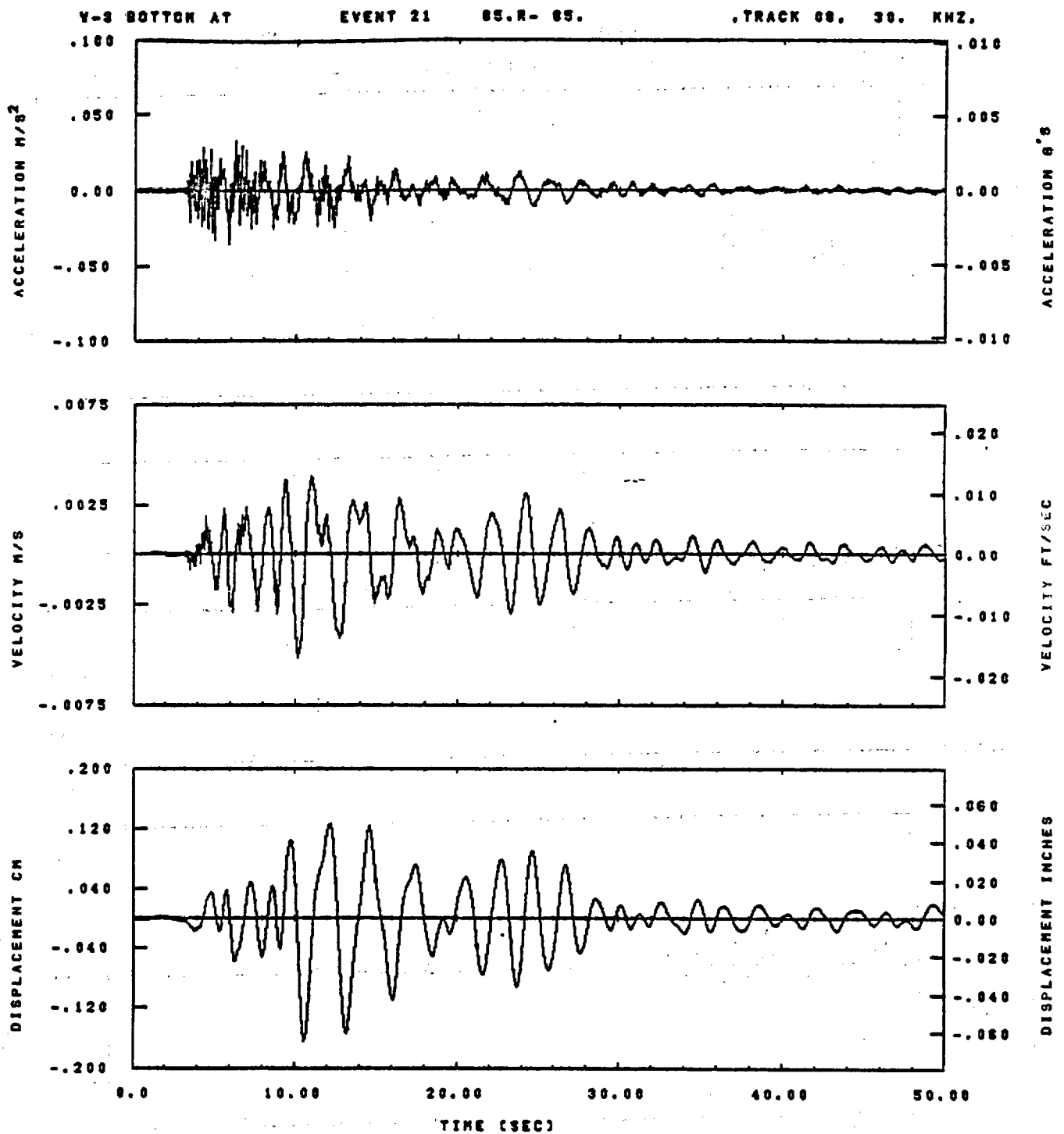


IDT= .0020	ODT=	FIX=	AAS= 0.
HPP= .3	BYH= .20	HLH= 417	ASB=
LPP= 10.	BYL= 2.	HLL= 1999	ASE=
VTS= .30	VTE= .200	FLL= -20.	VSE= 0.
DPS= 0.	DPE= 100.	FLH= 0	DSE= 0.

09.31.53.

07/02/82

Figure F-53

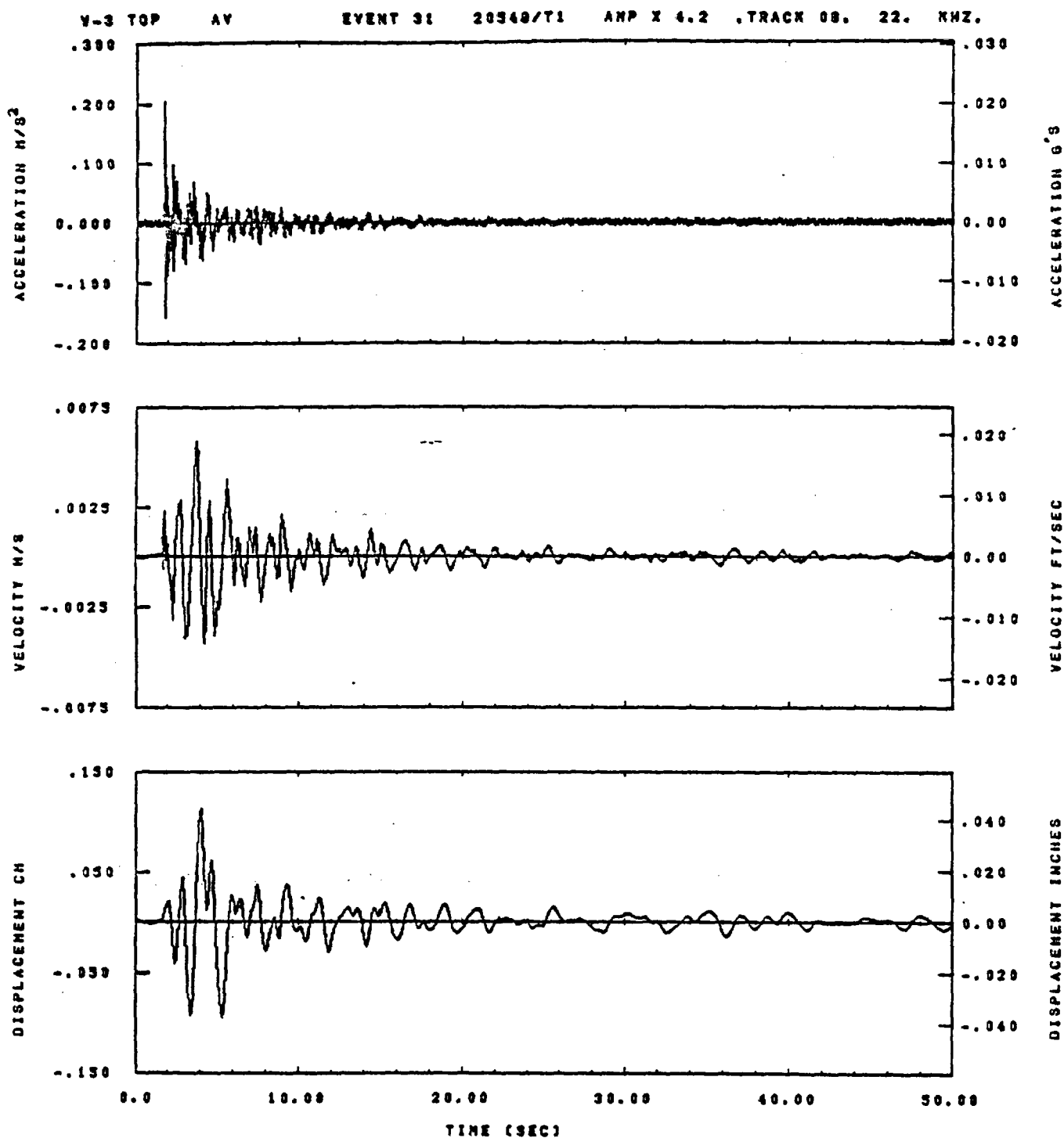


IDT= .0020	ODT=	FIX=	AAS= 0.
HPF= .3	SVH= .20	HLH= 417	ASB=
LPP= 10.	SVL= 2.	HLL= 1000	ASE=
VTS= .30	VTE= .200	FLL= -20.	VSE= 0.
DPS= 0.	OPE= 100.	FLH= 0	DSE= 0.

08.52.25.

07/02/82

Figure F-54

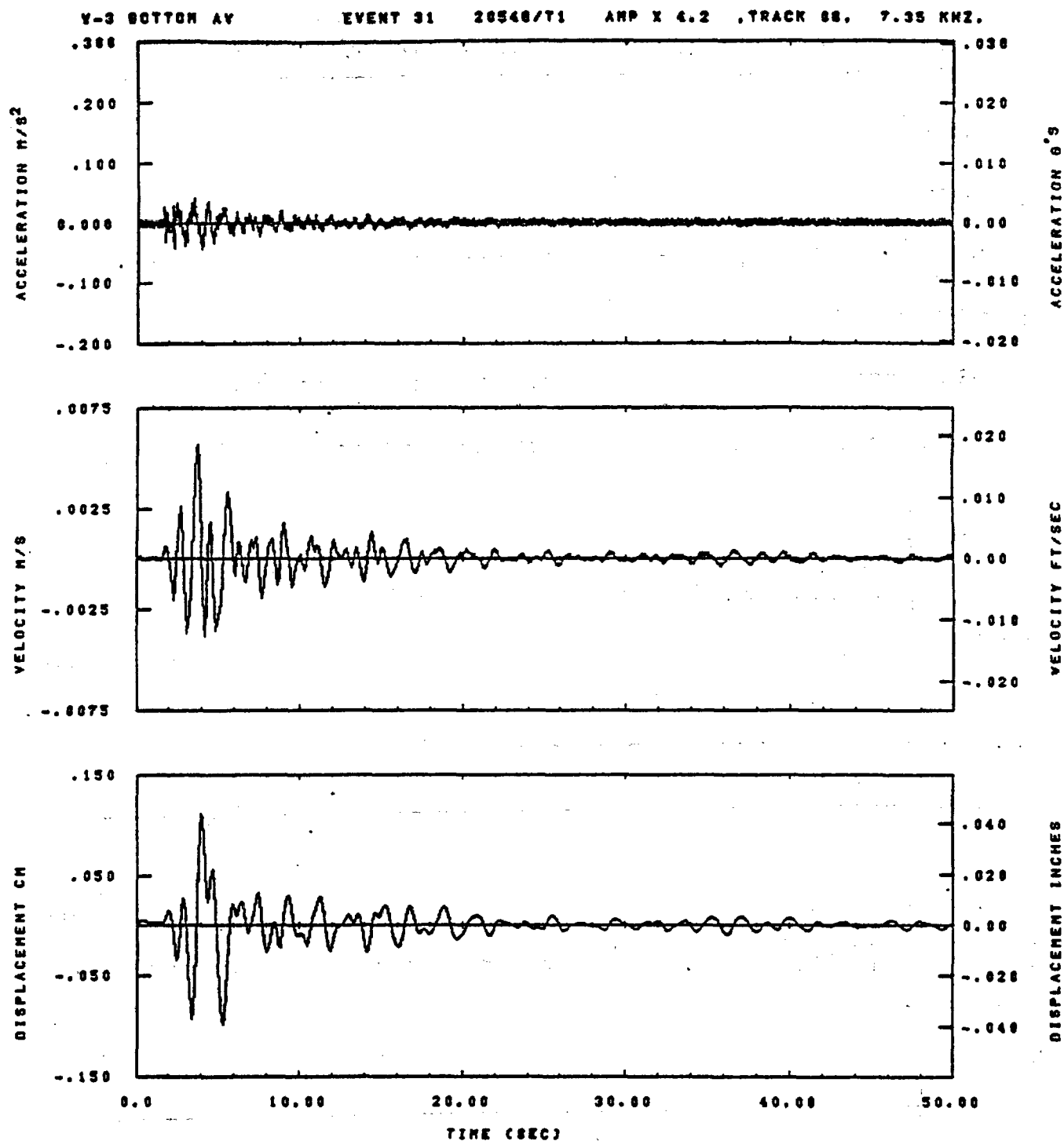


IDT= .0020	ODT= .003	FIX=	AAS= 0.
HPP= .25	BYH= .18	MLH= 143	ASB=
LPP= 31.	BYL= 7.	MLL= 2359	ASE=
YTS= .250	YTS= .188	PLL= -20.	VSE= 0.
DPS= 0.	DPE= 100.	PLH= 0	DSE= 0.

11.59.55.

08/26/92

Figure F-55

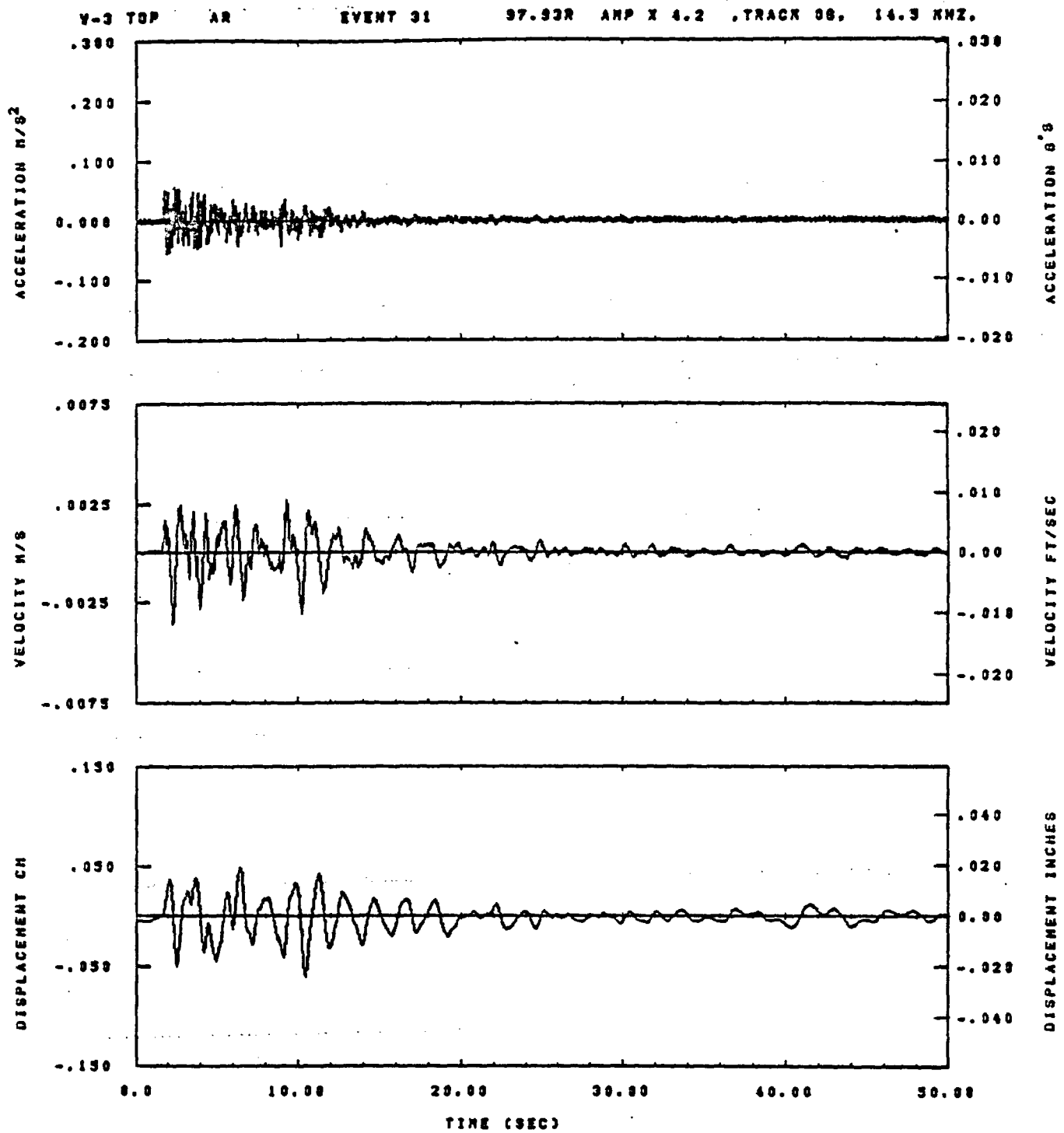


IDT= .0020	ODT= .005	FIX=	AAS= 0.
HFF= .25	BYH= .16	HLH= 143	ASB=
LFF= 31.	BYL= 7.	HLL= 2388	ASE=
VTB= .250	VTE= .166	FLL= -20.	VSE= 0.
DPE= 0.	DPE= 100.	FLH= 0	DSE= 0.

12.06.25.

06/24/82

Figure F-56

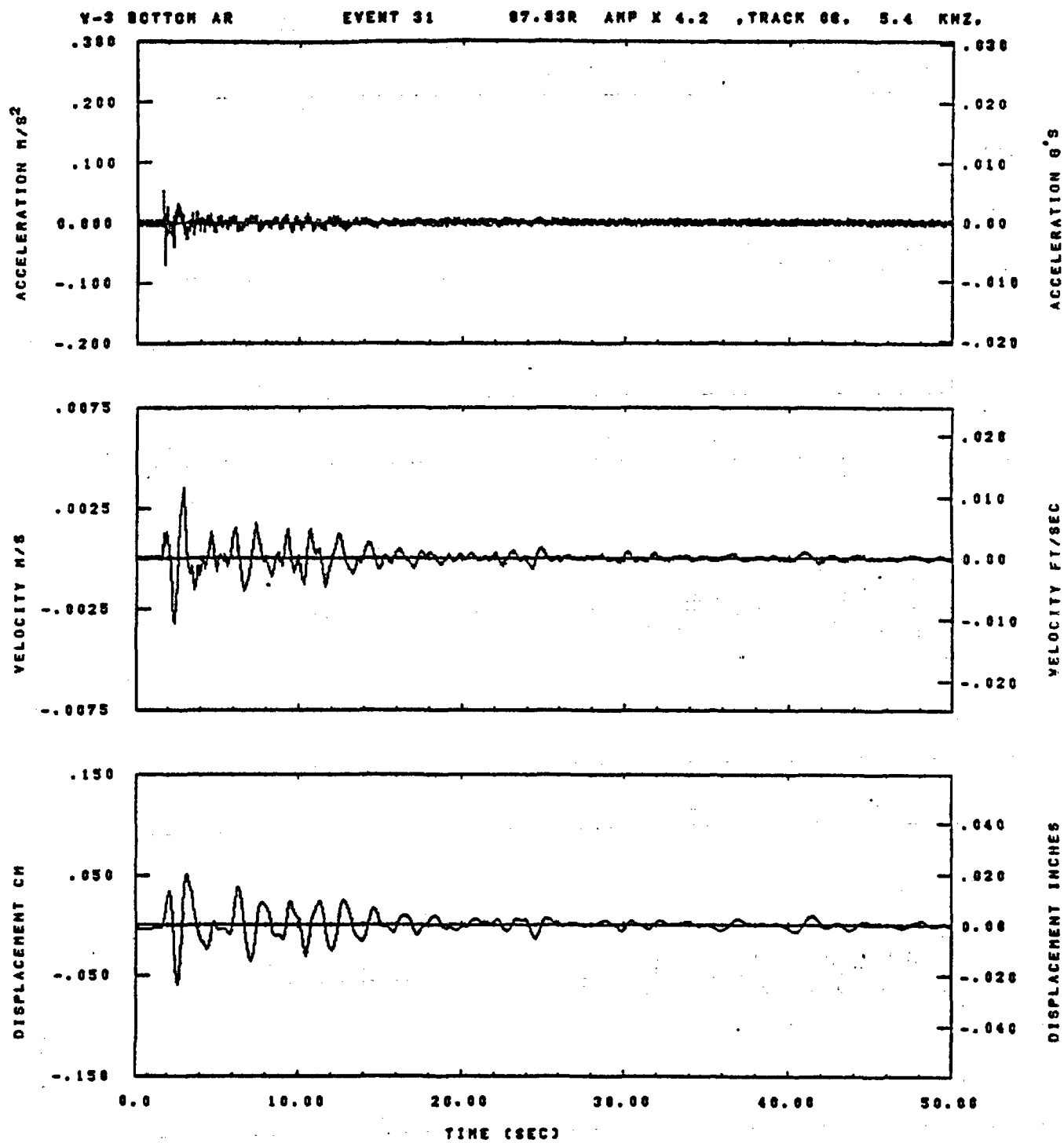


IDT= .0020	ODT= .003	FIX=	AAS= 0.
HPF= .25	BYH= .18	HLH= 143	ASB=
LPF= 31.	BYL= 7.	HLL= 2333	ASE=
VTB= .250	VTE= .188	FLL= -20.	VSE= 0.
DPS= 0.	DPE= 100.	FLH= 0	DSE= 0.

11.39.45.

06/26/92

Figure F-57

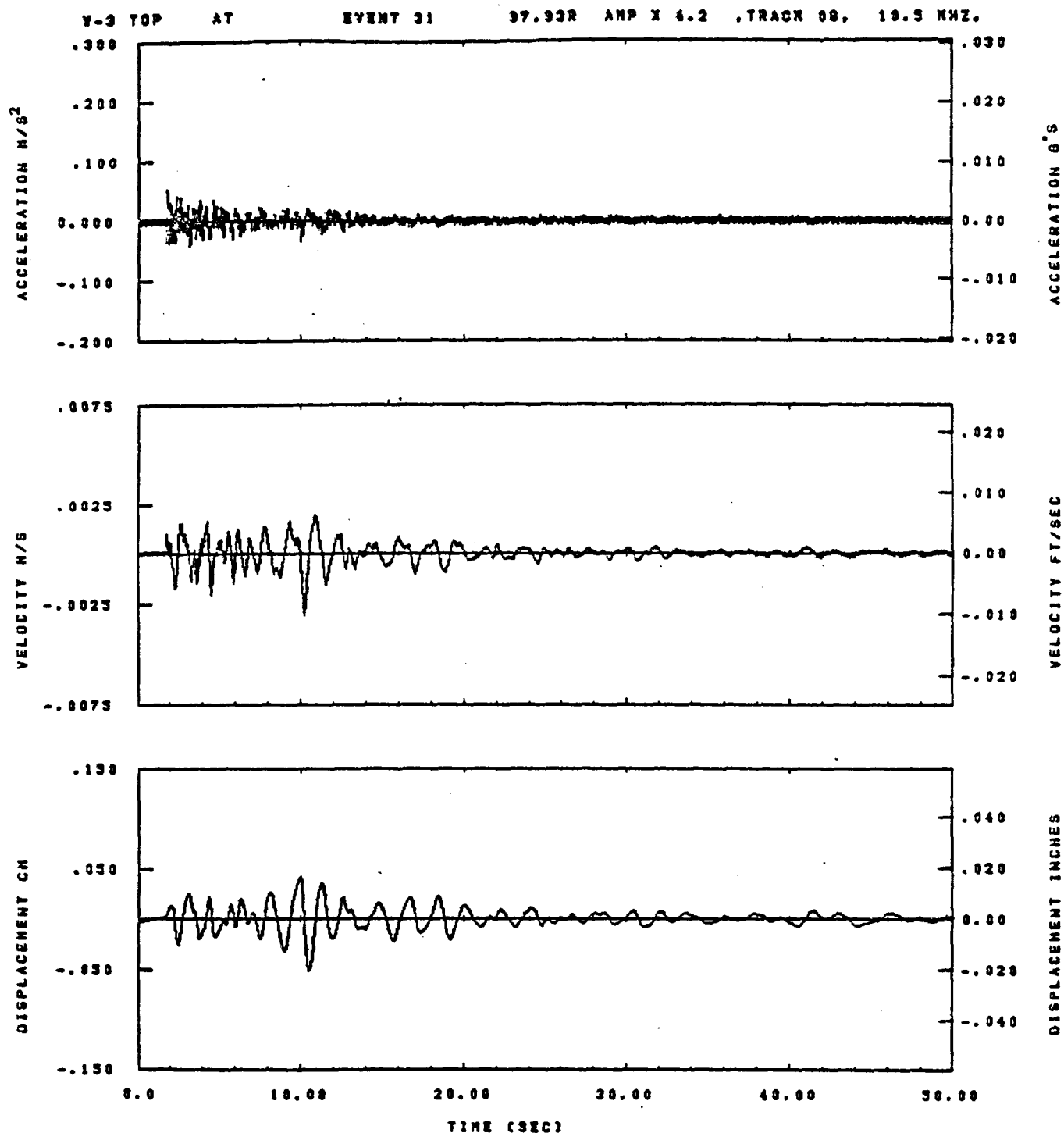


IDT= .0020	ODT= .005	FIX=	AAS= 0.
HPP= .25	BYH= .16	HLH= 143	ASB=
LPP= 31.	BYL= 7.	HLL= 2388	ASE=
VTS= .250	VTE= .166	FLL= -26.	VSE= 0.
DPS= 0.	DPE= 166.	FLH= 6	DSE= 0.

12.00.05.

06/24/82

Figure F-58

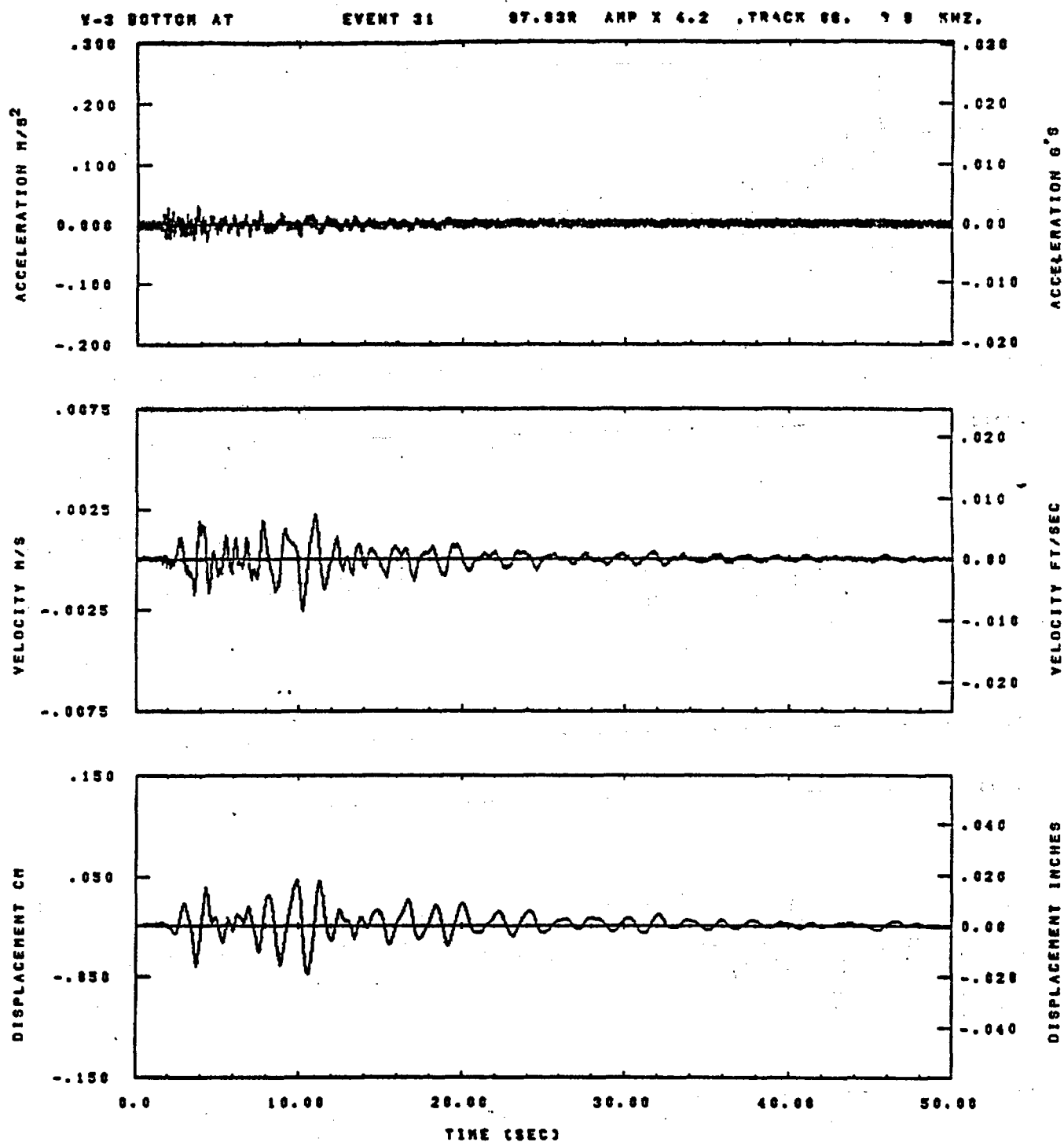


IDT= .0020	ODT= .005	FIX=	AAS= 0.
HPP= .25	BYN= .18	HLN= 143	ASB=
LPP= 31.	BYL= 7.	HLL= 2399	ASE=
VTB= .250	VTE= .188	FLL= -20.	VSE= 0.
DPS= 0.	DPE= 100.	FLH= 0	DSE= 0.

11.59.49.

08/24/92

Figure F-59

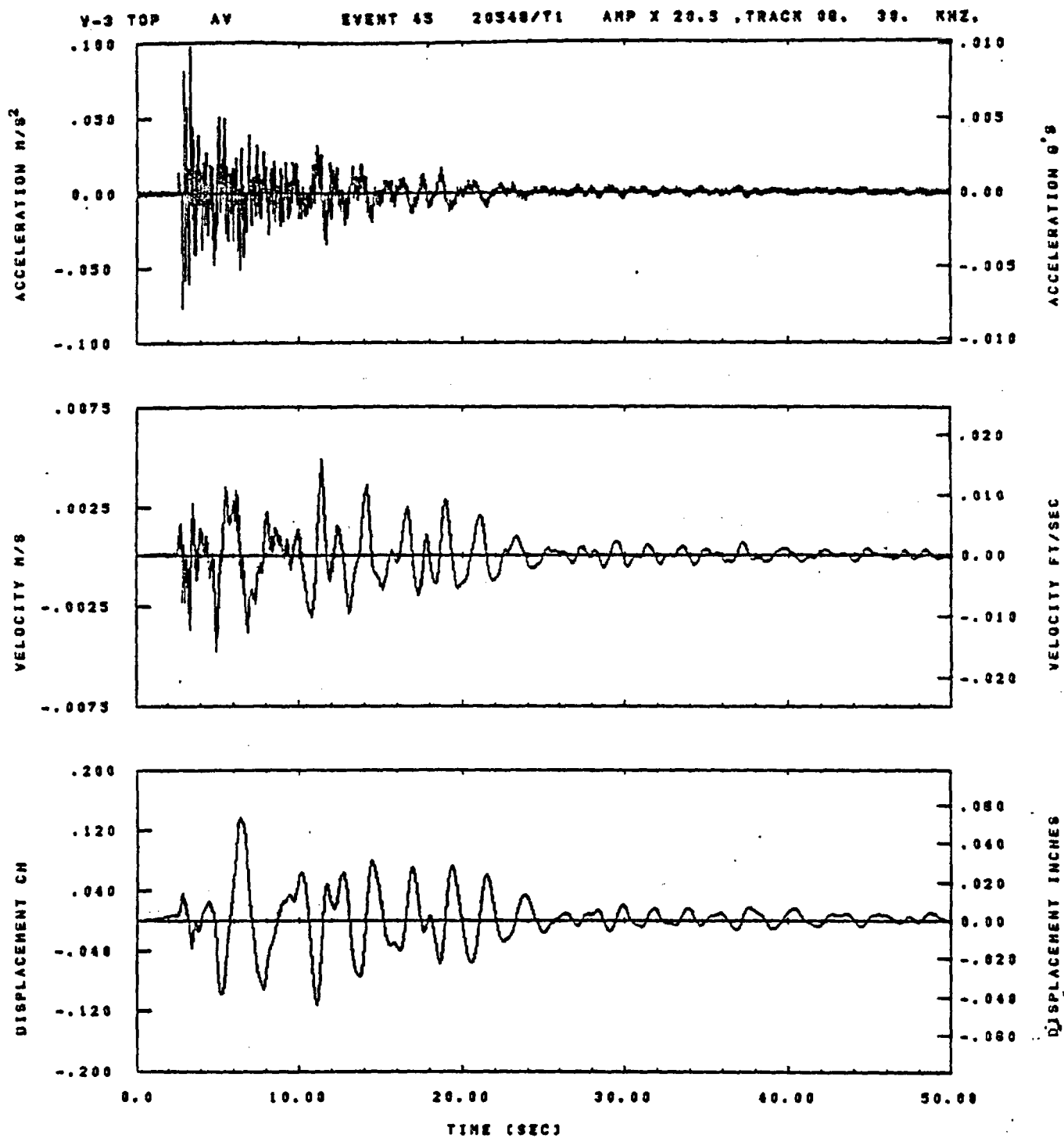


IDT= .0026	QDT= .005	FIX=	AAS= 0.
HPP= .25	BYH= .18	NLM= 143	ASB=
LPP= 31.	BVL= 7.	NLL= 2398	ASE=
VTS= .258	VTE= .168	FLL= -26.	VSE= 0.
DPS= 6.	DPE= 100.	FLH= 0	DSE= 0.

12.00.17.

06/24/82

Figure F-60

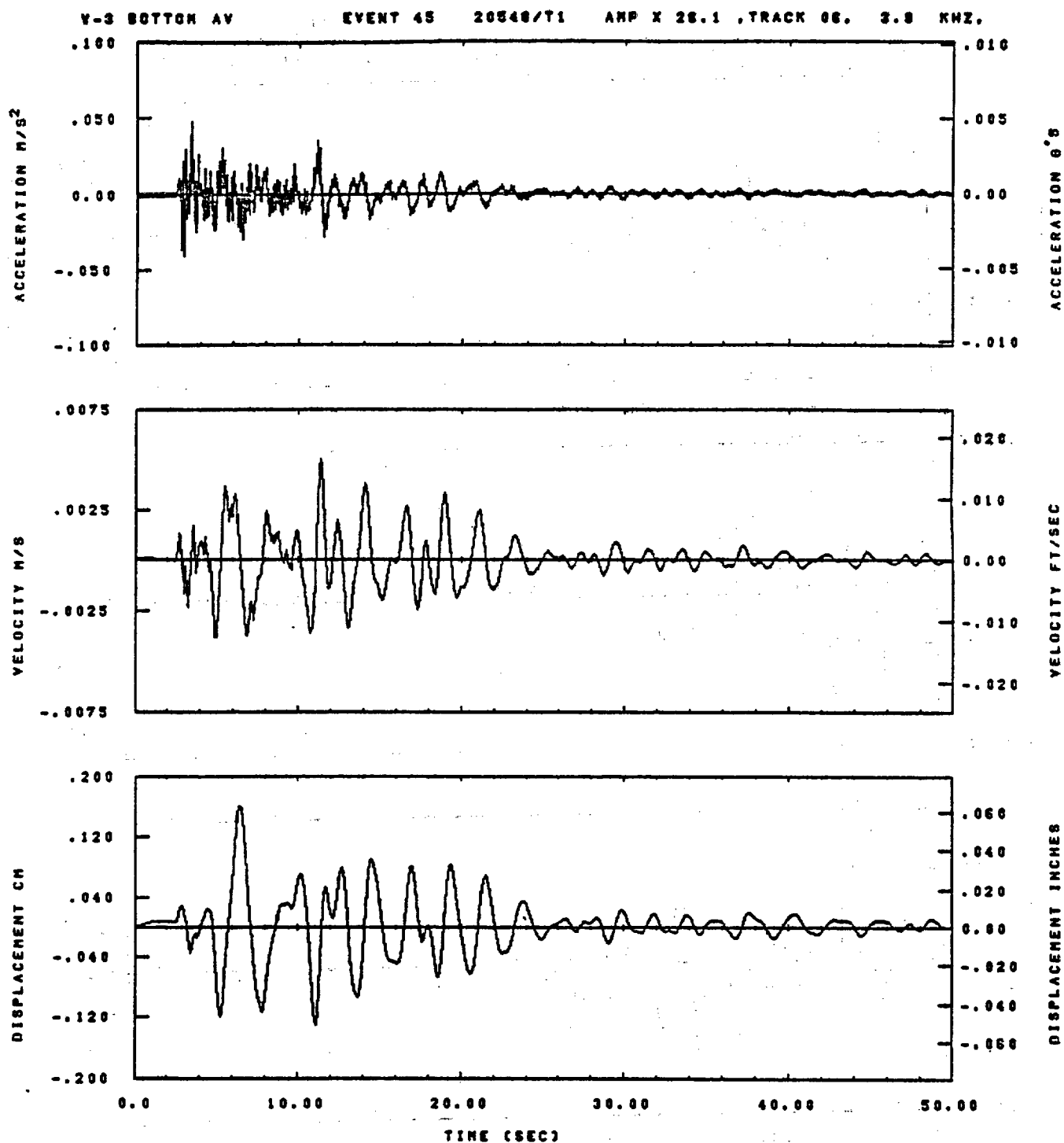


IDT= .0020	QDT= .003	FIX=	AAS= 0.
HPP= .20	BYH= .13	HLH= 33	ASB=
LPP= 45.	BYL= 10.	HLL= 2993	ASE=
VTB= .200	VTE= .133	FLL= -20.	VSE= 0.
DPB= 0.	OPE= 100.	FLH= 0	OSE= 0.

09.21.38.

06/23/92

Figure F-61

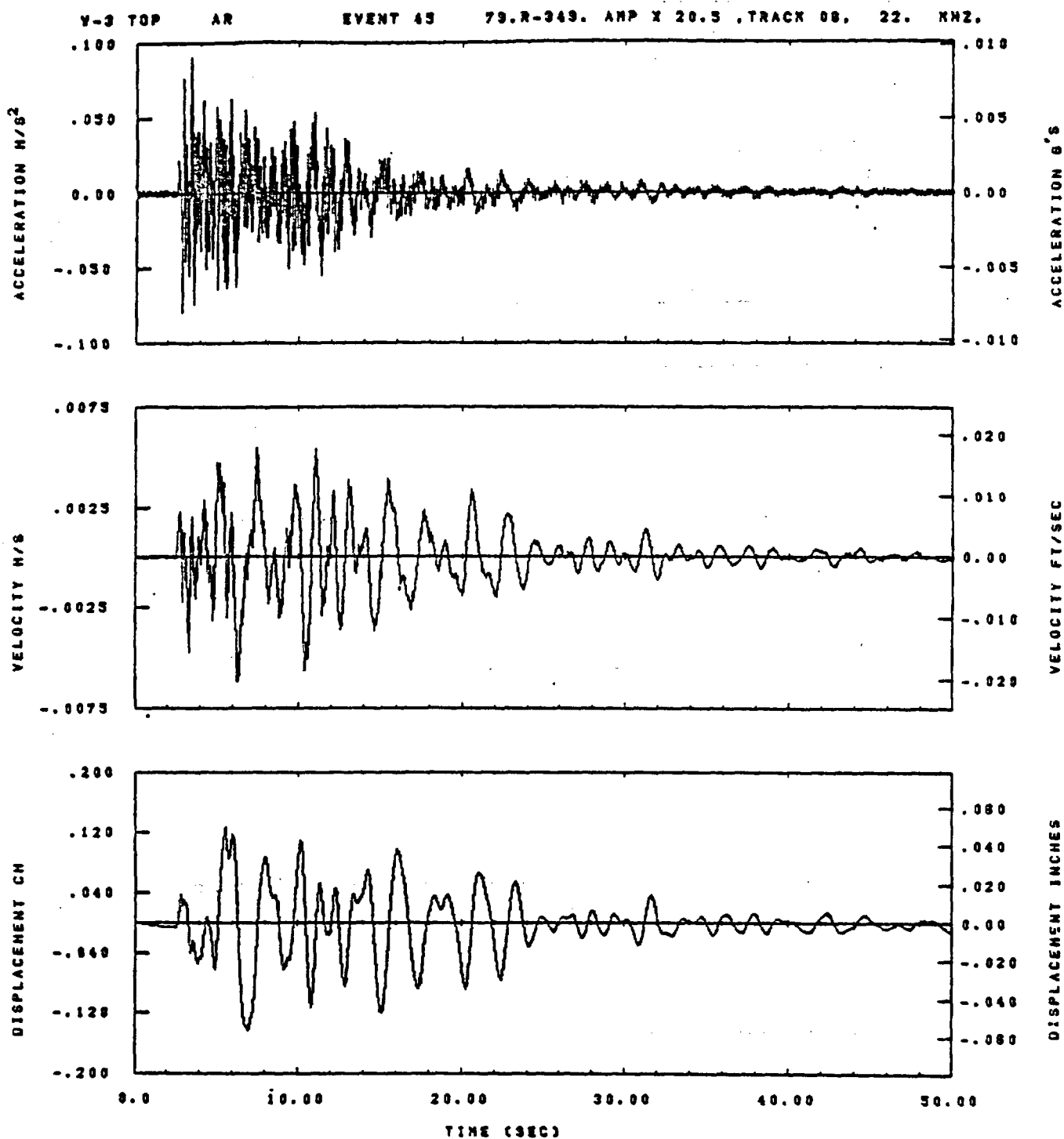


IDT= .0020	ODT= .005	FIX=	AAS= 0.
HPF= .20	BYH= .13	HLH= 99	ASS=
LPF= 45.	BYL= 10.	HLL= 2999	ASE=
VTB= .200	VTE= .133	FLL= -20.	VSE= 0.
OPB= 0.	OPE= 100.	FLH= 0	DSE= 0.

08.22.83.

06/23/82

Figure F-62

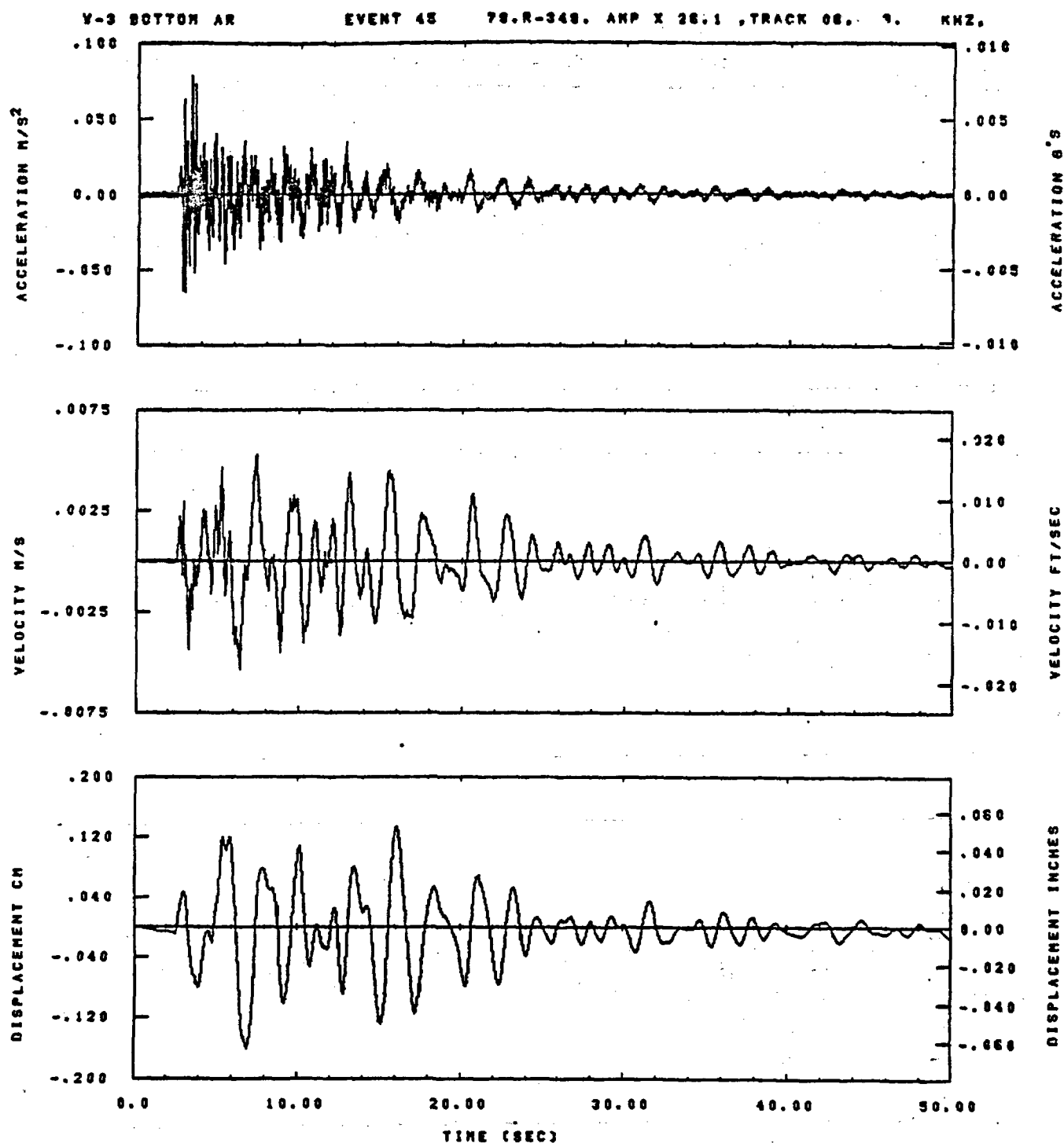


IOT= .0020	OOT= .005	FIX=	AAS= 0.
HPP= .20	BYN= .13	HLH= 99	ASB=
LPP= 43.	BYL= 10.	HLL= 2999	ASE=
VTS= .200	VTE= .133	PLL= -20.	VSE= 0.
OPS= 0.	OPE= 100.	PLH= 0	OSE= 0.

08.21.48.

08/23/92

Figure F-63

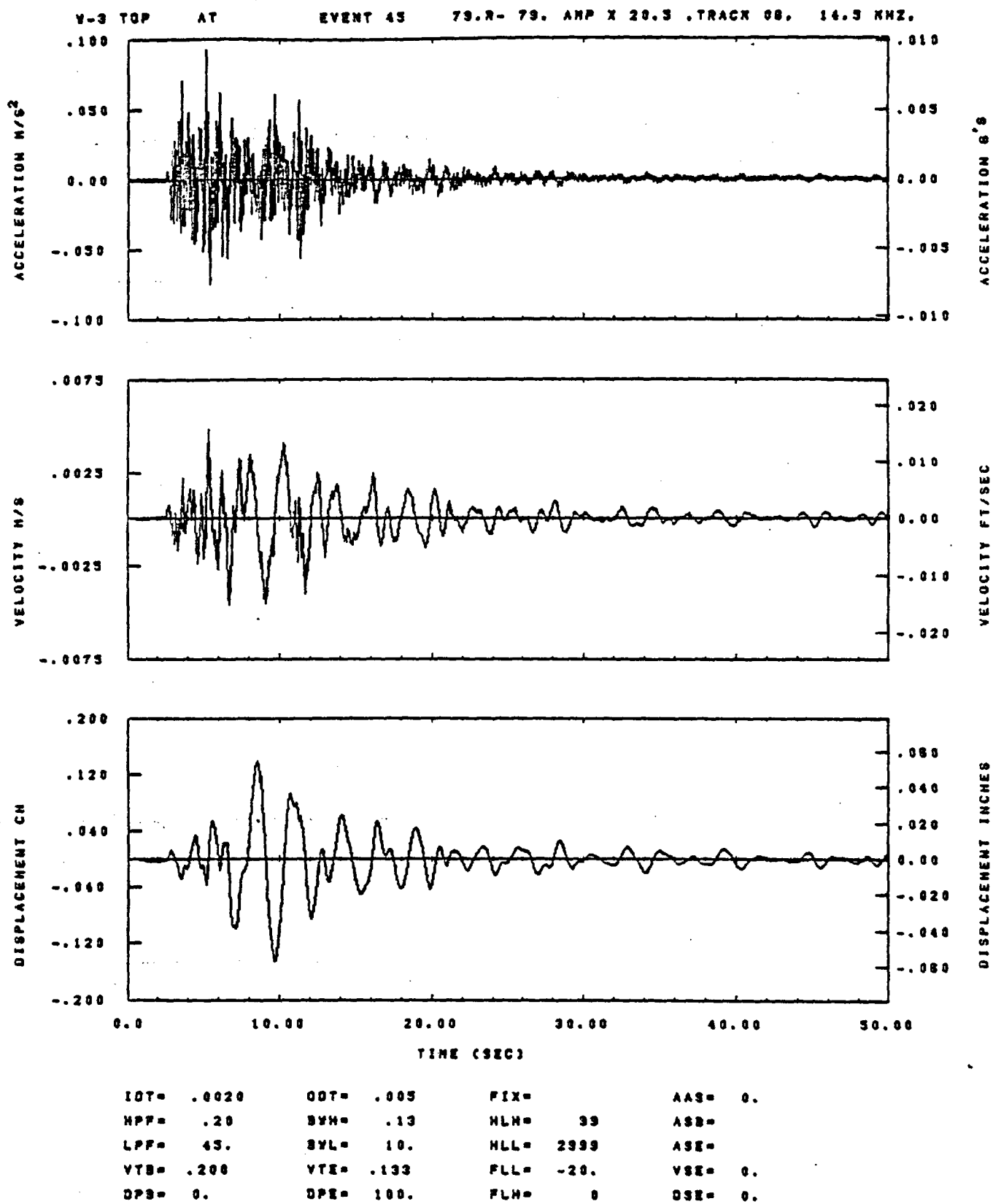


IDT= .0020	ODT= .005	FIX=	AAS= 0.
HFF= .20	BYH= .13	HLH= 99	ASB=
LFF= 45.	BYL= 10.	HLL= 2999	ASE=
VTS= .200	VTE= .133	FLL= -20.	VSE= 0.
DPS= 0.	DPE= 100.	FLH= 0	DSE= 0.

00.22.13.

06/23/82

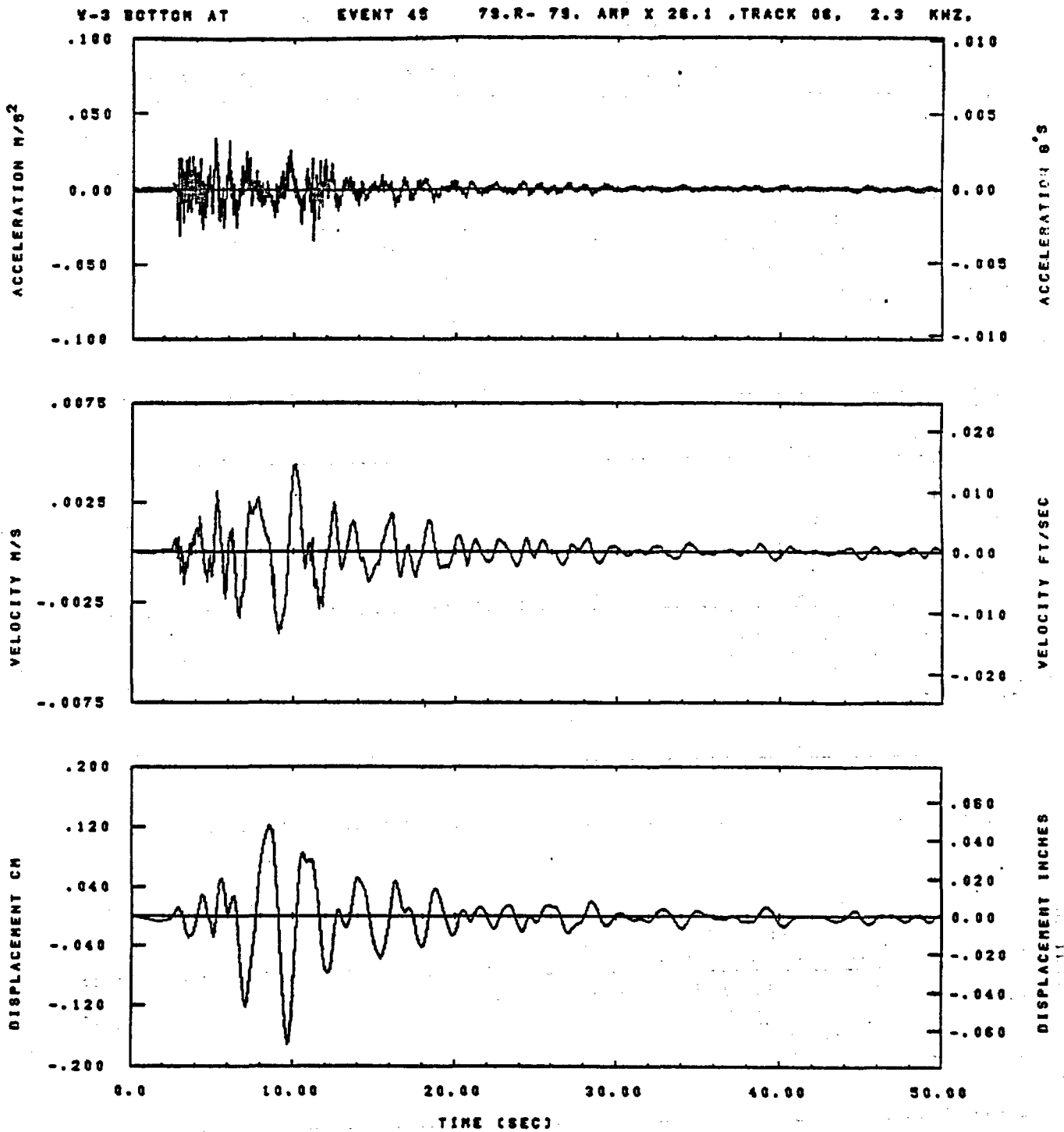
Figure F-64



08.21.55.

08/23/82

Figure F-65

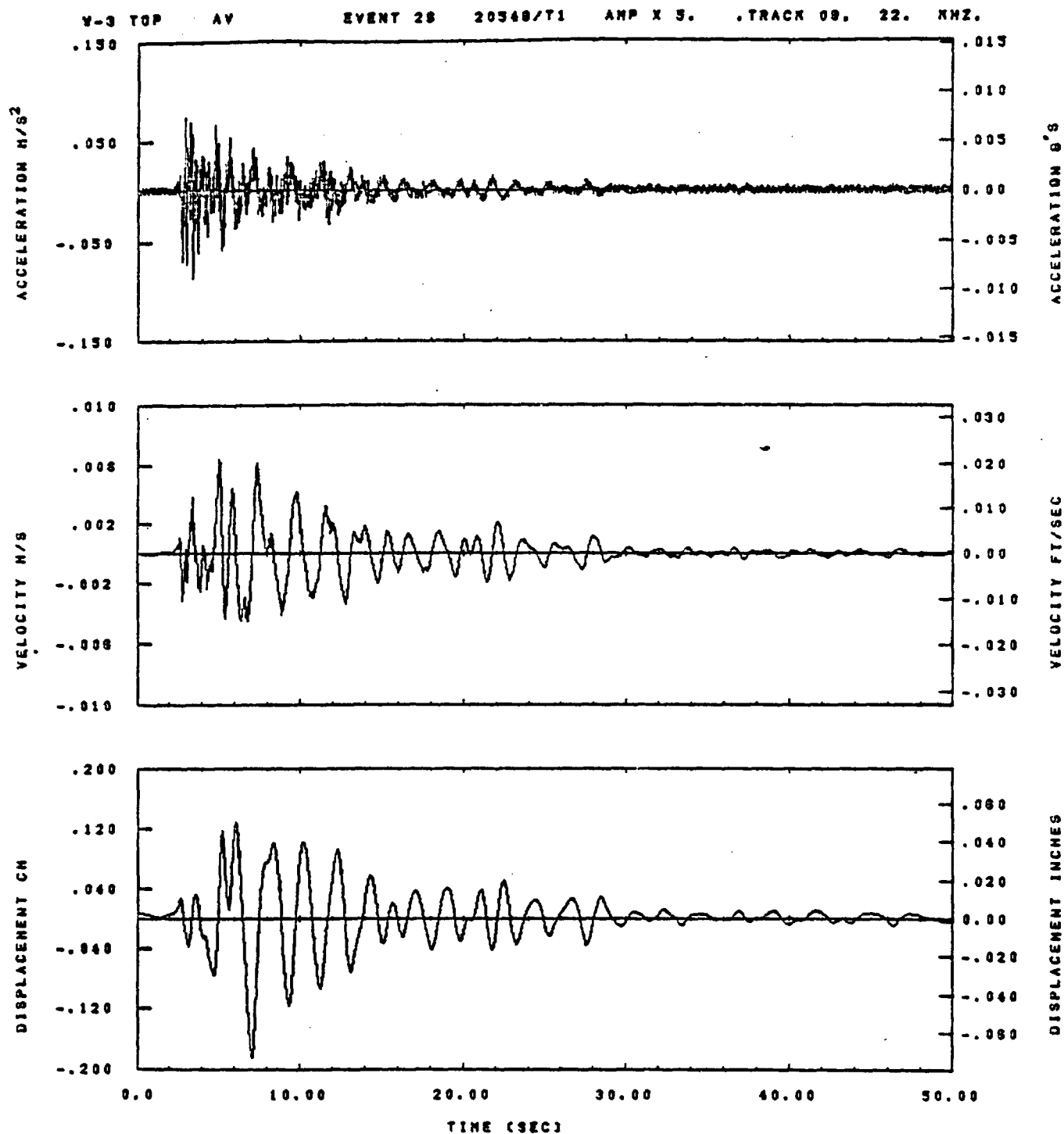


IDT= .0020	QDT= .005	FIX=	AAS= 0.
HPF= .20	BYH= .13	HLH= 99	ASB=
LPF= 45.	BYL= 10.	HLL= 2999	ASE=
YTS= .200	YTE= .133	FLL= -20.	VSE= 0.
DPS= 0.	DPE= 100.	FLH= 0	DSE= 0.

06.22.20.

06/23/82

Figure F-66



IDT= .0020	ODT= .005	FIX=	AAS= 0.
HPP= .20	BYH= .13	HLH= 187	ASB=
LPP= 27.	BYL= 8.	HLL= 2999	ASE=
VTB= .200	VTE= .133	FLL= -20.	VSE= 0.
DPB= 0.	DPE= 100.	FLH= A-.1	DSE= A+.1

08.02.44.

08/25/82

Figure F-67

Y-3 BOTTOM AV

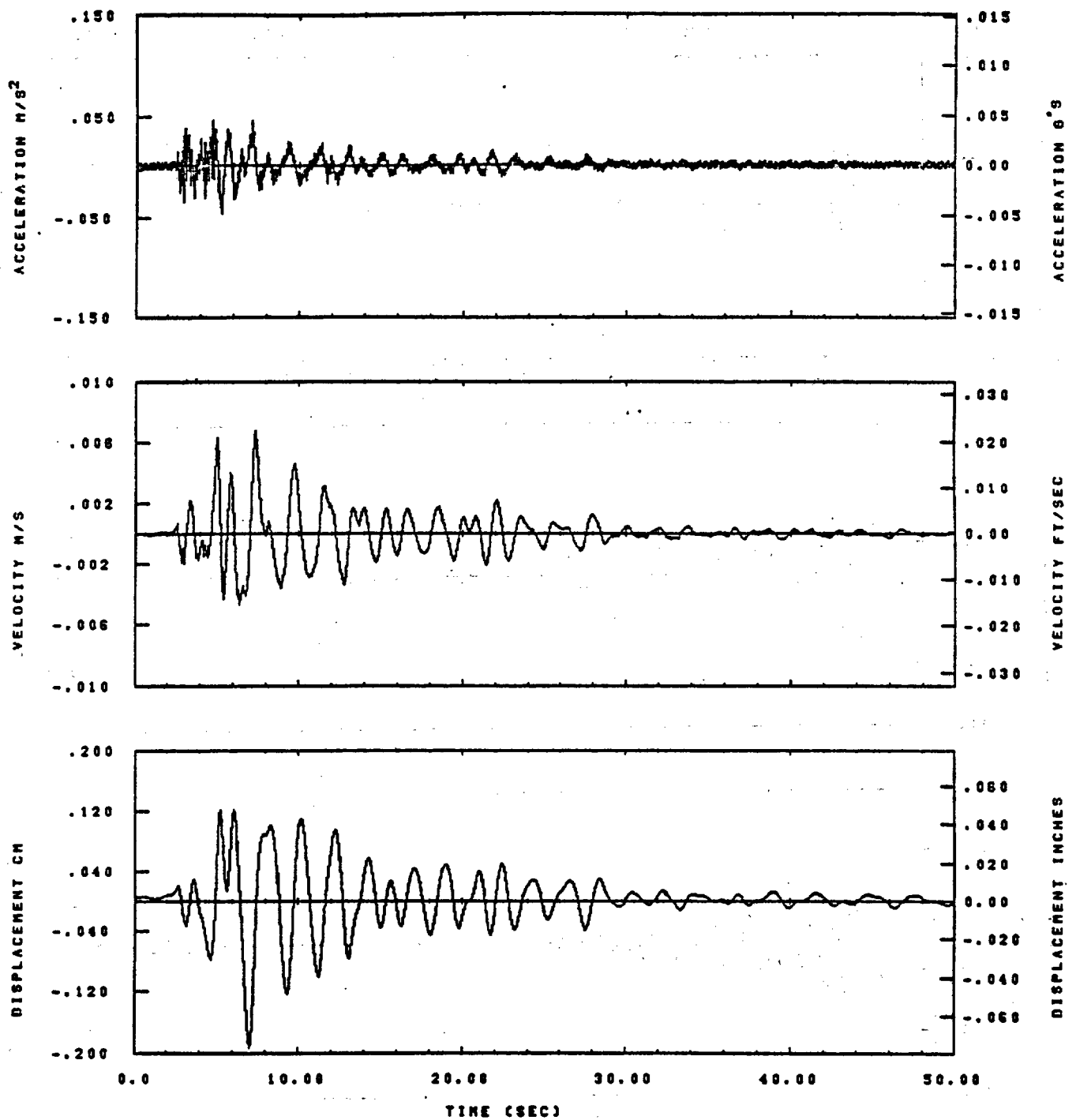
EVENT 26

20348/T1

AMP X 5.

.TRACK 08.

52.7 KHZ.

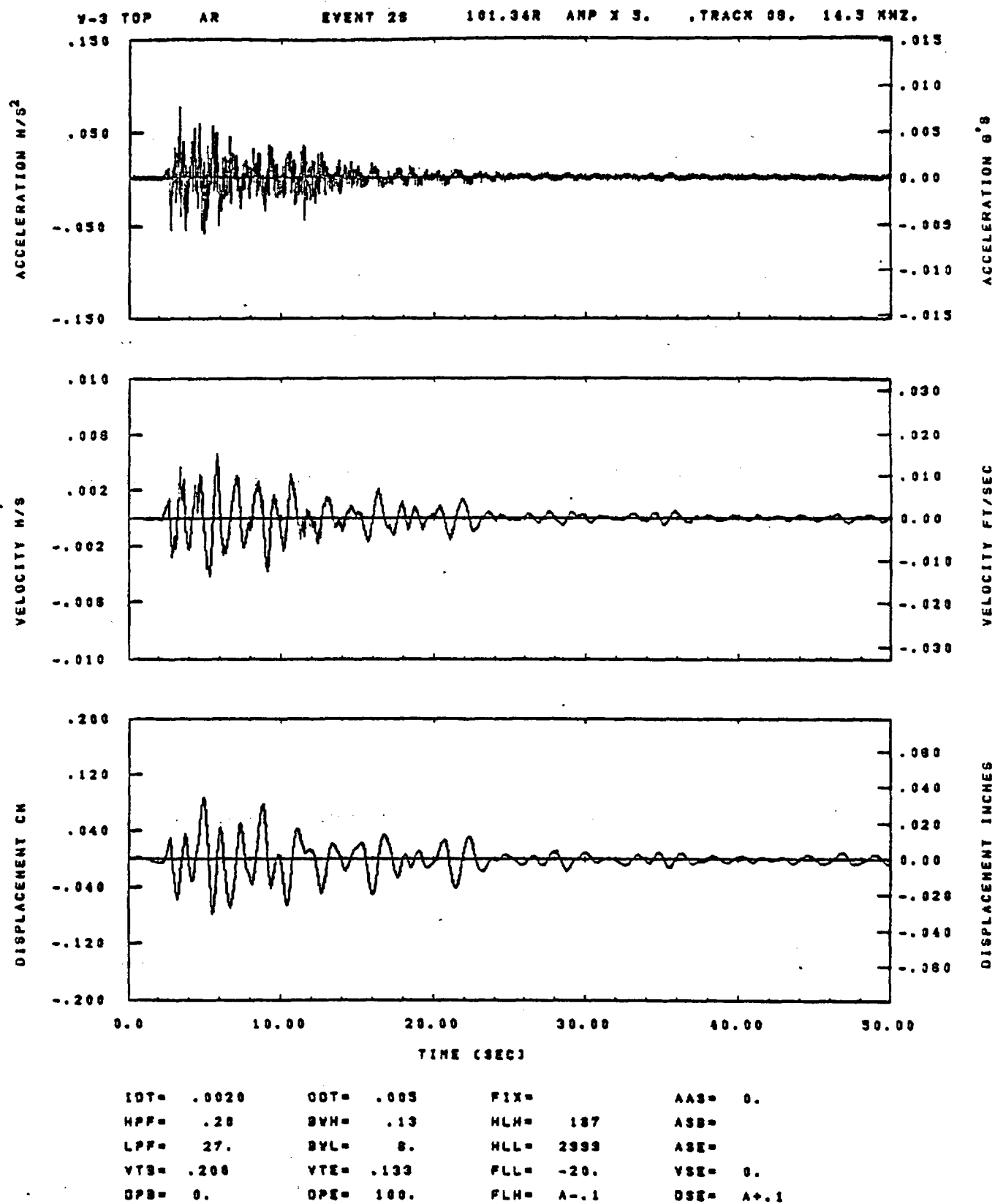


IDT= .0020	ODT= .005	FIX=	AAS= 0.
HPP= .20	BYH= .13	HLH= 167	ASS=
LPP= 27.	BYL= 6.	HLL= 2999	ASE=
VTS= .200	VTE= .133	FLL= -20.	VSE= 0.
DPS= 0.	DPE= 100.	FLH= A-.1	DSE= A+.1

00.04.16.

06/25/82

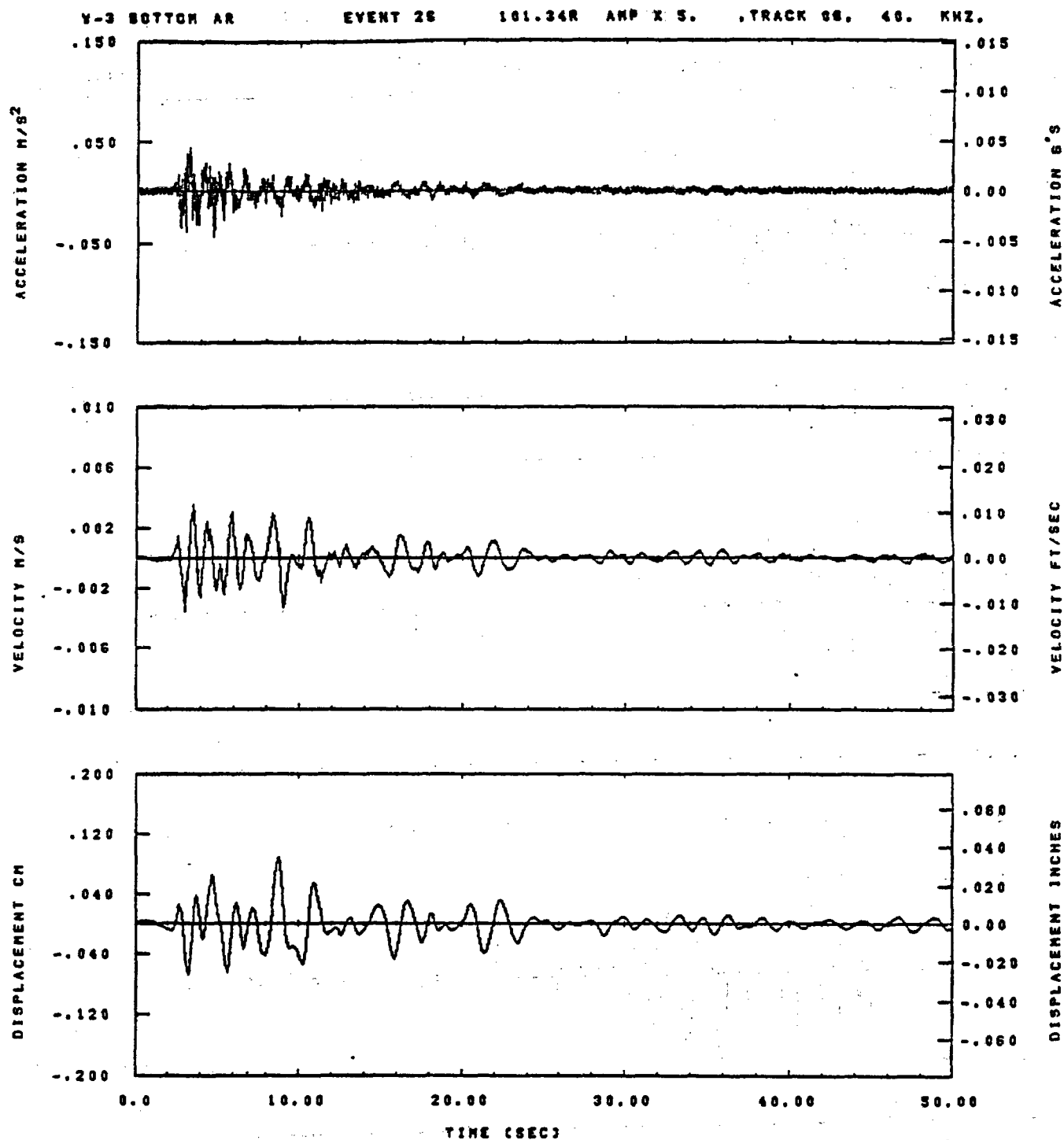
Figure F-68



08.03.18.

08/23/82

Figure F-69

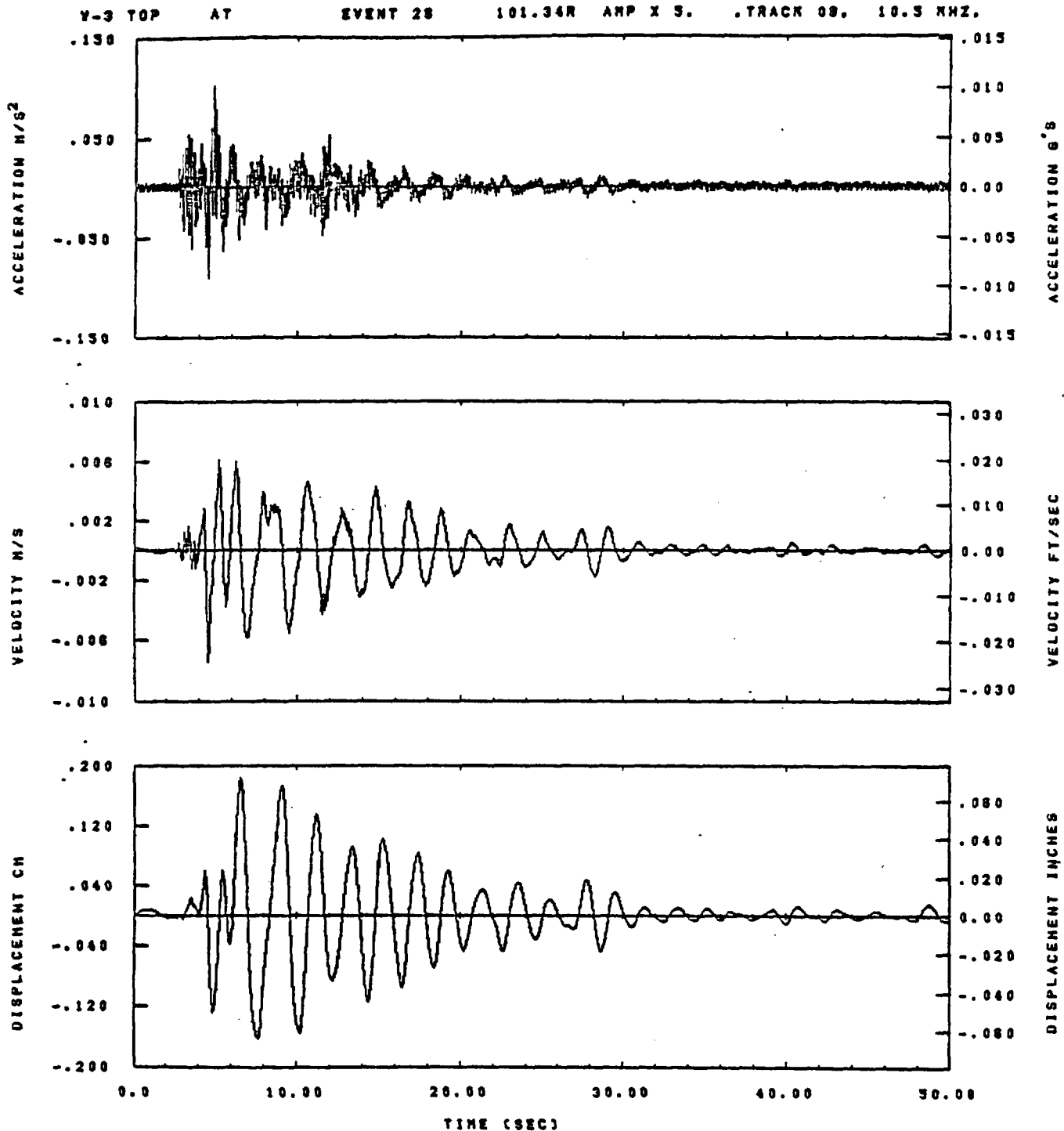


IDT= .0020	ODT= .005	FIX=	AAS= 0.
HPF= .20	BVM= .13	HLH= 167	ASB=
LPF= 27.	BVL= 6.	HLL= 2588	ASE=
VTS= .200	VTE= .133	FLL= -20.	VSE= 0.
DPS= 0.	DPE= 100.	PLH= A-.1	DSE= A+.1

08.03.43.

06/25/82

Figure F-70

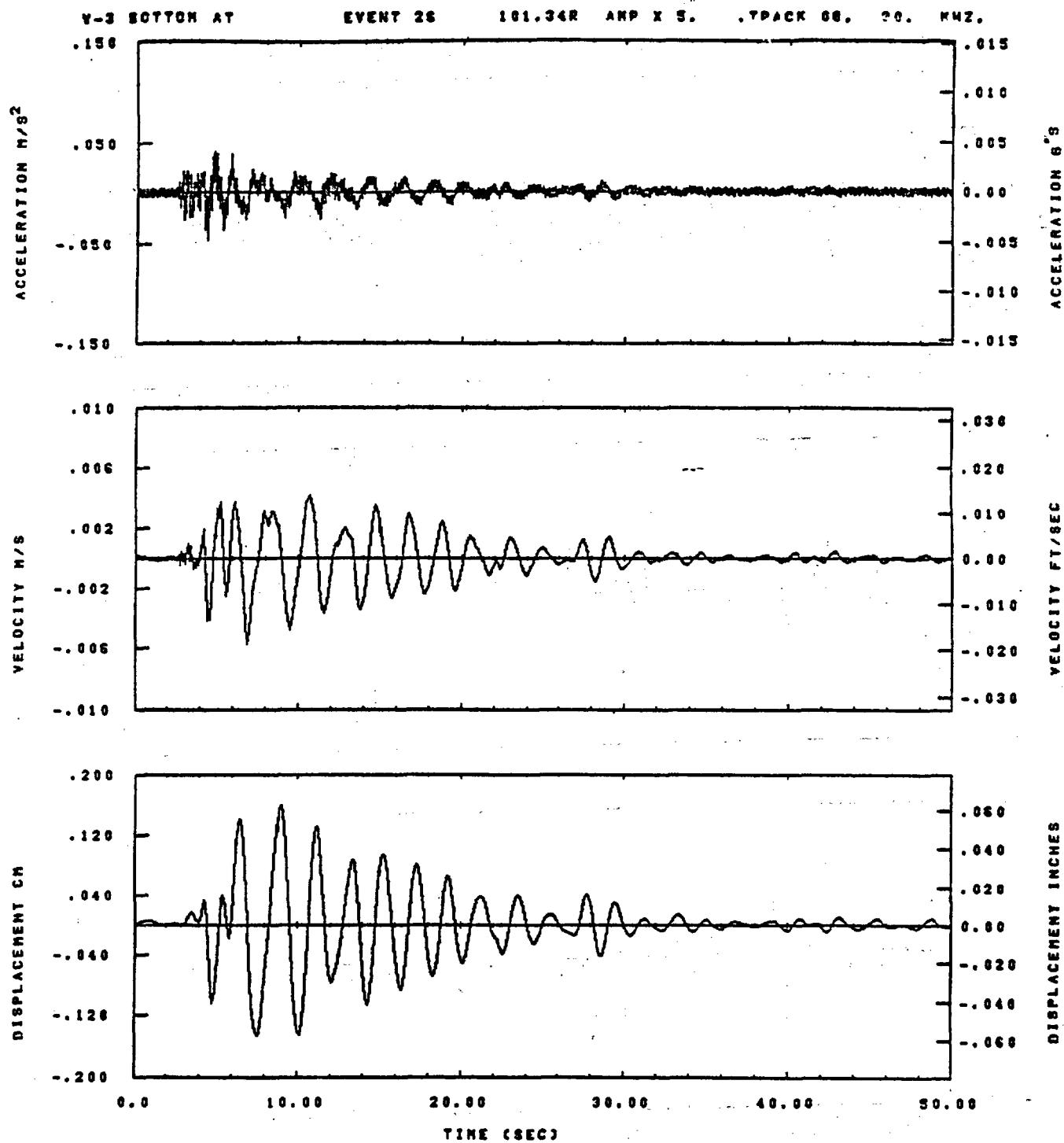


IDT= .0020	ODT= .005	FIX=	AAS= 0.
HPF= .20	BYH= .13	HLH= 187	ASB=
LPF= 27.	BYL= 8.	HLL= 2998	ASE=
VTS= .200	VTE= .133	FLL= -20.	VSE= 0.
DPS= 0.	DPE= 100.	FLH= A+.1	OSE= A+.1

08.03.38.

08/25/82

Figure F-71

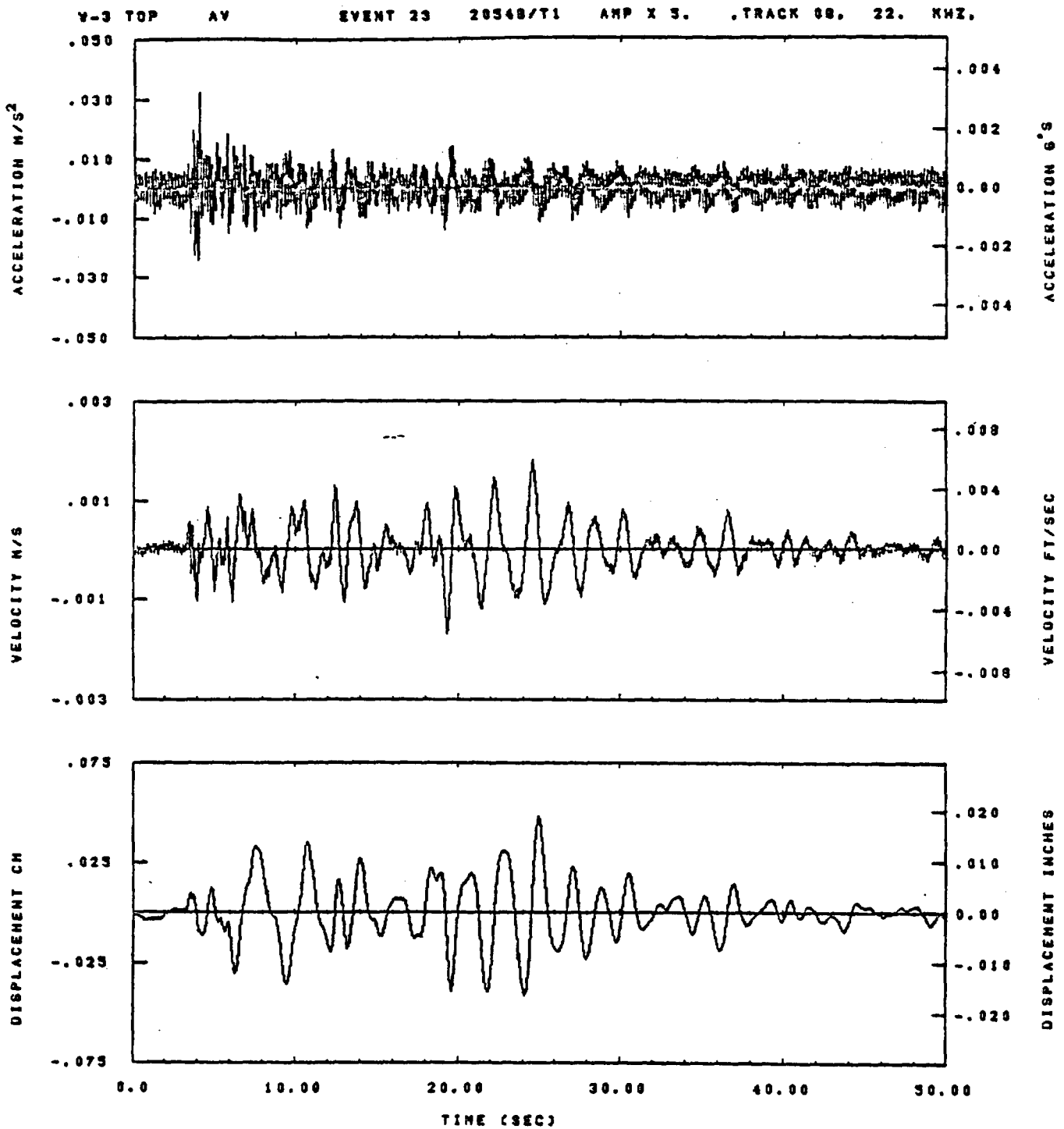


LOT= .0020	ODT= .005	FIX=	AAS= 0.
HPP= .20	BYH= .13	HLH= 167	ASB=
LPP= 27.	BVL= 6.	HLL= 2988	ASE=
YTB= .200	YTE= .133	FLL= -20.	VSE= 0.
DPS= 0.	OPE= 100.	FLH= A-.1	DSE= A+.1

08.04.02.

06/25/82

Figure F-72

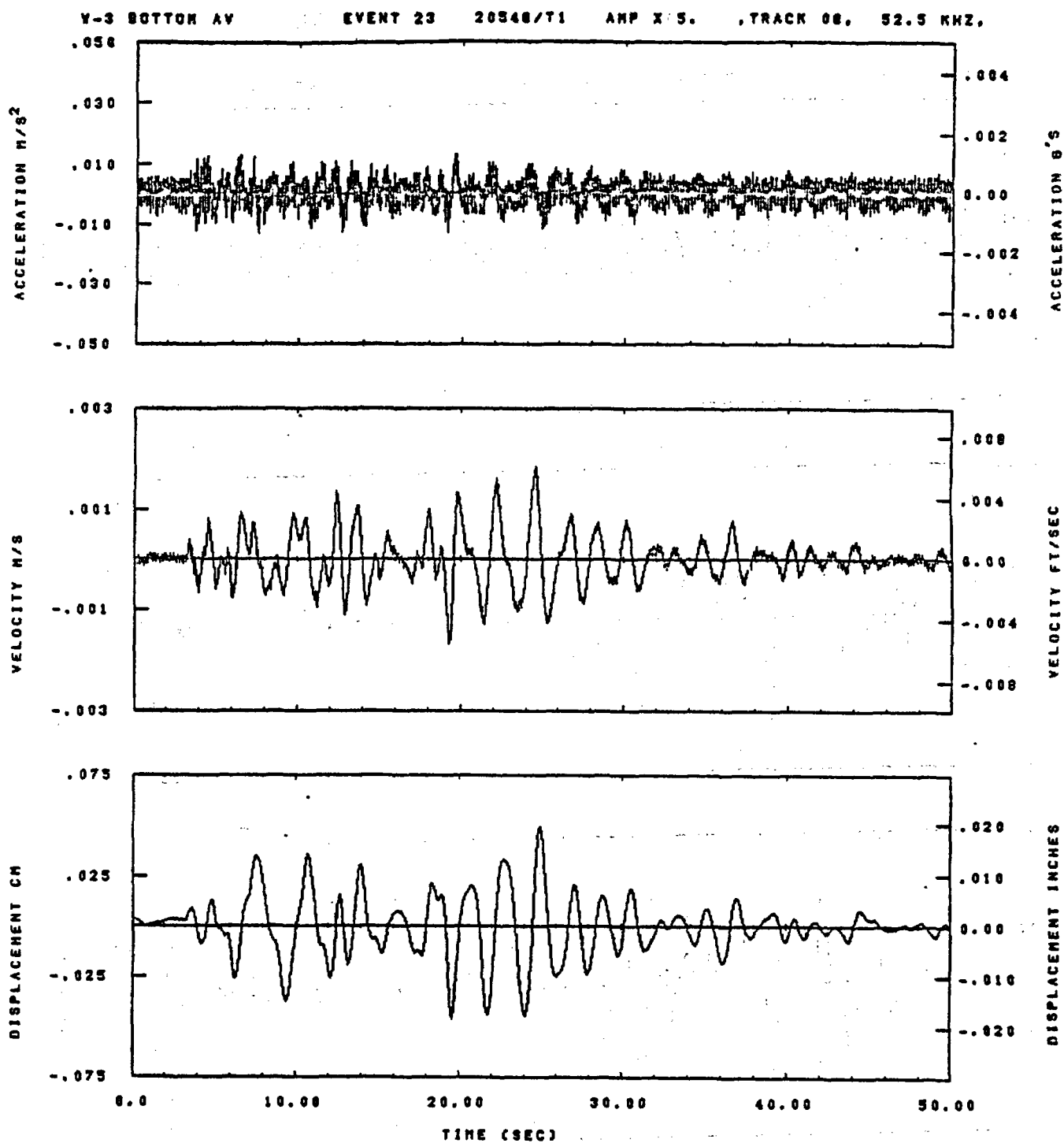


IDT= .0020	ODT= .005	FIX=	AAS= 0.
HPP= .2	BYM= .13	HLH= 201	ASB=
LPP= 22.	BYL= 5.	HLL= 2999	ASE=
VTB= .20	VTE= .133	FLL= -15.	VSE= 0.
DPS= 0.	DPE= 100.	FLH= 0	DSE= 0.

12.02.48.

08/30/92

Figure F-73

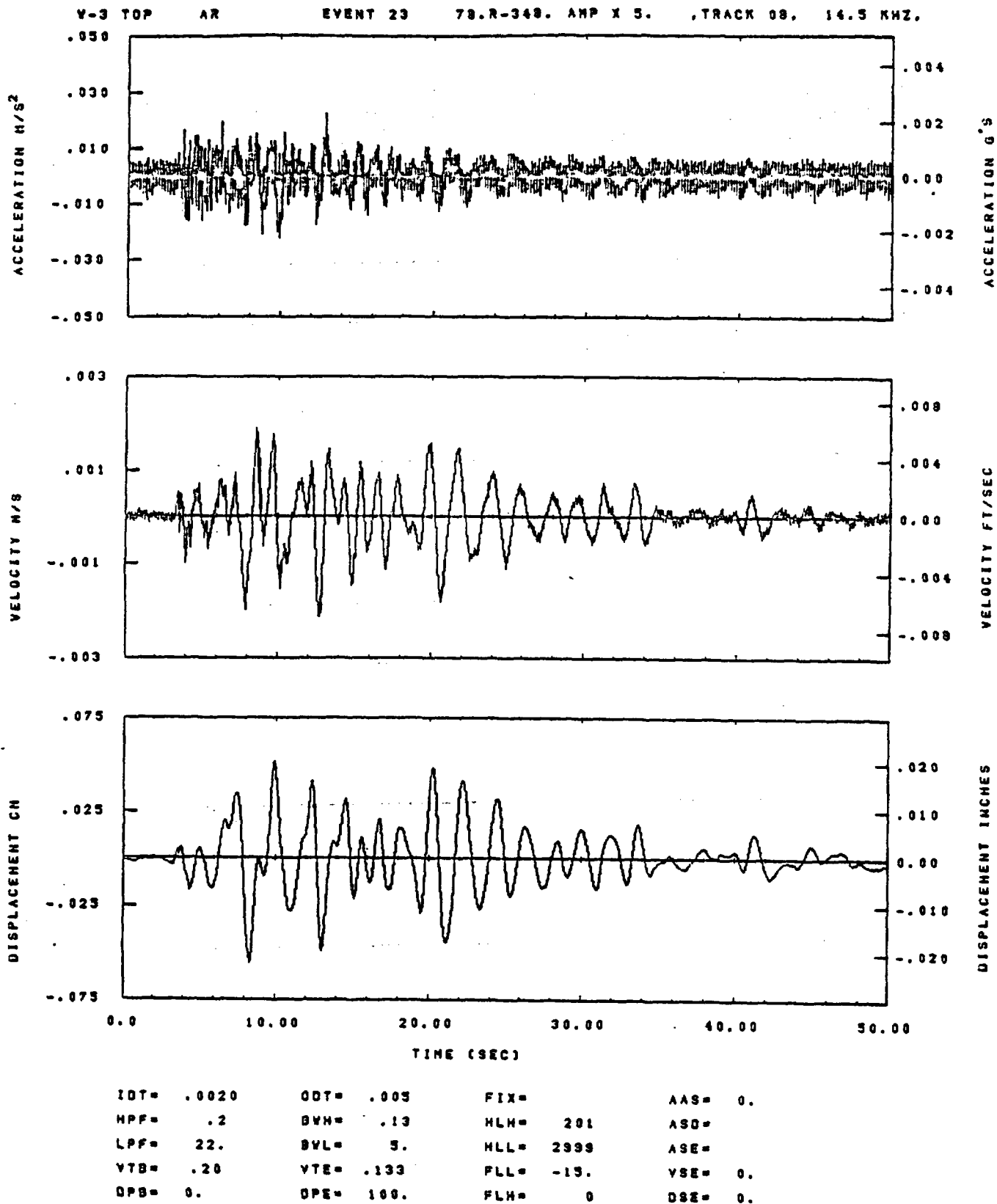


IDT= .0020	ODT= .005	FIX=	AAS= 0.
HPP= .2	SVH= .13	HLH= 201	ASB=
LPP= 22.	SVL= 5.	HLL= 2388	ASE=
VTB= .20	VTE= .133	PLL= -20.	VSE= 0.
OPB= 0.	OPE= 100.	FLH= 0	DSE= 0.

12.02.56.

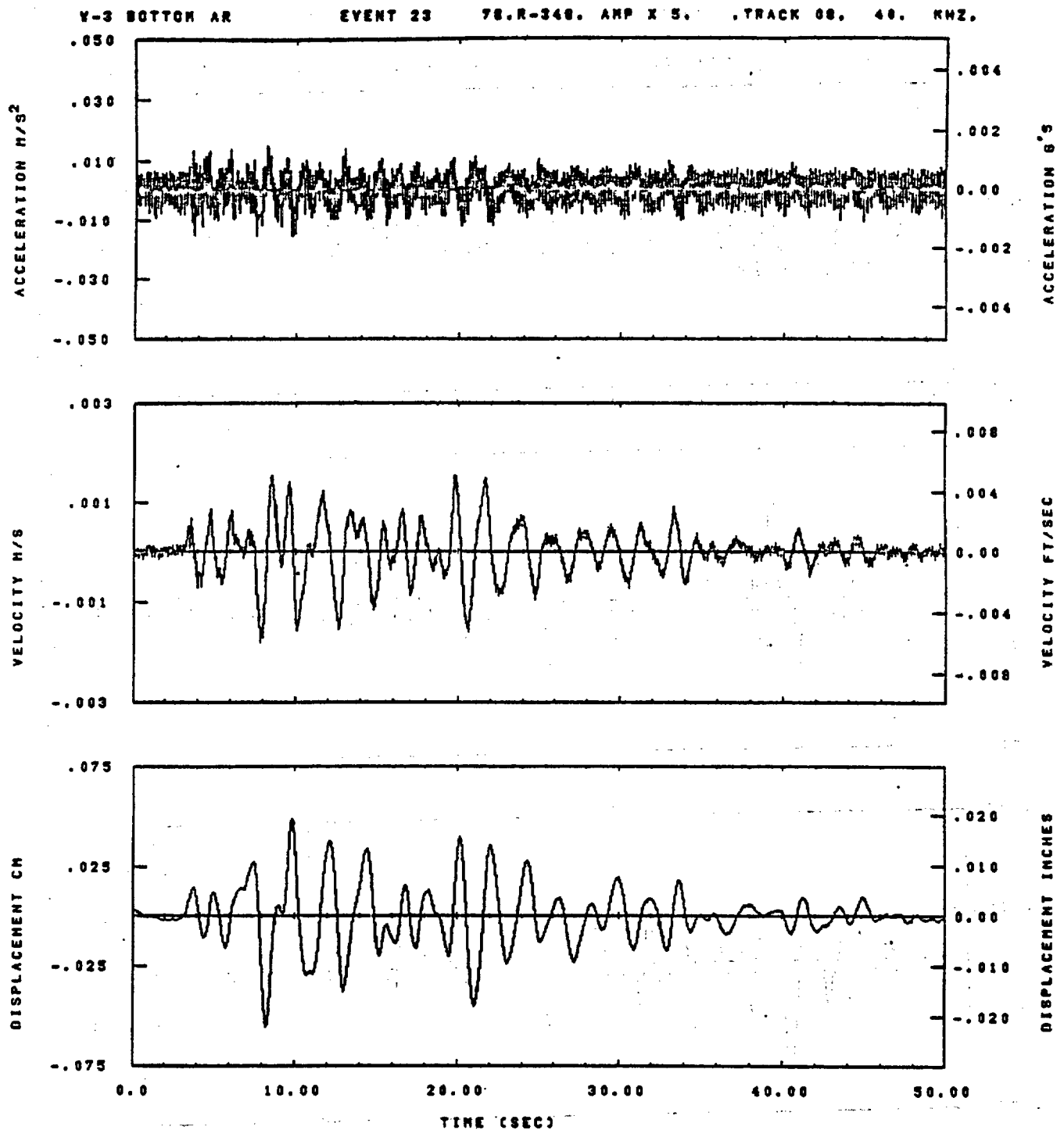
06/30/82

Figure F-74



12.03.08.

08/30/82

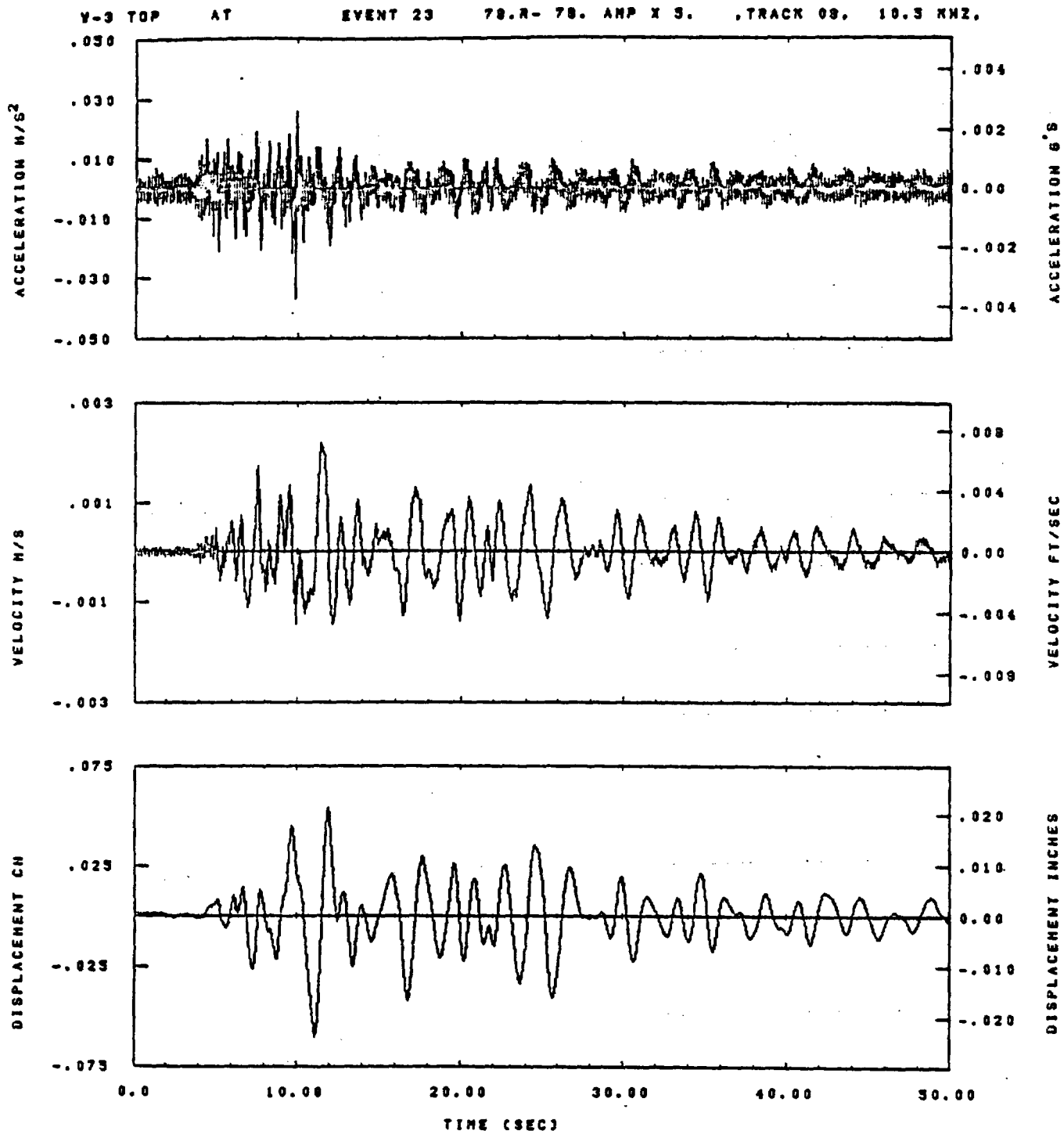


IDT= .0020	ODT= .005	FIX=	AAS= 0.
HPF= .2	SVH= .13	HLH= 201	ASB=
LPF= 22.	SVL= 5.	HLL= 2988	ASE=
VTB= .20	VTE= .133	PLL= -20.	VSE= 0.
DPS= 0.	DPE= 100.	FLH= 0	DSE= 0.

12.03.18.

06/30/82

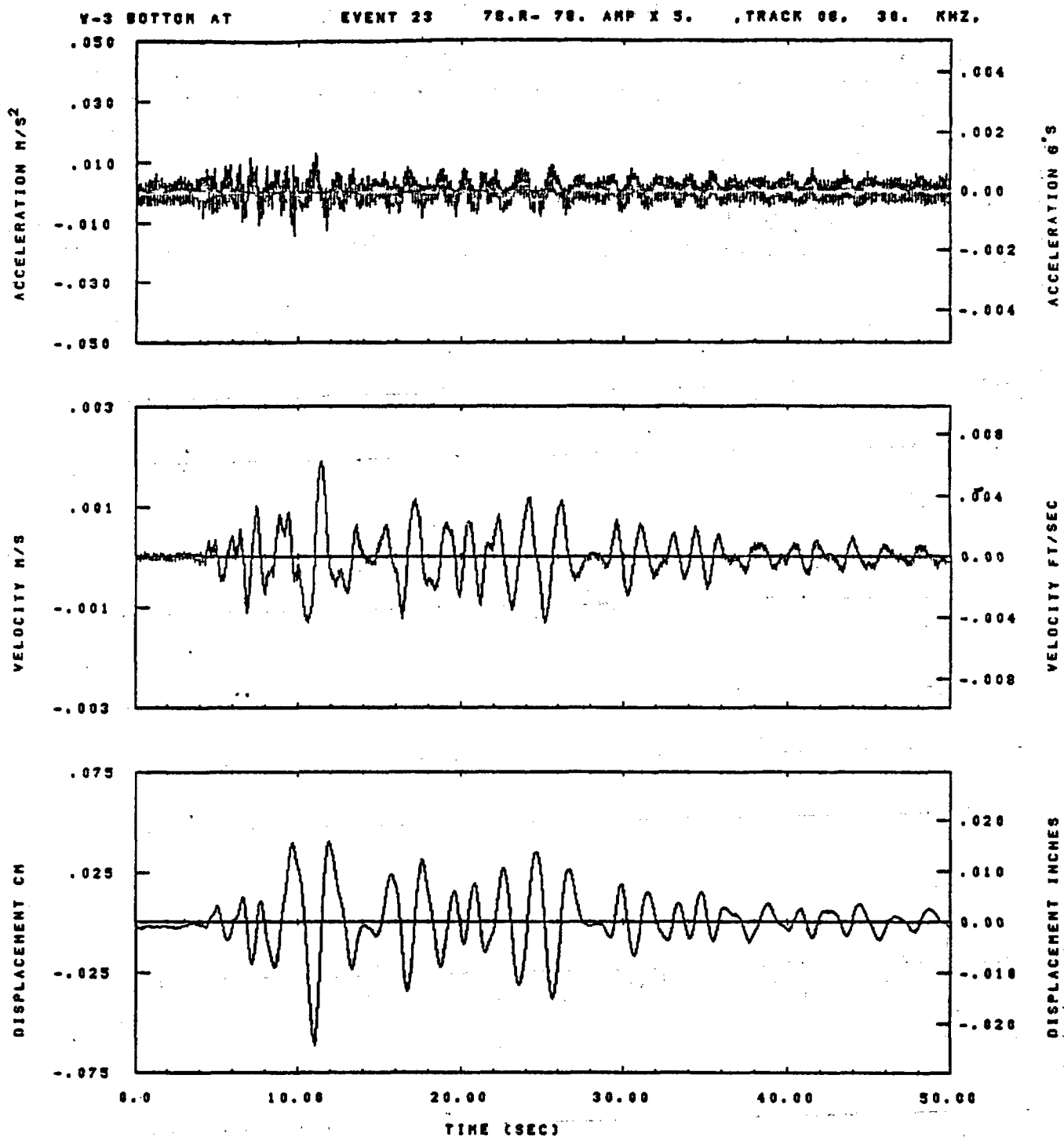
Figure F-76



IDT= .0020	ODT= .005	FIX=	AAS= 0.
HPF= .2	SVH= .13	HLH= 201	ASS=
LPF= 22.	SVL= 5.	HLL= 2999	ASE=
VTS= .20	VTE= .133	FLL= -15.	VSE= 0.
DPS= 0.	DPE= 100.	PLH= 0	DSE= 0.

12.03.31.

08/30/82

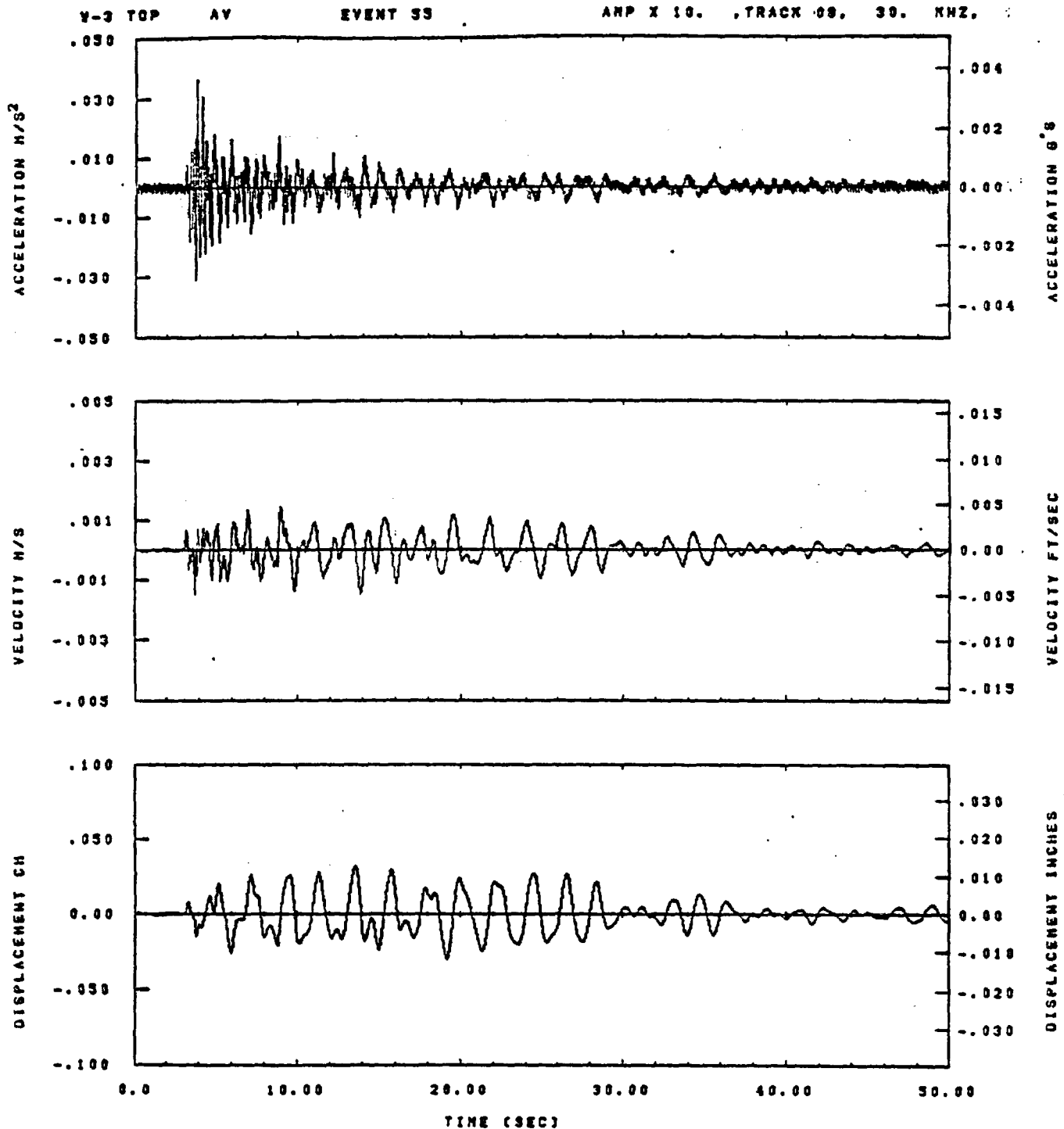


IDT= .0020	ODT= .005	FIX=	AAS= 0.
HPF= .2	BYM= .13	HLH= 201	AGB=
LPP= 22.	BYL= 5.	HLL= 2999	ASE=
VTB= .20	YTE= .133	FLL= -20.	VSE= 0.
DPS= 0.	DPE= 100.	FLH= 0	DSE= 0.

12.04.12.

06/30/82

Figure F-78

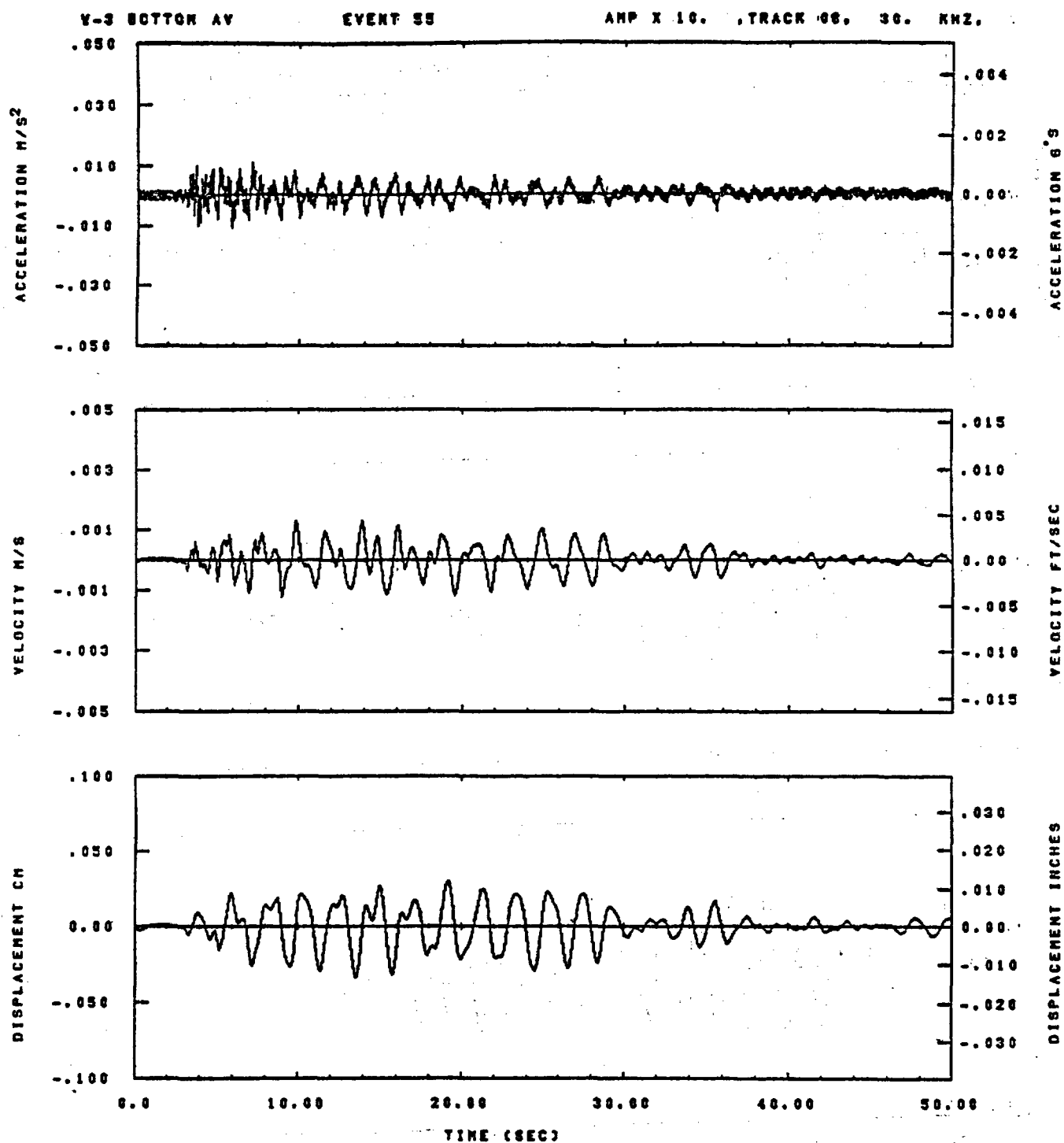


IDT= .0020	ODT= .0	FIX=	AAS=
HPP= .4	BYH= .28	HLH= 187	ASB=
LPP= 27.	BYL= 8.	HLL= 1493	ASE=
VTS= .48	VTE= .287	FLL=	VSE=
DPS=	DPE=	FLH= 0	DSE= 0.

12.24.33.

07/01/82

Figure F-79

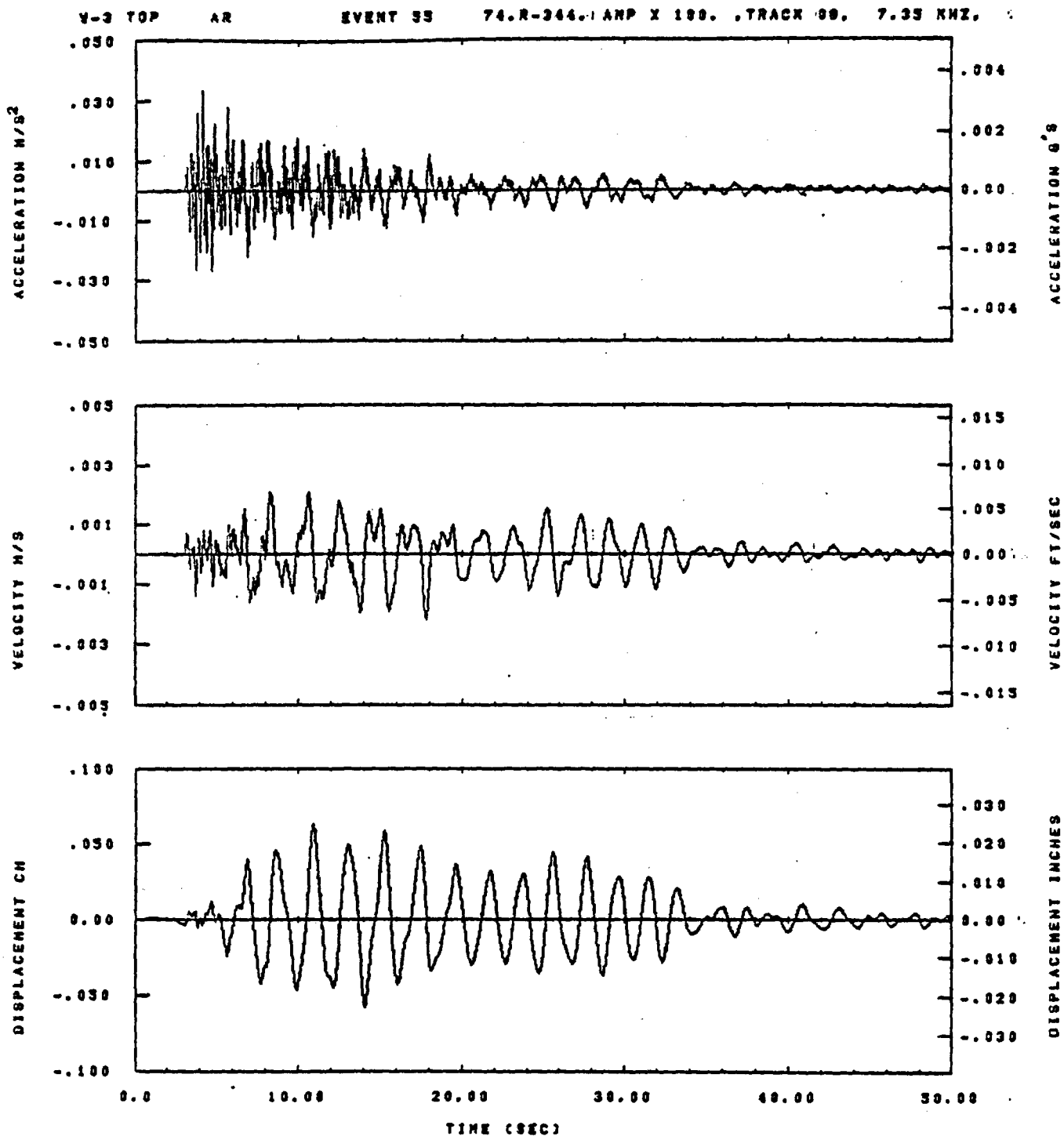


IDT= .0020	ODT= .0	FIX=	AAS=
HPF= .4	BYH= .28	HLH= 167	ASB=
LPF= 27.	BYL= 6.	HLL= 1488	ASE=
VTS= .48	VTE= .287	FLL=	VSE=
DPS=	DPE=	FLH= 0	DSE= 0.

12.24.48.

07/01/82

Figure F-80

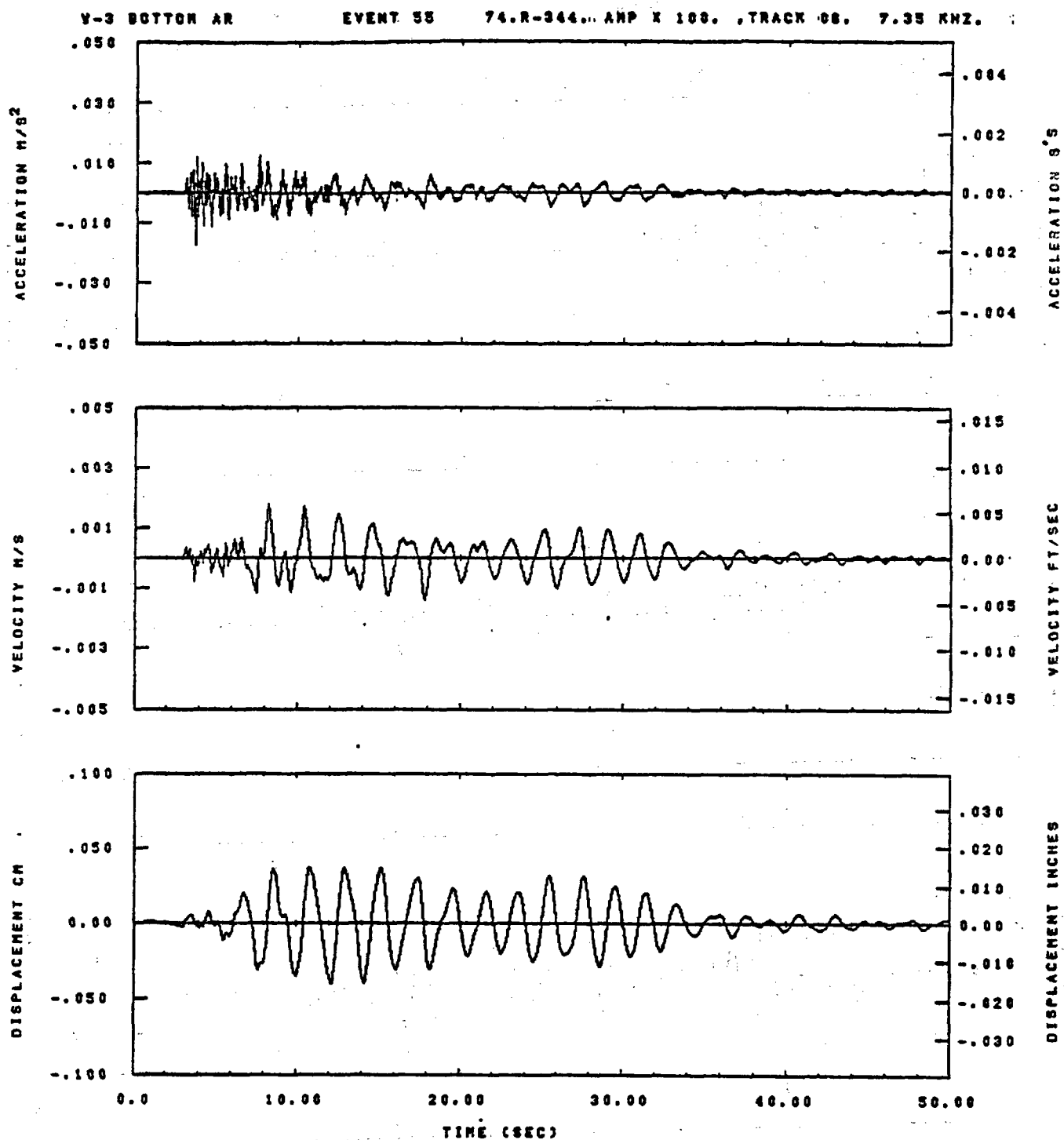


IST=	.0020	QDT=	.0	FIX=		AAS=	
HPP=	.4	SVH=	.28	HLH=	187	ASB=	
LPP=	27.	SVL=	8.	NLL=	1499	ASZ=	
VTS=	.48	VTE=	.287	PLL=		VSE=	
OPS=		OPE=		PLH=	8	OSE=	9.

12.24.99.

07/01/02

Figure F-81

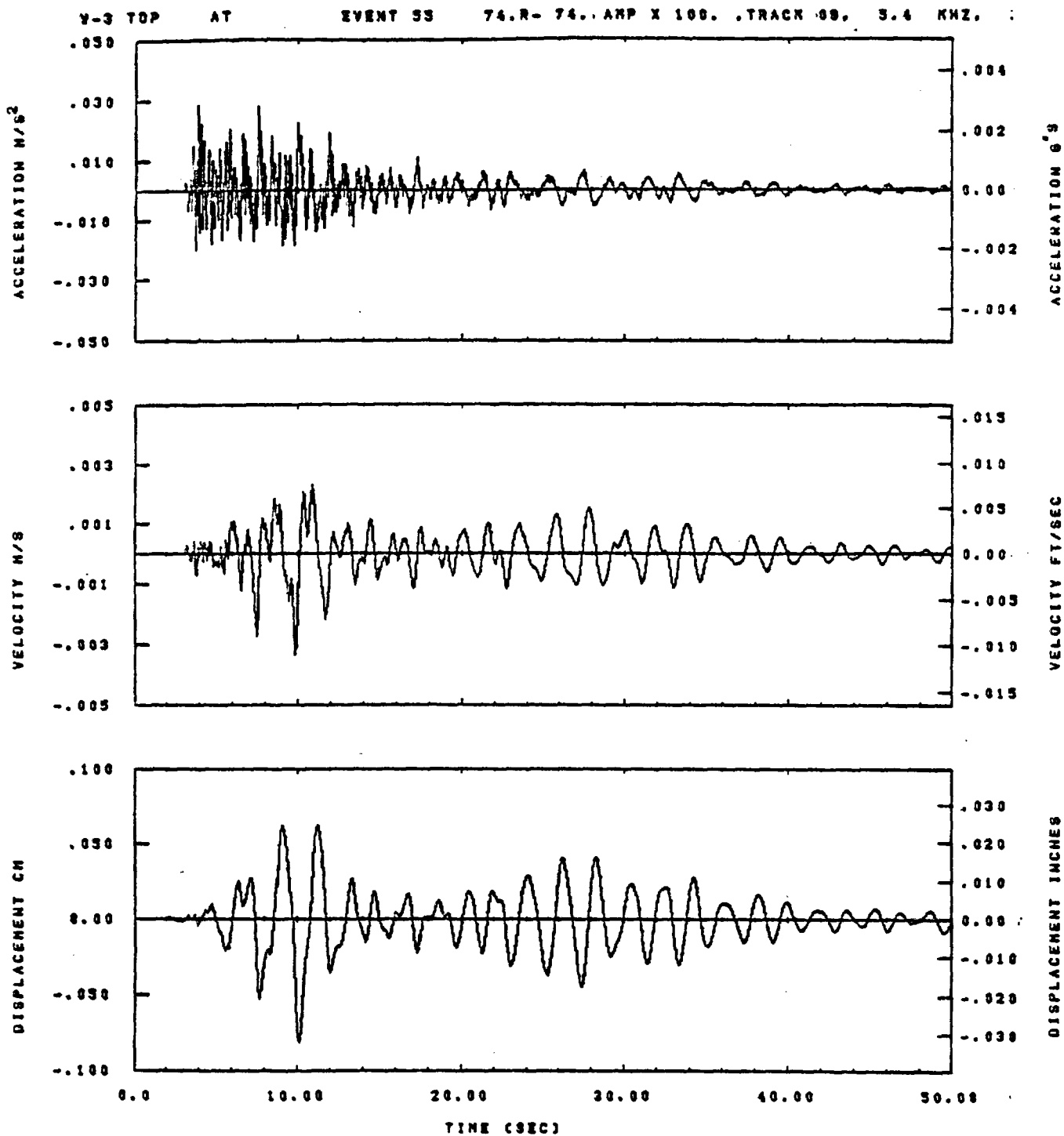


IDT= .0020	ODT= .0	FIX=	AAS=
HPF= .4	SVH= .25	HLH= 167	ASS=
LPF= 27.	BVL= 6.	HLL= 1488	ASE=
VTS= .40	VTE= .267	PLL=	VSE=
DPS=	OPE=	PLH= 0	DSE= 6.

12.25.35.

07/01/82

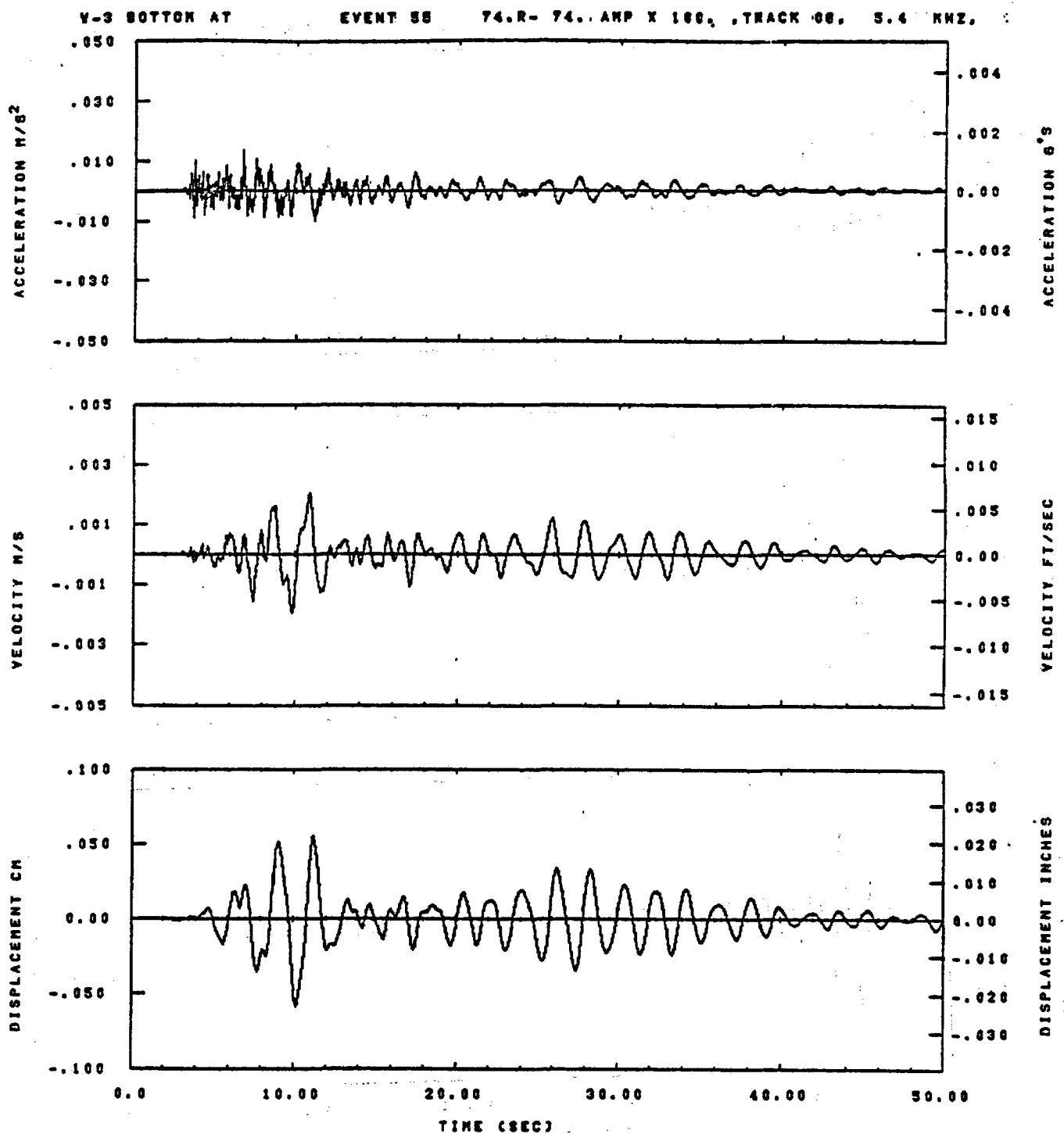
Figure F-82



IDT= .0020	OST= .0	FIX=	AAS=
HFF= .4	BYM= .28	HLH= 187	ASB=
LFF= 27.	BYL= 8.	HLL= 1493	ASZ=
VTB= .40	VTE= .287	PLL=	VSE=
DPS=	DPE=	PLH= 0	DSE= 0.

12.24.43.

07/01/92

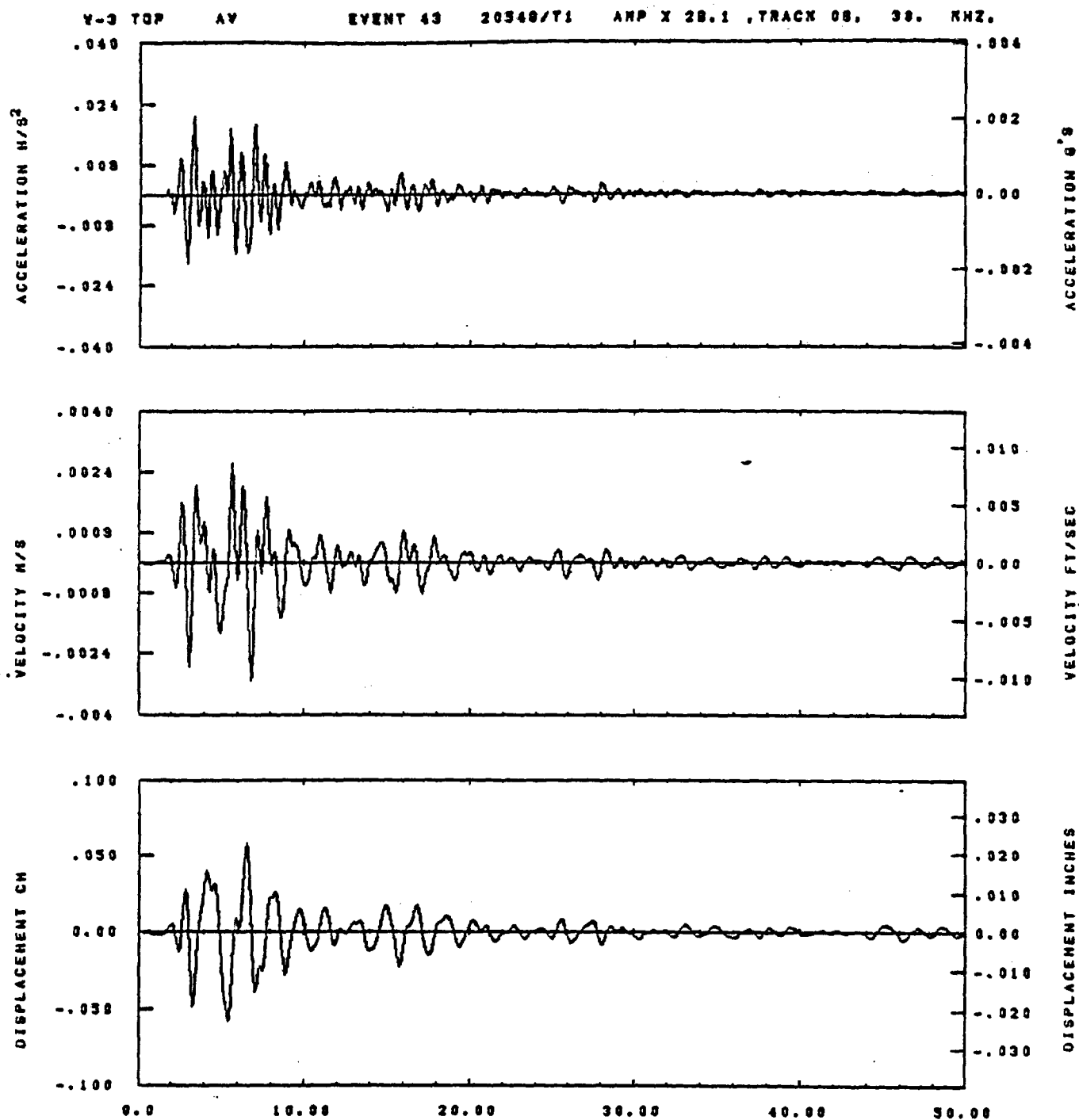


IDT= .0020	ODT= .0	FIX=	AAS=
HPF= .4	BVH= .26	HLH= 167	ASB=
LPF= 27.	BVL= 6.	HLL= 1488	ASE=
VTE= .48	VTE= .267	FLL=	VSE=
DPS=	DPE=	FLH= 0	DSE= 0.

12.25.47.

07/01/82

Figure F-84

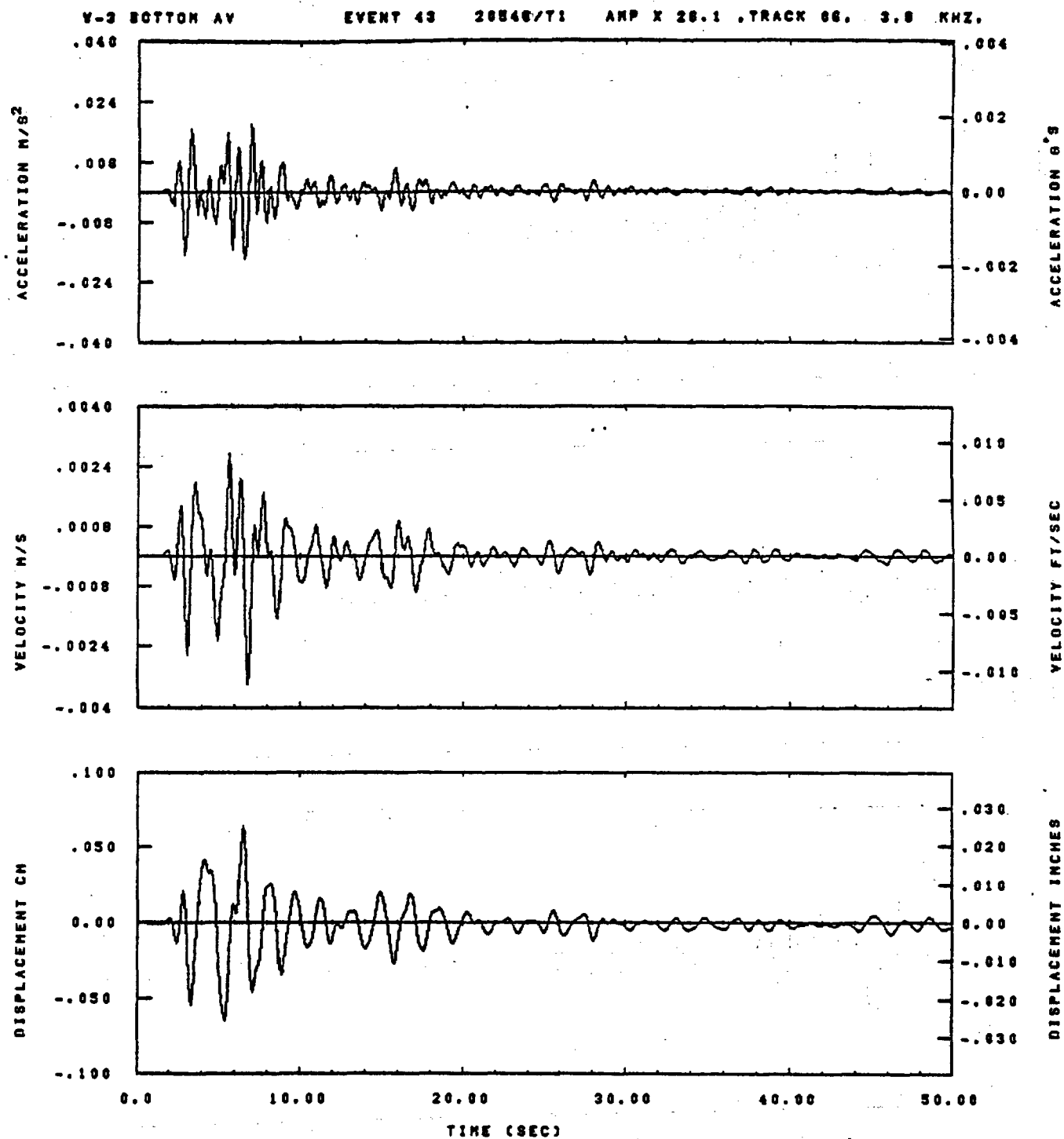


IDT= .0020	ODT=	FIX=	AAS= 0.
HPP= .20	BYH= .13	HLH= 417.	ASB=
LPP= 10.	BYL= 2.	HLL= 2889	ASE=
VTB= .280	VTE= .133	FLL= -20.	VSE= 0.
DPS= 0.	DPE= 100.	FLH= 0	DSE= 0.

10.47.17.

08/23/82

Figure F-85

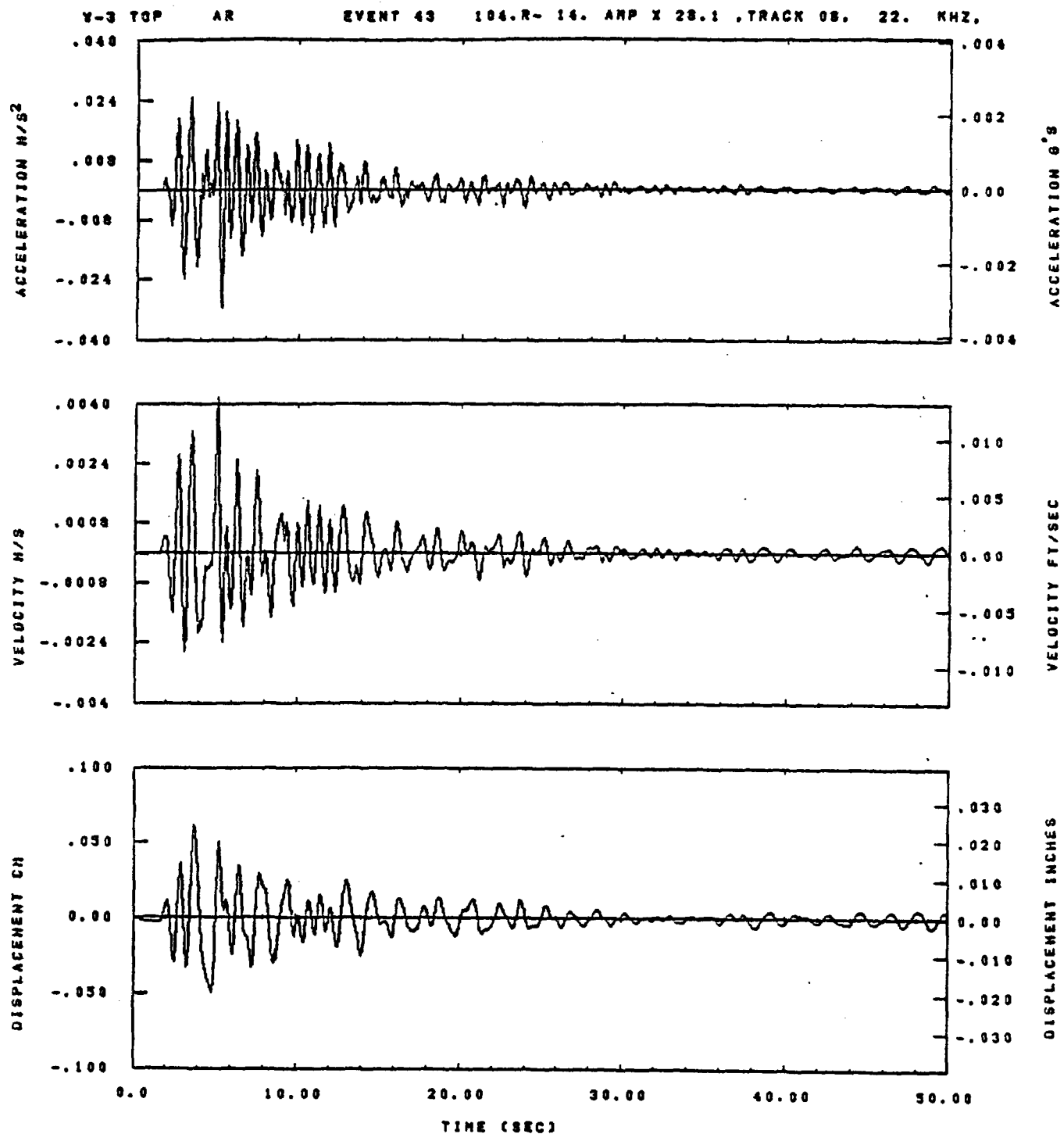


IDT= .0028	QDT=	FIX=	AAS= 0.
HPF= .20	SVH= .13	HLH= 417	ASB=
LPF= 10.	SVL= 2.	HLL= 2999	ASE=
VTB= .200	VTE= .133	FLL= -20.	VSE= 0.
OPB= 0.	DPE= 100.	FLH= 0	DSE= 0.

10.47.36.

06/23/82

Figure F-86

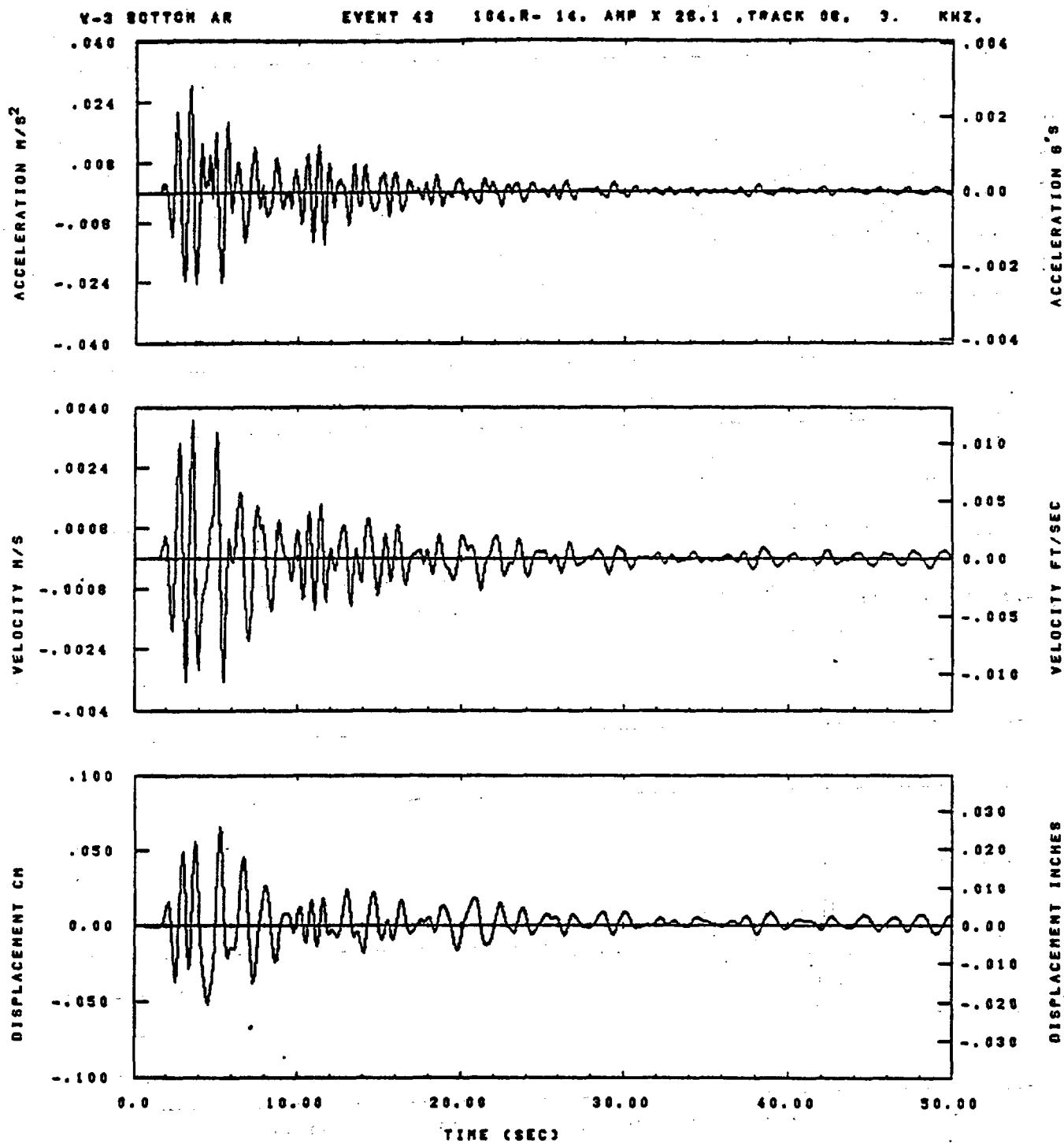


IDT= .0020	ODT=	FIX=	AAS= 0.
HPF= .20	BYH= .13	HLH= 417	ASB=
LPP= 10.	BYL= 2.	HLL= 2999	ASE=
VTS= .200	VTE= .133	FLL= -20.	VSE= 0.
OPS= 0.	OPE= 100.	FLH= 0	OSE= 0.

10.47.23.

08/23/82

Figure F-87

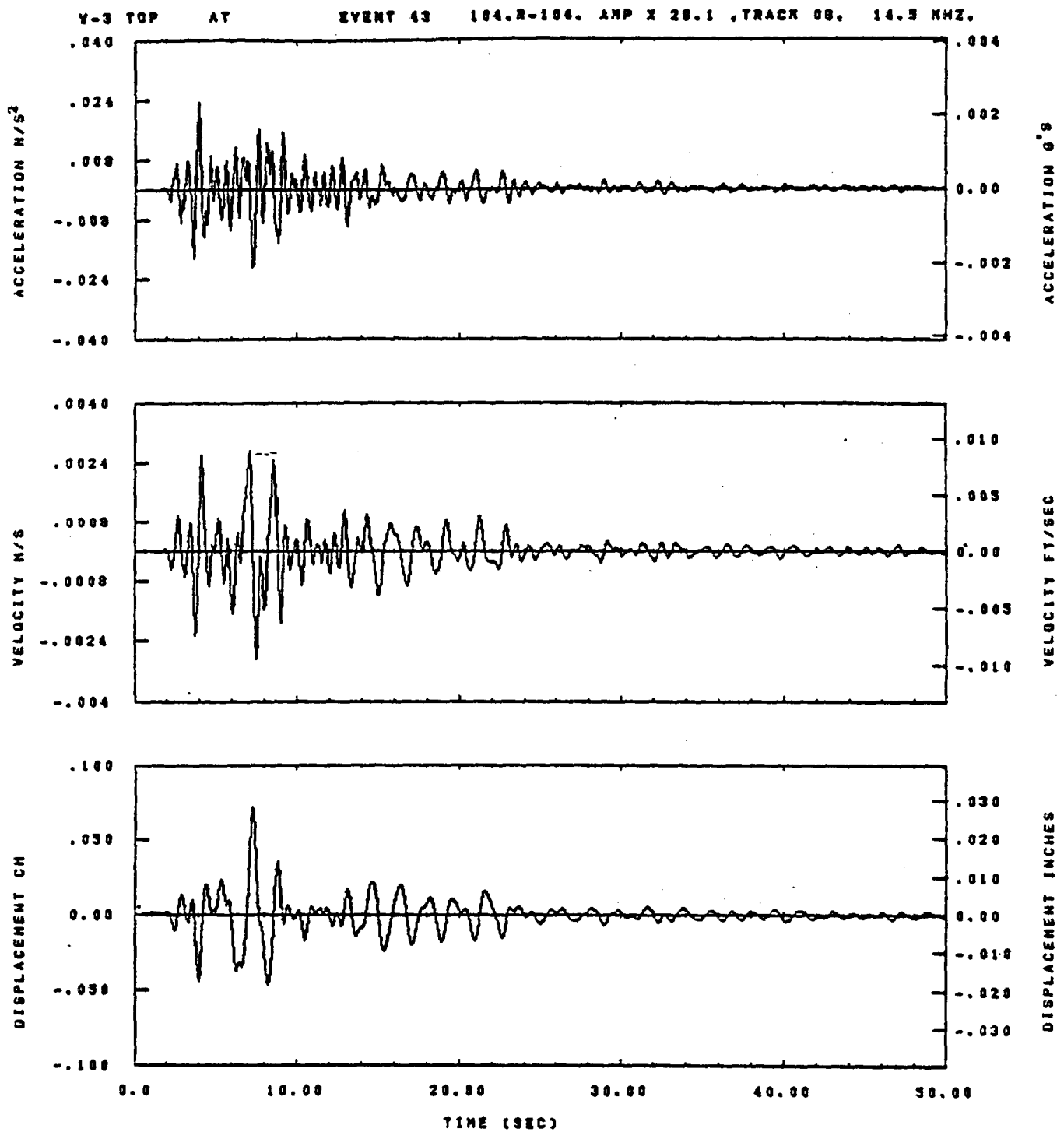


IDT= .0020	ODT=	FIX=	AAS= 0.
HPP= .20	BYH= .13	HLH= 417	ASB=
LPP= 10.	BYL= 2.	HLL= 2589	ASE=
VTS= .200	VTE= .133	FLL= -20.	VSE= 0.
DPS= 0.	DPE= 100.	FLH= 0	DSE= 0.

10.47.43.

06/23/82

Figure F-88

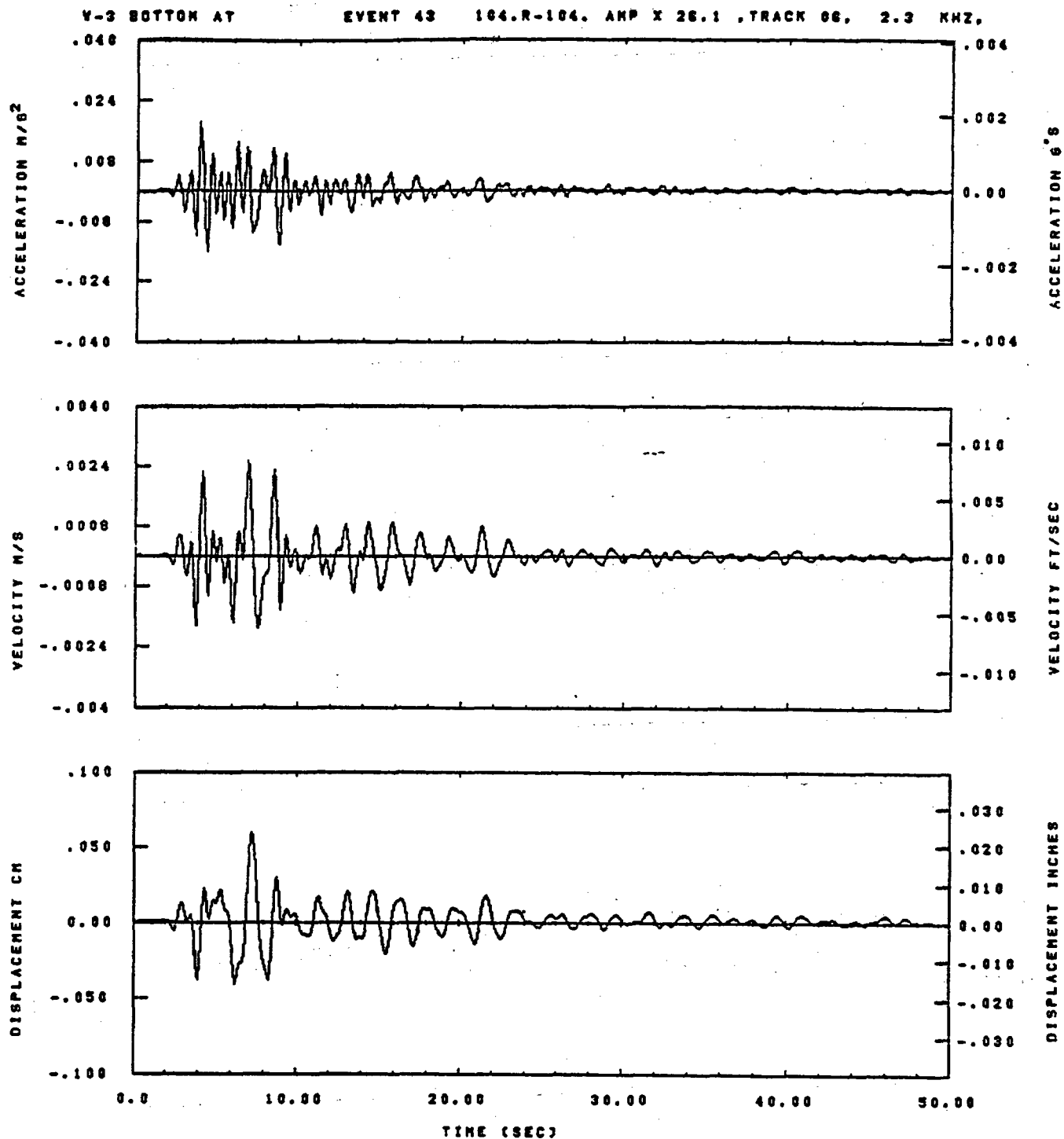


IDT= .0020	QDT=	FIX=	AAS= 0.
HPF= .20	BYH= .13	HLH= 417	ASB=
LPF= 10.	BYL= 2.	HLL= 2999	ASE=
VTS= .200	VTE= .133	FLL= -20.	VSE= 0.
DPS= 0.	DPE= 100.	FLH= 0	DSE= 0.

19.47.31.

06/23/82

Figure F-89

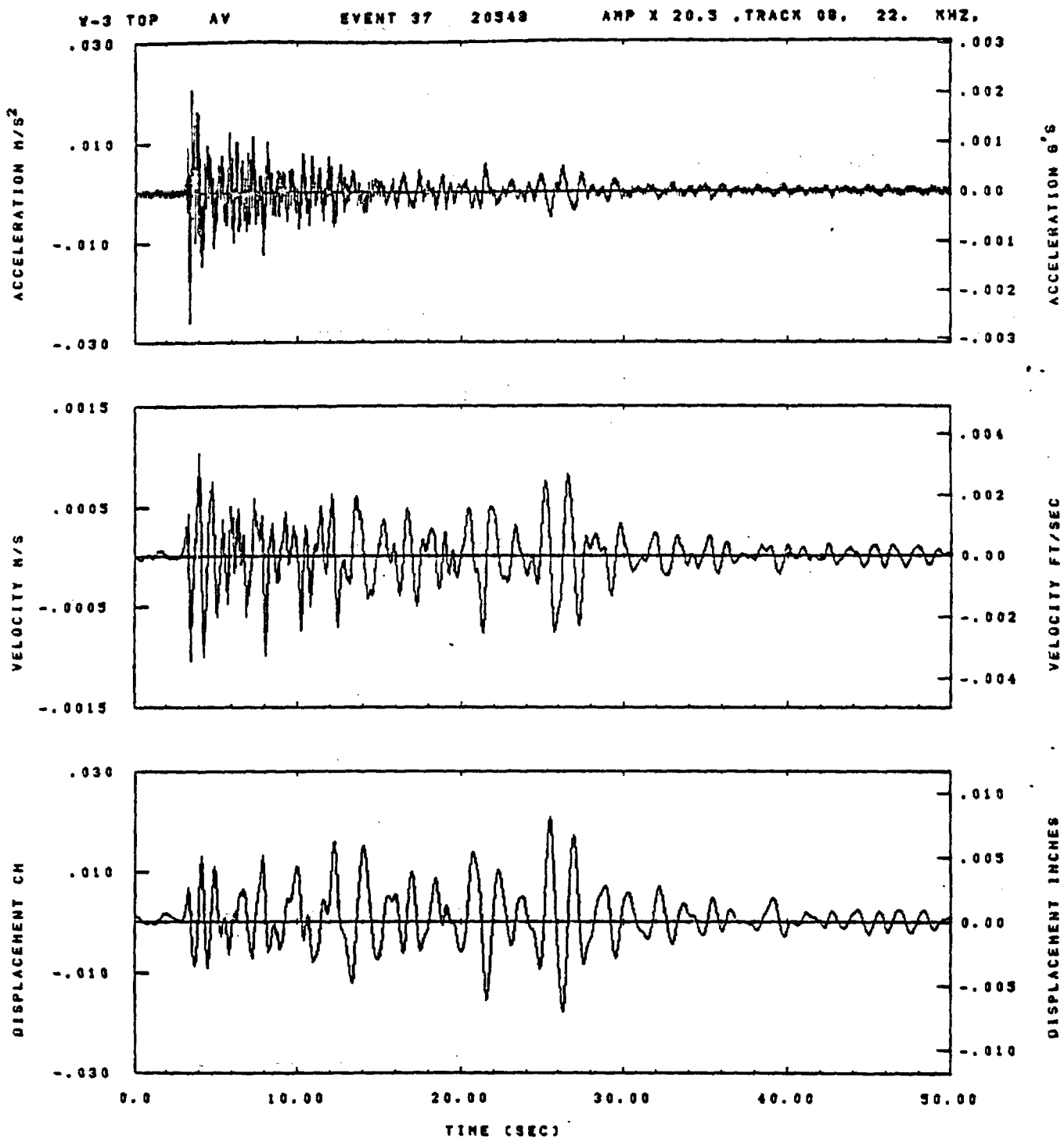


IDT= .0020	ODT=	FIX=	AAS= 0.
HPP= .20	BYH= .13	HLH= 417	ASS=
LPP= 10.	BYL= 2.	HLL= 2558	ASE=
VTS= .200	VTE= .133	FLL= -20.	VSE= 0.
DPS= 0.	DPE= 100.	FLH= 0	DSE= 0.

10.48.04.

06/23/82

Figure F-90

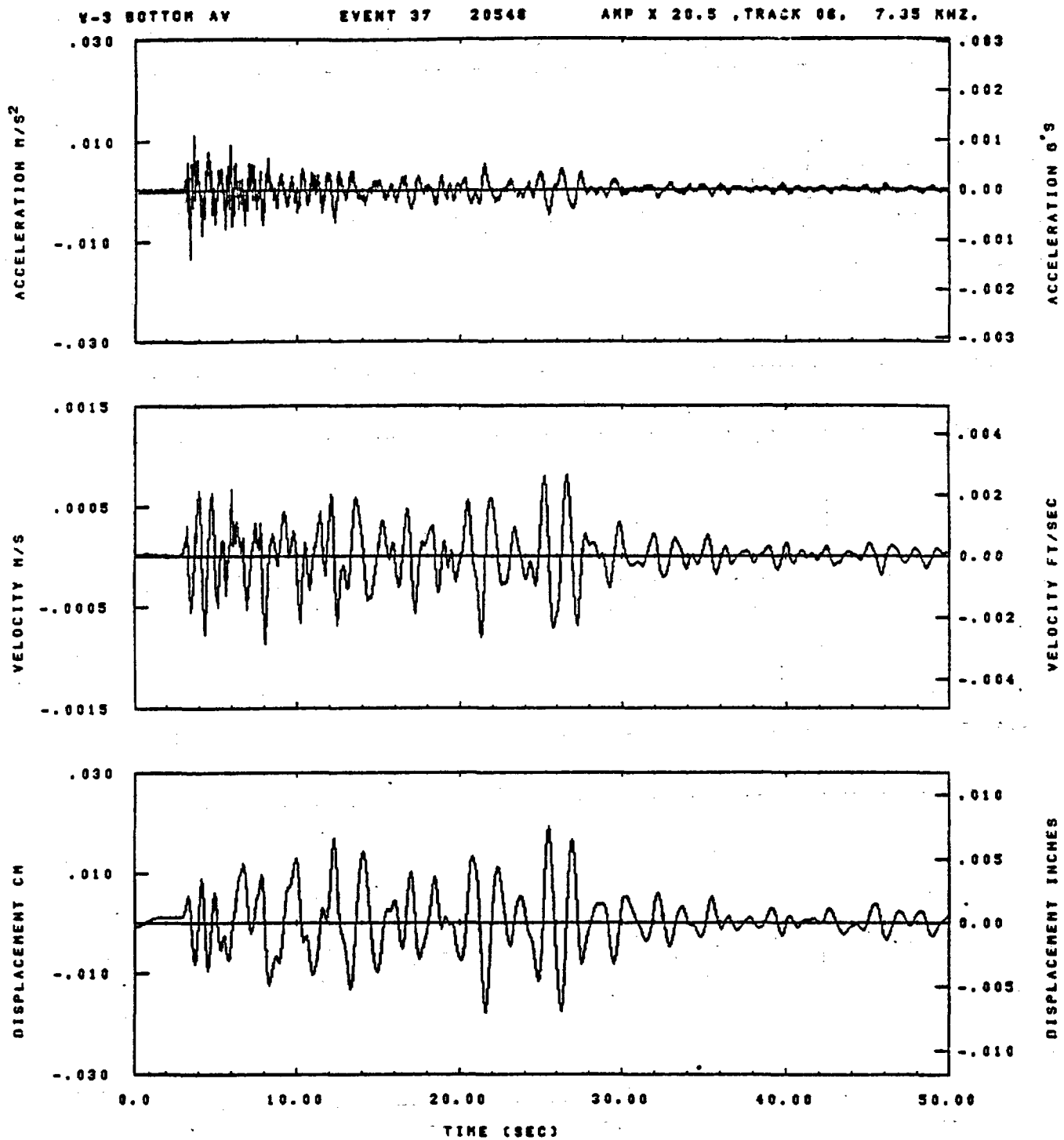


IDT= .0020	ODT= .005	FIX=	AAS= 0.
HPP= .50	BYH= .33	HLH= 187	ASB=
LPP= 27.	BYL= 8.	HLL= 1199	ASE=
VTS= .500	VTE= .333	FLL= -20.	VSE= 0.
OPS= 0.	OPE= 100.	FLH= 0	DSE= 0.

03.44.08

08/15/82

Figure F-91

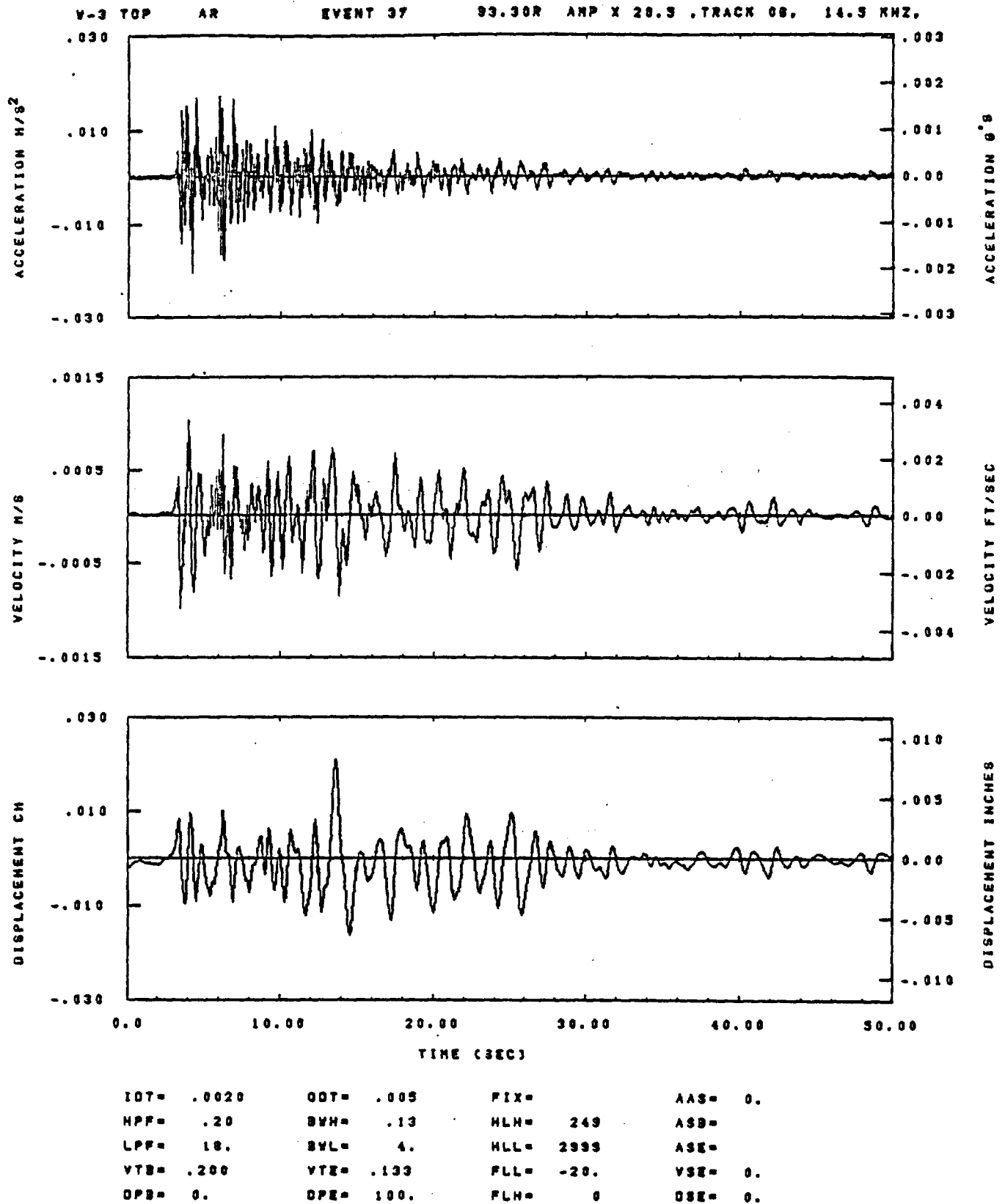


IDT= .0020	ODT= .005	FIX=	AAS= 0.
HPF= .20	BYH= .13	HLH= 248	ASB=
LPF= 18.	BYL= 4.	HLL= 2989	ASE=
VTB= .200	VTE= .133	FLL= -20.	VSE= 0.
DPE= 0.	DPE= 100.	FLH= 0	DSE= 0.

08.44.24

06/15/82

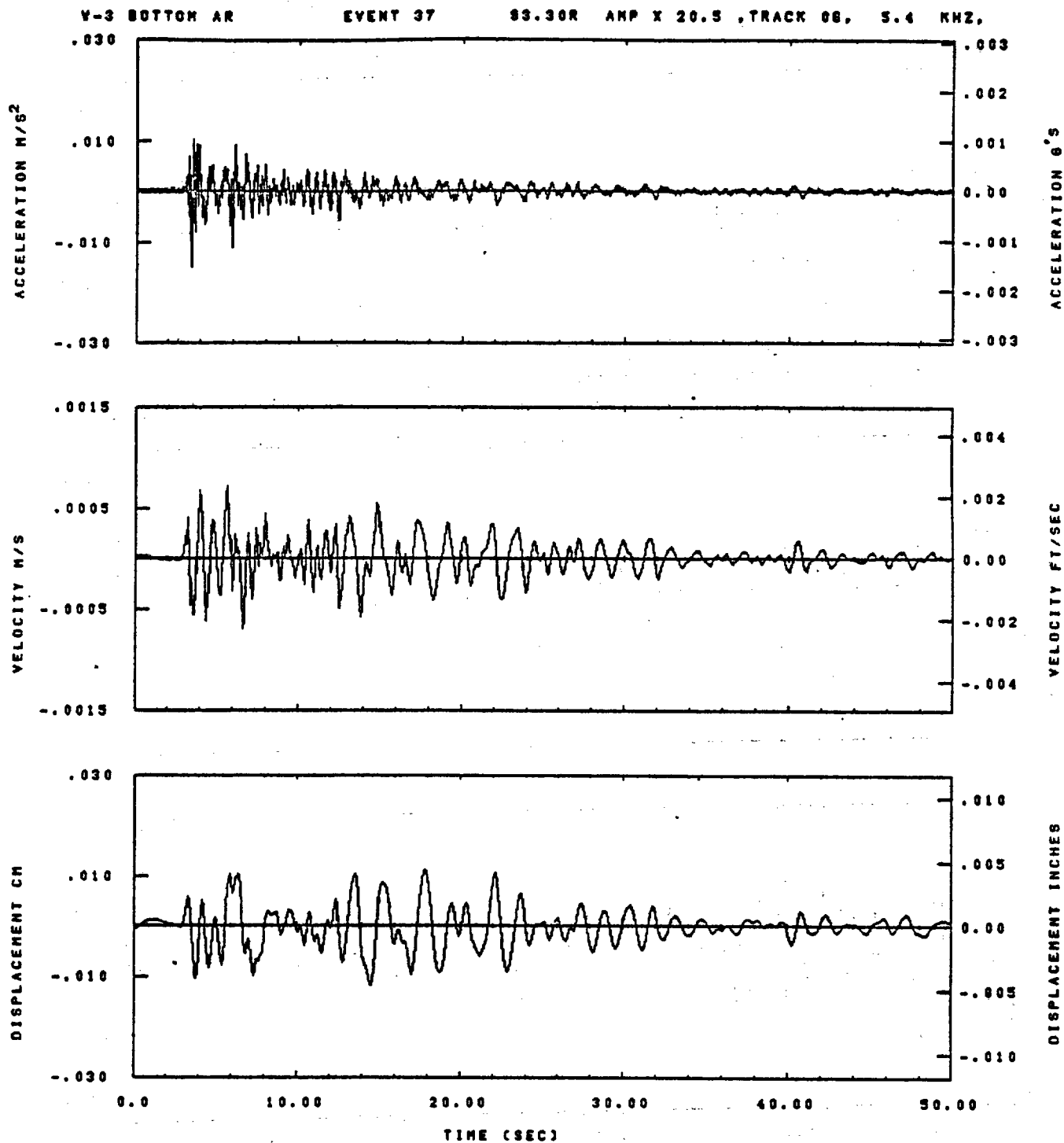
Figure F-92



09.43.47

06/15/82

Figure F-93

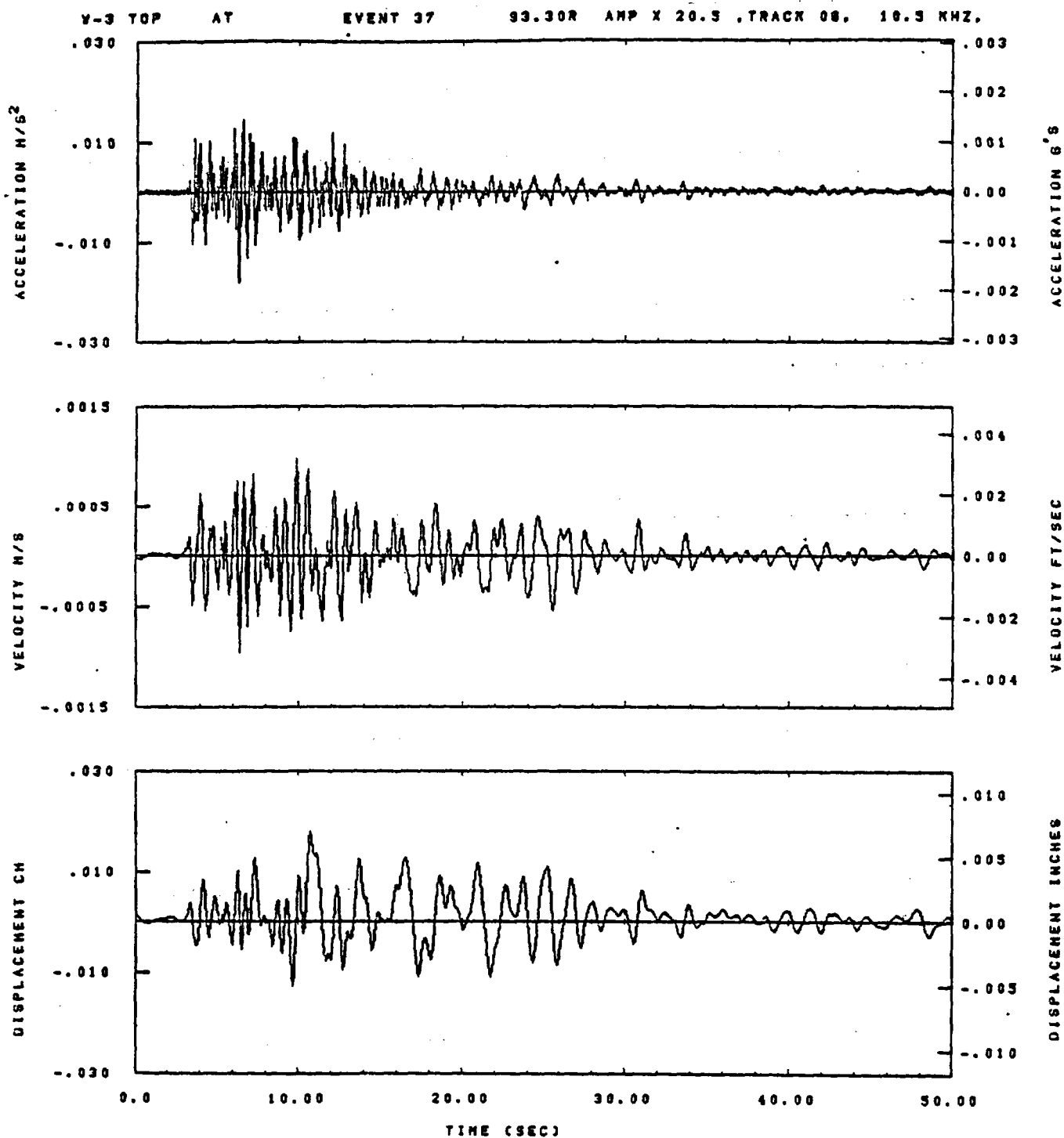


IDT= .0020	ODT= .005	FIX=	AAS= 0.
HPF= .20	SVH= .13	HLH= 249	ASE=
LPF= 18.	SVL= 4.	HLL= 2999	ASE=
VTS= .200	VTE= .133	FLL= -20.	VSE= 0.
DPS= 0.	DPE= 100.	FLH= 0	DSE= 0.

08.44.31

06/15/82

Figure F-94

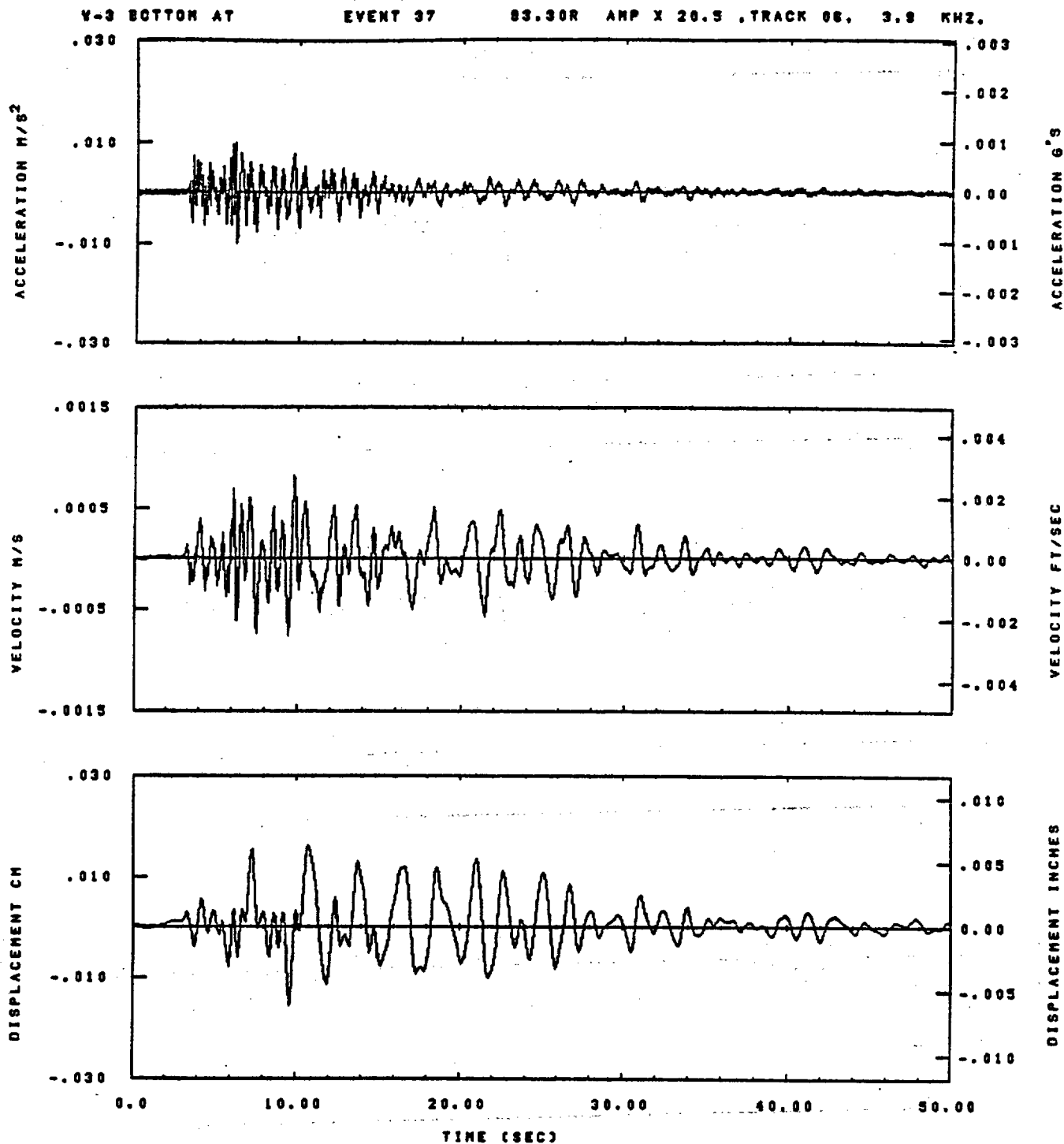


IOT= .0020	OOT= .005	FIX=	AAS= 0.
HPP= .20	SVH= .13	HLH= 249	ASB=
LPP= 10.	SVL= 4.	HLL= 2999	ASE=
VTS= .200	VTE= .133	FLL= -20.	VSE= 0.
DPS= 0.	DPE= 100.	FLH= 0	DSE= 0.

03.43.37

06/15/82

Figure F-95

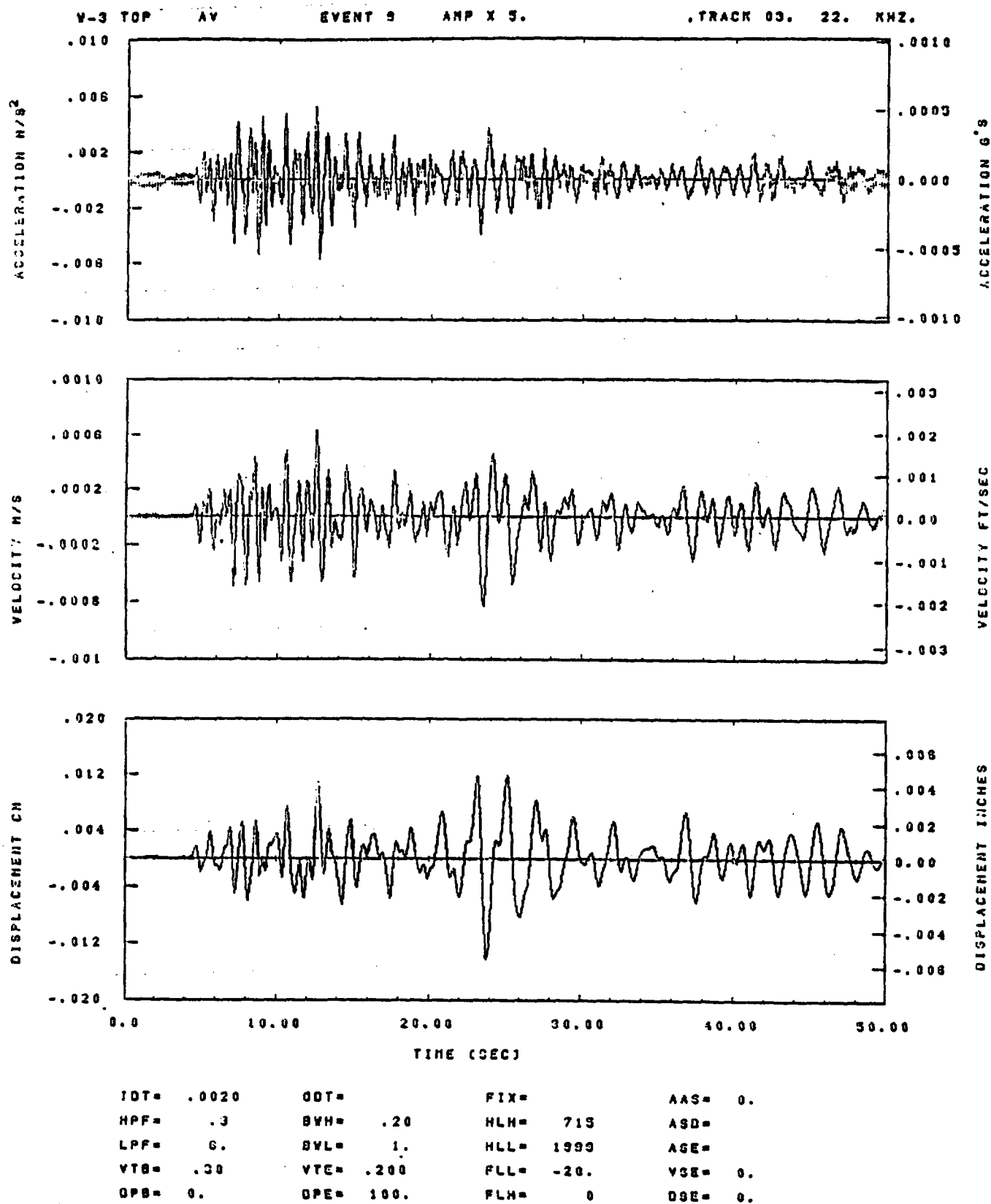


IDT= .0020	ODT= .005	FIX=	AAS= 0.
HPF= .20	BVN= .13	HLH= 249	ASB=
LPF= 18.	BYL= 4.	HLL= 2999	ASE=
VTB= .200	VTE= .133	FLL= -20.	VSE= 0.
DPS= 0.	DPE= 100.	FLH= 0	DSE= 0.

08.46.41

06/15/82

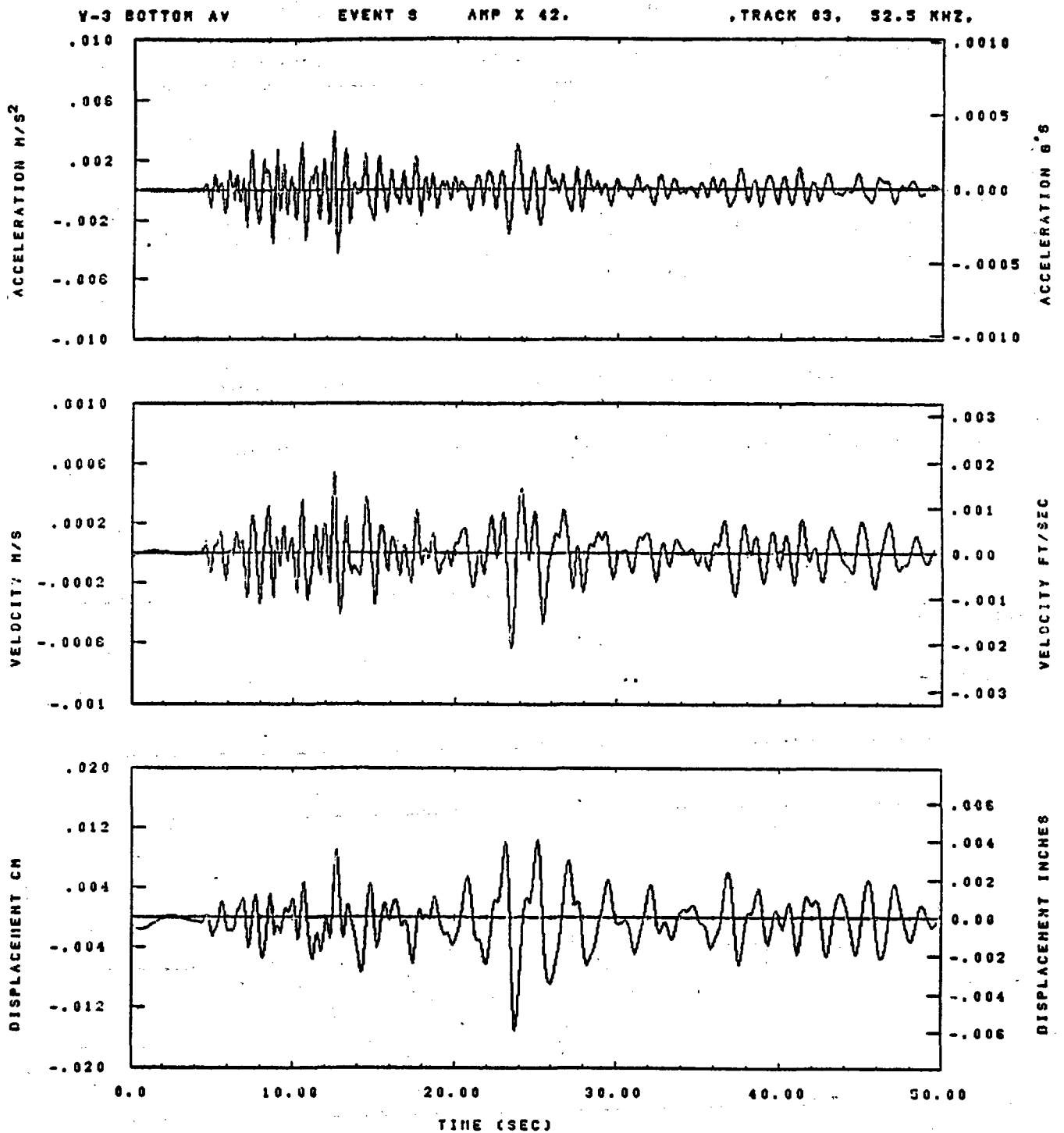
Figure F-96



08.37.12.

08/29/82

Figure F-97

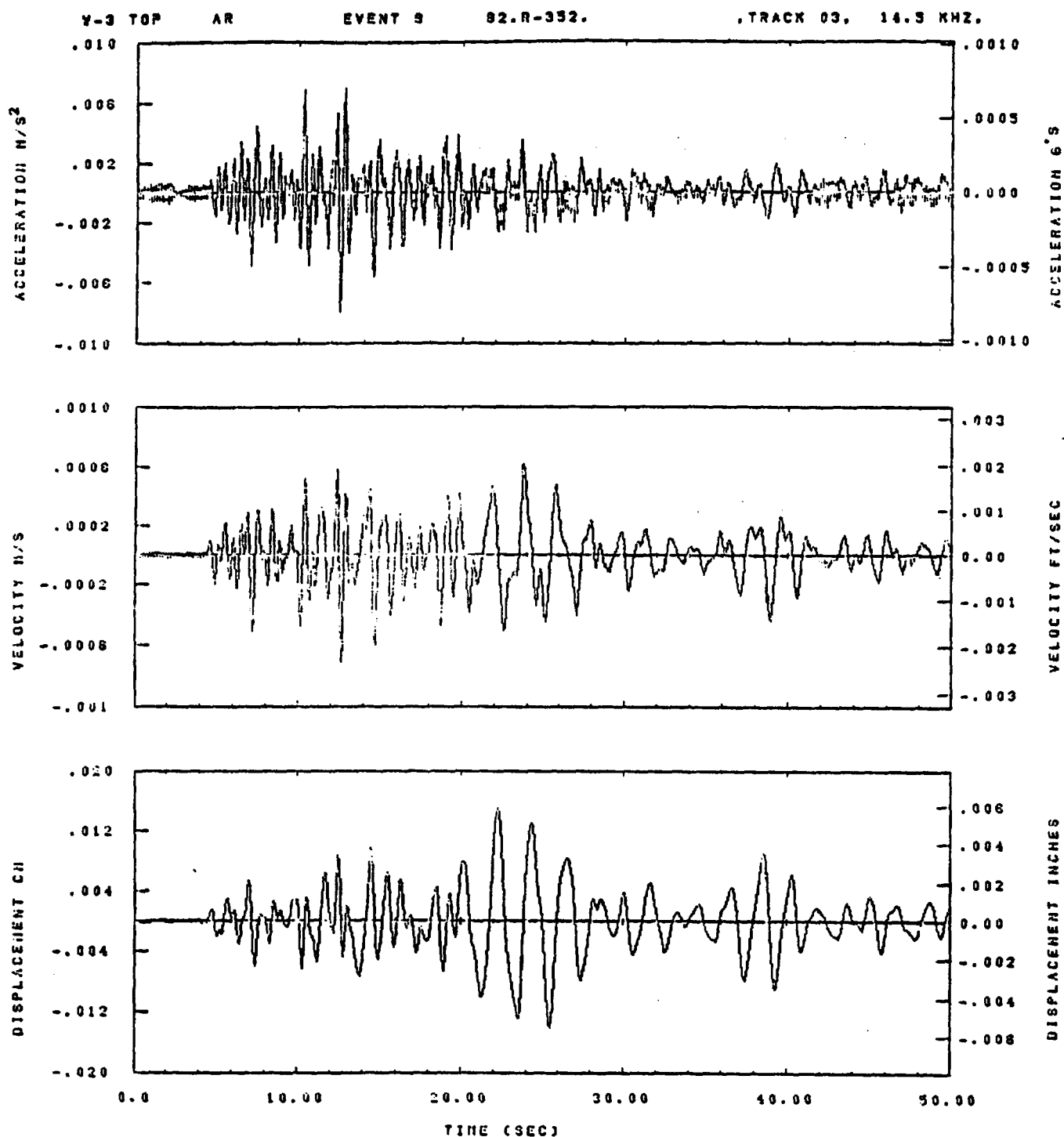


IDT= .0020	OOT=	FIX=	AAS= 0.
HPF= .3	BYH= .20	HLH= 713	ASD=
LPF= 6.	DVL= 1.	HLL= 1999	ASE=
VTB= .30	VTE= .200	FLL= -20.	VSE= 0.
OPD= 0.	DPE= 100.	FLH= 0	DSE= 0.

08,37.43.

06/28/82

Figure F-98



IDT= .0020	ODT=	FIX=	AAS= 0.
HPP= .3	DYN= .20	HLH= 713	ASB=
LPP= 6.	DYL= 1.	HLL= 1000	ASE=
VTB= .00	VTE= .200	FLL= -20.	VSE= 0.
OPD= 0.	DPE= 100.	FLH= 0	DSE= 0.

08.37.18.

08/29/82

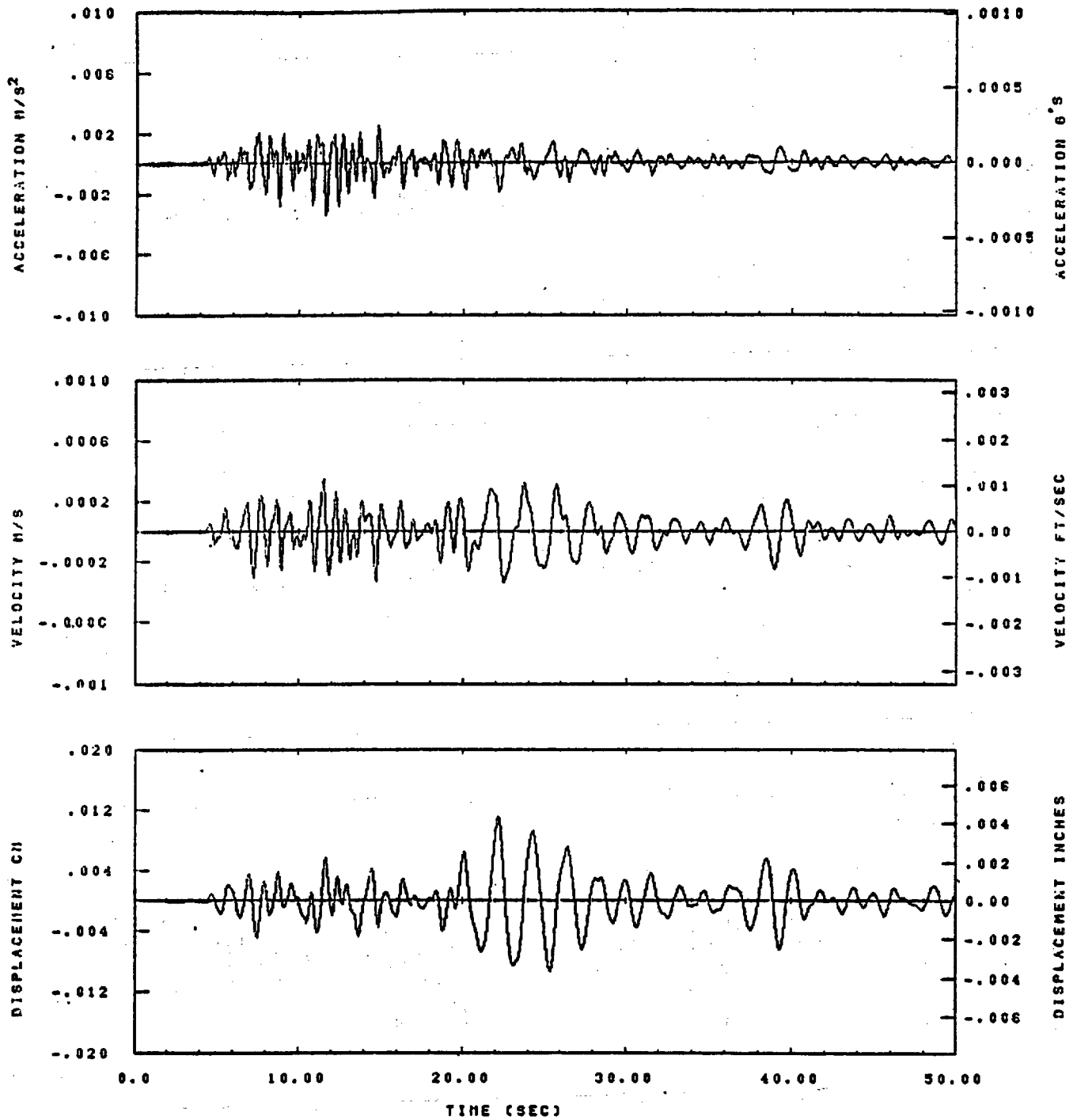
Figure F-99

Y-3 BOTTOM AR

EVENT 9

82.R-352.

, TRACK 03. 40. KHZ.

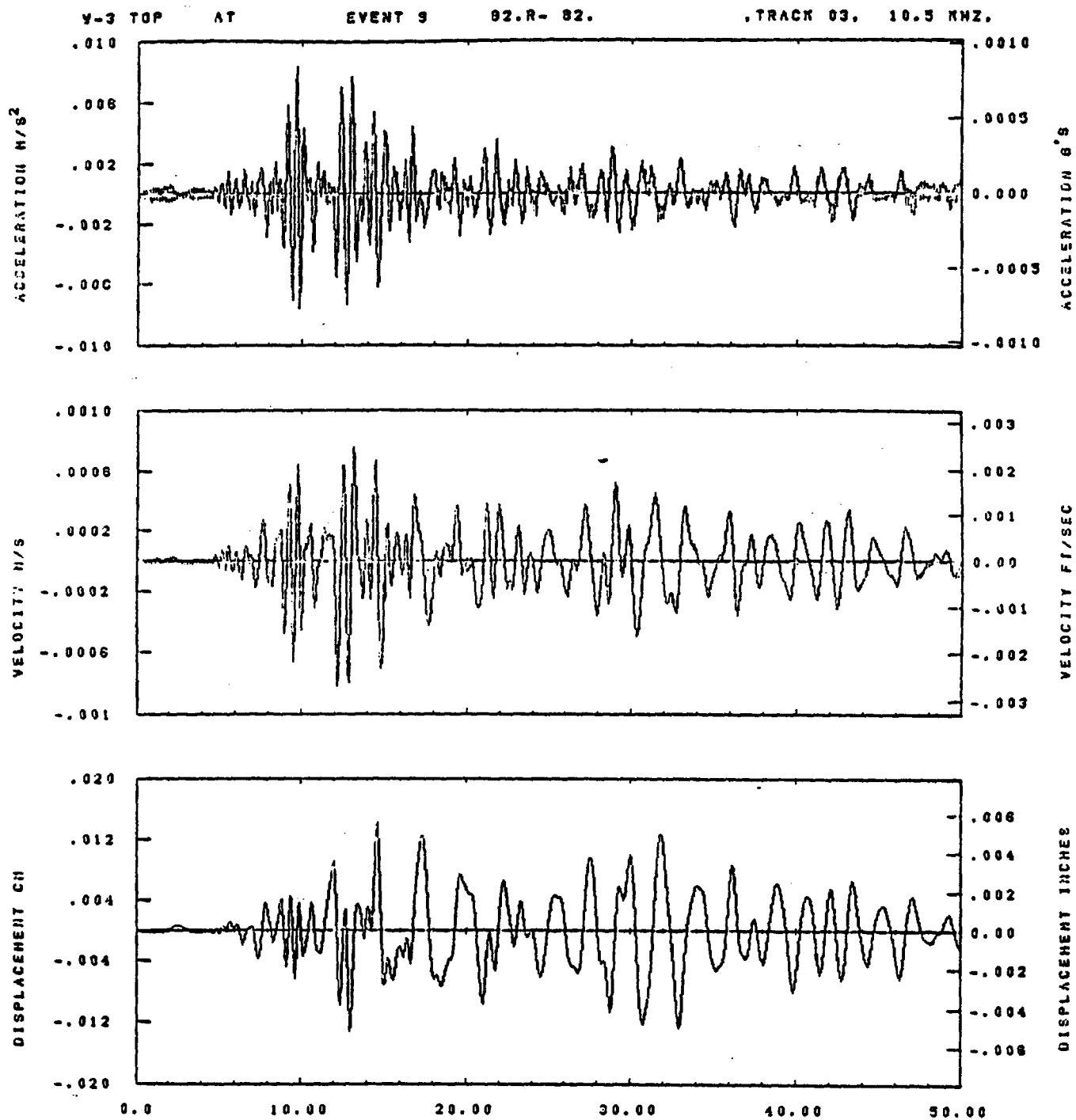


IDT=	.0020	ODT=		FIX=		AAS=	0.
HPF=	.3	BYH=	.20	HLH=	715	ASB=	
LPF=	6.	BYL=	1.	HLL=	1899	ASE=	
VTB=	.20	VTE=	.200	FLL=	-20.	VSE=	0.
DPS=	0.	DPE=	100.	FLH=	0	DSE=	0.

08.37.51.

06/29/82

Figure F-100

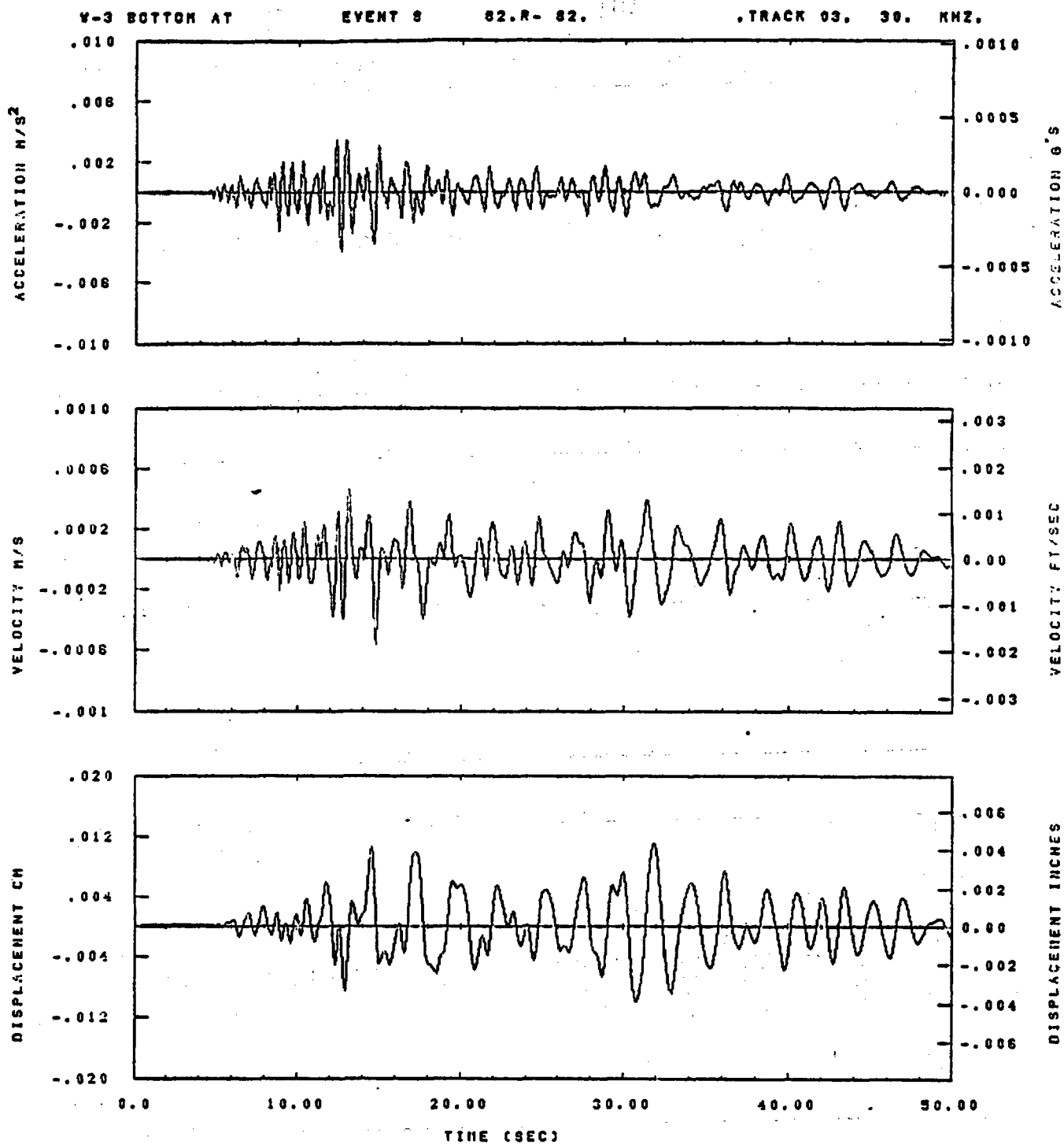


LOT= .0020	ODT=	FIX=	AAS= 0.
HPF= .3	BYH= .20	HLH= 713	ASB=
LPF= 6.	QWL= 1.	HLL= 1399	ASE=
VTS= .30	VTE= .200	FLL= -20.	VSE= 0.
OPB= 0.	OPE= 100.	FLH= 0	DSE= 0.

08.37.38.

08/23/82

Figure F-101

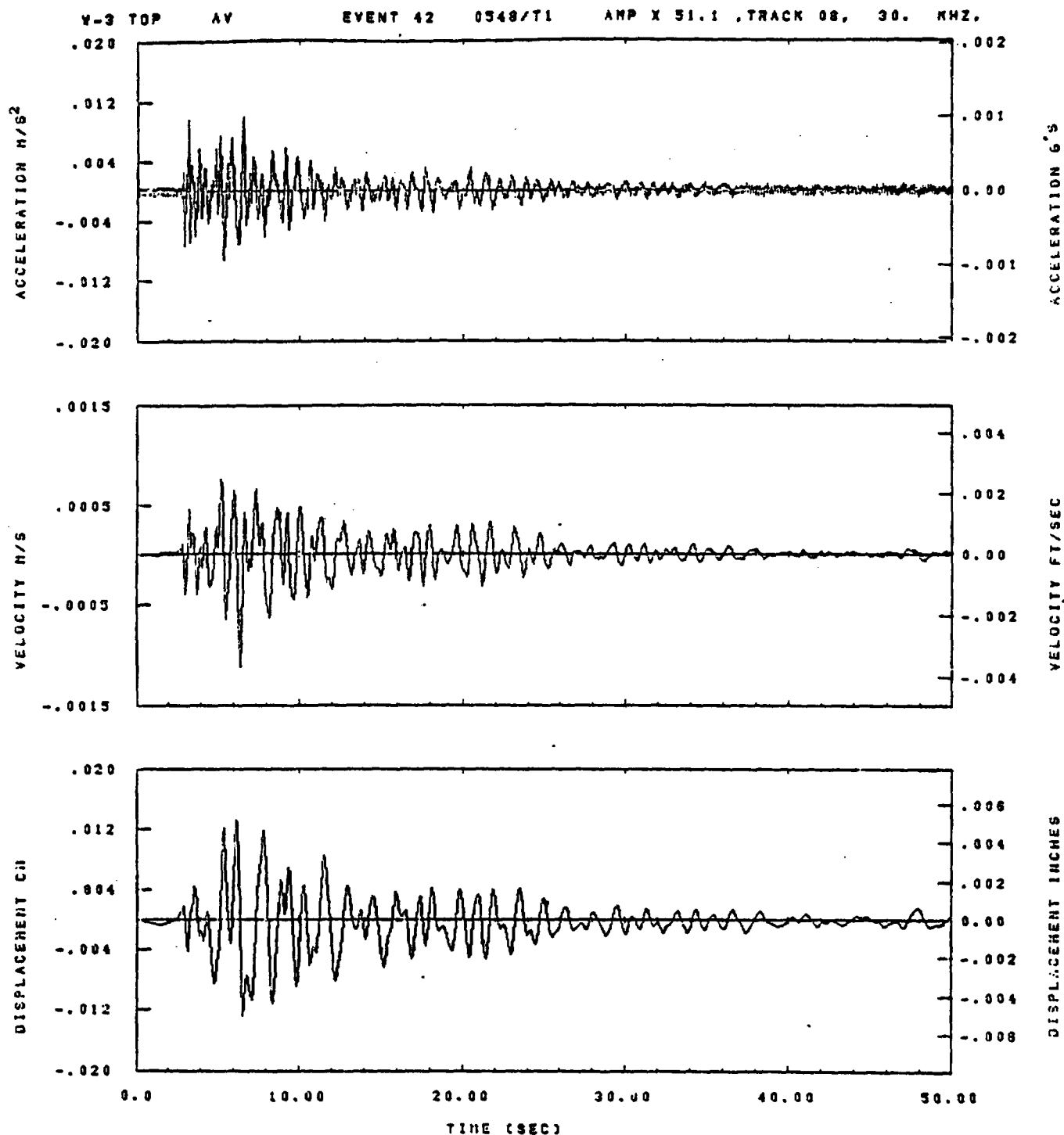


IDT= .0020	ODT=	FIX=	AAS= 0.
HPF= .3	QWH= .20	NLH= 715	ASD=
LPF= 6.	BYL= 1.	HLL= 1999	ASE=
VTB= .30	VTE= .200	FLL= -20.	VSE= 0.
OPB= 0.	DPE= 100.	FLH= 0	DSE= 0.

08.37.58.

86/29/82

Figure F-102

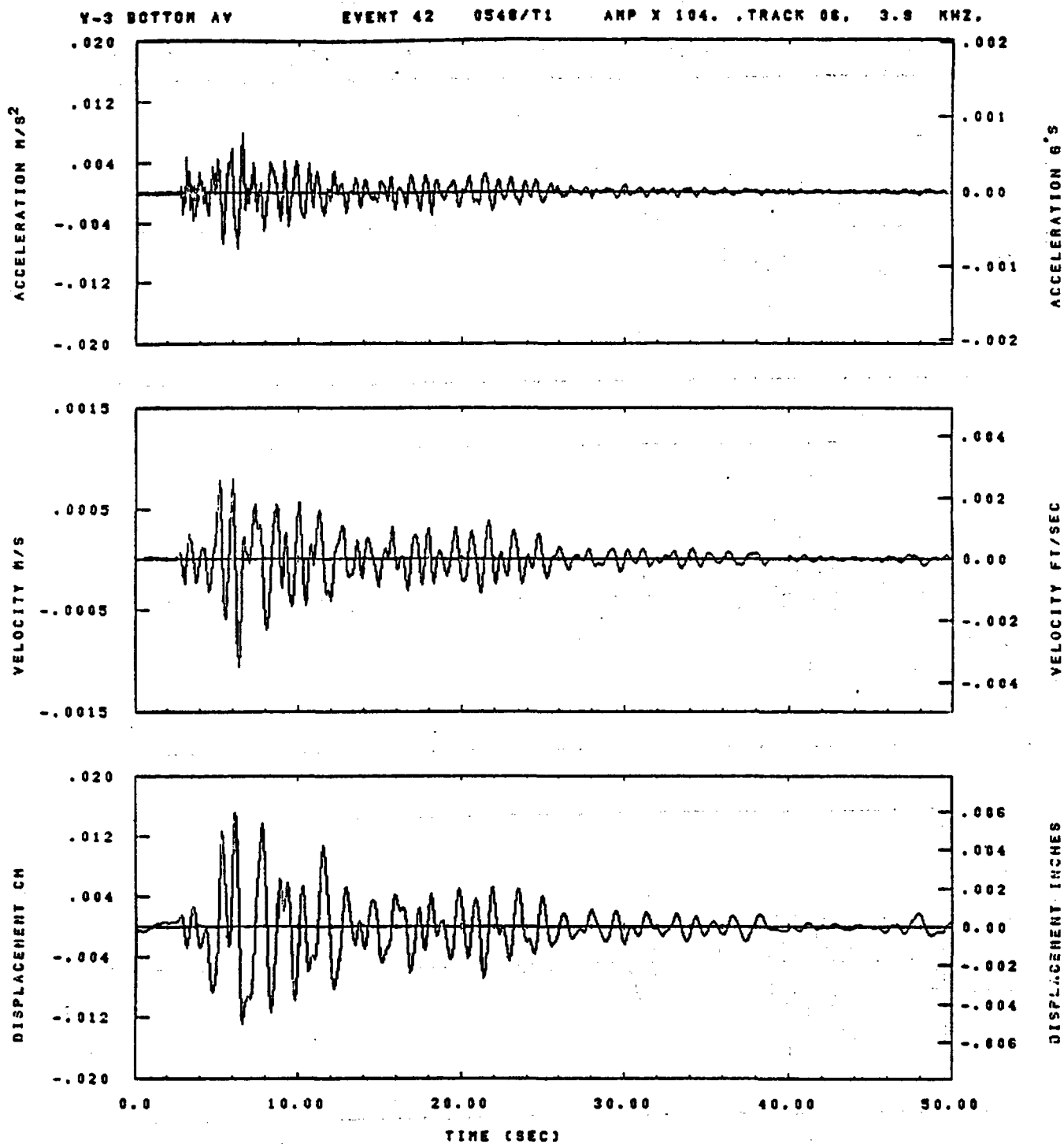


LOT= .0020	QOT= .0003	FIX=	AAS= 0.
HPP= .30	QWH= .20	MLH= 167	ASS=
LPP= 27.	SVL= 6.	NLL= 1999	ASE=
VTS= .300	VTE= .200	FLL= -20.	VSE= 0.
OPS= 0.	DPE= 100.	FLH= 0	OTE= 0.

13.08.32.

06/29/92

Figure F-103

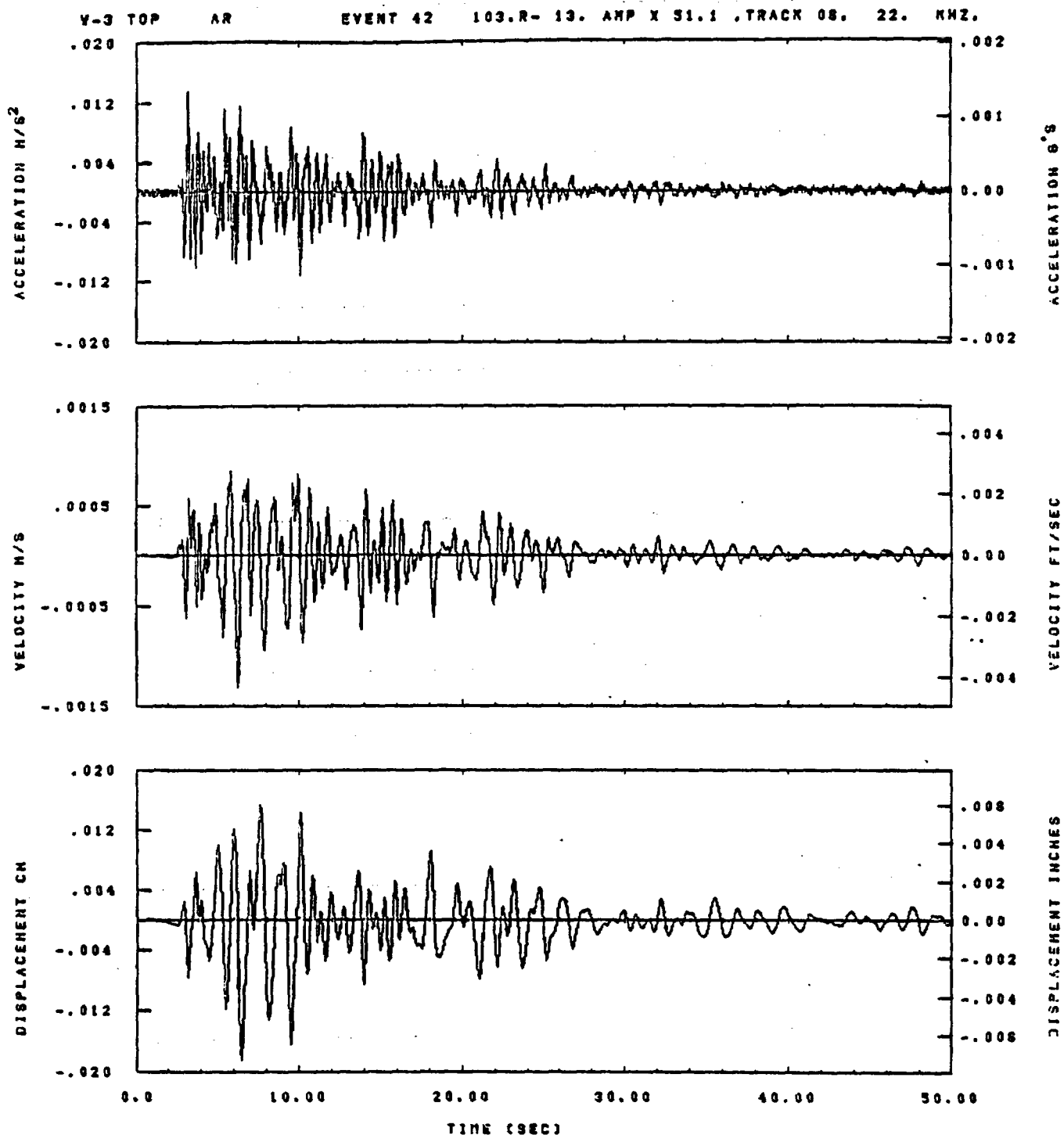


IDT= .0020	ODT=	FIX=	AAS= 0.
HPF= .25	BYH= .16	HLH= 333	ASB=
LPF= 13.	BYL= 3.	HLL= 2388	ASE=
VTB= .250	VTE= .166	FLL= -20.	VSE= 0.
OPS= 0.	DPE= 100.	FLH= 0	DSE= 0.

13.11.08.

06/28/82

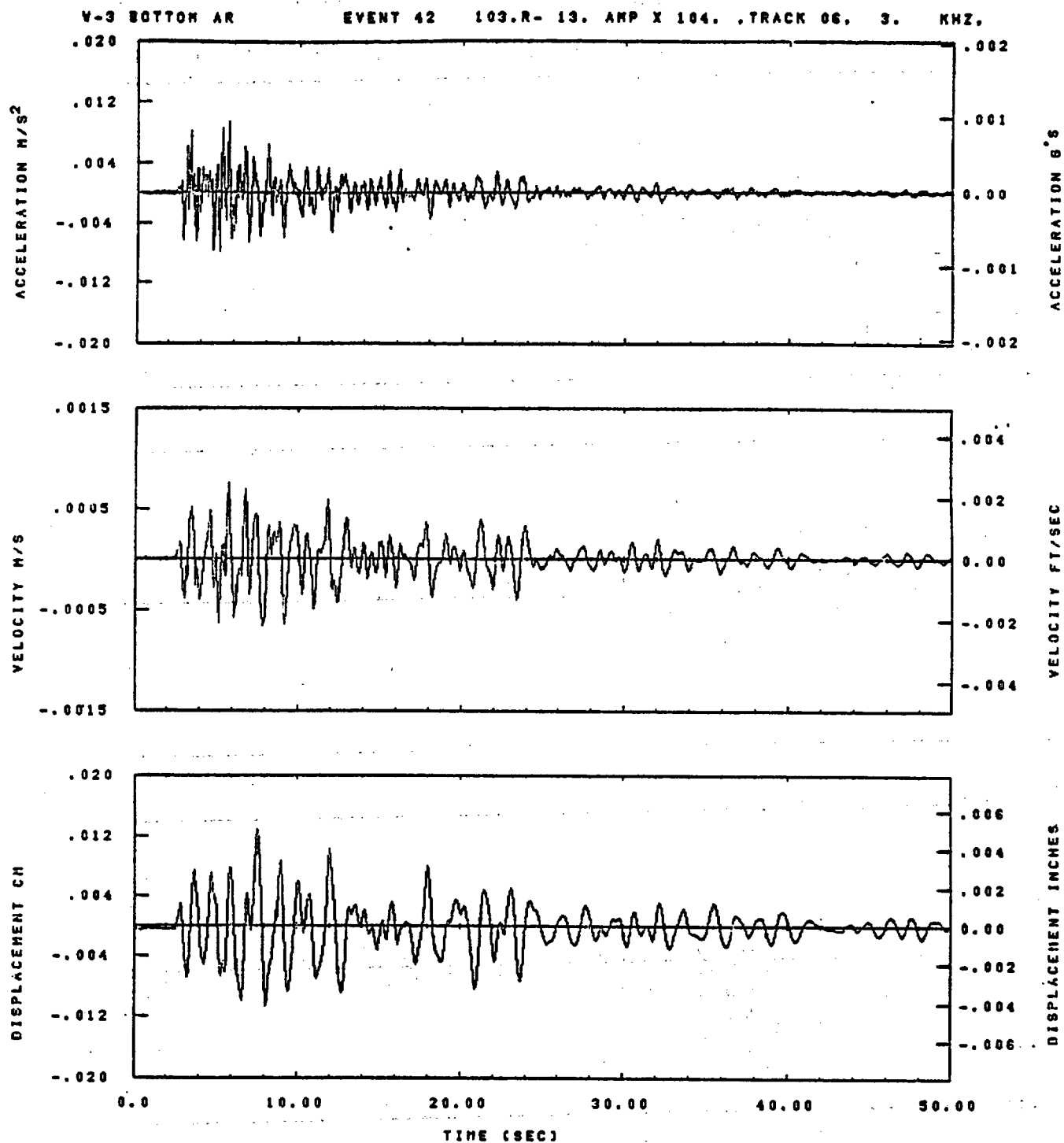
Figure F-104



IGT= .0020	QDT= .005	FIX=	AAS= 0.
HPP= .38	BVH= .20	HLN= 187	ASS=
LPP= 27.	BVL= 8.	HLL= 1999	ASE=
VTE= .300	YTE= .200	FLL= -20.	VSE= 0.
DPS= 0.	DPE= 100.	FLH= 0	DSE= 0.

13.03.02.

08/28/02

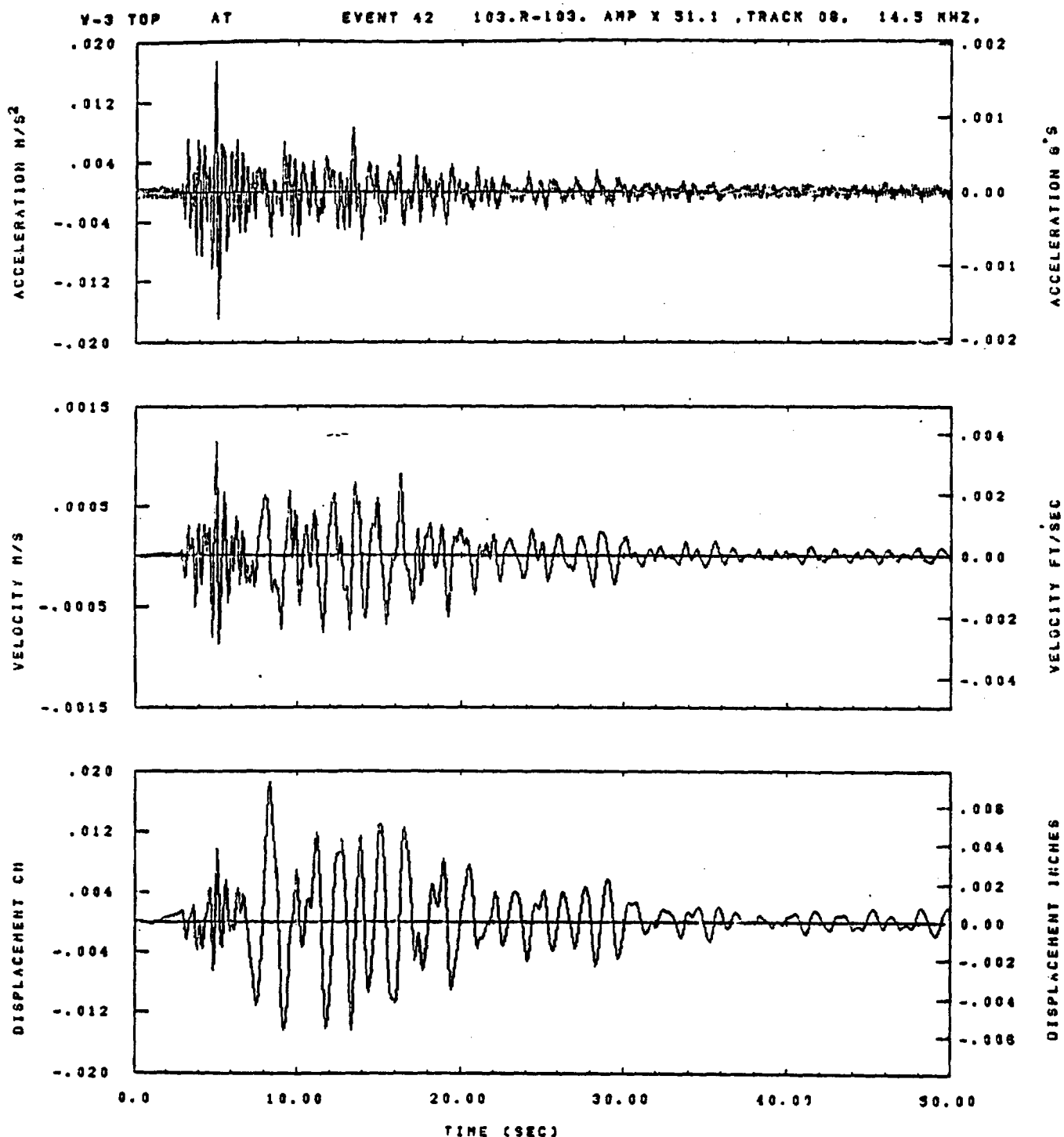


IDT= .0020	ODT=	FIX=	AAS= 0.
HPF= .25	BYH= .16	HLH= 333	ASB=
LPF= 13.	BVL= 3.	HLL= 2399	ASE=
YTB= .250	VTE= .166	FLL= -20.	VSE= 0.
OPB= 0.	OPE= 100.	FLH= 0	DSE= 0.

13.09.52.

06/28/82

Figure F-106

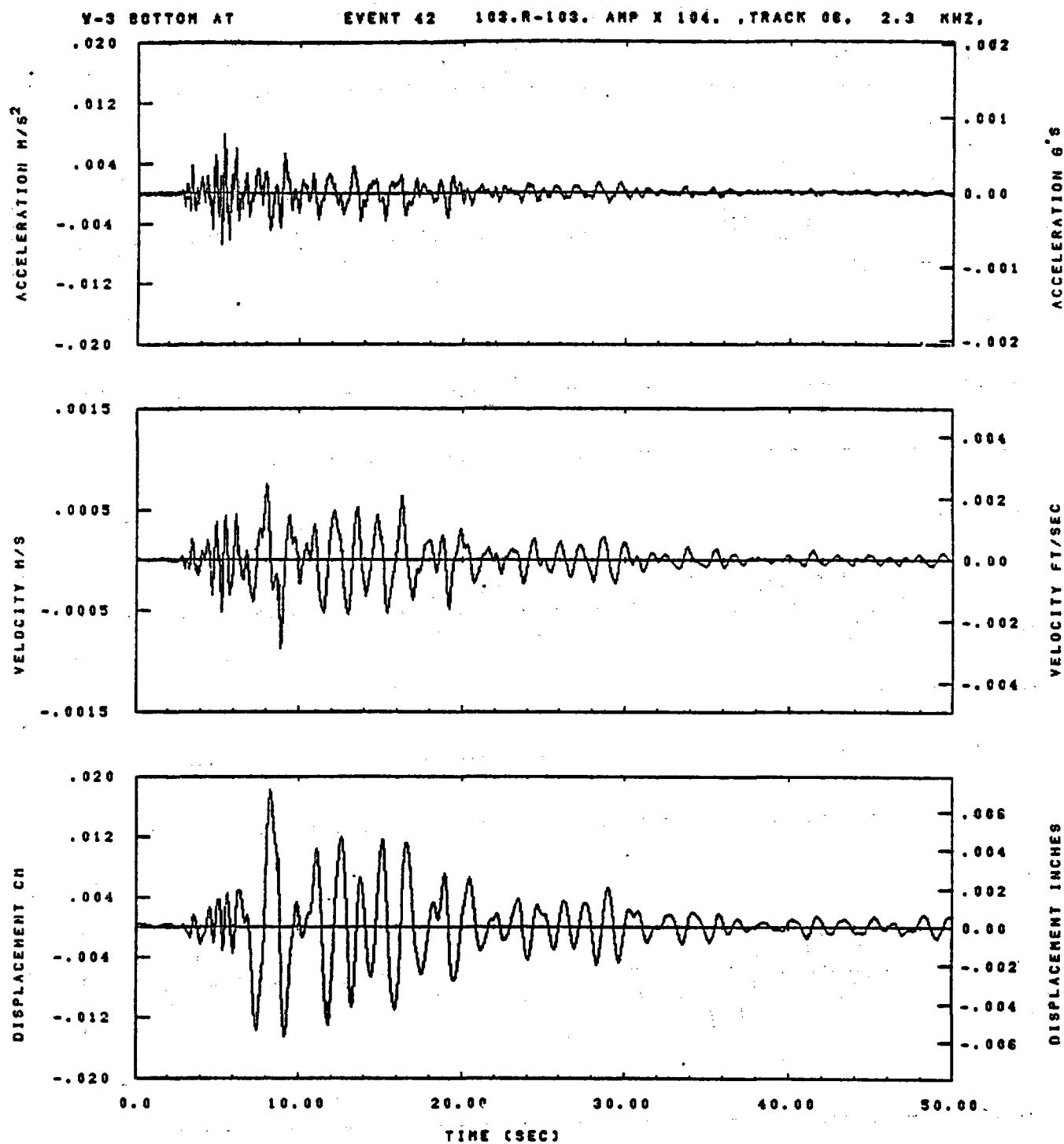


IDT= .0020	ODT= .005	FIX=	AAS= 0.
HPF= .30	QVM= .20	HLH= 187	ASB=
LPF= 27.	QVL= 0.	HLL= 1999	ASE=
VTS= .300	VTE= .200	FLL= -20.	VSE= 0.
DPS= 0.	DPE= 100.	FLH= 0	DSE= 0.

13.09.11.

08/28/82

Figure F-107

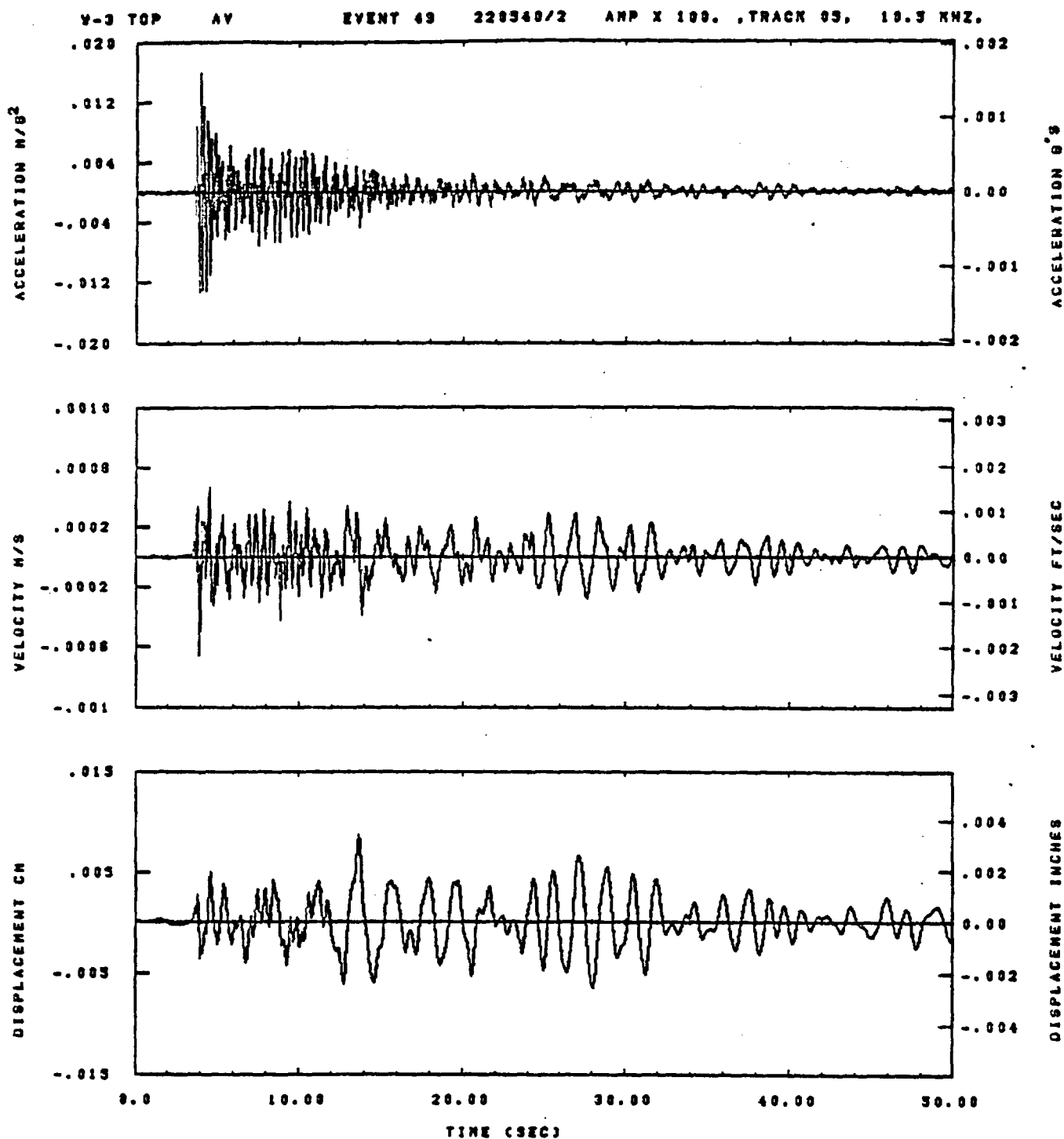


IDT= .0020	ODT=	FIX=	AAS= 0.
HPF= .25	BYH= .16	HLH= 333	ASS=
LPF= 13.	BYL= 3.	HLL= 2388	ASE=
VTB= .250	VTE= .166	FLL= -20.	VSE= 0.
OPB= 0.	DPE= 100.	FLH= 0	DSE= 0.

13.10.50.

06/28/82

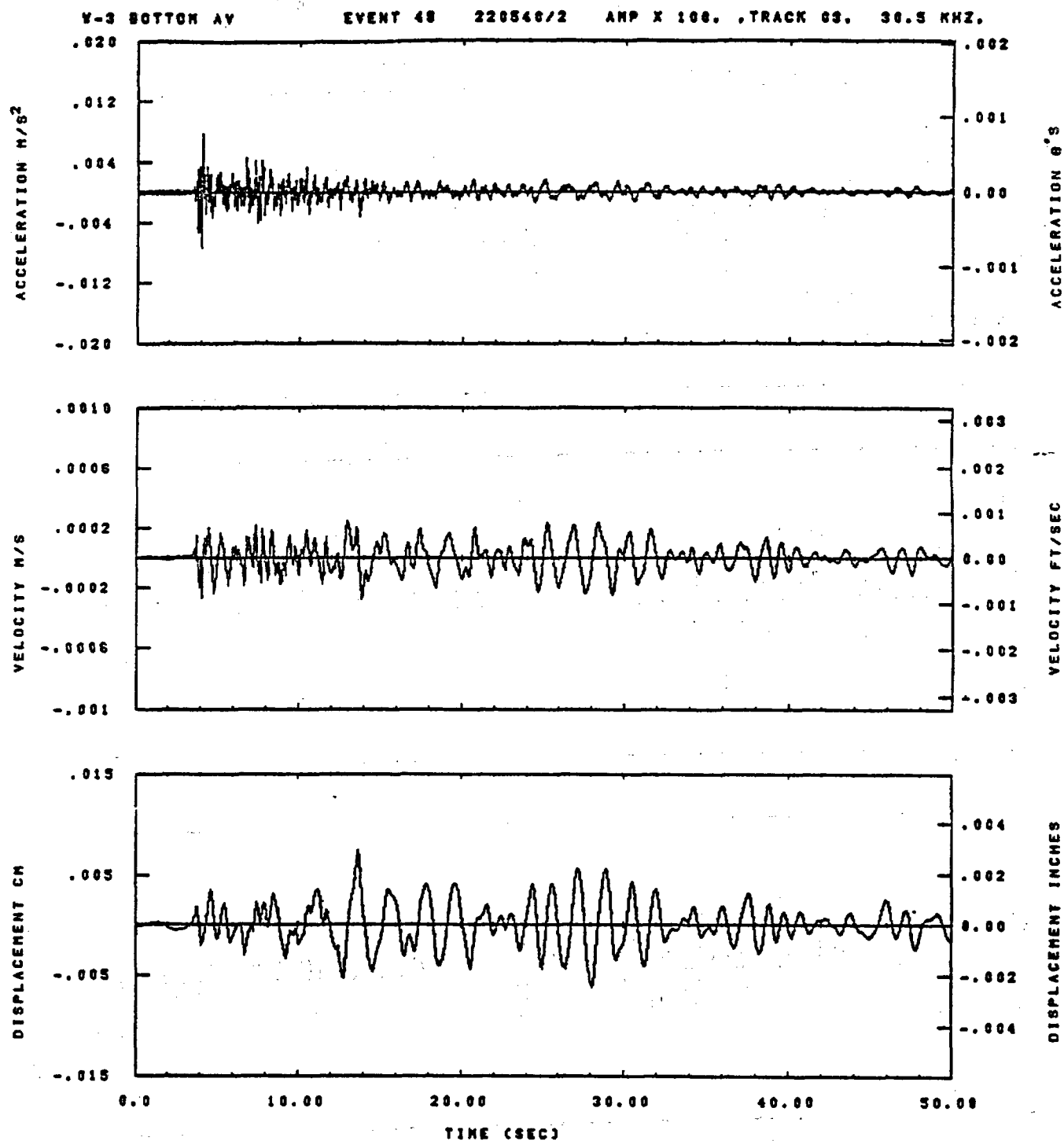
Figure F-108



IOD= .0020	ODT= .005	FIX=	AAS= 0.
HPP= .30	BYH= .20	HLH= 187	ASB=
LPP= 27.	BYL= 8.	HLL= 1333	ASZ=
VTB= .300	VTE= .200	FLL= -20.	VSE= 0.
DPB= 0.	DPE= 100.	FLH= 0	DSE= 0.

13.35.38.

08/30/82

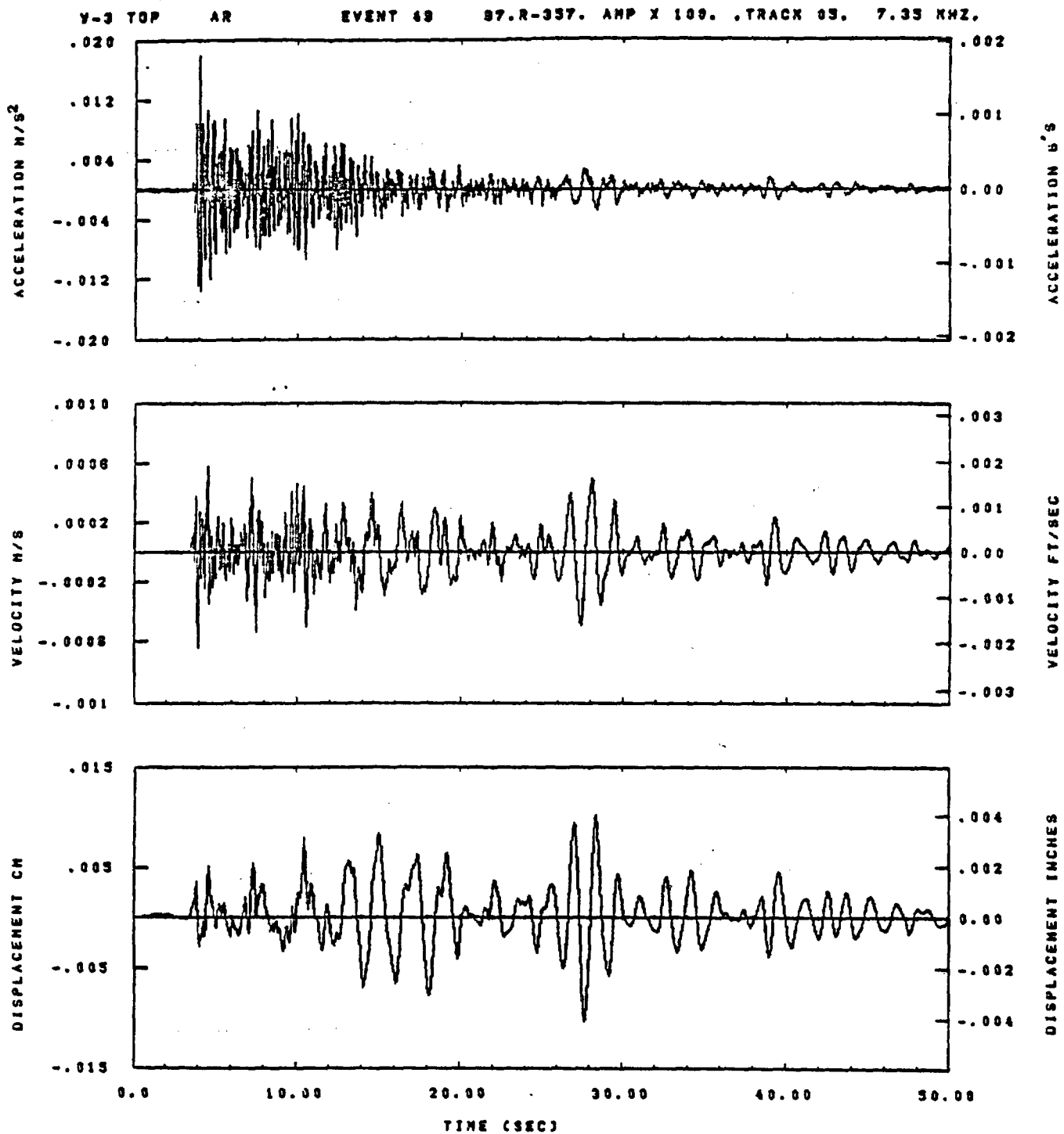


IDT= .0020	ODT= .005	FIX=	AAS= 0.
HPF= .30	BYH= .20	HLH= 167	ASS=
LPF= 27.	BYL= 6.	HLL= 1888	ASE=
VTB= .300	VTE= .200	FLL= -20.	VSE= 0.
DPE= 0.	DPE= 100.	FLH= 0	DSE= 0.

15.36.86.

06/30/82

Figure F-110

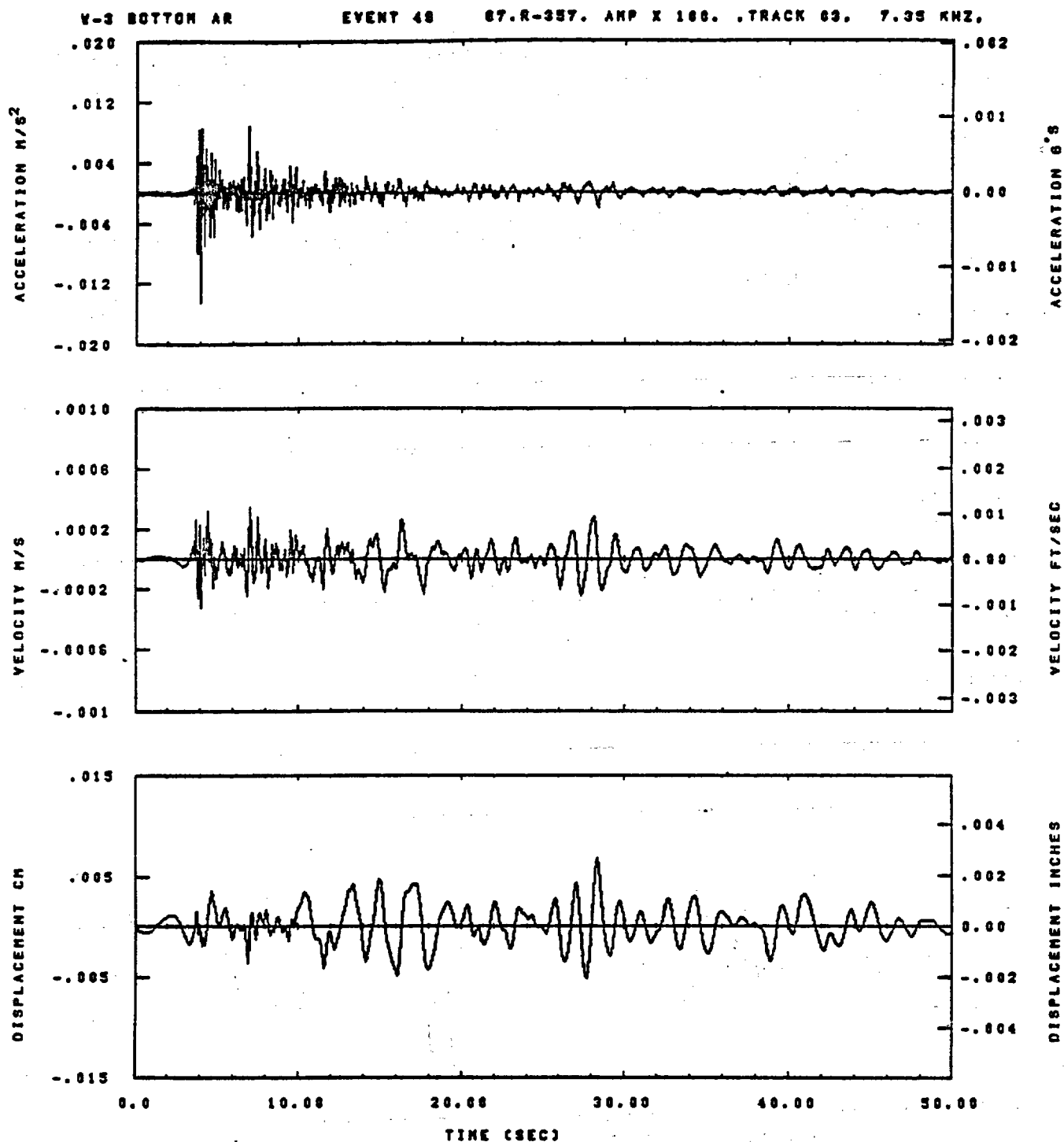


IDT= .0020	ODT= .003	FIX=	AAS= 0.
HPP= .30	BYH= .20	HLH= 187	ASS=
LPP= 27.	BYL= 8.	HLL= 1333	ASE=
VTB= .300	VTE= .200	FLL= -20.	VSE= 0.
DPS= 0.	DPE= 100.	FLH= 0	DSE= 0.

15.35.43.

06/30/82

Figure F-111

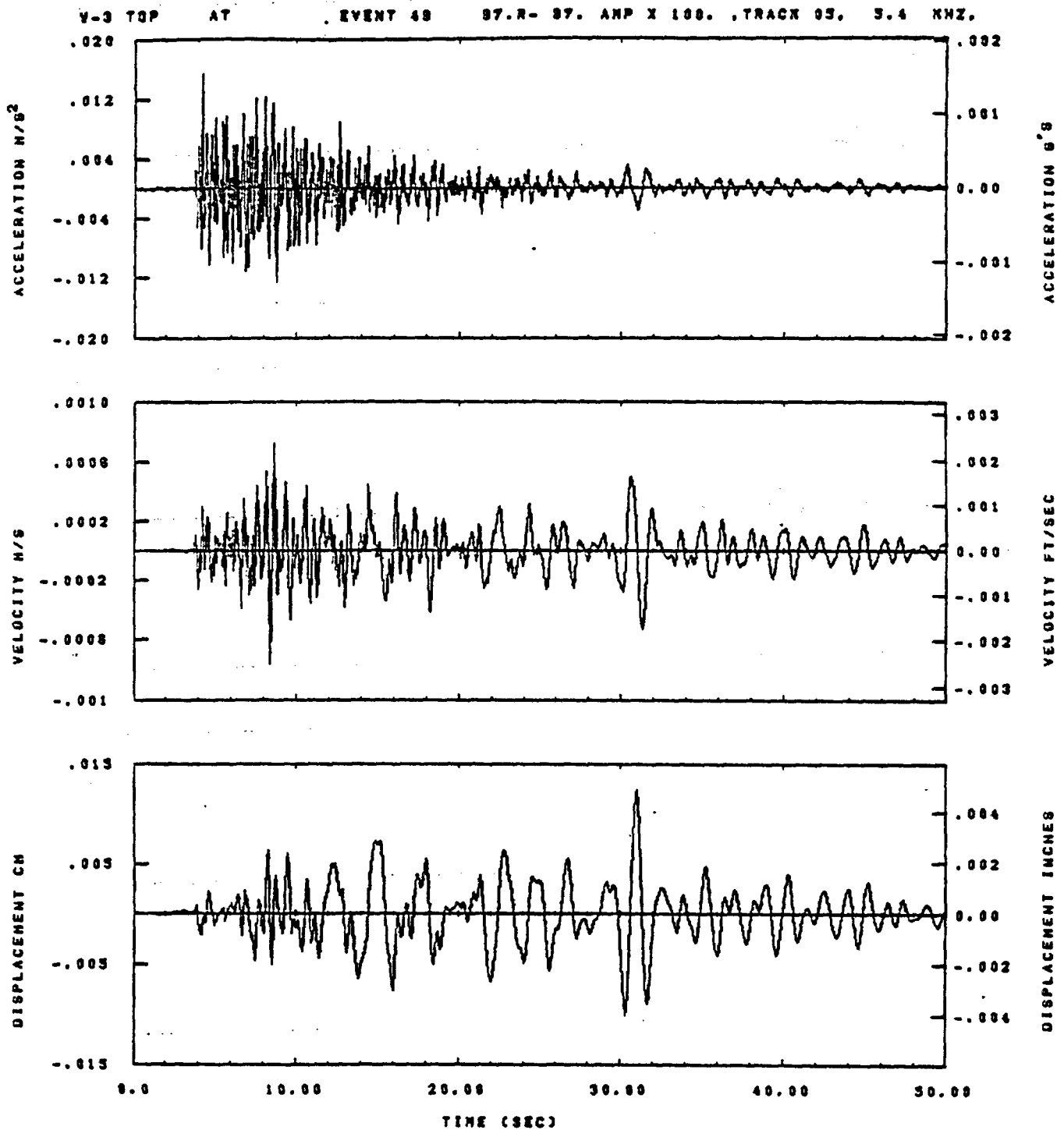


IDT= .0020	ODT= .005	FIX=	AAS= 0.
HPP= .30	BYH= .20	HLH= 167	ASB=
LPP= 27.	BYL= 6.	HLL= 1888	ASE=
VTE= .300	VTE= .200	FLL= -20.	VSE= 0.
DPE= 0.	DPE= 100.	FLH= 0	DSE= 0.

15.35.56.

06/30/82

Figure F-112

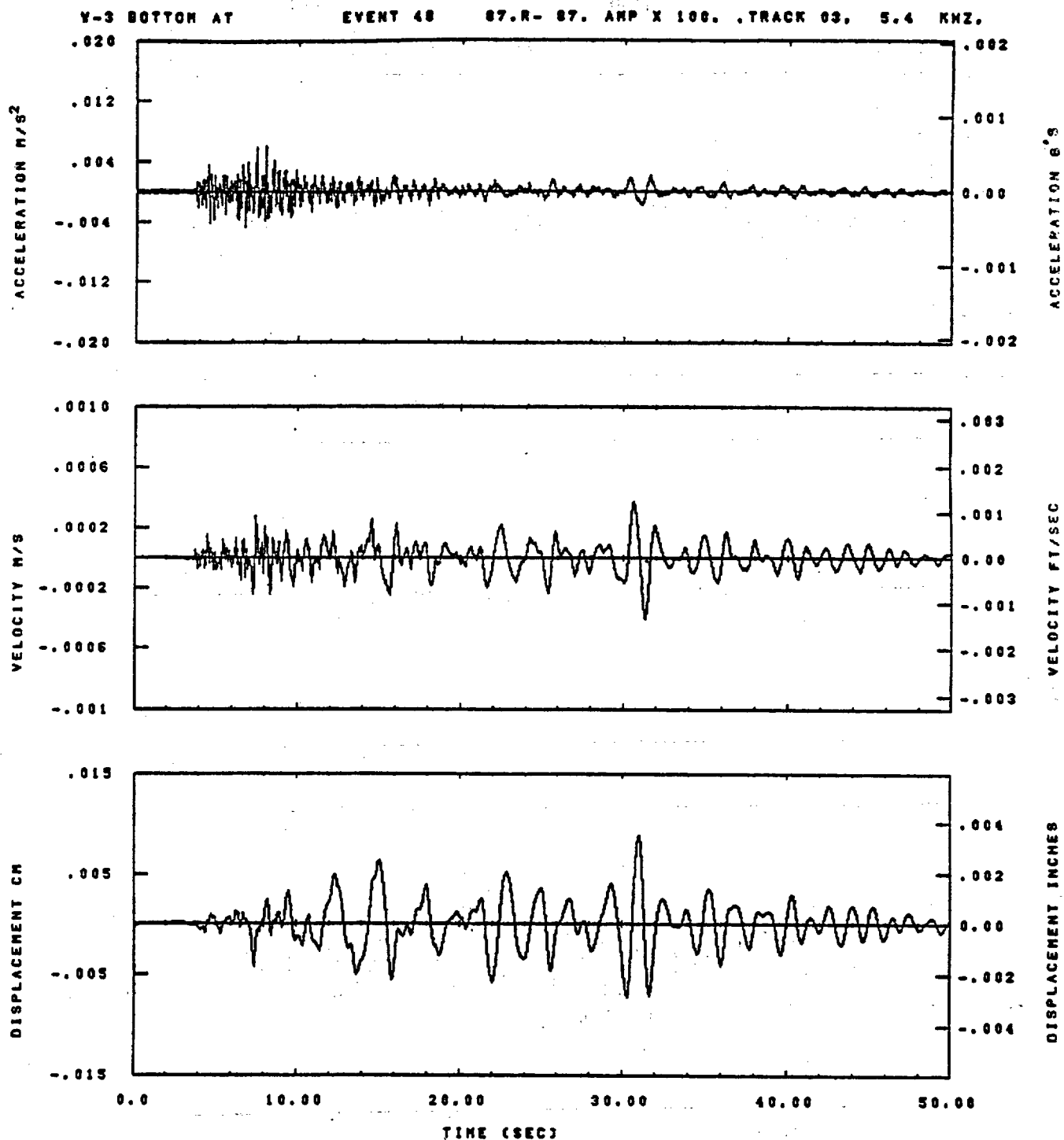


IDT= .0020	DDT= .003	FIX=	AAS= 0.
HPP= .30	BYH= .20	HLH= 187	ASS=
LPP= 27.	BYL= 8.	HLL= 1393	ASE=
VTB= .300	VTE= .200	FLL= -20.	VSE= 0.
OPB= 0.	OPE= 100.	FLH= 0	OSE= 0.

13.35.47.

08/30/82

Figure F-113

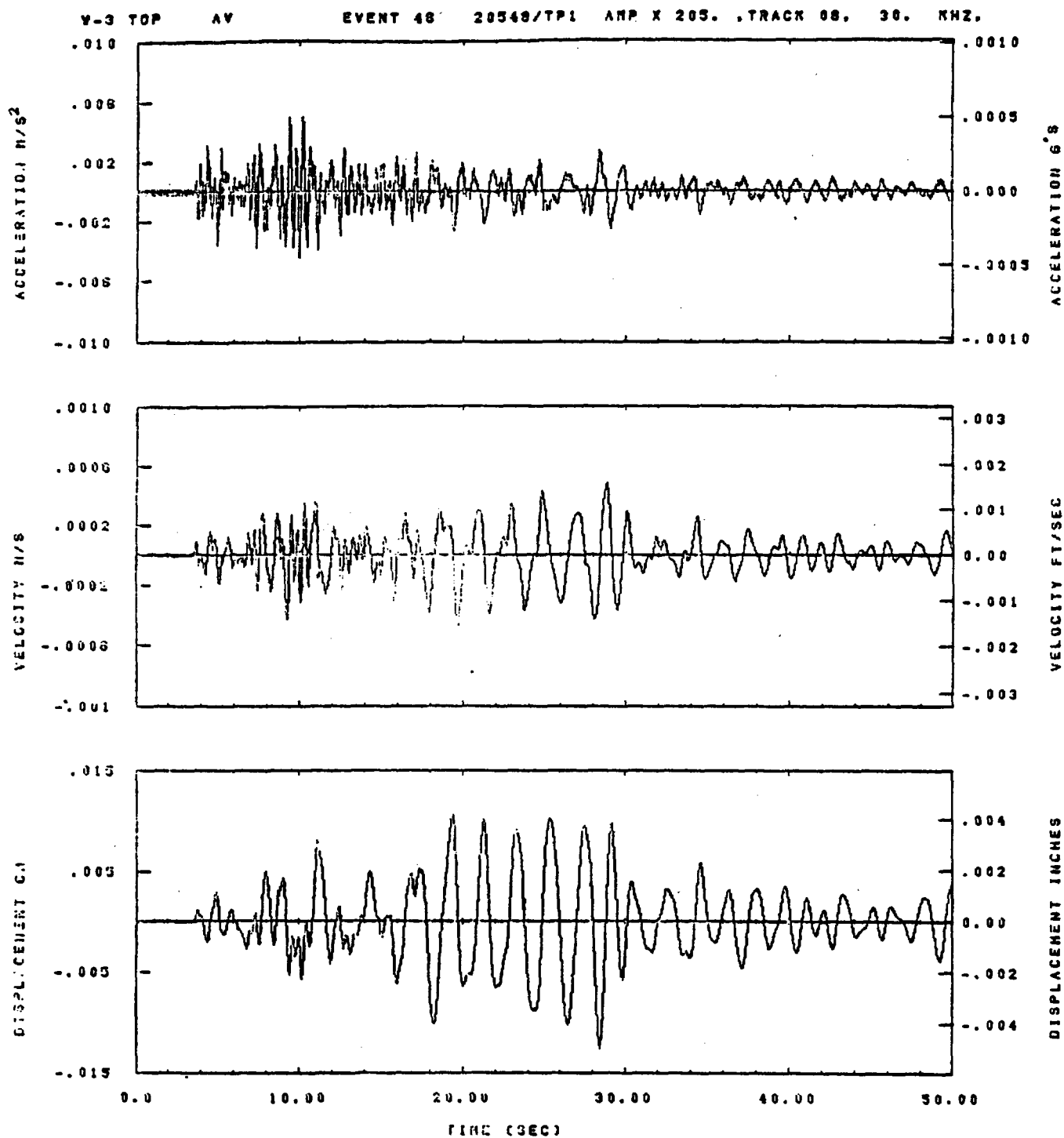


IDT= .0020	ODT= .005	FIX=	AAS= 0.
HPF= .30	BYH= .20	HLH= 167	ASB=
LPF= 27.	BYL= 6.	HLL= 1888	ASE=
VTS= .300	VTE= .200	FLL= -20.	VSE= 0.
OPS= 0.	DPE= 100.	FLH= 0	DSE= 0.

15.36.00.

06/30/82

Figure F-114

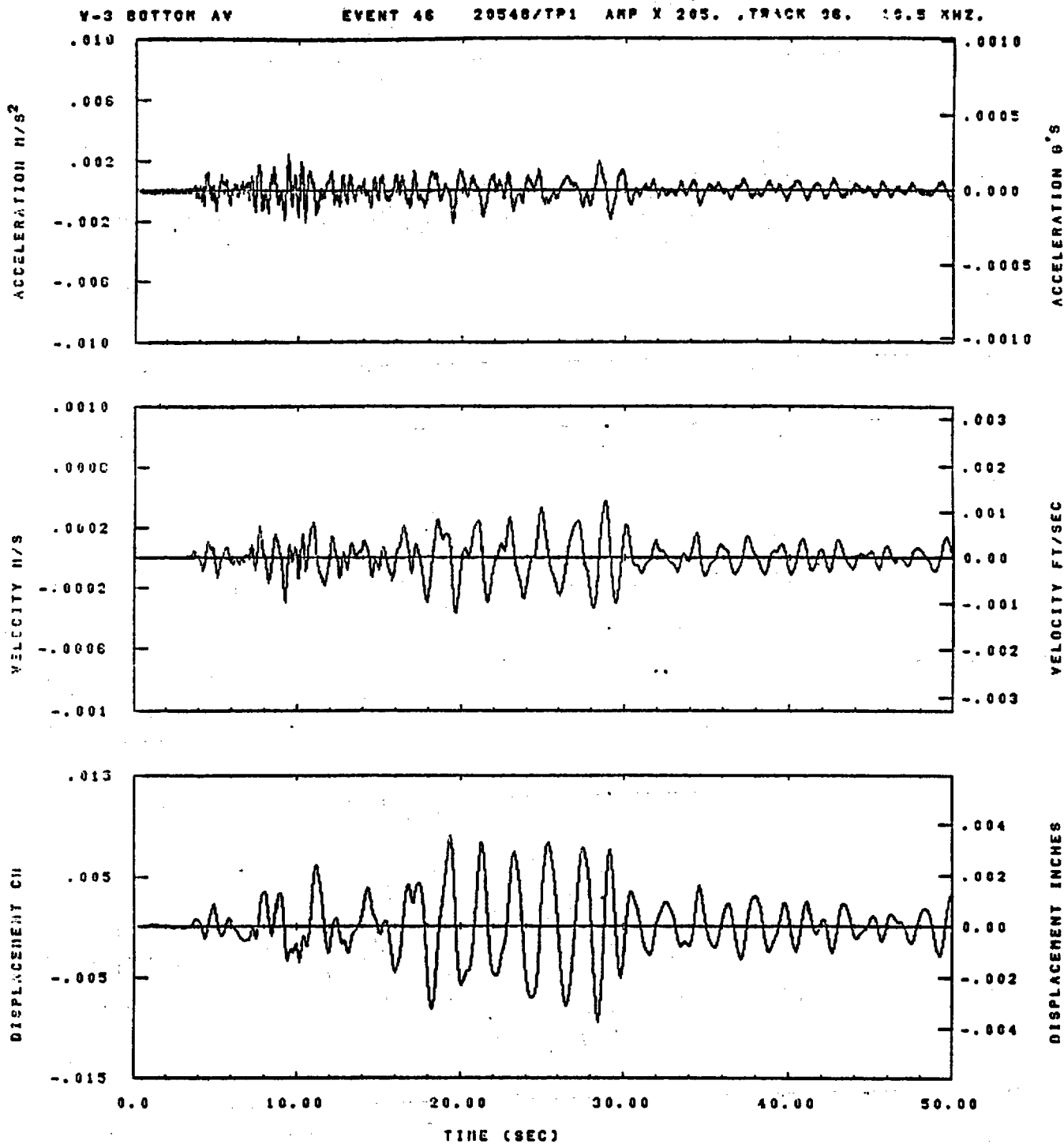


IDT= .0020	ODT= .003	FIX=	AAS= 0.
HPF= .30	QVH= .20	HLH= 201	ASB=
LPF= 22.	QVL= 3.	HLL= 1999	ASE=
VTB= .300	VTE= .200	FLL= -20.	VSE= 0.
DPB= 0.	DPE= 100.	FLH= 0	DSE= 0.

15.43.41.

06/21/82

Figure F-115

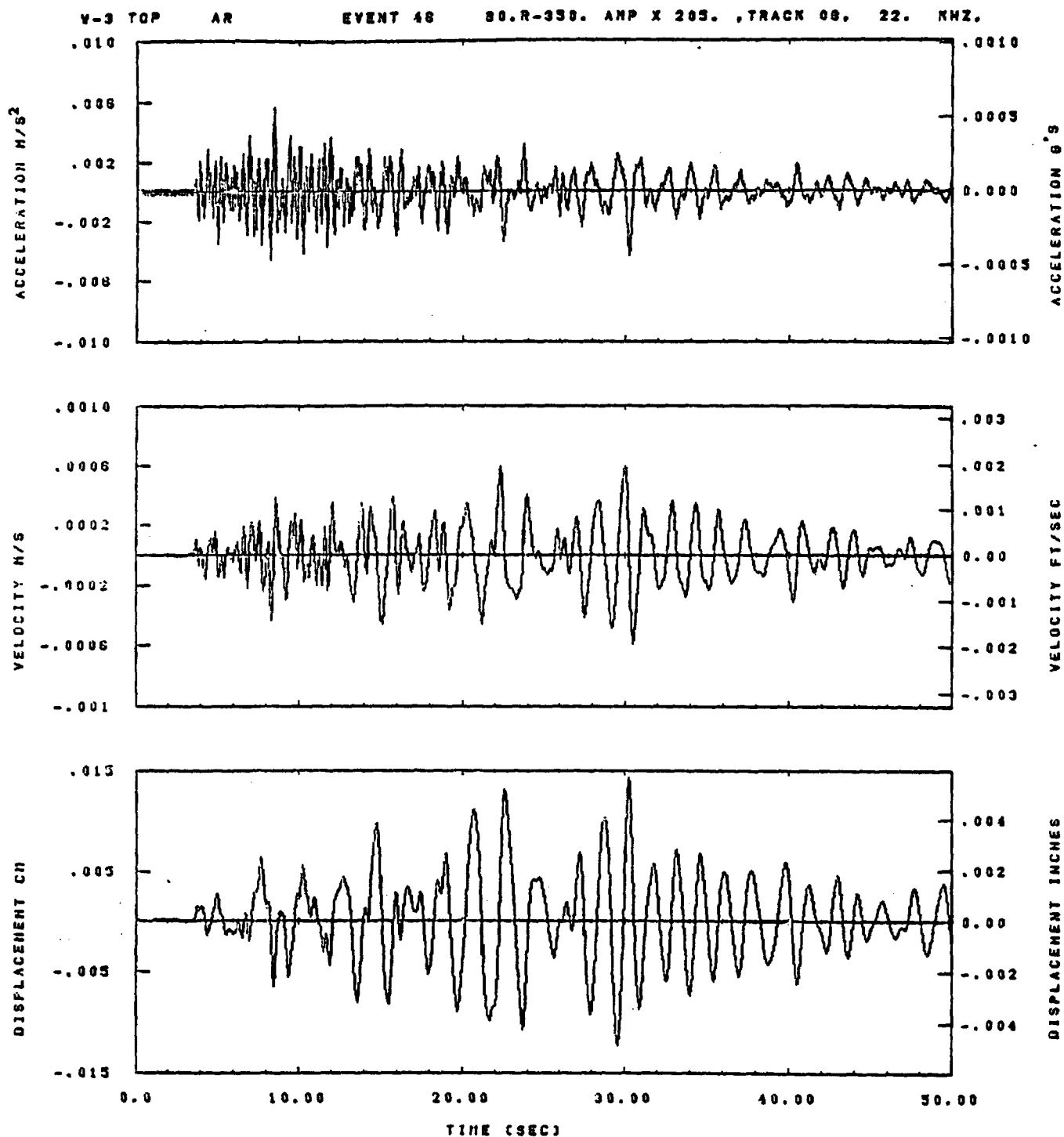


IOT= .0020	ODT= .005	FIX=	AAS= 0.
HPF= .30	BYH= .20	HLH= 201	ASB=
LPF= 22.	BYL= 5.	HLL= 1999	ASE=
VTB= .300	VTE= .200	FLL= -20.	VSE= 0.
DPB= 0.	OPE= 100.	FLH= 0	DSE= 0.

15.47.14.

06/21/82

Figure F-116

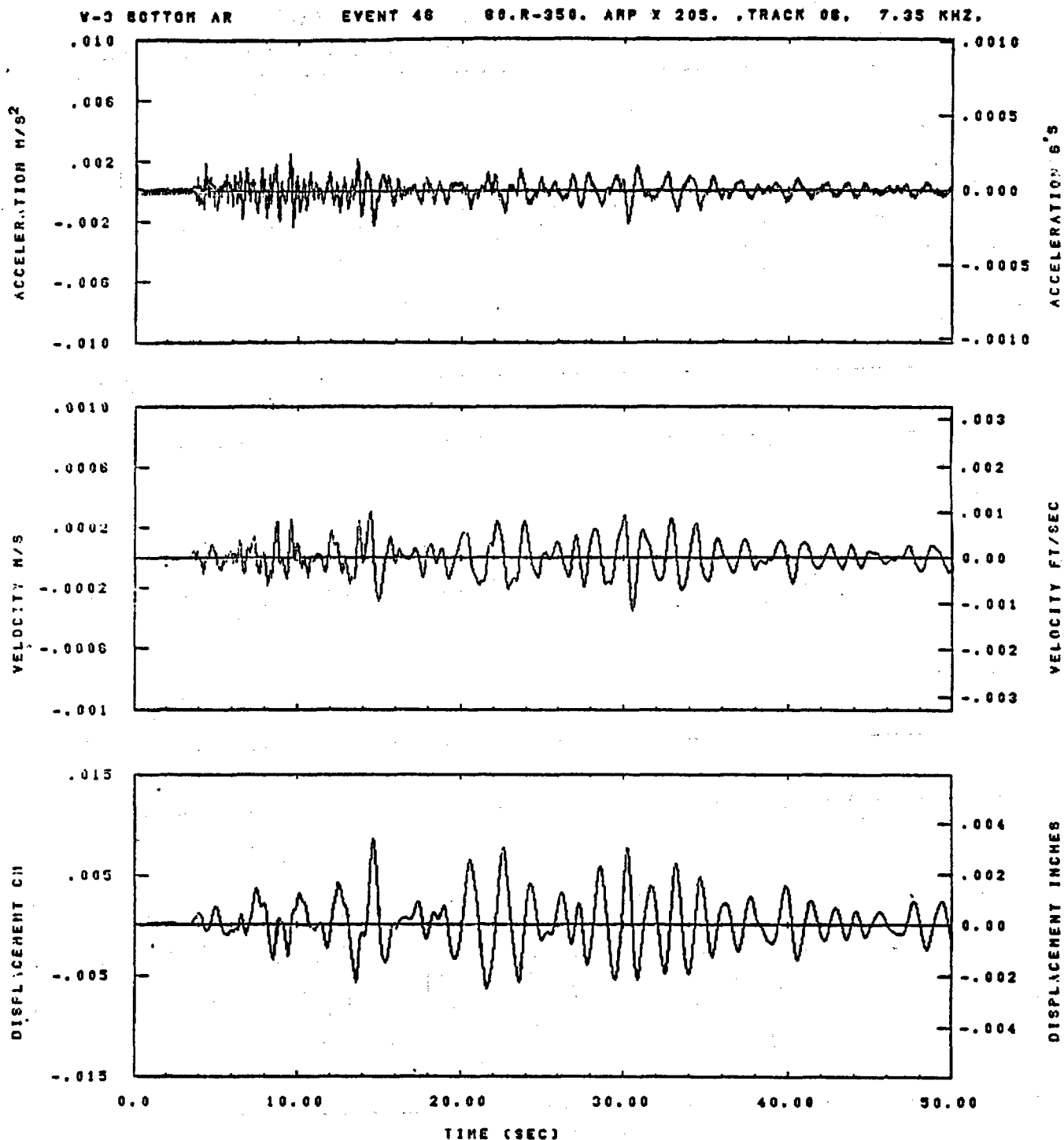


LOT= .0020	OOT= .003	FIX=	AAS= 0.
HPP= .30	BVH= .20	HLH= 201	ASB=
LPP= 22.	BVL= 5.	HLL= 1999	ASE=
VTB= .300	VTE= .200	FLL= -20.	VSE= 0.
DPB= 0.	DPE= 100.	FLH= 0	DSE= 0.

15.48.19.

08/21/82

Figure F-117

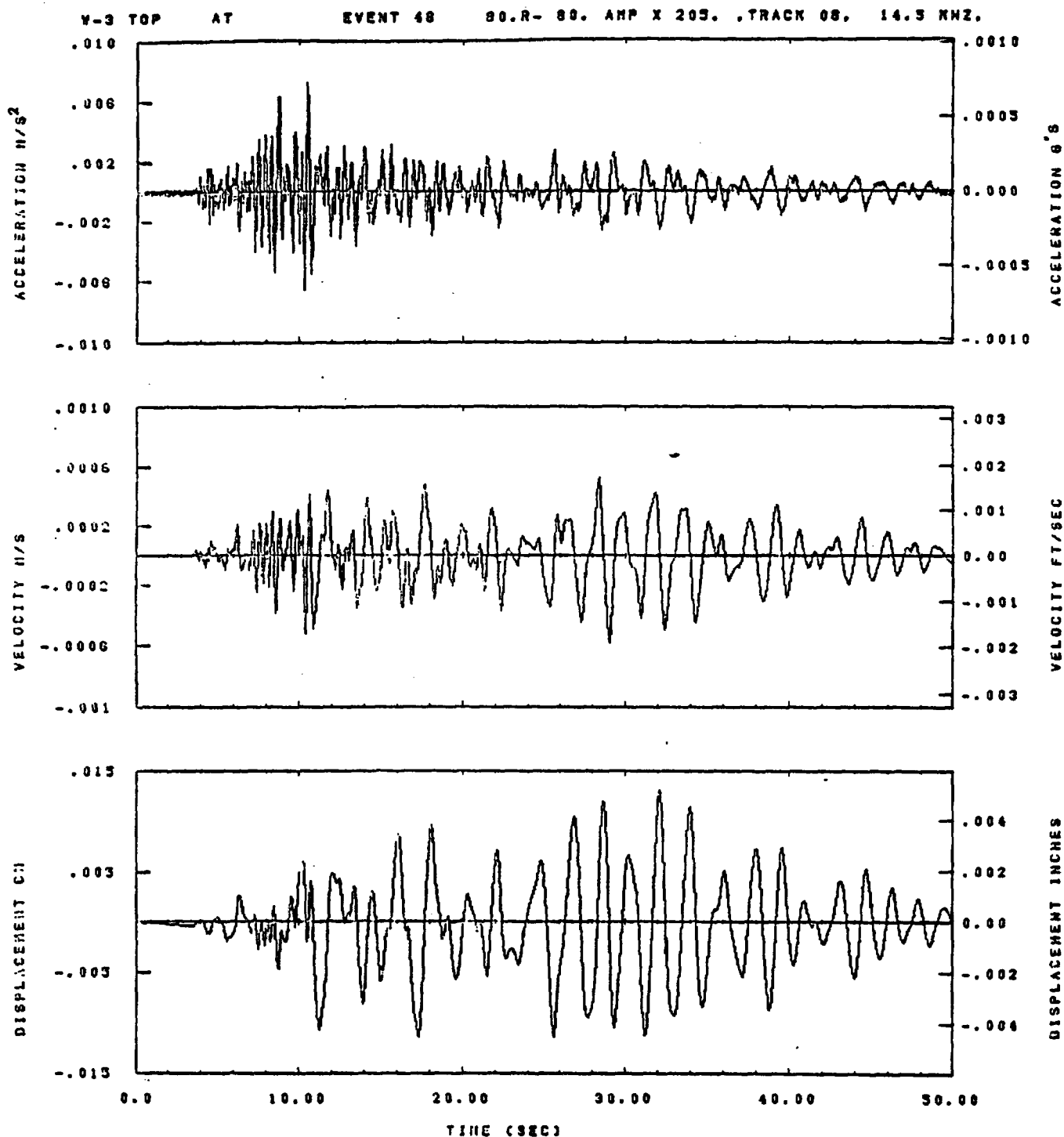


IDT= .0020	ODT= .005	FIX=	AAS= 0.
HPF= .30	BYH= .20	HLH= 201	ASS=
LPF= 22.	DYL= 3.	HLL= 1999	ASE=
VTB= .300	VTE= .200	FLL= -20.	VSE= 0.
OPB= 0.	DPE= 100.	FLH= 0	DSE= 0.

15.47.00.

06/21/82

Figure F-118

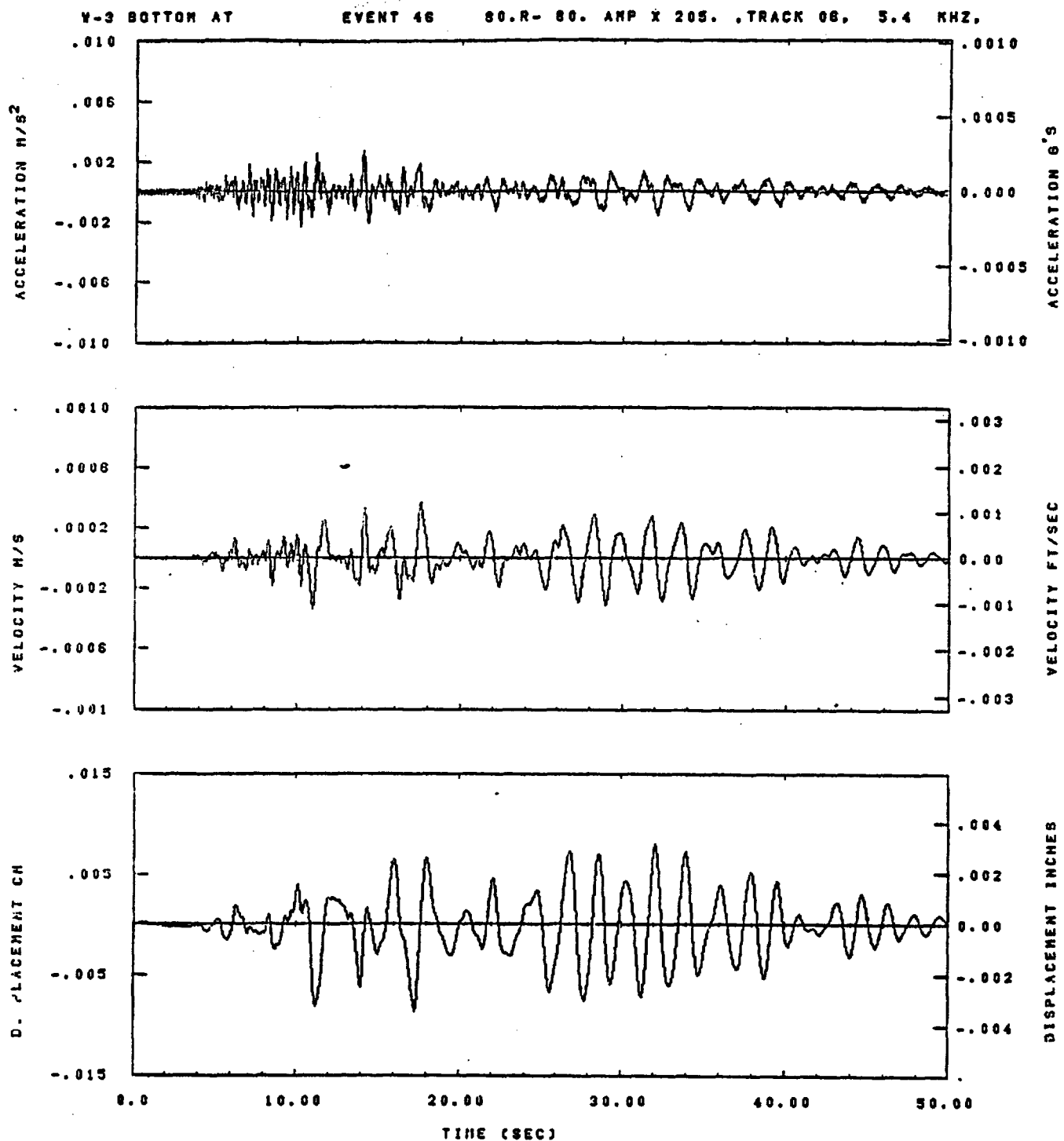


IDT= .0020	ODT= .003	FIX=	AAS= 0.
HPF= .30	BVN= .20	HLN= 201	ASB=
LPF= 22.	BVL= 3.	HLL= 1999	ASZ=
VTB= .300	VTE= .200	FLL= -20.	VSE= 0.
DPS= 0.	DPE= 100.	FLH= 0	DSE= 0.

13.48.33.

08/21/82

Figure F-119



IDT= .0020	ODT= .005	FIX=	AAS= 0.
HPF= .30	BYH= .20	HLH= 201	ASB=
LPF= 22.	BVL= 5.	HLL= 1999	ASE=
VTB= .300	YTE= .200	FLL= -20.	VSE= 0.
DPB= 0.	DPE= 100.	FLH= 0	DSE= 0.

15.47.06.

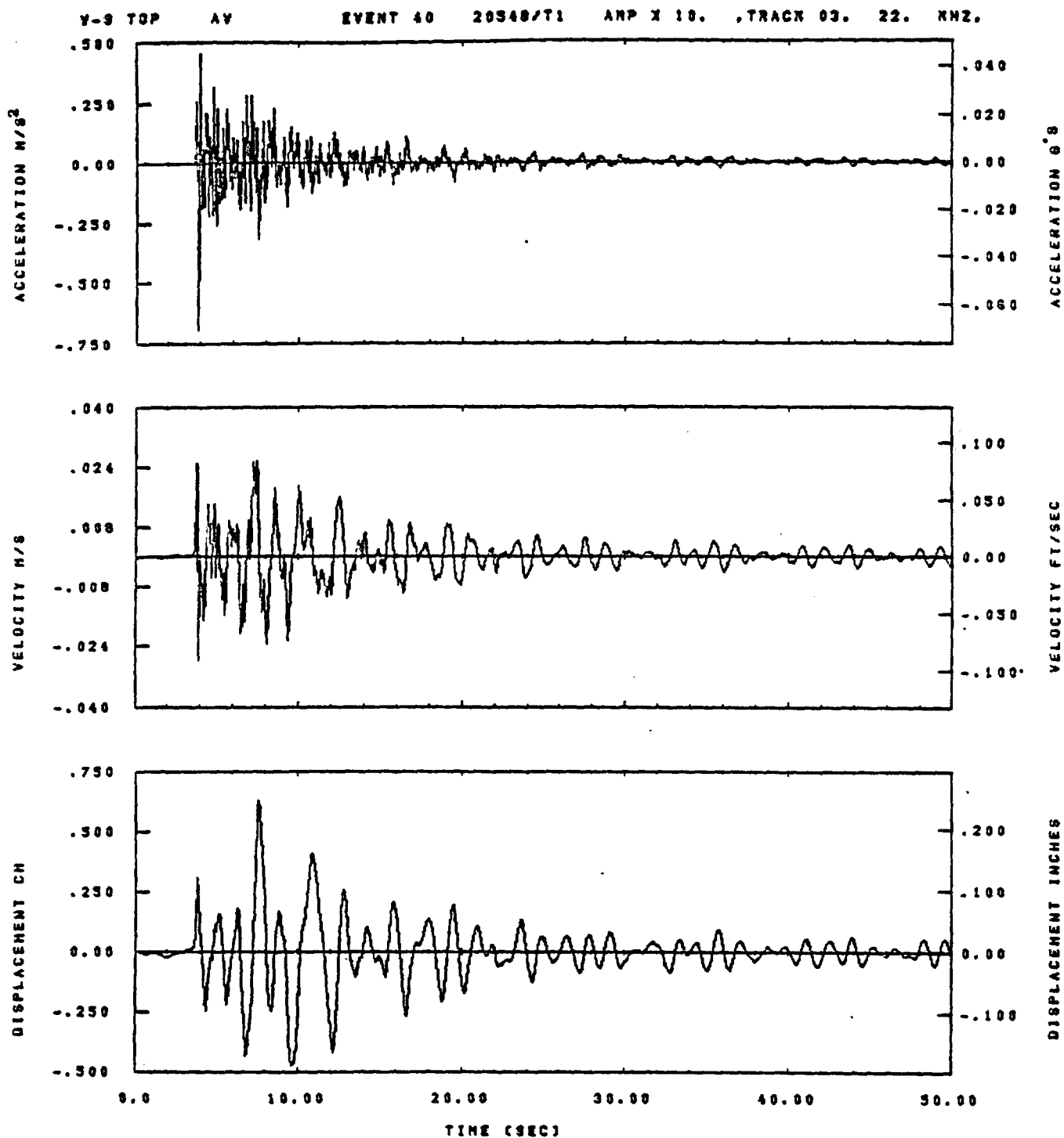
06/21/82

Figure F-120

APPENDIX G

COMPARISON OF TOP AND BOTTOM

WAVEFORMS AT STATION W-9

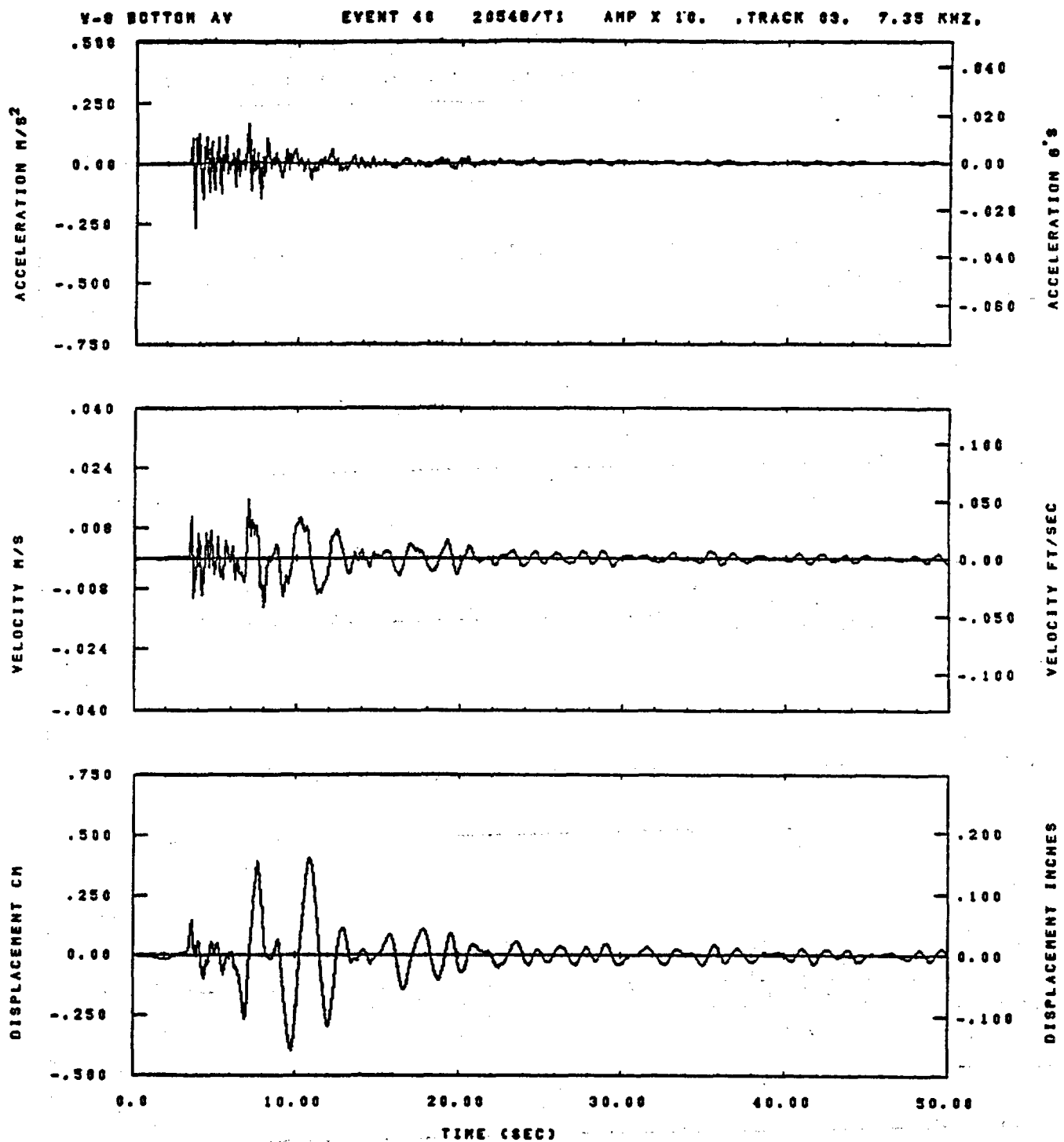


IDT= .0020	ODT= .003	FIX=	AAS= 0.
HPP= .25	BYH= .18	HLH= 187	ASB=
LPP= 27.	BVL= 8.	HLL= 2399	ASE=
VTB= .250	VTE= .188	PLL= -20.	VSE= 0.
OPS= 0.	OPE= 95.	FLH= 0	DSE= 0.

13.17.35.

08/25/82

Figure G-1

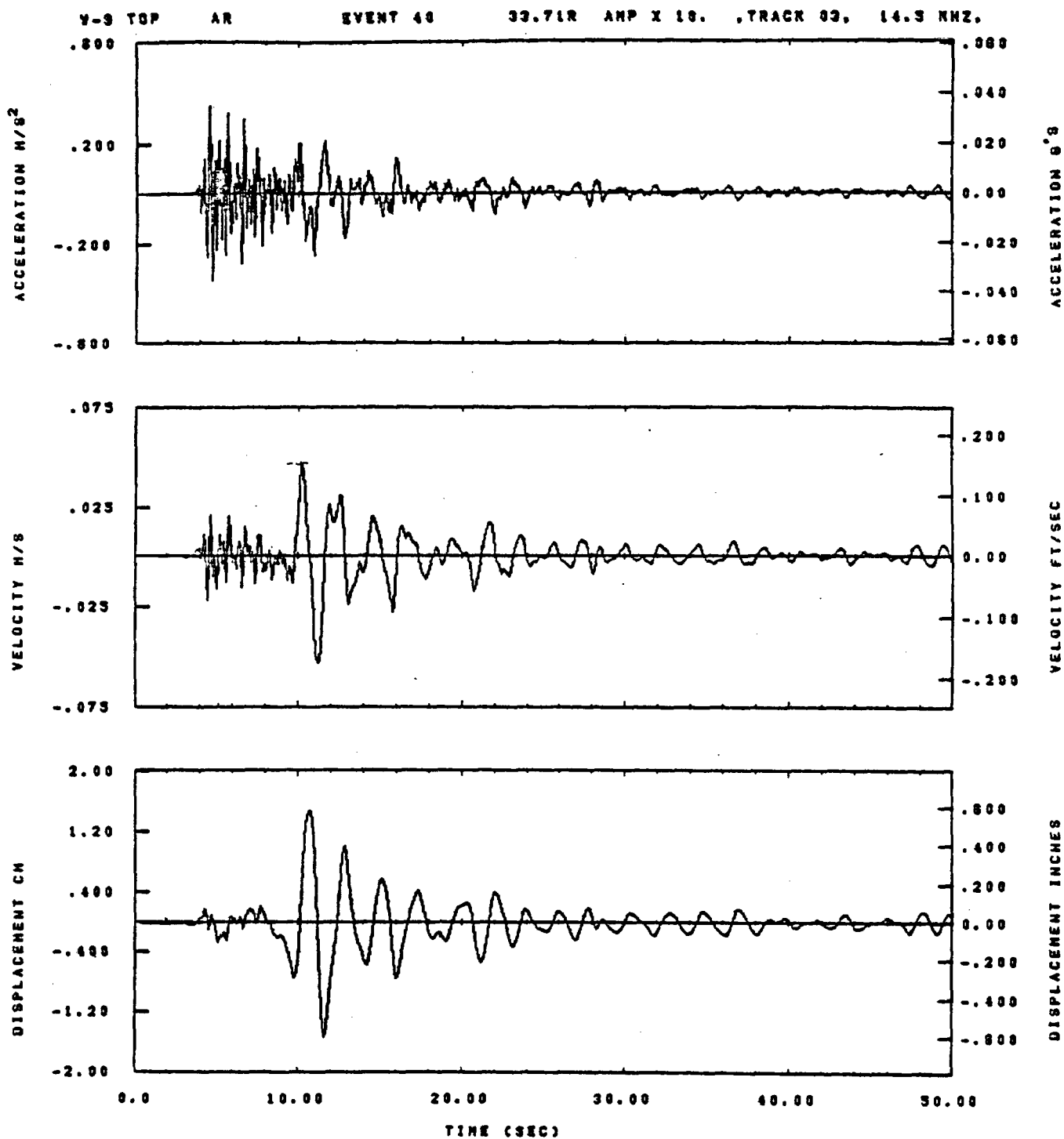


IDT= .0020	ODT= .005	FIX=	AAS= 0.
HPP= .25	BYH= .16	HLH= 167	ASB=
LPP= 27.	BYL= 6.	MLL= 2399	ASE=
VTS= .250	VTE= .166	FLL= -20.	VSE= 0.
DPS= 0.	DPE= 85.	FLH= 0	DSE= 0.

13.16.56.

06/25/82

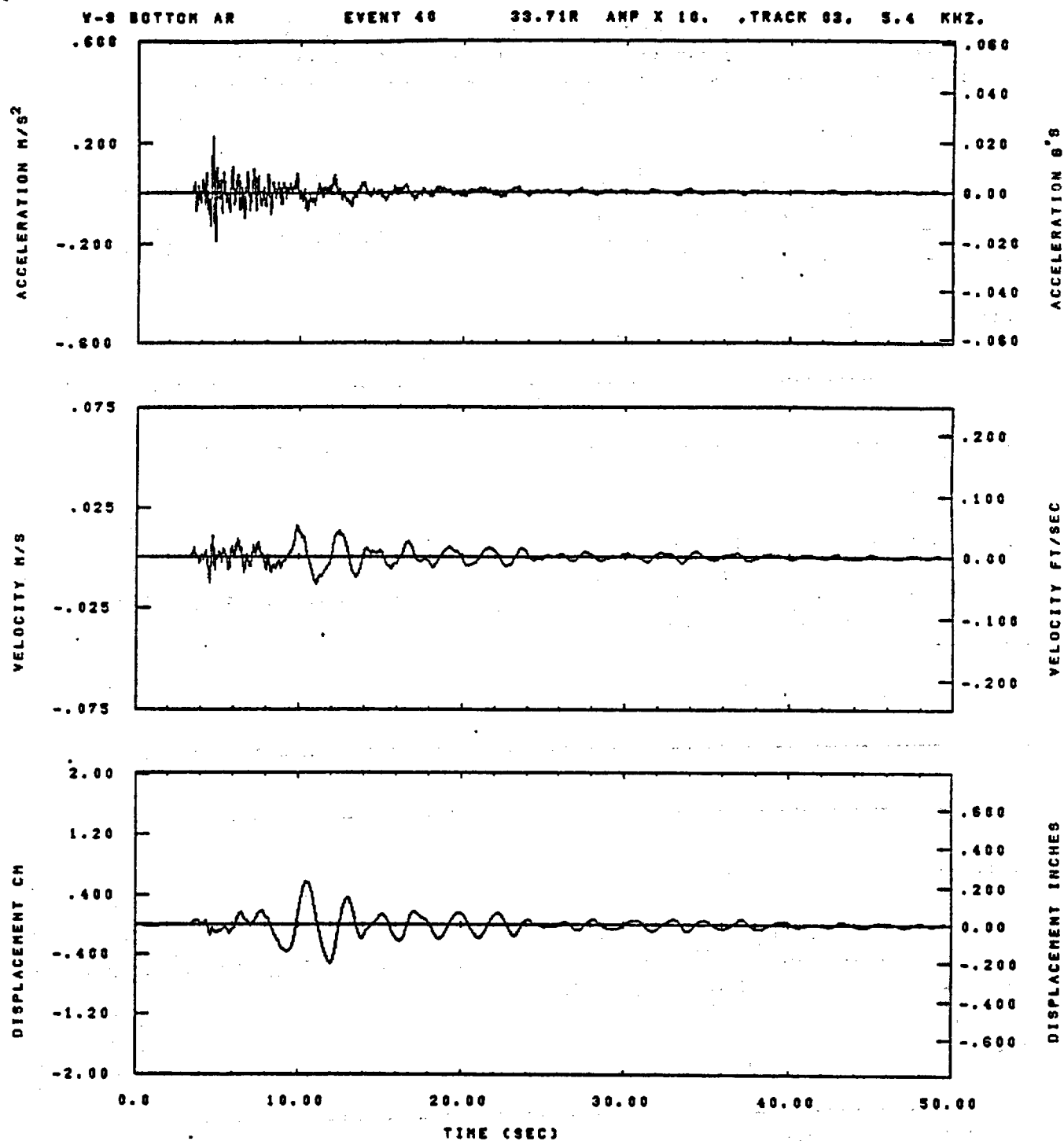
Figure G-2



IDT= .0020	ODT= .003	FIX=	AAS= 0.
HPF= .25	BYN= .18	HLH= 187	ASB=
LPF= 27.	BYL= 8.	HLL= 2399	ASE=
VTS= .250	VTE= .188	FLL= -20.	VSE= 0.
OPB= 0.	OPE= 95.	FLH= 0	DSE= 0.

13.17.33.

08/23/82

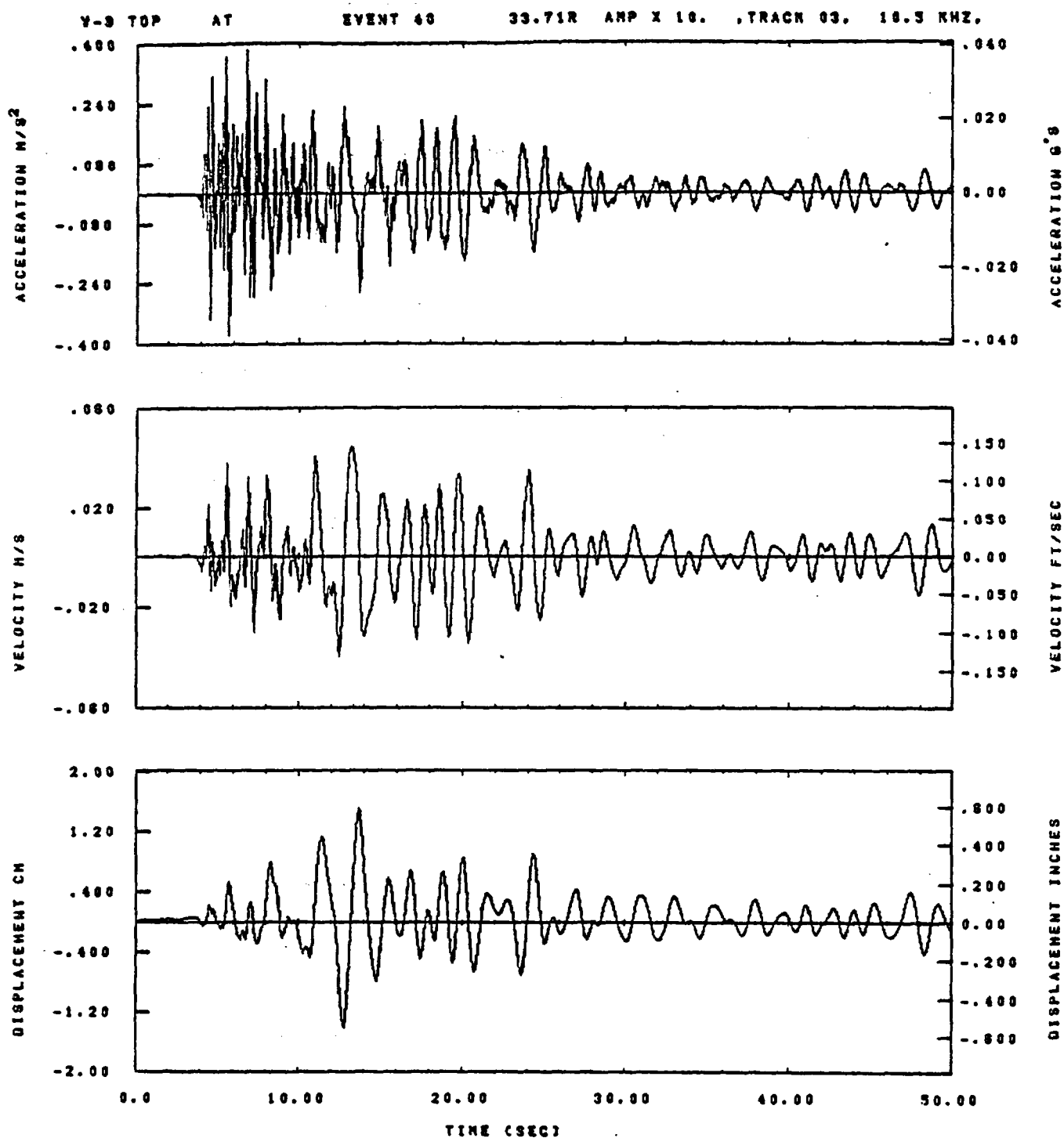


IDT= .0020	ODT= .005	FIX=	AAS= 0.
HPP= .25	SVH= .16	HLN= 167	ASB=
LPP= 27.	SVL= 6.	HLL= 2388	ASE=
VTS= .250	VTE= .166	FLL= -20.	VSE= 0.
DPS= 0.	OPE= 85.	FLH= 0	DSE= 0.

13.16.58.

06/25/82

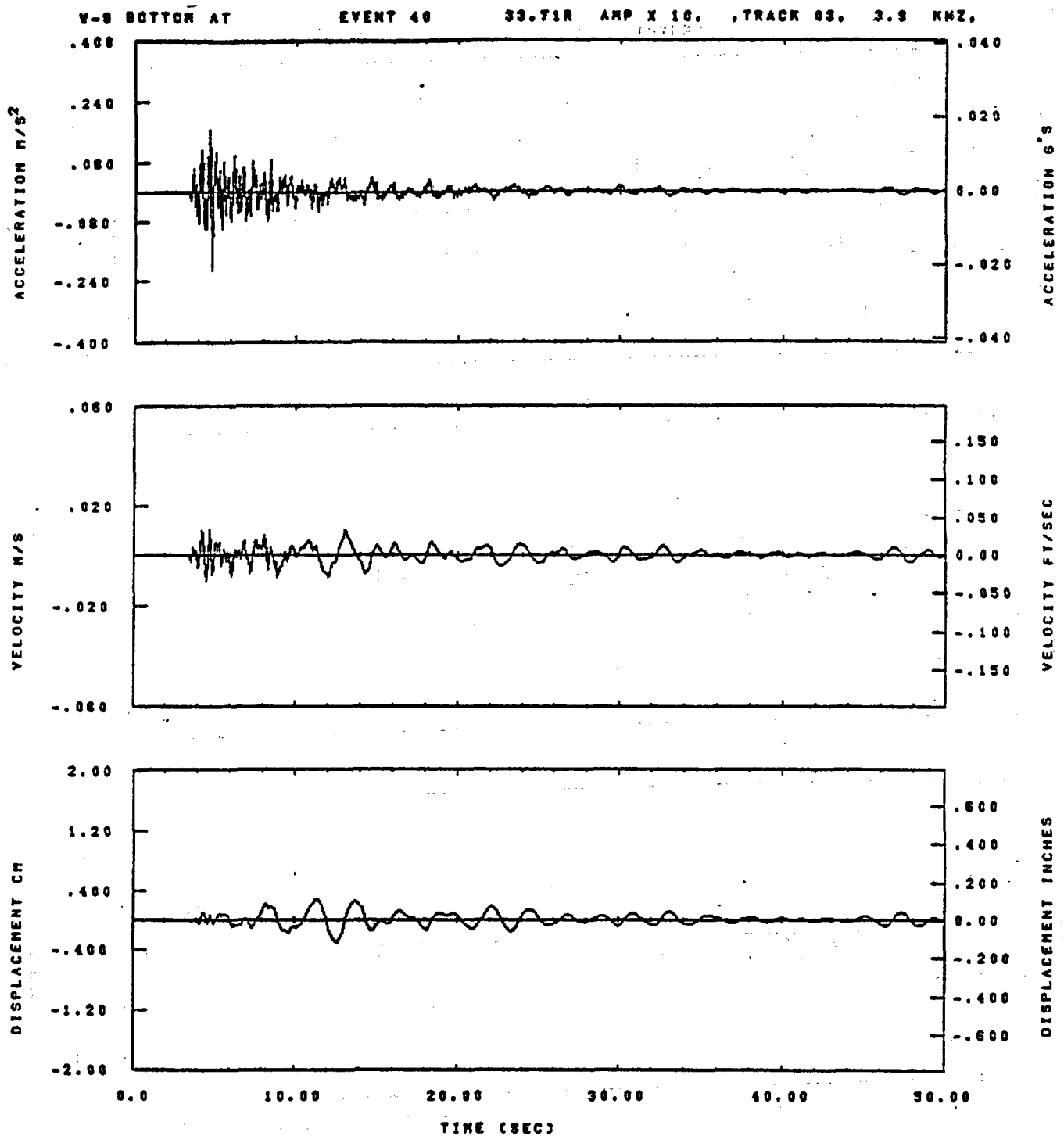
Figure G-4



IDY= .0020	ODY= .003	FIX=	AAS= 0.
HPP= .25	BYH= .18	HLH= 187	ASB=
LPP= 27.	BYL= 8.	HLL= 2399	ASE=
VTS= .250	VTE= .188	FLL= -20.	YSE= 0.
DPB= 0.	DPE= 95.	FLH= 0	DSE= 0.

13.17.48.

08/23/92

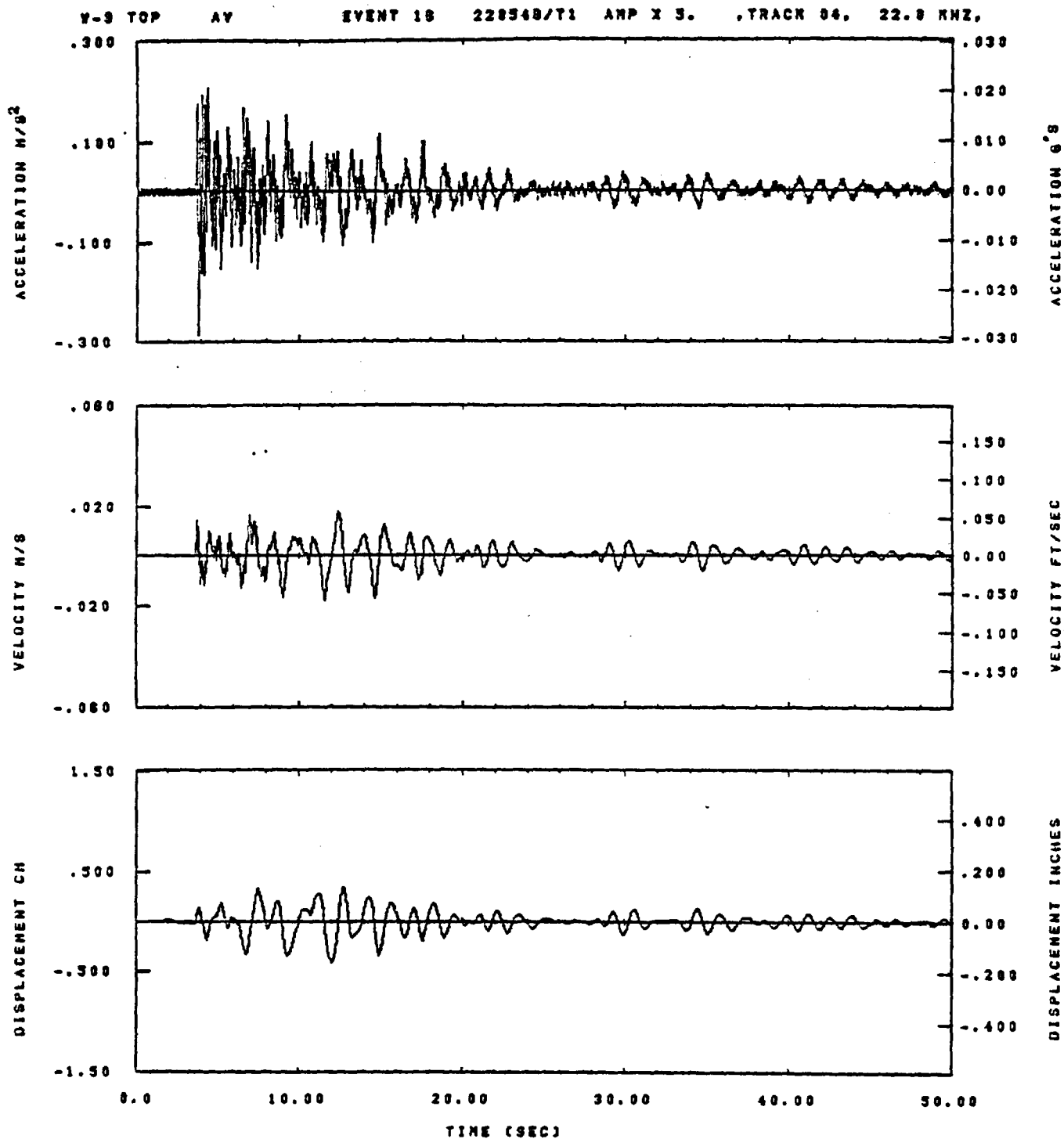


IDT= .0020	ODT= .005	FIX=	AAS= 0.
HPF= .25	BVH= .16	HLH= 167	ASB=
LPF= 27.	BVL= 6.	HLL= 2388	ASE=
VTB= .250	VTE= .166	FLL= -20.	VSE= 0.
DPS= 0.	DPE= 85.	FLH= 0	DSE= 0.

13.17.03.

06/25/82

Figure G-6

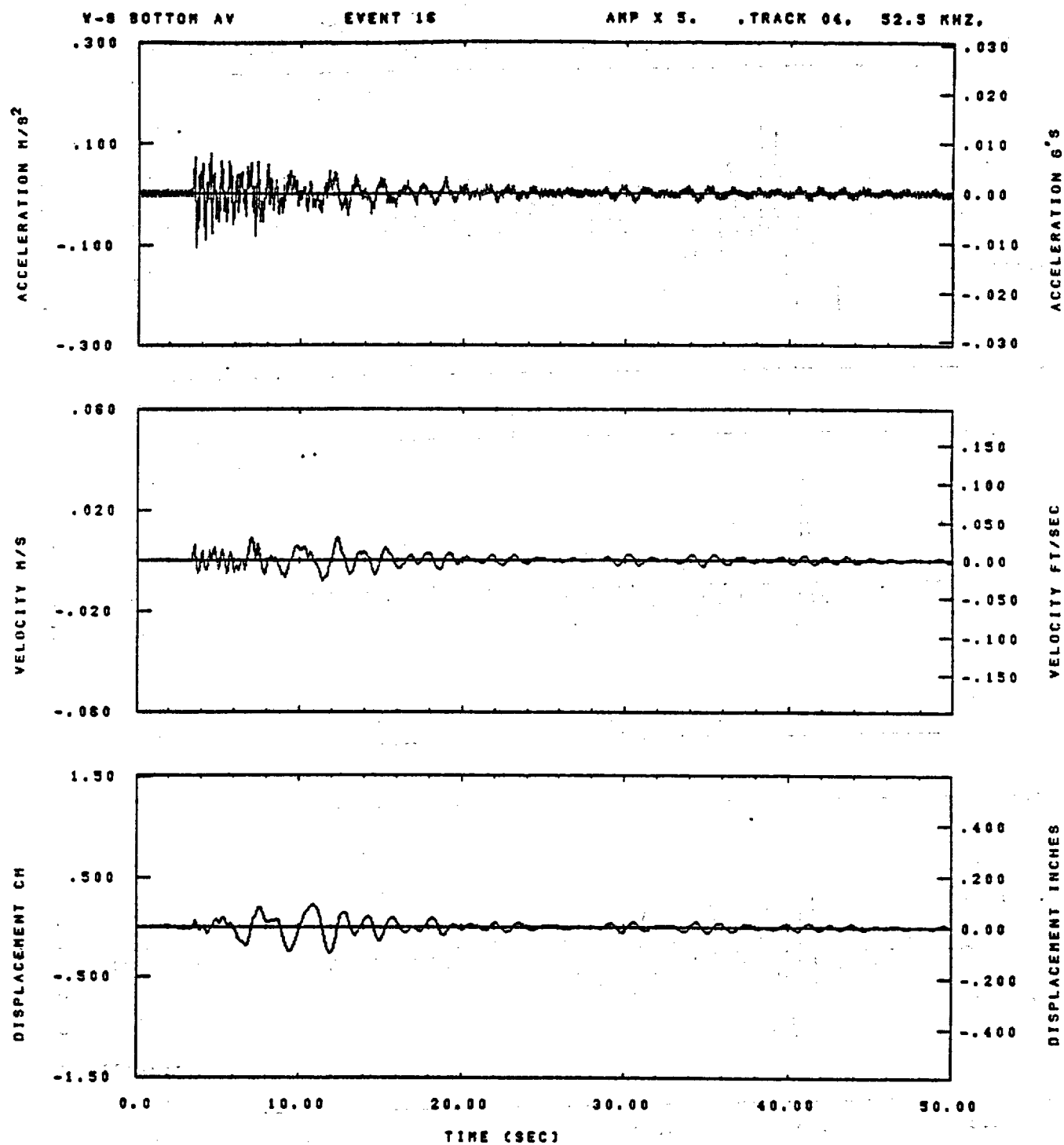


IDT= .0028	QDT=	FIX=	AAS= 0.
HPF= .3	BYH= .20	HLH= 187	ASS=
LPF= 27.	BYL= 8.	HLL= 1333	ASE=
VTB= .30	VTE= .208	FLL= -20.	VSE= 0.
DPS= 0.	DPE= 100.	FLH= 0	DSE= 0.

14.38.28.

07/89/82

Figure G-7

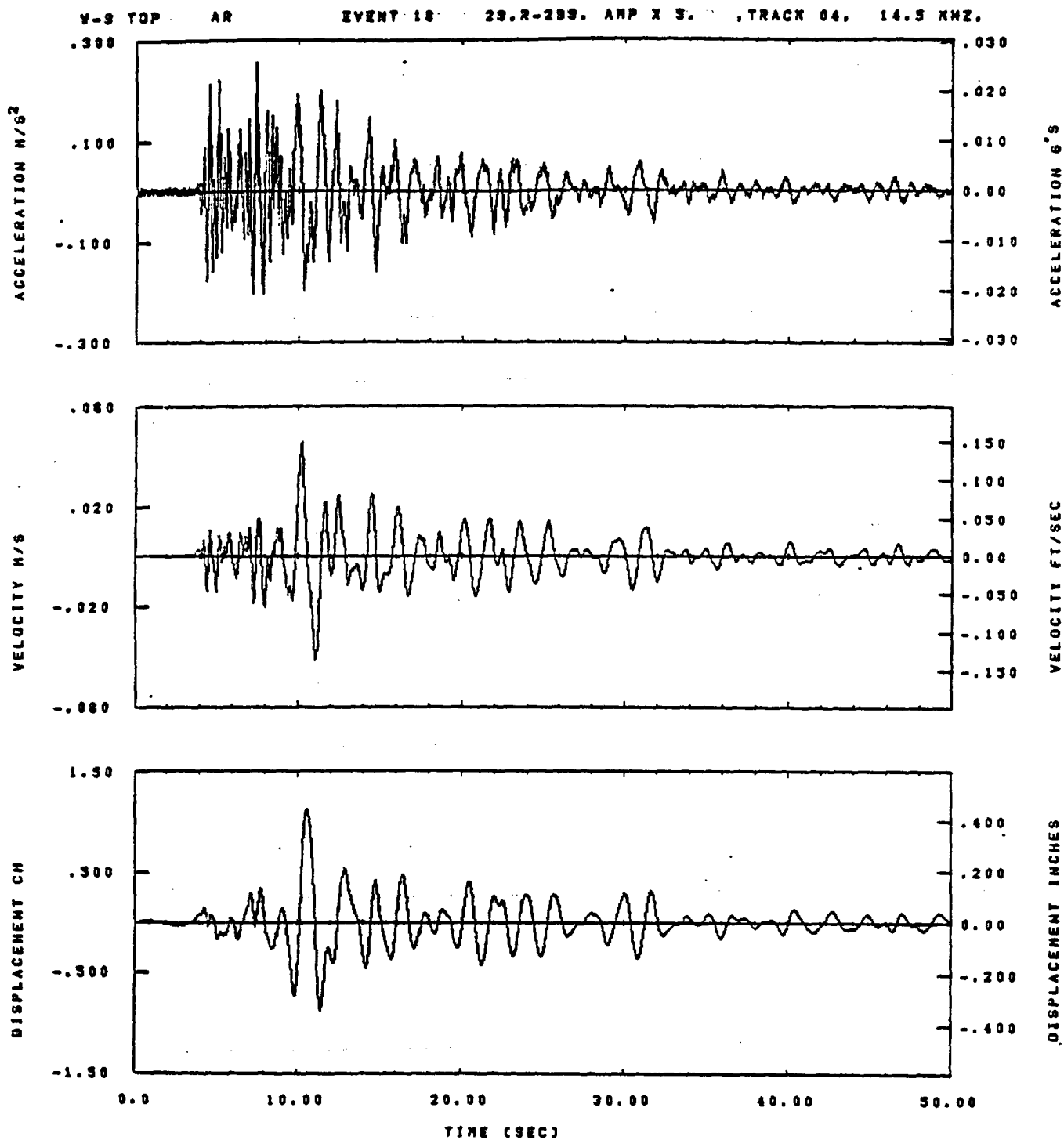


IDT=	.0020	ODT=		FIX=		AAS=	
HPP=	.3	BYH=	.20	HLH=	167	ASB=	
LPP=	27.	BYL=	6.	HLL=	1999	ASE=	
VTB=	.30	VTE=	.200	FLL=		VSE=	
DPS=		DPE=		FLH=	0	DSE=	0.

14.38.55.

07/08/82

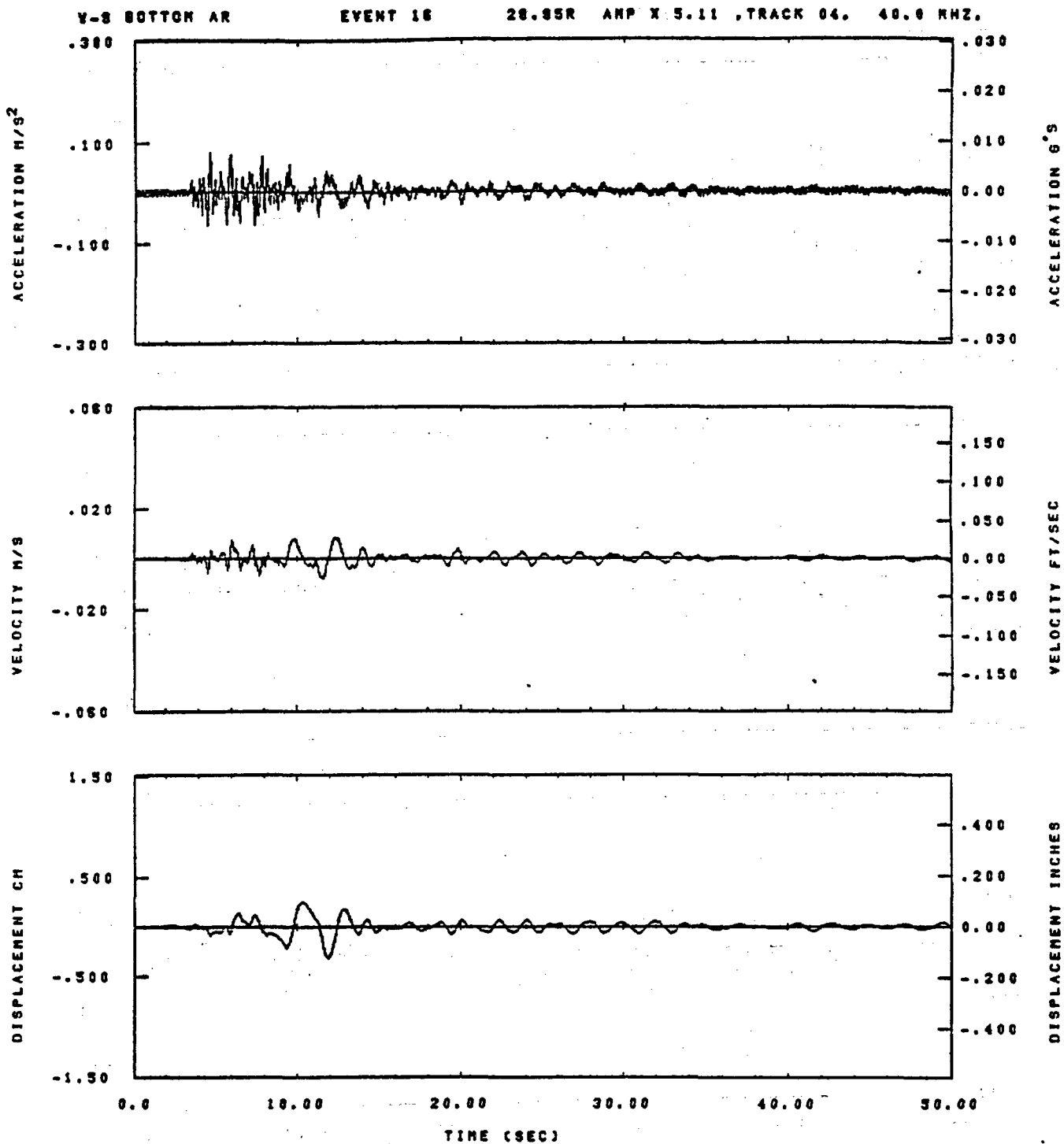
Figure G-8



IDT= .0020	ODT=	FIX=	AAS= 0.
HPP= .3	BVH= .20	HLH= 187	ASB=
LPP= 27.	BWL= 8.	HLL= 1999	ASE=
VTS= .30	VTE= .200	FLL= -20.	VSE= 0.
DPS= 0.	DPZ= 100.	FLH= 0	DSE= 0.

14.38.37.

07/09/82

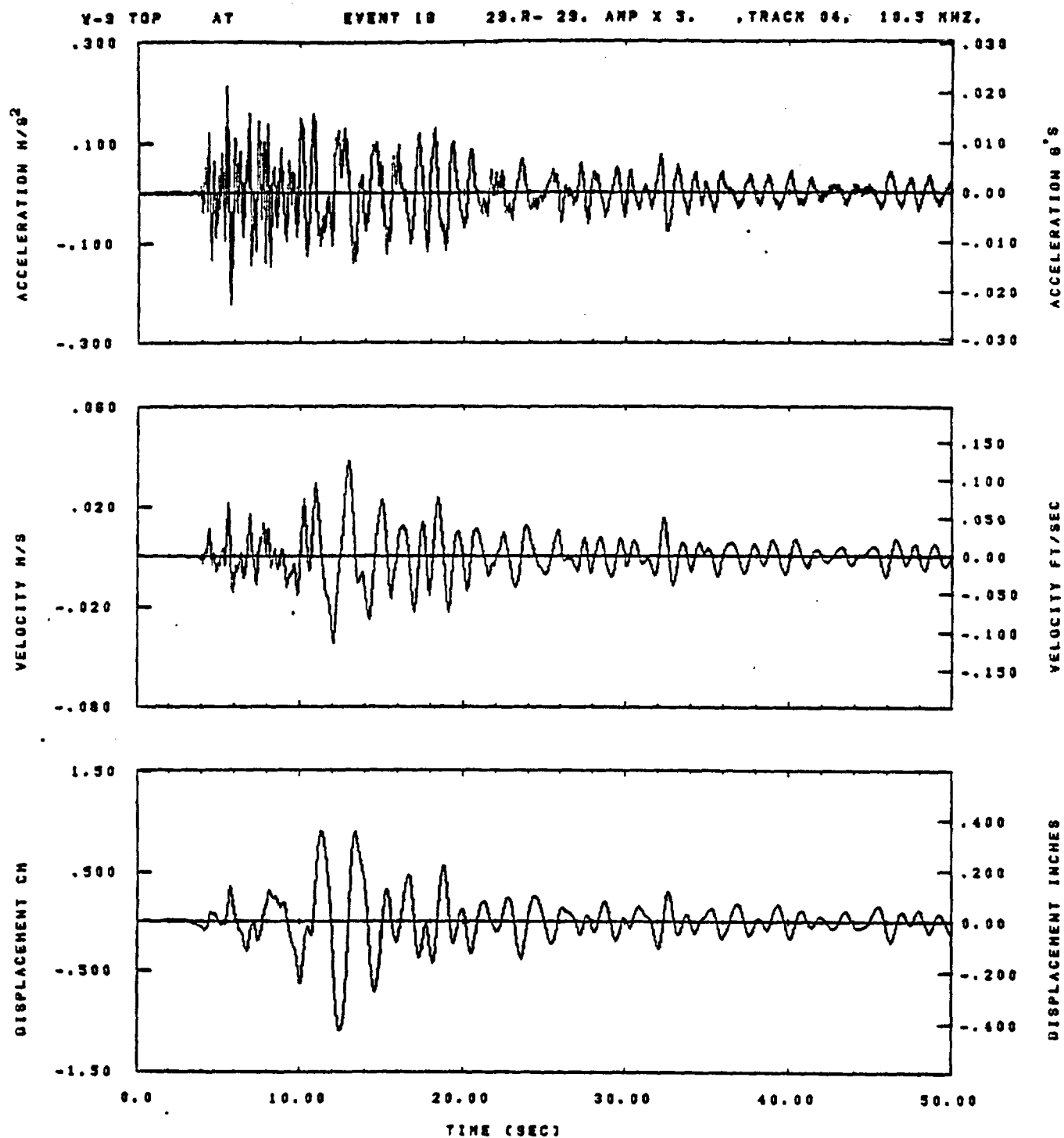


IDT= .0020	ODT= .005	FIX=	AAS= 0.
HPF= .20	BYH= .13	HLH= 251	ASB=
LPF= 18.	BYL= 4.	HLL= 2999	ASE=
VTS= .200	VTE= .133	FLL= -20.	VSE= 0.
DPS= 0.	DPE= 100.	FLH= A-.1	DSE= A+.1

14.38.06.

07/08/82

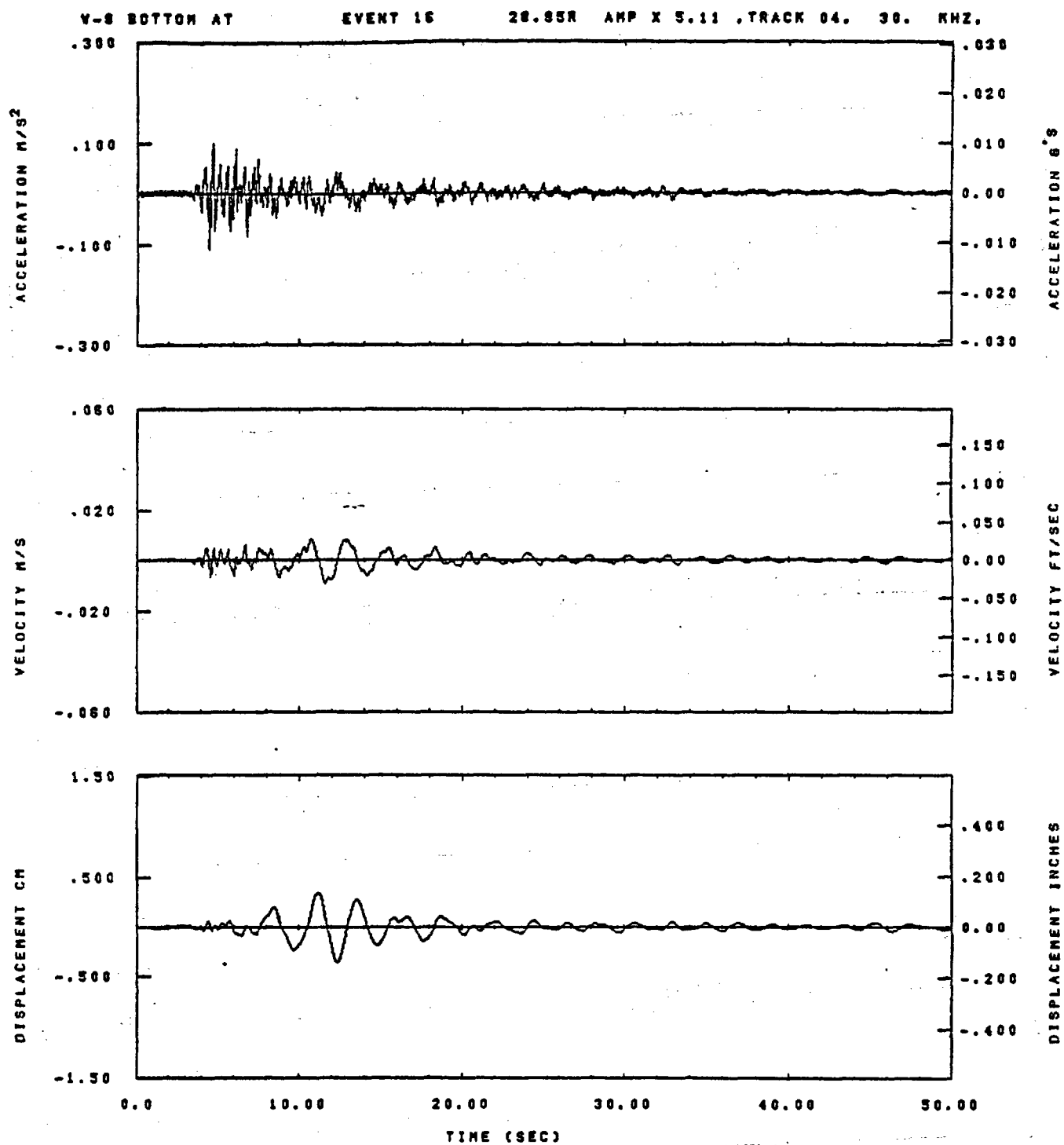
Figure G-10



IDT= .0020	ODT=	FIX=	AAS= 0.
HPF= .3	SVH= .20	HLH= 167	ASS=
LPF= 27.	SVL= 6.	HLL= 1999	ASE=
VTB= .30	VTE= .200	FLL= -20.	VSE= 0.
OPB= 0.	OPE= 100.	FLH= 0	DSE= 0.

14.38.47.

07/09/82

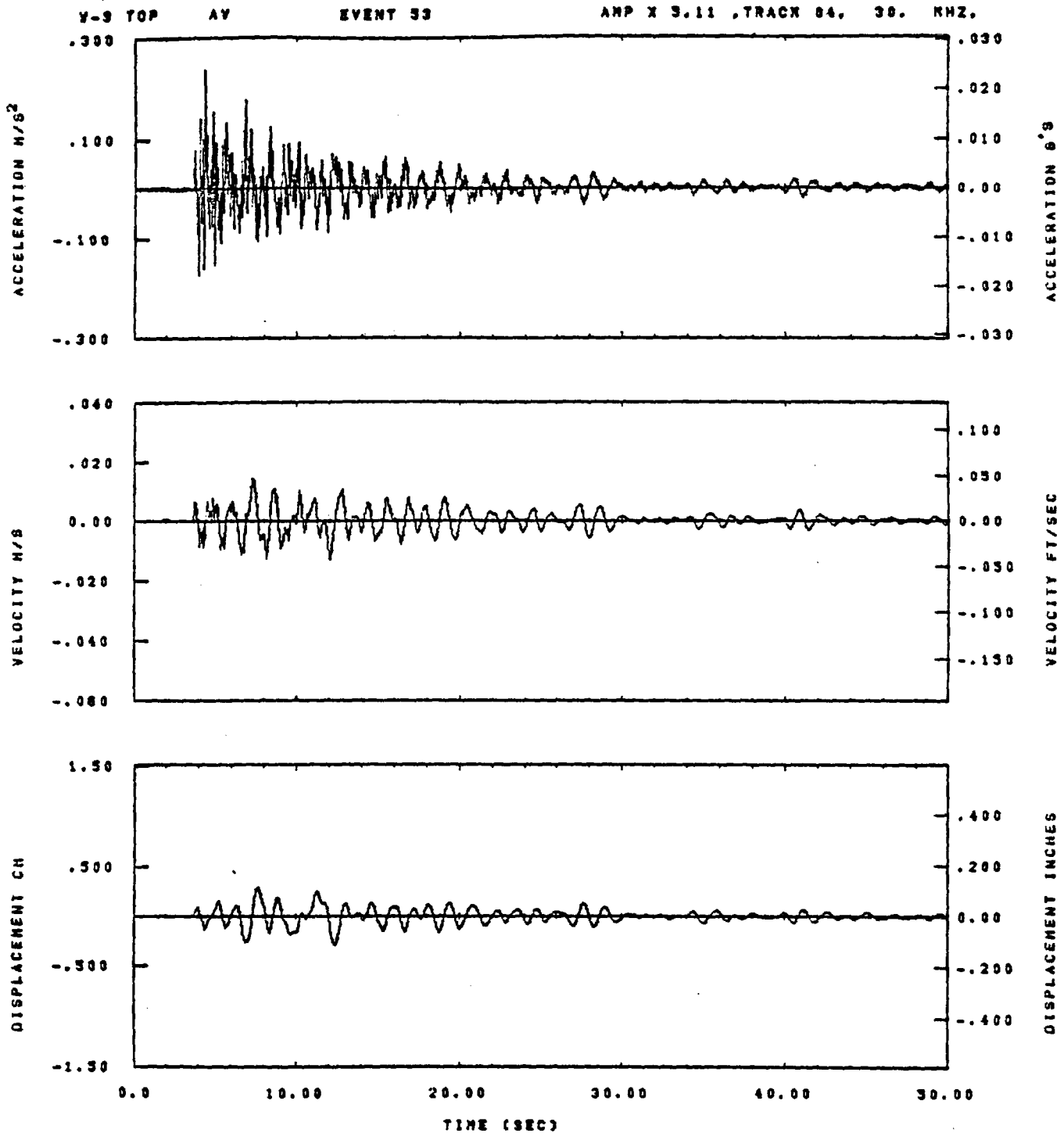


IDT= .0020	ODT= .005	FIX=	AAS= 0.
HPF= .20	BYH= .13	HLH= 251	ASB=
LPF= 18.	BVL= 4.	HLL= 2999	ASE=
VTB= .200	YTE= .133	FLL= -20.	VSE= 0.
OPS= 0.	OPE= 100.	FLH= A-.1	OSE= A+.1

14.38.18.

07/89/82

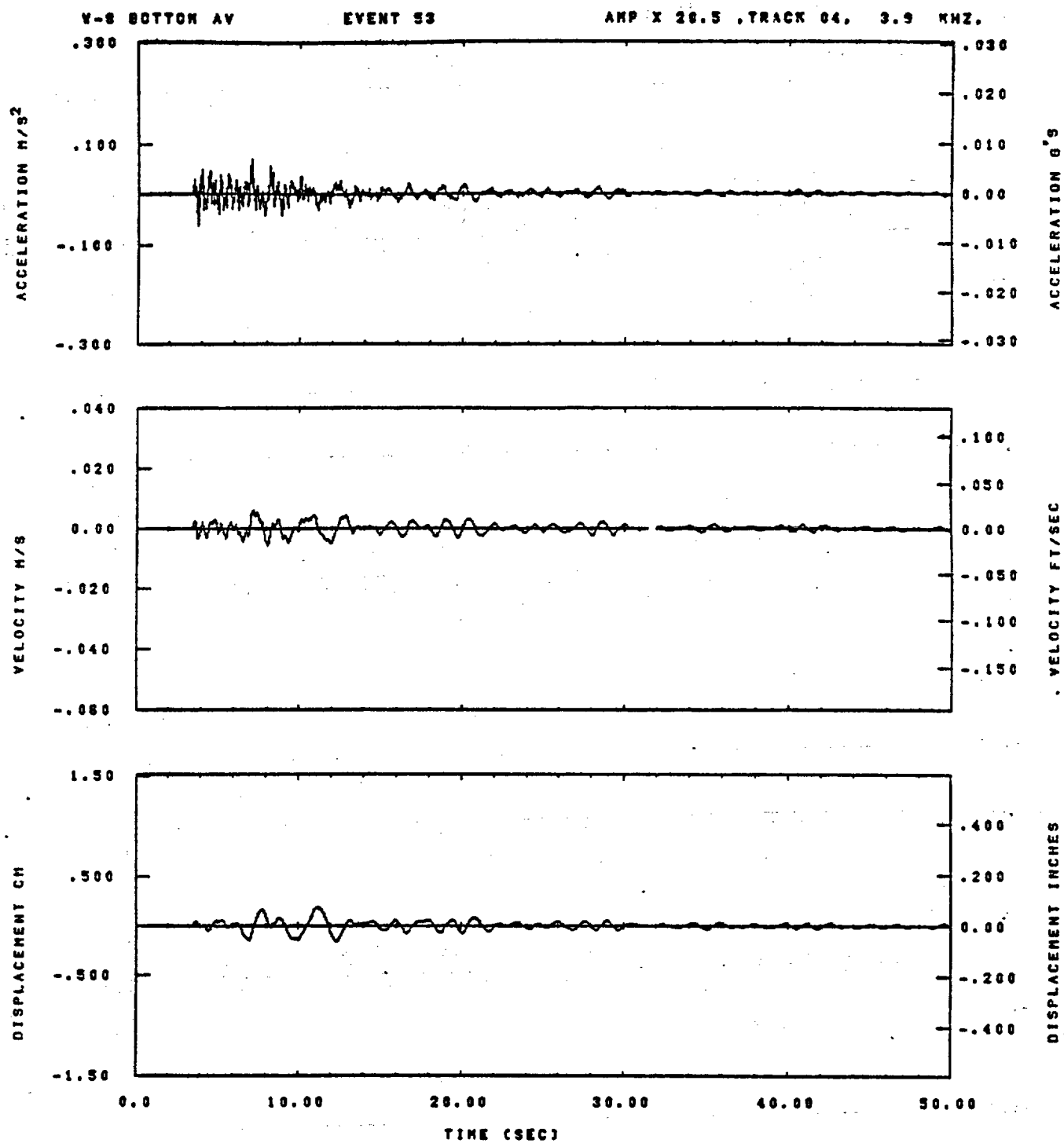
Figure G-12



IDT=	.0020	ODT=	.0	FIX=		AAS=	
HPP=	.3	BYH=	.20	HLH=	187	ASS=	
LPP=	27.	BYL=	8.	HLL=	1999	ASE=	
VTS=	.30	VTE=	.200	FLL=		VSE=	
OPS=		OPE=		FLH=	0	OSE=	0.

09.28.40.

07/07/92

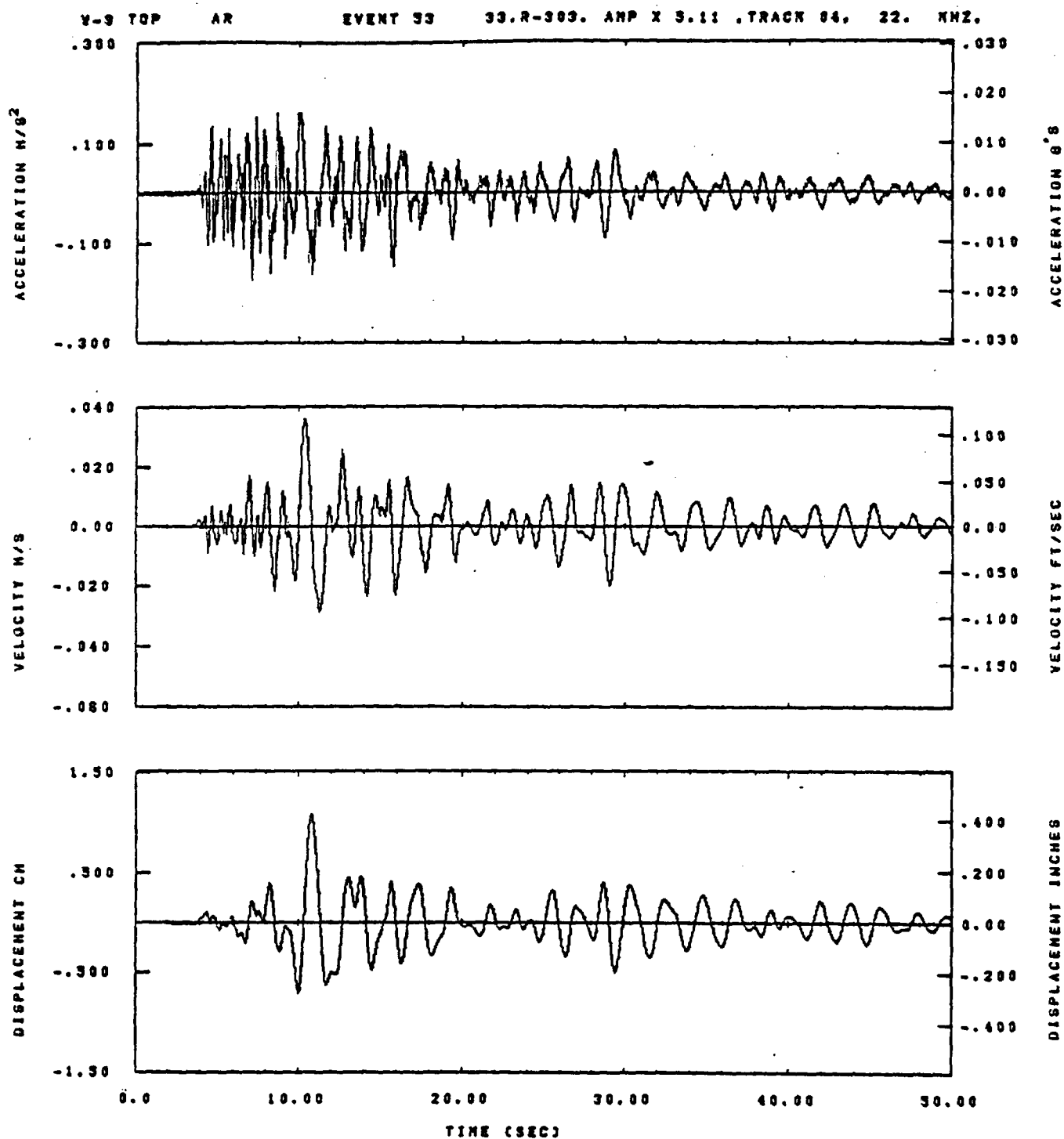


IDT= .0020	ODT= .0	FIX=	AAS=
HPP= .3	SVH= .20	HLH= 167	ASB=
LPP= 27.	SVL= 6.	HLL= 1999	ASE=
VTB= .30	VTE= .200	PLL=	VSE=
DPS=	OPE=	FLH= 0	DSE= 0.

08.26.54.

07/07/82

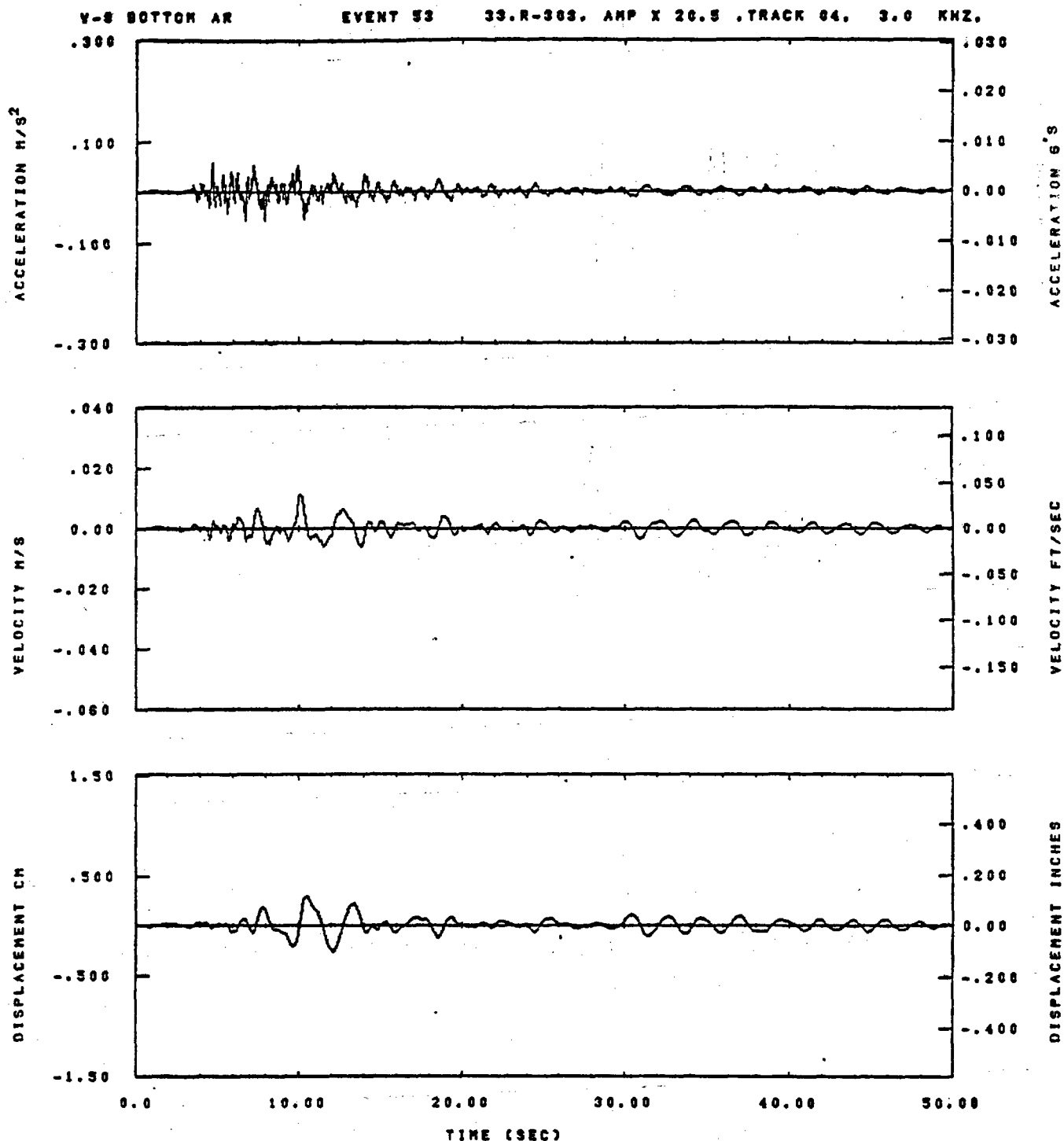
Figure G-14



IDT= .0020	ODT= .0	FIX=	AAS=
HPP= .3	SVH= .20	HLH= 187	ASB=
LPP= 27.	SVL= 8.	HLL= 1999	ASE=
VTS= .30	VTE= .200	FLL=	VSE=
OPS=	OPE=	FLH= 0	DSE= 0.

08.28.43.

07/07/82

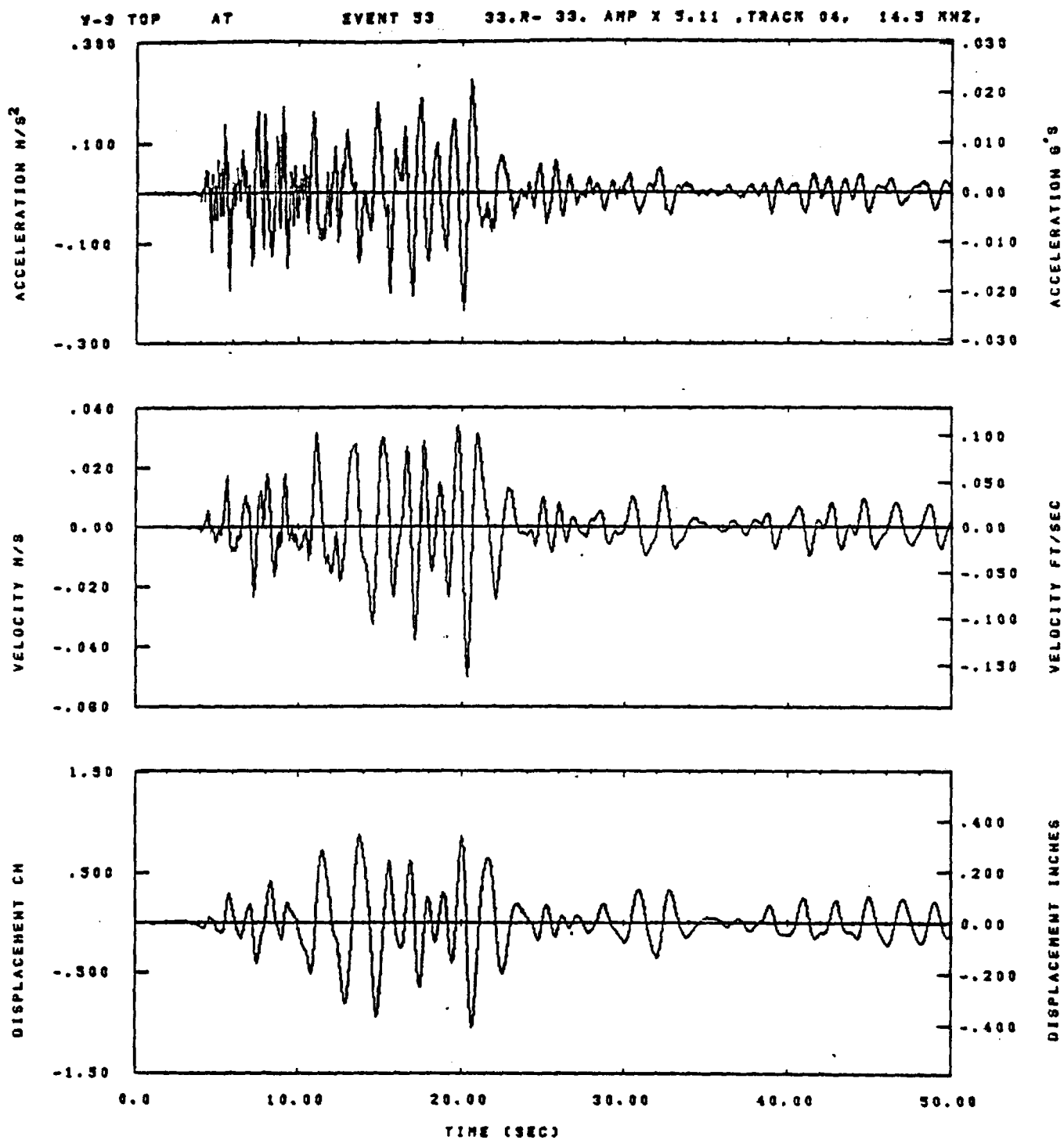


IDT= .0020	ODT= .0	FIX=	AAS=
HPP= .3	BYH= .20	HLH= 167	ASS=
LPP= 27.	BYL= 6.	HLL= 1999	ASE=
VTS= .30	VTE= .200	FLL=	VSE=
OPS=	OPE=	FLH= 0	DSE= 0.

06.26.59.

07/07/82

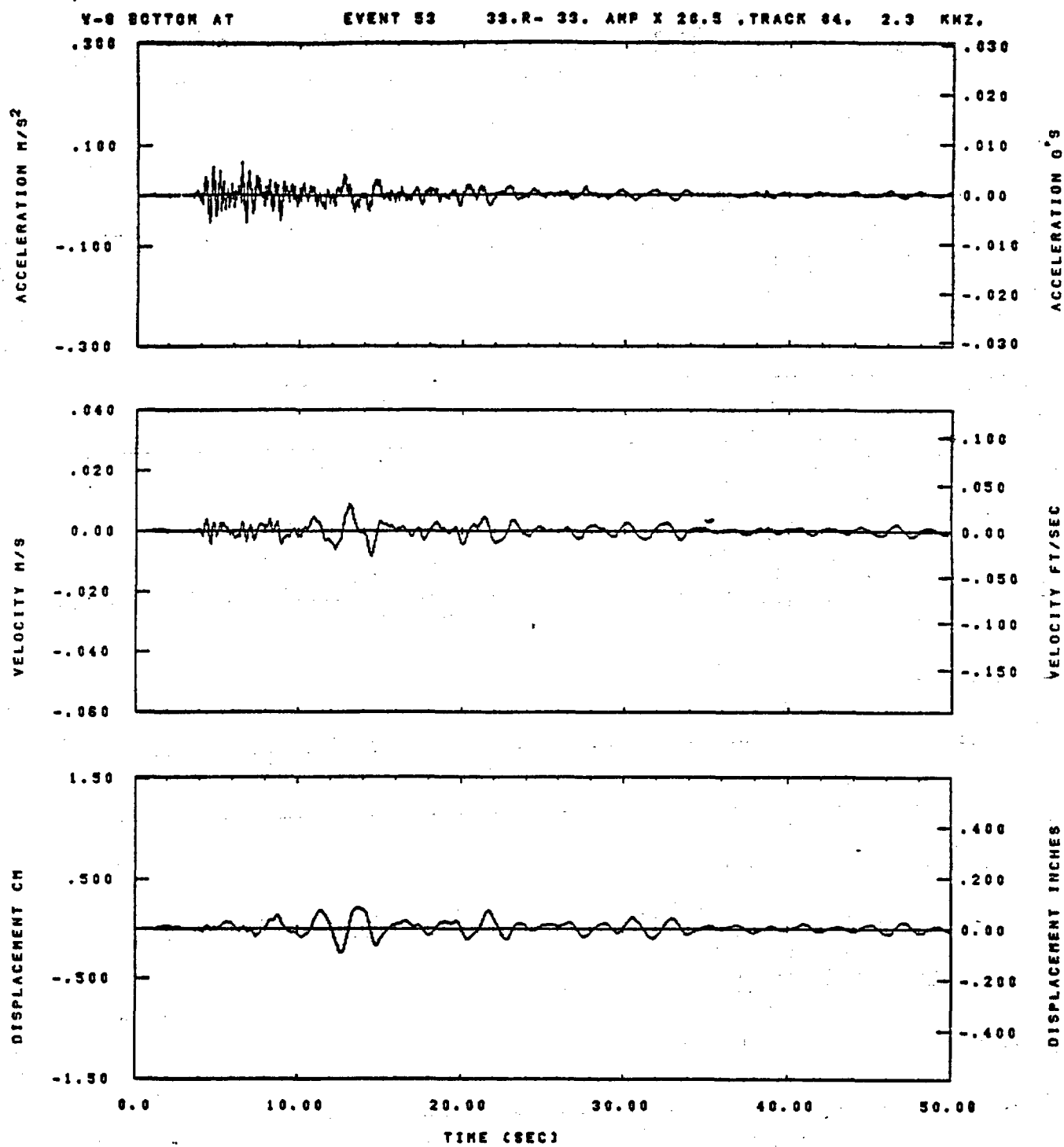
Figure G-16



IDT=	.0020	ODT=	.0	FIX=		AAS=	
HPF=	.3	BYH=	.20	HLH=	187	ASB=	
LPF=	27.	SVL=	6.	HLL=	1999	ASE=	
VTB=	.30	VTE=	.200	FLL=		VSE=	
OPB=		OPE=		FLH=	0	OSE=	0.

09.28.49.

07/07/02

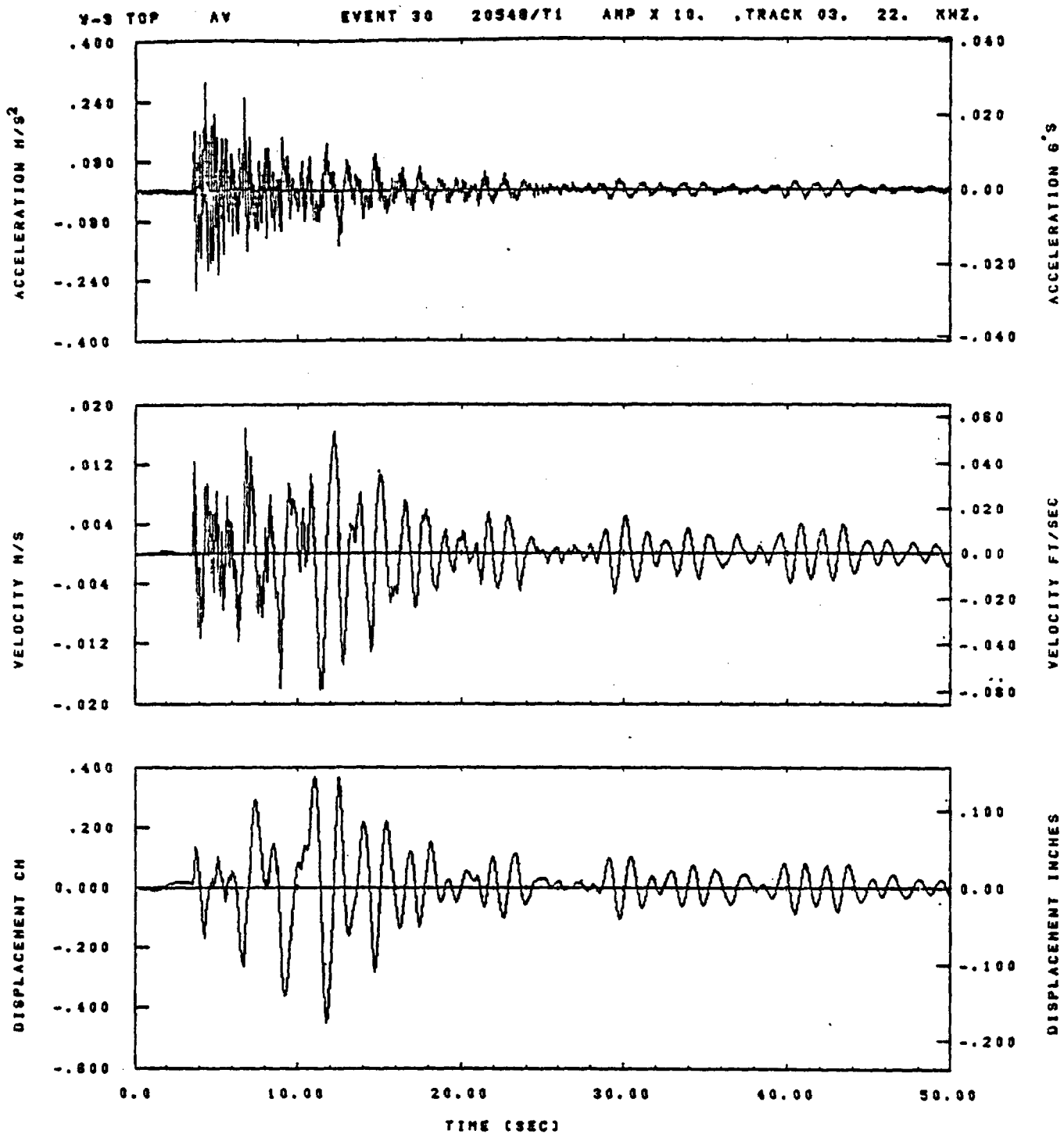


IDT= .0020	ODT= .0	FIX=	AAS=
HPP= .3	SVH= .20	HLN= 167	ASS=
LPF= 27.	SVL= 6.	HLL= 1998	ASE=
VTB= .30	VTE= .200	FLL=	VSE=
DPS=	DPE=	FLN= 0	DSE= 0.

08.27.94.

07/07/82

Figure G-18

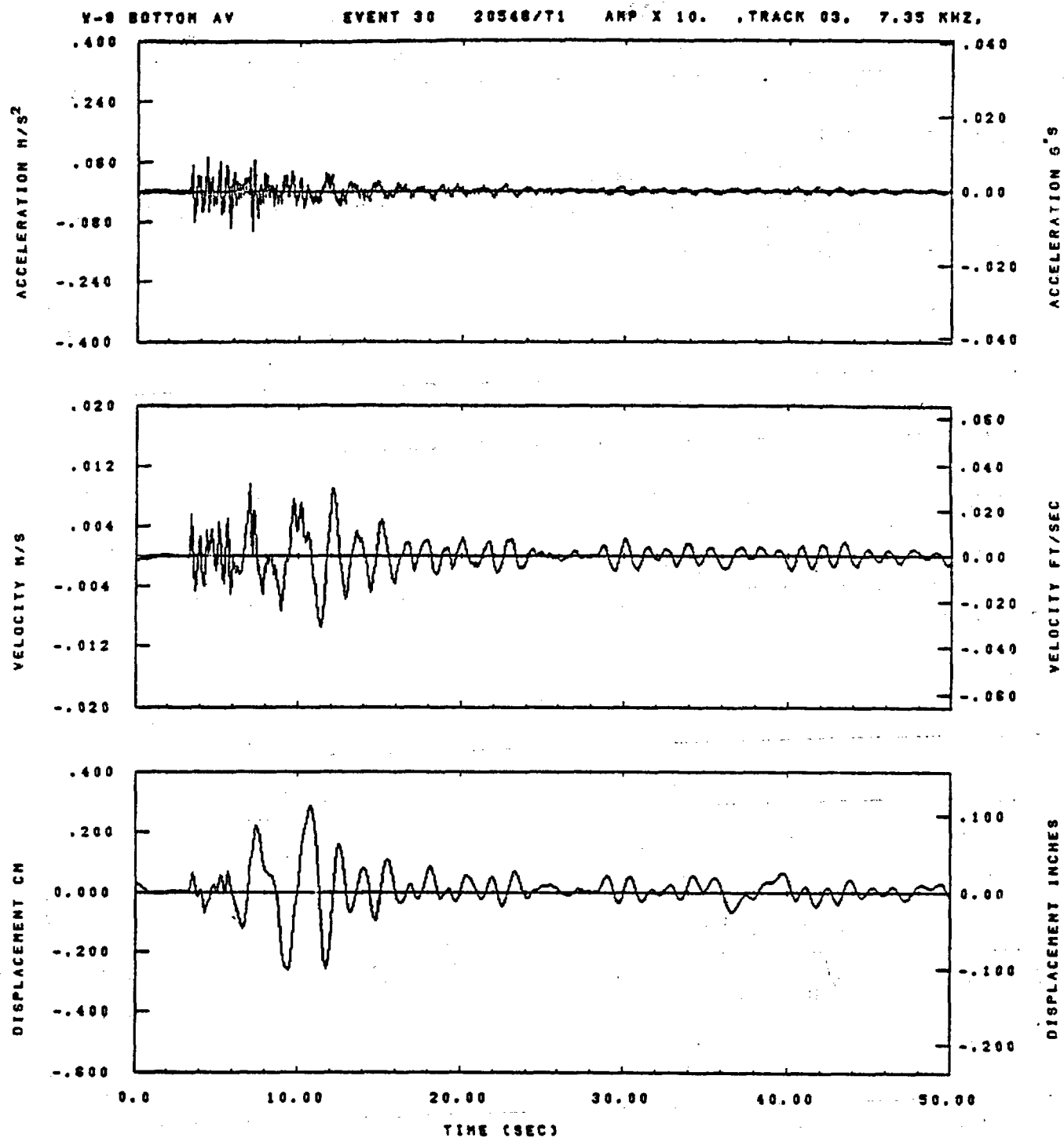


IDT= .0020	OOT= .005	FIX=	AAS= 0.
HPP= .20	BVH= .13	HLH= 125	ASB=
LPP= 36.	BVL= 8.	HLL= 2999	ASE=
VTS= .200	VTE= .133	FLL= -20.	VSE= 0.
OPS= 0.	OPE= 100.	FLH= 0	DSE= 0.

09.43.32.

08/30/82

Figure G-19

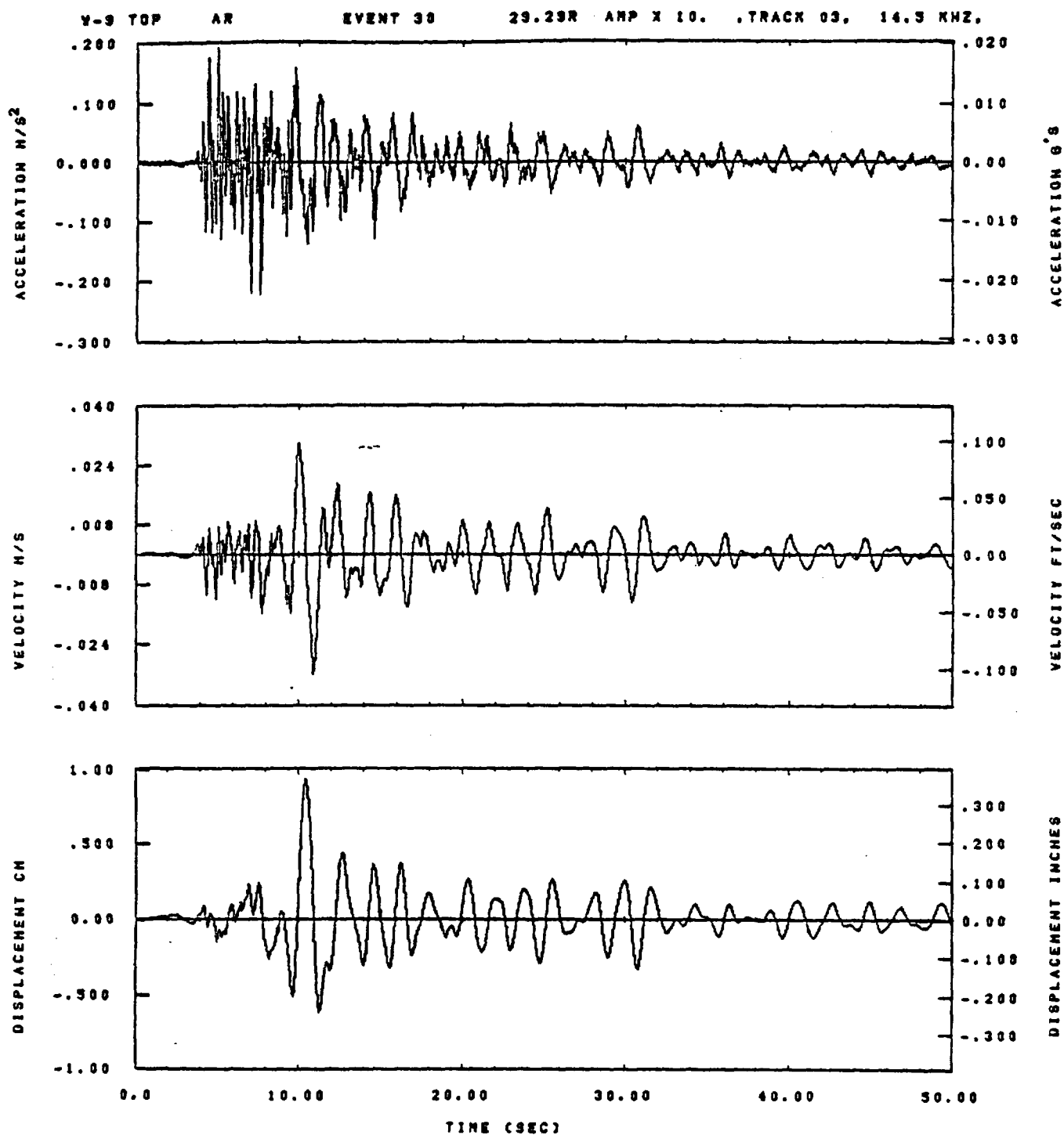


IDT= .0020	ODT= .005	FIX=	AAS= 0.
HPF= .20	BYH= .13	HLH= 125	ASB=
LPF= 36.	BYL= 8.	HLL= 2999	ASE=
VTS= .200	VTE= .133	FLL= -20.	VSE= 0.
DPS= 0.	DPE= 100.	FLH= 0	DSE= 0.

10.13.07.

06/30/82

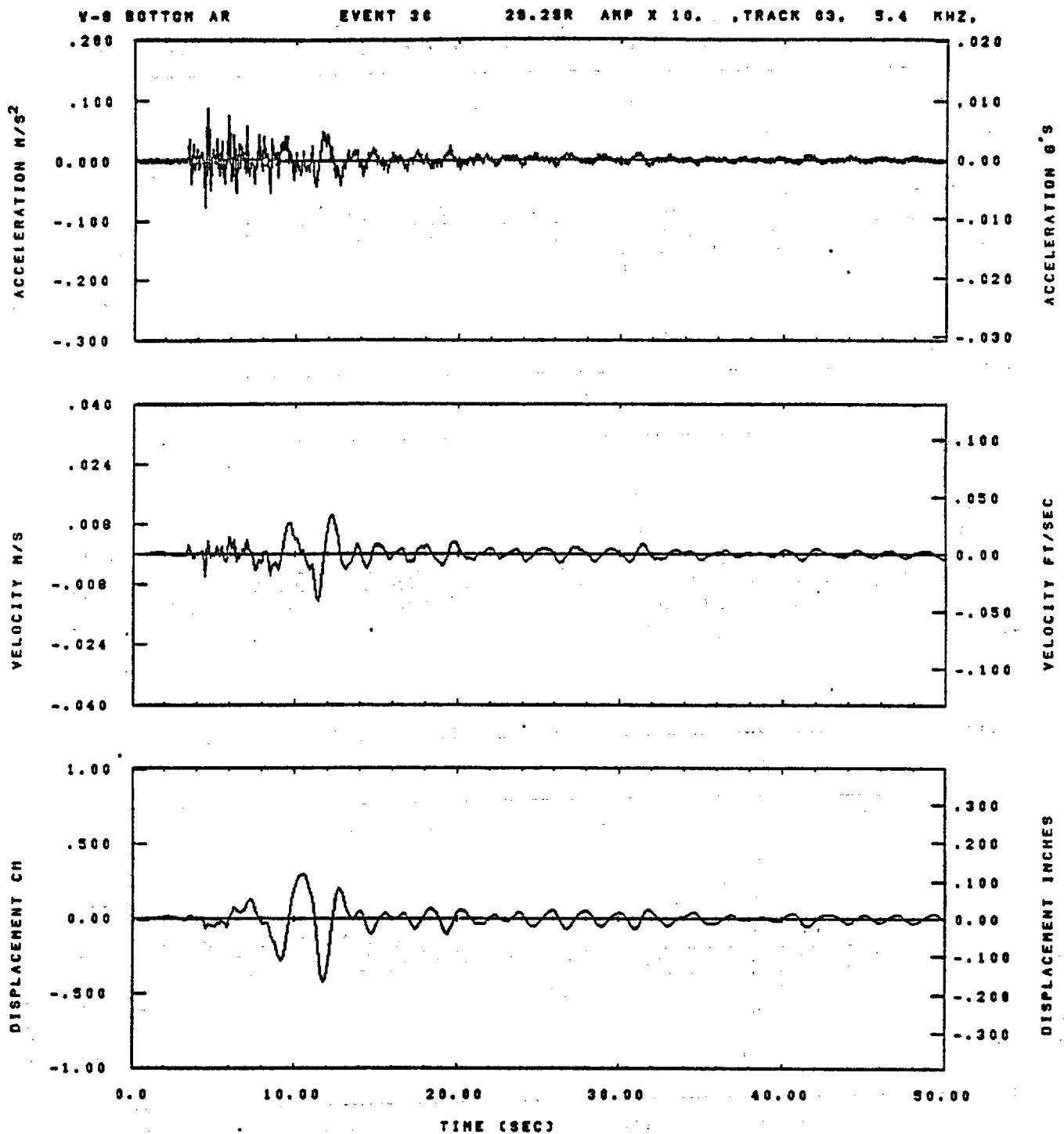
Figure G-20



IDT= .0020	QDT= .003	FIX=	AAS= 0.
HPF= .20	BVH= .13	HLH= 125	ASB=
LPF= 35.	BYL= 8.	HLL= 2999	ASE=
VTS= .200	VTE= .133	FLL= -20.	VSE= 0.
DPS= 0.	DPE= 100.	FLH= 0	DSE= 0.

09.43.23.

08/30/92

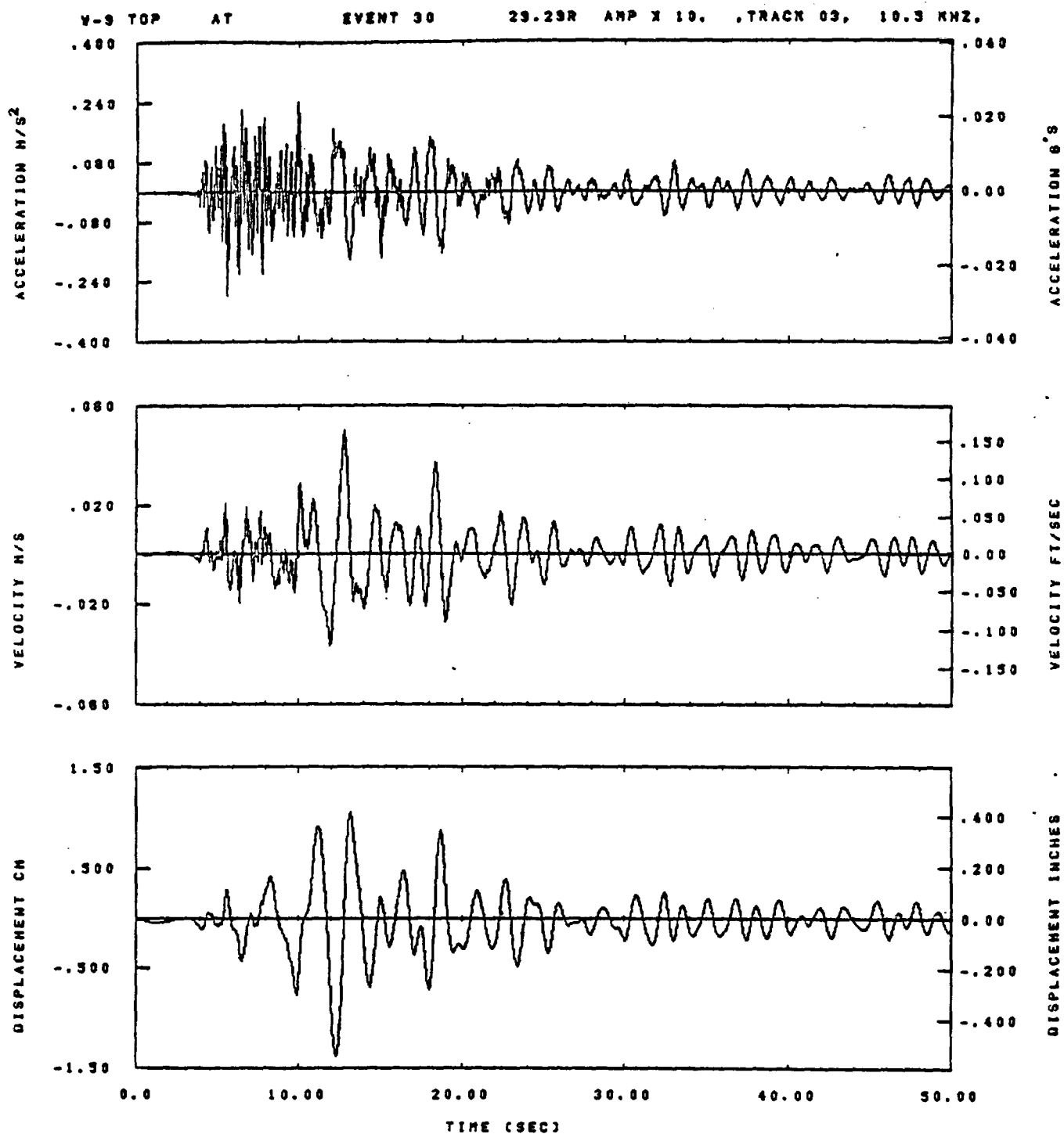


IDT= .0020	ODT= .005	FIX=	AAS= 0.
HFF= .20	BYH= .13	HLH= 125	ASB=
LFF= 36.	BYL= 8.	HLL= 2889	ASE=
VTS= .200	VTE= .133	PLL= -20.	VSE= 0.
DPS= 0.	DPE= 100.	PLH= 0	DSE= 0.

10.12.54.

06/30/82

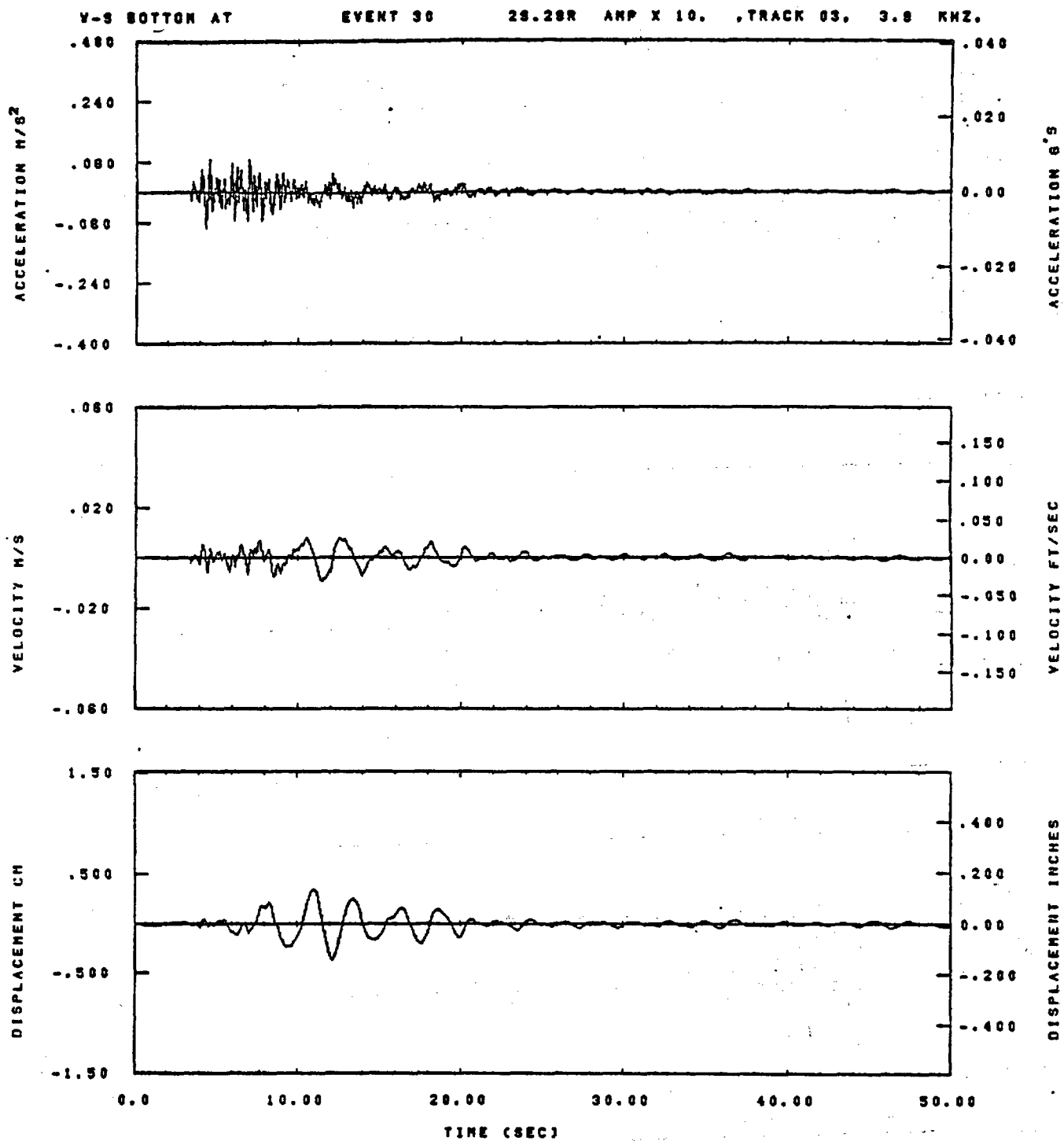
Figure G-22



IDT= .0020	OOT= .005	FIX=	AAS= 0.
HPP= .20	SVH= .13	HLH= 125	ASB=
LPP= 38.	SVL= 8.	HLL= 2999	ASE=
VTS= .200	VTE= .133	FLL= -20.	VSE= 0.
DPS= 0.	DPE= 100.	PLH= 0	OSE= 0.

09.43.27.

08/30/82

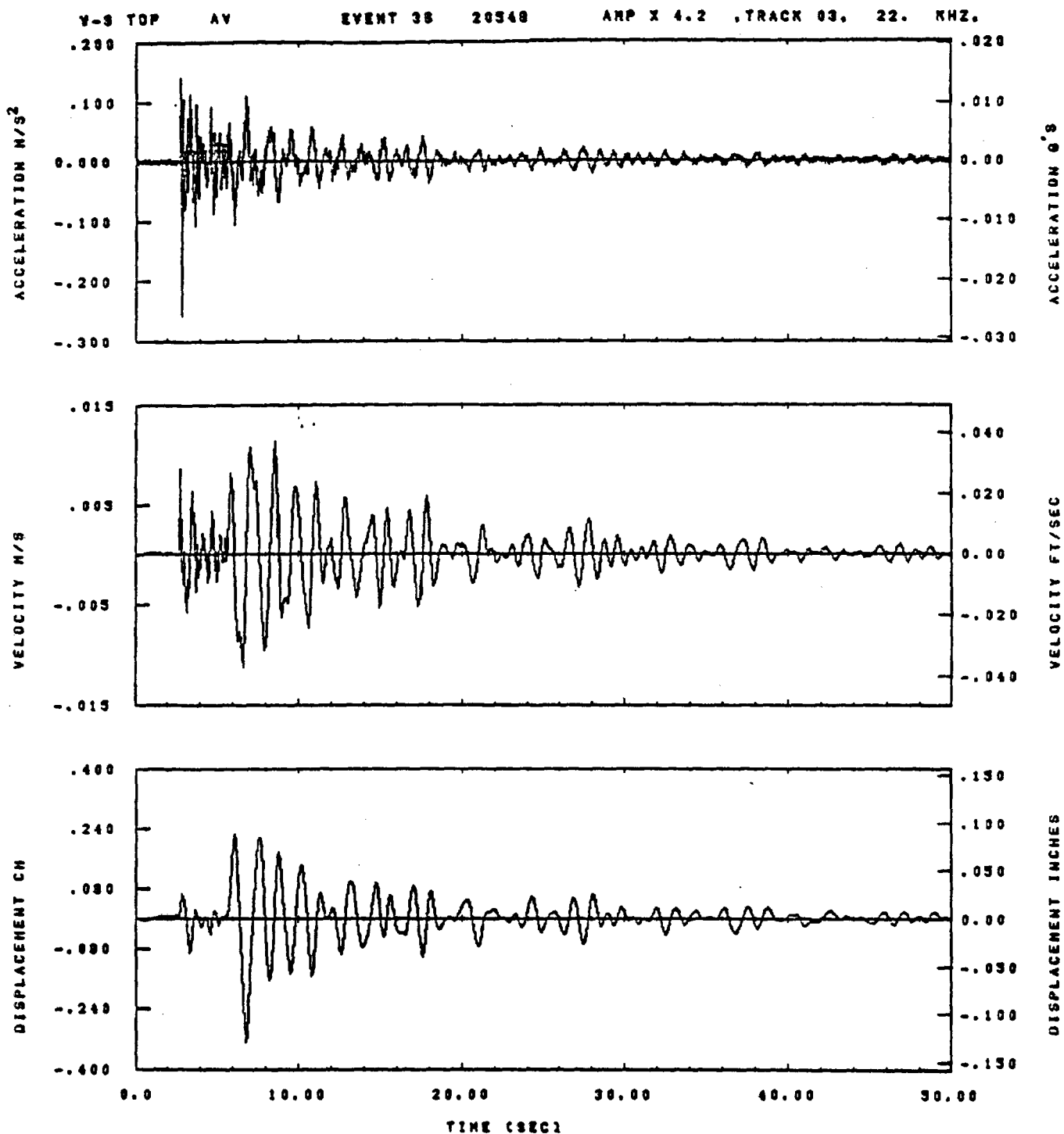


IDT= .0020	ODT= .005	FIX=	AAS= 0.
HPF= .20	BYH= .13	HLH= 125	ASB=
LPF= 36.	BVL= 8.	HLL= 2999	ASE=
VTB= .200	VTE= .133	FLL= -20.	VSE= 0.
DPS= 0.	DPE= 100.	FLH= 0	DSE= 0.

10.13.00.

06/30/82

Figure G-24

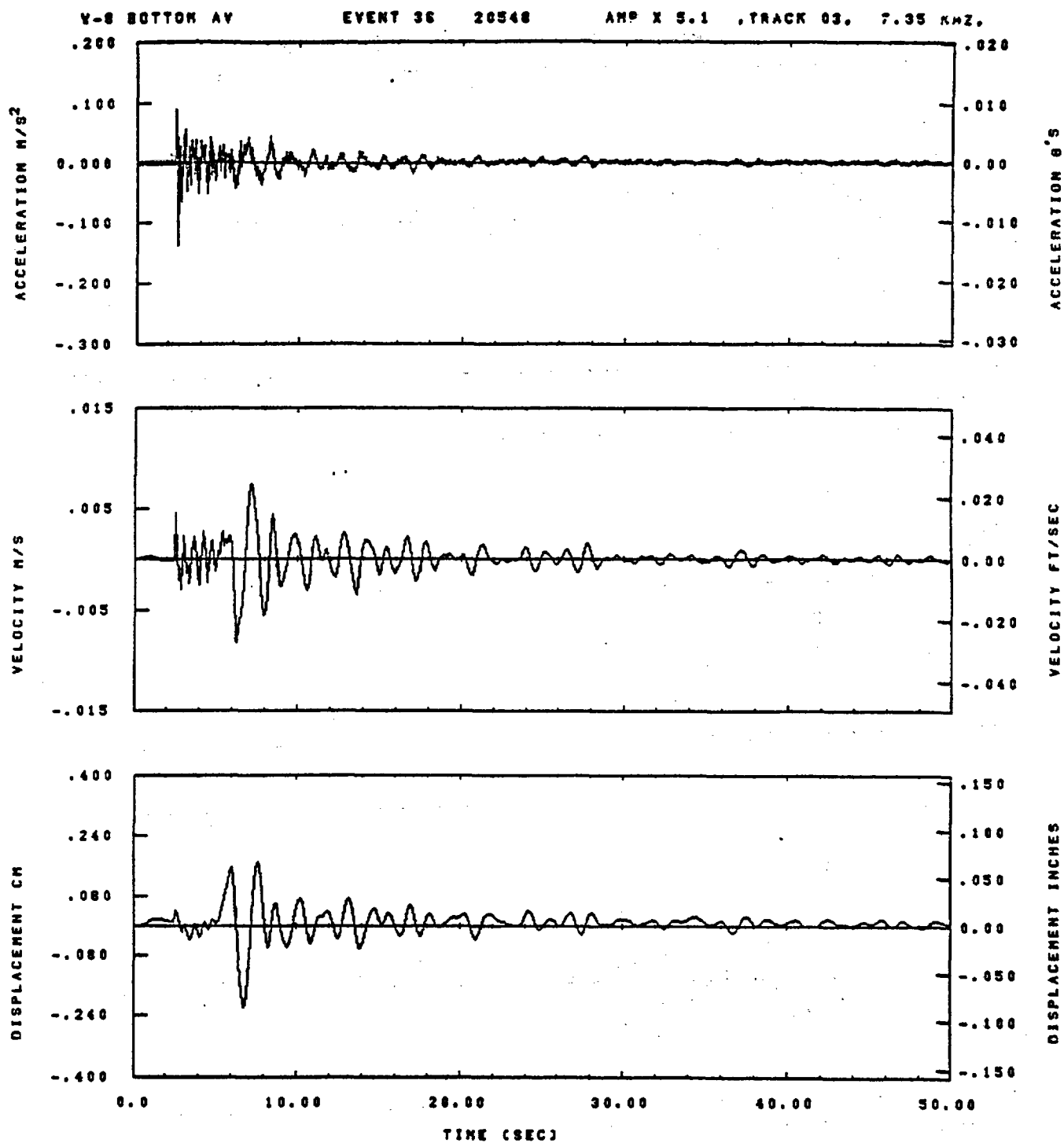


IDT= .0020	ODT= .003	FIX=	AAS= 0.
HPP= .25	BYN= .18	HLH= 143	ASB=
LPP= 31.	BYL= 7.	HLL= 2398	ASE=
VTS= .250	VTE= .188	FLL= -20.	VSE= 0.
DPS= 0.	DPE= 100.	FLH= 0	DSE= 0.

14.13.42.

08/23/82

Figure G-25

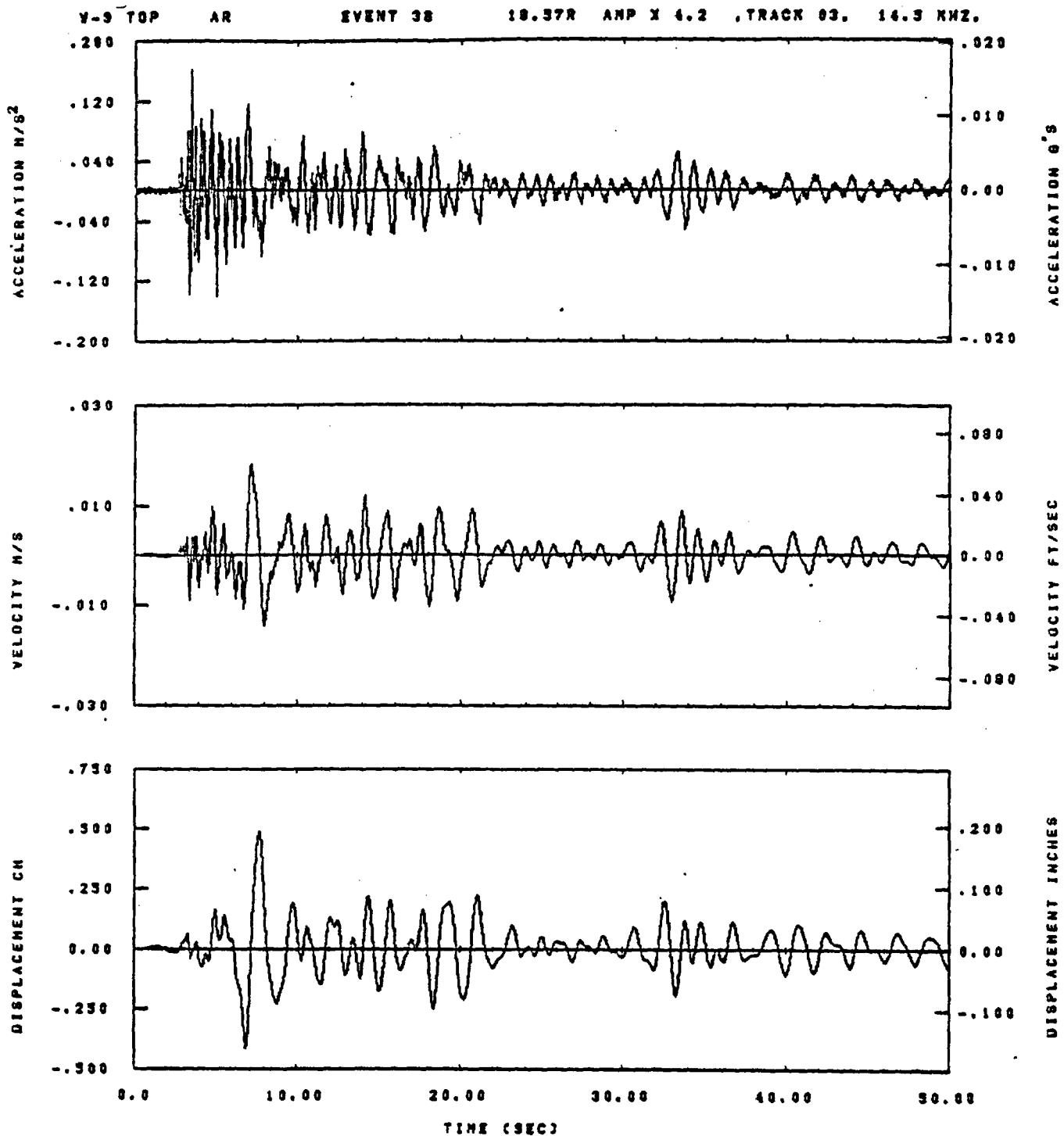


IDT= .0020	OOT= .005	FIX=	AAS= 0.
HPF= .25	BYH= .16	HLH= 143	ASB=
LPF= 31.	BVL= 7.	HLL= 2388	ASE=
VTS= .250	VTE= .166	FLL= -20.	VSE= 0.
DPS= 0.	DPE= 100.	FLH= 0	DSE= 0.

14.16.15.

06/23/82

Figure G-26

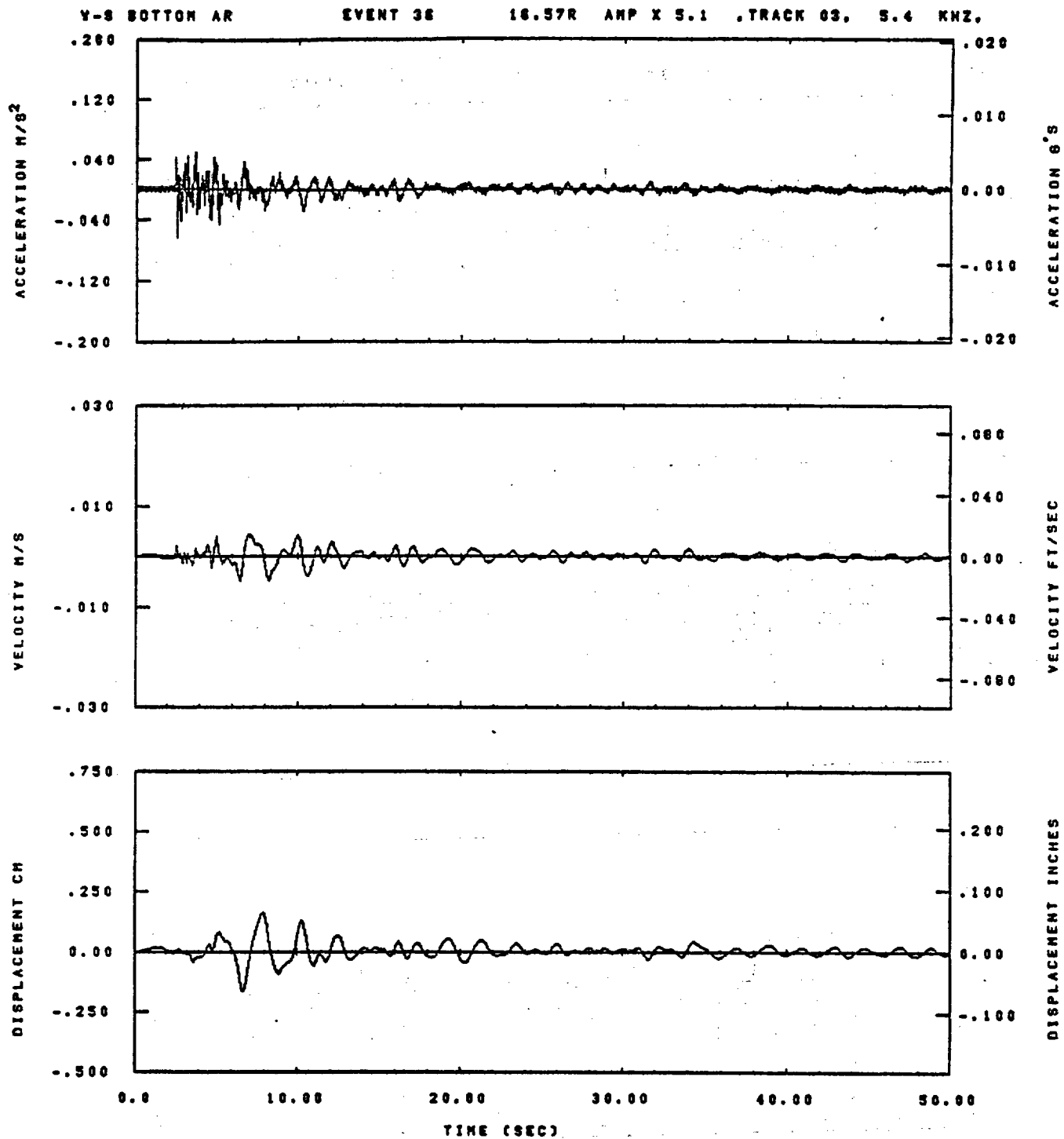


IDT= .0020	ODT= .003	FIX=	AAS= 0.
HPP= .25	BYH= .18	HLN= 143	ASB=
LPP= 31.	BYL= 7.	NLL= 2393	ASE=
VTB= .250	VTE= .188	FLL= -20.	VSE= 0.
DPS= 0.	DPE= 100.	PLH= 0	DSE= 0.

14.13.33.

08/23/92

Figure G-27

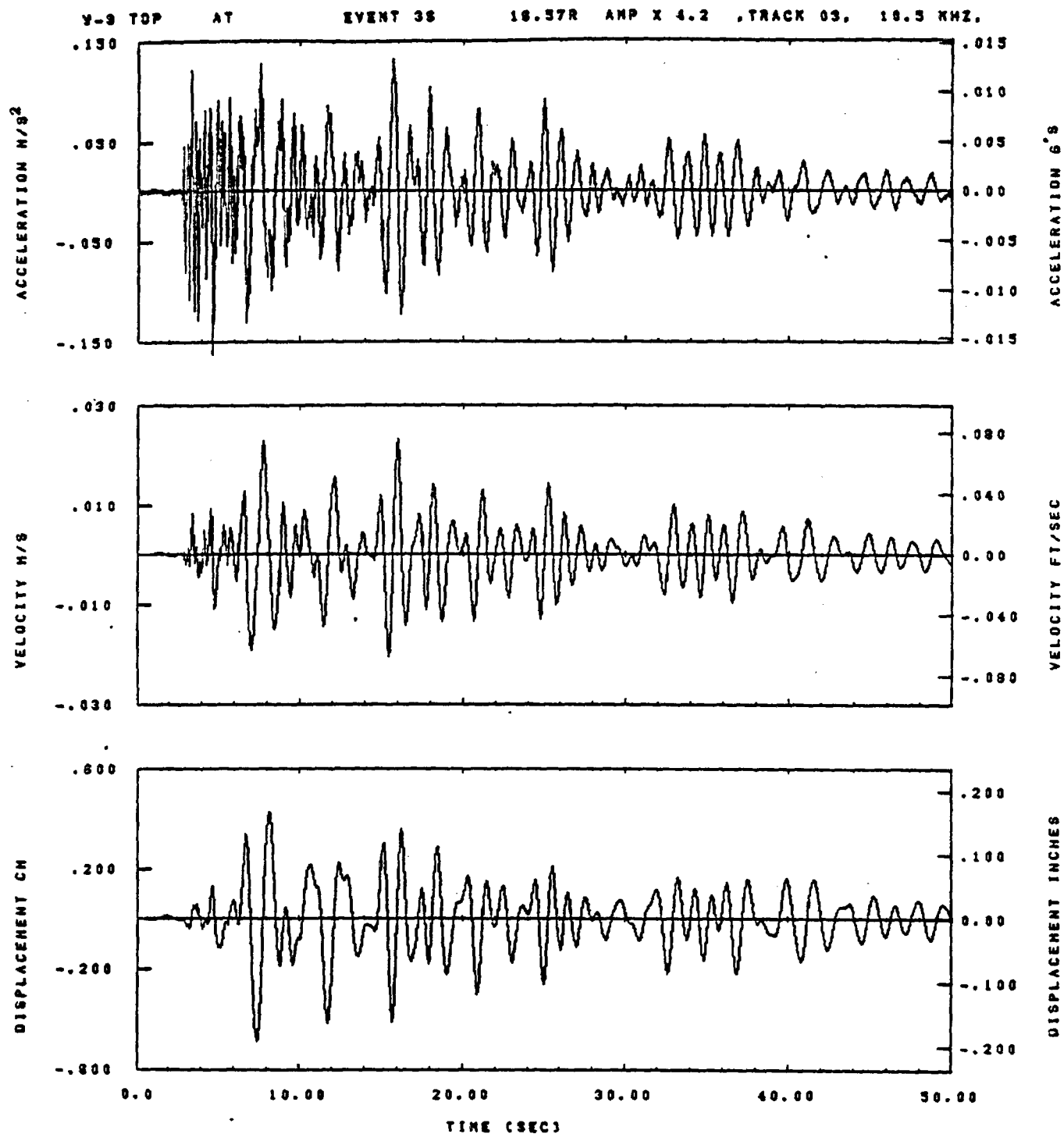


IDT= .0020	ODT= .005	FIX=	AAS= 0.
HPF= .25	EVH= .16	MLH= 143	ASS=
LPF= 31.	SVL= 7.	MLL= 2388	ASE=
VTS= .250	VTE= .166	FLL= -20.	VSE= 0.
OPS= 0.	OPE= 100.	FLH= 0	DSE= 0.

14.16.18.

06/23/82

Figure G-28



IDT= .0020	ODT= .005	FIX=	AAS= 0.
HPP= .25	SVH= .16	HLH= 143	ASB=
LPP= 31.	SVL= 7.	HLL= 2339	ASE=
VTB= .250	VTZ= .188	FLL= -20.	VSE= 0.
DPS= 0.	OPE= 100.	FLH= 0	DSE= 0.

14.14.15.

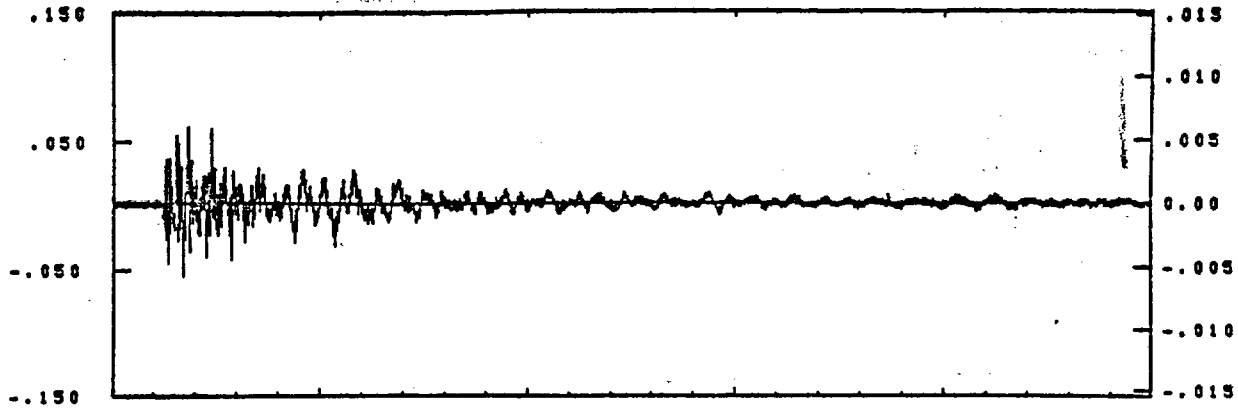
08/23/92

Figure G-29

Y-3 BOTTOM AT

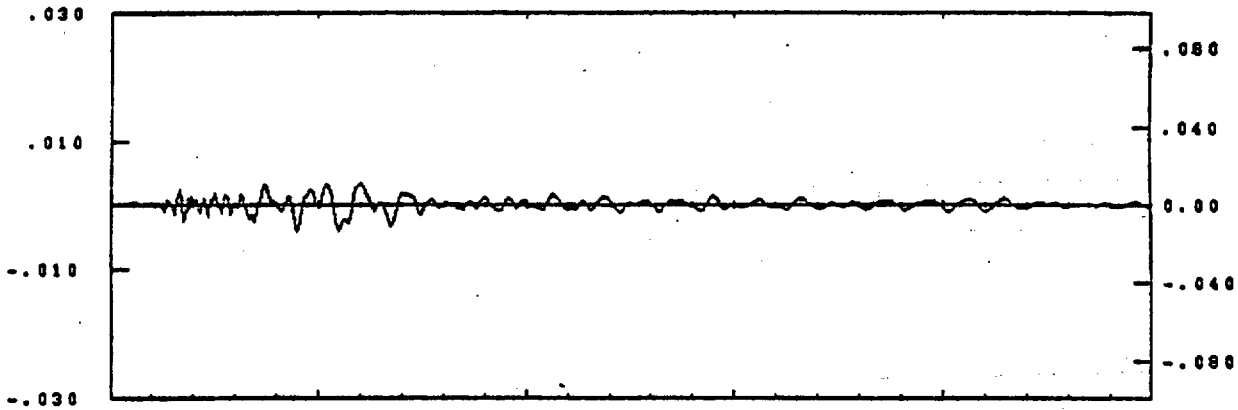
EVENT 36

16.57R AMP X 5.1 ,TRACK 03, 3.8 KHZ.

ACCELERATION M/S²

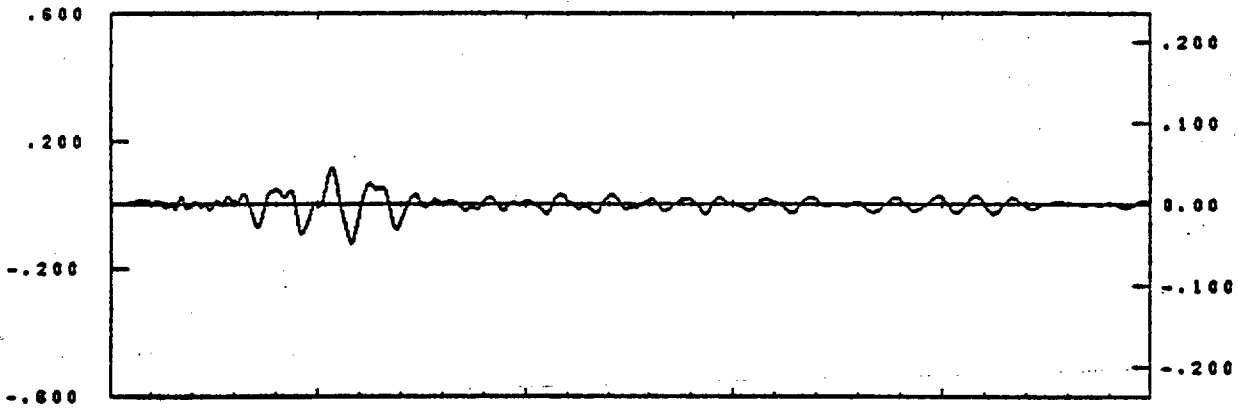
ACCELERATION G'S

VELOCITY M/S



VELOCITY FT/SEC

DISPLACEMENT CM



DISPLACEMENT INCHES

0.0 10.00 20.00 30.00 40.00 50.00

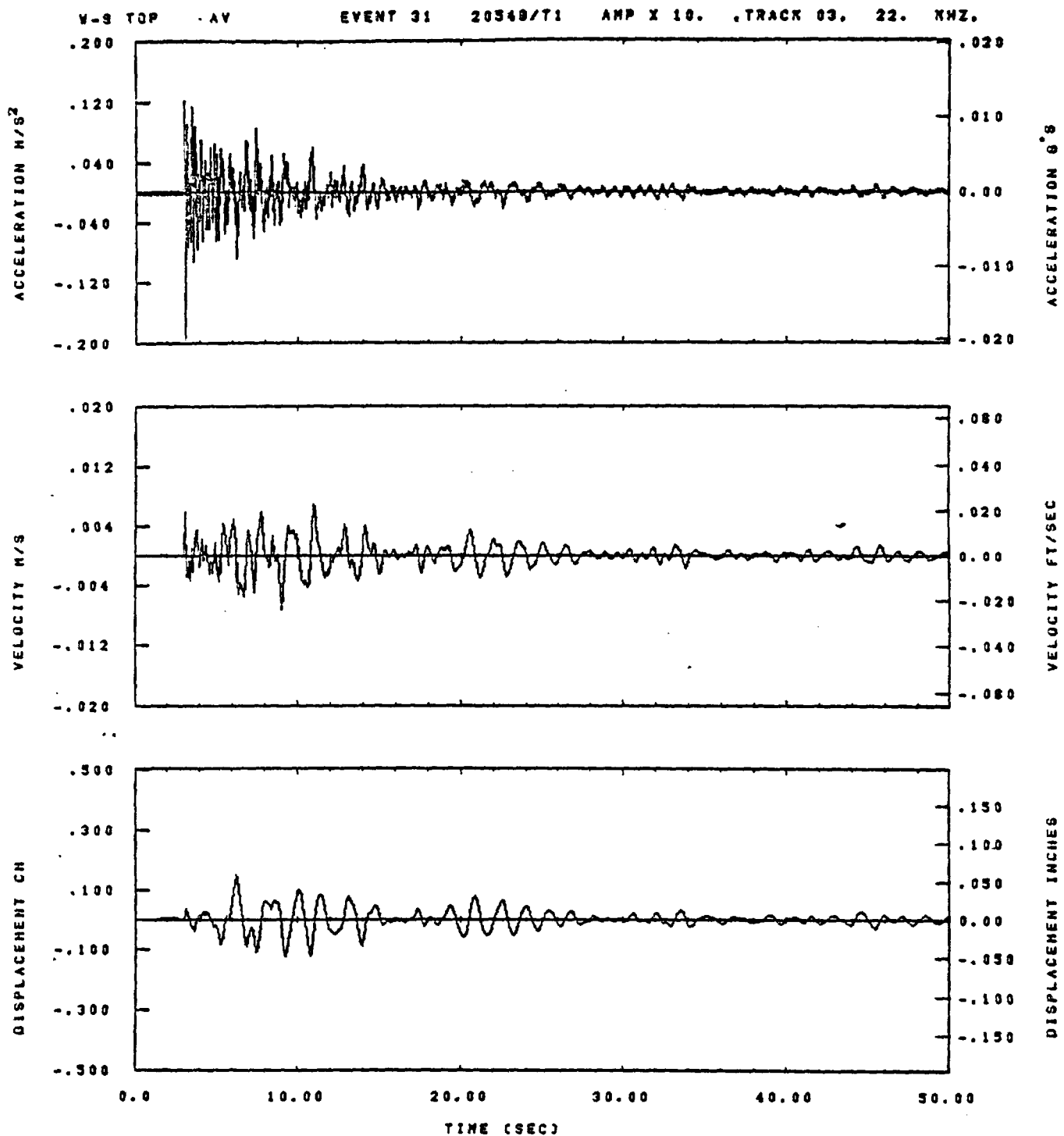
TIME (SEC)

IDT= .0020	ODT= .005	FIX=	AAS= 0.
HPF= .25	BYH= .16	HLH= 143	ASS=
LPF= 31.	BYL= 7.	HLL= 2388	ASE=
VTS= .250	VTE= .166	FLL= -20.	VSE= 0.
DPE= 0.	DPE= 100.	FLH= 0	DSE= 0.

14.16.25.

06/23/82

Figure G-30

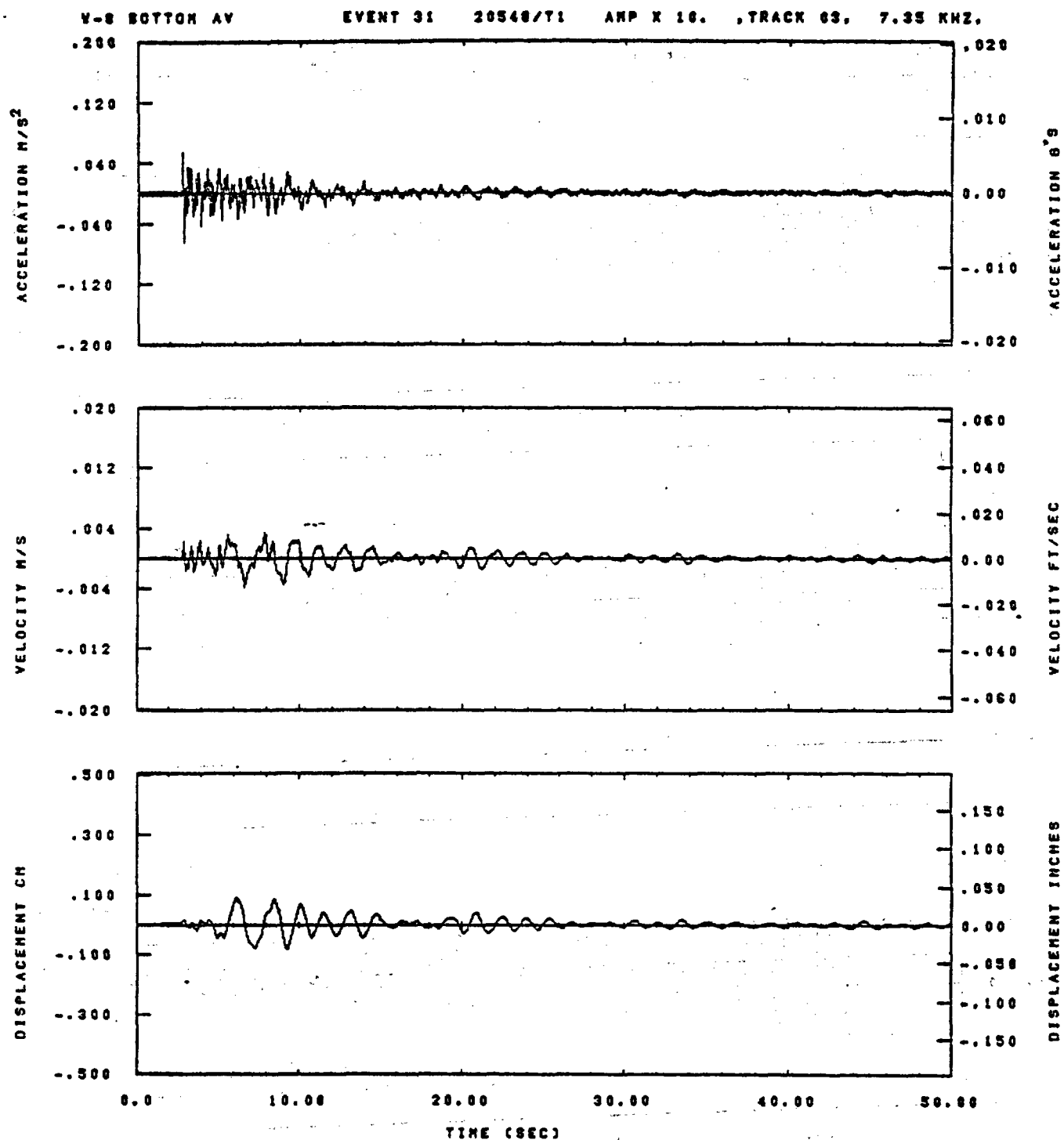


IDT= .0020	ODT= .005	FIX=	AAS= 0.
HPF= .25	SVH= .18	HLH= 143	ASB=
LPF= 31.	SVL= 7.	HLL= 2393	ASE=
VTB= .250	VTE= .188	FLL= -20.	VSE= 0.
OPS= 0.	OPE= 100.	FLH= 0	OSE= 0.

11.25.41.

08/24/92

Figure G-31

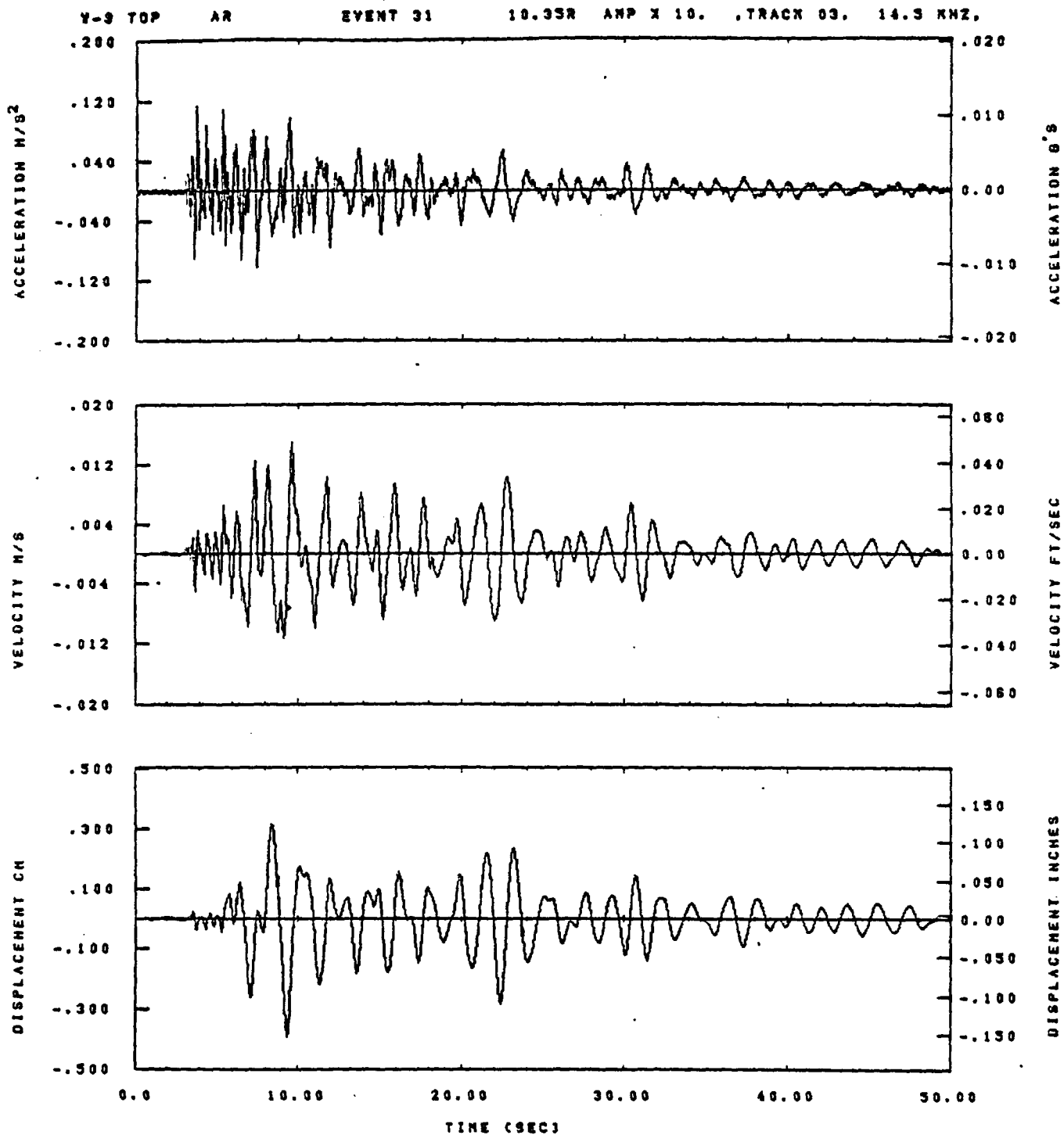


IDT= .0020	ODT= .005	FIX=	AAS= 0.
HPP= .25	BYH= .18	HLH= 143	ASH=
LPP= 31.	BYL= 7.	HLL= 2388	ASE=
VTB= .250	VTE= .188	FLL= -20.	VSE= 0.
DPS= 0.	DPE= 100.	FLH= 0	OSE= 0.

11.25.00.

06/24/82

Figure G-32

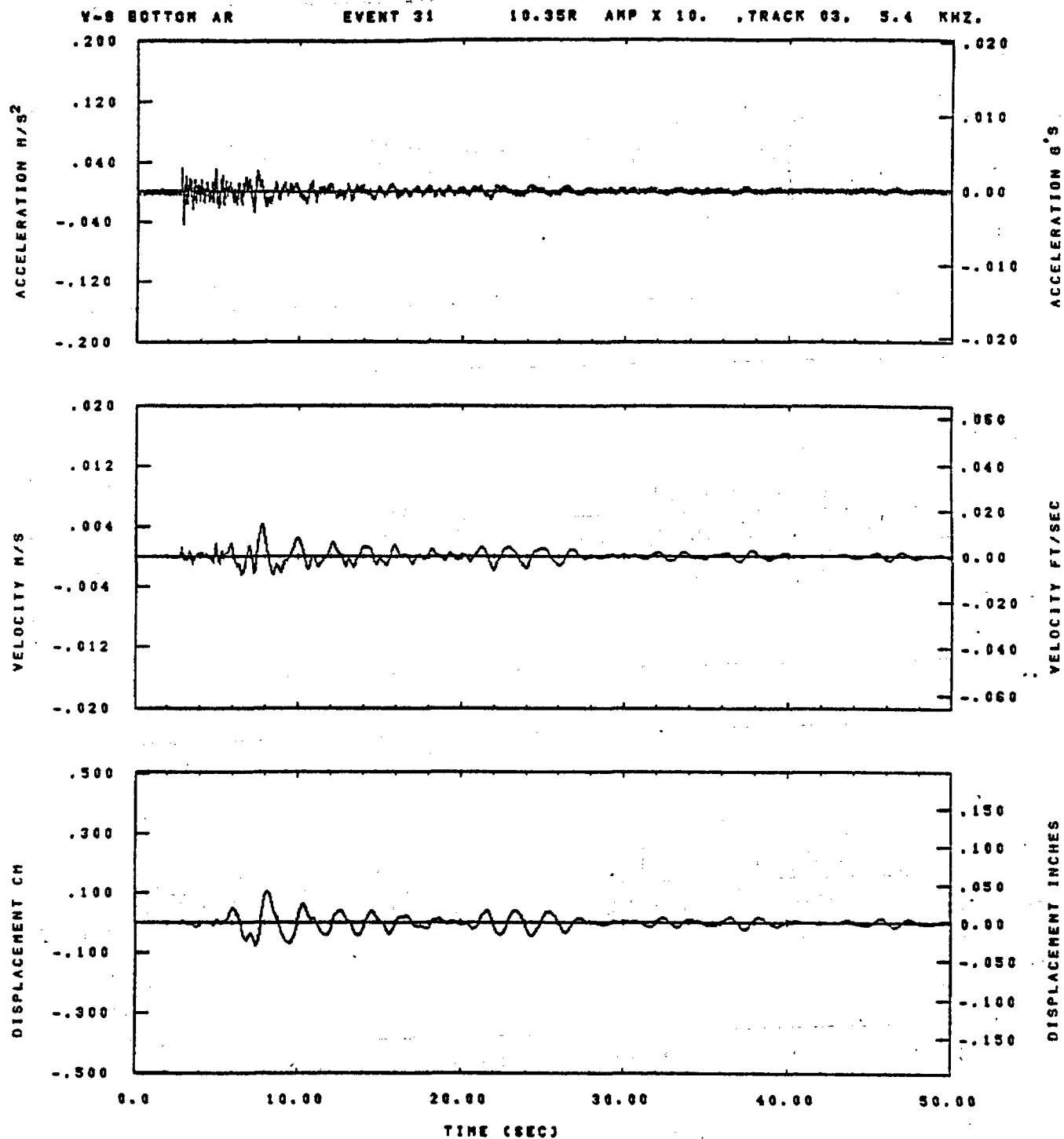


IDT= .0020	ODT= .003	FIX=	AAS= 0.
HPP= .25	SVH= .18	HLH= 143	ASS=
LPP= 31.	SVL= 7.	HLL= 2399	ASE=
VTB= .250	VTE= .188	FLL= -20.	VSE= 0.
OPB= 0.	OPE= 100.	FLH= 0	OSE= 0.

11.24.41.

08/24/82

Figure G-33

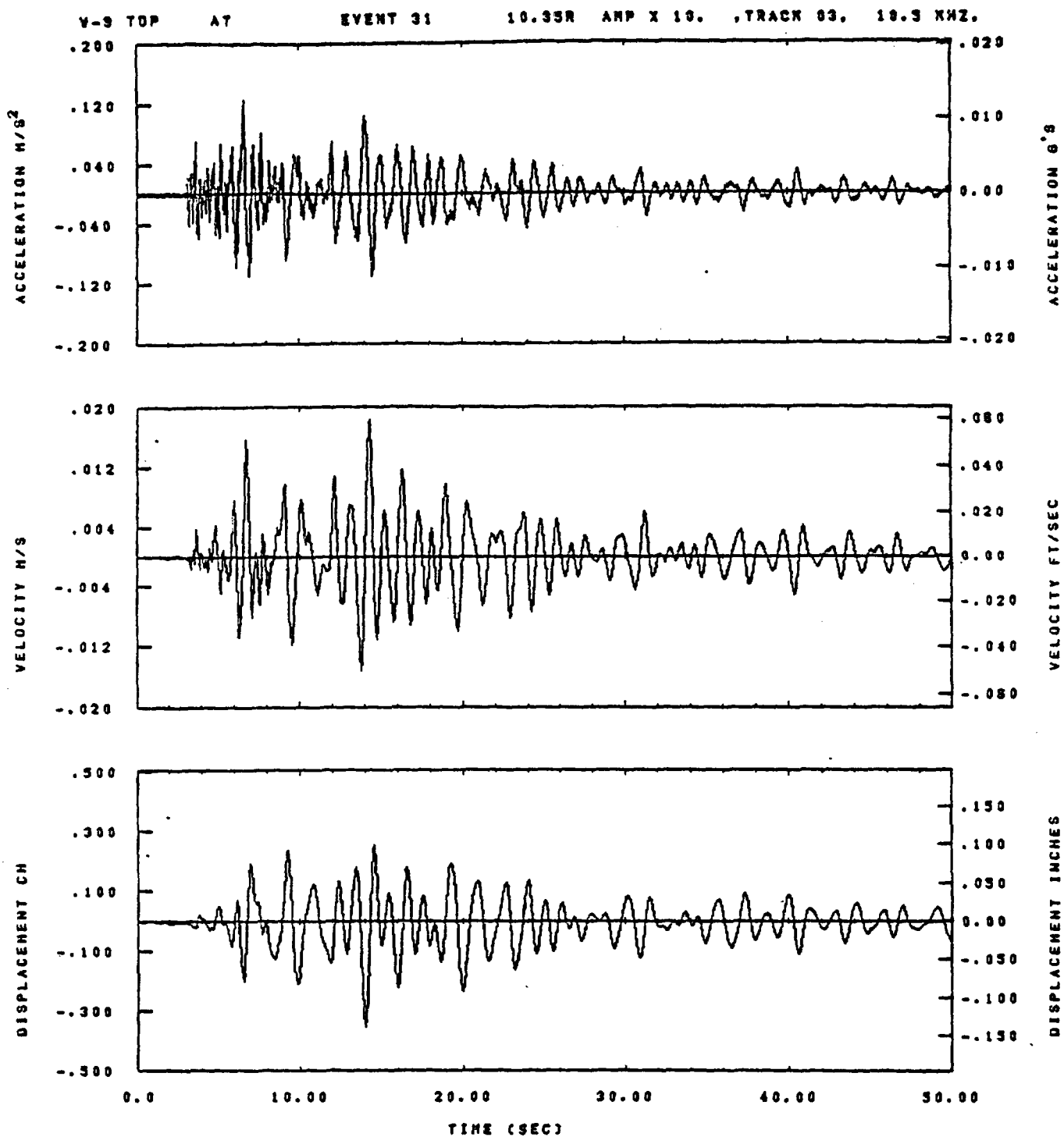


IDT= .0020	QDT= .005	FIX=	AAS= 0.
HPF= .25	SVH= .16	HLH= 143	ASS=
LPF= 31.	SVL= 7.	HLL= 2388	ASE=
VTS= .250	VTE= .166	FLL= -20.	VSE= 0.
DPS= 0.	DPE= 100.	FLH= 0	DSE= 0.

11.25.47.

06/24/82

Figure G-34

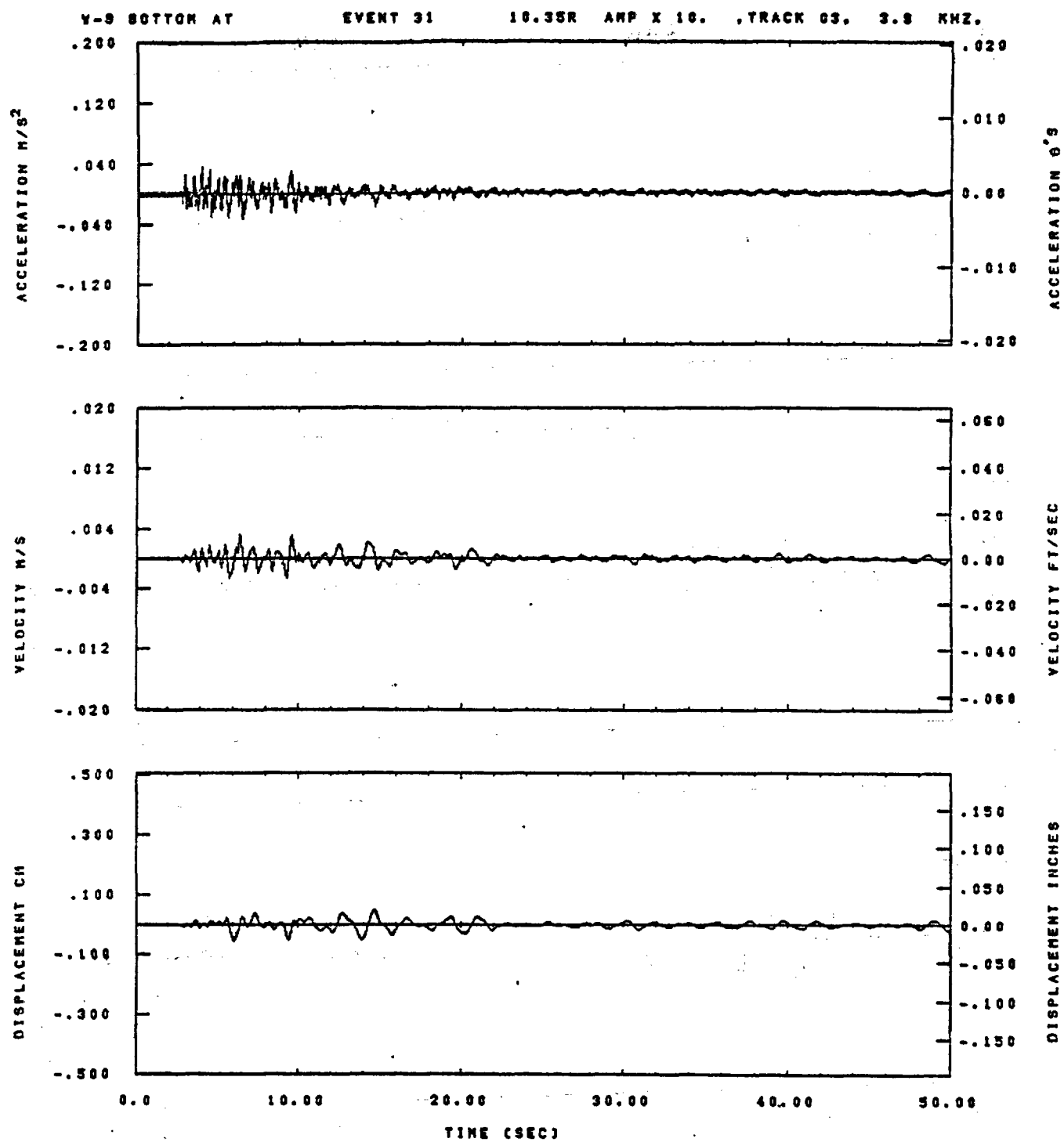


IDT= .0020	ODT= .003	FIX=	AAS= 0.
HPF= .25	SVH= .18	HLH= 143	ASB=
LPF= 31.	SVL= 7.	HLL= 2339	ASE=
VTS= .250	VTE= .188	FLL= -20.	VSE= 0.
OPB= 0.	OPE= 100.	FLH= 0	DSE= 0.

11.25.28.

08/26/92

Figure G-35

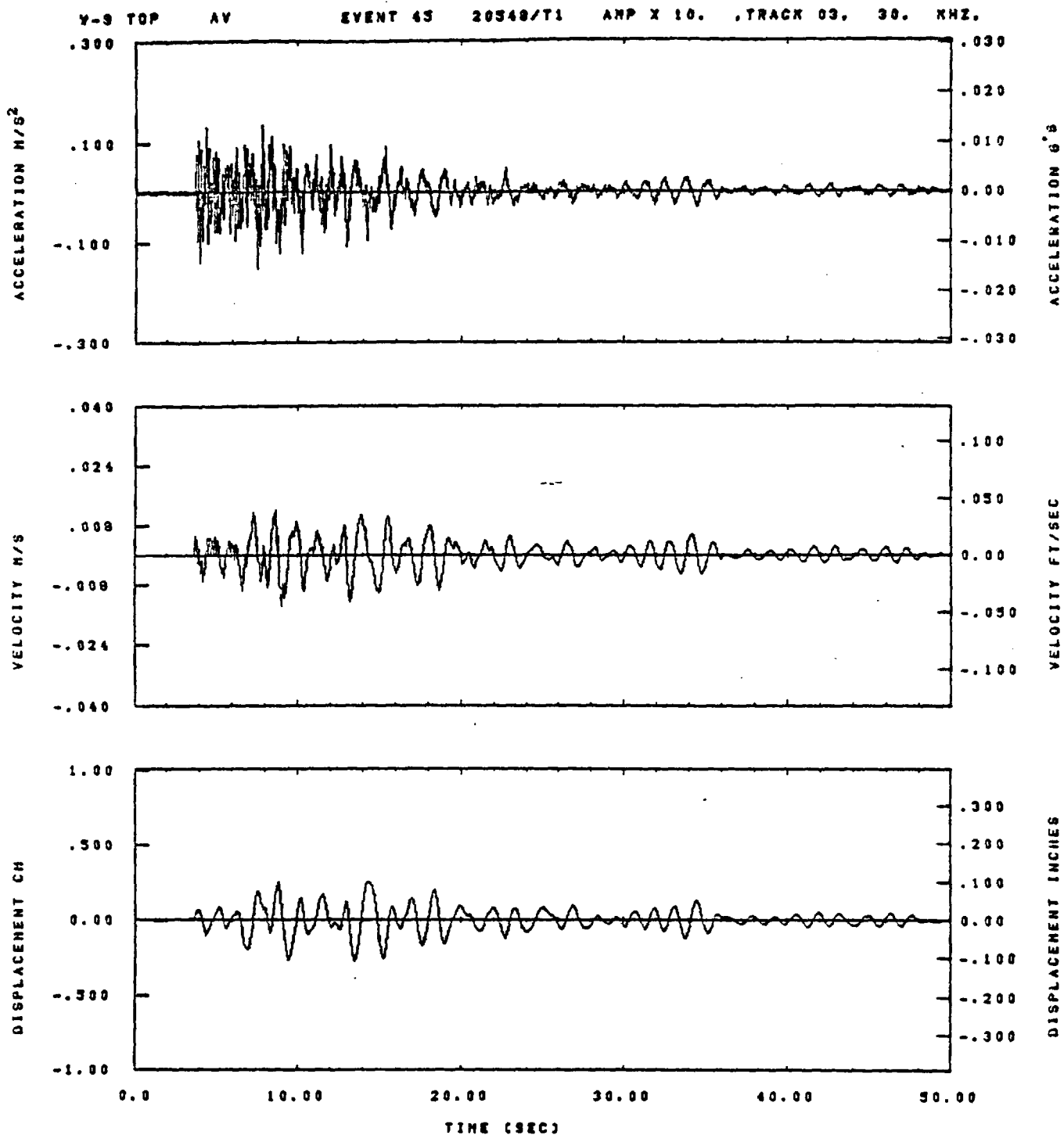


IDT= .0020	ODT= .005	FIX=	AAS= 0.
HPF= .25	BYH= .16	HLH= 143	ASB=
LPF= 31.	BYL= 7.	HLL= 2398	ASE=
VTB= .250	VTE= .166	FLL= -20.	VSE= 0.
DPS= 0.	DPE= 160.	FLH= 0	DSE= 0.

11.25.54.

06/24/82

Figure G-36

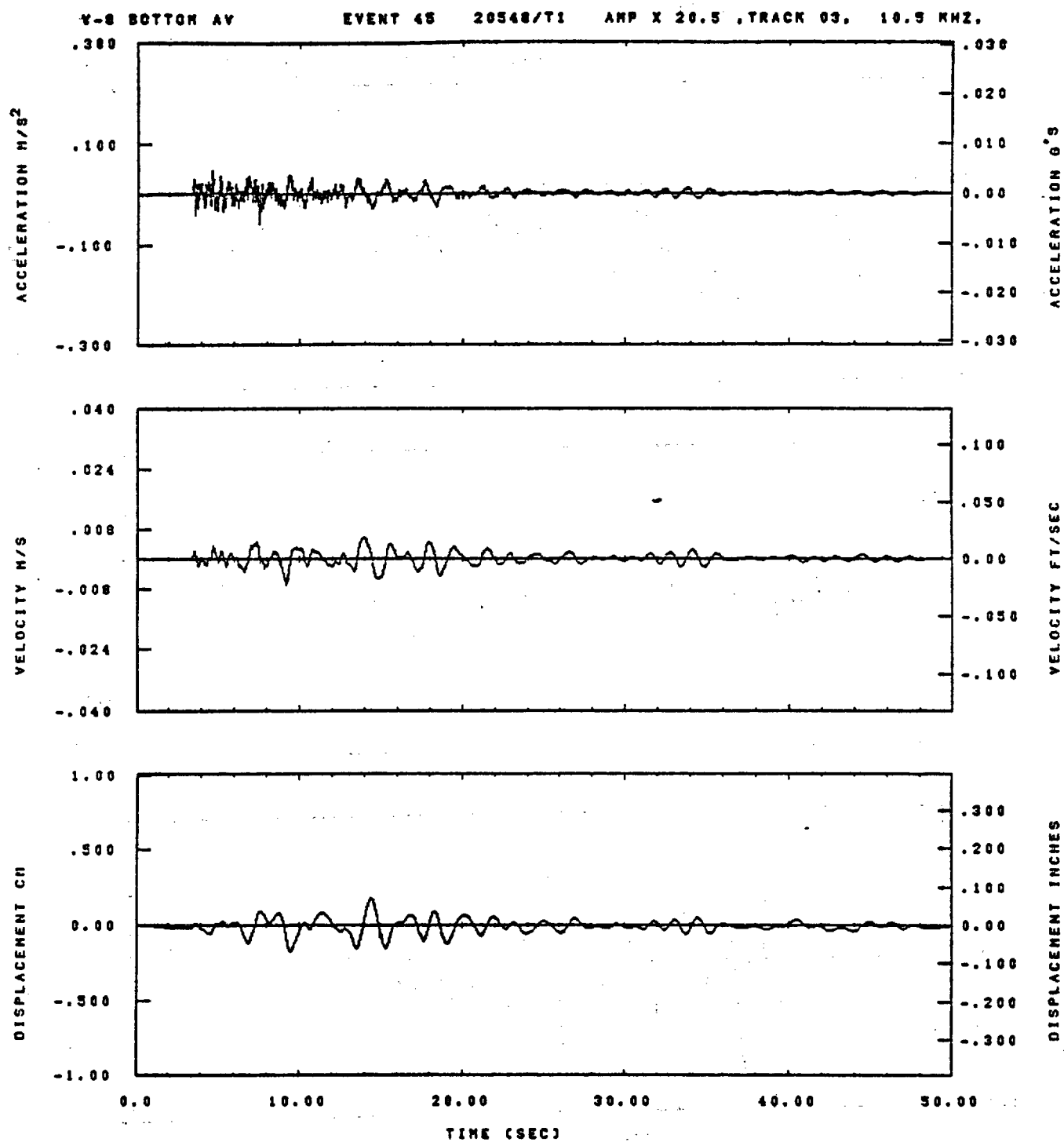


IDT= .0020	ODT= .005	FIX=	AAS= 0.
HPP= .2	BVH= .13	HLH= 33	ASB=
LPP= 45.	BVL= 10.	HLL= 2939	ASE=
VTB= .20	VTE= .133	FLL= -20.	VSE= 0.
OPS= 0.	OPE= 100.	FLH= 0	DSE= 0.

08.44.38.

08/23/82

Figure G-37

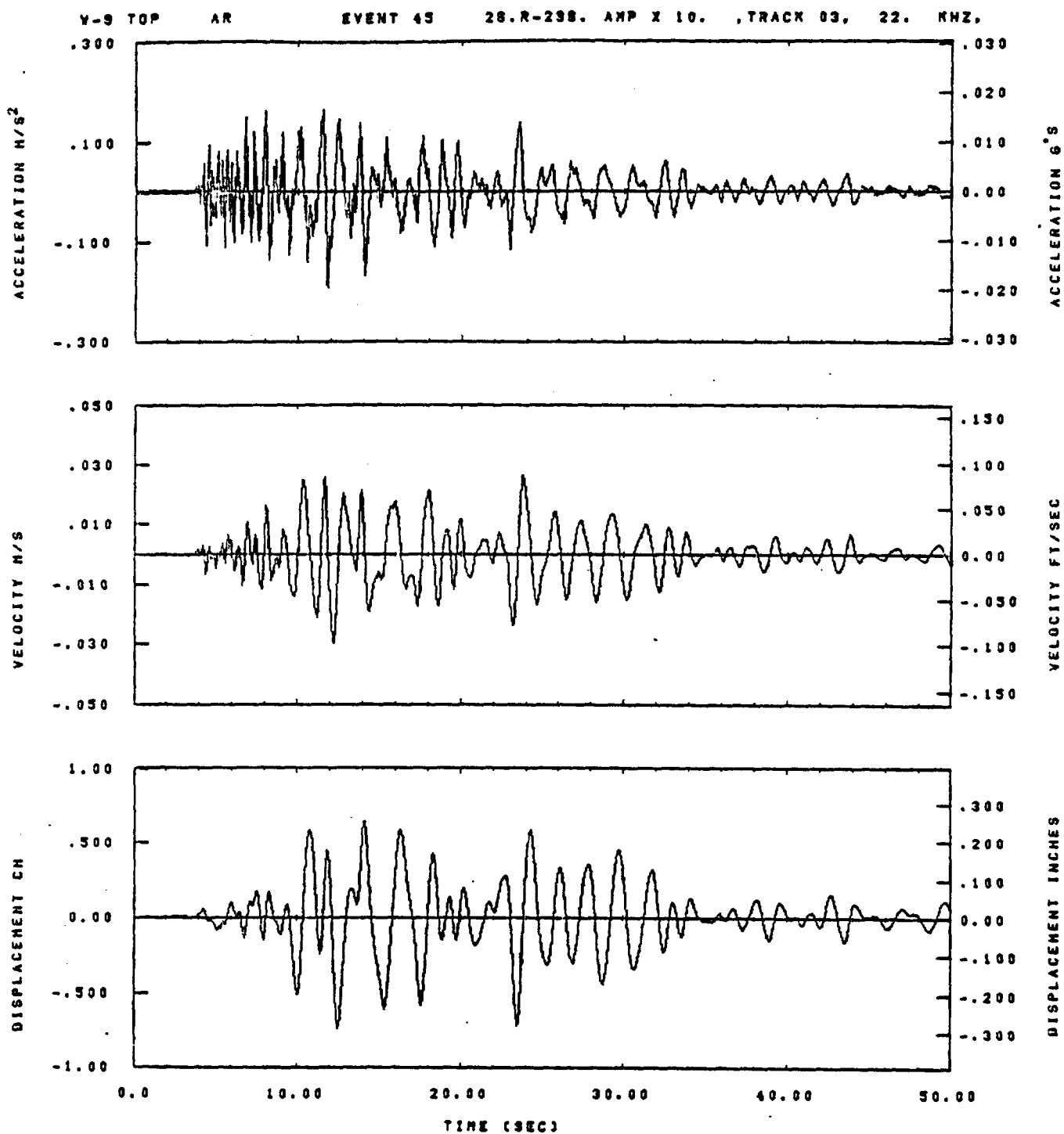


IDT= .0020	ODT= .005	FIX=	AAS= 0.
HPP= .2	SVH= .13	HLH= 89	ASB=
LPP= 45.	SVL= 10.	HLL= 2999	ASE=
VTB= .20	VTE= .133	FLL= -20.	VSE= 0.
DPS= 0.	DPE= 100.	FLH= 0	DSE= 0.

10.27.32.

06/23/82

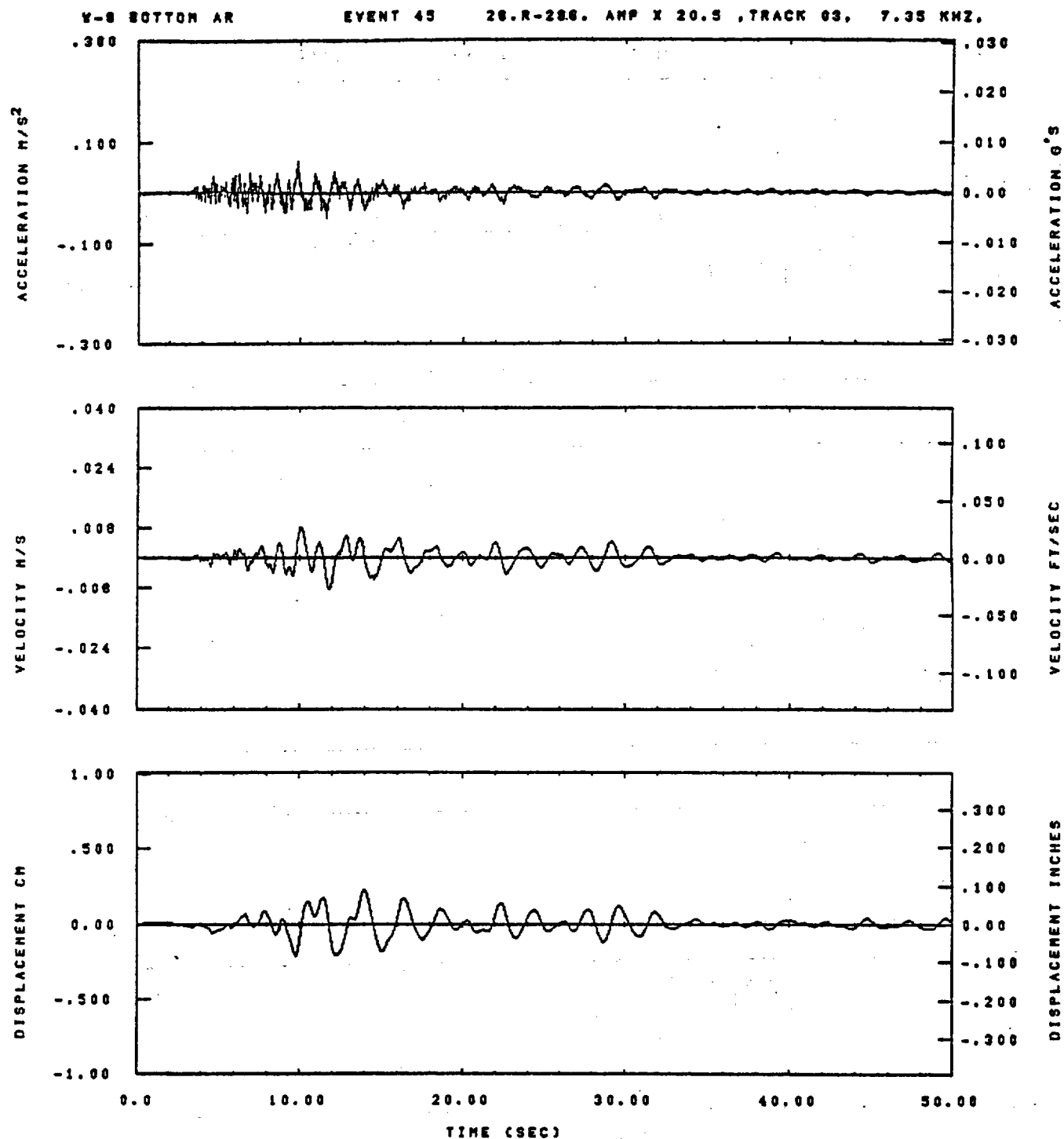
Figure G-38



IDT= .0020	ODT= .003	FIX=	AAS= 0.
HPF= .2	BYN= .13	HLH= 99	ASS=
LPF= 45.	SVL= 10.	HLL= 2999	ASE=
VTB= .20	VTE= .133	PLL= -20.	VSE= 0.
DPS= 0.	DPE= 100.	PLH= 0	DSE= 0.

12.13.37.

08/30/82

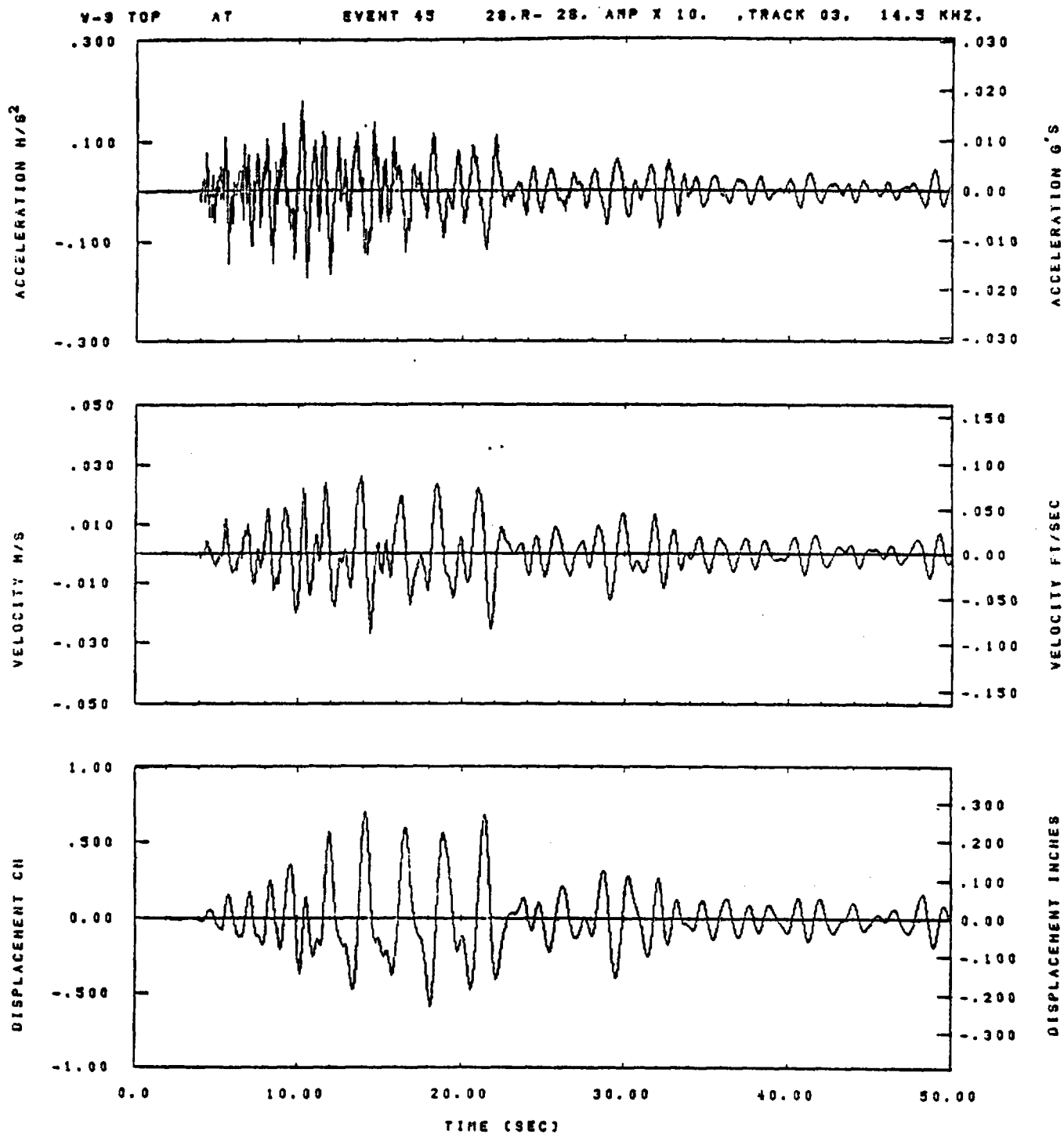


IDT= .0020	OOT= .005	FIX=	AAS= 0.
HPP= .20	BYH= .13	HLH= 89	ASS=
LPP= 45.	BYL= 10.	HLL= 2999	ASE=
VTB= .200	VTE= .133	FLL= -20.	VSE= 0.
DPS= 0.	DPE= 100.	FLH= 0	DSE= 0.

10.27.38.

06/23/82

Figure G-40

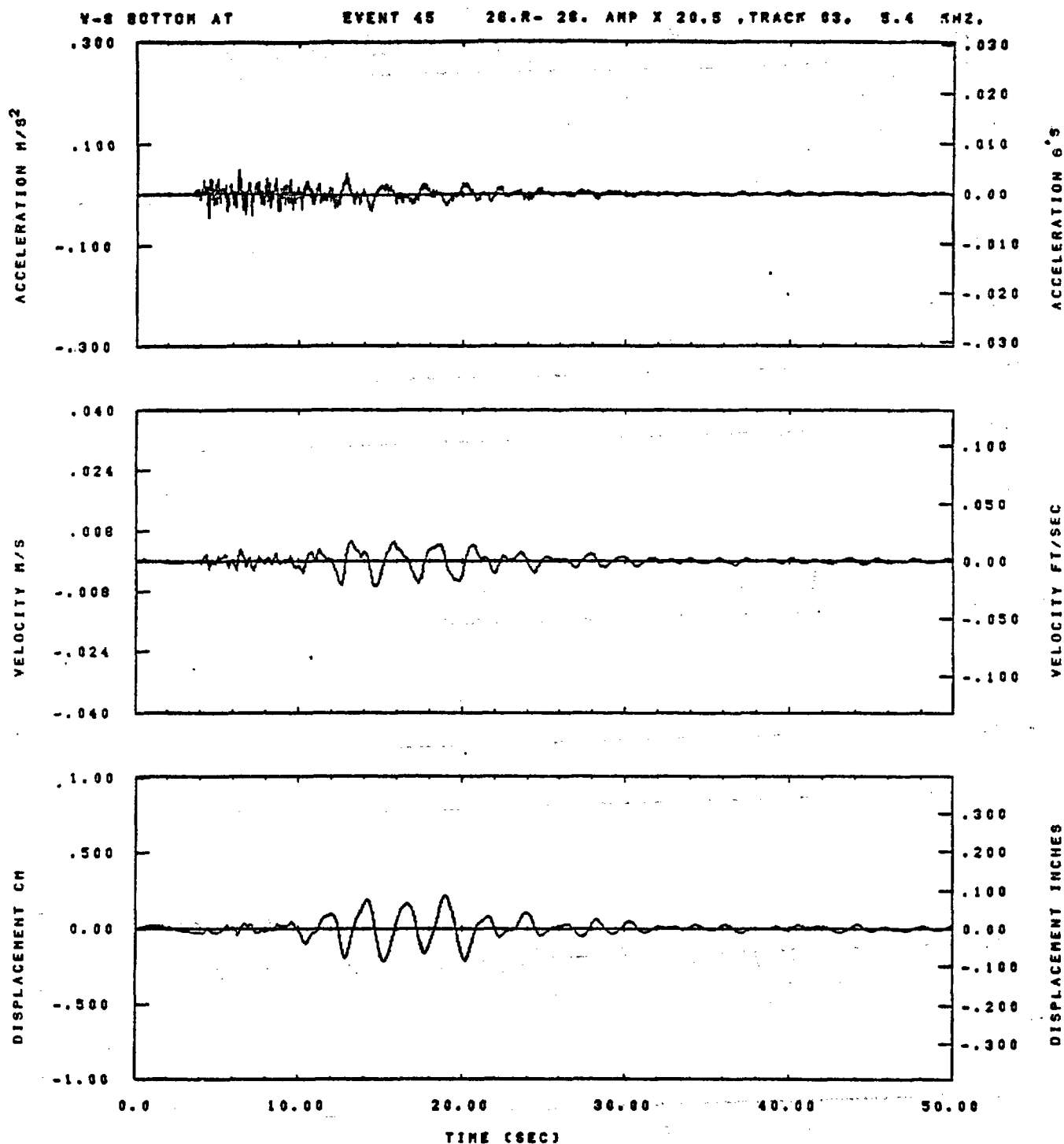


IDT= .0020	ODT= .0	FIX=	AAS=
HPF= .3	BYH= .20	HLH= 167	ASB=
LPF= 27.	BYL= 6.	HLL= 1999	ASE=
VTB= .30	VTE= .200	FLL=	VSE=
OPB=	OPE=	FLH= 0	DSE= 0.

12.13.42.

06/30/82

Figure G-41

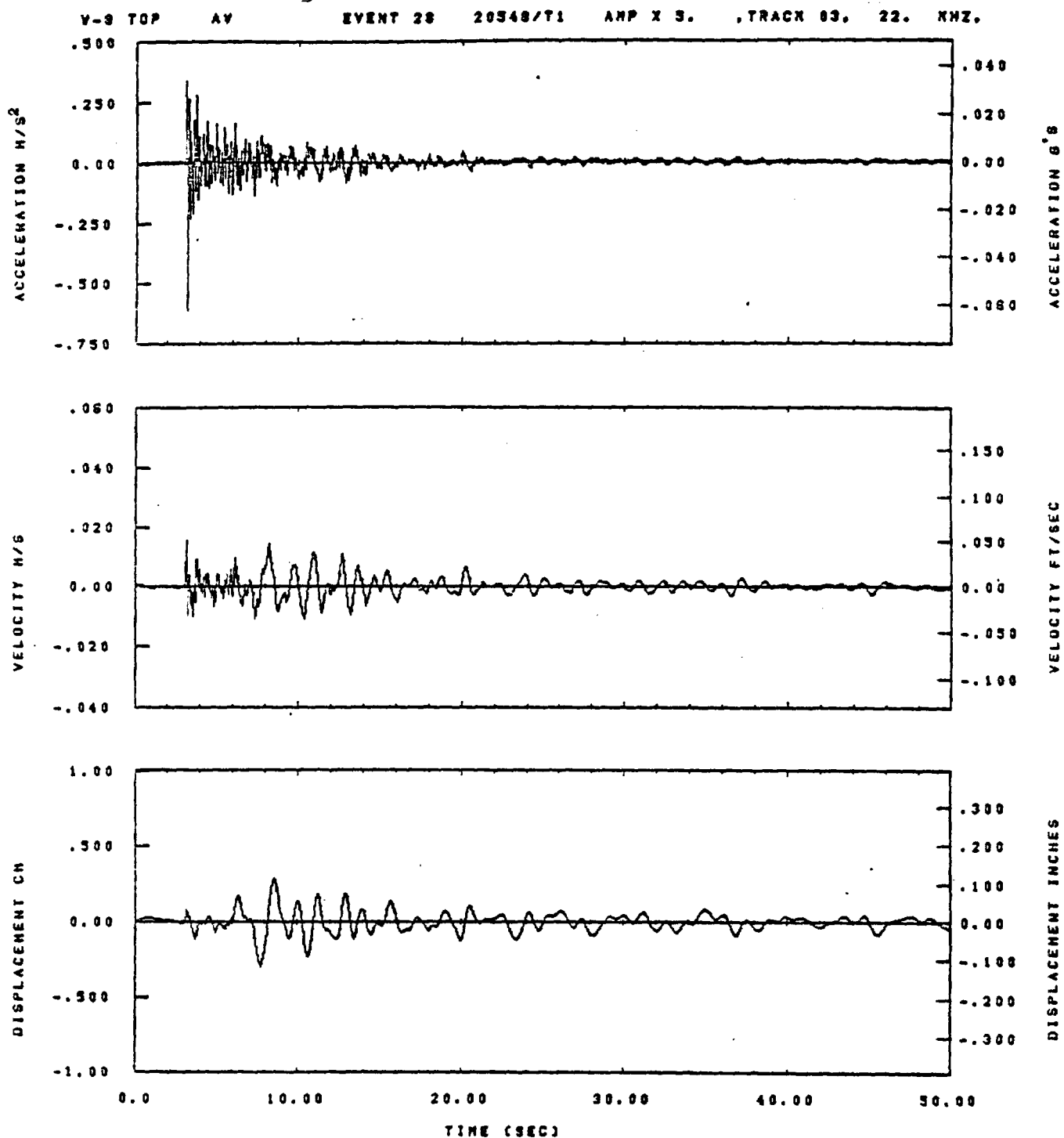


IDT= .0020	ODT= .005	FIX=	AAS= 0.
HPF= .20	BYH= .13	HLH= 99	ASB=
LPF= 45.	BYL= 10.	HLL= 2898	ASE=
VTB= .200	VTE= .133	FLL= -20.	VSE= 0.
DPS= 0.	DPE= 100.	FLH= 0	DSE= 0.

10.27.45.

06/23/82

Figure G-42

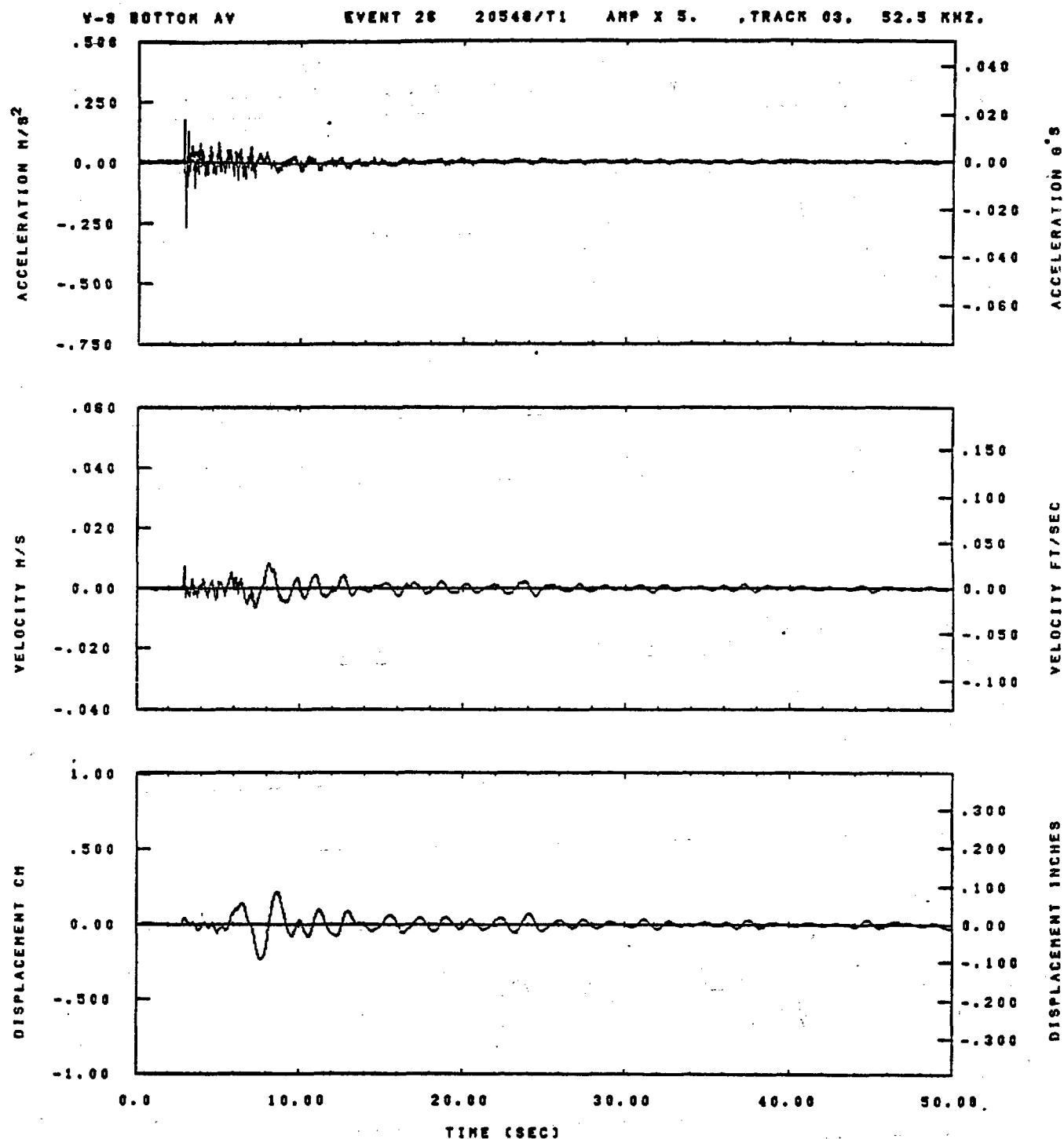


IDT= .0020	QDT= .005	FIX=	AAS= 0.
HPP= .20	SVH= .13	HLH= 187	ASS=
LPP= 27.	SVL= 8.	HLL= 2333	ASE=
VTS= .200	VTE= .133	FLL= -20.	VSE= 0.
OPS= 0.	OPE= 100.	FLH= A-.1	DSE= A+.1

08.04.47.

08/25/82

Figure G-43

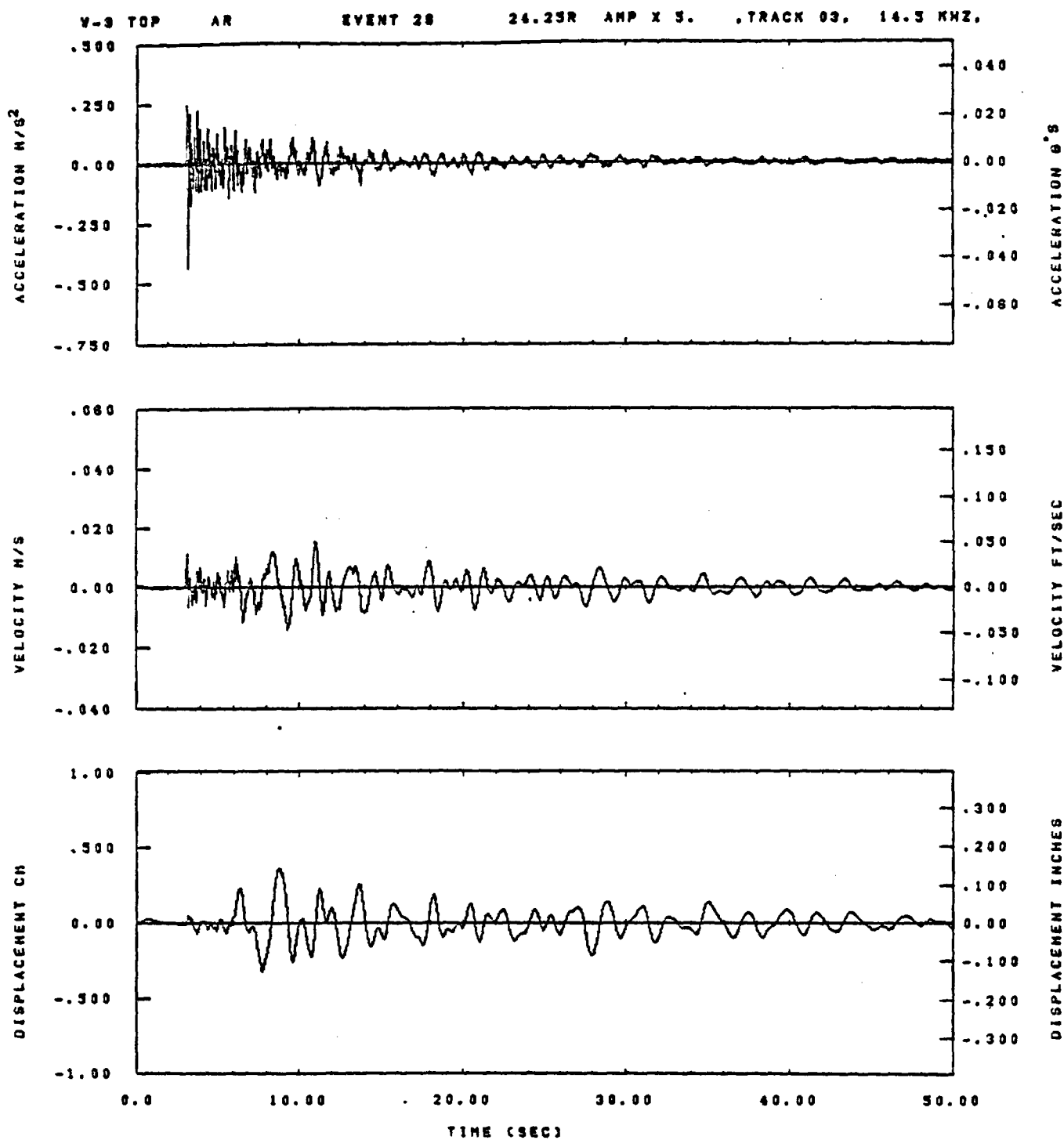


IDT= .0020	ODT= .005	FIX=	AAS= 0.
HPF= .20	BYH= .13	HLH= 167	ASB=
LPF= 27.	BVL= 6.	HLL= 2999	ASE=
VTS= .200	VTE= .133	FLL= -15.	VSE= 0.
DPS= 0.	DPE= 60.	FLH= A-.1	DSE= A+.1

08.04.57.

06/25/82

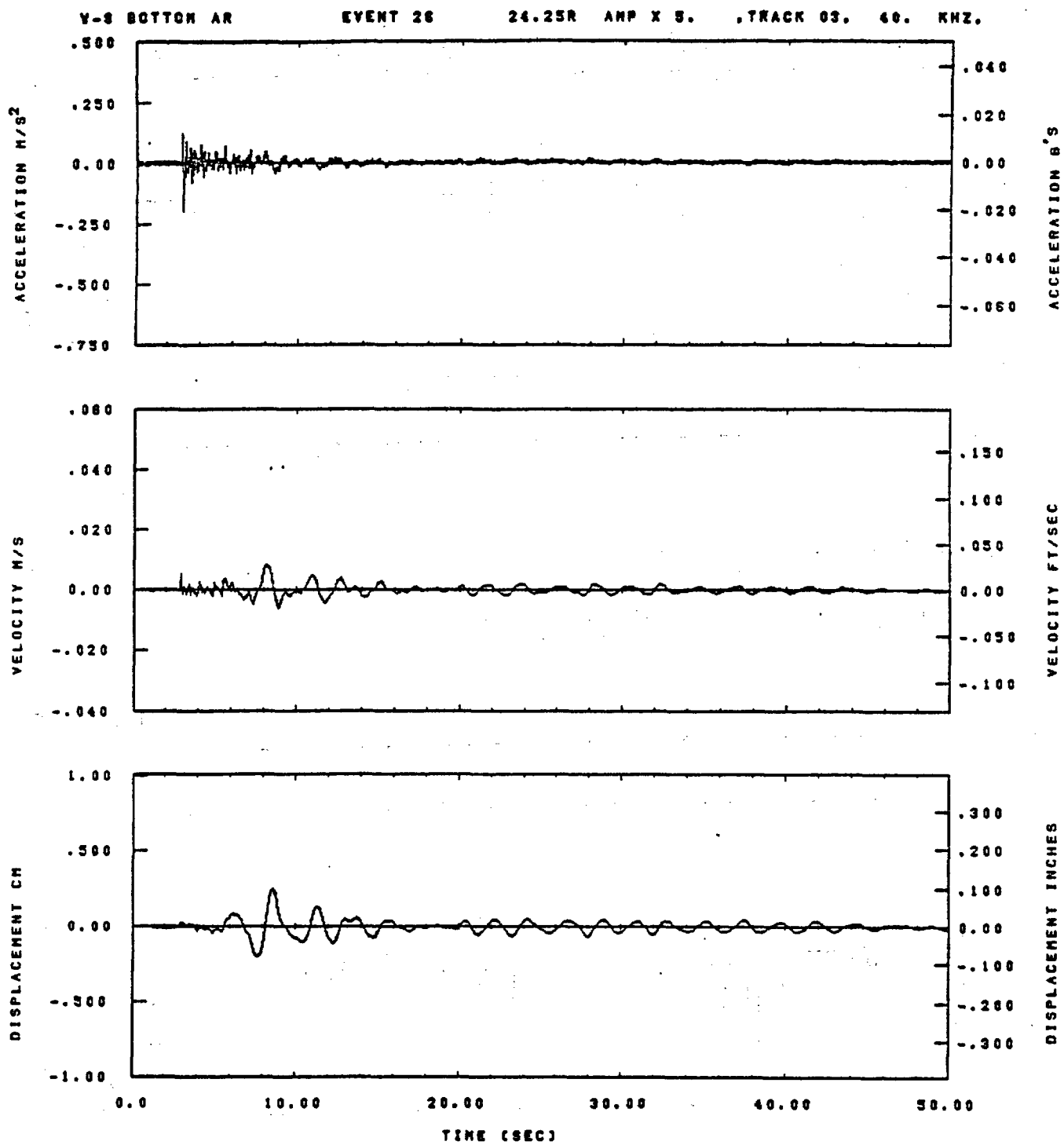
Figure G-44



IDT= .0020	ODT= .005	FIX=	AAS= 0.
HPP= .20	SVN= .13	MLN= 187	ASB=
LPF= 27.	SVL= 6.	MLL= 2998	ASE=
VTB= .200	VTE= .133	FLL= -20.	VSE= 0.
DPS= 0.	DPE= 100.	FLH= A+.1	DSE= A+.1

08.04.27.

08/23/92

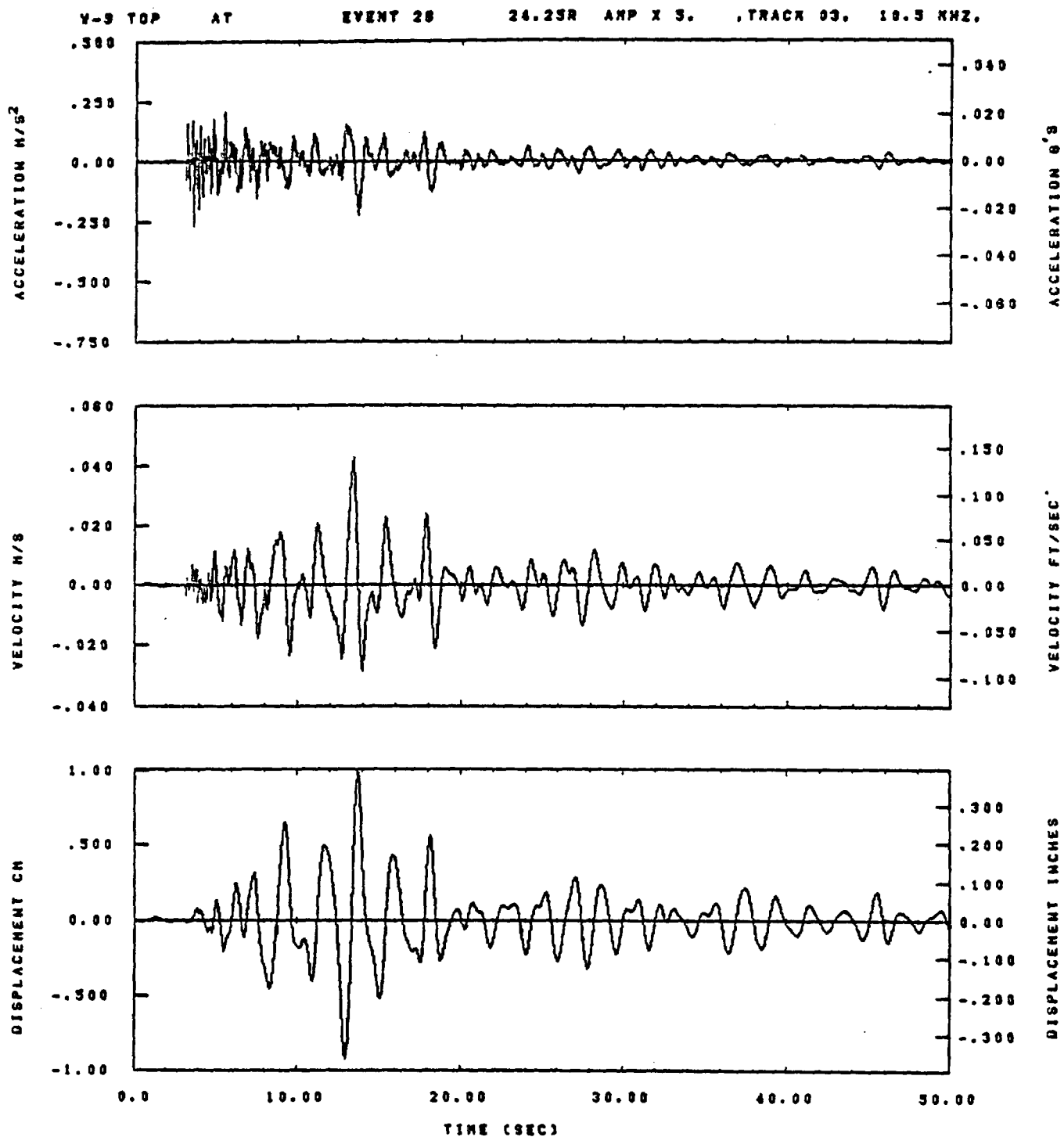


IDT= .0020	ODT= .005	FIX=	AAS= 0.
HPF= .20	BYH= .13	HLH= 167	ASH=
LPF= 27.	BYL= 6.	HLL= 2599	ASE=
YTB= .200	YTE= .133	FLL= -15.	VSE= 0.
DPS= 0.	DPE= 60.	FLH= A-.1	OSE= A+.1

08.05.07.

06/25/82

Figure G-46

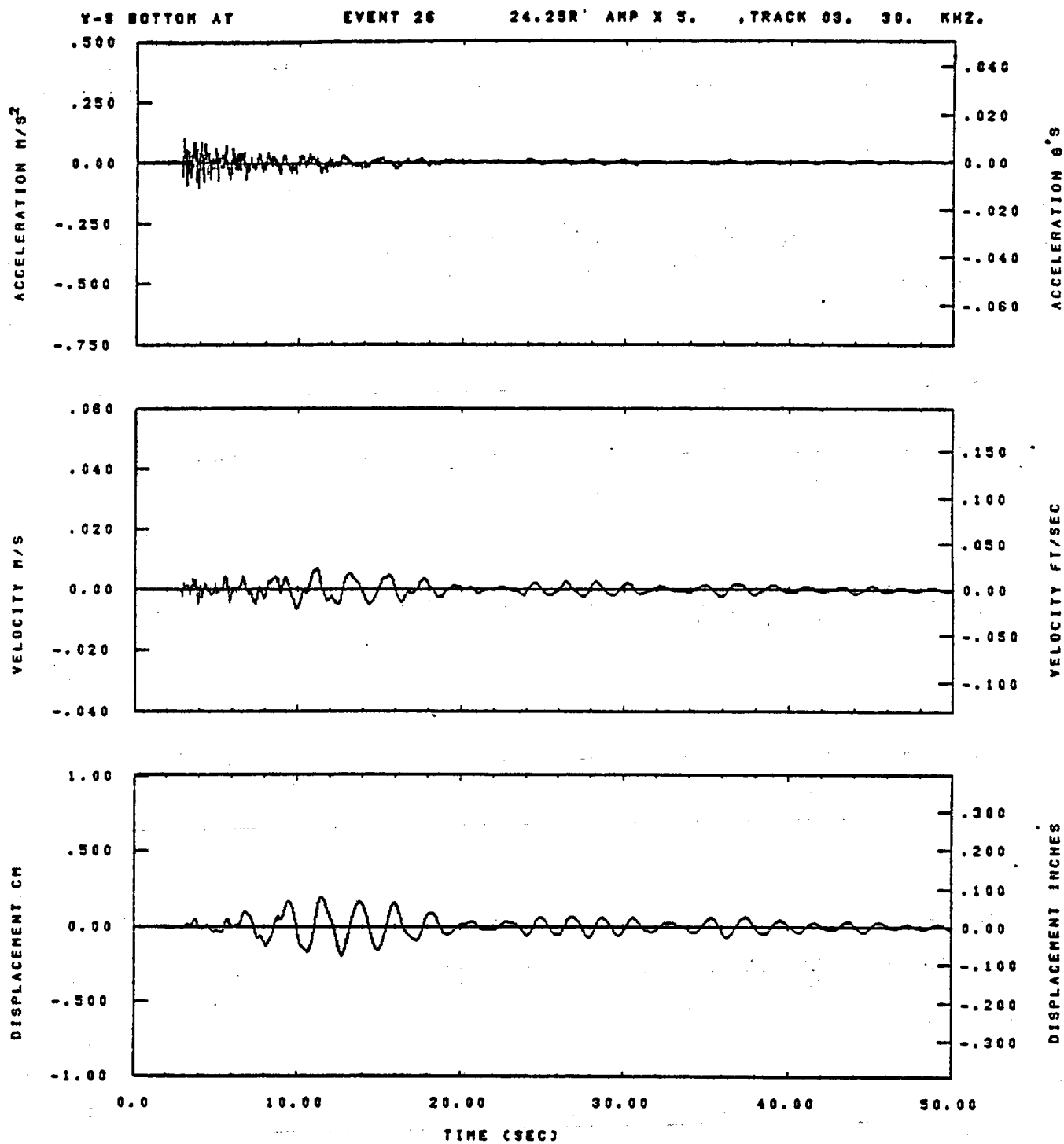


IDT= .0020	ODT= .005	FIX=	AAS= 0.
HPP= .20	BWH= .13	HLH= 187	ASB=
LPP= 27.	BVL= 8.	HLL= 2999	ASE=
VTB= .200	VTE= .133	FLL= -20.	VSE= 0.
OPB= 0.	OPE= 100.	FLH= A-.1	DSE= A+.1

08.04.35.

08/23/82

Figure G-47

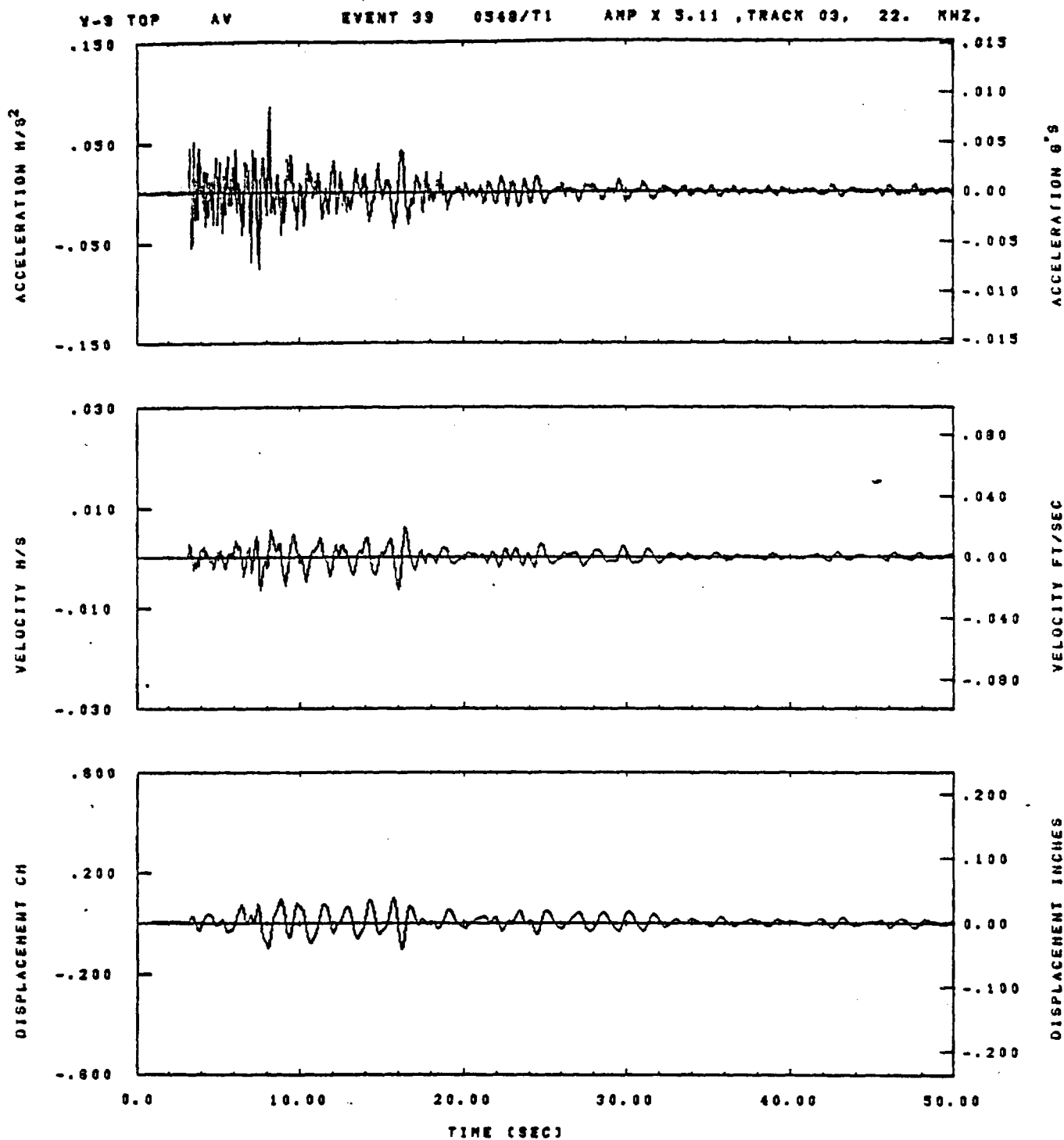


IDT= .0020	OOT= .005	FIX=	AAS= 0.
HPF= .20	SVH= .13	HLH= 167	ASB=
LPF= 27.	SVL= 6.	HLL= 2999	ASE=
VTB= .200	VTE= .133	FLL= -19.	VSE= 0.
DPB= 0.	DPE= 60.	FLH= A-.1	DSE= A+.1

06.05.17.

06/25/62

Figure G-48



IDT= .0020	QDT= .005	FIX=	AAS= 0.
HPP= .30	BYH= .20	HLH= 199	ASS=
LPP= 22.	BYL= 5.	HLL= 1999	ASE=
VTS= .300	VTE= .200	FLL= -20.	VSE= 0.
DPS= 0.	DPE= 100.	FLH= 0	DSE= 0.

14.58.48.

06/23/82

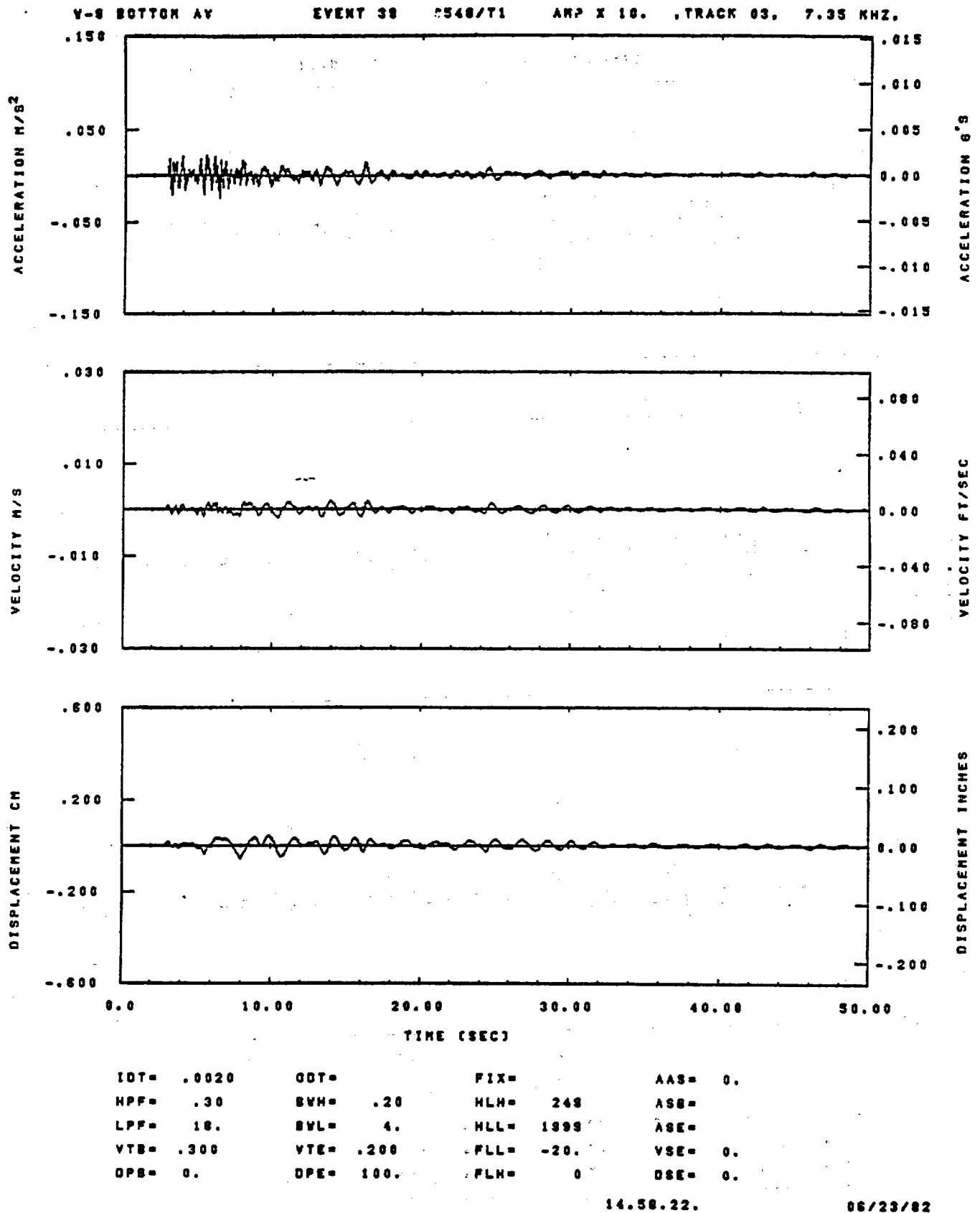
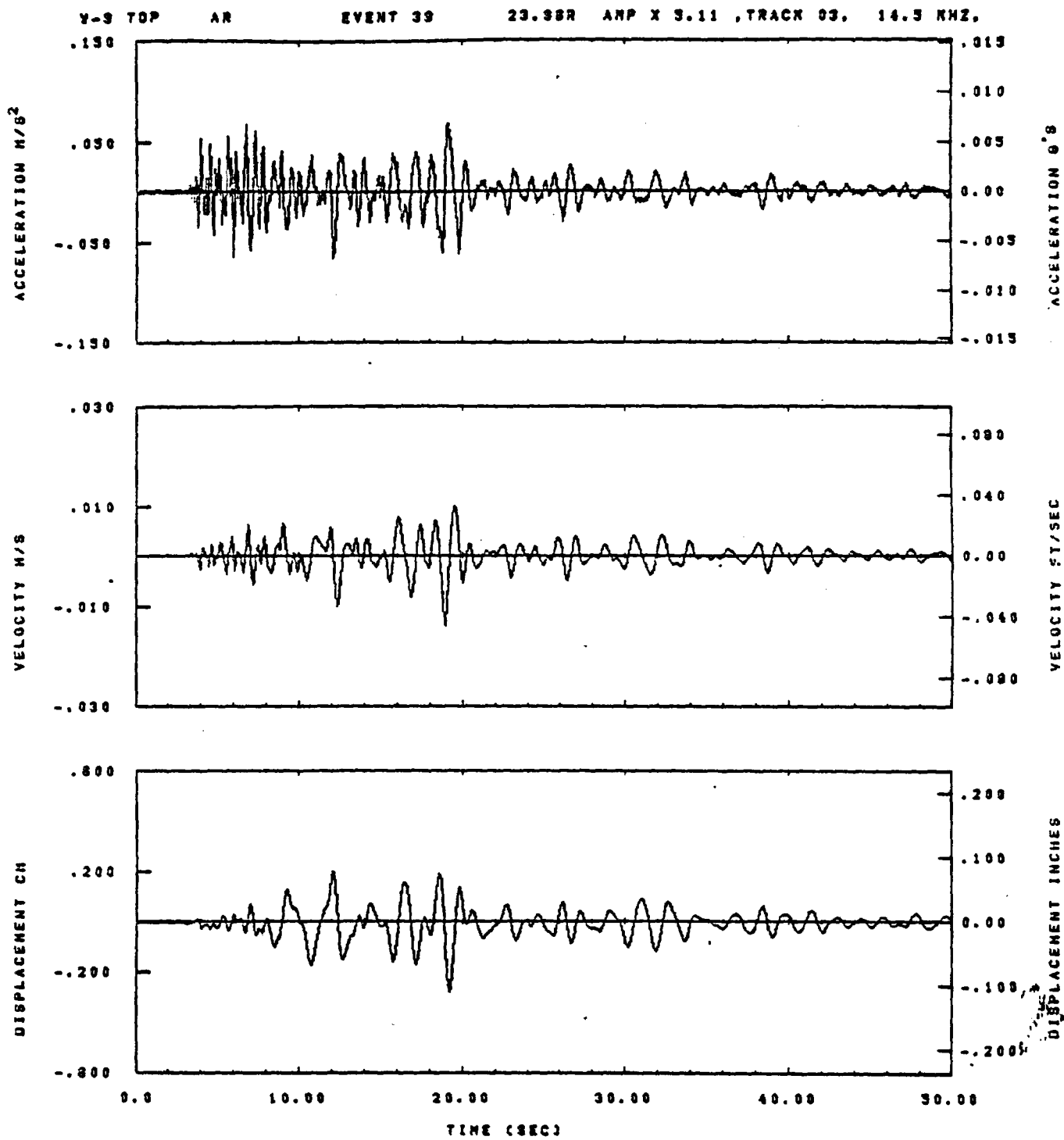


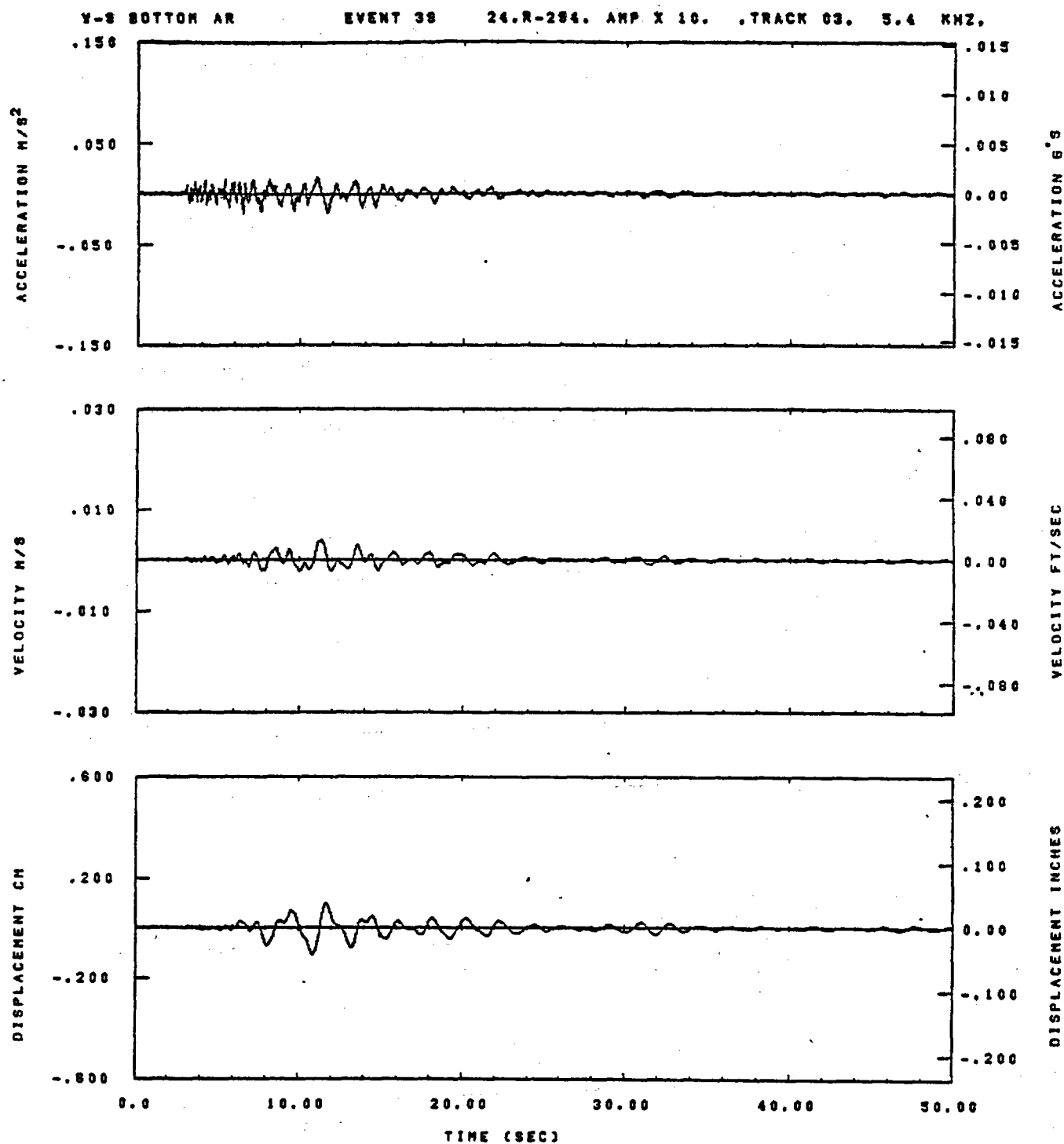
Figure G-50



IDT= .0020	ODT= .003	FIX=	AAS= 0.
HPP= .30	BYH= .20	HLH= 139	ASB=
LPP= 22.	BYL= 3.	HLL= 1333	ASE=
VTB= .300	VTE= .200	FLL= -20.	VSE= 0.
OPB= 0.	OPE= 100.	FLH= 0	DSE= 0.

14.58.10.

08/23/82

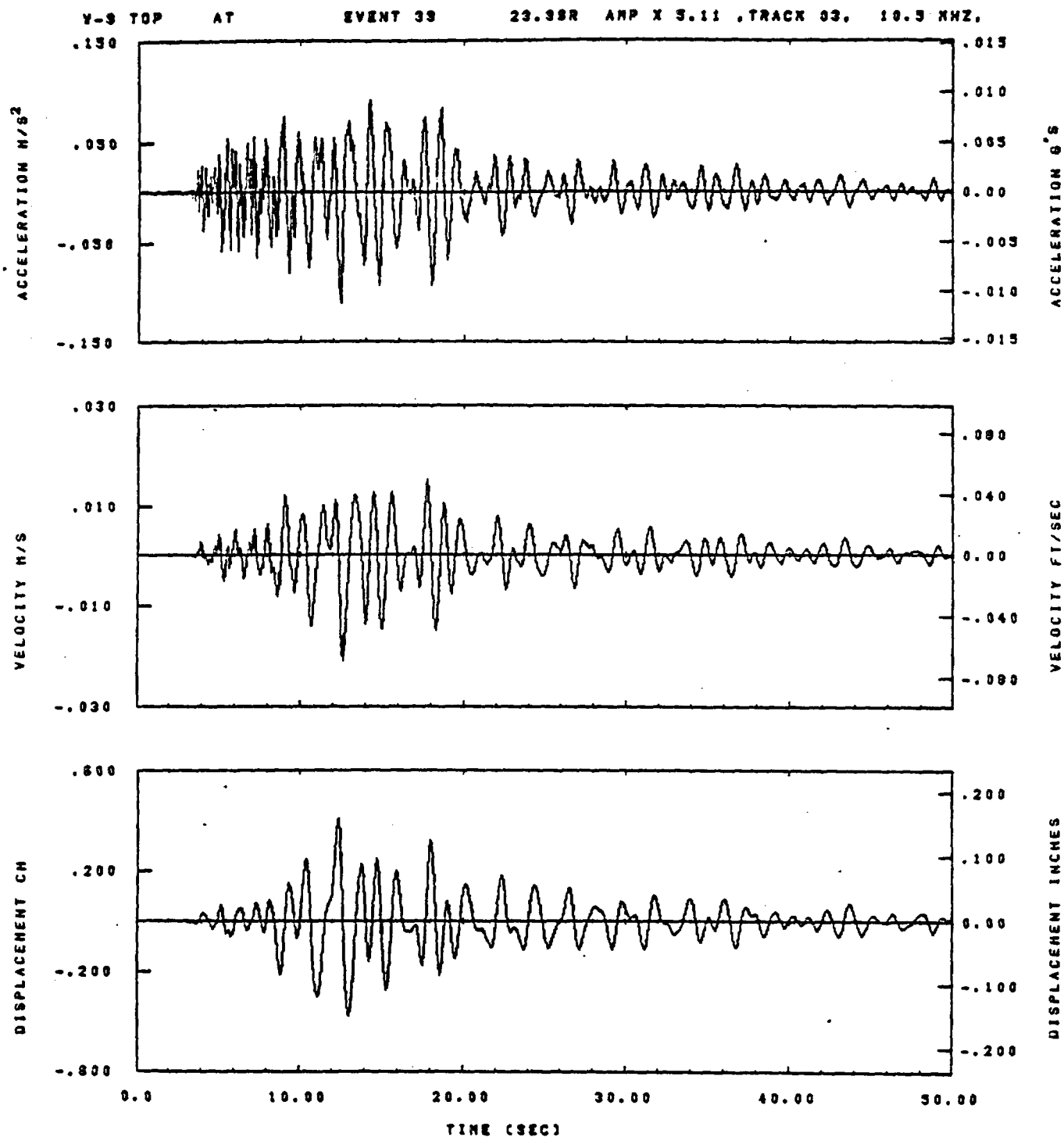


IDT= .0020	OOT=	FIX=	AAS= 0.
HPF= .30	BYH= .20	HLH= 248	ASB=
LPF= 18.	BYL= 4.	HLL= 1999	ASE=
VTS= .300	VTE= .200	PLL= -20.	VSE= 0.
OPS= 0.	DPE= 100.	FLH= 0	DSE= 0.

14.57.44.

06/23/82

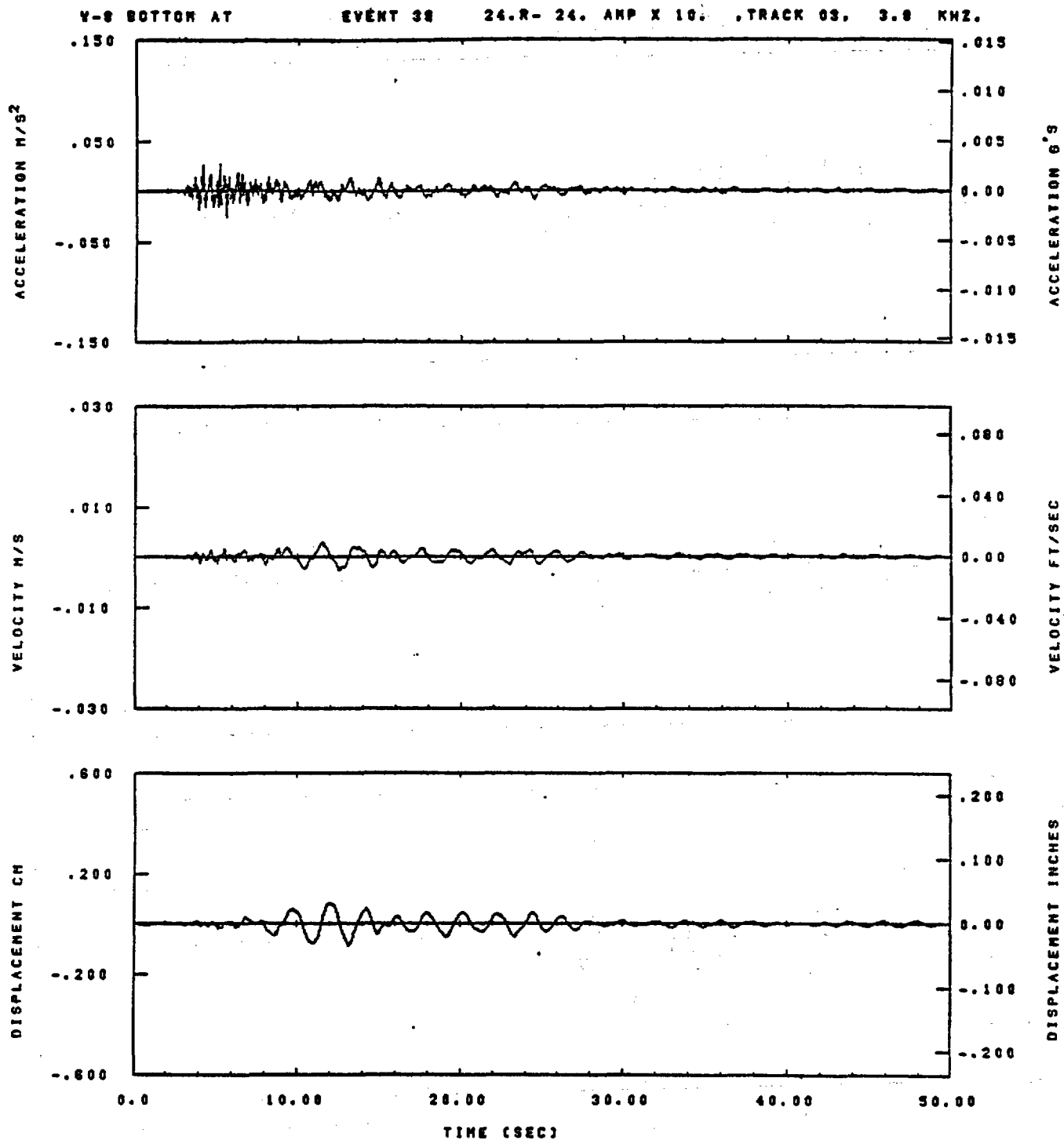
Figure G-52



IDT= .0020	ODT= .003	FIX=	AAS= 0.
HPP= .30	BYH= .20	HLH= 133	ASB=
LPP= 22.	BYL= 5.	HLL= 1993	ASE=
VTS= .300	VTE= .200	FLL= -20.	VSE= 0.
DPS= 0.	DPE= 100.	FLH= 0	OSE= 0.

14.38.17.

08/23/82

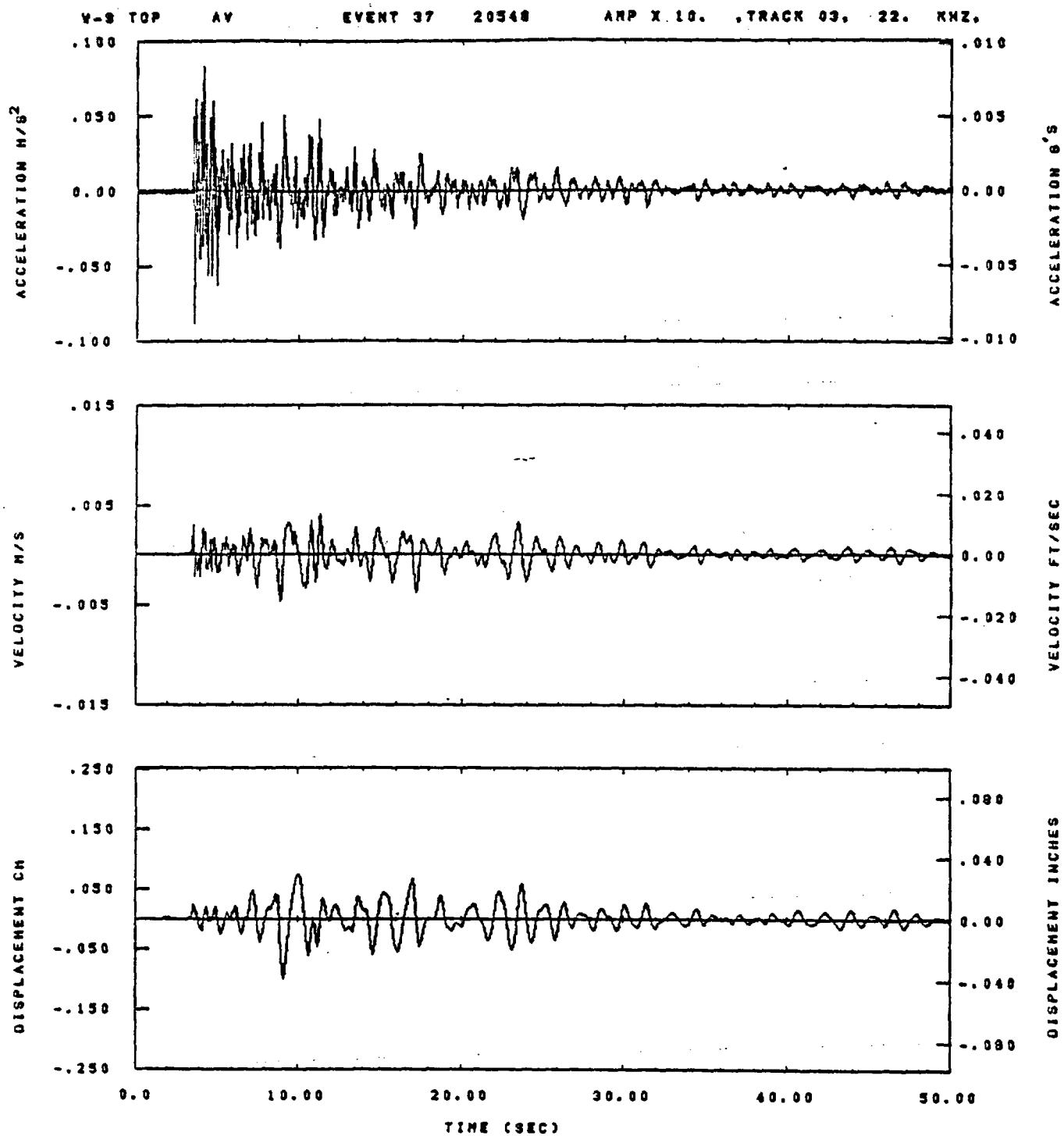


IDT= .0020	ODT=	FIX=	AAS= 0.
HPP= .30	SVN= .20	HLN= 248	ASS=
LPP= 18.	SVL= 4.	HLL= 1888	ASE=
VTS= .300	VTE= .200	FLL= -20.	VSE= 0.
OPS= 0.	OPE= 100.	FLH= 0	OSE= 0.

14.58.13.

06/23/82

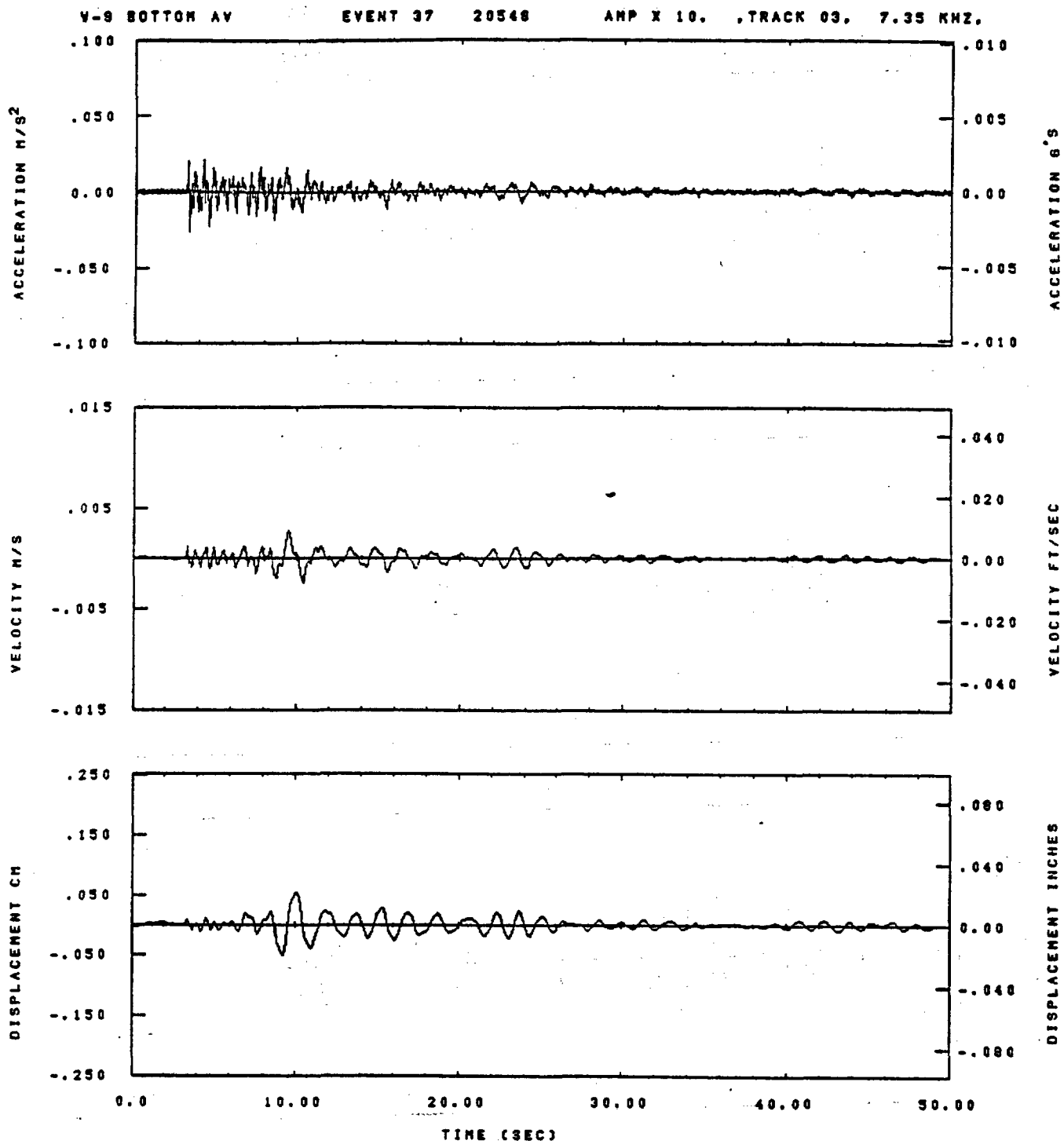
Figure G-54



IDT= .0020	ODT= .003	FIX=	AAS= 0.
HPF= .20	SVH= .13	HLH= 243	ASS=
LPF= 18.	SVL= 4.	HLL= 2333	ASE=
VTS= .200	VTE= .133	FLL= -20.	VSE= 0.
DPS= 0.	DPE= 100.	FLH= 0	DSE= 0.

09.45.00

08/15/82

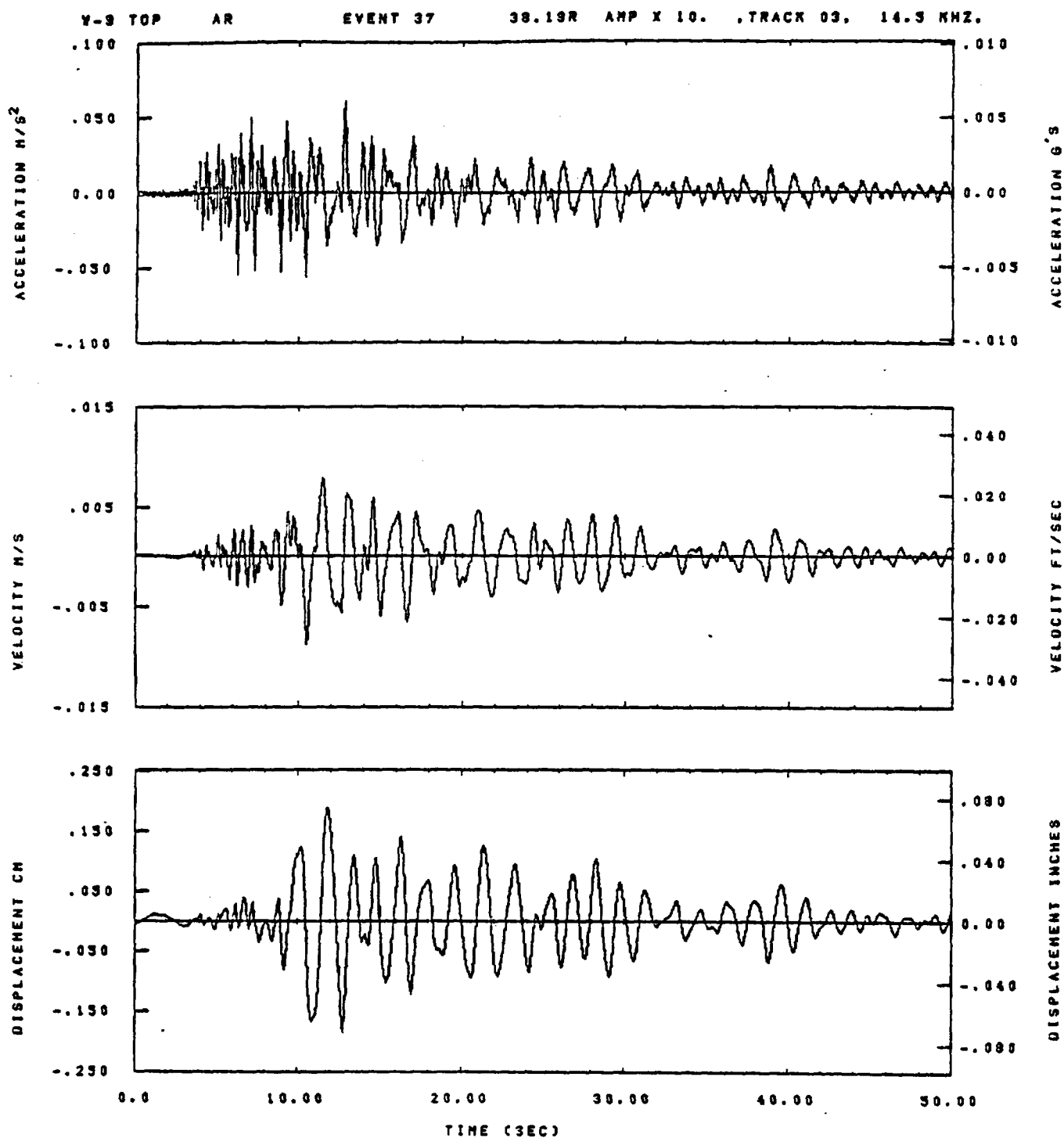


IDT= .0020	ODT= .005	FIX=	AAS= 0.
HPF= .20	SVH= .13	HLH= 248	ASB=
LPF= 18.	SVL= 4.	HLL= 2999	ASE=
VTS= .200	VTE= .133	FLL= -20.	VSE= 0.
DPS= 0.	DPE= 100.	FLH= 0	DSE= 0.

08.45.26

06/15/82

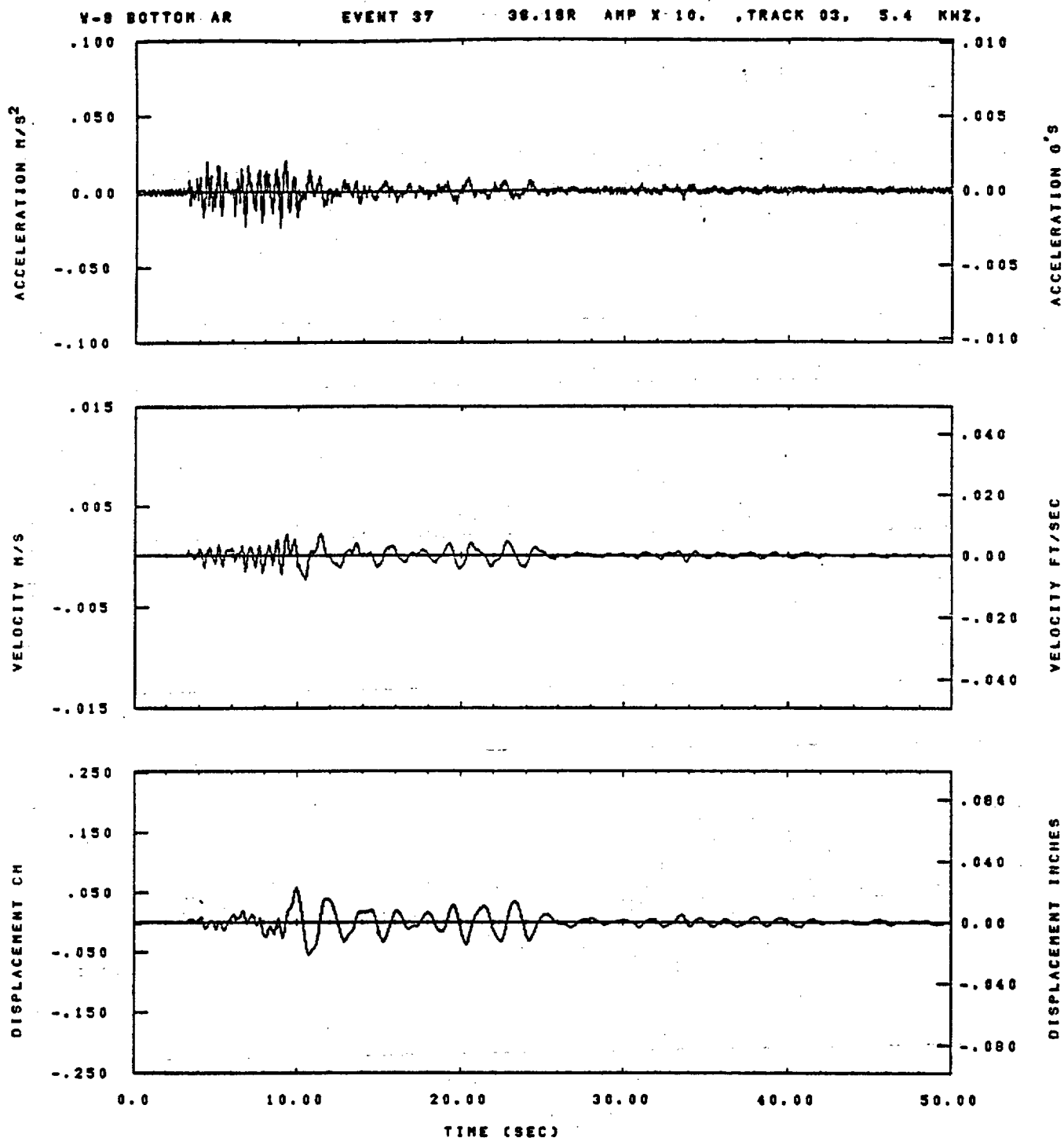
Figure G-56



IDT= .0020	ODT= .005	FIX=	AAS= 0.
HPP= .20	SVH= .13	HLH= 249	ASB=
LPP= 18.	SVL= 4.	HLL= 2999	ASE=
VTS= .200	VTE= .133	FLL= -20.	VSE= 0.
DPS= 0.	OPE= 100.	FLH= 0	OSE= 0.

09.44.49

06/15/82



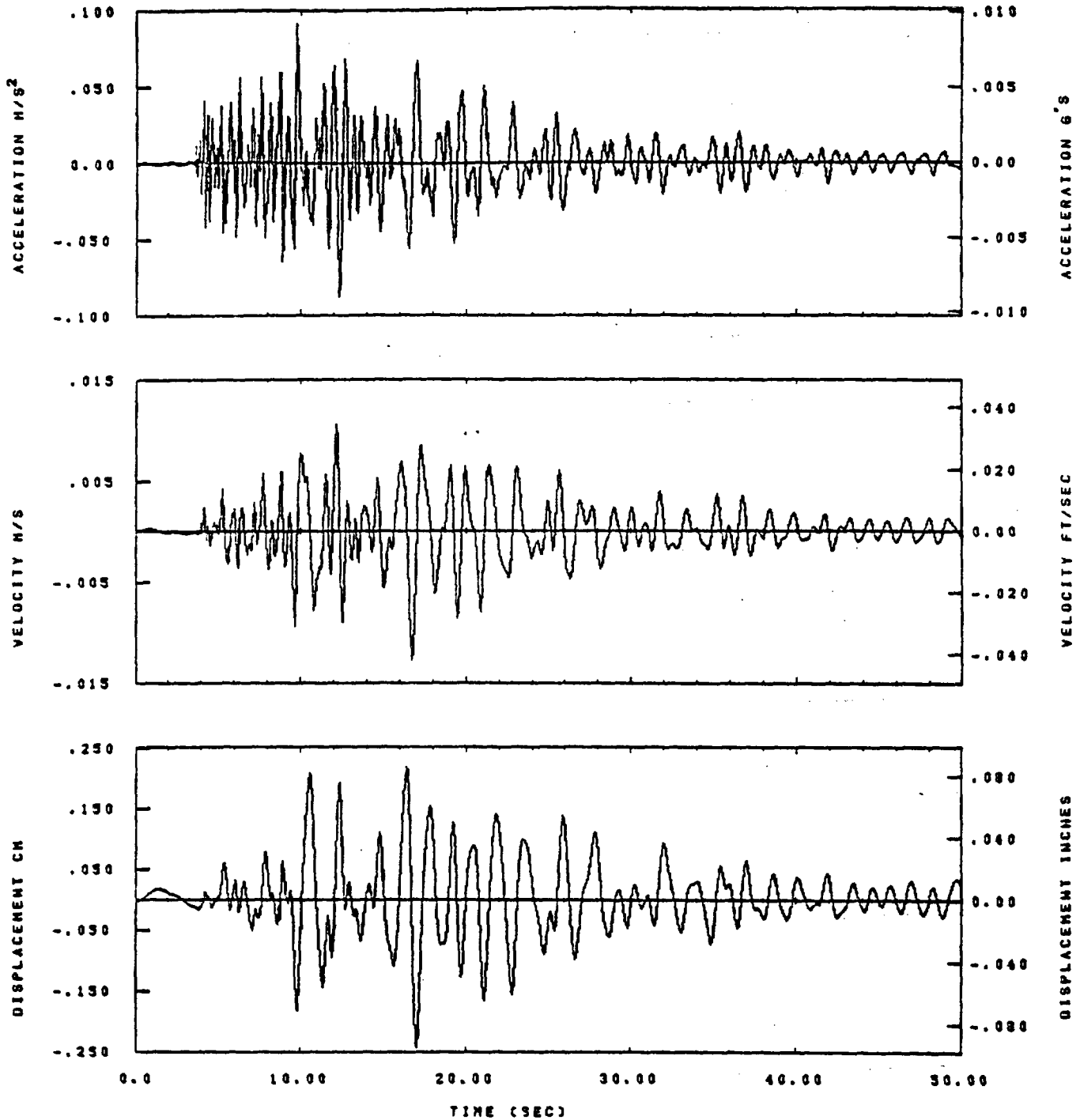
IDT= .0020	QDT= .005	FIX=	AAS= 0.
HPF= .20	BYH= .13	HLH= 249	ASB=
LPF= 18.	BYL= 4.	HLL= 2989	ASE=
VTS= .200	YTE= .133	FLL= -20.	VSE= 0.
DPS= 0.	DPE= 100.	FLH= 0	DSE= 0.

08.45.17

06/15/82

Figure G-58

Y-9 TOP AT EVENT 37 38.18R AMP X 10. , TRACK 03, 10.3 KHZ.

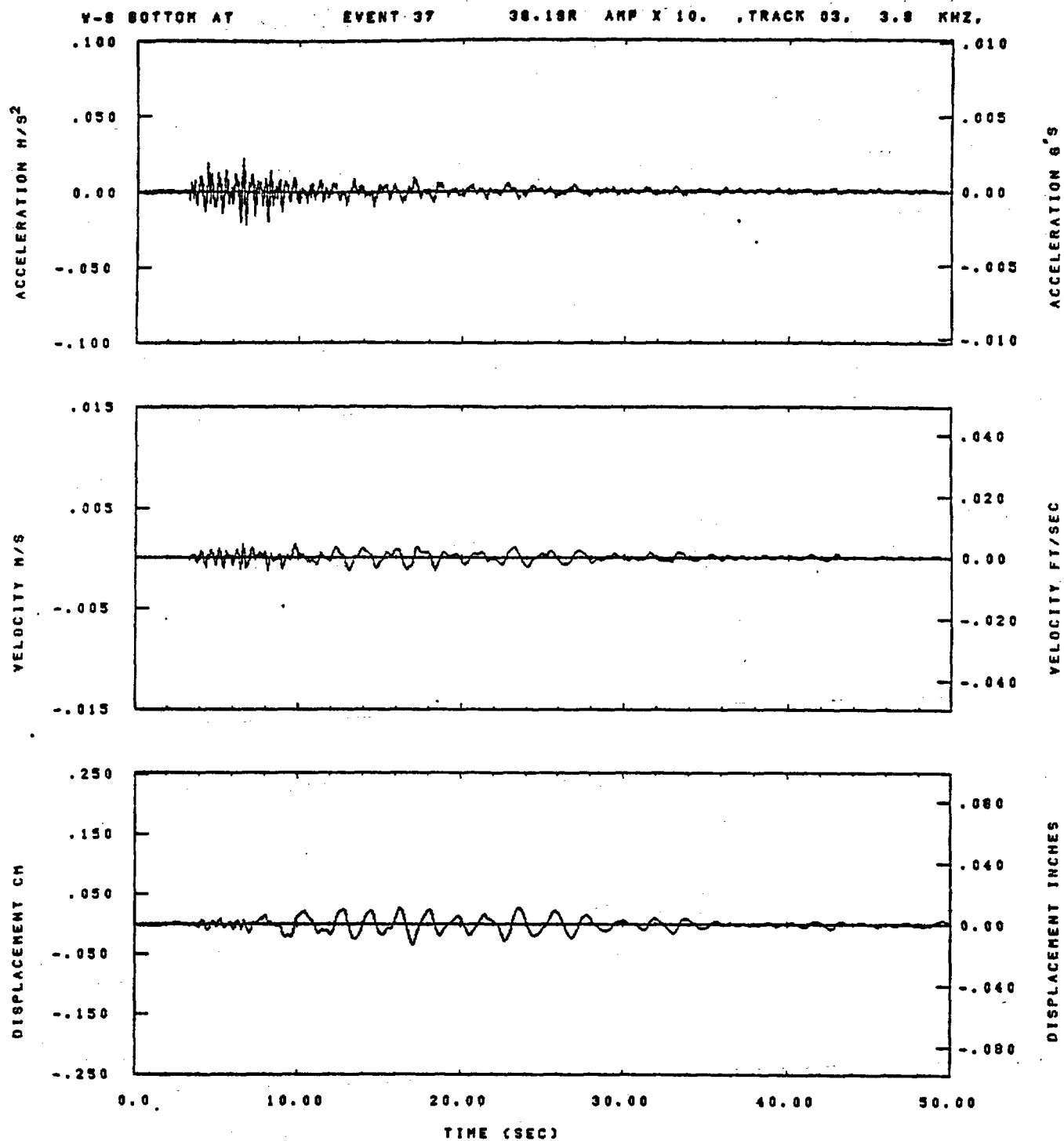


IQT= .0020	OOT= .005	FIX=	AAS= 0.
HPP= .20	SVH= .13	HLH= 249	ASS=
LPP= 18.	SVL= 4.	HLL= 2999	ASE=
YTB= .200	VTE= .133	FLL= -20.	VSE= 0.
DPS= 0.	DPE= 100.	FLH= 0	DSE= 0.

09.43.08

08/19/82

Figure G-59

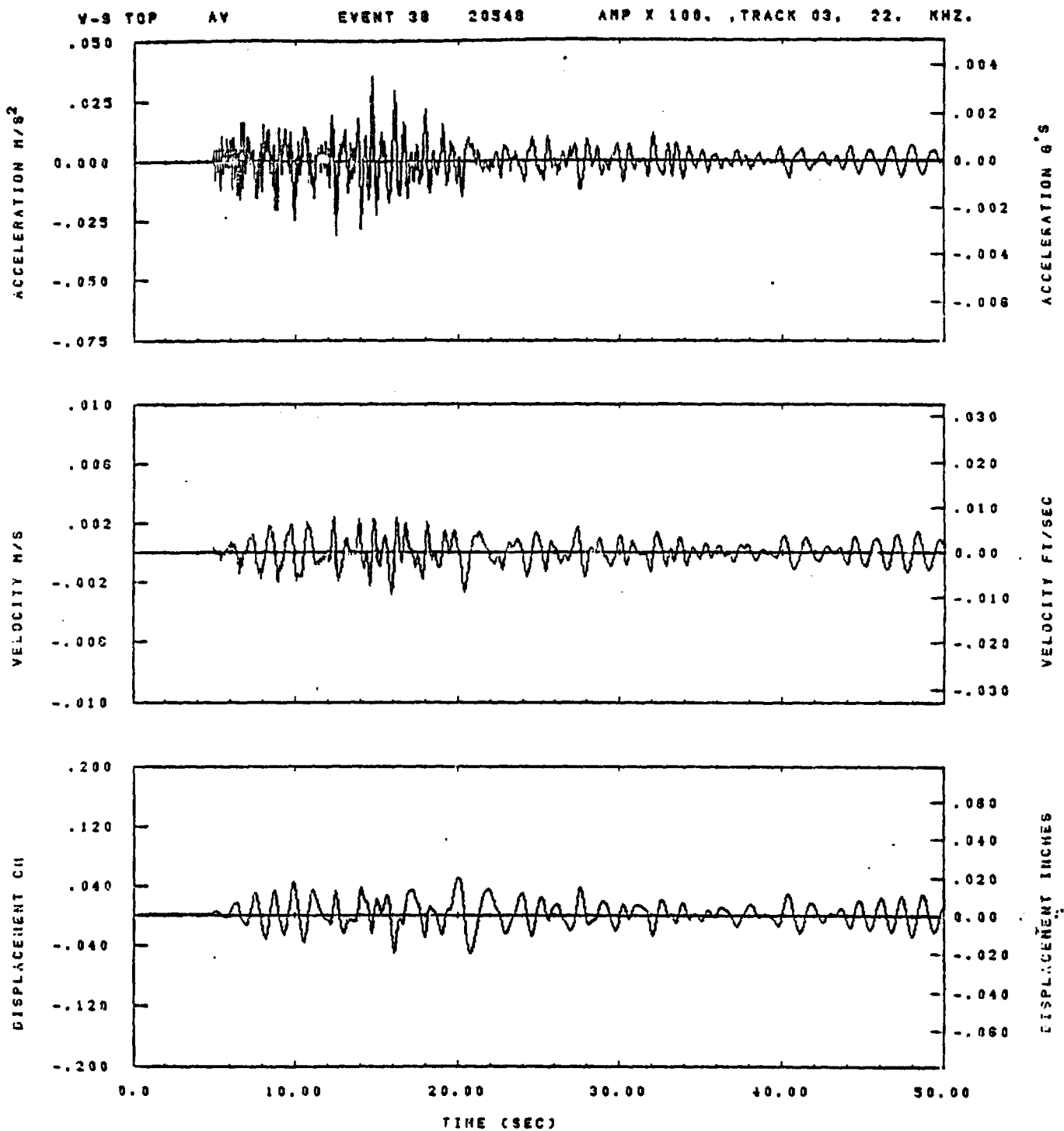


IDT= .0020	ODT= .005	FIX=	AAS= 0.
HPF= .20	SVH= .13	HLH= 249	ASB=
LPF= 18.	SVL= 4.	HLL= 2998	ASE=
VTB= .200	VTE= .133	FLL= -20.	VSE= 0.
DPS= 0.	DPE= 100.	FLH= 0	DSE= 0.

08.45.34

06/15/82

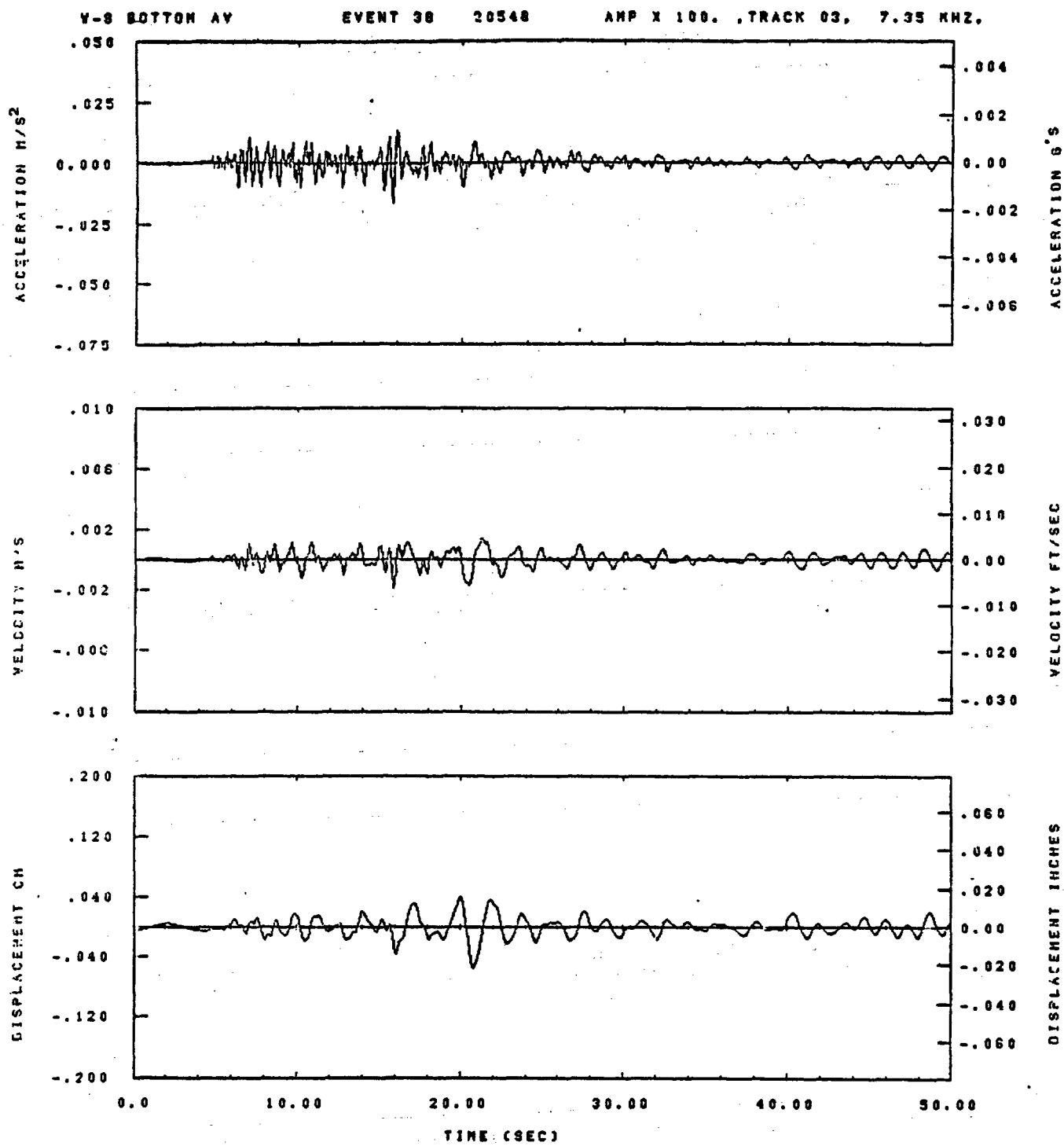
Figure G-60



IOT= .0020	OOT= .005	FIX=	AAS= 0.
HPF= .20	SVH= .13	HLH= 251	ASB=
LPF= 18.	SVL= 4.	HLL= 2399	ASE=
VTB= .200	VTE= .133	FLL= -20.	VSE= 0.
OPS= 0.	OPE= 100.	FLH= 0	DSE= 0.

10.08.01.

08/28/82

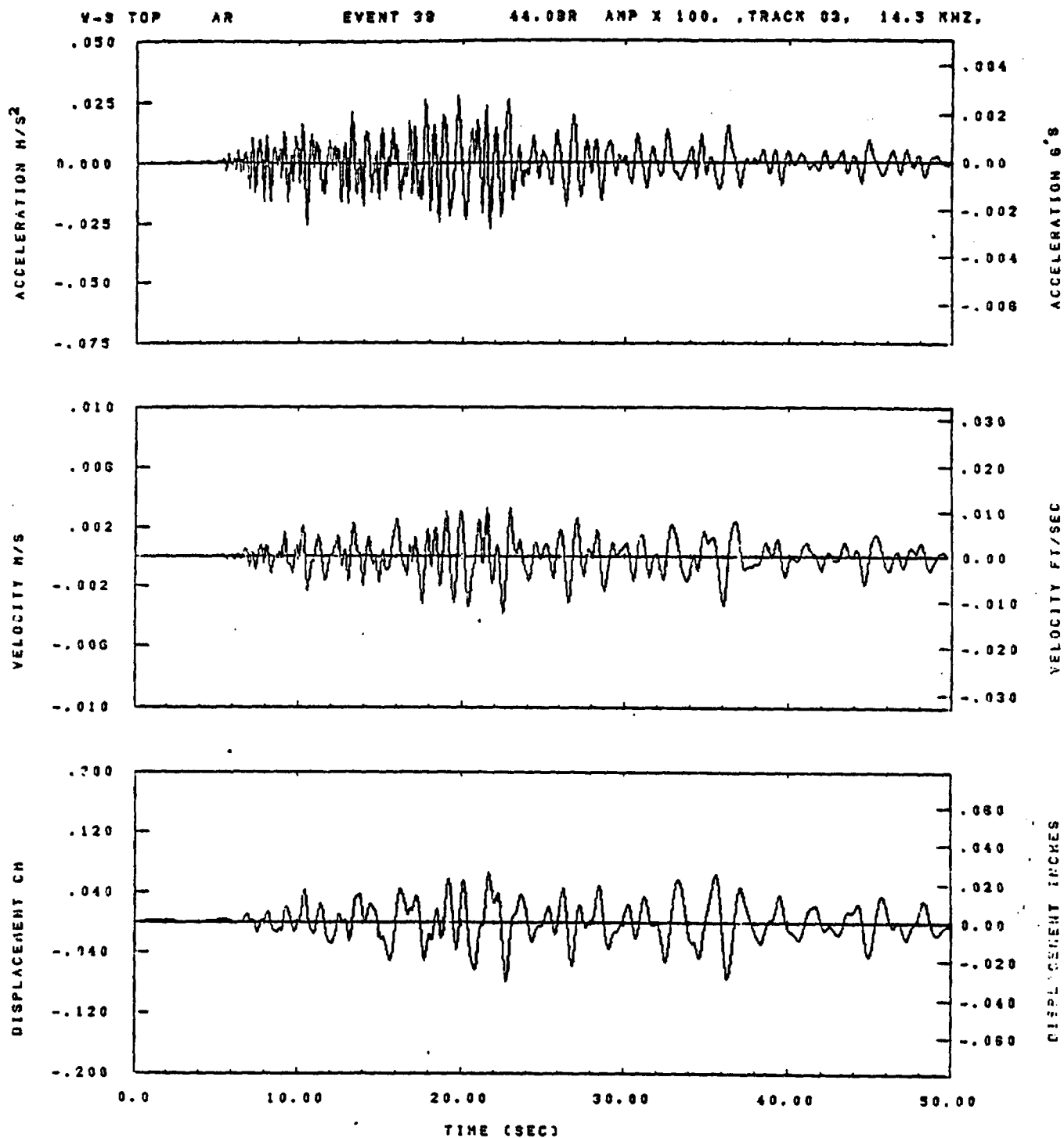


IDT= .0020	ODT= .005	FIX=	AAS= 0.
HPF= .20	BVH= .13	HLH= 251	ASB=
LPF= 10.	BVL= 4.	HLL= 2999	ASE=
VTB= .200	VTE= .133	FLL= -20.	VSE= 0.
DPS= 0.	DPE= 100.	FLH= 0	DSE= 0.

10.09.15.

06/28/82

Figure G-62

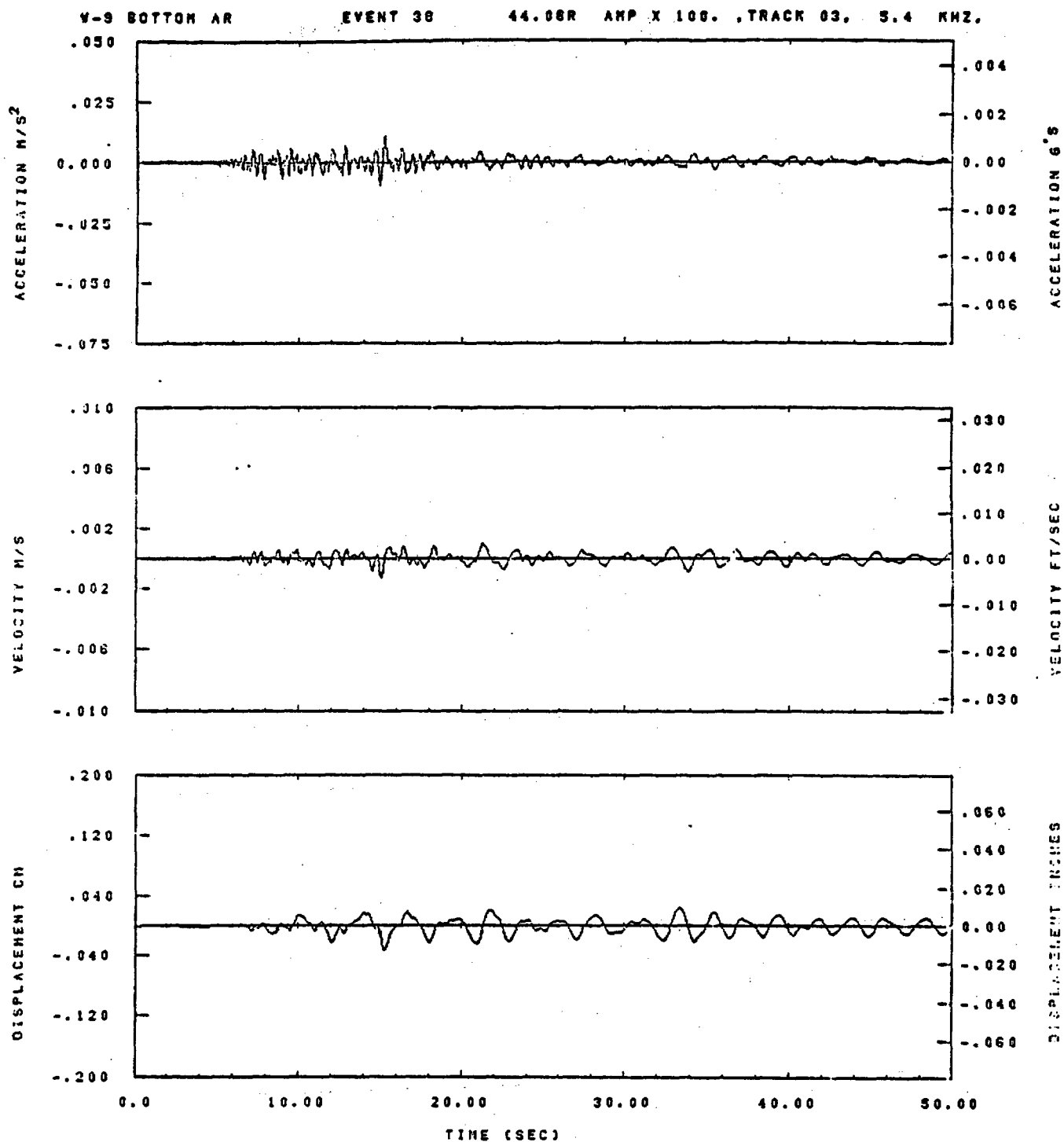


IDT= .0020	ODT= .005	FIX=	AAS= 0.
HPP= .20	SVH= .13	HLH= 251	ASB=
LPF= 10.	SVL= 4.	HLL= 2333	ASE=
VTS= .200	VTE= .133	FLH= -20.	VSE= 0.
DPS= 0.	DPE= 100.	FLH= 0	ORE= 0.

10.07.33.

08/28/82

Figure G-63

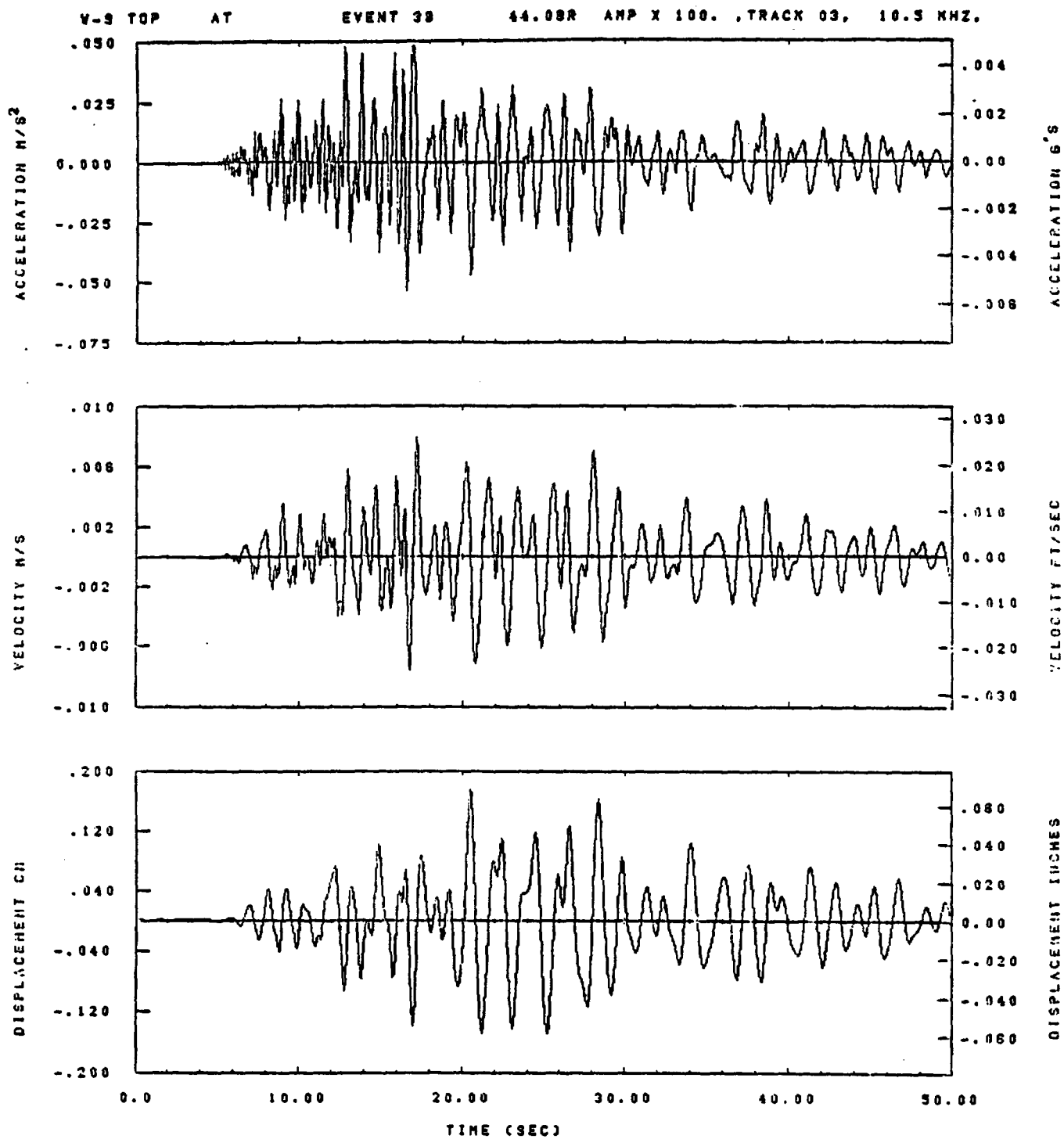


IDT= .0020	ODT= .005	FIX=	AAS= 0.
HPF= .20	BWH= .13	HLH= 251	ASB=
LPF= 18.	QWL= 4.	HLL= 2999	ASE=
VTB= .200	VTE= .133	FLL= -20.	VSE= 0.
OPB= 0.	OPE= 100.	FLH= 0	DSE= 0.

10.08.06.

05/28/82

Figure G-64

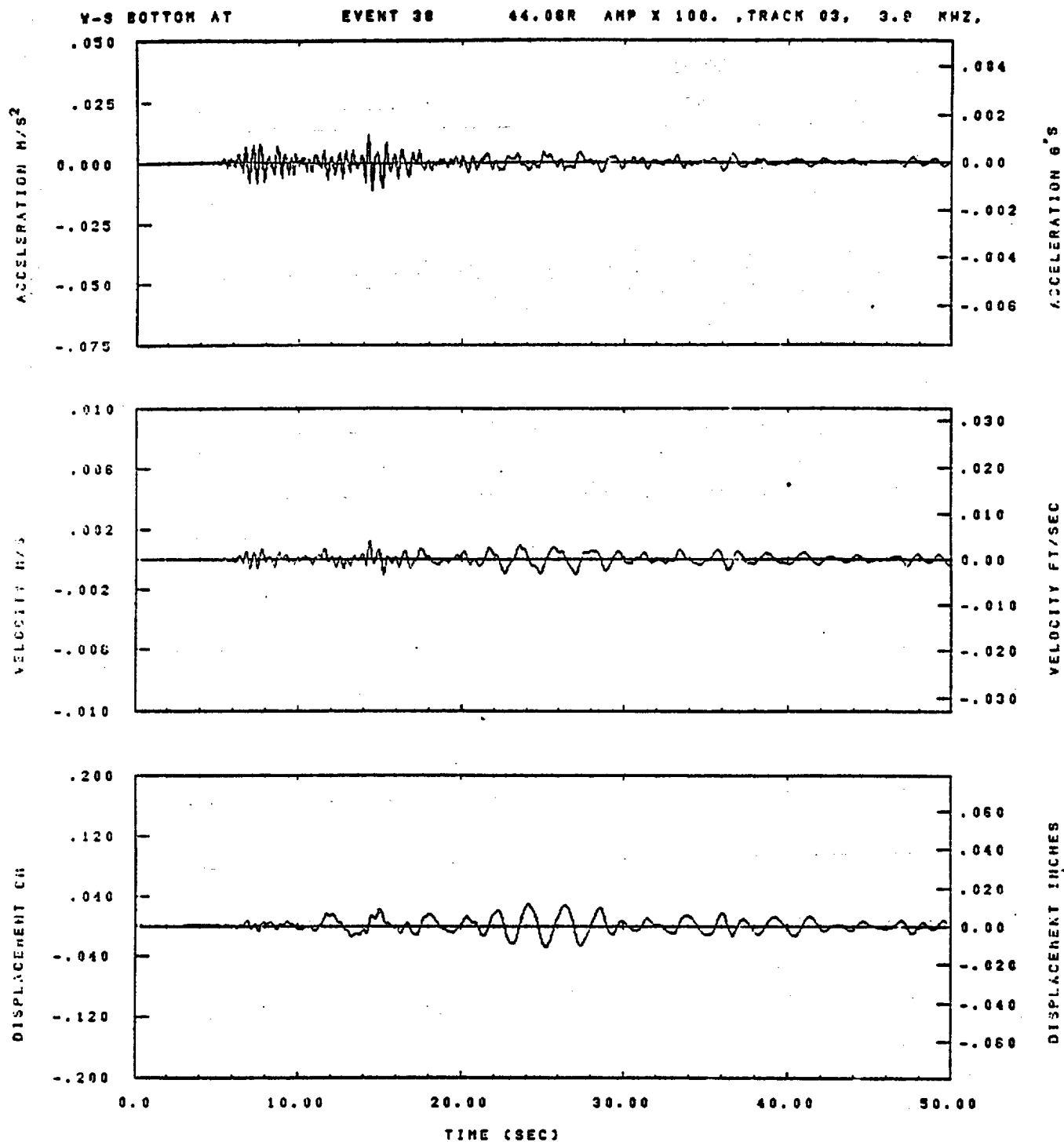


IDT= .0020	QDT= .005	FIX=	AAS= 0.
HPF= .20	QVH= .13	HLH= 251	ASB=
LPF= 18.	QVL= 4.	HLL= 2999	ASE=
VTB= .200	VTE= .133	FLL= -20.	VSE= 0.
QPB= 0.	DPE= 100.	FLH= 0	LSE= 0.

10.07.38.

08/28/82

Figure G-65



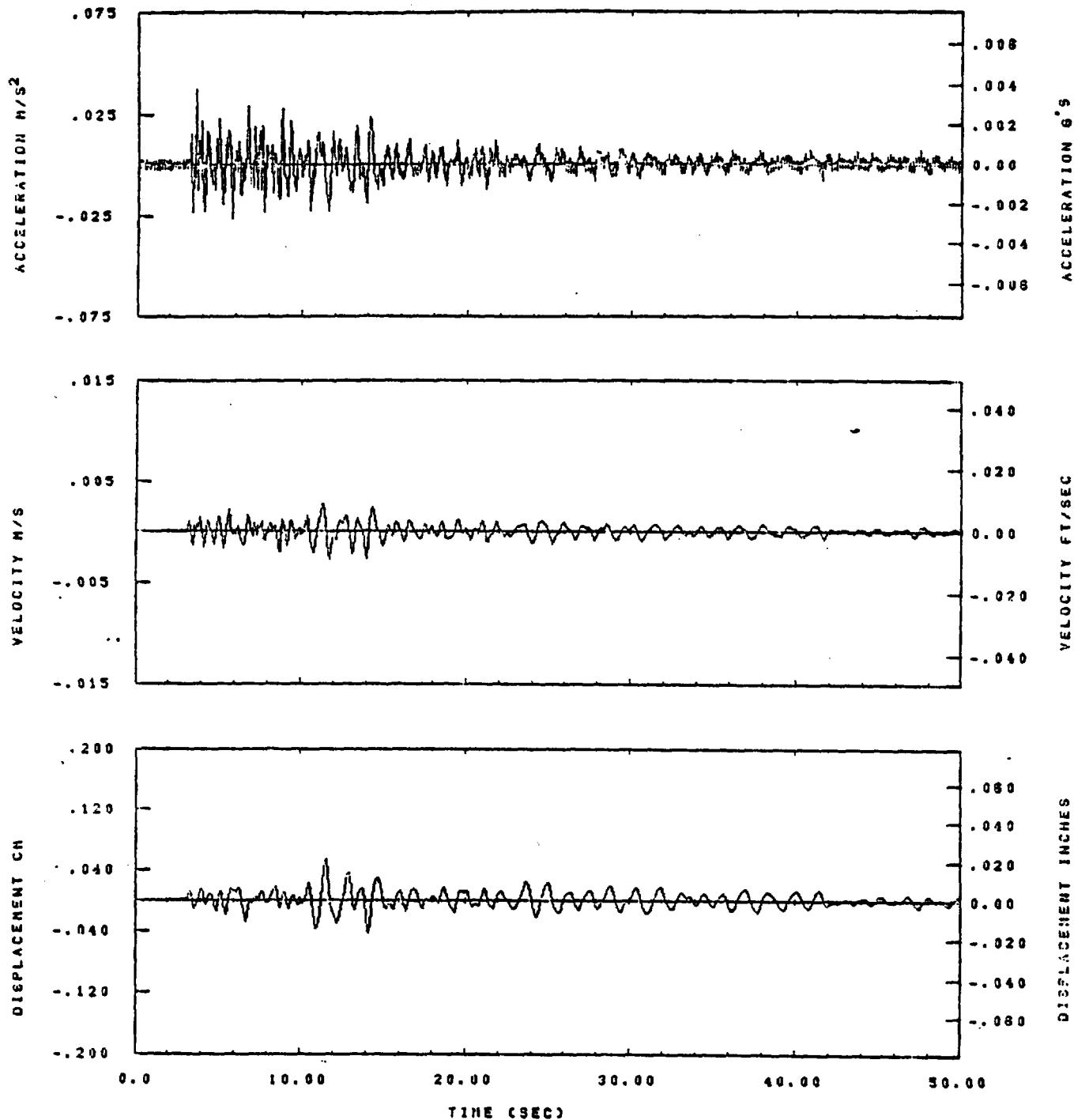
IDT= .0020	ODT= .005	FIX=	AAS= 0.
HPF= .20	BYH= .13	HLH= 251	ASB=
LPF= 18.	BYL= 4.	HLL= 2999	ASE=
VTB= .200	VTE= .133	FLL= -20.	VSE= 0.
DPS= 0.	DPE= 100.	FLH= 0	DCE= 0.

10.08.10.

06/28/82

Figure G-66

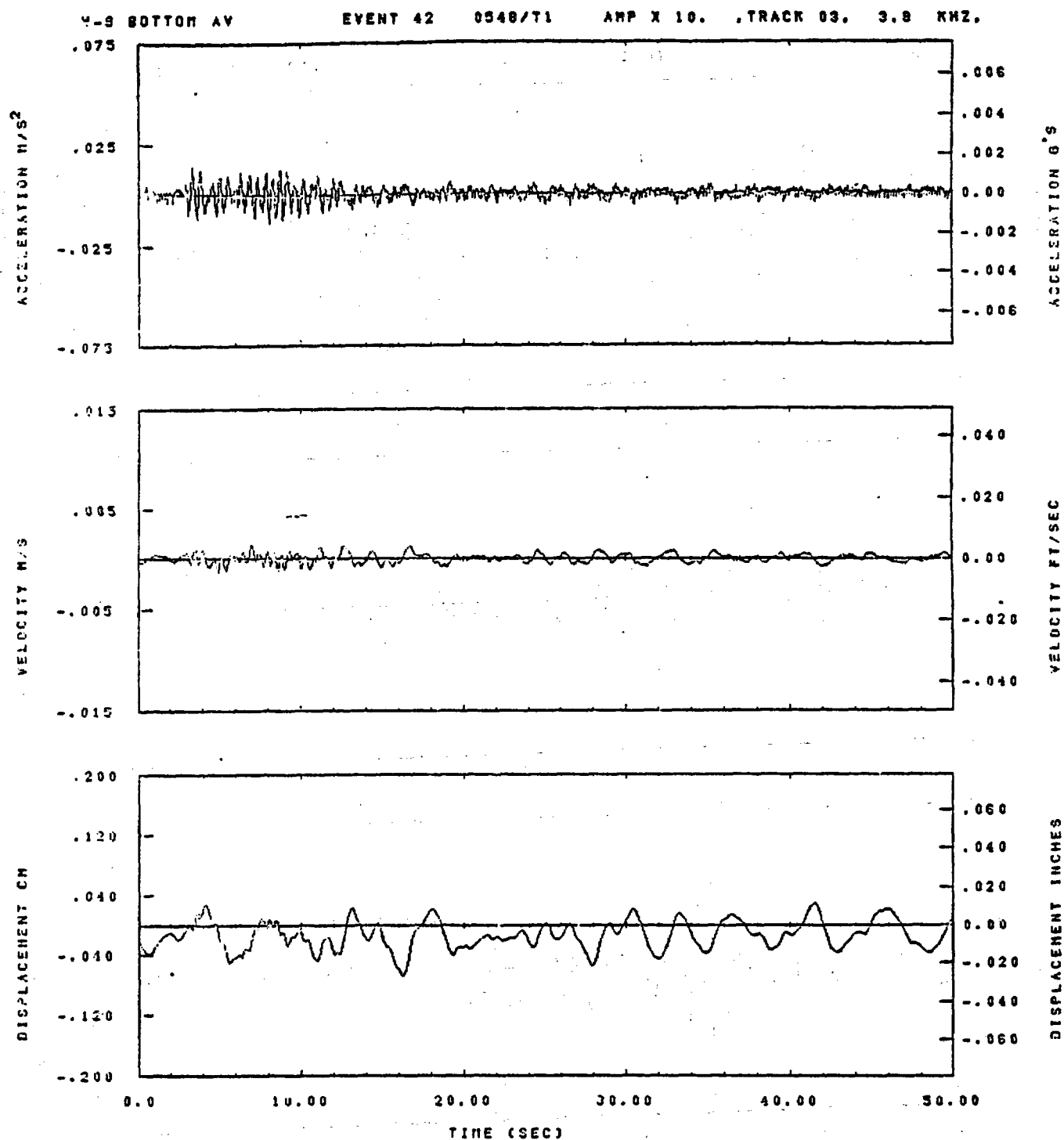
V-3 TOP AV EVENT 42 0348/T1 AMP X 5.11 ,TRACK 03. 30. KHZ.



IDT= .0020	ODT= .003	FIX=	AAS= 0.
MPF= .25	BWH= .18	HLH= 303	ASB=
LPF= 13.	BYL= 3.	HLL= 2399	ASE=
VTB= .250	VTE= .188	FLL= -20.	VSE= 0.
DPB= 0.	DPE= 100.	FLH= 0	DSE= 0.

13.20.19.

08/29/82

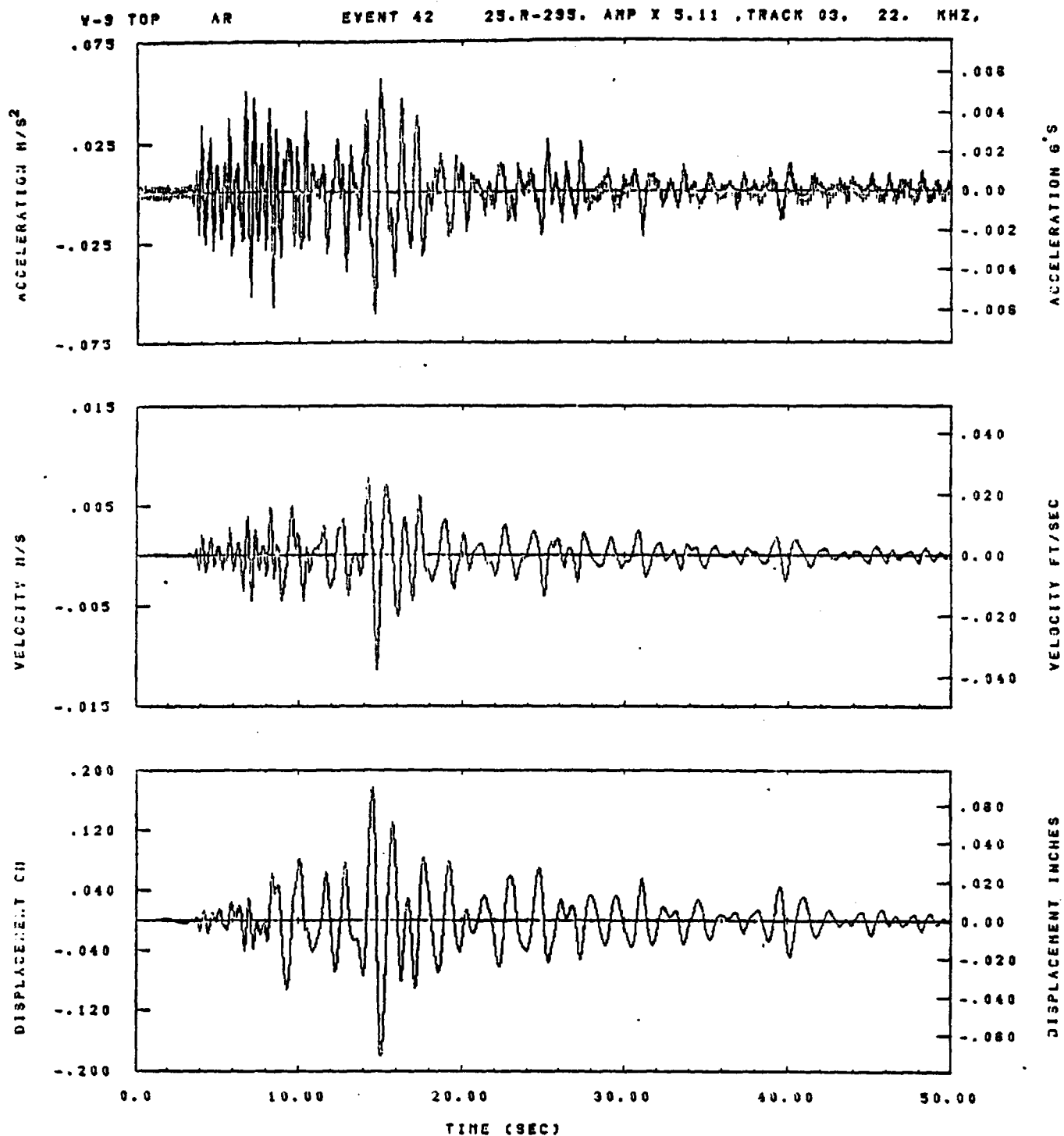


IDT= .0020	ODT= .005	FIX=	AAS= 0.
HPF= .25	BVH= .10	HLH= 333	ASB=
LPF= 12.	QVL= 0.	HLL= 2399	ASE=
VTB= .150	VTC= .160	FLL= -20.	VSE= 0.
DPB= 0.	DPE= 100.	FLH= 0	OGE= 0.

13.20.51.

06/28/82

Figure G-68



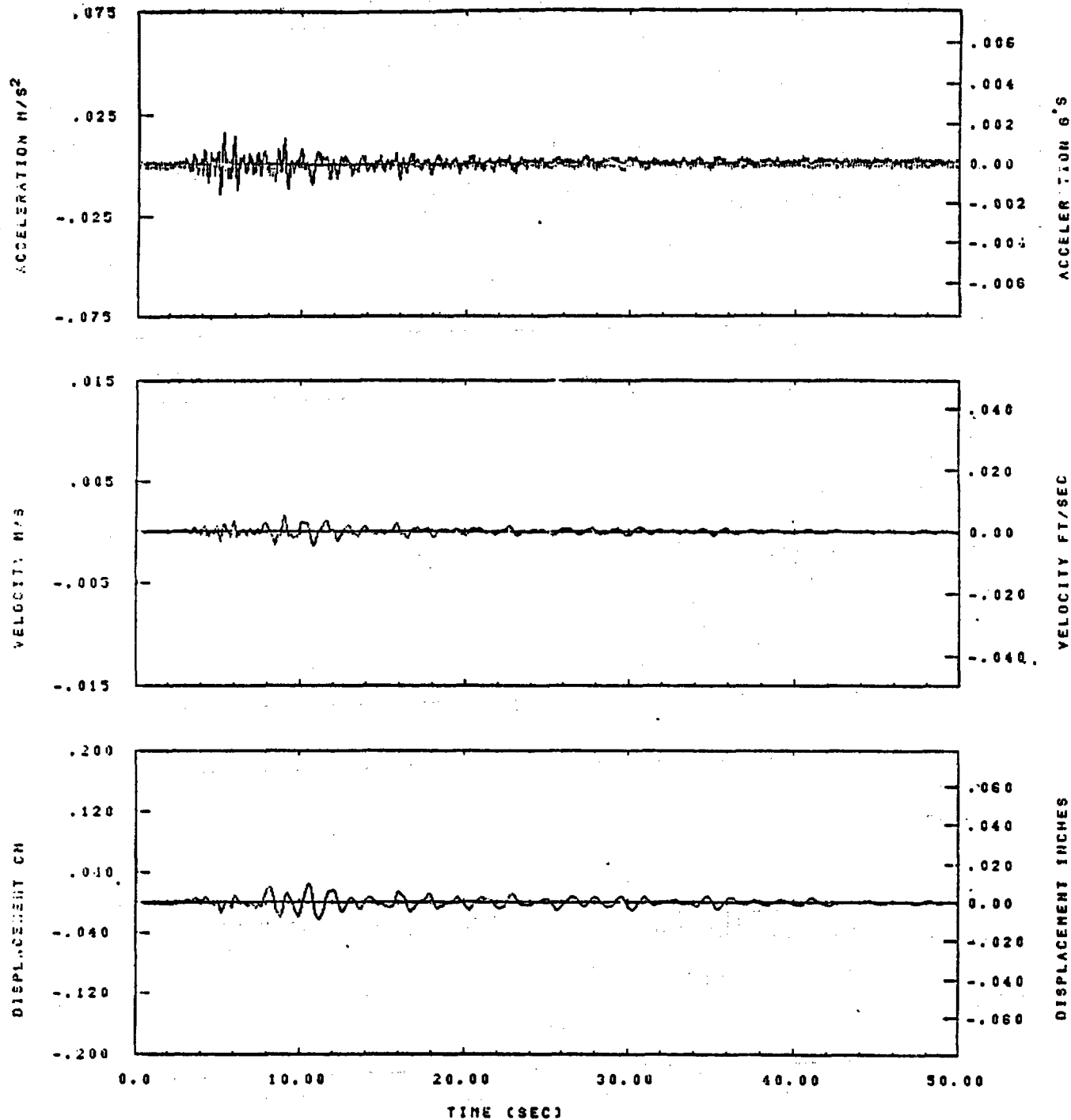
IDT= .0020	ODT= .003	FIX=	AAS= 0.
HPF= .25	QVH= .16	HLH= 333	ASD=
LPF= 13.	QVL= 3.	HLL= 2399	ASE=
VFB= .250	VTE= .160	FLL= -20.	VSE= 0.
OPD= 0.	OPE= 100.	FLH= 0	OSE= 0.

13.20.23.

08/28/92

Figure G-69

V-S BOTTOM AR EVENT 42 25.R-295. AMP X 10. TRACK 03. 3. KHZ.

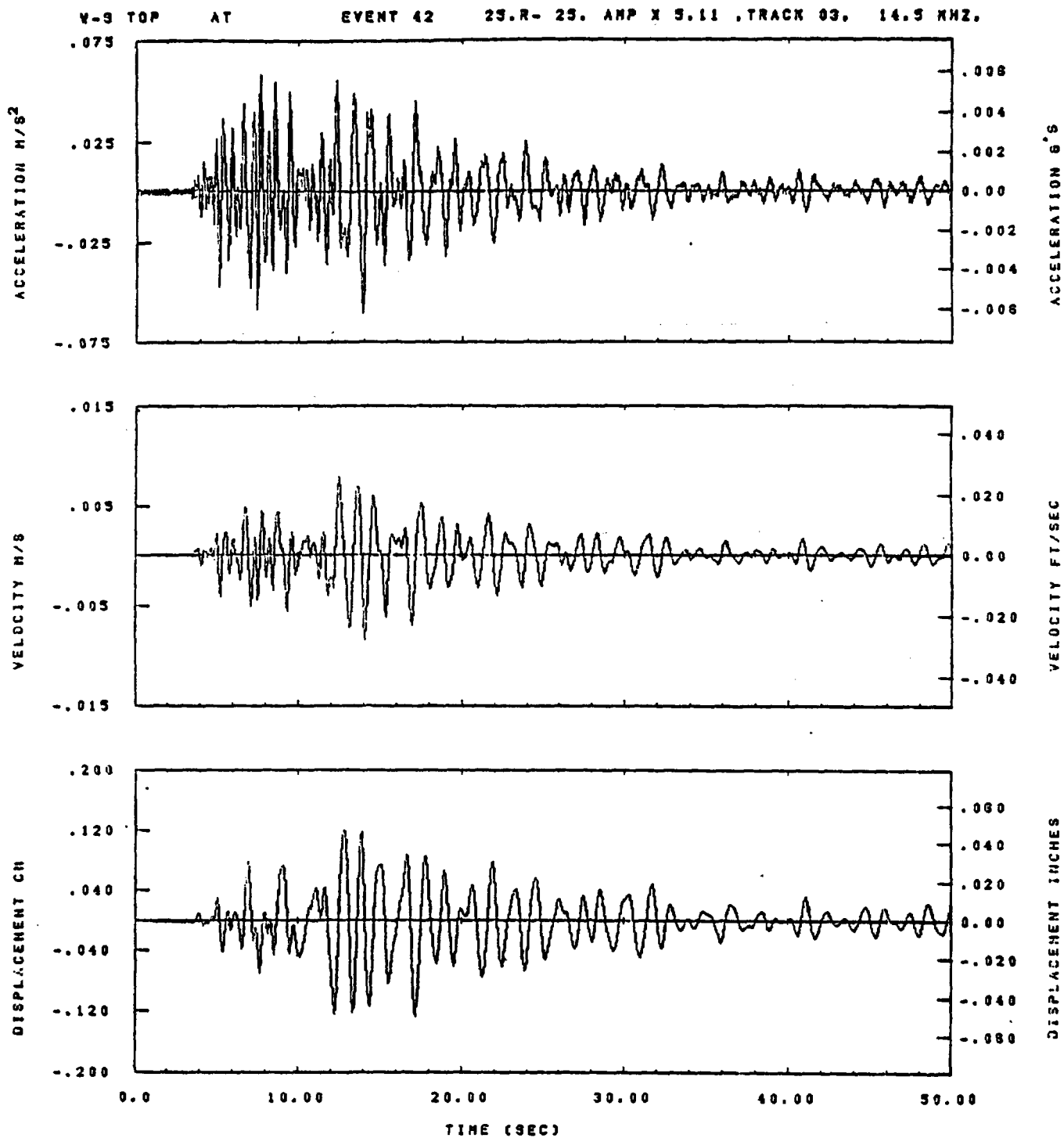


IDT= .0020	ODT= .005	FIX=	AA3= 0.
HPF= .25	BYH= .18	HLH= 333	ACB=
LPF= 13.	BYL= 3.	HLL= 2399	ASE=
VTB= .250	VTE= .166	FLL= -20.	YSE= 0.
DPB= 0.	DPE= 100.	FLH= 0	USE= 0.

13-20-40.

06/28/82

Figure G-70

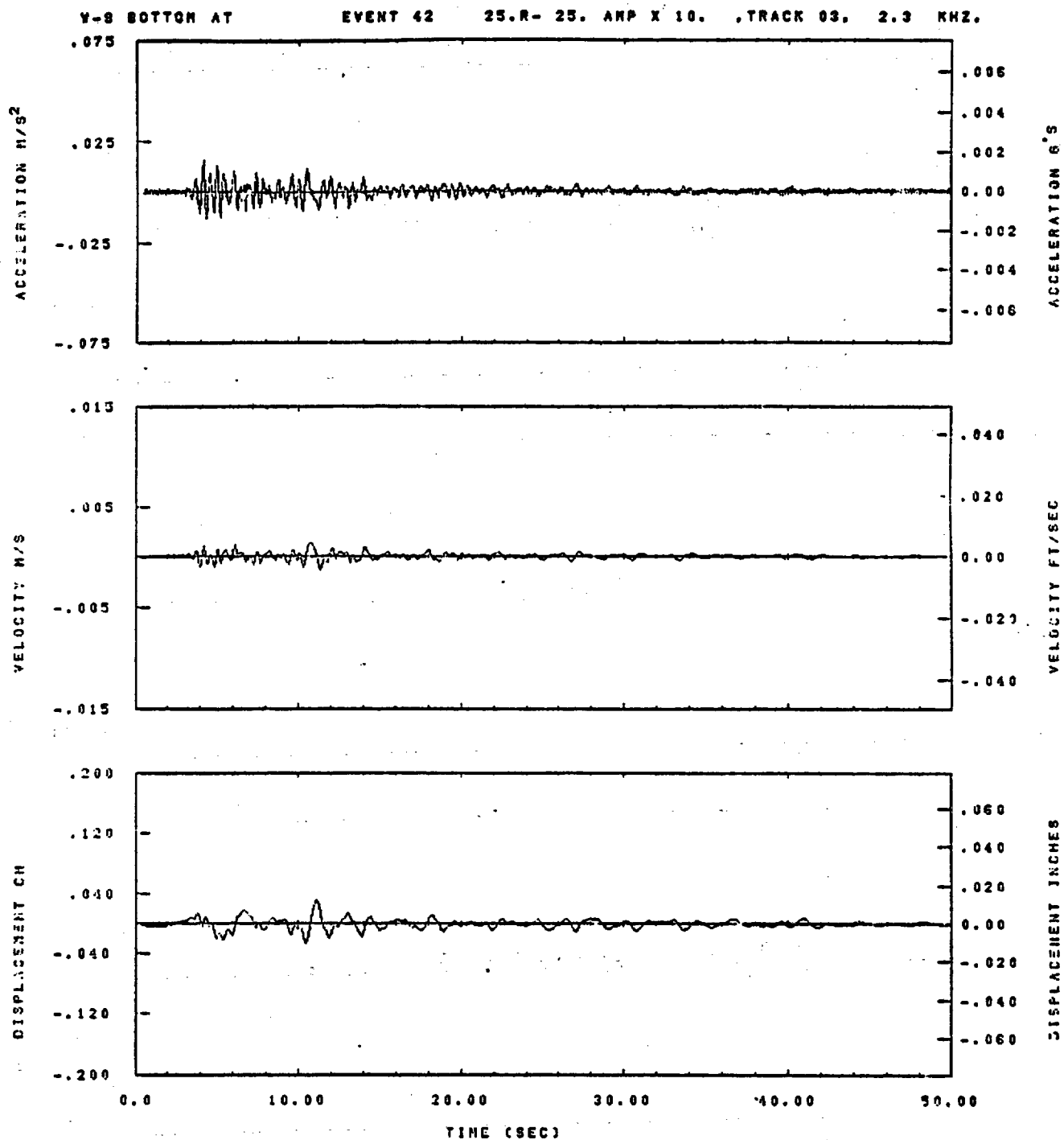


IDT= .0020	ODT= .005	FIX=	AAS= 0.
HPF= .25	DYH= .10	HLH= 333	ASB=
LPF= 13.	BVL= 3.	HLL= 2399	ASE=
VTB= .250	VTE= .168	FLL= -20.	VSE= 0.
OPS= 0.	OPE= 100.	FLH= 0	DSE= 0.

13.20.98.

08/28/82

Figure G-71

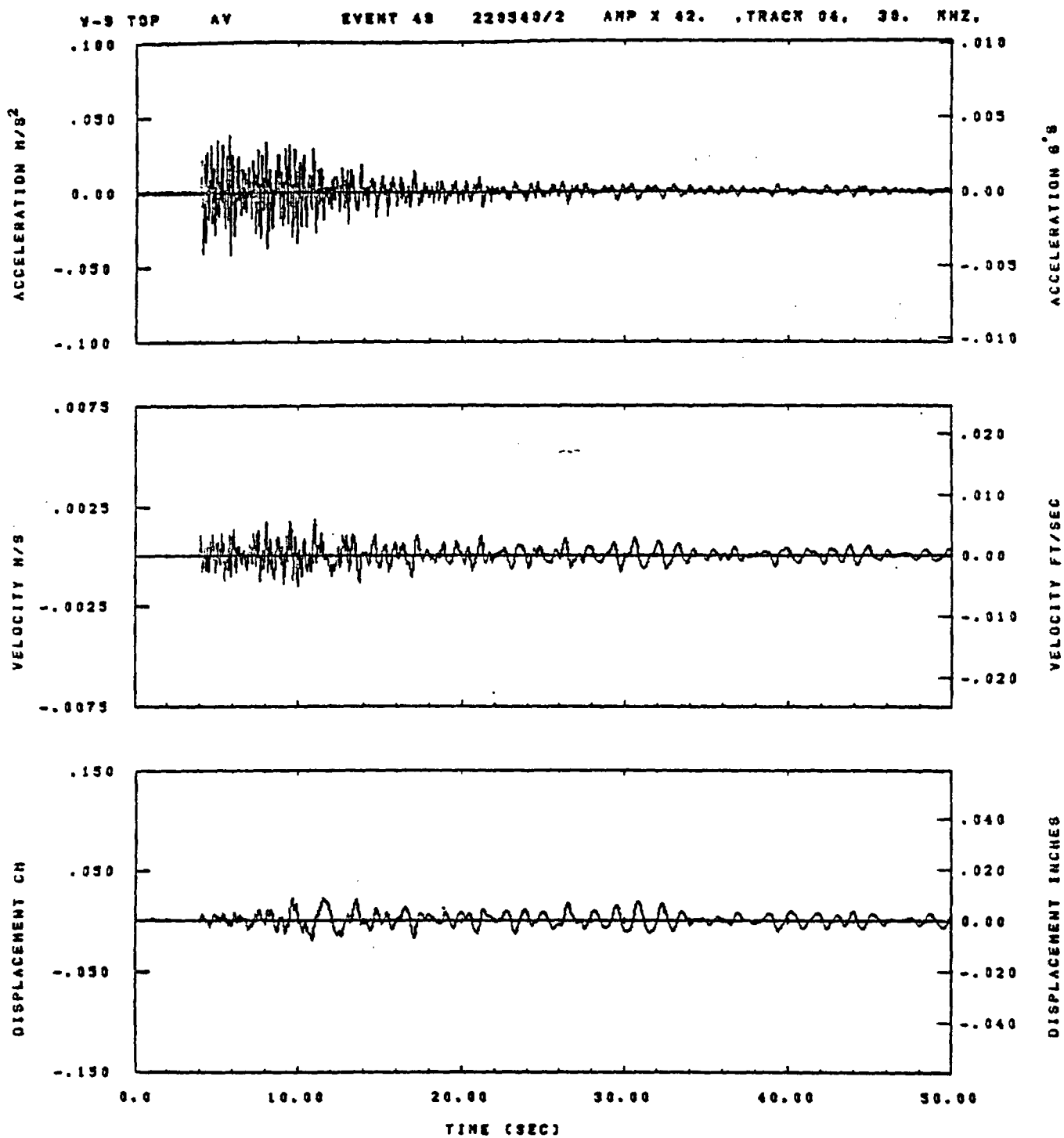


IDT= .0020	OOT= .005	FIX=	AAS= 0.
HPF= .25	BVM= .16	HLH= 333	ASB=
LPF= 13.	QVL= 3.	HLL= 2309	ASE=
VTD= .250	VTE= .166	FLL= -20.	VRE= 0.
DPS= 0.	DPE= 100.	FLH= 0	GGE= 0.

13.20.45.

06/28/82

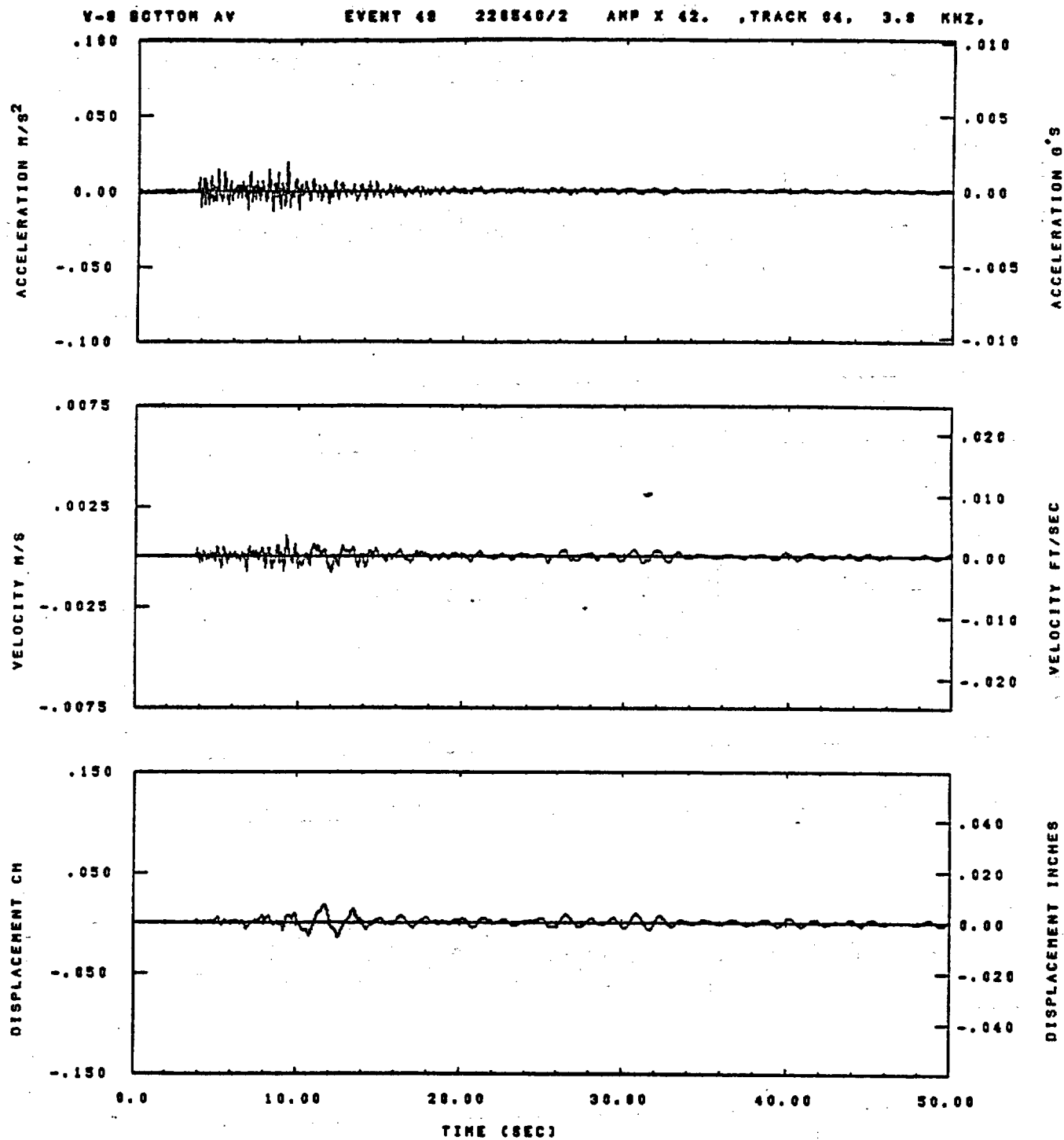
Figure G-72



IDT= .0020	ODT= .005	FIX=	AAS= 0.
MPF= .30	BWH= .20	HLH= 187	ASB=
LPF= 27.	BVL= 6.	HLL= 1339	ASE=
VTS= .300	VTE= .200	FLL= -20.	VSE= 0.
OPS= 0.	OPE= 100.	FLH= 0	OSE= 0.

13.35.33.

08/30/82

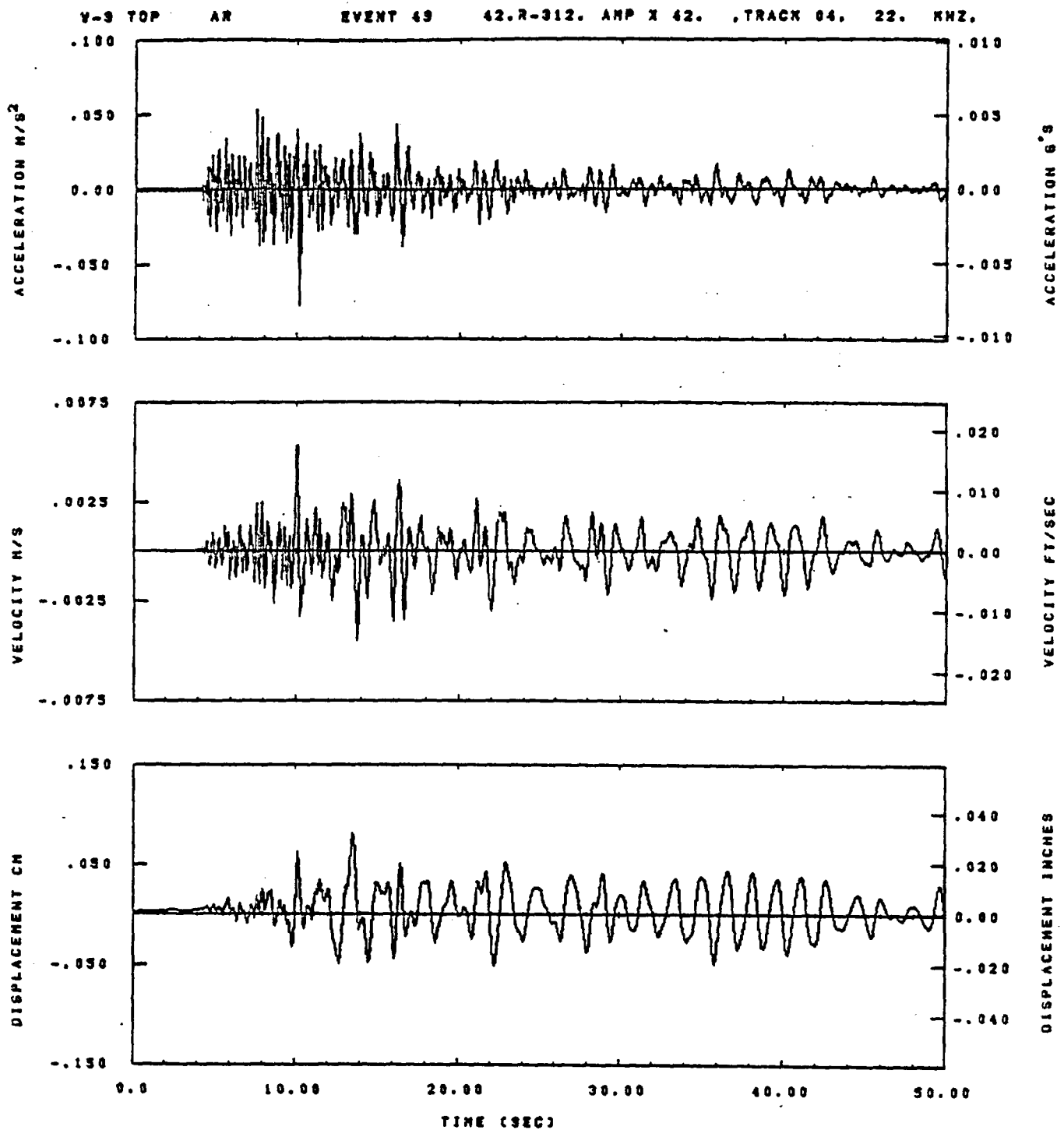


IDT= .0020	ODT= .005	FIX=	AAS= 0.
HPF= .30	BYH= .20	HLH= 187	ASH=
LPF= 27.	BYL= 6.	HLL= 1988	ASE=
VTS= .308	VTE= .208	FLL= -20.	VSE= 0.
DPS= 0.	DPE= 100.	FLH= 0	DSE= 0.

15.38.58.

06/30/82

Figure G-74



IDT= .0020	ODT= .005	FIX=	AAS= 0.
HPP= .30	BYH= .20	MLM= 187	ASB=
LPP= 27.	BYL= 6.	MLL= 1393	ASE=
YTS= .300	VTE= .200	PLL= -20.	VSE= 0.
OPS= 0.	OPE= 100.	PLH= 0	DSE= 0.

15.38.38.

08/30/82

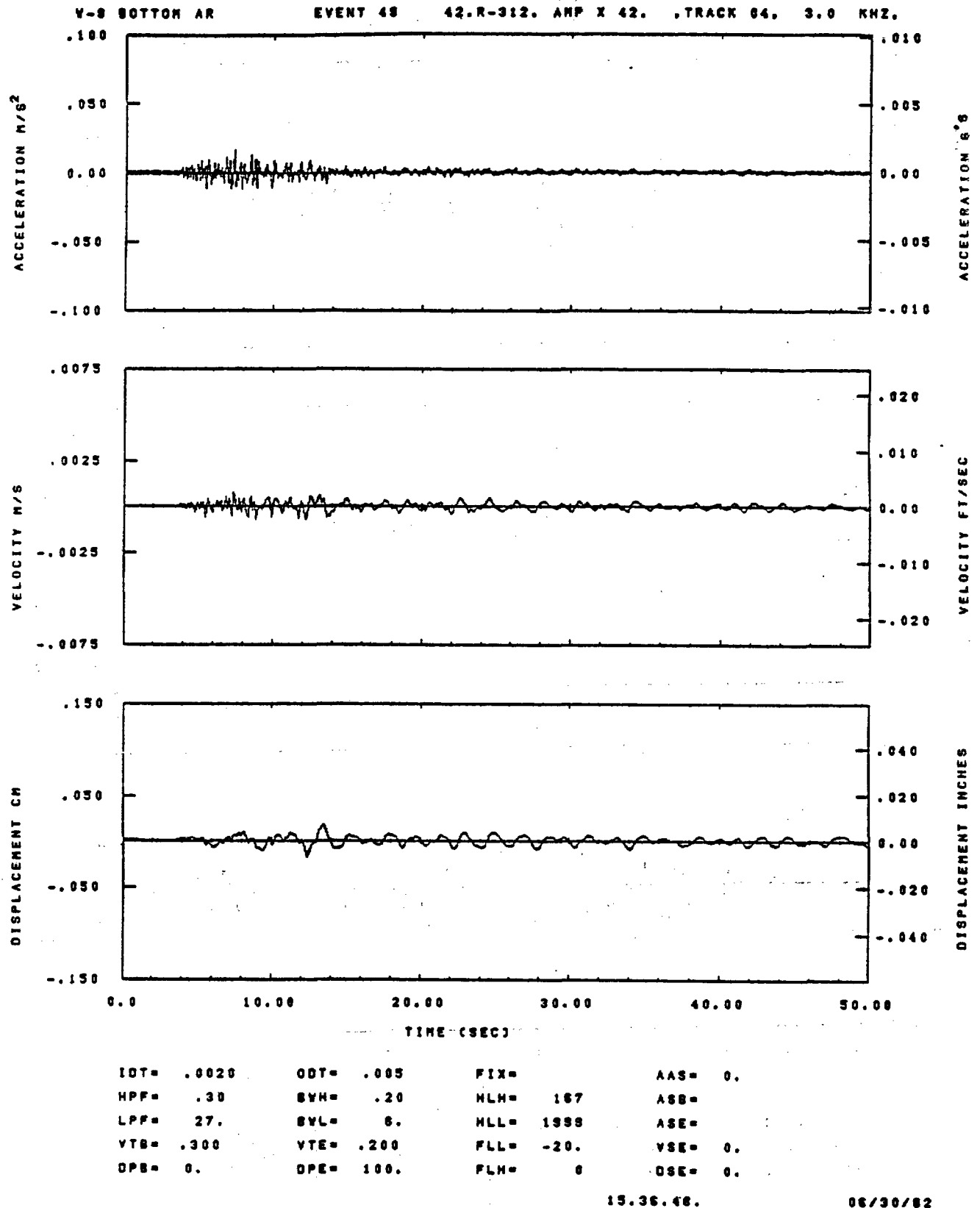
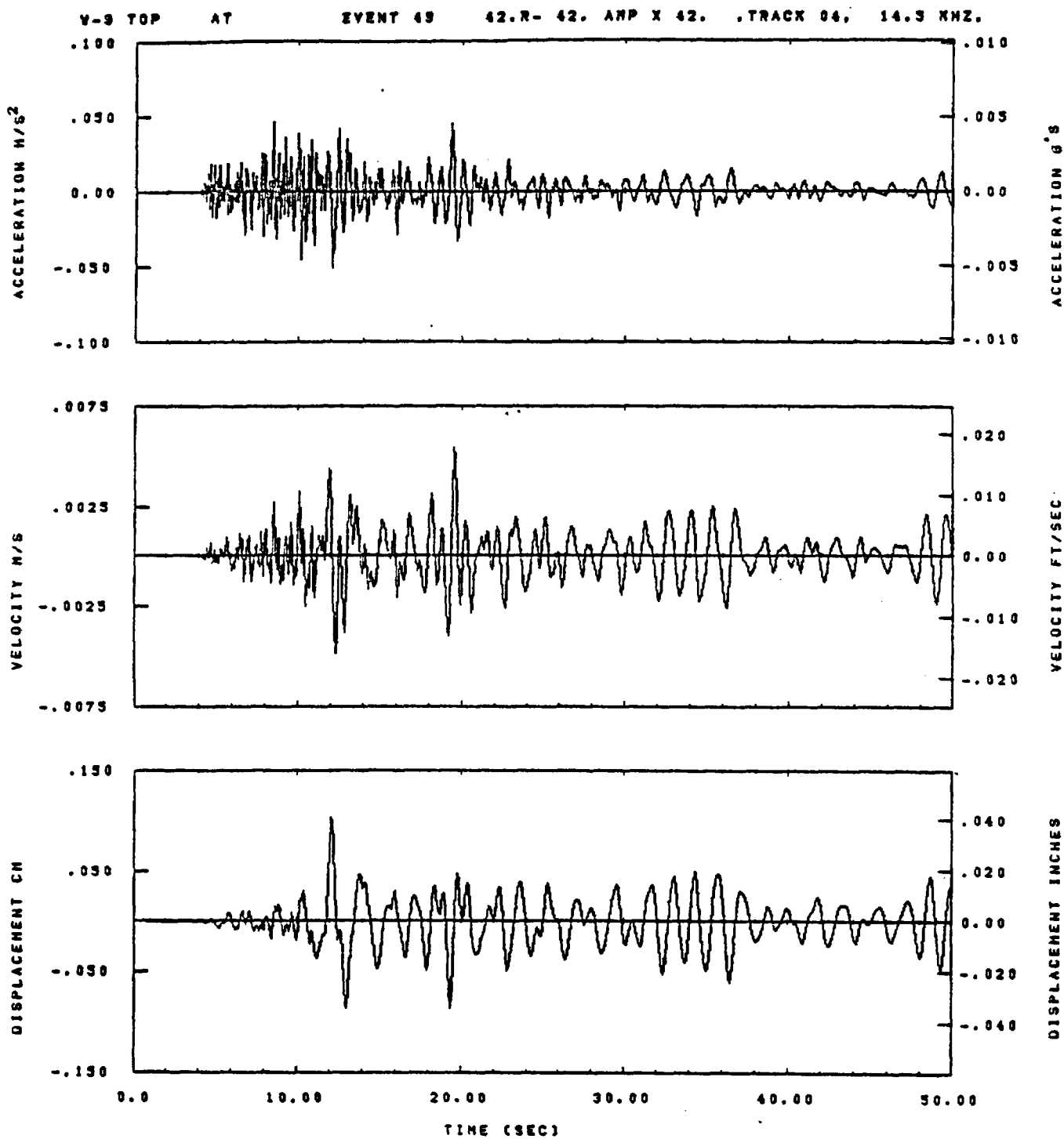


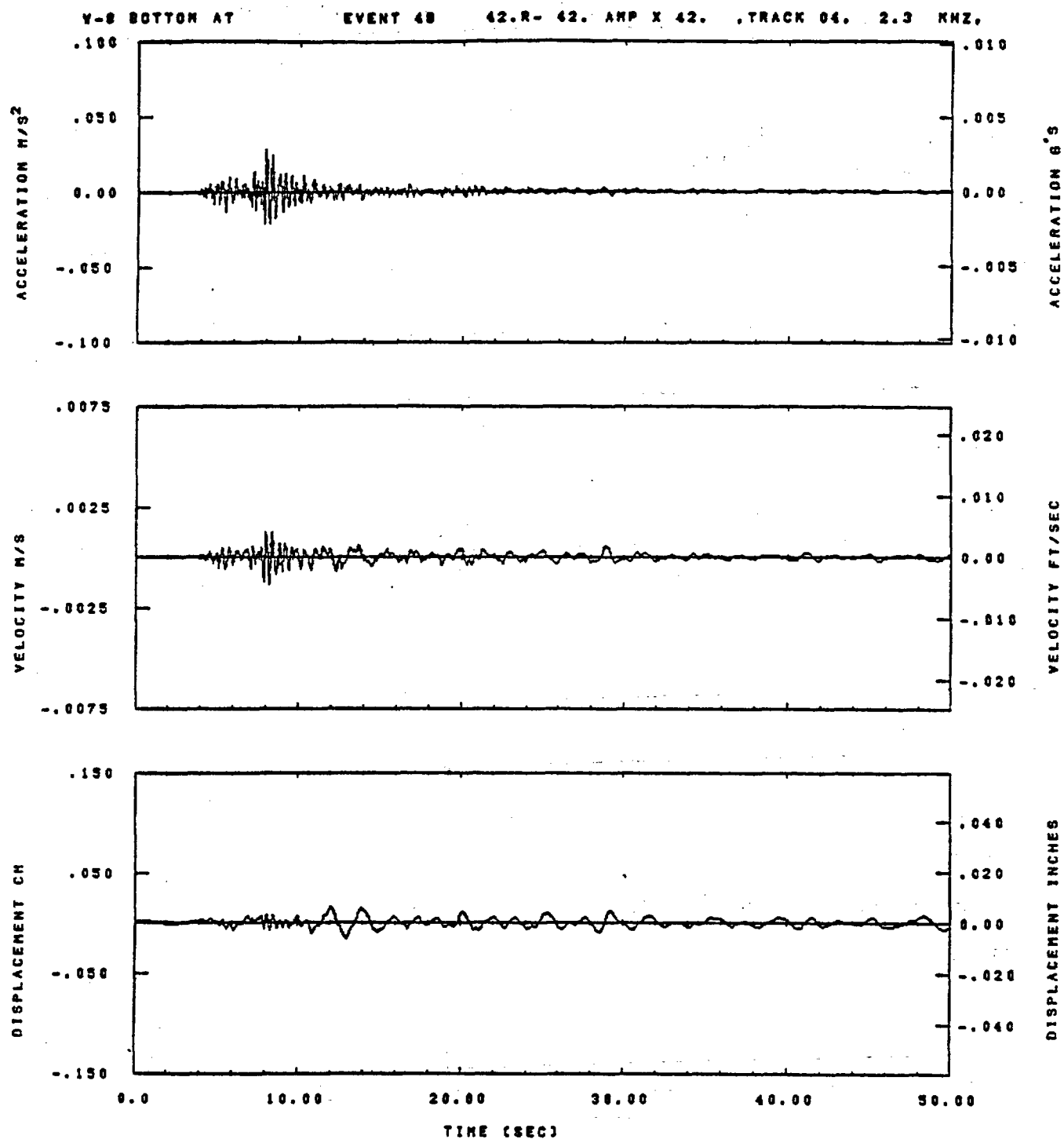
Figure G-76



IDT= .0020	ODT= .005	FIX=	AAS= 0.
HPP= .30	BVH= .20	HLH= 187	ASB=
LPP= 27.	BVL= 6.	HLL= 1999	ASE=
VTB= .300	VTE= .200	FLL= -20.	VSE= 0.
DPS= 0.	DPE= 100.	FLH= 0	DSE= 0.

13.38.42.

08/30/82

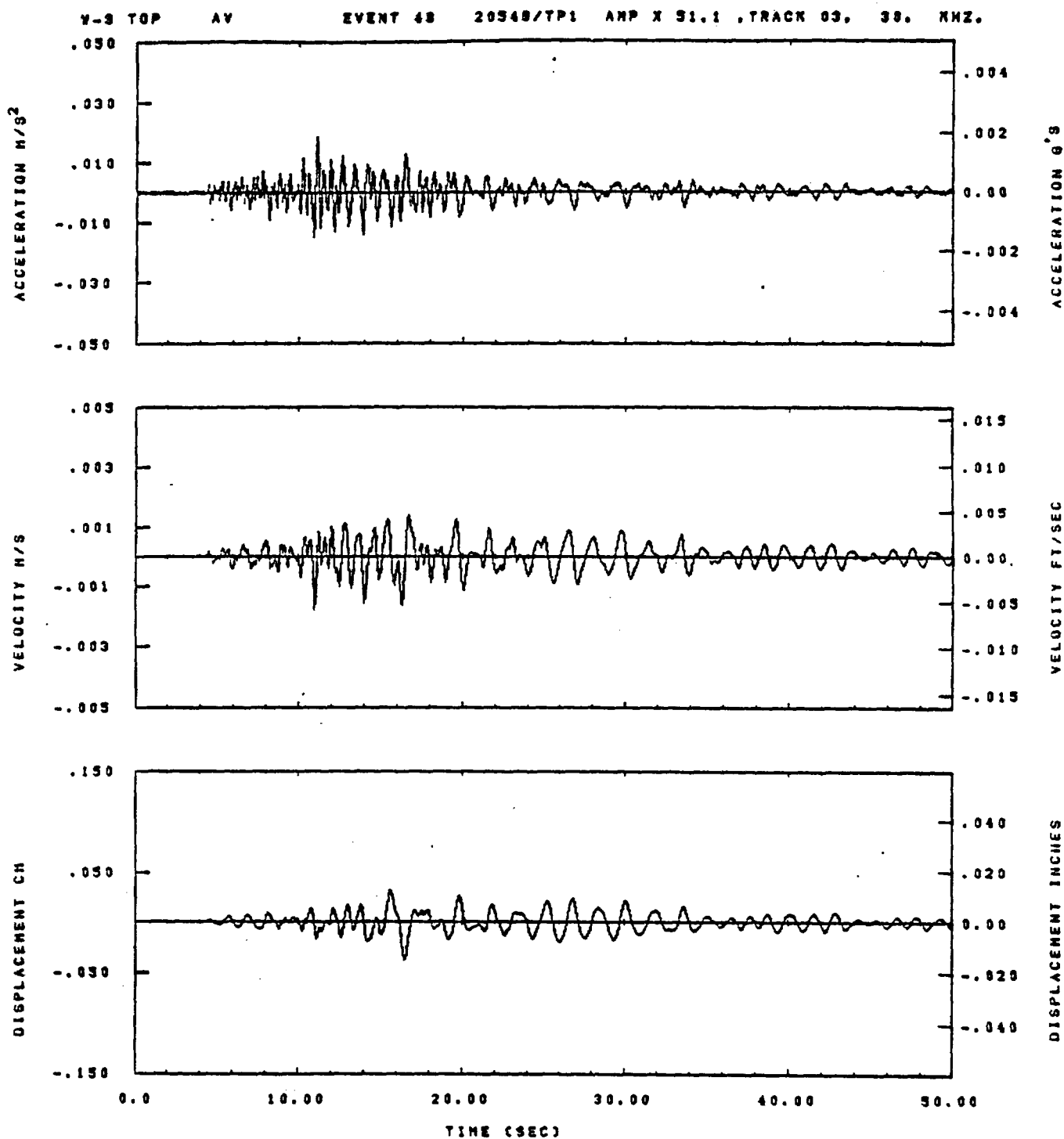


IDT= .0020	ODT= .005	FIX=	AAS= 0.
HPF= .30	SVH= .20	HLH= 167	ASS=
LPF= 27.	SVL= 6.	HLL= 1998	ASE=
VTE= .300	VTE= .200	FLL= -20.	VSE= 0.
DPE= 0.	DPE= 100.	PLH= 0	DSE= 0.

15.36.54.

06/30/82

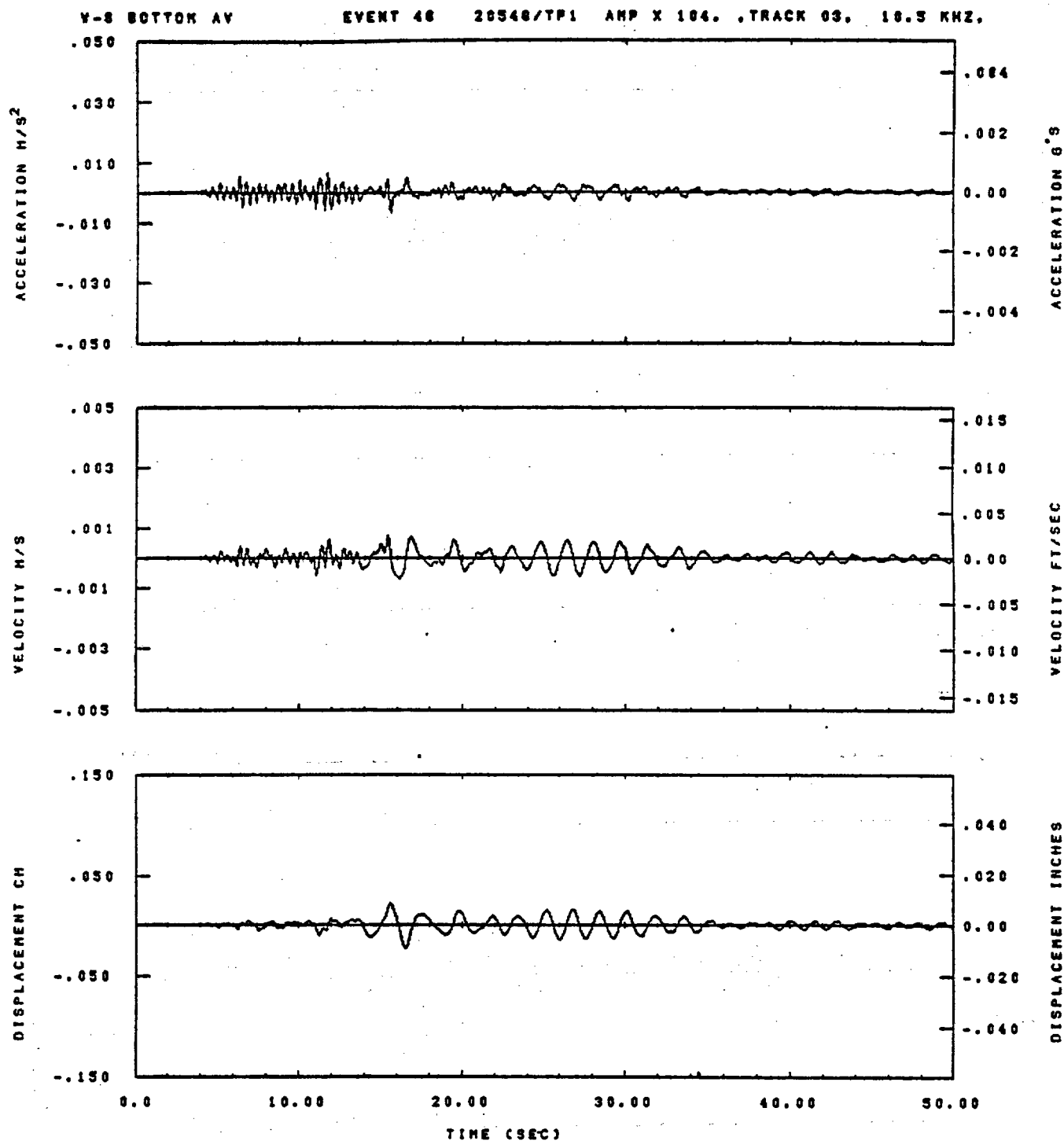
Figure G-78



IDT= .0020	ODT= .005	FIX=	AAS= 0.
HPF= .30	BVH= .20	HLH= 201	ASB=
LPF= 22.	BVL= 5.	HLL= 1999	ASE=
VTB= .300	VTE= .200	FLL= -20.	VSE= 0.
OPS= 0.	OPE= 100.	FLH= 0	OSE= 0.

09.23.03.

07/02/92

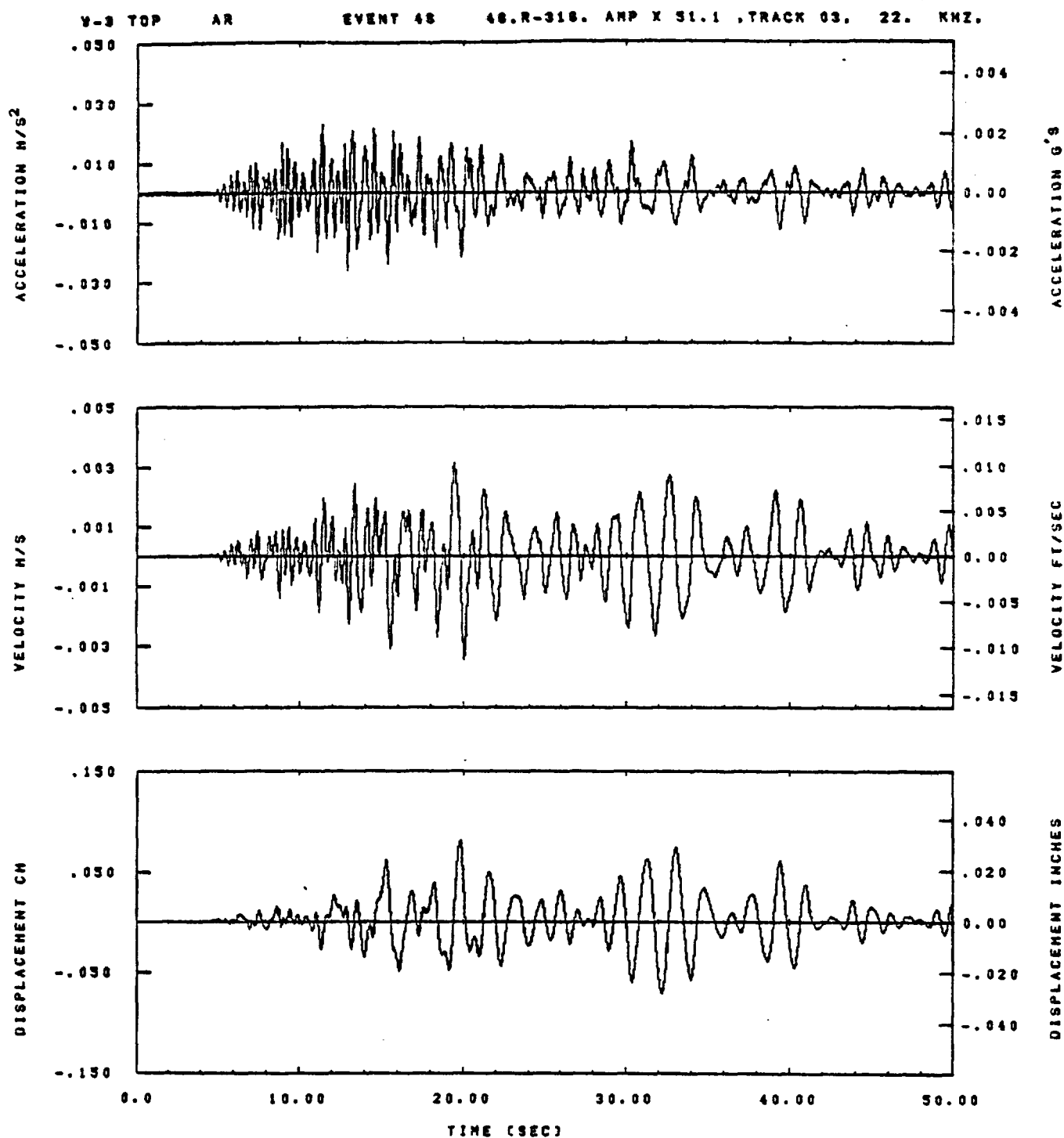


IDT= .0020	ODT= .0	FIX=	AAS=
HPF= .3	BYH= .20	HLH= 187	ASB=
LPF= 27.	BYL= 8.	HLL= 1999	ASE=
VTB= .30	VTE= .200	PLL=	VSE=
DPS=	DPE=	PLH= 0	DSE= 0.

09.25.23.

07/02/82

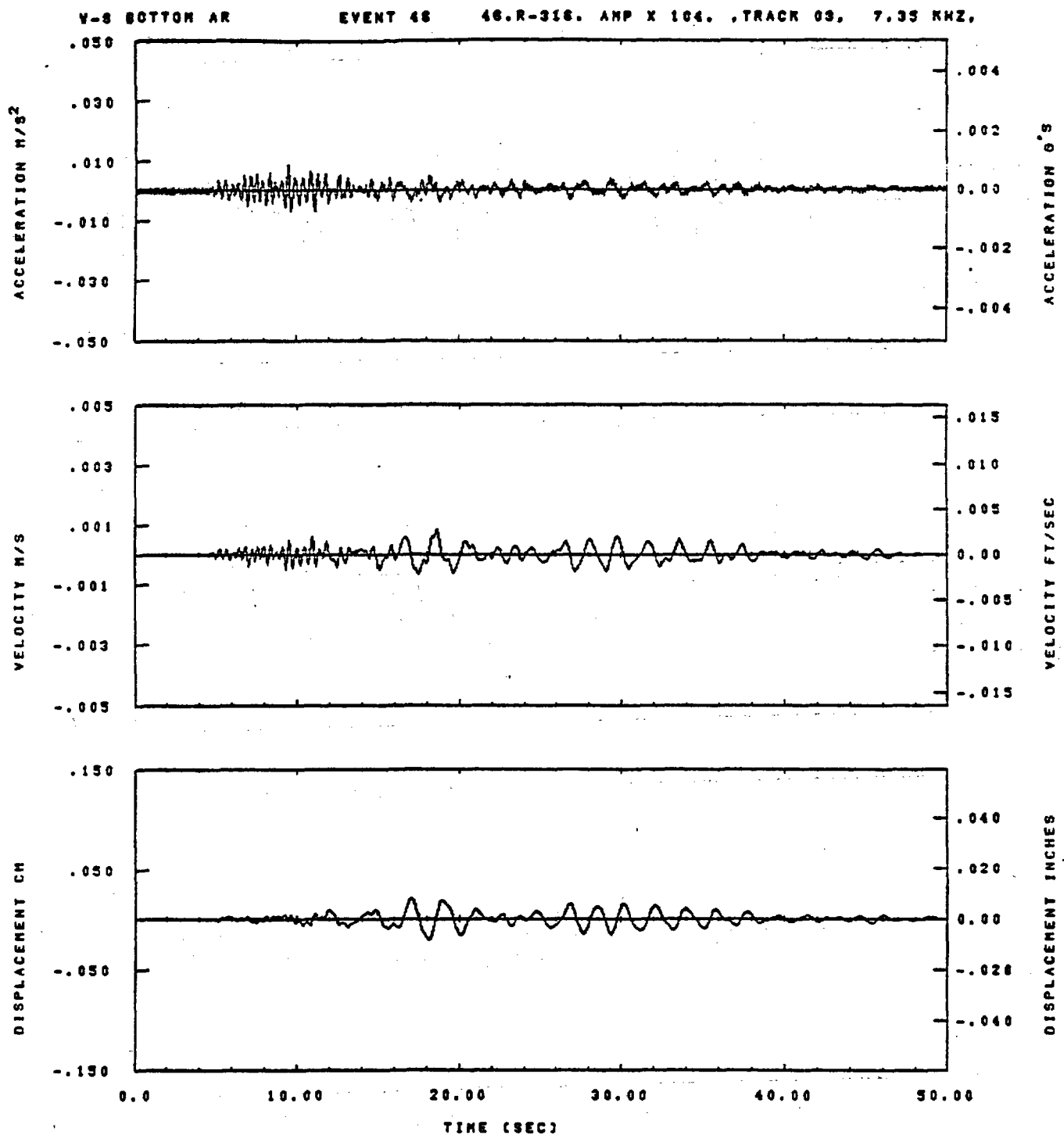
Figure G-80



IDT= .0020	OOT= .005	FIX=	AAS= 0.
HPP= .30	SVH= .20	HLH= 201	ASB=
LPP= 22.	SVL= 5.	HLL= 1999	ASE=
VTB= .300	VTE= .200	FLL= -20.	VSE= 0.
DPB= 0.	DPE= 100.	FLH= 0	DSE= 0.

09.29.12.

07/02/92



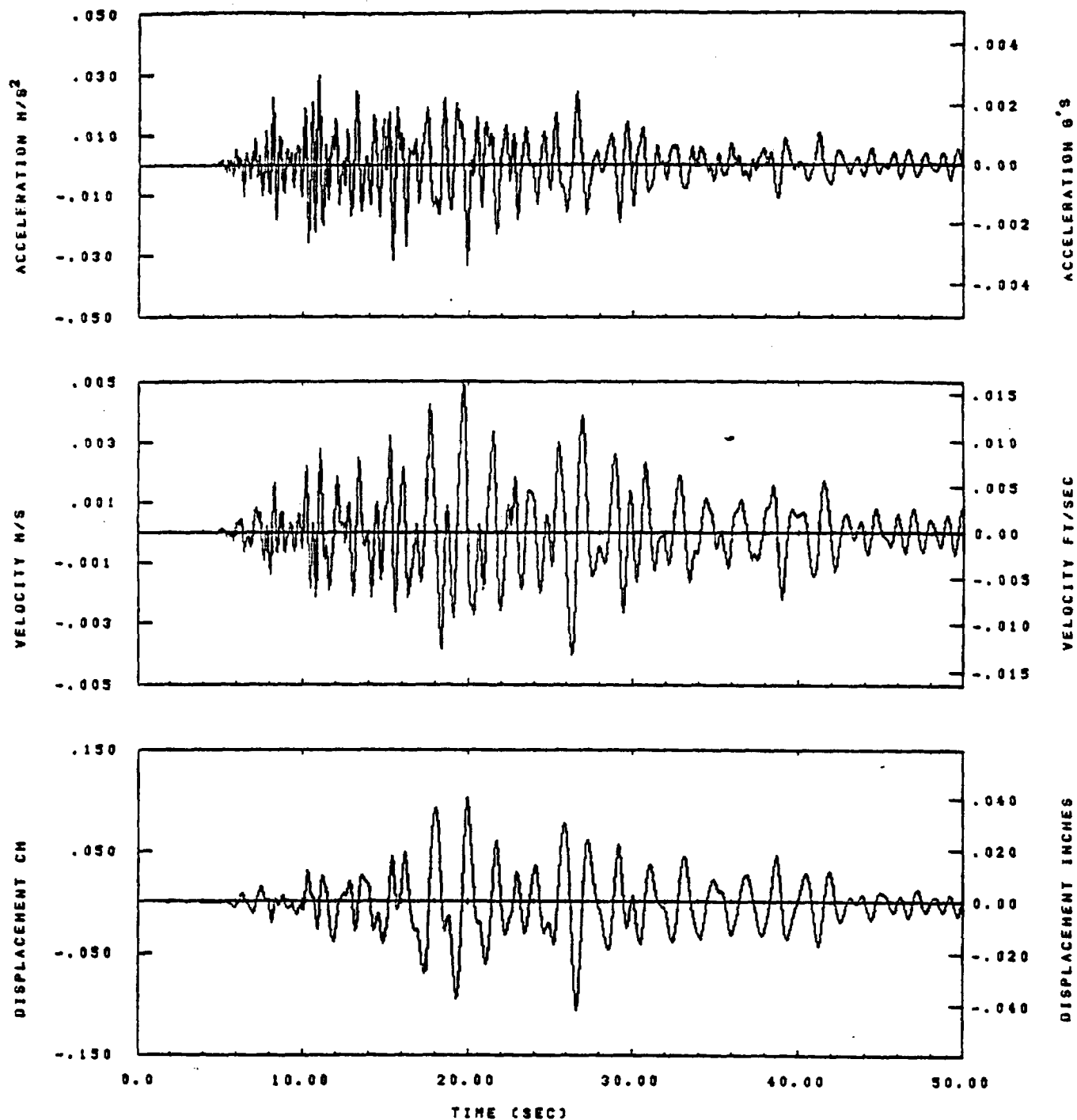
IDT= .0020	OOT= .0	FIX=	AAS=
HPP= .3	SVH= .20	HLH= 167	ASB=
LPP= 27.	SVL= 8.	HLL= 1998	ASE=
VTS= .30	VTE= .200	FLL=	VSE=
DPS=	DPE=	FLH= 0	DSE= 0.

08.28.27.

07/02/82

Figure G-82

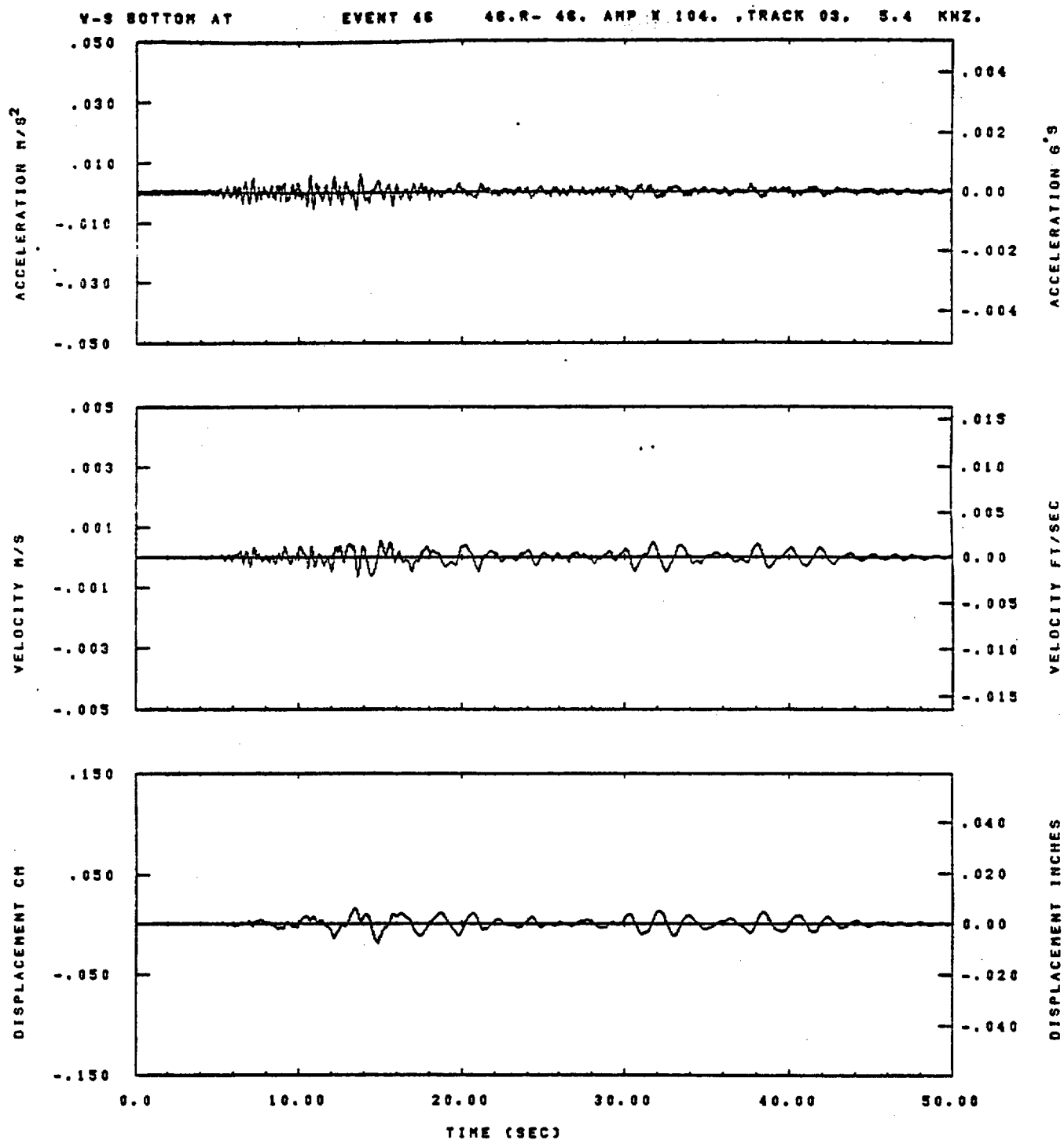
Y-S TOP AT EVENT 48 48.R- 48. AMP X 51.1 ,TRACK 03. 14.3 MHZ.



IOT= .0020	ODT= .003	FIX=	AAS= 0.
HFF= .30	SVH= .20	MLH= 201	ASS=
LFF= 22.	SVL= 5.	MLL= 1999	ASE=
VTS= .300	VTE= .200	FLL= -20.	VSE= 0.
DPS= 0.	DPE= 100.	FLH= 0	DSE= 0.

03.29.19.

07/02/92



IOT= .0020	QOT= .0	FIX=	AAS=
HPP= .3	BYH= .20	HLH= 167	ASH=
LPP= 27.	BYL= 6.	HLL= 1999	ASE=
VTS= .30	VTE= .200	FLL=	VSE=
DPS=	DPE=	FLH= 0	DSE= 0.

09.29.30.

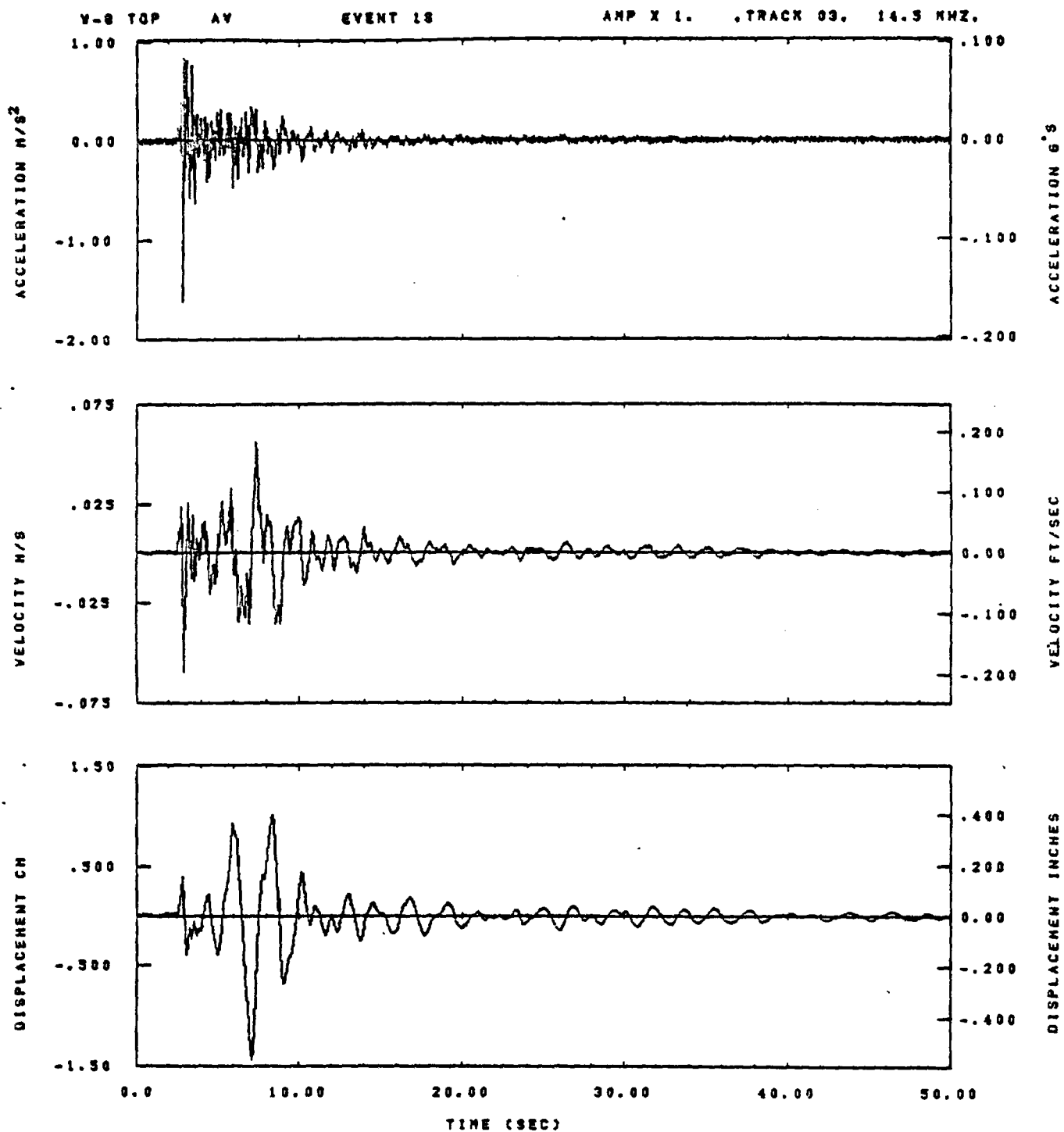
07/02/82

Figure G-84

APPENDIX H

COMPARISON OF TOP AND BOTTOM

WAVEFORMS AT STATION W-8

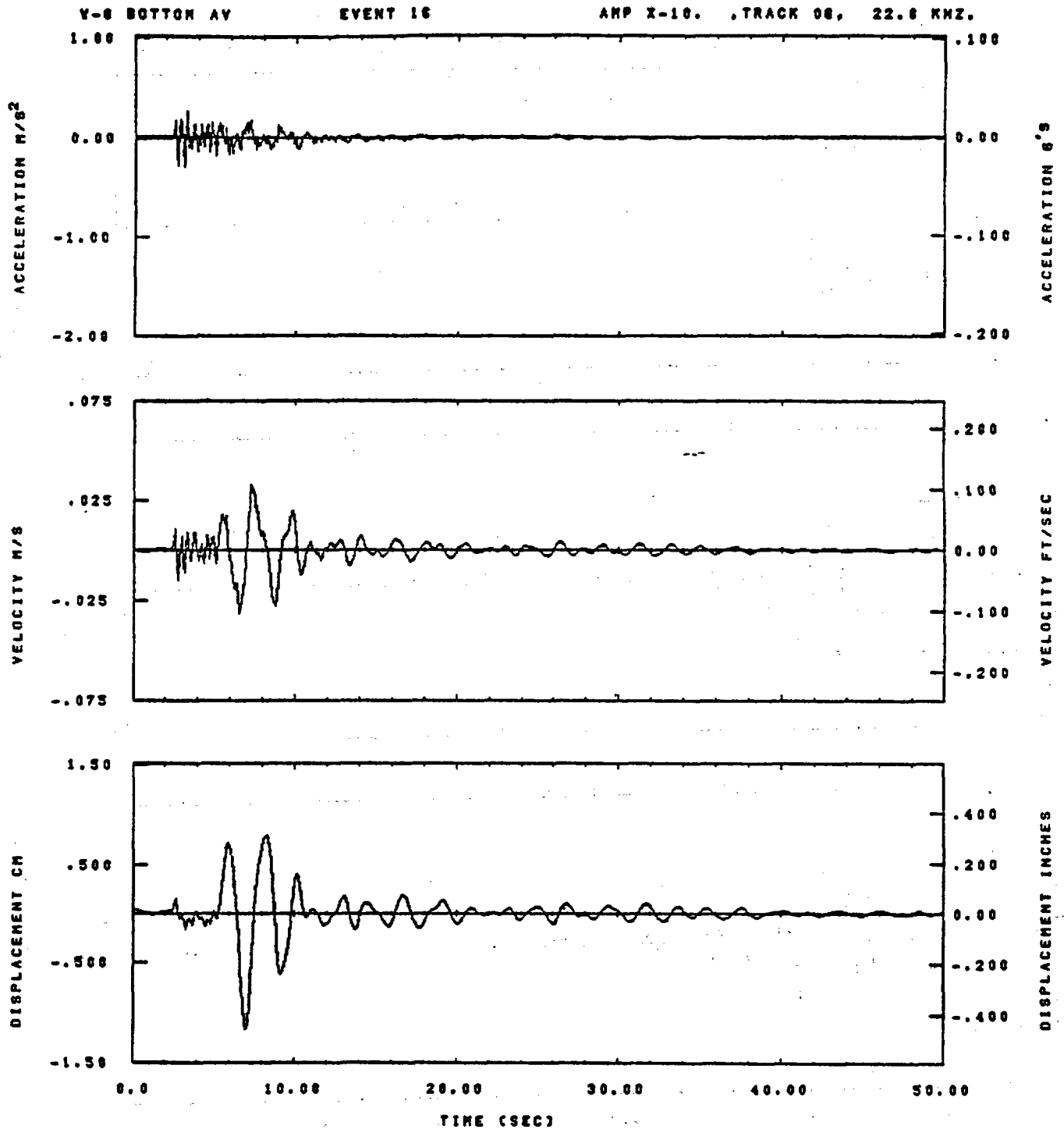


IDT= .0020	OOT= .005	FIX=	AAS= 0.
HPP= .20	BYH= .13	HLH= 231	ASB=
LPP= 18.	BYL= 4.	HLL= 2999	ASE=
VTB= .200	VTE= .133	FLL= -20.	VSE= 0.
DPS= 0.	DPE= 100.	FLH= A-.1	DSE= A+.1

13.53.18.

08/30/82

Figure H-1

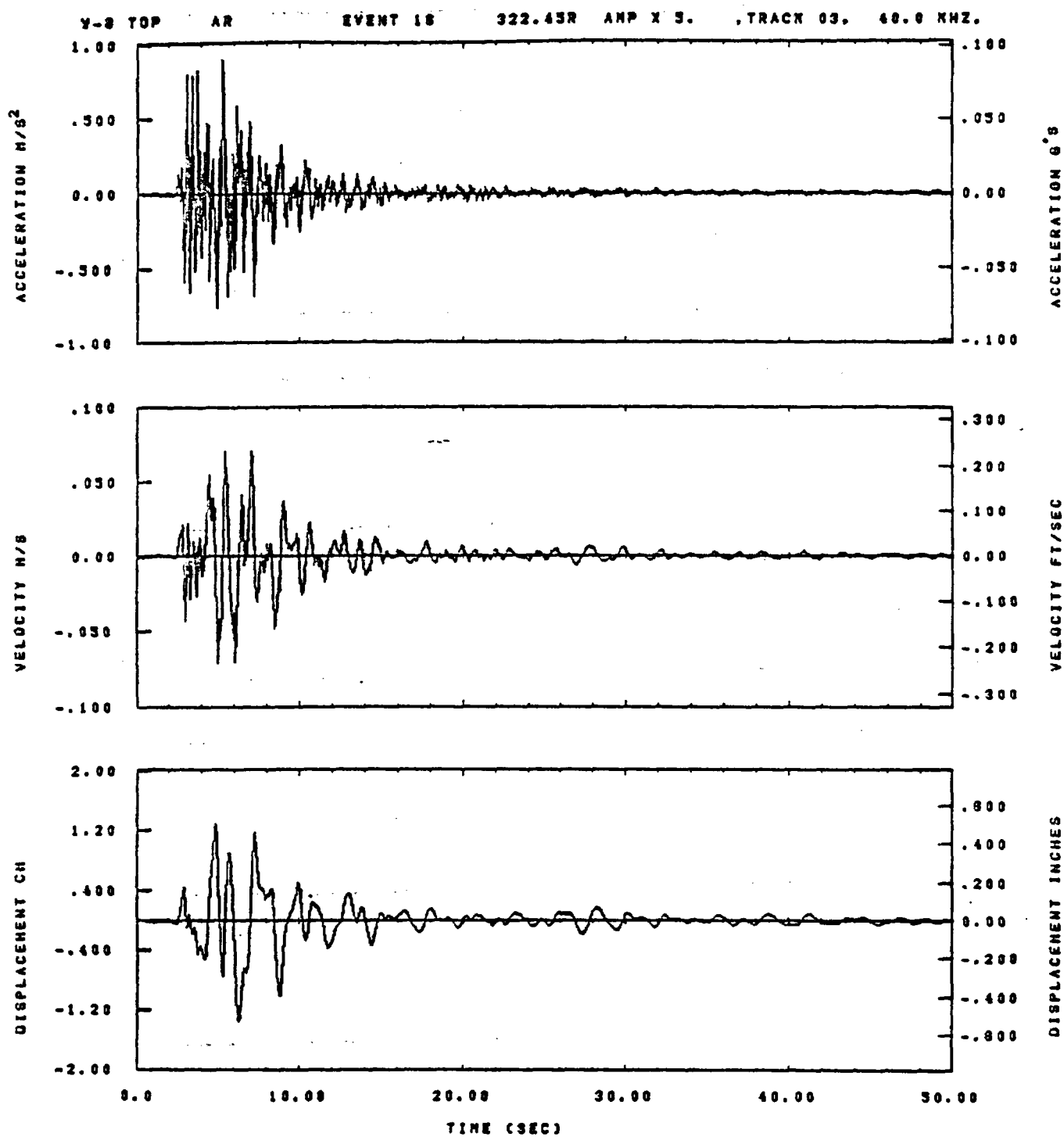


IDT= .0020	OOT= .005	FIX=	AAS= 0.
HPF= .20	SVH= .13	HLH= 251	ASB=
LPF= 18.	SVL= 4.	HLL= 2888	ASE=
VTB= .200	VTE= .133	FLL= -20.	VSE= 0.
DPS= 0.	DPE= 100.	FLH= A-.1	DSE= A+.1

13.53.02.

06/30/82

Figure H-2

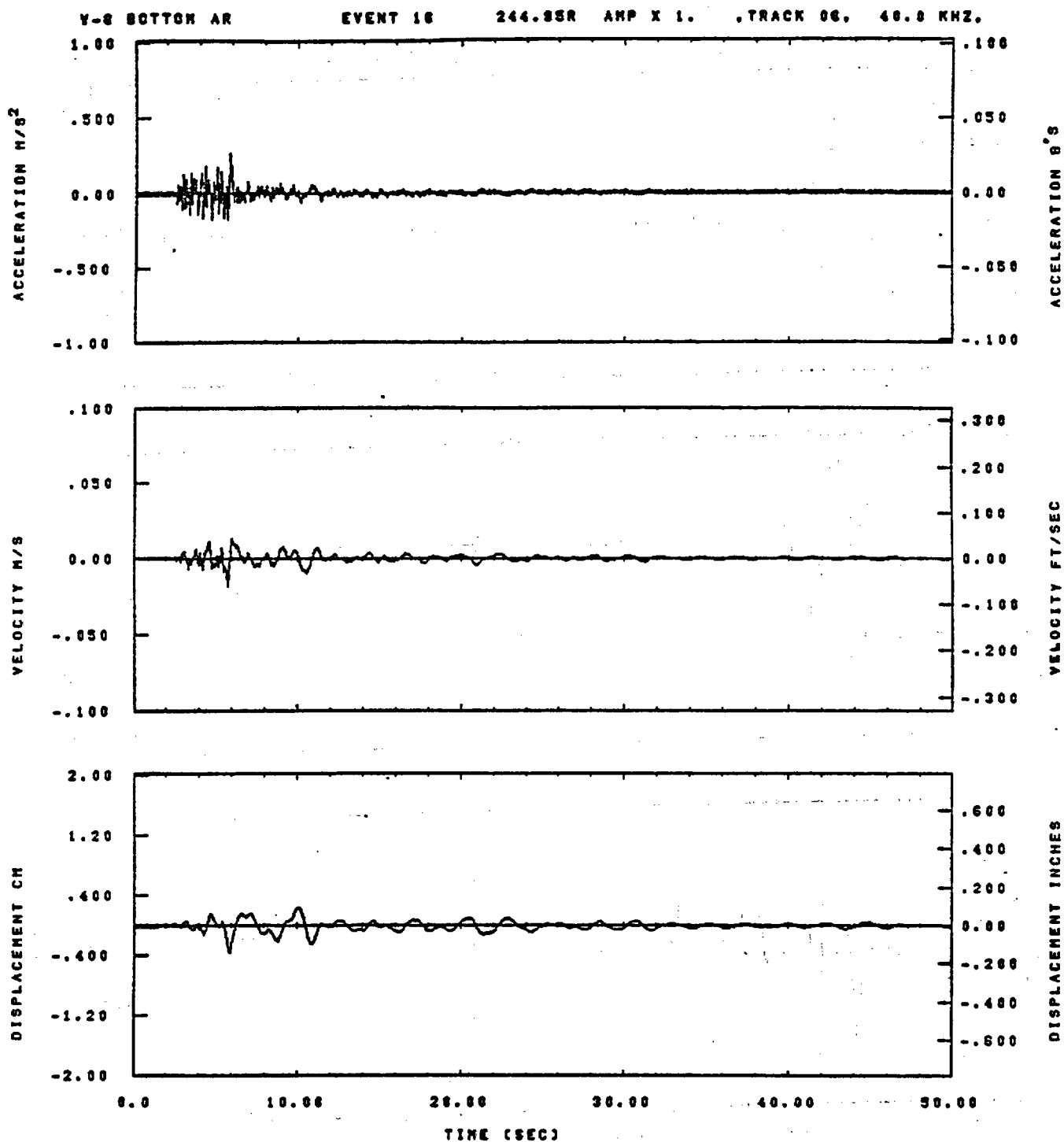


IDT= .0020	QDT= .003	FIX=	AAS= 0.
HPP= .20	BYM= .13	HLH= 251	ASB=
LPP= 18.	BYL= 6.	HLL= 2999	ASZ=
VTS= .200	VTE= .133	FLL= -20.	VSE= 0.
OPS= 0.	QPS= 100.	FLH= A-.1	QSE= A+.1

13.53.28.

08/30/82

Figure H-3

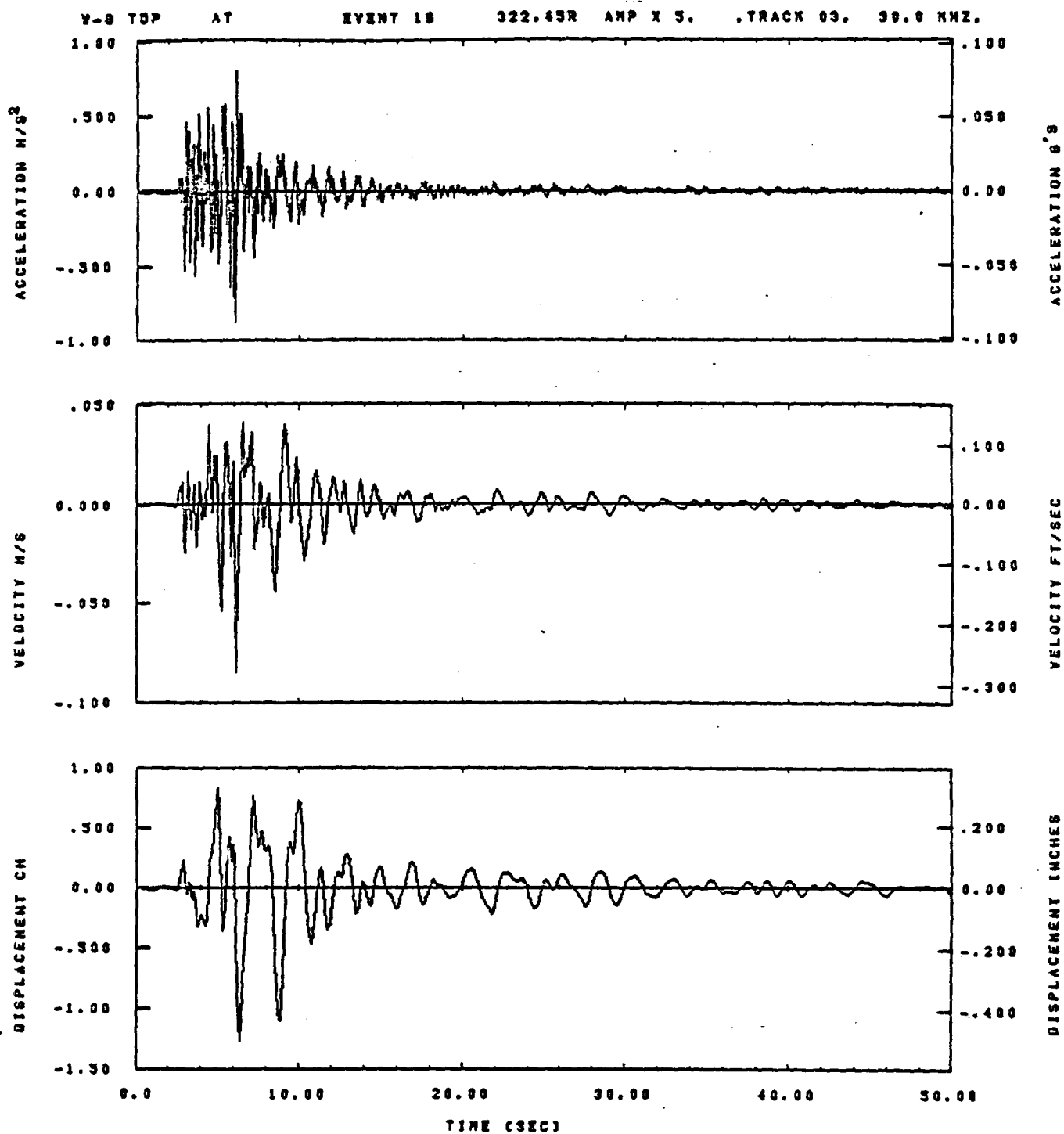


IDT= .0020	ODT= .005	FIX=	AAS= 0.
HPP= .20	BYH= .13	HLH= 251	ASS=
LPP= 18.	BYL= 4.	HLL= 2988	ASE=
VTS= .200	VTE= .133	FLL= -20.	VSE= 0.
DPS= 0.	DPE= 100.	FLH= A-.1	DSE= A+.1

13.53.10.

06/30/82

Figure H-4

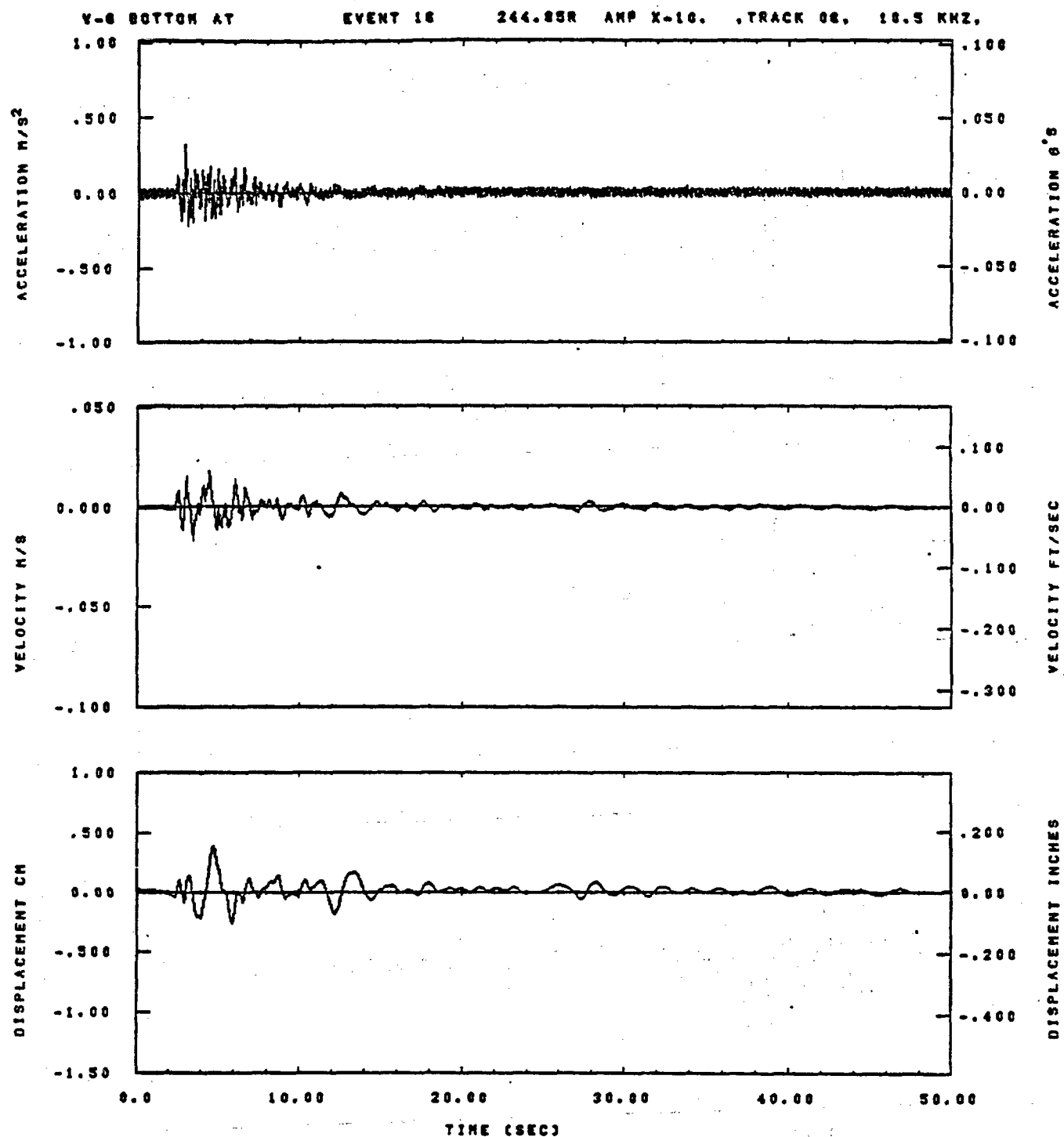


IDT= .0020	ODT= .003	FIX=	AAS= 0.
HPP= .20	BYH= .13	HLH= 251	ASS=
LPP= 18.	BYL= 4.	HLL= 2999	ASE=
VTB= .200	VTE= .133	FLL= -20.	VSE= 0.
DPS= 0.	DPE= 100.	FLH= A-.1	DSE= A+.1

13.53.59.

08/30/82

Figure H-5

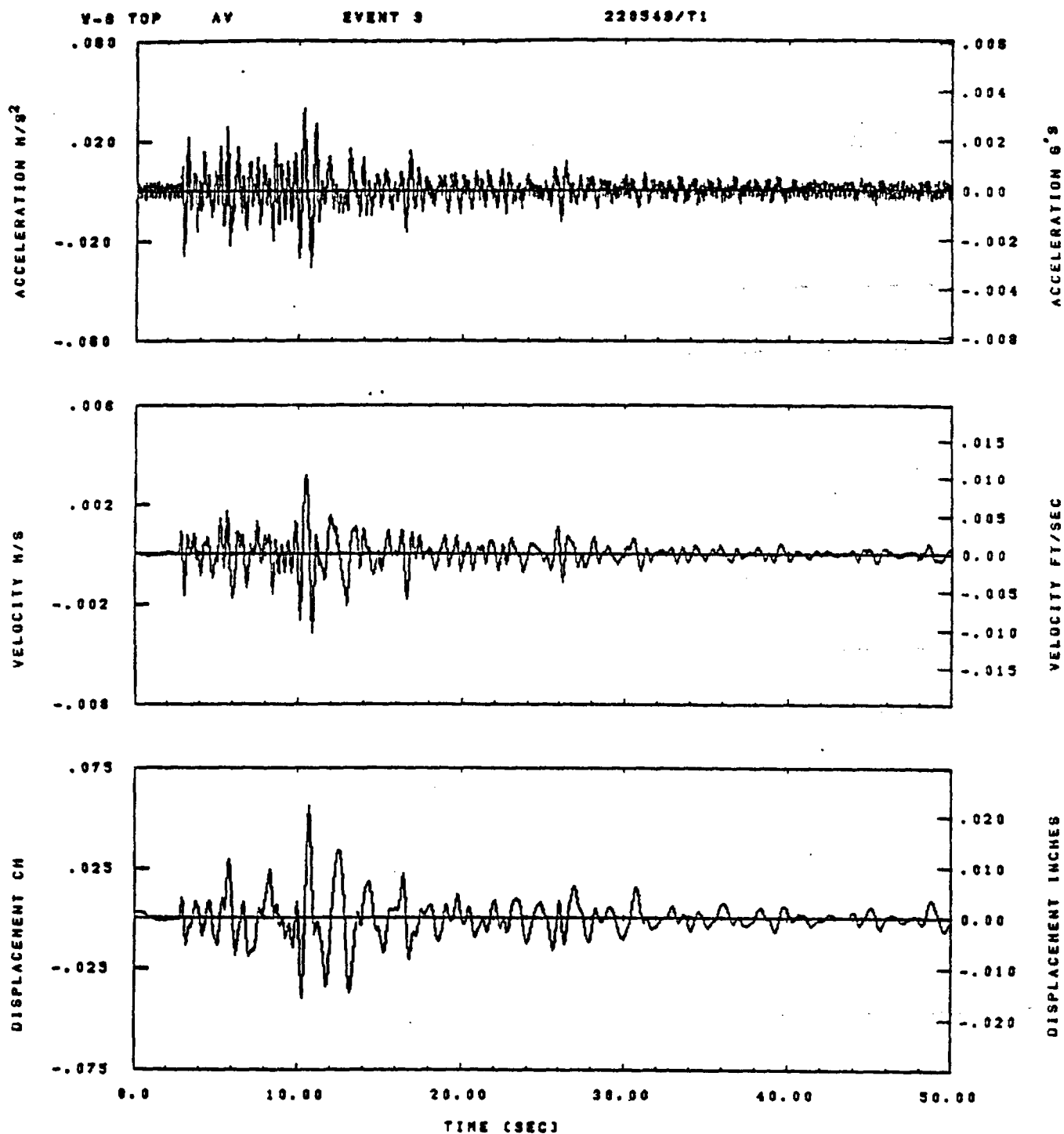


IDT= .0020	QDT= .005	FIX=	AAS= 0.
HPP= .20	BVH= .13	HLH= 251	ASB=
LPP= 18.	BVL= 4.	HLL= 2988	ASE=
VTS= .200	VTE= .133	FLL= -20.	VSE= 0.
DPS= 0.	DPE= 100.	FLH= A-.1	DSE= A+.1

13.54.15.

06/30/82

Figure H-6

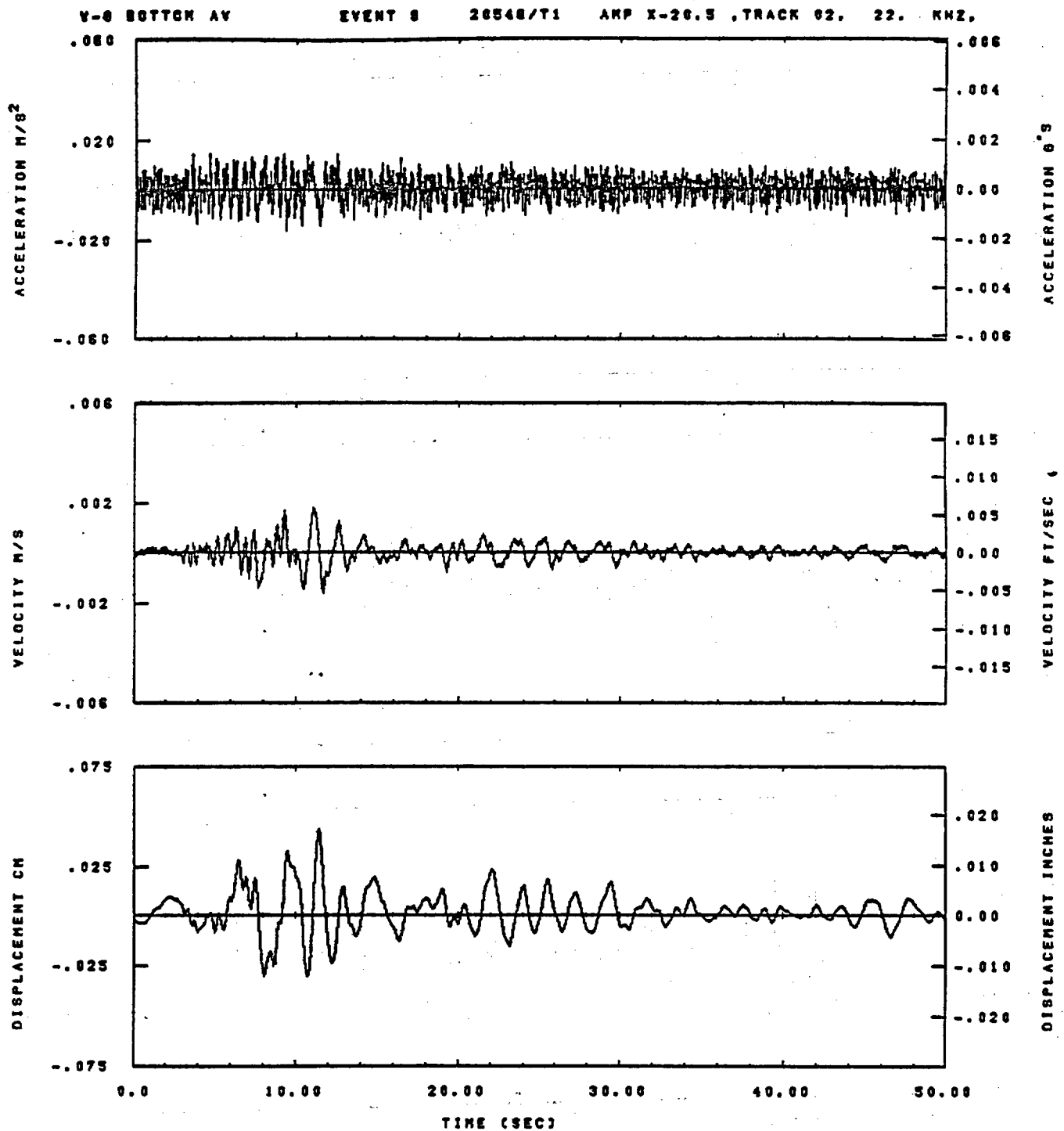


IOT= .0020	OOT=	FIX=	AAS= 0.
HPP= .3	BYN= .20	HLH= 187	ASB=
LPP= 27.	BYL= 8.	HLL= 1999	ASE=
VTS= .30	VTE= .200	FLL= -20.	VSE= 0.
DPS= 0.	DPE= 100.	FLH= 0	DSE= 0.

13.33.53.

07/02/82

Figure H-7

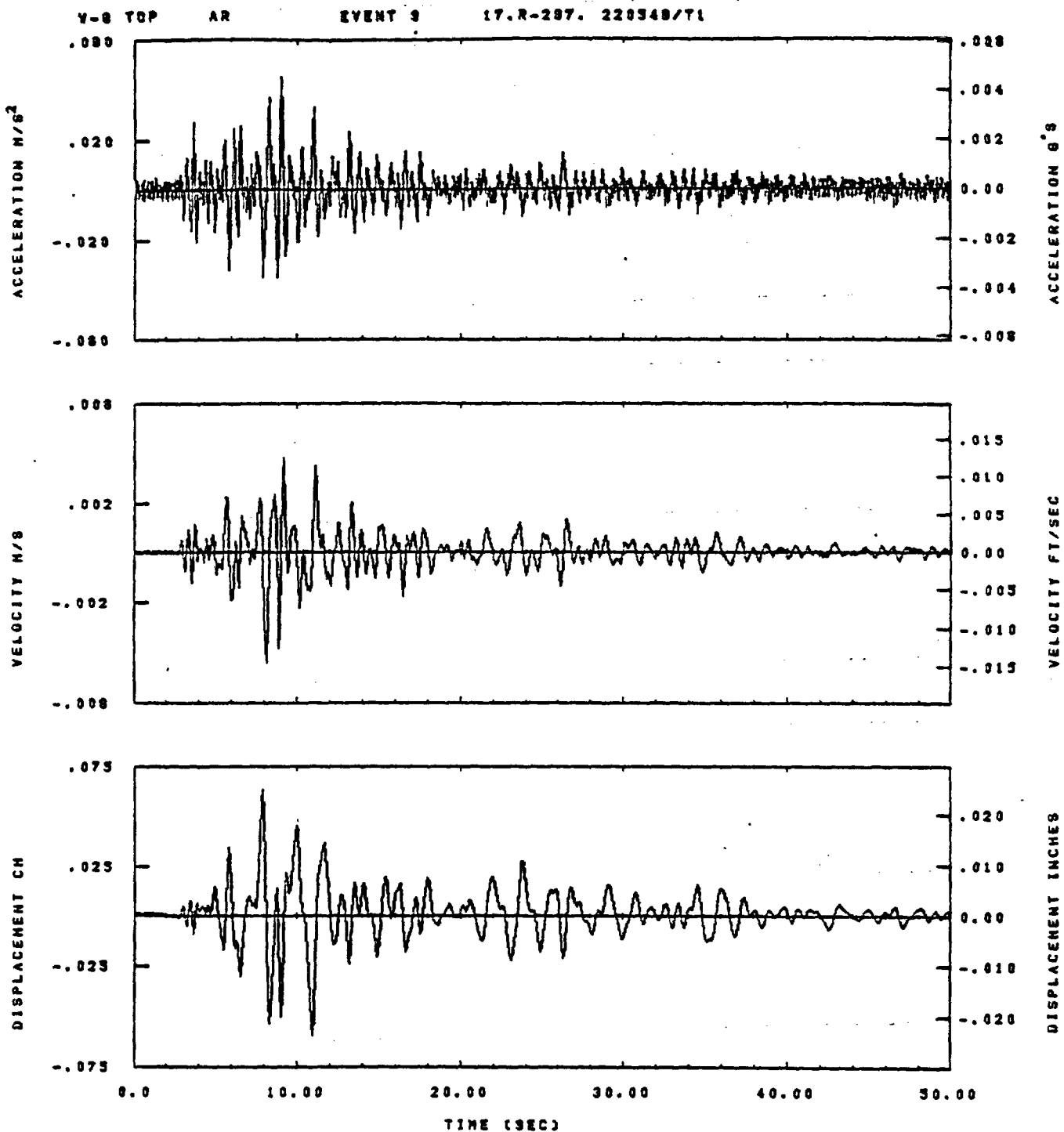


IDT= .0020	ODT=	FIX=	AAS= 0.
HPP= .3	SVH= .20	HLH= 167	ASB=
LPP= 27.	SVL= 6.	HLL= 1988	ASE=
VTB= .30	VTE= .200	FLL= -20.	VSE= 0.
DPS= 0.	DPE= 100.	FLH= 0	DSE= 0.

15.34.04.

07/02/02

Figure H-8



IDT= .0020	ODT=	FIX=	AAS= 0.
MPP= .3	BYH= .20	HLH= 187	ASB=
LPP= 27.	BYL= 6.	HLL= 1999	ASE=
VTB= .30	VTE= .200	FLL= -20.	VSE= 0.
DPS= 0.	DPE= 100.	FLH= 0	DSE= 0.

15.33.58.

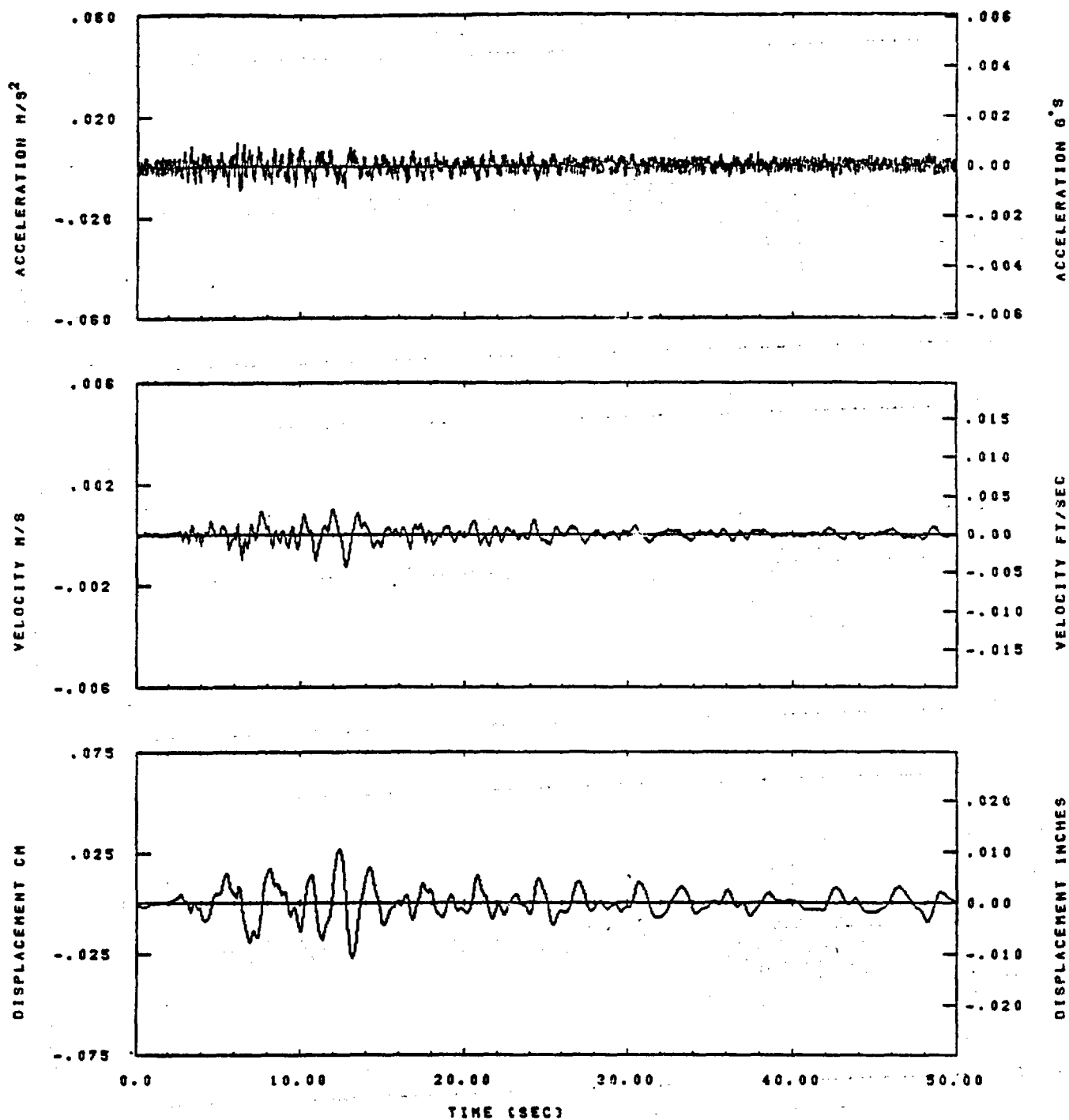
07/02/82

Figure H-9

Y-6 BOTTOM AR

EVENT 9

62.R-287. AMP X-20.5 ,TRACK 02. 14.5 KHZ,

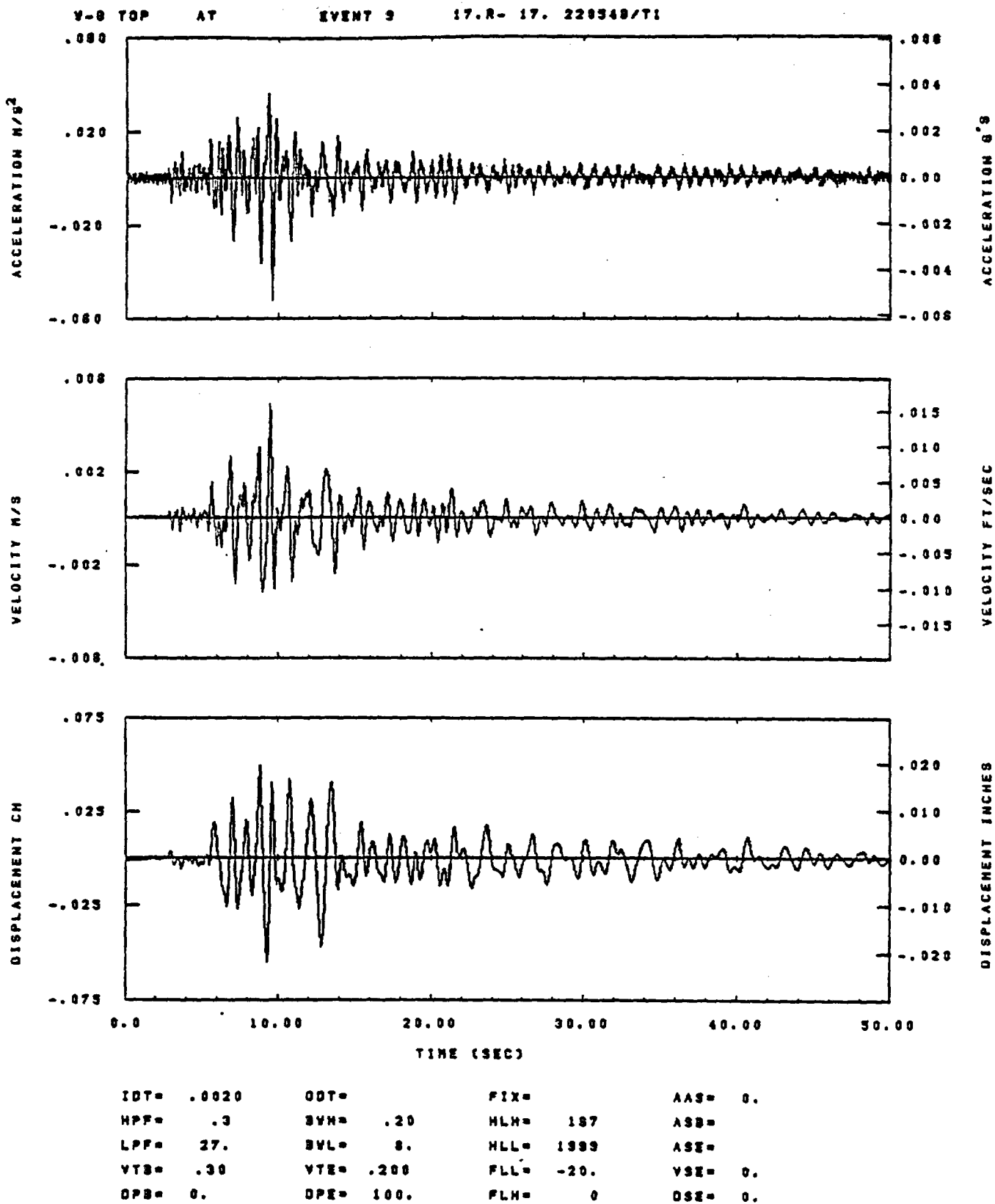


IDT= .0020	ODT=	FIX=	AAS= 0.
HPF= .3	SVH= .20	HLH= 167	RNG=
LPF= 27.	SVL= 6.	HLL= 1999	AZH=
VTS= .30	VTE= .200	FLL= -20.	VSE= 0.
DPS= 0.	DPE= 100.	FLH= 0	HLT=

08.08.07.

07/23/82

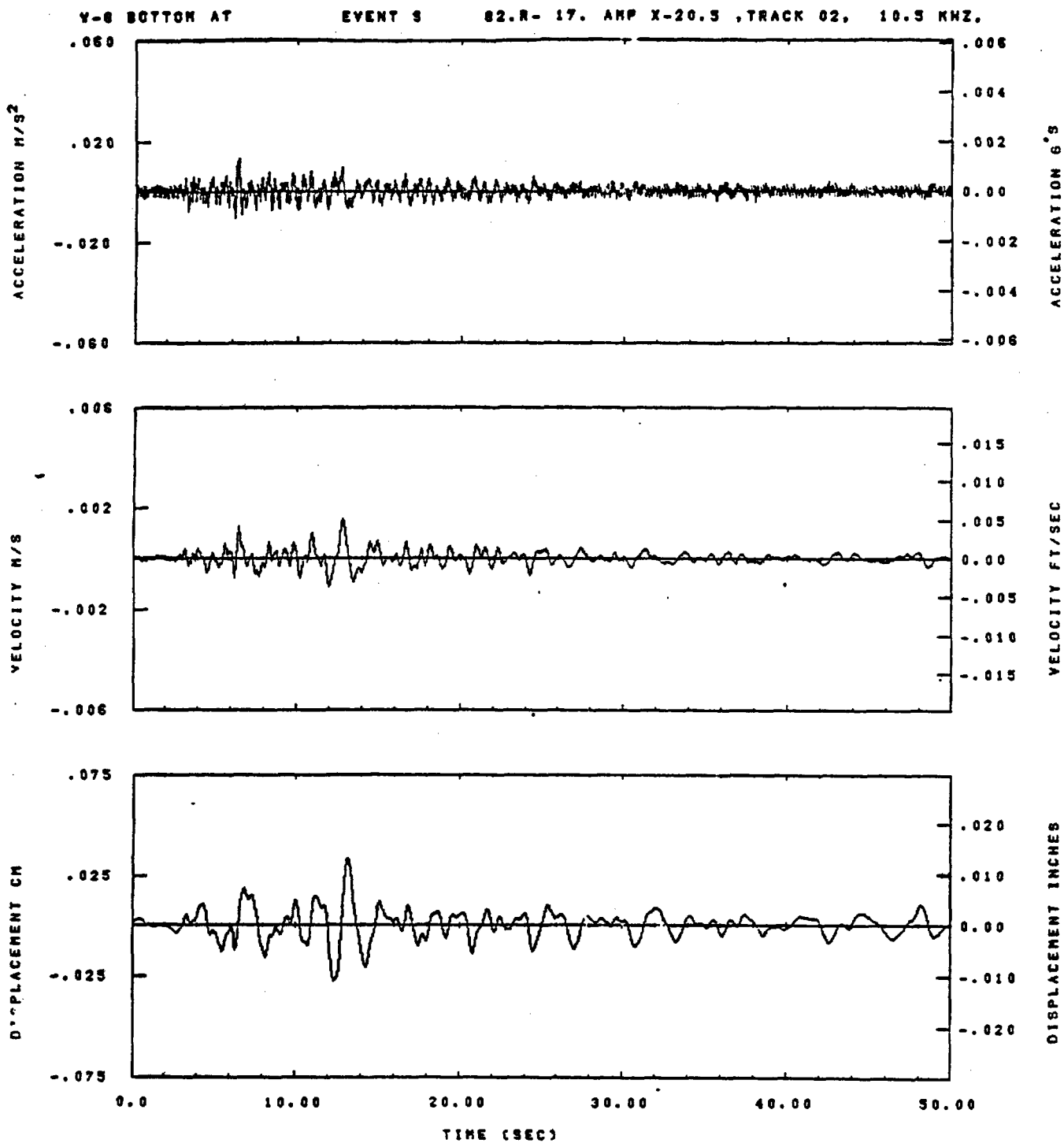
Figure H-10



15.34.00.

07/02/92

Figure H-11



IDT= .0020	ODT=	FIX=	AAS= 0.
HPF= .3	BVN= .20	HLN= 167	RNG=
LPF= 27.	BVL= 6.	HLL= 1998	AZH=
VTE= .30	VTE= .200	FLL= -20.	VSE= 0.
OPB= 0.	OPE= 100.	FLH= 0	MLT=

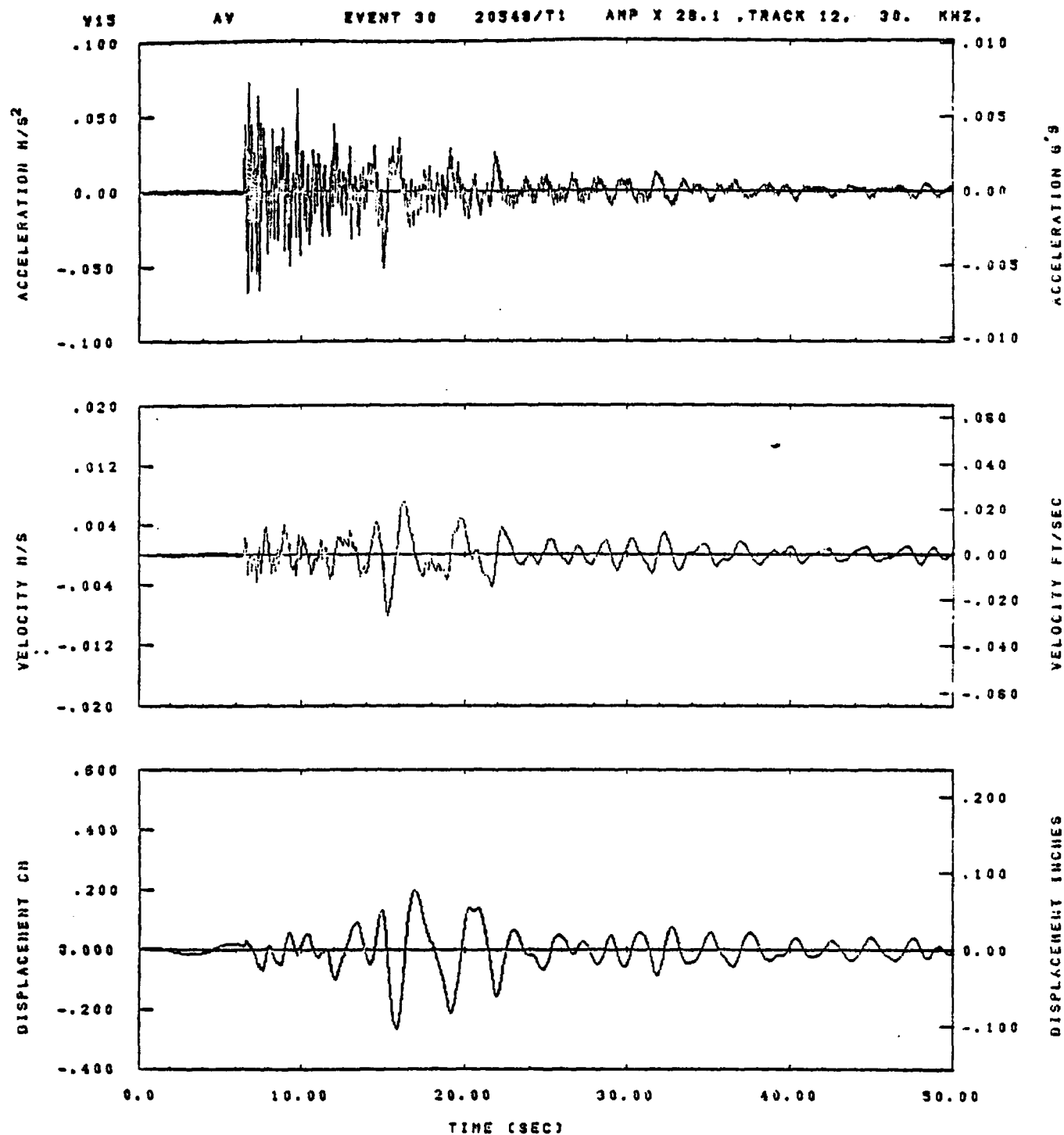
09.09.18.

07/23/82

Figure H-12

APPENDIX I

COMPARISON OF WAVEFORMS AT STATIONS W-15 AND W-16

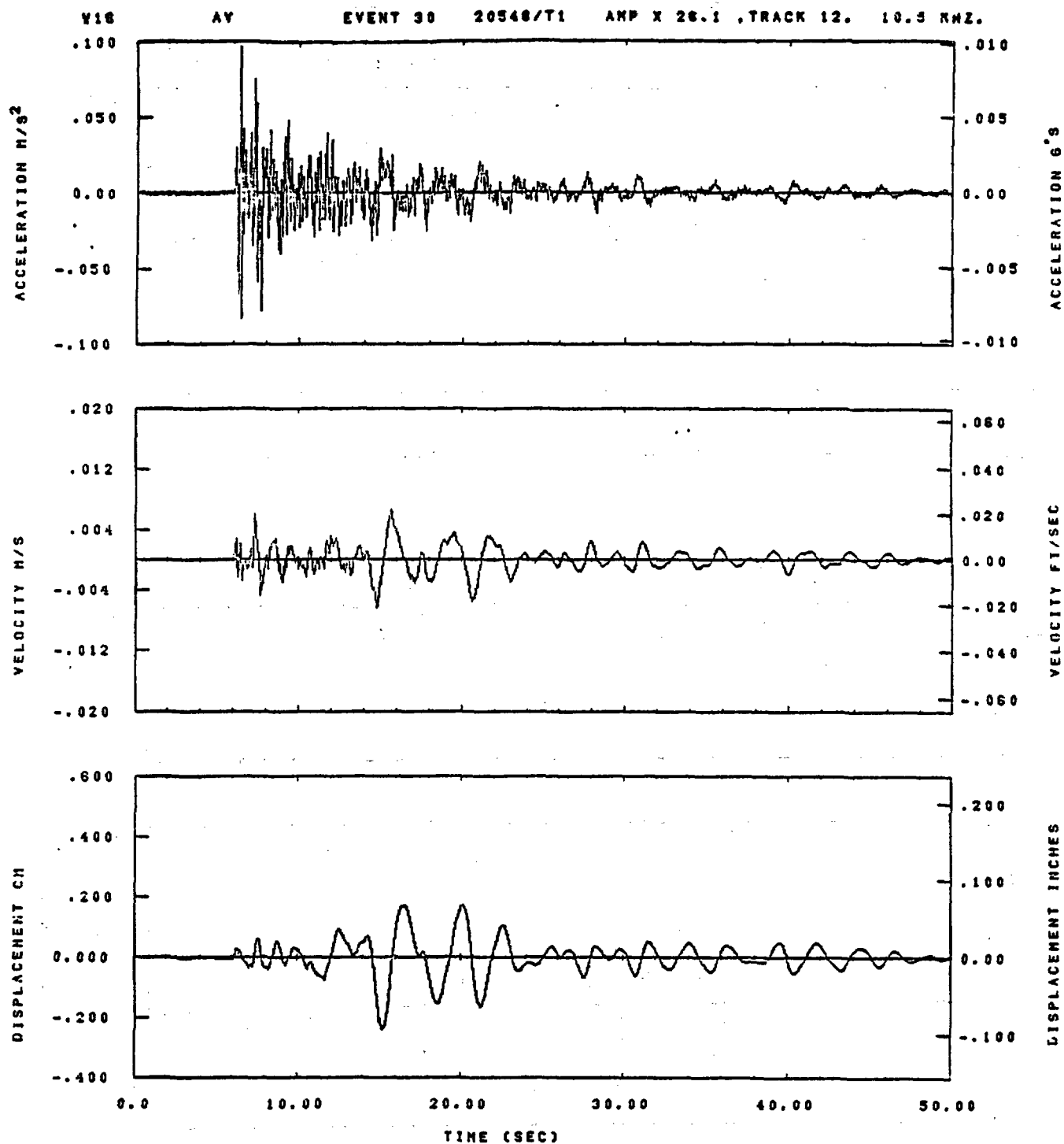


IOT= .0020	ODT= .005	FIX=	MIN=
HPF= .20	BYH= .13	MLH= 125	MAX=
LPF= 36.	BYL= 8.	MLL= 2999	AZM=
VTB= .200	VTE= .133	FLL= -20.	RNG=
OPB= 0.	DPE= 100.	FLH= 0	MLT=

13.29.12.

08/08/92

Figure I-1

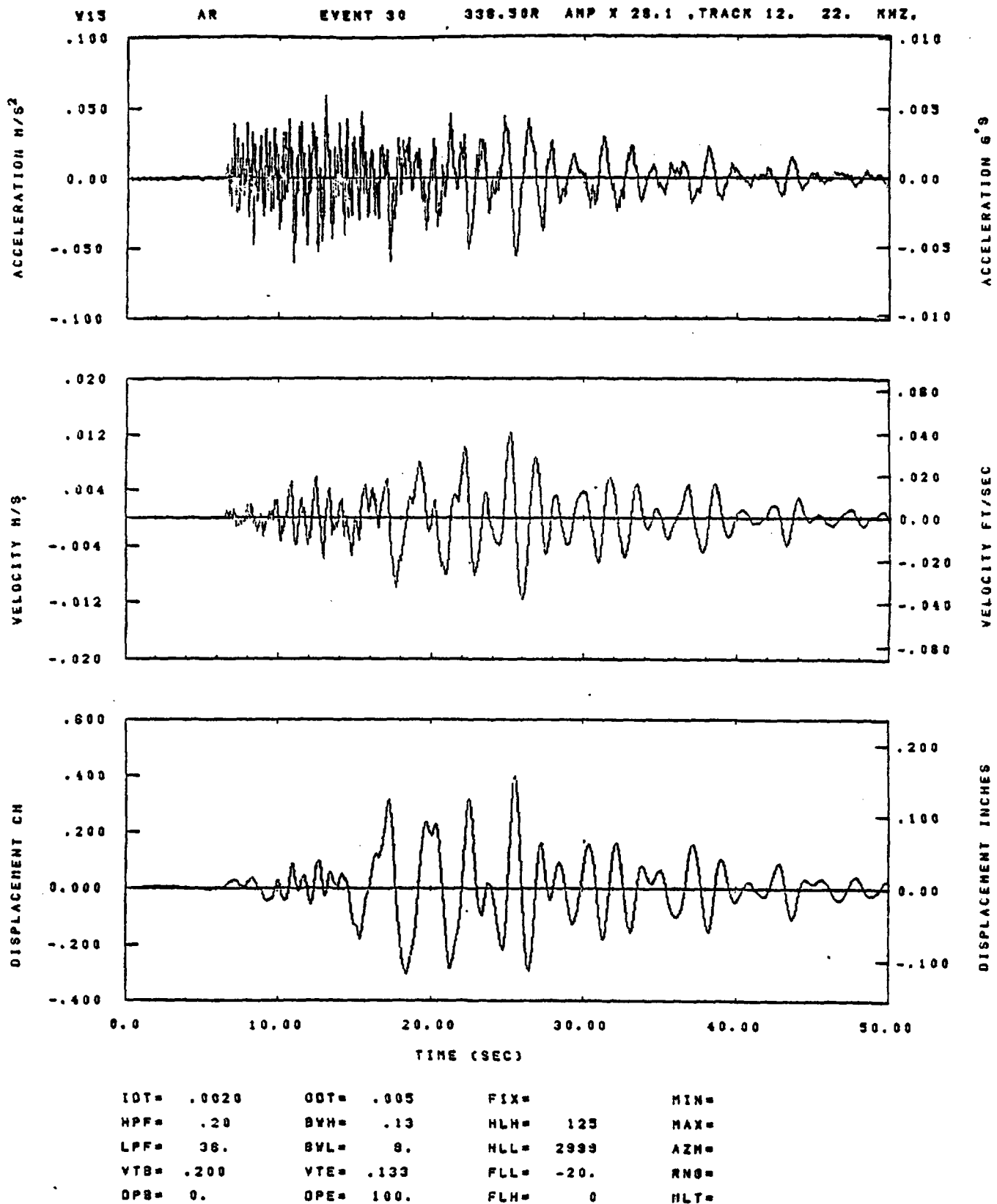


IDT= .0020	QDT= .005	FIX=	MIN=
HPF= .20	BYH= .13	HLH= 125	HAX=
LPF= 36.	BVL= 8.	HLL= 2999	AZN=
VTB= .200	YTE= .133	FLL= -20.	RNG=
DPS= 0.	OPE= 100.	FLH= 0	MLT=

13.28.16.

08/06/82

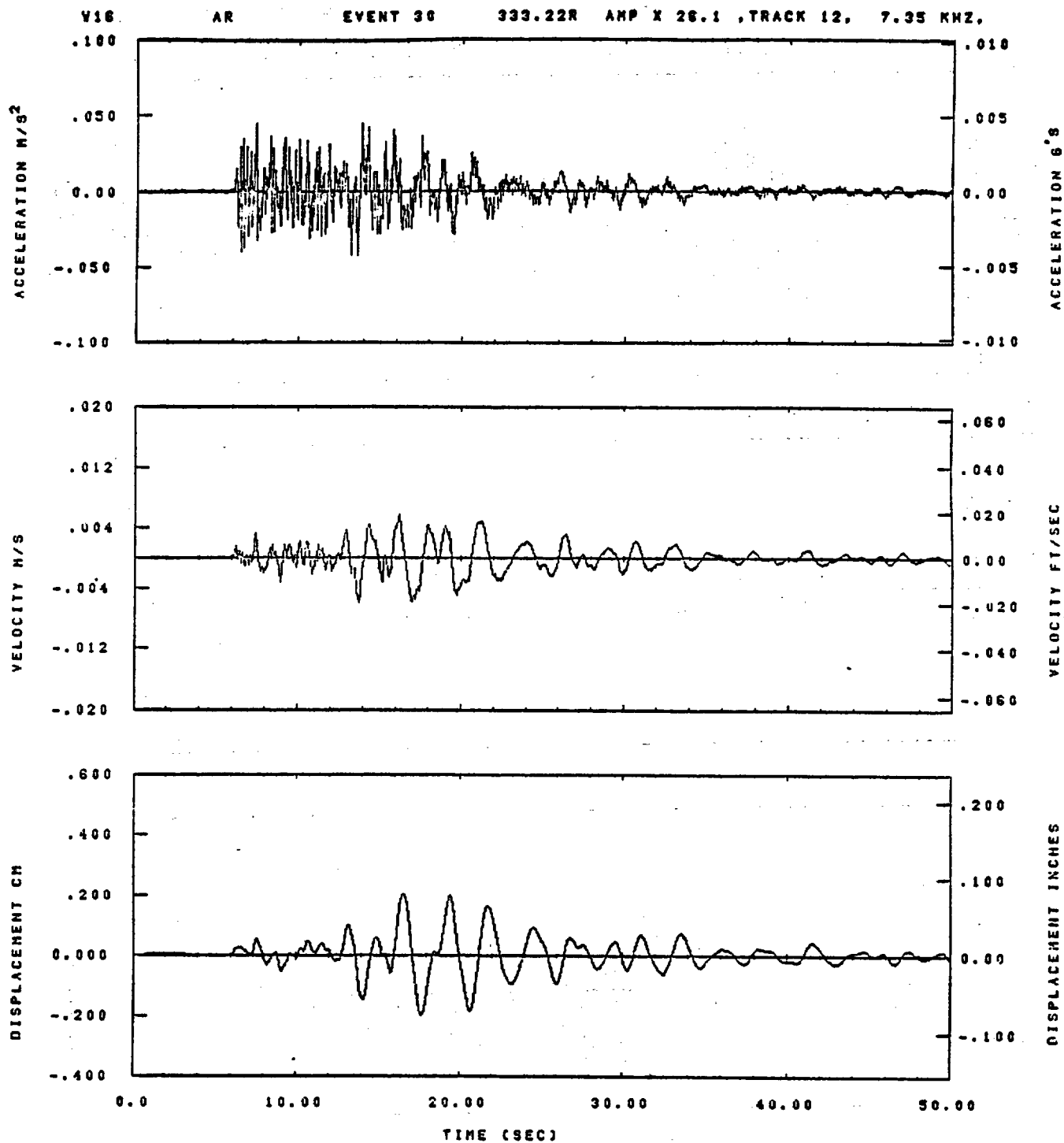
Figure I-2



13.29.08.

08/08/82

Figure I-3

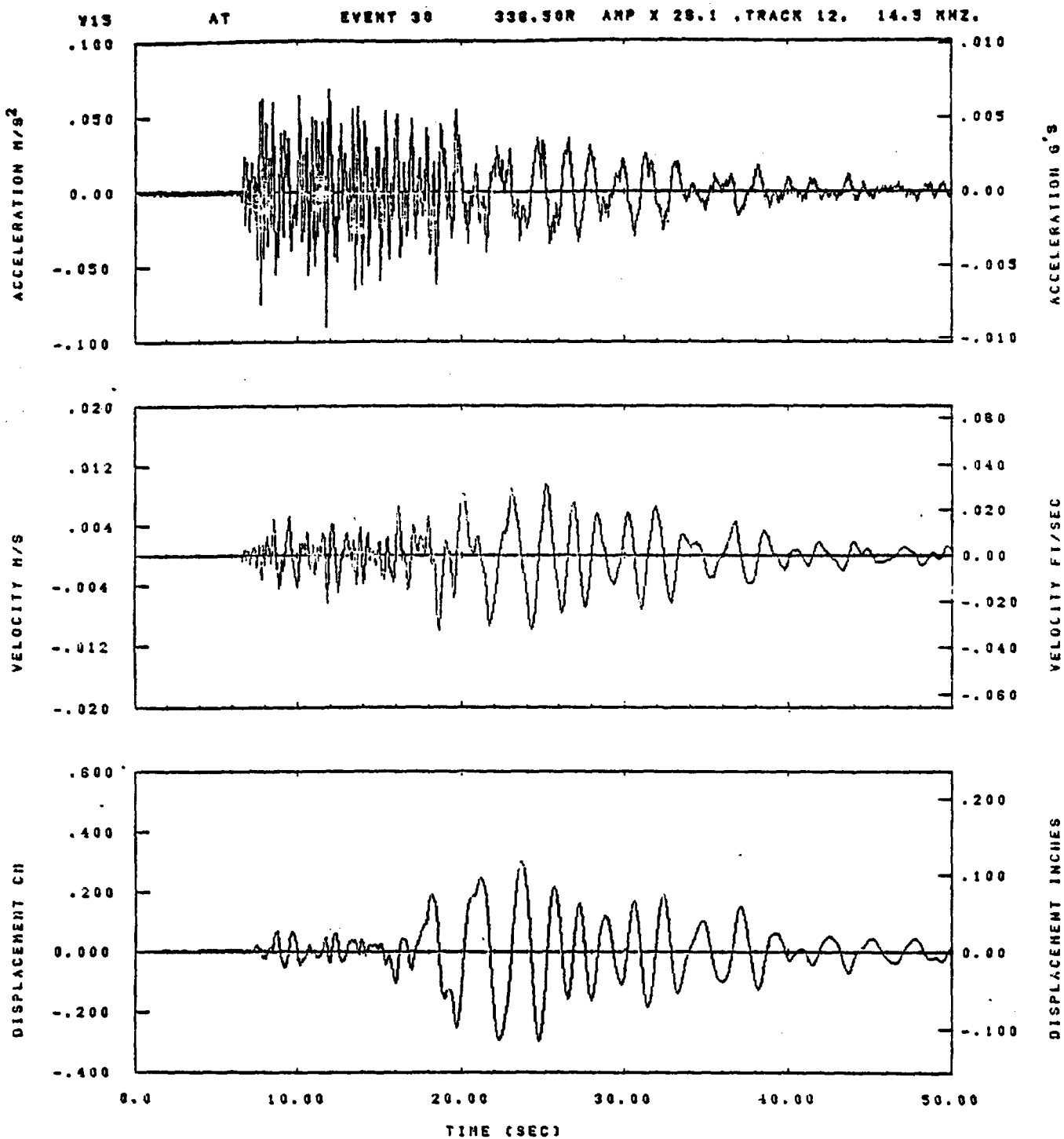


IDT= .0020	ODT= .005	FIX=	MIN=
HPF= .20	BVH= .13	HLH= 125	MAX=
LPF= 36.	BYL= 8.	HLL= 2999	AZN=
VTB= .200	VTE= .133	FLL= -20.	RNG=
DPB= 0.	DPE= 100.	FLH= 0	MLT=

13.29.25.

08/06/82

Figure I-4

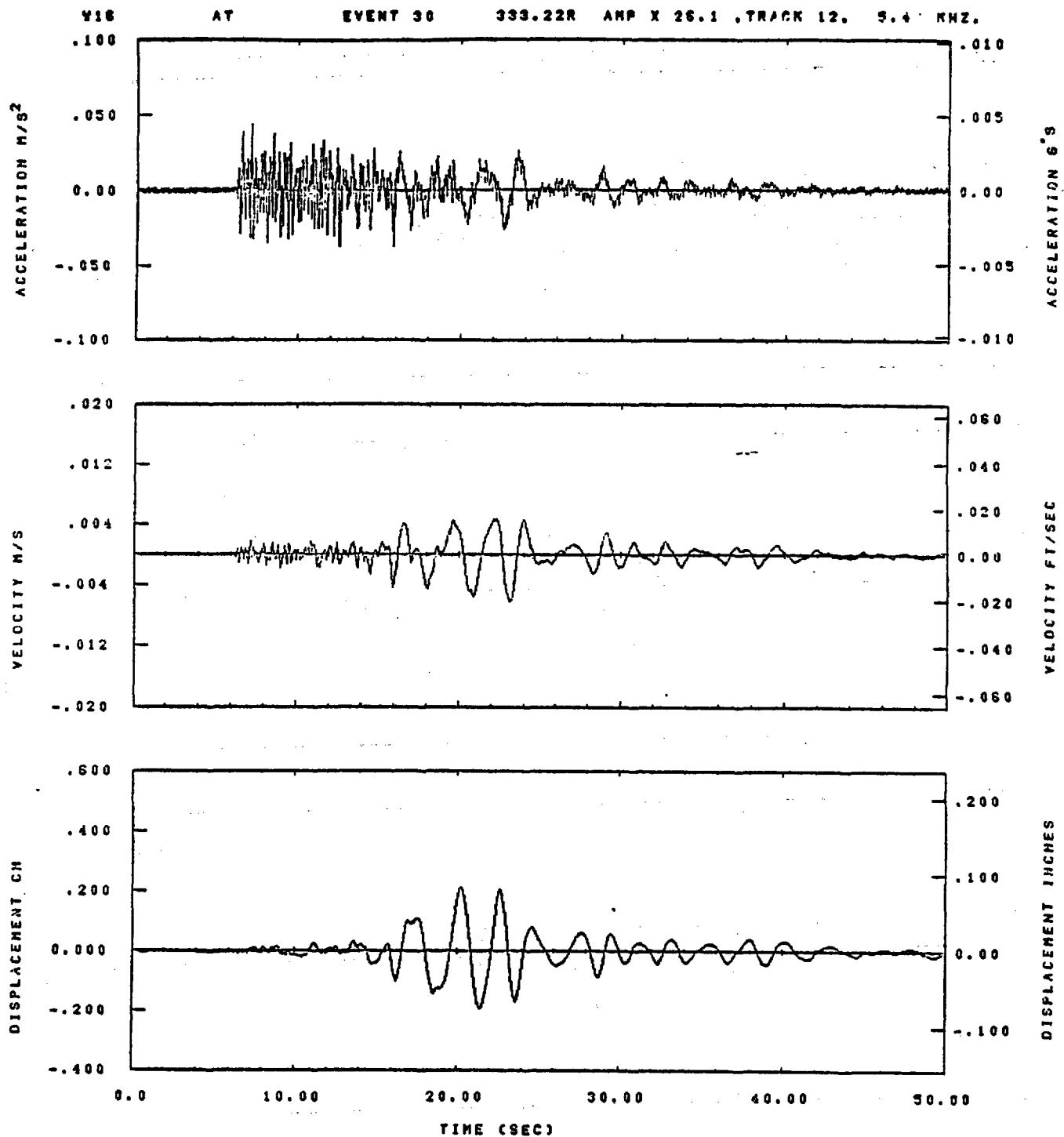


IOT= .0020	OOT= .005	FIX=	MIN=
HPF= .20	BYH= .13	HLH= 125	MAX=
LPF= 36.	BYL= 0.	HLL= 2989	AZH=
VTS= .200	VTE= .133	FLL= -20.	RNG=
DPB= 0.	OPE= 100.	FLH= 0	NLT=

13.28.59.

09/08/82

Figure I-5

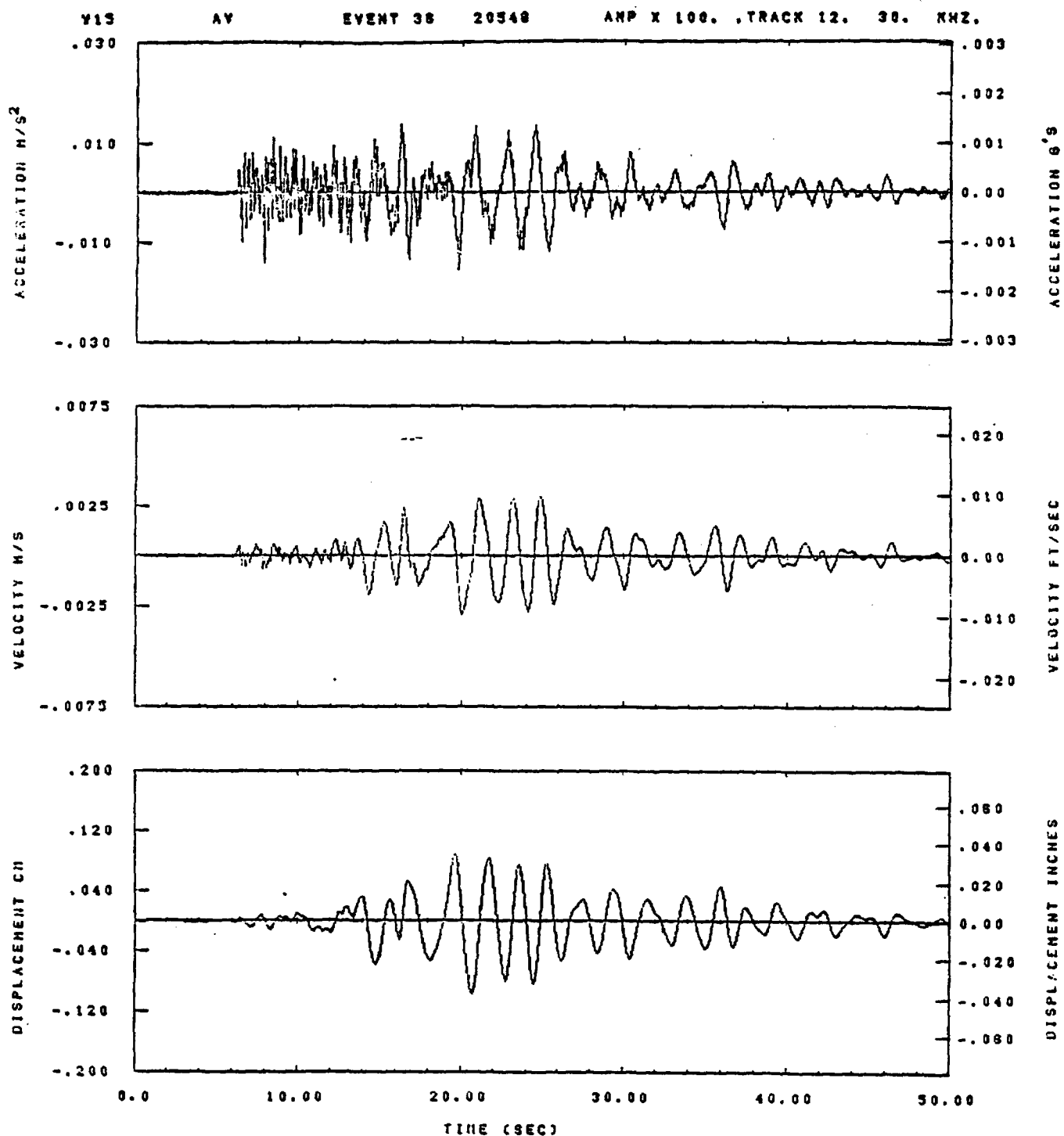


IDT= .0020	ODT= .005	FIX=	MIN=
HPF= .20	BYH= .13	HLH= 125	MAX=
LPF= 36.	BYL= 0.	HLL= 2888	AZN=
VTB= .200	VTE= .133	PLL= -20.	RNG=
OPB= 0.	DPE= 100.	FLH= 0	HLT=

13.29.20.

08/06/82

Figure I-6

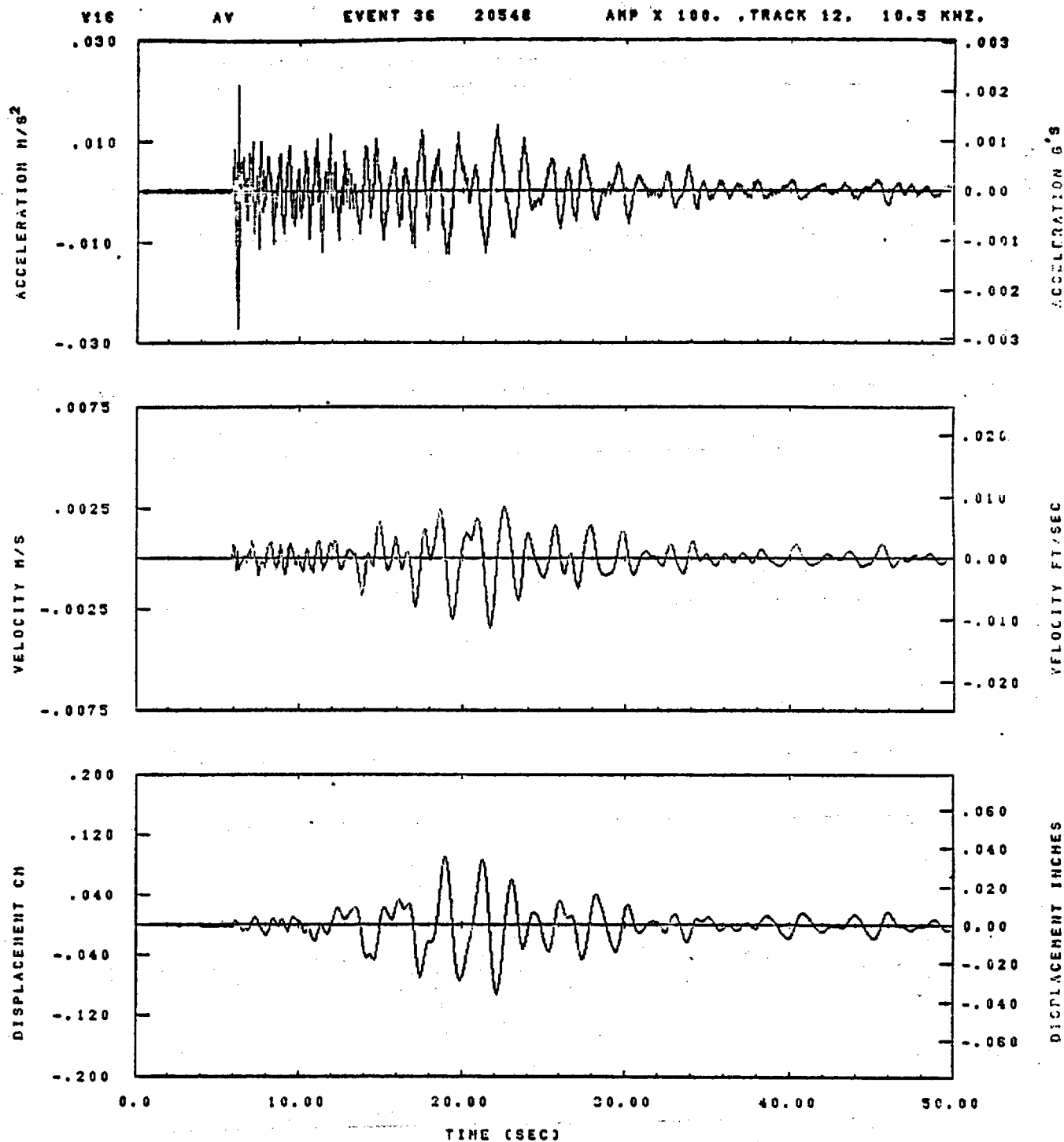


IDT= .0020	ODT= .003	FIX=	MIN=
HPF= .25	BYH= .18	HLH= 143	MAX=
LPF= 31.	QVL= 7.	HLL= 2399	AZII=
VTB= .250	VTE= .168	FLL= -20.	RNG=
OPB= 0.	OPE= 100.	FLH= 0	MLT=

14.24.29.

08/08/82

Figure I-7

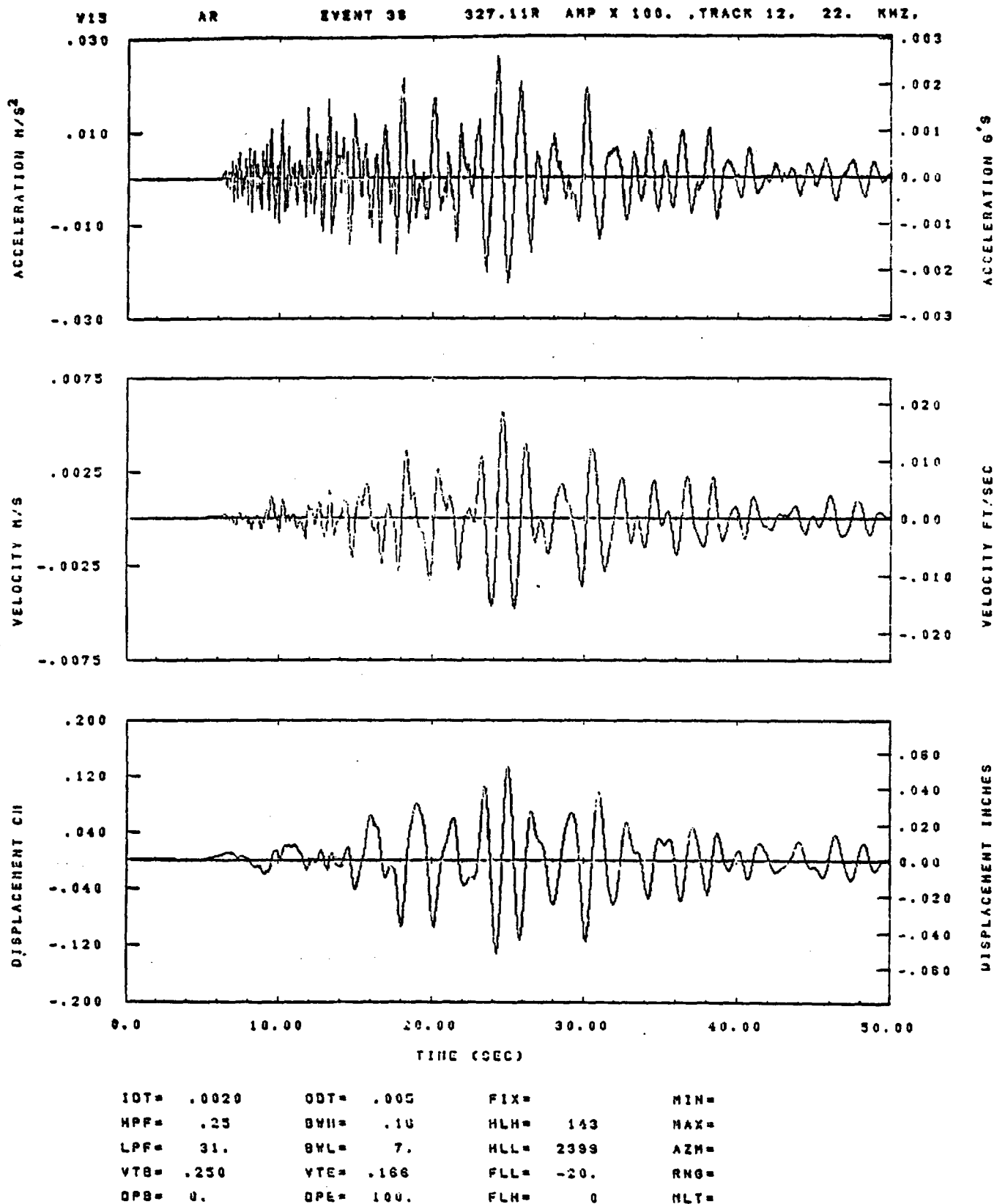


IDT= .0020	ODT= .005	FIX=	MIN=
HPF= .25	BWH= .16	HLH= 143	MAX=
LPF= 31.	BVL= 7.	HLL= 2399	AZH=
VTB= .250	VTE= .166	FLL= -20.	RNG=
OPB= 0.	DPE= 100.	FLH= 0	HLT=

14.25.20.

08/06/82

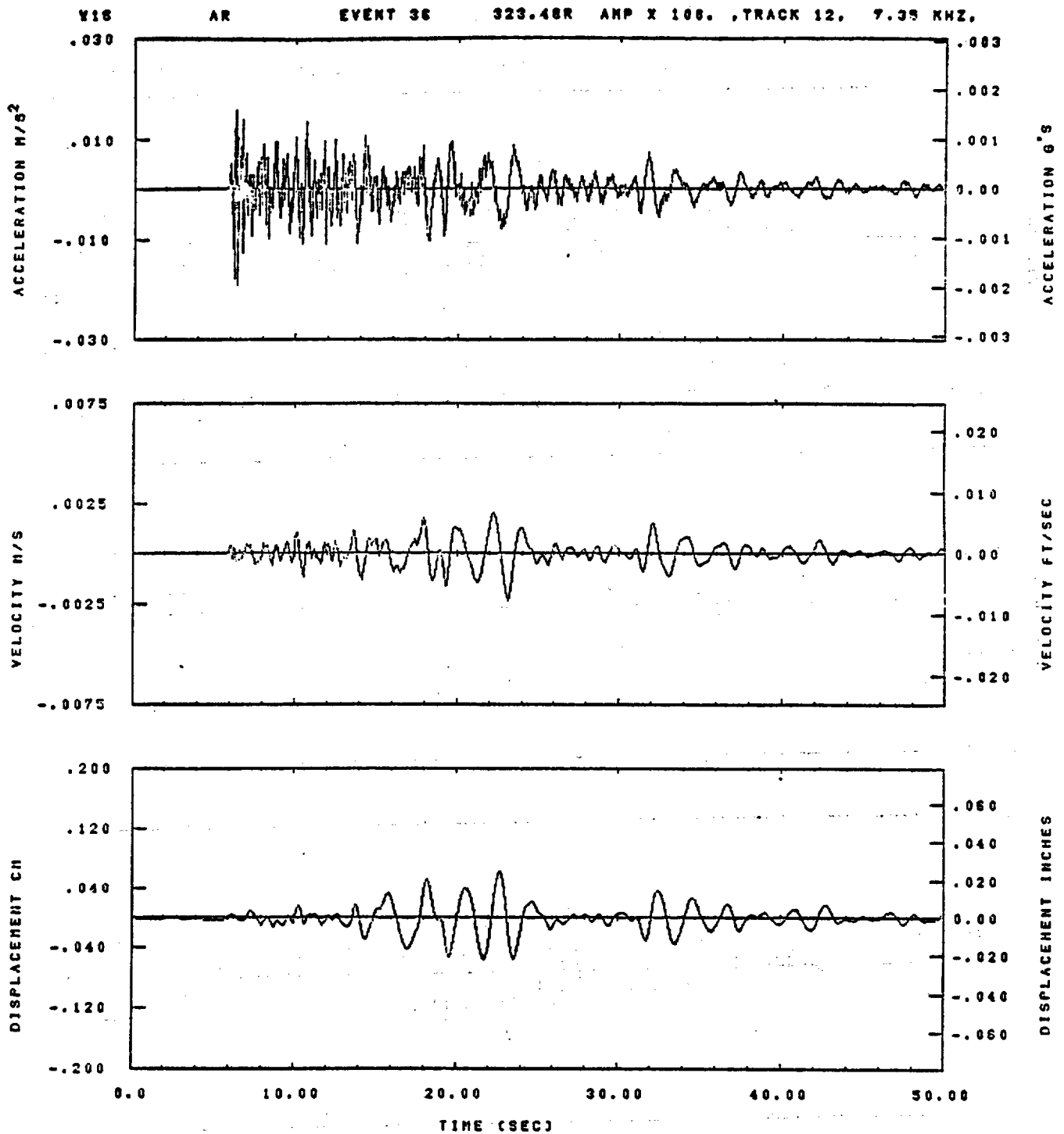
Figure I-8



14.22.35.

08/08/92

Figure I-9

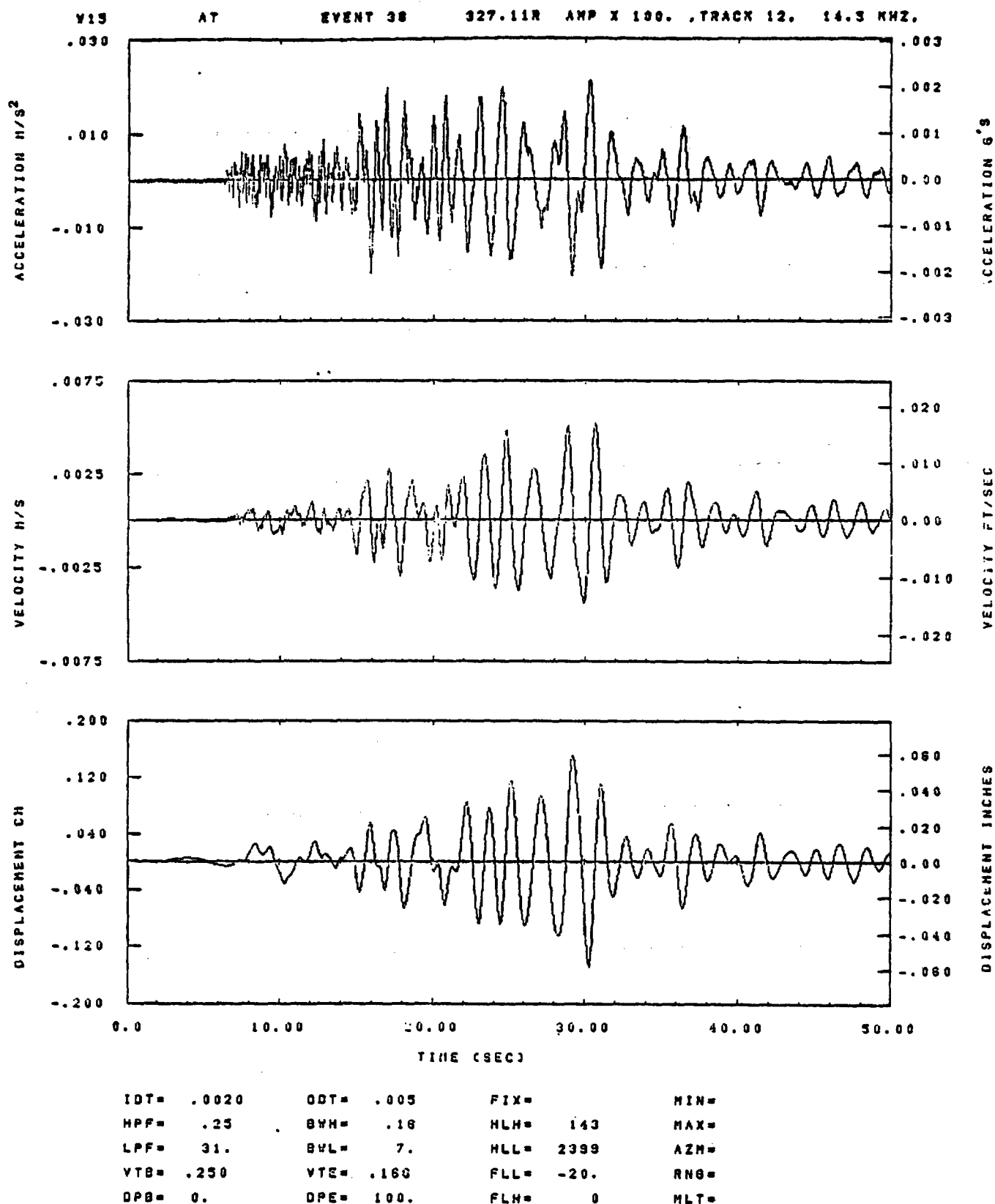


IOT= .0020	OOT= .005	FIX=	MIN=
HPF= .25	BYH= .16	HLN= 143	MAX=
LPF= 31.	BYL= 7.	HLL= 2399	AZM=
VTB= .250	VTE= .168	FLL= -20.	RNG=
DPB= 0.	DPE= 100.	FLH= 0	MLT=

14.24.56.

08/06/82

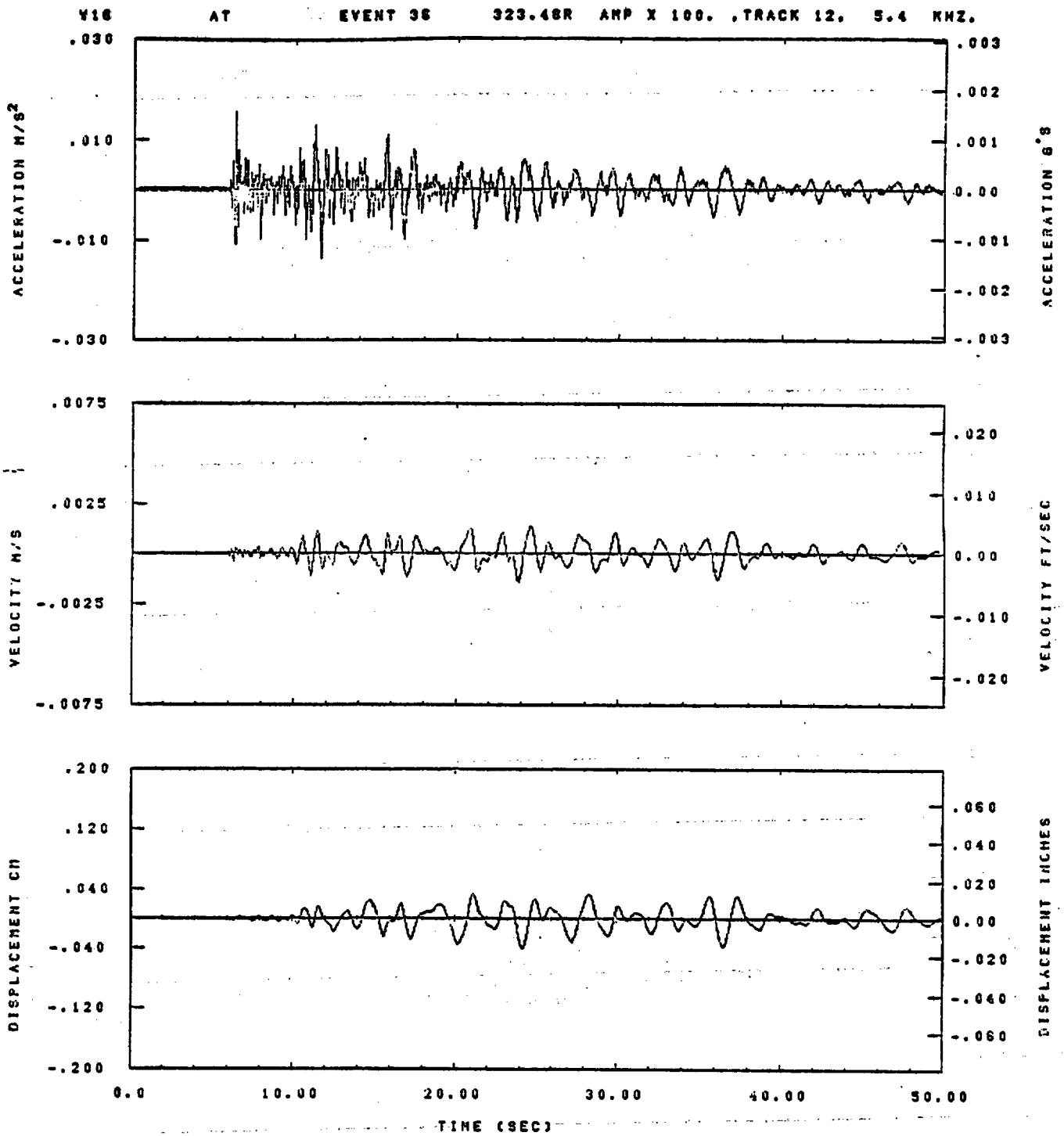
Figure I-10



14.23.07.

09/08/82

Figure I-11

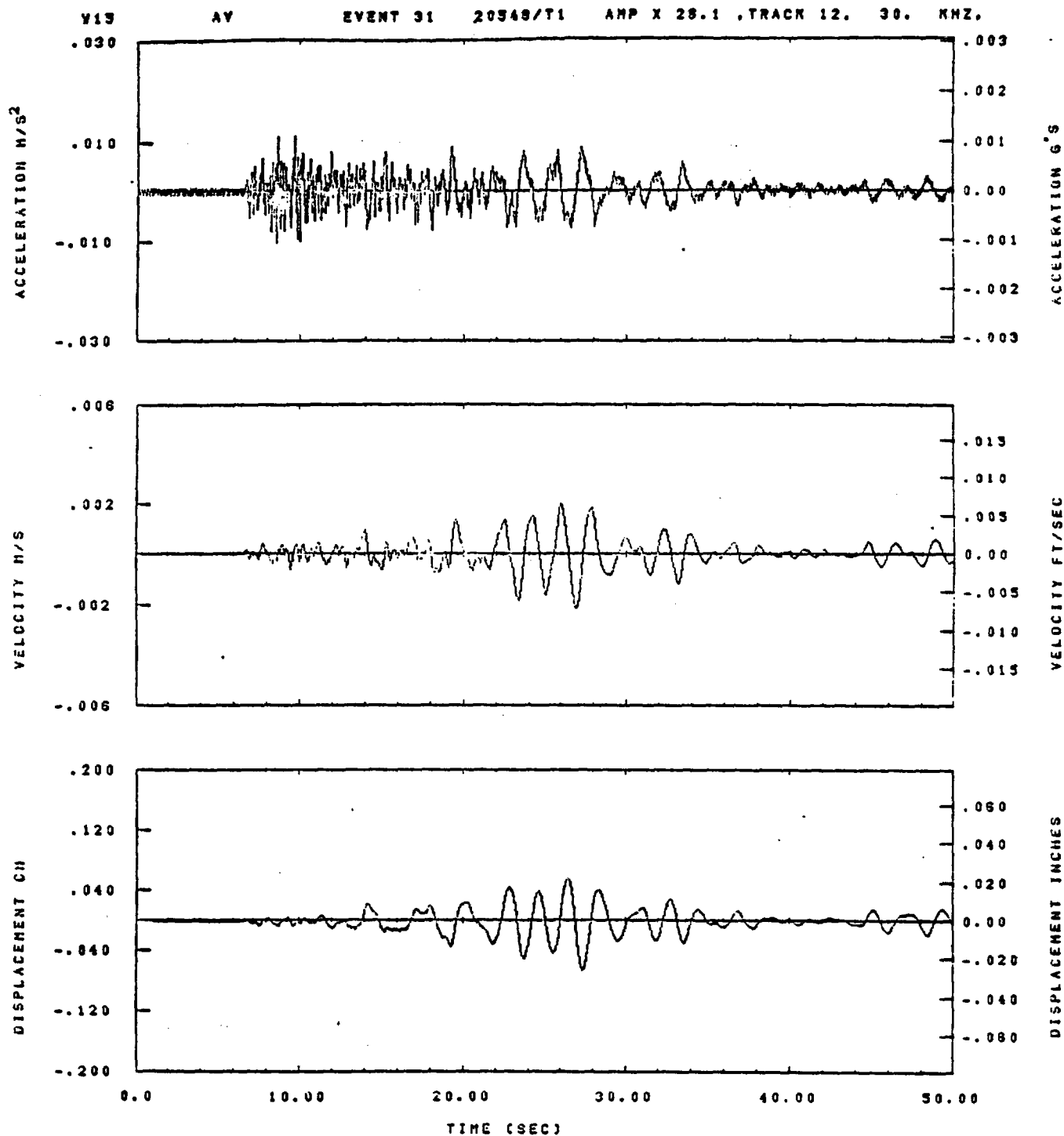


IDT= .0020	ODT= .005	FIX=	MIN=
HPF= .25	BYH= .18	HLH= 143	MAX=
LPF= 31.	BYL= 7.	HLL= 2399	AZH=
VTB= .250	VTE= .168	FLL= -20.	RNB=
OPB= 0.	DPE= 100.	FLH= 0	MLT=

14.25.13.

08/06/82

Figure I-12

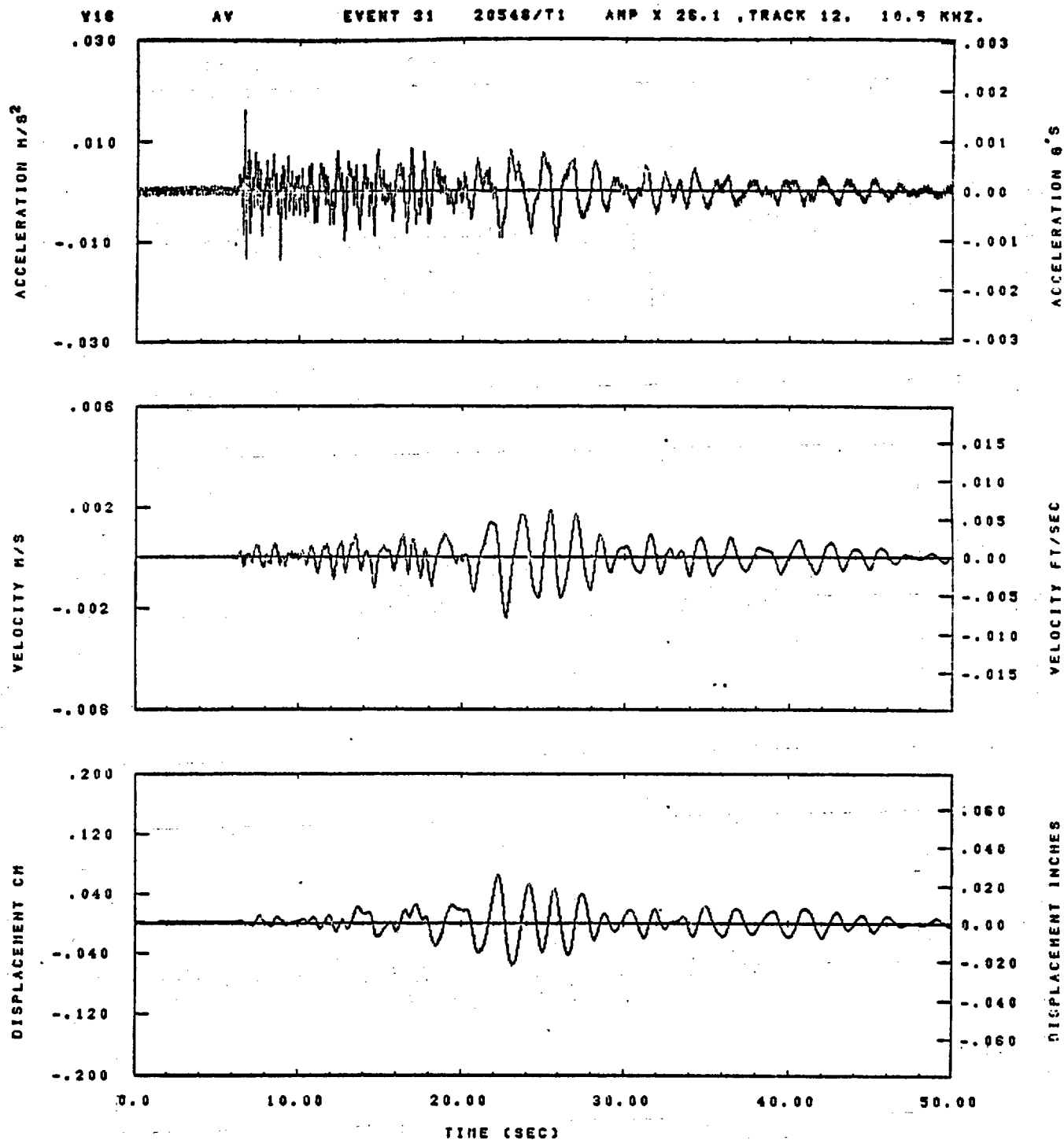


IDT= .0020	ODT= .005	FIX=	MIN=
HPF= .25	GVH= .18	HLH= 143	MAX=
LPF= 31.	BVL= 7.	HLL= 2399	AZN=
YTD= .250	YTE= .186	FLL= -20.	RNS=
DPB= 0.	OPE= 100.	FLH= 0	MLT=

14.03.91.

08/08/92

Figure I-13

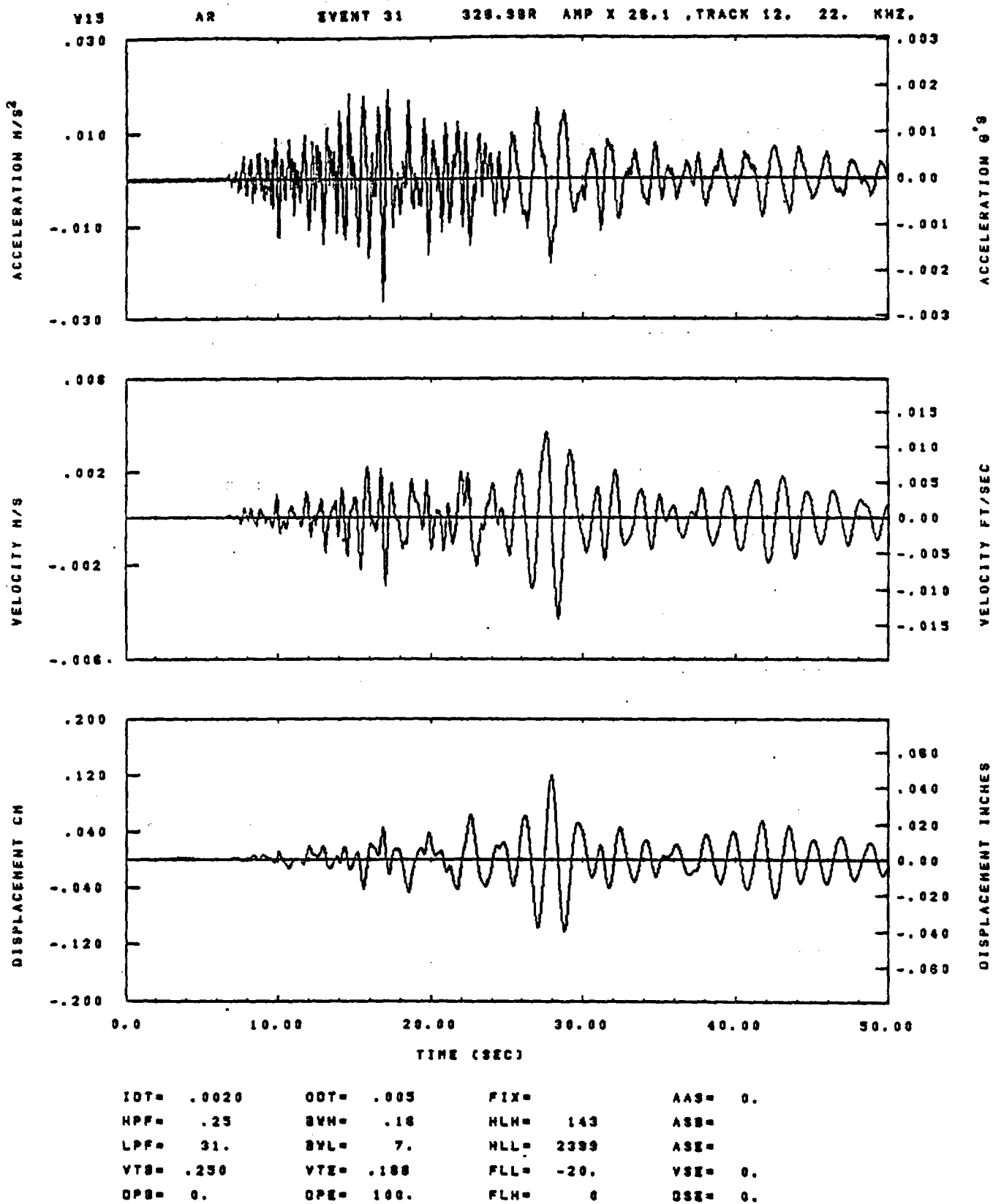


IDT= .0020	ODT= .005	FIX=	MIN=
HPF= .25	BYH= .16	HLH= 143	MAX=
LPF= 31.	BYL= 7.	NLL= 2399	AZN=
VTB= .250	VTE= .166	FLL= -20.	RNG=
DPB= 0.	DPE= 100.	FLH= 0	MLT=

14.03.58.

08/06/82

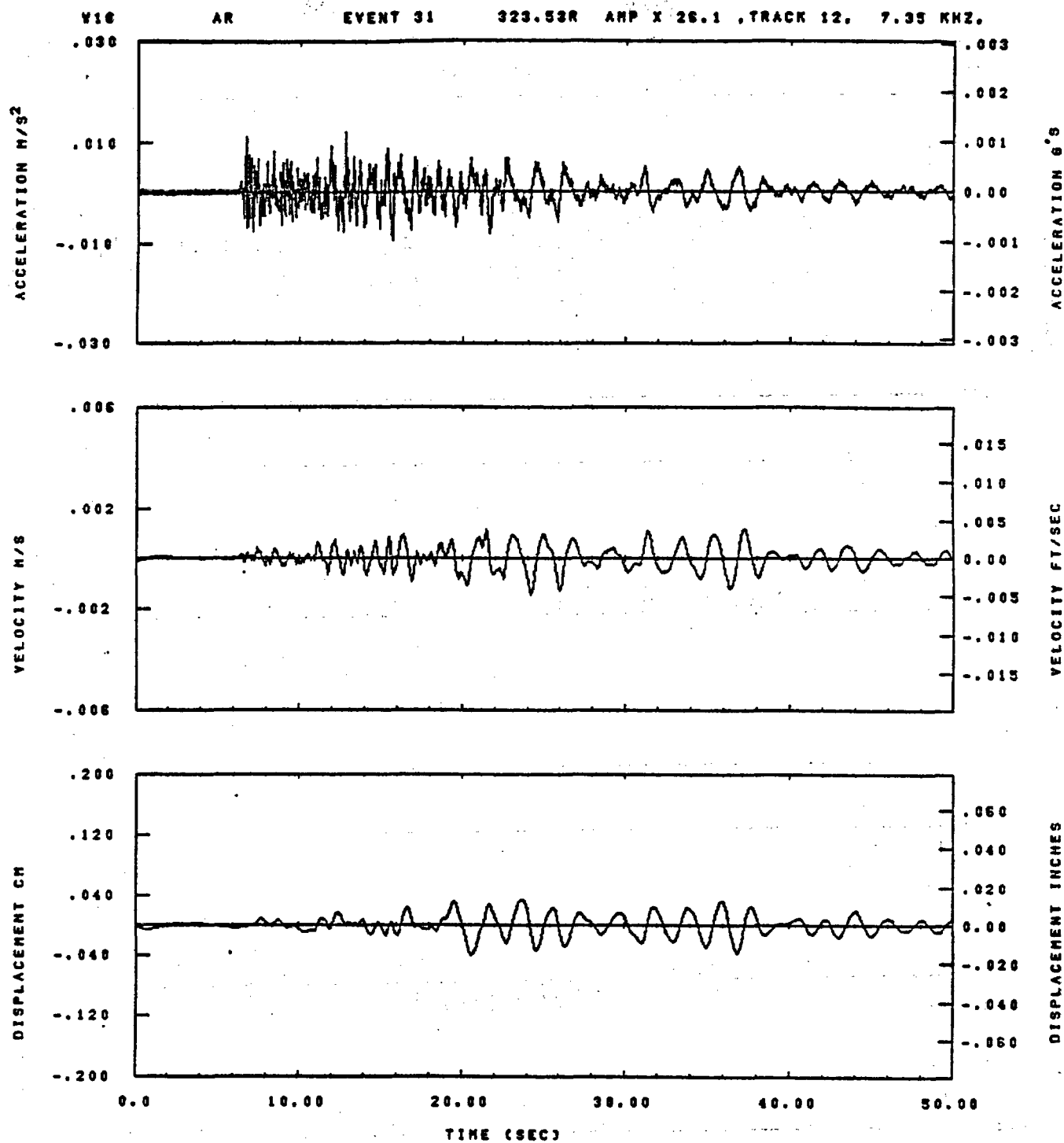
Figure I-14



15.39.41.

08/23/82

Figure I-15

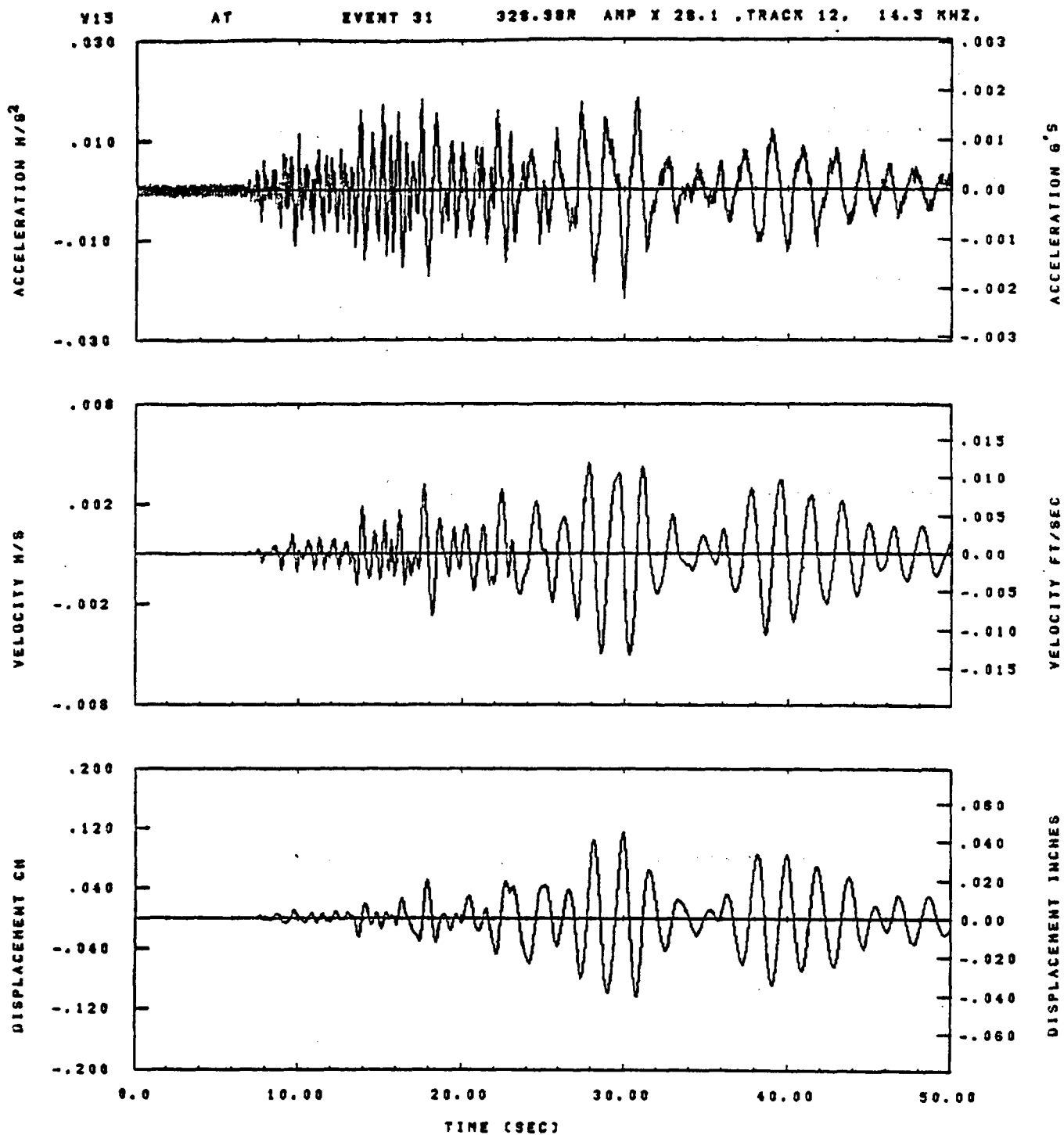


IDT= .0020	ODT= .005	FIX=	AAS= 0.
HPP= .25	BYH= .16	HLH= 143	ASB=
LPP= 31.	BYL= 7.	HLL= 2388	ASE=
VTE= .250	VTE= .166	FLL= -20.	VSE= 0.
DPS= 0.	DPE= 188.	FLH= 0	DSE= 0.

15.43.47.

06/23/62

Figure I-16

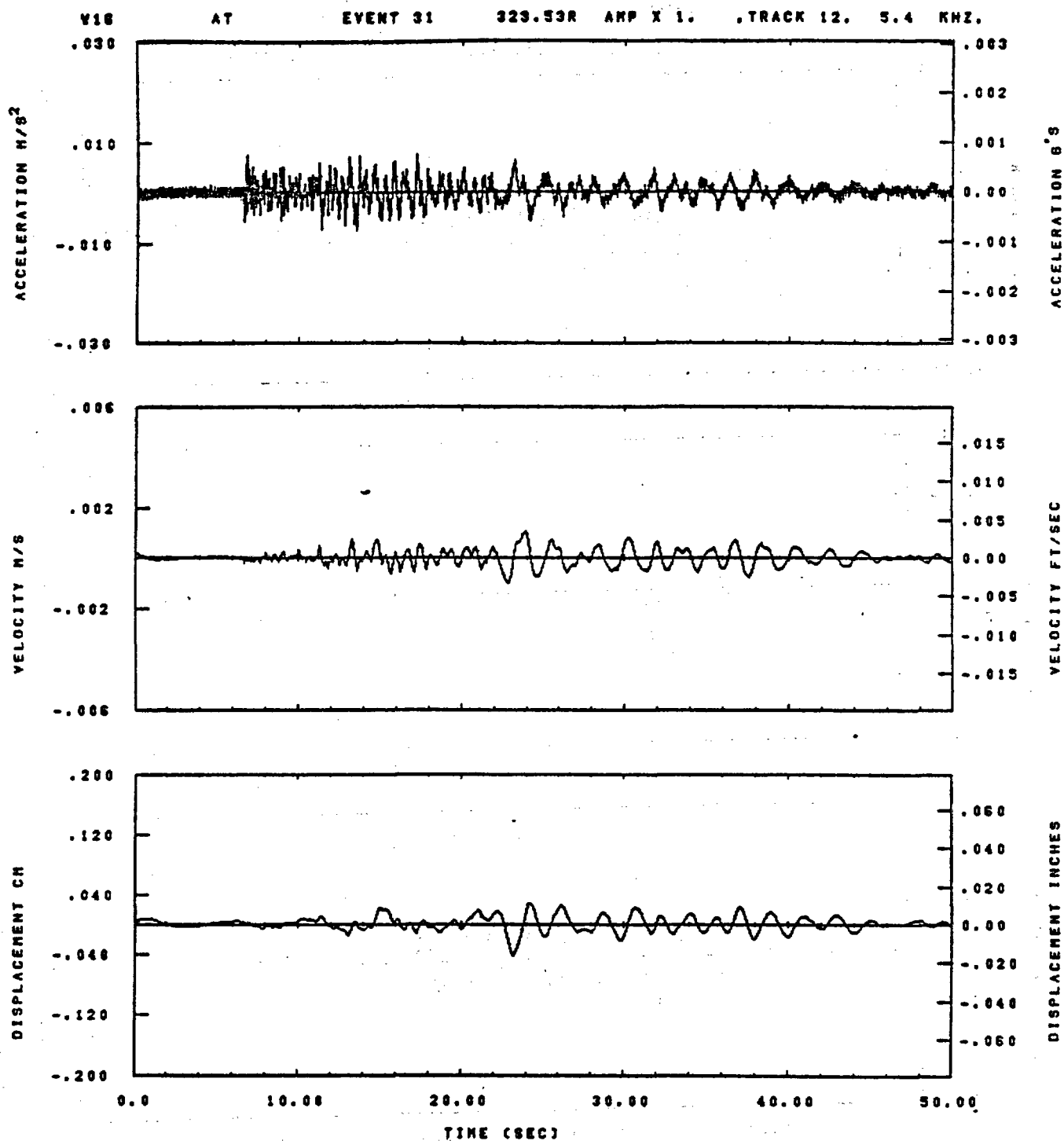


IDT= .0020	OOT= .003	FIX=	AAS= 0.
HPP= .25	SVH= .18	HLH= 143	ASS=
LPP= 31.	SVL= 7.	HLL= 2399	ASE=
VTS= .250	VTE= .188	FLL= -20.	VSE= 0.
DPS= 0.	DPE= 100.	FLH= 0	DSE= 0.

13.39.50.

08/23/82

Figure I-17

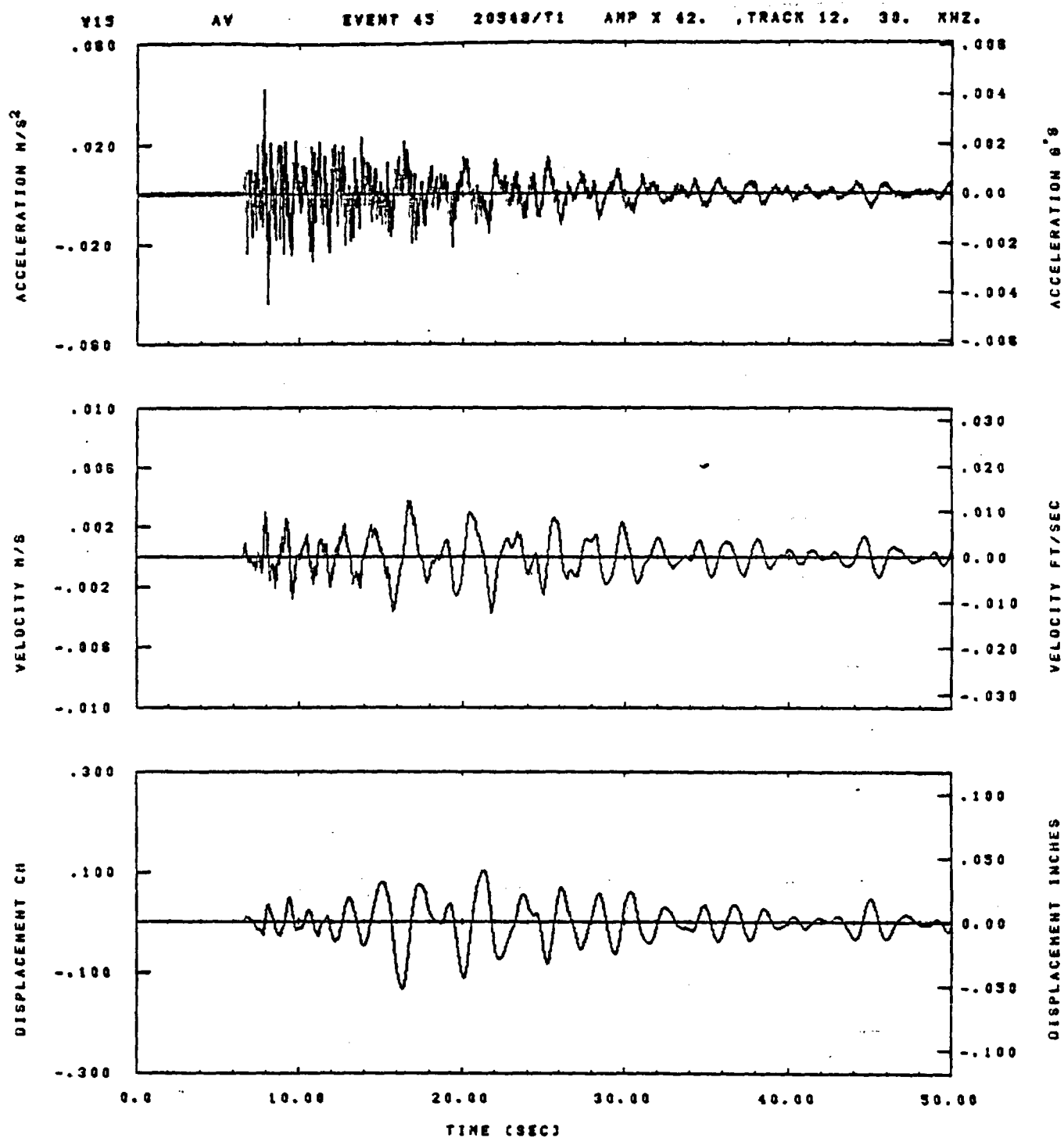


IDT= .0020	ODT= .005	FIX=	AAS= 0.
HPF= .25	BYH= .16	HLH= 143	ASS=
LPF= 31.	BYL= 7.	HLL= 2388	ASE=
VTE= .250	VTE= .166	FLL= -20.	VSE= 0.
DPE= 0.	DPE= 166.	FLH= 0	DSE= 0.

15.43.52.

06/23/82

Figure I-18

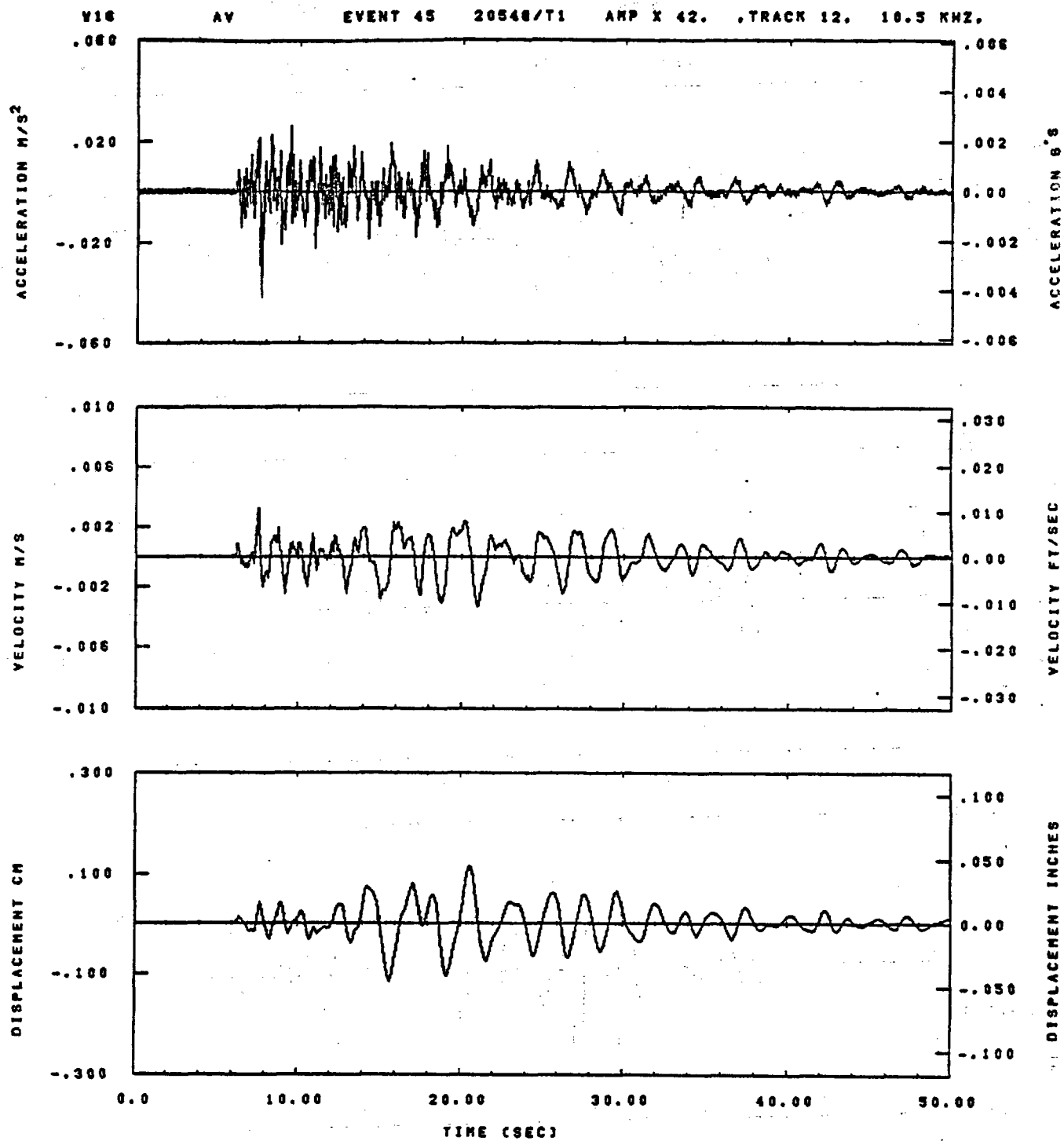


IDT= .0020	ODT= .005	FIX=	AAS= 0.
HPP= .20	BYH= .13	HLH= 99	ASS=
LPP= 45.	BYL= 10.	HLL= 2999	ASE=
VTB= .200	VTE= .133	FLL= -20.	VSE= 0.
DPB= 0.	DPE= 100.	FLH= 0	DSE= 0.

09.32.42.

08/23/82

Figure I-19

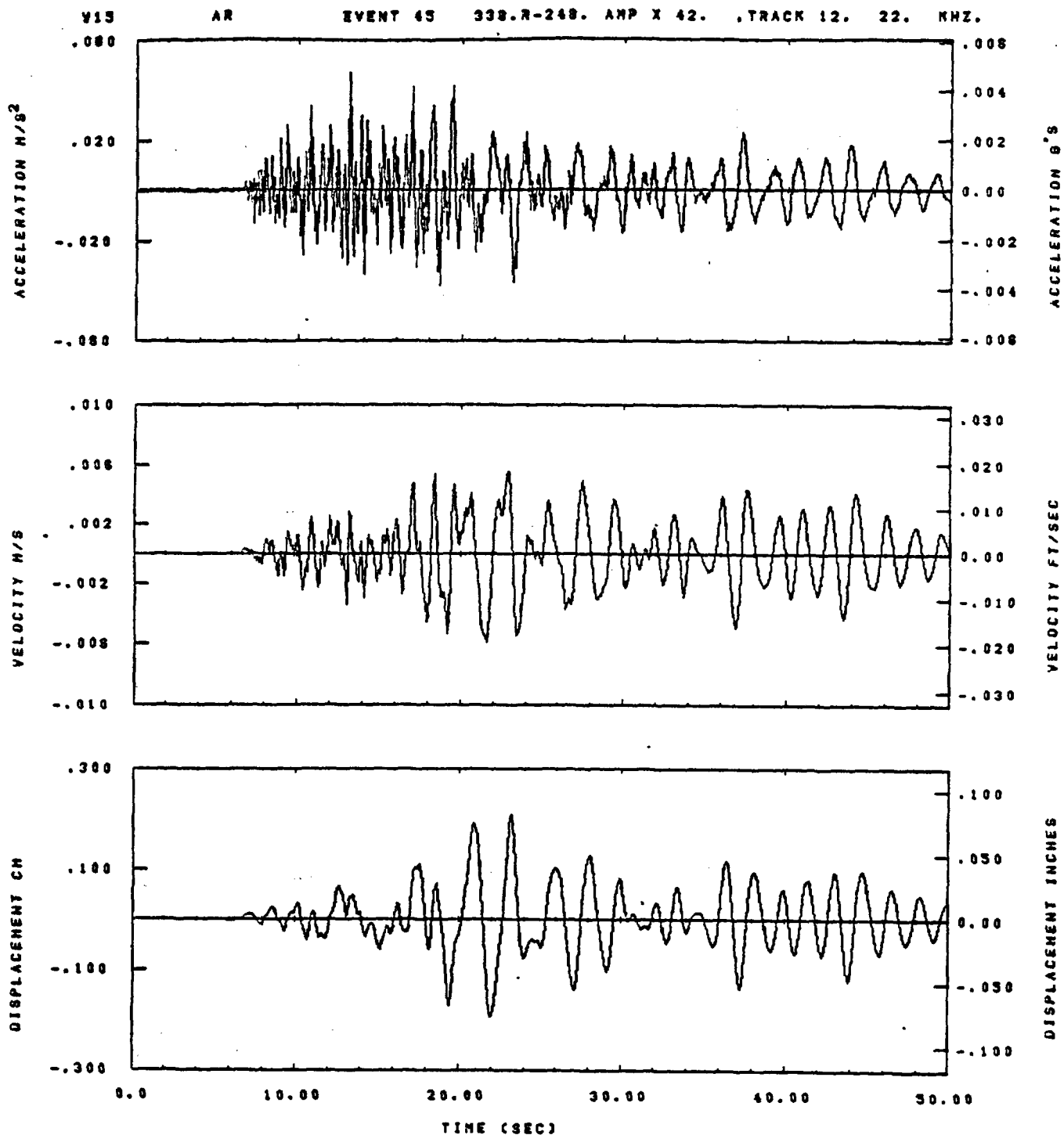


IDT= .0020	ODT= .005	FIX=	AAS= 0.
HPP= .20	BVH= .13	HLH= 89	ASS=
LPP= 45.	BYL= 10.	HLL= 2998	ASE=
VTS= .200	VTE= .133	FLL= -20.	VSE= 0.
DPS= 0.	DPE= 100.	FLH= 0	DSE= 0.

06.33.15.

06/23/82

Figure I-20

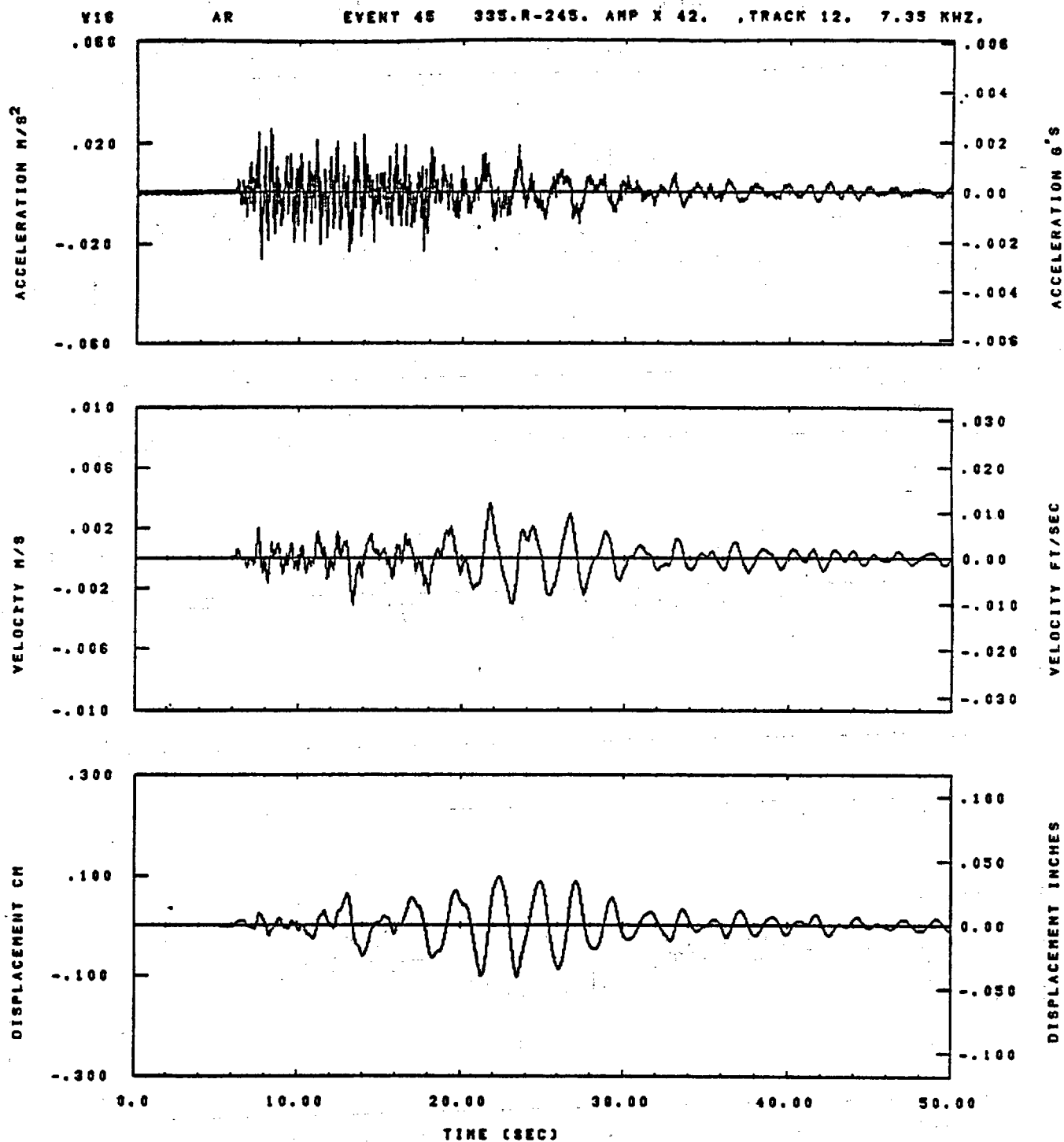


IDT= .0020	ODT= .005	FIX=	AAS= 0.
HPP= .20	BVH= .13	HLH= 99	ASS=
LPP= 45.	BVL= 10.	HLL= 2999	ASE=
VTS= .200	VTE= .133	FLL= -20.	VSE= 0.
OPB= 0.	OPE= 100.	FLH= 0	DSE= 0.

08.52.57.

08/23/82

Figure I-21

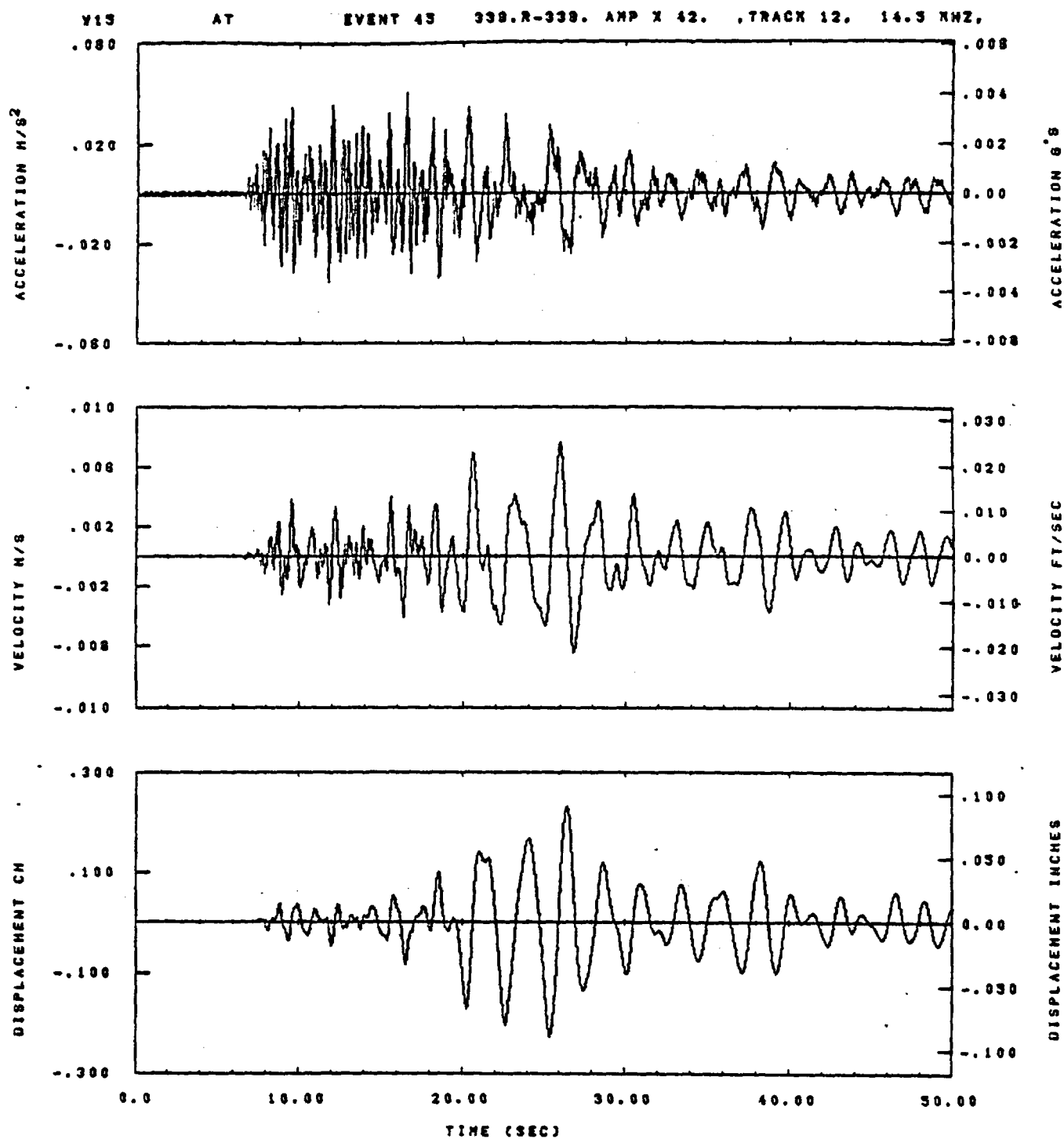


IDT= .0020	ODT= .005	FIX=	AAS= 0.
HPP= .20	SVH= .13	HLH= 33	ASB=
LPP= 45.	SVL= 10.	HLL= 2998	ASE=
VTB= .200	VTE= .133	FLL= -20.	VSE= 0.
DPS= 0.	DPE= 100.	FLH= 0	DSE= 0.

06.53.22.

06/23/82

Figure I-22

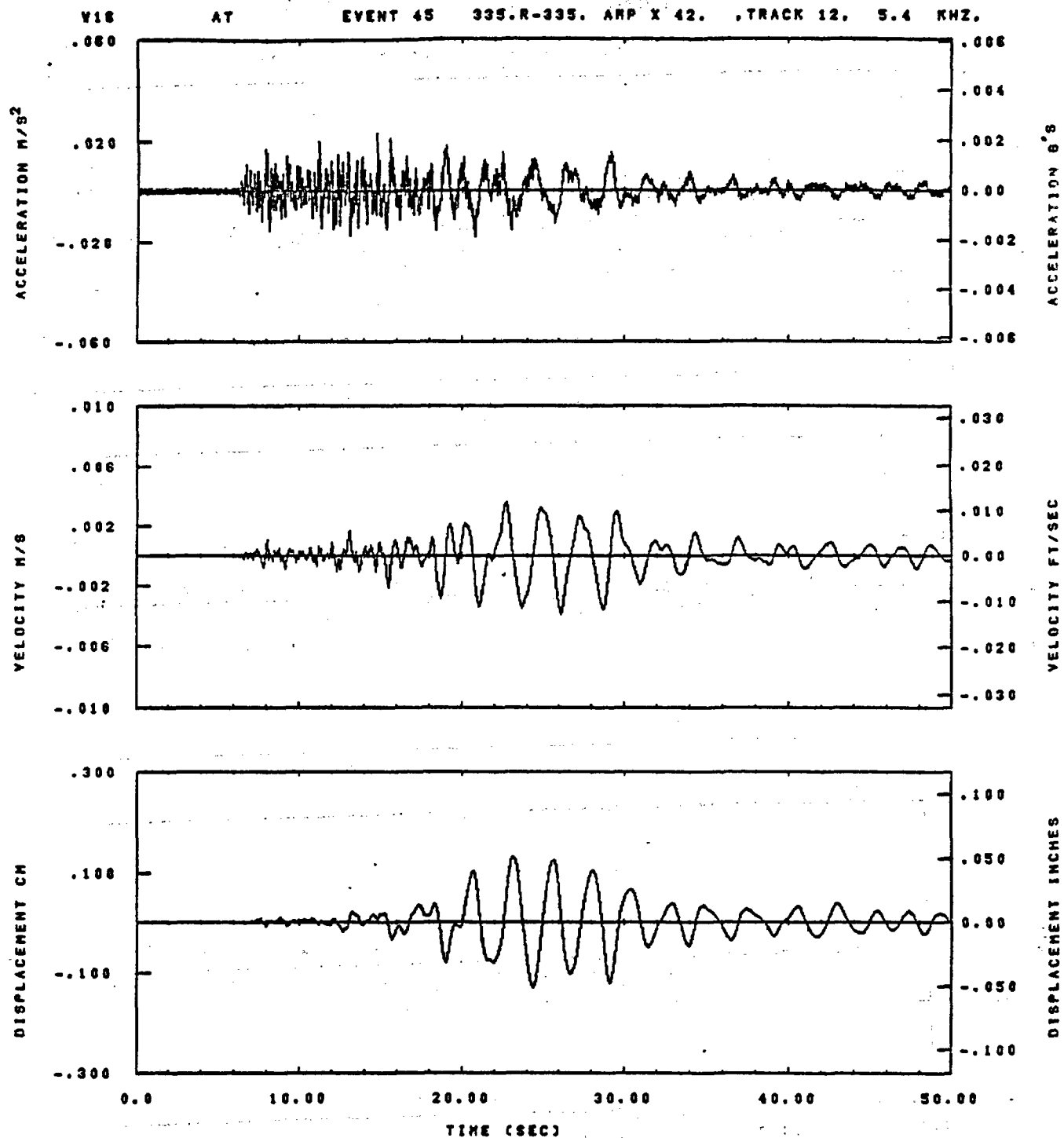


IDT= .0020	ODT= .005	FIX=	AAS= 0.
HPF= .20	BYH= .13	HLH= 99	ASB=
LPF= 45.	BYL= 10.	HLL= 2999	ASE=
VTS= .200	VTE= .133	FLL= -20.	VSE= 0.
OPB= 0.	OPE= 100.	FLH= 0	DSE= 0.

08.53.07.

08/23/82

Figure I-23

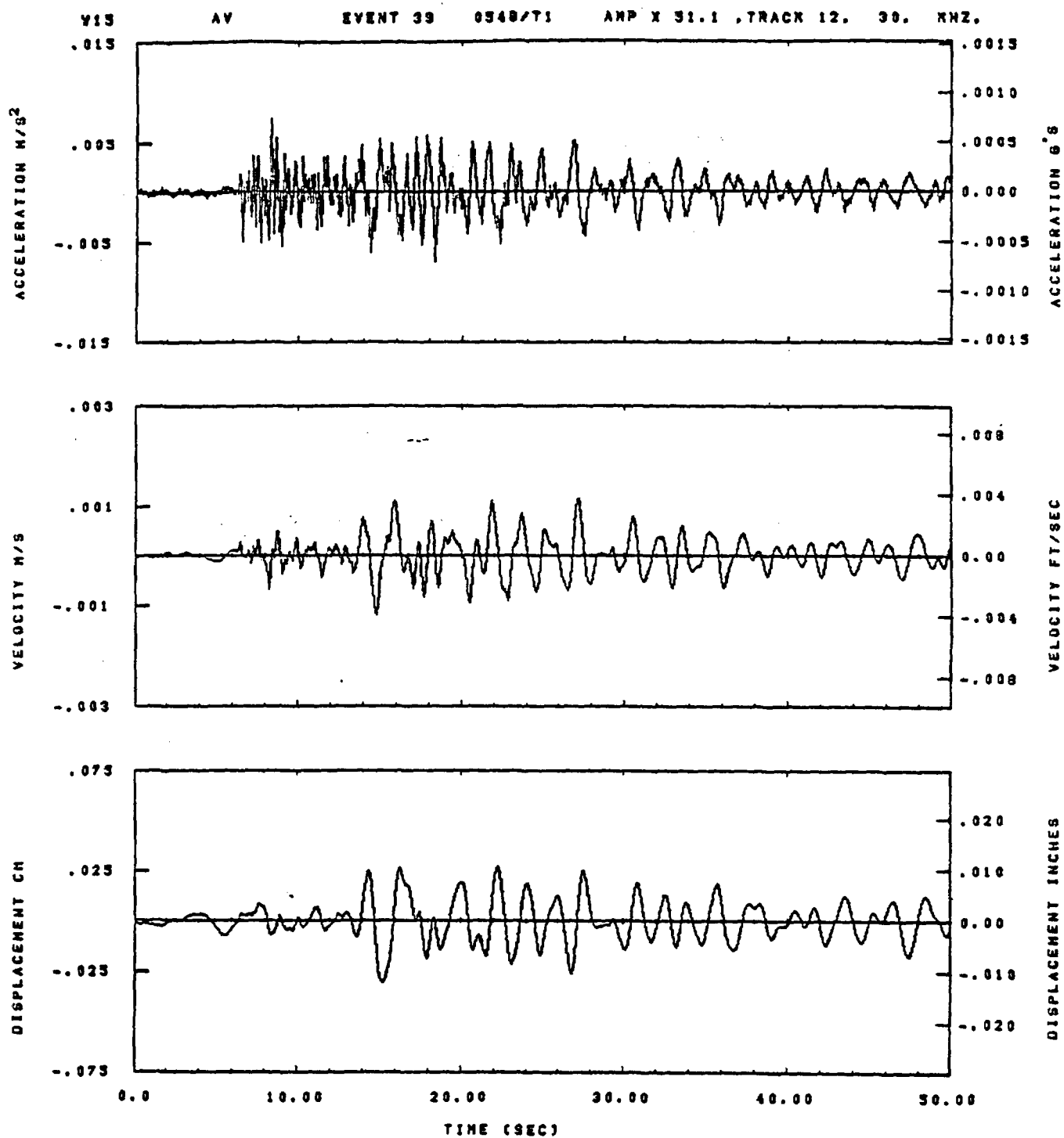


IDT= .0020	ODT= .005	FIX=	AAS= 0.
HPF= .20	BYH= .13	HLH= 99	ASB=
LPF= 45.	BYL= 10.	HLL= 2999	ASE=
VTS= .200	VTE= .133	FLL= -20.	VSE= 0.
DPS= 0.	DPE= 100.	FLH= 0	DSE= 0.

08.53.27.

08/23/82

Figure I-24

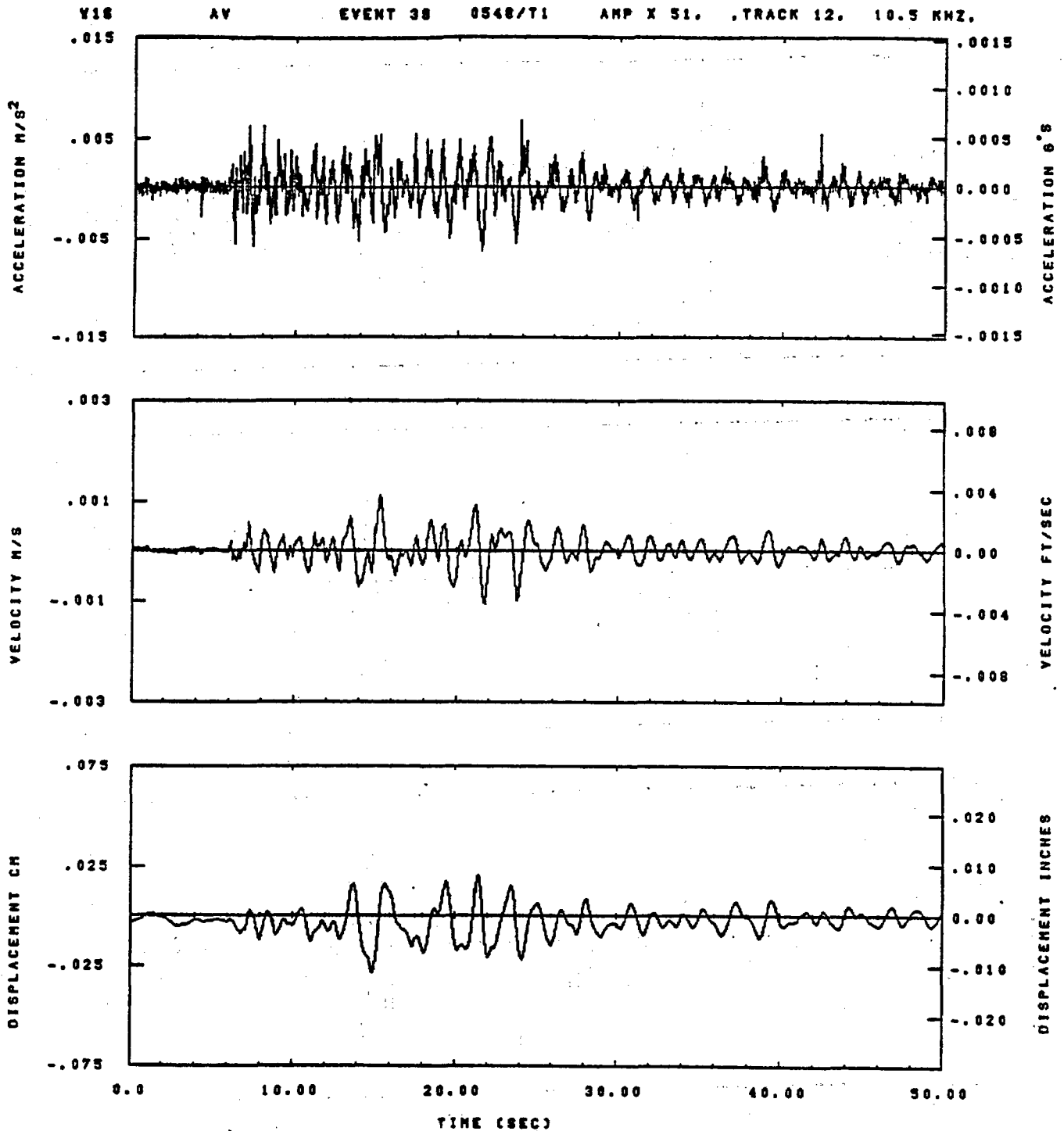


IDT= .0020	OOT=	FIX=	AAS= 0.
HPP= .30	BYH= .20	HLH= 249	ASS=
LPP= 18.	BVL= 4.	HLL= 1999	ASE=
VTS= .300	VTE= .200	FLL= -20.	VSE= 0.
OPB= 0.	OPE= -100.	FLH= 0	OSE= 0.

08.01.19.

08/24/82

Figure I-25

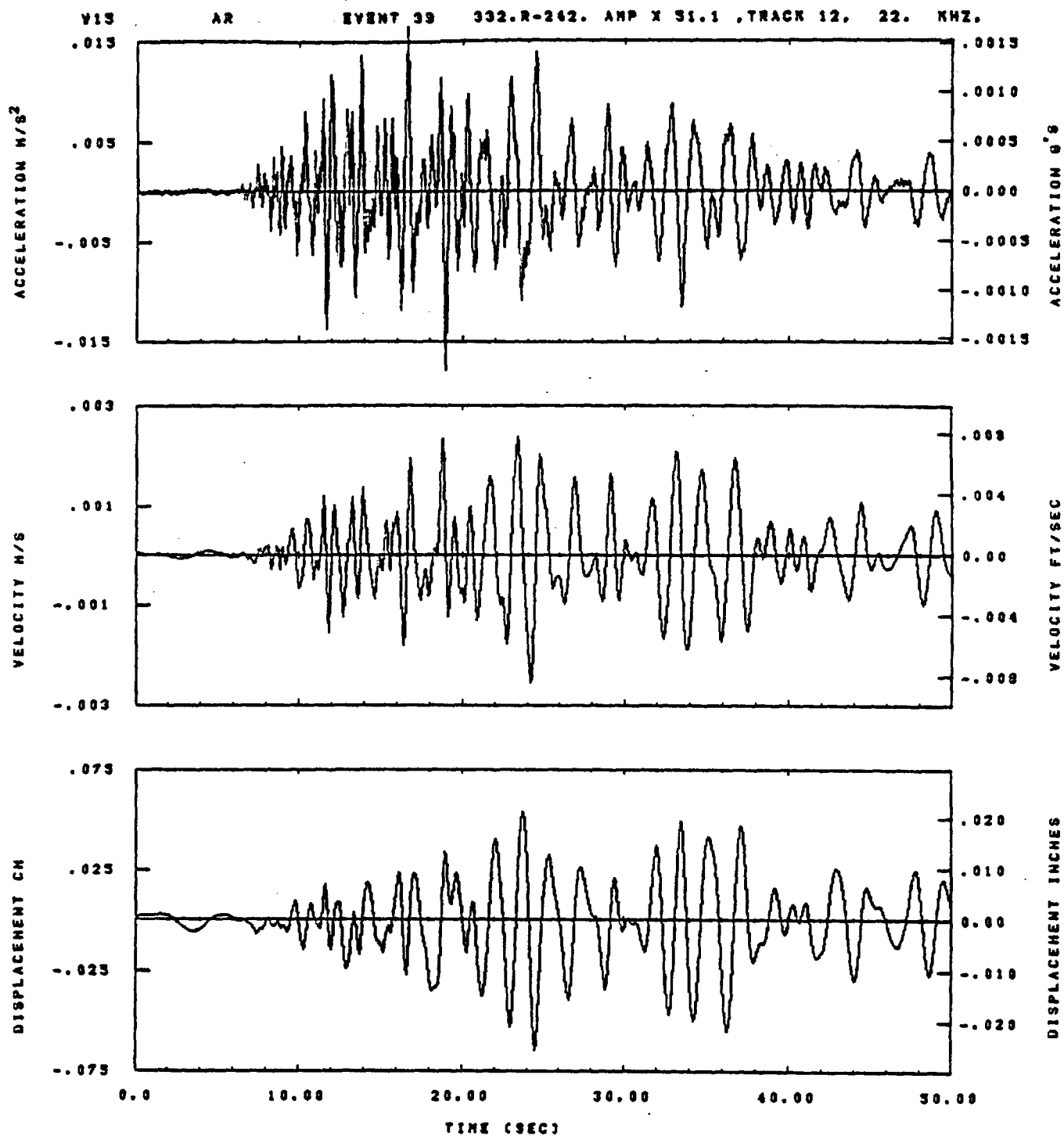


IDT= .0020	ODT=	FIX=	AAS= 0.
HPF= .30	BYH= .20	HLH= 249	ASB=
LPF= 18.	BYL= 4.	HLL= 1998	ASE=
YTS= .300	YTE= .208	FLL= -20.	VSE= 0.
DPS= 0.	DPE= 100.	FLH= 0	DSE= 0.

08.01.37.

06/24/82

Figure I-26

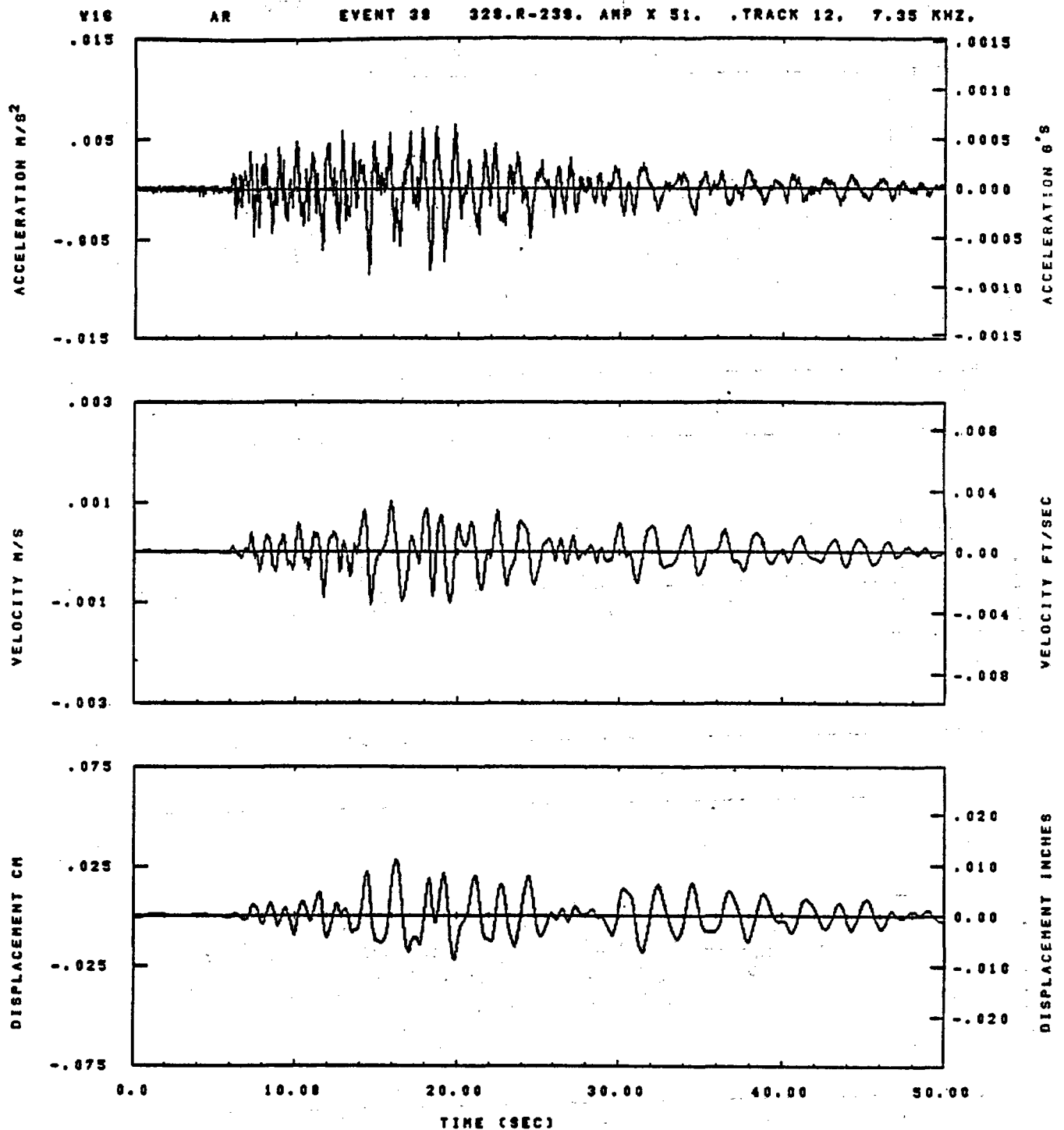


IDT= .0020	ODT=	FIX=	AAS= 0.
HPF= .30	BYN= .20	HLH= 249	ASB=
LPF= 19.	BYL= 4.	HLL= 1999	ASE=
VTB= .300	VTE= .200	FLL= -20.	VSE= 0.
DPS= 0.	DPE= 100.	FLH= 8	DSE= 0.

09.01.11.

08/24/92

Figure I-27

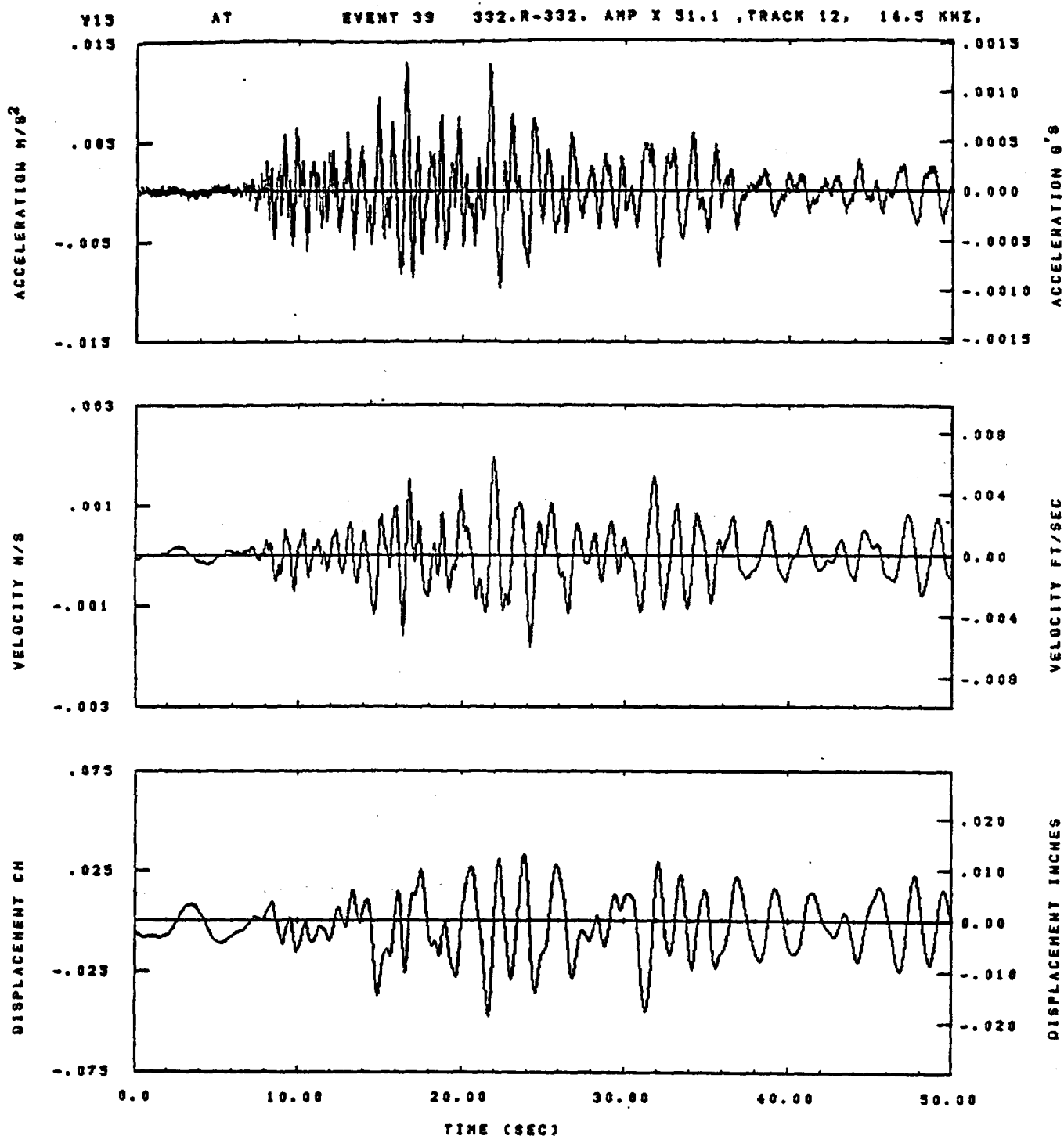


IDT= .0020	ODT=	FIX=	AAS= 0.
HPF= .30	BYH= .20	HLH= 248	ASB=
LPF= 18.	BYL= 4.	HLL= 1889	ASE=
VTS= .300	VTE= .200	FLL= -20.	VSE= 0.
DPS= 0.	DPE= 100.	FLH= 0	DSE= 0.

08.01.23.

06/24/82

Figure I-28

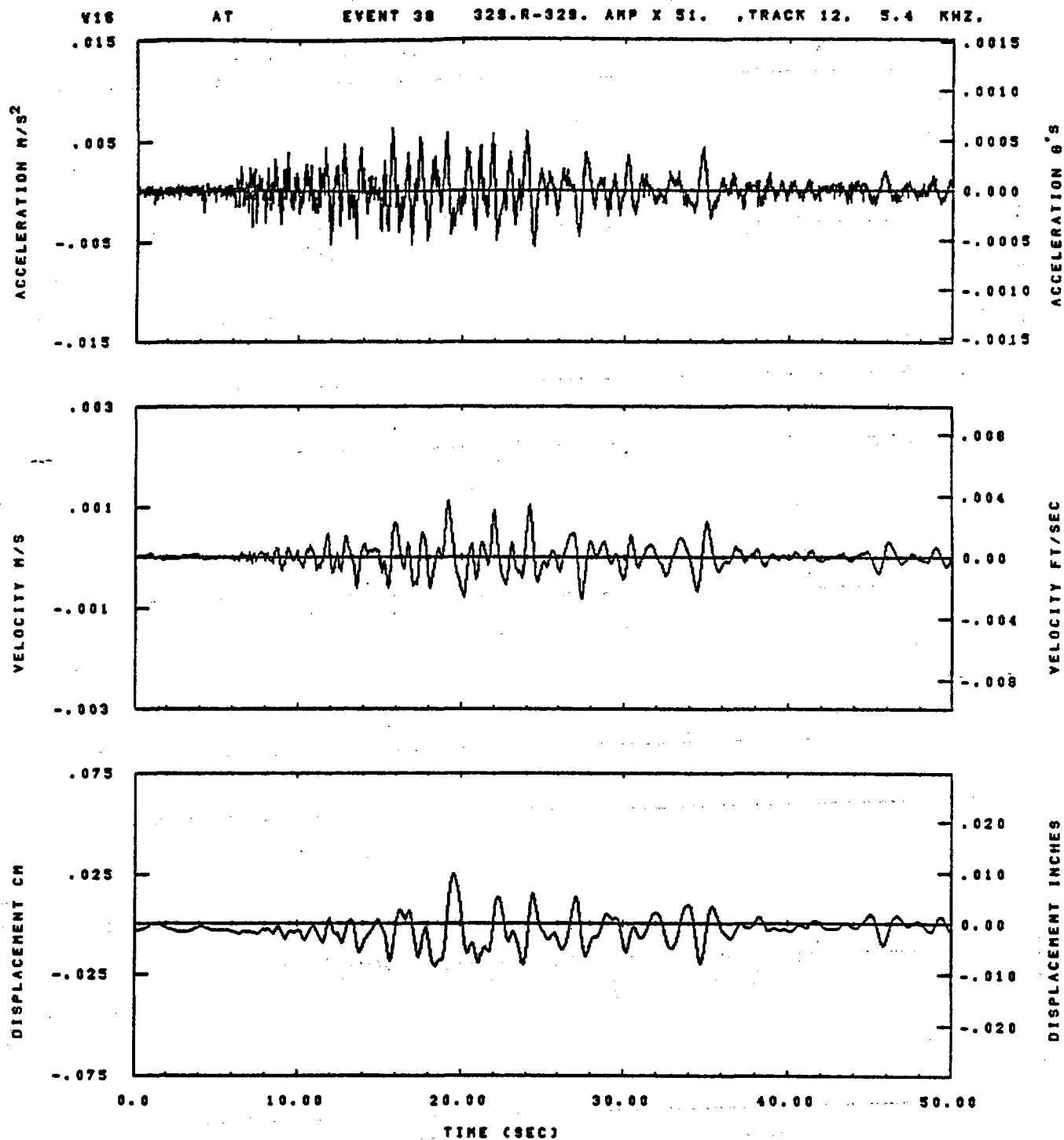


IDT= .0020	OOT=	FIX=	AAS= 0.
HPP= .30	BYH= .20	HLH= 249	ASE=
LPP= 10.	BYL= 4.	HLL= 1333	ASE=
VTS= .300	VTE= .200	FLL= -20.	VSE= 0.
DPS= 0.	DPE= 100.	FLH= 0	DSE= 0.

08.01.15.

08/24/82

Figure I-29

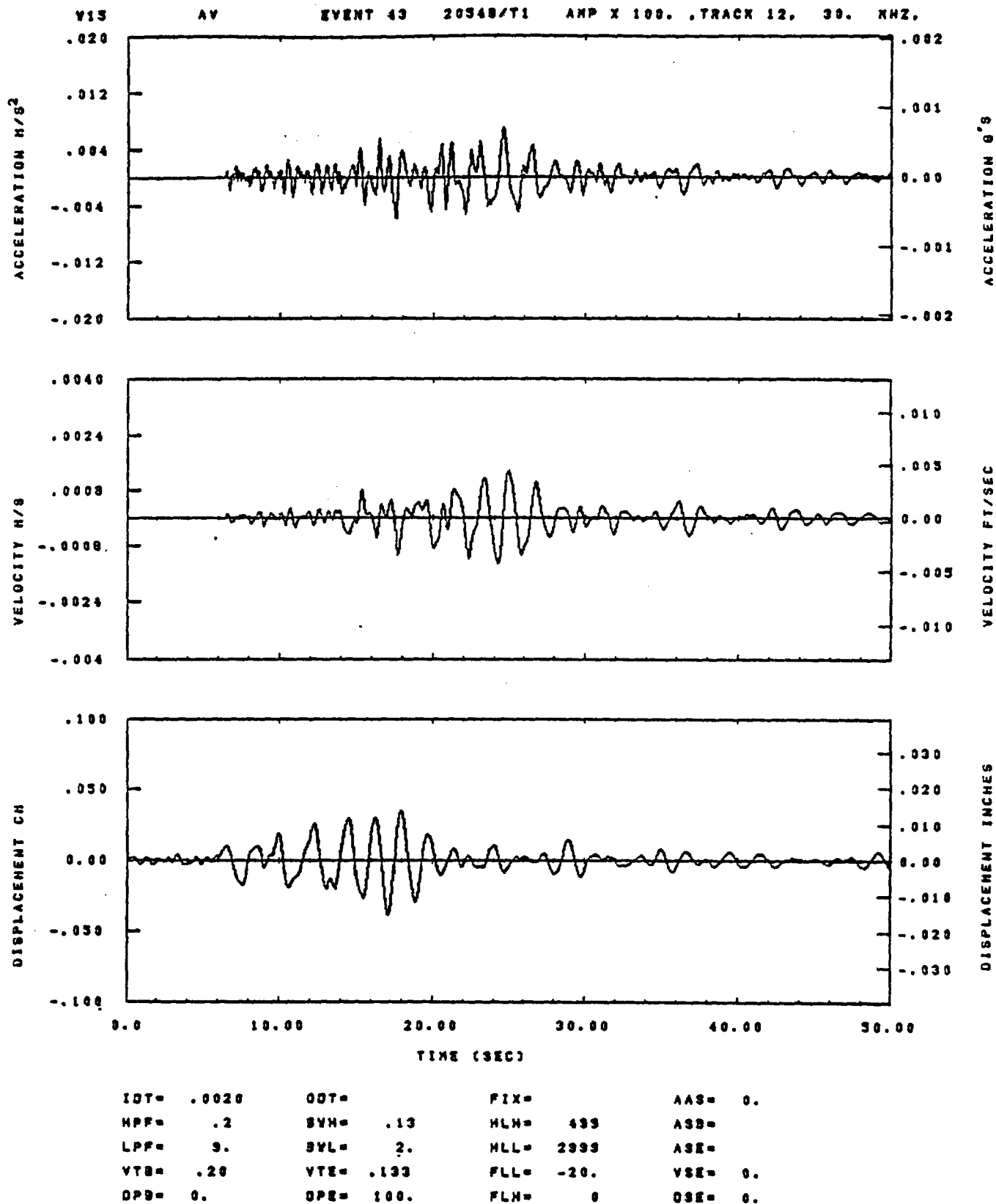


IDT= .0020	ODT=	FIX=	AAS= 0.
HPF= .30	BYN= .20	HLN= 249	ASB=
LPF= 16.	BYL= 4.	HLL= 1888	ASE=
VTS= .300	VTE= .200	FLL= -20.	VSE= 0.
DPS= 0.	DPE= 100.	FLH= 0	DSE= 0.

08.01.33.

06/24/82

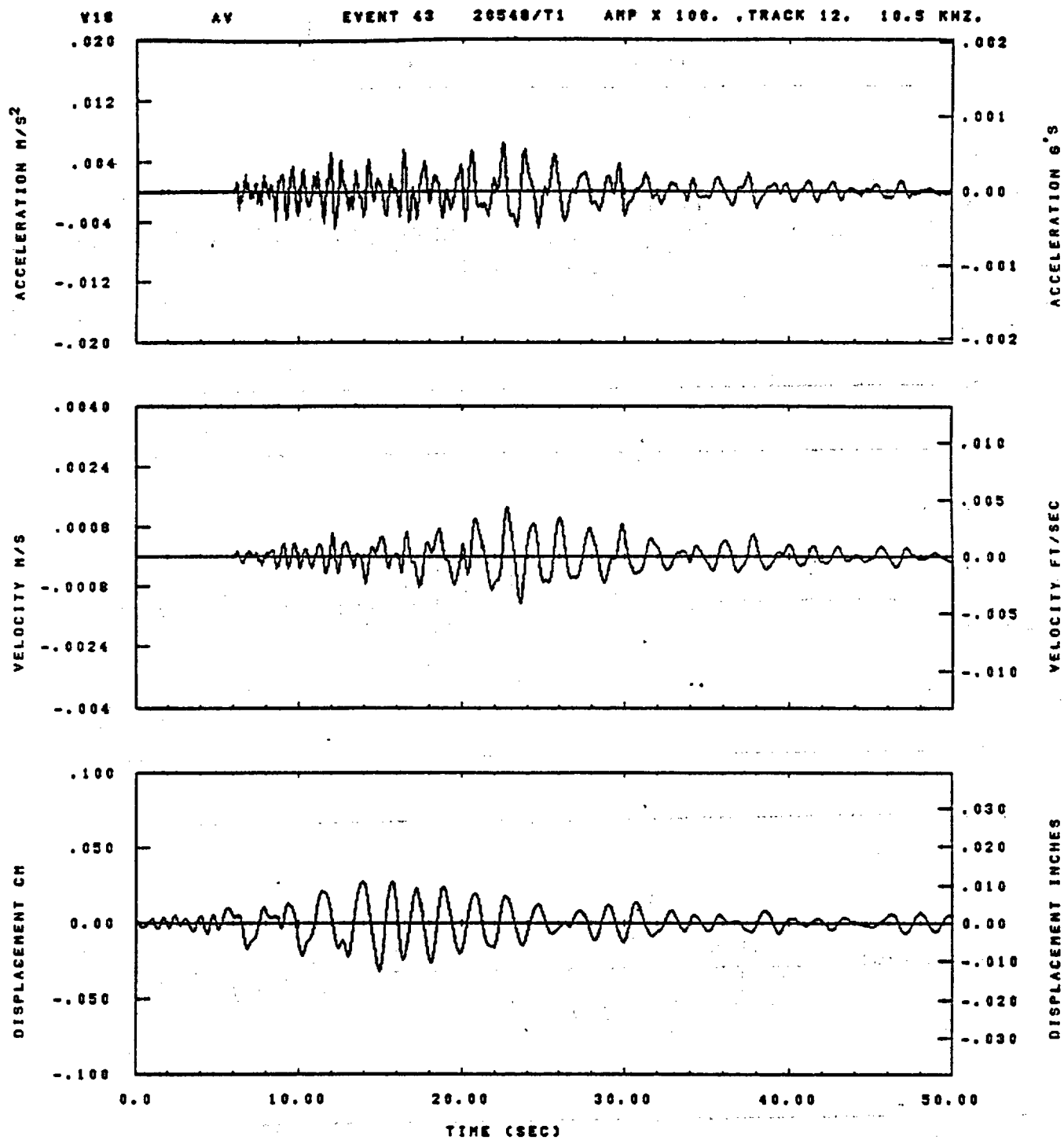
Figure I-30



10.49.33.

08/23/02

Figure I-31

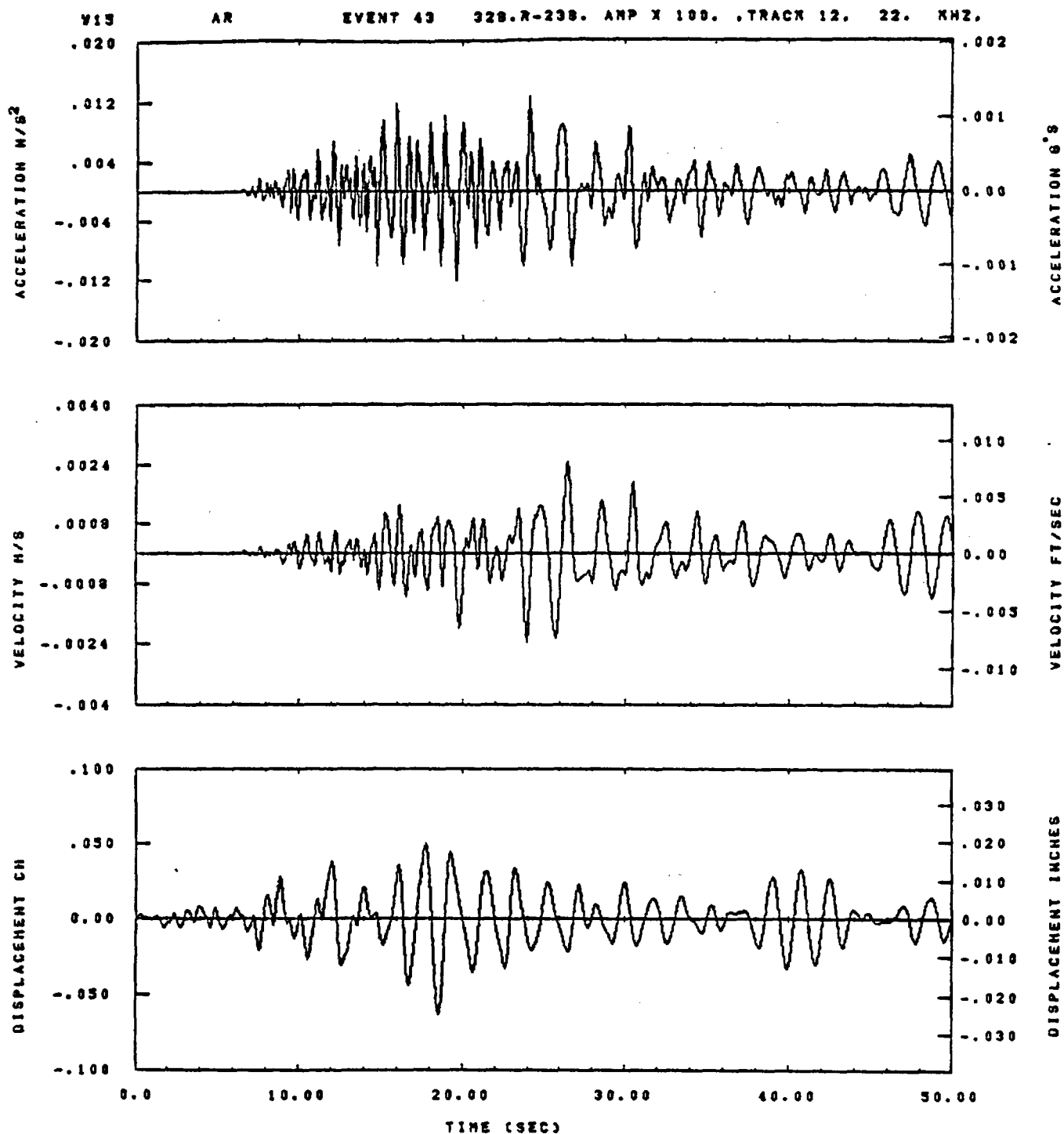


IDT= .0020	ODT=	FIX=	AAS= 0.
HPF= .2	BYH= .13	MLH= 489	ASB=
LPF= 9.	BYL= 2.	MLL= 2988	ASE=
VTB= .20	VTE= .133	FLL= -20.	VSE= 0.
DPS= 0.	OPE= 100.	FLH= 0	DSE= 0.

13.02.46.

06/23/82

Figure I-32

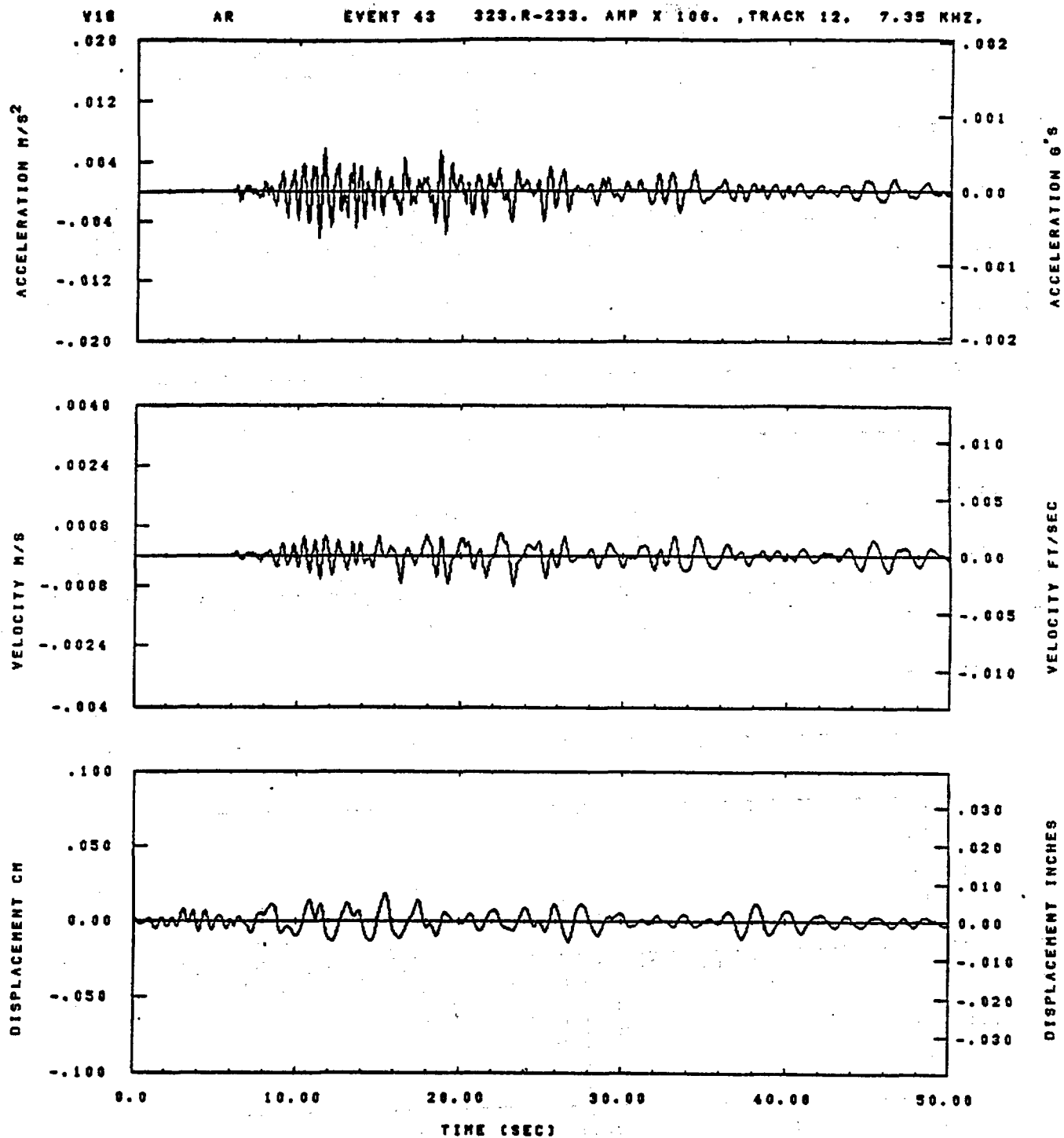


IDT= .0020	QDT=	FIX=	AAS= 0.
HPF= .2	SVH= .13	HLH= 433	ASB=
LPF= 9.	SVL= 2.	HLL= 2999	ASE=
VTB= .20	VTE= .133	FLL= -20.	VSE= 0.
OPB= 0.	OPE= 100.	FLH= 0	OSE= 0.

10.30.03.

08/23/82

Figure I-33

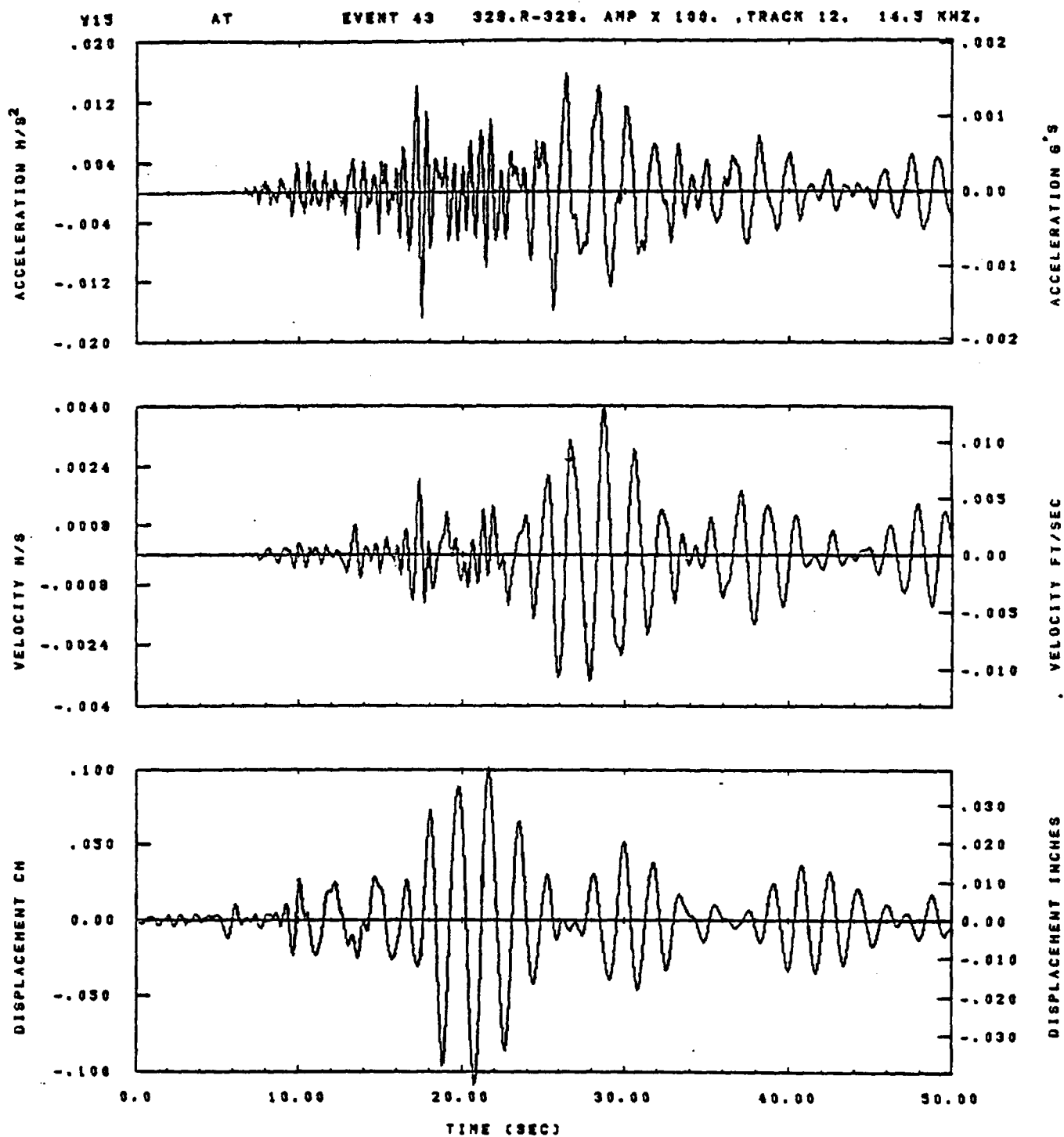


IDT= .0020	ODT=	FIX=	AAS= 0.
HPF= .2	BYH= .13	HLH= 499	ASB=
LPF= 8.	BYL= 2.	HLL= 2998	ASE=
VTS= .20	VTE= .133	FLL= -20.	VSE= 0.
DPS= 0.	DPE= 100.	FLH= 0	DSE= 0.

13.02.50.

06/23/82

Figure I-34

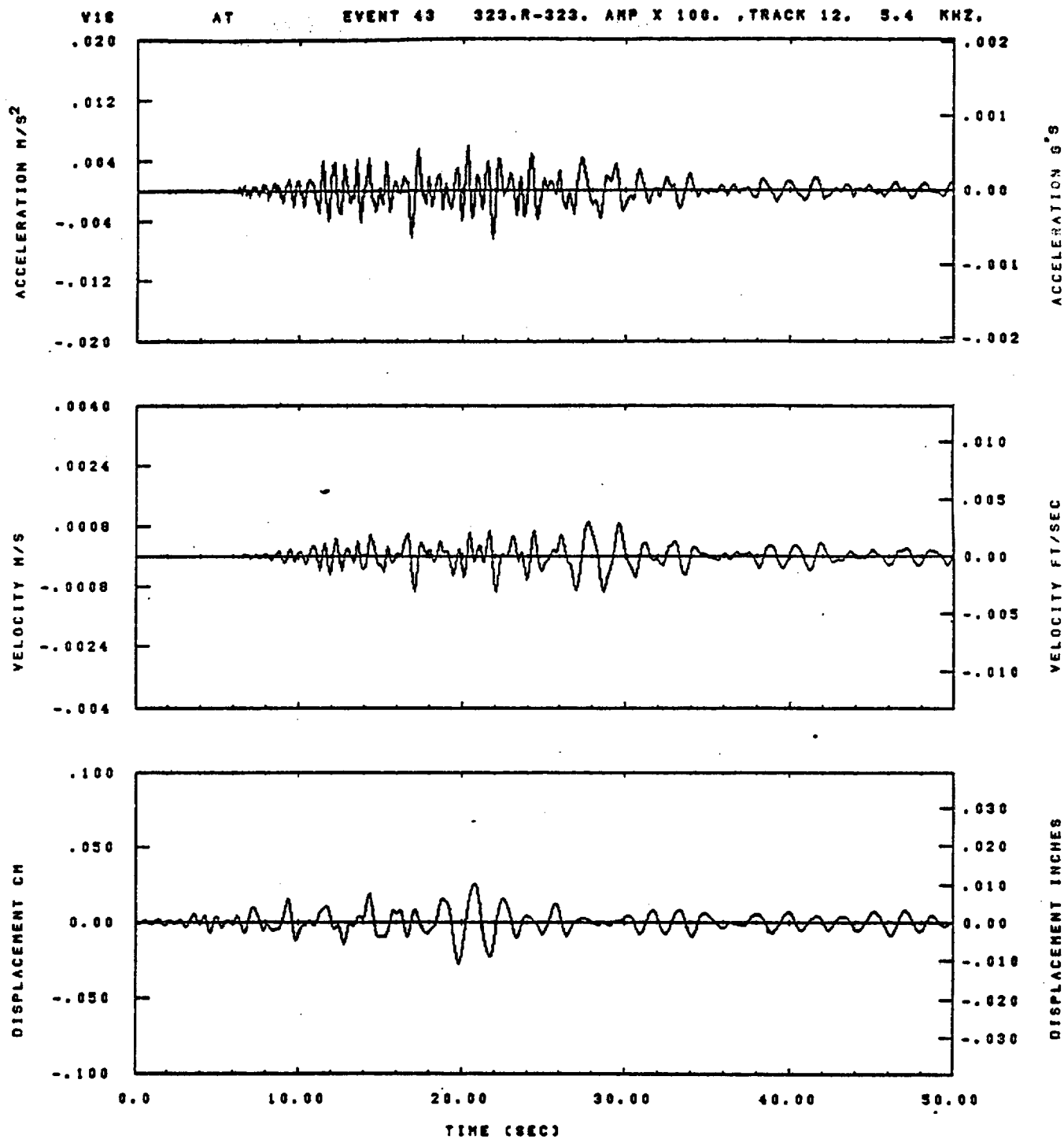


IDT= .0020	ODT=	FIX=	AAS= 0.
HPP= .2	BYH= .13	HLH= 499	ASB=
LPP= 9.	BYL= 2.	HLL= 2999	ASE=
VTB= .20	VTE= .133	FLL= -20.	VSE= 0.
DPS= 0.	OPE= 100.	FLH= 0	OSE= 0.

10.30.13.

08/23/82

Figure I-35



IDT= .0020	ODT=	FIX=	AAS= 0.
HPF= .2	BVN= .13	HLH= 499	ASB=
LPF= 9.	BVL= 2.	HLL= 2999	ASE=
VTB= .20	VTZ= .133	FLL= -20.	VSE= 0.
DPS= 0.	DPE= 100.	FLH= 0	DSE= 0.

13.08.35.

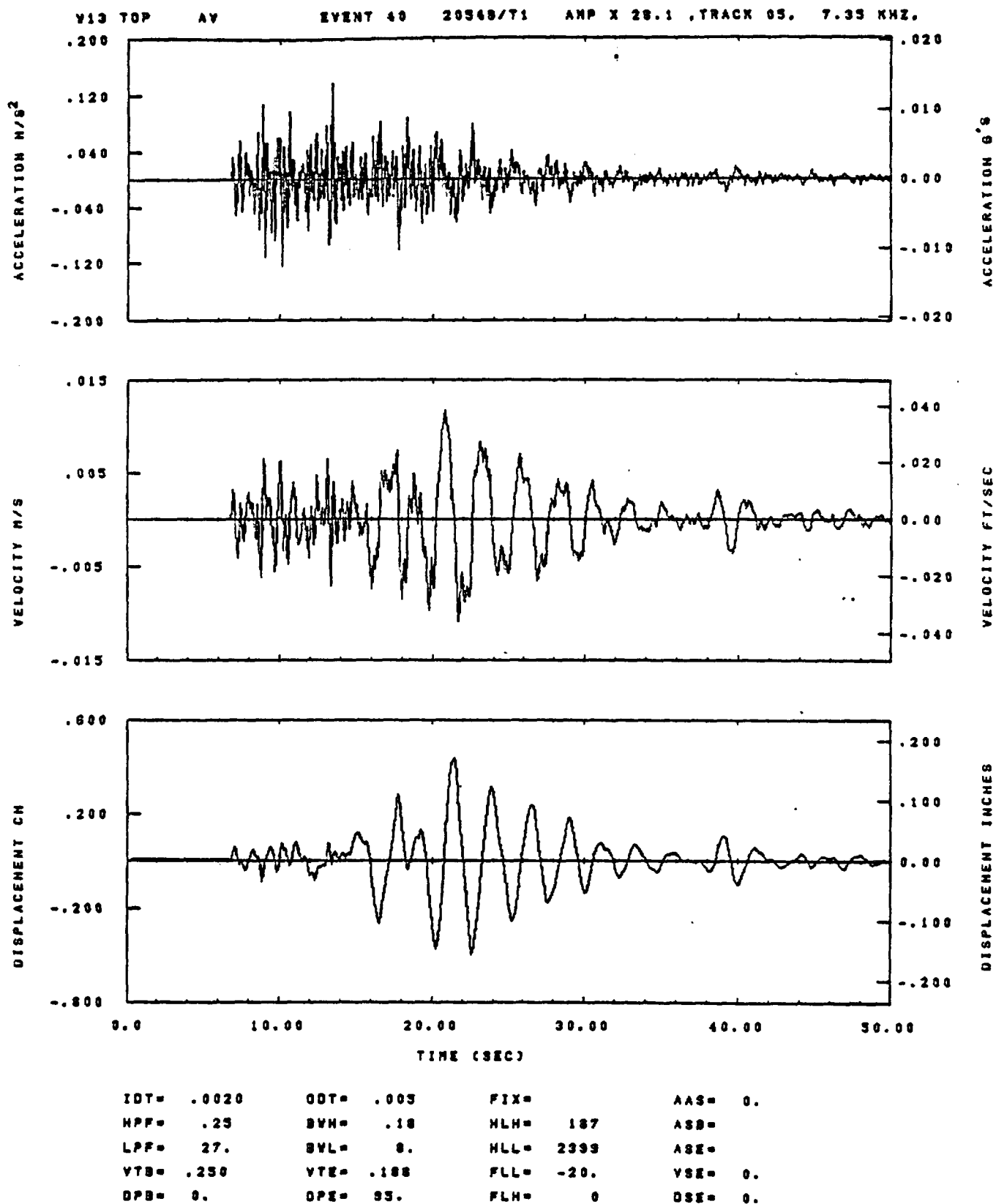
06/29/82

Figure I-36

APPENDIX J

COMPARISON OF TOP AND BOTTOM

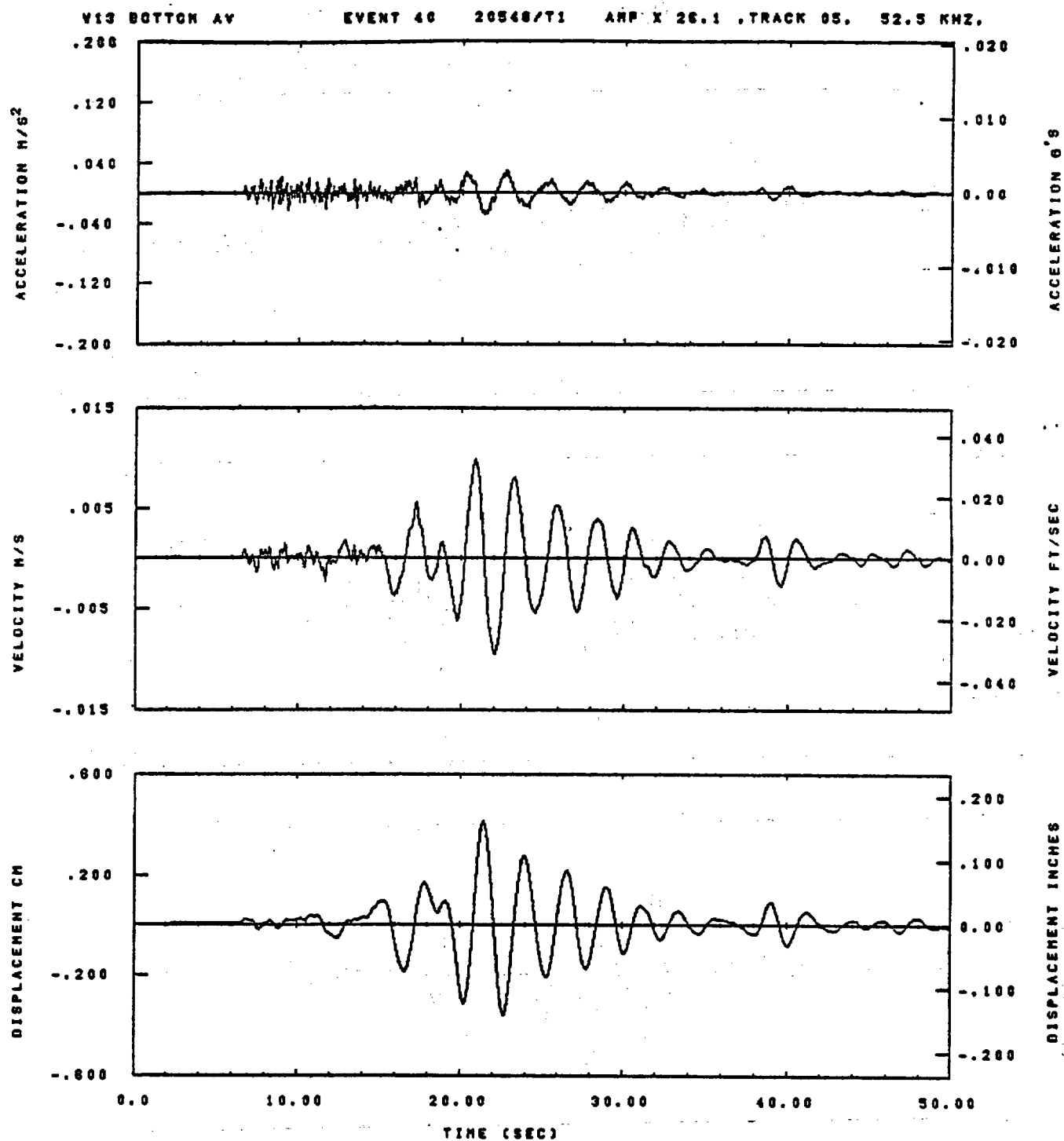
WAVEFORMS AT STATION W-13



11.08.10.

08/23/82

Figure J-1

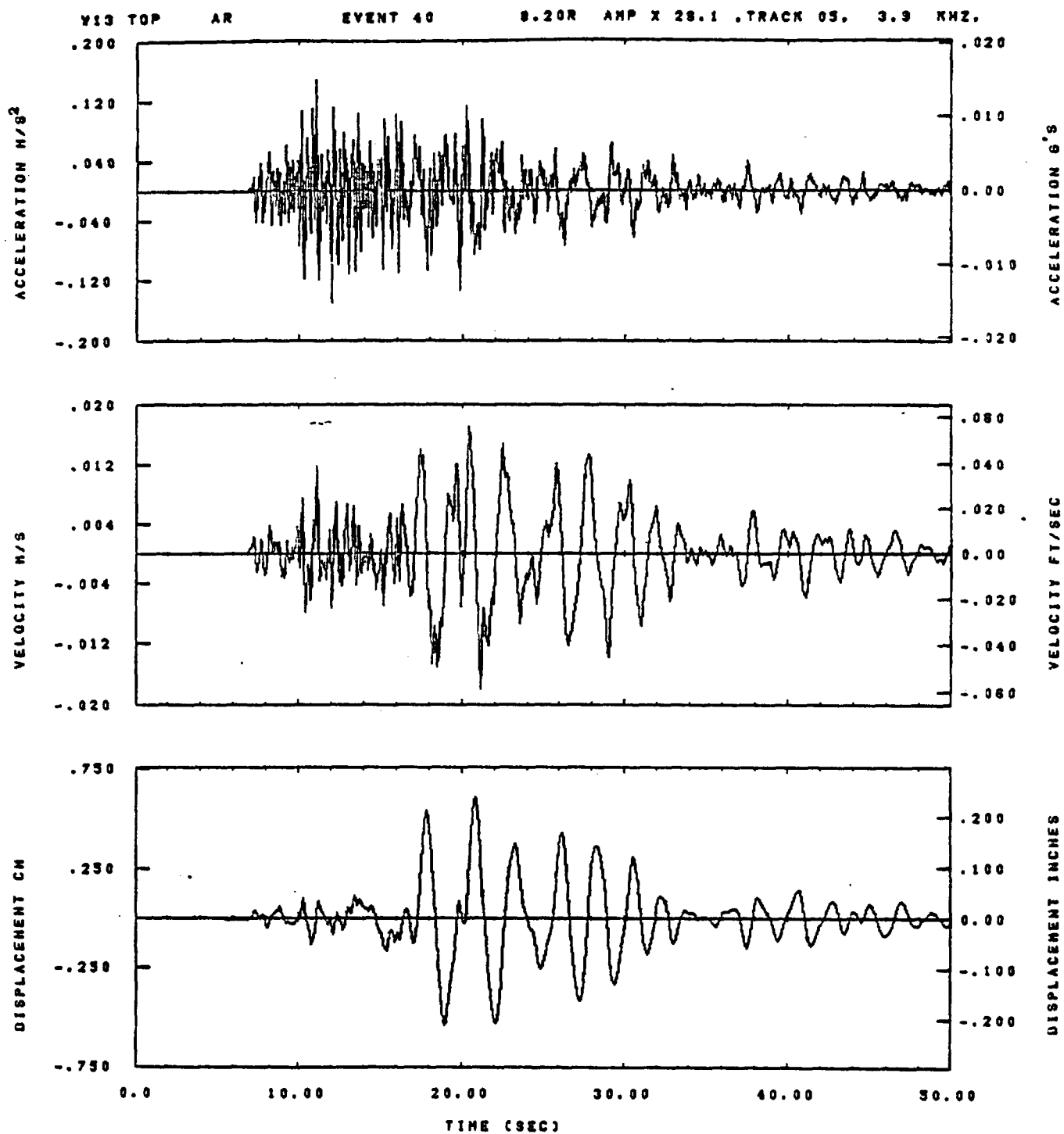


IDT= .0020	ODT= .005	FIX=	AAS= 0.
HPF= .25	BVN= .16	HLH= 167	ASB=
LPF= 27.	BVL= 6.	HLL= 2388	ASE=
VTB= .250	VTE= .166	FLL= -20.	VSE= 0.
DPS= 0.	DPE= 95.	FLH= 0	DSE= 0.

11.06.45.

06/29/82

Figure J-2

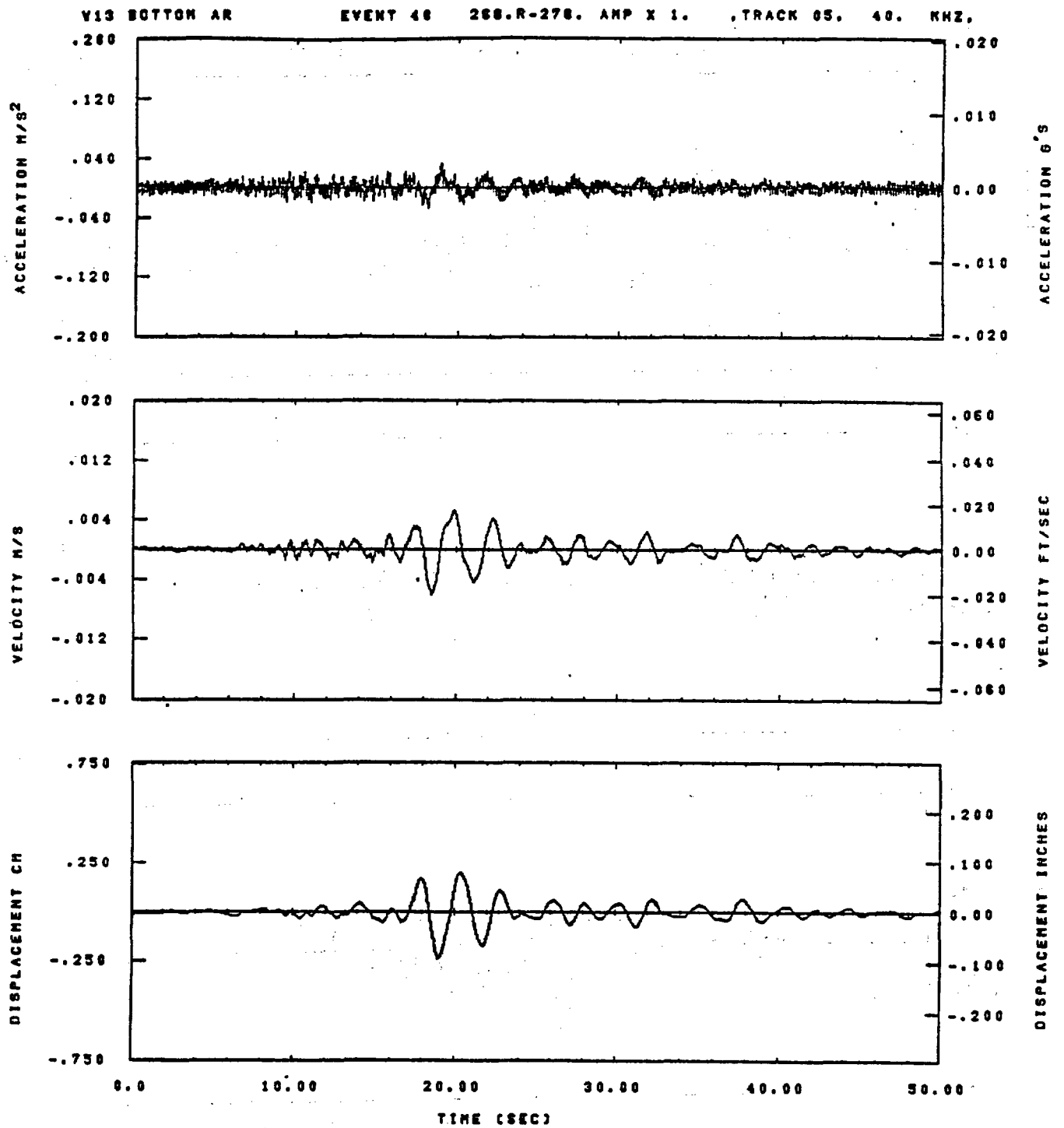


IDT= .0020	ODT= .005	FIX=	AAS= 0.
HPF= .25	BYH= .16	HLH= 167	ASB=
LPP= 27.	BYL= 8.	HLL= 2339	ASE=
VTB= .250	VTE= .188	FLL= -20.	VSE= 0.
OPB= 0.	OPE= 95.	FLH= 0	OSE= 0.

11.06.37.

08/23/92

Figure J-3



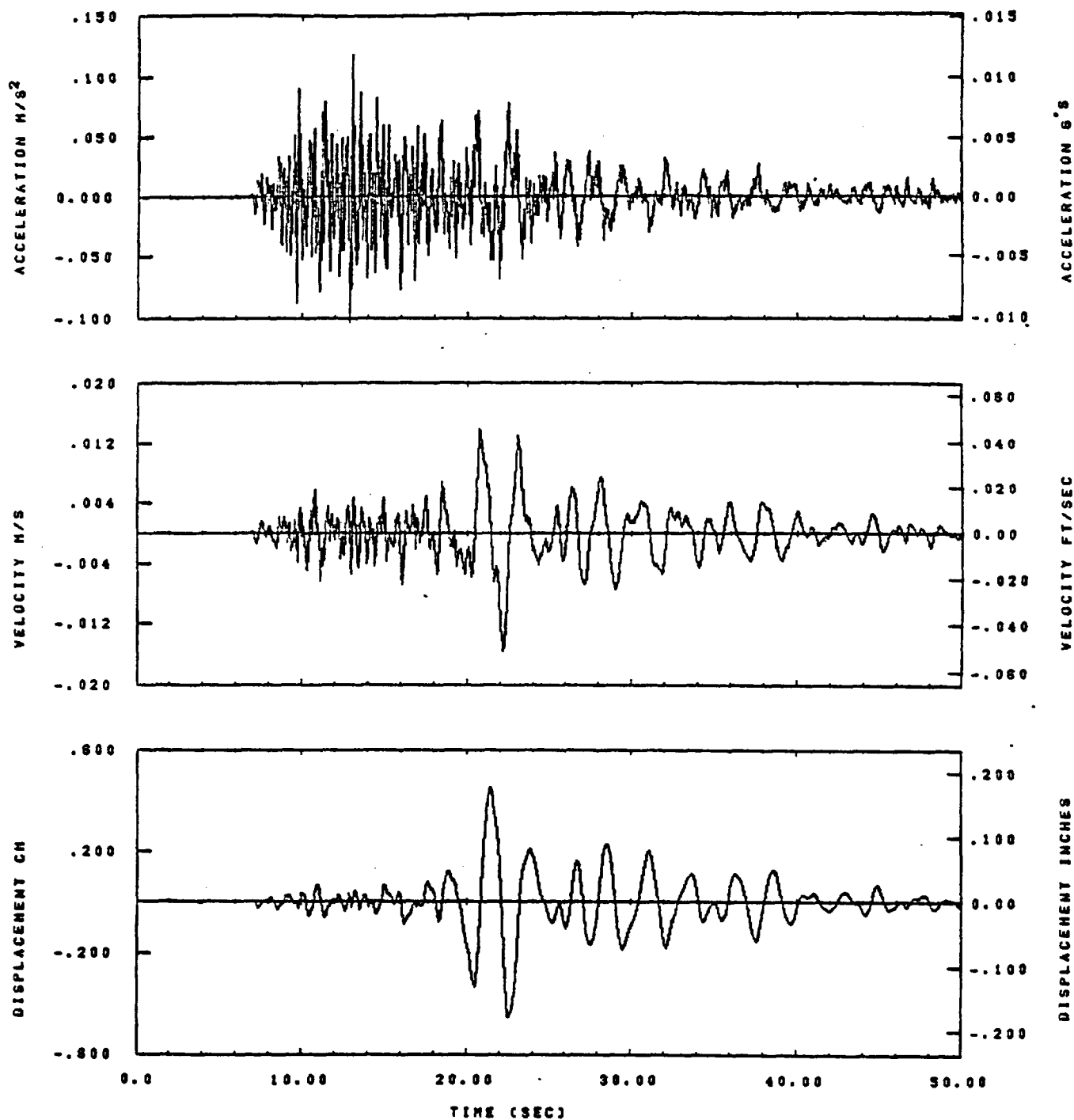
IDT= .0020	ODT= .005	FIX=	AAS= 0.
HPF= .3	BYH= .20	HLH= 167	ASS=
LPF= 27.	BYL= 6.	HLL= 1999	ASE=
VTS= .30	VTE= .200	FLL= -20.	VSE= 0.
DPE= 0.	DPE= 100.	FLH= 0	DSE= 0.

11.06.48.

06/23/82

Figure J-4

V13 TOP AT EVENT 40 8.20R AMP X 28.1 ,TRACK 05, 2.3 KHZ,

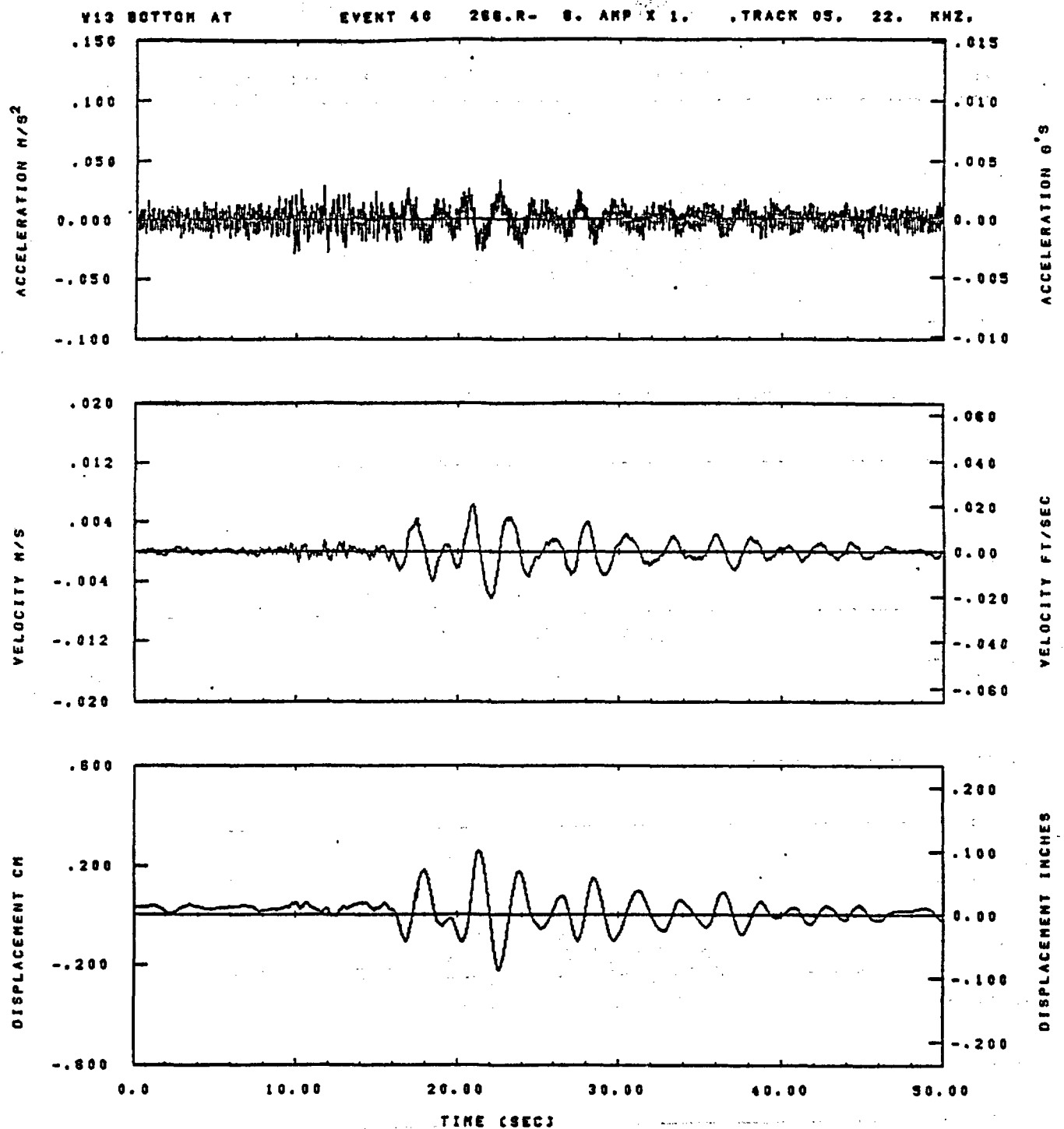


IDT= .0020	ODT= .005	FIX=	AAS= 0.
HPP= .25	BYH= .18	HLH= 187	ASS=
LPP= 27.	BYL= 8.	HLL= 2399	ASE=
VTB= .250	VTE= .188	FLL= -20.	VSE= 0.
DPS= 0.	DPE= 95.	FLH= 0	DSE= 0.

11.08.42.

08/23/92

Figure J-5

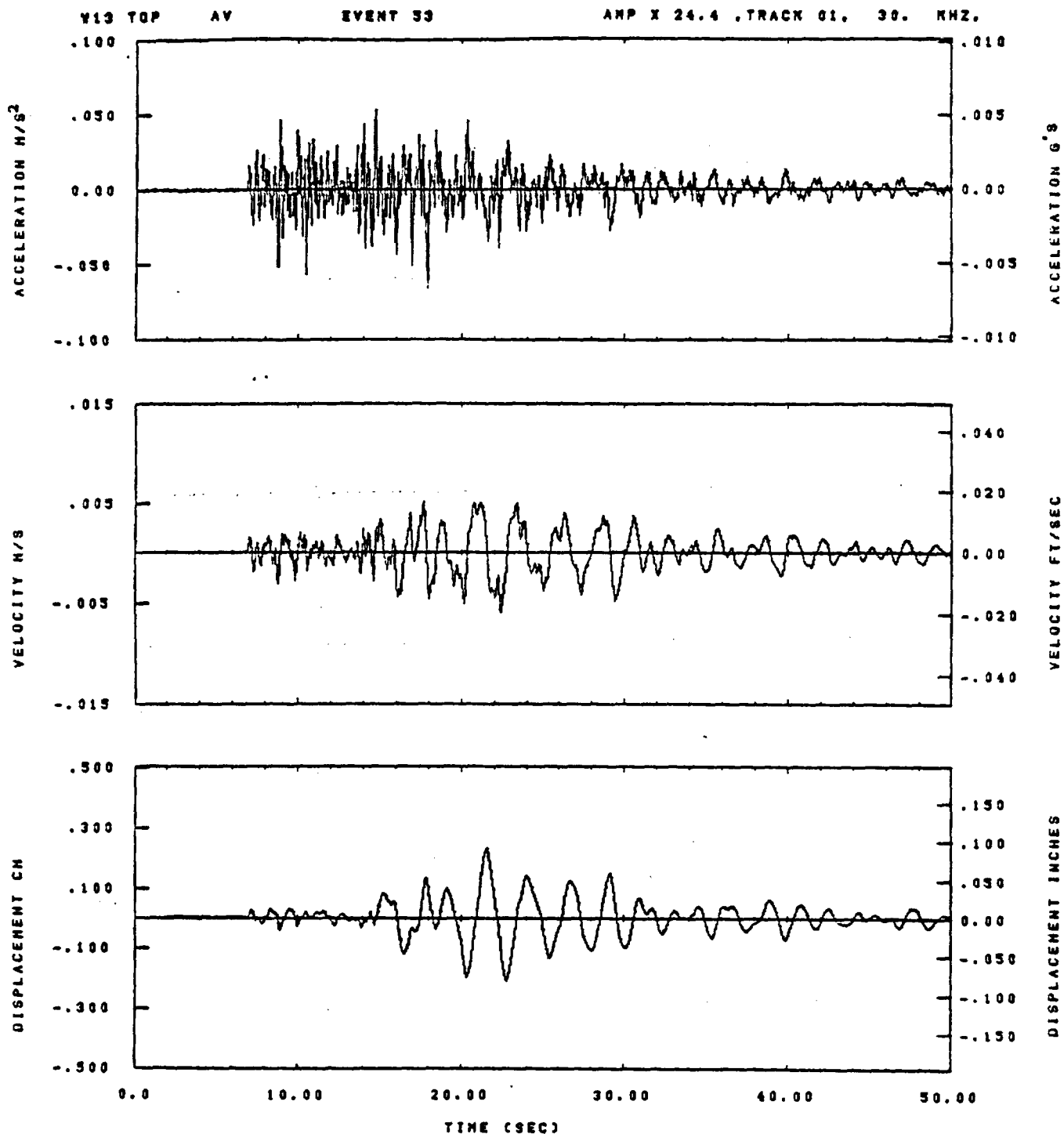


IDT= .0020	GDT= .005	FIX=	AAS= 0.
HPF= .3	BVH= .20	HLH= 167	ASS=
LPF= 27.	BVL= 8.	HLL= 1998	ASE=
VTB= .30	VTE= .200	FLL= -20.	VSE= 0.
DPS= 0.	DPE= 100.	FLH= 0	DSE= 0.

11.06.55.

05/23/82

Figure J-6

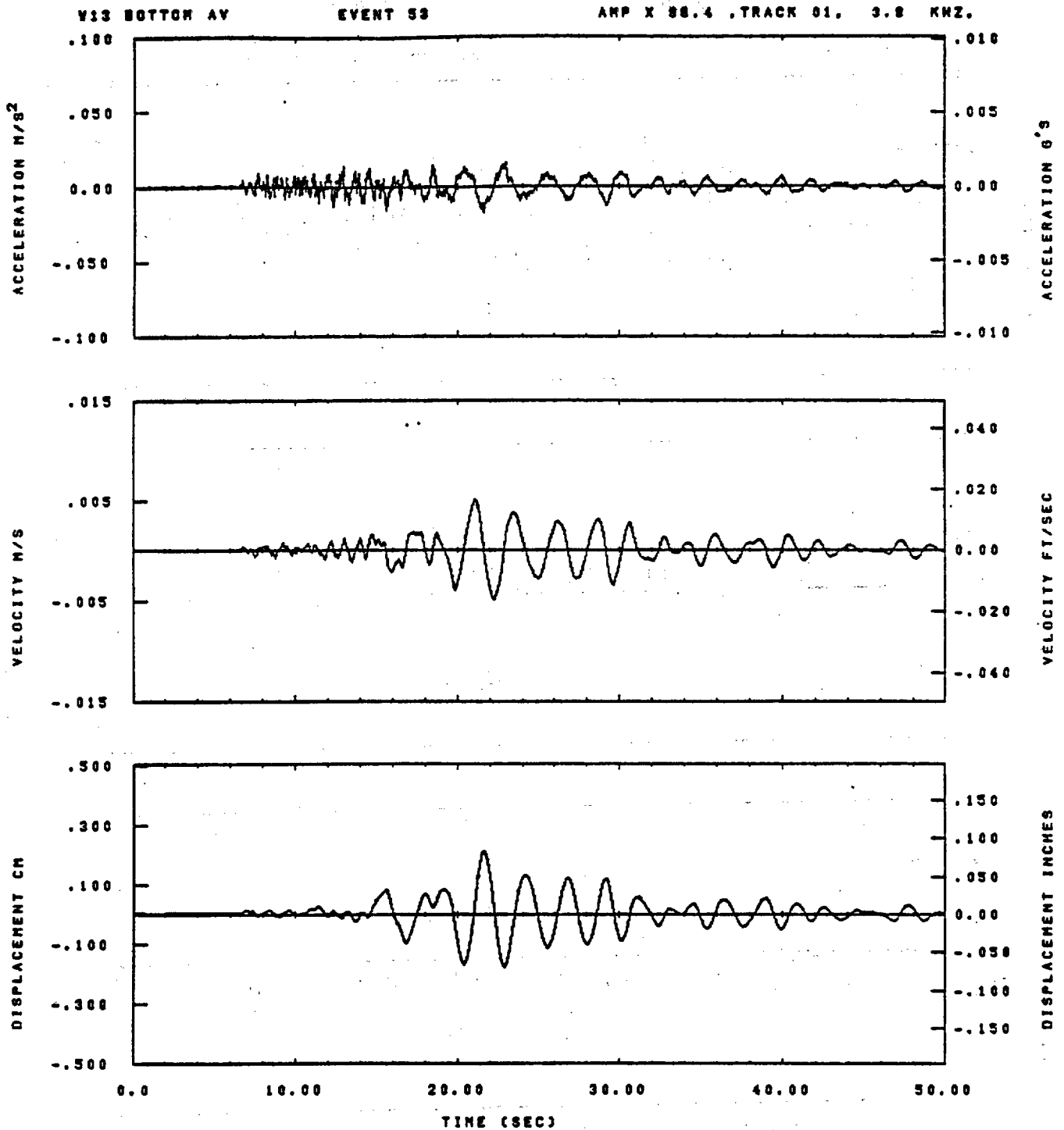


IDT= .0020	ODT= .0	FIX=	AAS=
HPP= .3	BVH= .20	HLH= 167	ASB=
LPP= 27.	BVL= 6.	HLL= 1999	ASE=
VTB= .30	VTE= .200	FLL=	VSE=
OPB=	OPZ=	FLH= 0	OSE= 0.

09.40.14.

07/02/92

Figure J-7

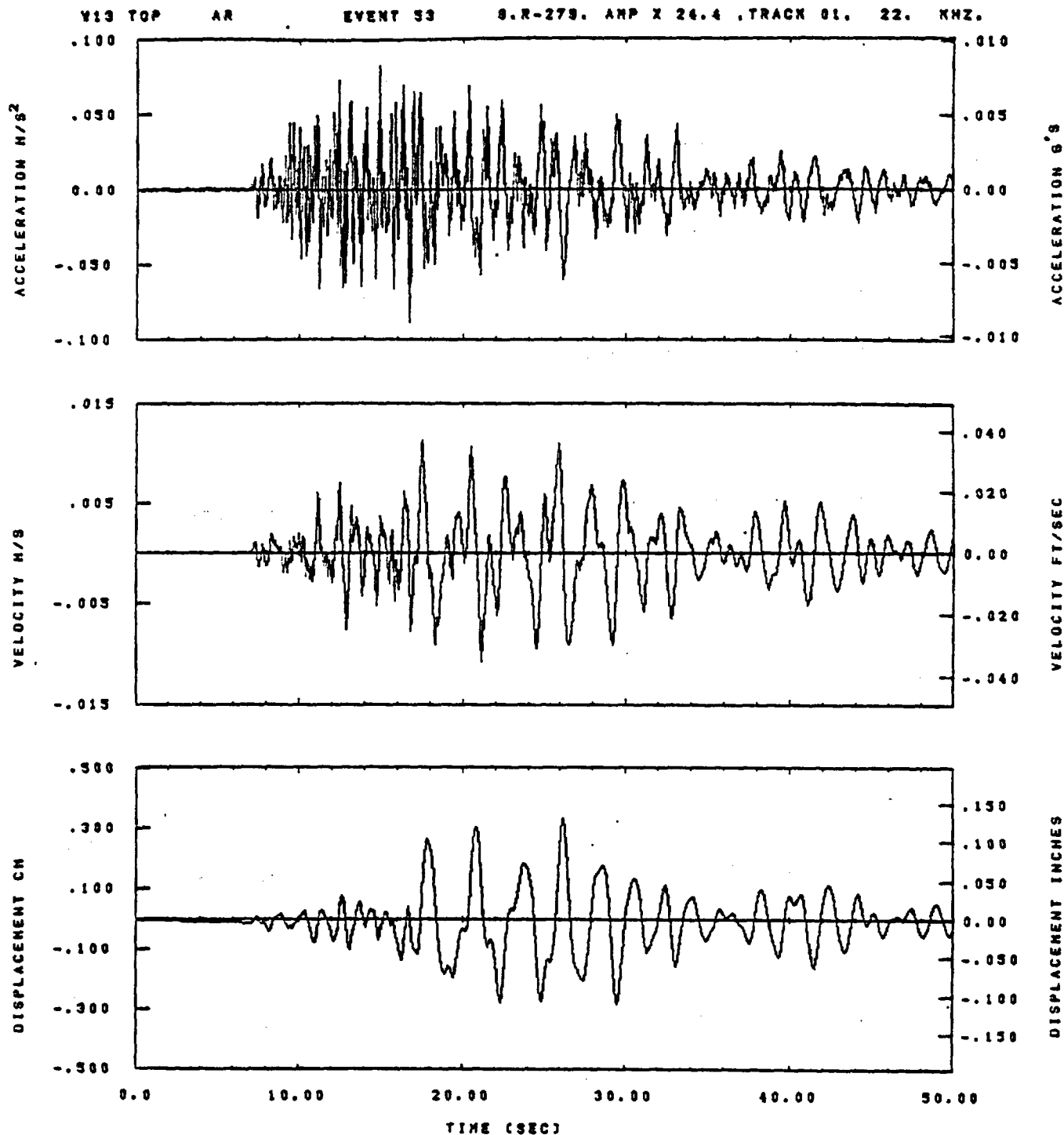


IDT= .0020	ODT= .0	FIX=	AAS=
HPF= .3	SVH= .20	HLH= 187	ASB=
LPF= 27.	SVL= 6.	HLL= 1998	ASE=
VTB= .30	VTE= .200	FLL=	VSE=
OPB=	DPE=	FLH= 0	DSE= 0.

08.40.43.

07/02/82

Figure J-8

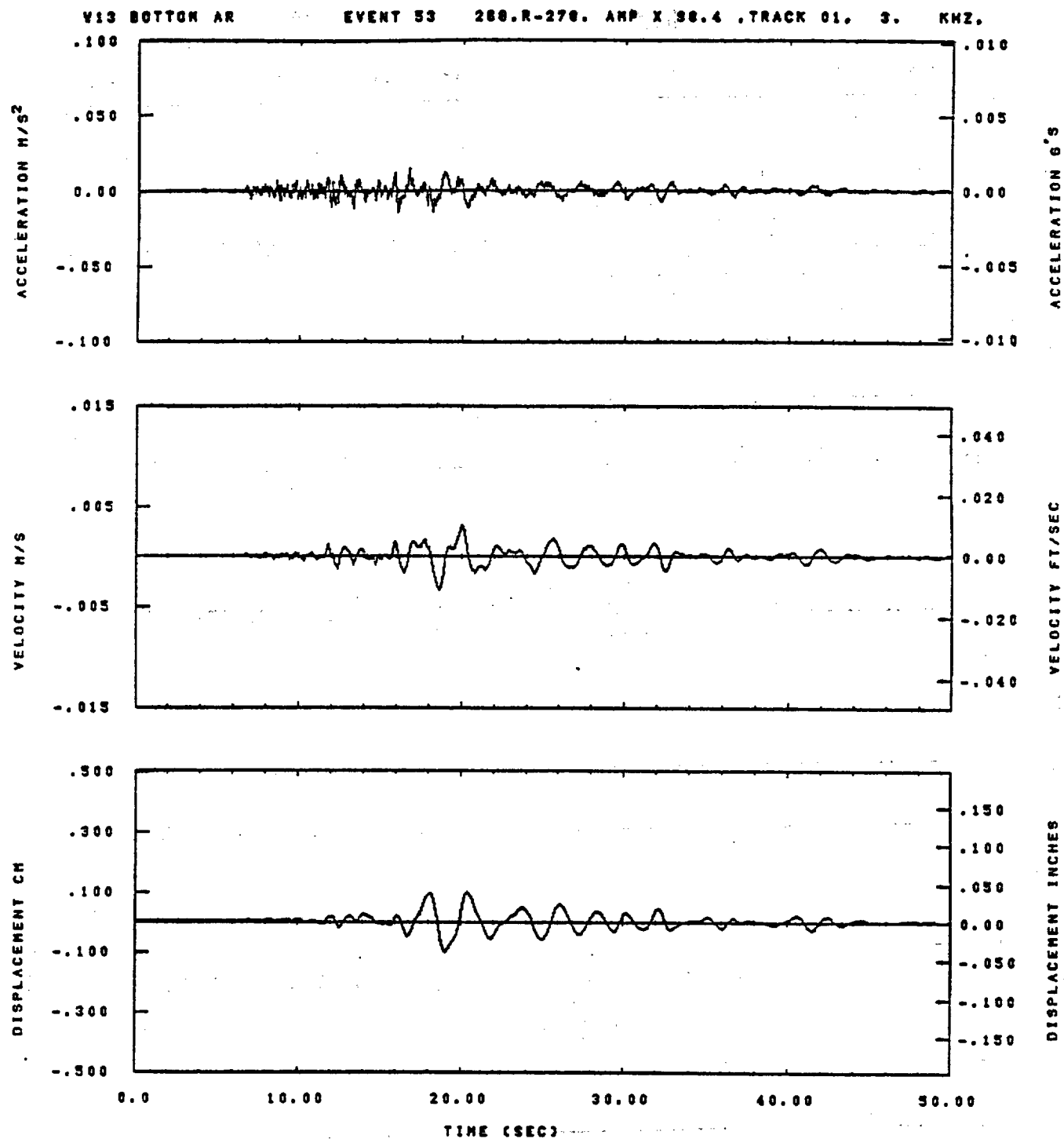


IDT= .0020	ODT= .0	FIX=	AAS=
HPP= .3	BYH= .20	HLH= 187	ASS=
LPP= 27.	BYL= 8.	HLL= 1939	ASE=
VTB= .30	VTE= .200	FLL=	VSE=
OPS=	DPE=	FLH= 0	DSE= 0.

09.40.18.

07/02/82

Figure J-9

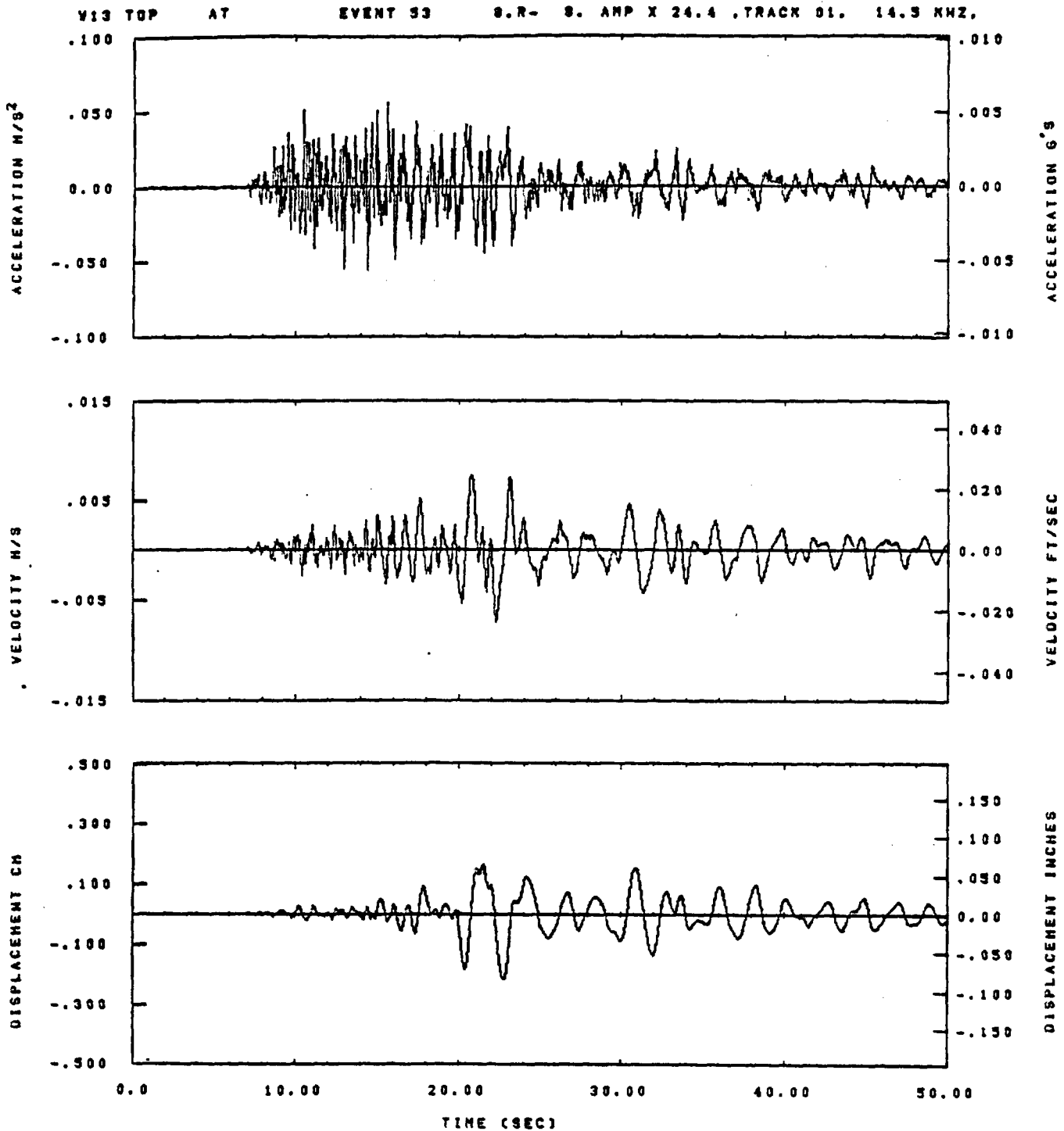


IDT= .0020	QDT= .0	FIX=	AAS=
HPF= .3	BYH= .20	HLH= 167	ASB=
LPF= 27.	BYL= 6.	HLL= 1989	ASE=
VTB= .30	YTE= .200	PLL=	VSE=
DPS=	DPE=	PLH= 0	DSE= 0.

09.40.50.

07/02/82

Figure J-10

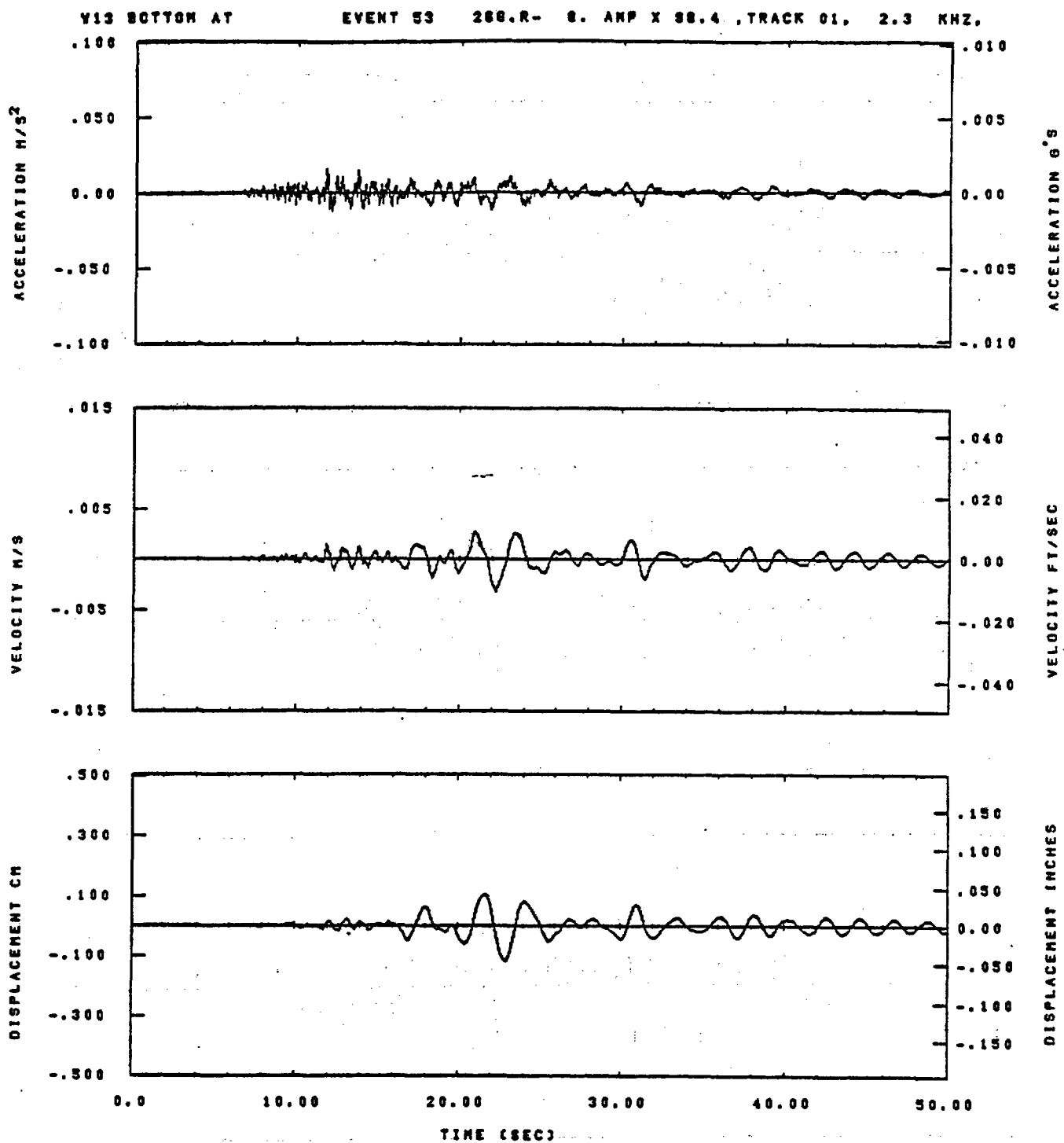


IOT= .0020	OOT= .0	FIX=	AAS=
HPP= .3	BYH= .20	HLH= 187	ASB=
LPP= 27.	BYL= 8.	HLL= 1999	ASE=
VTS= .38	VTE= .200	FLL=	VSE=
DPS=	DPE=	FLH= 0	DSE= 0.

09.40.22.

07/02/82

Figure J-11



IDT= .0020
HPF= .3
LPF= 27.
VTB= .38
DPB=

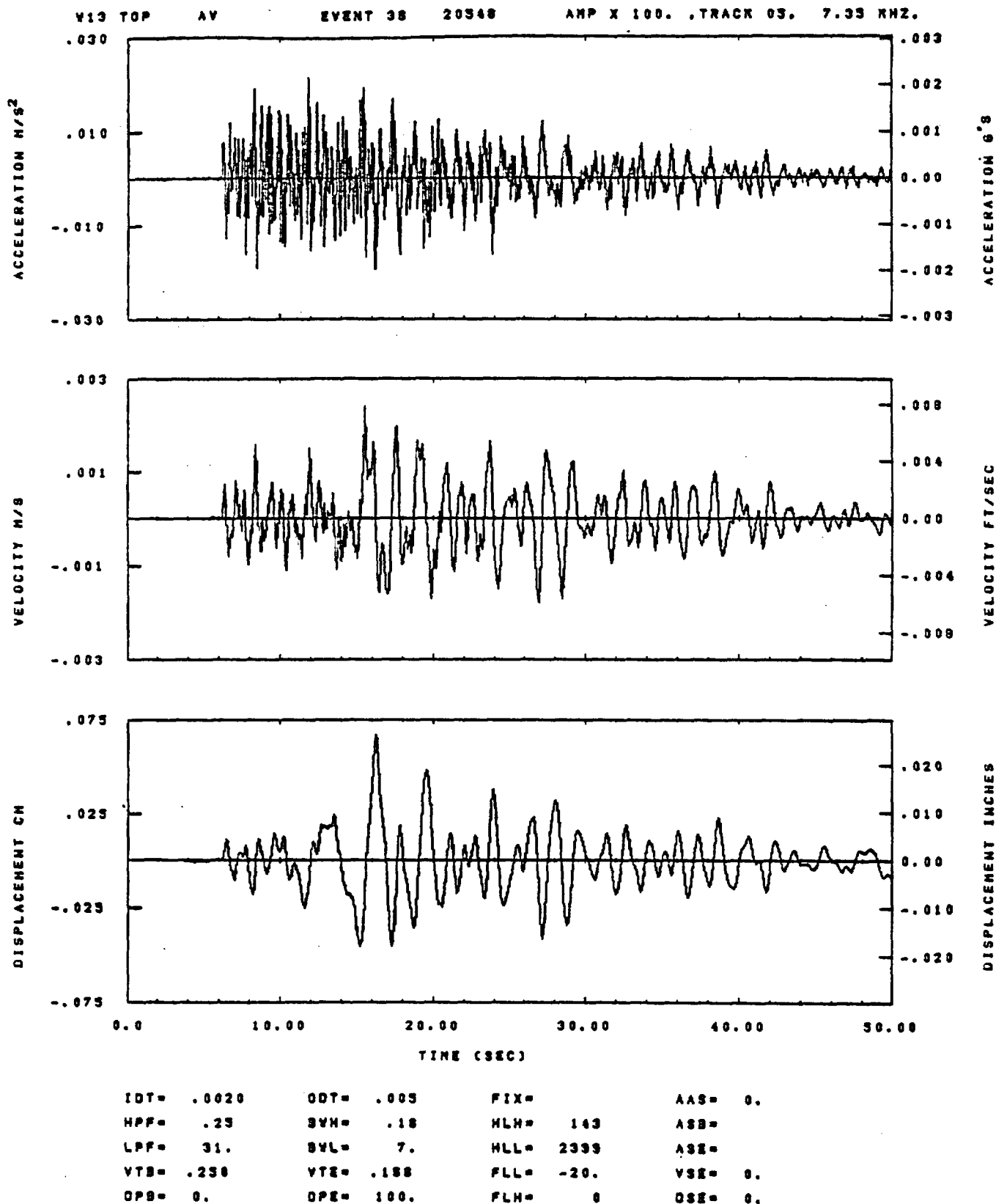
ODT= .0
BYH= .20
BYL= 6.
VTE= .200
DPE=

FIX= AAS=
HLH= 167 ASB=
HLL= 1898 ASE=
FLL= VSE=
FLH= 0 DSE= 0.

09.41.05.

07/02/82

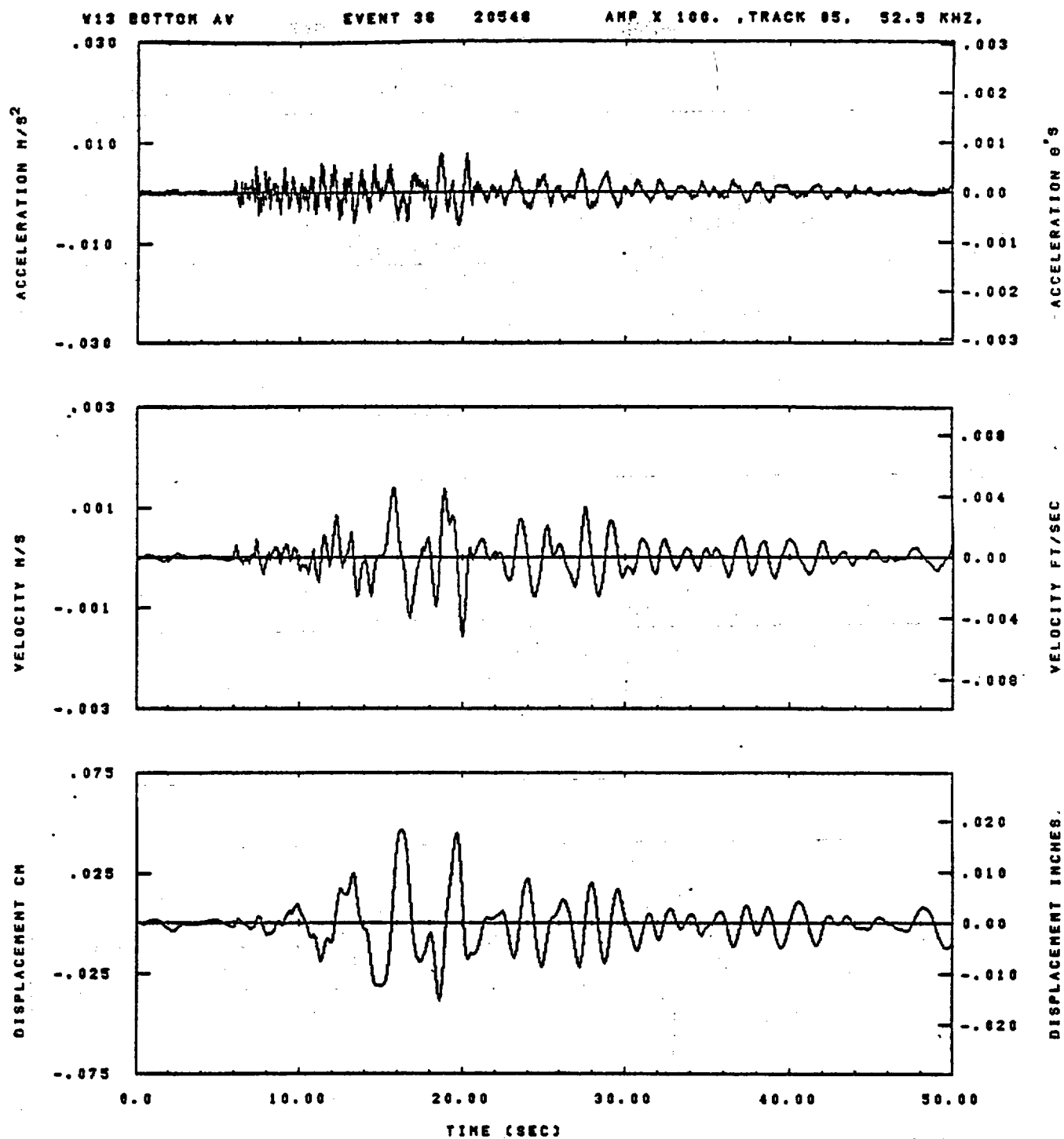
Figure J-12



10.10.00.

08/23/82

Figure J-13

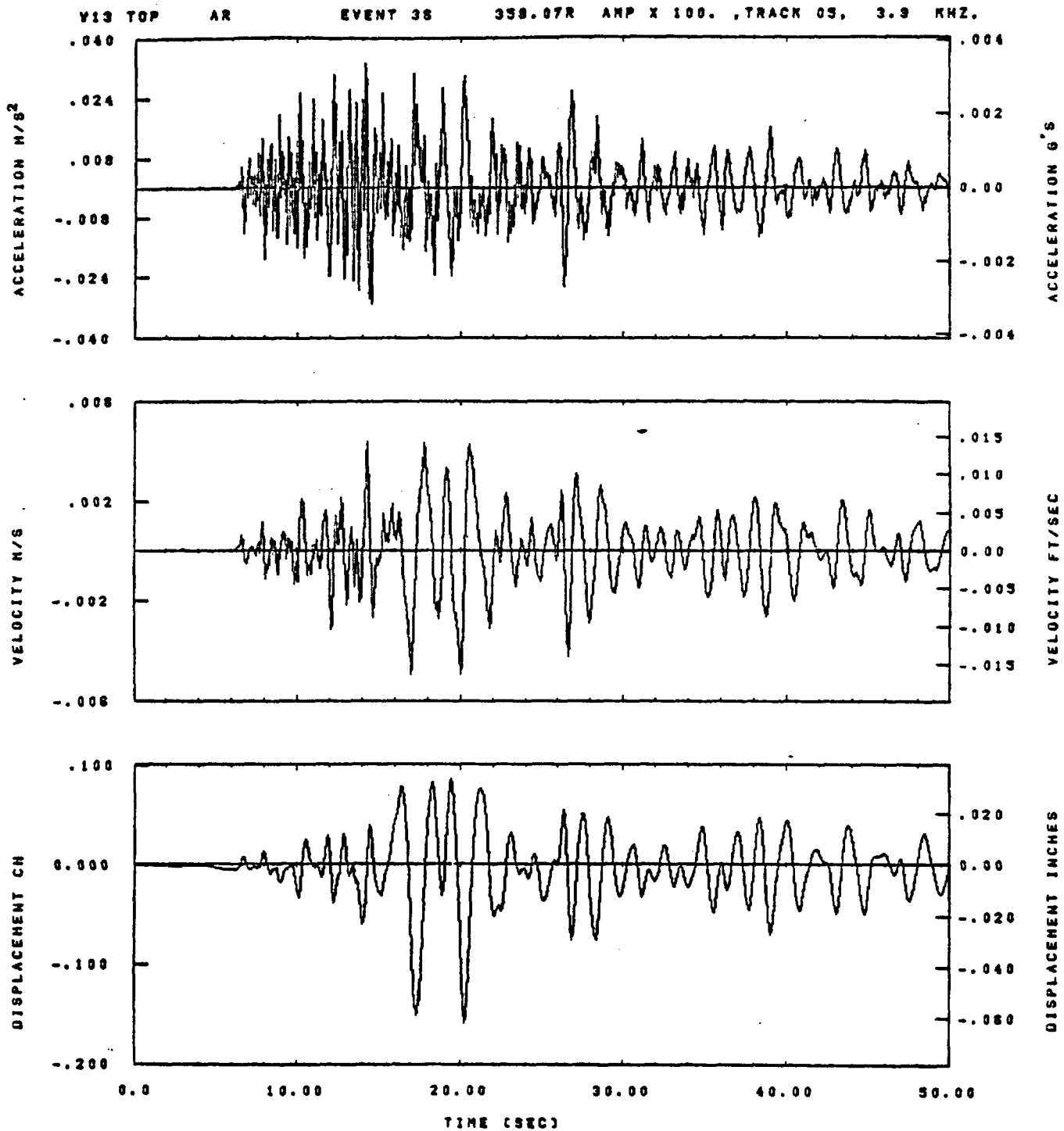


IDT= .0020	ODT= .005	FIX=	AAS= 0.
HPF= .25	BYH= .16	MLH= 143	ASB=
LPF= 31.	BYL= 7.	MLL= 2398	ASE=
VTS= .250	VTE= .166	FLL= -20.	VSE= 0.
OPB= 0.	OPE= 100.	FLN= 0	OSE= 0.

10.10.38.

06/23/82

Figure J-14

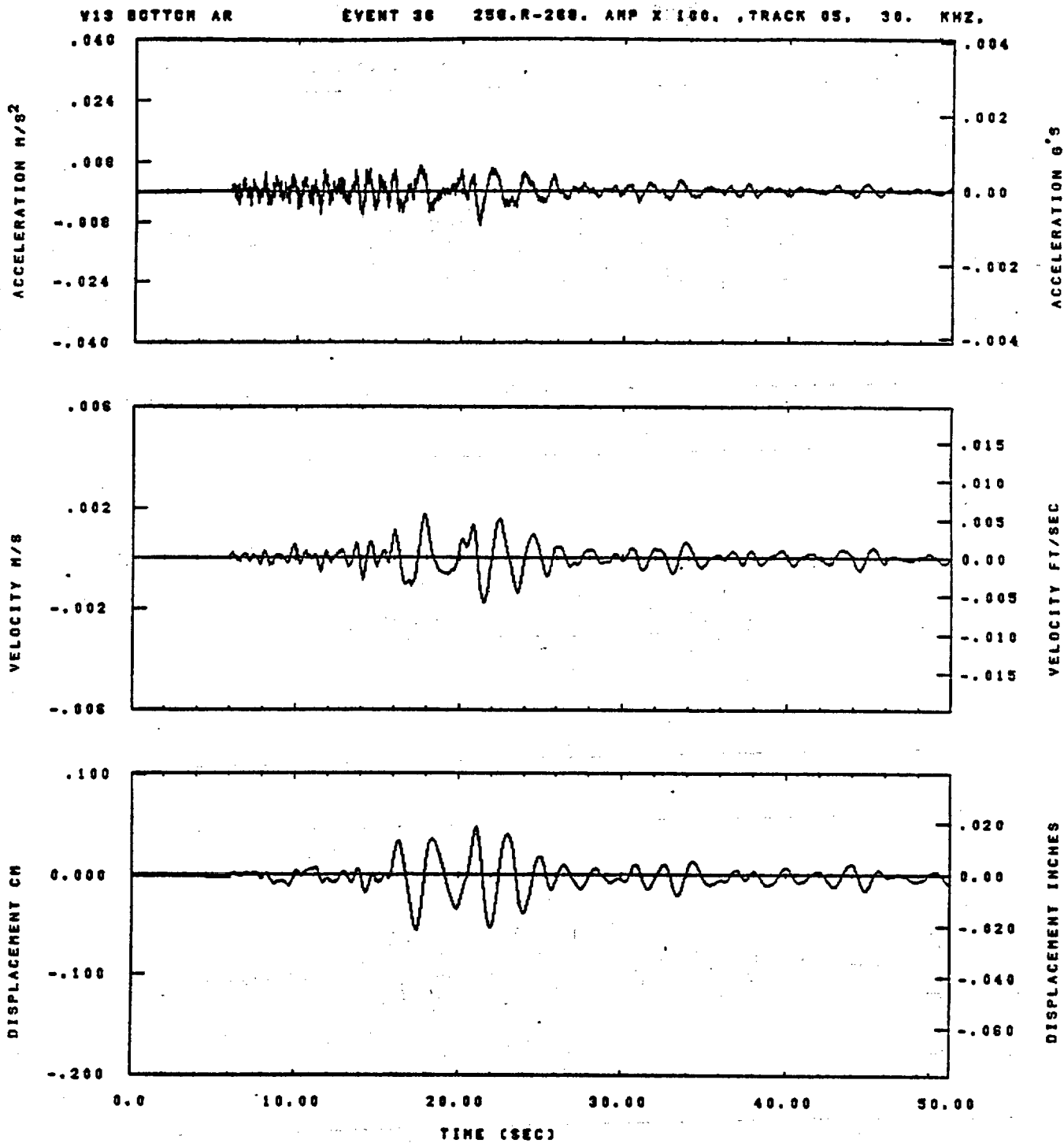


IDT= .0020	ODT= .005	FIX=	AAS= 0.
NPF= .23	BYM= .18	MLM= 143	ASB=
LPF= 31.	SVL= 7.	MLL= 2333	ASE=
VTS= .250	VTE= .168	FLL= -20.	VSE= 0.
DPE= 0.	DPE= 100.	FLM= 0	DSE= 0.

10.10.03.

08/23/82

Figure J-15

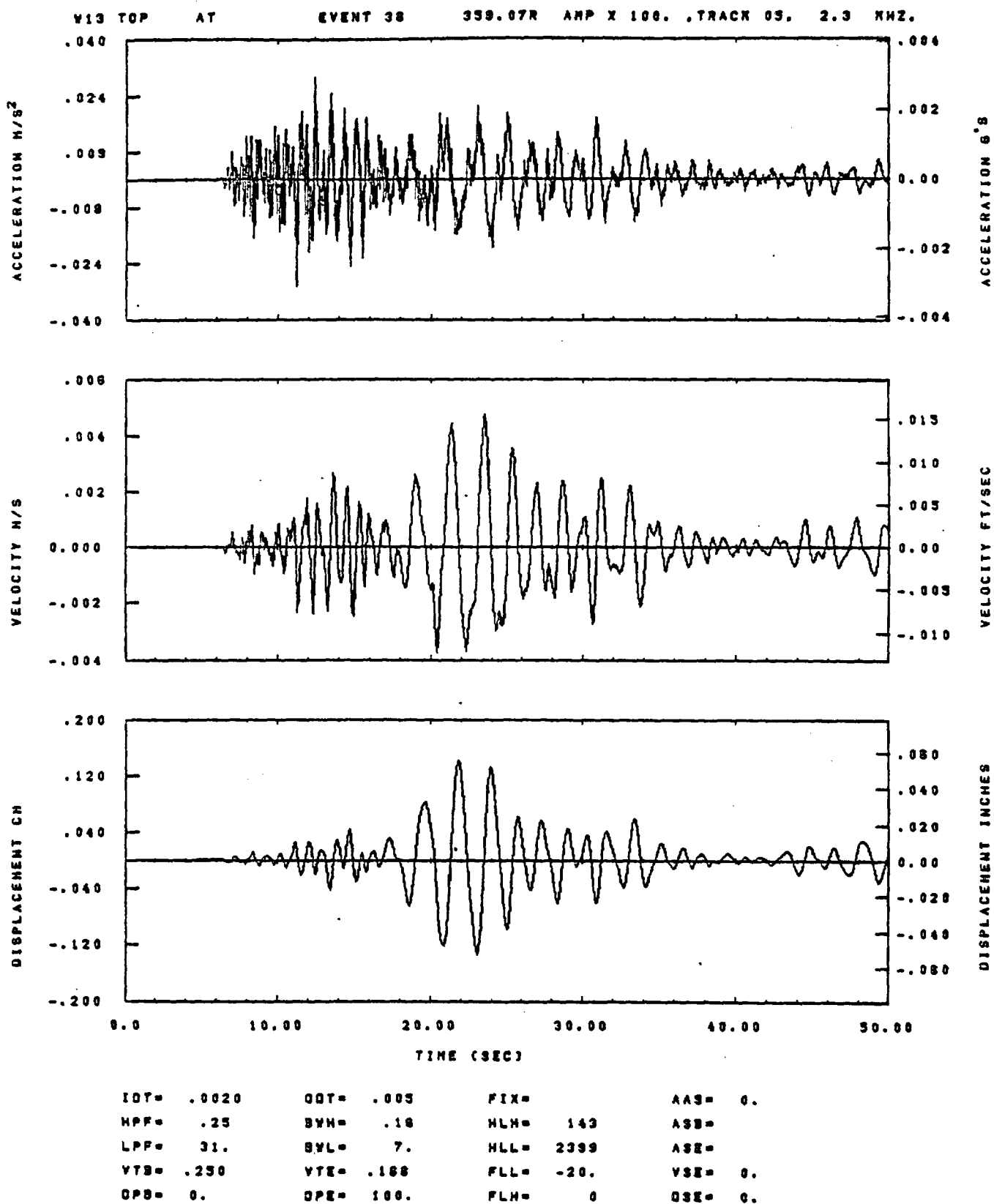


IOT= .0020	ODT= .005	FIX=	AAS= 0.
HPF= .25	SVN= .16	HLN= 143	ASS=
LPF= 31.	SVL= 7.	HLL= 2388	ASE=
VTB= .250	VTE= .166	FLL= -20.	VSE= 0.
DPS= 0.	DPE= 100.	FLH= 0	DSE= 0.

10.10.50.

06/29/82

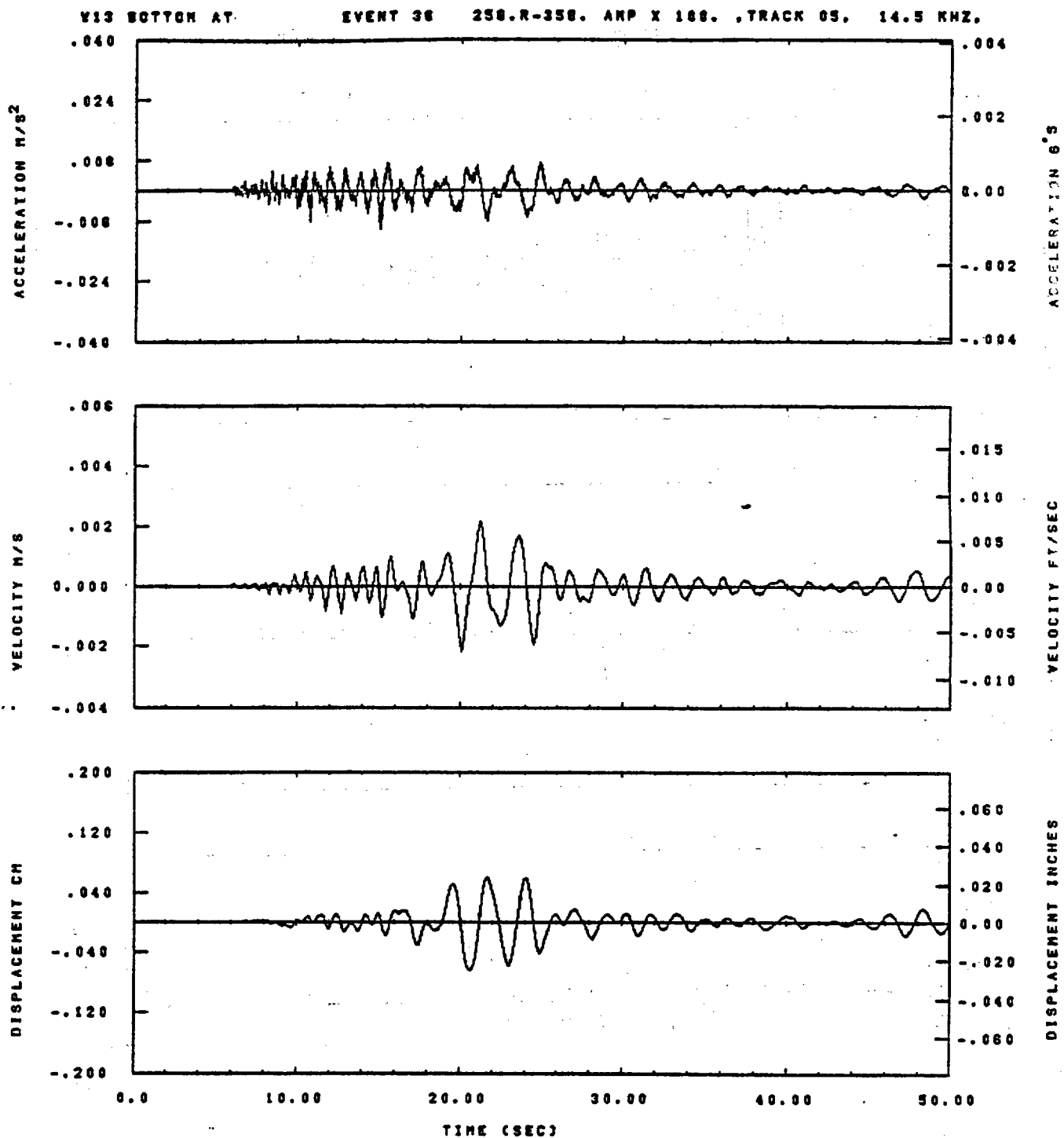
Figure J-16



10.10.12.

08/23/82

Figure J-17

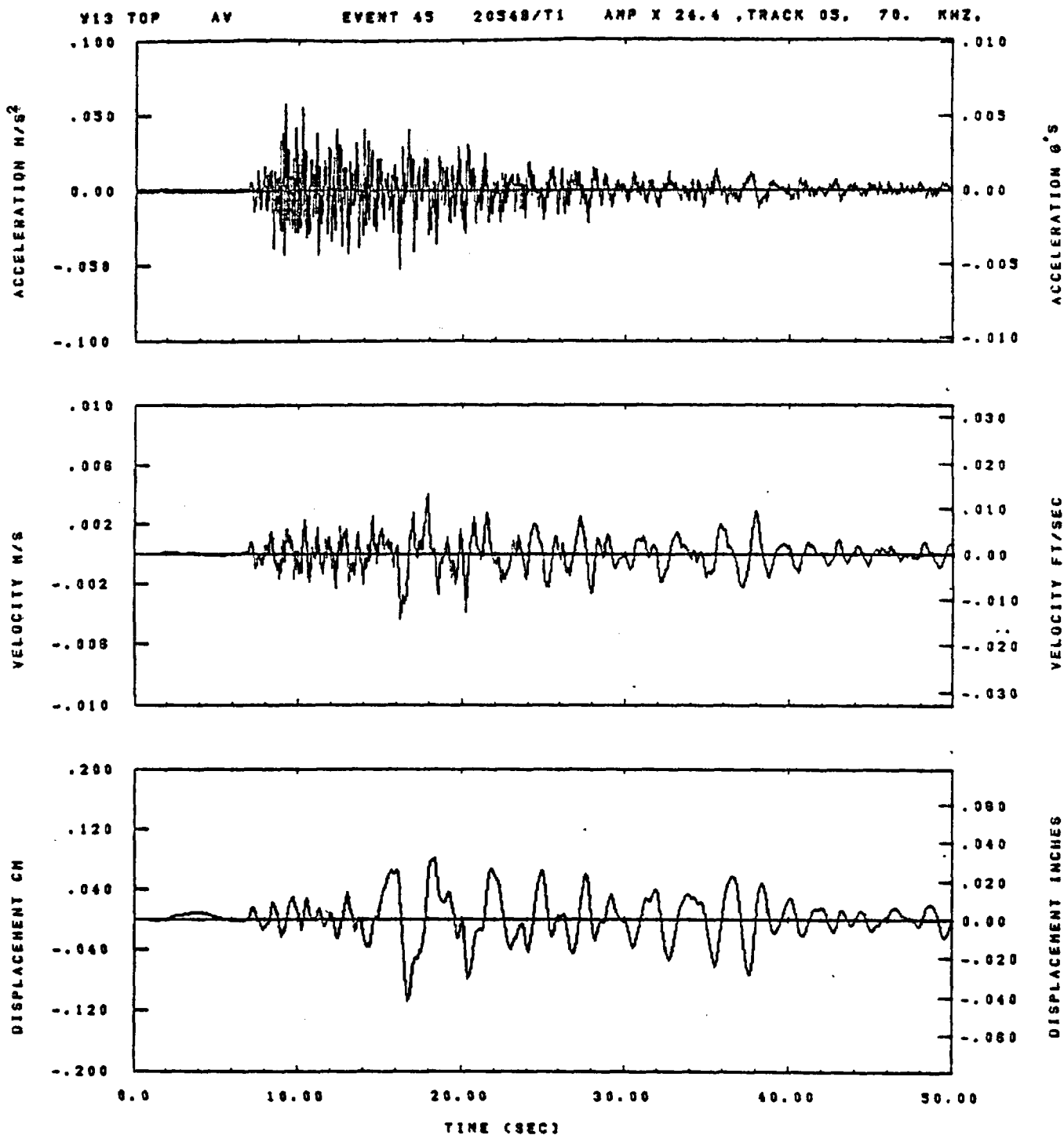


IDT= .0020	ODT= .005	FIX=	AAS= 0.
HPF= .25	BYH= .16	HLH= 143	ASB=
LPF= 31.	BYL= 7.	HLL= 2389	ASE=
VTS= .250	VTE= .166	FLL= -20.	VSE= 0.
DPS= 0.	DPE= 100.	FLH= 0	DSE= 0.

10.10.55.

06/23/82

Figure J-18

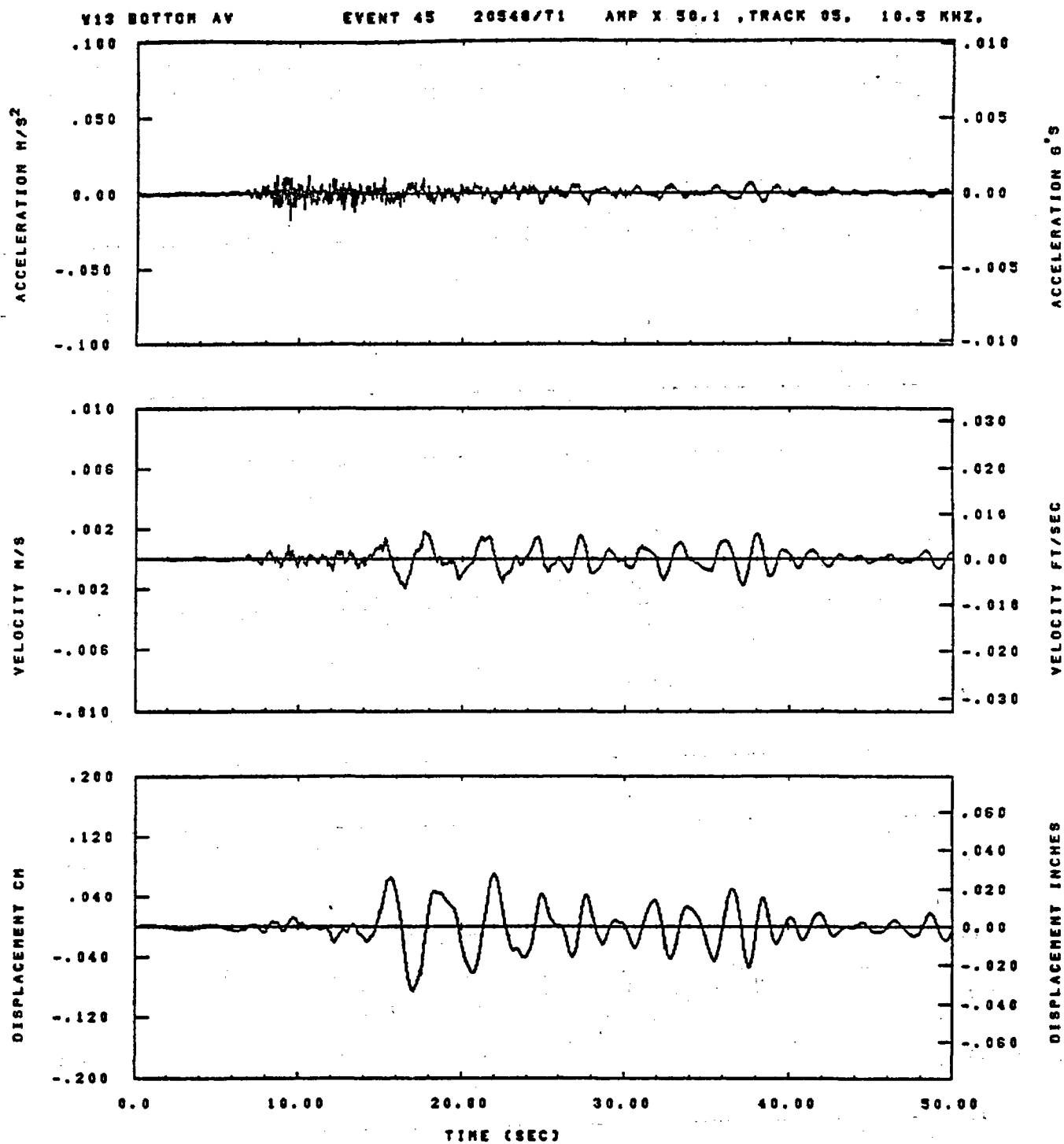


IDT= .0020	ODT= .003	FIX=	AAS= 0.
HPP= .20	BYH= .13	HLH= 33	ASB=
LPP= 45.	BYL= 10.	HLL= 2333	ASE=
VTB= .200	YTE= .133	FLL= -20.	VSE= 0.
DPB= 0.	DPE= 100.	FLH= 0	DSE= 0.

13.57.35.

08/22/82

Figure J-19



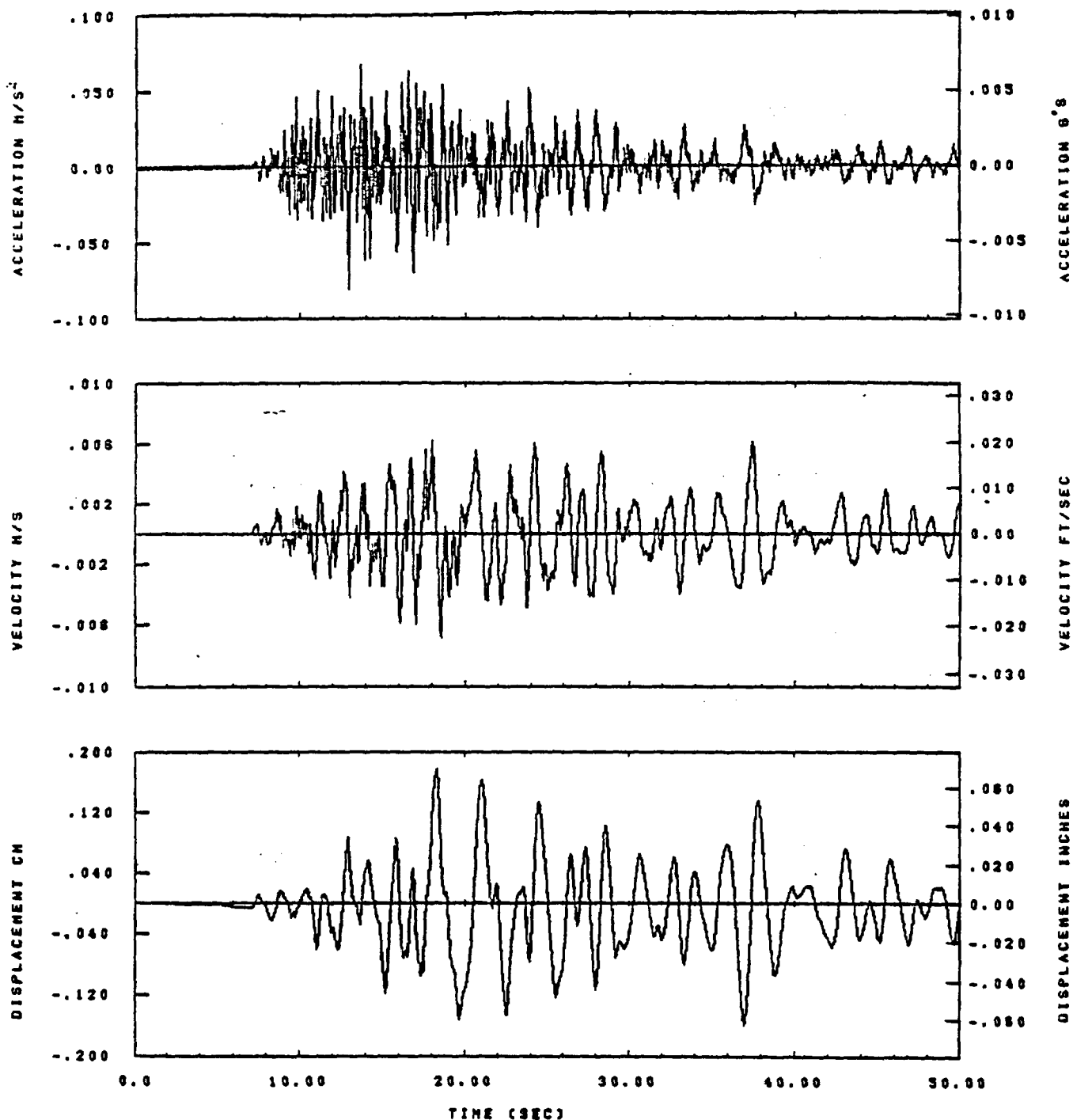
IDT= .0020	ODT= .005	FIX=	AAS= 0.
HPP= .20	BYH= .13	HLH= 88	ASB=
LPP= 45.	BYL= 10.	HLL= 2998	ASE=
VTB= .200	VTE= .138	FLL= -20.	VSE= 0.
DPS= 0.	DPE= 100.	FLH= 8	DSE= 0.

13.57.52.

06/22/82

Figure J-20

Y13 TOP AR EVENT 43 S.R-278. AMP X 24.4 .TRACK 05. 32.3 KHZ.

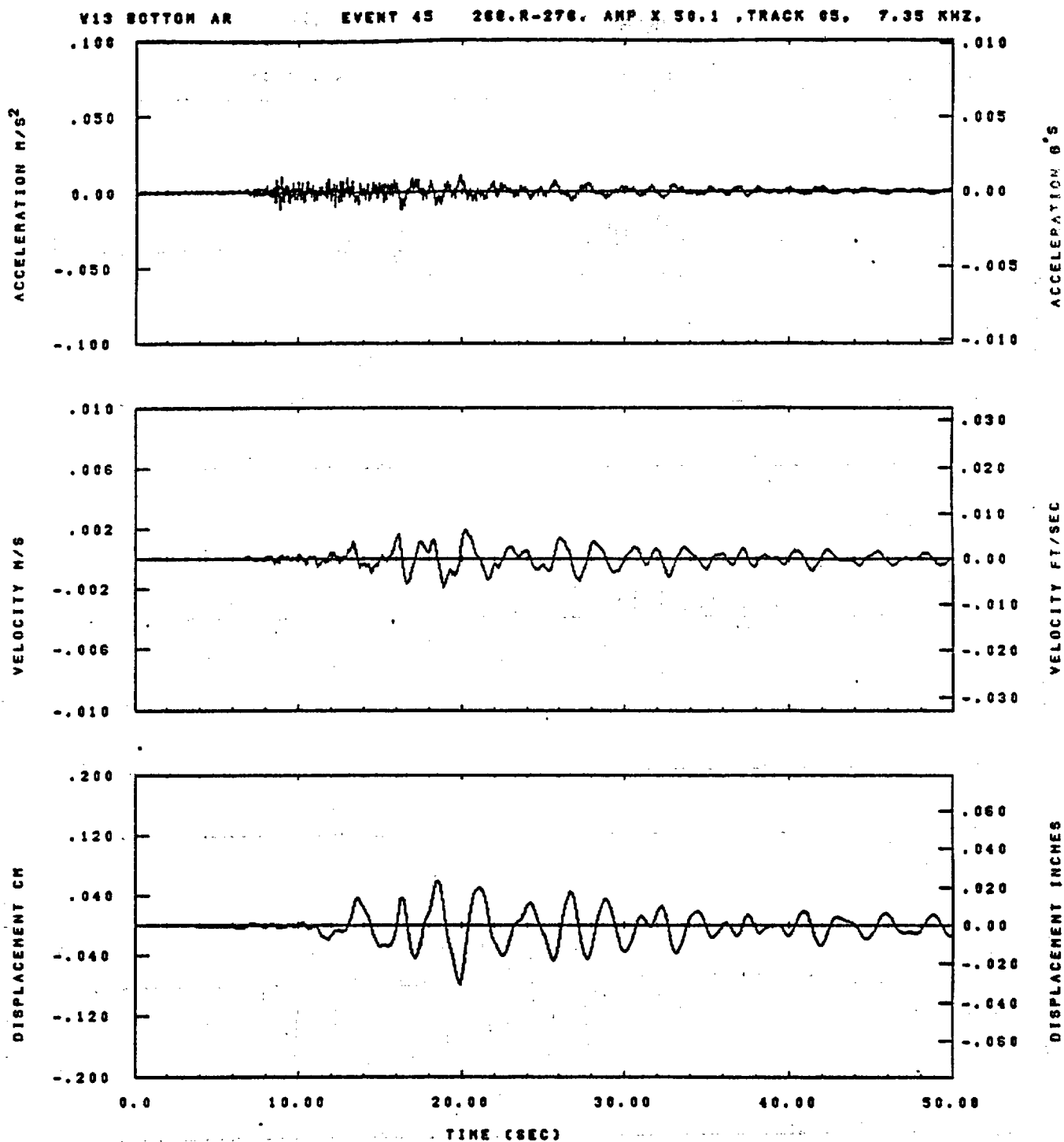


IOT= .0020	OOT= .003	FIX=	AAS= 0.
HPP= .20	BYH= .13	HLH= 33	ASB=
LPP= 45.	BYL= 10.	HLL= 2993	ASE=
VTS= .200	VTE= .133	FLL= -20.	VSE= 0.
OPS= 0.	OPE= 100.	FLH= 0	OSE= 0.

13.37.42.

08/22/82

Figure J-21

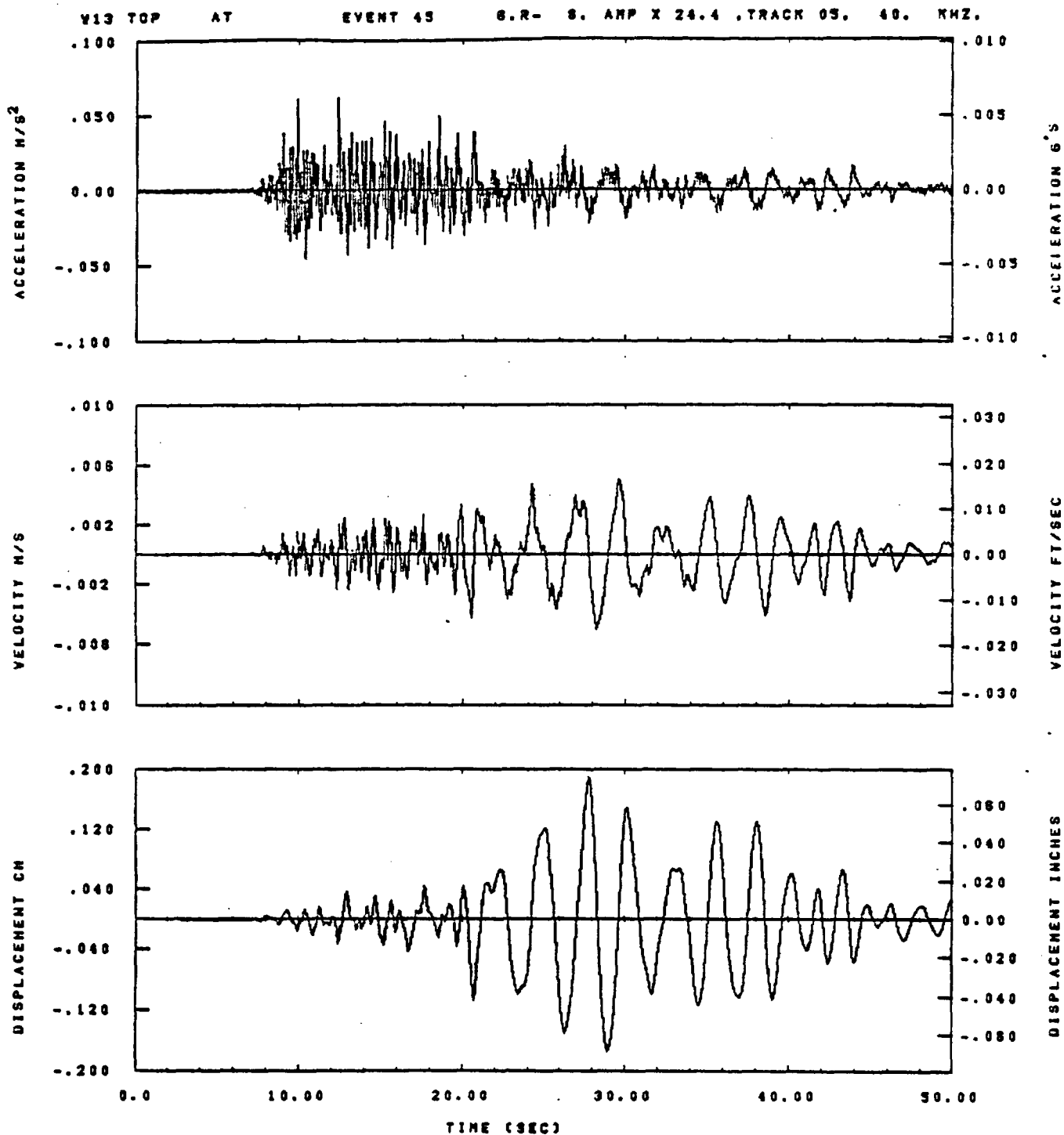


IDT= .0020	ODT= .005	FIX=	AAS= 0.
HPP= .20	BWH= .13	HLH= 99	ASS=
LPF= 45.	BYL= 10.	HLL= 2988	ASE=
VTS= .200	VTE= .133	FLL= -20.	VSE= 0.
DPE= 0.	DPE= 100.	FLH= 0	DSE= 0.

13.57.56.

06/22/82

Figure J-22

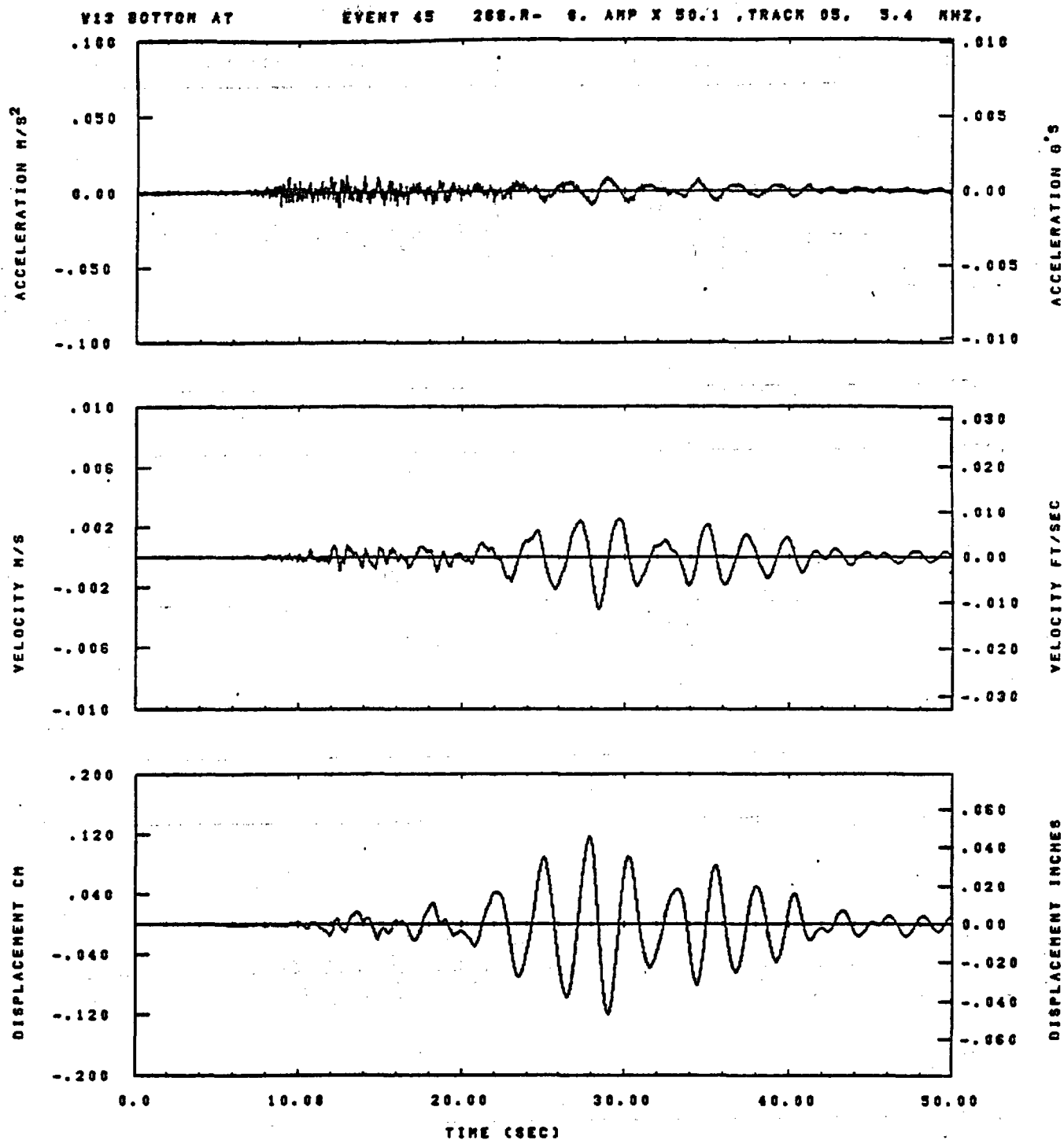


IDT= .0020	ODT= .003	FIX=	AAS= 0.
HPP= .20	BVH= .13	HLH= 33	ASB=
LPP= 43.	BVL= 10.	HLL= 2999	ASE=
VTB= .200	VTE= .133	FLL= -20.	VSE= 0.
OPS= 0.	DPE= 100.	FLH= 0	DSE= 0.

13.37.48.

08/22/82

Figure J-23

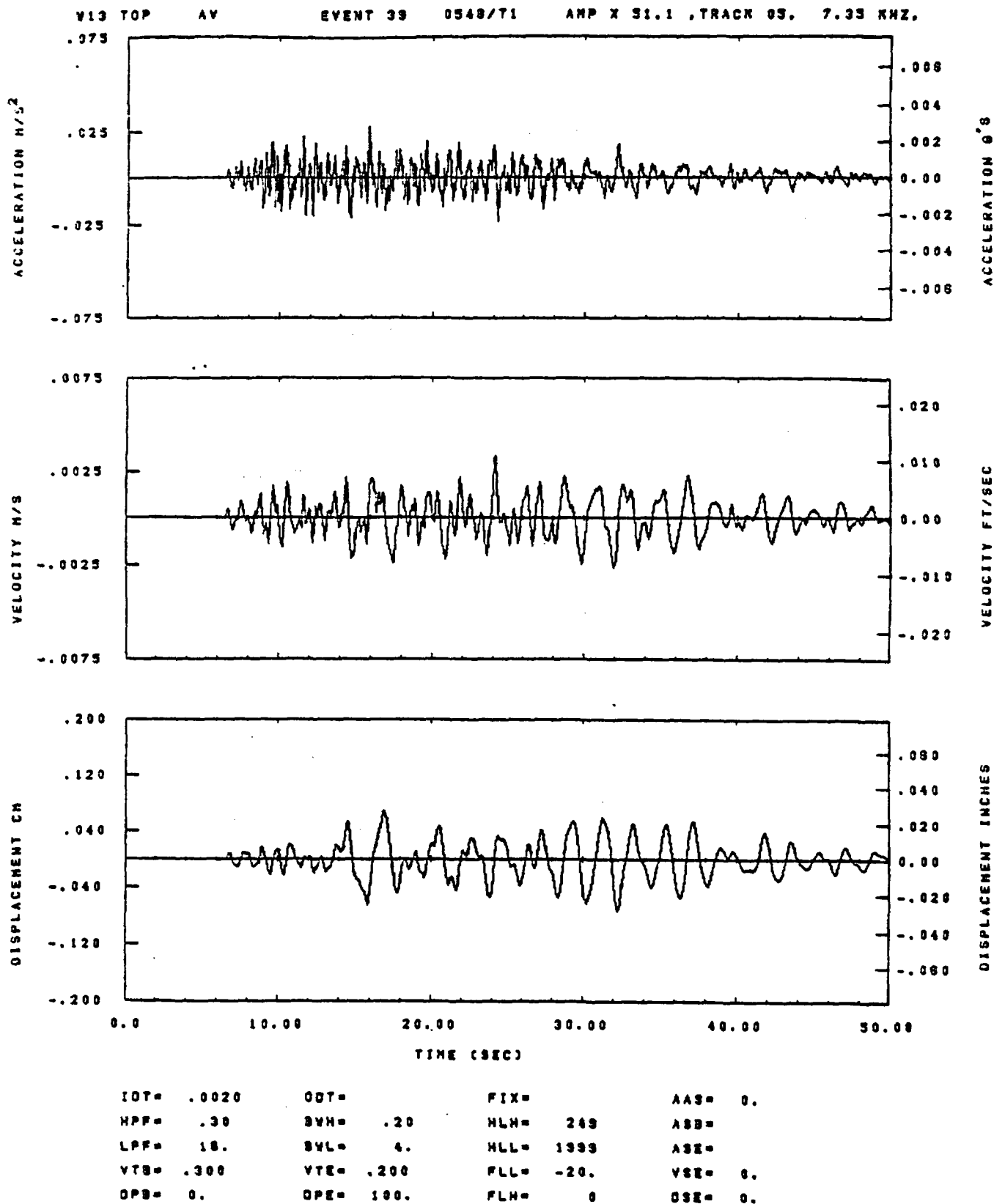


IDT= .0020	ODT= .005	FIX=	AAS= 0.
HFF= .20	BYH= .13	HLH= 88	ASB=
LFF= 45.	BYL= 10.	HLL= 2888	ASE=
VTB= .288	VTE= .133	FLL= -20.	VSE= 0.
DPS= 0.	DPE= 180.	FLH= 0	DSE= 0.

13.58.01.

06/22/02

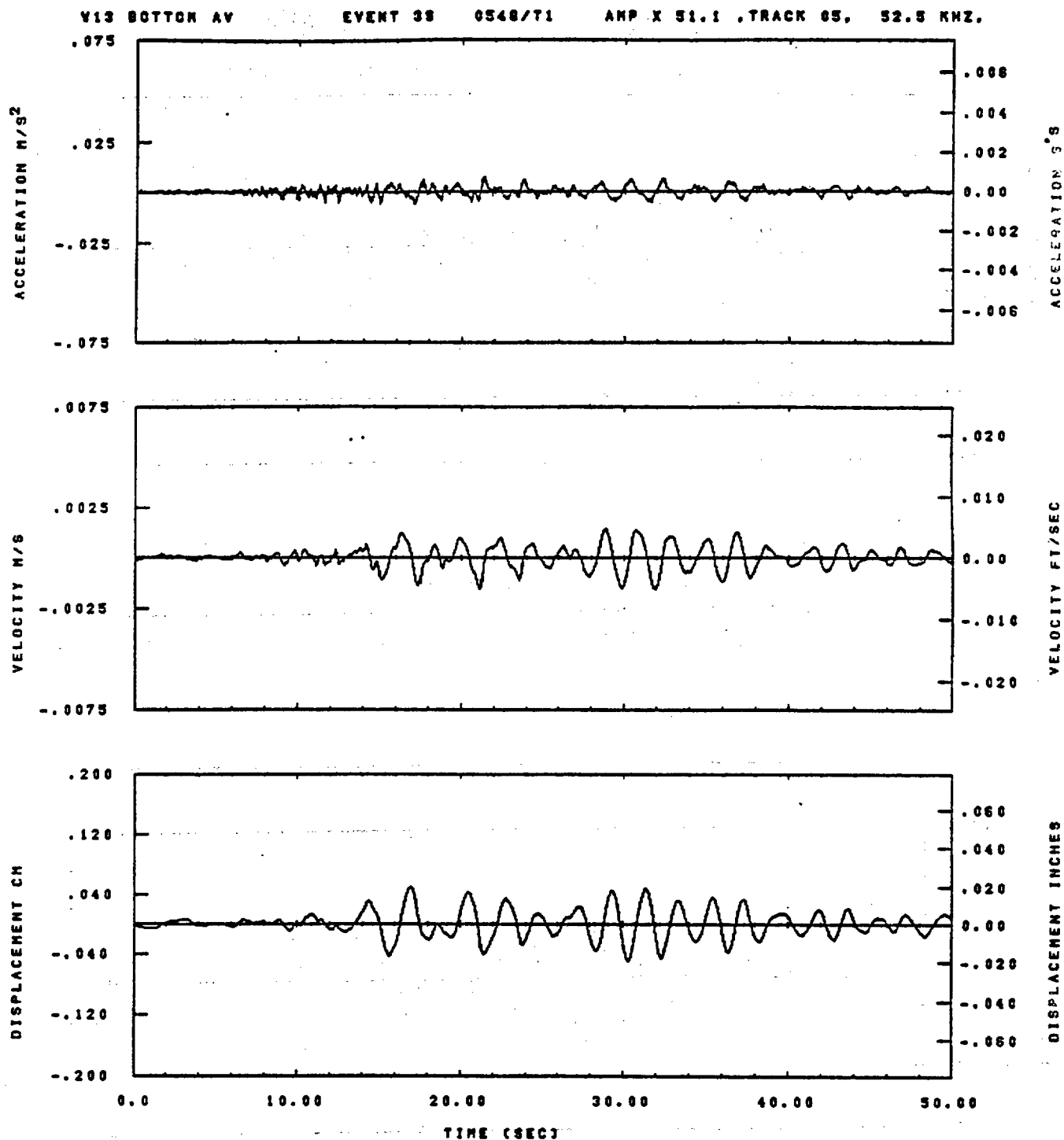
Figure J-24



11.38.03.

08/22/82

Figure J-25

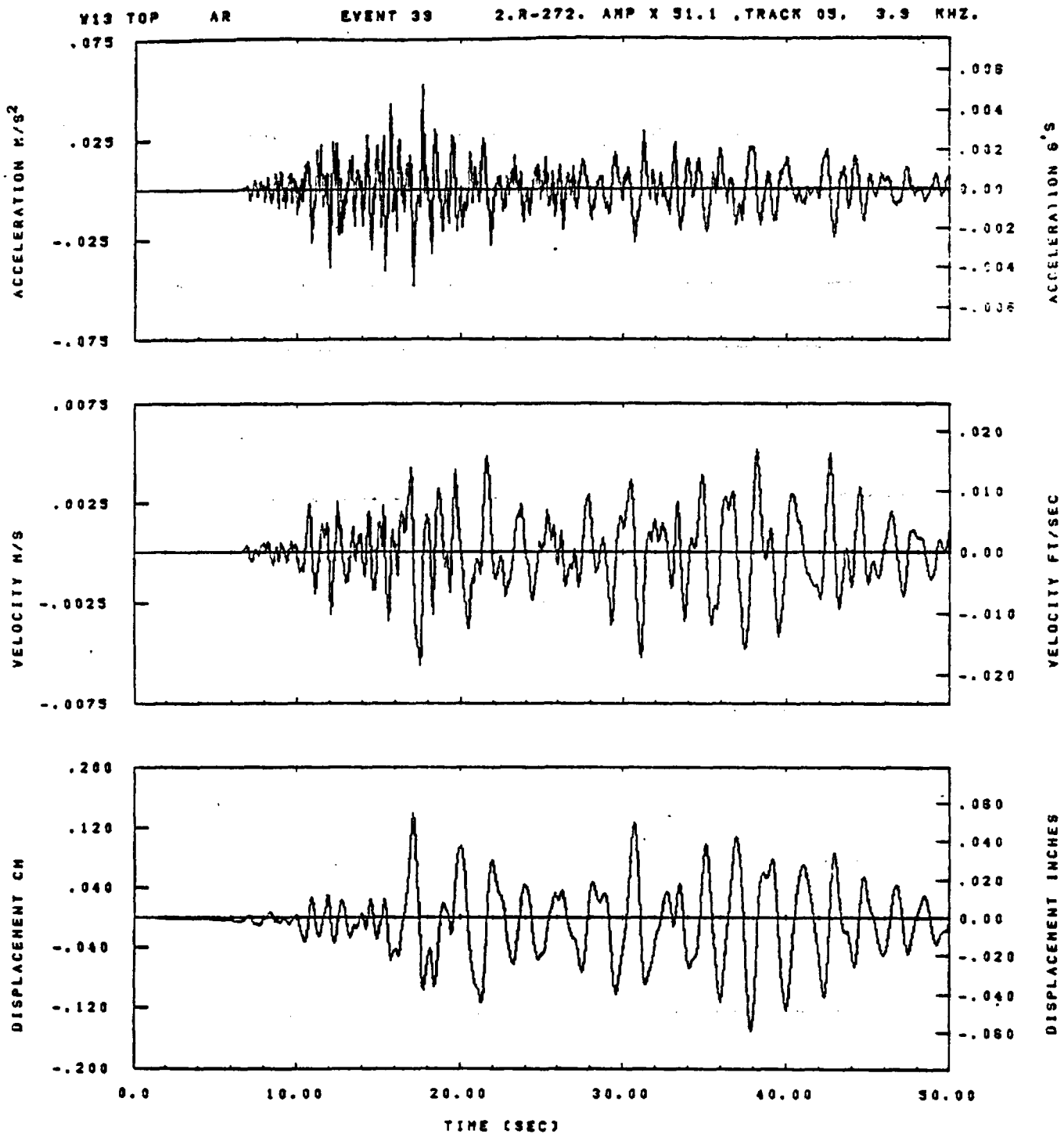


LOT= .0020	ODT= .005	FIX=	AAS= 0.
HPF= .30	BYH= .20	HLH= 188	ASB=
LPF= 22.	BYL= 5.	HLL= 1888	ASE=
VTS= .300	VTE= .200	FLL= -20.	VSE= 0.
DPS= 0.	DPE= 100.	FLH= 0	DSE= 0.

11.56.15.

06/22/02

Figure J-26

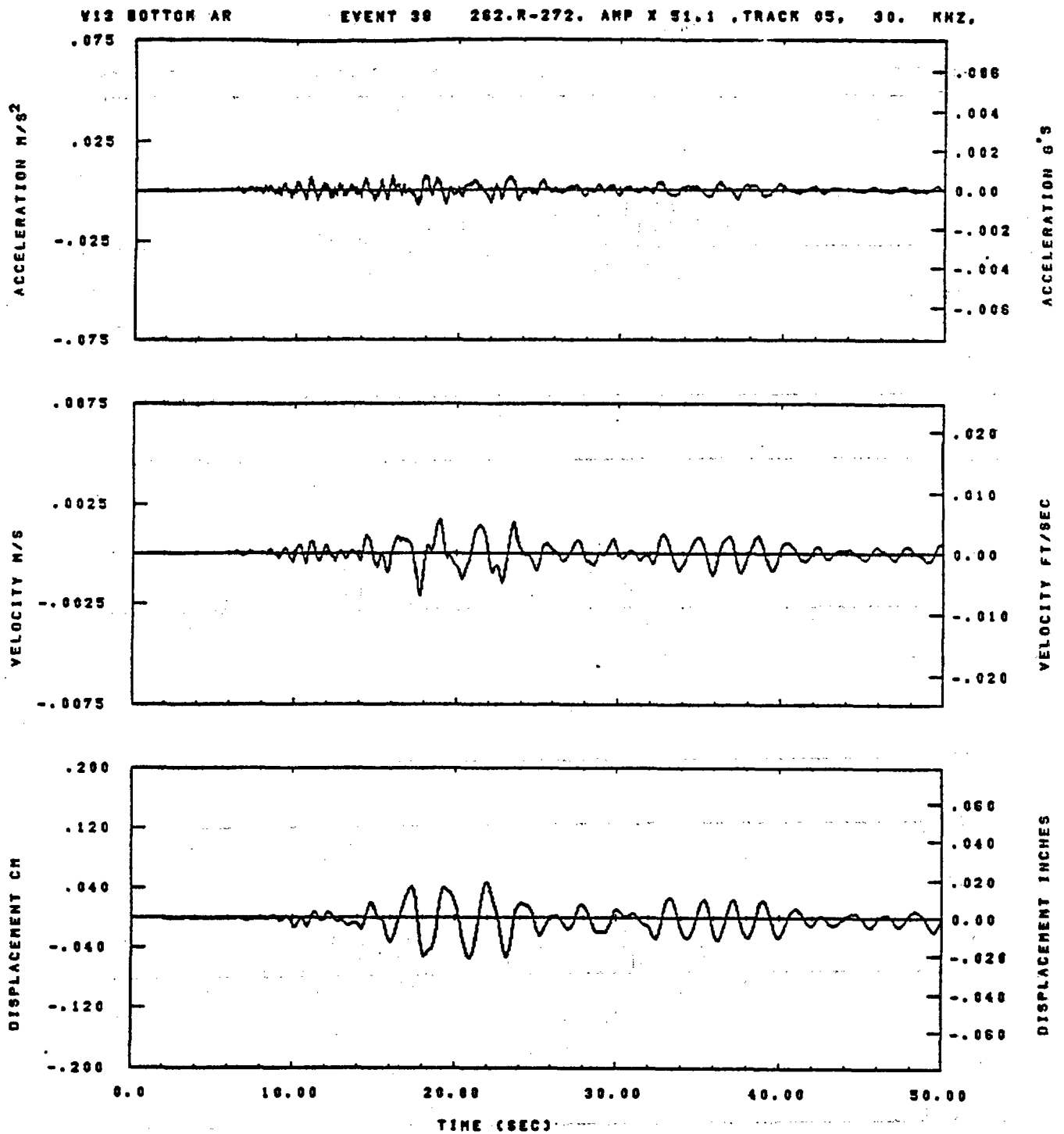


IDT= .0020	ODT=	FIX=	AAS= 0.
HPP= .30	SVH= .20	HLH= 249	ASB=
LPP= 18.	SVL= 4.	HLL= 1399	ASE=
VTS= .388	VTE= .200	FLL= -20.	VSE= 0.
OPS= 0.	OPE= 100.	FLH= 0	DSE= 0.

11.58.08.

06/22/82

Figure J-27



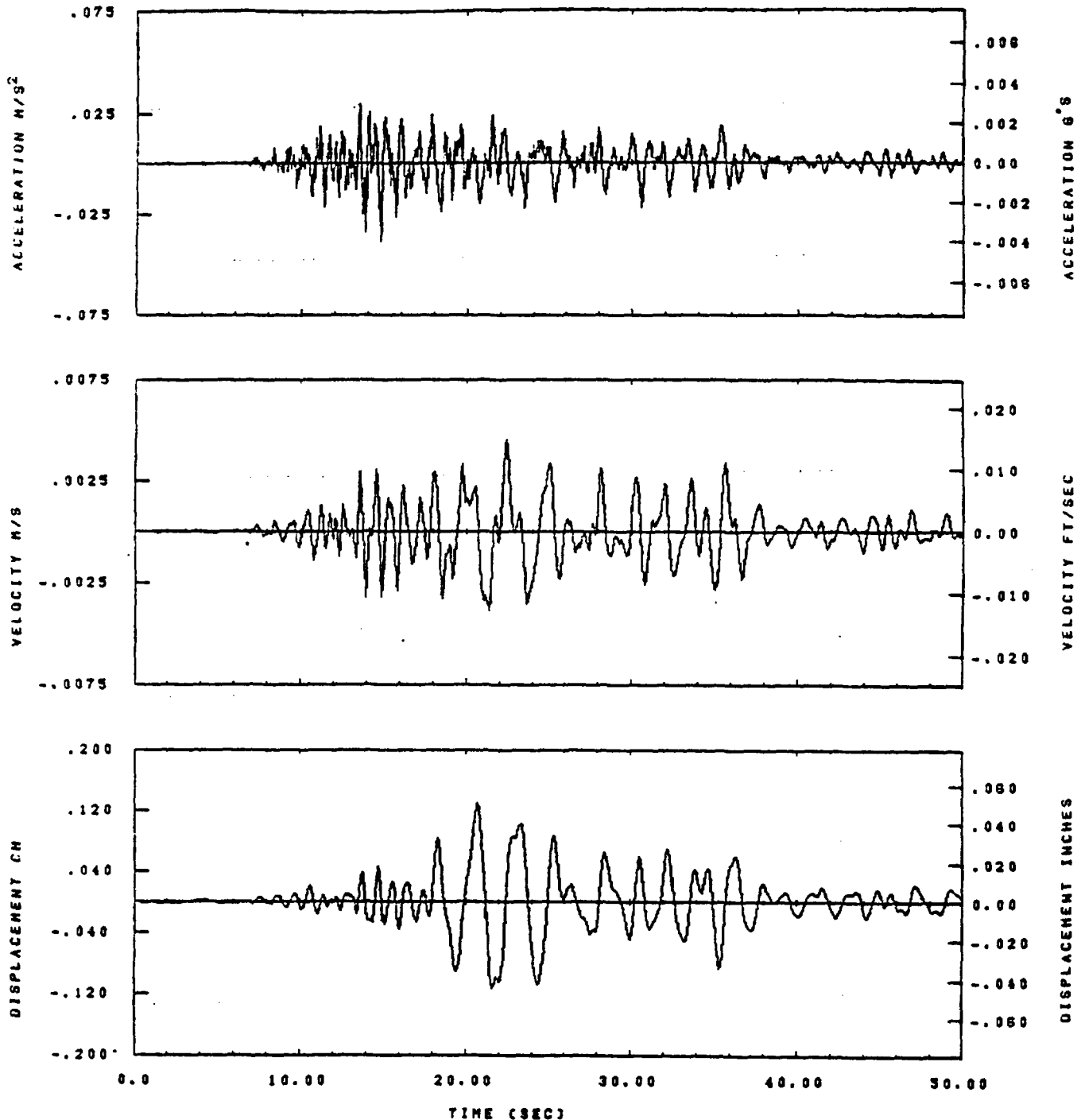
IDT= .0020	ODT= .005	FIX=	AAS= 0.
HPP= .30	BYH= .20	HLH= 188	ASS=
LPP= 22.	BYL= 5.	HLL= 1888	ASE=
VTB= .308	VTE= .208	FLL= -20.	VSE= 0.
DPS= 0.	DPE= 100.	FLH= 0	DSE= 0.

11.56.37.

06/22/82

Figure J-28

W13 TOP AT EVENT 33 2.R- 2. AMP X 51.1 .TRACK 05. 2.3 KHZ.

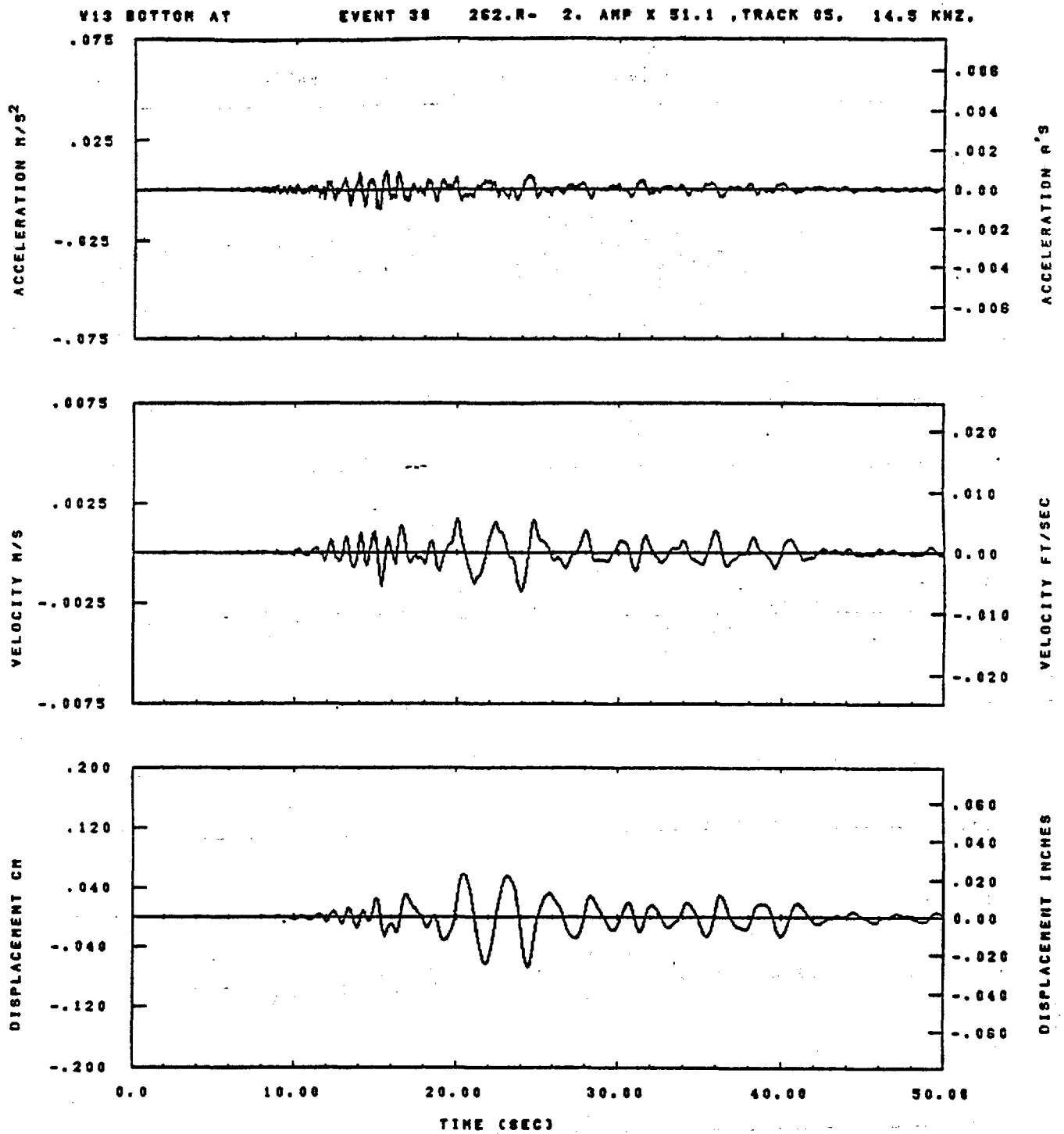


IDT=	.0020	ODT=		FIX=		AAS=	0.
HPP=	.30	SVN=	.20	HLN=	249	ASB=	
LPP=	18.	SVL=	4.	MLL=	1999	ASE=	
VTS=	.300	VTE=	.200	FLL=	-20.	VSE=	0.
OPS=	0.	OPE=	100.	FLN=	0	OSE=	0.

11.38.11.

08/22/92

Figure J-29

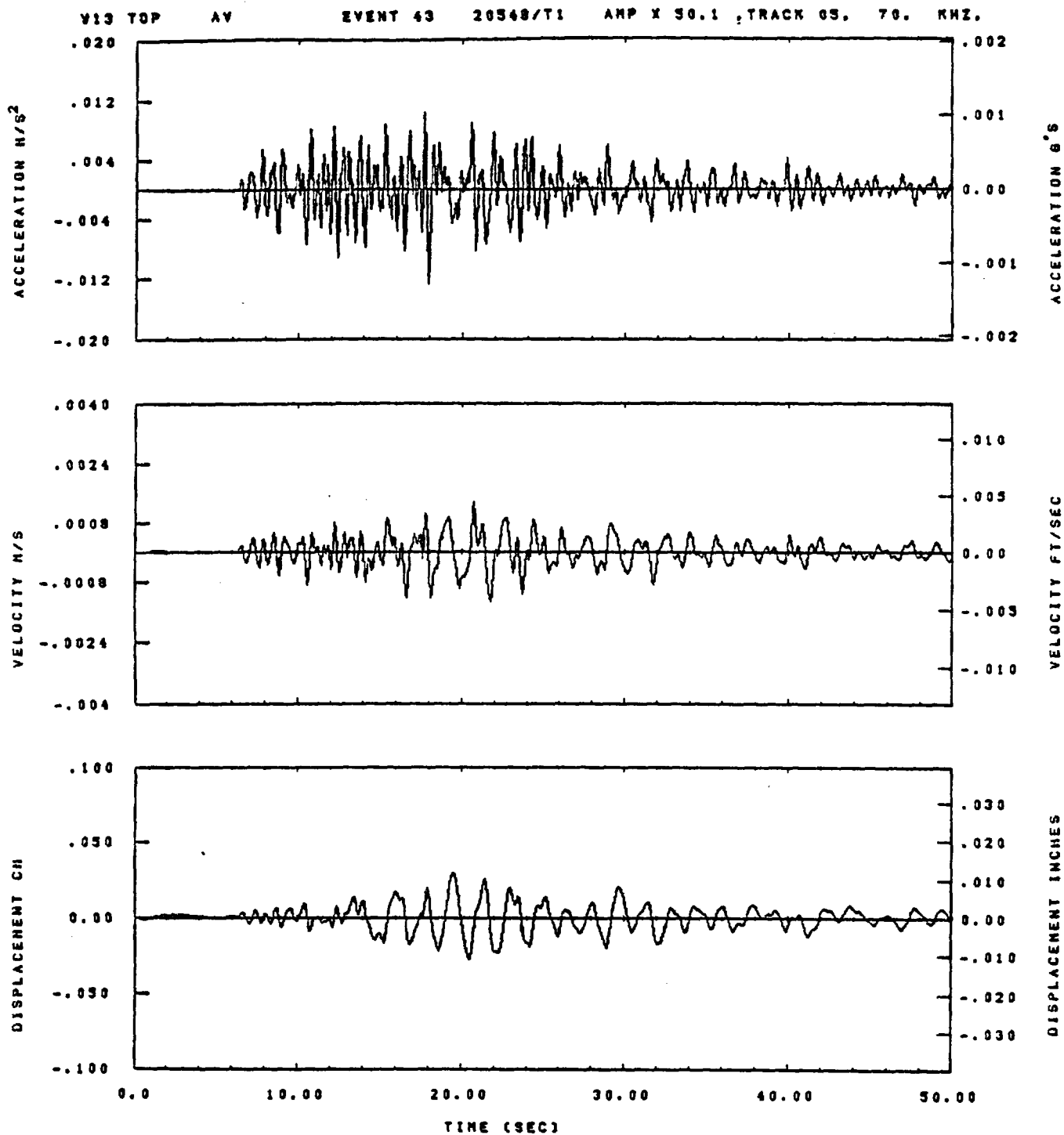


IDT= .0020	ODT= .005	FIX=	AAS= 0.
HPP= .30	BYH= .20	HLH= 199	ASB=
LPP= 22.	BVL= 5.	HLL= 1990	ASE=
VTB= .300	VTE= .200	FLL= -20.	VSE= 0.
DPS= 0.	DPE= 100.	FLH= 0	DSE= 0.

11.56.43.

06/22/82

Figure J-30

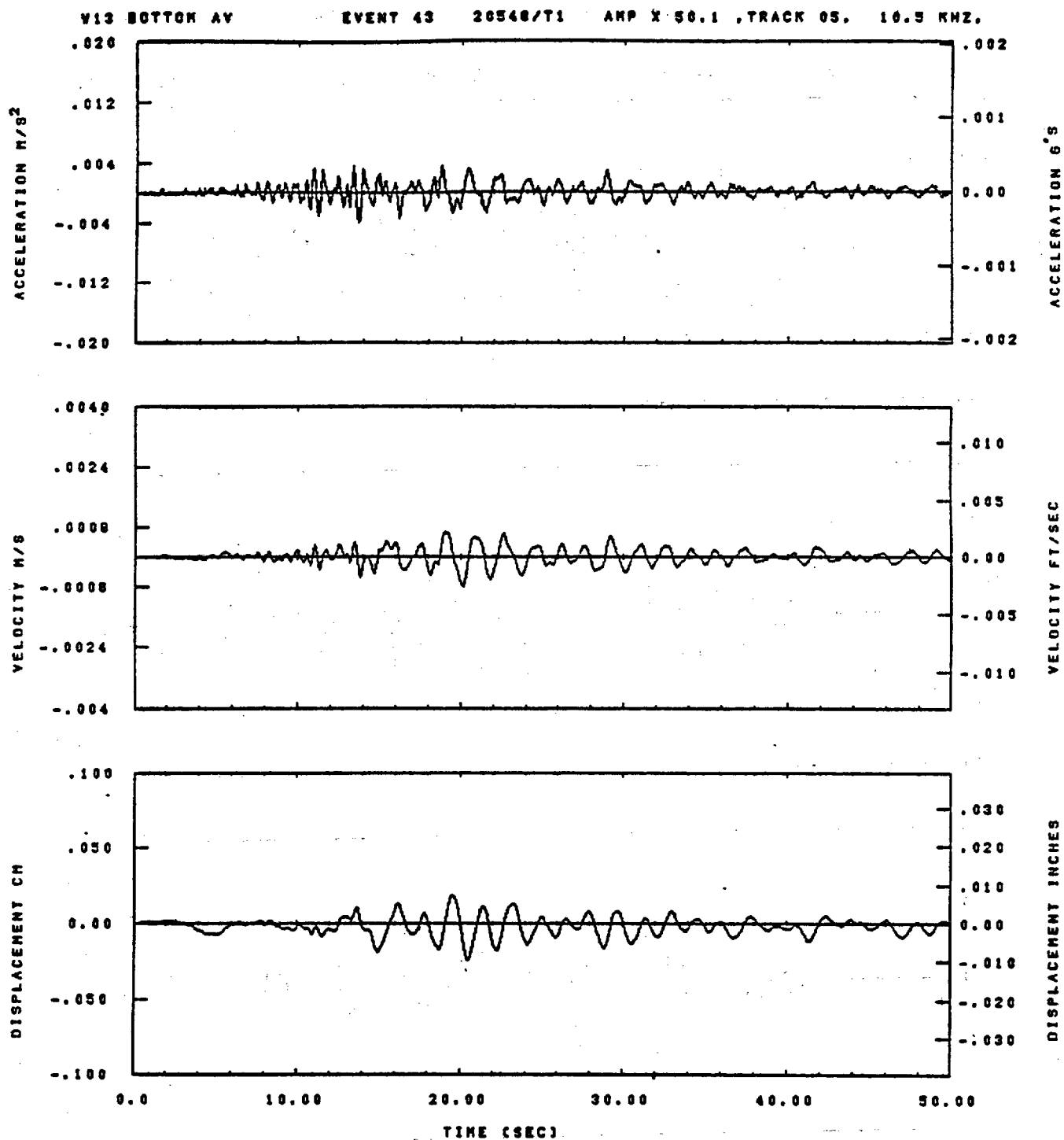


IDT= .0020	ODT= .005	FIX=	AAS= 0.
HPF= .20	BVN= .13	HLH= 417	ASB=
LPF= 10.	SVL= 2.	HLL= 2999	ASE=
VTB= .200	VTE= .133	FLL= -20.	VSE= 0.
DPS= 0.	DPE= 100.	FLH= 0	DSE= 0.

09.48.35.

08/23/82

Figure J-31

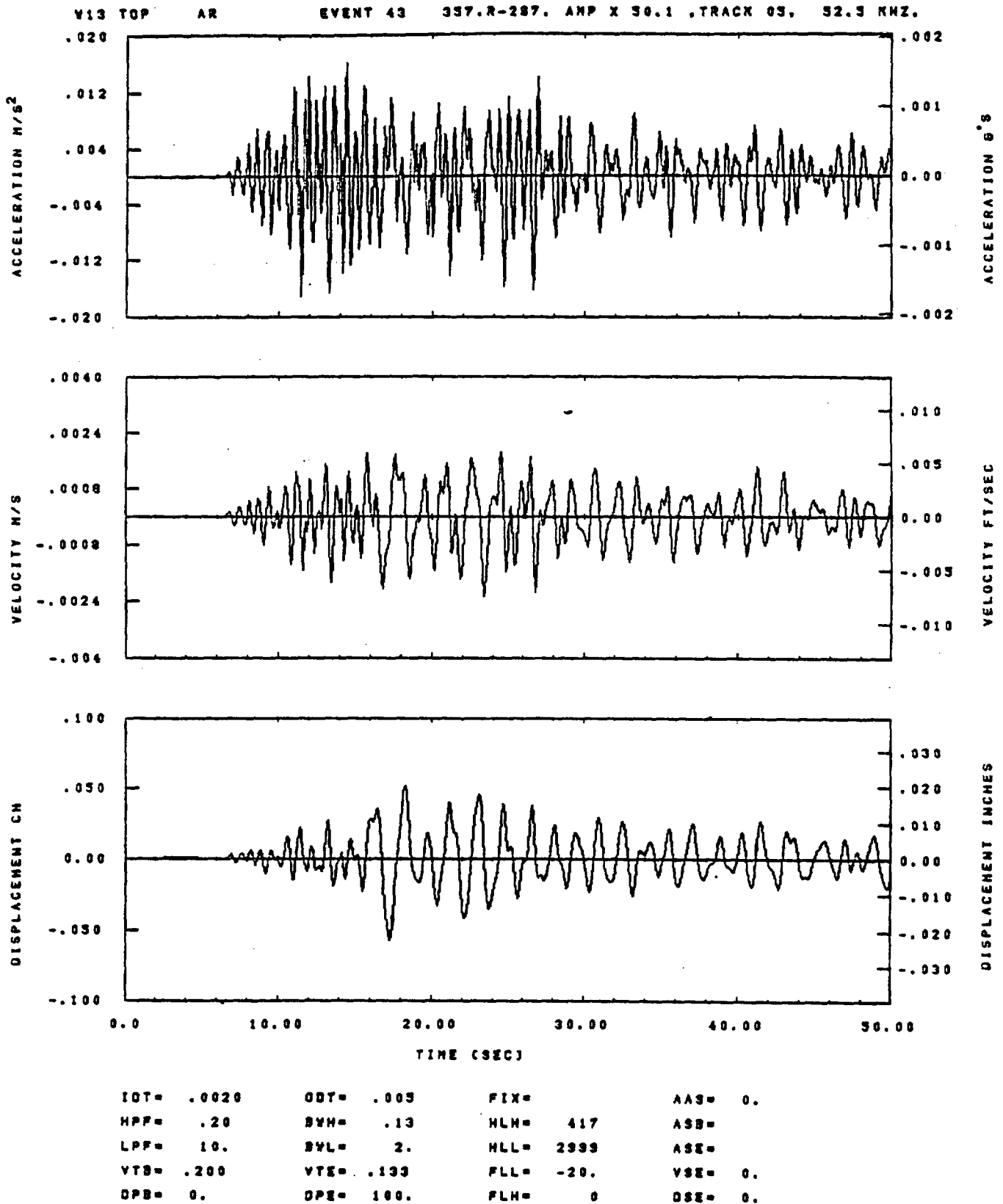


IDT= .0020	ODT= .005	FIX=	AAS= 0.
HPF= .20	SVH= .13	HLH= 417	ASS=
LPF= 10.	SVL= 2.	HLL= 2989	ASE=
VTS= .200	VTE= .133	FLL= -20.	VSE= 0.
DPS= 0.	DPE= 100.	FLH= 0	DSE= 0.

08.50.38.

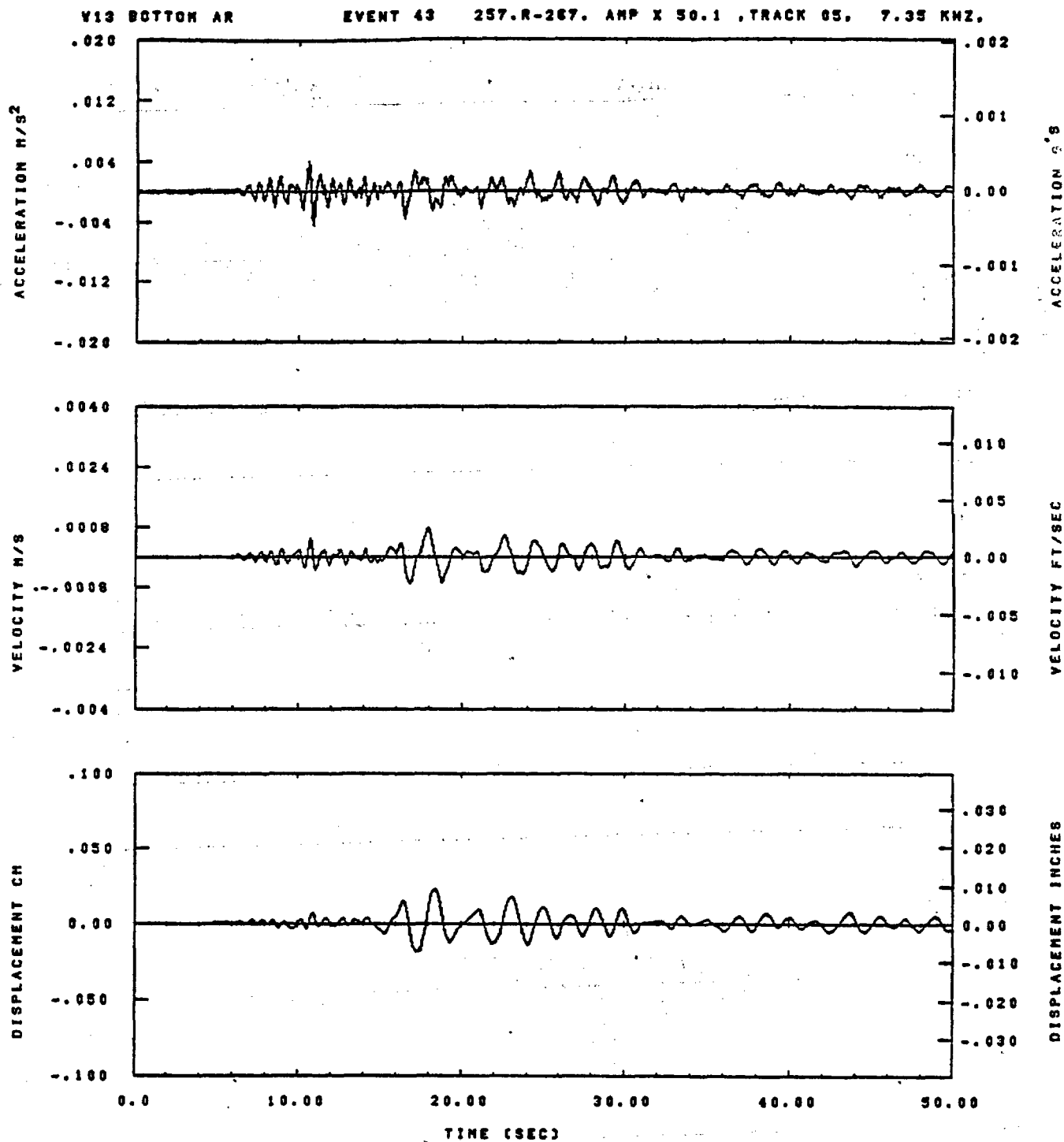
06/23/82

Figure J-32



08.48.45.

08/23/82

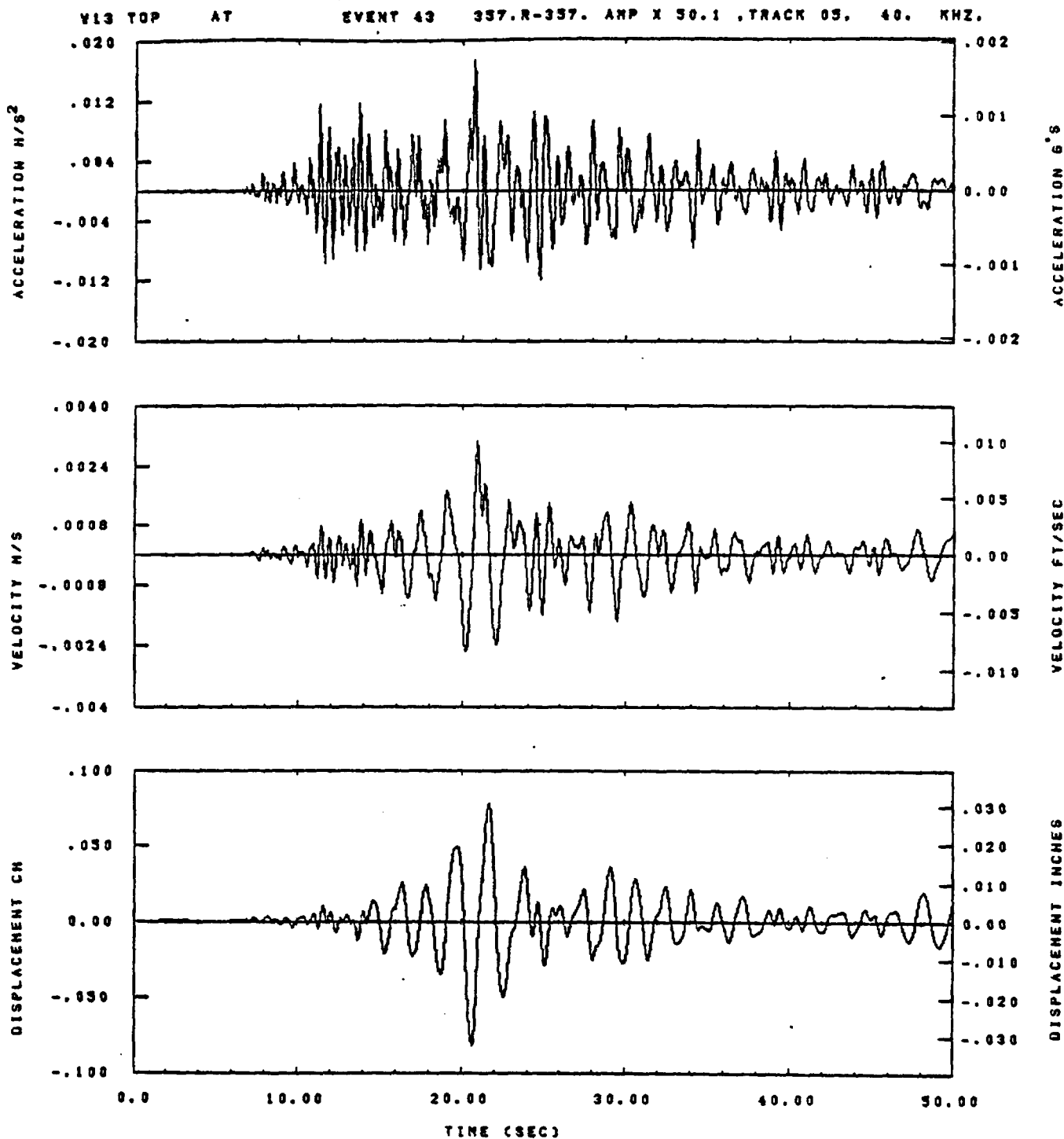


IDT= .0020	ODT= .005	FIX=	AAS= 0.
HPF= .20	BYH= .13	HLH= 417	ASB=
LPF= 10.	BYL= 2.	HLL= 2888	ASE=
VTS= .200	VTE= .133	FLL= -20.	VSE= 0.
DPS= 0.	OPE= 100.	FLH= 0	DSE= 0.

08.51.29.

06/23/82

Figure J-34

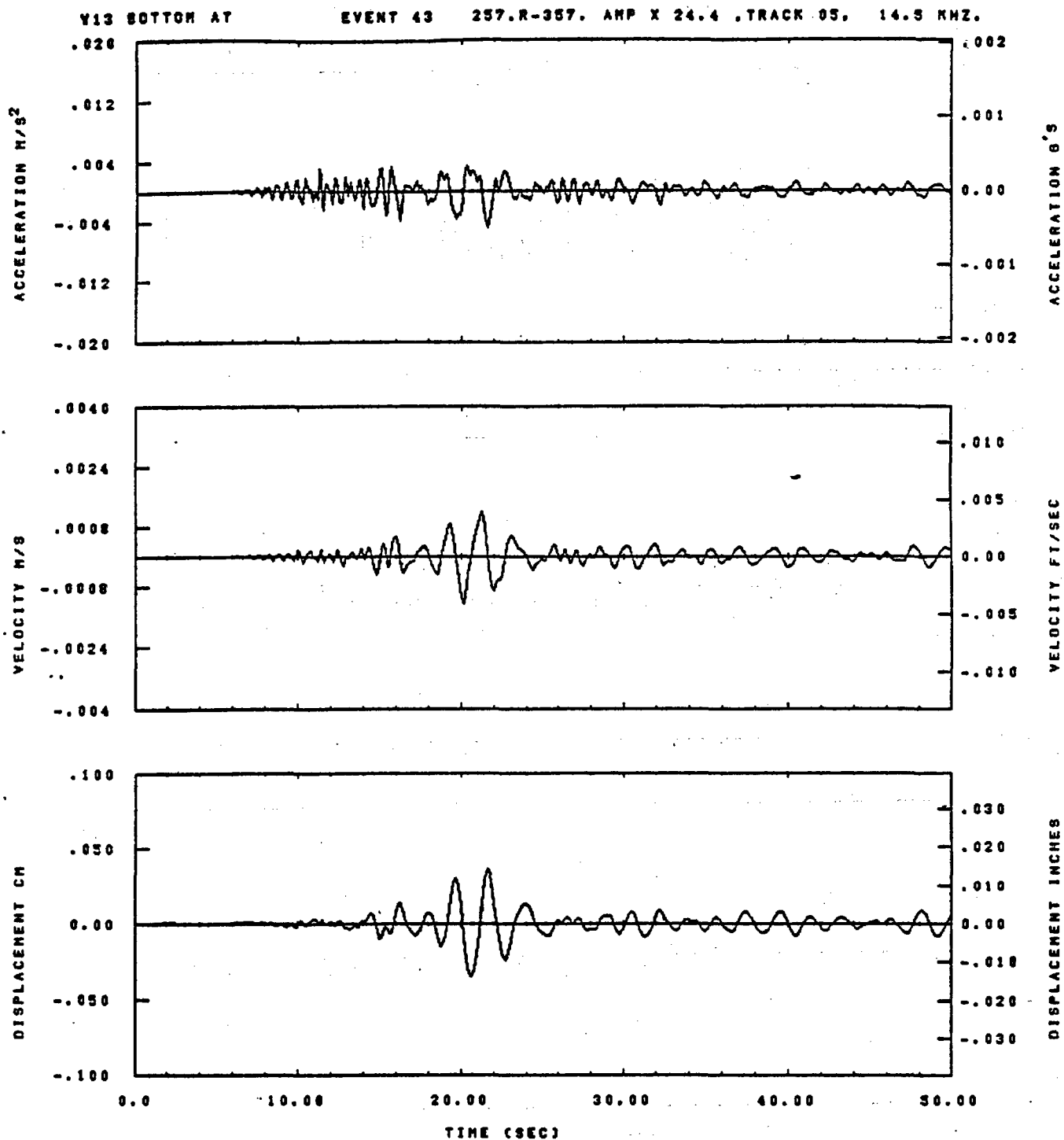


IOT= .0020	ODT= .005	FIX=	AAS= 0.
HPF= .20	BYH= .13	HLH= 417	ASB=
LPF= 10.	BYL= 2.	HLL= 2999	ASE=
VTS= .200	VTE= .133	FLL= -20.	VSE= 0.
DPS= 0.	DPE= 100.	FLH= 0	DSE= 0.

09.30.13.

06/23/82

Figure J-35

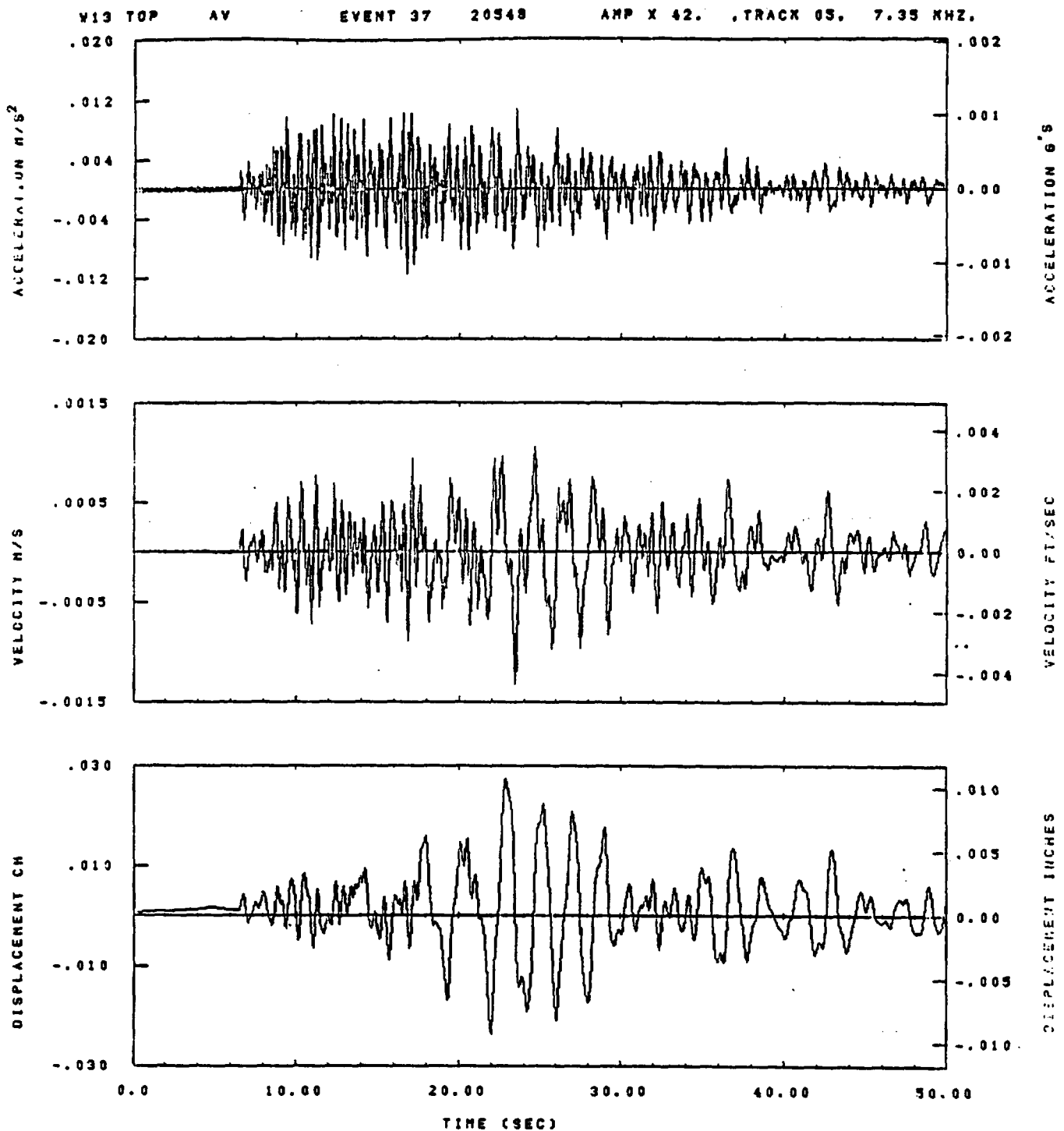


IDT= .0020	ODT= .005	FIX=	AAS= 0.
HPP= .20	BYH= .13	HLH= 417	ASB=
LPP= 10.	BYL= 2.	HLL= 2888	ASE=
VTS= .200	VTE= .133	PLL= -20.	VSE= 0.
DPS= 0.	DPE= 100.	PLH= 0	DSE= 0.

00.52.54.

06/23/82

Figure J-36

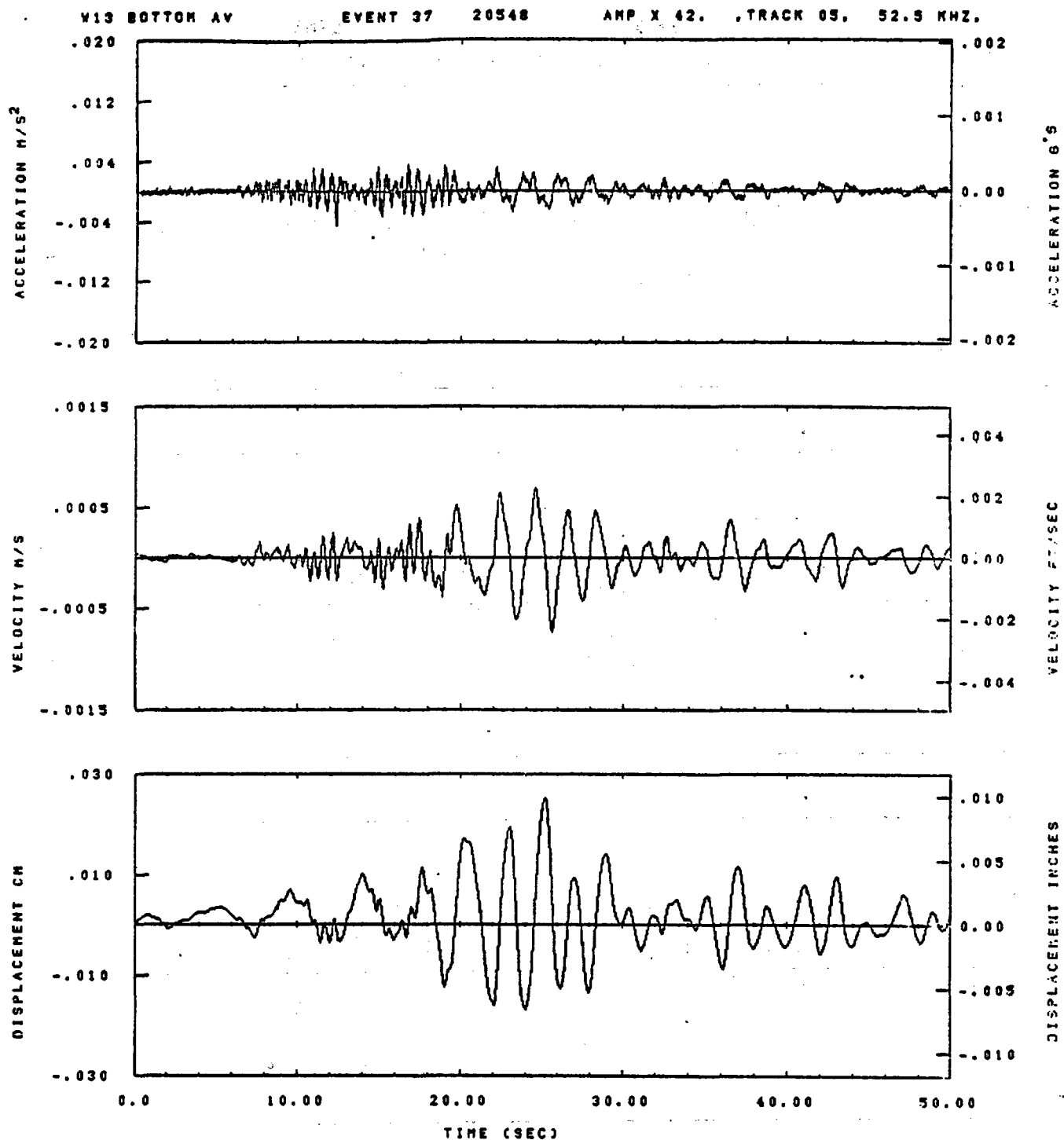


IDT= .0020	ODT= .005	FIX=	AAS= 0.
HPF= .20	BYH= .13	HLH= 243	ASB=
LPF= 18.	BYL= 4.	HLL= 2999	ASE=
YTB= .200	YTE= .133	FLL= -20.	VSE= 0.
DPS= 0.	DPE= 100.	FLH= 0	DSE= 0.

09.59.50.

08/17/82

Figure J-37

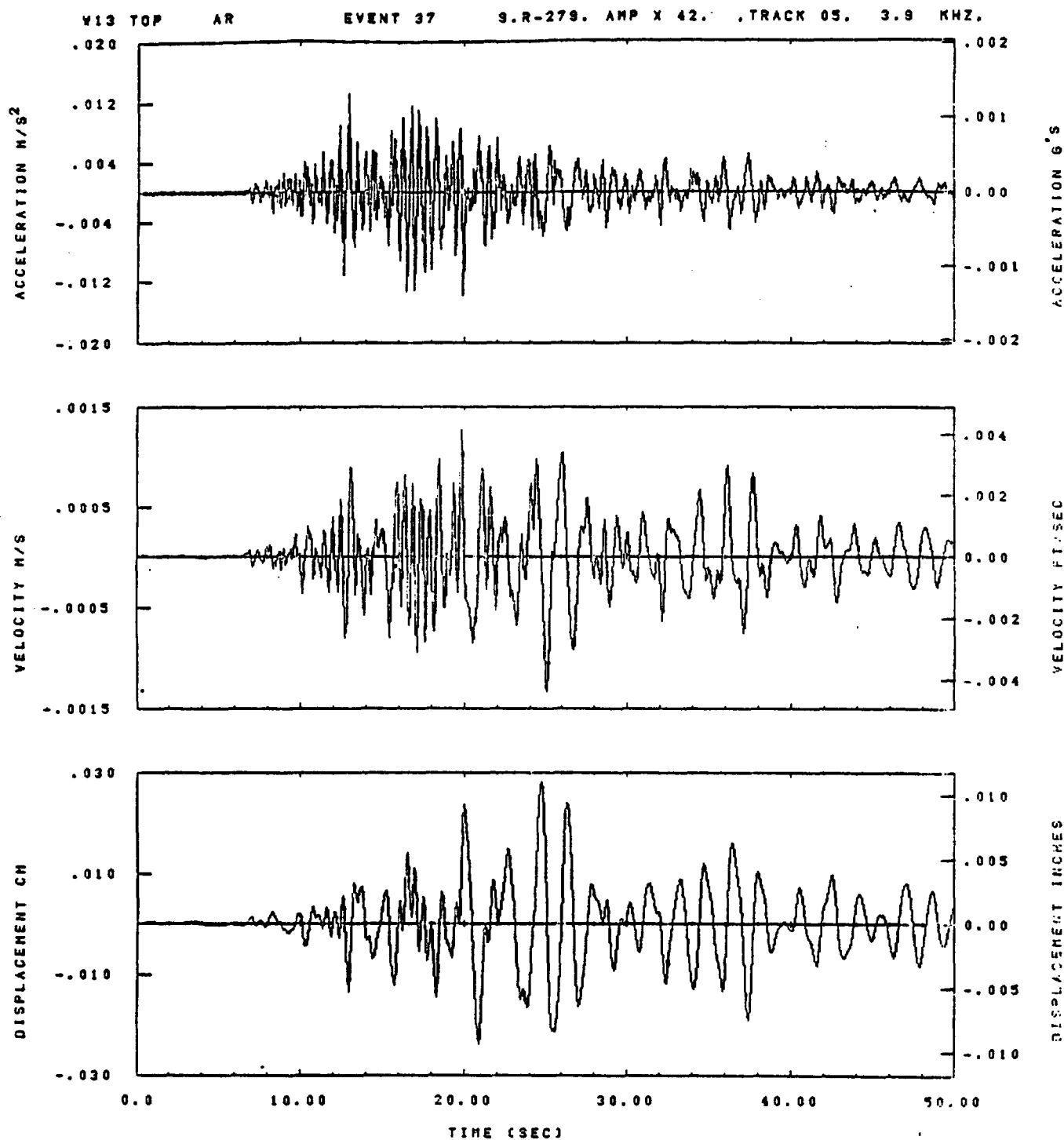


IOD= .0020	OOT= .005	FIX=	AAS= 0.
HPF= .20	BYH= .13	HLH= 249	ASB=
LPF= 18.	BVL= 4.	HLL= 2999	ASE=
VTS= .200	VTE= .133	FLL= -20.	VSE= 0.
DPS= 0.	DPE= 100.	FLH= 0	DSE= 0.

10.00.20.

06/17/82

Figure J-38

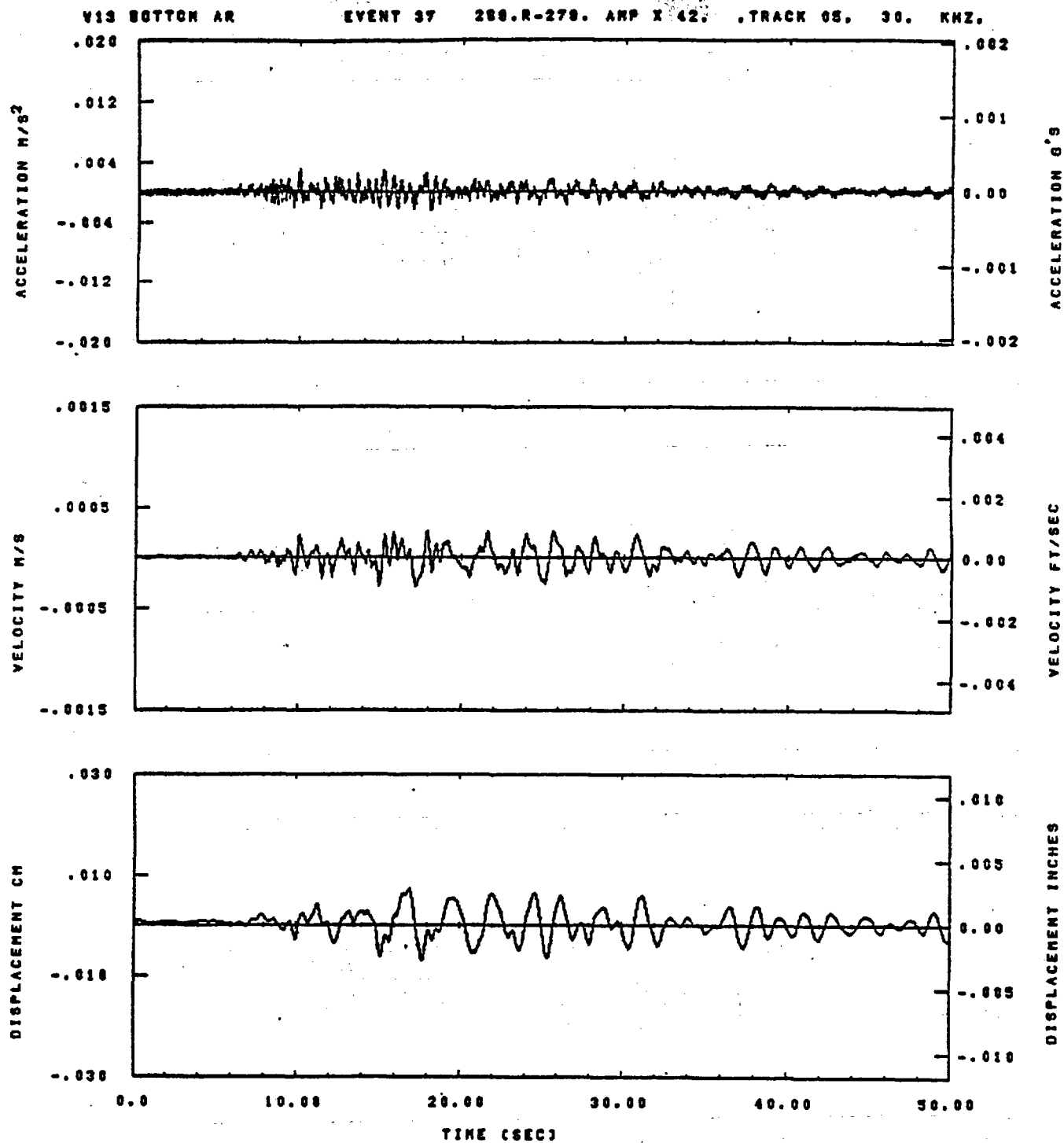


IDT= .0020	ODT= .005	FIX=	AAS= 0.
HPF= .2	BYH= .13	HLH= 249	ASB=
LPF= 18.	BVL= 4.	HLL= 2999	ASE=
YTS= .20	VTE= .133	FLL= -20.	VSE= 0.
DPD= 0.	DPE= 100.	FLH= 0	DSE= 0.

10.00.00.

06/17/92

Figure J-39

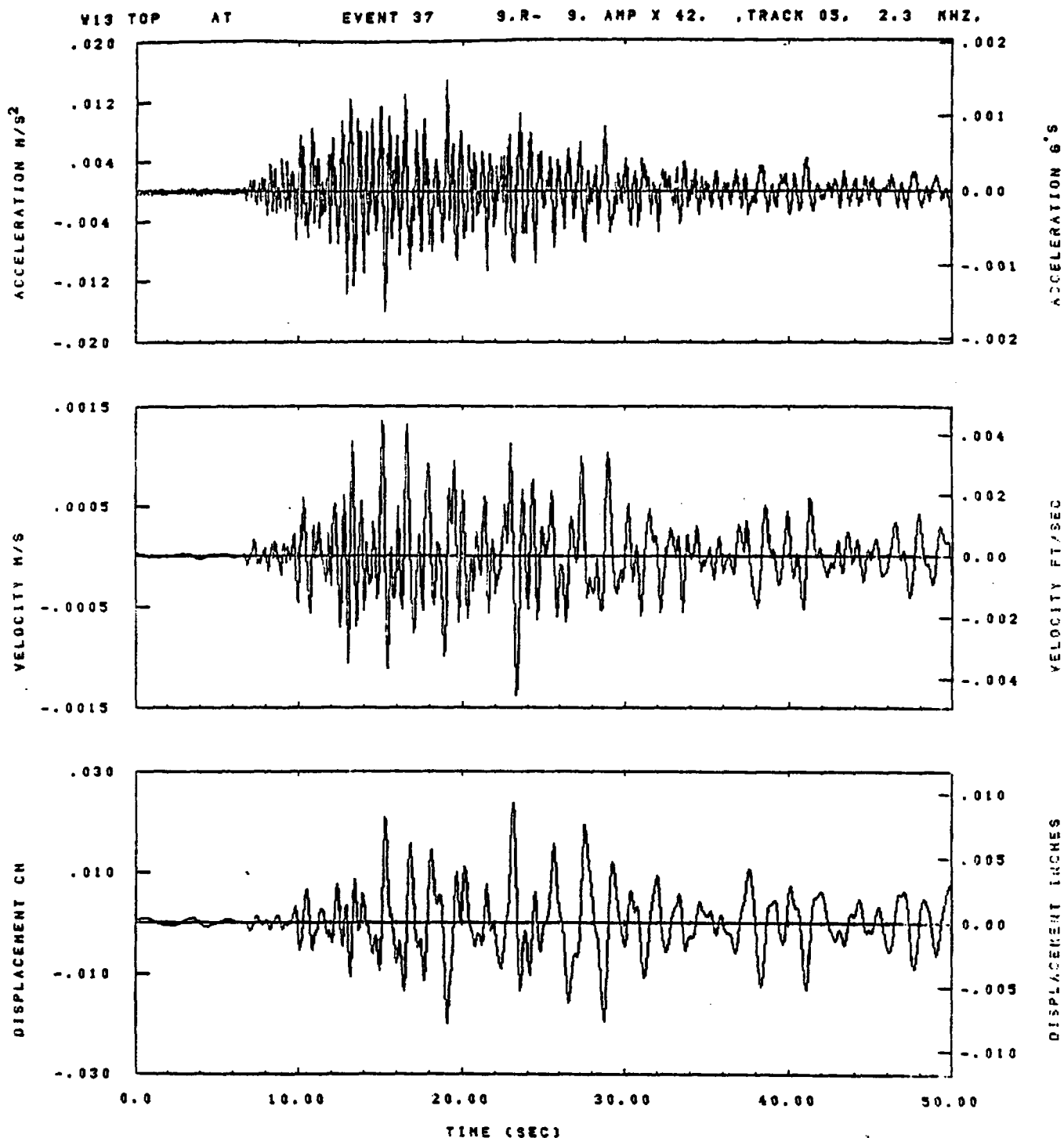


IDT= .0020	ODT= .0005	FIX=	AAS= 0.
HPP= .3	BYH= .20	HLH= 188	ASS=
LPP= 22.	BYL= 5.	HLL= 1888	ASE=
VTS= .38	VTE= .288	FLL= -20.	VSE= 0.
DPS= 0.	DPE= 188.	FLH= 0	DSE= 0.

13.58.02.

08/24/82

Figure J-40

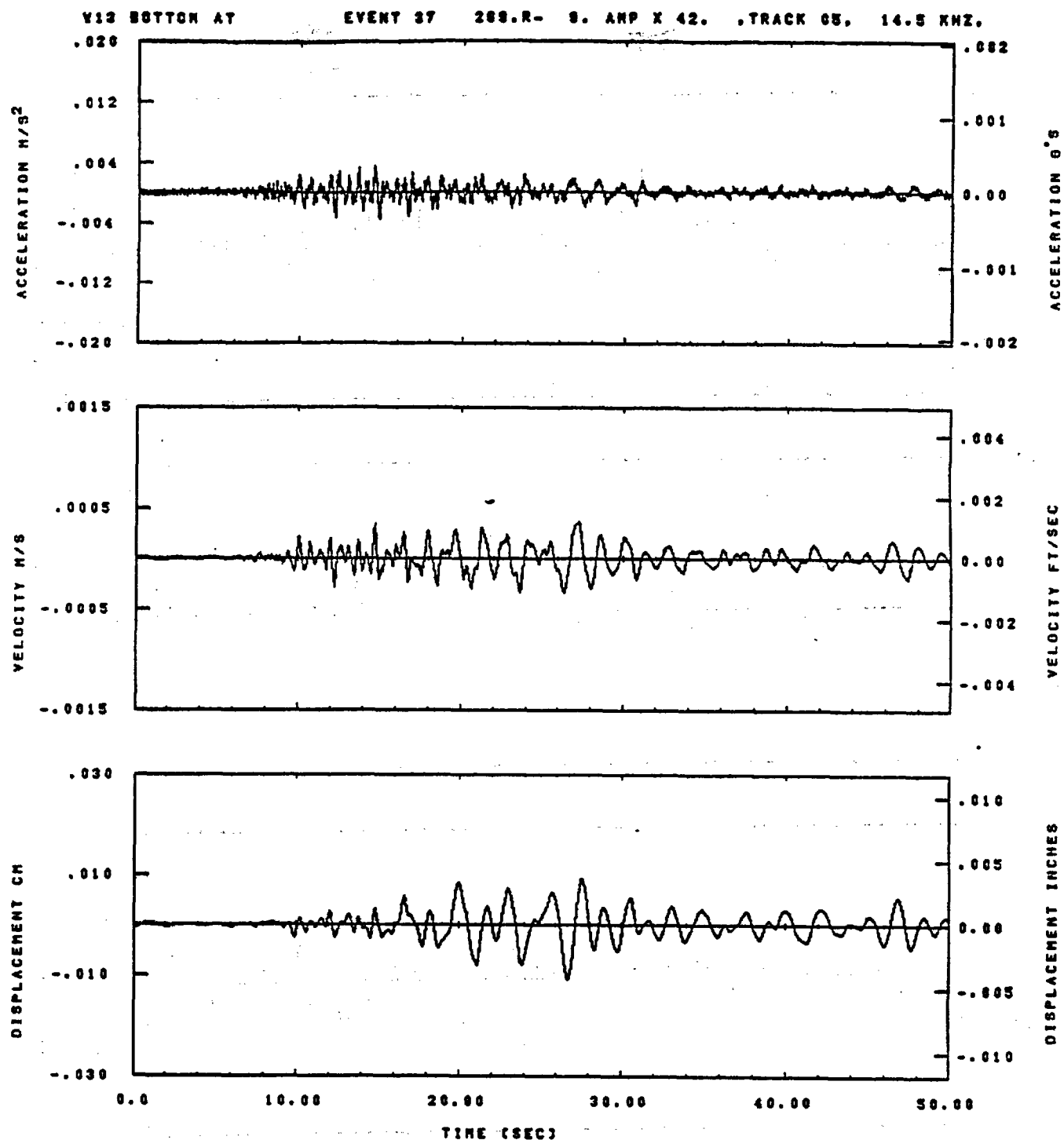


IDT= .0020	ODT= .005	FIX=	AAS= 0.
HPF= .4	BYH= .28	HLH= 187	ASS=
LPF= 27.	BYL= 6.	HLL= 1439	ASE=
VTS= .40	VTE= .287	FLL= -20.	VSE= 0.
DPS= 0.	DPE= 100.	FLH= 0	DSE= 0.

10.00.03.

06/17/82

Figure J-41



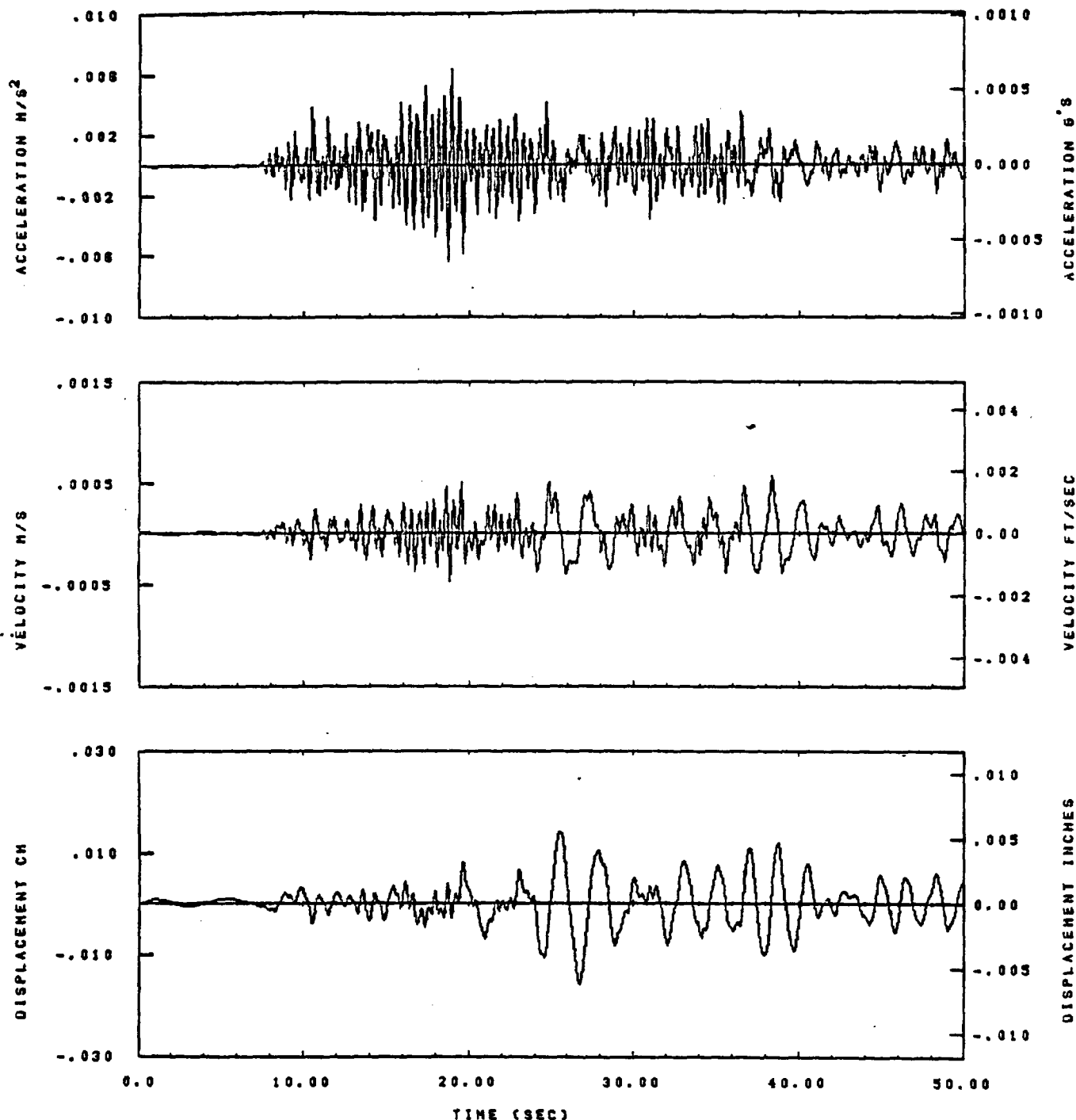
IDT= .0020	QDT= .005	FIX=	AAS= 0.
HPF= .3	SVN= .20	HLN= 188	ASS=
LPF= 22.	BVL= 5.	HLL= 1988	ASE=
VTS= .38	VTE= .200	FLL= -20.	VSE= 0.
DPS= 0.	DPE= 100.	FLH= 0	DSE= 0.

13.58.87.

06/24/82

Figure J-42

V13 TOP AV EVENT 48 20348/TPI AMP X 499. TRACK 05, 30. KHZ.

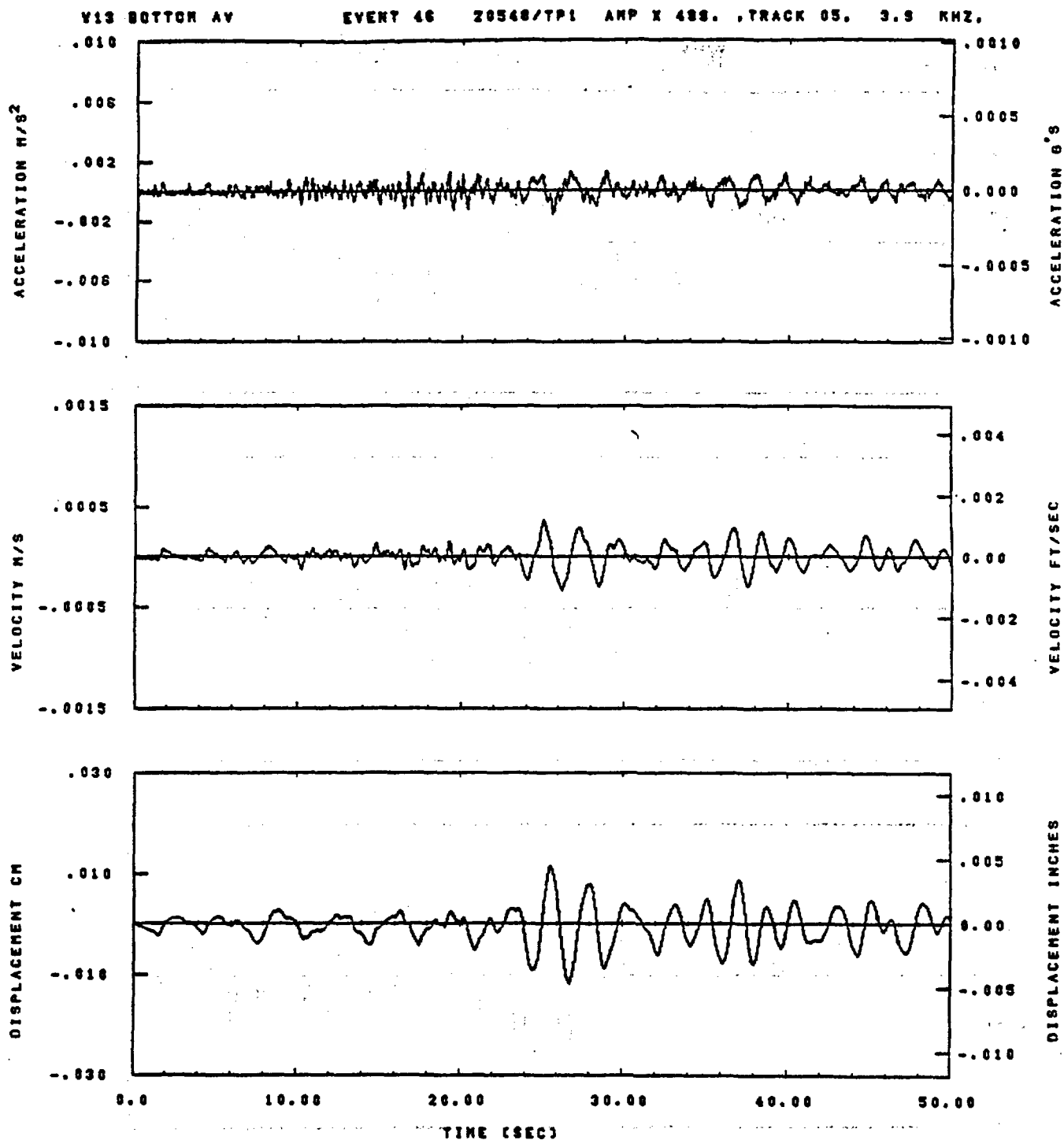


IDT= .0020	QDT= .0005	FIX=	AAS= 0.
HPP= .30	BYN= .20	HLN= 201	ASS=
LPP= 22.	BYL= 5.	HLL= 1999	ASE=
YTB= .300	YTS= .200	FLL= -12.	VSE= 0.
DPS= 0.	DPE= 100.	FLH= 0	DSE= 0.

07.58.25.

08/26/92

Figure J-43

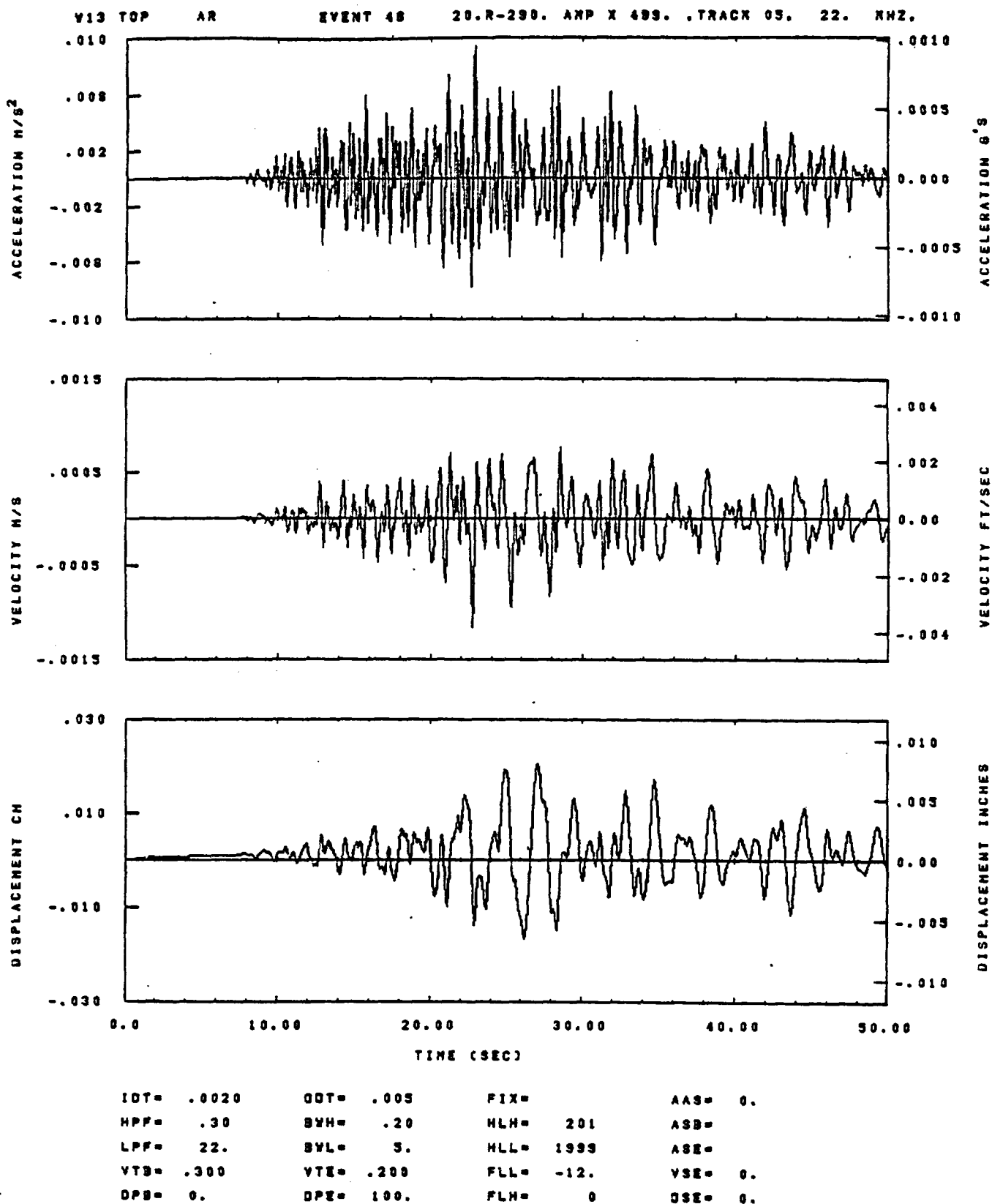


IDT= .0020	ODT= .005	FIX=	AAS= 0.
HPF= .30	BYH= .20	HLH= 201	ASH=
LPF= 22.	BYL= 5.	HLL= 1980	ASE=
VTS= .300	VTE= .200	FLL= -12.	VSE= 0.
DPS= 0.	OPE= 100.	FLH= 0	DSE= 0.

07.58.40.

06/24/82

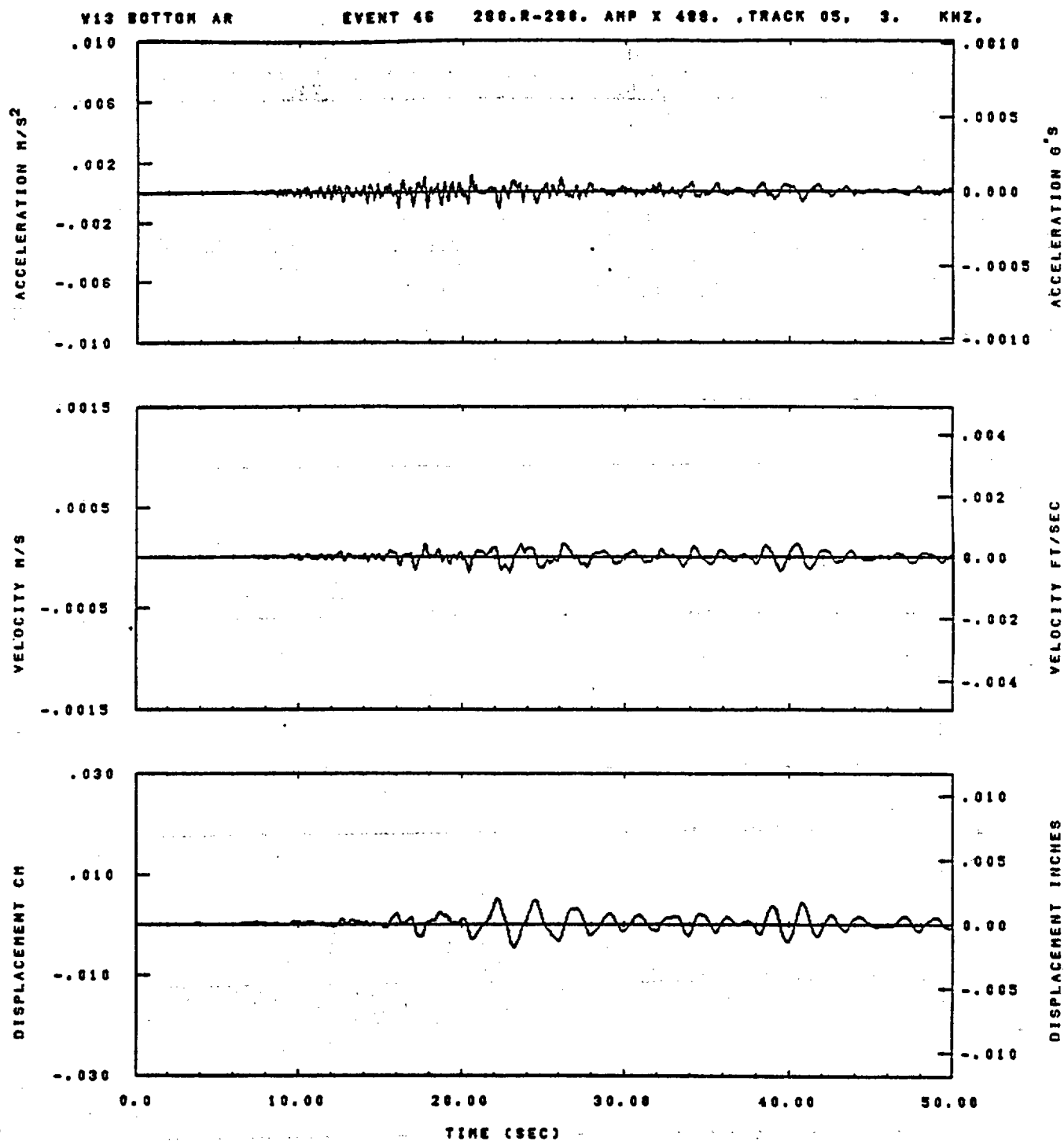
Figure J-44



07.58.31.

08/24/82

Figure J-45

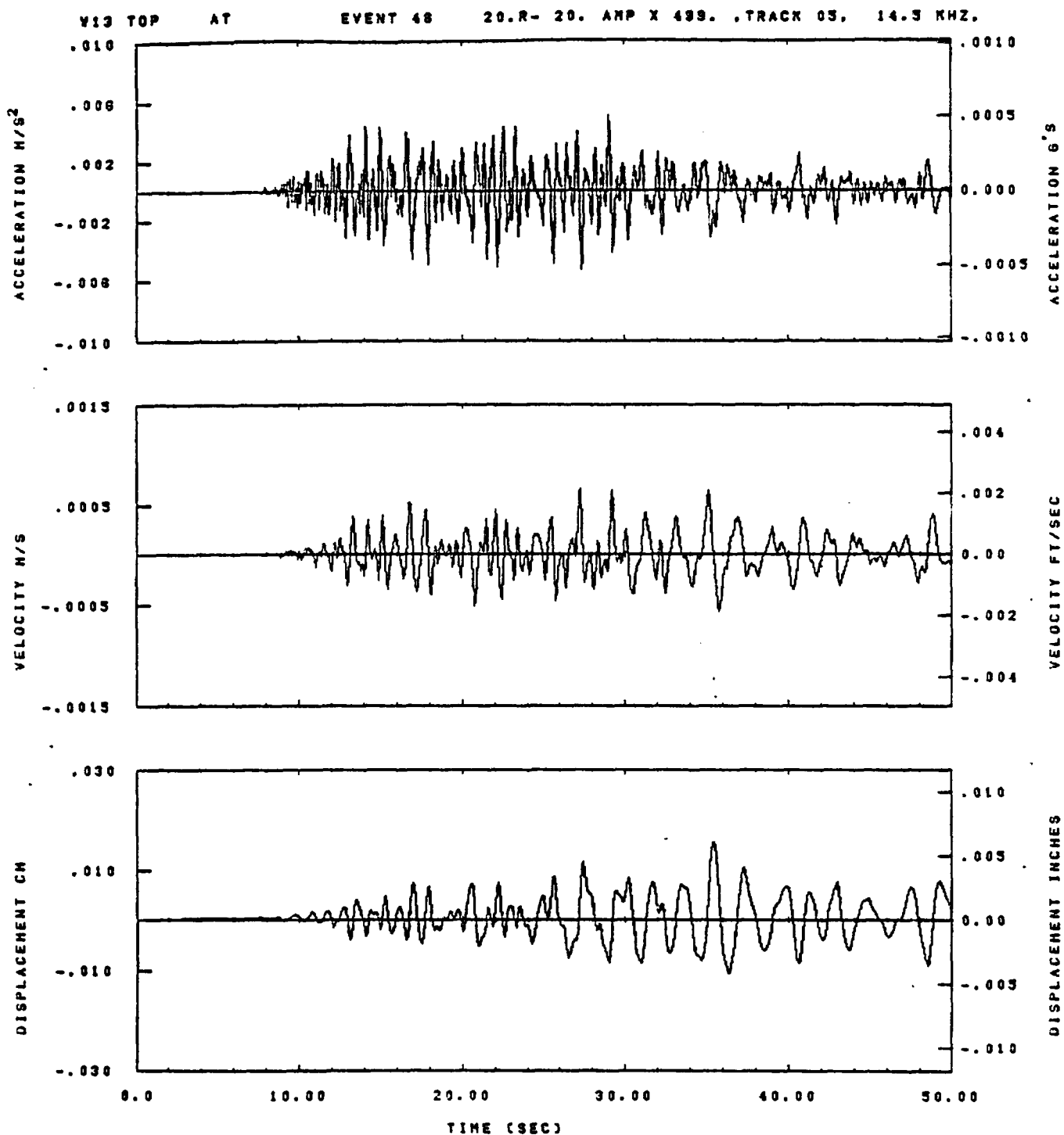


IDT= .0020	ODT= .005	FIX=	AAS= 0.
HPF= .30	BYH= .20	HLH= 201	ASB=
LPF= 22.	BVL= 5.	HLL= 1999	ASE=
VTB= .300	YTE= .200	FLL= -12.	VSE= 0.
DPS= 0.	DPE= 100.	FLH= 0	DSE= 0.

87.58.45.

06/24/82

Figure J-46

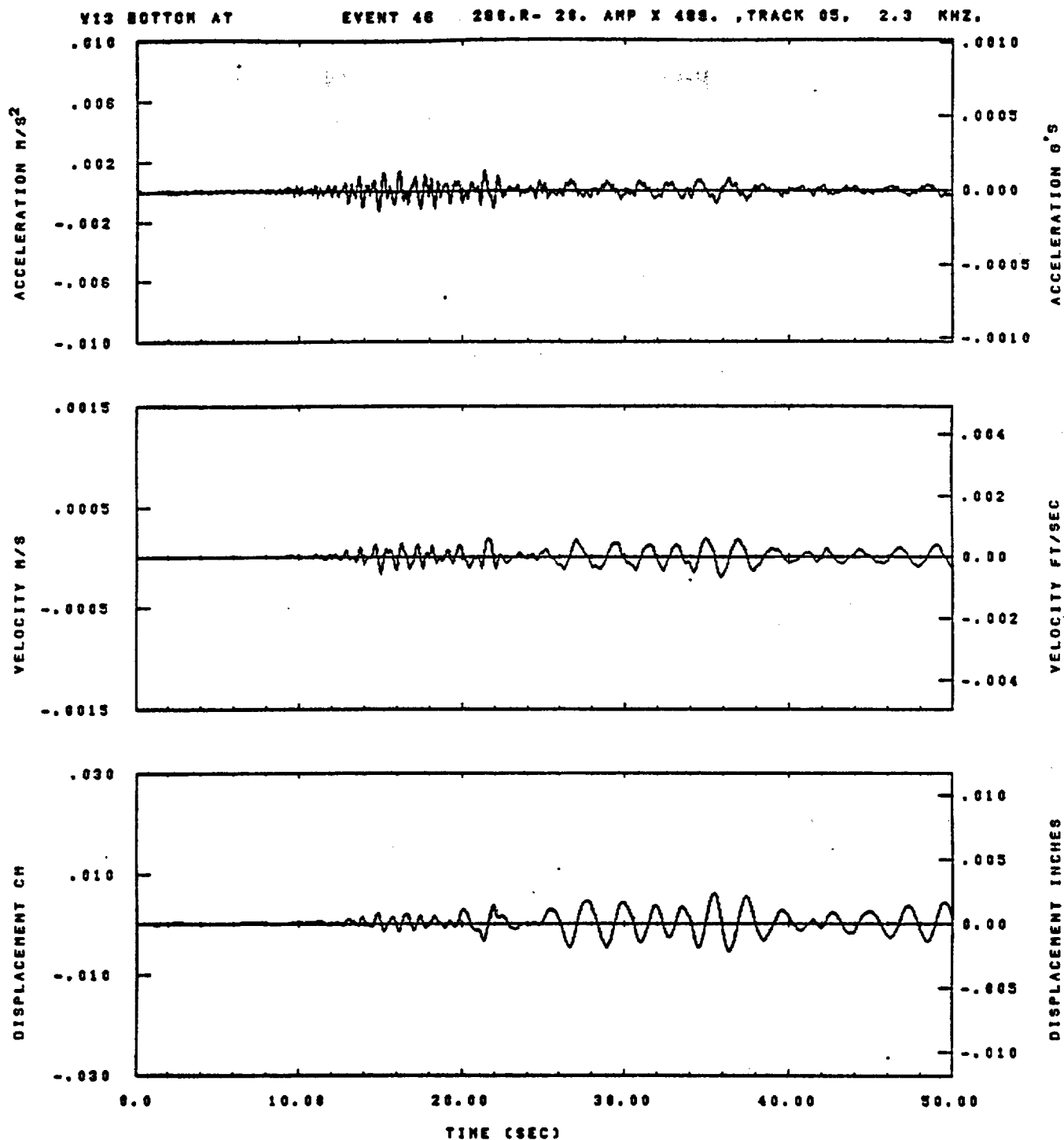


IDT= .0020	ODT= .005	FIX=	AAS= 0.
HPF= .30	BVN= .20	HLH= 201	ASB=
LPF= 22.	BYL= 5.	HLL= 1999	ASE=
VTS= .300	VTE= .200	FLL= -12.	VSE= 0.
OPS= 0.	OPE= 100.	FLH= 0	DSE= 0.

07.58.38.

08/26/82

Figure J-47



IDT= .0020	ODT= .005	FIX=	AAS= 0.
HFF= .30	BYH= .20	HLN= 201	ASB=
LPF= 22.	BYL= 5.	HLL= 1888	ASE=
VTS= .300	VTE= .200	FLL= -12.	VSE= 0.
DPS= 6.	DPE= 100.	FLH= 0	DSE= 0.

07.58.50.

08/24/82

Figure J-48

Distribution:

C. R. Cooley, Team Leader
Technology Development Team
Office of Waste Isolation
U. S. Department of Energy
NE-330
Germantown, MD 20767

R. Stein, Team Leader
Repository Projects Team
U. S. Department of Energy
NE-330
Germantown, MD 20767

W. W. Ballard, Jr., Director
Office of Waste Isolation
U. S. Department of Energy
NE-330
Germantown, MD 20767

F. E. Coffman, Deputy Ass't.
Secretary of Nuclear Waste
Management & Fuel Cycle Prog.
U. S. Department of Energy
NE-330
Germantown, MD 20767

J. O. Neff, Program Manager
National Waste Terminal
Storage Program Office
U. S. Department of Energy
505 King Avenue
Columbus, OH 43201

L. D. Ramspott
Technical Project Officer
Lawrence Livermore National
Laboratory
University of California
P.O. Box 808
Mail Stop L-204
Livermore, CA 94550

B. R. Erdal
Technical Project Officer
Los Alamos National Laboratory
University of California
P.O. Box 1663, MS-514
Los Alamos, NM 87545

G. L. Dixon, MS-954
Technical Project Officer
U. S. Geological Survey
P.O. Box 25046
Federal Center
Denver, CO 80225

W. E. Wilson, MS-416
U. S. Geological Survey
P.O. Box 25046
Federal Center
Denver, CO 80225

F. W. Muller
Technical Project Officer
Sandia National Laboratories
P.O. Box 5800
Organization 7417
Albuquerque, NM 87185

W. S. Twenhofel
820 Estes Street
Lakewood, CO 80215

K. Street, Jr., L-209
Lawrence Livermore National
Laboratory
P.O. Box 808
Livermore, CA 94550

D. C. Hoffman, MS-760
Los Alamos National Laboratory
University of California
P.O. Box 1663
Los Alamos, NM 87545

J. H. Anttonen, Asst. Manager
Projects & Facilities Management
U. S. Department of Energy
Richland Operations Office
P.O. Box 550
Richland, WA 99352

R. Deju
Rockwell International Atomic
International Division
Rockwell Hanford Operations
Richland, WA 99352

M. P. Kunich, Acting Dir. (3)
Waste Management Project Office
U. S. Department of Energy
P.O. Box 14100
Las Vegas, NV 89114

D. F. Miller, Director
Office of Public Affairs
U. S. Department of Energy
P.O. Box 14100
Las Vegas, NV 89114

R. H. Marks
U. S. Department of Energy
CP-1, MS-210
P.O. Box 14100
Las Vegas, NV 89114

B. W. Church, Director
Health Physics Division
U. S. Department of Energy
P.O. Box 14100
Las Vegas, NV 89114

D. A. Nowack (7)
U. S. Department of Energy
P.O. Box 14100
Las Vegas, NV 89114

A. E. Gurrola
Holmes & Narver, Inc.
P.O. Box 14340
Las Vegas, NV 89114

N. E. Carter
Battelle
Office of Nuclear Waste Isolation
505 King Avenue
Columbus, OH 43201

W. A. Carbiener
Battelle
Office of NWTIS Integration
505 King Avenue
Columbus, OH 43201

S. Goldsmith
Battelle
Office of Nuclear Waste Isolation
505 King Avenue
Columbus, OH 43201

ONWI Library (5)
Battelle
Office of Nuclear Waste Isolation
505 King Avenue
Columbus, OH 43201

R. M. Hill
State Planning Coordinator
Governor's Office of
Planning Coordination
State of Nevada
Capitol Complex
Carson City, NV 89170

S. A. Robinson
Department of Energy
State of Nevada
Capitol Complex
Carson City, NV 89170

A. R. Haki, Site Manager
Westinghouse-AEST
P.O. Box 708
Mail Stop 703
Mercury, NV 89023

S. M. Coplan (2)
High-Level Waste Management
Development Branch
Division of Waste Management
U. S. Nuclear Regulatory Commission
Washington, DC 20555

J. K. Kimball
Licensing Branch
U. S. Nuclear Regulatory Commission
Washington, DC 20555

Dr. Patrick A. Domenico
Geology Department
University of Illinois
Urbana, IL 61801

Dr. Lawrence T. Larson
Dept. of Geological Sciences
Mackay School of Mines
University of Nevada, Reno
Reno, NV 89557

Dr. Howard P. Ross
Earth Science Laboratory
University of Utah
Research Institute
420 Chipeta Way, Suite 120
Salt Lake City, UT 84108

Dr. Rudy C. Epis
Professor of Geology
Colorado School of Mines
Golden, CO 80401

Dr. Allan S. Ryall
Director, Seismological Lab
Mackay School of Mines
University of Nevada, Reno
Reno, NV 89507

Dr. H. Frank Morrison
Department of Geophysical Eng.
University of California
Berkeley, CA 94720

Dr. George A. Thompson
Department of Geophysics
365 Mitchell Bldg.
Stanford University
Stanford, CA 94305

Dr. Robert N. Farvolden
Dean of Science
University of Waterloo
Waterloo, Ontario
Canada N2L3G1

Dr. Konrad B. Krauskopf (Chairman)
Committee on Radioactive Waste
Management, NAS
Geology Department, 8-73
Stanford University
Stanford, CA 94305

Dr. John B. Farr
Western Geophysical Co.
P.O. Box 2469
Houston, TX 77001

WEAPONS TEST Distribution List

John A. Blume & Associates,
Engineers
130 Jessie Street (at New
Montgomery)
San Francisco, CA 94105

John G. Lewis
R & D Associates
P.O. Box 9695
Marina del Rey, CA 90291

Gyron L. Ristvet
Field Command
Defense Nuclear Agency
Attn: FCTK
Kirtland AFB, NM 87115

K. Olsen, MS-676
Los Alamos National Laboratory
P.O. Box 1663
Los Alamos, NM 87545

Frank J. Tokarz, L-799
Lawrence Livermore Natl. Lab.
P.O. Box 808
Livermore, CA 94550

Robert W. Newman
DOE/Nevada Operations Office
P.O. Box 14100
Las Vegas, NV 89114

Richard Navarro
Nevada Operations Office
U. S. Department of Energy
P.O. Box 14100
Las Vegas, NV 89114

Gilbert A. Bollinger
Dept. of Geology and Geophysics
Virginia Polytechnic Institute
and State University
Blacksburg, VA 24061

Bruce Bolt
University of California
Berkeley, CA 94720

Henry J. Degenkolb
H. J. Degenkolb & Associates
350 Sansome Street
San Francisco, CA 94104

Joseph A. Lahoud
Greenbriar Systems, Inc.
Fairfax Square
9940 Main Street
Fairfax, VA 22031

Tom McEvilly
University of California
Dept. of Geology & Geophysics
Berkeley, CA 94720

Leo J. O'Brien
Adaptronics, Inc.
1750 Old Meadow Road
McLean, VA 22102

Carl Romney
DARPA
1400 Wilson Blvd.
Arlington, VA 22209

G. F. Dickerson, Director
Division of Systems and
Technology
Internal Security Affairs
DP-52
1000 Independence Avenue SW
Washington, DC 20585

7100 C. D. Broyles
7110 J. D. Plimpton
7111 J. R. Banister
7111 J. W. Long
7111 L. J. Vortman (10)
7123 B. C. Benjamin
7124 J. W. Wistor
7417 F. W. Muller
9730 W. D. Weart
9733 D. M. Ellett
9760 R. W. Lynch
9761 L. W. Scully
9761 H. R. MacDougall
9764 R. C. Lincoln for J. T. Neal
9764 A. E. Stephenson
9764 R. M. Jefferson
8214 M. A. Pound
3141 L. J. Erickson (5)
3151 W. L. Garner (3)
for DOE/TIC (Unlimited
Release)
DOE/TIC (25) (C. H. Dalin, 3154-3)

